707739

ORAU 101

K. Morris Davis - ORAU DMSD Return to 1966

15-76-3090

RESEARCH REPORT

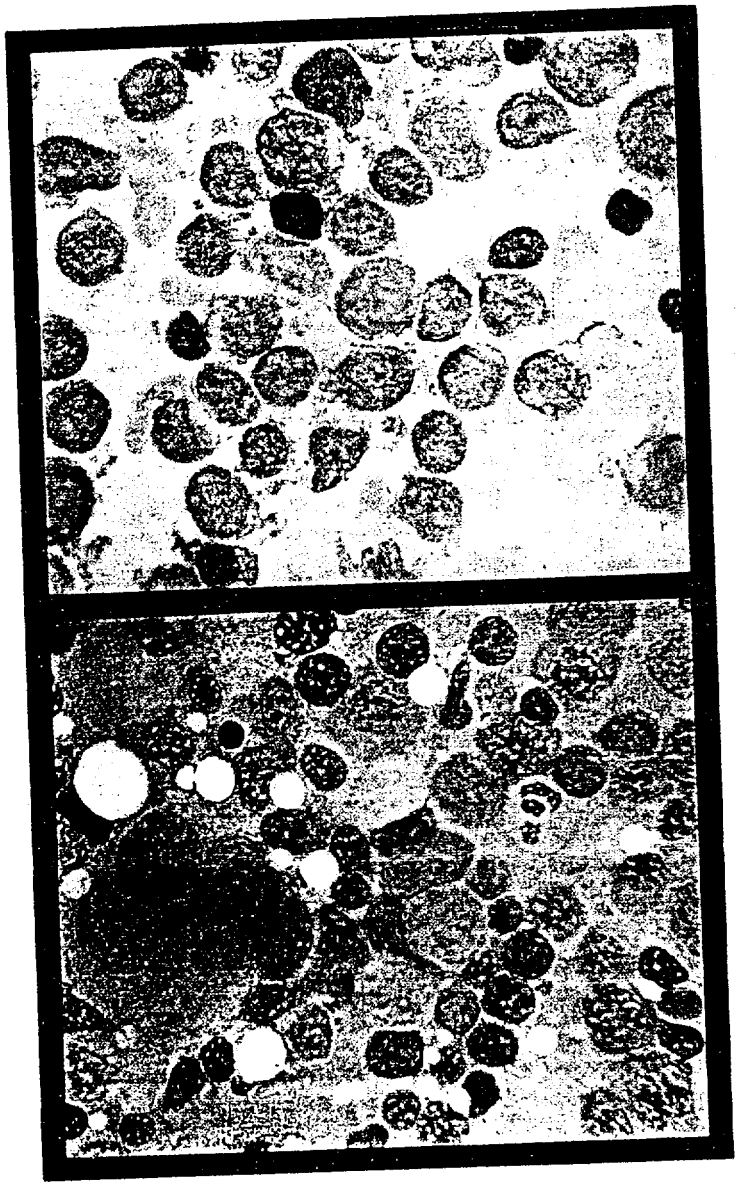

Medical Division

REPOSITORY Oak Ridge Institute for Science and Education, Medical Sciences Division

COLLECTION ORAU/Medical Sciences Division Vance Road Facility, Room 202A

BOX No. No folder title. Part 3 of 6

FOLDER Document No.: ORAU-30002

Oak Ridge Associated Universities

1027138

RESEARCH REPORT—MEDICAL DIVISION

Oak Ridge Associated Universities

FOR THE YEAR ENDING DECEMBER 31, 1966

Operating Under Contract With
The United States Atomic Energy Commission

1027139

ON THE COVER: *Photomicrographs of bone marrow aspirated from a man with acute leukemia. We are accustomed to think of acute leukemia as a diffuse process involving the entire cellular marrow. Yet in this patient, who improved during a course of chemotherapy, a noteworthy phenomenon was observed. Samples of the bone marrow in the trunk remained filled with leukemic cells (top photomicrograph). On the basis of clues from a bone-marrow scan, a sample was aspirated from the knee (bottom photomicrograph), and, surprisingly, active generation of normal blood precursors, especially red cell precursors, was discovered (see report on page 92). Here is direct evidence in man that sites normally occupied by fatty marrow are capable of producing normal hematopoietic cells in the face of persisting diffuse leukemic proliferation in the trunk marrow.*

ORAU–101

Single copies are available on request from:
Medical Division
Oak Ridge Associated Universities
Oak Ridge, Tenn. 37830

Printed in the United States of America
Price $3.00
Available from: Clearinghouse for Federal Scientific and Technical Information, Springfield, Virginia 22151

1027140

CONTENTS

	Page
ORGANIZATION OF RESEARCH	viii
INTRODUCTION	1
MECHANISMS OF RADIATION INJURY	5
Lipid Composition of the Blood Lymphocyte in Chronic Lymphocytic Leukemia. *F. Goswitz* and *F. Snyder.*	5
The Effect of Total-body Irradiation on Human Chromosomes: 1. Cytogenetic Studies of the Peripheral Leukocytes Seven Years After Total-body Irradiation. *K. O. Goh.*	8
Triglyceride Deposition in Irradiated Bone Marrow. *F. Snyder* and *R. Wood.*	12
A Study of Infections in Irradiated Patients. *E. Balish.*	14
Hematologic Effects of Total-body Irradiation in the Human Being. *G. A. Andrews, C. C. Lushbaugh, R. M. Kniseley* and *D. A. White.*	18
Radiation Exposure-rate Studies on Specific-Pathogen-Free Mice. *N. Gengozian, Elizabeth Allen* and *D. Carlson.*	23
Histologic Changes in Marrow After Total-body Irradiation of Marmosets: A Quantitative Stereologic Evaluation. *B. Nelson, Martha L. Lothrop* and *N. Gengozian.*	27
Vascular Radiation Syndrome. *C. C. Lushbaugh.*	30
The Absence of Sodium Loss After Massive Total-body Neutron Exposure of Rats. *C. C. Lushbaugh, H. D. Hodges, M. C. Yarbrough* and *W. D. Gibbs.*	34
STUDIES RELATED TO TREATMENT OF RADIATION INJURY	37
Radioprotective and Metabolic Studies of Alkenyl and Alkyl Ethers of Glycerol and Glycol. *F. Snyder* and *J. H. Arrington.*	37
Hemopoietic Spleen Colonies in the Rat. *F. V. Comas.*	38
Recovery of Lethally-irradiated Mice Given Fewer than One Million Syngeneic Bone-marrow Cells. *A. L. Kretchmar* and *W. R. Conover.*	41
Relation Between Rate of Erythroid Differentiation and Size of the Population of Hemopoietic Stem-Cells. *A. L. Kretchmar, Elizabeth M. Rupp* and *W. R. Conover.*	45

1027141

Serine-3-^{14}C Metabolism in Irradiation Chimeras: Respiration Pattern Analysis. *A. L. Kretchmar* and *C. E. Phipps*. 48
Computer Study of the Hemopoietic System of Rats Recovering from Total-body Irradiation. *J. P. OKunewick* and *A. L. Kretchmar*. 53
Effect of Phytohemagglutinin (PHA) on an Antibody-forming System. *N. Gengozian* and *K. F. Hübner*. 55
Human A-like Antigen on Marmoset Red Cells Detected with Rabbit Anti-Marmoset Saliva Serum. *C. B. Merritt* and *N. Gengozian*. 58
A Technique for Orthotopic Fitted Skin Grafts in the Marmoset. *R. Porter* and *N. Gengozian*. 62
Normal and Pathologic Intrauterine Development of Marmosets *(Saguinus fuscicollis)*. *C. C. Lushbaugh, Gretchen Humason, R. M. Kniseley* and *N. Gengozian*. 65

NASA STUDY ON RADIATION EFFECTS 69
Retrospective Study on Deleterious Radiation Effects in Man.... 69
Dosimetry Used in Equating Various Radiation Exposures for Determining Dose-Response Relationships. *W. L. Beck, R. J. Cloutier* and *F. V. Comas*. 70

MEDICAL RADIOISOTOPE DEVELOPMENT 74
Rhenium-188 as a Possible Diagnostic Agent. *R. L. Hayes* and *J. J. Rafter*. 74
Hydrous Ferric Oxide Colloid Labeled with Gallium-68. *R. L. Hayes, J. E. Carlton, J. J. Rafter* and *B. L. Byrd*. 78
Studies with Indium-113m. *R. L. Hayes* and *B. L. Byrd*. 81
Techniques to Provide Sterile and Pyrogen-free Radiopharmaceuticals from Long-lived Generators. *C. L. Edwards* and *R. L. Hayes*. 83
Binding of Gallium by Blood Serum. *R. E. Hartman* and *R. L. Hayes*. 84
Animal Toxicity Studies of a Ferric Oxide Colloid Suitable for Marrow Scanning. *B. Nelson, R. L. Hayes* and *C. L. Edwards*. 87

THERAPY WITH RADIATION 89
Total-body Irradiation. *F. V. Comas, C. L. Edwards, G. A. Andrews, Helen Vodopick* and *R. M. Kniseley*. 89
Spleen and Liver Irradiation in Chronic Granulocytic Leukemia.

1027142

F. V. Comas, C. L. Edwards, Helen Vodopick and *G. A. Andrews*. 90

ADIOISOTOPES IN DIAGNOSIS..... 92

Nonhomogeneity of Marrow in Acute Leukemia. *C. L. Edwards, Helen Vodopick* and *R. M. Kniseley*. 92

Bone-marrow Scanning with Radioactive Colloids. *R. M. Kniseley, C. L. Edwards, G. A. Andrews, R. Tanida* and *R. L. Hayes*. 96

Skeletal Scanning with Gallium-68 Citrate. *C. L. Edwards, J. Ahumada* and *R. L. Hayes*. 100

HEORETICAL AND EXPERIMENTAL STUDIES ON RETENTION AND DISTRIBUTION OF RADIONUCLIDES... 103

Turnover Compartmentalization. *P.-E. E. Bergner*. 103

Analog Computer Analysis of Human ^{51}Cr RBC Survival and Whole-body Retention Data. *C. C. Lushbaugh, W. D. Gibbs, W. Franz* and *P. -E. E. Bergner*. 106

Effect of Chromium on Rabbit Red Blood Cell Survival. *D. F. Opdyke, W. Franz, W. D. Gibbs, P.-E. E. Bergner* and *C. C. Lushbaugh*. 111

The Role of the Spleen in ^{51}Cr-Labeled Red Blood Cell Sequestration and Elimination by the Total Reticuloendothelial System. *C. C. Lushbaugh, W. D. Gibbs, C. L. Edwards, H. D. Hodges* and *R. F. Queener*. 115

A Two-year Study of Cesium-137 and Potassium in Normal Subjects. *W. D. Gibbs, H. D. Hodges, C. C. Lushbaugh* and *J. F. Quarles*. 117

ASIC STUDIES RELATED TO NEOPLASIA 120

A Search for Tumor Antigens Using an *In Vitro* Histocompatibility Test. *Helen Vodopick, Elizabeth M. Rupp, C. L. Edwards* and *N. Gengozian*. 120

Ch^{1} and Partial 21/15 Translocation: A Familial Study with One Member Having Acute Leukemia. *K. O. Goh*. 122

Chronic Lymphocytic Leukemia and Pseudodiploidy. *K. O. Goh*. 126

Additional Evidence of the Philadelphia Chromosome as a Postzygotic Abnormality in Identical Twins. *K. O. Goh, S. N. Swisher* and *E. C. Herman, Jr.* 129

Scope and Orientation of the Lipid Project. *F. Snyder*. 131

1027143

An Unidentified Lipid Prevalent in Tumors. *F. Snyder, E. A. Cress* and *N. Stephens*..... 131
Characterization and Identification of Glyceryl Ether Diesters Prevalent in Ehrlich Ascites Cells and Other Tumors. *R. Wood* and *F. Snyder*..... 133
The Incorporation of Labeled Lipids into a Glyceryl Ether Component of Ehrlich Ascites Cells. *F. Snyder* and *R. Wood*. .. 135
Metabolism of Alpha-Alkoxy Glyceryl Monoethers in Rat Liver, *In Vivo and In Vitro*. *F. Snyder* and *R. C. Pfleger*. 137
Chemical and Physical Properties of Isomeric Glyceryl Monoethers. *R. Wood* and *F. Snyder*. 138
The Synthesis of ^{14}C- and ^{3}H-Labeled Glyceryl Ethers. *E. O. Oswald, C. Piantadosi, C. E. Anderson* and *F. Snyder*..... 140
The GLC and TLC Resolution of Diastereoisomeric Polyhydroxystearates and Assignment of Configurations. *R. Wood, Enid L. Bever* and *F. Snyder*..... 140
GLC and TLC Analysis of Isopropylidene Derivatives of Isomeric Polyhydroxy Acids Derived from Positional and Geometrical Isomers of Unsaturated Fatty Acids. *R. Wood*. .. 142
The Quantitative Analysis of Long-chain Fatty Alcohols by Gas-Liquid Chromatography. *R. Wood*. 144
Cleavage of the 1- and 2-isomers of ^{14}C-Labeled Glyceryl Ethers by a Soluble Multienzyme System of Rat Liver. *R. C. Pfleger, F. Snyder* and *C. Piantadosi*..... 146
Volume Distribution of Normal and Leukemic Human Lymphocytes. *C. C. Lushbaugh, F. Goswitz, Martha L. Clevenger* and *Dorothy H. Lushbaugh*. 149

INSTRUMENT DEVELOPMENT AND METHODOLOGY... 154
An Automated System for Sample Collection and Computer Analysis of Thin-layer Radiochromatograms. *F. Snyder* and *Donna Bibler*. 154
An Improved Probe for Detecting Radioactivity at Surgery. *A. C. Morris, Jr*..... 156
Absolute Leukocyte Differential Counts by Rapid Electronic Sizing. *Dorothy H. Lushbaugh, C. L. Edwards* and *C. C. Lushbaugh*..... 158
Automated Hemolyzometers. 161
A. Automated RBC Osmotic Fragility Measurements Using a Linear-Gradient Device. *A. M. Webb* and *C. C. Lushbaugh*. 161

1027144

B. Micro Osmotic Fragility System for the Nonautomated Laboratory. *A. C. Morris, Jr.* and *C. C. Lushbaugh*. 164
Correction of Whole-body Counting Retention Studies with Radioisotope Tracers. *W. D. Gibbs, H. D. Hodges* and *C. C. Lushbaugh*. 166
A $4\pi^{32}$P-Labeled Diisopropylfluorophosphate (DFP) in Blood. *W. D. Gibbs* and *W. T. Pope*. 168

PUBLICATIONS 171

MEDICAL DIVISION EMPLOYEES 176

FELLOWSHIPS AND TERM APPOINTMENTS 177

RESEARCH PARTICIPANTS 178

STUDENT TRAINEES 178

CONSULTANTS AND COLLABORATORS 178

MEDICAL COMMITTEE, ORAU COUNCIL 182

ORAU MEDICAL PROGRAM REVIEW COMMITTEE 182

SEMINARS 183

SYMPOSIUM 188

AUTHOR INDEX 189

1027145

10271146

ORGANIZATION OF RESEARCH – ORAU MEDICAL DIVISION

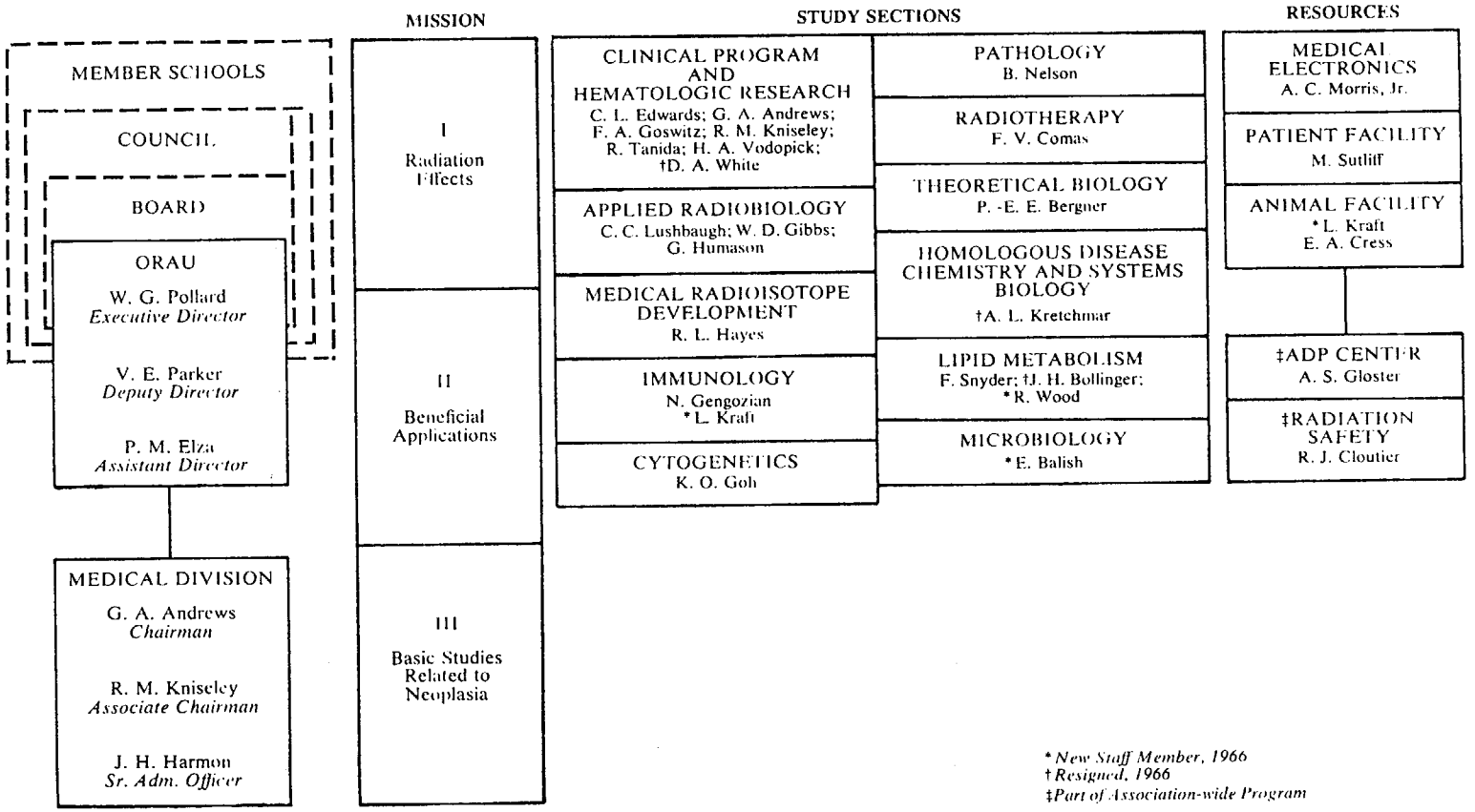

New Staff Member, 1966
†Resigned, 1966
‡Part of Association-wide Program

INTRODUCTION

THE DIVISION of Biology and Medicine of the United States Atomic Energy Commission supports laboratories for extensive biological research at several sites, a major one being at Oak Ridge. The ORAU Medical Division is one of these laboratories and it has, as a special feature, an active clinical investigational program. Most of the financial support comes from the Atomic Energy Commission; additional funds come from the National Aeronautics and Space Administration (human radiation effects), the National Institutes of Health (immunology program in marmosets), and the Armed Forces Epidemiologic Board (infections in patients with bone-marrow depression).

The program's major objectives fall within two broad categories: to obtain information on radiation effects, especially in the human being, and to advance the clinical uses of radioisotopes. The outline on page viii gives some of the relationships of the program.

During the year, three staff members who have made fine contributions to the Division program, left for other opportunities. Dr. James Bollinger, who had worked with the lipid group, moved to the Southwest Research Institute in San Antonio, Tex. Dr. David A. White, who carried most of the responsibility for outpatient care, is now in practice at the ıterville Clinic, Fredericktown, Pa. Dr. Arthur Kretchmar moved to . . University of Tennessee Memorial Research Center in Knoxville. He will continue to collaborate with the staff of the Medical Division. While here he was largely responsible for the introduction of work in theoretical and mathematical biology. Dr. Kretchmar, along with Howard Harmon, took the initial steps that led to the development of computer capabilities at Oak Ridge Associated Universities.

Joining the staff during the year were Dr. Lisbeth Kraft, Dr. Edward Balish, and Dr. Randall Wood. Dr. Kraft is a Doctor of Veterinary Medicine and she enjoys a fine reputation as an expert in animal care and in independent investigation, especially of infectious diseases in animals. Dr. Balish is a microbiologist who comes from a postdoctoral position at Argonne National Laboratory. He is developing the program on infections related to bone-marrow damage, especially that due to radiation injury. Dr. Wood had been on a postdoctoral program, working in lipid biochemistry at the Medical Division. He has now become part of the regular staff and has continued his research program with outstanding productivity.

The Medical Division's work is enhanced by productive collaborations with several scientists and institutions in Oak Ridge, Knoxville,

1027147

and at greater distances. During the year Dr. Frank Comas, radiotherapist at the Medical Division, was appointed as a staff member at the University of Tennessee Memorial Research Center, where he works one day per week, mainly in the teaching of residents. Other ties with this institution have developed or are planned. Dr. Fred Snyder and the lipid group at the Medical Division have increased their collaborative work with colleagues at the University of North Carolina.

Training activities in the Division are not emphasized in this report. We have continued to cooperate with the Special Training Division of ORAU and to provide teaching and clinical and laboratory experience for the medical courses given under the direction of Dr. Frank Goswitz. Longer periods of training in the Medical Division are provided in a variety of ways and the participants in these programs are listed on page 177.

The major symposium of the year was entitled *Compartments, Pools, and Spaces in Medical Physiology*. This was planned by Dr. C. C. Lushbaugh and Dr. Per-Erik E. Bergner, of the Medical Division staff, and Dr. W. Newlon Tauxe of the Mayo Clinic. Dr. Lushbaugh and Dr. Bergner are editing the proceedings of the meeting. The speakers included 14 from the United States and seven from other countries. Participants numbered 151, in addition to speakers, Medical Division staff members, and scientists from the Oak Ridge area.

An informal regional lipid meeting was sponsored by ORAU on March 29–30, 1966. The main purpose was to provide closer contact of faculty and graduate students engaged in lipid research within a few hundred miles of Oak Ridge, and attendance was limited to lipid groups from Vanderbilt University, University of Tennessee, University of North Carolina, University of South Carolina, and ORAU Medical Division. In addition to presentations by the participants, two invited lectures were arranged.

A low dose-rate human irradiator was built during the year with funds provided by AEC and NASA. This building consists of an outer shell 30 ft by 30 ft, an inner room 16 ft by 16 ft, plus supporting facilities. The entrance to the radiation area is through the hospital wing at the Medical Division. In the inner room there will be a homogeneous radiation field of radiation provided by 10 specially designed radiation sources. Patients can be irradiated for periods of from several hours to many days and can move about in a comfortable room during treatment. Special equipment for monitoring the patients is planned but not yet completed.

For some time the Medical Division has been seeking additional room, especially for laboratories and for experimental animals. Appropriate and needed growth in certain research activities has been prevented

1027148

by lack of space. Late in 1966, Oak Ridge Associated Universities purchased the building formerly used by Abbott Laboratories for development and production of radiopharmaceuticals (see page 4). This building includes 13,000 square feet, much of which is already divided into laboratories well fitted out for chemical and biological work. The newly-acquired building will be used mainly for the Medical Division, but will also house some other activities of ORAU. During the early months of 1967 some interior modifications will be made and we will begin to occupy this very welcome space.

The acquisition of this building from corporate funds, and the decision of the Board of Directors to build a new marmoset research building, are evidence of the very strong support the Division receives from Oak Ridge Associated Universities.

The following research report is in a form similar to that of the preceding two years. The results presented include a major portion of what has been accomplished, but do not cover all aspects of the ongoing program or all of the collaborative work. Most of the reports represent briefer versions of articles published, in press, or planned for publication.

The staff is again indebted to Betty Anderson, technical editor, and Rush King, photographer, for assistance in preparing this report.

GOULD A. ANDREWS
Chairman

1027149

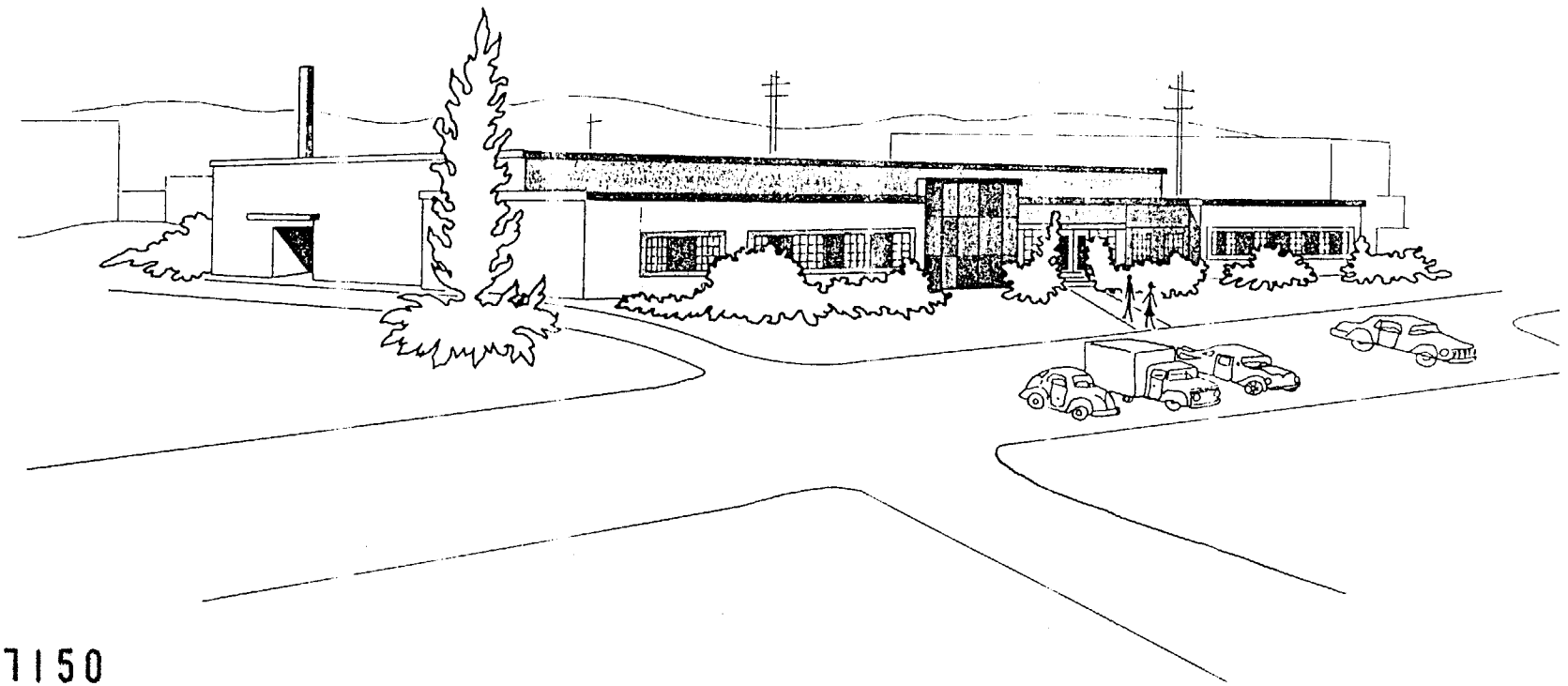

1027150

Artist's conception of new medical facility, Tyrone Road, Oak Ridge

MECHANISMS OF RADIATION INJURY

The work of the Division on mechanisms of radiation injury places most emphasis on acute effects. Hematologic, biochemical, immunologic and cytogenetic changes are investigated with the view toward (1) better management of unwanted radiation injury and (2) improved therapeutic use of radiation. Studies were done on human beings and several species of animals, and the experience is correlated where possible.

Lipid Composition of the Blood Lymphocyte in Chronic Lymphocytic Leukemia

F. Goswitz and F. Snyder

Lipids are structural components of all blood-cell membranes and organelles. The blood smears from patients with chronic lymphocytic leukemia manifest many "smudge" lymphocytes, but none or few of these cells are seen on normal blood smears. Possibly the membranes of these leukemic cells are more fragile than those of their normal counterparts, and hence they smudge when the cells are traumatized in the preparation of a blood smear. We have found significant differences in the lipid content and composition of the leukemic lymphocyte as compared with the normal lymphocyte. Therefore, we are considering the possibility that an abnormality in lipid chemistry contributes to making a cell more or less fragile by affecting the structure of its membrane.

The lymphocytes from 10 normal controls were obtained in yields ranging from 1 to 11% and with an average purity of 80% by removing the blood platelets by defibrination, the granulocytes by nylon-wool filtration, and the majority of erythrocytes by sedimentation and differential centrifugation. In nine patients with chronic lymphocytic leukemia, the lymphocytes were separated from the other cells by sedimentation and differential centrifugation with yields of nearly 40% and with a purity of almost 95%. Although the lymphocyte suspensions were contaminated with some erythrocytes, the lipid composition of only the lymphocytes could be calculated by subtracting the lipid values of a determined population of pure erythrocytes from those results of a de-

1027151

termined lymphocyte-erythrocyte mixture. With this method the composition of lipid per number of lymphocytes was obtained.

The lymphocyte-erythrocyte contaminated mixtures and the pure preparations of erythrocytes, which were also suspended in Eagle's buffer solution, were freeze-dried and their total lipids were extracted.[1] Thin-layer chromatography separated the extracted lipids into homologous lipid classes for analyses.

The total lipid content in the lymphocytes of healthy controls was significantly greater than that present in the lymphocytes of patients with chronic lymphocytic leukemia. *Table 1* illustrates that the mean of the total lipid content of normal lymphocytes was 0.8 mg/10^7 lymphocytes while the mean of the total lipid content of lymphocytes from patients with chronic lymphocytic leukemia was only 0.06 mg/10^7 lymphocytes. The concentrations of all individual lipid fractions were lower

TABLE 1

Total Lipid Content of Human Lymphocytes

Patient	WBC × 10^3 / mm^3 blood	WBC % lymphocytes	mg total lipid / 10^7 lymphocytes
Healthy Controls			
1	5.6	48	0.39
2	4.6	35	1.47
3	5.6	36	1.08
4	4.7	39	1.04
5	7.3	50	0.4
6	7.3	40	0.26
7	8.1	45	0.25
8	4.9	36	1.17
9	7.5	39	1.47
10	4.5	38	0.48
		Mean ± Standard Deviation	0.8 ± 0.55
Chronic Lymphocytic Leukemia			
A	16.7	88	0.02
B	129.2	96	0.01
C	202.5	97	0.02
D	216.5	97	0.05
E	35.9	94	0.06
F	91.5	84	0.04
G	18.2	88	0.16
H	210.0	100	0.08
I	29.0	98	0.13
		Mean ± Standard Deviation	0.06 ± 0.05

1027152

in leukemic cells but there were some qualitative differences in the lipid pattern; in leukemic cells fatty acids were relatively less reduced, and phospholipids were present in small amounts as compared with neutral lipids, as shown in *Table 2*. Although *Table 2* presents the mean percentage of the various lipid fractions for the normal and leukemic lymphocytes, it must be stressed that variations have been observed in these lymphocytes. Studies are in progress to determine the reasons for these changes, but now they are considered to be due either to the primary disease process or to the type of therapy prescibed for the disease. In addition, some lipid classes as yet uncharacterized and labeled as unknown in *Fig. 1* have been observed in the lymphocyte-erythrocyte contaminated mixtures.

We plan to investigate the significance of, and the mechanism responsible for, these differences and to determine whether all the lipid in the lymphocyte is located in the cell membrane as it is in the erythrocyte.

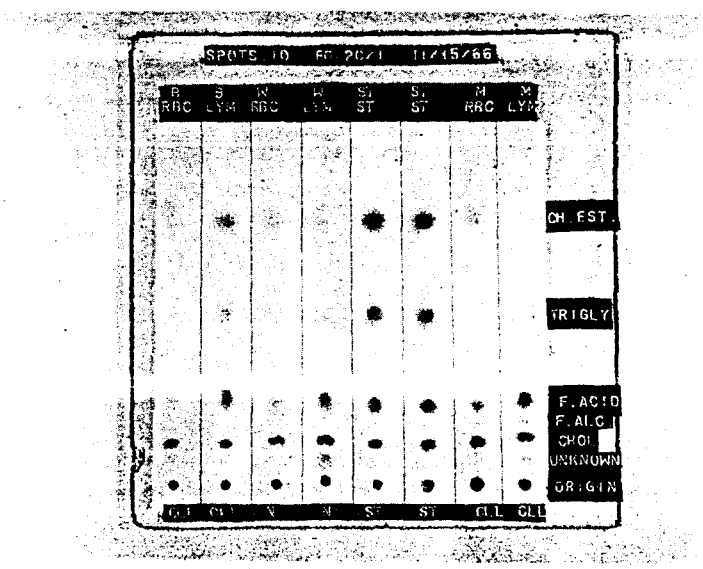

Fig. 1. Thin-layer chromatogram of neutral lipids extracted from the pure red blood cell preparation (RBC) and the lymphocyte-erythrocyte contaminated mixture (LYM) of patients B and M who have chronic lymphocytic leukemia (CLL) and of a normal (N) subject W. A known standard (ST) neutral lipid is used to identify and quantify the lipid fractions: cholesteryl esters (CH. EST.), triglycerides (TRIGLY), fatty acid (F. ACID), fatty alcohol (F. ALC.), cholesterol (CHOL.).

1027153

TABLE 2

Relative Distribution of Lipid in the Human Lymphocyte

Healthy Controls*		Chronic Lymphocytic Leukemia*
60%	Neutral lipid	70%
25%	Free steroids	25%
5%	Fatty acids	20%
10%	Triglycerides	10%
20%	Cholesterol esters	15%
40%	Phospholipid	30%
10%	Sphingomyelin	6%
25%	Lecithin	15%
5%	Cephalin	9%

*Mean percentage values of the lymphocytes studied.

REFERENCE

1. Snyder, F. and Piantadosi, C. Labeling and radiopurity of lipids. *In:* Advances in Lipid Research, Vol. 4, New York, Academic Press, 1966, pp. 257–283.

The Effect of Total-body Irradiation on Human Chromosomes: I. Cytogenetic Studies of the Peripheral Leukocytes Seven Years after Total-body Irradiation

K. O. Goh

A group of eight men accidentally exposed to mixed fast neutrons and gamma rays resulting in a total-body irradiation ranging between 22.8 and 365 rads has been the subject of several reports. A smaller G chromosome was found in three of these men and has been reported.[1] This is a report of the chromosomal aberrations found in the peripheral blood of the six men who are still available for our cytogenetic investigation.

Table 3 shows the distribution in the chromosomal analyses of these patients. Seventy-nine (15.4%) abnormal cells and 46 (9%) X_1 cells were seen in this investigation. A total of 116 chromosomal breakages was found in these 512 metaphases. The chromosomal breaks included fragments, in all patients *(Fig. 2)*; dicentrics, in four out of six patients

1027154

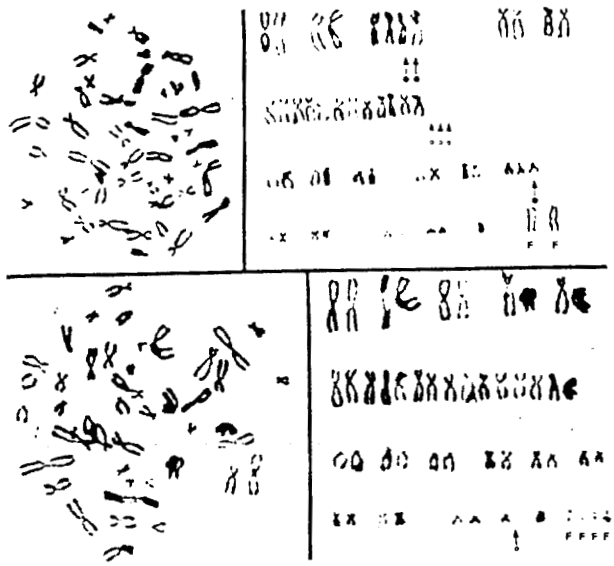

Fig. 2. Two metaphases and their karyotypes showing large fragments (acentric F) in the upper portion and small fragments in the lower portion. Additional chromosomes are marked by an arrow with a black circle and the missing chromosomes by an arrow with a white circle.

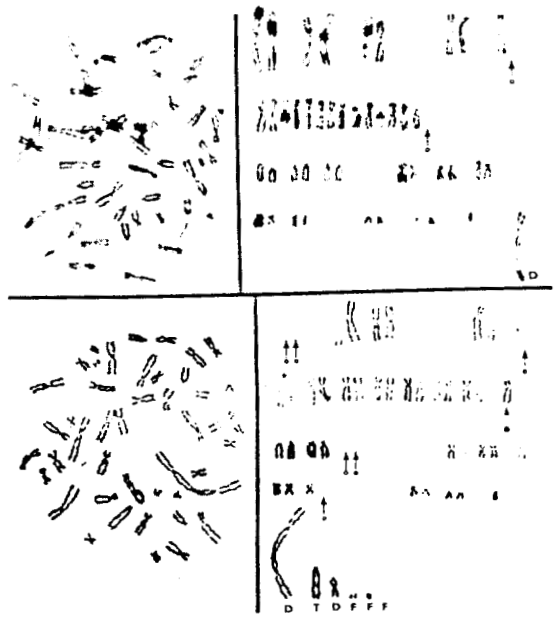

Fig. 3. Two metaphases and their karyotypes showing the dicentric chromosomes marked with D's.

1027155

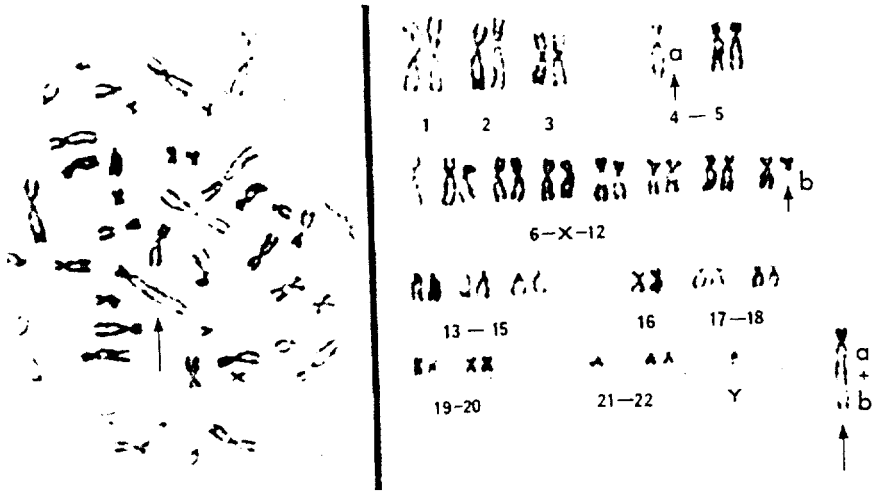

Fig. 4. A diploid metaphase and its karyotype showing a translocated chromosome (a + b). The abnormal chromosome probably is derived from the missing chromosome 4-5(a) and the long arm of a chromosome in 6-X-12(b).

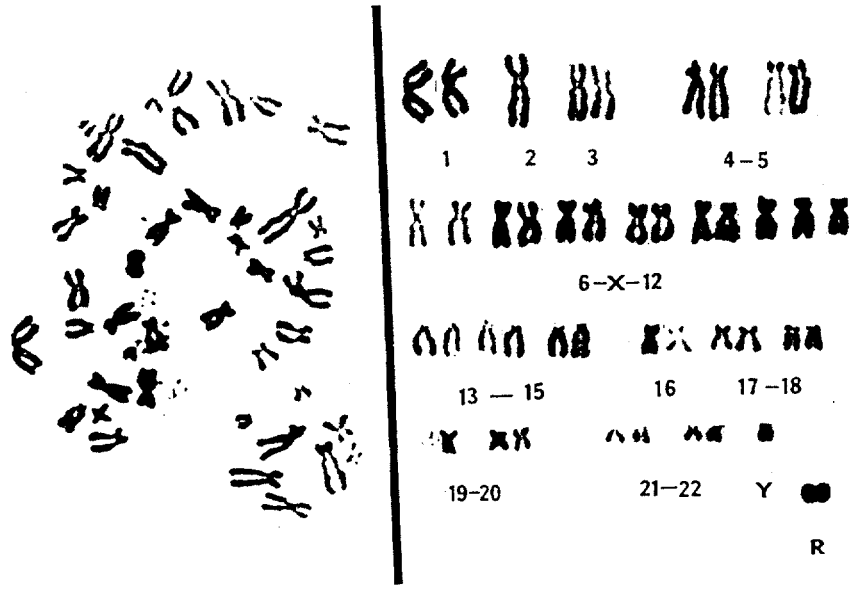

Fig. 5. Metaphase with 43 and a ring chromosome (R) and its karyotype.

1027156

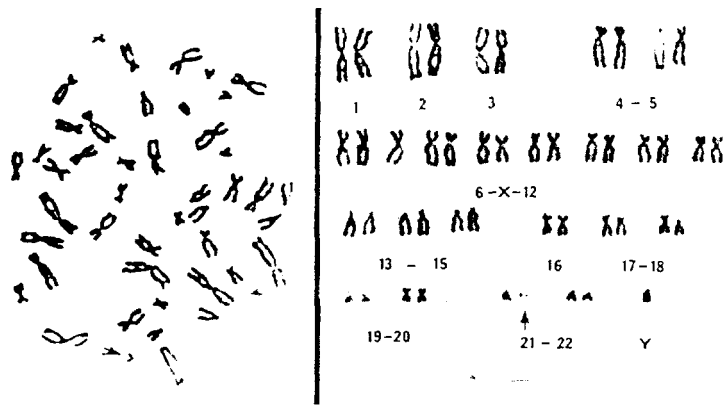

Fig. 6. A metaphase and its karyotype with a smaller G (21-22) chromosome (arrowed).

TABLE 3

Chromosomal Number and Frequency of Abnormal Cells

		Chromosome Number					Total	%M‡	Abn. Cells		X_1§	Cells‖
Code*	Doses†	<45	45	46	47	>47			No.	%	No.	%
A(40)	365(1250)	1	7	92	0	0	100	92	10	10	7	7
B(32)	270(1330)	0	10	90	0	0	100	90	10	10	5	5
C(39)	339(1710)	9	8	91	3		111	82	18	16.2	12	10.6
D(51)	327(1980)	2	2	23	1	0	28	82	10	36	5	18
E(35)	236(1050)	5	5	90	0	0	100	90	20	20	13	13
F(41)	68.5(2550)	1	3	69	0	0	73	95	11	15	4	5.5
	Total	18	35	455	4		512	89	79	15.4	46	9

* This coding has been used by others. The number inside the parentheses was the age at the time of exposure.
† Established doses of total-body irradiation in rads. The number inside the parentheses is the absolute lymphocyte per cubic millimeter 11 hr after the accident.
‡ Percentage of cells having a chromosomal number of 46 (diploid).
§ Cells having chromosomal aberrations (see text).
‖ Presumably first generation cells with chromosomal aberrations accompanied by fragments.

1027157

(Fig. 3); translocation, in all patients *(Fig. 4);* ring chromosomes, in four out of six patients *(Fig. 5);* and smaller G, in all patients *(Fig. 6).*

The frequency of these abnormalities is independent of the doses of irradiation received. The reason might be explained by several possibilities, some rather unlikely: (1) The total population of lymphocytes in each person at the time of radiation was different; (2) each person's lymphocytes might vary in their radiosensitivity; (3) maximum mitotic rates might vary among individuals (see *Fig. 58* of the section on Chronic Lymphocytic Leukemia and Pseudodiploidy, p. 126), hence different fractions of the patients' lymphocyte populations were examined; (4) severely damaged cells might have been eliminated from the circulation; and (5) at the time of the cytogenetic studies, a patient might have had some subclinical virus disease. In spite of these possibilities, the present observation supports those of others that chromosomal aberrations can be seen seven years after *in vivo* total-body irradiation.

REFERENCE

1. Goh, K. O. Smaller G chromosome in irradiated man. Lancet 1, 659–660, 1966.

Triglyceride Deposition in Irradiated Bone Marrow*

F. Snyder and R. Wood

Fatty acid metabolism in bone-marrow cells exposed to gamma radiation primarily involves formation of triglycerides. This metabolic alteration appears morphologically as an increased number of fat cells, which reach their maximum approximately one week after total-body irradiation (TBI).

The type of triglyceride deposited and the incorporation of palmitic-1-^{14}C acid into triglycerides are the subjects of this report. Femoral bone-marrow triglycerides were isolated by preparative thin-layer chromatography (TLC) from control and irradiated (800 R) Carworth Farms Nelson strain rats. The purified triglyceride fractions were separated further by $Ag(NH_3)_2^+$ TLC and by gas-liquid chromatography

---

*Abstract of paper presented at American Oil Chemists' Society fall meeting, 1966, Philadelphia, Pa.

1027158

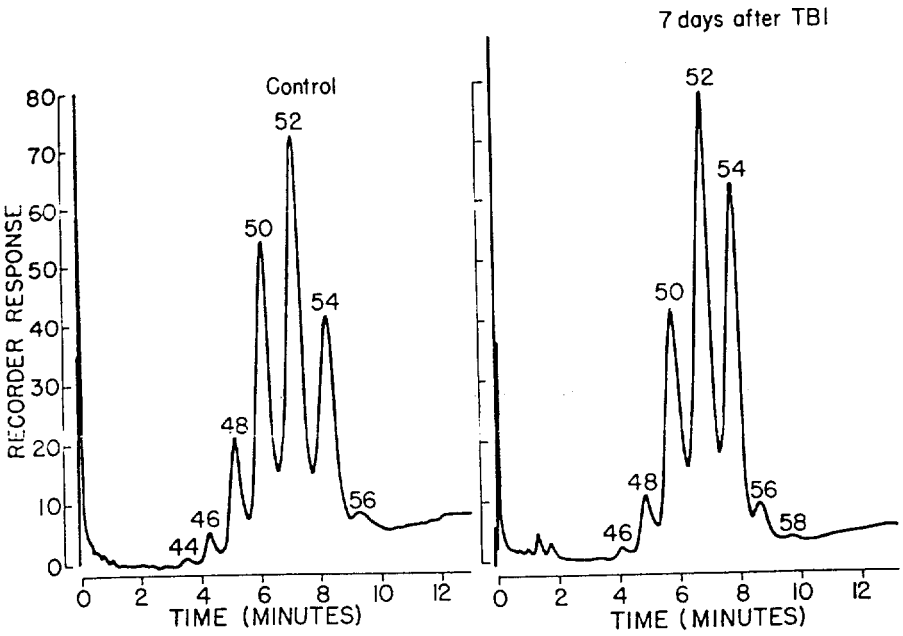

Fig. 7. Gas-liquid chromatograms of intact triglycerides isolated from control bone marrow (left) and irradiated bone marrow (right). The numbers above each peak refer to the total carbon number of the three acyl groupings of the triglyceride. The temperature was programed from 250-350°C manually during a period of 12 min. The shift in peak size to higher carbon numbers occurs after irradiation.

(GLC) with the use of a JXR-silicone liquid phase. The specific activities of the total triglyceride fraction were calculated as a function of time after irradiation and of time after injection of palmitic-1-^{14}C acid on the basis of TLC zonal scans and TLC photodensitometry. The specific activities demonstrated that the maximal period for triglyceride biosynthesis occurred between 3 and 4 days after TBI.

The degree of unsaturation in the triglyceride fraction did not appear to be affected by irradiation. However, GLC showed that the newly formed triglycerides deposited in the irradiated bone marrow had a somewhat higher carbon number than that found in control marrow *(Fig. 7)*.

1027159

A Study of Infections in Irradiated Patients

E. Balish

The most serious complication of sublethal total-body irradiation is infection. Many data exist on the increased susceptibility of, and infections that occur in, laboratory animals receiving sublethal and lethal doses of total-body irradiation. However, information is still meager on the etiology of infections in human beings after total-body irradiation at lethal and sublethal levels. Of particular interest are the infections that occur subsequent to accidental sublethal doses of total-body irradiation and that may account for possibly preventable deaths. This research project will be concerned with identifying the species of organisms involved in infections, as well as their portal of entry and response to therapy. The relative role played by commensal versus the exogenous microorganisms will be studied. Another important objective will be to ascertain whether changes in the microbial flora, which could result in the overgrowth of more virulent mutant species, might occur after treatment with total-body irradiation or local irradiation to areas of the digestive tract or the respiratory tract.

Several interesting results have shown up in the initial study of a patient treated with 100 R total-body irradiation (eight ^{137}Cs sources at 1 R/min) for chronic granulocytic leukemia. No antibiotics were given during this study and no infections were manifest. Blood samples before and after exposure were negative. A β-hemolytic *Staphylococcus albus* and *Klebsiella-Aerobacter* microorganisms were cultured from the urine two weeks after exposure. The numbers of the latter microorganisms were relatively small. However, urine samples before or immediately after (1 through 12 days) 100 R total-body irradiation were negative.

Throat cultures remained relatively stable after the exposure to 100 R. *Neisseria* and α- and β-hemolytic streptococci predominated in the throat before and for one month after exposure. Three days after exposure, β-hemolytic *Staphylococcus albus* appeared in nasal cultures. Before irradiation, a nonhemolytic *S. albus* and *Klebsiella-Aerobacter* (nonhemolytic) predominated. The β-hemolytic *S. albus* became the predominant microorganism isolated from nasal swabs within two weeks after the total-body irradiation *(Table 4)*.

Before irradiation, the predominant microorganism isolated from gastric secretions was *Candida albicans*. The flora did not show any change immediately after exposure *(Table 5)*. However, *Neisseria* and α-streptococci appeared as the predominant microbial flora after one day, and large populations of the latter organisms were observed up to three weeks after exposure. Moreover, during the latter period the

stomach contents were less acidic than bef
Three weeks after the exposure, *C. albi*
gastric secretions were more acidic. The
and its influence on the flora will be foll
gastric acid is supposed to kill a large nu
nisms. However, if acid flow is interfered
bacteria could accumulate in large number
to a person whose defense mechanisms ha

Table 6 shows the fecal microbial pr
predominant aerobic microorganism bef

TABLE 4

Predominant Microorganisms from Na
Exposure to 100 R Total-bo

Time (days)	Predominant Mi
−2	*S. albus* (nonh
−1 (Preirradiation)	*Klebsiella-Aero*
+1 (Postirradiation)	*Klebsiella-Aero*
+2	*Klebsiella-Aero*
+4	*S. albus* (β-he
	(nonhemolytic
+9	*S. albus* (nonh
+15	*S. albus* (β-he
+22	*S. albus* (β-he
+29	*S. albus* (β-he
+34	*S. albus* (β-he

TABLE 5

pH and Microflora of Gastric Secretions fro
Exposure to 100 R Total-bo

Time (days)	Total Aerobic count/ml	Pr Mic
−2	1.3×10^2	*Candida*
−1 (Preirradiation)	1.9×10^3	*Candida*
+1 (Postirradiation)	1.5×10^2	*Candida*
+2	5×10^4	*Neisseria* streptocc
+3	1×10^5	*Neisseria* streptocc
+22	3.7×10^5	*Neisseria* streptocc
+29	1.4×10^3	*Candida*
+36	6×10^2	*Candida*

1027160

stomach contents were less acidic than before and shortly after exposure. Three weeks after the exposure, *C. albicans* predominated again and gastric secretions were more acidic. The pH of the gastric secretions and its influence on the flora will be followed with great interest since gastric acid is supposed to kill a large number of swallowed microorganisms. However, if acid flow is interfered with by exposure to radiation, bacteria could accumulate in large numbers and might be a serious threat to a person whose defense mechanisms have been weakened.

Table 6 shows the fecal microbial profile. *Escherichia coli* was the predominant aerobic microorganism before the irradiation. However,

TABLE 4

Predominant Microorganisms from Nasal Swabs before and after Exposure to 100 R Total-body Irradiation

Time (days)	Predominant Microorganisms
−2	*S. albus* (nonhemolytic)
−1 (Preirradiation)	*Klebsiella-Aerobacter* (nonhemolytic)
+1 (Postirradiation)	*Klebsiella-Aerobacter* (nonhemolytic)
+2	*Klebsiella-Aerobacter* (nonhemolytic)
+4	*S. albus* (β-hemolytic) and *Klebsiella-Aerobacter* (nonhemolytic)
+9	*S. albus* (nonhemolytic) and *Klebsiella-Aerobacter*
15	*S. albus* (β-hemolytic)
+22	*S. albus* (β-hemolytic)
+29	*S. albus* (β-hemolytic)
+34	*S. albus* (β-hemolytic)

TABLE 5

pH and Microflora of Gastric Secretions from a Patient before and after Exposure to 100 R Total-body Irradiation

Time (days)	Total Aerobic count/ml	Predominant Microorganisms	pH of Stomach Contents
−2	1.3×10^2	*Candida albicans*	1.8
−1 (Preirradiation)	1.9×10^3	*Candida albicans*	3.0
+1 (Postirradiation)	1.5×10^2	*Candida albicans*	1.8
+2	5×10^4	*Neisseria* and α-hemolytic streptococci	5.8
+3	1×10^5	*Neisseria* and α-hemolytic streptococci	4.5
+22	3.7×10^5	*Neisseria* and α-hemolytic streptococci	3.5
+29	1.4×10^3	*Candida albicans*	1.8
+36	6×10^2	*Candida albicans*	2.0

1027161

after one day a β-hemolytic *S. albus* became prominent. This is quite unusual and further studies must be performed to ascertain its significance. This organism was present in the stool in large numbers for one week after irradiation. A β-hemolytic *S. albus* was isolated from nasal swabs of this same patient soon after irradiation *(Table 4). Escherichia coli,* which was a major component in the microflora before and for a short time after irradiation, was apparently inhibited by other microorganisms *(Table 6)* and was no longer the predominant aerobic bacterium.

Since these studies are in the initial phase, many more samples will have to be taken before any definite conclusions can be made. An important objective will be to ascertain whether the microorganisms isolated from postirradiation infections show any correlation with the predominant microflora.

Concurrent with the foregoing investigation, the microbial flora of a patient receiving a radiomimetic drug was also studied. This patient was treated with 150 mg Cytoxan daily, for a metastatic squamous cell carcinoma, from October 21 through December 31, 1966. No antibiotics were given and no infections were manifest during this time. Blood samples before and during therapy were negative. Sporadic, low populations of microorganisms of the *Klebsiella-Aerobacter* group were found in freshly voided urine samples. Throughout the observation period throat and nasal cultures showed that a β-hemolytic *S. albus* and

TABLE 6

Fecal Microflora from a Patient before and after 100 R Total-body Irradiation

Time (days)	Total Aerobic Colonies per g (dry wt)	Predominant Microorganisms
−2	1.9×10^7	*E. coli*
−1 (Preirradiation)	1.7×10^6	*E. coli*
+1 (Postirradiation)	3.9×10^7	β-hemolytic, *S. albus* (2.5×10^7)
+3	6.4×10^8	*E. coli* and *S. albus* (β-hemolytic)
+8	3.4×10^9	*E. coli* and *S. albus* (β-hemolytic)
+14	1.6×10^8	*Klebsiella-Aerobacter;* Fecal streptococci; *Proteus inconstans*
+21	1.2×10^7	*Coli-Aerogenes*
+28	6.1×10^7	*Streptococcus faecalis*
+35	6.6×10^6	*Coli-Aerogenes*

1027162

TABLE 7

Fecal Microflora of a Patient before and during Therapy with a Radiomimetic Drug (Cytoxan—150 mg/day)

Time (days)	Total Aerobic Count per g (dry wt)	Predominant Microorganism
−15	4.9×10^9	*E. coli*
−9	1.2×10^9	*E. coli*
−6	8.7×10^8	*E. coli*
−2	2.9×10^9	*E. coli*
(Cytoxan therapy started)		
+11	2.2×10^9	*E. coli* and *Klebsiella-Aerobacter*
+12	6.1×10^7	*E. coli* and *Proteus* sp.
+20	4.5×10^7	*E. coli*
+48	1.1×10^9	*E. coli*
+53	6.5×10^9	*E. coli*
+60	2.3×10^9	*E. coli*

α-hemolytic streptococci were the predominant microorganisms. Rectal swabs consistently showed a predominance of *E. coli* and gastric secretions were consistently positive for *C. albicans*. The pH of the gastric contents ranged between 1.5 and 2. *Table 7* shows the total aerobic population and the predominating microorganisms in the stool over the period of observation. *Escherichia coli* was the predominant aerobic microorganism throughout this time.

Numerous reports in the literature indicate that the microbial flora of humans remains relatively stable for a long time and that it is most difficult to remove or eliminate a resident strain of bacteria.[1–4] In this initial work we find after 100 R of total-body irradiation that the nasal, gastric and fecal microflora are altered. A rise in the pH of the gastric secretions was observed and may be a factor in the shift in the gastric microflora. If irradiation permits the overgrowth of bacteria in the stomach and small intestine, serious complications might arise since large populations of bacteria are not normally found in the small intestine.

REFERENCES

1. Zubrzycki, L. and Spaulding, E. H. Studies on the stability of the normal human fecal flora. J Bacteriol 83, 968–974, 1962.
2. Wilson, G. S. and Miles, A. A. Topley and Wilson principles of bacteriology and immunity. 4th ed. Williams and Wilkins Co., Baltimore, 1955, pp. 468, 2250, 2253.
3. Kraus, F. W. and Gaston, C. Individual constancy of numbers among oral flora. J Bacteriol 71, 703–707, 1956.
4. Sears, H. J. Persistence of individual strains of *Escherichia coli* in the intestinal tract of man. J Bacteriol 59, 293–301, 1949.

1027163

Hematologic Effects of Total-body Irradiation in the Human Being*

G. A. Andrews, C. C. Lushbaugh, R. M. Kniseley, and D. A. White

During the course of studies of total-body irradiation at the Medical Division, careful records have been kept of hematologic responses. Most of this information was obtained in patients with blood diseases; therefore the effects seen are not those that would be expected in the normal person. On the other hand, the responses may have considerable value in understanding the abnormal hematopoietic physiology of patients with blood diseases. To the extent that certain trends occur in all groups of patients, regardless of diagnosis, the findings are of value in pointing to general hematologic responses to total-body irradiation. These patients can be divided into three groups: (1) Those with chronic hematologic disorders, polycythemia vera, chronic leukemia, exposed to doses of 50 and 100 R; (2) those with various types of advanced neoplasm exposed to doses of 300 to 473 R; and (3) those with acute leukemia in relapse given exposures of from 206 to 384 R.

Most of the patients were irradiated in the cesium-137 total-body irradiator, which produces a uniform air dose. Dose rates were usually between 0.64 and 1.52 R/min. All the patients reported were given a single total-body exposure. Most of them were followed for a period of six weeks or longer, and none was given other forms of myelosuppressive therapy during this period.

Nonhematologic Malignancies. Figure 8 shows typical hematologic responses in the average value for four patients with cancer of various sorts (not primarily involving blood-forming tissues).

The hematologic effects are very much what one would expect in the normal. The improvement in hemoglobin was partially caused by transfusion, and therefore the red-cell values cannot be evaluated. It was our impression that these patients lacked the capacity for rapid and complete recovery that is seen in radiation accident victims, probably because as cancer patients they had been subjected to previous therapy with local irradiation and myelosuppressive drugs.

Polycythemia vera. Six patients with polycythemia vera were given 100 R exposures and the mean blood values are shown in *Fig. 9*. In these patients, the red-cell values had been lowered to acceptable levels by

*A condensed version of a presentation at the International Atomic Energy Agency Panel on *The Effects of Various Types of Ionizing Radiations from Different Sources on the Haematopoietic Tissues*, Vienna, Austria, May 17–20, 1966.

1027164

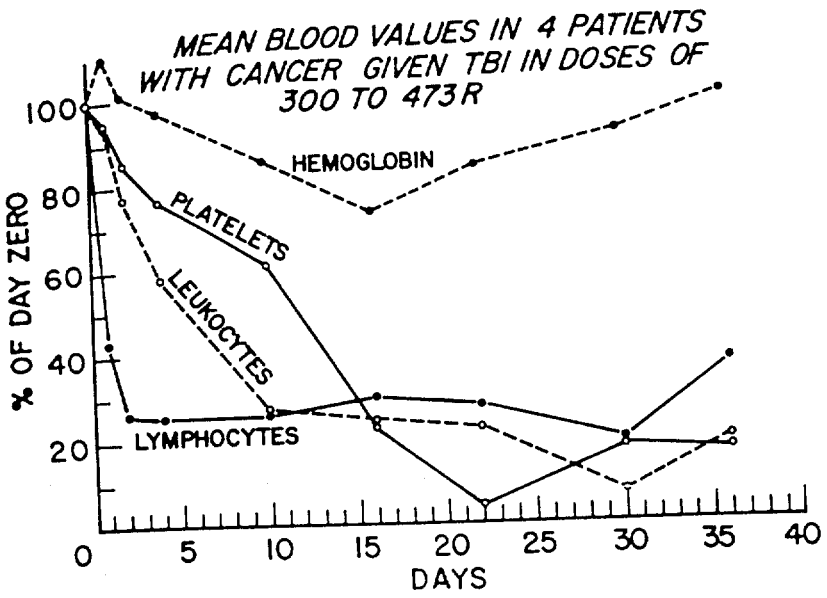

Fig. 8. Mean values for leukocytes, lymphocytes and platelets. Four patients with cancer treated with TBI, 300 to 470 R.

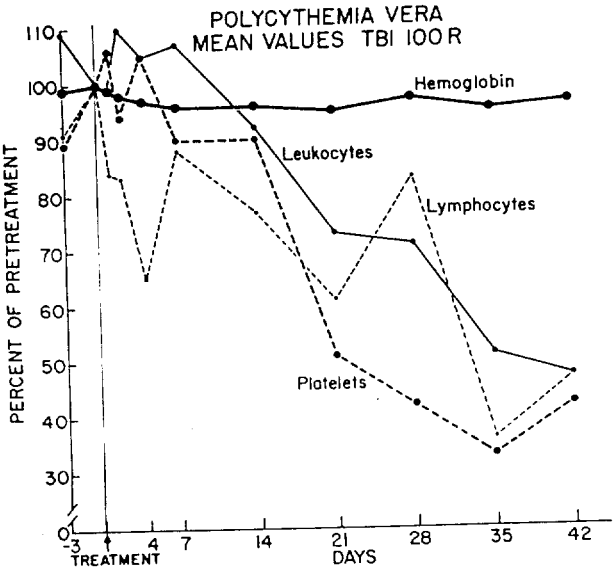

Fig. 9. Six patients with polycythemia vera—mean percentages of pretreatment levels for leukocytes, lymphocytes, platelets and hemoglobin.

1027165

phlebotomy before the treatment was given; this may explain the absence of any fall apparently due to radiation treatment. Clinically, the patients responded well in that symptoms were alleviated by the combined phlebotomy and radiation treatment.

Chronic Lymphocytic Leukemia. An interesting comparison was made between two groups of patients, one that received 50 R exposures, the other that received 100 R exposures. Although these two groups of patients are not identical in pretreatment status, it is believed that differences in response are truly related to the differences in dose. *Figure 10* shows that the platelet values were much more depressed in those that received 100 R. *Figure 11* shows that the degree of depression of the lymphocytes, however, was no different for the two radiation doses.

Chronic Granulocytic Leukemia. In a small group of patients with chronic granulocytic leukemia given 50 R, there was a gradual fall in leukocyte values during a period of about three weeks to about 50% of the pretreatment levels. Hemoglobin values improved slightly and platelet values showed a variable and erratic response.

Acute Leukemia. The patients with this disease divide into two groups, one group who had a distinct remission as a result of total-body irradiation and another group that showed no remission. *Figures 12 and 13* show the leukocyte values in these two groups of patients. It is not clear what underlying differences account for the remissions in one group and lack of remissions in the other. Almost all these patients had extensive pretreatment therapy with drugs and were in a late or near terminal stage of their disease. All had a large percentage of blast cells in the marrow at the time of treatment and most of the leukocytes in the peripheral blood were blast cells. In the group that had remissions *(Fig. 13)*, the rise in white count after day 20 consisted mostly of normal granulocytes, and platelet values showed an even more striking early rise, beginning on day 20.

These studies show some underlying patterns, even though there is pronounced variation, depending upon the disease state. The effect of radiation is always to depress hematologic values in some degree. In general, the levels of abnormal cells are more easily depressed than those of normal cells. For example, in chronic lymphocytic leukemia and chronic granulocytic leukemia, 50 R produces a distinct depression in the white blood count. Although data for normal persons at these dose levels are not readily available, limited information from radiation accidents suggests that it is very difficult to detect any effects of 50 R on the routine blood values; thus the abnormal lymphocytes and granulocytes of chronic leukemia appear more easily depressed by radiation. Furthermore, the time course of the depression of the lymphocyte values is quite

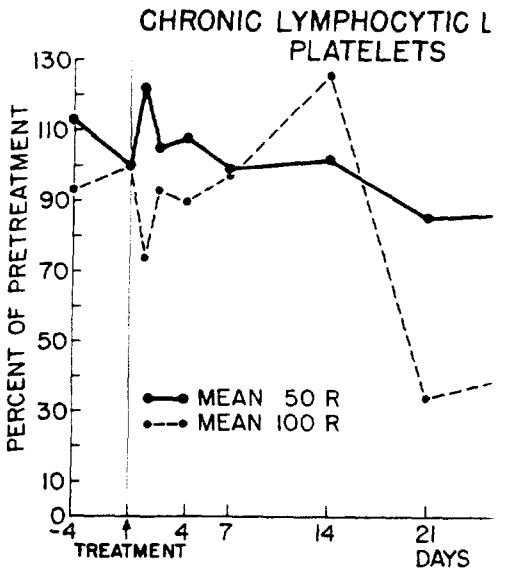

Fig. 10. Twenty-one patients with chronic lympho pressed as mean per cent of pretreatment doses of 50 R (13 patients) and 100 R (8 pati

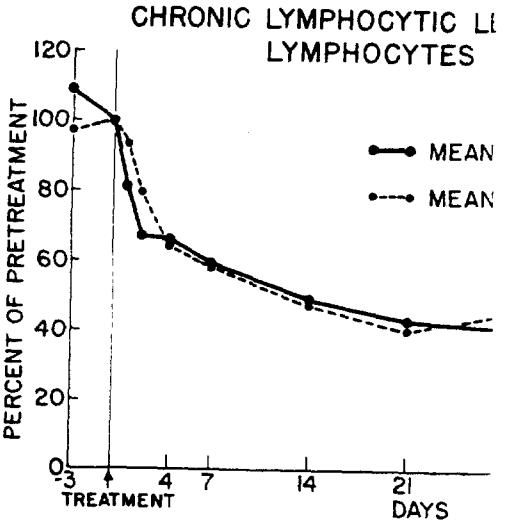

Fig. 11. Twenty-one patients with chronic lymphoc expressed as mean per cent of pretreatment doses of 50 (13 patients) and 100 R (8 patient

1027166

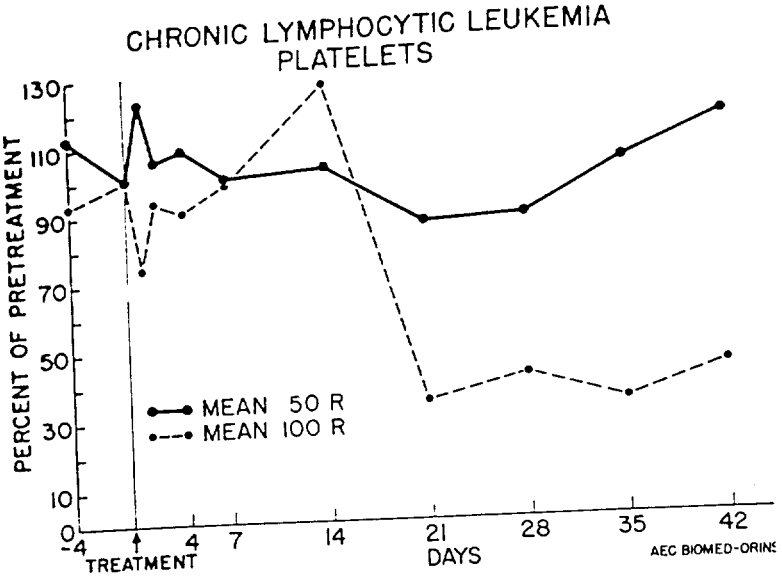

Fig. 10. Twenty-one patients with chronic lymphocytic leukemia; platelets expressed as mean per cent of pretreatment values. Patients given TBI in doses of 50 R (13 patients) and 100 R (8 patients).

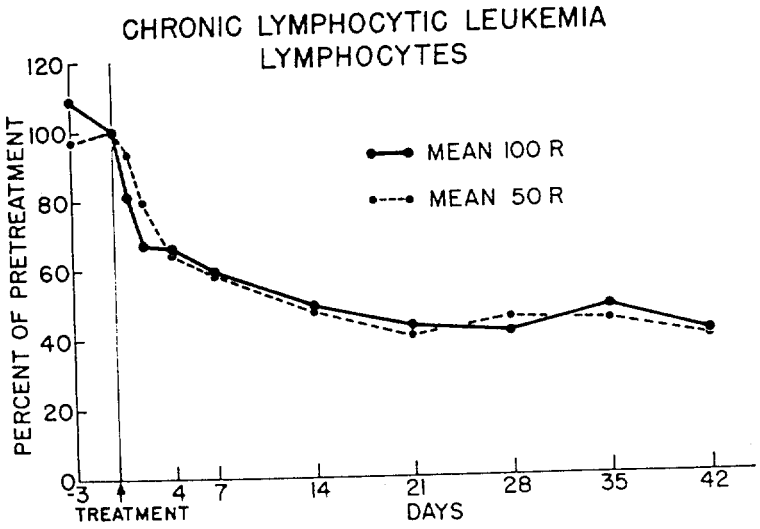

Fig. 11. Twenty-one patients with chronic lymphocytic leukemia; lymphocytes expressed as mean per cent of pretreatment values. Patients given TBI in doses of 50 (13 patients) and 100 R (8 patients).

1027167

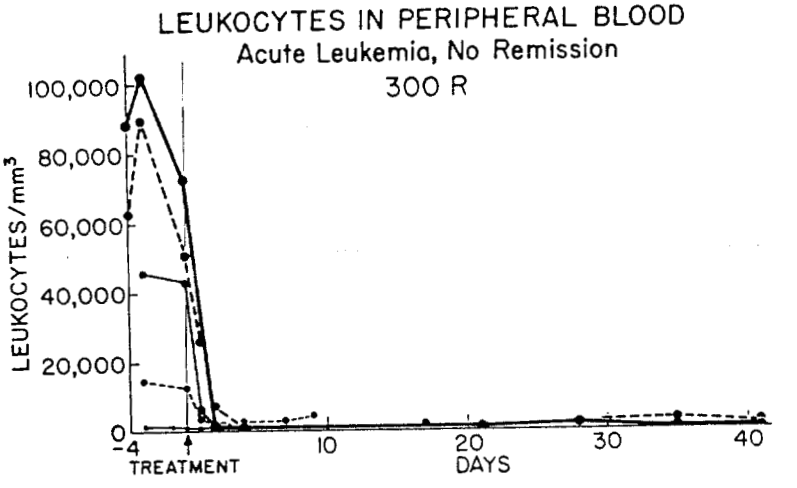

Fig. 12. Leukocyte values in five patients with acute leukemia exposed to 300 R who had no remission.

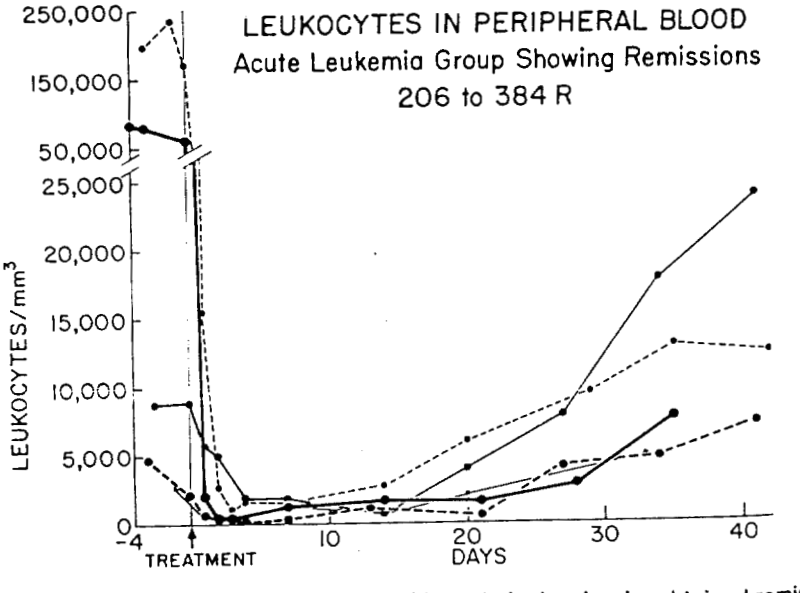

Fig. 13. Leukocyte values in five patients with acute leukemia who obtained remissions after exposure to 206–384 R.

1027168

similar to that of the granulocyte values, a gradual fall during a period of three weeks or so. In normal persons given higher doses producing easily detectible effects, there is a great difference, with the lymphocyte depression occuring promptly and the granulocyte depression more gradually.

Responses of platelet values appeared quite uniform in all these various diseases. There were differences in sensitivity, but the timing was usually such that the greatest depression occured at about four weeks after exposure.

The blast cells of acute leukemia in children always appear radiosensitive, although we have seen an example in an adult of blast cells that were only transiently depressed by a large dose of radiation. In children it is not clear whether or not the failure of recovery is due to a persistence of blast cells or to some other unknown mechanism that prevents initiation of regeneration. One of the most striking features of the large dose total-body irradiation studies in children is the fact that when remission does occur it begins at a remarkably early time after radiation—from 20 to 22 days. In most other situations, large doses of total-body irradiation, whether given to normal persons or persons with various diseases, are not accompanied by signs of increase in platelets and normal white cells until at least 30 days after exposure.

A great deal of further information is needed on the cytokinetic aspects of these varying hematologic responses to total-body irradiation. This information should be useful in understanding the underlying disease as well as in evaluating the possible benefits of radiation therapy.

Radiation Exposure-Rate Studies on Specific-Pathogen-Free Mice

N. Gengozian, Elizabeth Allen, and D. Carlson

We previously demonstrated the importance of radiation exposure rate in the therapeutic effectiveness of foreign marrow transfusions in lethally-irradiated animals. The higher exposure rates caused more depression of the immune mechanism and a greater probability of a marrow transplant; immunologic graft rejection was demonstrated at the lower radiation exposure rates. In these studies it had been noted, however, that among the control irradiated animals, death would occur as early as 5 and 6 days postirradiation, with 50% of the animals dying within

1027169

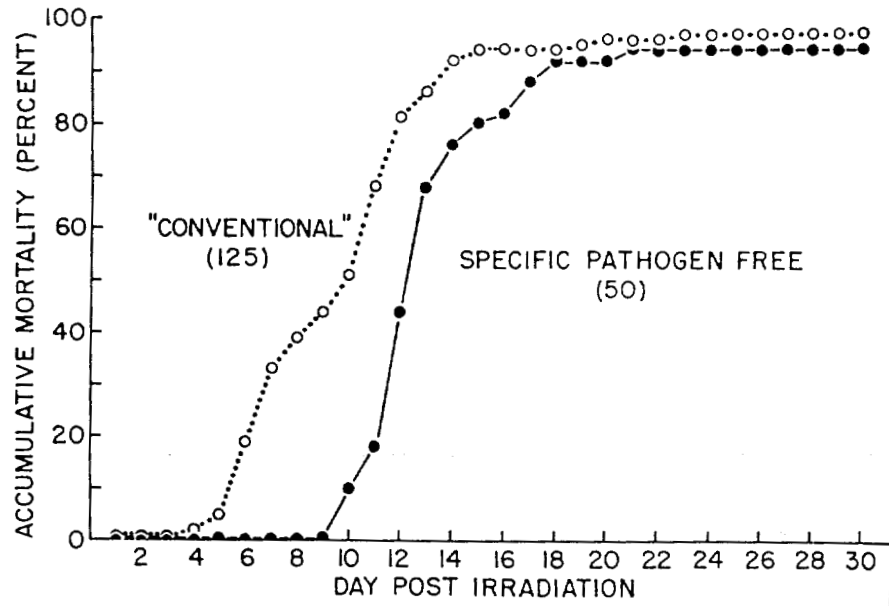

Fig. 14. Time-mortality sequence in "conventional" and specific-pathogen free mice following 1200 R at approximately 4 R/min. Numbers in parentheses represent the number of animals involved in the study.

10 days. At the levels of radiation used, the 30-day LD_{50} and LD_{100}, this was considered to be too early for the usual hemopoietic death, and the probability of infectious agents playing an unusual role in the mortality pattern was considered. A random testing of mice in our colony confirmed the presence of *Pseudomonas aeruginosa*, an agent that can lead to early deaths in irradiated animals. To confirm our previous interpretation of the radiation exposure-rate phenomenon, it was necessary to repeat certain studies in animals known to be free of specific pathogens.

Figure 14 shows mortality pattern of specific-pathogen free (SPF) mice (i.e., known to be free of *Pseudomonas* and *Salmonella*) and of mice that can be referred to as our earlier "conventional" type, after 1200 R at approximately 4 R/min. This dose was an LD_{99} for both groups of mice, but the onset of death in the two groups differed strikingly. Among the SPF mice, mortality did not begin until 10 days after irradiation, while within this time 50% of the conventional animals had died. Thus, with the SPF mice the mortality curve was shifted dramatically to the right with a greater slope. Similar alterations in the mortality pattern

1027170

FIC PATHOGEN FREE
(50)

18 20 22 24 26 28 30
DIATION

al" and specific-pathogen free R/min. Numbers in parentheses in the study.

ıe 30-day LD_{50} and LD_{100}, sual hemopoietic death, and unusual role in the mortality ıice in our colony confirmed agent that can lead to early r previous interpretation of t was necessary to repeat f specific pathogens. ıecific-pathogen free (SPF) ınd *Salmonella*) and of mice ntional" type, after 1200 R n LD_{99} for both groups of differed strikingly. Among 10 days after irradiation, al animals had died. Thus, shifted dramatically to the s in the mortality pattern

were observed even at lower radiation doses, such that the LD_{50} dose was raised considerably with SPF mice. At 20 R/min, the LD_{50} in the conventional mice was estimated to be 940 R and with the SPF mice, 1066 R; at 40 R/min, the LD_{50} was raised from 840 R to 1000 R, respectively, for the conventional and SPF mice.

In the next study, rat bone marrow was injected into SPF mice given a total radiation dose of 1050 at 3.7 R/min and 53 R/min; the results were compared to our previous data obtained in conventional mice given 900 R, a dose having an equivalent radiation control mortality. The results, shown in *Fig. 15*, indicate that irrespective of the different absolute dose of radiation used for the two groups of mice, the percentages of mortality and of successful grafts in the marrow-treated animals were the same. Graft rejection in the SPF mice given radiation at the lower exposure rate was observed, as would be expected if the radiation exposure-rate phenomenon were operating. This was also observed in the higher ex-

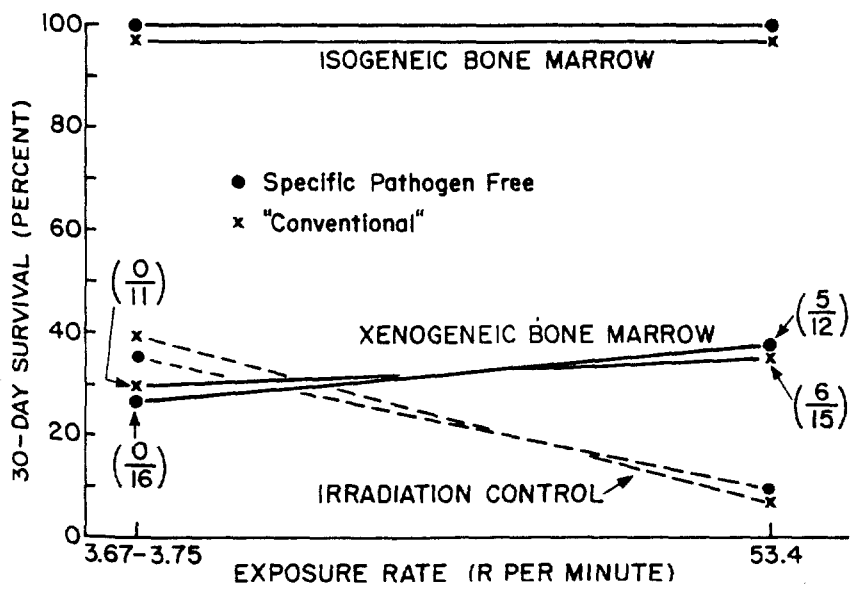

Fig. 15. Survival after irradiation and bone-marrow treatment of "conventional" and specific pathogen-free mice at 900 R and 1050 R, respectively. Xenogenic bone marrow indicates injection of rat bone marrow, and isogeneic bone marrow indicates marrow treatment from the same strain of mouse. (Numbers in parentheses indicate number of animals having a donor graft over number tested 30 days post-treatment.)

1027171

posure-rate group, the frequency being almost identical to that obtained previously with the conventional mice.

Since this study was performed in the radiation dose range below the LD_{100}, we next decided to determine whether the effect of exposure rate would be seen after 1200 R, a dose that would be 95 to 100% lethal at 4 R/min and 53 R/min. The results with the SPF mice in comparison to our previous data obtained in conventional mice are shown in *Fig. 16.* In both exposure-rate groups, the per cent survival was greater among the SPF mice. Also, at the low exposure rate of 3.7 R/min, graft rejection again was observed; four of 12 animals in the SPF group when tested at day 30 showed the absence of any rat cells in the peripheral blood. The parallelism of the curves for the SPF and conventional mice appears to suggest a similar relationship between the radiation exposure rate and the immune system, the higher survival in the SPF group at both exposure rates merely reflecting the greater survival value of noncontaminated animals.

Finally, the high radiation dose of 1200 R did not eliminate the ex-

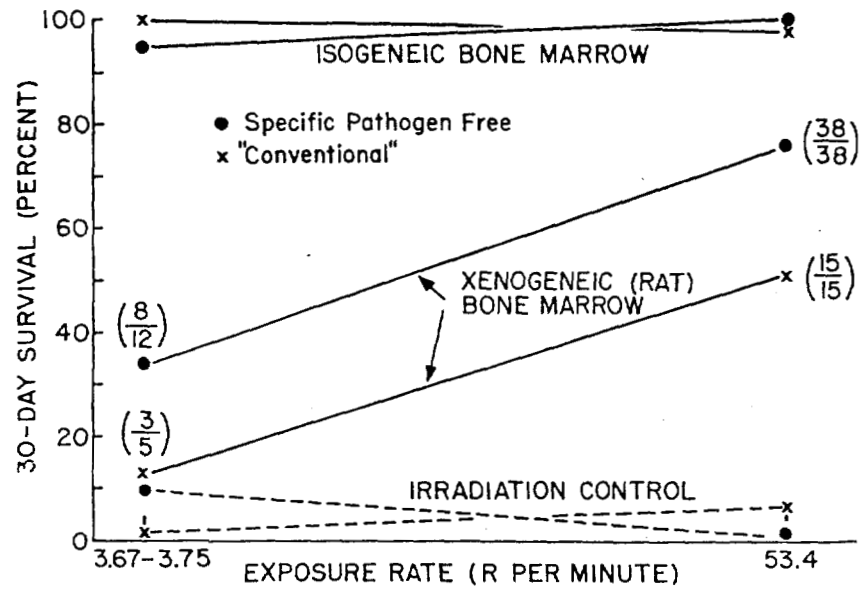

Fig. 16. Survival after 1200 R and bone-marrow treatment in "conventional" and specific-pathogen free mice. (Numbers in parentheses indicate number of animals having a donor graft over number tested 30 days post treatment.)

1027172

to 800 oil-immersion fields evenly spaced throughout a section. The percentage of hits on a component is a measure of the volume that component contributes to the specimen. Undoubtedly, the data are biased by artifacts, especially from the shrinkage of tissue in preparation. Whatever the inaccuracies of this method, it shows the simple dichotomous classification of marrow components as cellular and fatty to be inadequate for our purposes. Despite the scarcity of fat cells in the control animals, hemopoietic cells constituted less than half the marrow; the pointer also fell on red cells, vascular walls, supporting stromal structures and "space" between cells. In addition to red-cell precursors and cells in the granulocytic series, we classified megakaryocytes, histiocytes, lymphocytes, plasma cells, mitoses, blasts, degenerating forms and unidentified cells.

Some of the principal findings are depicted in the histogram *(Fig. 17)*. In addition to killed healthy animals, controls include nonirradiated marmosets found dead of infection or injury because all the irradiated marmosets were found dead or moribund, often with infection and hemorrhage. Depression of hemopoiesis is seen in the marrow of all those dying in the first month after irradiation, but marrow recovery seems complete in the 100-R animals dying much later. No benefit from marrow infusions is evident after 400 R. Exposure to 600 R and 800 R apparently permitted a homograft, with prolongation of life and the development of definite hemopoietic activity in the marrow, although none of the animals fully recovered.

These differential counts of cell types have an advantage over counts made from smears, in that they provide absolute values rather than relative numbers. They permit the observation, for example, that the increase in plasma cells in marrow smears after irradiation is not merely relative to the reduction in other cells, but is absolute. (In the noninfused marmosets in the 400- and 800-R groups, plasma cells averaged 2.4% of the marrow volume, the killed controls, 0.1%, and the controls found dead, 0.3%.)

Results of stereologic quantitation can also be expressed as the volume of each cell type per cubic millimeter of marrow, or, after determination of cell size, as the number of cells per cubic millimeter. The ratio between the numbers of two types of cells can also be calculated if their sizes are determined. Obviously, the ratio between the volumes of granulocytic cells and erythrocyte precursors is somewhat greater than the familiar "G-E" ratio based on numbers of cells in a smear from

1027173

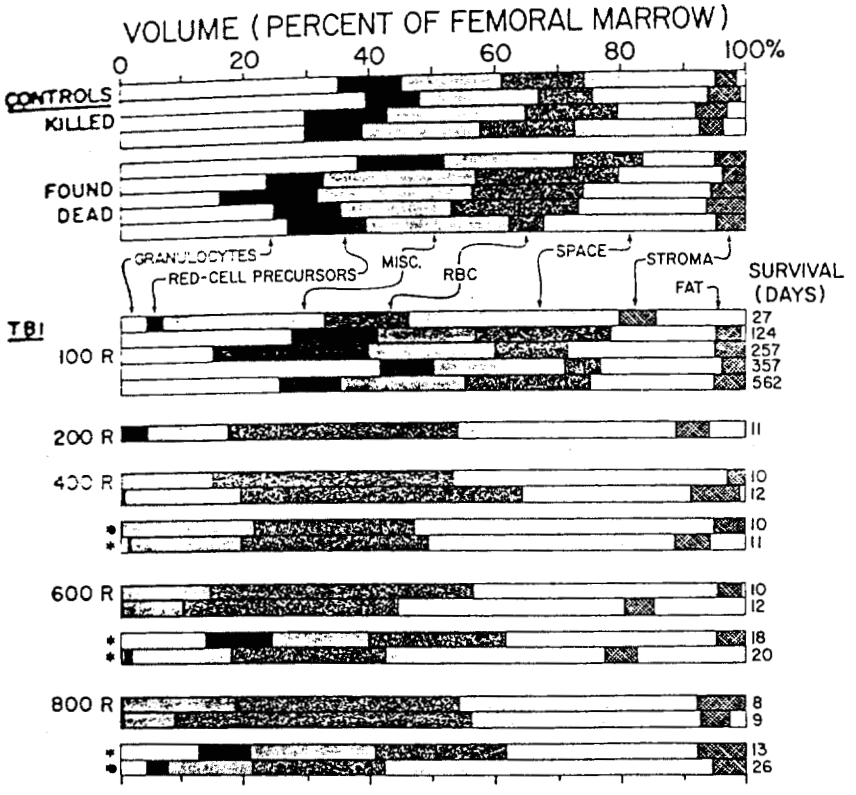

Fig. 17. Histologic changes in femoral marrow of marmosets after total-body irradiation. Each bar represents one animal. The day of death after irradiation is given at the right. Marmosets given infusions of marrow after total-body irradiation are designated by "M" at the left.

the same marrow, because granulocytes are larger than most red-cell precursors.

Of course, the unusual radiosensitivity of the marmoset is not yet elucidated, but stereologic quantitation is helpful for analysis of the histologic and cytologic changes related to the dramatic hemopoietic depression. Accurate quantitations of marrow cells were especially valuable in assessing attempts to transplant marrow after total-body irradiation: In two animals these histologic studies demonstrated foci of hemopoiesis.

1027174

supporting the conclusion derived from cytogenetic studies (sex chromosomes in the marrow post-mortem) that homografts were obtained.[5]

REFERENCES

1. Gengozian, N. and Batson, J. S. Effects of total-body irradiation on a small South American primate, *Saguinus fuscicollis*. Int J Radiat Biol, in press.
2. Custer, R. P. and Ahlfeldt, F. E. Studies on structure and function of bone marrow. II. Variations in cellularity in various bones with advancing years of life and their relative response to stimuli. J Lab Clin Med 17, 960–962, 1932.
3. Sturgeon, P. Volumetric and microscopic pattern of bone marrow in normal infants and children. Pediatrics 7, 774–781, 1951.
4. Hartsock, R., Smith E. B., and Petty, C. S. Normal variations with aging of the amount of hematopoietic tissue in bone marrow from the anterior iliac crest. Amer J Clin Path 43, 326–331, 1965.
5. Gengozian, N., Batson, J. S., and Nelson, Bill M. Bone-marrow grafting attempts in marmosets after total-body irradiation. Int J Radiat Biol, in press.

Vascular Radiation Syndrome

C. C. Lushbaugh

A retrospective study[1] of the case histories of the 1960 Los Alamos and 1964 Rhode Island nuclear criticality accident radiation victims revealed that 5000- and 10,000- rad doses induce hypotension, widespread vascular damage, shock, and death within two days. The pathologic changes indicated that these two cases must represent a previously undefined lethal subsyndrome of the acute radiation syndrome. It occurs in the dosage range between that causing the acute gastrointestinal and neurologic subsyndromes. Because meningeal and cortical vascular inflammatory changes occur as part of the total-body vascular damage, terminal neurologic symptoms appeared that led to the clinical suspicion of radiation-induced neurologic damage. However, only minimal evidence of cerebral or cerebellar neuronal damage and glial reaction was present. Death in both instances apparently resulted from increased intracranial pressure, cerebral anoxia, cardiac failure, and massive peripheral edema secondary to vascular damage.

Three major mechanisms of death have been recognized in humans after lethal radiation exposure: central nervous system injury, gastrointestinal mucosal loss and hematopoietic failure. At radiation exposure levels (300 to 800 R), which are known to result in death of animals within 30 days, or man within 60 days, death occurs from hemorrhage or

1027175

infection, secondary to hematopoietic injury. In man, the hematologic syndrome has been documented by clinical and pathologic studies after therapeutic and accidental exposure to ionizing radiation. Radiation between 1000 and 3000 R denudes the intestinal mucosa and results in septicemia and electrolyte imbalance causing death within five days in animals and within two weeks in man.

At exposures higher than 3000 R, deaths in animals or man within 24 to 48 hr are considered secondary to cerebral and cerebellar damage. After exposure to more than 5000 R, most animals manifest a neurologic syndrome: malaise, weakness, ataxia and prostration are progressive. Finally, such animals become unresponsive and die with convulsive manifestations. Pathologic changes in such instances include meningeal leukocytic exudates, necrosis of cerebellar granular cells, oligodendroglial and cortical neurone lysis, and progressive cerebral edema. This syndrome and its pathologic basis is well defined in monkeys but has not been seen in man. No human deaths have been attributed *per se* to the neurologic syndrome as it is known in animals. Although the early deaths of some Hiroshima and Nagasaki victims may possibly have occurred in this manner, clinical records during the first two days and postmortem examination during the first week after the detonations were not made.

The accidents related to this study were basically similar criticality excursions that occurred when fissionable material in a reclamation process was unintentionally caused to flow into unsafe geometric volumes. The integrated total-body doses differed by a factor of two (dose of Patient 1 was ≈4900 rads; dose of Patient 2 was ≈8800 rads). The doses to the heart were two or more times larger. The clinical courses, however, were so similar and unique that the same morphologic damage must have resulted. Postexposure hemoconcentration was followed by a return to normal hematocrit levels, but in spite of 14 liters of fluid administered intravenously to Patient 1, and 9 liters to Patient 2, neither man showed signs of hemodilution but tended to hemoconcentrate.

This progressive leakage into an expanding extravascular space was quite obvious clinically. These men suffered from severe shock as is illustrated graphically by the blood pressure changes. Patient 1 initially had an extremely low blood pressure (40/10) which never reached normotensive levels. Patient 2 was hypertensive on hospital admission but within 6 hr required vasopressor drugs to combat the steady decline in his blood pressure. In both men, a relatively stable but lower than normal systolic pressure was maintainable during the first postirradiation day, chiefly by vasopressor drugs and intravenous fluids, but diastolic pressures were often difficult to measure. Terminally, both men had low unstable blood pressures, which were difficult to measure. Patient 2 had no discernible blood pressure for 6 hr before death.

1027176

The most conspicuous gross postmortem findings related to the cardiovascular, lymphopoietic and hemopoietic systems, and interstitial tissues and spaces. There was extensive extravascular interstitial accumulations of fluid, bilateral hydrothorax, pericardial effusion, and ascites. Both had a serofibrinous pericarditis. Microscopically, fibrin and polymorphonuclear leukocytes were scattered in patchy fashion in the epicardium of the right ventricle, auricle, and atrium, and between muscle fibers, usually near blood vessels *(Fig. 18)*.

Most of the medium-sized arteries stained pale histologically because of swollen smooth muscle layers. This intracellular edema was also seen in the muscularis of the small and large intestine where the ganglionic cells of the intramuscular plexuses were similarly affected. In many areas, polymorphonuclear leukocyte exudation was found where it could be considered only evidence of primary endothelial damage. The small venules of the meninges are an excellent example of this change, for they

Fig. 18. Right ventricular myocardium showing interstitial leukocyte exudation and edema (PAS, X400).

1027177

Fig. 19. Cerebral meningeal blood vessels and exudate of morphonuclear leukocytes (PAS, X400).

were collared by neutrophils in the absence of demonstrably damaged tissue *(Fig. 19)*.

The brains were grossly normal and microscopic changes were minimal in both patients. The endothelial cells of capillaries sometimes were prominent. Debris was present in extravascular histiocytes. Cerebellar granule cells did not show necrosis or any decrease in number. Diffusely scattered extravascular polymorphonuclear leukocytes were increased in the meninges and around some of the cortical blood vessels, slightly greater in amount than the infiltrations in the viscera. These sections were reviewed by several consultants in neuropathology that agreed in general that cytologic evidence of primary neuronal and granule-cell damage was minimal or questionable, while vascular changes and meningeal leukocytic exudation were present but mild in comparison to the changes in monkeys and lower animals irradiated at the level of these patient's exposures. These findings lead us to the conclusion that periph-

1027178

eral and organic vascular damage was the dominant radiation lesion underlying the hypotensive shock and rapid death within two days.

REFERENCE

1. Fanger, H. and Lushbaugh, C. C. Radiation death from cardiovascular shock following a criticality accident: Report of the second death from a newly defined human radiation death syndrome, Archives of Pathology, in press.

The Absence of Sodium Loss After Massive Total-body Neutron Exposure of Rats.

C. C. Lushbaugh, H. D. Hodges, M. C. Yarbrough, and W. D. Gibbs

Electrolyte loss is so well accepted as the basic lethal mechanism in radiation-induced gastrointestinal syndrome that evidence questioning the validity of this concept is not taken seriously. Previously we showed that the turnover and loss of ^{22}Na and ^{42}K-labeled electrolyte were reduced instead of increased in rats after X-ray exposures in the range of 1000 to 8000 R.[1] In fact, the heavily irradiated animals appeared to conserve electrolytes to balance decreased electrolyte intake due to reduced food consumption. Starved unirradiated rats had electrolyte retention curves identical with those of the heavily-irradiated ones.

These experiments, however, might conceivably be erroneous because the radioactive labels may not have had sufficient time to equilibrate with the exchangeable mass of electrolyte in the gastrointestinal tissues before radiation exposure. We decided, therefore, to repeat the study with fission neutrons as the means of producing gastrointestinal damage and ^{24}Na activation simultaneously.

Three groups of rats were exposed to fission neutrons from an unclad criticality assembly.* Two groups received 100 rads/rat and one group 1200 rads/rat. All rats exposed to 1200 rads (3600? rem) died between 68 and 75 hr after exposure and had small-intestinal mucosal denudation. One 100-rad group was allowed food and water ad libitum while the other was pair fed with the 1200-rad group. The rats in all groups were

* Exposures were made by John A. Auxier and John W. Poston, Health Physics Division, Oak Ridge National Laboratory.

1027179

whole-body counted and individual retention curves were determined for neutron-activated sodium-24. When all 1200-rad rats were dead, the others were killed and residual ^{24}Na distribution in gastrointestinal tract, liver, and the rest of the body in all animals was assayed.

The data in *Table 8* show that no significantly different loss in body weight occurred in the 1200-rad rat in comparison with the 100-rad pair-fed controls. Both groups lost only 20% of their neutron-induced ^{24}Na whole-body radioactivity while the 100-rad group fed ad libitum lost 50%, as shown in *Fig. 20*; the whole-body ^{24}Na retention curves show that the 1200-rad rats did not develop a sodium leak. There was no chance for any significant quantity of nontagged sodium to be excreted before equilibrium was reached, since ^{24}Na was produced wherever the neutrons penetrated and sodium was present. In *Table 9*, showing the residual distribution of the ^{24}Na in the animals 68 to 72 hr after exposure, there is a slight but not significant decrease in the amount of sodium in the small and large intestines and contents of the heavily irradiated rats. The shift of 60% of the hepatic sodium to "rest of body" in these animals was an

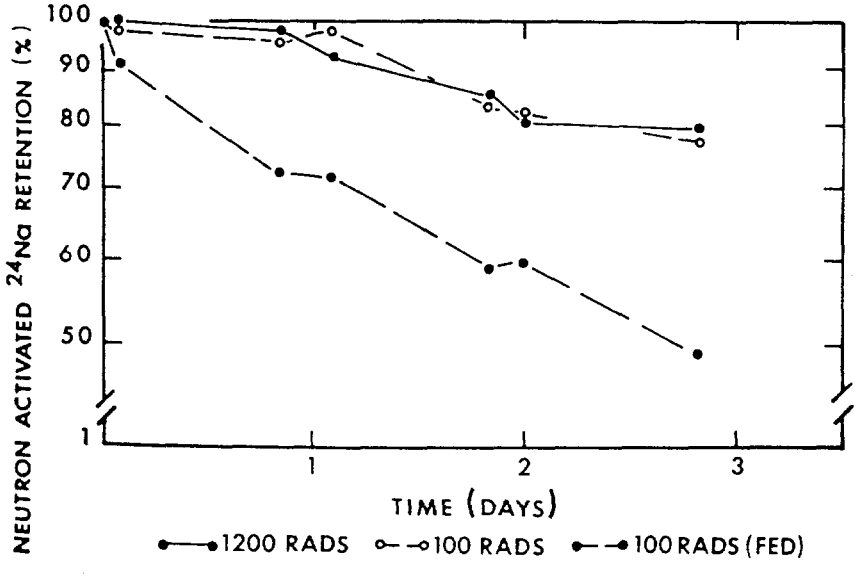

Fig. 20. Graph ^{24}Na retention in rats exposed at the doses shown to fission neutrons from an unclad criticality assembly. The 1200-rad rats and the 100-rad rats pair-fed with them lost the labeled sodium at a much slower rate than the 100-rad rats allowed free access to food.

1027180

unexpected finding that merits reinvestigation, since if true, a severe hepatic extracellular sodium and water loss would have had to occur. Sodium loss from the whole body, however, cannot be the cause of death of these rats in the gastrointestinal syndrome as commonly presumed.

TABLE 8

Progressive Body-weight Loss (%) and Food Consumption (g) in Neutron Irradiated and Food Restricted Rats.

Time After Exposure	Dosage (Rads)					
	1200		100*		100	
	Body Wt.	Food	Body Wt.	Food	Body Wt.	Food
(hr)	(− %)	(+ g)	(− %)	(+ g)	(− %)	(+ g)
20	1.5	4.5	5.8	—	0.5	9.6
44	6.8	8.0	11.3	4.5	2.7	18.9
68	13.8	10.5	12.5	8.0	1.8	33.4

*Pair fed with rats exposed to 1200 rads.

TABLE 9

Residual ^{24}Na Distribution in Rats 68 hr After Neutron Exposure

Dose Group	Gut*		Liver		Rest of Body	
	(% ^{24}Na)	(% BW)†	(% ^{24}Na)	(% BW)	(% ^{24}Na)	(% BW)
100 rad (fed)	13	7	11	7	76	87
100 rad (pair fed)‡	13	5	13	5	74	91
1200 rad (fed)	11	5	5	5	84	90

* Pylorus to anus with contents.
† Body weight.
‡ With 1200-rad group.

REFERENCE

1. Lushbaugh, C. C., Sutton, J., and Richmond, C. R. The question of electrolyte loss in the intestinal death syndrome of radiation damage, Radiat Res 13, 814–824, 1960.

1027181

Studies Related to the Treatment of Radiation Injury

The objective is to prevent or correct the damage caused by radiation; to a large extent the effort is focused on the infections and hemorrhagic manifestations of total-body irradiation. Since a major goal is to treat radiation injury with hemopoietic grafts, we are pursuing animal studies on the prevention, mechanisms, and treatment of the complications of "secondary" or homologous disease.

These investigations have led us into cytokinetics with significant findings that are basic in hemopoiesis. Immunologic studies related to chimerism in marmosets also provide fundamental information related to transplantation. Clinical studies with irradiated patients elucidate mechanisms of marrow depression, and some blood diseases characterized by severe bone-marrow depression also are of interest because they simulate the irradiated state.

Radioprotective and Metabolic Studies of Alkenyl and Alkyl Ethers of Glycerol and Glycol*

F. Snyder and J. H. Arrington†

Numerous reports in the literature indicate that glyceryl monoethers have hemopoietic and radioprotective activities. Much of the early work was conducted with a limited number of experimental animals and improper controls. The glyceryl ethers used were seldom characterized chemically according to their class or molecular purity. In our biochemical studies of the ether bond in rats, we examined the radioprotective actions of a number of lipids, including synthetic and naturally occurring alkyl and alkenyl nonphosphatide ethers of glycerol. The purity of all lipids was determined by thin-layer and gas-liquid chromatography. Daily injections of the lipids were given orally in corn oil immediately after intubation of glucose to stimulate absorption. On a few occasions, some of the test compounds were administered intraperitoneally, intramuscularly, or subcutaneously.

In experiments with the purified triglycerides, fatty acids, alkyl ethers

*To be presented at the Radiation Research Meeting, San Juan, Puerto Rico, May, 1967.

†Research participant, Albany State College, Albany, Ga.

1027182

of glycerol or glycol, or the crude fish oil from the dogfish liver, we were unable to confirm earlier work reporting the radioprotective action of glyceryl ethers[1] and other lipids.[2] Our evaluation of radioprotection was based on the ability of the lipids to alleviate the leukopenia occurring in rats exposed to total-body irradiation (50, 100, 150, 200, and 800 R). After oral intubation of the alkyl ethers, we found almost complete enzymatic cleavage of the ether bond by mucosal and liver cells. The products of this cleavage were fatty acids, fatty alcohols, and fatty aldehydes.

REFERENCES

1. Brohult, A. Alkoxyglycerols and their use in radiation treatment. Acta Radiol Suppl 223, 1963, 99 pp.
2. Ashikawa, J. K. and Anderson, O. K. Postirradiation protection of x-irradiated mice with olive oil. Radiat Res 13, 99–107, 1960.

Hemopoietic Spleen Colonies in the Rat

F. V. Comas

Till and McCulloch[1] first demonstrated the capability of bone-marrow stem cells to form clones in the spleen of heavily irradiated mice. This method is an adaptation of classic tissue-culture techniques to an *in vivo* system, and has been especially suitable for testing the radiosensitivity of bone-marrow cells. The experiments here reported were designed to extend the spleen-colony technique to another animal species, the rat.

Groups of young adult Fisher-334 rats were given graded doses of total-body irradiation, between 856 and 1432 rads. The animals were killed 10, 12, and 14 days after irradiation to determine whether their spleens would show hemopoietic colonies derived from surviving bone-marrow stem cells that had migrated and colonized in the spleen (endogenous colonies). Such colonies were found in almost all the spleens, but their number was not related to radiation dose. The vast majority of these endogenous colonies were very small, seldom exceeding one millimeter in diameter.

In another series of experiments, groups of rats were given 1400 rads of total-body irradiation, and were immediately injected intravenously with isologous bone-marrow cells obtained from donor rats. A fraction of

1027183

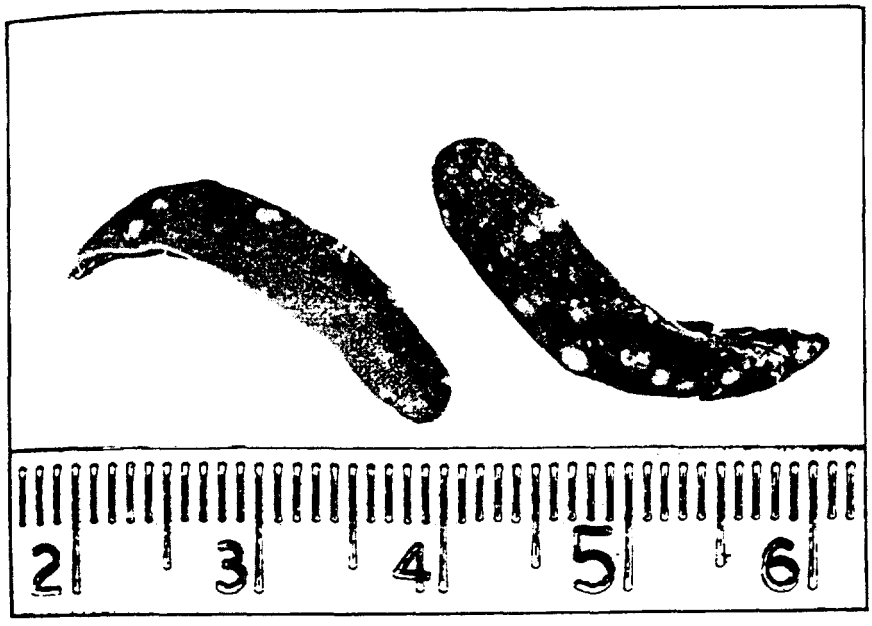

Fig. 21. Exogenous hemopoietic colonies in a rat spleen, 12 days after injection of 4×10^5 nucleated bone-marrow cells. Metric scale, in centimeters.

these injected cells went to and proliferated in the spleen of the recipient animals forming well-defined exogenous spleen colonies *(Fig. 21)*. To assist in discriminating against the endogenous colonies that also appeared in these rats, only colonies measuring over 1 mm in diameter were scored. The mean number of exogenous spleen colonies was 4.4 per 10^5 bone-marrow cells injected.

To test for linearity of response, groups of rats were injected with 1 to 8×10^5 bone-marrow cells in graded doses. The results *(Fig. 22)* indicate that within the limits of the size of the inocula used, the number of colonies per spleen varied linearly with the number of cells injected. The slope of the regression line was 4.4 (95% confidence limits: 3.5–5.3), indicating that for each increment of 10^5 cells injected, an average of 4.4 additional spleen colonies appeared.

These results indicate that the spleen-colony technique can be used in the rat. Endogenous colonies include such a large proportion that are too small to be counted that they are not suitable for quantitative evaluation. Exogenous colonies, however, constitute a useful radiobiological system.

1027184

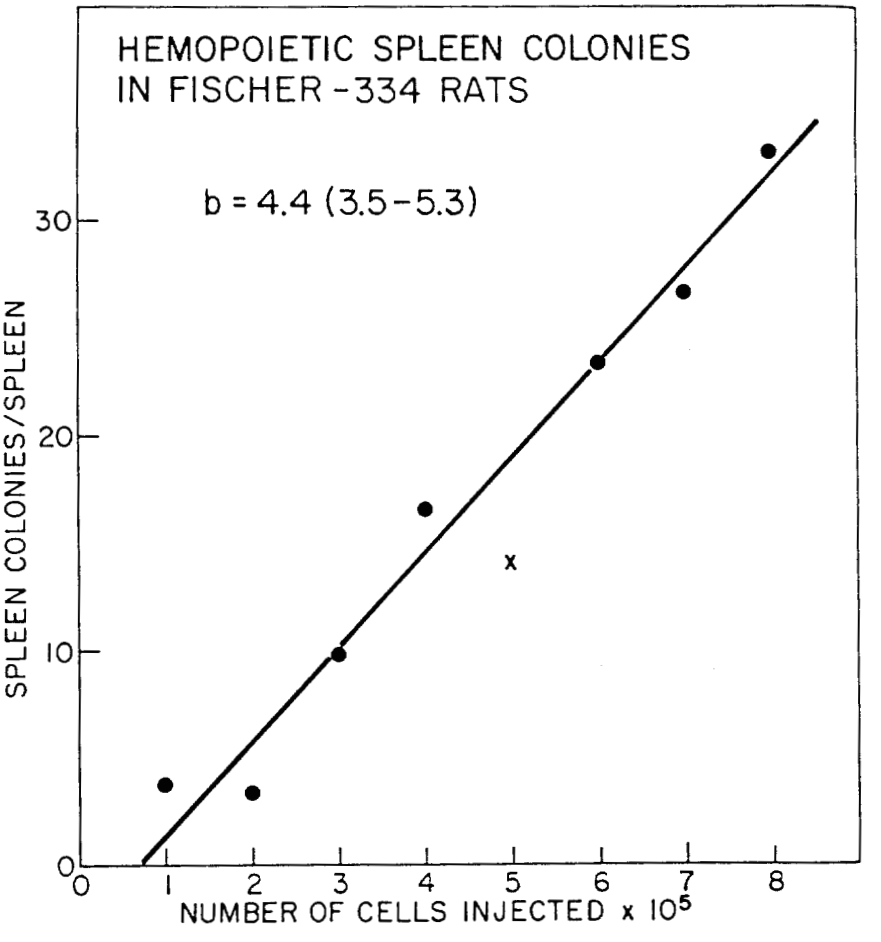

Fig. 22. Relation between number of spleen colonies per spleen and number of nucleated rat bone-marrow cells. The equation for the regression line is $Y = -2.9 + 4.4(X)$.

REFERENCE

1. Till, J. E. and McCulloch, E. A. A direct measurement of the radiation sensitivity of normal mouse bone marrow cells. Radiat Res 14, 213–222, 1961.

1027185

Recovery of Lethally-Irradiated Mice Given Fewer Than One Million Syngeneic Bone-marrow Cells

A. L. Kretchmar and W. R. Conover**

We have previously reported[1] that when lethally irradiated mice were given fewer than 1×10^6 syngeneic bone-marrow cells there is a significant so-called "secondary mortality." Although the mortality in our experiments was not, in general, as great as that reported by Barnes, et al.,[2] we did confirm their observations in several respects. We do not think, however, that "secondary disease," as seen in irradiated mice given allogeneic bone-marrow cells, occurred in any of our experiments.

As shown in *Table 10*, the mortality pattern among lethally irradiated mice given allogeneic bone-marrow cells differs from that of similarly irradiated mice given syngeneic cells. It should be noted that over approximately the same range of "secondary mortality"† (6 to 76% in the

*Present address: Memorial Research Center, University of Tennessee; work carried out in collaboration with mammalian recovery section, Biology Division, Oak Ridge National Laboratory.

†Primary mortality was calculated as: $\frac{\text{number dead at 20 days}}{\text{number in the experiment}} \times 100$; second mortality was: $\frac{\text{number dying 21 to 100 days}}{\text{number in experiment} - \text{number dead at 20 days.}}$ Thus, secondary mortality is calculated as per cent of the surviving population *at 20 days*.

TABLE 10

Primary and Secondary Mortality Among Lethally Irradiated Mice Given Bone-marrow Cells

Bone-marrow Treatment		Primary Mortality (Death 0–20 days)	Secondary Mortality (Death 21–100 days)
		%	%
Syngeneic	1×10^6	4	6
	1.5×10^5	13	5
	1×10^5*	27	23
	1×10^5*	76	76
Allogeneic†		3	17
		12	43
		9	58
		20	87

*See Table 11.

†We are indebted to C. C. Congdon, M. A. Kastenbaum, and D. A. Gardiner for the mortality data from which these calculations were made.

1027186

syngeneic group compared with 17 to 87% in the allogeneic group) there is a relatively high "primary mortality" among mice given syngeneic marrow. Indeed, there is a strong correlation between primary and secondary mortality in these animals, and the probability of death 21 to 100 days after irradiation and marrow treatment is about the same as for 0 to 20 days. If allogeneic cells are given, however, the probability of death 21 to 100 days is several times higher than of death 0 to 20 days after treatment.

This result suggested that the mortality seen in the animals given inadequate doses of syngeneic bone-marrow cells is due to suboptimal recovery. *Table 11* presents data showing that the hemopoietic system of lethally irradiated mice given inadequate doses of syngeneic cells may not recover in a qualitative way, even though it may perhaps recover quantitatively, as suggested by total nucleated cell counts in the femur. The donor animals for the "reconstituted" hemopoietic cells were mice that had survived 29 to 32 weeks after lethal total-body irradiation

TABLE 11

Test for Qualitative Recovery of Hemopoietic System of Lethally Irradiated Mice Given 1 × 10^5 Syngeneic Bone-marrow Cells

Test	Result		
	% Mortality		
1. Protection of lethally irradiated mice	0–20 days	21–100 days	
1 × 10^5 normal cells	27	23	
1 × 10^5 "reconstituted" cells*	76	76	
2. Spleen Colony Assay	CFU/10^5 cells		
normal cells	17		
"reconstituted" cells	10		
3. Response to repeated bleeding	Ht	Hb	Retic†
control levels	50.3	16.2	0.5
normal (after 4th bleeding)	46.4	13.7	8.5
X-ray + 1 × 10^5 IBM − 70 days (after 4th bleeding)	39.2	10.4	7.4

* "Reconstituted" cells are the hemic cells obtained from bone marrow of mice 29 to 32 weeks after lethal irradiation and treatment with 1 × 10^5 syngeneic bone-marrow cells from normal donors.

† Per cent reticulocytes determined by counting (brilliant cresyl blue blood films) times the hematocrit.

1027187

(950 R) and injection of 1×10^5 syngeneic marrow cells taken from normal unirradiated animals. Thus, the reconstituted cells could be considered as having been passaged once through syngeneic recipients. The first test shown in *Table 11* indicates that 1×10^5 of these reconstituted marrow cells are not so effective in protecting lethally irradiated mice as 1×10^5 normal marrow cells. Therefore, marrow has not fully recovered its protective capabilities even after 29 to 32 weeks. The second test shows that the marrow of mice protected from lethal irradiation by 1×10^5 syngeneic hemopoietic cells and surviving 29 to 32 weeks contains only 10/17 as many cells that can form gross spleen colonies; again we find a qualitative deficiency of reconstituted marrow. Finally, recovered mice cannot withstand repeated bleeding as well as normal mice can. Thus, we have shown that the marrow of mice that have survived lethal irradiation after injection of inadequate doses of syngeneic hemopoietic cells is deficient in its ability to protect other lethally irradiated mice, in its spleen colony-forming potential, and in its erythropoietic capacity under stress of repeated bleeding.

Finally, the lymphoid system of lethally irradiated and inadequately protected mice is often deficient. Barnes, et al.,[2] particularly, have discussed this and, in addition, find extensive amyloid deposits in organs of inadequately protected animals. We have not found amyloid in histologic sections of spleen, lymph nodes, thymus, and bone marrow (the only organs studied in our experiments), but have found poor recovery of lymphopoiesis in spleen, lymph nodes, and thymus of inadequately protected mice. As *Table 12* shows, 29 of 40 animals given an inadequate dose of syngeneic cells had thymus and lymph node weights in the normal range. Twenty of these gained weight after treatment, and nine either failed to gain in body weight or lost weight 35 to 84 days after treatment. Thus, normal weight of thymus and lymph nodes did not prevent loss of body weight.

On the other hand, all animals with poor recovery of weight of thymus or lymph nodes, or both, failed to gain or lost body weight. Thus, of the 20 animals that lost weight in this group of marginally protected lethally irradiated mice, 11 had poor recovery in weight of thymus or thymus and lymph nodes. Despite this general relation, we did not find a correlation between the amount of body weight lost and the weight of thymus or lymph nodes.

Our observations suggest that among lethally irradiated mice treated with inadequate doses of syngeneic cells, suboptimal recovery of hemopoietic and lymphoid systems is common. The marrow treatment may have been sufficient to carry animals through the period of acute irradiation mortality but not sufficient to permit optimal recovery in the hemic

1027188

TABLE 12

Recovery of Lymph-Node and Thymus Weight in Mice Given Lethal Irradiation and 1.5×10^6 Syngeneic Bone-marrow Cells and Killed 35 to 84 Days Later

Lymph-Node and Thymus Weight	Number of Animals Showing	
	Body-Weight Gain	Body-Weight Loss
Lymph Node (6–15 mg) Thymus (20–40 mg)	20	9
Lymph Node (less than 6 mg) Thymus (less than 20 mg)		5
Lymph Node (6–15 mg) Thymus (less than 20 mg)		6

Data are from a serial sacrifice study in which one-half the animals had either failed to gain or had lost body weight at the day of sacrifice as compared with the initial body weight.

and possibly other systems not studied in our experiments. The delayed (i.e., 20 to 100 days) mortality and weight loss might be a consequence of this suboptimal recovery and have no special relevance to the question of the pathogenesis of secondary disease as seen in lethally irradiated mice given allogeneic bone-marrow cells.

REFERENCES

1. Kretchmar, A. L. and Conover, W. R. Secondary mortality and body weight loss in lethally irradiated mice given small doses of isologous bone-marrow cells. USAEC Report ORINS-53, 1965, pp. 50–51.
2. Barnes, D. W. H., Loutit, J. R., and Micklem, H. S. "Secondary disease" of radiation chimeras: A syndrome due to lymphoid aplasia. Ann NY Acad Sci 99,374–385, 1962.

1027189

Relation Between Rate of Erythroid Differentiation and Size of the Population of Hemopoietic Stem-cells

A. L. Kretchmar, Elizabeth M. Rupp, and W. R. Conover**

The concept that a single progenitor cell type ("stem cell") is the source of the various differentiated elements of the fixed hemopoietic tissue would seem to require that the size of the population of stem cells depends, in part, on the rate at which cells differentiate and leave the stem-cell pool. If no primitive cells were differentiating into erythroid elements, the population of primitive cells might reasonably be expected to increase, and if erythroid differentiation were accelerated, the population should decrease, temporarily at least. We might also expect that increasing the requirement for erythroid differentiation might decrease the rate of recovery of the hemopoietic system after X irradiation.

These possibilities are being studied in polycythemic animals whose red-cell production is minimal and in lethally irradiated mice given isologous bone marrow and then bled during the postirradiation recovery to increase the stimulus for erythroid differentiation. Although the results reported here are preliminary, they do indicate that the size of the population of hemic cells that can give rise to gross spleen colonies[1] changes in accordance with the expectations indicated.

Mice were lethally irradiated (950 R total-body X irradiation) and then given 20×10^6 isologous bone-marrow cells from normal donors. They were allowed various times to recover before erythropoiesis was stimulated by bleeding. Approximately 1/3 of the blood volume (0.5 ml) was withdrawn from the retro-orbital venous sinus of each animal on four separate occasions. The second 0.5 ml was taken three days after the first, the third, four days after the second, and the fourth, three days after the third. This schedule of bleeding (0.5 ml every three to four days) requires a three- or four-fold increase in rate of erythropoiesis if an approximately normal red-cell mass is to be maintained.

In all groups the same schedule of bleeding was maintained; the only variation was in the interval between initial treatment (irradiation plus bone marrow) and the beginning of bleeding. The number of nucleated cells recoverable from both femurs and tibias of these mice was measured immediately after the first bleeding (unstimulated mice) and again after the fourth bleeding (erythropoiesis stimulated for 10 days). In addition, the number of colony-forming units (CFU) in 4×10^4 of these cells was

* Present address: Memorial Research Center, University of Tennessee; work carried out in collaboration with mammalian recovery section, Biology Division, Oak Ridge National Laboratory.

1027190

measured by the Till and McCulloch spleen-assay technique.[1] From these data, the total number of colony-forming units in both femurs and tibias of the recovering animals could be calculated.

Other mice, not irradiated, were made polycythemic by keeping them in a hypoxic environment in cages covered with silicone rubber membranes.* When these polycythemic mice are returned to a normal environment, erythroid differentiation practically ceases. Total nucleated cells in the femurs and spleens of these animals were determined and the number of colony-forming units was measured as indicated. These measurements were made five days after the polycythemic mice had been returned to normal atmosphere when erythropoiesis was minimal.

The results are plotted in *Figs. 23 and 24*. The number of nucleated cells in this aliquot of the marrow space (two femurs and two tibias) of mice given 20×10^6 isologous marrow cells after lethal irradiation *(Fig. 23)* recovers rapidly and "overshoots" to levels above normal by 10 days. Elevated total nucleated-cell counts persisted from 15 to 45 days. In contrast, the subpopulation that can form spleen colonies recovers rapidly at first and reaches normal numbers 45 days after irradiation and bone-marrow treatment. At 10 and 15 days, the population of colony formers is only about 80% of normal size.

When erythropoiesis was stimulated by bleeding and this pressure for erythroid differentiation was maintained for 10 days, the rate of recovery in the marrow populations was significantly altered. The number of nucleated cells in the marrow space did not exceed normal and no "overshoot" was noted. The recovery of the subpopulation of marrow cells that could form spleen colonies was delayed and did not reach 80% of normal until 25 days.

The data summarized in *Fig. 24* show that the fraction of bone marrow and spleen cells able to form spleen colonies increases when mice made polycythemic by hypoxia are returned to a normal atmosphere. Thus, under the conditions of these experiments at least, we have shown that the population of cells that can form spleen colonies decreases when erythroid differentiation is stimulated and increases when erythroid differentiation is decreased.

These results have important implications relative to control of the size of marrow-cell populations and to the question of whether differentiation occurs from a homogeneous pool of primitive progenitors or from a

*We are indebted to R. Lange and T. P. McDonald for help in preparing these mice.

1027191

progenitor pool that contains subclasses of erythropoietin-sensitive cells and colony-forming cells. Although much further work is needed before these implications can be discussed fully, the probability that a primitive cell will leave the colony-forming pool for differentiated cell lines remains less than 0.5 even when the pressure for erythroid differentiation is considerably increased by bleeding. This maintenance of the non-differentiating stem-cell pool is vital to the recovery of the animal, for the hemopoietic system can regenerate only if more than one-half the proliferating primitive cells can escape differentiation. What protects the primitive marrow population from these pressures leading to differentiation?

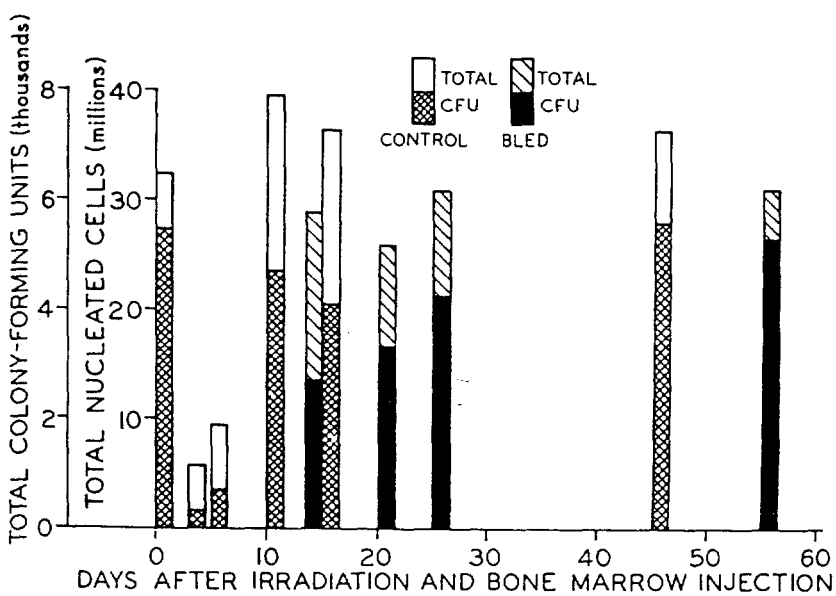

Fig. 23. Rate of recovery of total nucleated cells (open bar) and colony-forming units (CFU) (cross hatch) in the marrow space of both femurs and both tibias of mice given 20×10^6 isologous marrow cells after 950 R total-body X irradiation. Mice with erythropoiesis stimulated by bleeding for 10 days before measurement show less rapid recovery in total nucleated cells and colony-forming units. Compare bars for bled animals at 15, 20, 25 and 55 days with bars for control animals at 10, 15 and 45 days. Control untreated mice have 32×10^6 total nucleated cells and 5.4×10^3 colony-forming units in this aliquot of the marrow space (bar shown at 0 time).

1027192

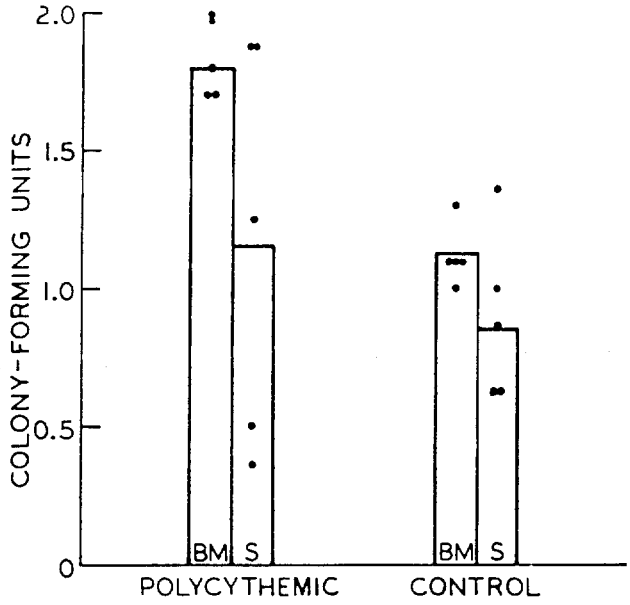

Fig. 24. Colony-forming units per 10^4 bone-marrow cells (BM) or per 10^5 spleen cells (S) in normal mice made polycythemic by caging in a hypoxic environment compared with control mice. The assays were performed five days after the polycythemic mice had been returned to a normal atmospheric environment.

REFERENCE

1. Till, J. E. and McCulloch, E. A. A direct measurement of the radiation sensitivity of normal mouse bone marrow cells. Radiat Res 14, 213–222, 1961.

Serine-3-^{14}C Metabolism in Irradiation Chimeras: Respiration Pattern Analysis

A. L. Kretchmar and C. E. Phipps*

We have reported previously[1] a study of serine-3-^{14}C metabolism in normal mice with the use of the experimental technique of respiration pattern analysis. To study the metabolism of a compound with this tech-

*Present address: Memorial Research Center, University of Tennessee, Knoxville.

1027193

nique, one follows the specific activity of the expired CO_2 after the injection of the compound labeled with carbon-14. We found that by simultaneously injecting unlabeled compounds that were metabolically closely related to serine, information about certain specific reactions could be obtained from *in vivo* experiments.

Figure 25 shows, in outline, the metabolic pathways relevant to this discussion. From this group of reactions, the ^{14}C of the third carbon atom of serine could reach the respiratory CO_2 pool by reaction with tetrahydrofolic acid (THFA) through the formyl-THFA pathway to formate. Ordinarily, the free formate pool in tissues is very small and formate is rapidly oxidized to CO_2. The rate of appearance in the respiratory CO_2 of an animal of ^{14}C from injected serine will clearly depend upon many factors, among which are the relative activities of all the enzymes of these and other pathways for serine, glycine, and formate metabolism. The pool sizes of each of the intermediates must also be taken into account, and the free serine and glycine concentration in liver, plasma, and muscle have been measured in other experiments with irradiation chimeras.[2]

Control factors undoubtedly exist *in vivo* that influence the relative importance (in terms of carbon atom flux) of the various alternative pathways. Because of this complexity, respiration pattern analysis cannot be expected to give very detailed and quantitative information about the metabolism of serine, glycine, or other compounds of intermediary

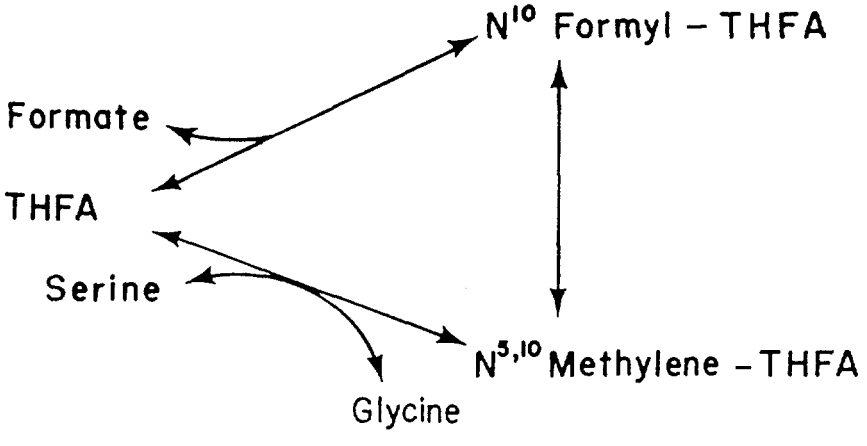

Fig. 25. Outline of the metabolic relationship of serine, glycine, and formate in a cycle of folic acid (THFA) reactions.

1027194

metabolism. The technique can, however, give useful qualitative and, as this report shows, quite suggestive information. Morever, it has the advantage of being a nondestructive analytical tool that can be applied with relatively minor disturbance to the intact organism.

The techniques used in this study were as previously described.[1] Three groups of mice (8 to 10 animals in each group) were studied: normal unirradiated mice and lethally irradiated animals (950 R total-body X irradiation) given either isologous bone-marrow (IBM) cells (20×10^6) or homologous (HBM) cells (20×10^6).

As *Fig. 26* shows and as reported previously,[1] the simultaneous injection of unlabeled compounds with the labeled serine influences the respiration pattern in a specific way. The results are consistent with the following interpretation. When glycine is injected with the labeled serine, $N^{5,10}$ methylene-THFA tends to react with the glycine, thus inhibiting the appearance in the formate pool of ^{14}C from serine-3-^{14}C. *Figure 26* shows that, with added glycine present, the specific activity of respira-

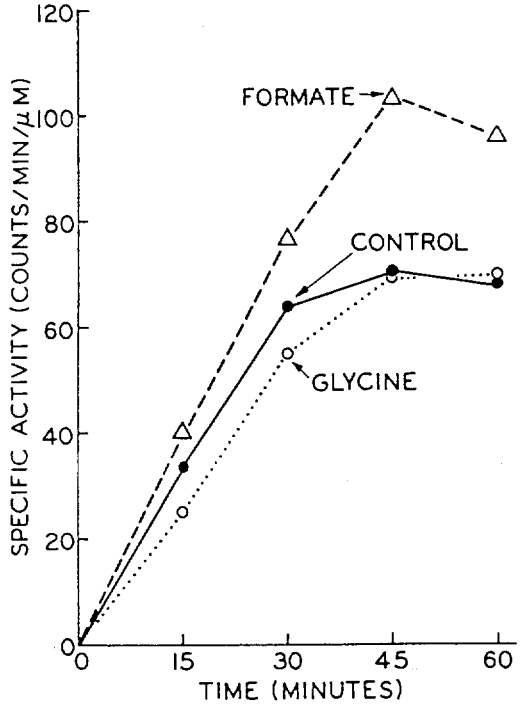

Fig. 26. The effect of unlabeled compounds (ammonium formate and glycine) when injected simultaneously with serine-3-^{14}C on the ^{14}C activity in respiratory CO_2 or normal mice. The curve labeled "control" is the specific activity of respiratory CO_2 of normal mice. The curve labeled "control" is the specific activity of respiratory CO_2 in normal mice when serine alone was injected.

1027195

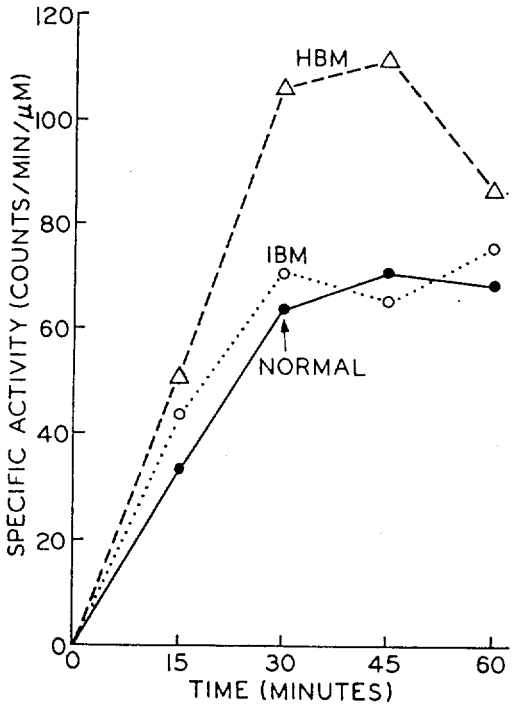

Fig. 27. The specific activity of respiratory CO_2 after injection of serine-3-^{14}C in normal mice and in lethally irradiated animals given isologous bone-marrow cells (IBM) or homologous cells (HBM).

tory CO_2 is lower than the control for 45 min, as expected. On the other hand, when ammonium formate is injected with the labeled serine, THFA can react with the serine and the N^{10} formyl-THFA pool becomes more highly labeled, and ^{14}C in this pool would tend to become "trapped" in the expanded tissue formate pool and would rapidly be oxidized to $^{14}CO_2$. *Figure 26* shows that, when formate was injected with the labeled serine, the specific activity of respiratory CO_2 was greater for 60 min than when labeled serine alone was injected. The bicarbonate pool of the animal is, of course, much larger than the formate pool so that the addition of cold CO_2 from the injected formate is relatively less important than the "trapping effect" of the increase in tissue formate.

Figure 27 shows that serine metabolism in irradiated mice treated with homologous bone-marrow cells is altered (21 days after treatment). Similarly irradiated mice given isologous bone marrow have a nearly

1027196

normal respiration pattern. The greater specific activity of respiratory CO_2 of mice treated with homologous marrow could be due to less dilution of the injected serine since we have previously shown[2] that, at 21 days, the concentration of free serine of liver tissue of chimeras is only about one-half that of normal mice or of irradiated animals given isologous marrow. However, the effect of injecting unlabeled glycine or formate is different *(Table 13)*.

As shown in *Fig. 26* and in the first and fourth lines in *Table 13*, in normal animals the simultaneous injection of glycine delays the appearance of ^{14}C from injected serine-3-^{14}C in respiratory CO_2, whereas the injection of formate increases ^{14}C in respiratory CO_2. The results are similar in lethally irradiated mice treated with isologous bone marrow. In irradiated mice given homologous marrow, however, the effect of glycine is several times greater and the effect of formate is reversed. Thus, in chimeras, both glycine and formate decrease the rate of appearance of ^{14}C from serine into respiratory CO_2. This suggests the possibility that in chimeras the metabolic system of *Fig. 25* is somehow set to favor the production of serine and THFA.

TABLE 13

The Effect of Unabeled Compounds on the Specific Activity of Respiratory CO_2

"Cold" Compound	Group	Time After Injection (minutes)			
		15	30	45	60
Glycine	Normal	−8.5	−8.6	−1.2	+1.7
	IBM	−13.3	−7.6	+14.6	+8.2
	HBM	−4.3	−48.2	−23.4	+4.9
Formate	Normal	+6.8	+13.4	+32.4	+27.8
	IBM	+9.1	+22.2	+30.7	+27.8
	HBM	−1.1	−1.6	−25.0	+11.3

The numbers in the table are the differences in specific activity, counts/min/μM, at the times indicated between animals injected with serine-3-^{14}C alone and injected with serine-3-^{14}C solutions containing unlabeled glycine or ammonium formate. Three groups of animals were studied: normal, irradiated and then given isologous bone-marrow cells (IBM), and irradiated mice treated with homologous cells (HBM).

1027197

To understand the biochemical details of this change in the metabolism of serine in chimeras will require experiments of a different kind from those reported here, but respiration pattern analysis provides a useful tool for the survey of compounds whose metabolism might be altered in chimeras, and the results suggest specific reactions for further study.

REFERENCES

1. Kretchmar, A. L. and Phipps, C. E. Serine-3-^{14}C metabolism in mice as determined by respiration pattern analysis. USAEC Report ORINS-53, pp. 51–53.
2. Kretchmar, A. L. and Congdon, C. C. The levels of free aspartic acid, glycine, and serine in tissues of bone marrow chimeras. Transplantation 1, 298–305, 1963.

Computer Study of the Hemopoietic System of Rats Recovering from Total-body Irradiation

J. P. OKunewick and A. L. Kretchmar†*

The model of hemopoiesis reported previously[1] has been used as a basis for a study of the oscillatory behavior of the recovery of the ability to incorporate ^{59}Fe into the red blood cells after 100 R total-body irradiation.[2] Several significant modifications were made in the original model to accommodate more realistically the problem of recovery in sublethally irradiated animals; the original model was intended for application to recovery in lethally irradiated mice given unirradiated bone-marrow cells intravenously after irradiation.

The S population (normal hemopoietic stem cells) was assumed to be subdivided after irradiation into the S′ cells (uninjured irradiated stem cells) and the S″ cells. The S″ cells were considered to be injured and were assumed to undergo "reproductive death," i.e., to die after one or several divisions. The number of divisions was made a parameter of the model and hence could be changed according to the assumptions being tested.

*Present address: Armed Forces Radiobiology Research Institute; National Naval Medical Center.

†Present address: Memorial Research Center, University of Tennessee, Knoxville.

1027198

The D population, i.e., cells committed to erythroid differentiation but still able to divide, included a D′ population of cells derived from the S′ or S″ population after irradiation. The other populations (N, R′, R and RBC) were the same as for the previous model with suitable changes in estimated size, time lags, and life span of red blood cells to bring the assumptions more into line with experimental data available for the hemopoietic system of the rat.

Figure 28 shows output from the computer depicting the changes with time after irradiation in the stem cell and differentiated-dividing

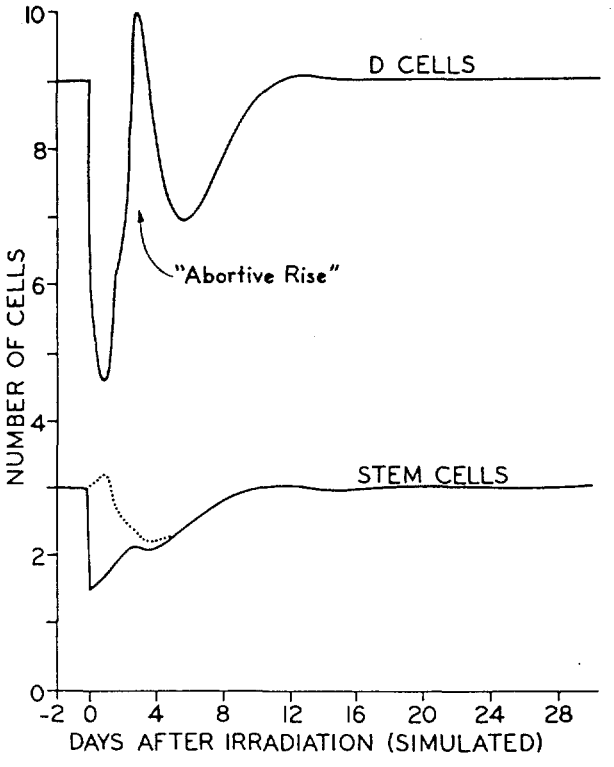

Fig. 28. *Computer output for the model discussed in the text.* Irradiation was simulated at day 0. The assumption was made that 50% of the stem-cell population was injured and would die after division as differentiated cells. This assumption leads to a prominent "abortive rise" in the D population (dividing—differentiated bone-marrow cells). The dotted line in the 0 to 6 day region of the curve for stem cells is for the total stem-cell population (injured + uninjured). The solid line represents uninjured stem cells.

1027199

(D) populations. Of particular interest was the "abortive rise" in the D population at about three days after irradiation owing to the assumption that injured stem cells can differentiate after irradiation.

Certain further significant changes in the model and in the program for the computer analysis have been made by personnel of the Rand Corporation's Aero-Astronautics Department and will be the subject of a forthcoming report.[3]

REFERENCES

1. Kretchmar, A. L. A model of hemopoiesis for mammalian recovery experiments. USAEC Report ORINS-53, 1966, p. 41.
2. Hennessy, T. F. and OKunewick, J. P. Radioiron study of erythropoiesis after x-irradiation, USAEC Report UCLA-383, 1956.
3. OKunewick, J. P. in preparation.

Effect of Phytohemagglutinin (PHA) on an Antibody-forming System

N. Gengozian and K. F. Hübner

Several investigators have shown the blastogenic and mitogenic effects of phytohemagglutinin (PHA) on human and animal lymphocytes under a variety of culture conditions. These cellular events are preceded by synthesis of RNA and DNA, and in human cells, the production of gamma globulin has been reported. The striking morphologic and biochemical parallelism between the PHA-treated lymphocytes and those of antigen-stimulated lymphocytes led us to consider the effect of PHA on an antibody-forming system.

Figure 29 shows the response to *Salmonella* typhoid antigen of normal mice and of those treated with PHA 24 hr before or after antigen injection. In both PHA-treated groups there was a suppressive effect on the immune response. This suppression, however, was only slight and temporary when the PHA was given after antigen injection, the most apparent effect being a delay in the formation of 7S (2-mercaptothanol resistant) antibody. In the mice given PHA before antigen injection, there was a significant depression in the total amount of antibody formed and a delay of approximately three weeks before the formation of 7S antibody.

As shown in *Fig. 30 (A and B)*, the anamnestic response was studied in mice receiving a normal primary antigenic stimulus and in those treated with PHA 24 hr before the primary antigen injection. In those groups that

1027200

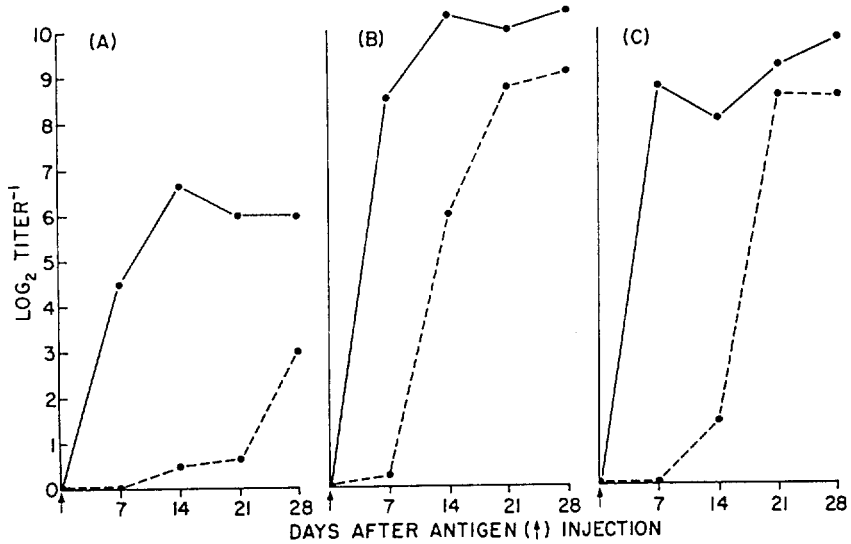

Fig. 29. Effect of PHA on antibody response to *Salmonella* typhoid antigen in mice.
(A). PHA treatment one day before antigen injection.
(B). No PHA treatment.
(C). PHA treatment one day after antigen injection.
Solid lines indicate titration for total antibody. Dashed lines indicate titration for antibody after 2-mercaptothanol (2-ME) treatment of serum. Reduction in titer after 2-ME treatment indicates presence of 19S antibody; 7S antibody is considered to be resistant to 2-ME treatment.

were not exposed to PHA during the primary response *(Fig. 30A)* it can be seen that (a) injection of PHA alone on day 56 did not affect the antibody being formed (amount and type) as a result of the previous primary antigen injection, i.e., there was an absence of a nonspecific anamnestic response; and (b) injection of PHA at the time of the secondary stimulus of antigen (PHA given 8 hr before antigen) had only a temporary suppressive effect on the anamnestic response, the antibody level reaching control values 21 and 28 days after the booster stimulus. Similar results were obtained with mice treated with PHA during the primary response *(Fig. 30B)*. Thus, the suppression induced by PHA in the primary response had no effect on the subsequent anamnestic response, with or without additional PHA treatment at the time of the secondary antigenic stimulus. Indeed, the amounts of antibody formed (7S and 19S) were almost identical in both groups of mice.

Additional studies revealed that with a smaller primary antigen injection, PHA suppressed completely the formation of 7S antibody. The

1027201

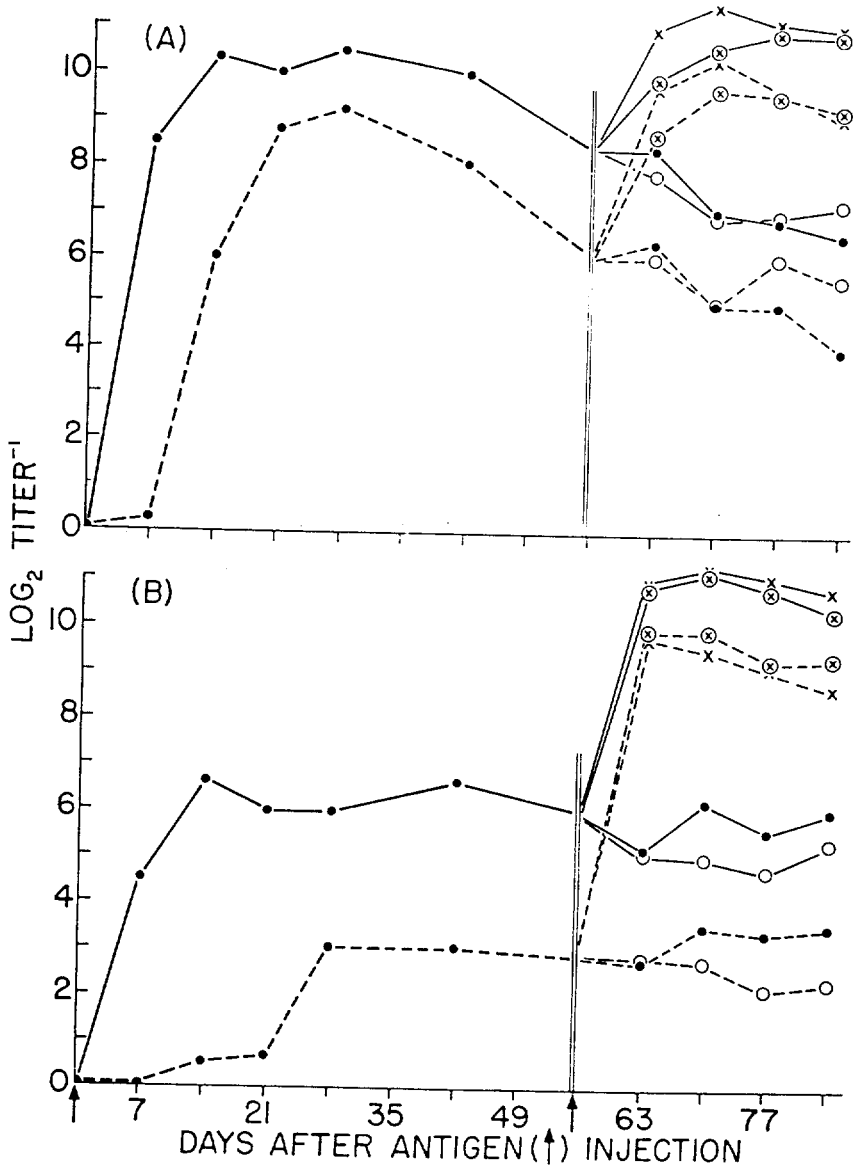

Fig. 30. Effect of PHA on the primary and secondary response to *Salmonella* typhoid antigen in mice.
(A). Mice not treated with PHA during the primary response.
(B). Mice treated with PHA during the primary response.
Procedures performed on day 56 for secondary response studies:
Closed circles (●_____●), no treatment with PHA or antigen; open circles (○_____○), injected with PHA only; X's (X_____X), injected with antigen only; open circles with X (⊗_____⊗), injected with PHA and antigen. Solid lines indicate titration for total antibody, dashed lines indicate titration for antibody after 2-ME treatment of serum.

1027202

anamnestic response in mice so treated was also striking in that only 19S antibody was formed, suggesting that PHA somehow modified the cellular immune mechanism so that 7S antibody production was completely suppressed.

In summary, if 7S antibody production was achieved in the primary response after PHA treatment (as shown in *Fig. 30*) with a strong antigenic stimulus, PHA did not abolish 7S antibody production in the secondary response, the levels of antibody attained being comparable to those of the nontreated control group. If, however, 7S production was suppressed with PHA treatment during the primary immunization, subsequent stimulation with the antigen for the anamnestic response resulted only in 19S antibody formation. Finally, it should be noted that PHA alone did not elicit a nonspecific anamnestic response in mice previously sensitized to an antigen. Parallel studies with cultivation of antibody-forming cells in *in vivo* diffusion chambers revealed essentially the same effects of PHA as were observed in the intact animal.

Human A-like Antigen on Marmoset Red Cells Detected with Rabbit Anti-marmoset Saliva Serum

C. B. Merritt and N. Gengozian*

Previously we demonstrated that the marmoset, *Saguinus fuscicollis*,† had human A-like antigen in its saliva, in the serum of young (10 weeks old) but not of adults, and on its red blood cells. In contrast, a human B-like antigen has been found only on its red cells. Since the saliva contained considerable quantities of the A-like antigen, it was postulated that, by immunization of rabbits with this substance, a reagent might be made for further investigation of the A-like antigen system of the marmosets.

---

* Student trainee from Tulane University School of Medicine, New Orleans, La.

† Previously designated by us as *Tamarinus nigricollis*. Recent communication with Dr. P. Hershkovitz,[1] Chicago Natural History Museum, Chicago, Ill., suggests that the marmosets in our colony should be identified as *Saguinus fuscicollis* of the *Saguinus nigricollis* group. *Saguinus* is considered to be the oldest valid generic name (synonyms: *Leontocebus, Marikina, Oedipomidas, Tamarin,* and *Tamarinus*) for all marmosets. Dr. Hershkovitz identifies three species among the hairy-faced "white lipped" members of the *Saguinus nigricollis* groups, these being *S. graellsi, S. nigricollis,* and *S. fuscicollis* (Hershkovitz 1966).

1027203

The immune reagent produced was tested against human and marmoset red cells and yielded the results shown in *Table 14*. The unabsorbed reagent reacted most strongly against human A cells, and slightly with B cells and marmoset cells. Absorption with A cells removed es-

TABLE 14

Reactions of Rabbit Anti-saliva Reagent with Papainized Red Cells Before and After Absorptions with Papainized Red Cells

Antiserum	Log_2 $Titer^{-1}$ Versus Following Red Cells: A	B	O	Marmoset
Unabsorbed	12	8–9	2–3	6–8
A-Absorbed	<2	1–2	<2	<2
B-Absorbed	11	2	<2	3
O-Absorbed	12	6–7	0	6
Marmoset-Absorbed	10	5	3–4	0

sentially all serum reactivity for either human or marmoset cells, while absorption with B cells had little effect on the reaction of the reagent for A cells, but removed reactivity for B and O cells and diminished the reactivity for marmoset cells. This suggests that the reagent contained a specific anti-A-like antibody, and perhaps a small amount of specific anti-B activity, which also reacted with the marmoset cells. The presence of both specific anti-A and anti-B antibodies in the reagent is further shown by the reactions after absorption with O cells. These cells removed only nonspecific antihuman activity and left strong reactivity against A, B, and marmoset cells. Absorption with marmoset cells removed some of the anti-A and anti-B activity but did not affect the reactivity of the reagent with O cells. These reactions clearly indicate an anti-A-like antibody in the antiserum, as would be expected from the presence of the A-like antigen in the immunizing saliva. In addition, anti-B and anti-marmoset specificities are also present, but their relation to the anti-A is not clear.

To evaluate more clearly the specificities of the rabbit anti-saliva reagent, eluates from human and marmoset red cells that had been reacted with the reagent were prepared and tested with the results shown in *Table 15*. The eluate from human A cells reacted only with A cells. The eluate from B cells had moderate anti-B and anti-marmoset activity, and of special interest, contained a large amount of anti-A activity, strongly suggesting a cross-reacting type of antibody with both A and B specificity. The eluates from O cells appeared to possess only nonspecific anti-human activity. In eluates from marmoset cells most of the activity

1027204

recovered was against human A cells, suggesting again that the marmoset cells have an A-like factor.

To further investigate the specificities of the anti-saliva reagent, inhibition tests were performed with human and marmoset salivas containing

TABLE 15

Reactions of Eluates of Rabbit Anti-saliva Reagent from Human and Marmoset Red Cells

Eluted from	Log_2 Titer^{-1} Versus Following Red Cells: A	B	O	Marmoset
A Cells*	5	<2	<2	<2
B Cells*	9	4	<2	4
O Cells	4	4	4	<2
Marmoset Cells	9	4	3	2

*Eluates from A and B cells were made with O-absorbed anti-saliva. All cells used for absorption or testing were papainized.

specific blood-group substances. As in the inhibition tests previously described, the system was a mixture of anti-serum, the anti-saliva reagent, and saliva containing A, B, or H substance. After incubating the anti-serum and saliva, this mixture was tested against human and marmoset red cells. The presence of antigens in the saliva that reacted with the anti-saliva reagent would inactivate the antibodies in the reagent for the red cells with which the mixture was subsequently incubated. In the situations where the anti-saliva does not react with the salivary antigen with which it is incubated, agglutination of the added red cells subsequently occurs and indicates the absence of inhibiting substances. The effects of various salivas in inhibiting the ability of the anti-saliva reagent to agglutinate human and marmoset red cells is shown in *Table 16*. Human A saliva inhibited slightly the ability of the reagent to agglutinate human A cells and marmoset cells. Human B saliva had no inhibitory effects on the activity of the anti-saliva reagent. Human O saliva, however, specifically inhibited the ability of the anti-saliva reagent to agglutinate human O cells, but did not affect reactivity against A, B, or marmoset cells. Marmoset saliva produced only minimal inhibition of reactivity against A and marmoset cells.

These results are perhaps most striking in showing marked inhibition of anti-O activity by human group O saliva, indicating that the anti-saliva reagent contained a quantity of anti-H antibody, presumably produced in response to the stimulus of H-like antigen in the marmoset saliva used

1027205

for immunization. Unfortunately, the preimmunization rabbit serum was not available for testing and therefore the presence of anti-H in the rabbit before immunization cannot be definitely excluded. Normally, however, rabbit serum does not contain detectable amounts of anti-H

TABLE 16

Inhibition Tests of Human and Marmoset Salivas for Substances Reacting against Rabbit Anti-marmoset Saliva Reagent

Test System and Cells	$(Log_2)^{-1}$ Saliva Dilution										Control
	1	2	3	4	5	6	7	8	9	10	
I. Rabbit Anti-Saliva + Human A Saliva vs.											
A Cells	2±	4±	4±	4±	4+	→					4+
B Cells	4+	4+	→								4+
O Cells	4±	4+	→								4+
Marmoset Cells	±	3+	3+	4±	4±	4+	→				4+
II. Rabbit Anti-Saliva + Human B Saliva vs.											
A Cells	4+	→									4+
B Cells	4+	→									4+
O Cells	4+	→									4+
Marmoset Cells	4+	→									4+
III. Rabbit Anti-Saliva + Human O Saliva vs.											
A Cells	4+	→									4+
B Cells	4+	→									4+
O Cells	–	–	–	–	–	–	–	1±	1±	4±	4+
Marmoset Cells	4+	→									4+
IV. Rabbit Anti-Saliva + Marmoset Saliva vs.											
A Cells	4±	4±	4+	→							4+
B Cells	4+	→									4+
O Cells	4+	→									4+
Marmoset Cells	4±	4±	4+	→							4+

1027206

activity; therefore, that present in the anti-saliva was probably a result of the immunization.

The inhibition system used was found to be much more sensitive if a much more dilute anti-saliva reagent was used. Therefore such a system was used to test the ability of various salivas to inhibit the anti-A activity of this reagent. The results of these tests showed more clearly the ability of both human A saliva and marmoset saliva to inhibit the anti-A activity. This confirms the presence of an A-like antigen in marmoset saliva and emphasizes the presence of a predominantly anti-A-like activity in the immune reagent.

REFERENCE

1. Hershkovitz, P. Taxonomic notes on tamarins, genus *Saguinus* (Callithricidae, Primates), with descriptions of four new forms. Folia Primat 4, 381–395, 1966.

A Technique for Orthotopic, Fitted Skin Grafts in the Marmoset

R. Porter and N. Gengozian

The natural blood chimerism in the marmoset, resulting from the fraternal twinning and placental vascular anastomoses between the young, suggests that a state of immunologic tolerance exists between the two genetically determined, different blood-forming systems. Whether this tolerance will extend to skin homografts is yet to be determined. In anticipation of skin homograft studies between related and unrelated marmosets, it was necessary to develop a reproducible control autograft procedure for experimental homograft studies. This report describes briefly the development of a successful autograft technique using adult male and female marmosets, *Saguinus fuscicollis*,* imported from South America and maintained in our colony from 2 to 18 months.

Selection site for grafting. A choice of a thoracic ventrolateral graft-bed site as optimal was based on the following criteria: (1) adequate supply of blood and lymph for graft healing by "first intention"; (2) subgraft mechanical support afforded by rib cage; (3) anatomical situation to easily cover and prevent mechanical removal during the early stages of primary union of the graft skin to the host bed.

Because future demands of homografting require a simultaneous con-

* See footnote on Page 58.

1027207

trol autograft for comparison, both right and left sides of the chest wall were autografted.

Skin grafting procedure. The animal is first calmed by a tranquilizing drug. The hair is close-clipped from the levels of the axillae to the mid-abdomen. This area is washed with surgical soap, and the chest-hair stubble is removed with a dipilatory cream, followed by terminal surgical soap scrub.

The animal is taped to a holding device and covered with a sterile drape having a 2½-in. aperture. Loose hair is removed by touching adhesive tape to the dried skin. The skin is prepared for surgery by applying clear aqueous thimerosal (1:1000) and then dried with 70% alcohol. No-touch sterile technique is followed throughout.

The exact site to be excised is injected intradermally with 0.5 ml of a local anaesthetic. To obtain a skin specimen of uniform size, intended sites are marked with a 9 mm cork borer dipped in dye. A very sharp No. 15 scalpel is used to cut through the dermis as close below the epidermis as possible leaving an area of dermis with intact attendant vessels. The excised skin is not otherwise prepared and is placed on a covered sterile saline-dampened gauze until used. The donor site becomes a recipient site without further preparation. After bleeding of the graft bed has subsided, the defect is closed by fixing a graft with the hair follicles in reverse direction in place with four interrupted tie-down stitches and as many uninterrupted stitches (usually 10) as necessary. The uninterrupted stitch serves as a "purse string" by also holding the edge of the defect in the skin from expanding.

Thimerosal (1:1000) is used to cleanse the sites, which are then circumscribed with a water-soluble antibacterial ointment and covered by one piece of sterile petroleum jelly impregnated cloth. Over this lubricating dressing, two opened 2-in. × 2-in., dry gauze squares are placed. This dressing is then covered for protection with one piece of plaster of paris bandage, 3-in. wide. Snug-fitting, crossed harness straps made of folded plaster of paris bandage are applied over the shoulders and covered with another piece of plaster of paris bandage around the chest. The second plaster bandage holds the loose ends of the straps securely in place, the harness is tied front and back with twine to form a round collar *(Fig. 31)*. Before the plaster is completely hard (5 min) it is kneaded until pliable for the sake of comfort. The animal is returned to an isolation cage. The entire grafting procedure is completed in approximately 1 hr.

First inspection. After seven days the graft should be well united to the bed and the cast can be removed. To capture the animal with as little excitement as possible, it is coaxed into a side-cage box that can be re-

1027208

Fig. 31. Photograph of marmoset immediately after grafting and covering with plaster of paris bandage.

Fig. 32. Photograph of an autograft with excellent hair growth two months after grafting.

1027209

moved and has a tight fitting slide door. An inhalant anaesthetic is introduced into the box. When the animal is quiet, the cast is rapidly cut away, grafts are photographed, and sutures are removed. The sites are cleansed with surgical soap and coated lightly with antibacterial ointment. This procedure requires approximately 5 to 6 min.

The animal is released into a clean cage and left by itself for one week. It may be net-captured for graft inspection after the tenth postgraft day.

In more than two dozen double autografted marmosets only one graft was lost to partial mechanical removal, self-inflicted in the first hour after removal of the cast. The remainder are well taken and growing hair. *Figure 32* shows an autograft in its 60th day.

Normal and Pathologic Intrauterine Development of Marmosets *(Saguinus fuscicollis).*

C. C. Lushbaugh, Gretchen Humason, R. M. Kniseley, and N. Gengozian

Knowledge of normal development, morphology and physiology is far from complete for any species of the Hapaloid New-World monkeys. The successful development of an experimental marmoset colony here now affords a unique opportunity to study growth and disease in these animals. Although these histopathologic studies are a by-product of a broad immunologic investigation of natural blood chimerism, they are aiding[1] also in understanding the high incidence of reproductive failure that has been the experience here and elsewhere in breeding these animals.

Gross and histologic examinations were made of all products of conception, embryonal, fetal, neonatal, and adult deaths in the colony. To date, 112 animals have been autopsied to determine (1) the major causes of fetal and neonatal deaths; and (2) the nature of senescent processes.

Definition of the diseases of intrauterine origin requires correlation of organogenesis with gestational time, but there is no agreement on average length of normal gestation and average size of the full-term newborn in the various *Saguinus* species. We have had to assume crown-rump (CR) length to be an approximation of fetal age and determine indirectly an asymptotic, full-term length at birth. On the basis of 46 *S. fuscicollis* young delivered in the last year, we estimate that the full-term "maximum" CR length at birth is 11 cm, while 10.5 cm is the expected common

1027210

size of normal young at full term. *Figure 33* shows, however, that almost half the dead infants were less than 8 cm CR length and only 20% were larger than 10 cm CR.

Time of viability, defined as pulmonary maturity, or the time (or CR size) when the cuboidal epithelium of pulmonary alveolar walls disappears while capillary proliferation becomes prominent, was found to be at 8 cm CR length. Pulmonary developmental stages in respect to fetal size in *S. fuscicollis* are approximately:

1. Bronchial budding—1.5 cm CR length
2. Bronchiolar budding—5.5
3. Atrial budding—6.0
4. Alveolar development—6.5
5. Cuboidal epithelial "dilution"—7.5
6. Mature appearance—8.0

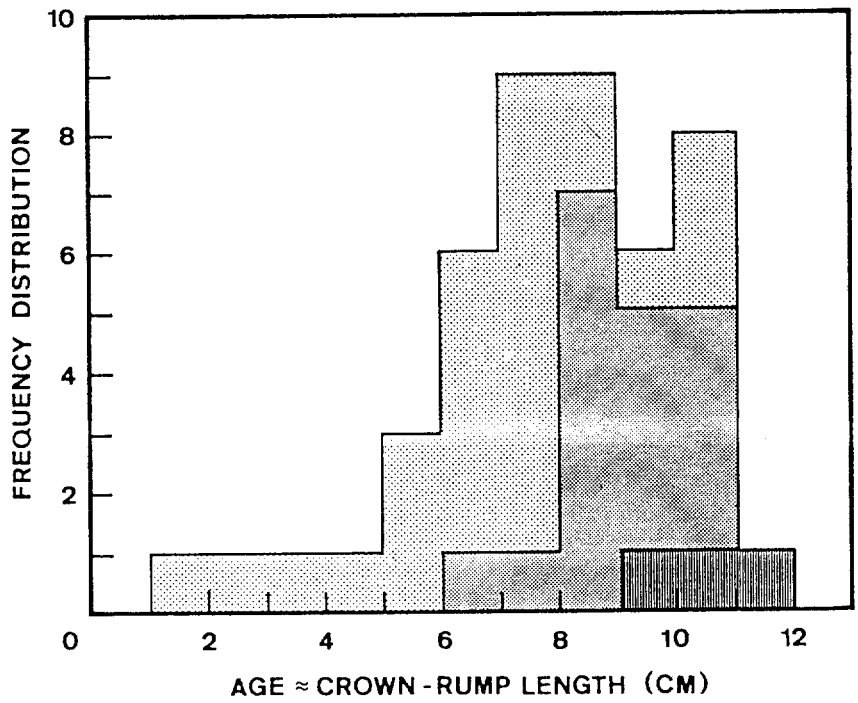

Fig. 33. Histogram of the size (age) distribution of marmoset (*S. fuscicollis*) young at autopsy. Three animals (shown darkest) of the total of 46 specimens were liveborn and died within a week of birth. These animals and the 17 in the other dark area had pathologic (increased) amounts of iron (Prussian Blue-positive material) diffusely in all hepatic parenchymal cells and are presumed to have had hemolytic anemia (43.5%). (Age of viability is approximately 8 cm CR stage.)

1027211

In only 4 of 24 animals larger than 8.0 cm was there previability as evidenced by persisting prominent alveolar epithelium. Any evidence of passive pulmonary aeration resulting from stresses during birth was not seen, however, until 8.6 cm CR length. Although such pulmonary aeration was usually incomplete, it was commonly found in young at 9.0 cm CR. Extensive aeration from attempted postnatal breathing was found in those greater than 9.5 cm CR. Amniotic debris was present in alveoli of 8.5 cm CR and larger marmosets—a sign of prenatal anoxia. These findings suggest that marmoset young shorter than 8.0 cm CR are previable and those longer than 8.0 cm but less than 10.0 cm are premature but viable.

Although the cause of all abortions (previable births) are not determinable, since some can be due to unknown lethal genetic mechanisms, a major cause appears to be anoxia, which leads to cardiac failure and massive hepatic passive congestion. Underlying causes for this anoxia may relate to multiple conceptions, double placentas, placental vascular anastomoses, and partial placental abruptions. Disparity in sizes of twins, the phenomenon of infants with small pale livers while their twins have large engorged livers, and subcapsular hepatic hemorrhages suggest such mechanisms as the "transfusion syndrome" and hypo- and hypervolemia from intranatal uterine contractions pumping blood into the already born twin from the intrauterine one and its placenta.

Chronic fetal hypoxia may be also postulated to result from obstruction to placental blood flow by numerous huge islands of proliferating erythroblasts that are present in marmoset placentas from fetal size 1.5 to 9.0 cm CR. Our study extends Hill's[2] and Wislocki's[3] limited observations concerning a normal placental stage of erythropoiesis in these primates. Our material contains abundant evidence that after yolk-sac erythropoiesis, erythroblastic stem cells next develop in the marmoset placenta. The disappearance of these erythropoietic islands is accompanied by hepatic erythroblast development. Bone-marrow erythroblastic stem-cell development is delayed until about the 9.0 to 10 cm CR stage near term. This delay in marrow neoerythrogenesis might portend severe neonatal anemia ("anemia of prematurity") in this species. The invariable occurrence, larger size, and widespread distribution of erythroblastic stem-cell islands in both placentas require the concept of "blood" chimerism to be expanded to include intrauterine sharing of a large erythroblastic stem-cell pool rather than just intermixing of peripherally circulating leukocytes and erythrocytes.

The normal occurrence of intraplacental and intrahepatic erythroblastic proliferation, in addition, complicates the morphologic diagnosis of hemolytic anemia of the newborn. The inconsistent persistence of placental erythroblasts beyond the 9.0 cm CR stage could be a conse-

1027212

quence of severe hypoxia from multiple causes, but the presence of large amounts of iron in hepatic parenchymal cells and renal proximal convoluted tubules suggests that hemolytic disease afflicts many of the premature viable but stillborn infants. In *Fig. 33* the two dark areas define the frequency distribution of heavily iron-laden livers in respect to fetal size (or age). In immunogenic hemolytic disease of the newborn such a hemosiderosis should occur in the last third of the pregnancy as it does here. The incidence of 20/46, however, is extraordinarily high, and other factors than red-cell antigens and antibody mechanisms may be needed to explain it. Only a few of these animals had detectable antibodies on their red cells, but in many instances of human hemolytic disease of the newborn such antibodies are not found, particularly in partially macerated stillborn.

Correlations of the embryonic and fetal development of other organ systems with age are needed. A preliminary study of the lymphopoietic system has disclosed that lymph-node and splenic development is relatively delayed in this animal compared to that of man and mouse. Whether this retarded development is related to, or responsible for, the production of the chimeric tolerant state will be determinable when known non-chimeric singlings can be studied in large numbers.

REFERENCES

1. Gengozian, N., Lushbaugh, C. C., Humason, G. L., and Kniseley, R. M. 'Erythroblastosis foetalis' in the primate, *Tamarinus nigricollis*, Nature 209, 731–732, 1966.
2. Hill, J. P. The developmental history of primates, Croonian Lecture, Phil Trans Roy Soc, London, Series B, 221, 45–175, 1932.
3. Wislocki, G. B. Hemopoiesis in the chorionic villi of the placenta of Platyrrhine monkeys, Anat Rec 85, 349–363, 1943.

1027213

NASA Study on Radiation Effects

Retrospective Study on Deleterious Radiation Effects in Man

The great need for more precise knowledge about the radiosensitivity of man gave rise to a retrospective search for human radiation-exposure data that could be analyzed by rigidly imposed statistical methods. This study, supported jointly by the National Aeronautics and Space Administration and the U. S. Atomic Energy Commission, is now in its third year. The commencement of the Apollo program for human exploration of the moon's surface has created deadline pressures for completion of the part of the study focused on the effects of single and repeated exposures within an eight-day period.

Previously we reported two such studies in which first we used only data obtained from the hospital records of 100 patients treated at the Medical Division of Oak Ridge Associated Universities, and then combined that study with similar data obtained from the University of Cincinnati and the City of Hope Hospital, Duarte, Calif. We are now in process of expanding the study to include a total of about 1000 such hospital observations. We anticipate that this large amount of data will increase the accuracy of our statistical analysis so that greater reliance can be placed upon the correctness of the estimates now underlying shielding requirements of space vehicles. We also expect that correlation of medical and nursing observations of untoward changes in this large group of patients after the various levels of radiation exposure will enable predictions to be made of the kinds and severity of physiologic responses to be expected in normal man in certain radiation fields. We hope that such knowledge will supply on-ground monitors a basis for deciding whether or not an astronaut showing symptoms of distress in space is suffering from radiation exposure rather than from some other stress.

In the interest of giving our results to date the widest and earliest dissemination, the dose-response relations developed for symptoms of the human prodromal response were incorporated in Chapter 5.2.2 "Prodromal Response" and Chapter 6.0 "Lethality" in *Space Radiation Hazards*, a book to be published soon (March 1967) by the National Research Council, National Academy of Sciences under the editorship of W. H. Langham and Douglas Grahn (C. C. Lushbaugh and G. A. Andrews).

The responsibility for data storage, retrieval and programming analysis

1027214

has been transferred from the Mathematics Division of Oak Ridge National Laboratory to personnel of the Data Processing Center of Oak Ridge Associated Universities. The computer facilities of ORNL are still required to handle the large volume of data and perform the required analyses and statistical evaluations (A. S. Gloster and Donna Bibler).

The data under study are from 27 participating institutions that have provided 1226 usable patient charts out of 1274 obtained (Evalyn Repplinger and Dorothy Vola). At present, approximately one-half million dose-correlated observations are in the study, although not all information from all charts has been completely encoded. This volume of data required development of an efficient data management system to obtain analytic results in reasonable time periods. This development has paralleled a search for more appropriate statistical methods of data analysis for this kind of study. Probit analysis, the method used so far, was neither designed nor intended to be used in retrospect so that deviations from implied assumptions are not ascertainable with it. Even so, our use of probit analysis appears justified by its widespread use in experimental radiobiology so that relative comparisons can be made between sick and well persons and various species of small and large animals. We are also applying methods used in testing of inanimate engineering components for reliability and durability. The Weibull density function that describes wear-out failure rather than chance failure, predicting the time that any rate of failure will be evident, seems most promising, since most symptoms and signs of biological distress can be considered as evidence for "wear-out" of a homeostatic physiologic system (E. Frome).

The following abstract of one of our studies is included because it illustrates one of the many complex problems that must be solved as a basis for this program.

During the year, further refinement has been achieved in the estimates of doses required for production of specific prodromal effects. These new estimates will not be reported in detail here because they will be refined still further in the future as larger numbers of patients are analyzed.

Dosimetry Used in Equating Various Radiation Exposures for Determining Dose-Response Relationships

W. Beck, R. Cloutier, and F. V. Comas

The factor that can affect most the validity of our retrospective determination of human dose-response relations is the accuracy of each dose

1027215

estimate. The statistical analysis commonly used in such studies contains the assumption that the independent variable, dose, is known precisely while the biological response may not be accurately measured.

The retrospective study was divided into four phases. Phase I was a pilot study of only 100 single exposures of less than 24 hr in patients at the Medical Division.[1] Phase II was an extension of this study to test the feasibility of using data from other hospitals, and also included only single radiation exposures.[2] Phase III, now being completed, includes single and fractionated exposures (greater than one day and less than eight days). Phase IV is planned to study protracted exposures where exposure time was greater than eight days.

Phase I. Phase I was composed of 93 single-exposure cases of therapeutically administered total-body irradiation (TBI) and seven cases of accidental TBI. Eighty-four of these were treated with the Division's medium-exposure-rate total-body irradiator,[3] and the other nine were treated with the Division's cobalt-60 temporary irradiator.[4]

The dose estimates for the 93 patients were based on a dosimetric study by Hayes, et al.[4] The dosimetric system consisted of an aqueous ferrous sulfate solution (Fricke dosimeter) within a plexiglass phantom. The absorbed dose to the solution was taken as the patient's dose when he was exposed to the same amount of radiation.

Using this technique we determined the whole-body average dose (WBAD), and the midepigastric dose for all 93 patients. The WBAD is an estimate of the average energy absorbed per gram of tissue, where the average is taken for every gram of tissue in the body. The midepigastric dose is an estimate of the average energy absorbed per gram in the upper abdominal compartment.

The dose estimates for the seven accident cases were determined by a mock-up of the accident at its site.[5]

Phase II. Phase II extended the pilot study by the addition of 11 new ORAU cases, 29 from Cincinnati General Hospital, Cincinnati, Ohio, and 23 from the City of Hope Medical Center, Duarte, Calif., bringing the total number of patients in the study to 163.

The dose estimates for the new ORAU cases were made with the same technique described in Phase I. However, all the ORAU dose estimates were modified for patient size. The size-correction factors were determined from the experimental measurements of the absorbed doses in three phantoms representative of an adult, an adolescent and a child.

The dose estimates for the Cincinnati and the City of Hope cases were based on a comparison of phantom depth-dose measurements made at each facility.

1027216

Phase III. The addition of about 600 patients from 21 institutions with both single and fractionated exposures brought the total number under study to more than 750. Approximately 50 treatment techniques were used, and "dosage" was recorded in more than 15 different units. To make these doses comparable to those in Phase I and II, it was necessary to convert the variously reported doses to total-body average dose.

Table 17 shows the dose distribution of the 504 cases for whom total-body average doses have now been estimated.

TABLE 17

Dose Distribution of 504 Cases

Whole-body Average Dose (in rads)	Number of Cases
0–25	149
26–50	108
51–75	90
76–100	19
101–125	17
126–150	36
151–200	19
201–250	26
251–300	4
301–400	15
401–500	7
501–700	7
701–900	2
901–1100	3
1101–1300	2
	504

Of the 600 new cases, only 66 were treated with gamma rays from isotopic sources and 39 of these were from institutions included in Phase II. We estimated the absorbed dose for 40 of these on the basis of experimental phantom measurements made at each facility. No dose estimates for the other 26 patients could be made owing to lack of phantom data.

Doses were estimated for 310 of 535 cases of X-ray TBI with the use of a method developed by Mayneord.[6] Mayneord's method was experimentally verified by phantom measurements before its use. With it we estimated the total-body average dose for all cases of bilateral X-ray TBI having qualities expressed as half-value layers of from 0.5 mm to

1027217

4.2 mm of copper. For most of the other cases of X-ray TBI, the free-air exposure is the only "dosage" parameter available.

There were only 34 cases of the 757 single exposures to be considered in Phase III for whom we were not able to estimate either the total-body average dose or the free-air exposure, less than a 5% loss of cases due to insufficient dosimetry data.

REFERENCES

1. Lushbaugh, C. C., Roth, R., Andrews, G. A., Kniseley, R. M. Preliminary Report: A retrospective evaluation of the radiosensitivity of man based on therapeutic and accidental whole-body irradiation. NASA Report, July 1, 1964.
2. Lushbaugh, C. C., Comas, F., Saenger, E. L., Jacobs, M., Hofstra, R., and Andrews, G. A. Radiosensitivity of man by extrapolation from studies of total-body irradiation of patients. Radiat Res 27, 487–488, 1966, Abstr. Aa-2.
3. Brucer, M. A total-body irradiator. Int J Appl Radiat 10, 99–105, 1961.
4. Hayes, R. L., Oddie, T. H., and Brucer, M. Dose comparison of two total-body irradiation facilities. Int J Appl Radiat 15, 313–318, 1964.
5. Hurst, G. S., Ritchie, R. H., and Emerson, L. C. Accidental radiation excursion at the Y-12 Plant III. Determination of radiation doses. Health Physics 2, 121–133, 1959.
6. Mayneord, W. V. and Clarkson, J. R. Energy absorption. II Part I. Integral dose when the whole body is irradiated. Brit J Radiol 17, 151–157, 1944.

1027218

›isotope Development

bjective of developing improved radioactive
sis and therapy, and performing fundamental
dies necessary to achieve these objectives.
rk with gallium-68 has been quite promising.
hemical forms it may prove useful in several
ons. The work on bone deposition of gallium
uestions must be answered before it can be
inical use. Other new radionuclides under
ım, each offering some potential advantages
els such as technetium-99m.

sible Diagnostic Agent

emely useful in diagnostic procedures, the
only a short useful life ($t_{1/2}$ parent ^{99}Mo =
$_2$ = 17 hr) can be obtained from a generator
l at the Oak Ridge National Laboratory
^{188}W.[1] Rhenium is chemically similar to
adiation dose from ^{188}Re is higher than that
ided advantage in that its parent, ^{188}W, has
ı that of ^{99}Mo ($t_{1/2}$ ^{188}W = 70 days). Rhe
photon emission and some associated high
principal photon emitted has an energy of
nd excretion of ^{188}Re in the perrhenate form,
NL generator, has been studied in various
tion is similar to that of ^{99m}Tc with concen
ach, and salivary glands. *Figure 34* shows a
ı of a dog. The thyroid and salivary glands
nium-188 is excreted through the urine, is
n both the feces and urine. *Figure 35* shows
at administered ^{188}Re perrhenate and a sim
ministered ^{99m}Tc pertechnetate showing the
e gut. Tracer studies of the body retention

1027219

^{188}Re perrhenate by man have also been made. *Figure 36* shows the body retention of orally administered ^{188}Re perrhenate in a normal human volunteer subject. Half times were approximately 10 hr.

A ^{188}Re sulfur colloid can be prepared by the hydrogen sulfide technique; its distribution in animals resembles that of ^{99m}Tc sulfur sol.

not legible in original.

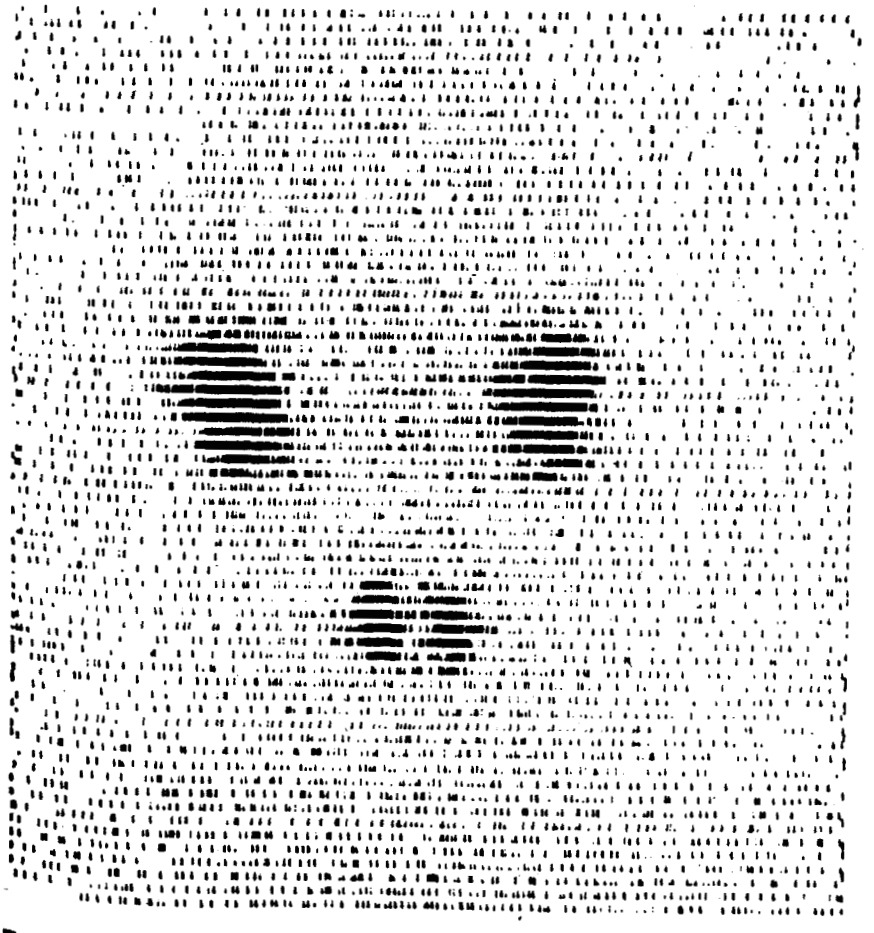

Fig. 34. Neck scan of dog 4 hr. after administration of ^{188}Re in perrhenate form. Salivary glands and thyroid lobes are clearly defined.

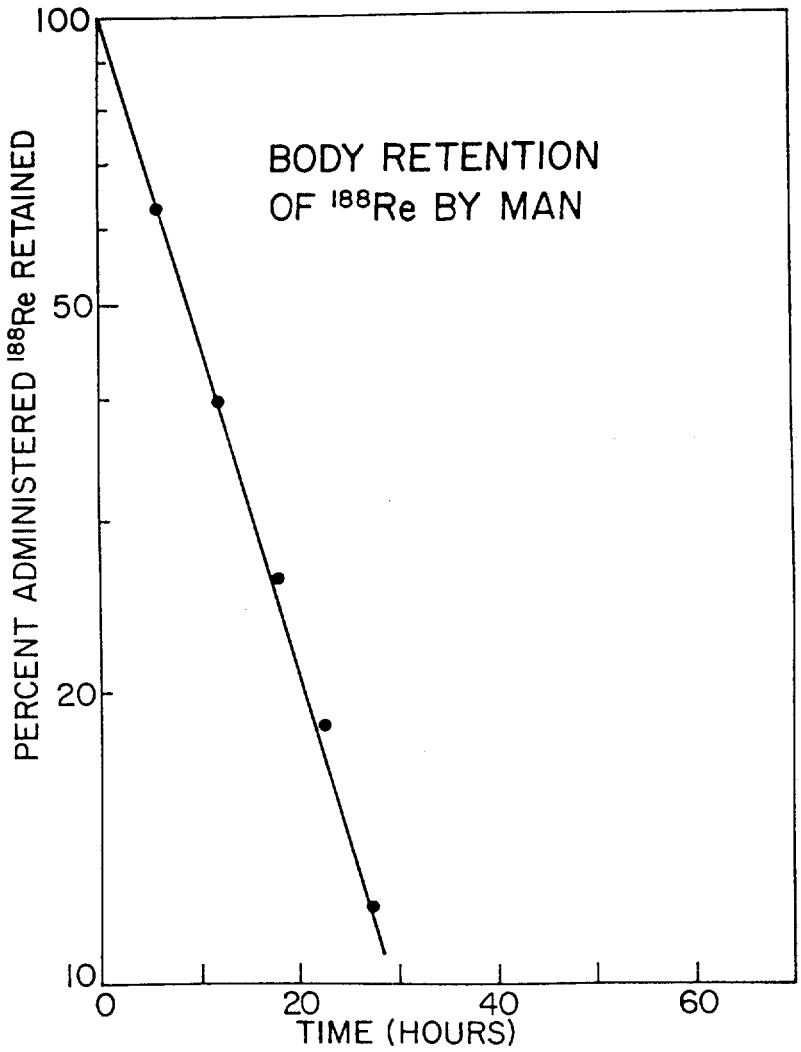

Fig. 36. Body retention of tracer ^{188}Re (5 microcuries) by volunteer subject as measured indirectly by excretion.

REFERENCE

1. Lewis, R. W. and Eldridge, J. S. Production of 70-day tungsten-188 and development of a 17 hour rhenium-188 radioisotope generator. J Nucl Med 7, 804, 1966.

1027220

Hydrous Ferric Oxide Colloid Labeled with Gallium-68

R. L. Hayes, J. E. Carlton, J. J. Rafter, and B. L. Byrd

The hydroxides of polyvalent metals are often used in scavenging and purification processes. Precipitation of ferric hydroxide is frequently used in separation procedures for a number of radionuclides, especially those in a carrier-free or high-specific-activity state. Quite stable colloidal preparations of hydrous ferric oxide are readily prepared by the hydrolysis of ferric salts. When this particular colloid is formed in the presence of ionic gallium-68, the gallium is bound to the colloid particles. The radioactivity in such preparations will not dialyze and remains bound to the colloid in *in vivo* systems as well. The particle size of the colloid may be varied by control of the rate of hydrolysis through alterations in ferric salt concentration, heating rate, and presence or absence of stabilizer.

Gallium-68 in this colloidal form is of interest as an agent for bone-marrow scanning. Because of its short half-life ($t_{1/2} = 68$ min), the radiation dose to the patient will be reasonably low even with multimillicurie amounts. Gallium-68 is readily available from a nuclide generator (parent, ^{68}Ge) having a long useful life ($t_{1/2} = 280$ days). The factors that influence the biologic distribution of these ^{68}Ga-labeled hydrous ferric oxide preparations are being investigated in detail with emphasis on the enhancement of their deposition in bone marrow. The results should also apply to ferric oxide colloids labeled with other radionuclides.

It is well known that the clearance of colloids from the blood is profoundly affected by the total number of particles administered. When short-lived radionuclides are used in scanning of the reticuloendothelial system, the blood disappearance rate should be rapid enough to permit scanning before too great a portion of the activity has decayed. *Figure 37* shows the blood clearance of one particular preparation of ^{68}Ga-labeled hydrous ferric oxide colloid in the rabbit. The disappearance is quite rapid with a half-time of 9 min, a rate well suited to the use of ^{68}Ga.

Decreasing the number of particles administered tends to hasten the blood clearance. The total number of particles administered also has quite a dramatic effect on the relative amount of colloid deposited in the bone marrow as shown in *Table 18*. As the amount of colloid administered was increased there was a corresponding increase in the percentage localized in bone marrow at one hour after intravenous administration. At the highest dose, the blood activity was somewhat elevated. The blood

1027221

level data in *Fig. 37* correspond to those for the 1 mg/kg dose level in *Table 18*.

Others have reported that colloids of small particle size tend to be preferentially taken up by bone marrow. From *Table 18* it is apparent

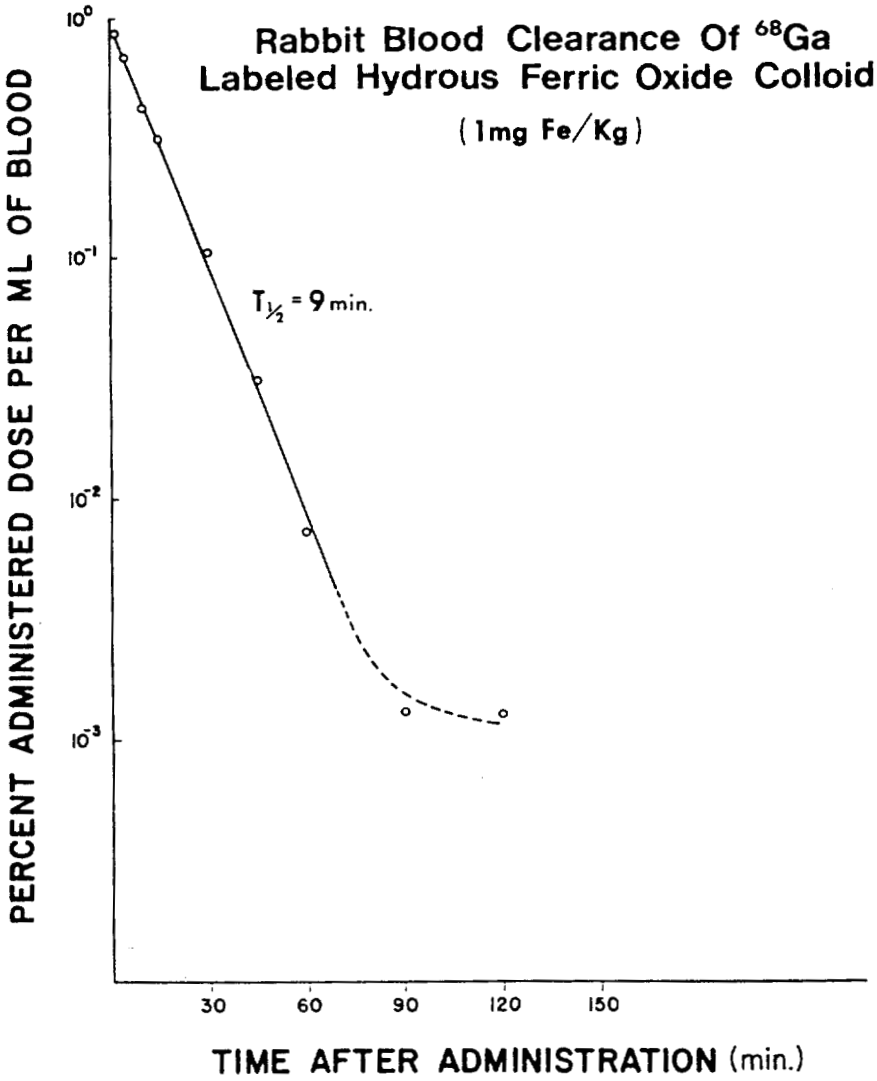

Fig. 37. Blood concentration of ^{68}Ga-labeled hydrous ferric oxide colloid in the rabbit as a function of time. Each point is the average of three measurements.

1027222

shows the results of a study of the effect of dextran on the distribution of colloid in the rabbit. The data indicate an optimum level of dextran for maximum bone marrow deposition. Similar results have been obtained with other stabilizers.

Studies with Indium-113m

R. L. Hayes and B. L. Byrd

Short-lived ^{113m}In, now available from a nuclide generator, is promising as a possible diagnostic agent. Its 1.7-hr half-life would be near optimum for many procedures. Further, its parent, ^{113}Sn, has a half-life of 118 days, providing a long useful life for the generator system. Indium-113m decays with a single gamma emission having an energy of 390 keV. It can be separated from parent ^{113}Sn deposited on hydrous zirconium oxide in 70 to 80% yield by elution with dilute acid. Contamination levels of only 4×10^{-4}% have been consistently observed in our laboratory. Exploratory studies in animals of the distribution of ^{113m}In in various forms are now in progress.

In microgram amounts, indium in the citrate form is diffusely distributed in the rat with the highest level in the blood occurring at 2 hr after intravenous injection. The use of carrier indium to improve early clearance from the blood and enhanced deposition in the bone (as with gallium) is not feasible because indium is toxic. However gallium, which is chemically similar to indium, can act as a pseudo carrier for indium. With a level of 5 mg/kg of gallium (citrate) the distribution of ^{113m}In citrate in the rat approaches that of ^{68}Ga under similar conditions, indicating that ^{113m}In may find use as a bone-scanning agent.

Indium-113m can be used as a label for hydrous ferric oxide colloid. Its use in this form as a possible agent for bone-marrow scanning is being investigated. Marrow-liver concentration ratios of 0.5 have been achieved; however blood levels at early periods (2 hr) after intravenous injection have been too high for use of this preparation as a practical scanning agent.

The excretion of ^{113m}In in the ethylenediaminetetraacetic acid form (EDTA) by the rat has also been investigated. *Figure 38* shows the

1027223

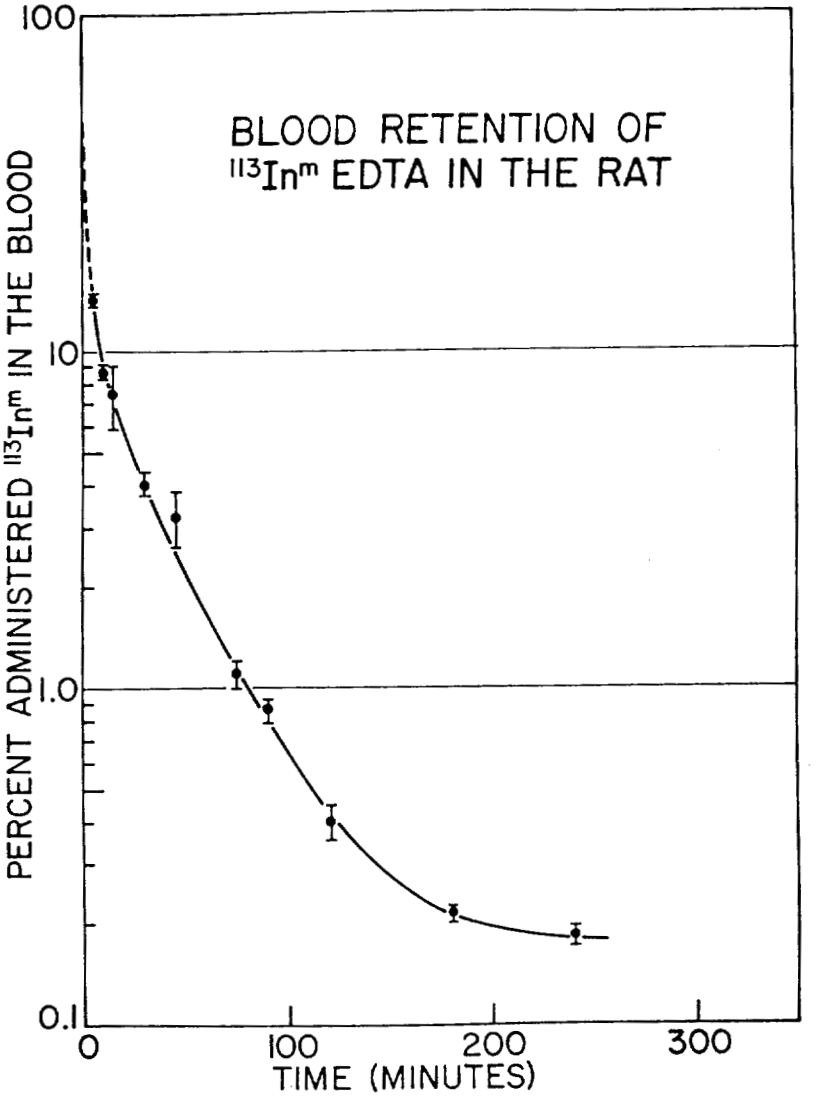

Fig. 38. Blood retention of ^{113m}In EDTA in the rat.

retention of ^{113m}In in the blood as a function of time; the whole-body retention parallels the blood level. These results resemble those obtained with ^{68}Ga EDTA, and it is possible that, as with ^{68}Ga, ^{113m}In in the EDTA form may be suitable as a brain-scanning agent.

1027224

Techniques to Provide Sterile and Pyrogen-free Radiopharmaceuticals from Long-lived Generators

C. L. Edwards and R. L. Hayes

The advent of radionuclide generators has greatly extended the availability and increased use of short half-lived radionuclides in nuclear medicine. As a result major progress has been made both from the standpoint of improving established procedures and in developing new applications of radioisotopes to clinical medicine.

New problems have been created also. Heretofore most radiopharmaceuticals have had half-lives sufficiently long to allow for quality-control testing similar to that for stable pharmaceuticals. The testing for pyrogenicity and sterility was largely the responsibility of the producer. The user rarely had to be concerned about the pharmaceutical acceptability of the preparation. However, the production of short-lived radionuclides in the nuclear-medicine laboratory places the burden of quality control on the user. Yet because of the short half-lives, the standard procedures for testing pyrogenicity and sterility as prescribed by the U.S.P. are not applicable. The radioactivity would be lost owing to decay before testing could be completed.

One approach to the problem, which has been used commercially, has been the sterile, pyrogen-free generator supplied with a closed system for elution with sterile, pyrogen-free eluant. Relatively few entries over a fairly brief period with the usual aseptic techniques allow little opportunity for contamination by microorganisms or pyrogens. Its acceptability is similar to that of the multiple-dose vial of stable pharmaceuticals.

The problem of quality control for short half-lived radiopharmaceuticals is greater for generators having long useful lives, e.g., the germanium-68-gallium-68, and the tin-113-indium-113m generators. Both have useful lives measured in months. The large number of elutions over extended periods increases greatly the chance for contamination. For maximum yield the generators should be kept wet between elutions, which further enhances the opportunity of pyrogenic contamination. Neither pyrogens nor microorganisms can be detected by present methods in the brief time between the eluting procedure and the administration of the isotope.

Our experience with the gallium-68 generator has led us to institute the following program:

(1) The eluate is cultured in Sabouraud's and thioglycolate solutions twice weekly, the first eluate on Monday and the last on Friday.

When an organism is cultured from the eluate, subsequent eluates are withheld from patient use until the organism is identified, the source of the contamination is found, and subsequent eluates are sterile for 10

1027225

days. To date we have no evidence of actual contamination of the generator by microorganisms and each positive culture has resulted from faulty handling of the culture media or eluate.

(2) A 10% aliquot of each dose is held for pyrogen testing in event of a febrile reaction. Although this is less desirable than testing beforehand, if a fever occurs after a dose, it helps to identify a pyrogen as the cause of the fever. Once the presence of a pyrogen has been demonstrated, techniques and materials are reexamined to find the sources of the pyrogen and take proper steps to eliminate them. Subsequent doses are withheld until shown to be free of the pyrogen.

(3) Only sterile and pyrogen-free reagents (wherever possible commercial pharmaceuticals for parenteral use) are used to prepare the radiopharmaceutical. Likewise, all tubing, containers, and syringes are of either sterile, pyrogen-free disposable plastic or glass, or metal that can be washed, autoclaved, and stored in sterile dry wrappings.

(4) The generator is stored and all elutions are made within a sterile glove box. Although the generator is equipped with a cap to prevent drying out and should prevent air-borne contaminants while in place, each of the frequent entries offers an opportunity for air-borne or accidental contamination. Any contamination of the generator poses a threat of pyrogenicity of the eluate and requires a long and expensive procedure of decontamination and testing before the generator can be used again for radiopharmaceutical production.

(5) The sterility of the final preparation is assured by 0.22μ filtration.

Although this entire procedure has not been implemented at ORAU for a sufficiently long time to establish its efficacy, less rigorous procedures have been inadequate.

Binding of Gallium by Blood Serum

R. E. Hartman and R. L. Hayes*

Previous animal work with gallium in the citrate form has shown that ^{68}Ga may be used as a skeletal scanning agent if sufficient stable gallium is administered with the radionuclide.[1] It has been shown in the rat, rabbit, and dog that when small amounts of gallium are administered, the distribution tends to be diffuse and consequently a poor one for scanning

*Summer Research Participant, St. Bonaventure University, St. Bonaventure, N.Y.

1027226

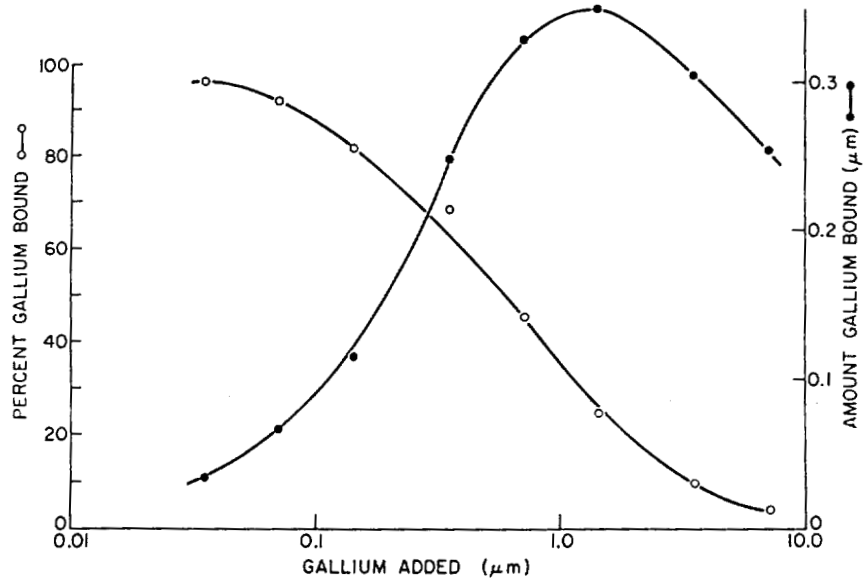

Fig. 39. Equilibrium dialysis study of the effect of gallium (citrate form) concentration on the binding of gallium by rabbit blood serum. Equal volume of gallium citrate normal saline and sera dialyzed against each other. Molar ratio of citrate to gallium was 3:1.

purposes. Ultrafiltration, gel filtration, equilibrium dialysis, and electrophoresis have been used to test the hypothesis that the lack of specific localization in bone at low levels of gallium is due to the binding of gallium by blood serum proteins, making it relatively unavailable for concentration in bone. *Figure 39* shows the results of an equilibrium dialysis study of the binding of gallium (citrate form) by rabbit blood sera with ^{72}Ga as a tracer. As the gallium concentration was increased, the percentage of gallium bound decreased. The absolute binding of gallium reached a saturation level and then showed a decrease. This decrease was probably due to the excess citrate associated with the larger amounts of gallium. *Figure 40* shows histograms of ^{72}Ga counting rates obtained when electrophoresis was carried out on mixtures of gallium citrate plus rabbit serum and gallium citrate plus saline. These are superimposed on the serum protein electrophoretic pattern obtained at the same time. *Figure 40* indicates that the major portion of the serum binding occured with the alpha and beta globulin fractions.

Individual blood serum fractions have been investigated for their gallium-binding activity. The results are shown in *Table 19*. Albumin and gamma globulin had no capacity for binding but the various alpha and beta

1027227

TABLE 19

Gallium Binding by Rabbit Serum Fractions

Serum Fraction	Concentration*	Ga Added	Ga Bound
	%(W/V)	($\mu M \times 10^{-2}$)	($\mu M \times 10^{-2}$)
Albumin	5.0	1.3	0.0
Gamma Globulin	2.0	1.3	0.0
III, β Globulin	2.0	1.3	0.2
IV-1, α Globulin	2.0	1.3	1.2
IV-4, α and β Globulin	2.0	6.6	5.1
Transferrin	0.3	1.3	1.0

*10 ml portions used.

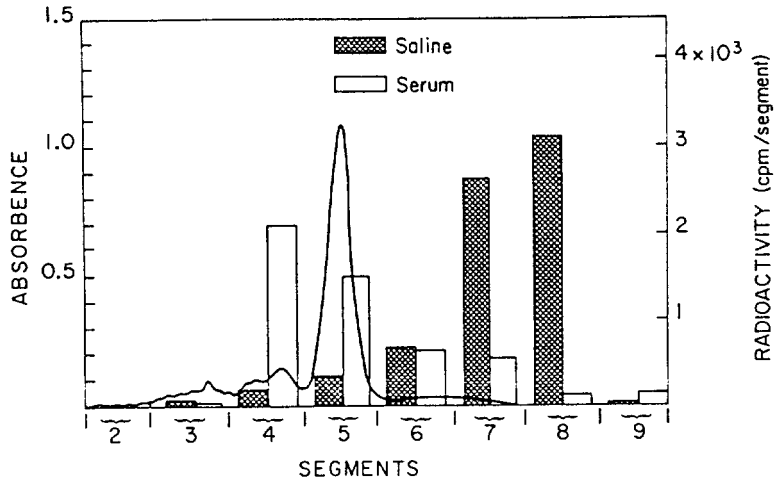

Fig. 40. Electrophoresis of gallium citrate–rabbit serum and gallium citrate–saline with ^{72}Ga as a tracer.

globulin fractions showed distinct activity. Transferrin was particularly avid in binding. Other studies have shown that iron competes with gallium for binding sites on transferrin.

REFERENCE

1. Hayes, R. L. Isotopes of gallium. *In:* Radioactive Pharmaceuticals. AEC Symposium Series No. 6, CONF-651111, 1966, pp. 603–618.

1027228

Animal Toxicity Studies of a Ferric Oxide Colloid Suitable for Marrow Scanning

B. Nelson, R. L. Hayes, and C. L. Edwards

Hayes, et al., have shown colloidal hydrous ferric oxide labeled with ^{68}Ga to be a good agent for scanning the marrow of rabbits.[1] Much of the colloid localizes in the liver and spleen after intravenous injection, but marrow deposition can be enhanced by controlling the particle size and number of the particles and the nature and quantity of the lyophilic stabilizer. This report concerns studies in rabbits and dogs of the metabolism of colloidal hydrous ferric oxide relevant to its possible toxicity.

Doses of up to 10 mg/kg (10 times the dose proposed for human use)

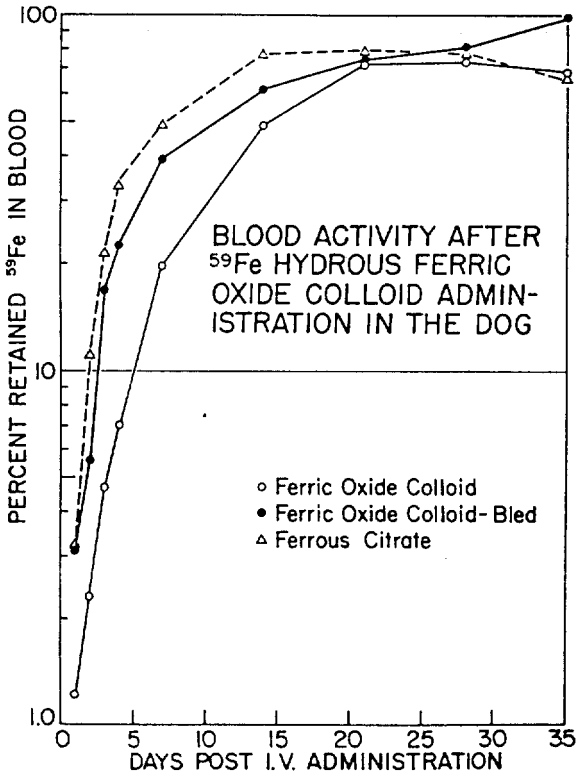

Fig. 41. Half the iron given a healthy dog intravenously as a colloid was incorporated in red cells in about 15 days. A dog made iron deficient by repeated phlebotomy had even more rapid incorporation of the same dose (1 mg/kg), approaching the utilization of a tracer dose of ferrous citrate.

1027229

were injected intravenously into rabbits and dogs without deleterious effects. Animals were killed at appropriate intervals and histologic studies demonstrated aggregates of iron-containing (Prussian blue positive) material in the histiocytes of the marrow, liver and spleen within 2 hr after injection. No reaction to the aggregates was noted and no significant histologic abnormalities were detected in the lungs, adrenals, or kidneys.

The intracellular iron-positive aggregates were resorbed and no excess of stainable iron remained in tissues 35 days after an intravenous dose of 1 mg/kg. This resorption was also demonstrated by giving colloid prepared from radioiron. As shown in *Fig. 41*, the tracer entered the iron pool after a brief delay and was incorporated into the erythrocytes. Incorporation of the iron into red cells was also increased in the rabbit made iron deficient by bleeding.

These results suggest that toxicity of colloidal ferric oxide will not be a problem in scanning human marrow. Thus the toxicity of the whole preparation should be negligible, since only pharmacologically insignificant amounts of radionuclide (e.g., carrier-free ^{68}Ga) will be bound to the colloid for clinical use.

REFERENCE

1. Hayes, R. L., Carlton, J. E., and Rafter, J. J. Scanning with hydrous ferric oxide colloid labeled with gallium-68, J Nucl Med 7, 335–336, 1966.

1027230

Therapy with Radiation

This is a long range and continuing program which has as its objective the improved treatment of disease by means of radiation, both internal and external. Main areas of effort are (1) the best use of total-body irradiation in the treatment of lymphoma, leukemia and polycythemia; (2) local external irradiation therapy for certain types of cancer, including application of experimental methods based on animal studies; (3) assessment of total-body irradiation as compared with splenic irradiation for chronic granulocytic leukemia; and (4) continued investigations of the best use of internal radioisotopes for malignant disease, especially radioiodine for thyroid cancer.

Total-body Irradiation

F. V. Comas, C. L. Edwards, G. A. Andrews, Helen Vodopick, and R. M. Kniseley

The study of total-body irradiation has continued and *Table 20* indicates the numbers of patients treated this year in the various diagnostic categories, and a summary of the experience of previous years.

No large doses were given this year. Several children with acute leukemia are being carried on combined drug therapy. We plan to offer

TABLE 20

Total-body Irradiation Treatments Given at the Medical Division

	50 R	100 R	200 R	300–900 R	Total
Through 1965:	29	56	3	25	113
Calendar Yr 1966:					
Acute Leukemia					
Chronic lymphocytic leukemia		3			
Chronic granulocytic leukemia		2			
Lymphosarcoma		2			
Multiple myeloma					
Polycythemia vera		1			
Thrombocytosis		1			
Lymphoma	1				
Total					10
					123

1027231

high dose (300 R) total-body irradiation to these patients when it becomes apparent that no further remissions can be expected from drug therapy.

It has been possible to treat two patients with chronic granulocytic leukemia with 100 R to compare the results with those in a small series treated earlier with 50 R.

Specific research results of the total-body irradiation program are covered to a considerable extent in other portions of this publication.

Spleen and Liver Irradiation in Chronic Granulocytic Leukemia

F. V. Comas, C. L. Edwards, Helen Vodopick, and G. A. Andrews

Irradiation of the spleen in patients with chronic granulocytic leukemia results in a lowering of the peripheral white cell count. The purpose of this study is to quantitate this effect and to clarify its mechanism.

The study protocol consists of irradiating the spleen and liver alternatively to compare the effects of spleen irradiation with that of irradiating an organ other than the spleen. The radiation dose is adjusted so that the product of the midplane dose (in rads) by the volume irradiated (in cm^3) equals 4×10^6. This dose is divided in 10 equal fractions to be given in a period of three weeks. The blood count is followed at close intervals for at least 75 days and bone marrow is aspirated before and several times after irradiation.

(1) Constancy of response after spleen irradiation is striking.
   (a) The white cell count begins to fall immediately after the first radiation dose, and continues dropping in an exponential manner, with a half-time of nine days, for the next six weeks, after which it begins to rise again.
   (b) Regardless of the pretreatment count, the lowest white cell count attained is between 3 and 7% of the initial value, *Table 21*.
   (c) The platelet count decreases much less, to a mean value of 36% of the initial count, and its fall is neither immediate nor exponential.
   (d) The myeloerythroid ratio in the bone marrow always decreases.
   (e) The spleen volume shrinks to about 17% of its pretreatment volume.

1027232

TABLE 21

White Cell Count Relative to Preirradiation Values 3 Weeks After Spleen and Liver Irradiation with 4×10^4 ergs (nominal)

	No. of Patients	Mean	95% Conf. Lim.
Spleen	8	5.0%	2.6 – 7.4
Liver	6	38.1%	8.1 – 68.1
		$P < 0.01$	

Range of spleen control counts: 72,000 – 243,000
Range of liver control counts: 67,000 – 224,000

(2) The response to liver irradiation is variable, but in general the white cell count and bone-marrow changes are much less pronounced than after spleen irradiation.

These results indicate that the response to spleen irradiation in patients with chronic granulocytic leukemia is highly predictable if the radiation factors are kept constant (dose, time, and volume). The patient's general condition and severity of the disease do not seem to influence the response, provided the changes observed in the white cell count are normalized to the pretreatment value. The results do not provide enough information yet to explain the mechanism of effect.

1027233

Radioisotopes in Diagnosis

The objective is to apply radioisotopic test compounds in (1) the detection of tumors, (2) the measurement of functional disorders, and (3) the diagnosis of metabolic defects. The agents are radioactive compounds, either already available or newly synthesized and tested in animals; the subjects are patients in the Medical Division's research hospital; and the procedures involved emphasize whole-body counting and scanning. Special techniques for radioassay and autoradiography on biopsy and autopsy material are applied to these problems.

Nonhomogeneity of Marrow in Acute Leukemia

C. L. Edwards, Helen Vodopick, and R. M. Kniseley

Acute leukemia, we are accustomed to think, is a diffuse and homogeneous involvement of the entire cellular marrow. Ordinarily, in any one patient, samples aspirated from different sites show little variation in the type of the cells present. Aided by bone-marrow scanning we have encountered a situation that varies from this pattern and is of extreme interest to students of acute leukemia.

The patient, a 49-year-old man, after an acute recurring febrile illness in March and April 1965, treated with antibiotics, was found to have acute aleukemic leukemia. Blood values showed a moderate pancytopenia, but abnormal leukocytes in the blood were not sufficient to make the diagnosis obvious. He was treated with 6-mercaptopurine and several transfusions. Gradually his blood values and general condition improved. In October he had a hemoglobin of 14.3 grams with platelets 185,000/mm^3 and leukocytes of 3650/mm^3. In spite of the clinical and hematological improvement, the bone-marrow aspirates from the posterior iliac spines and sternum showed acute leukemic cells almost exclusively. On October 20, 1965 *(Fig. 42)*, a bone-marrow scan with the use of technetium-99m sulfur sol colloid showed decreased uptake of the tracer compound in the usual marrow sites and an unusual concentration in the region of the knees. Aspiration from the proximal right tibia (November 5, 1965, see *Fig. 43A*) disclosed a marrow of increased cellularity with a pronounced erythroid hyperplasia. Megakaryocytes and granulopoietic cells were present though moderately decreased.

1027234

Scattered leukemic cells were seen among the normal elements, but the picture was in striking contrast to aspirates taken from the sternum and iliac spines *(Fig. 43B)*. Repeat aspiration one month later (December 4,

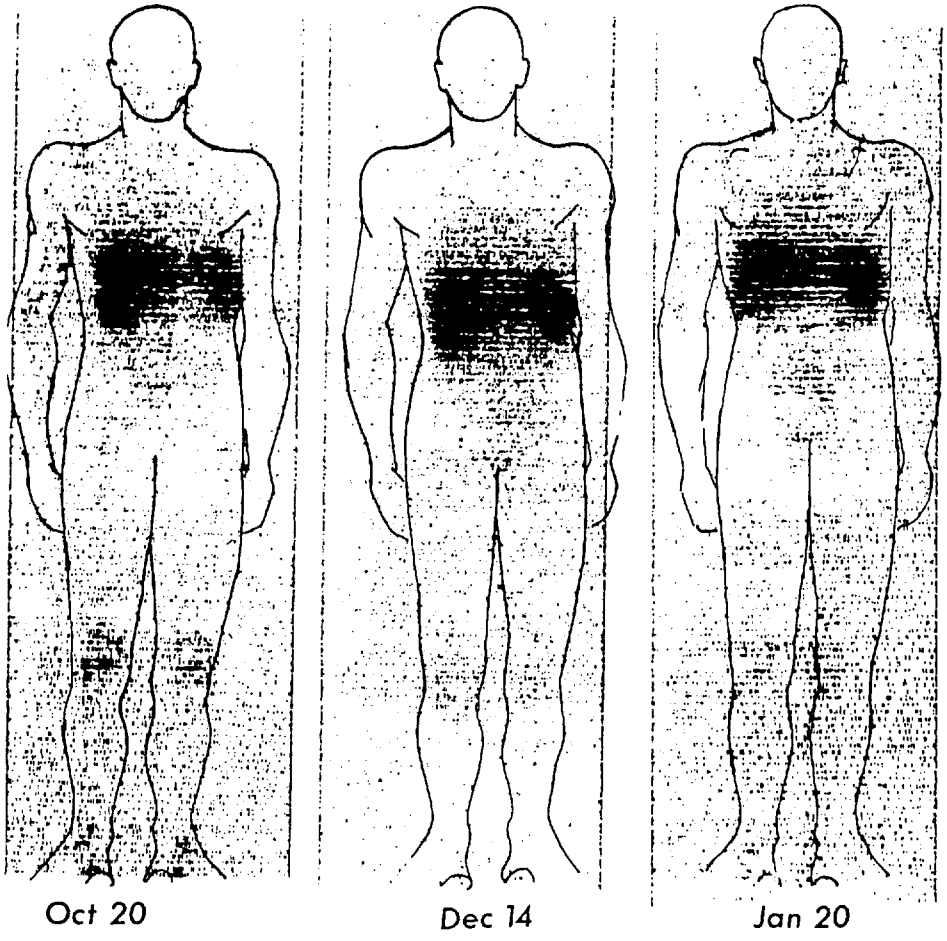

Fig. 42. Sequential whole-body bone-marrow scans in a 49-year-old man with acute leukemia.

1027235

1965) from the proximal end of the right tibia showed the diffuse leukemic pattern that had been encountered in aspirates from other sites and this correlated with deterioration of the patient's hematologic and clinical status. In spite of continued supportive and chemotherapeutic efforts, his condition continued to decline. Death occurred on February 22, 1966.

Until recent years, scanning the marrow organ had not been customary or feasible, and observers have been unable to adequately understand those patients who have evidence in the blood of a good deal of normal hematopoiesis when the marrow appears completely filled with blast cells. (This is not limited to patients responding to therapy.) In this patient, the marrow scan provided a direct explanation for the clinical hematologic response and pointed to the site of compensatory normal hemopoietic activity in the region of the knees. Furthermore, correlation was good between the subsequent marrow scan and the later

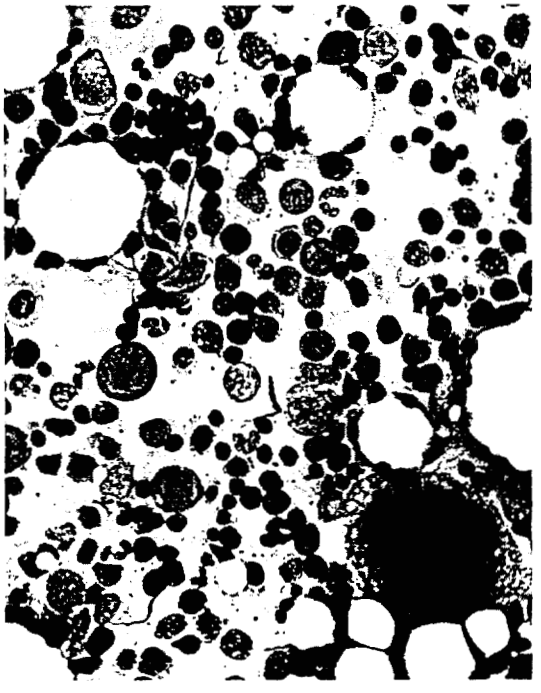

Fig. 43A. Marrow aspirate in November, 1965, from proximal tibia showing erythroid hyperplasia. Note the presence of megakaryocyte and granulocytic precursors.

1027236

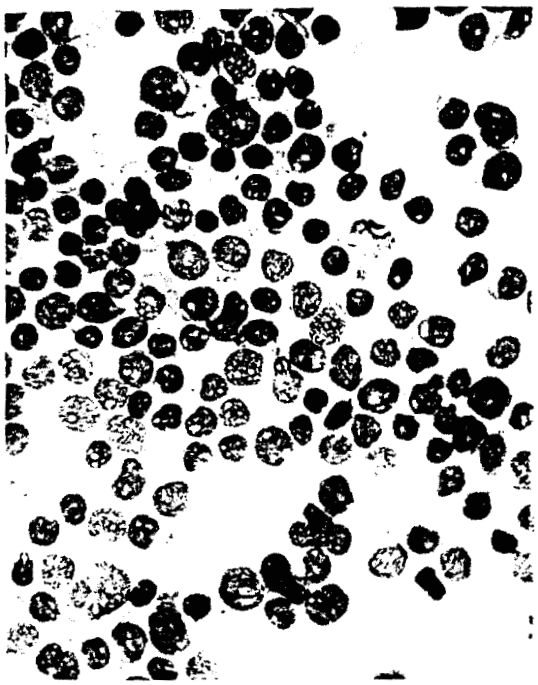

Fig. 43B. Aspirate on October 29, 1965, from sternum showing the diffuse proliferation of blast cells, and absence of normal hemopoietic activity.

tibial marrow aspirate. As the patient relapsed the scan showed less activity around the knees, and the marrow contained a much larger proportion of blast cells.

This study demonstrates the usefulness of the bone-marrow scanning technique in broadening our understanding of a hematologic process. It also suggests that in the pathogenesis of acute leukemia, fatty marrow is capable of responding with the production of normal sustaining hemopoietic elements in the face of persisting diffuse leukemic infiltrations of the marrow in the trunk regions. These observations raise an interesting speculation that perhaps some patients with acute leukemia under optimal management, even though incurable, may be amenable to more prolonged palliation if a greater and more persisting colonization of fatty marrow with normal elements can be achieved or if therapy can be directed selectively to the more abnormal areas of marrow.

1027237

Bone-marrow Scanning with Radioactive Colloids

R. M. Kniseley, C. L. Edwards, G. A. Andrews, R. Tanida, and R. L. Hayes

Bone-marrow scanning, as a nondestructive technique of delineating the hemopoietic marrow organ in patients, yields information helpful to the clinician and investigator.[1] Two fundamentally different radiopharmaceutical approaches to bone-marrow scanning are possible: (1) radioactive isotopes of iron and (2) colloids labeled with radioisotopes. The former is based on the fact that with active hematopoiesis, most of a tracer dose of iron injected intravenously is transported to the bone marrow and incorporated in erythrocytes unless there is an iron excess. On the other hand, colloids are removed from the blood by the reticuloendothelial cells of the liver, spleen, and bone marrow. There is ample evidence that in normal animals and in many clinical conditions the distribution of radiocolloids in the bone marrow closely correlates with the distribution of erythropoiesis as detected by the distribution of radioiron or "red marrow."

Of the two approaches to bone-marrow scanning, that of using radioiron has the more appeal because of greater interest in the distribution of the erythropoietic marrow. Iron-52, however, is the only isotope of iron that can be given in quantities sufficient for area scanning, but owing to its short half-life and difficulties in its production, it is limited to only a few institutions. For general use, radiocolloids are more promising.

There are, therefore, two basic problems toward which our attention has been focused in 1966: (1) correlation of bone-marrow distribution of radiocolloids and radioiron in various abnormal situations and (2) improved radiocolloids for scanning of bone marrow.

Iron-59 is a readily available isotope, but owing to its long effective half-life and radiation, it may be given in doses of only 0.05 millicuries or less, activity too small for practical rectilinear scanning with present equipment. Profile scans, however, can be made with the Division's linear scanner. Comparing a ^{59}Fe scan with the radiocolloid scan permits us to correlate the distribution of "erythropoietic marrow" and the "phagocytic marrow."

An example of a patient in whom there was a discrepancy is a woman, age 19, with an aplastic anemia following chloramphenicol therapy. In *Fig. 44*, the whole-body scan after the intravenous injection of technetium-99m sulfur-sol colloid shows (as did the profile scan) the usual distribution of the colloid in the liver, spleen and the bone marrow of the trunk. The profile scan with ^{59}Fe exhibits localization in the liver but little in the normal sites of hemopoiesis. The group at Donner Laboratory using ^{52}Fe and technetium colloid have even more graphi-

1027238

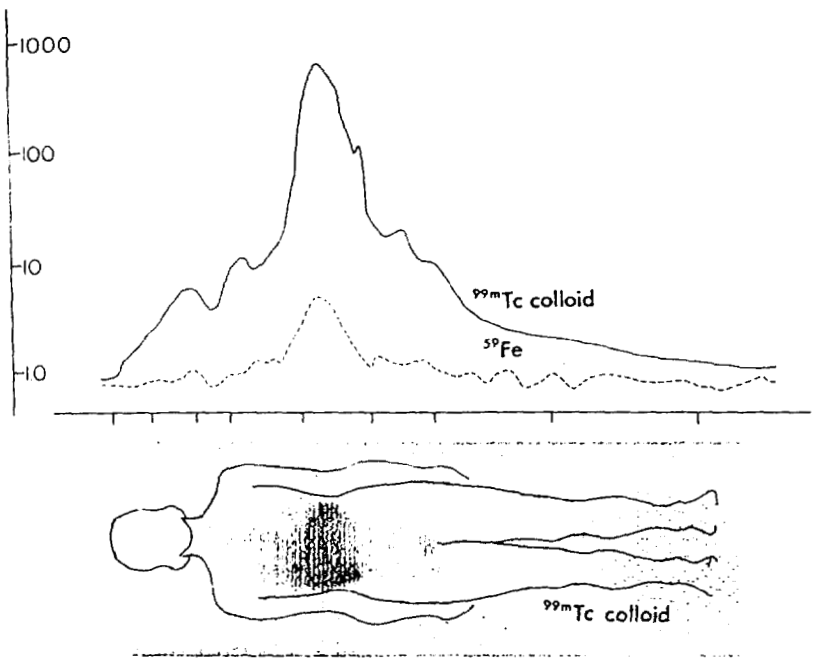

Fig. 44. Whole-body scan and linear scans of a 19-year-old woman with aplastic anemia subsequent to therapy with chloramphenicol. The distribution of colloid follows the usual pattern in the trunk region. The ^{59}Fe fails to localize in the usual regions of hemopoiesis.

cally demonstrated differences in marrow patterns in certain disorders.[2]

During the past year, 48 scan studies were performed on patients with various hematologic disorders. Although we have encountered some unexpected abnormalities and variations in the distribution of the marrow, we have been generally disappointed in the quality of the technetium-99m scans with the use of present equipment. Most of these scans were made with a sulfur colloid of ^{99m}Tc to take advantage of its radiation characteristics that allow a larger millicurie dose with less irradiation compared to ^{198}Au. Our scans with ^{99m}Tc sulfur colloid have been inferior to those made with the ^{198}Au colloid. The suspected reasons are the physical characteristics of the colloid giving a higher blood level (less completely removed), nonuniformity of the colloidal preparations and the attenuation of the 140 keV gamma at varying depths of bone, with considerable scatter being detected without discrimination from the photopeak.

1027239

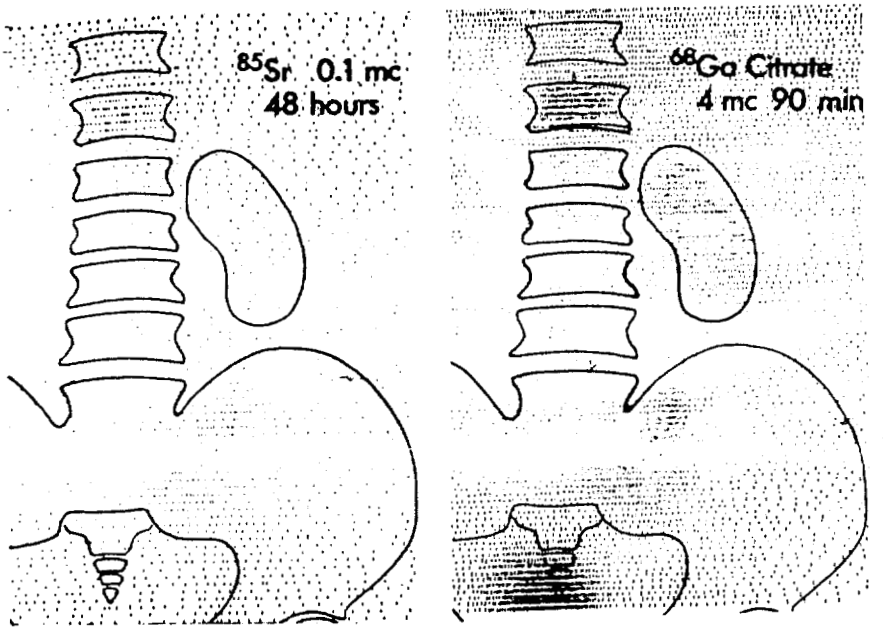

Fig. 47. Comparative scans made with ^{68}Ga citrate and ^{85}Sr of a patient with metastatic prostatic carcinoma indicating lesions in the first lumbar vertebra and the left sacroiliac region.

The uncertainty of chemical toxicity of the carrier gallium mitigates recommendation of broad usage of this preparation as yet. An LD_{10} of 20 mg/kg body weight was suggested by Brucer, et al., in 1953.[3] Chemical toxicity was thought to be responsible for the bone-marrow depression and dermatitis seen in patients who had received gallium-72 as treatment of osteogenic sarcoma. They also observed lethal nephritis in dogs given much smaller doses of gallium than those given to any other species.

We have seen no evidence of nephritis or dermatitis in patients at the 2 to 4 mg/kg level. Eight patients have been found to have an unexplained, temporary depression of white blood cell values (to below 5000 mm^3 or to 50% of preinfusion value) within the first 60 days after the infusion. All had significant malignant disorders and six had ma-

1027240

lignant diseases of the lymphatic or hematopoietic systems. Observations on more patients without bone-marrow involvement will have to be completed before a definite conclusion can be drawn regarding the effect, if any, of the stable gallium carrier upon the bone marrow.

REFERENCES

1. Hayes, R. L., Carlton, J. E., and Byrd, B. L. Bone scanning with gallium-68: A carrier effect. J Nucl Med 6, 605–610, 1965.
2. Edwards, C. L., Hayes, R. L., Ahumada, J., and Kniseley, R. M. Gallium-68 citrate: A clincially useful skeletal scanning agent. J Nucl Med 7, 363–364, 1966, Abstr. L-1.
3. Brucer, M., Andrews, G. A., and Bruner, H. D., and others. A study of gallium^{72}. Radiology 61, 534–613, 1953.

1027241

Theoretical and Experimental Studies on Retention and Distribution of Radionuclides

The objective is to determine quantitatively the patterns of absorption, distribution and excretion for tracer metals, radionuclides of medical interest, and environmental and occupational contaminants. Much of the work is on human beings, either normal persons or patients. Whole-body counting, combined with chemical and radioassay data, is a major research tool.

Emphasis is given to theoretical approaches and mathematical models that can be used to clarify the interpretation of experimental data.

Turnover Compartmentalization

P.-E. E. Bergner

A method for determination of the total-body pool size from tracer data has previously been reported.[1,2] Compared to the classic dilution technique, the method has the advantage of being precise from a physico-mathematical viewpoint, but it suffers from several disadvantages.

According to the theory, the whole-body mass of a substance is obtained from corresponding tracer data according to the equation:

$$\text{(Whole body mass)} = \frac{\text{(Total area under the whole-body retention curve)}}{\text{(Total area under the specific-activity curve)}}$$

where the specific activity refers to a time invariant, but otherwise arbitrary, subsystem or compartment. Consequently, the theory states that one has to observe the complete tracer process, from the start of experiment to the time when no significant amount of tracer remains in the organism. However:

(i) Tracer data do not reflect the whole metabolic pool but rather a smaller part having a sufficiently rapid turnover to be effectual during the time of experimental observations. The right hand side of the equation is therefore not likely to give the whole-body mass, but a smaller quantity—the "exchangeable mass." This quantity still lacks a physical definition of its own and, consequently, the physical significance of the equation becomes obscure in many practical applications.

(ii) In most tracer studies, the curves cannot be followed long enough to give reasonable estimates of the two integrals.

1027242

(iii) Different functions can give the same area (integral) and consequently, the equation "pays no attention" to the shapes of curves. In other words, tracer data contain more information than is revealed by the equation.

The most common method used to solve such difficulties is linear first order compartment analysis (LFCA). The organism is considered as consisting of a number of so-called compartments, each of which is homogeneous (well-stirred). Several objections may be raised against this approach and, recently, Marshall[3] has outlined a different one for calcium metabolism. Instead of considering the metabolic pool as subdivided into compartments in morphological and chemical terms, Marshall suggests considering compartmentalization in terms of "turnover times," or "mean-transit times" in the language used by Zierler.[4] Marshall works with a specific problem and the method does not seem to be valid for general use. In the following, I outline a modification of Marshall's approach that seems to possess the desired generality. The emerging theory has a solid physical significance, based on previous works[5-7] and the resulting representation is applicable to a broad class of systems, no matter whether or not they are homogeneous (well-stirred).

Assume that the start of experiment (i.e., the supply of tracer) takes place at the time $t = 0$, and that the whole-body retention curve is observed until the time $t = T$. Consider a subdivision of this time period: $0 < t_1 < t_2 < \ldots < t_{n-1} < t_n = T$. Then, one can meaningfully ask for the size and kinetics (turnover rate) of that part of the whole-body pool, the particles of which leave the system somewhere during the time t_{i-1} to t_i ($i = 1, 2, \ldots, n$; $t_0 = 0$). It can be shown[8] that such relative sizes and turnovers can be obtained from whole-body data alone. If, in addition, the specific activity curve is also obtained in some arbitrary but time-invariant part of the system, these relative values are then transformed into absolute numbers.

One ends up with a representation of whole-body retention data, according to the principles illustrated by the following diagram:

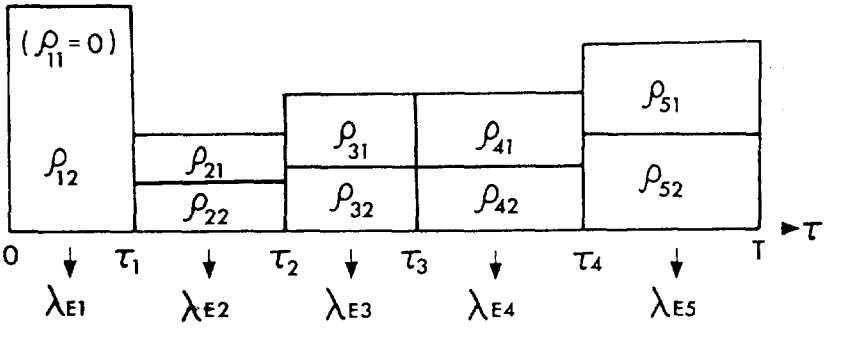

1027243

where the area of each rectangle is equal to the relative size of the compartment, and the length of each arrow equals the relative turnover, $\rho_{ij} \cdot \lambda_{Ei}$. Each compartment is divided into two subcompartments, so that, for instance, ρ_{21} is the relative size of that part of the whole-body pool made up of the particles that have stayed in the system a time less or equal to t_1, but will leave the system between t_1 and t_2; ρ_{22} then stands for the relative size of that part of the pool made up of the particles that have stayed a time greater than t_1, and will leave the system before t_2; λ_{Ei} stands for the turnover factor of compartment ρ_{i2}, i.e., the mean exit probability with respect to steady state distribution of mother substance in ρ_{i2}.

The partition of the total time interval (0,T) is a matter of each investigator's personal choice and is governed partly by the quality of data (i.e., what "resolution" they allow). This approach at last makes possible a description of metabolic whole-body pools that can be made as detailed as is motivated by data and goal of experiment. The objections (i)–(iii) appear to be positively met and the concept "exchangeable mass" is given a precise definition, requiring only that a time interval be specified. For instance, exchangeable mass may mean $\rho_{31} + \rho_{32}$ or, if the total time interval (0,T) is considered $\rho_{12} + \rho_{21} + \ldots + \rho_{51} + \rho_{52}$.

In this representation the difference between the homogeneous (well-stirred) and the nonhomogeneous system becomes quantitative rather than qualitative. Thus, when the system is homogeneous, in the sense that the complete retention curve is described by a single exponential t-function, all λ_{Ei} become equal, and the corresponding compartment sizes decrease exponentially.

REFERENCES

1. Bergner, P.-E. E. Exchangeable mass: Determination without assumption of isotopic equilibrium. Science 150, 1048–1050, 1965.
2. Bergner, P.-E. E. Exchangeable mass: Determination without assumption of isotopic equilibrium. USAEC Report, ORINS-53, pp. 103–104.
3. Marshall, J. H. Calcium pools and the power function. *In:* Compartments, pools and Spaces in Medical Physiology (Eds. C. C. Lushbaugh, P.-E. E. Bergner). AEC Symposium Series CONF-661010, in press.
4. Zierler, K. L. Effect of circulatory beds on tracer experiments on noncompartmental analysis. Ann NY Acad Sci 108, 106–116, 1963.
5. Bergner, P.-E. E. Tracer dynamics and the determination of pool-sizes and turnover factors. J Theor Biol 6, 137–158, 1964.
6. Bergner, P.-E. E. Ergodic properties of the tracer system. Report presented at the Biometric Society meeting in Tallahassee, Fla., 1964.
7. Bergner, P.-E. E. On the ergodic properties of the tracer system. *In:* USAEC Report ORINS-53, 1965, pp. 102–103.
8. Detailed report in preparation.

1027244

Analog Computer Analysis of Human ^{51}Cr RBC Survival and Whole-body Retention Data

C. C. Lushbaugh, W. D. Gibbs, W. Franz, and P.-E. E. Bergner*

As previously reported,[1] simultaneous measurements of whole-blood and whole-body radioactivity, after intravenous injection of ^{51}Cr-labeled red blood cells (RBC), offer an opportunity for a rather detailed description of mechanisms for destruction of RBC. Our working hypothesis has been that in the population of chromium-labeled RBC a certain fraction of cells are "damaged" by the chromium-labeling procedure. The chromium-damaged cells are assumed to have two simultaneous independent removal mechanisms: senescence, as for any undamaged RBC, and a removal mechanism that destroys RBC independently of age.

According to hypothesis, these two destructive processes occur in two *functionally* different parts of the reticuloendothelial (RE) system, denoted by U_1 and U_2, where U_1 takes care of random destruction and U_2, of senescence. About 40% of the function of U_1 appears to be located in the spleen.

One possible realization of these arguments is shown in *Fig. 48* where $S_1 + S_2$ is the population of labeled RBC, S_1 denotes the RBC subpopulation damaged by chromium, and S_2 that undamaged. The flux into U_2 is induced by the senescence process, and implies a linear survival curve as observed by ohe Ashby technique. The flux into U_1 is induced by damage from chromium ν and by some inherent random mechanism due to disease (λ') and is assumed to follow first order kinetics with the rate-constant $\lambda' + \nu$. The parameter λ'' is the rate constant of random loss of RBC due to bleeding, or "elution" of chromium if this occurs. The rate constants κ_1, κ_2 are clearance of label from U_1 and U_2 respectively: the sum of these two fluxes is the total-body physiologic excretion of chromium label from the globin molecule.

The most serious assumption made in constructing this model is the linearity in the fluxes into U_1, and from U_1 and U_2 to the environment. However, because these fluxes are irreversible, one can expect a positive correlation between the parameters of the model and the corresponding physiologic functions, even if the actual kinetics is nonlinear. The existence of a valid correspondence with the true physiologic system can be verified only by experiments, and this constitutes the main objective

* Department of Chemical Engineering, University of Tennessee, Knoxville, Tenn.

1027245

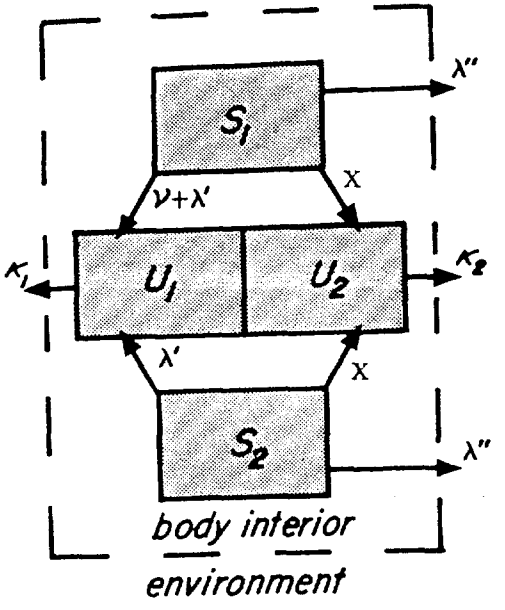

Fig. 48. Diagram of the model of ^{51}Cr-RBC survival in normal or diseased men. The parameters and symbols are defined in the text.

of the analysis of clinical data of ^{51}Cr-RBC survival studies described in the following:

With the use of the methods developed previously,[2] the model in *Fig. 48* gives rise to the following set of differential equations:

$$\dot{s}_1 = -(\nu+\lambda)s_1 - \lambda s_1^0 e^{-\nu t}/\{e^{\lambda x} - 1\} \quad (1)$$

$$\dot{s}_2 = -\lambda s_2 - \lambda s_2^0/\{\ \} \quad (2)$$

$$\dot{u}_1 = (\nu+\lambda')s_1 + \lambda' s_2 - \kappa_1 u_1 \quad (3)$$

$$\dot{u}_2 = \lambda s_2^0 + \lambda s_1^0 e^{-\nu t}/\{\ \} - \kappa_2 u_2 \quad (4)$$

$\lambda \equiv \lambda' + \lambda''$

where s_i and u_i stand for the corresponding amounts of label in s_i and u_i ($i = 1, 2$); s_i^0 and u_i^0 denote the corresponding initial amounts (at the time $t = 0$). The experimentally observed curves are b(t), the whole-blood activity $s_1 + s_2$ and w(t), the whole-body activity $s_1 + s_2 + u_1 + u_2$, as shown in *Fig. 49*. Eight parameters must be estimated on the basis of such data, and one would expect difficulties concerning the uniqueness of the estimates. However, with an analog computer, and trial and error adjustments of the potentiometers until good fits are obtained, we have obtained, with only one or two exceptions, remarkably stable estimates.

1027246

The solid curves in *Fig. 49*, generated by the analog computer, are shown fitted to corresponding experimental data in a typical study where the RBC were labeled with ^{51}Cr early and late in the course of acute leukemia.

Twenty-four ^{51}Cr-RBC retention studies in patients were analyzed by this technique. As shown in *Table 22*, five of the 24 were normal volunteers without disease but two of these were normally menstruating women (group 1); four were men with jaundice from viral or degenerative hepatic diseases (group 2); two were patients with acute leukemia with cortisone-produced clinical but not hematologic remission (group 3); six studies were in four patients with acute leukemia with moderate to severe symptoms of their disease (group 4); four patients had acquired hemolytic anemia without leukemia (group 5); two patients had polycythemia rubra vera (group 6); and one patient (group 7) had anemia associated with giant follicular lymphosarcoma. The dose of ^{51}Cr and the range of RBC mass estimates for the groups are also shown.

TABLE 22

Groups of Patients Studied

Group Number	Diagnostic Description	Number Studies	^{51}Cr Dose (μCi)		RBC Mass ($\times 10^3$ ml)	
			(mean)	(range)	(mean)	(range)
1	Normal	5	289	245–320	2.1	1.8–2.7
2	Jaundice $\bar{s}$ anemia	4	218	161–369	1.7	1.0–2.3
3	Acute leukemia $\bar{s}$ symptoms	2	300	238–360	1.3	1.2–1.5
4	Acute leukemia $\bar{c}$ symptoms	6	270	78–460	1.1	0.9–1.4
5	Hemolytic anemia $\bar{s}$ leukemia	4	205	50–268	1.0	0.9–1.3
6	Polycythemia vera	2	128	94–163	2.4	
7	Anemia and giant follicular lymphoma	1	123		1.5	

The analysis of the results of the analog solution of these ^{51}Cr-RBC retention data is summarized in *Fig. 50, A–C*, to allow visual comparison of the means and ranges of the parameters of the model obtained from the analog computer fits to the data shown in *Fig. 49*. The solid horizontal line in each graph denotes the mean value obtained for the group of five normal people. *Figure 50 A* shows the relative sizes of S_1^0, the chromium damaged fraction of the labeled RBC; X, the RBC age of senescence; $T_{50}(w)$ for the ^{51}Cr label within the whole body and $T_{50}(b)$ for the ^{51}Cr-RBC label in the peripheral blood. *Figure 50B* shows the rate

1027247

constants for the random removal of chromium damaged RBC (ν) and diseased RBC (λ'), and random loss of label from the whole body as from hemorrhage (λ''). In *Fig. 50C*, the rate constants are shown for κ_1 and κ_2 that depict the RE-systems excretion rates from U_1 and U_2 respectively.

These results support the hypothesis that parameter ν may be looked upon as a measure of the "efficiency" of the RE system to take care of chromium damaged normal or diseased RBC. As one would expect,

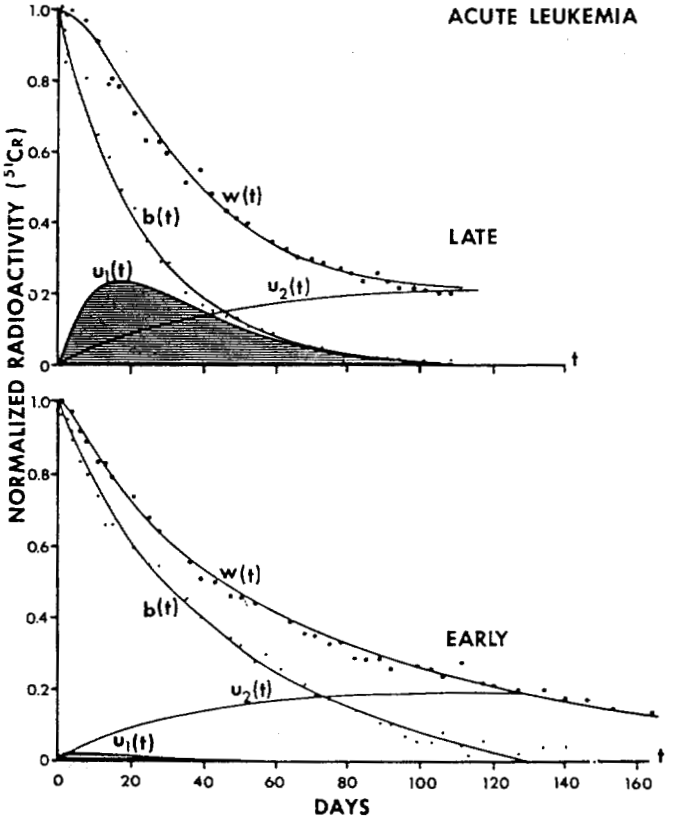

Fig. 49. Curves generated by analog computer to fit blood and whole-body retention data of ^{51}Cr-RBC in a patient with acute myelogenous leukemia early in her disease when cortisone therapy was effective, and six months later when cortisone was ineffective and severe debilitation was present. The turnover of randomly destroyed RBC is described by the shaded areas [u_1 (t)] in each study.

1027248

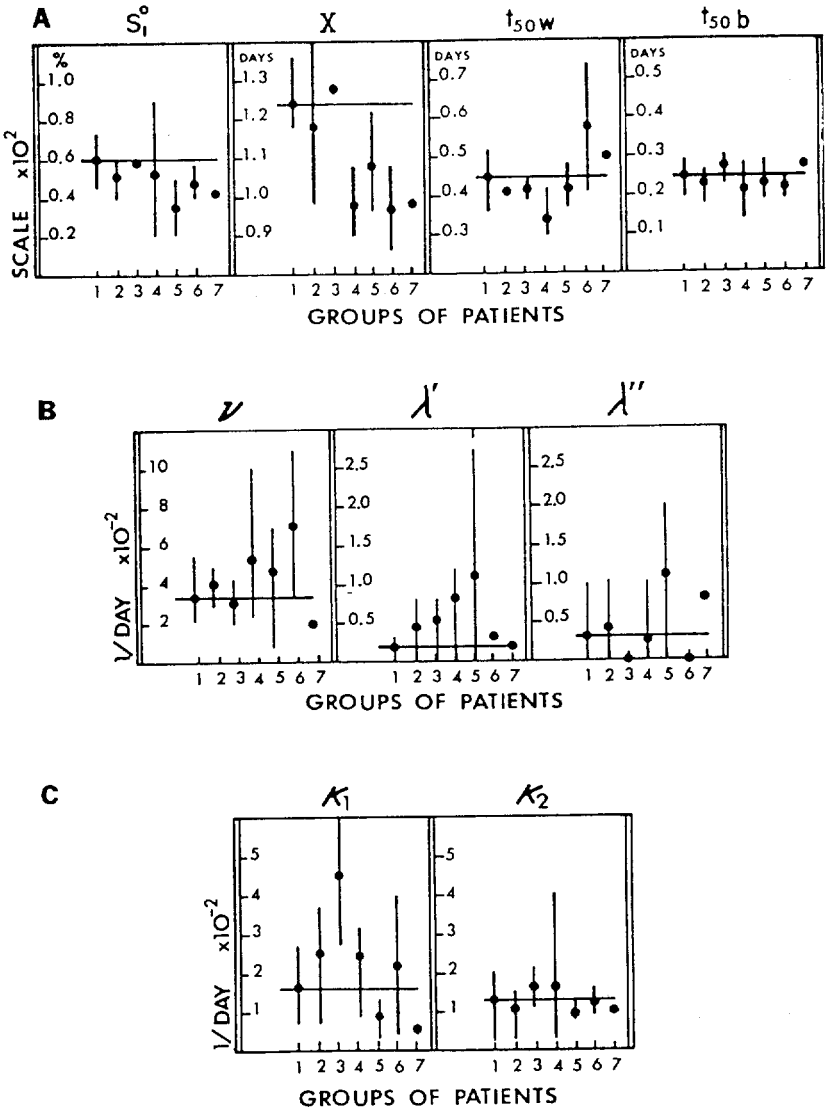

Fig. 50. Comparison of the means and parameters of the model obtained from analog computer fits of the data according to diagnostic groups of patients. The solid horizontal line in each graph denotes the mean value for the group of five normal people; see text for further description.

1027249

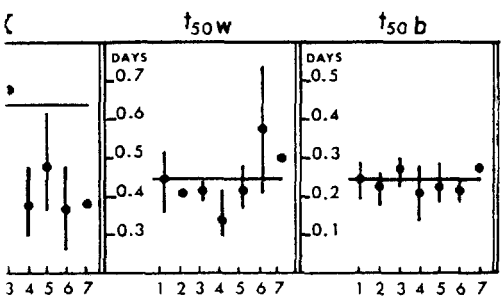

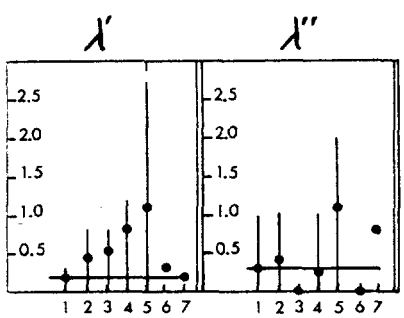

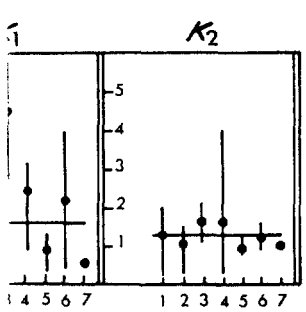

s and parameters of the model obtained from e data according to diagnostic groups of patients. in each graph denotes the mean value for the le; see text for further description.

ν is increased in the hematologic diseases studied here, since the presence of diseased RBC in the blood induces an increased RE-system random-removal activity $\nu + \lambda'$. Similarly, the RE digestive and excretory mechanism, κ_1 is also increased. In agreement with the hypothesis that essentially only U_1 is involved in random removal of damaged RBC, κ_2 is not increased significantly. Since X (RBC age of senescence) exhibits a systematic shortening, there must be a change of RBC metabolism in these diseases.

In contrast to these meaningful variations in the parameters measured by the model, the more familiar T_{50} values (see *Fig. 50A*) commonly used in hematologic diagnosis do not afford comparable information.

REFERENCES

1. Lawson, J. D., Bergner, P.-E. E., Lushbaugh, C. C., Gibbs, W. D., and Lushbaugh, D. H. A mathematical description of the discrepancy between whole-body and peripheral blood retention of ^{51}Cr given as labeled red cells. USAEC Report ORINS-53, 1965, pp. 107–112.
2. Bergner, P.-E. E. On stationary and non-stationary red cells survival curves. J Theor Biol 9, 366–388, 1965.

Effect of Chromium on Rabbit Red Blood Cell Survival

D. F. Opdyke, W. Franz,† W. D. Gibbs, P.-E. E. Bergner, and C. C. Lushbaugh*

There is abundant historical medical documentation that the toxicity of chromium results from protein binding by this highly reactive metal ion. In fact, "chromation" of proteins renders them insoluble, difficult to hydrolyze, necrotizing and autoantigenic.[1] In addition, some RBC enzyme systems are inhibited by substrate binding with minute amounts of chromium.[2] Nevertheless, it is generally accepted that ^{51}Cr labeling of proteins and cells does not denature them but produces such a flimsy bond that a significant portion of the tracer is lost by "elution" instead of by red blood cell (RBC) death. Studies revealing that the contrary is true are either ignored or their results are misinterpreted.

* Summer Research Participant from the New Jersey College of Medicine and Dentistry, Jersey City, N. J.

† Department of Chemical Engineering, University of Tennessee, Knoxville, Tenn.

Whole-body counting studies done simultaneously with blood-retention studies of ^{51}Cr-labeled RBC in normal and diseased men and animals show that, as ^{51}Cr-labeled RBC are removed from the blood randomly, they are retained in the reticuloendothelial system for a long time as the tracer is slowly excreted.[3] A recent study by Owen, et al.,[4] shows further that the iron in the hemoglobin of such cells is freed and returned to the iron pool immediately while the chromated-globulin fragment remains "undigested" in the RE system.

The successful trial in patients of our previously reported description of this peculiar behavior of chromium-labeled RBC suggested that the

TABLE 23

Experimental Rabbit Groups and Amounts of Chromium Carrier Used

Group	Number Rabbits	Chromium Carrier added/ml RBC (μg)
1	4*	*none*
2	4	10
3	2	100
4	4*	500
5	4	1000

*One animal died before completion of the study.

hypothesis might be tested further by purposefully damaging RBC with excess chromium carrier. According to theory[5] it would be possible thereby to force all labeled RBC into the damaged fraction so that $s_1^0 = 1.0$ and $s_2^0 = 0$. Normal animals would appear falsely then to have hemolytic disease. The following investigation, therefore, was done:

The 18 rabbits used in this analytical study were each given 35 ml of ^{51}Cr-labeled blood (hematocrit 35 to 40%) from a donor pool of 670 ml obtained from 9 other rabbits. The recipients were divided into five groups according to the amount of chromium carrier per milliliter of RBC that was added in the labeling procedure *(Table 23)*. The tracer radioactivity was kept constant (35 microcuries per rabbit) in each labeled sample. Blood and whole-body radioactivity were determined as near simultaneously as possible after intravenous administration of the labeled blood at 15 min; 1, 3, and 7 days; and at weekly intervals thereafter for 21 weeks. The blood and whole-body ^{51}Cr-retention data for each rabbit were analyzed with the use of the analog computer line-fitting procedure and theoretical model previously described for human ^{51}Cr-RBC survival.

These attempts showed that the rabbit data gave a very large λ'' value suggesting that a large amount of hemorrhage had occurred. Since no

1027251

healthy rabbit could possibly have such a large value of λ'' and no hemorrhage was observed, we had to assume that this value resulted from the heavy chromium load: the large amount of chromium induces hemolysis, and whenever intravascular hemolysis occurs rapidly, haptoglobin is consequently saturated; renal hemoglobin excretion then results so that the loss of the RBC label to the environment resembles hemorrhage or "elution".[4] Hence, this large λ'', induced by the label, is a characteristic not of mother substance but of tracer (the labeled RBC), as is ν. It therefore becomes necessary to reformulate some portions of the model, and the following equations were derived (the symbols being the same as in the preceding report):

$$\dot{s}_1 = -(\nu + \lambda)s_1 - \lambda' s_1^0 e^{-(\nu + \lambda'')t} / \{e^{\lambda' X} - 1\} \quad (1)$$

$$\dot{s}_2 = -\lambda s_2 - \lambda' s_2^0 e^{-\lambda'' t} / \{\ \} \quad (2)$$

$$\dot{u}_1 = (\nu + \lambda')s_1 + \lambda' s_2 - \kappa_1 u_1 \quad (3)$$

$$\dot{u}_2 = \lambda' e^{-\lambda'' t}(s_1^0 e^{-\nu t} + s_2^0) / \{\ \} - \kappa_2 u_2 \quad (4)$$

$\lambda = \lambda' + \lambda''$

In *Fig. 51*, typical data are presented for blood and whole-body retention of the ^{51}Cr-RBC label from a rabbit given a high specific-activity

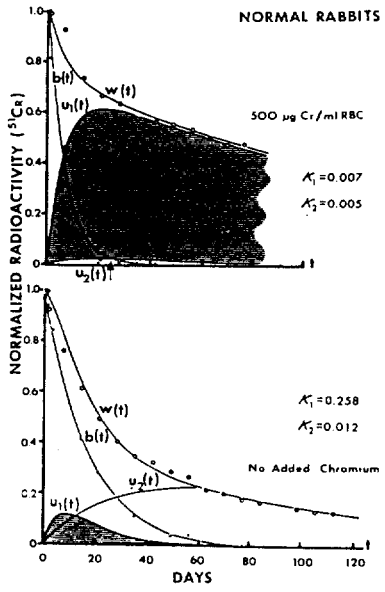

Fig. 51. Whole-body and blood ^{51}Cr-RBC retention curves with and without chromium added, analyzed by analog computer to determine the flux of label through RE system, U_1 and U_2, in rabbits (U_1 shaded).

1027252

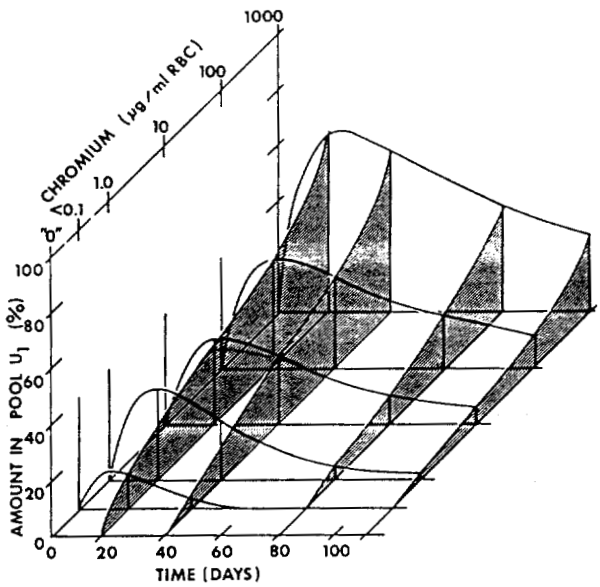

Fig. 52. Shaded planes drawn 20, 40, 80 and 100 days after ^{51}Cr + Cr-RBC labeling to show that the amount of label in RE compartment U_1 is determinable by the amount of chromium used.

label and a low specific-activity label (500 μg of chromium carrier per milliliter of injected RBC). The analog computer solution using the modified model shows that the additional chromium caused such a rapid disappearance of the ^{51}Cr-RBC from the blood into the compartment U_1 of the RE system that nonrandom removal of senescent cells was insignificant (U_2). The retention of ^{51}Cr-labeled RBC and their fragments (globulin?) was increased by the large chromium dose perhaps because of reduced ability of the U_1 RE compartment to excrete these denatured proteins as reflected in a reduced value of κ_1 as shown.

Fig. 52 shows the "toxic" effect (shaded planes) of increasing amounts of chromium per RBC labeled upon the relative amounts of ^{51}Cr label to be found in the RE system, U_1, at 20, 40, 80, and 100 days after injection of the labeled RBC. This increasingly rapid input and prolonged retention explains the large disparity between the blood and whole-body radioactivity shown previously and in *Fig. 51*.

REFERENCES

1. Hueper, W. C. Occupational Tumors and Allied Diseases, Springfield, Ill., Charles C Thomas, 1942, pp. 408–415.

1027253

2. Kontras, G. A., Haltori, M., Schneider, A. S., Ebaugh, F. G., Jr., and Valentine, W. M. Studies on chromated erythrocytes. Effect of sodium chromate of erythrocyte glutathione reductase. J Clin Invest 43, 323–331, 1964.
3. Lushbaugh, C. C., Marvin, H., and Hale, D. B. The life span of the radiochromated erythrocyte. Fed Proc 18, 1935, 1959 (abstr.).
4. Owen, C. A., Jr., Orvis, A. L., and Kiely, J. M. Sequestration of erythrocytes by rat spleen. Amer J Physiol 211, 237–280, 1966.
5. Lushbaugh, C. C., Gibbs, W. D., Franz, W., and Bergner, P.-E. E. Analog computer analysis of human ^{51}Cr RBC survival and whole-body retention data (this report).

The Role of the Spleen in ^{51}Cr-Labeled Red Blood Cell Sequestration and Elimination by the Total Reticuloendothelial System

C. C. Lushbaugh, W. D. Gibbs, C. L. Edwards, H. D. Hodges, and R. F. Queener

Since erythrocyte (RBC) sequestration does not occur at all in normal man,[1] the diagnosis of hypersplenism by demonstration of an abnormal rate of RBC removal would be straightforward if a noninjurious gamma-emitting radioactive RBC label were available. Chromium-51 seemed at first to be the long-sought RBC label because it was inexpensive, had a gamma energy that could be collimated for external counting, and could be assayed with equipment commonly used. At once, however, the chromium label was found to act differently than had been expected: its use produced curvilinear instead of linear regressions of RBC survival, and although a theory of "elution" was coined to explain the apparently random loss of ^{51}Cr-RBC in the absence of disease, it failed to explain the "normal" sequestration of ^{51}Cr-RBC in "normal" persons.

Several studies have now challenged the "elution" theory by showing that the lives of some chromium-labeled RBC in the peripheral blood are shortened as if they were damaged by disease or heat. The altered RBC are removed by the reticuloendothelial system, an unknown portion being sequestered by the spleen. The disparity between simultaneous blood and whole-body counts can be used to define the relative amount of labeled blood in the reticuloendothelial system. In attempting to determine the metabolic fate of the chromated RBC fragments, we have measured by whole-body counter the ^{51}Cr retention in 20 patients undergoing splenic scanning and RBC-survival studies. *Figure 53* shows the arithmetic means of whole-body retention of 10 patients with various hema-

1027254

tologic diseases who received "unheated" autologous ^{51}Cr-labeled RBC and those of eight patients who received "heated" autologous ^{51}Cr-labeled RBC for splenic scanning. It also shows the retention pattern of a patient who received heat-treated ^{51}Cr-RBC two years after splenectomy and another splenectomized for thrombocytopenia three days after receiving heat-treated ^{51}Cr-RBC.

These preliminary analyses indicate that after five days all patients had the same whole-body T_{50} of 44 ± 1 day and that (1) the label of the heated RBC was excreted initially at a faster rate than that of unheated RBC; (2) splenectomy three days after administration of heated RBC removed about 25 to 30% of label retained in the body although the spleen weighed only 160 grams; and (3) a patient two years after splenectomy for idiopathic thrombocytopenia processed the ^{51}Cr-labeled, heat-treated RBC with 87% of the intact reticuloendothelial system efficiency. Our

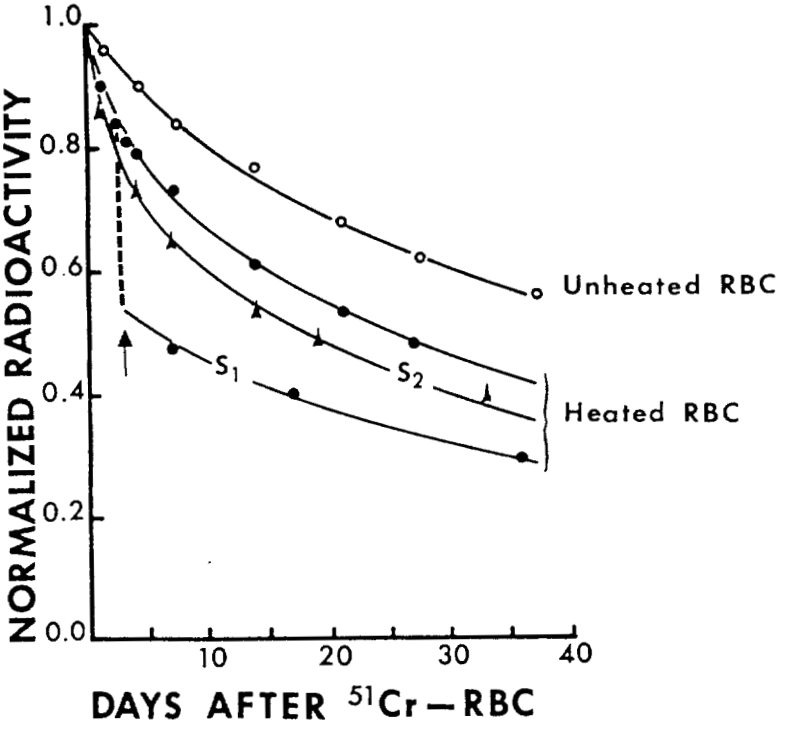

Fig. 53. Whole-body retention of ^{51}Cr-labeled red cells; for unheated RBC (10 patients); for heat-treated RBC (10 patients). One patient (S_1) had splenectomy at three days; another (S_2) had splenectomy two years previously.

1027255

other studies based on a theoretical physical model for describing the fate of chromium-damaged RBC in various groups of hematologic diseases (this report) agree with these findings, thus defining for the first time the relative magnitudes of splenic versus hepatic and bone-marrow RBC sequestration and catabolism.

REFERENCE

1. Crosby, W. H. The use of radioactive tagged red cells and platelets to study the phenomenon of sequestration. *In:* International Conference on Peaceful Uses of Atomic Energy. Vol. 10, 1955, pp. 378–381.

A Two-year Study of Cesium-137 and Potassium in Normal Subjects

W. D. Gibbs, H. D. Hodges, C. C. Lushbaugh, and J. F. Quarles

The potassium and cesium-137 content of normal persons was studied in the low-level whole-body counter during 1965 and 1966 with a total of 416 measurements. Average values for the two years showed only small differences in mean potassium content, mean weight, and mean lean body mass, indicating that the two groups were similar and that comparisons would be valid. Nearly all the persons counted in 1966 were also counted in 1965. About one-third of the measurements were made in January of each year; the remainder were done mostly during the period February-September of each year. The relative number of men and women counted in any month varied only slightly during the period of this study.

The mean total-body cesium-137 content of both men and women was lower in 1966 than in 1965, reflecting the well-known world-wide decrease of cesium-137 in the environment *(Table 24)*. However, the magnitude of the decrease is greater in men than in women, suggesting that the turnover rate is more rapid in men. In 1966, the mean cesium-137 total-body content of men was 61.5% of the 1965 content while that of women was 77.6%. The mean cesium-137 concentration expressed as nanocuries per kilogram of lean body mass for these years shows that the 1966 level was 58.6% in men and 76.2% in women of the 1965 level. The fact that these numbers agree very closely for men (61.5:58.6) and women (77.6:

1027256

76.2) indicates that the composition of the groups for the two years was comparable.

The mean cesium-137 per kilogram of lean body mass was the same for both men and women in 1966. We have not as yet completed analysis of these data with respect to age or diet.

Total body potassium was calculated from whole-body potassium-40 measurements. All calculations of lean body mass are based on the value of potassium content of lean tissue given by Forbes, et al.,[1] of 68.1 mEq/kg. Other values have been reported[2,3] of 63 mEq/kg and 73 mEq/kg.

Figure 54 shows the relation between lean body mass and body weight for men and women. The fat content of men ranges from 10 to 48% with a mean of 27%, and of women from 27 to 65% with a mean of 39%. The ranges reported by Forbes, et al., were men, 16 to 48%, and women, 24 to 67%. The figure shows that only 10 men had a fat content less than 15%. These men were all less than 30 years old, hard-working laborers, and oriental visitors who consume diets known to be poor in

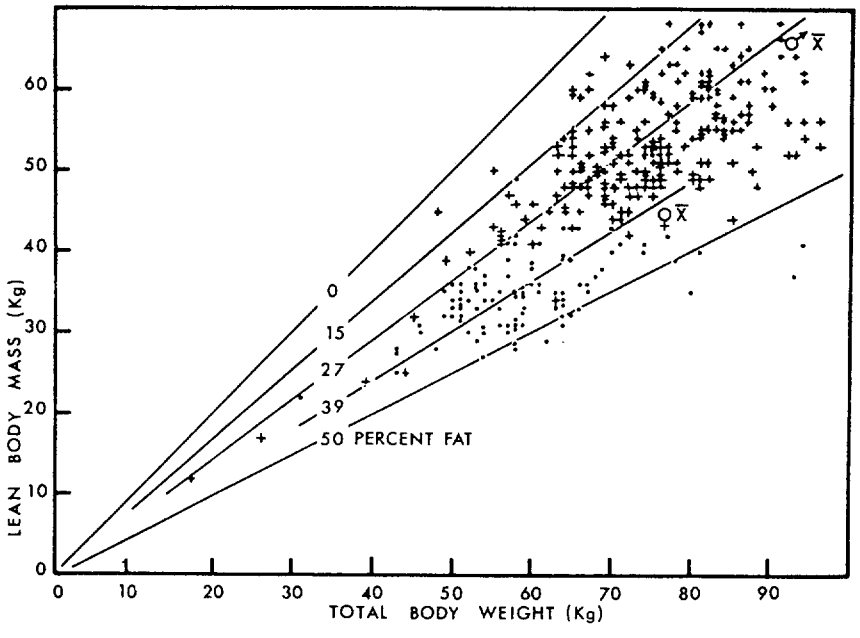

Fig. 54. Graph showing the relation of lean body mass to total body weight in normal men (+) and women (.) The mean (X) fat content is 27% in men and 39% in women.

1027257

BASIC STUDIES RELATED TO NEOPLASIA

There are underlying basic questions about neoplasia that continually emerge in the context of the specific research projects in the Division. Thus this section includes reports in the disciplines of lipid chemistry, cytogenetics, and immunology.

A Search for Tumor Antigens Using An *In Vitro* Histocompatibility Test

Helen Vodopick, Elizabeth M. Rupp, and N. Gengozian

As a supplement to experimental clinical immunotherapy for leukemia and solid tumors,[1] a procedure is required to demonstrate whether or not an immune response to the malignant cells can be produced in the lymphocytes of the donor. Since drug therapy is given in conjunction with the infusion of homologous lymphocytes, it is difficult to evaluate the relative contribution of each in promoting a remission. If the donor lymphocytes do prove beneficial, it will be important to have information on the mechanism of the immunotherapeutic effect.

An *in vitro* histocompatibility test (mixed leukocyte culture test)[2,3] using blood lymphocytes is being investigated to determine its feasibility for demonstrating tumor specific antigens after immunization of a potential donor with malignant cells. Lymphocytes obtained from two persons are allowed to react under sterile conditions in a controlled CO_2-temperature environment. Histoincompatibility between the two persons is indicated by a blastic transformation (of some of the lymphocytes) which is associated with DNA increased synthesis that can be measured by ^{14}C thymidine incorporation. Sensitization resulting from immunization of one person with leukocyte antigens of another should therefore be demonstrable as a greater histoincompatibility reaction.

Preliminary tests with the technique dealt with the reactivity between two lymphocyte populations when both were viable and capable of reacting immunologically (two-way system) and when one was inactivated and prevented from responding to the antigens of the other (one-way

1027258

system). Inactivation was accomplished with Mitomycin C.[4] With normal unrelated persons it was found that the total incorporation of thymidine in lymphocytes was usually greater in the one-way stimulation system than in the two-way system. This result would suggest that an inhibition of maximal response occurs when both populations are viable and reacting. The reasons for this are not yet known and under investigation.

The one-way system was subsequently used to study the response of lymphocytes to lymphocytes, lymphocytes to tumor cells, and tumor cells to lymphocytes. In one study, lymphocytes from an unrelated person showed a greater reaction to tumor cells (malignant melanoma treated with Mitomycin C) than did lymphocytes from a person related to the patient. The reaction of the unrelated lymphocytes stimulated by tumor cells inhibited with Mitomycin C was significantly greater than the reaction of these same normal lymphocytes to blood lymphocytes (Mitomycin C treated) obtained from the patient bearing the tumor. This reaction would suggest that this tumor tissue does indeed contain some antigenic substance absent from the patient's lymphocytes. Such an increase in reaction cannot be attributed to incompatibility due to differences in blood isoantigens since both stimulating cells, lymphocytes and tumor, came from the same patient. Finally, the control autologous combination, that is, the patient's blood lymphocytes incubated with his own tumor cells, showed the least reaction, indicating failure of the patient's lymphocytes to recognize his "tumor specific antigens." These data are summarized in *Table 25*.

Attempts to apply this reaction to lymphocytes sensitized *in vivo* to tumor tissue are now in progress. Also being evaluated is the use of

TABLE 25

Studies of a Patient with Malignant Melanoma

Viable Reacting Cells	Stimulating Cells Treated With Mitomycin C		
	Normal Lymphocytes (Related to Patient)	Patient's Lymphocytes	Tumor Cells
Normal Lymphocytes Unrelated to Patient		+++	++++++
Normal Lymphocytes From Mother of Patient		+	++
Patient's Lymphocytes	+		0

The symbols used (0, +, etc.) are arbitrary values to denote relative incorporation of ^{14}C thymidine after 24-hr incubation into 2×10^6 viable reacting cells per culture tube.

1027259

cells, lymphocytes and tumor cells, preserved by slow-freeze liquid nitrogen and stored for prolonged periods.

REFERENCES

1. Edwards, C. L., Congdon, C. C., Gengozian, N., Vodopick, H., and Andrews, G. A. Immunotherapy of acute leukemia: An experimental approach. USAEC Report ORINS-53, 81–83, 1965.
2. Bain, B., Vas, M. R., and Lowenstein, L. The development of large immature mononuclear cells in mixed leukocyte cultures. Blood 23, 108–116, 1964.
3. Bach, F. H. and Hirschhorn, K. Lymphocyte interactions: A potential histocompatibility test in vitro. Science 143, 813–818, 1964.
4. Bach, F. H. and Voynow, N. K. One-way stimulation in mixed leukocyte cultures. Science 153, 545–547, 1966.

Ch^1 and Partial 21/15 Translocation: A Familial Study with One Member Having Acute Leukemia

K. O. Goh

A smaller G chromosome, probably evolving from a deletion of the short arm of a normal G chromosome, has been reported in familial chronic lymphocytic leukemia (CLL) and is called "Ch^1".[1] A similar abnormal chromosome was found in a phenotypically normal 4½-year-old girl with acute lymphoblastic leukemia. However, in addition to this smaller G chromosome, a normal D chromosome was replaced by an abnormal one that had a short arm, which was shorter than any member of the C and longer than any member of the D chromosome group *(Fig. 55)*. The abnormality of the D chromosome was interpreted as a translocation. Both abnormal chromosomes were seen in cultured peripheral-blood leukocytes, direct bone marrow, and cultured bone marrow *(Table 26)*.

Autoradiographic studies[2] of the peripheral-blood leukocytes indicate that in the smaller G chromosome synthesis of deoxyribonucleic acid (DNA) is late and in the translocated D it is early *(Fig. 56)*. These abnormal chromosomes were also found in the patient's father and her paternal grandmother *(Table 26* and *Fig. 57)*.

The translocation of a segment of the long arm of a G chromosome to the short arm of a D chromosome has been reported in two patients having some features of mongolism, but without leukemia.[3,4] These two patients also had four morphologically normal G chromosomes; thus,

1027260

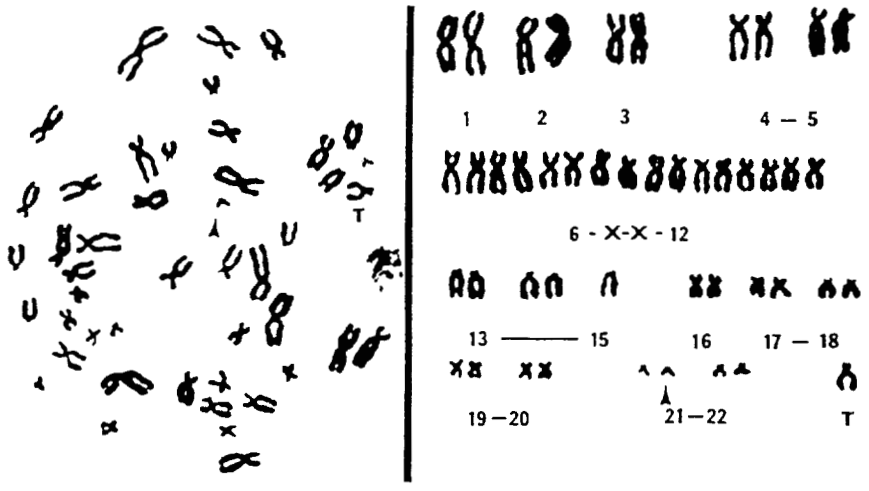

Fig. 55. Metaphase and karyotype obtained from the patient's bone marrow. A smaller G chromosome is marked with an arrow head, and a translocated chromosome (T) is also seen.

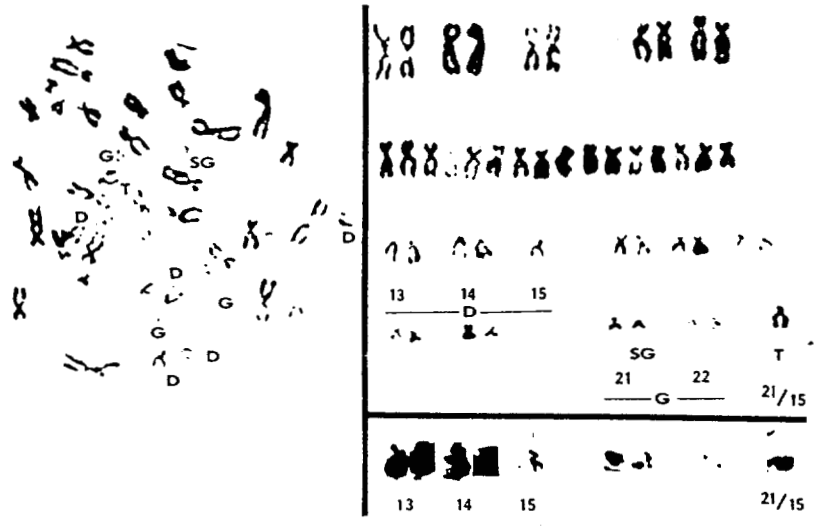

Fig. 56. Metaphase and karyotype obtained from the patient's peripheral blood. The last row at the right are the D, G, and the translocated chromosomes after autoradiographic development.

102726l

there was a net gain of genetic material. Furthermore, the cytogenetic studies of the mother (phenotypic normal) of one[4] suggested that the gained material was part of the long arm of a G chromosome.

A smaller G chromosome called the Philadelphia, or Ph^1 chromosome, has been found in patients with chronic myelocytic leukemia.[5] Its production has been postulated to be a deletion of the long arm of a normal G chromosome. The mechanism of its production may be analogous to that of the smaller G chromosome found in irradiated man.[6] The deleted long arm of the G chromosome apparently is lost since translocation of the deleted part has been reported in only two metaphases with the Ph^1 chromosome.[7] This translocation, however, has not been seen in any of the more than 2,000 Philadelphia-positive metaphases analyzed in our laboratory. Hence, in the Philadelphia-positive metaphases of chronic myelocytic leukemia, there is a net loss of genetic material of the long arm of a G chromosome.

TABLE 26

Chromosomal Analyses of the Family

Subjects	Metaphases* Obtained	Chromosome Number No. of Cells					Total	% Modal†	Smaller G‡		Translocation§	
		<45	45	46	47	>47			No.	%	No.	%
III_3	BMD	0	2	15	0	0	17	88	17	100	17	100
	BMC	0	0	33	1	1	35	94	34	97	29	83
	PBC	0	2	70	0	0	72	97	72	100	72	100
III_2	PBC	0	0	18	1	1	20	90	0		0	
III_1	PBC	0	1	19	2	0	22	86	0		0	
II_1	PBC	0	0	70	0	0	70	100	0		0	
II_2	PBC	1	4	16	0	2	23	70	20	87	17	74
	BMD	1	10	49	0	0	60	82	57	95	56	93
I_1	PBC	0	8	56	1	0	65	86	58	89	35	54
I_2	PBC	2	0	64	2	1	69	93	0		0	

* BMD = Direct bone-marrow preparation; BMC = Bone-marrow culture; PBC = Peripheral blood leukocyte culture.
† Percentage of cells having a normal diploid chromosomal number.
‡ A G chromosome ended abruptly at centromere region.
§ A D chromosome with a longer than normal short arm.

The present cytogenetic findings contrast with those previously reported in that they involve the translocation of the short arm of a G chromosome. This translocation results in neither a gain nor a loss of any morphologic genetic material. However, the possibility remains that a small segment of either a D or G chromosome, undetected with the cytogenetic techniques now available, is lost during the translocation.

It is unlikely that the abnormal chromosomes found here are related to the patient's leukemia, since neither the phenotypically normal father

1027262

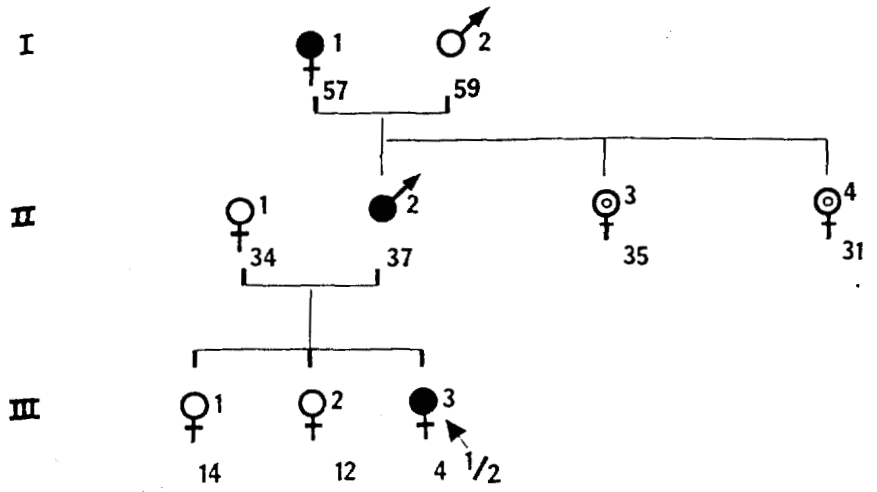

Fig. 57. Pedigree of the members of the patient's (marked with an arrow) family. Members 11_3 and 11_4 were not available for cytogenetic studies. The number in the lower right of each symbol is the age of the member. Cytogenetically normal members are indicated with white circles, and the black-circled members are carriers.

nor the paternal grandmother, who are carriers of these abnormal chromosomes, have any evidence of the disease. However, it is possible that the carriers of these two familial abnormal chromosomes may be predisposed to leukemia. The follow-up studies in this family may illuminate the problem.

REFERENCES

1. Gunz, F. W., Fitzgerald, P. H., and Adams, A. An abnormal chromosome in chronic lymphocytic leukaemia. Brit Med J 2, 1097–1099, 1962.
2. Morishima, A., Grumbach, M. M., and Taylor, J. H. Asynchronous duplication of human chromosomes and the origin of sex chromatin. Proc Nat Acad Sci 48, 756–763, 1962.
3. Shaw, M. W. Familial monogolism. Cytogenetics 1, 141–179, 1962.
4. Finley, S. C., Finley, W. H., Rosecrans, C. J., and Phillips, C. Exceptional intelligence in a mongoloid child of a family with a 13–15/partial 21 (D/partial G) translocation. New Engl J Med 272, 1089–1092, 1965.
5. Nowell, P. C. and Hungerford, D. A. A minute chromosome in human chronic granulocytic leukemia. Science 132, 1497, 1960.
6. Goh, K. O. Smaller G chromosome in irradiated man. Lancet 1, 659–660, 1966.
7. Ohno, S., Trujillo, J. M., Kaplan, W. D., Kinosita, R., and Stenius, C. Nucleolus-organisers in the causation of chromosomal anomalies in man. Lancet 1, 123–126, 1961.

1027263

Chronic Lymphocytic Leukemia and Pseudodiploidy*†

K. O. Goh

Cytogenetic studies in chronic lymphocytic leukemia (CLL) have not been so rewarding in the past as in chronic myelocytic leukemia where a specific abnormal chromosome was seen. The difficulty in studying CLL probably resulted from: (1) poor mitotic rate of the cultured peripheral lymphocytes of CLL patients with standard *in vitro* techniques; (2) few mitoses found in the direct preparations of bone marrow; and (3) the occasional metaphases seen in the direct bone-marrow preparations were probably the mitotic myeloid and erythroid cells. However, with the use of a modified standard leukocyte culture method by terminating at 3, 4, 5 and 6 days, adequate mitoses were obtained for cytogenetic studies from the peripheral-blood leukocytes of patients with CLL.

The maximum mitotic rate in the normal controls occurred in the third and fourth days *(Fig. 58)*. A lower mitotic rate was seen in every CLL patient during these days. However, with prolonged incubation, the

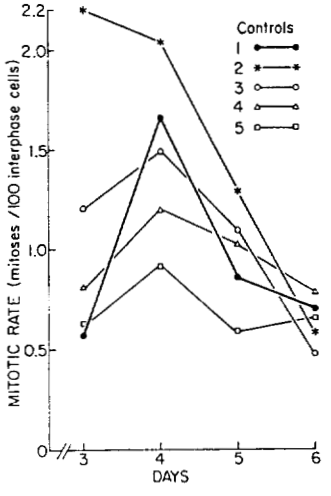

Fig. 58. The mitotic rates of the peripheral leukocytes of five normal young adults incubated with phytohemagglutinin and terminated at different intervals.

---

* Part of this study was done while associated with the University of Rochester School of Medicine and Dentistry, Rochester, N.Y.

† In press. J Lab Clin Med.

1027264

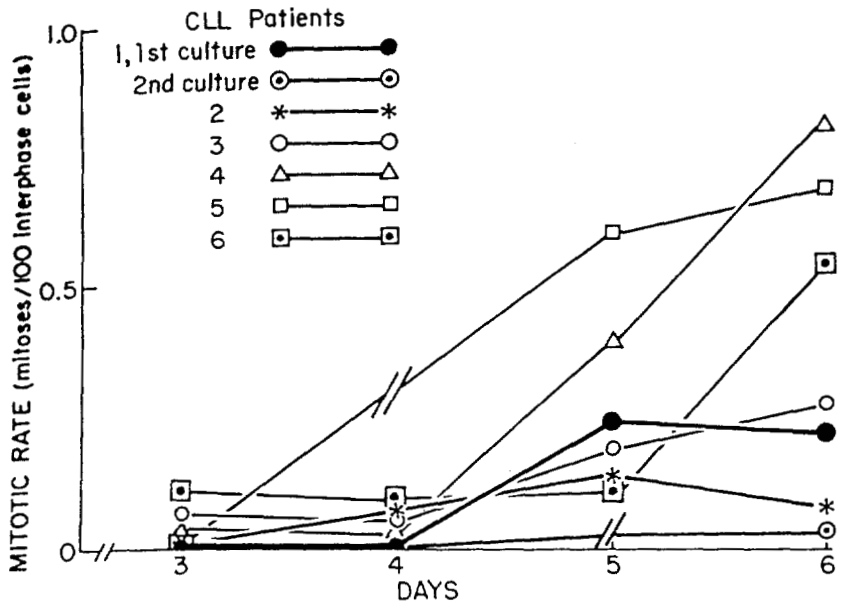

Fig. 59. The mitotic rate of the peripheral leukocytes of six CLL patients incubated with phytohemagglutinin and terminated at different intervals.

mitotic rate decreased in normals, while it increased in CLL patients *(Fig. 59)*.

Cytogenetic analyses of the karyotypes of the five-day and six-day metaphases of the normal controls showed only 3.1% pseudodiploidy (metaphases having a normal diploid chromosomal number, but with one or more abnormal chromosomes, or missing or additional chromosomes, or both, in one or more of the seven major chromosomal groups), while 44% was seen in the patients with CLL *(Fig. 60)*. Three of the six patients have not been treated with any antileukemic therapy. These findings suggest that lymphocytes from patients with CLL are capable of undergoing mitosis, that their mitotic rates are slower than those of normal controls, and that their cytogenetic patterns (based on karyotypic examination) are those of pseudodiploidy.

The mechanism by which phytohemagglutinin (PHA) stimulates mitosis may involve its "antigenic" effect[1] rather than its effect as a hemagglutinin agent.[2] Therefore, the present finding of a slower mitotic rate of the lymphocytes from CLL patients under PHA stimulation might explain the observation of an increase in "takes" and survival of homolo-

1027265

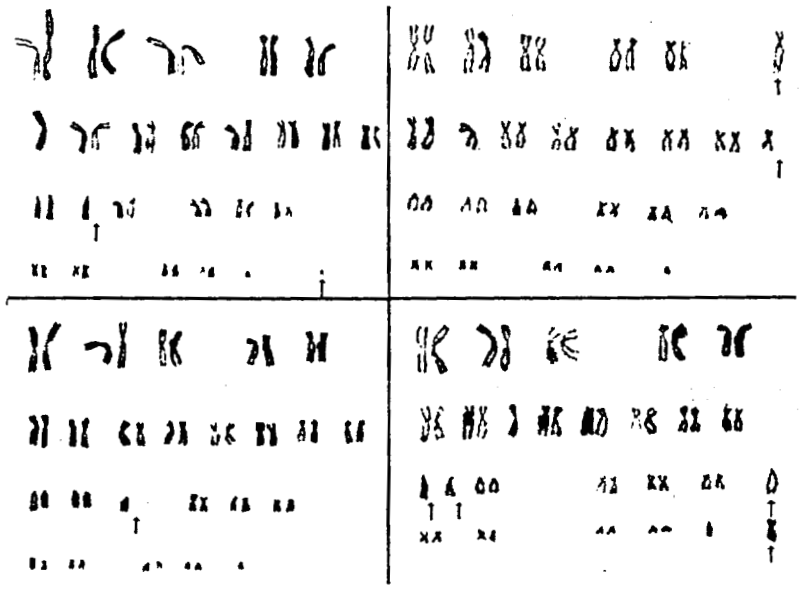

Fig. 60. Four pseudodiploid karyotypes of Case 1. One of the chromosomes in group 13-15 is replaced by a very small abnormal mesocentric chromosome (upper left) and by a chromosome of group 6-X-12 (lower left). At least one chromosome in group D is replaced by a chromosome of the other group (lower right).

gous skin graft in patients with malignant lymphoproliferative disorder.[3] The lymphocytes of these patients probably respond poorly to the antigenic stimulation of the homologous graft. Also, the poor responsiveness of the CLL lymphocytes to the antigenic stimulation might theoretically explain the frequent clinical findings of a second primary malignancy in patients with CLL.[4]

REFERENCES

1. Elves, M. W., Roath, S., and Israels, M. C. G. The response of lymphocytes to antigen challenge in vitro. Lancet 1, 806–807, 1963.
2. Hirschhorn, K., Bach, F., Kolodny, R. L., Firschein, I. L., and Hashem, N. Immune response and mitosis of human peripheral blood lymphocytes in vitro. Science 142, 1185–1187, 1963.
3. Miller, D. G., Lizardo, J. G., and Snyderman, R. K. Homologous and heterologous skin transplantation in patients with lymphomatous disease. J Nat Cancer Inst 26, 569–583, 1961.
4. Gunz, F. W. and Angus, H. B. Leukemia and cancer in the same patient. Cancer 18, 145–152, 1965.

1027266

Additional Evidence of the Philadelphia Chromosome as a Postzygotic Abnormality in Identical Twins

K. O. Goh, S. N. Swisher, and E. C. Herman, Jr.†*

An abnormal chromosome was observed in chronic myelocytic leukemia (CML) and called Ph[1] by Nowell and Hungerford.[1] The mechanism of its production conceivably may be analogous to the production of a smaller G chromosome found in patients accidentally exposed to total-body irradiation.[2] If so, it indicates that the Ph[1] chromosome is an acquired abnormality rather than a prezygotic abnormality. This postulation was supported by our finding that there was no Ph[1] chromosome in a normal identical twin whose leukemic twin showed typical Ph[1] chromosome.[3] We now report the cytogenetic studies of another set of identical twins (H twins), one having CML, and we also present the follow-up report on the cytogenetic studies of the surviving unaffected P twin of our first set.[3]

Table 27 summarizes the distribution of cytogenetic studies of the H twins from different material. A typical Ph[1] chromosome was seen

TABLE 27

Distribution of the Philadelphia (Ph[1]) Chromosomes in Identical H Twins

Materials	CML		Normal	
	Ph[1]	No*	Ph[1]	No
Bone Marrow				
Direct	38	40	0	28
Incubated	8	8	0	50
Peripheral leukocyte culture	31	34		0†
Total	77	82	0	78

*Number of cells analyzed.
†No mitosis was seen.

in the diseased twin *(Fig. 61)*, but it was not seen in the normal twin. In the normal P twin, 7½ years after the diagnosis of his CML twin, 20 metaphases from direct bone marrow and 40 metaphases from incubated bone marrow were negative for Ph[1] chromosome. There was a possibility that the absence of Ph[1] chromosome in the studies of these two normal

*University of Rochester School of Medicine and Dentistry, Rochester, N.Y.
†Mary Imogene Bassett Hospital, Cooperstown, N.Y., and Columbia University College of Physicians and Surgeons, New York, N.Y.

1027267

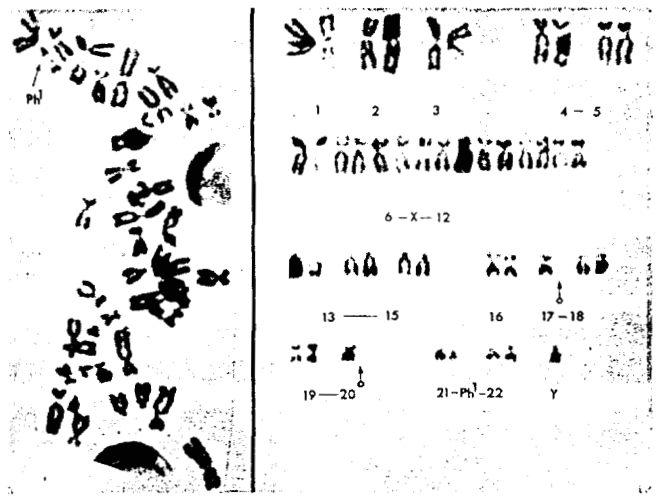

Fig. 61. A hypodiploid (44) metaphase and its karyotype obtained from the bone marrow of the diseased H twin showing a Ph¹ chromosome.

twins reflected the cytogenetic pattern of their lymphocytes. However, in our present studies, to avoid the misleading results that might have been obtained from the study of metaphases coming predominantly from lymphocytes, the metaphases of the normal twins were obtained from the direct bone-marrow preparations and from bone-marrow material incubated for only a short time and without PHA. Thus, we believe that the Ph¹ chromosome is absent in the nonlymphocytic cells of these two normal twins. These findings and the two sets reported by others[4,5] support our original suggestion that the Ph¹ chromosome is an acquired postzygotic chromosomal abnormality associated with chronic myelocytic leukemia.

REFERENCES

1. Nowell, P. C. and Hungerford, D. A. A minute chromosome in human chronic granulocytic leukemia. Science 132, 1497, 1960.
2. Goh, K. O. Smaller G chromosome in irradiated man. Lancet 1, 659–660, 1966.
3. Goh, K. O. and Swisher, S. N. Identical twins and chronic myelocytic leukemia: Chromosomal studies of a patient with chronic myelocytic leukemia and his normal identical twin. Arch Intern Med 115, 475–478, 1965.
4. Jacobs, E. M., Luce, J. K., and Cailleau, R. Chromosomel abnormalities in human cancer: Report of a patient with chronic myelocytic leukemia and his nonleukemic monozygotic twin. Cancer 19, 869–876, 1966.
5. Woodliff, H. J., Dougan, L. and Onesti, P. Cytogenetic studies in twins, one with chronic granulocytic leukaemia (abstract). Nature 211, 533, 1966.

1027268

Scope and Orientation of the Lipid Project

F. Snyder

The over-all objective of the lipid program is to elucidate the chemical, physical and metabolic properties of glyceryl ethers and other lipids in relation to cell structure and function in normal, neoplastic, virus-infected and irradiated cells. The main project is focused on the diacyl glyceryl alkyl monoethers and related lipids, and has included the following work: chemical synthesis (^{14}C, ^{3}H, and unlabeled), determination of chemical and physical properties, study of enzymatic cleavage of isomeric glyceryl ethers by a soluble liver enzyme system, survey of the occurrence of glyceryl ethers in tumors, and investigation of the metabolism of the ether bond in tumors. The tumor work is also providing quantitative data on the lipid composition of a wide spectrum of animal and human cancers.

An investigation is also being done on the biochemical mechanism of fat-cell formation in bone marrow after irradiation and in hematologic disorders. Certain aspects of the program have been carried out in collaboration with the University of North Carolina, the University of Minnesota, the University of Tennessee, and the molecular anatomy project at Oak Ridge National Laboratory. The first graduate student from the University of Tennessee (Memphis) will start work on his Ph.D. research requirements after this semester.

The following ten reports present work from the lipid qroup. Other reports of work from these investigators are found under other headings (see pages 5, 12 and 37).

An Unidentified Lipid Prevalent in Tumors*

F. Snyder, E. A. Cress, and N. Stephens

An unidentified lipid was found in five different tumor sources examined. It was not found in liver, bone marrow, or plasma from tumor-bearing animals, nor in the extracellular fluid supporting growth of Ehrlich ascites cells *(Fig. 62)*. The polarity of the unidentified component was similar to that of a glyceryl ether diester, and it was isolated in milligram amounts by preparative thin-layer chromatography. Methyl esters of fatty acids, vinyl ether diesters, or quinones were not found in the structural makeup of this lipid.

---

*Abstract of article published in *Lipids* 1, 381–386, 1966.

1027269

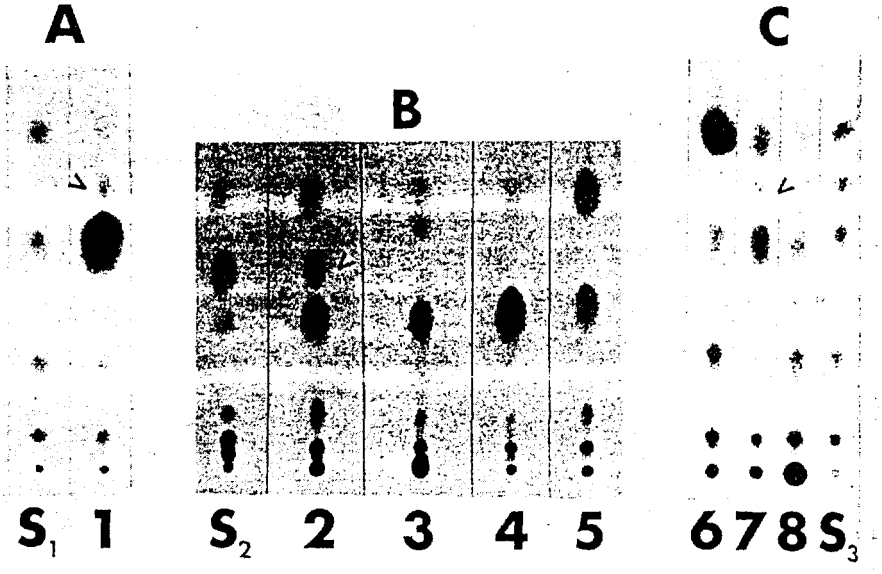

Fig. 62. Thin-layer chromatograms of total lipid extracts from (A) human lymphosarcoma (Lane 1), (B) irradiated rat tumor (Lane 2) and (C) Ehrlich ascites cells (Lane 7). The < designates the unknown lipid component (above triglycerides) prevalent in all tumors examined. The TLC patterns of total lipids from other tissues or fluids are *Plate B*—rat liver (Lane 3), rat femoral bone marrow (Lane 4), and rat plasma (Lane 5); *Plate C*—EAC extracellular fluid (Lane 6) and mouse liver (Lane 8). S_1 is a mixed lipid standard (from bottom to top) containing lecithin, cholesterol, oleic acid, triolein and cholesteryl oleate. S_2 is a mixed lipid standard containing S_1 components plus 1-hexadecanol (third component from bottom) and dipalmitoyl batyl alcohol (sixth component from bottom at same R_f as unknown tumor lipid). S_3 is a mixed lipid standard containing S_1 components plus dipalmitoly batyl alcohol (fifth component from bottom at same R_f as unknown tumor lipid). Although the lipid patterns from the Walker-256 sarcoma and the R-3259 tumor (*both tumors transplantable in rats*) *are not shown in the chromatogram*, they, too, exhibited an unidentified spot having an identical R_f to that observed in the tumor lipids shown here.

Thin-layer chromatography of the purified unidentified tumor lipid on Ag-impregnated silica layers revealed two main components of intermediary unsaturation. Saponification of the unidentified tumor lipid, when water washing was omitted, yielded two components that migrated at R_f's identical to those of free fatty acids and dihydroxy glyceryl monoethers. Neither acetate-1-^{14}C nor palmitic-1-^{14}C acid (single injections) was found to be incorporated into the unidentified lipid of a mature rat tumor.

1027270

Characterization and Identification of Glyceryl Ether Diesters Prevalent in Ehrlich Ascites Cells and Other Tumors*

R. Wood and F. Snyder

A previously unidentified neutral lipid prevalent in tumor tissues has been isolated from Ehrlich ascites cells and unequivocally identified as a lipid class of glyceryl ether diesters containing various degrees of unsaturation, and ranging in approximate molecular weight from 760 to 990. The glyceryl ether diester fraction was shown to be free of neutral plasmalogens.

The tumor lipid was subjected to saponification, transesterification, and lithium aluminum hydride reduction *(Fig. 63)*. The glyceryl mono-

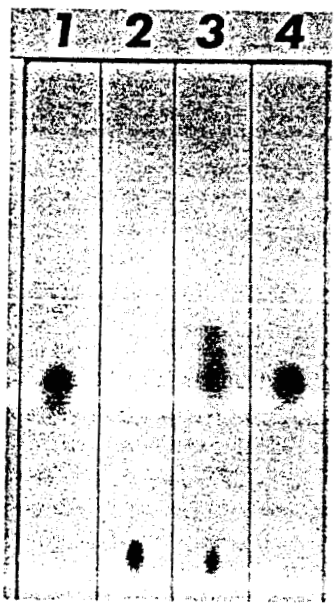

Fig. 63. Thin-layer chromatoplate of the products resulting from Lithium aluminum hydride reduction of the unidentified tumor lipid (Lane 3) and tripalmitin (Lane 4). Standards shown in Lanes 1 and 2 are hexadecanol and synthetic glyceryl monoethers, respectively. The solvent system was chloroform-methanol 98:2 (v/v).

ethers following deacylation were found to be the 1-isomers ranging in hydrocarbon chain length from C_{12} to C_{24}. Saturated and mono- and polyunsaturated fatty acids ranging in chain length from C_{12} to C_{24} carbon atoms were esterified to the glyceryl monoether. Gas-liquid chromatog-

* Published in ACS Abstracts, 152nd Meeting, New York, C-257, 1966.

1027271

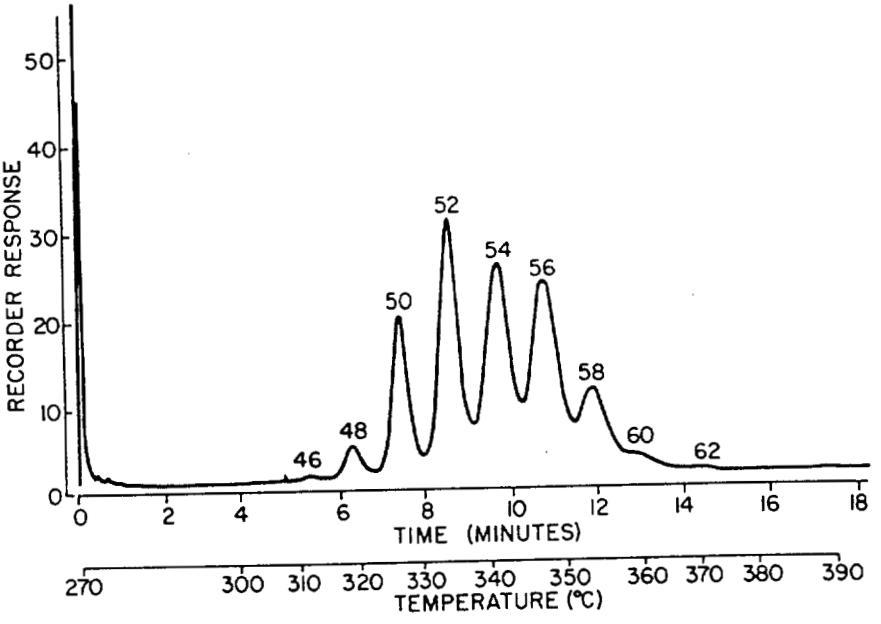

Fig. 64. Gas-liquid chromatogram tracing obtained for the intact unhydrogenated tumor lipid. The carbon numbers are above each peak.

raphy *(Fig. 64)*, thin-layer chromatography, and nuclear magnetic resonance and infrared spectroscopy were used to characterize and identify the intact tumor lipid and its derived products.

1027272

The Incorporation of Labeled Lipids into a Glyceryl Ether Component of Ehrlich Ascites Cells*

F. Snyder and R. Wood

Our group has reported the occurrence of an unidentified lipid prevalent in tumors. Recently, this unidentified lipid component, as found in Ehrlich ascites cells (EAC), has been tentatively identified as a glyceryl ether diester (GED); the chemical and physical evidence for identification of this structure is presented elsewhere in this report (p. 133).

*Published in ACS Abstracts, 152nd meeting, New York, C-258, 1966.

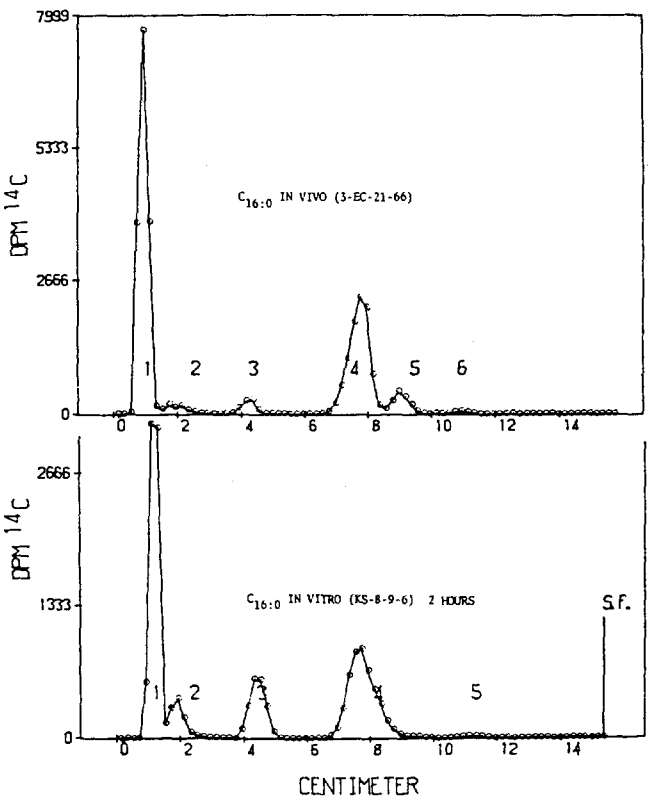

Fig. 65. The incorporation of palmitic-1-^{14}C acid into lipids of Ehrlich ascites cells grown *in vivo* and *in vitro*. The peak numbers in the upper TLC zonal profile represent (1) origin, (2) diglycerides, (3) fatty acids, (4) triglycerides, (5) glyceryl ether diesters and (6) cholesteryl esters. The peak numbers in the lower TLC zonal profile represent (1) origin, (2) diglycerides, (3) fatty acids, (4) triglycerides with a shoulder peak of glyceryl ether diester, and (5) cholesteryl esters. The S.F. designates the solvent front.

1027273

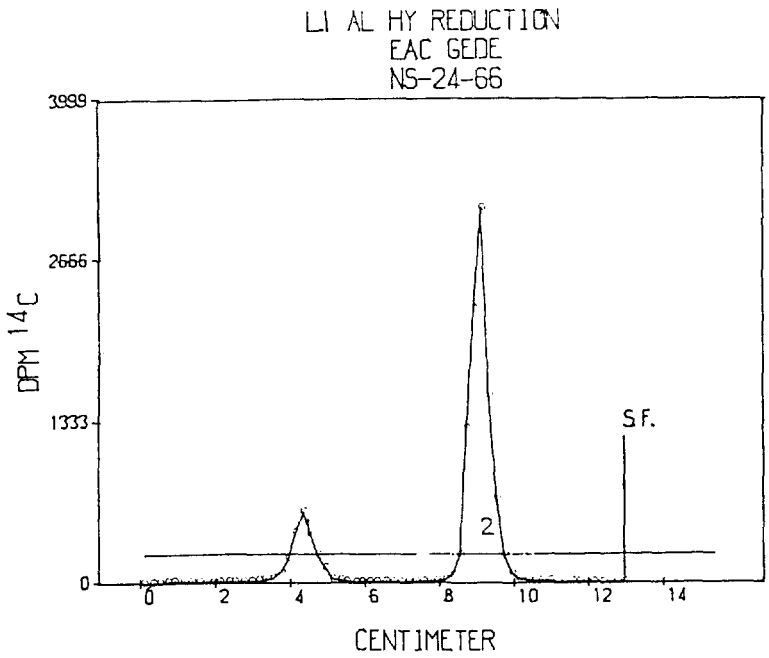

Fig. 66. A zonal ^{14}C profile of products detected after $LiAlH_4$ reduction of purified ^{14}C-labeled glyceryl ether diesters that had been isolated from Ehrlich ascites cells. The activity in peak 1 represents the deacylated glyceryl ether and the activity in peak 2 represents fatty alcohols.

The significant quantity of glyceryl ethers found in EAC has suggested these carcinoma cells as a useful biological system for studying the biosynthesis of the ether bond in lipids. We have examined the *in vivo* incorporation of the following ^{14}C-labeled compounds into the diacyl glyceryl ether fraction of EAC: fatty acids ($C_{10:0}$, $C_{14:0}$, $C_{16:0}$, $C_{18:0}$, $C_{18:1}$), fatty alcohols ($C_{18:0}$, $C_{16:0}$), triglycerides ($C_{18:0}$, $C_{18:1}$), glycerol, propionate, ethylene glycol, glucose, formate and acetate. A single injection, or eight repeated daily injections, of the labeled compounds was given intraperitoneally to white Swiss mice bearing EAC. Thin-layer chromatographic zonal scans (2-mm) were used to determine the percentage of label incorporated into the GED of EAC, EAC fluid, and livers from EAC-bearing mice. All the labeled lipids were found to be incorporated into the GED of EAC (2–10% of the total lipid ^{14}C of EAC), but not into the EAC fluid or into the livers from EAC-bearing mice. None of the ^{14}C from acetate, glucose, glycerol, propionate, ethylene glycol, or formate was found in the GED fraction. After administration of the $C_{16:0}$ acid *(Fig. 65)*, 25–50% of the ^{14}C in GED resided in the glyceryl ethers liberated by $LiAlH_4$ *(Fig. 66)* or ethanolic KOH.

1027274

Metabolism of Alpha-Alkoxy Glyceryl Monoethers in Rat Liver, *in vivo* and *in vitro*.*

F. Snyder and R. C. Pfleger

An investigation of the metabolism of ^{14}C and ^{3}H-labeled 1-isomers of C_{16} and C_{18} α-alkoxy monoethers, administered intravenously and added to liver slices, showed extensive cleavage of the ether bond in rat liver *(Fig. 67)*. Approximately 99% cleavage of the $C_{16:0}$ ether bond

* Abstract of article published in *Lipids* 1, 328–334, 1966.

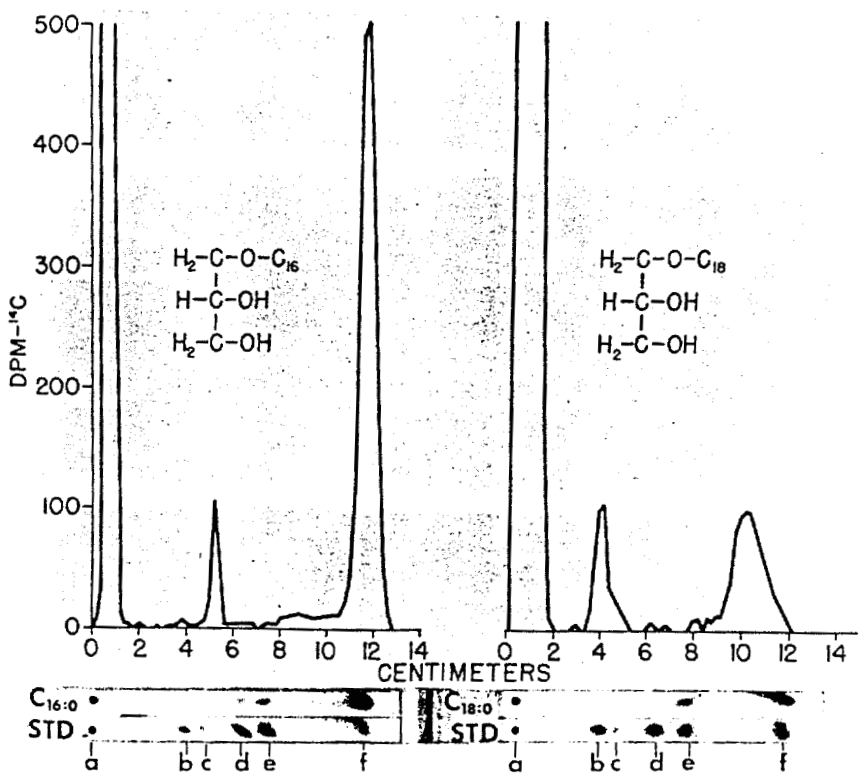

Fig. 67. Zonal scans (2-mm) of thin-layer chromatograms of total liver lipids 6 hr after intravenous chimyl-1-^{14}C (2-^{3}H-glyceryl) alcohol (LEFT scan) or batyl-1-^{14}C alcohol (RIGHT scan) injections. The arabic letters designate lipid classes based on known standards (STD): (a) phospholipids, (b) monoglycerides, (c) glyceryl ethers, (d) free fatty acids, (e) fatty alcohols, (f) triglycerides. $C_{16:0}$ is a sample of liver lipids from chimyl-alcohol injected rat. $C_{18:0}$ is sample of liver lipids from batyl-alcohol-injected rat. Chromatograms were developed in a solvent system of hexane: diethyl ether: methanol: acetic acid (80: 20: 10:1 v/v/v/v/).

1027275

and approximately 94% cleavage of the $C_{18:0}$ ether bond occurred in rat liver within 6 hr after intravenous injection. With doubly labeled chimyl alcohol (^3H and ^{14}C), acetylation and subsequent acetolysis demonstrated that less than 0.92% of the phosphatides and less than 1.52% of total lipid radioactivity were in the form of alkoxy glycerols. Long-chain fatty alcohols and fatty acids were the principal products of the ether cleavage in the liver.

The relative rate of ^{14}C incorporation from chimyl alcohol and batyl alcohol into triglycerides and phospholipids, respectively, demonstrates that the palmitic (from chimyl alcohol) and stearic (from batyl alcohol) acids formed after cleavage enter the free fatty acid pool. The liver contained most of the radioactive label in the lecithin and cephalin of the microsomal fraction. Incubation of the labeled batyl or chimyl alcohols with liver slices resulted in the same products as in the *in vivo* experiments. Less than 1.4% of the C_{16} and C_{18} alkoxyglycerols was oxidized to $^{14}CO_2$ during a 3-hr incubation.

In view of the extensive cleavage of the ether bond by liver, the hemopoietic and radioprotective activities reported for the alkoxyglycerols should be reevaluated in terms of their metabolic products.

Chemical and Physical Properties of Isomeric Glyceryl Monoethers*

R. Wood and F. Snyder

Long-chain saturated and mono- and di-unsaturated 1- and 2-glyceryl monoethers were synthesized by reacting 1, 2-isopropylidene and 1, 3-benzylidene glycerol potassium salts with alkyl halides in the preparation of the saturated, and with alkenyl-p-toluene sulfonates in the preparation of the unsaturated, followed by hydrolysis of the blocking groups with boric acid. The progress of the reaction was monitored by gas-liquid chromatography (GLC) of the reaction mixture. All the 2-glyceryl ethers except two had not been prepared previously. Normal propyl and 3-pentyl octadecyl ethers also were synthesized to aid in the interpretation of infrared (IR) and nuclear magnetic resonance (NMR) spectra.

Purity of all the ethers prepared after purification by preparative thin-layer chromatography (TLC) and crystallization was found to be

* Presented at the American Oil Chemists' Society fall meeting, 1966, Philadelphia, Pa.

1027276

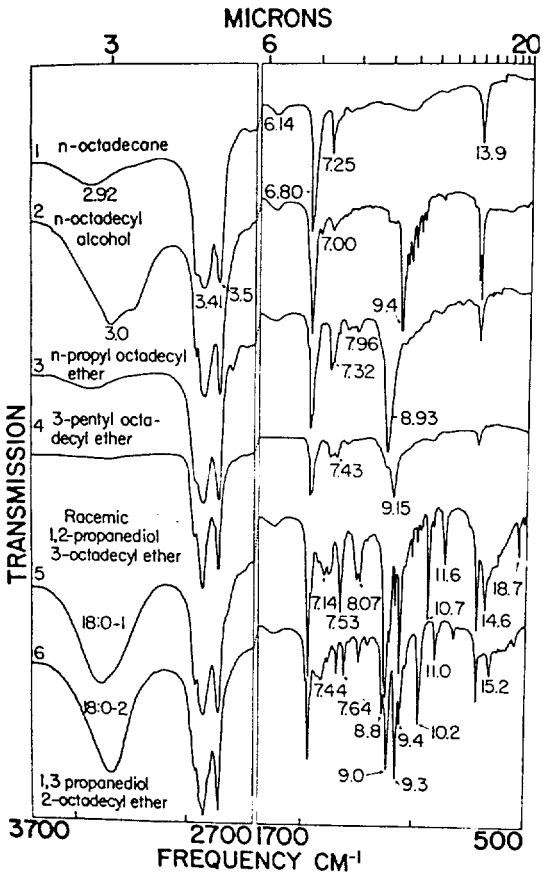

Fig. 68. IR spectra of 18:0-1 and 18:0-2 isomeric glyceryl ethers and compounds with individual functional groups found in the two isomeric ethers.

greater than 95%, as determined by TLC and GLC, supported by NMR and IR spectra. The isomeric 1- and 2-glyceryl ethers were separated on Silica Gel G adsorbent layers impregnated with either sodium arsenite or boric acid, and their TLC behavior was interpreted on the basis of the polarity of the complexes formed. Melting-point determinations indicated more than one polymorphic form. Comparison of IR *(Fig. 68)* and NMR spectra of the saturated and unsaturated isomeric glyceryl ethers, and various derivatives demonstrated the applicability of these spectroscopy methods for characterization and structural determination, in addition to distinguishing between the two isomeric forms.

1027277

The Synthesis of ^{14}C- and ^{3}H-labeled Glyceryl Ethers*

E. O. Oswald,† C. Piantadosi,‡ C. E. Anderson,† and F. Snyder

The racemic ^{14}C- and ^{3}H-labeled alpha and beta derivatives of octadecyl glyceryl ether (batyl alcohol) and of hexadecyl glyceryl ether (chimyl alcohol) of high specific activity were synthesized by treating the appropriate alkyl halides with a large excess of the potassium salts of isopropylidene or benzylidene glycerol. By use of the trifluoroacetic anhydride esterification procedure, the labeled diesters of alpha and beta octadecyl and hexadecyl glyceryl ethers were prepared. The labeled monoesters of beta octadecyl and of beta hexadecyl glyceryl ethers were isolated from the reaction mixtures by silicic acid column chromatography.

* Abstract of article published in *Lipids* 1, 241-246, 1966.

†From the Department of Biochemistry, University of North Carolina, Chapel Hill, N.C.
‡From the Department of Medicinal Chemistry, University of North Carolina, Chapel Hill, N.C.

The GLC and TLC Resolution of Diastereoisomeric Polyhydroxystearates and Assignment of Configurations*

R. Wood, Enid L. Bever,† and F. Snyder

Trifluoroacetate (TFA) derivatives of methyl 12-hydroxystearate, methylricinoleate, five positional isomers of methyl *threo-* and *erythro-*dihydroxystearate, four diastereoisomeric methyl 9, 10-12-trihydroxystearates, and four racemic diastereoisomeric methyl 9, 10-12, 13-tetrahydroxystearates were prepared and analyzed by gas-liquid chromatography (GLC). The isomeric *threo-* and *erythro-*dihydroxystearates that had not previously been resolved by GLC were separated. Excellent resolution of the diastereoisomeric pairs of methyl *threo-* and *erythro-*9, 10-12-tri- and methyl *erythro, erythro-* and *threo, threo-*9, 10-12, 13-tetra-hydroxystearates was obtained by GLC of their TFA derivatives. Analyses of these high molecular-weight compounds were

* Abstract of article published in *Lipids* 1, 399-408, 1966.

† Research participant from Lawrence University, Appleton, Wis.

T

Physical and Chemical Properties of Dia
Alkaline Permanganate Ox

Cpd. No.	Parent Acid†	Di-, tri- and tetra-hydroxystearate	Relative & Absolut Configurati
1.	18:1 (9c)	*erythro*-9, 10-	
2.	18:1 (9t)	*threo*-9, 10-	
3.	18:1 (9t) 12-OH	(9-S, 10-S, 12-R)‡ *threo*-9, 10- *threo*-10, 12-	
4.	18:1 (9t) 12-OH	(9-R, 10-R, 12-R)‡ *threo*-9, 10- *erythro*-10, 12-	
5.	18:1 (9c) 12-OH	(9-S, 10-R, 12-R)‡ *erythro*-9, 10- *erythro*-10, 12-	
6.	18:1 (9c) 12-OH	(9-R, 10-S, 12-R)‡ *erythro*-9, 10- *threo*-10, 12-	
7.	18:2 (9t, 12t)	*threo*-9, 10- *erythro*-10, 12- *threo*-12, 13-	
8.	18:2 (9t, 12t)	*threo*-9, 10- *threo*-10, 12- *threo*-12, 13-	
9.	18:2 (9c, 12c)	*erythro*-9, 10- *erythro*-10, 12- *erythro*-12, 13-	
10.	18:2 (9c, 12c)	*erythro*-9, 10- *threo*-10, 12- *erythro*-12, 13-	

*Heavy lines separate synthetic diastereoiso
†The number and letter in parenthesis repre
‡Cahn-Ingold-Prelog system of designating
§Melting points represent the uncorrected n
* Literature melting points.

1027278

carried out on polar and nonpolar packed columns used routinely for methyl ester analysis.

The various methyl mono-, di-, tri-, and tetra-hydroxystearate esters were also analyzed by thin-layer chromatography (TLC) on Silica Gel G adsorbent layers and on Silica Gel G impregnated with sodium arsenite. Relative and absolute configurations were assigned to the various diastereoisomeric tri- and tetra-hydroxystearates based on information obtained from GLC, TLC, synthetic ratios, and molecular-model data *(Table 28)*.

A micro hydroxylation method that gives quantitative yields of *threo-* and *erythro*-dihydroxy acids from various concentrations of C_{18} monoene geometrical isomers was developed. Subsequent GLC analysis of the isomeric methyl dihydroxy TFA derivatives allows the quantitative determination of double-bond configuration on small samples without expensive or specialized equipment.

GLC and TLC Analysis of Isopropylidene Derivatives of Isomeric Polyhydroxy Acids Derived from Positional and Geometrical Isomers of Unsaturated Fatty Acids

R. Wood

Gas-liquid chromatography (GLC) and thin-layer chromatography (TLC) were used to investigate the isopropylidene derivatives of nine isomeric dihydroxy esters, four methyl 9, 10-12-trihydroxystearates, and eight methyl 9, 10-12, 13-tetrahydroxystearates prepared from unsaturated fatty acids. This method resolves polyhydroxy acids not previously possible, and is particularly useful for determining the position of double bonds and geometric configurations of intact fatty acids.

All GLC analyses were carried out with liquid phases of ethylene glycol succinate methyl silicone polymer (EGSS-X) and methyl silicone polymer (SE-30) packed columns, which are normally used for methyl ester analysis. The isopropylidenes derived from *cis* and *trans* monounsaturated fatty acids were easily separated on both EGSS-X and SE-30 columns. Positional isomers were not separated on either liquid phase but were resolved by TLC *(Fig. 69)*. The trifluoroacetate derivatives of the odd hydroxyl group of the isopropylidenes prepared from the four isomeric trihydroxy esters were resolved by GLC. Four of the

1027279

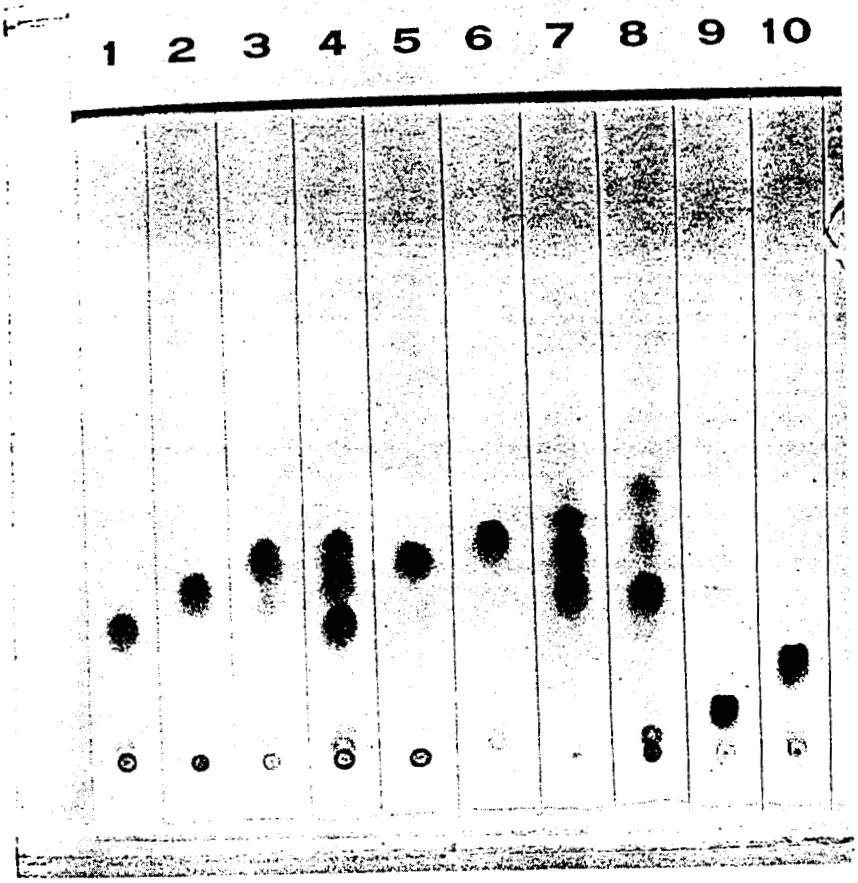

Fig. 69. Thin-layer chromatograms of isopropylidene fatty esters derived from (1) petroselenic; (2) oleic; (3) *cis*-vaccenic; (4) mixture of 1, 2, and 3; (5) elaidic; (6) *trans*-vaccenic; (7) mixture; (8) palmitoleic; (9) linoleic; and (10) linoelaidic acids. Solvent system was hexane-diethyl ether-30% aqueous ammonium hydroxide 90:12:0.25 (v/v/v/).

eight isopropylidenes derived from the four geometric isomers of linoleic acid were resolved on the EGSS-X column; the other four isomers eluted as a single peak.

1027280

The Quantitative Analysis of Long-chain Fatty Alcohols by Gas-Liquid Chromatography

R. Wood

Trifluoroacetate (TFA) and trimethylsilyl ether (TMS) derivatives of saturated and mono- and poly-unsaturated fatty alcohols ranging in chain length from C_{14} to C_{20} were analyzed quantitatively by gas-liquid chromatography (GLC) *(Table 29)*. The TFA and TMS derivatives were prepared quickly and quantitatively at room temperature according to previously described trifluoroacetylating and trimethylsilating procedures.[1–3]

Unlike glyceryl ethers and polyhydroxy acids,[1,2] the stable alcohol TFA derivatives can be stored and samples for GLC can be injected in hexane containing 1% trifluoroacetic anhydride without breakdown. This eliminates solvent peak tailing caused by trifluoroacetic anhydride and trifluoroacetic acid, allowing analysis of shorter chain alcohols.

Analyses were carried out on columns (5 ft × 1/8 in.) containing 15% ethylene glycol succinate methyl silicone polymer (EGSS-X) and 5% methyl silicone polymer (SE-30) liquid phases operating at 130 and 190°C for both derivatives. The TFA derivatives are superior to the TMS

TABLE 29

*GLC Analysis of Saturated and Unsaturated Fatty Alcohols as Their Trifluoroacetate (TFA) and Trimethylsilyl Ether (TMS) Derivatives**

Alcohol	Known Wt. %	Known Molar%	% TMS Found	% TFA Found
	Saturated Alchol Mixture			
Myristyl (14:0)†	15.4	18.7	19.8	17.8
Palmityl (16:0)	23.1	24.8	23.6	23.8
Stearyl (18.0)	30.8	29.6	30.4	29.3
Arachidyl (20:0)	30.8	26.8	26.0	29.0
	Unsaturated Alcohol Mixture			
Palmitoleyl (16:1)	15.4	16.7	16.3	18.7
Oleyl (18:1)	23.1	22.6	23.1	21.7
Linoleyl (18:2)	30.8	30.4	30.2	29.7
Linolenyl (18:3)	30.8	30.4	30.2	29.7

*Analyses were carried our at 130 C on a 5ft × 1/8 in. Pyrex column packed with 15% ethylene glycol succinate methyl silicone polymer (EGSS-X) coated on 100-120 mesh Gas-Chrom-P.

†Shorthand system of nomenclature; the first number separated by a colon represents the number of carbon atoms in the hydrocarbon chain and the second number represents the number of double bonds in the chain.

1027281

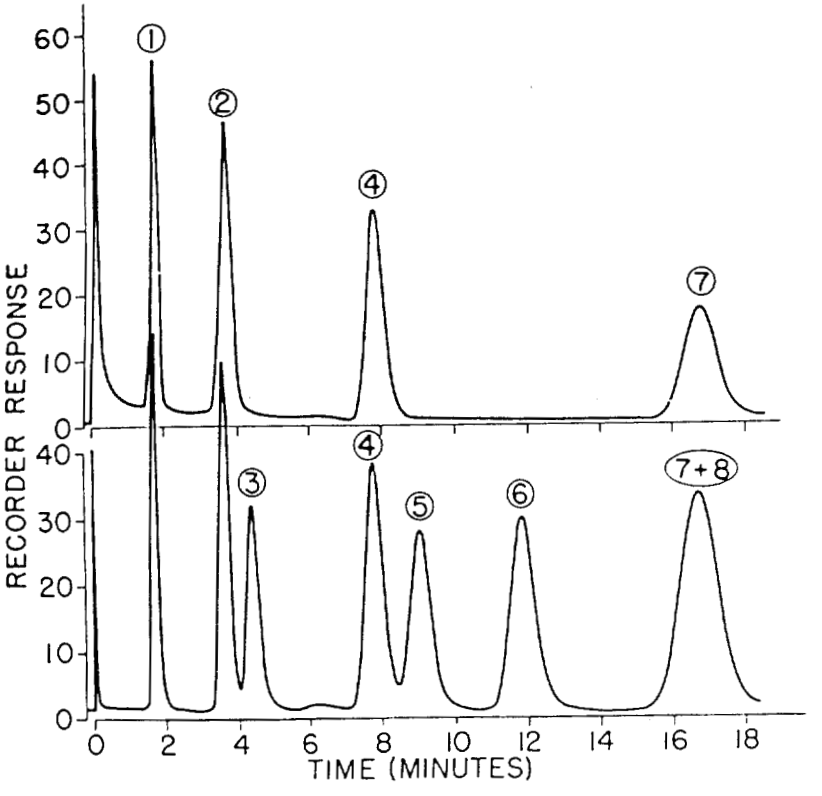

Fig. 70. The two chromatogram tracings depict the analysis of a mixture of long-chain fatty alcohols as their trifluoroacetate (TFA) derivatives. The numbered alcohol peaks are (1) myristyl; (2) palmityl; (3) palmitoleyl; (4) stearyl; (5) oleyl; (6) linoleyl; (7) arachidyl; and (8) linolenyl. Analyses were made on a 5 ft × 1/8 in. Pyrex column packed with 15% EGSS-X coated on 100-120 mesh Gas-Chrom-P operating at 130°C.

derivatives for the quantitative analysis of long-chain fatty alcohol mixtures. The TFA derivatives of the alcohols that are difficult to separate, the saturated and corresponding monounsaturated, were easily resolved on the EGSS-X liquid phase *(Fig. 70)*, but not on the SE-30; TMS derivatives were not resolved satisfactorily on either liquid phase. Both TFA and TMS derivatives of polyunsaturated fatty alcohols give quantitative GLC results *(Table 29* and *Fig. 70)*.

The TFA derivatives have proved useful for the analysis of fatty alcohol mixtures liberated by $LiAlH_4$ reduction of glyceryl ether diesters

1027282

isolated from Ehrlich ascites tumor cells[4] and are applicable for the analysis of alcohols formed during the biocleavage of glyceryl ethers.[5]

REFERENCES

1. Wood, R. and Snyder, F. Gas-liquid chromatographic analysis of long-chain isomeric glyceryl monoethers. Lipids 1, 62–72, 1966.
2. Wood, R., Bever, E. L., and Snyder, F. The GLC and TLC resolution of diastereoisomeric polyhydroxystearates and assignment of configurations. Lipids 1, 399–408, 1966.
3. Wood, R. D., Raju, P. K., and Reiser, R. Gas-liquid chromatographic analysis of monoglycerides as their trimethylsilyl ether derivatives. J Amer Oil Chem Soc 42, 161–165, 1965.
4. Wood, R. and Snyder, F. Characterization and tentative identification of a lipid ether present in Ehrlich ascites cells and other tumors. ACS Abstracts, 152nd Meeting, N.Y., C-257, 1966.
5. Snyder, F. and Pfleger, R. C. Metabolism of α-alkoxy glyceryl monoethers in rat liver, *in vivo* and *in vitro*. Lipids 1, 328–334, 1966.

Cleavage of the 1- and 2-isomers of ^{14}C-labeled Glyceryl Ethers by a Soluble Multienzyme System of Rat Liver*

R. C. Pfleger,† F. Snyder, and C. Piantadosi‡

Initial *in vivo* metabolic studies of the 1- and 2-isomers of the $C_{16:0}$ and $C_{18:0}$ glyceryl ethers revealed that rat liver cleaves the ether bond even more extensively and rapidly than do mucosal cells.[1] We have examined this cleavage in more detail in cell-free liver preparations from a number of species. Our data confirm the work of Tietz, *et al.*[2] on the pteridine cofactor requirements for microsomal enzymatic cleavage of the ether bond, but also demonstrate that the enzyme system involved can readily be washed away from the microsomes *(Fig. 71)*.

This soluble ether-cleaving enzymatic system, defined by electron microscopy and zonal centrifugation, cleaves the 2-isomers and the $C_{16:0}$ ether chain to a slightly greater extent than the 1-isomers and the $C_{18:0}$ chain. The main ^{14}C products were fatty acids and fatty alcohols. They were produced in a sytem containing the soluble enzymes, pteridine,

* Abstract for Seventh International Congress of Biochemistry, Tokyo, Japan, August 19–25, 1967. (Material from the dissertation for the Ph.D. degree of R. C. Pfleger.)

† Oak Ridge graduate fellow under appointment with ORAU.

‡ From the Department of Medicinal Chemistry, University of North Carolina, Chapel Hill, N. C.

1027283

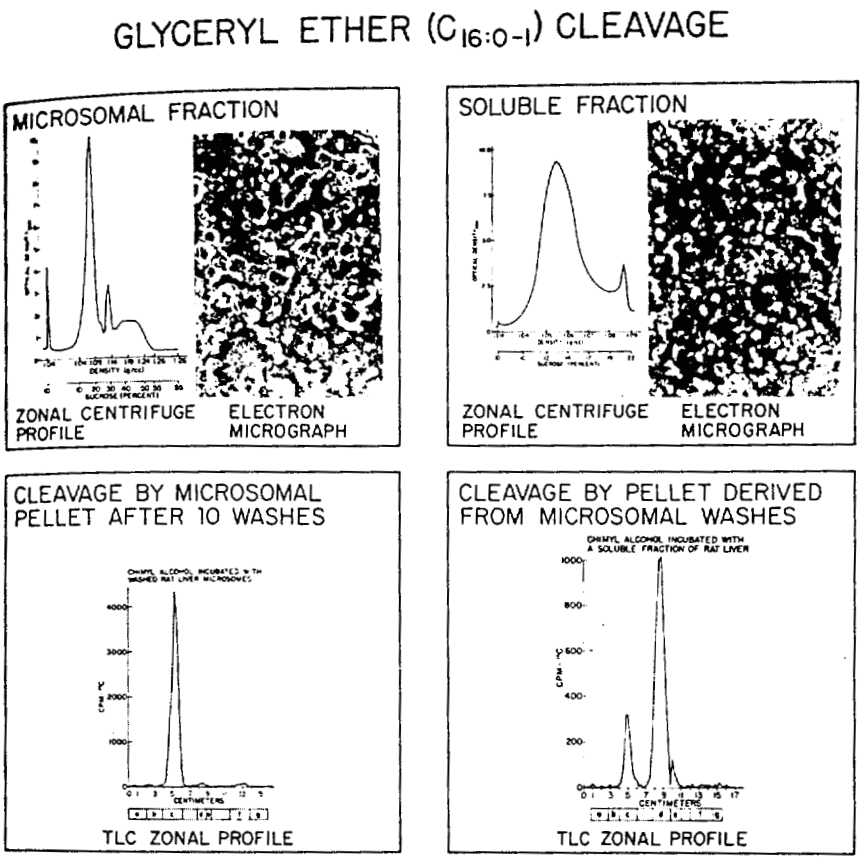

Fig. 71. The biocleavage of 1-^{14}C-chimyl alcohol (2-^{3}H-glyceryl) by a soluble enzyme fraction of rat liver. The zonal centrifuge profile indicates (1) floating lipid at 1.04 density, (2) soluble protein at 1.04–1.08 density, (3) smooth-surfaced microsomes at 1.14 density, (4) rough-surfaced microsomes at 1.14–1.24 density, and (5) material having the same density as red cell ghosts at 1.08–1.09 density. The electron micrograph at the left shows the presence of microsomes and at the right the presence of only soluble protein. The TLC zonal profile show the intact chimyl alcohol peak at 3–6 cm, the fatty acid peak at 7–9 cm, and the fatty alcohol peak at 10–11 cm.

NAD, glucose-6-PO_4, NADP, and glucose-6-P-dehydrogenase for generating NADPH. The palmitic acid formed from the $C_{16:0}$ glyceryl ether contined 98% of the ^{14}C in the fatty acid fraction. When we omitted NAD from the system, ^{14}C-labeled fatty aldehydes built up and ^{14}C-labeled fatty acids decreased *(Fig. 72)*; and we found more of the ^{14}C in fatty alcohols.

1027284

The NADPH required for the reduction of the pteridine cofactor involved in ether cleavage also appears to be required for the reduction of the fatty aldehyde to the alcohol. Only the liver and intestine possess significant quantities of the ether-cleaving enzyme, and its activity varies considerably according to species.

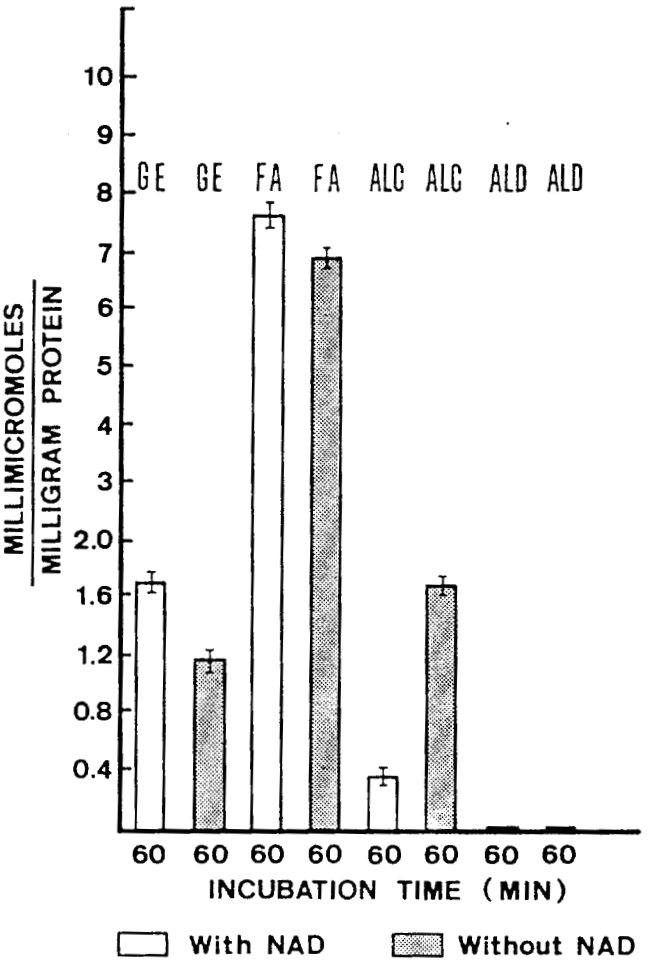

Fig. 72. The formation of fatty acids, fatty alcohols, and fatty aldehydes in the presence and absence of NAD during the biocleavage of the 1-isomer of doubly labeled (^{3}H, ^{14}C) alcohol by a soluble enzyme system isolated from rat liver. The incubation period was one hour. Symbols: GE—glyceryl ether [1-chimyl-1-^{14}C-(2-^{3}H-glycerol)-alcohol], FA—fatty acid, ALC—fatty alcohol, ALD—fatty aldehyde, and NAD—nicotinamide adenine dinucleotide.

1027285

ACKNOWLEDGEMENT

The authors are indebted to Norman G. Anderson, ORNL Biophysical Separations Laboratory, for permitting us to use the zonal centrifuge, and to W. W. Harris, ORNL, for the preparation and interpretation of the electron micrographs.

REFERENCES

1. Snyder, F. and Pfleger, R. C. Metabolism of α-alkoxy glyceryl monoethers in rat liver, *in vivo* and *in vitro*. Lipids 1, 328–334, 1966.
2. Tietz, A., Lindberg, M., and Kennedy, E. P. A new pteridine-requiring enzyme system for the oxidation of glyceryl ethers. J Biol Chem 239, 4081–4090, 1964.

Volume Distribution of Normal and Leukemic Human Lymphocytes

C. C. Lushbaugh, F. Goswitz, Martha L. Clevenger, and Dorothy H. Lushbaugh

Measurements of cellular volume based on the Coulter principle allow cellular populations to be studied with statistical and mathematical methods that define the population variance more precisely than has been previously possible. The true *in vivo* distribution of size variance of any cellular population of course cannot be measured because our present techniques are inadequate. Although the Coulter method measures *in vitro* cellular suspensions whose cellular volumes have been altered to an unknown degree by methods of collection, counting medium, physical trauma, chemical concentrations, etc., it appears to be freer from artifactually introduced, uncontrollable changes in these volumes than any other method. Kubitschek[1] and Van Dilla[2] have introduced modifications of many of the originally proposed aperture currents, aperture sensor diameters, and fluid driving pressures,[3] that appear to improve the resolution of the system without necessitating the use of high-aperture currents as suggested by Lushbaugh.[4–6]

Using high-aperture currents, standard equipment, and conditions used in clinical hematology laboratories for making blood counts, we can, however, obtain highly reproducible frequency distributions of blood cell volumes with small coefficients of population size variance. The use of a large-aperture diameter (100 microns) also avoids the plugging that is frequently experienced with apertures less than 50 microns in diameter. In addition, the high-aperture current defines a second subpopulation of

1027286

large RBC that appears to reflect electrically induced permeability changes in an immature RBC population. Mature RBC do not show this capability. The single, normally skewed distribution of lymphocyte populations shown here with the use of the same conditions that produce bimodal RBC population distributions supports the contention that the latter appearance is a physiologic phenomenon of the RBC rather than a systems artifact.

In this study, normal human lymphocytes were sized after collection from thoracic duct lymph into: (1) empty heparinized tubes; (2) an equal volume of heparinized and 0.9% saline at pH 6.7; (3) an equal volume of heparinized Eagles culture medium; and (4) an equal volume of 2.5% glutaraldehyde in 0.9% saline at pH 6.7. About 30 min after collection the cell suspensions were diluted in the usual way with 0.9% saline at pH 6.7 and sized with the pulse-height analyzer system *(Table 30, Fig. 73)*.

Lymphocytes from five patients with chronic lymphocytic leukemia

TABLE 30

Parameters of Cellular Volume Distribution of Normal Human Lymphocytes From Thoracic Duct Lymph

Lymph Collected Into:	Incidence at Modal Size	Cellular Volume		Coefficients		Volume Ratio
	F(max.) (percent/ch)	Mode (channel)*	Mean	Variance (δ/μ)	Skewness (γ)	L/RBC
1. Heparin only	6.61	36	42	0.14	0.25	2.4
2. Heparin and 0.9% Saline (pH 6.7)	7.78	36	40	0.12	0.27	2.1
3. Heparin and Eagles Medium	7.43	36	40	0.12	0.28	2.0
4. 2.5% Glutaraldehyde and 0.9% Saline (pH 6.7)	5.43	38	44	0.15	0.30	2.1

*Pulse-height analyzer channel $\simeq 4.8\mu^3$

were also studied. The lymphocytes were selectively concentrated in the suspensions by means of sedimentation and centrifugation as described elsewhere in this report.[7]

In *Table 31*, the initial lymphocyte counts, differential percentages, and lymphocyte concentration and residual RBC "contamination" finally obtained are shown under *A. Hematologic Measurements*. When the cells were sized by the Coulter method this RBC residuum was deleted from the lymphocyte population profiles by means of the well-known system of "background-erase" of the pulse-height analyzer. The results are

1027287

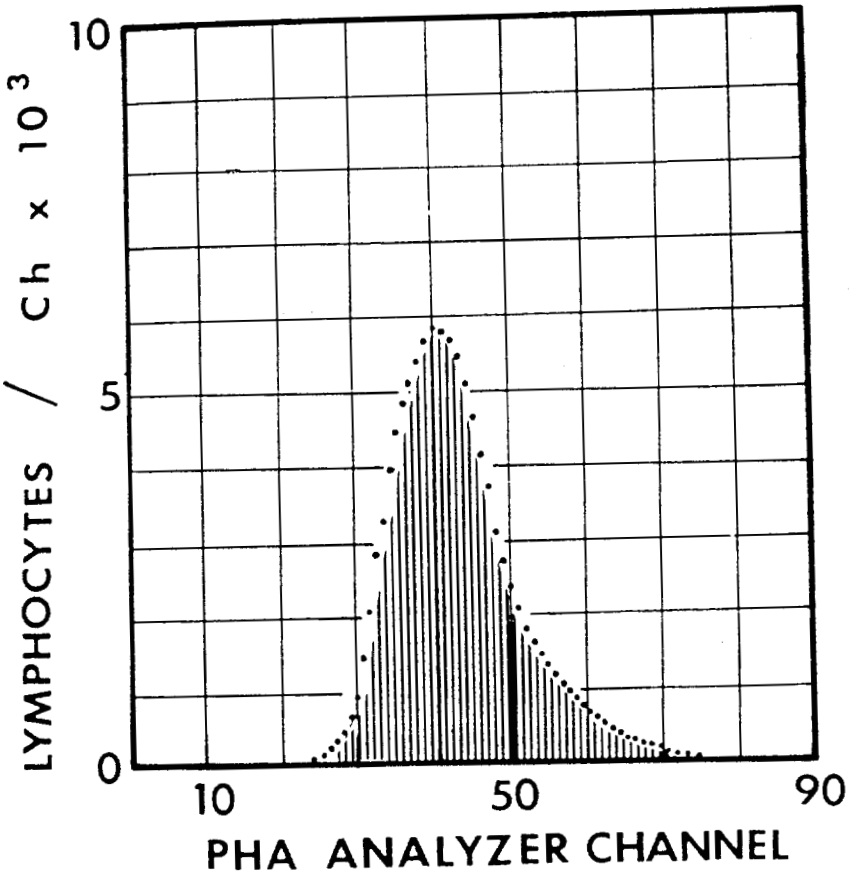

Fig. 73. Histogram of frequency of lymphocytic volumes (normal thoracic duct lymphocytes) shown as lymphocytes/pulse height analyzer channel under conditions where one channel $\simeq 4.48\mu^3$.

shown under *B. Cell-Size Measurements* in *Table 31*. The ratio of the modal lymphocyte to the modal RBC size shown as the L/RBC ratio, ranges from 2.0 to 2.4 and averages about 2.2. Variance and degree of skewness of the leukemic lymphocytes were only slightly increased above normal in some of the samples. These differences are probably not significant in view of the different method of preparation and collection used. The lower frequency of cells of the modal size and the occurrence of the mode and mean in a larger channel are significant differences, and they indicate that the leukemic lymphocytes were slightly (about $30\mu^3$) larger than the normal ones from the thoracic duct. Further study is required to

1027288

determine whether this difference reflects the "leukemic" change, the different millieu, or the different procedures. We are inclined to believe from this study that the lymphocyte of chronic lymphatic leukemia shows no real difference from the normal in size and frequency distribution of cell volumes.

The parameters of population size distribution defined here for lymphocytes from the thoracic-duct lymph of a normal person and those from the blood of five patients with chronic lymphatic leukemia correspond well with those reported recently for lymphocytes as "leukocyte peak I" in the blood of a normal person by Van Dilla and Hardin.[8] The agreement is particularly remarkable in view of the different sizing systems and different RBC size distributions we used for reference in determining the mean volume of the lymphocyte relative to RBC. Only the lymphocytes from Patient 1 exceeded the range (0.10–0.20) of the coefficient of cell population volume variance suggested as being normal by Kubitschek according to Van Dilla.[8] The coefficients of variance of other lymphocyte population distributions were tightly grouped about 0.14

TABLE 31

Parameters of Cellular Volume Distributions of Chronic Lymphatic Leukemic Lymphocytes Collected by Sedimentation and Centrifugation

A. Hematologic Measurements

Patient	WBC ($\times 10^3/mm^3$)	Lymphs (%)	Smudges (%)	Concentration Lymphs/RBC ($\times 10^4/mm^3$)
1	125	99	29	837/930
1	350	99	36	440/42
2	16	88	84	19/2
3	78	89	18	57/9
4	124	98	16	74/131
5	138	96	13	16/9

B. Cell Size Measurements

Patient	Incidence at Modal Size	Cellular Volume		Coefficients		Volume Ratio
	F(max.) (%/ch)	Mode (channel)*	Mean	Variance (δ/μ)	Skewness (γ)	L/RBC
1	3.22	43	51	0.22	0.35	2.2
1	3.53	43	50	0.20	0.34	2.2
2	5.16	41	47	0.12	0.28	2.4
3	4.47	40	47	0.15	0.28	2.2
4	5.02	37	43	0.14	0.21	2.1
5	4.46	38	45	0.16	0.37	2.1

*PHA Channel $\simeq 4.8\mu^3$

1027289

(range 0.12 to 0.16). In all patients but one (Patient 4) the distribution of volumes of lymphocytes was slightly more skewed than that described for normal human blood lymphocytes. This increased skewness probably results, however, from the known presence of (3 to 4%) granulocytes in these concentrated samples and is not necessarily a characteristic of leukemia lymphocytes.

REFERENCES

1. Kubitschek, H. E. Electronic measurement of particle size. Research 13, 128–135, 1960.
2. Van Dilla, M. A., Basmann, N. J., and Fulwyler, M. J. Electronic cell sizing: I. Effect of aperture current. II. Influence of physical phenomena on measured spectra: III. Erythrocytes. Los Alamos Scientific Laboratory Report LA-3132-MS, 1964, pp. 182–204.
3. Brecher, G., et al., Size distribution of erythrocytes. Ann N Y Acad Sci 99, 242–261, 1962.
4. Lushbaugh, C. C., Maddy, J. A., and Basmann, N. J. Electronic measurement of cellular volumes. I. Calibration of the apparatus. Blood 20, 233–240, 1962.
5. Lushbaugh, C. C., Basmann, N. J., and Glascock, B. Electronic measurement of cellular volumes. II. Frequency distribution of erythrocyte volumes. Blood 20, 241–248, 1962.
6. Lushbaugh, C. C. and Lushbaugh, D. B. Rapid electronic red blood cell sizing as an aid in clinical diagnosis. Southern Med J 28, 1208–1212, 1965.
7. Goswitz, F. and Snyder, F. Lipid composition of the blood lymphocyte in chronic lymphocytic leukemia (this report).
8. Van Dilla, M. A. and Hardin, J. M. Volume distribution of normal human erythrocytes and leucocytes. Los Alamos Scientific Laboratory Report LA-3610-MS, 1966, pp. 234–238.

1027290

Instrument Development and Methodology

The Medical Division's research efforts require new tools and new methods, some of which must be designed by the investigator for the particular problem at hand. Investigators at the Medical Division are fortunate to have the excellent shop facilities of the ORAU Technical Services Department and consultation with experts in other laboratories in Oak Ridge.

These endeavors are essential to our research, and some results may be useful to investigators elsewhere. One objective is to develop and apply refined instrumentation for detecting and localizing radioactivity to meet specific needs in the research effort. Examples have been scanning systems, whole-body counting facilities, and other detection apparatus for quantitating the radioactivity in an organ. Some developments are not directly related to measurement of radioactivity.

An Automated System for Sample Collection and Computer Analysis of Thin-layer Radiochromatograms*

F. Snyder and Donna Bibler

An automatic scraper for collecting minute zones of absorbent along thin-layer chromatographic lanes for subsequent radioisotopic or chemical measurements has now been combined with a direct data acquisition system. Remotely located liquid scintillation spectrometers transmit their data by means of a dedicated telephone circuit to an IBM 026 Card Punch in our data processing center.

Programs using an IBM 7090 computer, and a Benson-Lehner Electroplotter have been developed, providing radiometric analysis of small (1- and 2-mm) and large TLC zones, and graphically producing exact scaled replicas of the radioisotopic distribution along the chromatographic lanes from the punched-card data. The programed analysis includes the conversion of counts per minute to disintegrations per minute, the com-

* Abstract of article published in *Separation Science* 1, 709–722, 1966, and presented at the ACS 19th Annual Summer Symposium on Separation Techniques, Edmonton, Canada, 1966.

1027291

putation of the radioisotopic distribution on chromatograms, recovery of activity from TLC plates, and determination of specific activity. Application of this system of analysis is illustrated for the separation of synthetic derivatives of ^{14}C-labeled glyceryl ethers and of products of a lipase-catalyzed reaction *(Fig. 74)*

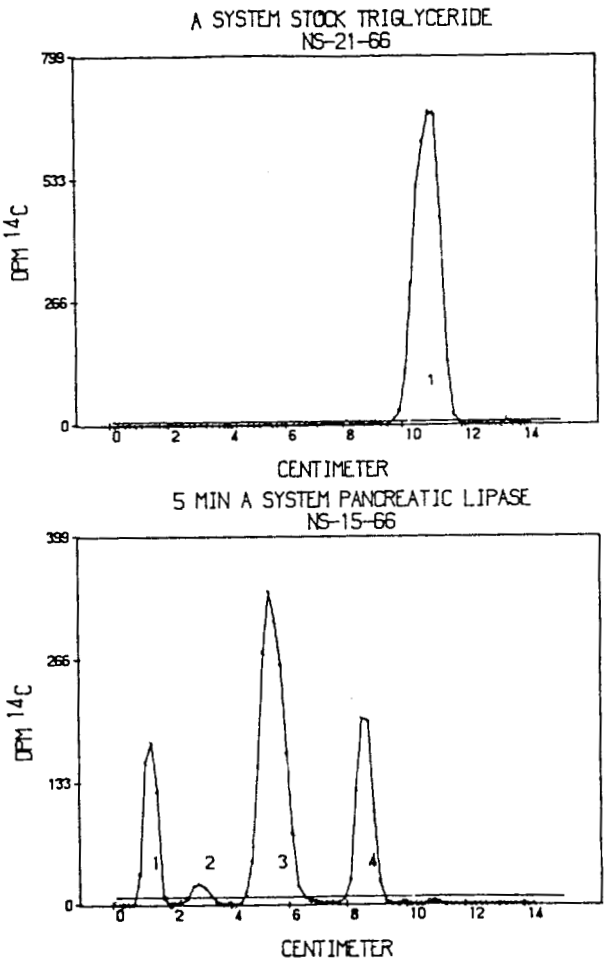

Fig. 74. Carbon-14 zonal scans of a lipase catalyzed reaction involving ^{14}C-carboxy-labeled tripalmitin. The upper scan shows the purity of the substrate before lipase attack. The lower scan shows the products obtained after a 5-min. incubation at 37°: (1) monopalmitin; (2) dipalmitin; (3) palmitic acid; (4) tripalmitin. Chromatographic development: Separations were made in a solvent system of hexane: diethyl ether: acetic acid (80:20:1 v/v/v).

1027292

An Improved Probe for Detecting Radioactivity at Surgery

A. C. Morris, Jr.

In the study of thyroid disease, a surgical probe detector is needed to seek out bits of functioning and metastatic tissue. For the past 10 years we have used a surgical probe developed by C. C. Harris and others of the Medical Nuclear Instrument Development Group, Oak Ridge National Laboratory. This probe has become unreliable owing to its age, and a newer miniaturized version with transistor circuitry is under development. It uses a small cesium iodide crystal measuring 0.220 in. in diameter by 3/8 in. long, mounted in the end of a long, 1/4 in.-diameter tube. Surrounding the detector crystal is an annular-shaped collimator made of a high-Z material that may be applied or removed depending on the requirement of the surgeon.

Light induced by gamma or beta rays in the cesium iodide detector is coupled back through a light pipe to a miniature, 1/2 in.-diameter photomultiplier tube. The main part of the probe contains the voltage-divider network for the photomultiplier tube and the high-voltage decoupling circuitry. The preamplifier, however, now is located remotely so that the probe can be kept small *(Fig. 75)*. By suitable decoupling circuitry, both

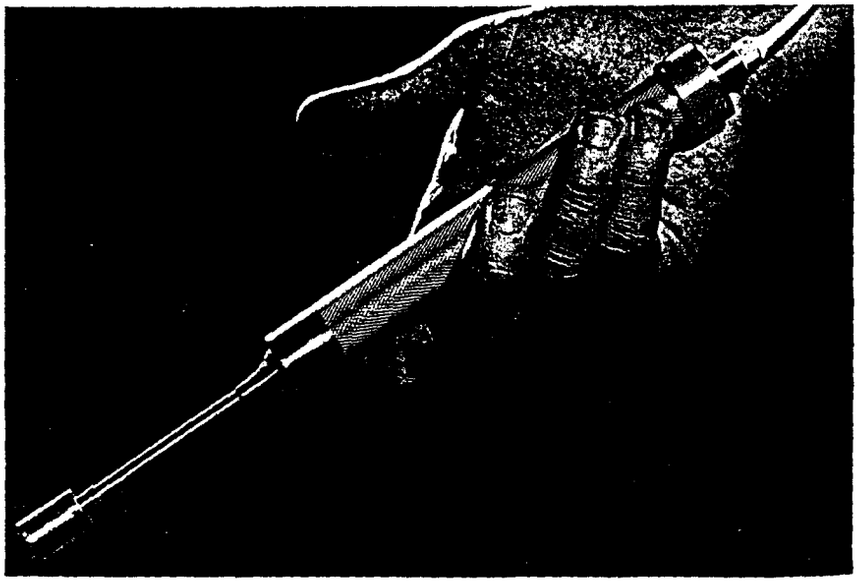

Fig. 75. Miniaturized surgical probe unit.

1027293

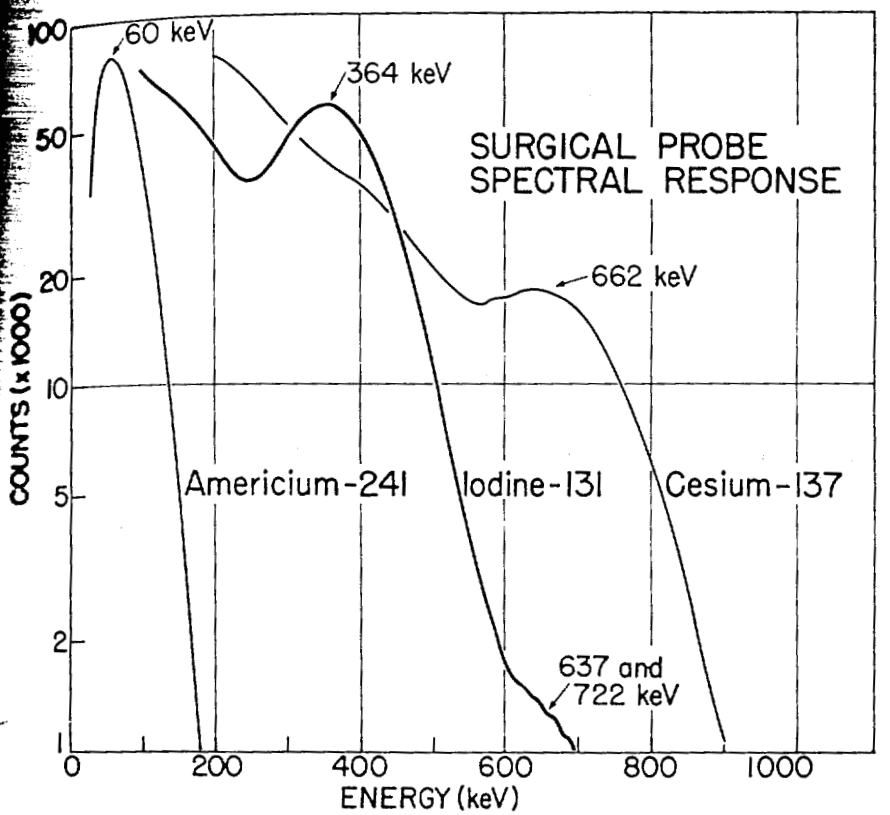

Fig. 76. Spectral response of the new surgical probe.

the high-voltage supply to the probe and signals from the probe are carried on one coaxial cable. A charge-type preamplifier at the instrument end of the cable removes the electrical signals generated by the photomultiplier tube. A 12-ft cable length can be used without deleterious signal effects. The unit is undergoing operational tests.

The spectra in *Fig. 76* show the output of this probe from three different radioisotopes; the response to americium-241 is quite sharp but, because of the small crystal size, there is a degradation in peak response as one goes to the higher energies of ^{131}I and ^{137}Cs. The response to ^{131}I is most important because it is the major isotope used for our thyroid surgery; it is about as good as can be expected with the small crystal and long light pipe. Further tests will be made on the probe's sensitivity to position and magnetic fields, and to its ability to withstand immersion in antiseptic solutions.

1027294

Other work is now being directed toward assembling the external amplifying and audio-pitch control circuits for use with this probe. This external circuitry will signal the presence of radioisotope concentrations to the surgeon by means of a rising audio pitch, permitting him to hear the response of the probe.

Absolute Leukocyte Differential Counts by Rapid Electronic Sizing

Dorothy H. Lushbaugh, C. L. Edwards, and C. C. Lushbaugh

A procedure has been developed for making absolute leukocyte differentials with the use of an electronic Coulter transducer and a pulse-height analyzer system. The entire determination requires 15 min and can be completely automated. The results can be displayed photographically so normal and abnormal distribution patterns can be recognized instantly without resort to mathematical analysis.

Twenty lambda of heparinized whole blood is diluted to 100 ml with normal saline (1:5000 dilution) buffered at pH 6.7. We then add 0.6 ml of a detergent solution.* Ten minutes are allowed to elapse for complete hemolysis to occur. The remaining white blood cell suspension is then passed at a standard rate of 1 ml/26 sec for 3 min through a 100 μ in diameter Coulter-sensor aperture through which a 2.85 mA current is being generated. The electrical pulses caused by increase in resistance as WBC pass through the aperture are analyzed after pulse shaping† and stored in a 100-channel memory bank of a 400-channel pulse-height analyzer.‡

The numbers of cells counted per channel are printed out automatically, are displayed as the frequency distribution of WBC volumes on an oscilloscope, and are photographed.¶ The counts per channel are printed out automatically if a numerical record is desired.

To avoid sizing a variable number of erythrocytic ghosts and debris, the sensitivity of the pulse-height analyzer is adjusted so that no pulses

---

* Blood diluent, WBC, detergent type—Fisher Scientific Co.
† RIDL (Nuclear Chicago) pulse shaper, amplifier, and discriminator module.
‡ RIDL (Nuclear Chicago) 400-Channel Pulse-Height Analyzer.
¶ Polaroid Corporation Land Camera, Film #3000.

1027295

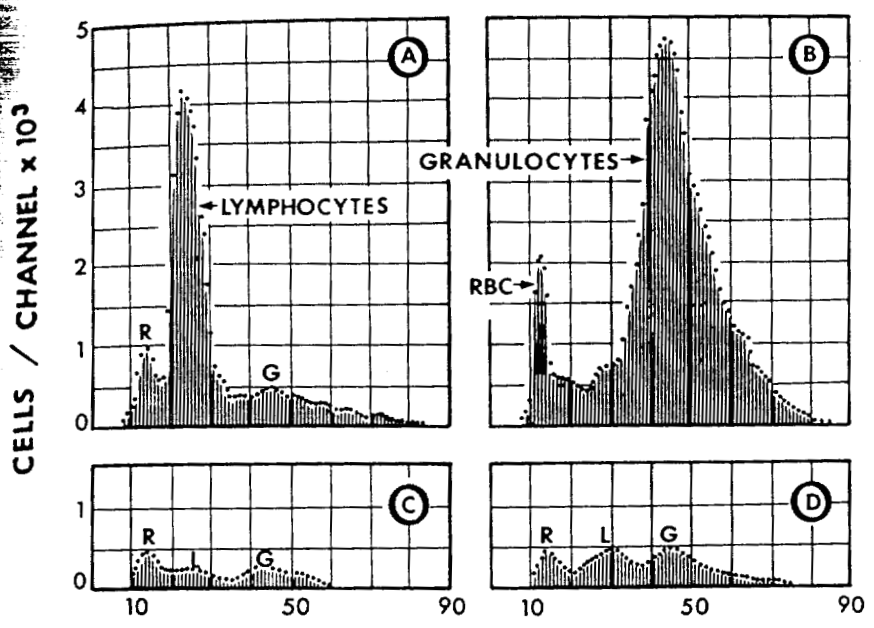

Fig. 77. Electronically produced "absolute leukocyte differentials": (A) chronic lymphocytic leukemia; (B) chronic granulocytic leukemia; (C) low normal white blood cell count; and (D) high normal white cell count. The RBC debris peak has been truncated in each.

are stored in the first 10 channels. With the suggested cell dilution and a fluid driving pressure of ≃ 12 mm Hg, the dead time of the pulse-height analyzer will vary between 4 and 9%, depending on the WBC count. Under these conditions, losses in cell sizing and counting due to coincidence of particles in the aperture do not alter the population profiles enough to interfere with practical usefulness.

In *Fig. 77*, four typical absolute WBC differentials (frequency cell-volume distributions) are shown as counts per 3 min per channel in (A) a patient with chronic lymphocytic leukemia in relapse; (B) a patient with chronic granulocytic leukemia in relapse; (C) a normal person; and (D) a patient with an increased WBC count but normal differential.

1027296

All distributions are bimodal if the peak of RBC debris around Channel 11 is ignored. The first population of WBC of smaller volume is composed principally of lymphocytes, the second one granulocytes and monocytes. The distributions in each are skewed toward the higher channels so that mean cell volume does not correspond to the modal volume.

These results indicate that this procedure generates clinically useful information concerning the number and kinds (sizes) of WBC present per cubic millimeter. The technique displays graphically the absolute WBC differential count as total lymphocytes versus granulocytes plus monocytes in a way that could also be calculated from a differential count of a Wright-stained blood film done microscopically, and the total white blood cell count per cubic millimeter. The amount of technical effort in the two procedures is, however, vastly different; very little is expended with the electronic automated system that produces an approximate answer graphically and numerically without need for staining, counting, calculating and transcribing.

The detergent solution hemolyzes the RBC and reduces both lymphocyte and granulocyte volume by a factor of about 2.5 and is used here to keep the technique simple by obviating changes in aperture current, amplification settings, aperture sizes, etc., from those commonly used in a hospital clinical laboratory doing Coulter blood-cell counting.

1027297

Automated Hemolyzometers

The next two reports are related and have the same bibliography.

To minimize laboratory delay in data production for rapid detection of RBC abnormalities, automated devices that determine RBC osmotic fragility can decrease the usual 24- to 48-hr time requirement for this determination to less than 30 min. A commercial device[1] available for making such rapid determinations has proved application in detecting "outdated" blood in blood banks but uses a minute membranous diffusion chamber that prevents simultaneous determination of other end points such as measurement of ^{59}Fe, ^{51}Cr, or ^{32}P liberation. The studies reported here record our progress in satisfying this need for an automated RBC osmotic-fragility measuring system that is rapid, automatic, precise and easy to analyze, and where many measurements can be made simultaneously upon the RBC hemolysate.

A. Automated RBC Osmotic Fragility Measurements Using a Linear-gradient Device

A. M. Webb and C. C. Lushbaugh

Previously[2] we reported a semiautomated device for determining RBC osmotic fragility. The saline concentration in the RBC exposure chamber decreased logarithmically with time because of the constant fluid-pumping rate used. Because a linearly decreasing gradient would effect a hemolysis rate more easily analyzed mathematically, a mixing device such as is used in elution chromatography[3] was designed to produce such a gradient for RBC exposure. The dilution device consists of two chambers separated by a slanting partition and connected to a common discharge tube. The slanted partition determines the cross-sectional area and volume of solution delivered by each chamber. When liquid is slowly withdrawn through the discharge tube, the salt concentration is determined by the relative volume contributed by each chamber. When two solutions of similar specific gravity but different concentration are placed in the chambers, the more concentrated solution can be decreased linearly at any rate in respect to time. *Figure 78* depicts three linear gradients produced with three commonly used types of solutes: a radioactive tracer (^{131}I), saline solution, and a dye ($KMnO_4$).

1027298

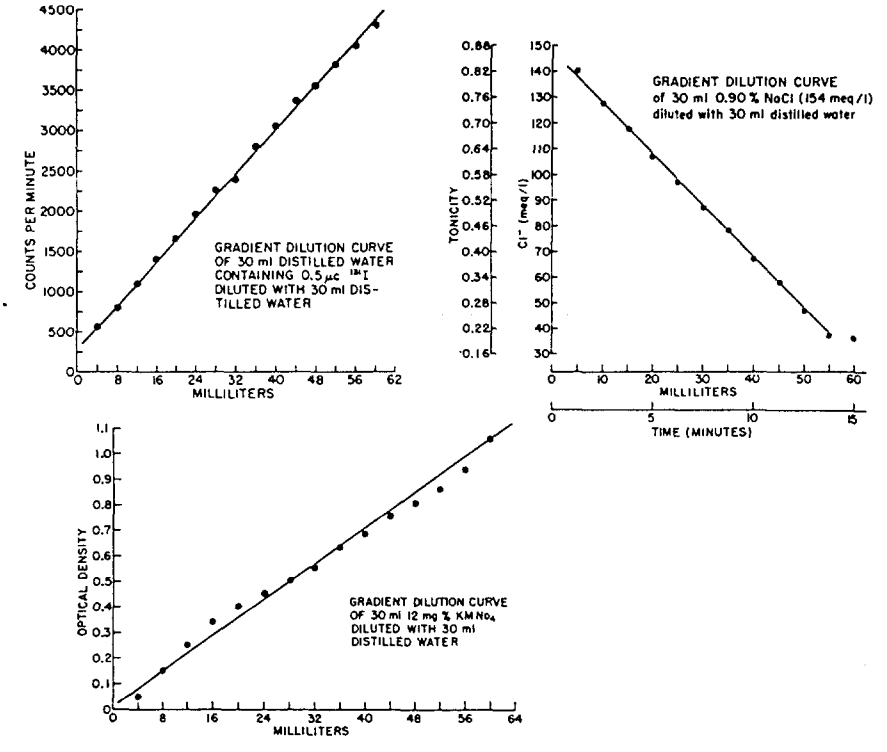

Fig. 78. Solutions of similar specific gravities show linearly decreasing concentrations using the linear gradient dilution device.

An automated system was then designed with mixing coils, constant-flow pumps, a flow-cell colorimeter and a strip chart recorder with this gradient chamber; it provides completely automatic determination of osmotic fragility *(Fig. 79)*.

Commercially available bottles of normal saline and distilled water (prepared for intravenous injection) are connected to the dilution device by lengths of tubing. The bottles are inverted in a ring stand to permit gravity filling of the chambers. Stopcocks attached to the discharge tubes facilitate the filling of the chambers and prevent intermixing of the solutions before the start of the analysis. Each chamber is filled separately to the overflow mark with its solution and the stopcock is closed. Approximately 8 ml of blood is placed in the sample mixing cup and mixed very slowly to prevent sedimentation of the cells. The recorder connected to the colorimeter has a 630-millimicron interference filter and is set at 50% transmission with distilled water.

1027299

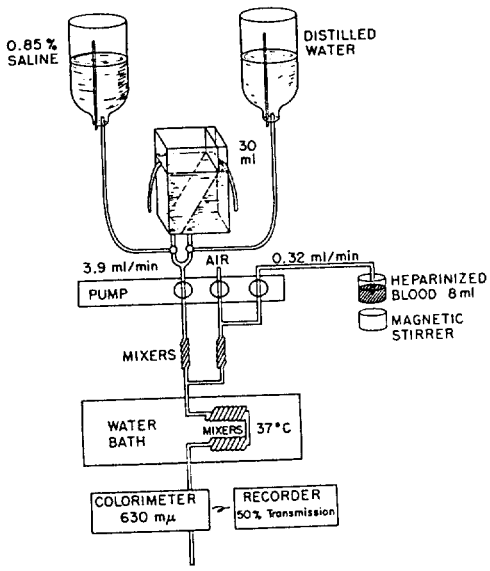

Fig. 79. Flow diagram and components used in the automatic determination of erythrocyte osmotic fragility.

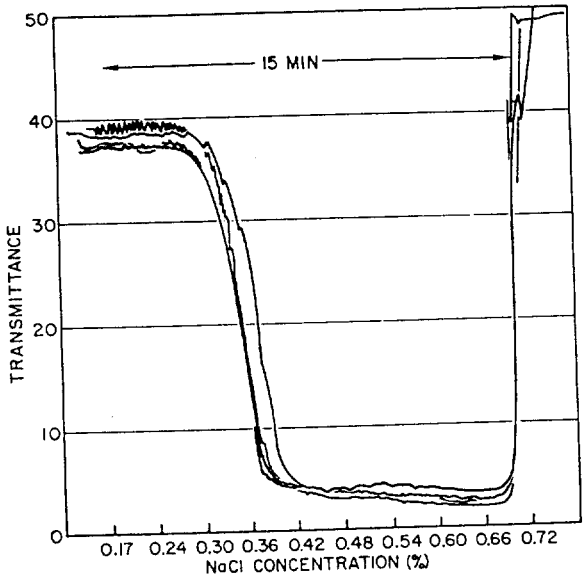

Fig. 80. Reproducibility of four analyses of the same blood.

1027300

The stopcocks of the discharge tube are opened simultaneously and the pump is started. The colorimeter readings are recorded continuously until all the diluent has passed through the colorimeter. The per cent transmission is recorded as a function of time, beginning with no hemolysis and a minimal transmission and proceeding to a maximal reading, indicating total hemolysis. The determination is complete within 15 min, and after a fast rinse of the system with distilled water or saline, the next determination can be started.

The time base of the strip chart is transformed to saline concentration units by chloride determinations on samples collected at appropriate time intervals. Repeated analyses show that with this system the RBC are exposed at first to a saline concentration of 0.72% that decreases linearly to 0.17% in 15 min.

Typical fragility curves produced with four different samples of the same normal blood are shown in *Fig. 80*. A shift of the rising curve to the left or right would indicate increased or decreased RBC resistance to hemolysis. From this tracing a precise estimate of the saline concentration that causes hemolysis of 50% of the RBC sample can be determined by graphic probit regression analysis. For all practical purposes, the time (or saline concentration) corresponding to one-half of maximum light transmittance is a good estimate of mean corpuscular fragility.

B. Micro Osmotic Fragility System for the Nonautomated Laboratory

A. C. Morris, Jr. and C. C. Lushbaugh

Our previous automated hemolyzometers[2,4] have required 2 to 8 ml of blood, a volume that precludes using the methods often when the patient is anemic or when the animal being studied is small. We have, therefore, developed a "lysing chamber" consisting simply of a Millipore* filter assembly and filters to hold a minute blood sample in the stream of a decreasing saline gradient. Such a chamber inserted in line with the effluent from the gradient chamber[4] would reduce the required RBC sample size almost a millionfold and still permit simultaneous measurements of light transmission, hemoglobin content and radioactivity of the hemolysate effluent.

In evaluating the use of this filter system as a lysing chamber, an *in vitro* test system was designed that is proving to have unexpected labora-

* Millipore Corp., Bedford, Mass.

1027301

discharge tube are opened simultaneously and colorimeter readings are recorded continuously passed through the colorimeter. The per cent s a function of time, beginning with no hemolyission and proceeding to a maximal reading, The determination is complete within 15 min, system with distilled water or saline, the next ed.

ip chart is transformed to saline concentration itions on samples collected at appropriate time es show that with this system the RBC are oncentration of 0.72% that decreases linearly

produced with four different samples of the vn in *Fig. 80*. A shift of the rising curve to the increased or decreased RBC resistance to a precise estimate of the saline concentration % of the RBC sample can be determined by nalysis. For all practical purposes, the time orresponding to one-half of maximum light nate of mean corpuscular fragility.

---

ity System for the Nonautomated

shbaugh

emolyzometers[2,4] have required 2 to 8 ml ludes using the methods often when the e animal being studied is small. We have, g chamber" consisting simply of a Millirs to hold a minute blood sample in the gradient. Such a chamber inserted in line lient chamber[4] would reduce the required ionfold and still permit simultaneous meas- hemoglobin content and radioactivity of

s filter system as a lysing chamber, an *in* hat is proving to have unexpected labora-

1027302

tory usefulness as well as requiring no other equipment than a test-tube rack, test tubes, Millipore-filter holder for syringes, Millipore filters and prefilters, and a 10-ml syringe that has an easily moving plunger *(Fig. 81)*. A 100-gram weight placed on the plunger of the loaded syringe produces a flow of solution that does not cause mechanical damage to RBC. Typical frequency polygons of amount of hemolysis (optical density at 415 mμ) in relation to saline concentration are obtained that define normo- hyper- and hyposensitive RBC populations *(Fig. 82)*. The unusually increased sensitivity of RBC to hemolysis in this system seems to be caused by: (1) the abrupt stepwise changes in saline concentration we used; and (2) the presence of wetting agents such as Triton X-100 in the Millipore filters.[5] This discrepancy does not, however, alter the usefulness of the method in defining relative osmotic fragility for most clinical purposes.

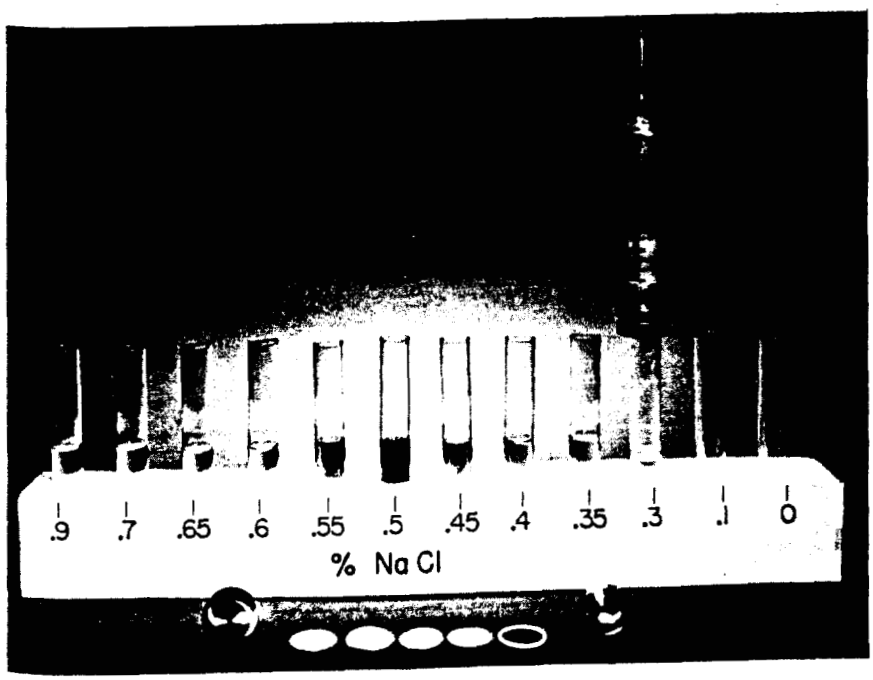

Fig. 81. Photograph of the micro osmotic fragilometry system in operation: 10 ml of 0.3 NaCl solution is being pushed at constant rate through the lysing chamber into the appropriately labeled test tube. The tube at 0.5 NaCl with highest hemoglobin concentration measured by colorimeter defines maximum hemolysis per change in saline concentration. The separate components of the lysing chamber, a Millipore filter assembly, are shown in the foreground.

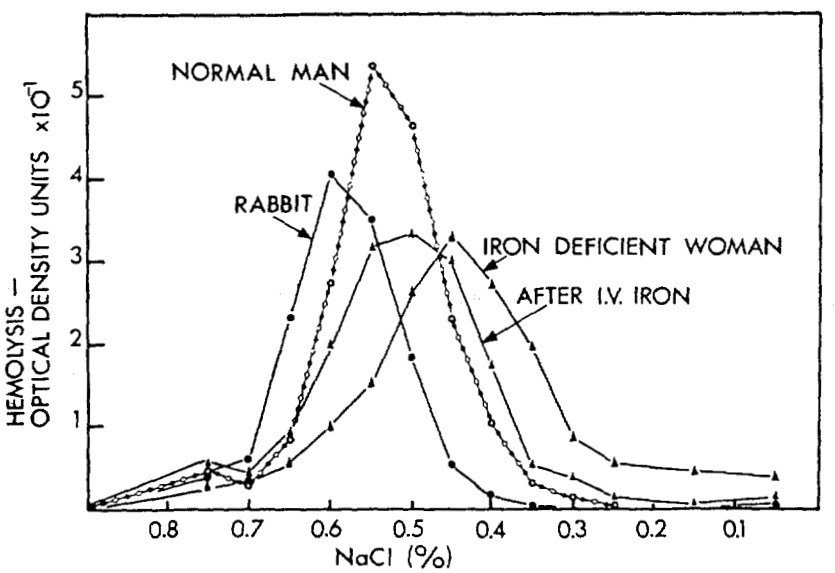

Fig. 82. Frequency polygons of the amount of hemolysis produced progressively with 10 ml washes of decreasing NaCl concentrations using four blood samples that show decreased, normal and increased osmotic resistance by this method.

REFERENCES

1. Danon, D. A rapid micro method for recording red cell osmotic fragility by continuous decrease of salt concentration. J Clin Path 16, 377–382, 1963.
2. Morris, A. C., Jr., Lushbaugh, C. C., Lushbaugh, D. H., and Corley, R. H. A rapid electronic method for measuring red-cell fragility in hemolytic systems. USAEC Report ORINS-53, 1965, pp. 149–154.
3. Bock, R. M. and Ling, N-S. Devices for gradient elution in chromatography. Anal Chem 26, 1543–1546, 1954.
4. Webb, A. and Lushbaugh, C. C., A. Automated RBC osmotic fragility measurements using a linear-gradient device (this report).
5. Cahn, R. D. Detergents in membrane filters, Science 155, 195–196, 1967.

Correction of Whole-body Counting Retention Studies with Radioisotope Tracers

W. D. Gibbs, H. D. Hodges, and C. C. Lushbaugh

The initial whole-body count after the ingestion or injection of a radioactive tracer is usually used as the 100% reference point for subsequent

1027303

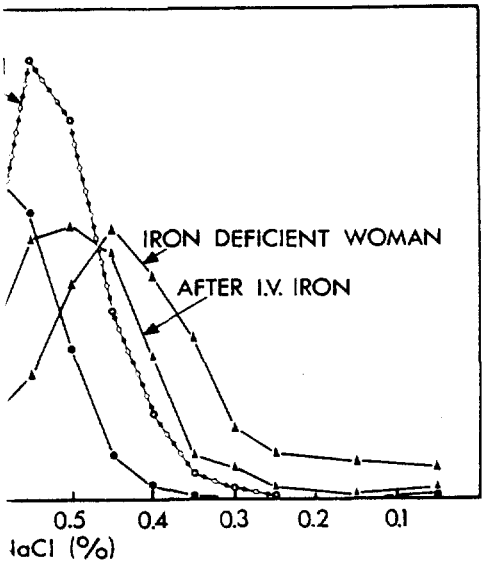

e amount of hemolysis produced progressively reasing NaCl concentrations using four blood sed, normal and increased osmotic resistance

for recording red cell osmotic fragility by continuous in Path 16, 377–382, 1963.
C., Lushbaugh, D. H., and Corley, R. H. A rapid l-cell fragility in hemolytic systems. USAEC Report

ices for gradient elution in chromatography. Anal

A. Automated RBC osmotic fragility measurements eport).
ine filters, Science 155, 195–196, 1967.

Counting Retention Studies

S

C. C. Lushbaugh

it after the ingestion or injection of a radio- the 100% reference point for subsequent

1027304

determinations. Erroneous final values can be produced by changes in counting efficiency resulting from changing distribution of the radioactivity in the body as time passes. The error in such determinations can be large as +50% if the initial count is erroneously low or −50% if the initial count is erroneously high. Various methods have been suggested for reducing and controlling the size of this error.[1] The most recent one[2] suggests that a small intravenous calibration dose of the tracer be counted in the subject before an oral dose is given. This method will provide correct results only when the oral dose becomes reasonably well diffused.

We have been developing a technique that will give correct results for the diffuse initial intravenous dose that becomes localized, as well as for the localized initial oral dose that becomes diffused. We have studied this problem with the use of radioactive point sources in man-sized compartmented water phantoms in a multicrystal whole-body counter.[3,4] Multichannel energy spectrum counts were made with a point source of ^{59}Fe located at 30 different positions in the phantom. The results when the counts in the photopeaks (1.0–1.4 MeV) are used are shown in *Table 32*,

TABLE 32

Per cent Response from ^{59}Fe Point Source in Water Phantom

Body Section	A. Peak Response*			B. Scatter Response†		
	Front (%)	Center (%)	Back (%)	Front (%)	Center (%)	Back (%)
Left Leg	134.9	132.4	154.2	101.1	109.0	112.1
Right Leg	136.8	128.0	151.3	103.9	107.6	110.6
Left Thigh	128.7	118.9	143.4	99.0	104.3	107.5
Right Thigh	131.4	119.0	141.1	101.0	103.4	103.4
Pelvis	123.2	102.1	141.9	98.3	103.0	107.5
Trunk	127.1	100.0	142.0	97.8	100.0	106.1
Neck	125.5	109.3	141.3	104.2	102.0	104.1
Head	136.7	108.2	143.8	99.6	99.6	104.8
Left Arm	134.4	125.5	134.1	102.0	106.5	105.8
Right Arm	137.1	137.2	129.7	103.9	109.7	104.9

*1.0–1.4 Mev
†0.6–1.0 Mev

expressed as per cent of the reference count obtained when the source is in the center of the trunk compartment. Differences of as much as +54% are observed. The table also shows our results when the counts in a specific portion of the Compton scatter (0.6–1.0 MeV) are used. With this alteration in counting method the maximum difference is only +12%. When these data are then corrected for the mass of each of the 10 phantom compartments, to simulate uniform distribution, the count difference

between a uniform distribution and a point source in the stomach is +28% with the photopeak counts but only +3% with the Compton scatter (0.6–1.0 MeV) as shown here.

REFERENCES

1. Lushbaugh, C. C. and Hale, D. B. Determination of absorbability of oral radioiron in health and disease in man by whole-body scintillometry. *In:* Radioactivity in Man (George R. Meneely and Shirley M. Linde, eds.), Springfield, Ill., Charles C Thomas, 1965, pp. 417–429.
2. Pollack, S., Balcerzak, S. P., and Crosby, W. H. Fe^{59} absorption in human subjects using total-body counting technic. Blood 28: 94–97, 1966.
3. Morris, A. C., Jr. and Ross, D. A. The design of a low-background whole-body counting facility. USAEC Report ORINS-51, January 1966, 49 pp.
4. Gibbs, W. D., Lushbaugh, C. C., and Morris, A. C., Jr. Preliminary efficiency and calibration studies with a new whole-body counter with an ultralow background shield. J Nucl Med 6, 337, 1965.

A 4π ^{32}P-Labeled Diisopropylfluorophosphate (DFP) in Blood

W. D. Gibbs and W. T. Pope

Although numerous commercial counters are available for measuring beta activity in a sample, none is highly efficient for measuring ^{32}P in a large sample of unhemolyzed, unbleached whole blood. Liquid scintillation counting systems are easily quenched by small amounts of opaque suspensions of cells or hemoglobin. End-window Geiger counters require drying the blood sample on planchets and have 2π (50%) counting efficiency at most. The canning metal of NaI crystals shields out most beta particle energies and makes the use of such systems impractical.

In addition to the inadequacies of these available electronic counting devices, the problem of assaying ^{32}P-labeled diisopropylfluorophosphate (^{32}P-DFP) as a red cell (RBC) label has the complication of low specific activity/RBC caused by the limited capacity of the RBC cholinesterase system for DFP and the low specific activity (200 to 250 microcuries ^{32}P/mgDFP) of commercially available ^{32}P-labeled DFP. The problem is complicated further if *in vitro* instead of *in vivo* RBC labeling is used; the resulting RBC activity then obtained is initially in the order of 2 nanocuries/ml of blood. In addition, the short half time of this RBC label (about 10 days) leads to the requirement of increasingly long counting times to maintain a predetermined statistical accuracy.

Since accurate quantitation of this small amount of beta activity is required for our purposes,[1,2] we need a system that will have high abso-

1027305

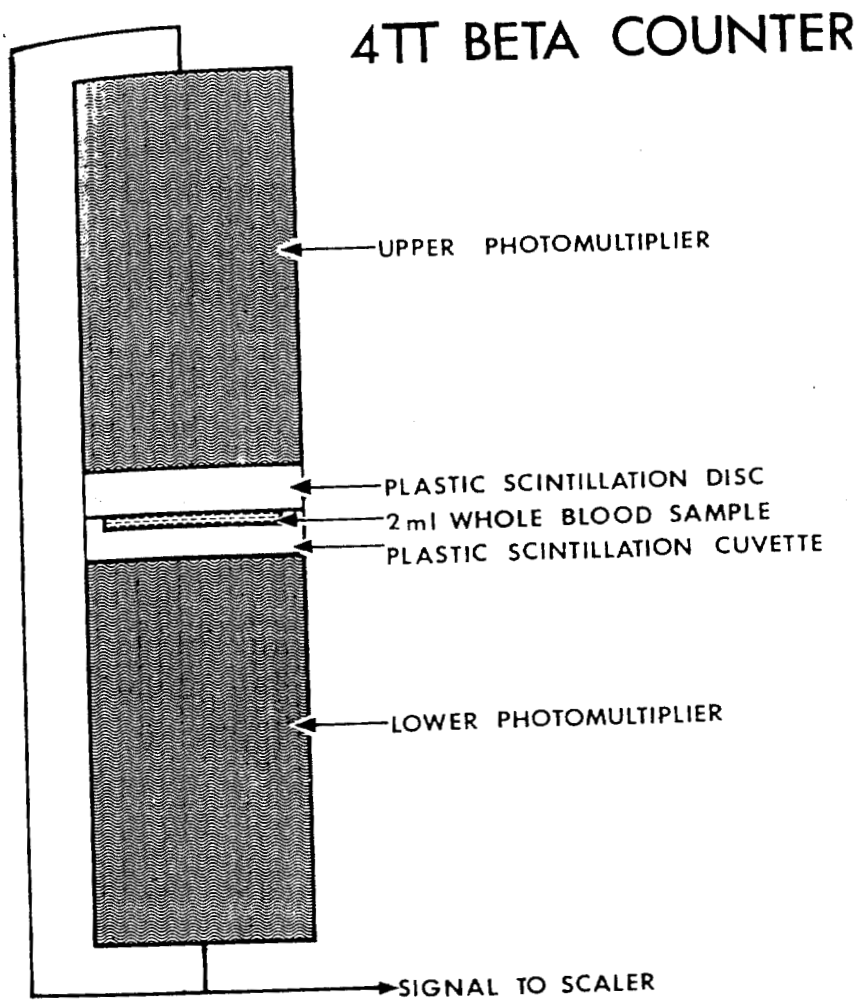

Fig. 83. Block diagram of 4π beta counter.

lute counting efficiency and will allow use of comparatively large volume samples of whole blood. We have developed an instrument that accepts samples as large as 2 ml and detects ^{32}P with an efficiency of 70 to 75%. *Figure 83* shows a block diagram of this device. It consists of two 2-in. diameter photomultiplier tubes (DuMont 6292), two 2-in. diameter discs (0.5 in. thick) of NE102 plastic scintillator and a scaler. The photomultipliers and plastic scintillators are enclosed in a light-proof lead shield. The combined outputs of the photomultipliers are put directly into a scaler.

1027306

With the photomultipliers used it is not necessary to have preamplification of the pulses from the photons produced by the ^{32}P beta particles in the plastic scintillator. The high voltage supply to the photomultipliers is interrupted by a switch that breaks the circuit when the shield door is opened for sample changing.

The upper photomultiplier can be manually moved in the vertical direction to allow samples to be changed. The upper disc of plastic scintillator (2-in. diameter × 3/8-in. thick) is optically coupled by silicone oil and permanently attached to the upper photomultiplier tube.

The lower detector disc is removable and has a depression 40 mm in diameter and 3 mm deep. This cuvette volume of 3.77 ml holds 2 ml of blood without its touching the upper detector surface.

Decontamination of this cuvette is accomplished easily because its inside surface is kept lightly coated with silicone oil. Forty cuvettes fabricated at the same time have identical counting efficiency and are consequently interchangeable. These cuvettes are optically coupled to the face of the lower photomultiplier with one drop of silicone oil each time a sample is counted.

The absolute counting efficiency of this system for ^{32}P was found to be about 75%. This 25% loss of theoretical maximum efficiency is inherent in the response characteristics of plastic scintillator and self-absorption by the blood sample. The optimum thickness of such discs and cuvettes for different beta energies has not been determined, but thickness of the plastic detectors must influence counting efficiency of this system. The basic principle used here, however, should be applicable to counting systems for beta emitting isotopes other than ^{32}P, although preamplification may be necessary for those of low energy. Theoretically, however, the system should have approximately 15% efficiency for ^{14}C.

REFERENCES

1. Lushbaugh, C. C., Scott, W. L., Yarbrough, M. C., Queener, R., and Gibbs, W. D. Feasibility of using *in vivo* $DF^{32}P$ and whole-body counting in red-cell survival studies. USAEC Report ORINS-53, 1965, pp. 112–114.
2. Lushbaugh, C. C., Queener, R., and Gibbs, W. D. An *in vitro* method for $DF^{32}P$ labeling of red cells for intravenous administration. USAEC Report ORINS-53, 1965, pp. 115–117.

1027307

Publications

From the Medical Division
Oak Ridge Associated Universities

1966

Reprints from the open literature and additional information on publications can be obtained by writing Mrs. Edward H. Anderson, Technical Editor, Medical Division, Oak Ridge Associated Universities, Box 117, Oak Ridge, Tennessee 37830. Complete lists of Medical Division publications are available.

PUBLICATIONS IN JOURNALS

Andrews, G. A. Treatment of radiation injury. J Miss Med Ass 7, 534–538, 1966.

Bergner, P. -E. E. Tracer theory: A review. Isotop Radiat Technol 3, 245–262, 1966.

Bollinger, J. N. Incorporation of dietary lineoleic acid into Triglycerides of irradiated bone marrow. Radiat Res 28, 121–131, 1966.

Gengozian, N. Formation of isohaemagglutinins in the marmoset, *Tamarinus nigricollis*. Nature 209, 722–723, 1966.

Gengozian, N., Lushbaugh, C. C., Humason, G. L., and Kniseley, R. M. 'Erythroblastosis foetalis' in the primate, *Tamarinus nigricollis*. Nature 209, 731–732, 1966.

Goh, K. O. Smaller G chromosome in irradiated man. Lancet 1, 659–660, March 19, 1966.

Harris, W. W., Anderson, N. G., Bartlett, T. W., Rutenberg, E. L., McCauley, L. L., and Kniseley, R. M. Unusual particles in human plasma from leukemia and lymphosarcoma. Nat Cancer Inst Monogr 21, 389–394, 1966.

Johnson, G. T. and Kyker, G. C. The mechanism of cerium uptake by *Saccharomyces cerevisiae*. Mycologia 58, 91–99, 1966.

Kniseley, R. M., Andrews, G. A., Tanida, R., Edwards, C. L., and Kyker, G. C. Delineation of active marrow by whole-body scanning with radioactive colloids. J Nucl Med 7, 575–582, 1966.

Kretchmar, A. L. Erythropoietin: Hypothesis of action tested by analog computer. Science 152, 367–370, 1966.

Nelson, B., Cosgrove, G. E., and Gengozian, N. Diseases of an imported primate *Tamarinus nigricollis*. Lab Animal Care 16, 255–275, 1966.

Oswald, E. O., Piantadosi, C., Anderson, C. E., and Snyder, F. The synthesis of ^{14}C- and ^{3}H-labeled glycerol ethers. Lipids 1, 241–246, 1966.

Rogers, W. A., Jr. and Nelson, B. Strongyloidiasis and malignant lymphoma: "Opportunistic infection" by a nematode. JAMA 195, 685–687, Feb. 21, 1966.

Snyder, F. A comparison of zonal scans and strip scans of thin-layer chromatograms. Separation Sci 1, 655–657, 1966.

Snyder, F. Triglyceride biosynthesis in irradiated bone marrow. Radiat Res 27, 375–383, 1966.

1027308

Snyder, F., Cress, E. A., and Stephens, N. An unidentified lipid prevalent in tumors. Lipids 1, 381–386, 1966.

Snyder, F. and Pfleger, R. C. Metabolism of α-alkoxy glyceryl monoethers in rat liver, in vivo and in vitro. Lipids 1, 328–334, 1966.

Snyder, F. and Piantadosi, C. Labeling and radiopurity of lipids. Advan Lipid Res 4, 257–283, 1966.

Snyder, F. and Smith, D. An automated system for sample collection and computer analysis of thin-layer radiochromatograms. Separation Sci 1, 709–722, 1966.

Wood, R., Bever, E. L., and Snyder, F. The GLC and TLC resolution of diastereoisomeric polyhydroxystearates and assignment of configurations. Lipids 1, 399–408, 1966.

Wood, R. and Snyder, F. Gas-liquid chromatographic analysis of long chain isomeric glyceryl monoethers. Lipids 1, 62–72, 1966.

Wood, R. and Snyder, F. A modified applicator for the uniform coating of thin-layer plates. J Chromatog 21, 318–319, 1966.

Wood, R. and Snyder, F. Modified silver ion thin-layer chromatography. J Amer Oil Chem Soc 43, 53–54, 1966.

GOVERNMENT DOCUMENTS

Morris, A. C., Jr. and Ross, D. A. The design of a low-background whole-body counting facility. USAEC Report ORINS-51, January 1966, 49 pp.

Radioactive Pharmaceuticals. Proceedings of a symposium held at the Oak Ridge Institute of Nuclear Studies, an operating unit of Oak Ridge Associated Universities, Edited by Gould A. Andrews, Ralph M. Kniseley and Henry N. Wagner, Jr. (Elizabeth B. Anderson, Technical Editor) AEC Symposium Series No. 6, CONF-651111, 1966.

CHAPTERS

Hayes, R. L. Radioisotopes of gallium. In: Radioactive Pharmaceuticals. Edited by G. A. Andrews, R. M. Kniseley, and H. N. Wagner, Jr. AEC Symposium Series No. 6, CONF-651111, April 1966, pp. 603–618.

Kyker, G. C. and Rafter, J. J. Colloidal properties of the lanthanides. In: Radioactive Pharmaceuticals. Edited by G. A. Andrews, R. M. Kniseley, and H. N. Wagner, Jr. AEC Symposium Series No. 6, CONF-651111, April 1966, pp. 503–524.

Snyder, F. and Piantadosi, C. The synthesis and purity of labeled lipids. In: Radioactive Pharmaceuticals. Edited by G. A. Andrews, R. M. Kniseley, and H. N. Wagner, Jr. AEC Symposium Series No. 6, CONF-651111, April 1966, pp. 553–565.

PUBLISHED ABSTRACTS

Cloutier, R. J. and Dalton, C. P. Radiation safety problems connected with the medical use of radioisotopes. Health Physics 12, 1835, 1966.

Cloutier, R. J. and Watson, E. E. Measurement of plutonium in wounds: Self-absorption by plutonium. Health Physics 12, 1203, 1966.

Edwards, C. L., Congdon, C. C., Gengozian, N., Vodopick, H., and Andrews, G. A. The treatment of acute leukemia: An experimental immunologic approach. Exp Hematol 9. 23–24, 1966.

Edwards, C. L., Hayes, R., Ahumada, J., and Kniseley, R. M. Gallium-68 citrate: A clinically useful skeletal scanning agent. J Nucl Med 7, 363–364, 1966, Abstr. L-1.

1027309

Gengozian, N. Isohemagglutinin formation in the marmoset, *T. nigricollis*. Fed Proc 25, 435, 1966, Abstr. 1386.

Goh, K. O. Inner chromosomal structure of the somatic metaphase of mammals: A light microscopic observation. Clin Res 14, 310, 1966.

Hayes, R. L., Carlton, J. E., and Rafter, J. J. Scanning with hydrous ferric oxide colloid labeled with gallium-68. J Nucl Med 7, 335–336, 1966, Abstr. C-1.

Hayes, R. L. and Rafter, J. J. Rhenium-188 as a possible diagnostic agent. J Nucl Med 7, 797, 1966, Abstr. 15.

Kretchmar, A. L. A model of hemopoiesis for mammalian recovery experiments. Exp Hematol 9, 42–44, 1966.

Kretchmar, A. L. and Conover, W. R. Secondary mortality and body-weight loss in lethally irradiated mice given small doses of isologous bone marrow cells. Exp Hematol 10, 11–12, 1966.

Lushbaugh, C. C., Comas, F., Saenger, E. L., Jacobs, M., Hofstra, R., and Andrews, G. A. Radiosensitivity of man by extrapolation from studies of total-body irradiation of patients. Radiat Res 27, 487–488, 1966, Abstr. Aa 2.

Merritt, C., Gengozian, N., and Hampton, J. Human A- and B-like antigens and antibodies in marmoset serum. Fed Proc 25, 345, 1966, Abstr. 1385.

Pfleger, R. C., Piantadosi, C., and Snyder, F. The metabolism of α-alkoxy glyceryl monoethers in rat liver. J Amer Oil Chem Soc 43, 140A, 1966.

Snyder, F. Triglyceride and phospholipid biosynthesis in irradiated bone marrow. Radiat Res 27, 523, 1966.

Snyder, F., Cheng, S., and Piantadosi, C. An unusual lipid present in Ehrlich ascites cells and other tumors. J Amer Oil Chem Soc 43, 140A, 1966.

Snyder, F. and Wood, R. The incorporation of labeled lipids into a glyceryl ether component of Ehrlich ascites cells. ACS Abstracts, 152nd Meeting, N.Y., C-258, 1966.

Webb, A. M. and Lushbaugh, C. C. Automated measurement of erythrocyte fragility using a linearly decreasing salt gradient. Clin Chem 12, 538, 1966.

Wood, R., Bever, E. L. and Snyder, F. The resolution of long-chain isomeric polyhydroxy acids by GLC. J Amer Oil Chem Soc 43, 139A, 1966.

Wood, R. and Snyder, F. Characterization and tentative identification of a lipid ether present in Ehrlich ascites cells and other tumors. ACS Abstracts, 152nd Meeting, N.Y., C-257, 1966.

MISCELLANEOUS

Kniseley, R. M. Book Review: Progress in Atomic Medicine, Vol. I, edited by John H. Lawrence, M.D., New York, Grune and Stratton, 1965. Amer J Clin Path 45, 487, 1966.

Nelson, B. and Takasugi, M. Letter to the editor. New Engl J Med 274, 110, January 13, 1966.

IN PRESS

Andrews, G. A. Book Review: Progress in Medical Radioisotope Scanning, Vol. II, IAEA, Vienna, 1964. Health Physics.

Andrews, G. A. Radiation accidents and their management. Radiat Res.

1027310

Andrews, G. A. Total-body irradiation in the human being. Proceedings of the XI International Congress of Radiology, held in Rome, September, 1965, Amsterdam, Excerpta Medica Foundations.

Andrews, G. A., Lushbaugh, C. C., Kniseley, R. M., White, D. A., and Friedman, B. I. Hematologic effects of total-body irradiation in the human being. IAEA Panel on the Effects of Various Types of Ionizing Radiations from Different Sources on the Hematopoietic Tissues, Vienna, May, 1966.

Bergner, P. -E. E. The concepts of mass, volume, and concentration. In: Compartments, Pools, and Spaces in Medical Physiology. Edited by C. C. Lushbaugh and P. -E. E. Bergner. AEC Symposium Series CONF-661010.

Cheng, S., Piantadosi, C., and Snyder, F. Lipid droplets and glyceryl ether diesters in Ehrlich ascites cells grown in tissue culture. Lipids.

Cloutier, R. J. and Dalton, C. P. Radiation safety problems connected with medical use of radioisotopes. In: Proceedings of the First International Congress of the International Radiation Protection Association. Pergamon Press.

Compartments, Pools, and Spaces in Medical Physiology. Proceedings of a symposium held at the Oak Ridge Institute of Nuclear Studies, an operating unit of Oak Ridge Associated Universities, October 24–27, 1966. Edited by C. C. Lushbaugh and P. -E. E. Bergner. AEC Symposium Series CONF-661010.

Fanger, H. and Lushbaugh, C. C. Radiation death from cardiac shock following a criticality accident: Report of a second death from a newly defined human radiation death syndrome. Arch Pathol.

Gengozian, N. and Batson, J. S. Effects of total-body irradiation on a small South American primate, *Saguinus fuscicollis*. Int J Radiat Biol.

Gengozian, N., Batson, J. S., and Nelson, B. M. Bone-marrow grafting attempts in marmosets after total-body irradiation. Int J Radiat Biol.

Goh, K. O. Cytogenetic studies in chronic lymphocytic leukemia: Nonspecific pseudodiploid chromosomal pattern. J Lab Clin Med.

Goh, K. O. Inner chromosomal structures in the somatic metaphase of rat kangaroo (*Potorous tridaclylis*): A light microscopic observation. Cytologia.

Kniseley, R. M. Diseases of the bone marrow. In: Principles of Nuclear Medicine. Edited by H. N. Wagner, Jr., Philadelphia, W. B. Saunders.

Likuski, H. J., Debons, A. F., and Cloutier, R. J. The inhibitory effect of 2-deoxy-D-glucose and 2-amino-2-deoxy-D-glucose on gold-thioglucose induced hypothalmic obesity in mice. Amer J Physiol.

Lim, J., Piantadosi, C., and Snyder, F. A comparison of phospholipid biosynthesis in irradiated bone marrow and liver. Proc Soc Exp Biol Med.

Lushbaugh, C. C., Cloutier, R. J., Humason, G. L., Langham, J., and Guzak, S. Histopathologic study of intradermal plutonium metal deposits: Their conjectured fate. Ann N Y Acad Sci.

Lushbaugh, C. C. and Comas, F. Clinical studies of radiation effects in man: A preliminary report of a retrospective search for dose-response relationships in the prodromal syndrome. Radiat Res.

Pfannenstiel, P., Sitterson, B. W., and Andrews, G. A. The use of iodine-130 to study the effects of thyroid-stimulating hormone in patients with thyroid cancer. J Nucl Med.

Pfleger, R. C. and Snyder, F. Lipid turnover in an isolated population of irradiated bone marrow cells. Radiat Res.

1027311

Snyder, F. Thin-layer chromatography: A review of radioassay. Advances in Tracer Methodology, Vol. 4.

Uchiyama, G., Hitchcock, A. A. C., and Morris, A. C., Jr. Clinical results with a color-recording rescanner. J Nucl Med.

Wood, R. and Snyder, F. Chemical and physical properties of isomeric glyceryl monoethers. Lipids.

1027312

Medical Division Employees

Scientific Staff

Elizabeth Allen, B.S.
Gould A. Andrews, M.D.
Mildred Bailey
Edward Balish, Ph.D.
Margaret Bateman, B.S.
Jerre Batson, B.S.
William L. Beck, Jr., B.S.
Per-Erik Bergner, M.D.
Billy L. Byrd, B.S.
James E. Carlton, B.S.
Kay Clayton, B.S.
Martha Clevenger, B.S.
Frank V. Comas, M.D.
Edgar Cress, B.S.
Rachel Dixon
C. Lowell Edwards, M.D.
William Fishback
Nazareth Gengozian, Ph.D.
William D. Gibbs, B.S.
Kong-oo Goh, M.D.
Francis A. Goswitz, M.D.
Charles T. Greene, B.A.
Robert Harlow, B.S.
Oliver Hawkins
Raymond L. Hayes, Ph.D.
Joyce Hewins, A.B.
Harold Hodges, B.S.
Elizabeth Holloway
Gretchen Humason, M.A.
Marjorie Ketelle, B.S.
Ralph M. Kniseley, M.D.
Lisbeth Kraft, D.V.M.
Dorothy Litton
C.C. Lushbaugh, M.D., Ph.D.
Dorothy Lushbaugh, B.S.
Boyd Malone, B.S.
J. E. McCarter
Sallie McCaskill
Anita Moehl, B.S.
A. C. Morris, Jr., M.S.E.
Bill M. Nelson, M.D.
Etna Palmer, M.D.
Ted A. Pearson, M.S.
Charles Phipps, B.S.
Raymond Pfleger, M.S.
William Pope
Richard Queener
John Rafter, B.S.
Evalyn Repplinger, M.B.
Mack Ruffner
Elizabeth M. Rupp, B.A.
Thomas A. Smith
Mary Smyser, B.S.
Fred L. Snyder, Ph.D.
Margo Steinman, M.S.
Nelson Stephens, B.S.
Ryosaku Tanida, M.D.
Mary Thomas, B.S.
Melvin Van Woert, M.D.
Helen Vodopick, M.D.
Mary Alyce Watkins, A.B.
Allen Webb, B.S.
James White
Randall Wood, Ph.D.
Martin Yarbrough, B.S.

Nursing and Patient Care

Lucy Amburn
Margie Bagley, R.N.
Helen Brinker, R.N.
James Cozart
Mary Nell Craig, R.N.
John Dean
Thelma Eden, R.N.
Mable Helton, R.N.
Marilyn Mackley, R.N.
Barbara Nance, R.N.
Beuna Pack
Garfield Porter
Naomi Presnell, R.N.
Mary Rogers, R.N.
Lillie P. Simmons
Elaine Stoetzel, R.N.
Mary E. Sutliff, R.N.
Eria Winters, R.N.
Lillie I. Woods

1027313

Administrative, Editorial, Medical Records, and Secretarial

Elizabeth B. Anderson, M.S.
Frances Banner
Kenneth L. Burton, B.S.
Blanche Carden
Frances Darr
Laura P. Edwards
J. Howard Harmon
Mary Lynn Helton
Wanda Hodge
Julia Hopper
Ann Lake, B.S.
Willa Fae Loveday
Kathryn McCulloch, B.A.
Maryrose McGown
Ruth C. Paire
Emily Roemer
Evelyn Sipe
Mona Smith
Lana Toburen
Dorothy Vola
Patsy White

Custodial and Animal Care

Willie Barnett
Mark Brewer
Willie J. Brooks
Isaiah Caldwell
Jerry Constance
James Graham
Clarence Hamilton
Fred Hamilton
Renfro Henderson
James Kline
Carlos McGhee
James Rather
Jerry Steele
J. R. Stevens
William Walker

Fellowships and Term Appointments

Resident Physicians (Massachusetts General Hospital):
- Joseph Ferrucci, M.D.
- Donald Fleischli, M.D.
- Milton Weiner, M.D.

Trainees in Clinical Investigation:
- Milton H. Dunsky, M.D. (began July 1, 1966)
- B. V. Suryanarayana, M.D. (to July 1966)
- Myosaku Takasugi, M.D. (to July 1966)
- Amiram Ur, M.D. (began October 1966)

Picker Foundation Fellow:
- Noboru Arimizu, M.D.

Damon Runyon Fellow:
- Yasuhiko Ito, M.D.

Abbott Fellows:
- Karen Fu
- William Kean

AEC Predoctoral Fellow:
- Raymond Porter, M.S.

PHS Fellow:
- Donald Carlson, M.S.

1027314

Research Participants—1966

James H. Arrington
Albany State College
Albany, Ga.

Enid L. Bever
Lawrence University
Appleton, Wis.

Ronald E. Hartman
St. Bonaventure University
St. Bonaventure, N.Y.

David F. Opdyke
New Jersey College of Medicine and Dentistry
Jersey City

Student Trainees—1966

James Allen Kimble
Sterling College
Sterling, Kan.

Martha Lee Lothrop
Texas Woman's University
Denton

Margaret Meir
College of St. Catherine
St. Paul, Minn.

Ann Suzette Morrow
Western Kentucky State College
Bowling Green

Johnnie Mae Neals
Bethune-Cookman College
Daytona Beach, Fla.

Christina Louise Reda
Kansas State Teachers College
Pittsburgh

Kathleen A. Schmidt
Our Lady of the Lake College
San Antonio, Tex.

Consultants and Collaborators—1966

Norman G. Anderson, Ph.D.
Biology Division
Oak Ridge National Laboratory

John A. Auxier, M.S.
Health Physics
Oak Ridge National Laboratory

Fritz H. Bach, Ph.D.
Laboratory of Genetics
University of Wisconsin
Madison

Robert C. Baldridge, Ph.D.
Department of Biochemistry
Temple University School of Medicine
Philadelphia, Pa.

Robert P. Ball, M.D.
Radiology Department
Oak Ridge Hospital

Jere M. Bauer, M.D.
University of Michigan School of Medicine
Ann Arbor

W. J. Baumann, Ph.D.
University of Minnesota
Hormel Institute
Austin

M. A Bender, Ph.D.
Biology Division
Oak Ridge National Laboratory

1027315

R. R. Bigelow, M.D.
Medical Arts Building
Oak Ridge

B. B. Blevins, D.D.S.
Medical Arts Building
Oak Ridge

Matthew Block, M.D.
Division of Hematology
University of Colorado Medical Center
Denver

Donald Brown, M.D.
Department of Radiology
University of Colorado Medical Center
Denver

Louis Bryan, M.D.
Doctors Building
Oak Ridge

Jimmy E. Camper, B.A.
Hatchery Biologist
National Fish Hatchery
Pisgah Forest, N.C.

Amoz I. Chernoff, M.D.
Director of Research
U.T. Memorial Research Center
Knoxville, Tenn.

C. C. Congdon, M.D.
Biology Division
Oak Ridge National Laboratory

Betty M. Cooper, M.D.
Northwest Texas Hospital
Amarillo

G. E. Cosgrove, M.D.
Biology Division
Oak Ridge National Laboratory

Dexter Davis, M.D.
Medical Arts Building
Oak Ridge

Albert F. Debons, Ph.D.
Department of Surgery and Physiology
Veterans Administration Hospital
Brooklyn, N.Y.

Wilhelmina F. Dunning, Ph.D.
Cancer Research Laboratory
Professor of Experimental Pathology
University of Miami
Coral Gables, Fla.

Earl Eversole, Jr., M.D.
Medical Arts Building
Oak Ridge

Herbert Fanger, M.D.
Institute of Pathology
Rhode Island Hospital
Providence

Warren L. Franz, M.S.
Department of Chemical Engineering
University of Tennessee
Knoxville

Ben I. Friedman, M.D.
Department of Radiology
University of Cincinnati
School of Medicine
Cincinnati, Ohio

Warren Glaser, M.D.
Department of Medicine
State University of New York College of Medicine
Downstate Medical Center
Brooklyn

Douglas Grahn, Ph.D.
Division of Biological and Medical Research
Argonne National Laboratory
Argonne, Ill.

Nathan S. Hall, Ph.D.
Laboratory Director
UT-AEC Agricultural Research Laboratory
Oak Ridge

George T. Harrell, M.D.
Milton S. Hershey Medical Center
Pennsylvania State University
Hershey

C. Craig Harris, M.S.
Medical Nuclear Instrumentation Group
Oak Ridge National Laboratory

Warren W. Harris, Ph.D.
Biophysics Separations Laboratory
Oak Ridge National Laboratory

Ernest L. Hendrix, M.D.
Medical Arts Building
Oak Ridge

1027316

John U. Hidalgo, M.S.
Tulane University
Bio-Medical Computing System
New Orleans, La.

Dorris H. Hutchison, Ph.D.
Division of Experimental Chemotherapy
Sloan Kettering Institute for Cancer Research
Rye, N.Y.

Melville L. Jacobs, M.D.
City of Hope Medical Center
Duarte, Calif.

Raymond A. Johnson, M.D.
Medical Arts Building
Oak Ridge

Marvin A. Kastenbaum, Ph.D.
Mathematics Division
Oak Ridge National Laboratory

Bergene Kawin, Ph.D.
Veterans Administration Hospital
Washington, D.C.

Herbert D. Kerman, M.D.
Halifax District Hospital
Daytona Beach, Fla.

Avery P. King, M.D.
Medical Arts Building
Oak Ridge

Alfred P. Kraus, M.D.
University of Tennessee
Memphis

Robert D. Lange, M.D.
U. T. Memorial Research Center
Knoxville, Tenn.

Wright Langham, Ph.D.
Los Alamos Scientific Laboratory
Albuquerque, N.M.

Henry J. Likusky, Ph.D.
Downstate Medical Center
New York City

Stuart W. Lippincott, M.D.
Department of Radiation Biology
Richmond, Va.

Helmut Mangold, Ph.D.
University of Minnesota
Hormel Institute
Austin

Margaret Maynard, M.D.
Dermatologist
Medical Arts Building
Knoxville, Tenn.

Christopher B. Merritt, B.S.
Tulane Medical School
Department of Radiology
New Orleans, La.

Isadore Meschan, M.D.
Department of Radiology
Bowman Gray School of Medicine
Wake Forest College
Winston-Salem, N.C.

Enrico Milhich, M.D.
Roswell Park Memorial Institute
Buffalo, N.Y.

William O. Miller, M.D.
Urologist
606 Main Ave., S.W.
Knoxville, Tenn.

George R. Minor, M.D.
Department of Surgery
University of Virginia Hospital
Charlottesville

William C. Moloney, M.D.
Director
Hematology Laboratory
Boston City Hospital
Boston, Mass.

K. Z. Morgan, Ph.D.
Health Physics Division
Oak Ridge National Laboratory

Dana W. Nance, M.D.
Oak Ridge Hospital

Robert W. Newman, M.D.
Medical Arts Building
Knoxville, Tenn.

Robert Nordlie, Ph.D.
Department of Biochemistry
University of North Dakota
Grand Forks

Richard A. Obenour, M.D.
Knoxville, Tenn.

Thomas H. Oddie, D.Sc.
Department of Radiology
University of Arkansas Medical Center
Little Rock

1027317

T. T. Odell, Ph.D.
Biology Division
Oak Ridge National Laboratory

Charles Oderr, M.D.
Oak Ridge Hospital

James P. OKunewick, Ph.D.
Experimental Pathology Department
Armed Forces Radiobiology Research Institute
National Naval Medical Center
Bethesda, Md.

Howard Pearson, M.D.
University of Florida
Gainesville

Claude Piantadosi, Ph.D.
Department of Medicinal Chemistry
University of North Carolina
Chapel Hill

Orville Privett, Ph.D.
University of Minnesota
Hormel Institute
Austin

W. W. Pugh, Jr., M.D.
Doctors Building
Oak Ridge

D. A. Ross, Ph.D., M.D.
Medical Nuclear Instrumentation Group
Oak Ridge National Laboratory

Henry B. Ruley, M.D.
Medical Arts Building
Oak Ridge

Eugene L. Saenger, M.D.
Radioisotope Laboratory
General Hospital
Cincinnati, Ohio

H. H. O. Schmidt, Ph.D.
University of Minnesota
Hormel Institute
Austin

N. G. Scott, Ph.D.
Chemical Technology Division
Oak Ridge National Laboratory

C. W. Sensenbach, M.D.
Medical Arts Building
Oak Ridge

Leigh Simmons, D.V.M.
Biology Division
Oak Ridge National Laboratory

Norman Simon, M.D.
945 Fifth Avenue
New York, N.Y.

W. Eidson Smith, M.D.
Blount Professional Building
Knoxville, Tenn.

Walter S. Snyder, Ph.D.
Health Physics Division
Oak Ridge National Laboratory

Alan Solomon, M.D.
U.T. Memorial Research Center
Knoxville, Tenn.

Ben H. Spargo, M.D.
Department of Pathology
University of Chicago
Chicago, Ill.

Paul Spray, M.D.
Doctors Building
Oak Ridge

P. E. Steiner, M.D.
Department of Pathology
University of Pennsylvania School of Medicine
Philadelphia

George M. Stevens, III, M.D.
Doctors Building
Oak Ridge

W. N. Tauxe, M.D.
Section of Clinical Pathology
Mayo Clinic
Rochester, Minn.

William M. Tipton, M.D.
522 West Church Street
Knoxville, Tenn.

Joe E. Tittle, M.D.
Doctors Building
Oak Ridge, Tenn.

V. R. R. Uppuluri, Ph.D.
Mathematics Division
Oak Ridge National Laboratory

A. C. Upton, M.D.
Biology Division
Oak Ridge National Laboratory

1027318

Henry N. Wagner, Jr., M.D.
Division of Nuclear Medicine
Johns Hopkins Hospital
Baltimore, Md.

George E. Watson, Ph.D.
Curator, Division of Birds
Smithsonian Institution
Washington, D.C.

H. Stephen Weens, M.D.
Emory University School of Medicine
Atlanta, Ga.

Trevor Williams, Ph.D.
Duke University
Durham, N.C.

Medical Committee, ORAU Council

Fearghus T. O'Foghluda (Chairman)
Medical College of Virginia

R. H. Alden
University of Tennessee Medical Units

Lewis Anderson
Duke University

Maxwell Dauer
University of Miami

R. B. Escue
North Texas State University

Kenneth A. Fry
Texas Woman's University

R. B. Platt
Emory University

R. D. Sloan
University of Mississippi Medical School

J. L. McCarthy
Southern Methodist University

Joseph C. Morris
Tulane University

ORAU Medical Program Review Committee for 1966

Joseph F. Ross (Chairman)
University of California, Los Angeles

Howard L. Andrews
Puerto Rico Nuclear Center

Sidney Fleischer
Vanderbilt University

E. Richard King
Medical College of Virginia

Harold J. Morowitz
Yale University

Eugene Saenger
University of Cincinnati

Robert E. Stevenson
National Cancer Institute

David W. Talmage
University of Colorado Medical Center

1027319

Medical Division Conferences – 1966

January 6: Mathematical descriptions of the consequences of radiation dose protraction – HAL HOLLISTER, chief of technical analysis branch, Division of Biology and Medicine, Atomic Energy Commission, Washington, D.C.

January 13: Chromosome studies in malignant lymphomas – A. G. BAIKIE, University of Melbourne, Victoria, Australia.

January 20: Radiation induced chromosomal aberrations in man – MARGO STEINMAN, research assistant, cytogenetics, Division staff.

January 27: Lipids and the blood cells – FRANK GOSWITZ, Special Training Division staff.

February 3: Gallium-68 scanning of the reticuloendothelial system – RAY HAYES, Division staff.

February 10: Mode of action of erythropoietin – ARTHUR L. KRETCHMAR, Division staff.

February 17: Report of the Atomic Energy Commission Biomedical Directors' meeting – RALPH M. KNISELEY, Division staff.

February 24: Clinical applications of the scintillation camera – A. GOTTSCHALK, University of Chicago, department of radiology.

March 10: Current work at Oak Ridge National Laboratory in nuclear medical instrumentation – C. CRAIG HARRIS, Oak Ridge National Laboratory.

March 17: The GLC and TLC resolution of diastereoisomeric polyhydroxystearates and assignment of configurations – RANDALL WOOD, Division staff.

March 24: Clinical iron absorption – MASAYUKI TAKASUGI, Division staff.

March 31: Histocompatibility testing – HELEN VODOPICK, Division staff.

April 7: A lipid found exclusively in tumors – FRED SNYDER, Division staff.

April 14: Intermittent corticosteroid therapy in the malignant lymphocytic diseases – DAVID A. WHITE, Division staff.

May 5: The metabolic fate of ether-containing lipids—RAYMOND C. PFLEGER, Division staff.

May 12: Irradiation of liver and spleen in chronic myeloid leukemia—F. COMAS, Division staff.

May 19: Comparison of gamma ray and neutron exposures of large animals—D. G. BROWN, University of Tennessee Agricultural Research Laboratory.

May 25: Metabolic interrelationships of polyunsaturated fatty acids—R. R. BRENNER, National University of La Plata, Argentina.

May 26: Bone scanning with gallium-68 citrate—C. LOWELL EDWARDS, Division staff.

June 2: Immunologic studies in the marmoset—N. GENGOZIAN, Division staff.

June 9: Clinical evaluation of anemic patients using radioisotopes—FRANCIS GOSWITZ, Special Training Division staff.

June 16: Qualitative identification of the chromosomes of malignant cells with ^{3}H-autoradiography—ISAO YAMANE, professor of microbiology, Research Institute, Tohoku University, Kitayobancho, Sendai, Japan.

June 23: The effect of oxygen and carbon dioxide on proteinase biosynthesis by *Streptococcus faecalis* var. *liquifaciens*—RONALD E. HARTMAN, summer research participant.

June 30: Splenic contraction and the optical density of blood—DAVID F. OPDYKE, summer research participant.

July 7: Cumulative mortality following lethal irradiation and low doses of isologous bone marrow—ARTHUR L. KRETCHMAR, Division staff.

July 14: Occurrence and metabolism of glyceryl ethers in Ehrlich ascites carcinoma cells—FRED SNYDER, Division staff.

July 21: Physiological monitoring for the low-dose rate facility—A. C. MORRIS, JR., Division staff.

July 28: A histologic method for quantitation of changes in marrow after irradiation—B. NELSON and M. LOTHROP, Division staff.

August 4: The toxicity of the chromium-51 RBC label—DAVID F. OPDYKE, New Jersey College of Medicine and Dentistry, Jersey City, N.J.

August 11: Studies on the genetics of radiation resistance—JOHN B. STORER, Jackson Laboratory, Bar Harbor, Maine.

1027321

August 18: Lipids of the human blood lymphocyte—FRANCIS GOSWITZ, Special Training Division staff.

August 19: *In vitro* survival studies of the leukemia lymphocyte—JAMES KIMBLE (Dr. Goswitz), Methyl-green pyronin-Y stain used in hematology and acute radiography—MARGARET MEIER (Dr. Vodopick), The LD_{50} of C_3H mice—JOHNNIE NEALS (Dr. Comas), Possibility of a plasmic factor causing chromosomal aberrations in irradiated persons—CHRISTINA REDA (Dr. Goh), Labeling of lipids in Ehrlich ascites carcinoma cells *in vitro*—KATHLEEN SCHMIDT (Dr. Snyder), An analog computer model for analysis of chromium-51 red cell survival and whole-body retention data—SUZETTE MORROW (Mr. Gibbs), all were summer college trainees.

August 25: A color re-scanner for clinical use—C. C. HARRIS, ORNL Medical Nuclear Instrumentation Group.

September 1: Characterization and tentative identification of the lipid ether present in Ehrlich ascites cells and other tumors—RANDALL WOOD, Division staff.

September 8: Hematologic effects of total-body irradiation—GOULD A. ANDREWS, Division staff.

September 15: Tracer dynamics—PER-ERIK BERGNER, Division staff.

September 22: A progress report on the low exposure rate total-body irradiation facility—ROGER CLOUTIER, Radiation Safety Officer, Division staff.

September 29: Factors affecting deposition of colloid in bone marrow—RAYMOND L. HAYES, Division staff.

October 6: Selected splenic studies in chronic granulocytic leukemia—C. LOWELL EDWARDS, Division staff.

October 13: Current knowledge of the gamma globulins—ALAN SOLOMON, U. T. Memorial Research Center, Knoxville, Tenn.

October 19: Space radiation hazards—WRIGHT LANGHAM, Los Alamos Scientific Laboratory, Los Alamos, New Mexico.

October 20: Scintillation camera studies of the kidneys and pancreas—MALCOLM R. POWELL, University of California School of Medicine, San Francisco, California.

October 28: ^{198}Au liver scanning in amebic abscesses and tumors—EFRAIM OTERO-RUIZ, Instituto Nacional de Cancerologia, Bogota, Colombia.

November 3: A biomedical approach to information theory, with clarification of terms used by computor programmers—FRED W. BROWN, ORAU staff.

1027322

November 10: Infections of germ-free animals with *Candida albicans*—EDWARD BALISH, Division staff.

November 17: Epidemiologic aspects of disease in laboratory animals—LISBETH KRAFT, Division staff.

November 30: Studies with experimental leukemia in the rat—WILLIAM MOLONEY, professor of clinical medicine, Tufts Medical School, director of clinical laboratories at Boston City Hospital.

December 1: Electronic red cell sizing: theoretical and practical aspects—GERSHOM ZAJICEK, NIH International Postdoctoral Research Fellow in Mathematical Biology, The Hebrew University, Hadassah Medical School, Israel.

December 8: Quantitative counting in the presence of coincidence—summing scintillation—D. A. ROSS, ORNL Medical Instrumentation Group.

December 15: Scintillation camera studies of the lung and bone marrow—A. MIALE, JR., Department of Radiobiology, Georgetown University School of Medicine.

December 20: Biocleavage of the lipid ether bond by a soluble multienzyme system—FRED SNYDER, Division staff.

December 17: More about the coulter counter and RBC populations—C. C. LUSHBAUGH, Division staff.

Lipid Seminars—1966

February 8: Recent data and interpretation of lipid biosynthesis occurring in irradiated bone marrow—FRED SNYDER, Medical Division, ORAU.

February 24: Proposed investigation of blood cell lipids and their relationship to radioactivity—FRANK GOSWITZ, Medical Division, ORAU.

March 10: The GLC and TLC resolution of diastereoisomeric polyhydroxystearates and assignment of configuration—RANDALL WOOD, Medical Division, ORAU.

April 5: Tumor lipids—J. N. BOLLINGER, Medical Division, ORAU.

April 19: Resolution of long-chain isomeric polyhydroxy acid by gas-liquid chromatography—RANDALL WOOD, Medical Division, ORAU.

1027323

April 19: The metabolism of α-alkoxy glyceryl monoethers in rat liver—RAYMOND PFLEGER, Oak Ridge Graduate Fellow, ORAU.

April 19: An unusual lipid present in Ehrlich ascites cells and other tumors—FRED SNYDER, Medical Division, ORAU.

May 25: Metabolic inter-relationships of polyunsaturated fatty acids—R. R. BRENNER, National Laboratory of La Plata, La Plata, Argentina.

July 19: Determination on structure and position of monoene double bonds—RANDALL WOOD, Medical Division, ORAU.

August 2: Lipids of the human body lymphocyte—FRANK GOSWITZ, Medical Division, ORAU.

August 15: Radioprotection studies of glyceryl ethers and related lipids—JAMES ARRINGTON, Research Participant, ORAU.

August 23: Labeling of lipids in Ehrlich ascites carcinoma cells, *in vitro*—KATHLEEN SCHMIDT, Student Trainee, ORAU.

October 11: Oxygen tension in tumor cells—FRANK COMAS, Medical Division, ORAU.

October 25: Glyceryl ether cleavage by a soluble protein fraction (defined by zonal centrifugation and electron microscopy) of rat liver—RAYMOND PFLEGER, Oak Ridge Graduate Fellow, ORAU.

November 3: Effects of various hormonal therapies and acute fasting on levels of liver microsomal glucose-6-phosphatase, inorganic-pyrophosphate-glucose-phosphotransferase and on lipid phosphate levels: an attempted correlation—ROBERT C. NORDLIE, Department of Biochemistry, University of North Dakota, Grand Forks, North Dakota.

November 23: *In vivo* and *in vitro* fatty acid metabolism of adipose tissue—MILTON DUNSKY, Medical Division, ORAU.

December 13: Further lipid studies in the human blood lymphocyte—FRANK GOSWITZ, Medical Division, ORAU.

1027324

Symposium

Symposium October 24–27, 1966 *Compartments, Pools, and Spaces in Medical Physiology*

Edited by: C. C. Lushbaugh and P.-E. E. Bergner
Elizabeth B. Anderson, Technical Editor

In press, AEC Symposium Series CONF-661010

Regional Lipid Meeting

March 29–30, 1966

Speaker—Affiliation	*Title of Talk*
Gerald. L. Feldman Department of Ophthalmology School of Medicine Baylor University	(1) *A Survey of Lipid Methodology* (2) *Lipids of the Eye and Their Biological Implications*
Norman G. Anderson Biology Division Oak Ridge National Laboratory	*Cell Fractionation in Zonal Centrifuges*

LEGAL NOTICE

This report was prepared as an account of Government sponsored work. Neither the United States, nor the Commission, nor any person acting on behalf of the commission:

A. Makes any warranty or representation, expressed or implied, with respect to the accuracy, completeness, or usefulness of the information contained in this report, or that the use of any information, apparatus, method, or process disclosed in this report may not infringe privately owned rights; or

B. Assumes any liabilities with respect to the use of, or for damages resulting from the use of any information, apparatus, method, or process disclosed in this report.

As used in the above, "person acting on behalf of the Commission" includes any employee or contractor of the Commission, or employee of such contractor, to the extent that such employee or contractor of the Commission, or employee of such contractor prepares, disseminates, or provides access to, any information pursuant to his employment or contract with the Commission, or his employment with such contractor.

1027325

Author Index

Ahumada, J. 100
Allen, Elizabeth 23
Anderson, C. E. 140
Andrews, G. A. 18, 89, 90, 96
Arrington, J. H. 37
Balish, E. 14
Beck, W. L. 70
Bergner, P.-E. E. 103, 106, 111
Bever, Enid L. 140
Bibler, Donna 154
Byrd, B. L. 78, 81
Carlson, D. 23
Carlton, J. E. 78
Clevenger, Martha L. 149
Cloutier, R. J. 70
Comas, F. V. 38, 70, 89, 90
Conover, W. R. 41, 45
Cress, E. A. 131
Edwards, C. L. 83, 87, 89, 90, 92, 96, 100, 115, 120, 158
Franz, W. 106, 111
Gengozian, N. 23, 27, 55, 58, 62, 65, 120
Gibbs, W. D. 34, 106, 111, 115, 117, 166, 168
Goh, K. O. 8, 122, 126, 129
Goswitz, F. 5, 149
Hartman, R. E. 84
Hayes, R. L. 74, 78, 81, 83, 84, 87, 96, 100
Herman, E. C., Jr. 129
Hodges, H. D. 34, 115, 117, 166
Hübner, K. F. 55
Humason, Gretchen 65
Kniseley, R. M. 18, 65, 89, 92, 96
Kretchmar, A. L. 41, 45, 48, 53
Lothrop, Martha L. 27
Lushbaugh, C. C. 18, 30, 34, 65, 106, 111, 115, 117, 149, 158, 161, 164, 166
Lushbaugh, Dorothy H. 149, 158
Merritt, C. B. 58
Morris, A. C., Jr. 156, 164
Nelson, B. 27, 87
OKunewick, J. P. 53
Opdyke, D. F. 111
Oswald, E. O. 140
Pfleger, R. C. 137, 146
Phipps, C. E. 48
Piantadosi, C. 140, 146
Pope, W. T. 168
Porter, R. 62
Quarles, J. F. 117
Queener, R. F. 115
Rafter, J. J. 74, 78
Rupp, Elizabeth M. 45, 120
Snyder, F. 5, 12, 37, 131, 133, 135, 137, 138, 140, 146, 154
Stephens, N. 131
Swisher, S. H. 129
Tanida, R. 96

1027326

Vodopick, Helen 89, 90, 92, 120
Webb, A. M. 161
White, D. A. 18
Wood, R. 12, 135, 138, 140, 142, 144
Yarbrough, M. C. 34

1027327

1969 RESEARCH REPORT

Oak Ridge Associated Universities

REPOSITORY Oak Ridge Institute for Science and Education, Medical Sciences Division

COLLECTION Oak Ridge Associated Universities Annual Research Reports, Medical and Health Sciences Division

BOX No. Vance Road Facility, Room 202A

FOLDER No folder title. Document no. ORAU-30002, Part 6 of 6

10273328

1021329

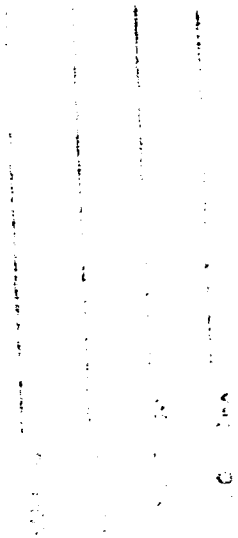

ON THE COVER: The development of gallium-67 as a tumor-localizing agent currently is a major research topic. Left: a whole-body scan showing normal uptake in skeleton and liver, and also uptake in lymphoblastic lymphoma (Burkitt's type) involving lymph nodes of the right side of the neck, inguinal region, mediastinum, and epigastrium. Right upper: electron micrographic autoradiogram of gallium-67 localized in electron-dense bodies in phagocytic cells that occupy the mesenteric lymph node of a leukemic AKR mouse. Right lower: a scan of a hamster carrying an adenovirus-30-induced tumor in the left foreleg; collaborative work with Dr. Norman Anderson's MAN group at ORNL.

ORAU-110

1969 RESEARCH REPORT

medical division

For the year ending December 31, 1969

Operating under contract with The United States Atomic Energy Commission

NOTICE

This report contains preliminary data and was prepared primarily to record the year's work, and is not intended as a substitute for publication in the open literature. It is subject to revision and does not represent a final report. Please do not quote from or refer to this work in open literature without permission from individual authors to reference the material as a personal communication.

ORAU-110

Requests for single copies of this report from organizations or individuals engaged in educational, professional, or research activities or programs as covered by this report may be directed to:

Medical Division
Oak Ridge Associated Universities
Oak Ridge, Tennessee 37830

Printed in the United States of America

Price $3.00

Available from: Clearinghouse for Federal Scientific and Technical Information, Springfield, Virginia 22151

1027330

CONTENTS

	Page
ORGANIZATION OF RESEARCH	IV
INTRODUCTION	1
RADIATION EFFECTS AND RELATED TOPICS	5
Clinical Total-Body Irradiation	5
Infections in Irradiated Patients	16
Dosimetry Studies and Monitoring	46
Applied Radiobiology	53
Radiation Immunology and Marrow Transplantation	57
Experimental Hematology	71
RESEARCH IN NUCLEAR MEDICINE	81
Radiopharmaceutical Development	81
Clinical Investigations in Nuclear Medicine	99
Whole-Body Counting	106
Instrumentation and Computer Technology	118
BASIC STUDIES RELATED TO RADIATION, NEOPLASIA, AND METABOLISM	130
Biological Chemistry	130
Marmoset Research Project	144
Ultrastructural Studies of Tumors	163
Induced Cytogenetic Abnormalities	169
Rapid Effects of Insulin on the Hypothalamic Satiety Center	179
Hemodialysis Cancer Therapy–Collaborative Project with ORNL	180
PUBLICATIONS	183
MEDICAL DIVISION CONFERENCES–1969	193
LIPID SEMINARS–1969	196
REGIONAL LIPID MEETING–1969	197
FELLOWSHIPS AND TERM APPOINTMENTS	198
RESEARCH PARTICIPANTS–1969	198
STUDENT TRAINEES–1969	199
ORAU MEDICAL DIVISION ADVISORY COMMITTEE	199
MEDICAL COMMITTEE, ORAU COUNCIL	200
MEDICAL DIVISION EMPLOYEES	200
CONSULTANTS AND COLLABORATORS–1969	202

NOTE: Numbered references in the text may be located in the list of publications beginning on page 183.

ORGANIZATION OF RESEARCH

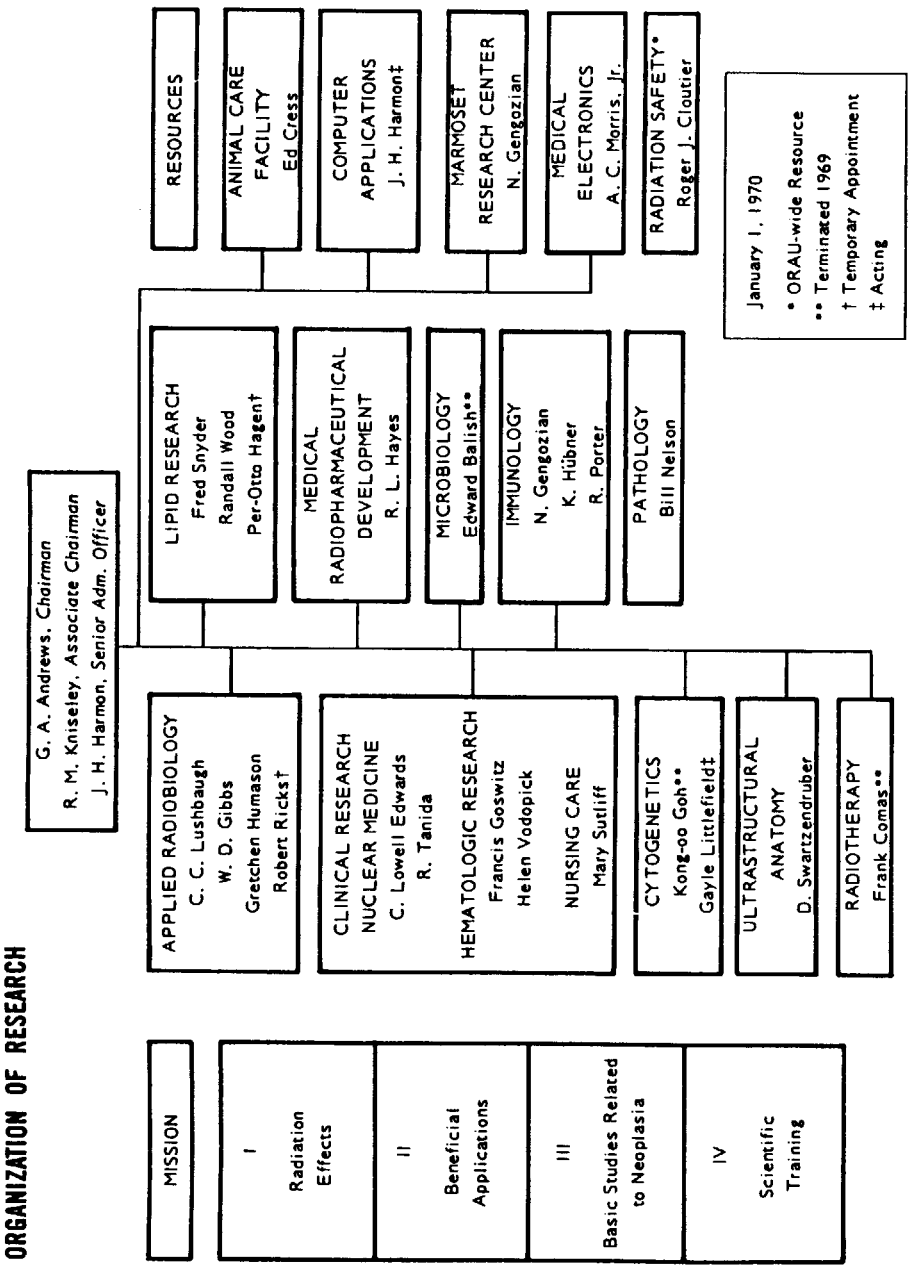

1027331

INTRODUCTION

The Medical Division operates a major biomedical program encompassing both clinical studies and related basic research, mainly devoted to effects of radiation and beneficial applications of radiation. The principal source of support is the United States Atomic Energy Commission. Our principal research objectives are (1) to delineate mechanisms of radiation injury, especially in man, and to devise improved methods of treating radiation injury; (2) to advance the beneficial applications of radiation for diagnosis and therapy; (3) to pursue selected basic studies, particularly ones related to cancer, that arise out of the ongoing program; and (4) to provide training in research for students, scientists, and physicians. The Division feels an obligation to contribute where possible to the pool, not only of investigators, but of physicians with knowledge of nuclear medicine.

This year, in an effort to provide a more unified picture of our current activities, we are trying a new format for our Research Report, with less emphasis than previously on separate units of research and more on continuity of presentation. The three main headings and the chapters under them identify the major research areas of the Division.

To our regret this year we must report several significant losses from our senior group. Dr. Frank Comas, after 11 years as our Research Radiotherapist, was lured to the University of Tennessee Memorial Hospital in Knoxville. Fortunately our ties with him are maintained and in the interim, until his replacement is selected, he provides an important consultative resource. We hope that he will continue indefinitely to have a close working relation with the Medical Division program. He has been a loyal staff member, and is a good friend, and a valuable collaborator in our program. Dr. Kong-oo Goh, who headed our Cytogenetics program, was unable to resist the persistent recruiting efforts of the University of Rochester from whence he previously came to the Medical Division. In his 5 years with us he devoted his full energies to cytogenetic problems, contributing a significant body of knowledge to his field. Dr. Per-Erik Bergner resigned in June 1969 to accept a position on the staff of the Rockland State Hospital, Orangeburg, New York. Dr. Bergner had come to us from the Karolinski Institute in Sweden in 1964. He had brought an unusual kind of luster to our staff, working on theoretical aspects of life processes. With mathematical tools he was reexamining old assumptions and constructing new hypotheses that may quite significantly affect the nature of experimental designs of future biomedical studies. His papers generated lively interest among the small group of theoretical biologists. Lastly, the University of Wisconsin recruited Dr. Edward Balish for their Department of Microbiology in the Medical School. Ed came here from a postdoctoral appointment at the Argonne National Laboratory, launching our effort in microbiology. He has built a fine group, and his laboratories and instrumentation have enhanced the Division resources.

While we are pleased that other institutions recognize the skills of our staff members, we are aware that their departure has been a

significant loss. Concurrently, the Medical Division has not escaped the fiscal crisis that is broadly affecting research in the nation. Although there has been no decrease in the basic support from the Division of Biology and Medicine of AEC, the inflationary spiral of the last 2 years has caught up with us. As we adjusted our salary rate ranges upward to compete, last year and again this year, the full impact on the current budget means that we must postpone replacing certain of these key positions.

We were pleased to have two staff additions in 1969. In February Dr. Gayle Littlefield came to us from the Medical College of Georgia to join the Cytogenetics project. Her presence assures the continued work on the important question concerning chromosomal breakages in women taking oral contraceptives, a project supported by the National Institutes of Health. Also joining the staff was Dr. Robert Ricks who had in two previous summers been a guest at the Medical Division as a Research Participant. Holding a Ph.D. in Zoology from Arkansas State University, he adds new strength to Dr. Lushbaugh's radiobiology group.

We were pleased that Dr. Jere Bauer, Associate Professor of Internal Medicine from the University of Michigan Medical School, chose to spend a six-month sabbatical at the Medical Division during 1969. Dr. Bauer was accompanied by Mr. Frank Nakamura, research associate, who will stay on for an additional three months. Their work is on an approach to tumor therapy by deprivation of specific amino acids, the deprivation to be accomplished by dialysis against specific enzymes. The work is going forward in collaboration with our staff members and with Drs. Stanfield Rogers, James Regan, and Conrad Richter of the Biology Division of Oak Ridge National Laboratory.

In 1969 the Atomic Energy Commission built a new addition to the Lipid Laboratory and we expect to occupy it in the first week of January 1970. Providing approximately 1200 square feet of additional laboratory space, the unit has special hoods for chromatography and is designed for unusually accurate humidity control, essential for adsorption chromatography. At the main Medical Division site a small addition to the building was provided by the AEC including a walk-in cold room for Microbiology and a special cold autoradiography room for Radiopharmaceutical Development. High-quality animal autoradiograms can be prepared for showing distributions of new radionuclides and experimental labeled compounds.

Training activities continued. Dr. Donald E. Carlson completed his Public Health Postdoctoral Fellowship with our Immunology group under Dr. Gengozian, and was appointed to the faculty of Southwestern Medical School in Dallas. Dr. David Mardon, on finishing his Public Health Service Postdoctoral Fellowship in December 1969 with Dr. Balish in Microbiology, accepted a position at the Virginia Commonwealth University in Richmond. Dr. Ten-ching Lu Lee continues on her Public Health Service Postdoctoral Fellowship with the Lipid Project, as does Dr. James Soodsma, who holds an AEC Postdoctoral Fellowship. In Immunology we are host to four University of Tennessee graduate students, Nancy Basford, Charles Gottlieb, John Kateley, and Mike Yurconic. In the Lipid Project Robert Wykle, M.S., continues his AEC Predoctoral

1027332

Fellowship, working toward his Ph.D. degree from the University of Tennessee Medical Units at Memphis. During 1969 Dr. Nasser Tehranian, who came from Boston University, held one of the Postresident Assistantships in Clinical Investigation. Dr. Gifford Ammermann, formerly at Chicago Wesley Memorial Hospital, arrived July 1 to begin his one-year appointment as a Postresident Assistant in Clinical Investigation. Dr. Yukio Tateno, from the University of Chiba, Japan, began his one-year Fellowship supported by the Damon Runyon Foundation; he is assigned to nuclear medicine instrumentation. During the year there were three Medical Student Fellows in Nuclear Medicine. This program was supported in 1969 by Abbott Laboratories and Neisler Radiopharmaceuticals. Assigned to the Medical Division from the University Participation Office of ORAU were four Research Participants from faculties of colleges and universities during the summer quarter, as well as six undergraduate college students in the College Trainee Program.

This year the Medical Division, with a grant from the Bureau of Radiological Health, presented its 12th major symposium in nuclear medicine, under joint sponsorship by the Atomic Energy Commission and the Public Health Service. The meeting was held December 8-11 on the topic, Medical Radionuclides: Radiation Dose and Effects.

The Fourth Annual Regional Meeting on Lipids was again sponsored by the Division.

Approximately 24 papers were presented at regional or national meetings and staff members attended more than 68 meetings during the year. Our senior staff continue to serve on a variety of advisory committees or as consultants to the National Institutes of Health or other programs. Foreign travel, reduced from previous years, still permitted us to be represented at several important international meetings. The Division Chairman presented a paper in Vienna at a Symposium on Handling Radiation Accidents, sponsored jointly by the International Atomic Energy Agency and the World Health Organization. Dr. C. C. Lushbaugh presented a paper in Hakone, Japan, at the Japanese-United States Seminar on Experimental Cancer of the Stomach. Dr. Ryosaku Tanida, while on a personal trip to Japan, attended the Sixth International Congress of Chemotherapy. Dr. Vodopick presented a paper in Vienna at the International Atomic Energy Agency Symposium on In Vitro Procedures with Radioisotopes in Clinical Medicine and Research. The Division was represented by Dr. C. L. Edwards and Dr. N. Gengozian at the Symposium sponsored by the Cooperative Group on Bone-Marrow Transplantation in Man and also attended the Colloquium on White Blood Cell Transfusions and Treatment of Acute Leukemia; both of these meetings were in Paris.

The support for the Medical Division activities comes from increasingly diverse sources. We operate under the ORAU contract with the Atomic Energy Commission receiving our funding base from the Division of Biology and Medicine, of which Dr. John Totter is the Director. The NASA project, Radiosensitivity in Man, directed by Dr. Lushbaugh, enters its sixth year. The contract to study Infections in Irradiated Patients is funded through the Department of the Army Medical Research

and Development Command. At the Marmoset Research Center Dr. Gengozian pursues his immunologic research under an NIH grant, Immunology of Hematopoietic Chimerism in Tamarins, and in addition is a beneficiary of support from corporate funds to maintain the colony. Dr. Snyder has a grant from the American Cancer Society on The Occurrence, Metabolism, and Function of Glyceryl Ethers in Neoplasms, and participates in an NIH grant to the University of North Carolina, with Dr. Claude Piantadosi, on Basic Studies on Alkoxy Alkenyloxy Glycerol Ethers and Derivatives. A contract with the National Institute of Child Health and Human Development supports the project, Chromosome Breaks in Women Taking Contraceptives.

A prime goal for future years continues to be enhanced cooperative activities with the Oak Ridge National Laboratory. We have fruitful collaborations under way and a number of others in prospect. With greater demands from the public to see biomedical research demonstrate its relevance to human needs, we anticipate the need to expand the Medical Division.

Gould A. Andrews
Chairman

1027333

CLINICAL TOTAL-BODY IRRADIATION

The Medical Division, as a major aspect of its program, has been investigating total-body irradiation in man. In seeking to better understand man's radiosensitivity, we hope to improve ways of controlling or palliating leukemias, lymphomas, and related disorders, as well as to devise effective treatments for radiation accidents. We have the experience gained a number of years ago when high-dose irradiations were given in early efforts, largely unsuccessful, to achieve marrow transplants. We also have had first-hand experience with radiation accident victims, and have added to our own collection of data the world-wide available information on radiation accidents. In addition, in a retrospective study we collected and analyzed the irradiation responses of patients treated with total-body irradiation at many centers throughout the nation.

In recent years, and currently, our effort has included a series of clinical experiments with single doses of total-body irradiation at 2 dose rates and currently an assessment of the effects of protracted low-exposure rates and fractionated exposures.

Low-Exposure-Rate and Fractionated Irradiation

We have completed the trials in which we exposed patients either to 50 or 100 R at 1.5 R/min in the medium-exposure-rate irradiator (METBI); these data now serve as a reference of comparison for the current low-exposure-rate irradiations (LETBI) at 1.5 R/hr and also for the fractionated METBI exposures which provide daily doses totaling the same as the continuous LETBI exposures -- about 30 R/day. The care of these patients and the collection of data involves a large number of Medical Division staff members -- physicians, nurses, aides, research associates, and technologists, and all of them do a vital job.

During 1969 eight patients were treated in LETBI with exposures of 100 to 250 R, and these paragraphs describe our current views of the responses (C. L. Edwards, G. A. Andrews, Helen Vodopick, Francis A. Goswitz, C. C. Lushbaugh, and R. M. Kniseley). These bring the number of patient treatments up to 24 (Table 1). The patients resided in the facility 83 to 211 hr. One patient was removed from the facility within 6 hr of beginning treatment because of acute pulmonary symptoms from bronchitis and emphysema thought at the time to be possibly due to pulmonary embolus or myocardial infarction. No treatments had to be discontinued because of the patient's intolerance of the confinement, or the rate of exposure.

Six of the patients received benefit from the treatment that could be assessed clinically as improvement in blood values, reduction in tumor mass, or improved sense of well-being. Of those receiving 250 R, two had transient reduction of their tumors (lymphomas), but also serious depression of the normal blood elements during the treatment and the

six weeks after irradiation. Both these patients had lymphosarcoma, circulating lymphosarcoma cells, and an infiltration of the bone marrow by immature lymphocytes. One, a 55-year-old man in whom the diagnosis was first made in 1964, had received numerous treatments with portal irradiation as well as cyclophosphamide off and on for 6 months. During the 250 R exposure in LETBI, he experienced some nausea and headache; there was only moderate regression of his tumors but severe depression of his platelet count and granulocyte count. Before the irradiation primitive cells in his blood had increased noticeably, and by the 24th day he had a leukemic blood picture. Prednisone and vincristine were added to the regimen but he developed a gram-negative septicemia and died on the 40th day.

The other patient with lymphosarcoma (61-year-old man), who experienced little apparent benefit from the irradiation, had known of his disease for only three months. He had received a brief course of chlorambucil but was otherwise untreated. He experienced no untoward symptoms during the exposure, but by the 11th day his total WBC count had dropped to less than 1,000 from 8,100 at day 0. His platelet count also fell and reached a nadir of 5×10^3/cu mm at day 31. He required 14 transfusions during the 6 weeks of observation. Despite the profound changes in his circulating blood, postirradiation bone-marrow aspirate was comprised almost entirely of lymphoid elements of varying morphology. He has since then been treated with prednisone and Cytoxan and has continued to work.

The response of the total WBC for all the patients exposed to 250 R in LETBI is shown in Fig. 1. An average response (excluding the two patients just described) is also shown. The individual responses are remarkably similar considering that the patients have several different diseases. Figure 2 shows the individual and average platelet response to 250 R in LETBI. Here there apparently is a greater individual variation. Figures 3 and 4 show the WBC and platelet data for patients treated with 100 R in LETBI. The initial WBC response through 11 days is similar to that for 250 R. The average WBC response then levels off with recovery beginning between days 18 and 24, an event that does not occur after 250 R until days 45 to 52. A more remarkable finding is how little an effect on the platelet count is seen after 100 R in LETBI.

These results indicate the relative ineffectiveness of a single 100-R exposure in LETBI for these diseases. This finding may be weighted because six of these patients had a myeloproliferative disorder. We have suspected a dose-rate effect in chronic granulocytic leukemia (CGL) as reported in last year's research report. On the other hand, the single 250-R exposure produces profound effects on the blood elements and two patients in addition to the two described above experienced untoward thrombocytopenia. Both these patients were elderly, 75 and 79 years, and had received previous marrow-damaging treatment, busulfan plus total-body irradiation in one, and busulfan alone in the other.

Five patients were exposed to a dose of 150 R (Table 1). These were patients with myeloproliferative disorders, either primary thrombocytosis (PHT), polycythemia vera (PRV), or CGL, with only a

TABLE 1

PATIENTS TREATED IN LETBI

Pt.	Age	Sex	Diag.	Exp. (R)	Exp. (Hr)	Residence (Hrs)	Rads Syndrome GI	Improvement: Well-being	Improvement: Tumor or Blood Count	Nadir: WBC (day)	Nadir: %	Platelet (day)
1	76	M	CLL	100	67	73	59	0	+	38(2w)	33	(31)
2	77	M	CLL	100	66	80	59	0	+	53(11)	20	(38)
3	79	M	LS	100	68	83	59	0	+	54(16)	71	(31)
4	69	M	LS	100	67	76	59	0	+	57(50)	65	(2w)
5	12	M	CGL	100	67	74	59	0*	+	47(9)	10*	(4)
6	45	F	CGL	100	67	79	59	0*	+	96(2w)	82	(38)
7	55	F	CGL	100	70	77	59	0*	+	83(18)	109	(51)
8	83	F	CGL	100	69	79	59	0*	+	39(1w)	111	(16)
9	66	F	CGL	100	69	79	59	0†	+	41(16)	50	(11)
10	60	M	PRV	100	66	80	59	0	+	44(45)	79	(31)
11	28	M	CGL	150	100	118	89	0*	++	11(11)	29	(2w)
12	59	M	PRV	150	103	116	89	0	++			
13	61	M	PHT	150	100	116	89	0	++	50(38)	2w	(38)
14	62	M	PHT	150	103	119	89	0	++	55(38)	28	(31)
15	61	F	PHT	150	100	12w	89	0	++	30(w5)	1w	(52)
16	62	M	LS	250	170	202	1w8	0	+	31(38)	15	(31)
17	59	F	LS	250	166	208	1w8	0	++	2w(w3)	w	(31)
18	55	M	LS	250	163	19w	1w8	+	++	26(1w)	1.0(39)	
19	61	M	LS	250	163	197	1w8	0	+	11(16)	w	(31)
20	52	M	CGL	250	165	211	1w8	0*	+++	w(w5)	2w	(38)
21	61	M	PRV	250	170	202	1w8	0	+++	21(w9)	35	(30)
22	59	F	PRV	230	15w	177	136	0†	+++	15(w5)	18	(2w)
23	75	M	PRV	250	169	208	1w8	0*	+++	10(w5)	2.5(31)	
24	78	F	PRV	250	166	200	1w8	+	+++	6(52)	0.7(38)	

* Preexposure nausea that recurred at random intervals.
† Had transient bout of nausea during gastric wash for bacteriologic studies.
‡ Had CVA with vomiting on last day after showing clinical improvement.

[a] Myleran started day w5.
[b] Blood transfusions required during and after Rx.
[c] Teletherapy to neck on day 21; died day w6.
[d] Died day w0. Required transfusion day 25; Prednisone day 25; Vincristine day 31.
[e] Required transfusion day 18.
[f] CVA on day 8.

1027334

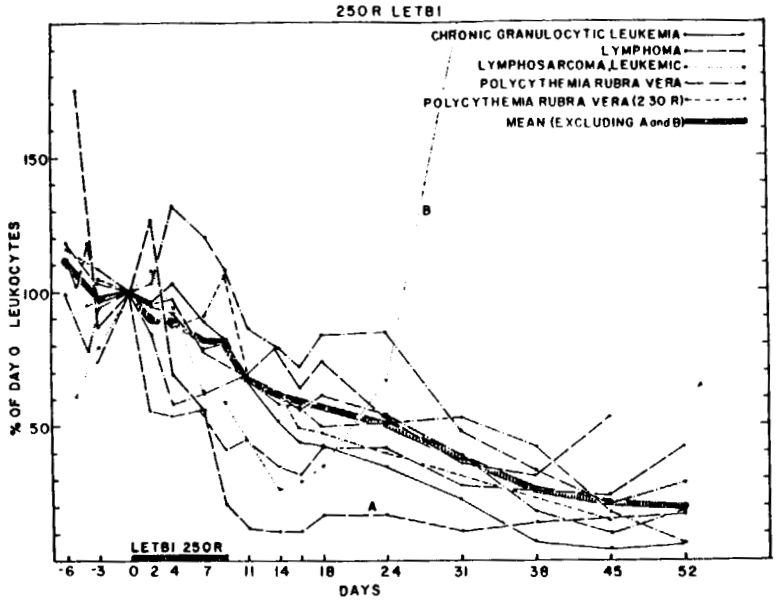

Fig. 1. The effect of 250 R total-body irradiation at 1.5 R/hr on leukocyte levels. Individual variations in absolute numbers require the use of percentages of pretreatment value for purposes of comparison. Two atypical patients, A and B, with rapid shifts in the disease state were excluded from the mean value.

moderate elevation of the WBC count. Each of these patients had beneficial response in terms of a decrease in the WBC or platelet count. None developed severe thrombocytopenia or gastrointestinal symptoms. One patient did complain of recurrence of a headache during the exposure.

In 1969 we initiated a new protocol giving patients daily exposures of 30 R in METBI at 1.5 R/min. We are looking for a dose-rate effect that may differ from LETBI. Obviously, short daily treatments are much more practical than prolonged ones.

One patient with reticulum cell sarcoma had responded very well to 250 R in LETBI previously. When her symptoms later became much worse she was treated with cyclophosphamide for 3 months. Because she was too weak to manage in the LETBI facility she was then treated in the METBI with 250 R in divided doses of approximately 30 R per day over 8 days. No remission from her disease followed this exposure and she died with severe thrombocytopenia and leukopenia.

Four patients have been treated in METBI with 30 R/day to a total of 150 R (5 days) and one patient has been exposed at 25 R for 4 days

1027335

(100 R), Table 2. Three of these patients had CGL and one PHT. Each of these had significant improvement in the blood-cell values without extreme leukopenia or thrombocytopenia. In one patient with lymphosarcoma and bone-marrow infiltration, who had been treated previously with nitrogen mustard, platelets dropped to 20,000/cu mm and leukocytes to less than 2,000/cu mm. She also required RBC transfusions. Her tumors decreased during and after the irradiation but the response was very transient. Each of the patients treated with fractionated doses in METBI (Fx METBI) experienced at least anorexia by the fourth exposure and one had severe nausea and emesis after the third dose.

Of those treated in LETBI, our best results have been in patients with PRV, PHT, and CGL. Remissions or periods until further treatment is required, over more than 18 months, have been obtained in patients with PRV, 10 months in PHT, and 5 months in CGL. Single exposures of 100 R in LETBI appear to be without sufficient effect to be regarded as therapy. That there is a brief effect on the tumor size in some lymphomas and on the WBC in some patients with CGL without a similar platelet count effect suggests carefully timed repeated exposures 100 R may increase the therapeutic index. As expected

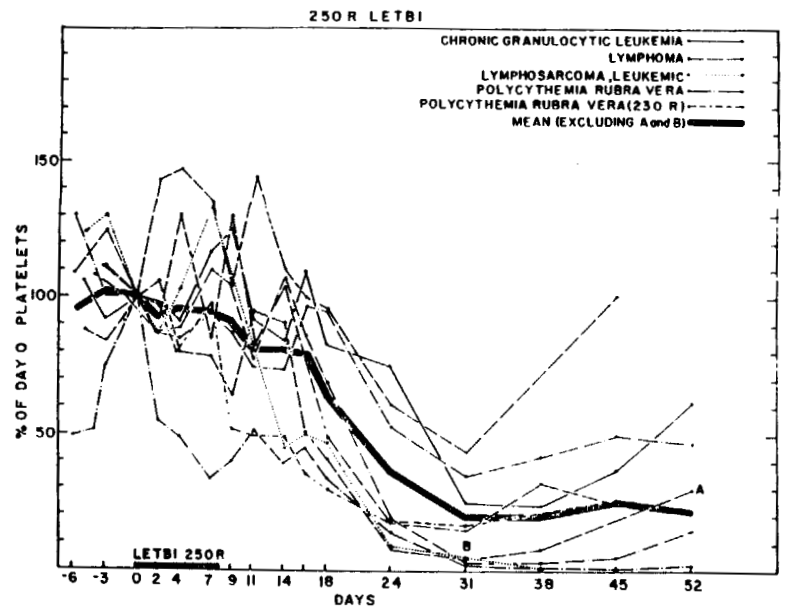

Fig. 2. The effect of 250 R total-body irradiation at 1.5 R/hr on platelets. Two atypical patients, A and B, with rapid shifts in the disease state were excluded from the mean value.

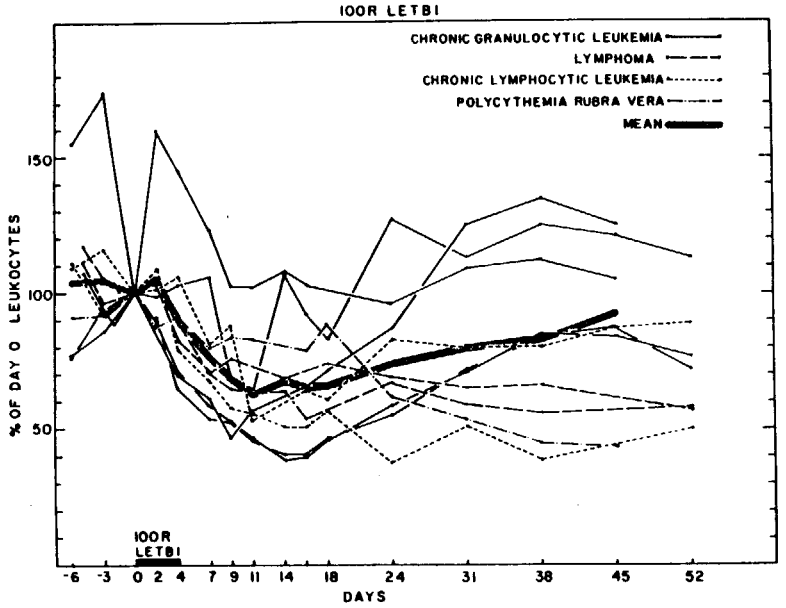

Fig. 3. The effects of 100 R total-body irradiation at 1.5 R/hr upon blood leukocytes in 10 patients with chronic granulocytic leukemia (CGL), chronic lymphocytic leukemia (CLL), polycythemia rubra vera (PRV), or lymphoma.

the 250-R exposure has the greatest and most prolonged effect on the blood values. However, in some patients the effect of 250 R was greater than we had predicted, depressing the blood values to below expected levels. In late stages of these diseases the 150-R exposure may be preferable since it has been clinically effective in four patients while not producing the severe depression seen with 250-R exposure. In untreated polycythemia attended by thrombocytosis, with 250-R exposure, however, we have obtained remissions lasting a year or longer.

Radiobiologic Inferences

The applied radiobiologic study program in connection with these therapeutic studies using total-body irradiation focused this year upon obtaining information that might help define better the relative efficacy of single exposures, daily fractionated exposures, and protracted low-dose-rate exposures (C. C. Lushbaugh). Numerous observations in clinical radiotherapy and experimental radiobiology have demonstrated that fractionated exposures given over periods of time longer than several days or weeks are much less efficient in producing hematologic and gastrointestinal damage and, therefore, much more tolerable than the same total dose given in a single exposure in less

1027336

than 1 day. Few studies, however, have been made in human radiotherapy or animal radiobiology that can be used to predict with certainty whether discontinuous rapidly delivered daily exposures are more or less efficient than continuous slowly delivered daily exposures of the same magnitude. Loss of damage-producing efficiency of radiation delivered at slow rates is considered to result chiefly from steady repair of a relatively smaller amount of induced damage. Since it is also assumed that repair proceeds more rapidly during completely radiation-free intervals, there might be no observable differences in effectiveness if (1) radiation exposure periods were short and rest periods long, or (2) if the radiation exposure periods were long and rest periods short or nonexistent. Accordingly, it is common practice for radiation health physicists to smooth out pulsed, repeated exposure patterns by expressing the exposure in terms of the averaged daily exposure rate as though the dose had been accumulated evenly. The studies this year indicate, however, that this practice is unwarranted. Fractionated daily exposures in the medium-exposure total-body irradiator produce greater hematologic depressions and greater gastrointestinal distress than the same dose protracted slowly over the same exposure period. This greater damaging effect

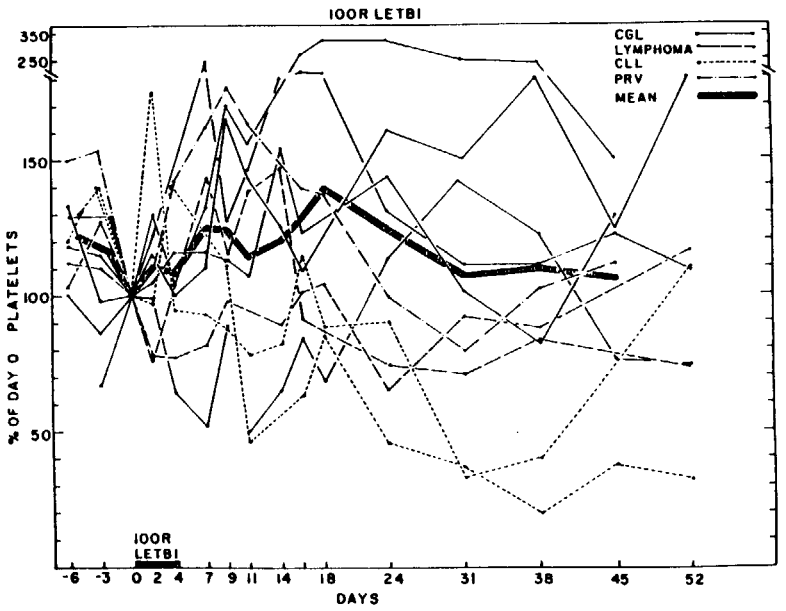

Fig. 4. The effects of 100 R total-body irradiation at 1.5 R/hr upon platelets in 10 patients with chronic granulocytic leukemia (CGL), chronic lymphocytic leukemia (CLL), polycythemia rubra vera (PRV), or lymphoma.

TABLE 2

FRACTIONATED THERAPY IN METBI

Pt.	Age	Sex	Diag.	Exp. (R)	Daily Fractions	R per Fraction	Rads	GI Syndrome	Improvement Well-being	Improvement Tumor or Red Blood Count	Nadir WBC	Nadir Platelet
											% (day)	% (day)
1	47	F	CGL	100	4	25	70	+	+	+	31(18)	60 (43)
2	60	F	LS	150	5	30	109	++	0	+	18(38)	14 (31)
3	48	F	CGL	150	5	30	110	+++	++	++	2(52)	34 (38)
4	68	F	CGL	150	5	30	107	+	+++	++	19(38)	28 (31)
5	63	M	PHT	150	5	30	106	+	+	++	38(35)	11 (24)
6	60	F	LS	250	8	30	176	+	-*	0	3.0(30)	1.0(30)

* Died at day 30.

of discontinuous irradiation might be restricted only to man since he has a slow rate of repair compared to the rapid repair kinetics of the mouse. We attempt, therefore, to test this explanation by pair-irradiating mice in the two facilities at rapid and slow exposure rates, 3.7 R/min (intermittent), and 0.025 R/min (continuous) so that the mice received 18, 36, and 64 R exposures daily. In these experiments the mice were irradiated until death and the mean of the survival times was determined. Changes were studied in weight of total body, testis, and spleen, in peripheral blood values of WBC, RBC, Hgb, Hmct, MCV, RBC size distribution, and histologic appearance of the gastrointestinal tract and hematopoietic organs. Weight loss and death occurred earlier as the result of hematologic failure in the mice exposed to the fractionated daily doses (METBI) than in the mice exposed continuously (22 out of 24 hours/day) in the low-exposure total-body irradiator to the same daily and total doses. Although some aspects of this study are still incompletely analyzed, these observations are sufficiently complete to suggest tentatively that the earlier deaths are due to less effectual hematopoietic repair in discontinuous irradiation. Reparative bone-marrow attempts in the mice exposed to the daily fractions seem more exuberant but fail to produce adequate numbers of erythrocytes in replacement of daily senescent losses. This observation is also confirmed in part by a parallel study of the iron metabolism of pair-irradiated rats exposed by the two irradiation techniques.

In addition to studying the therapeutic efficacy of total-body irradiation in malignant blood dyscrasias, we have been searching for clinical and laboratory observations of biologic effects that are altered in degree by changing the dose rate. Many biologic responses are known from experimental animal studies to be decreased in severity by a decrease in exposure rate even though the same total dose is accumulated. Few such dose-rate-dependent effects have been studied directly in man except for erythema and desquamation of the skin, which were extensively evaluated by Strandquist, Ellis, and others. On the basis of the experimental work of Lamerton in rats,

1027337

and Sacher and others in mice, it could be predicted that reducing the exposure rate would lessen the incidence and severity of the symptoms of the prodromal response (acute radiation sickness). The LETBI facility was designed on the basis of this prediction. We have found it difficult to obtain any evidence that any untoward gastrointestinal effects are produced by the low LETBI rate of 1.5 R/hr even though total exposures have been given that would cause severe GI distress when given quickly. Earlier in this chapter clinical experience with this low-dose-rate facility is reported along with our new use of the other more rapid irradiator (METBI), as a means of giving TBI in discontinuous, daily, rapidly delivered fractions rather than in a single short or long continuous exposure. In accumulating this clinical experience, several patients have now been irradiated in both irradiators and given the same and different total doses in single and multiple exposures. Although these exposures in the same patient have been as much as a year or more apart, and the status of the patient's disease has not been exactly the same each time, the records of these patients seem to show that whether or not total-body irradiation therapy causes acute gastrointestinal sickness depends on the rate of the daily exposure as well as on the size of the daily exposure. In one patient, for example, exposure to 100 R at 1.5 R/min in a single exposure caused severe prodromal sickness; exposure to 30 R/day at 1.5 R/min also caused severe prodromal sickness but not until the third and fourth daily exposure. Exposure to 30 R/day at 1.5 R/hr (continuous exposure for about 20 of each 24 hours), however, for five days 150 R did not cause prodromal symptoms even though the total dose from this exposure exceeded the earlier threshold level for this patient. Whether the 1.5 R/hr (0.025 R/min) exposure rate if continued would eventually cause a high incidence of the prodromal syndrome cannot be determined because hematologic effects after 250-R exposures have been sufficiently extensive to indicate that larger than 250-R exposures at the low-exposure rate (1.5 R/hr) are unwarranted and in some radiosensitive stages of disease processes would be intolerable.

In the group of patients that have been irradiated in both irradiators, the data suggest a similar relation between response and dose rate for hematologic effects, although not so well defined as that for nausea and vomiting. In Fig. 5, for example, the changes in total white blood cell count were graphed for the same patient with chronic granulocytic leukemia who was irradiated with 100 R on three separate occasions in A. (METBI) 1.5 R/min/63 min, in B. 1.5 R/min/$\sim$17 min on 4 successive days, and in C. 1.5 R/hr for $\sim$20 hr/day for 3+ days. Because her initial total WBC were slightly different each time, the counts have been normalized and graphed on a logarithmic scale as fraction of initial count. The effect of irradiation schedule A was greater than that of schedule B which was greater than that of schedule C, showing that a rapidly delivered exposure was more efficient in producing bone-marrow damage than a slower one in this patient. The decrease in efficiency between A and B can be interpreted to mean, from the viewpoint of experimental radiobiology, that some of the damage produced each day was repaired before the next exposure. In schedule C, the greater loss of efficiency must mean that the damage produced at the slower rate (0.025 R/min vs. 1.5

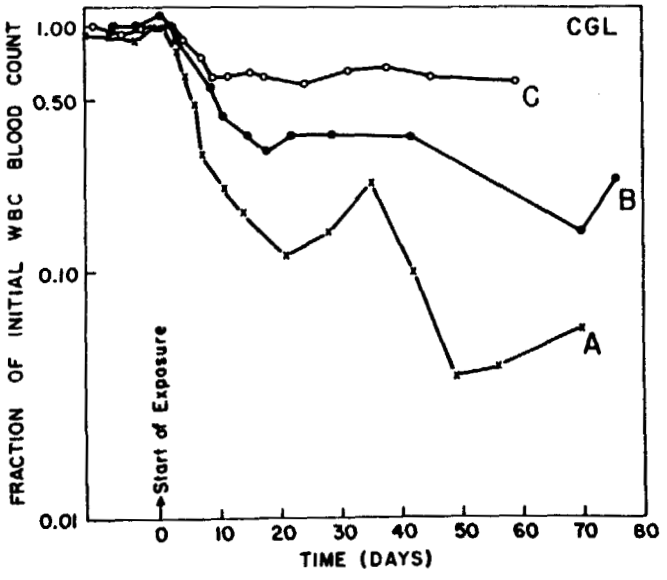

Fig. 5. Graph of the relative changes in total WBC count of the same patient after separate 100 R TBI exposures: (A) Single 67-min exposure at 1.5 R/min; (B) Four daily exposures to 25 R/day (17 min) at 1.5 R/min; and (C) Three and a quarter daily exposures (20 hr/day) at 1.5 R/hr.

R/min) is either less severe or more easily repaired than that caused by the higher rate even though the daily doses were the same.

Hematologic data of other patients in several instances now allow us to compare the effects at different total doses given at different rates and make it possible to estimate the exposures that produce comparable effects (or are isoeffective). A first attempt has been made to relate such isoeffective doses using various formulas or mathematical models. Because most data on the effects of irradiating large animals seem to fit Bateman's cube root of dose rate this model has been used in our studies. According to Bateman -

$$\text{Isoeffective dose}_x = \text{Dose}_\infty \left(1 + \frac{k}{\sqrt[3]{x}}\right)$$

where x equals the specific dose rate and k is the slope constant of the isoeffective dose line. This slope constant, in respect to dose rate can be obtained from a best-fitted regression line to data where doses required for the same biologic effect (e.g. ED_{10} for some symptoms, LD_{50}, etc.) have been measured at two or more different dose rates. This model fits the data of Strandquist, Ellis, and others who have determined the doses required at various exposure

1021338

rates to cause moist desquamation of human skin. When dose rate is scaled empirically as the cube root a linear isoefficient line is obtained with a slope constant (k) of 1.0. Coincidentally, this k value corresponds closely with that for the relation of change in LD_{50} to change in dose rate for numerous mouse radiation lethality experiments. When dose-rate, lethality data from sheep (that are radiosensitive) and swine (that are resistant to fractionated radiation) are used, k values of 0.65 and 1.35, respectively, are obtained. Although too few systems have been tried from this empirical point of view, the k values derived thus far appear to vary in size directly with the amount of radiation exposure required at some fixed rate for a particular effect. The size of the k value thus seems to reflect the radioresistance of the underlying biologic systems involved in the response being measured and, if so, is also a relative measure of its reparability. In other words, a small k value is associated with a system that is radiosensitive and repairs slowly so that large changes in dose rate have little effect on the isoeffective dose size.

In experimental radiotherapeutic studies of the relative effectiveness of different rates of total-body irradiation in patients with malignant lympho- and myeloproliferative diseases, isoeffective doses for hematologic effects have been obtained in a few instances at two dose rates, namely 1.5 R/min and 0.025 R/min. When we use percentage decrease in peripheral blood white cell or platelet count in the same persons as indices, a 100-R TBI at 1.5 R/min (METBI) appears to be isoeffective with 150-R TBI at 0.025 R/min (LETBI) so we can check Bateman's model. The need for knowing the effective dose at infinite rate in Bateman's formula is avoided by simple arithmetic. The two isoeffective, directly determined doses delivered at different rates are used to derive the slope factor, k, for the biologic response being studied, according to the formula:

$$\frac{D_1}{\left(1 + \frac{k}{\sqrt[3]{\text{Rate}_1}}\right)} = \frac{D_2}{\left(1 + \frac{k}{\sqrt[3]{\text{Rate}_2}}\right)}$$

Where D_1 and D_2 are isoeffective doses at rate 1 and rate 2 respectively. The solution using these clinically observed isoeffective doses is

$$\frac{100}{\left(1 + \frac{k}{\sqrt[3]{1.5}}\right)} = \frac{150}{\left(1 + \frac{k}{\sqrt[3]{0.025}}\right)}$$

This calculation shows k = 0.237. With this k value, 100 R at 1.5 R/min is isoeffective with 150 R at 1.5 R/hr as in LETBI. If one now assumes a factor of 2 correction of k for normal man's radioresistance over that of a patient so that k equals ~ 0.475, (the isoeffective dose also doubles) then the isoeffective doses for comparable hematologic effects for normal healthy men can be estimated and

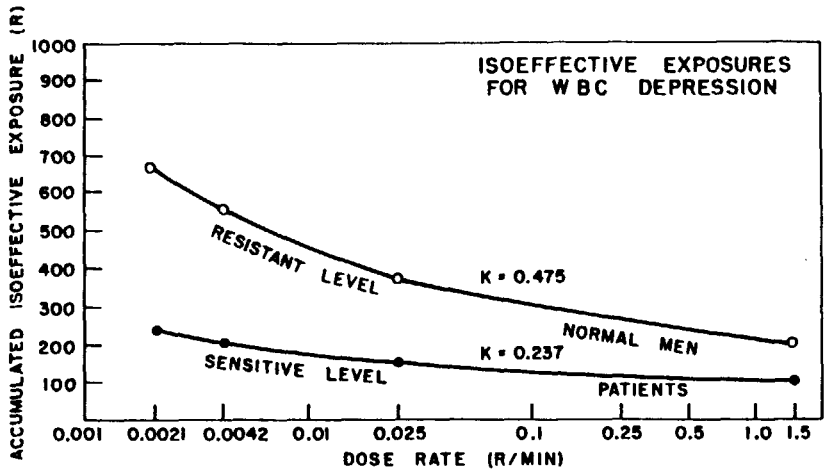

Fig. 6. Graph of the derived relation between dose rate and accumulated exposure for isoeffective WBC count depression in patients and normal men, with the assumption that observed WBC responses in TBI patients with chronic granulocytic leukemia represent a 2-fold increased radiosensitivity. These lines are based on Bateman's empirical model relating isoeffective doses to a modified ratio of the cube root of dose rate.

extrapolations made to the 3.0 and 6.0 R/day levels of exposure, which are considered by some as tolerable for long periods of time. As shown in Fig. 6, these extrapolations from our clinical observations applied to Bateman's model do not support the tolerability of the 3.0 R/day exposure level. They imply that the leukemic patient would be showing clinically severe hematologic damage in about 80 days and that normal man would have accumulated undesirable hematologic damage in less than 240 days.

INFECTIONS IN IRRADIATED PATIENTS

Two cardinal complications of the hematopoietic syndrome are infection and hemorrhage. Our project in Microbiology concentrates on acquiring data that will help us to prevent or control the infections that follow radiation exposures. Therefore, we are surveying comprehensively those patients who have received radiation. Closely related are the investigations on Candida albicans, an increasingly troublesome pathogenic yeast that infects not only immunosuppressed patients but also increasing numbers of patients who have been on intensive and prolonged antibiotic treatment.

1027339

Bacterial Flora and Humoral Elements

A major effort continues to characterize the bacterial flora of irradiated patients (Edward Balish, Ted A. Pearson, and Jean McIntyre). We summarize here the microbiologic and immunologic data on patients who were exposed to the following doses of irradiation: one at 353 R and one at 150 R in the medium-exposure-rate total-body irradiator (METBI) (1.5 R/min); four at 250 R in the low-exposure-rate total-body irradiator (LETBI) (1.5 R/hr); two splenic irradiations, one of 410 rads and another of 665 rads.

The microflora of patient 1 (150 R total body) was normal and consistent in the nares, throat and mouth, gastric washings, and feces. However we recovered Diplococcus pneumoniae from nasal swabs before and for 13 days after irradiation. Pseudomonas aeruginosa and beta hemolytic streptococci were present in his urine before irradiation, but we saw no dramatic increase in these microorganisms. This patient suffered no infectious complications. Patient 2 received a total-body dose of 353 R for advanced acute leukemia unresponsive to conventional therapy. Because he was very ill, the complete microbiologic assays could not be carried out. His flora was also normal except for D. pneumoniae and C. albicans in the throat, but they did not persist. Bacterial flora did not change dramatically after irradiation. However, a Fusobacterium sp. was cultured from his blood 9 days before death (26 days after exposure). It had not been detected earlier in any of our assays of flora. A postmortem blood culture revealed Escherichia coli. Candida albicans was cultured from esophageal lesions but not from any blood specimens.

Of four patients who received 250 R in the LETBI facility only one (a 65-year-old man with lymphosarcoma) developed a serious infection after exposure. The flora of the mouth and throat was normal and consistent except for an Enterobacter sp. and D. pneumoniae, neither becoming predominant. The fecal flora also remained stable during the study. The patient died 33 days after exposure. An Enterobacter group A was isolated from his blood 19 days postirradiation; serologically and biochemically it resembled the Enterobacter in the gastrointestinal tract. Escherichia coli was isolated at 24 days. Just before death another Enterobacter was obtained from the blood. This strain was more resistant to Chloramphenicol, nalidixic acid, and nitrofurantoin but more sensitive to kanamycin. Of the latter antibiotics only Chloramphenicol was used. The antibiotic resistance is hard to assess. Perhaps the patient acquired the second Enterobacter on the ward. Possibly the incidence of the resistant Enterobacter species in the small intestine had increased; it could easily have escaped our sampling procedures. The other three patients who received 250 R TBI showed some changes in the numbers and types of microorganisms. Transient species were encountered before and after irradiation but none were able to persist.

The two patients who received partial-body irradiation for therapy of chronic granulocytic leukemia both had stable throat and nasal flora. The stomach washings of one showed a flora resembling that of the mouth and throat. Gastric washings were not obtained from the other patient.

The fecal microflora of both remained stable with some transient species encountered. No infections occurred in these two patients.

Another aspect of our study has been to determine any changes occurring in the biochemical characteristics of the isolated microorganisms (gram negative bacilli in the family Enterobacteriaceae): indole production, citrate utilization, hydrogen sulfide production, formation of acetyl-methylcarbinol, motility, urea hydrolysis, amino acid decarboxylation, and fermentation of carbohydrates. To date we have looked at the gram negative bacilli isolated from eight irradiated patients. In general, the characteristics of most species remain stable throughout the study with some exceptions.

An atypical Escherichia coli was isolated from urine and feces of a patient with lymphosarcoma exposed to 150 roentgens in the METBI facility. Before irradiation, and 10 days postirradiation, it failed to produce gas from fermented carbohydrates, was motile, and decarboxylated lysine. Yet isolates from day 14 to the end of the study (48 days), now produced gas in carbohydrate media, were nonmotile, and failed to decarboxylate lysine. The colonial morphology of this "new" strain was identical with the "original" strain but it had changed biochemically. Radiation exposure of the patient may have contributed somehow to the appearance of this "new" strain of E. coli.

We were gratified to see no infectious complications in our recent previously reported studies on irradiated patients and radiation accident victims even though two of the accident victims were exposed to doses believed to be equivalent to 550 R total-body irradiation. However, we detected alterations of the microflora after as little as 50 R total-body irradiation. We have seen an apparent relation between gastric acidity, which decreased after total-body irradiation, and the microorganisms in gastric washings. As the acidity decreased, larger numbers of bacteria were cultured from washings. Also the anaerobic components of the bacterial flora are affected by total-body irradiation more than the aerobic ones. Incidences of C. albicans in the flora of irradiated patients also increased.

Studies were carried out to determine whether patients had agglutinating and bactericidal antibodies against bacteria from their microflora and whether these antibodies would be affected by total-body irradiation (Edward Balish and Ted A. Pearson). After 150 R TBI, agglutinins in the serum of patient 1 were very low for a Klebsiella sp. isolated from urine and feces (Table 3). We found good titers against an E. coli (stool) and Pseudomonas aeruginosa (urine); these titers decreased after irradiation but returned to preirradiation values after 1 week for the P. aeruginosa and 2 weeks for E. coli. No bactericidal activity appeared against P. aeruginosa before or after irradiation, but there was good killing activity against the E. coli in all serum samples. We found no alteration in agglutination titers with serum collected from patient 4 (250 R TBI) before, during, and after exposure, but all titers were low (Table 4). Several of the bacterial strains used were isolated from his blood about 20 to 25 days after irradiation and just before death. This patient's serum had no capacity to kill the Enterobacter sp. (5/3) or E. coli isolated

1027340

TABLE 3

Serum Agglutination Titers Against Bacteria Isolated from the Microflora of Patient 1 Before and After 150 R Total-Body Irradiation (1.5 R/min)

Time Days	Microorganisms Used			
	Klebsiella (Urine)*	*E. coli* (Stool)*	*P. aeruginosa* (Urine)*	*Klebsiella* (Stool)*
-6	16†	256	256	8
-3	16	128	128	16
-1	16	128	64	8
+4	16	128	64	8
+7	8	32	256	8
+11	2	32	128	4
+14	8	64	128	8
+16	8	128	64	4
+18	16	512	256	16
+24	8	256	128	16
+31	8	256	256	16

* Source of microorganism

† Reciprocal of highest titer showing agglutination.

from his blood. Antibody titers against Staphylococcus aureus (nares) decreased after the start of irradiation therapy in patient 3 (250 R TBI) but increased about 11 days later. Agglutinins against gram negative bacteria in this patient's serum did not change and we could detect no bactericidal activity. Agglutinin titers of serum from patient 5 (250 R TBI) against E. coli (feces) dropped dramatically (10-fold) 4 days after exposure; by day 9 the titer returned to pre-irradiation levels (Table 5). Although titers were high, there were no bactericidal antibodies against this organism. A Citrobacter freundii isolated from rectal swabs also elicited a high antibody titer; we saw good bactericidal activity against C. freundii in all serum specimens except for 3 days before and 2 days after irradiation.

Sera from patient 8 (665 rads partial-body irradiation) was able to kill a nonhemolytic E. coli isolated from her urine but not a beta hemolytic strain also from urine. However, agglutination titers were low (2) against the nonhemolytic strain yet moderately high (64 to 128) against the hemolytic strain (Table 6).

We are now using a serum-sensitive microorganism, E. coli "Texas," as a test organism in bactericidal studies. Preliminary

TABLE 4

Serum Agglutination Titers Against Bacteria Isolated from the Microflora of Patient 4 Before and After 250 R Total-Body Irradiation (1.5 R/hr)

Time Days		Microorganisms Used				
		Enterobacter (Blood - 4/24)*	*Enterobacter* (Blood - 5/3)	*E. coli* (Blood-4/28)	*E. coli* (Stool)	*S. aureus* (Nares)
-6		16†	64	2	2	32
-4		16	64	2	2	32
-3		16	64	2	16	16
0	250 R TBI	16	32	2	8	16
+2	250 R TBI	16	32	4	8	32
+4	250 R TBI	16	32	2	8	32
+7		16	32	2	8	16
+9		16	64	4	8	16
+11		32	32	4	16	32
+14		16	64	2	8	32
+16		16	64	4	16	32
+18		16	32	4	16	32
+24		16	64	2	16	16

* Source and strain of organism

† Reciprocal of highest titer showing agglutination

data show that in serum samples there are active bactericidins against this organism that do not kill members of the patient's own microflora. Since complement is necessary for lysis of gram negative bacteria by serum, then the serum that kills E. coli "Texas" has adequate levels of complement, but may not possess specific antibodies against microorganisms from the patient's microflora.

Studies on the plasma proteins, immunoglobulins, complement, and transferrin of three accidentally irradiated humans are now complete (Edward Balish and Stuart Chaskes). These three men were exposed while working with a Van de Graaff accelerator. Victim A was exposed to about 100 to 200 R total-body irradiation (TBI), B to about 550 R TBI, and C to about 550 R TBI, receiving much higher doses to his hands and feet (~5000 R). The total plasma protein (Biuret) fluctuated

1027341

TABLE 5

Serum Agglutination Titers Against Bacteria Isolated from the Microflora of Patient 5 Before and After 250 R Total-Body Irradiation (1.5 R/hr)

Time Days		Microorganisms	
		Citrobacter freundii (Feces) *	*Escherichia coli* (Stool) *
-5		256†	1024
-3		1024	1024
+2	250 R TBI	512	1024
+4	250 R TBI	1024	1024
+7	250 R TBI	1024	128
+9		256	1024
+14		1024	1024
+18		1024	1024
+31		1024	512
+38		1024	256

* Source of microorganism

† Reciprocal of highest titer showing agglutination

TABLE 6

Serum Agglutination Titers Against Bacteria Isolated from the Microflora of Patient 8 Who Received 665 rads of Splenic Irradiation

Time Days	Microorganisms			
	Beta hemolytic *E. coli* (Urine)*	Nonhemolytic *E. coli* (Urine)*	*Klebsiella* (Stool)*	*S. aureus* (Nares)*
+1	128†	2	128	1024
+2	64	0	256	512
+5	128	2	256	512
+7	128	2	128	512
+9	64	2	128	256
+12	64	2	128	256
+14	128	2	128	256

* Source of microorganism

† Reciprocal of highest titer showing agglutination

TABLE 7

Variability of Plasma Proteins Within a 6-month Period After Accidental Total-Body Irradiation

Plasma Protein	Normal Range	Patient A Highest Level	Patient A Lowest Level	Patient B Highest Level	Patient B Lowest Level	Patient C Highest Level	Patient C Lowest Level
IgG	1200 ± 300	2230*	540	1726	426	4160	171
IgA	288 ± 121	390	93	468	67	1700	540
IgM	80 ± 29	210	58	230	37	43	18
Complement C'3	145 ± 22	208	125	248	69	500	93
Transferrin	280 ± 67	254	115	268	71	210	59

* mg/100 ml plasma

TABLE 8

Germ-Tube Formation by *Candida* Species in Defined Liquid Culture Media and Human Serum

Organism	GSB + L-alpha-amino-n-butyric acid	GSB (no nitrogen source)	Human Serum*
C. albicans (8 strains)	64† (44-86)	8	89 (78-97)
C. albicans (10259)‡	91	33	96
C. stellatoidea (5 strains)	6 (0-14)	15	60 (0-100)
C. tropicalis (3 strains)	4	0	10
C. pseudotropicalis	0	0	0
C. parapsilosis	0	0	0
C. krusei	0	0	0
C. guilliermondii	0	0	0

* Diluted to 1/2 concentration with distilled water

† Percent germ tubes formed at 3 hr in static culture at 37°C

‡ Filamentous mutant

1027342

widely in all three. However, the low-dose victim had the widest range in values (9.88 to 5.00 g/100 ml) during the 6-month period. Protein electrophoretic studies were performed on the plasma from the three men. Alpha 2, beta, and gamma proteins of patient C became elevated 17 days after exposure and remained high throughout the 6-month study. More significantly, these fractions fluctuated appreciably after day 17. His albumin values were below normal for about 6 months. The patterns are shown in Fig. 7. The bone-marrow transplant and the high dose to his hands and feet may have a bearing on some of these abnormalities in the plasma proteins. We saw no drastic alterations of total plasma proteins for patients A and B. However, their electrophoretic patterns did vary, showing small changes in the shapes of the peaks and, on several occasions, small additional peaks. Patients A and B had similar patterns. The patterns of patient B are shown in Fig. 8. After the exposure, IgG, IgA, and IgM levels in all three patients were unstable, fluctuating at least 2 to 4-fold (see Fig. 9, 10, 11, and 12). Usually the low values were obtained 20 to 30 days after exposure. Patient C (Fig. 11) had exceptionally high values for IgG and IgA and low values for IgM. The values for IgM were not so low as those in patients A and B. Possibly the marrow infusion may have been responsible for the increased levels of IgG and IgA observed in patient C. However, the low levels of IgM in C's plasma, even after the marrow graft, suggest that the marrow injected into patient C did not contain, or was not the source of, cells capable of producing IgM. Figure 12 demonstrates how the levels of complement (C'3) and transferrin fluctuated above and below the normal values. All three victims had consistently low transferrin levels when compared to the normal range of 220 to 340 mg/100 ml. Complement (C'3) levels were also affected. Table 7 shows the values of the immunoglobulins, complement (C'3), and transferrin for 6 months after exposure and better indicates the pronounced variations in these three men.

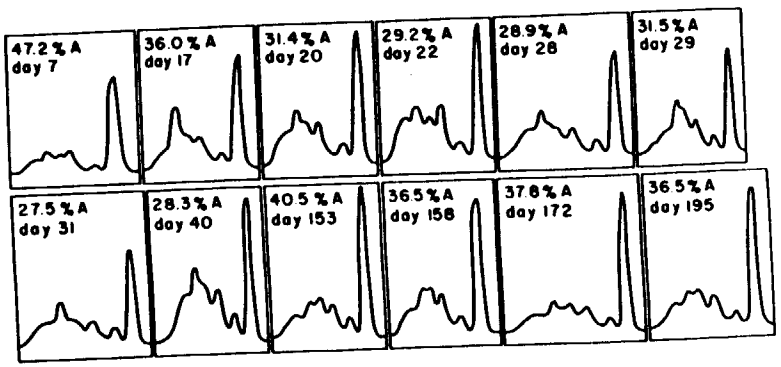

Fig. 7. Protein electrophoresis patterns of plasma from radiation accident victim C, exposed to 550 R total-body irradiation and 5000 R to his hands and feet.

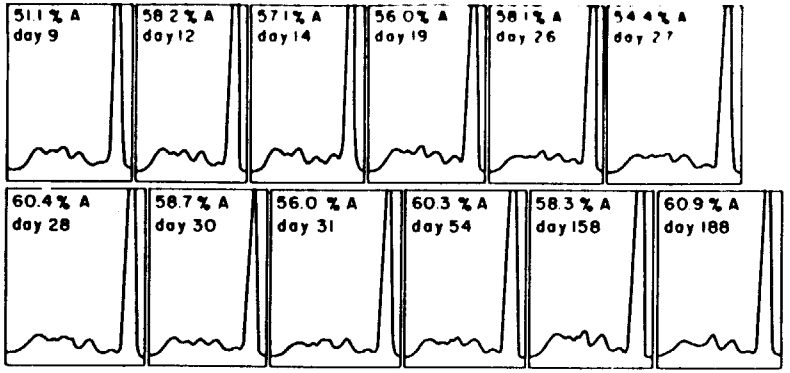

Fig. 8. Protein electrophoresis patterns of plasma from accident victim B after exposure to 550 R total-body irradiation.

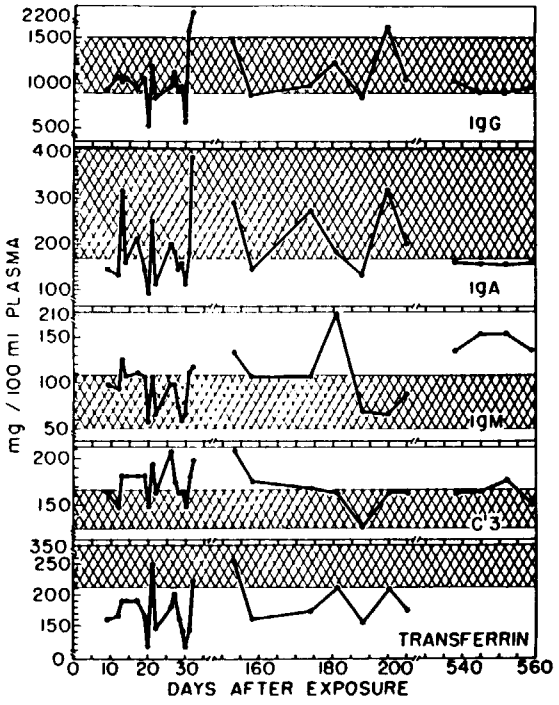

Fig. 9. Levels of immunoglobulins (IgG, IgA, IgM), complement (C'3), and transferrin in the plasma of low-dose victim A (100 to 200 R). The shaded areas indicate the normal range of values.

1027343

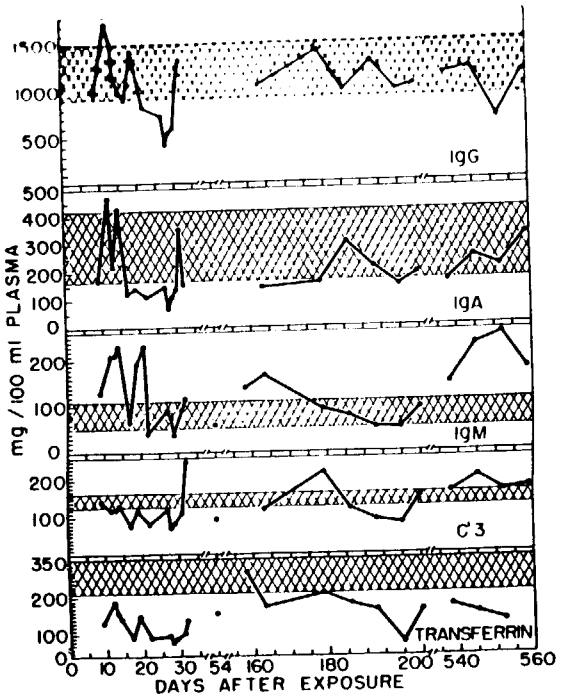

Fig. 10. Levels of immunoglobulins (IgG, IgA, IgM), complement (C'3), and transferrin in the plasma of high-dose victim B (550 R). The shaded areas indicate the normal range of values.

We have also studied the immunoglobulins, complement (C'3), and transferrin levels of patients exposed to total- and partial-body irradiation in the METBI and LETBI facilities at the Medical Division. Preliminary results with 14 patients show several dramatic increases or decreases in the levels of immunoglobulins, complement (C'3), and transferrin. Three patients had stable values for all proteins over a 6-week period after treatment. We observed infections in all patients who had low IgM levels (below 15/mg per 100 ml of serum) before radiation. Definite conclusions cannot be reached until more patients are studied. Here we present three examples, one exposed in LETBI, one in METBI, and one given splenic irradiation. A 59-year-old woman (patient 9) with malignant lymphoma, treated with 250 R total-body irradiation in the LETBI facility (1.5 R/hr), had low levels of IgG, IgA, and IgM and high levels of C'3 and normal levels of transferrin before treatment. The IgM and IgA levels decreased noticeably and IgG and transferrin levels increased significantly after irradiation (Fig. 13). The C'3 levels showed smaller variations. A 63-year-old man (patient 1) with idiopathic thrombocythemia exposed to 150 R

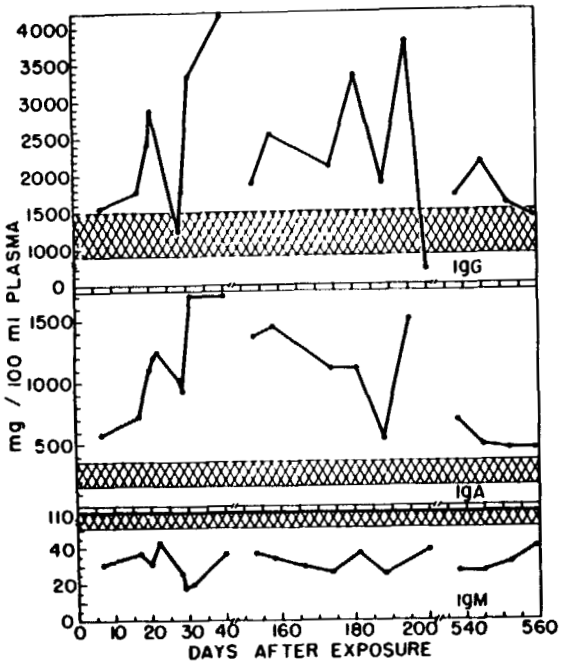

Fig. 11. Levels of IgG, IgA, and IgM in the plasma of high-dose victim C after irradiation and marrow grafts. The shaded areas indicate the normal range of values.

total-body irradiation in the METBI facility (1.5 R/min), had elevated IgG levels, normal IgA levels and low IgM levels before irradiation. We saw no change in the already depressed levels of IgM after treatment; however, both IgG and IgA levels significantly increased by 13 and 31 days (Fig. 14). A 63-year-old woman (patient 7) with chronic granulocytic leukemia treated with partial-body irradiation (410 rads to the spleen), had normal or slightly elevated immunoglobulins (IgG, IgA, and IgM) and C'3 before treatment. The IgA levels decreased after irradiation and reached the lowest level at day 9. The IgG, IgM, and C'3 levels fluctuated appreciably and on day 9 were at their lowest level (Fig. 15).

The half lives of IgG, IgA, and IgM in normal persons are 23, 6, and 5 days. In the accident victims short immunoglobulin half-lives are indicated by rapid increases and decreases. Apparent dramatic anabolic and catabolic imbalances have occurred. Immunoglobulin levels are reported by others to be stable for the average person, varying ± 17% of their mean over a 6-month period. All 3 radiation accident victims showed more than ± 17% variation within the first 3 months. Eighteen months after irradiation the immunoglobulins from low-dose victim A appeared to have stabilized but those of B and C were still showing pronounced variation. This report agrees with previous reported data, that the total gamma fraction decreases during the 30 days after total-body irradiation. However, a new finding is the long-term instability of immunoglobulin levels. We hope that animal experiments in progress will clarify this.

In contrast, our patients treated for blood diseases with total-body irradiation have not shown many rapid rises and falls in immunoglobulin levels, although significant changes have occurred. This difference from the accident patients can probably be attributed to the lower amounts of therapeutic radiation employed, the lower dose rate, and the fractionation of the dose. Only patient 7 who received splenic irradiation shows changes that approach those of the accident victims.

Morphogenesis and Pathogenicity of Candida Albicans

The other principal facet of our research in microbiology deals with morphogenesis and pathogenicity of Candida albicans. Germ-tube production by this yeast occurs in mammalian serum and serum substitutes, plasma, egg white, and human saliva, and it is often used to

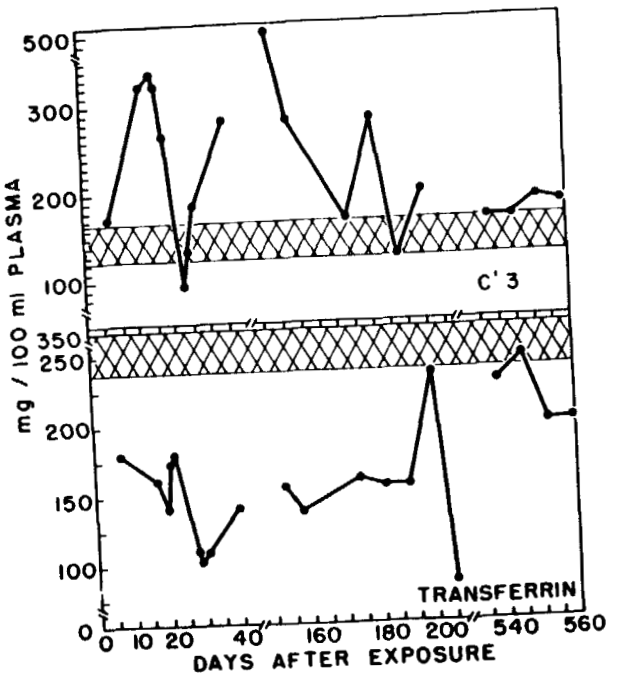

Fig. 12. Complement (C'3) and transferrin levels in the plasma of high-dose victim C. The shaded areas indicate the normal range of values.

1027344

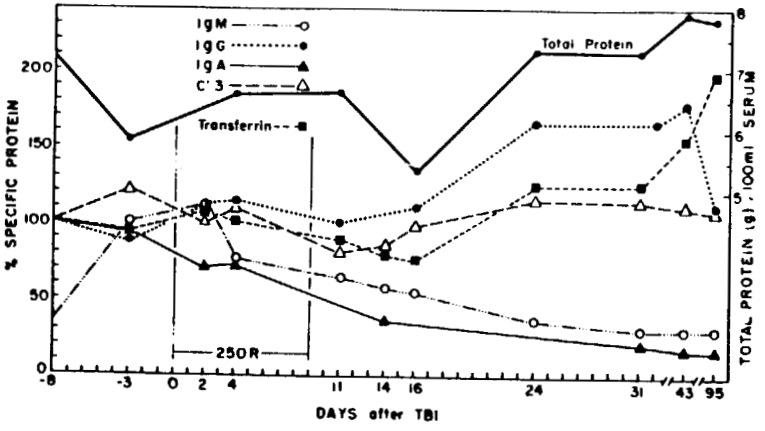

Fig. 13. Effect of 250 R total-body irradiation (1.5 R/hr) on the levels of immunoglobulins (IgG, IgA, IgM), complement (C'3), and transferrin. Three days before treatment the protein concentrations (mg/100 ml of serum) were 290 mg for IgG, 170 mg for IgA, 53 mg for IgM, 215 mg for C'3, and 308 mg for transferrin.

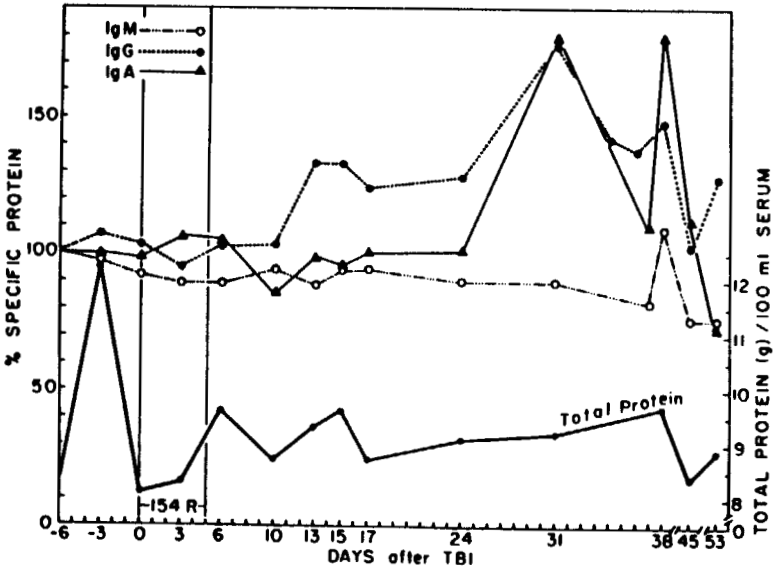

Fig. 14. Effect of 150 R total-body irradiation (1.5 R/min) on the levels of immunoglobulins (IgG, IgA, IgM). Before irradiation (day 0) the protein concentrations (mg/100 ml of serum) were 1795 mg for IgG, 210 mg for IgA, and 32 mg for IgM.

1027345

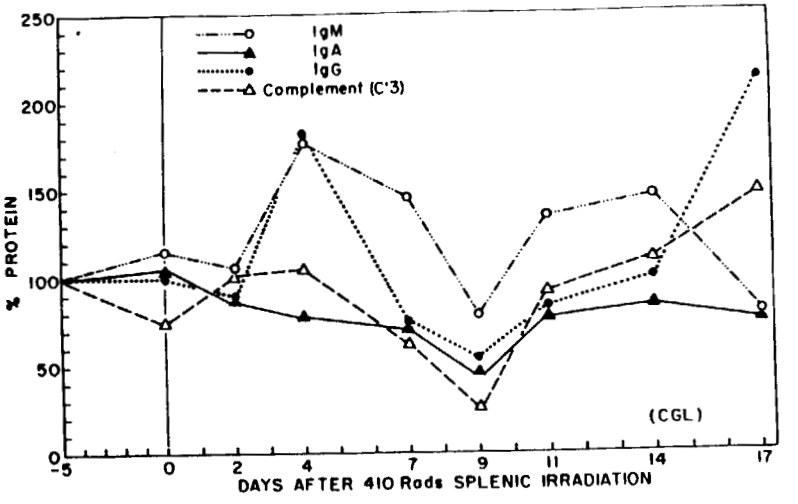

Fig. 15. Influence of 410 rads of splenic irradiation on the levels of IgG, IgA, IgM, and complement (C'3). Before irradiation (day 0) the protein concentrations (mg/100 ml of serum) were 1328 mg for IgG, 170 mg for IgA, 184 mg for IgM, and 158 for C'3.

aid in its clinical identification. Our research group has studied germ-tube production (or pseudohyphal growth) of typical C. albicans strains and of other Candida species in a defined liquid culture medium containing a single amino acid as the sole nitrogen source (Edward Balish, David N. Mardon, and Kathryn Hurst). Table 8 shows the capacity of Candida species to form germ tubes in glucose-salts-biotin (GSB) medium containing L-alpha-amino-n-butyric acid as the nitrogen source, GSB medium containing no nitrogen source, and human serum. In human serum, C. albicans produced typical long, curved germ tubes with a percentage range between 78 and 97. When GSB medium without a nitrogen source was used, the filamentous mutant (10259) produced a substantial number of filamentous cells and the "typical" C. albicans strains produced an average of 8% germ tubes. When L-alpha-amino-n-butyric acid was added to basal GSB medium, all strains produced germ tubes; however, they were shorter and less curved at 3 hr than those formed in human serum. In the first hour of growth C. albicans 10236-Y formed germ tubes faster in human serum than in GSB medium plus L-alpha-amino-n-butyric acid; after 1 hr similar numbers of germ tubes were produced in the two media.

Of other species of Candida, only C. stellatoidea formed germ tubes in appreciable numbers. This species produced the highest percentage of germ tubes in GSB medium with no nitrogen source and more in human serum than in GSB medium containing L-alpha-amino-n-butyric acid. Candida tropicalis and C. krusei did not make germ tubes, but formed elongated septate cells. The difference between germ tubes of C.

albicans and the elongated forms produced by C. stellatoidea, C. tropicalis, and C. krusei is shown in Fig. 16. With GSB as the basic medium, added gamma-amino-butyric acid as the nitrogen source caused C. albicans to form fewer germ tubes than did added L-alpha-amino-n-butyric acid. With L-methionine added to the GSB medium results were similar, for most strains of C. albicans, to those obtained

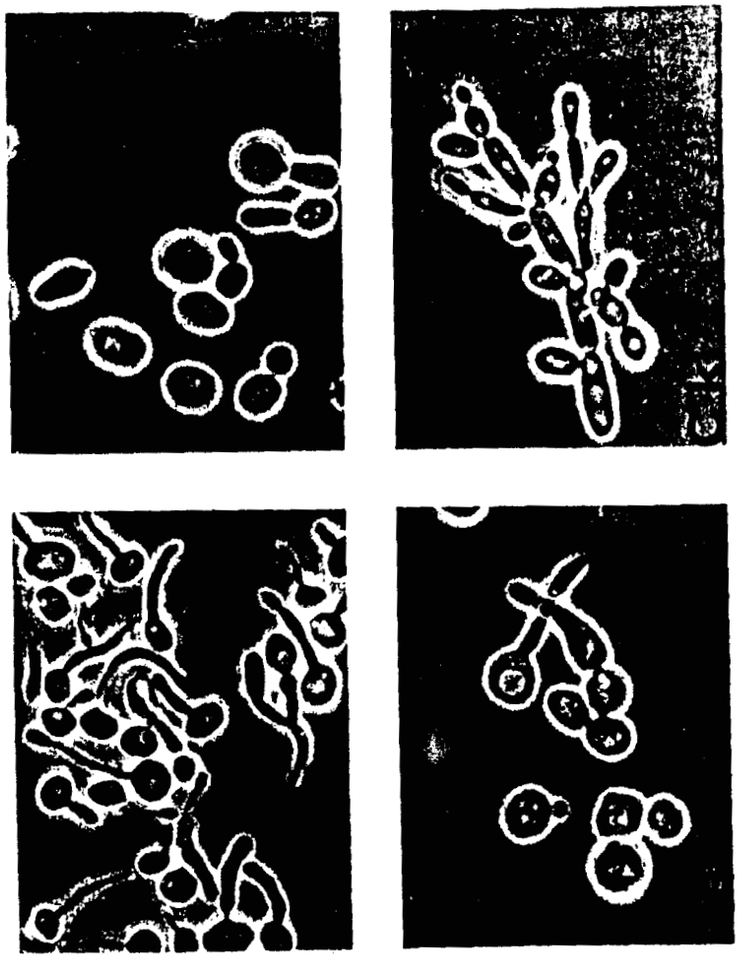

Fig. 16. Cellular morphology of four Candida species after 4 hr in L-alpha-amino-n-butyric acid medium at 37° C. Phase contrast 750 x.

1027346

in GSB medium with L-alpha-amino-n-butyric acid. When the other Candida species were tested, only C. stellatoidea produced a significant number of germ tubes. Unlike C. albicans, C. stellatoidea formed more germ tubes in Sabouraud dextrose broth than in GSB medium containing L-alpha-amino-n-butyric acid.

To study further the effect of the culture medium on germ-tube production, we grew three strains of C. albicans and six other Candida species on standard laboratory culture media and in GSB medium containing ammonium chloride as the nitrogen source. When cultured in GSB plus L-alpha-amino-n-butyric acid medium C. albicans produced significantly more germ tubes if the initial inoculum had been grown in Sabouraud dextrose agar rather than in Sabouraud dextrose broth or GSB medium with NH_4Cl. Growth of the initial inoculum on sheep blood agar (BBL) also resulted in poor formation of germ-tubes. In contrast to C. albicans, C. stellatoidea produced more germ tubes in GSB medium containing L-alpha-amino-n-butyric acid when the inoculum had been previously grown in GSB medium plus ammonium chloride than when it had been grown on Sabouraud dextrose agar.

Size of inoculum is an important factor in the formation of germ tubes by C. albicans in serum. Therefore, we kept the inoculum size between 2 and 6 x 10^6 cells/ml. Cell concentrations between 5 x 10^5 and 5 x 10^6 cells/ml for C. albicans strain 10231-Y were optimal. This range is lower than other investigators observed with C. albicans in serum and may help to explain the wider percentage range for germ-tube formation by C. albicans strains in GSB plus L-alpha-amino-n-butyric acid medium than in human serum (Table 8). Germ-tubes did not appear significantly at 28° C with any of the Candida cultures when L-alpha-amino-n-butyric acid was the nitrogen source in the GSB culture medium. These results resemble those that others have observed with C. albicans in serum at 30° C.

The effect of pH on germ-tube production by all Candida cultures in GSB medium containing L-alpha-amino-n-butyric acid was tested at pH 5.7 and 6.95. With most strains of C. albicans, the percentage of germ-tube formation was slightly higher at pH 6.95 (5 to 20% higher depending upon the strain) compared to that at pH 5.7. No significant differences in germ-tube formation occurred at these two pH values with any of the other Candida species, except C. stellatoidea 11006, which produced substantially more germ tubes at pH 6.95 than at 5.7.

We determined the rates of incorporation of ^{14}C-1- and ^{14}C-3-labeled alpha-amino-n-butyric acid during germ-tube formation by C. albicans. The relative incorporation of these two carbon atoms was normalized as to specific activities, allowing us to compare the incorporation of the ^{14}C-1 and ^{14}C-3 carbon atoms. During germ-tube formation (0 to 4 hr) approximately twice as many ^{14}C-3 atoms as ^{14}C-1 atoms appeared in the cellular residues. However, the rate of incorporation of both labeled carbon atoms was nearly equal at 6 and at 16 hr. Between 6 and 16 hr blastospore formation increased so that the cultures were more than 50% yeast-like by 16 hr of incubation.

In summary, we have described a minimal culture medium (GSB plus L-alpha-amino-n-butyric acid) in which C. albicans consistently

forms more germ tubes than C. stellatoidea. The minimal defined liquid culture medium excludes the complex nutritional factors present in other media (particularly serum) used to study germ tube production and therefore is a valuable tool for investigating and defining the biochemical basis for morphogenesis of C. albicans.

We have observed (Edward Balish, David N. Mardon, and Kathryn Hurst) that the cellular morphology of a biochemical variant of Candida albicans can be controlled by passing carbon dioxide through the culture

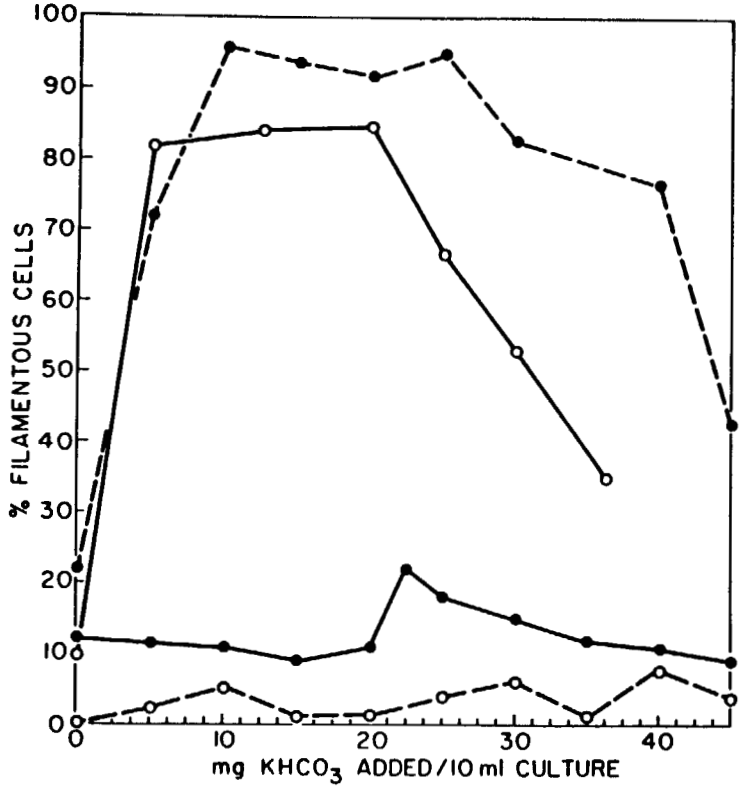

Fig. 17. Effect of carbon dioxide on dimorphism. Cultures grown for 5 hr at 37° C in GSB medium containing 0.025% Sabouraud dextrose medium. The inocula were grown in complete GSB medium.

●——● *C. albicans 10231-C* o——o *C. albicans 10261*
●– – –● *C. albicans 10231-Y* o– – –o *C. tropicalis 7347*

1027347

system or by growing the variant in media containing selected individual amino acids or ammonium sulfate as the sole nitrogen source. Since the variant resembled C. tropicalis in several respects, the effects of carbon dioxide and selected amino acids on the cellular morphology of a typical strain of C. tropicalis, several strains of C. albicans, and five other Candida species were also tested. Carbon dioxide initiated filamentous growth (germ tubes) of C. albicans 10231-Y and 10261, but not of 10231-C or C. tropicalis 7347 (Fig. 17). The percentage of filamentous cells obtained with 10231-Y and 10261 depended upon the quantity of bicarbonate added. Another C. albicans isolate (10231-F) was similar to 10231-Y in its response to potassium bicarbonate. The results with strain 10231-C resembled those previously observed (D. N. Mardon, A. W. Phillips, E. Balish, in press, J Bacteriol) when an inoculum was grown in GSB medium. However, in that earlier investigation, which employed a flow of carbon dioxide and oxygen through the culture system at a ratio of 2:1, we demonstrated that strain 10231-C could be induced to form predominately pseudohyphal cells in Sabouraud dextrose broth rather than GSB medium. In the present study we saw similar numbers of germ tubes in C. albicans isolates 10231-Y and 10231-F from Sabouraud dextrose broth or GSB medium. On the other hand, C. tropicalis 7347 did not form filamentous cells in the presence of carbon dioxide with either a GSB or Sabouraud dextrose broth inoculum. The greatest incorporation of $^{14}CO_2$ occurred in yeast-like cells of C. albicans 10231-C. Similarly yeast-like cells of C. tropicalis 7347 also incorporated relatively large amounts of this labeled compound. Less $^{14}CO_2$ was found in cells of the two isolates of C. albicans that produced germ tubes (10231-Y and 10231-F). The highest rate of incorporation of $^{14}CO_2$ by all four organisms occurred during the first 3 hr of growth. The maximum amount of $^{14}CO_2$ incorporated per milligram of cell solids was as follows: C. albicans 10231-C, 2.38%; C. tropicalis 7347, 1.58%; C. albicans 10231-F, 1.35%; and C. albicans 10231-Y, 1.01%. Table 9 shows the effect of carbon dioxide on filament production with the three isolates of C. albicans 10231 and C. tropicalis 7347 when various nitrogen sources were added to the GSB culture medium. Cultures of two C. albicans isolates (10231-Y and 10231-F) consisted predominantly of germ tubes with all additives tested. In the basal GSB culture medium without any added compounds, 10231-Y was predominantly yeast-like while 10231-F still displayed many germ tubes. In general, we have observed that strain 10231-F has a greater tendency toward filamentous growth than 10231-Y as shown in Table 9, where GSB medium without the usual ammonium sulfate (that is, containing no nitrogen source) was used. Even in this culture, a substantial number of germ tubes was observed owing to their presence in the 10231-F inoculum. The biochemical variant of C. albicans (10231-C) formed pseudohyphal cells (not germ tubes) only when Sabouraud dextrose broth or thioglycollate medium was added to the GSB medium, while C. tropicalis did not exhibit filamentous morphology under any of the test conditions. The cellular morphology of these four organisms grown in GSB plus 0.025% Sabouraud dextrose medium with and without carbon dioxide is shown in Fig. 18. With this medium at 28° C in the presence and absence of carbon dioxide, none of the organisms produced filamentous cells, although up to 25% pseudohyphal cells appeared in cultures of the C. albicans variant 10231-C.

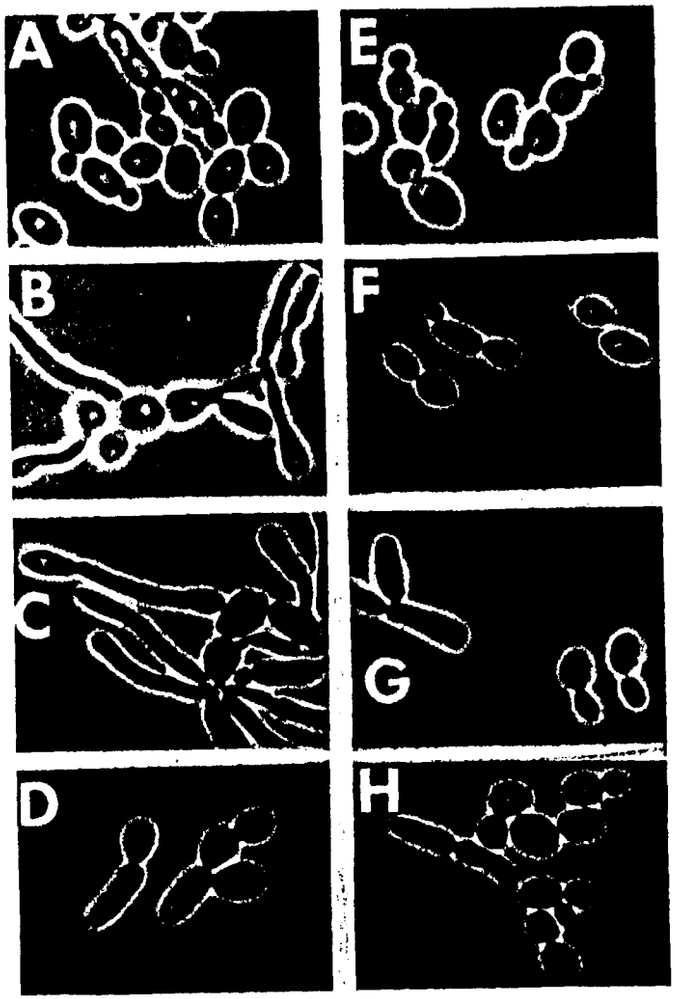

Fig. 18. Effect of carbon dioxide on cellular morphology. Growth was in GSB medium plus 0.025% Sabouraud dextrose medium. All are phase contrast 750 x.

With bicarbonate added

A. C. albicans 10231-C
B. C. albicans 10231-Y
C. C. albicans 10231-F
D. C. tropicalis 7347

Without bicarbonate

E. C. albicans 10231-C
F. C. albicans 10231-Y
G. C. albicans 10231-F
H. C. tropicalis 7347

1027348

The preceding experiments have established that carbon dioxide can direct dimorphism of C. albicans strains 10231-Y, 10231-F, and 10261. We subsequently tested the effect of carbon dioxide on three other strains of C. albicans and six other species of Candida and found that carbon dioxide initiated filamentous growth with all C. albicans strains. Cultures of a filamentous mutant of C. albicans (ATCC 10259) were predominantly filamentous whether carbon dioxide was added or omitted. Of six other Candida species tested for germ-tube production when bicarbonate was added, only C. stellatoidea 11006 produced germ tubes. However, this strain of C. stellatoidea made more germ tubes in control cultures without carbon dioxide than with added bicarbonate. Carbon dioxide induced cultures of C. tropicalis and C. krusei to form elongated cells; but being substantially shorter and thicker, they were readily distinguishable from germ tubes.

We previously reported that certain amino acids used as the sole nitrogen source could cause cellular elongation of a C. albicans variant (10231-C). On comparing the morphology of three isolates of C. albicans 10231 and C. tropicalis 7347 grown on selected nitrogen sources, C. albicans 10231-Y was yeast-like regardless of the nitrogen source while C. albicans 10231-F and 10231-C were predominantly filamentous with L-methionine, glycine, L-serine, L-ornithine, L-tyrosine, or L-phenylalanine. Also 10231-F was predominantly filamentous when L-proline, L-glutamic acid or L-glutamine was the sole nitrogen source. C. tropicalis 7347 produced some filamentous cells with L-methionine, L-phenylalanine, and L-tyrosine. Apparently the three organisms whose cellular morphology could be altered were most filamentous when L-methionine or L-phenylalanine was the nitrogen source and most yeast-like when ammonium salts (ammonium sulfate and ammonium chloride) were used. On the basis of these results, we tested ammonium chloride and L-methionine for their effects on the cellular morphology of four other strains of C. albicans and six other Candida species. Only C. albicans 10231-F and the filamentous mutant 10259 formed many filamentous cells in media containing ammonium chloride as the sole nitrogen source. However, when L-methionine was used, the biochemical variant of C. albicans (10231-C) and both strains of C. tropicalis tested, in addition to the filamentous strains of C. albicans (10231-F and 10259), produced a substantial percentage of filamentous cells. In the carbon dioxide studies we observed that C. albicans 10231-Y and 10231-F produced germ tubes at 37° C but not at 28° C. This prompted us to determine the cellular morphology of the three isolates of C. albicans 10231 and C. tropicalis 7347 at temperatures between 28° and 42° C in GSB medium containing methionine as the sole nitrogen source. C. albicans 10231-Y maintained yeast-like morphology at all temperatures tested. In contrast 10231-F was filamentous at 37° C, less so at 34° C, and yeast-like at 31° C and 28° C. C. albicans 10231-C was predominantly filamentous between 37° C and 28° C although the cells were shorter and thicker at 34° C and 37°C than at 31° C or 28° C. C. tropicalis 7347 produced some filamentous cells at all temperatures between 37° C and 28° C but was predominantly filamentous only at 28° C and 31° C. The cellular morphology of these four organisms at 28° C and 37° C is shown in Fig. 19. In addition to the obvious differences in mor-

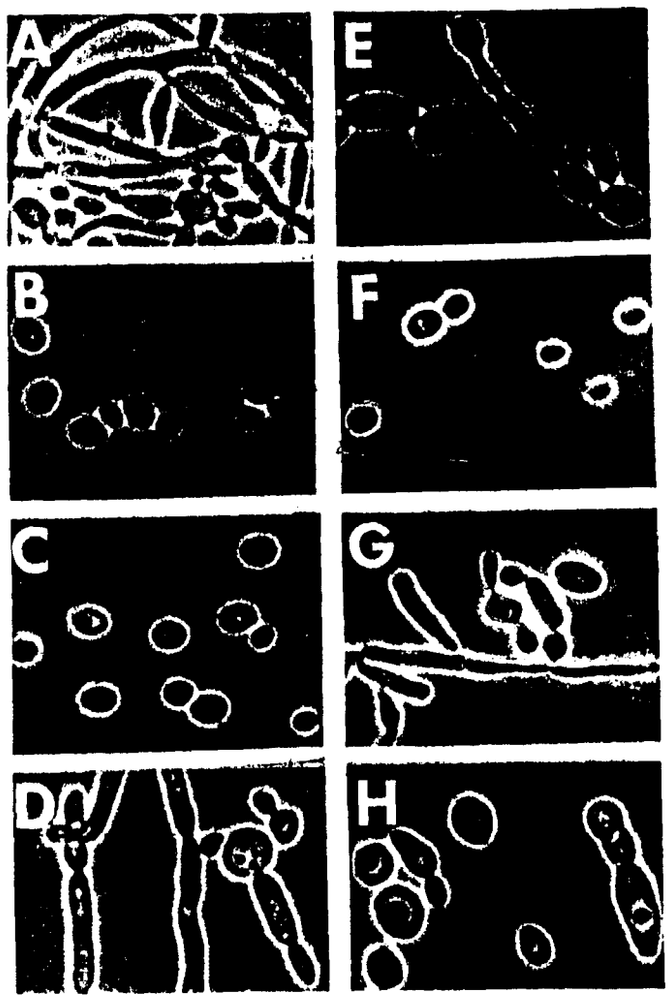

Fig. 19. Effects of temperature on cellular morphology. Growth was for 16 hr in GSB medium containing L-methionine as the nitrogen source. Phase contrast 750 x.

At 28° C	At 37° C
A. C. albicans 10231-C	E. C. albicans 10231-C
B. C. albicans 10231-Y	F. C. albicans 10231-Y
C. C. albicans 10231-F	G. C. albicans 10231-F
D. C. tropicalis 7347	H. C. tropicalis 7347

1027349

phology of C. albicans 10231-C, 10231-F, and C. tropicalis 7347 at 37° C and 28° C, large round dark areas were visible within all four organisms when they were grown at 37° C in media containing L-methionine as the nitrogen source. With the possible exception of C. albicans 10231-Y, these dark areas were absent in cells grown at 28° C.

The enzymatic transfer of a methyl group from adenosyl-L-methionine or methylmethionine to homocysteine has been demonstrated in extracts from yeast, bacteria, and in green plants. This enzyme synthesizes methionine from homocysteine in a manner that is different from mammalian and some microbial systems that require methyl-tetrahydrofolic acid and vitamin B_{12} or a B_{12} derivative plus methyl-tetrahydrofolate and adenosylmethionine. The enzyme may be important to the morphogenesis and virulence of C. albicans since we have shown that methionine stimulates filamentous growth. This cellular form predominates in infected tissues. In addition different levels of methionine in cell walls and different amounts of adenosylmethionine in vacuoles have been observed in yeast and filamentous forms of this organism. Our current studies on methionine biosynthesis in C. albicans were performed to determine the levels of homocysteine methyltransferase in crude cell-free extracts from six isolates representative of the wide variability often observed among strains of C. albicans (David N. Mardon, Edward Balish, and Kathryn Hurst). Although some of these strains were "filamentous mutants" we could obtain more than 85% yeast-like cultures with all six, for comparative purposes, when they were grown on Sabouraud dextrose agar. Thus we could observe enzyme levels in yeast-phase cells grown in a culture medium of the same composition, and the results should serve as base enzyme levels in future studies of sulfur metabolism during dimorphism.

Three cultures of C. albicans (10231-C, 10231-Y, and 10231-F) isolated from an ATCC 10231 culture were used throughout this investigation, as well as C. albicans ATCC 10261, 10259 (designated 10259-S), and 10259-R, a rough non-chlamydospore-producing strain isolated from C. albicans ATCC 10259. These six strains were selected because of differences in chlamydospore production, sucrose fermentation, germ-tube formation, and colonial morphology. We determined some of the optimal conditions for the enzyme assay by using crude cell-free extracts. The effect of pH on methyltransferase activity with C. albicans strains 10231-C and 10261 and different methyl donors was measured. For strain 10261, methyltransferase activity increased up to pH 9.4 when methylmethionine was the methyl donor. With adenosylmethionine the activity decreased at pH values above 7.30, presumably because of its decomposition under alkaline conditions. The results with the four other C. albicans isolates were comparable. With C. albicans 10231-C, however, methyltransferase activity increased sharply above pH 8.4 when methylmethionine was the methyl donor and when adenosylmethionine was used at pH values above pH 7.4. We selected pH 7.4 as the most appropriate pH for our standard reaction mixtures. Thirty-seven degrees centigrade was selected since higher temperatures can degrade adenosylmethionine. We did, however, examine the relative activity of homocysteine methyltrans-

ferase in extracts from all strains with methylmethionine as the methyl donor at 7-degree intervals between 23° C and 44° C. Essentially no activity occurred at 23° C with enzyme from all strains. At 44° C some cell-free extracts showed approximately twice as much methyltransferase activity as at 37° C but the extracts from other strains were erratic. In view of these results and since we wished to standardize our assay system for use with both adenosylmethionine and methylmethionine, 37° C was selected as the incubation temperature. The relation between protein concentration (of cell-free extracts) and methyltransferase activity was similar for adenosylmethionine and methylmethionine in all strains. With strain 10261, a 2-fold increase in protein from 150 to 300 μg of protein reaction mixture caused a doubling of enzyme activity. However, above 300 μg of protein the rate of methionine synthesis was slower. We therefore selected 250 μg protein per reaction mixture for the standard assay system.

Figure 20 shows a Lineweaver Burke plot of substrate (homocysteine) concentration and methyltransferase activity with an extract from strain 10261; we obtained similar results with extracts from the other

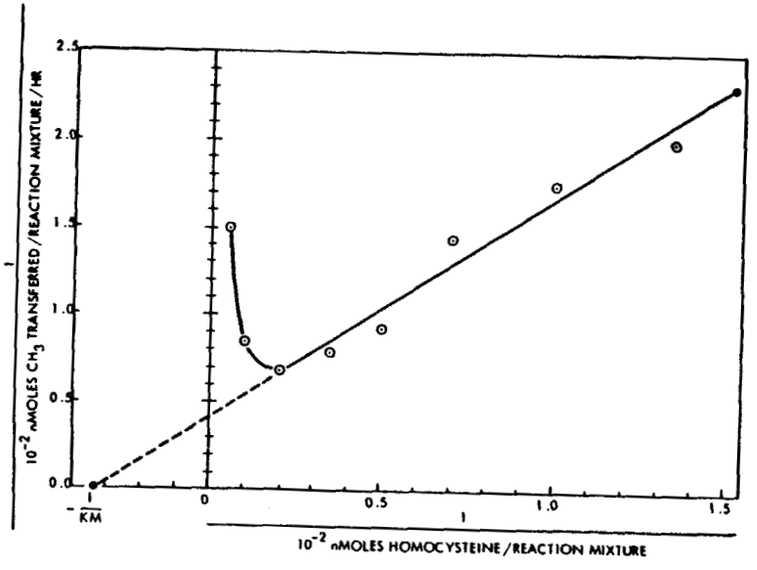

Fig. 20. Effect of homocysteine concentration on homocysteine methyltransferase activity in cell-free extracts from C. albicans ATCC 10261. Components/0.5 ml reaction mixture were L-homocysteine at the desired concentration; methylmethionine, 2 μmoles; C. albicans protein, 250 μg; KH_2PO_4-K_2HPO_4, 30 μmoles at pH 7.4; and dithiothreitol, 1 μmole. Incubated 1 hr at 37° C.

1027350

strains of C. albicans. Data obtained with methylmethionine as the methyl donor were used to calculate the approximate K_m value for the reaction ($\sim 7 \times 10^{-4}$ M) with strain 10261. The K_m, when adenosylmethionine was the methyl donor, was not determined, since enzymes that decompose adenosylmethionine were also present in these crude cell-free extracts. Above a concentration of 1000 n moles of homocysteine, substantial inhibition was observed; therefore we chose this level of substrate concentration, or a lower one.

When homocysteine methyltransferase activity versus time was measured, and when methylmethionine and adenosylmethionine were methyl donors, a linear relation was observed up to 3 hr with all strains of C. albicans with strain 10259-R; however, the activity was only about three-fourths that observed with the other strains at any time. For this experiment, reaction mixtures contained a total volume of 3 ml rather than 0.5 ml. At approximately 3 hr of incubation, the reaction rate decreased when the methyl donor was adenosylmethionine, owing to its depletion by side reactions. An incubation period between 0.5 and 2.5 hr resulted in proportional amounts of methyl groups transferred to homocysteine from either methylmethionine or adenosylmethionine.

The specific activity of enzyme from all strains with each methyl donor is shown in Table 10. We derived these values from experiments under standard assay conditions. The cell-free extracts were obtained from predominantly yeast-like cultures of all organisms grown on Sabouraud dextrose agar and allowed us to draw a comparative base line of enzyme activity in these strains for future studies of enzyme changes during dimorphism of C. albicans. Table 10 shows a slightly lower enzyme activity with adenosylmethionine than with methylmethionine. There was also a smaller range in enzyme activity (445-583) with methylmethionine than with adenosylmethionine (391-544), although in all experiments the values were within 30% of each other for all strains. These results indicated that homocysteine methyltransferase activity was similar in extracts from yeast-like cells of all strains.

Studies indicate that both L-homocysteine thiolactone and L-homocystine could replace L-homocysteine as the methyl acceptor. Further investigation of the methyltransferase reaction with ^{14}C-carboxyl labeled L-homocystine suggested that nonenzymatic reduction of homocystine to homocysteine occurred in reaction mixtures containing dithiothreitol. However, such an effect was not observed with homocysteine thiolactone. A small amount of methyltransferase activity appeared with L-cystathionine when adenosylmethionine was the methyl donor. None of the other potential methyl acceptors tested (L-cysteine, reduced L-glutathionine, oxidized L-glutathione, or dithiothreitol) were active in the methyltransferase reaction. The inability of the latter compounds to accept a methyl group is significant since relatively large amounts of glutathione or cysteine could be present in our crude cell-free extracts and since dithiothreitol was added to the standard reaction mixtures. Similar results were obtained for the other C. albicans strains with all potential acceptors except L-cystathio-

TABLE 9

Initiation of Filamentous Growth by Carbon Dioxide In Selected Culture Media*

Addition to GSB Culture Medium	Organisms *C. albicans* 10231-Y	*C. albicans* 10231-F	*C. albicans* 10231-C	*C. tropicalis* 7347
0.025% Sabouraud Dextrose Broth	5†	5	1	0
0.025% Yeast Extract	5	5	0	0
0.025% Vitamin-Free‡ Casamino Acids	5	5	0	0
0.025% Thioglycollate	5	5	2	0
0.008% AA Mixture	5	4	0	0
None	2	3	0	0
None - the usual Ammonium Sulfate Omitted	0	1	0	0

* 10 mg carbon dioxide was generated in each 25-ml Erlenmeyer flask by the addition of 0.45 ml 0.5 M $KHCO_3$ to 9.45 ml of GSB or modified GSB medium containing 0.45 ml of 0.5 N HCl at 4°C.

† Filamentous cells in cultures after 5 hr at 37°C.
0 = 0-15% 3 = 50-70%
1 = 15-30% 4 = 70-85%
2 = 30-50% 5 = 85-100%

‡ Comparable results were obtained with 0.008% vitamin-free casamino acids.

nine, where no activity was observed with strain 10231-Y.

Although L-methionine is the product of the homocysteine methyltransferase reaction, we tested 12 analogs of methionine in addition to L-methionine for inhibiting methyltransferase activity in reaction mixtures. Between 65 and 86% inhibition was observed when 2 µmoles of L-methionine, DL-methionine, L-methionine methylester, L-methionine ethylester, or N-hydroxy-methyl-DL-methionine was added to reaction mixtures containing either methylmethionine or adenosylmethionine. We found similar results with the two methyl donors when the other C. albicans strains were tested. Two other compounds, L-ethionine and S-methyl-L-cysteine also caused a small amount of inhibition, while L-methionine sulfoxide, N-formyl-L-methionine, N-acetyl-DL-methionine, DL-metheninol, S-ethyl-L-cysteine, and alpha-hydroxy-mercaptobutyrate did not inhibit the methyltransferase reaction. Figure 21 shows that competitive inhibition by L-methionine occurred when methylmethionine was the methyl donor and with two different concentrations of homocysteine. The K_i for strain 10261 under these

1027351

TABLE 10

Homocysteine Methyltransferase Activity in Cell-Free Extracts*

C. albicans Strain	N Moles CH_3 Transferred/mg Protein/hr† Methyl Donor: Methylmethionine	Adenosylmethionine
10231-C	524	394
10231-F	461	439
10231-Y	501	470
10259-R	445	391
10259-S	583	544
10261	474	505

* Reaction mixtures contained 1 µmole adenosylmethionine, or 2 µmoles methylmethionine : 250 µg protein : 30 µmoles potassium phosphate buffer, pH 7.4 : and 1 µmole dithiothreitol in a total volume of 0.5 ml.

† Reaction mixtures were incubated for 1 hr at 37°C. Each value represents an average of three assays.

TABLE 11

Methylmethionine : Homocysteine Methyltransferase Activity In Cell-Free Extracts from *Candida*

Candida Species	Nitrogen Source in GSB Culture Medium: NH_4Cl	NH_4Cl + L-Methionine	L-methionine
tropicalis	156*	215	20
stellatoidea	142	136	330
pseudotropicalis	-96†	14	-1
parapsilosis	-24	-34	246
krusei	-47	-22	-18
guilliermondii	-228	-169	-23

* Nmoles CH_3 transferred/mg protein/hr

† Indicate that methylmethionine was degraded or altered enzymatically.

conditions was $\sim 5 \times 10^{-4}$ M. This experiment was not performed with adenosylmethionine as the methyl donor because of interference from side reactions which degrade adenosylmethionine in our system.

We have established that C. albicans can form methionine from homocysteine via the enzyme adenosylmethionine (or methylmethionine): homocysteine methyltransferase (EC 2.1.1.e) and that C. albicans can accumulate adenosylmethionine (AM) and degrade it enzymatically. We undertook to determine whether other Candida species could carry out the same reactions as C. albicans (Edward Balish, David N. Mardon, and Margaret Wilusz*).

* Summer Student from Chestnut Hill College, Philadelphia, Pa. 19118.

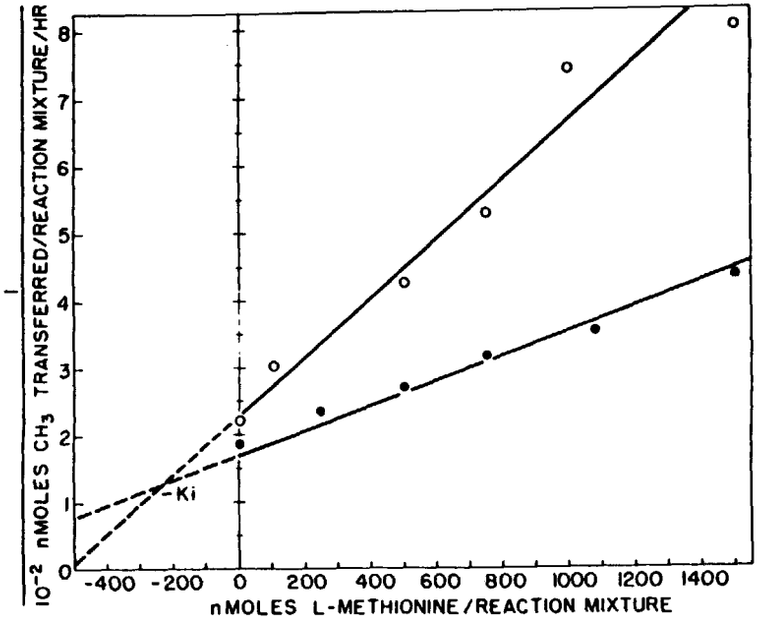

Fig. 21. Inhibition of homocysteine methyltransferase activity in cell-free extracts from C. albicans ATCC 10261 by L-methionine. Components/ 0.5 ml reaction mixture were L-homocysteine, either 0.5 µmole or 1.0 µmole; methylmethionine, 2.0 µmoles; C. albicans protein, 250 µg; KH_2PO_4-K_2HPO_4, 30 µmoles at pH 7.4; dithiothreitol, 1 µmole; L-methionine at the desired concentration. Incubated 1 hr at 37° C.

o——o 1.0 µmole L-homocysteine

•——• 0.5 µmole L-homocysteine

1027352

Of cell-free extracts from six other Candida species only those from C. tropicalis and C. stellatoidea had the enzymatic capacity to form methionine from methylmethionine (MM), and homocysteine via the methyltransferase reaction (Table 11). The cell-free extracts were prepared from cells grown in a defined medium with ammonium chloride as the nitrogen source. The negative values in Table 11 demonstrate that cell-free extracts from C. pseudotropicalis, C. parapsilosis, C. krusei, and C. guillermondii could degrade or alter MM enzymatically much more than could those from C. tropicalis and C. stellatoidea. Table 11 also shows that C. pseudotropicalis and C. parapsilosis could be induced to form methionine from homocysteine and MM when methionine was added to the growth medium. Candida tropicalis also showed increased homocysteine methyltransferase activity with MM when methionine was added to the glucose-salts-biotin-NH_4Cl medium. With C. stellatoidea methyltransferase activity increased when methionine was used as the sole source of nitrogen (Table 11).

Table 12 shows the amount of methionine formed when AM was the methyl donor in the enzymatic formation of methionine from homocysteine. Cell-free extracts from C. tropicalis, C. stellatoidea, C. pseudotropicalis, and C. krusei all could form methionine from homocysteine via a methyltransferase reaction from AM. Only C. parapsilosis was unable to carry out the reaction. However, as indicated by the negative values in Table 12, C. parapsilosis was able to degrade AM enzymatically. With several species, methionine supplementation of the growth medium stimulated AM-homocysteine methyltransferase activity (Table 12). When methionine was the sole nitrogen source, most strains again showed increased methyltransferase activity, except for C. krusei. All cell-free extracts (except C. krusei) degraded AM enzymatically, and methionine supplementation inhibited AM splitting activity, except for C. krusei. Cell-free extracts of C. krusei did have increased splitting activity when the organism was grown in medium with methionine as sole nitrogen source. Our previous studies showed that C. albicans can accumulate AM in their vacuoles. With all the Candida species tested, AM was present in vacuoles. Methionine in the growth medium enhanced AM accumulation except with C. pseudotropicalis, in which it caused inhibition. There are some interesting differences in methionine biosynthesis and adenosylmethionine metabolism between various Candida species and C. albicans. Candida albicans is the organism most frequently associated with infections in man. The metabolic differences we have observed may bear importantly on their pathogenicity.

Previously we noted a contradiction with earlier data on levels of homocysteine methyltransferase activity in cell-free extracts from yeast-like and filamentous cells of C. albicans. That is, some filamentous isolates had higher levels of this enzyme than extracts from yeast-like cells, while extracts from other filamentous isolates contained much less enzymatic activity than those from yeast-like cells. These differences might be explained partly by inherent strain

TABLE 12

Adenosylmethionine : Homocysteine Methyltransferase Activity In Cell-Free Extracts from *Candida*

Candida Species	Nitrogen Source in GSB Culture Medium		
	NH_4Cl	NH_4Cl + L-Methionine	L-Methionine
tropicalis	5*	23	41
stellatoidea	100	130	346
pseudotropicalis	88	138	157
parapsilosis	-286†	-254	-177
krusei	417	189	417
guilliermondii	-109	133	181

* Nmoles CH_3 transferred/mg protein/hr

† Indicates that adenosylmethionine was degraded or altered enzymatically

differences and variability in the culture and assay conditions. Therefore, in a new experiment (David N. Mardon, Edward Balish, and Brenda Joan Marks), we adopted the assay conditions for homocysteine methyltransferase described in an earlier paragraph with extracts from cells grown at 37° C for 16 hr in a GSB culture medium containing glycine as the sole nitrogen source. Among six strains of C. albicans, two (10231-C and 10259-R) failed to produce chlamydospores or form germ tubes. These physiologic characteristics (chlamydospore and germ-tube formation) usually are found in virulent strains of C. albicans. Extracts from the two atypical strains (10231-C and 10259-R) also contain less homocysteine methyltransferase activity than extracts from either yeast-like or filamentous strains of C. albicans that produce chlamydospores and form germ tubes. These results suggest a close relation between methionine metabolism, chlamydospore production, and virulence of C. albicans.

To further test this hypothesis we used three sulfur amino acid auxotrophs of C. albicans. One (7-NMU-I) has been previously described and the others were obtained from Dr. A. Sarachek of Wichita State University, Kansas. None of these organisms produced chlamydospores on corn meal agar, but when it was supplemented with L-methionine, S-adenosyl-L-methionine, L-homocysteine, L-cystathionine, or a combination of L-cysteine + L-homoserine, all three mutants produced chlamydospores (Table 13). One of the auxotrophs (7-NMU-I) also produced chlamydospores when corn meal medium was supplemented with L-homoserine alone. We believe that the results represent a specific role (or roles) of these compounds in chlamydospore formation

1027353

rather than merely a general growth requirement. This premise is supported (Table 14), showing results with a minimal glucose-salts-biotin medium supplemented with various amino acids; growth of the auxotrophs was determined by the methods of Bolinder; two amino acids (L-homoserine and L-homocysteine), which initiated chlamydospore production on corn meal agar, could not stimulate growth of the auxotrophs in minimal medium. Conversely, L-cysteine promoted growth of two of the auxotrophs but this amino acid did not initiate chlamydospore formation on corn meal agar (Table 14). However, some of these results may be due to differences in cellular permeability for cells grown on different media and will require further investigation. Because these auxotrophs could not grow in minimal medium supplemented with glycine, we could not compare their homocysteine methyltransferase activities with those of the six prototrophic strains. We have also found the three methionine auxotrophs to be as pathogenic for mice as prototrophic strains of C. albicans. This characteristic is lacking in C.

TABLE 13

Chlamydospore Formation by Sulfur Amino Acid Auxotrophs *

Supplement	Chlamydospore Formation		
	7-NMU-I	W-D-1	W-D-2
None	-	-	-
L-cysteine	-	-	-
L-homoserine	+	-	-
L-cysteine + L-homoserine†	+	+	+
L-serine	-	-	-
L-homocysteine	+	+	+
L-serine + L-homocysteine†	+	+	+
L-cystathionine	+	+	+
L-methionine	+	+	+
S-adenosyl-L-methionine‡	+	+	+
S-adenosylhomocysteine‡	-	-	-
S-methylthioadenosine‡	-	-	-

* 200 µg/ml of supplement was added to corn meal + 1% tween 80 agar then incubated 4 days at 23°C

† 100 µg/ml of each

‡ 4 µg/ml

TABLE 14

Growth of Sulfur Amino Acid Auxotrophs

In Supplemented Minimal Medium*

Supplement	Radius of Growth in MM		
	7-NMU-1	W-D-1	W-D-2
None	–	–	–
L-cysteine	–	5	5
L-homoserine	–	–	–
L-cysteine + L-homoserine†	–	3	3
L-serine	–	–	–
L-homocysteine	–	–	–
L-serine + L-homocysteine†	–	–	–
L-cystathionine	4	6	6
L-methionine	6	6	6
S-adenosyl-L-methionine	7	8	8
S-adenosylhomocysteine	–	–	–
5-methylthioadenosine	–	–	–

* Each supplement was at a concentration of 10 µg/ml in GSB minimal medium and was added to wells (7 mm d) in plates containing GSB medium + 3% agar and incubated 24 hr at 23°C.

† 5 µg/ml of each amino acid

albicans isolates (10231-C and 10259-R), which also failed to produce chlamydospores.

Our investigations to date provide evidence for a hypothesis that methionine metabolism, morphogenesis, and the relative virulence of C. albicans strains are intimately associated.

DOSIMETRY STUDIES AND MONITORING

To properly characterize the radiosensitivity of man, close cooperation among the health physicists, electronic engineers, and biomedical disciplines is required. To detect signs of stress in patients as they undergo radiation we have been obliged to create an instrument system for physiologic monitoring, and to precisely define the radiation that our patients receive. We have continued with dose measurements of our two total-body irradiators; our objective is to have truly adequate dosimetry,

1027354

a requirement that has been lacking in many earlier studies of radiation effects in man.

Human Organ Dose Estimates in Irradiators

Although the two irradiators used in our irradiation program were specifically designed for total-body irradiation, they differ in some respects: the medium-exposure-rate total-body irradiator (METBI) has eight cesium-137 sources producing an exposure rate of 1.5 R/min in a small exposure volume; the low-exposure-rate total-body irradiator (LETBI) has 10 cobalt-60 sources giving an exposure rate of 1.5 R/hr in a large volume. To determine the absorbed dose to organs of patients treated in these irradiators, parallel dosimetry studies were made with an Alderson Rando phantom and thermoluminescent dosimetry (W. L. Beck, Tom R. Stokes, Roger J. Cloutier, and C. C. Lushbaugh).

The Rando phantom, having standard-man dimensions, is constructed of tissue-equivalent plastic with an implanted skeleton and density-adjusted lung spaces. It is sliced transversely into 2.5-cm thick sections, each with holes in a 3- x 3-cm grid for insertion of dosimeters. Extruded LiF dosimeters were used to make all point dose measurements. We have previously reported the techniques for calibration and use of these dosimeters (USAEC Report CONF-680920, 1968, pp. 976-989).

Before estimating organ doses, we first had to locate dosimeter sites in volumes corresponding to the organs by comparing bone structure in roentgenograms of each phantom section with bone structure and organ locations given in standard anatomy texts. Dosimeters were placed in every grid hole within the volumes defined as organs. Except for the bone marrow, the average rad response of all dosimeters in an organ was defined as the average organ dose. The marrow dose had to be calculated by a weighted average since it is not uniformly distributed in a single well-defined volume. We first measured the average dose to each marrow compartment and then weighted each dose by the amount of active marrow in the compartment. The active marrow distribution was taken from a study by R. E. Ellis (Ellis, R. E. Phys Med Biol 5, 255, 1961). The average organ doses and their ranges, determined from several exposures in each irradiator, are given in Table 15.

We have shown that equal exposures in each irradiator produce almost (± 5%) equal absorbed doses to the head and chest of a patient; but the more centrally located organs such as the stomach, intestines, kidneys, and spleen receive approximately 20% greater dose in METBI than in LETBI. The liver and bone marrow get a dose about 10% higher in METBI.

Using these dosimetry data we can now compare the clinical responses of patients treated in these two irradiators on a critical organ-dose basis. Any differences seen can be attributed to dose-rate effects with far more reliability than when the comparison is made on an exposure basis.

TABLE 15

ORGAN DOSES IN TWO TOTAL-BODY IRRADIATION FACILITIES

Organ	Number of Dosimeters	Dose in Rads/100 R at Center of Exposure Field			
		METBI		LETBI	
		Average	Range	Average	Range
Bone Marrow	137	64	53-86	58	40-90
Cerebellum	9	77	74-81	75	72-77
Cerebrum	21	75	70-79	78	74-83
Heart	16	66	58-70	63	58-71
Intestines	107	67	54-76	54	46-61
Kidneys	6	66	62-70	52	51-54
Lenses of eyes	2	87	85-90	90	89-92
Liver	42	67	61-78	59	53-68
Lungs	185	67	58-77	64	56-77
Skin (above sternum)	2	73	72-75	82	80-83
Skin (front waist)	2	74	72-75	74	73-75
Spleen	7	69	64-73	55	53-57
Stomach	34	64	59-69	52	47-58
Thyroid	2	76	75-77	78	76-80

Physiologic Monitoring

The Instrumentation Department has continued to improve and upgrade the physiologic monitoring system used in the low-exposure total-body irradiator (LETBI). Additional signal connections have been made from the monitoring electronics to the IBM-1800 computer. Moreover, we have added lines from each rate meter, switch, and relay on the radiation-control console so the computer can monitor all operational functions. Any change can be sensed and dealt with through appropriate programs.

Our engineering staff is now evaluating a pair of subminiaturized physiologic couplers, obtained through the NASA Manned Space Flight Center in Houston, which are designed to condition signals of the electrocardiogram and pulmonary impedance functions. The size of the two units together is about that of a cough-drop box and we intend to mount them on a webbed belt worn about the patient's waist. Their proximity to the patient's electrodes will help reduce the 60-Hz interference seen on some of our recordings. Two 12-volt automobile storage batteries

1027355

supply power -- an addition we hope will give a more interference-free and safe operation. Ordinarily these small units are worn in an instrumented vest under an astronaut's spaceflight suit. We are pleased to have an opportunity to evaluate and perhaps later use these remarkable devices.

In recent months we began to expand our monitoring system, formerly limited to the LETBI facility, to measure patient reactions to therapy in the medium-exposure-rate total-body irradiator (METBI). The METBI exposures are 60 times faster than the 1.5 R/hr rate in our LETBI room. Past experience has shown that patients exposed to the higher dose rates, in METBI, develop some of the nausea and vomiting of radiation sickness. Soon we will begin examining some of these effects with a new mobile system for physiologic monitoring, which incorporates circuits for recording physiologic variables not included in the stationary LETBI monitor. It is movable to any location within our hospital complex, and with it we can also collect data for pre- and postirradiation studies.

A small room adjoining the LETBI facility was recently equipped with signal cables to the LETBI monitor so that base-line and other experimental data can be taken outside the irradiator. This small physiologic monitoring laboratory gives us the opportunity to study some radiation effects in greater detail. If needed, the new mobile monitoring system can be used in this room too.

Figure 22 shows a plan view of these physiologic monitoring facilities at the ORAU hospital along with an indication of routes for No. 4 gage wire grounding cables that have recently been installed to exhance safety.

Power Spectrum of Impedance Pneumograph

Changes in the power spectrum of the impedance pneumograph trace during radiation-induced gastrointestinal (GI) distress are being analyzed in our irradiated patients (Robert C. Ricks and C. C. Lushbaugh). One method for physiologically evaluating radiation stress is to analyze the changes in respiratory patterns, and it is generally agreed that various forms of stress including exercise, gastrointestinal distress, and pain result in altered breathing. Until recently most respiratory studies used data obtained from the impedance pneumograph (Geddes, L. A. and Hoff, H. E. A J Med Electron 3, 16-17, 1964 and Geddes, L. A., et al. Aerospace Med 33, 28-33, 1962) with visual interpretation serving as the basis for analysis.

Recent techniques in analysis of respiratory impedance have indicated that the pulmonary impedance waveform is more complex than previously described, and is better interpreted by power-spectral analysis. In using this technique we obtained sequential analog traces of pulmonary impedance before, during, and after single and fractionated total-body exposures of patients with chronic granulocytic leukemia to gamma irradiation. After analog-digital conversion the power spectra of 4-min segments of trace were computed as previously described (21).

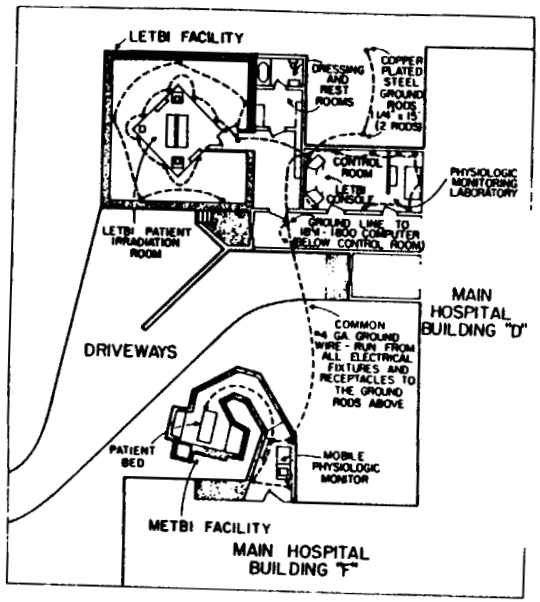

Fig. 22. Safety-grounding system for physiologic monitoring facilities at the ORAU hospital.

A patient receiving low-exposure-rate therapeutic radiation treatment (LETBI) served as a test subject for evaluation of low-dose-rate influence on GI distress. Treatment was protracted over 8 days with 30 R at 1.5 R/hr given daily. No untoward physiologic symptoms occurred and the pulmonary impedance power spectra remained normal (Fig. 23).

In another patient being treated in the METBI facility, definite alterations in respiratory waveform occurred after daily doses of 30 R (1.5 R/min) when GI distress developed. The increase in respiratory amplitude and variance, combined with the decrease in frequency resulted in large shifts in power spectra (Fig. 24). The postexposure power spectra not only show radiation-induced nausea (as expressed by altered breathing), but correlate well with descriptions of GI distress given by the patient (Table 16). As indicated by the patient's description and by graphic data, nausea subsided greatly when oral chlorpromazine was administered before the fifth radiation fractionation period. However, although the power spectral analysis showed no differences in pre- and postexposure traces, the patient did experience mild nausea. These observations indicate that spectral analysis of the pulmonary impedance pneumograph can be used in a patient-monitoring system to detect the onset and severity of radiation-induced GI distress and that these changes are dose-rate dependent.

102735b

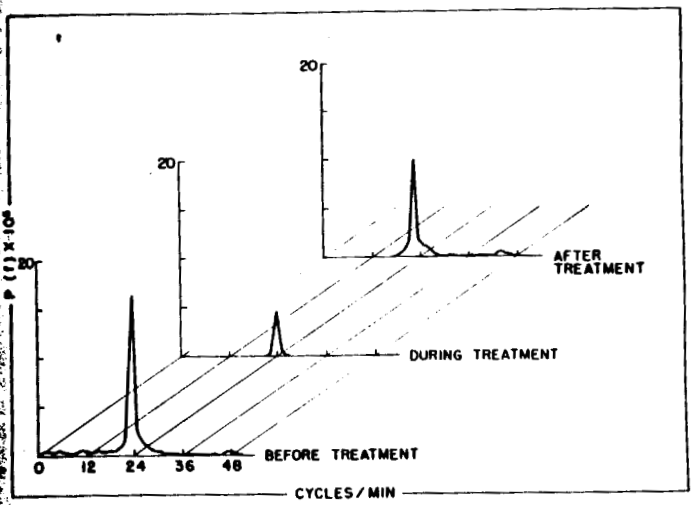

Fig. 23. Graphic representation of pulmonary impedance power spectra obtained before, during (midtreatment), and after treatment with 30 R daily for 8 days at 1.5 R/hr.

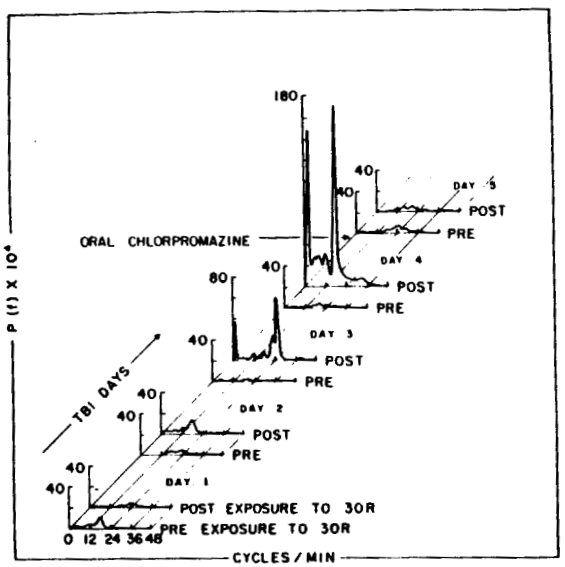

Fig. 24. Graphic correlation of severity of nausea with pulmonary impedance power spectra before and 15 min after 20-min exposures to 30 R (1.5 R/min) on 5 consecutive days (total exposure 150 R). On the fifth day the patient was on oral chlorpromazine therapy for radiation sickness.

TABLE 16

Patient Descriptions of GI Distress Following Daily Treatment with 30 R (1.5 R/min) for 5 Days

Accumulated Exposure	Described GI distress
Post 30 R	none
Post 60 R	mild
Post 90 R	moderate
Post 120 R	severe
Post 150 R	mild

Health Physics Aspects of Low-Energy Accelerators

In a somewhat separate but related effort, the health physics aspects of low-energy accelerators have been described by members of the ORAU Radiation Safety group at the conference on "The Use of Small Accelerators for Training and Research" (James D. Berger, Evelyn E. Watson, and Roger J. Cloutier. USAEC Report CONF-680411, pp. 112-137, 1968) sponsored by ORAU in April 1968. The paper dealt mainly with Cockcroft-Walton accelerators, similar to the unit located at the ORAU Special Training Division.

The low-energy accelerator is chiefly used as a high-yield, fast neutron source for activation analysis, neutron irradiation, and studies of neutron characteristics. Neutrons are produced by bombarding deuterium or tritium targets with a beam of deuterons. The deuterium reaction, $D(d,n)^3He$, produces 2.6-MeV neutrons at a yield of up to 10^9 n/sec. Fourteen-MeV neutrons are obtained from the $T(d,n)^4He$ reaction with a yield of about 10^{11} n/sec. This latter reaction results in a high radiation rate of approximately 200 rem/hr at 1 meter from the target. Shielding calculations and measurements in the ORAU accelerator facility indicate that approximately 150 cm of concrete is required to reduce the radiation levels to an acceptable value of 2.5 mrem/hr.

Capture gamma rays, decay of activation products, and X rays produced by backstreaming electrons are additional sources of radiation from the low-energy accelerator. Radiation levels outside the accelerator facility caused by these sources will be adequately attenuated by the neutron shielding. However, during operations requiring access to the machine and immediately after neutron production, these radiations may pose an exposure problem to those entering the accelerator room.

The tritium targets, 5 to 25 curies, used in neutron generators are a source of contamination and potential internal radiation exposure. Some of the tritium escapes during bombardment and deposits on internal surfaces of the accelerator and in components of the vacuum system. To evaluate its potential hazard in the vacuum system, samples of forepump oil from 42 accelerator installations were analyzed.

1027357

The results (38) indicate that millicurie quantities of tritium may be present in the vacuum pumps necessitating care when these units are serviced.

In an attempt to reduce tritium levels in the pump oil, we have installed on the ORAU accelerator a molecular sieve cartridge, described by Zimmerman in the proceedings of the accelerator conference (pp. 138-143). Since the installation of this cartridge, the tritium concentration has been reduced by a factor of 10.

APPLIED RADIOBIOLOGY

Our clinical observation is now well established that patients have more extensive WBC and platelet depressions and severe gastrointestinal distress in METBI than in LETBI. This difference is found even when the daily exposures are the same. It implies that greater damage per R is being produced by the 60-fold faster rate of METBI and accumulating faster than in that of LETBI. Elsewhere in this report, we show that these observations fit Bateman's dose-rate/response model that allows predictions of effects in man from presently untestable extremely low and high dose rates.

Damage and Repair in Relation to Exposure Patterns

In parallel to these studies in man we have made experimental studies in mice to determine the accumulation rates of gastrointestinal (GI) and marrow damage when we use the discontinuous METBI fractionated daily exposures and the continuous LETBI exposures (Lydia Corrill, C. C. Lushbaugh, Tom R. Stokes, Dorothy Lushbaugh, and Gretchen Humason). Mice were used because of the approximately equal dosage to marrow and all parts of the gut from the same exposure field whose strength was easily determined by thermoluminescent dosimetry. Multiple cellular replicating systems were studied in them simultaneously to see whether the length of the radiation-free interval would allow their more rapidly repairing systems to negate the greater damaging effect of the higher dose rate. The same daily dose level was studied with C57 and Blk 6 Cum mice irradiated continuously at 0.8, 1.6, and 3.2 R/hr in LETBI and others pair-irradiated with identical doses per day delivered at about 4.0 R/min. Multiple criteria for determining GI and bone-marrow repair levels were used: intestinal crypt mitotic index, intestinal weight, histopathology of necropsy sections, peripheral blood-cell counts and morphology, splenic weight, formation of endogenous erythroblast colonies in the spleen, ^3H-thymidine incorporation in replicating cells and testicular weight. These data were correlated with changes in total body weight and after-survival times in relation to accumulated dose. Two ages of mice were used: 50-day old (radiosensitive) mice, and 120-day old (radioresistant) mice.

Our findings did not support our initial thesis that the mouse would withstand the fractionated high-dose-rate daily exposures better than the continuous low-dose-rate ones. The germinal epithelium of the

mouse testis and the white blood-cell levels proved too radiosensitive to show any evidence of repair in either system of exposure at the dose rates used. Changes in intestinal length, weight, and crypt mitoses, on the other hand, seemed to indicate equal levels of good repair. Significant differences in response were found in changes in total body weight (Fig. 25), RBC indices and size distribution, splenic weight (Fig. 26), and numbers of endogenous erythroblast colonies, and in mean after-survival times. At a dose (35 R/day) that was half that critical for the adult mice (70 R/day) the young mice showed these responses to a pronounced extent.

The data are still incomplete for the lowest exposure groups. The data from the other two exposure levels show that almost all deaths were due to erythroblastic failure to replenish RBC lost through senescence. As anemia developed, progressive loss in total body weight occurred. Splenic size increased and then decreased as endogenous splenic erythroblastic clones arose and disappeared. Red blood cell sizing showed that these abortive splenic colonies were correlated in time with the appearance of macrocytic red cells that

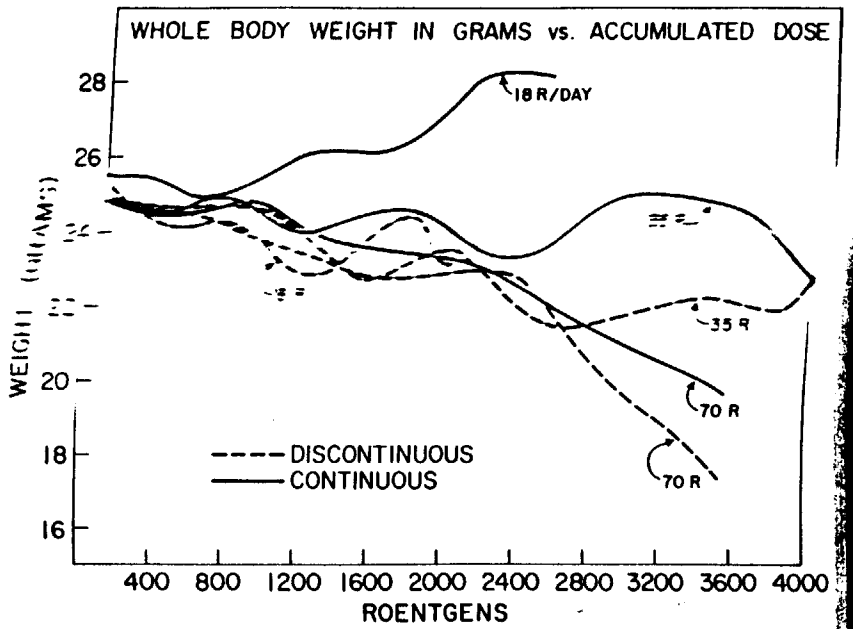

Fig. 25. Smoothed averages of the body weights of mice exposed discontinuously and continuously to total-body irradiation with the same daily doses. In every instance the mice given their daily exposure quickly (3.7 R/min) lost weight more rapidly than those exposed for 22 hr day.

1027358

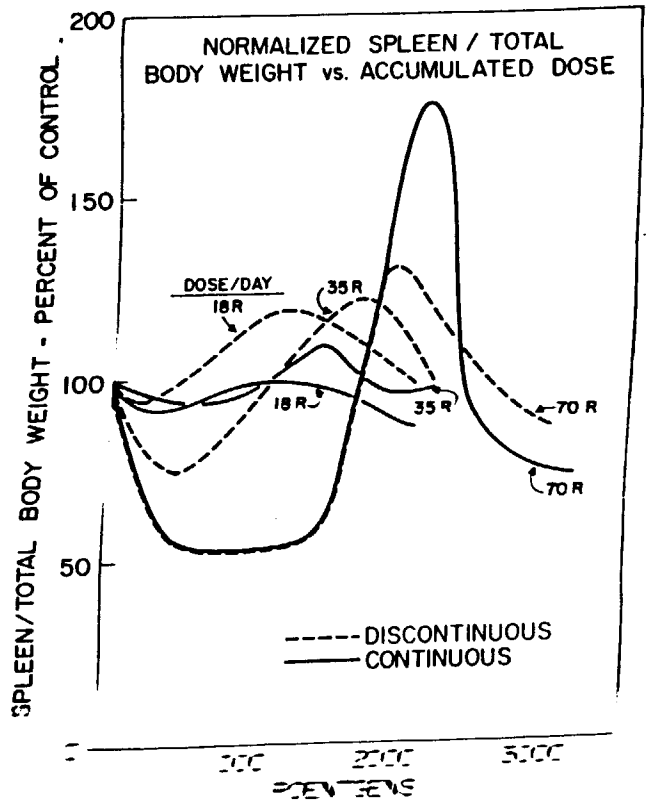

Fig. 26. Smoothed averages of changes in splenic weight of mice during discontinuous (METBI), and continuous (LETBI) gamma irradiation. They are expressed as spleen total-body-weight ratios to correct for the fluctuations in total-body weight shown in Fig. 25.

approached mouse fetal RBC in size. No deaths due to infection were found even though all mice had severe leukopenia and thrombocytopenia at all these exposure levels and patterns. In addition none had granulocytic myelopoietic hyperplasia as a measurable reparative response.

All signs of reparative responses and failures in these systems just described occurred at lower accumulated doses and elapsed times in the mice exposed to 35 and 70 R/day discontinuously at 4.0 R/min than in mice exposed to the same daily dose continuous at 1.5 R/hr.

Although these experiments are incomplete and need extension to obtain larger numbers for statistical purposes, the results seem to show that in the mouse, as well as man, discontinuous radiation

exposures at high dose rates are more deleterious than the same daily dose given continuously at a low dose rate. Since no differences are seen qualitatively in the repairing systems, it would seem that the lower continuous exposure causes less cellular damage by providing time between "hits" for intracellular repair to occur before the second hit. As a result less lethal cellular damage results and less replication by surviving cells is demanded in the critical cellular system.

Our observations on changes in body weight suggest that the higher radiosensitivity of the young animal may be due to greater somatic growth demands for protein synthesis in addition to that of its smaller, still-developing stem-cell population as previously demonstrated by Yuhas and Storer. Such demands would be a drain on its smaller stem-cell pool while; conversely, adequate reparative cellular replication would retard maturation of other systems.

Effect of Dose Rate and Fractionation on Iron Kinetics

In characterizing the effects of radiation on the erythropoietic system, we have examined the effect of dose rate and exposure fractionation on plasma iron kinetics in rats and man (Robert C. Ricks, C. L. Edwards, and C. C. Lushbaugh). Nondestructive methods of measuring radiation-induced physiologic changes are necessary for comparative radiobiologic studies involving man. Radiation-induced changes in serum iron transport can be assessed by measuring sequentially the serum iron and the disappearance rates for a ^{59}Fe tracer provided the radiation dose does not appreciably alter iron absorption or the mobilization of iron stores. Wasserman and Rashkoff previously suggested that plasma radioiron clearance provides a sensitive index of hematopoiesis (Brit J Haemat 1, 86, 1955). Lockner found that plasma iron levels remain rather constant except for diurnal variations in RBC production (Brit J Haemat 12, 646, 1966); Lajtha and Suit reported that failure of iron incorporation into early normoblasts causes an increase in the plasma iron (Brit J Haemat 1, 55, 1955). Therefore, in this study we assumed that the change in serum iron levels after total-body irradiation resulted from the changes in iron incorporation into red-cell precursors owing to the radiation-induced effects on red blood-cell formation. The effects on the erythropoietic system of single prompt (high-dose-rate) exposures, continuous protracted exposures at low dose rates, and fractionated daily exposures at high dose rates were studied in selected patients with chronic leukemia who were receiving therapeutic total-body irradiation and in mature male albino rats.

Our studies show that a single prompt exposure of 300 R TBI in the rat is sufficient to cause a significant increase in the serum iron within 6 hr postirradiation and this increase indicates an early erythropoietic depression. The serum iron reaches a peak of 268 μg per 100 ml (control value 130 μg per 100 ml) at 4 days postirradiation with the onset of recovery evident by 5 days. At the same time there is a steady prolongation of the radioiron disappearance rate reaching a maximum T/2 of 150 min (control value T/2 = 74) at 4 days postirradiation. At 5 days,

1027359

the data suggest considerable recovery with no significant difference in the serum iron and radioiron disappearance rate between irradiates and controls. This rate is assumed to indicate a recovery of erythropoietic activity.

Likewise, a 100 R single exposure (1.5 R/min) METBI in man appears to produce erythron suppression as evidenced by an increase in the serum iron similar to that caused by 300 R TBI in the rat. On the other hand, in eight patients exposures up to a total of 150 R, either fractionated METBI or protracted LETBI (1.5 R/hr) at 30 R/day failed to produce a similar effect. In rats an accumulated exposure of 600 R at 30 R/day failed to produce this effect. In fact, the 30 R daily exposures appear to stimulate increased erythron activity in the rat. Although not a constant finding over the 20-day fractionation period, there is some lowering of serum iron levels and shortening of ^{59}Fe disappearance times. The total serum iron clearance values in rats receiving 30 R/day exposures, either METBI or LETBI, do not increase significantly. However, a slight increase does occur when 360 R LETBI is accumulated as protracted exposure and when 420 R METBI is accumulated in fractionated exposures.

Daily exposures of 70 R at 3.6 R/min suppresses erythropoiesis in rats as indicated by the ^{59}Fe disappearance time when about 300 R is accumulated, but with further daily exposures the plasma iron disappearance time returns to normal range at day 7 (490 R accumulated exposure) and remains normal through 28 days (1960 R exposure). Indications are that the rat erythron adjusts to this level of daily damage. However, unlike after acute irradiation, the serum iron rises slowly reaching a peak at day 13 (910 R accumulated exposure) when the ^{59}Fe disappearance time has returned to control levels. When the serum iron levels and ^{59}Fe disappearance values are combined as the total iron clearance rate, we find the clearance lowest (0.36 μg/min) at day 4 (280 R accumulated exposure) when the $T\frac{1}{2}$ value is highest. After further daily exposures of 70 R the serum iron clearance rate rises to a maximum of 1.9 μg/min when 300 R more are accumulated. With protracted irradiation, daily exposures of 70 R at 3.6 R/hr, the rat erythron seems to respond similarly to 70 R/day at 3.6 R/min. The response to the protracted exposure occurs later, after 490 R accumulated exposure, and is less severe; the iron clearance-rate nadir is 0.8 μg/min.

These data suggest that the rat erythron can temporarily compensate to pulsed radiation up to 70 R/day; that exposures in this range affect the erythron and iron transport mechanisms in a way different from acute exposure to 300 R; and that exposures of 30 R/day cause too little damage to the erythron to be detected in altered iron transport values.

RADIATION IMMUNOLOGY AND MARROW TRANSPLANTATION

The immunology project has evolved from the objective of obtaining therapeutic marrow transplants, both in man and experimental animals, after exposure to lethal total-body irradiation. During the past few

years our emphasis has been placed in three basic research areas: (1) evaluation of various quantitative and qualitative parameters of radiation to suppress the immune response; (2) in vitro and in vivo studies of cellular immunologic incompatibility; and (3) use of anti-lymphocyte serum to delineate host-graft interactions in stable radiation chimeras and in the induction of chimerism after radiation.

Although the effects of total-body irradiation on the immune system of a variety of animal species is well documented, relatively little attention has been given to factors such as the quality of radiation and the rate at which it is administered to the animal. Previously we have demonstrated with ^{60}Co and ^{137}Cs gamma radiation that immune suppression depends not only upon the total dose but also upon the dose rate. Using the rejection of xenogeneic or allogeneic marrow grafts as an index of immunologic activity, we obtained more efficient host suppression if 900 R or 950 R irradiation was given at 53.4 R/min rather than at 3.65 R/min or 39.7 R/min (Science 146, 663, 1964 and Transplantation 7, 259, 1969). Also, antibody formation to sheep erythrocytes was more suppressed by radiation given at 72 R/min than at 8 R/min, the effect appearing over a total exposure range of 400 R to 800 R (Symposium on Dose Rate in Mammalian Radiation Biology. USAEC Report CONF-680410, 1968, pp. 16.1-16.22).

X-Ray and Neutron Effects on Mouse Immune System

Having documented the dependence of immunity on the dose and dose rate of low LET radiation, we recently studied similar parameters with two other types of radiation, X rays (250 kvp) and fission spectrum neutrons† (Charles F. Gottlieb* and N. Gengozian). Adult mice were irradiated with either X rays or neutrons to varying total doses, at three or four different dose rates, and then injected with sheep red blood cells (RBC) within 2 to 3 hr after exposure. At weekly intervals for 5 weeks the mice were bled for serum and the antibody titers were determined. The highest serum dilution yielding detectable agglutination of the red-cell antigen was taken as the endpoint. Figure 27 shows the responses after 165 rads of neutron irradiation. The absence of a dose-rate effect is clearly evident. Similar experiments using doses of 55, 220, and 880 rads also showed no dose-rate dependence, the immune suppression being proportional only to the total dose. In contrast to neutron radiation, we observed a definite dose-rate effect with 500 rads of X irradiation, the higher the dose rate the greater was the immune suppression (Fig. 28). The responses after 450, 600, and 750 rads of X rays were also determined, with all doses showing some dose-rate effect.

Comparing the responses after varying doses and dose rates, we used integral $\log_2$ titers, this being the area under the time-$\log_2$ titer curve between 7 and 35 days. Figure 29 shows the integral

* Predoctoral Graduate Student, University of Tennessee.

† From the Health Physics Reactor of ORNL.

1027360

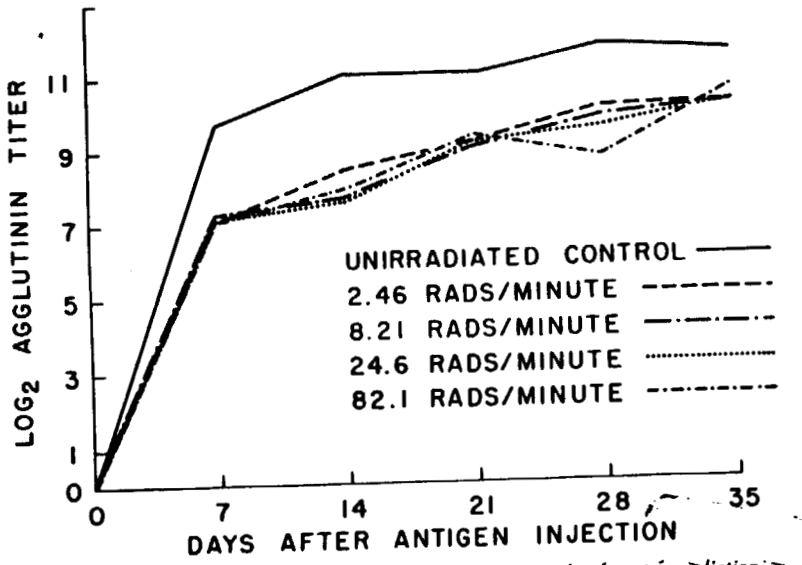

Fig. 27. Antibody formation to sheep RBC in mice after 165 rads of neutron radiation given at varying exposure rates.

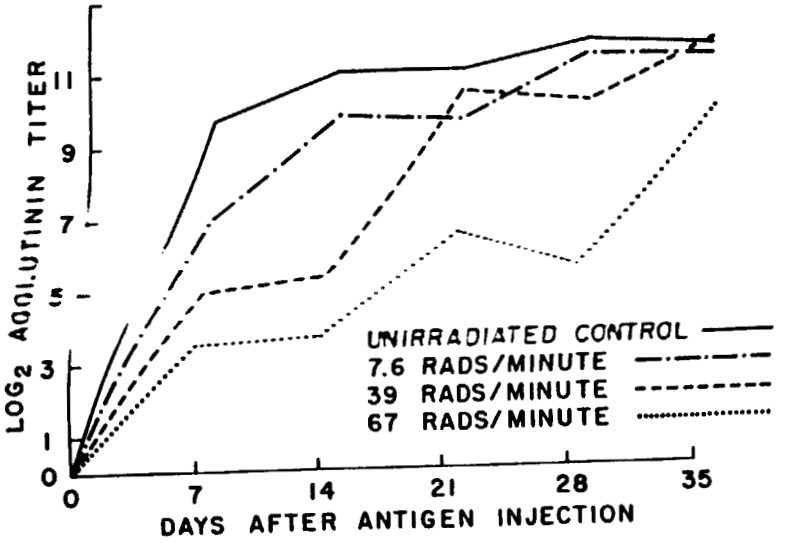

Fig. 28. Antibody formation to sheep RBC in mice after 500 rads of X irradiation given at varying exposure rates.

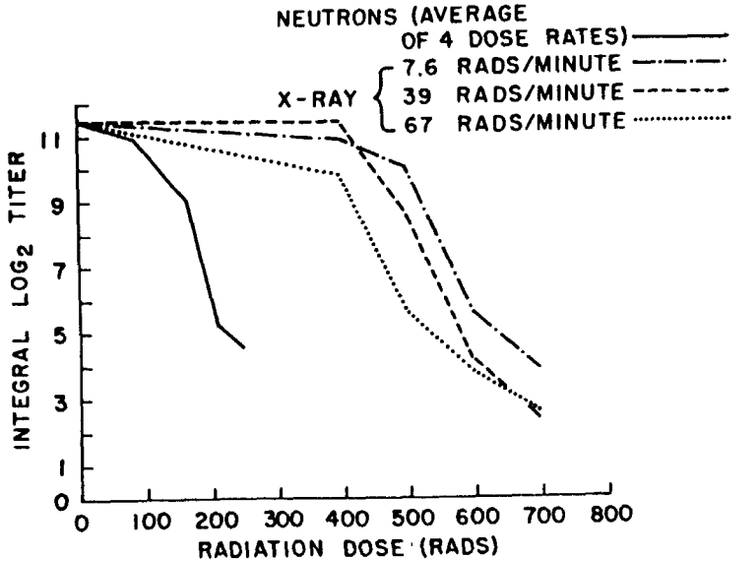

Fig. 29. Immune capacity of mice after different doses of neutron or X-ray irradiation given at varying rates.

titers as a function of radiation dose for neutrons and X rays. Because no neutron rate-effect was observed, the four dose rates (2.46, 8.21, 24.6, and 82.1 rads/min) were averaged to obtain a single curve. For X rays, each dose rate (7.6, 39, and 67 rads/min) was plotted separately to emphasize the rate differences. The maximum difference of 22-fold occurred at 500 rads, with slight differences apparent at the other doses. Other work from our laboratory with ^{60}Co radiation has shown a 60-fold difference in response when 670 rads was given at either 7.6 or 67 rads/min. Thus, the dose-rate phenomenon is dependent on radiation quality, with ^{60}Co (60-fold) > X rays (20-fold) > neutrons (0-fold).

These studies also show that neutrons are a more effective immunosuppressant rad for rad than either X or gamma radiation (Fig. 29). A survey of the literature in radiation immunology reveals that virtually nothing has been reported previously about the immunosuppressive effects of neutron radiation. In 1959, Vogel, Jordan, and Lesher (Proc. 2nd Australian Conf. on Rad. Biol. Acad. Press, p. 221) in reporting attempts to protect neutron-irradiated mice by marrow transplantation, suggested that neutrons may be a more effective depressant than either X or gamma rays. Their experiments were inconclusive, not having been designed to test radiation immunosuppression. Only recently, Miller and Jaroslow (Proc. of Symposium on Neutrons in Radiobiology. UT-AEC, ORNL, in press) reported

1027361

that the anti-sheep RBC response in neutron irradiated mice was slightly below normal when tested 100 to 300 days after exposure. Their objective was primarily to assess any delayed effects of radiation, rather than the acute, immediate effects reported here. Additional preliminary data from our laboratory confirm the greater immunosuppressive action of neutron irradiation in that significant depression of antibody formation occurs even when the exposure is given 3 days after antigen injection, an effect not observed with either X or gamma rays. The greater neutron radiation-mediated damage to the immune system and the apparent absence of any rate effect, in contrast to effects noted with X and gamma rays, correlate with radiation-induced mortality studies. Thus in our laboratory the $LD_{50/30}$ is 225 rads for neutrons, 800 to 900 rads for X rays, and 900 to 1200 rads for ^{60}Co, the latter two being dependent on the dose rate.

Detection of Graft-vs-Host Reaction in Mice

The studies reported in an earlier paragraph revealed the importance of radiation exposure rates in attaining adequate immunosuppression and its relevance to achieving foreign marrow transplants in mice. Thus, although at a low exposure rate the level of radiation given may be lethal, sufficient host activity may remain to result in a slow, yet often complete rejection of the graft. This rejection process was identified primarily by anti-graft antibodies in the serum several weeks after disappearance of the graft. We recognize, however, that any residual host immune capacity would be expected to make its presence felt immediately after exposure to the foreign-graft antigens. Our previous studies have indeed indicated that both host anti-graft and graft anti-host reactions may occur within 1 day after radiation exposure and bone-marrow grafting (Proc Soc Exp Biol Med 126, 135, 1967). In this earlier work we used the sensitive Jerne plaque technique to identify individual host or donor cells that react against foreign antigens. The early host and donor immune reactivity, although present, was not, however, as great as had been anticipated. In evaluating the procedures used, we decided that the conditions of the Jerne technique were not optimal for detecting the antigen-antibody systems involved in our radiation chimeras. Therefore, a subsequent extensive study was performed in analyzing the technique itself relative to our system. This resulted in the surprising finding that to detect antibody-forming cells optimally, the Jerne procedure requires different conditions for different antigen-antibody systems (16). With these new results we reevaluated our initial approach to this early host-graft incompatibility reaction in radiation chimeras. We decided to use Young and Friedman's modification of the Jerne procedure, which would provide additional sensitivity; rather than teasing the splenic tissue and suspending individual antibody-forming cells, thinly cut sections of a rapidly frozen spleen were used permitting the detection of discrete foci of antibody-forming cells (Germinal Centers in Immune Responses. Springer-Verlag, New York, 1967, p. 102). Rather than attempting to detect antibody-forming cells derived from bone-marrow cells injected into irradiated mice, we proceeded to establish the feasibility of this approach by injecting lymphoid cells known to have high numbers of immune-competent cells.

The present study incorporated three new factors designed to enhance the sensitivity of detection of immunologic activity of foreign cells in the irradiated recipient: (1) use of optimal conditions for the Jerne technique; (2) use of spleen sections rather than individually suspended cells; and (3) use of foreign lymphoid cells known to contain immune competent cells (Karl F. Hübner and N. Gengozian). This work was limited to studying only the early graft-anti-host reaction. Mice were given 950 R total-body X irradiation and then injected with either xenogeneic (rat) or allogeneic spleen cells 24 hr later. In the xenogenic system, 50×10^6 normal rat spleen cells were injected intravenously, and in the allogeneic system, 100×10^6 spleen cells from sensitized donors were injected intravenously and intraperitoneally. We killed mice daily for 8 days after cell transfer; after weighing each spleen we immediately froze it to an object disk of a Cryo Cut microtome at -18° C and cut sections 8 micrometers thick at 200 micrometer intervals along the longitudinal axis of the spleen and attached them to microscope slides. The slices were then covered with a thin layer of 0.7% agar containing the target RBC and complement (C'), human C' for the xenogeneic system, and guinea pig C' for the allogeneic system. A duplicate set of slides was prepared without C' for the experimental and for the control spleen sections. All preparations were incubated at 37° C and examined for hemolytic foci every 15 min.

During the first 3 days after injection of the cells the spleens of irradiated mice treated with rat spleen cells showed some hemolytic activity directed against mouse RBC. On days 1 and 2 after the cell transfer, diffuse hemolysis of the RBC in the agar layer appeared over the entire spleen slice in the presence of C'. On the third day after cell transfer the hemolytic activity over the spleen slices was less diffuse, indicating the beginning of a focal pattern; on day 4 clear confluent hemolytic foci appeared in the red-cell agar layer over the spleen. This focal pattern of hemolytic activity persisted thereafter. We did not attempt to count the number of foci because some were rather small, and confluent patterns were observed over many of the spleen slices; however, the number of foci increased on days 6 and 7 of the observation period.

The experiments with allogeneic spleen cells indicated a much weaker initial diffuse hemolytic activity against the host's RBC during the first 4 days, and foci did not appear before day 5. With a limited number of animals (3 per day) we could see hemolytic foci on days 5, 6, and 7. Figure 30 shows hemolytic foci over a spleen slice of an A/Sn mouse 5 days after the transfer of DBA_2 spleen cells. Spleen slices of normal mice and of mice that were irradiated but not treated with foreign cells did not show any hemolytic activity. All reactions performed in the absence of C' were also negative.

These observations indicate a complement-dependent reaction of the recipient's spleen against his own red cells, most likely due to specific antibody produced by the transplanted allogeneic or xenogeneic spleen cells. Thus, the feasibility of detecting early graft immune reactivity has been established; applying this approach to the study of graft-versus-host (GvH) or host-versus-graft (HvG) reactions in lethally irradiated mice treated with foreign bone marrow appears to

1027362

Fig. 30. Foci of graft anti-host activity in the spleen of an irradiated mouse injected with allogeneic spleen cells 5 days earlier.

be in order. The secondary-disease syndrome in many species of animals involves typically a rapid weight loss, hunched posture, piloerection, splenomegaly, and bloody diarrhea, signs that have limited significance and not offering quantitation of the pathophysiological events of a GvH reaction. Further, histologic examination of tissues from an animal with a secondary disease reaction offers merely a subjective evaluation of the process. Our studies appear to offer a means of specifically detecting in situ early or late ongoing GvH or HvG reactions with an excellent opportunity to define the morphology and origin of the cells involved.

Attempts to Abrogate Tolerance in Radiation Chimeras

Although transplantation of foreign bone marrow in irradiated animals eventually leads to secondary disease of varying degrees of

severity in most animals, a few will recover with no apparent ill effects and yet have a full transplant. In both xenogeneic (rat-mouse) and allogeneic long-term chimeras, however, spontaneous reversions to host hematopoietic systems do sometimes occur though infrequently and over an extended period; the cause and mechanism are not known. Is it an ultimate expression of a dormant, yet potentially reactive host immune system eliminating the foreign cells, or a "defective transplant" susceptible to any physiologic demand favoring residual host elements?

A study was undertaken in an attempt to gain some insight into this problem and better understand the conditions necessary to achieve a permanent therapeutic transplant (N. Gengozian and Charles C Congdon*). Long-term xenogeneic rat-mouse radiation chimeras having a complete rat-marrow transplant as indicated by tests on peripheral red blood cells, lymphocytes, and granulocytes were injected with varying doses of host (mouse) lymphoid cells (spleen and lymph-node cells). Three groups of chimeras received either 160×10^6, 10×10^6, or 1×10^6 mouse lymphoid cells intraperitoneally. At varying intervals after injection the animals were weighed, observed clinically, and tested for rat or mouse cells in the blood. Those receiving only 1×10^6 spleen cells showed no ill effects with no detectable change in the status of their foreign rat transplant. All of four chimeras that had received 120×10^6 spleen cells and, in addition, 40×10^6 lymph-node cells, showed a loss in body weight 9 days later (Fig. 31A). All had become severely anemic (hematocrits 14%-23%) by that time, and two died on day 10. The remaining two had approximately 25% mouse-type RBC in their circulation on day 9 and by day 13 all RBC were of mouse origin. The hematocrits were 25% and 28%. By day 25 the hematocrits had returned to 43%, paralleling the gradual increase in body weight, and these two animals went on to clinical recovery. Another group of four were injected with 10×10^6 mouse spleen cells (Fig. 31B). The severity of the wasting disease was less pronounced than with the high dose of cells as judged by gross appearance and a more gradual weight loss. However, three animals eventually died without any sign of replacement of rat-type tissues. The fourth animal had 100% rat-type cells on day 14, but when tested on day 22 had predominantly mouse-type RBC and by day 30 rat RBC could not be detected.

Two chimeras that had reverted to a mouse system as a result of treatment with a high dose of cells were subsequently injected with sheep RBC; both showed an excellent antibody response comparable to that of normal mice, which is in contrast to the known immunologic incapabilities of rat-mouse radiation chimeras.

This experiment demonstrated a reseeding of host hemopoietic elements in rat-mouse radiation chimeras after injection of mouse spleen and lymph-node cells. Since, however, spontaneous reversions are known to occur in this model, we invoked the thesis that all rat-mouse chimeras must contain a small surviving seed of mouse-type elements; therefore, activation and regeneration of these cells

---

* ORNL Biology Division

1027363

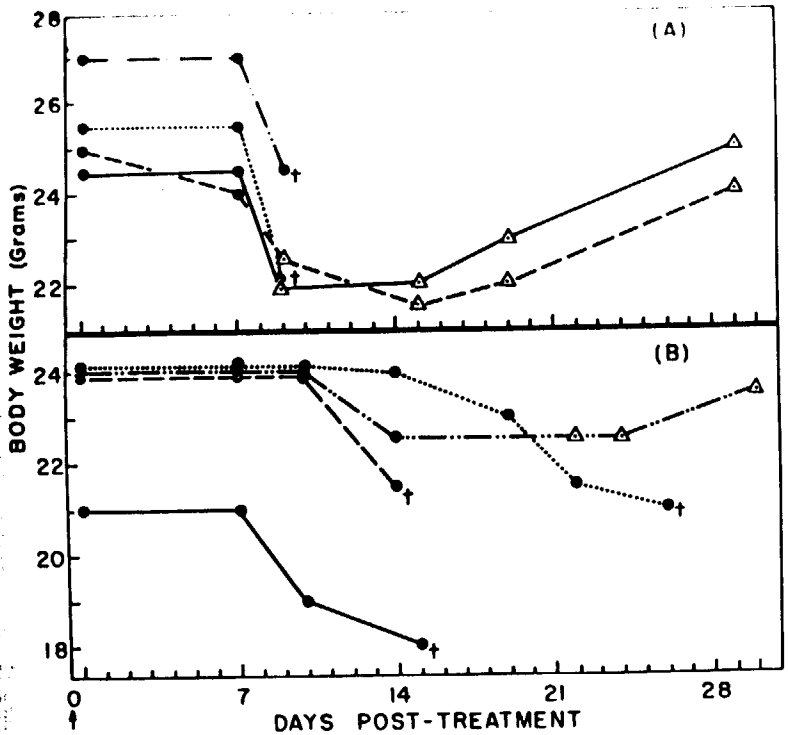

Fig. 31. (A, B). Chimerism reversal and body-weight changes in radiation rat-mouse chimeras injected with mouse lymphoid cells. A. 120×10^6 spleen cells and 40×10^6 lymph node cells; B. 10×10^6 spleen cells. Triangles indicate loss of rat RBC and reversal to mouse hemopoietic system. † indicates death of animal.

may be induced upon removal or destruction of the predominating chimeric rat tissues, without recourse to injection of spleen cells. The possibility of creating a reversion to host-type blood-forming cells with a mouse anti-rat lymphocyte serum (M-ARLS) was investigated. Such an antiserum would be completely syngeneic to the rat-mouse chimera since a bidirectional donor-host tolerance presumably exists.

More than 20 chimeras have been injected with M-ARLS and we will report here the data from only a few, representative of the reactions observed. The M-ARLS dose, 0.25 ml per inoculum and the routes, intraperitoneal and subcutaneous, were chosen empirically; since, however, the primary aim was not to induce a wasting syndrome but rather to effect chimerism reversal, the duration of treatment varied with the clinical course of each animal. The plan was to give three injections each week on alternating days until the condition of the animal warranted otherwise.

All chimeras responded strikingly to the M-ARLS as evidenced by loss in body weight, gross appearance, and hematologic effects. Some died within 1 to 2 days posttreatment, but one animal lived for 70 days under continuous treatment. One-half the mice died within 14 days of the initial injection. Figure 32 shows the effect of M-ARLS treatment of a chimera for 18 days; the characteristic responses were an early lymphopenia, marked neutrophilic response, anemia, and a gradual weight loss. The animal died 10 days after the last injection without any sign of recovery. The major pathologic processes seen at autopsy were bone-marrow necrosis and depletion of lymphatic tissues. Occasional animals died with relatively little evidence of bone-marrow necrosis. Chimeras treated with normal mouse serum showed cellular marrow at autopsy. Pathologic changes were absent in normal rats injected with normal mouse serum but normal rats receiving M-ARLS showed moderate lymphocyte depletion in lymphatic tissues in the few animals examined.

Several chimeras were treated with normal mouse serum as a control procedure. The response of one over a 30-day period is also shown in Fig. 32. Aside from a slight neutrophilic granulocytosis the first 4 days, normal serum treatment had no adverse effects. Similarly, normal mice injected with M-ARLS over an 80-day period showed no ill effects as gauged by body-weight increase, appearance, and hematologic values (data not shown).

None of the chimeras treated with M-ARLS has shown replacement of rat hemopoietic tissue by mouse elements. We tested for species-type RBC and neutrophils at regular intervals. We also removed mesenteric lymph nodes from a few animals that died and tested them with species specific antisera reagents; mouse lymphocytes could not be detected.

Much emphasis has been placed on the immunosuppressive potency of a variety of antilymphocyte sera (ALS) while the apparent cross-reactivity and physiologic effects of such sera on hemopoietic cell lines other than those of lymphoid origin have been minimized. Our studies show the potential marrow toxicity of ALS, and suggest further that the foreign marrow radiation chimera may be more uniquely sensitive to ALS than a normal animal. The fact that our experimental model allowed for a completely syngeneic relation between the host and ALS donor and therefore obviated any immune elimination of the ALS offers an explanation for its potent effect in the chimera. That this interpretation may not be entirely valid, however, is suggested by the following: (1) mortality was obtained with several chimeras within the first week of treatment and some died after only a single injection; (2) treatment of normal, young rats (80 g) with ALS on an equivalent body-weight basis has not resulted in anemia or mortality, although lymphopenia has been obtained in some animals; and (3) parallel histologic studies on rats and chimeras killed after varying intervals of ALS treatment show the chimera's hemopoietic system to be more severely damaged. Whether this is due to an innate deficiency in the regenerative capabilities of rat hemopoietic tissue in its foreign environment as contrasted to a normal "home" environment is not yet known.

1027364

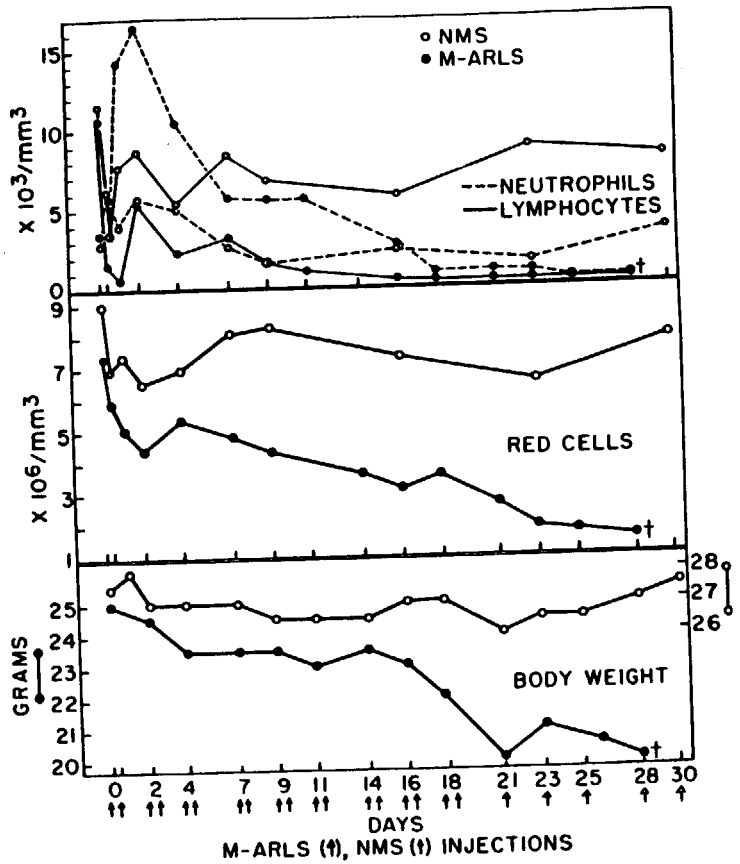

Fig. 32. Hematologic and body-weight changes in rat-mouse chimeras treated with either M-ARLS (solid arrows) or normal mouse serum, NMS (open arrows). † indicates death of animal.

Even though we failed to achieve chimerism reversal with the ALS, our original thesis that a break of tolerance could be induced by a negative feedback mechanism may still be valid. Indeed, the model chosen may have been too restrictive in that an insufficient number of original host cells were present in the chimera. Studies in chimeras having stable, more equivalent populations of both donor and host type elements are needed.

In Vitro Histocompatibility Test

We have continued work in the effort to develop an in vitro histocompatibility test in a search for tumor antigen (Helen Vodopick,

Elizabeth M. Rupp, and N. Gengozian). Evidence for the presence of tumor-specific antigens in animals with tumors is positive. However, unequivocal demonstration of tumor specificity has been possible only in autologous and syngeneic systems since in any homologous system, tumor specificities may be masked by strain-specific or species-specific antigens.

How does one demonstrate tumor-specific, in contrast to strain-specific or organ-specific, antigens?

The various methods of demonstrating tumor-specific antigens in animals are divided into two main groups - the in vivo and the in vitro tests. The former use transplantation methods, not usually practical in humans. Even if one restricts such tests to patients with cancer, the results may be misleading. If a patient cannot respond sufficiently to control his own tumor, then can he really respond to another tumor? In vitro tests eliminate some of the difficulties of in vivo studies, especially the need to use a patient or other human in the test system, but at times add their own problems.

The in vitro tests depend on the occurrence, concentration, and localization of the antigen in the tumor cell, and require the presence of surface antigen in the tumors. In a different approach we have used an in vitro culture technique originally devised as a histocompatibility test by Bach and Hirschhorn (Science 143, 813, 1964), and Bain, et al. (Blood 23, 108, 1964). They showed that a reaction occurred between different populations of mature lymphocytes, which transformed into blast cells capable of synthesizing DNA. This DNA formation can be assessed by incorporation of radioactively labeled thymidine: the greater the incompatibility of the cells, the greater the reaction that occurred. Initially, we used normal lymphocytes (37): first, a bi-directional study in which both populations were uninhibited; second, a unidirectional study in which one of the two lymphocyte populations was inhibited with an alkylating agent, mitomycin C. The reciprocal unidirectional reactions were also measured. When compared to the bidirectional results the uninhibited lymphocyte population of the uni-directional system yielded a greater or equal reaction in 23 out of 30 tests. We believe that maximal antigenic stimulation could be achieved in such a unidirectional system.

As an extension of these studies, we are attempting to use this method as a means of detecting tumor antigen. We obtained tumor tissue from patients with various malignant diseases and minced the tumor into fine particles with two scapels. These cells were suspended in tissue-culture medium TC 199. The particulate material was allowed to settle out and the supernatant suspension was used. We also isolated circulating lymphocytes from the blood of these same patients.

Healthy volunteers provided normal lymphocytes. These cells, presumed to be immunologically competent, were left uninhibited so that they could respond to the stimulus of the inhibited cells. The following combinations of cells were evaluated:

1027365

Untreated		Mitomycin C treated
Normal lymphocytes	vs	Patient's lymphocytes
Normal lymphocytes	vs	Patient's tumor
Patient's lymphocytes	vs	Autologous tumor
Patient's lymphocytes	vs	Normal lymphocytes

When sufficient cells were available, we were also able to test the response of the patient's lymphocytes to inhibited normal lymphocytes.

To minimize other stimulating factors in the unidirectional studies the culture medium TC 199 in which both cell populations were suspended contained 20% plasma autologous to the responding cells.

Blastic transformation was measured by carbon-14-labeled thymidine incorporation as described previously. The nucleoprotein of the cultured cells was isolated quantitatively and then counted in a liquid scintillation spectrometer. Final radioactivity was expressed as counts per minute per 4 million cells per culture tube.

In Figure 33, the results of five of the ten studies performed are depicted. Set 6a and b and set 7a and b are comparative studies using the same population of cells except that in set a no inhibition was used (bidirectional reaction) and in set b inhibited cells were used (unidirectional reaction). The pattern of response was the same in sets a and b but the degree of response was greater in set b in which

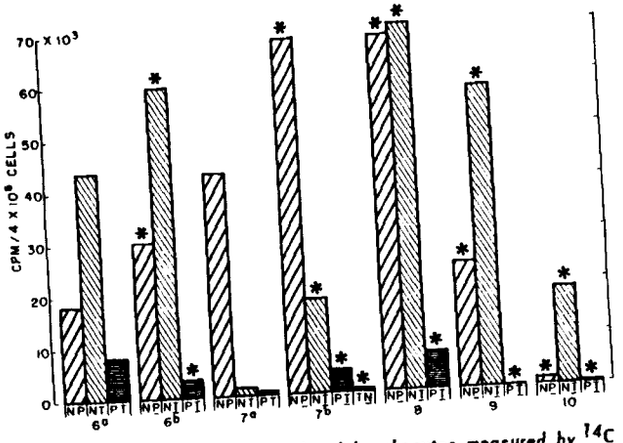

Fig. 33. Blastic transformation of stimulated lymphocytes measured by ^{14}C thymidine uptake. N refers to the normal lymphocyte population, P to the patient's circulating lymphocytes, and T to malignant tumor. The asterisk above the column indicates that one population had been inhibited with mitomycin C and the underscored letter below the column denotes which population was inhibited.

one inhibited population was used. Thus suppression of one cell population allowed maximal response of the remaining uninhibited cell line while mutual inhibition as well as stimulation occurs when both cell populations are allowed to react against each other.

In sets 6, 9, and 10, the tumor stimulated greater response of the normal lymphocyte population than did the patient's lymphocytes; similar results occurred in 5 other tumor studies. Set 7 was the only exception to this finding: this patient was different from the others in that he had two malignant diseases, lymphoma and a poorly differentiated skin cancer that had metastasized widely. The latter cancer was used in this study. The patient's lymphoma was under control at that time. The aggressive skin tumor produced less response than the patient's lymphocytes when reacted against normal cells. Either because of the already existing lymphoma or because this tumor failed to provide a strong antigenic stimulus, he was defenseless against it. In this patient, we could also show that the tumor was not stimulated by normal lymphocytes.

In set 8, relatively little difference was seen in the stimulation of normal lymphocytes by inhibited circulating lymphocytes of a patient with lymphosarcoma or by his inhibited lymph nodal cells. The lymphocytes in his blood may have represented the same population of cells obtained from his lymph node.

One would expect little reaction between a patient's lymphocytes and autologous tumor since the major histocompatibility antigens would be identical and the tumor antigens would be presumably weak. Therefore, the question arises -- can the lymphocytes of the tumor-bearing patient respond at all? When patient lymphocytes were challenged by inhibited normal lymphocytes, we observed a response. The lymphocytes of patients with malignant tumors responded less when stimulated by inhibited normal lymphocytes than did normal lymphocytes stimulated by inhibited lymphocytes of the patient.

For comparison, lymphocytes from patients with nonmalignant disease were also studied similarly. In these studies we used lymph nodes from patients with no malignant tumor and their circulating lymphocytes. The lymphocytes from the lymph node produced a greater response than that patient's circulating lymphocytes when each was reacted against the same normal lymphocytes. We know that antigens are trapped in lymph nodes and such added antigen would explain this finding. Hence, lymph nodes may be a poor control tissue. One difference from tumor was that these lymph-node cells could be stimulated by normal homologous lymphocytes.

In summary malignant tumor cells cause greater stimulation of normal, immunologically competent lymphocytes than do circulating lymphocytes from the tumor-bearing patients. Since the isoantigens of the tumor and the lymphocytes of the tumor-bearing patient are the same, the difference in the observed reactions suggests "tumor antigens." We hope that this kind of test will prove useful in future attempts at finding tumor antigen in humans. Such identification could play a role in the treatment of cancer by immunotherapy.

10273bb

EXPERIMENTAL HEMATOLOGY

The work in experimental hematology is related to the major clinical projects dealing with radiation effects in man, particularly in patients with disseminated disorders such as chronic leukemia or polycythemia rubra vera. The in vivo studies using labeled blood cells have been concerned principally with granulocytic leukemia and the underlying mechanisms of the therapeutic response. Distinct from this approach is our development of computer-assisted determinations of the differences in the profiles of populations of RBC; changes in erythropoiesis caused by therapy or progression of disease are reflected in altered profiles, easily visualized by electronic sizing. This technique may provide us with a new tool in assessing the kinetics of the erythron as it is stressed by radiation or disease process.

Autoradiographic Localization of DFP in Leukocytes

Microscopic autoradiography offers a valuable tool in studying the kinetics of leukemic cells. One experiment here reported dealt with autoradiographic localization of tritiated diisopropylfluorophosphate (DFP) in leukocytes of chronic granulocytic leukemia (Helen Vodopick, Elizabeth Rupp, and F. Goswitz). Phosphorus-32-DFP has been used as a leukocyte label for more than 10 years. Early studies done by Kurth and co-workers (Proc Soc Exp Biol Med 107, 422, 1961) demonstrated that during in vitro incubation of blood of normal persons, polymorphonuclear (PMN) neutrophils preferentially incorporated DFP labeled with tritium. Autoradiograms showed PMN neutrophils were labeled but eosinophils and basophils were not. Monocytes were lightly labeled and lymphocytes were not labeled above background. Blood from patients with chronic granulocytic leukemia was similarly exposed to tritiated DFP and analyzed by autoradiography. In the same blood sample, the immature cells, promyelocytes and myelocytes, which are not present in normal blood, had twice the labeling index of metamyelocytes and PMN neutrophils. The reason for this distribution of DFP is unknown, but may be related to cell concentration of cholinesterase to which DFP irreversibly binds.

We needed information about the relative concentration of the ^{32}P-DFP in the various granulocytic elements for analyzing mathematically our radioisotopic disappearance curves from previous leukokinetic studies in chronic granulocytic leukemia. Morphological "compartments" although thought to be concatenated do behave differently depending upon the stage of maturation.

Samples from a patient with chronic granulocytic leukemia were incubated in vitro for 1 hr with tritiated DFP (specific activity 4.82 Ci/mM); concentrations of the compound having 1.97, 3.93, and 7.86 microCi tritium per milliliter were added to a constant volume of leukocyte-rich plasma each containing the same number of cells. Then we prepared microscopic autoradiograms from each concentration, and developed them after 3 days of exposure. Scoring of cells (grain counting) could be done only on preparations from the 1.97-microcurie concentrations; labeling was too heavy at higher concentrations. The cells labeled were tabulated according to numbers of silver grains

per cell. Only neutrophilic leukocytes were labeled; the average grain count per cell was 23, 10, 9, and 8 for myelocytes, metamyelocytes, bands, and PMN leukocytes respectively (Table 17).

TABLE 17

Differential and Grain Counts of Granulocytes on Autoradiograms

Cell Type* Neutrophils	Differential %	Avg. Grains/Cell**
Myelocyte	16.6	23 ± 4.0
Metamyelocyte	21.6	10 ± 3.0
Band	20.2	9 ± 2.5
Polymorphonuclear	41.6	8 ± 2.5

* 100 scored for each cell type.

** Comparable area of background grains has been subtracted from each labeled cell.

Of the four cell types labeled, cell division occurs only in myelocytes which contained approximately twice as many grains per cell as the others. After mitosis, each daughter cell would presumably contain half the number of grains per cell. This number of grains would be the same as that found over the other maturing cells. These results, which concur with the findings of Kurth, will be helpful in the following paragraphs in analyzing the data on leukokinetics in chronic granulocytic leukemia.

Leukokinetics in Leukemia After Splenic Irradiation

We have a continuing study of the leukokinetics of our patients with chronic granulocytic leukemia (H. Vodopick, E. Rupp, F. Comas, F. Goswitz, and C. L. Edwards). In the past year, further studies on the mechanism of splenic irradiation in seven patients with chronic granulocytic leukemia (CGL) in relapse have been completed. The initial design of the experiments included three different studies using the ^{32}P diisopropylfluorophosphate (DFP) cell labeling technique on each patient. For each study one unit of blood ($\sim$500 ml) was removed from the patient and was labeled with ^{32}P-DFP. The cells labeled in vitro were reinfused into the same patient either (1) immediately before or (2) immediately after a single dose of splenic irradiation ranging between 100 and 700 rads. The third study followed in vitro irradiation of labeled blood cells with 500 or 1000 rads before their return to the patient who in this instance was not irradiated.

A control disappearance curve of the granulocytes was determined on each of these patients before the listed studies. The control curves usually were biphasic showing an initial fast fall and a second slower component with a half-disappearance time as long as 90 hr. In other leukokinetic studies, normal persons have been shown to have a more rapid loss of labeled granulocytes (half-disappearance time 4 to 10 hr) which follows a single exponential curve.

1027367

All seven leukemic patients have had a pretreatment control study and one study of granulocyte survival with infusion of labeled cells immediately after the completion of splenic irradiation. Six of these patients during another exacerbation of their disease also have had granulocyte survival studies in which the tagged cells were reinfused immediately before splenic irradiation. The seventh patient was excluded from these studies because of wide spontaneous fluctuations of her white blood cell count. Two patients of this original group have received a unit of irradiated blood (one at 500 rads, one at 1,000 rads) containing their own labeled cells. Two other patients have since died with blast-cell transformation of their disease.

Each patient's granulocyte disappearance curves obtained in association with splenic irradiation were compared to his own control curve. In six studies, labeled cells infused immediately after splenic irradiation left the circulation at a slower rate than the labeled cells during the control period. The seventh patient, however, had a faster disappearance of labeled cells after the treatment than during the control study.

In the six studies where the labeled cells were reinfused just before splenic irradiation, the granulocyte disappearance curves paralleled the control curves. An example of curves in one patient is shown in Fig. 34. The granulocyte disappearance curves in two patients after the return of tagged blood irradiated in vitro also paralleled the control curves. These differences require some explanation.

The disappearance curve of labeled granulocytes is affected by the influx of cells from an unlabeled precursor pool (dilution effect) and the removal rate of the circulating granulocytes, both labeled and unlabeled (utilization effect). By altering the ratio of labeled to unlabeled granulocytes, the disappearance curve can be shortened or lengthened. The finding in six posttreatment studies (labeled cells given after splenic irradiation) that the tagged granulocytes were removed more slowly suggests either decreased production of unlabeled cells or a decreased destruction of labeled cells. Soon after their reinfusion the labeled cells equilibrate with the unlabeled pool and since the total white blood cell count falls after splenic irradiation, decreased destruction cannot explain this finding. Therefore, decreased input of unlabeled cells because of decreased production by their unlabeled precursors would result in an apparent lengthening of the survival of the labeled cells, which is observed. Decreased production could be the result of direct damage to these circulating precursors passing through the field of irradiation or to an inhibitory effect exerted either by the irradiated spleen itself or by dying granulocytes.

In the other six pretreatment studies (labeled cells infused before splenic irradiation) the granulocyte disappearance curves fell parallel to the control curves. Here, the labeled cells were irradiated along with the unlabeled cells passing through the spleen. Presumably these two populations were in equilibrium during this time. Since the rate of removal of labeled granulocytes was parallel to the control rate, accelerated destruction of the circulating cells passing through the spleen during irradiation can not be supported. However, the total

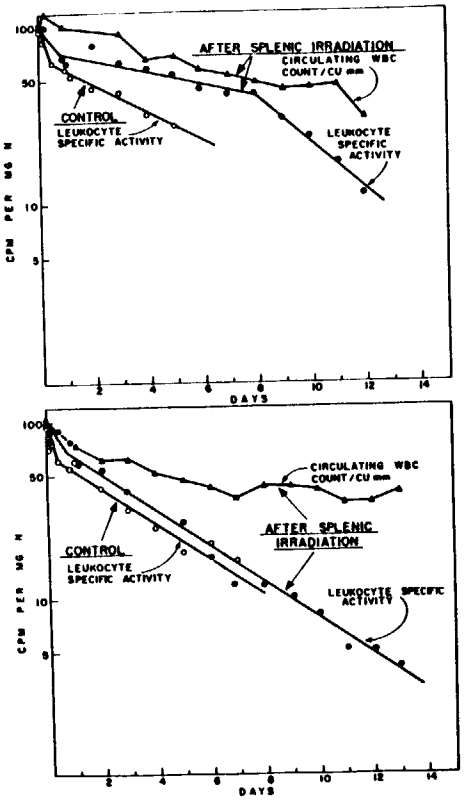

Fig. 34. Leukokinetic studies using ^{32}P-DFP in CGL. All data have been normalized on the basis that the T_o values represent 100%. The top half of this figure shows in order of appearance: the fall of the circulating white blood cells after splenic irradiation, the loss of labeled granulocytes infused after splenic irradiation, and the pretreatment granulocyte disappearance curve during the control period. A slower disappearance of the labeled granulocytes is seen after splenic irradiation than was observed during the control period. The lower half of the illustration shows the same sequence of curves as the upper portion. The middle curve, however, represents the loss of labeled granulocytes infused just before splenic irradiation. This curve was parallel to the control pretreatment granulocyte disappearance curve. Control curves were obtained before each separate study.

blood granulocyte count does fall, while it does not during the control period. Since increased destruction cannot be supported, decreased production must again be implicated. The finding that the labeled blood irradiated in vitro is removed at the same rate as in the control study would also support the conclusion that accelerated destruction is not

1027368

a factor in the fall in granulocyte levels after splenic irradiation.

All the studies thus far performed indicate that the main mechanism accounting for the fall of the leukocyte count after splenic irradiation is reduced production by precursor cells and not direct destruction of the already circulating cells. Further statistical analysis will help in our present provisional interpretation.

Another study on chronic granulocytic leukemia was undertaken to describe the changes in number of granulocytes (WBC) that occur in the blood after splenic irradiation (Frank V. Comas, C. L. Edwards, and Helen Vodopick). This study is limited to an analysis of those changes occurring during the first 39 days after irradiation.

Thirteen patients were irradiated with a single dose 28 different times. The radiation dose was adjusted to each patient in the following way: the product of the mid-spleen dose (in rads) times the volume of tissue irradiated (in cm^3) was kept constant. Patients were given either 1.0×10^6 rads x cm^3, or 1.6×10^6 rads x cm^3. The actual rad doses ranged between 100 and 700 rads. To facilitate the analysis of the data, all blood counts were normalized by taking the preradiation count to be 100, and by grouping all the patients together.

On the day after splenic irradiation the WBC had begun to decrease, and this decrease continued for about 5 weeks. The rate of decrease, however, was not constant, and the data could not be fitted by either a linear or a simple exponential equation. In all patients the relation between number of WBC/mm^3 with postradiation day described a continuously curving line with a slope that was fast at first and slow at later postradiation times. A simple model was proposed to explain these observations.

The WBC in blood (N) is made up of two components: B and S. Component B is the WBC originating from nonirradiated tissues (mostly bone marrow); component S is the WBC originating from tissues that were, or are to be, irradiated (mostly spleen).

Therefore:

$$N = B + S \qquad (1)$$

and at time zero, just preceding the spleen irradiation, the starting condition is

$$N_o = B_o + S_o \qquad (2)$$

We now assume that B cells are not affected by irradiation because their rate of influx into the blood is equal to their rate of disappearance. Therefore, $B = B_o$ at all times. The S cells, however, diminish in number because the irradiation has reduced the influx greatly; and on the other hand they keep on leaving from the blood at their normal rate, that we call (β). This can be written as:

$$N = B_o + S_o e^{-\beta t} \qquad (3)$$

According to this model the number of WBC should be decreasing almost exponentially shortly after irradiation because the term ($S_o e^{-\beta t}$)

changes rapidly at first, especially if there are more S than B cells in the blood. At later times, however, the daily decrease of S cells is rather small in absolute numbers, and therefore the number of WBC (N) changes but little with time. This is in accord with our data.

According to Eq. 3, a time should come when the WBC remain stationary at a level equal to the number of B cells originally present, because practically all S cells should have disappeared. In fact, however, at about the fourth to sixth postradiation week the WBC begin to increase, presumably owing to cell proliferation in the compartments from which S cells originate (mostly spleen). This "regenerating" phase is not being considered here.

By combining Eq. 3 with Eq. 2, one can derive the value of S_o, that is:

$$S_o = \frac{N_o - N}{(1-e^{-\beta t})} \qquad (4)$$

If the value of β were known, the size of S_o, compared to N_o, could be determined. We calculated β to amount to a decrease in S cells of 17% per day. If we apply this constant to Eq. 4 and solve for S_o, the best estimate of the number of S cells initially circulating in the blood is 75. In other words, in our patients during spleen irradiation, approximately 75% of all leukemic cells were irradiated. Figure 35 shows a plot of the observed difference between the preirradiation and postirradiation blood counts. The continuous line represents the predicted values, taken from Eq. 4. The fit is fairly good, especially during the early postradiation days. At later times individual differences from patient to patient made for greater scatter of the data.

Electronic Sizing and Distributions of Erythrocytes

Electronic cell sizing and distribution has provided a tool for detecting altered production of red cells in irradiated patients with polycythemia (Dorothy Lushbaugh, C. L. Edwards, and C. C. Lushbaugh). After acute total-body exposure there is usually little or no change in size, number, and hemoglobin content of red cells. The long life ($\sim$120 days) of the human RBC is not shortened by the exposure, so unless hemorrhage occurs the RBC levels are maintained while erythroblastic tissues recover and new RBC production begins. If there is any morphologic change in newly produced postirradiation RBC's, it is too subtle or infrequent to be recognized. In patients with polycythemia rubra vera, however, therapy by external photons and internal radioisotopes (or chemotherapy by cytotoxic drugs) affects the abnormal elements of the hematopoietic system so that normal RBC are produced at a rate that gradually returns the various parameters of circulating RBC mass to normal.

The course of this therapeutic effect is detectable and described in an objective, simply-reported manner by automated analysis of the RBC size profile. Elsewhere in this report are described some new electronic and engineering improvements in our methods. By detecting nonlinearity or changes in pulse/particle size ratios, they greatly enhance day to day accuracy. The methods of data reduction and analysis of profile differences, although we have previously described them, do need some

1027369

explanation if last year's report is not at hand: First, we determine the 100-channel RBC size distribution with normal blood, then reduce this to the decile distribution of number of pulse-height analyzer channels so that each group of channels contains 10% of the 100,000 RBC that are sized. For example, the first decile is composed of the first 23 channels while the second and third are composed of only one channel each, although all three groups contain 10% of the RBC distribution. This normal decile distribution is stored for later computer use. When the RBC size profile of a patient is determined, the data from the 100-channel pulse-height analyzer memory (number RBC/specific channel number) are compared with this normal decile distribution. The computer first determines the number or percentage of RBC found in the previously defined decile channel groups. The numbers normally expected (10,000+ or 10% ± 2% depending on the decile being used) are then subtracted from the newly determined values. Then these differences are squared, divided by the "expected" value and summed as in a determination of a chi-square goodness-of-fit. The resulting single number is small (less than 4.0) if there is no statistically valid difference between the test result and

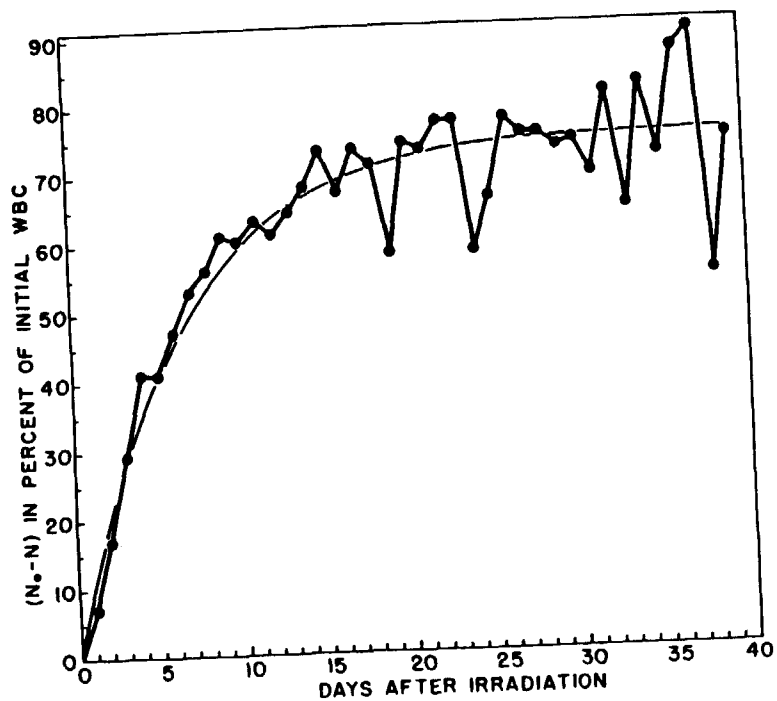

Fig. 35. Difference between the WBC count before radiation and at consecutive days after irradiation of the spleen. The continuous line was computed from Equation 4.

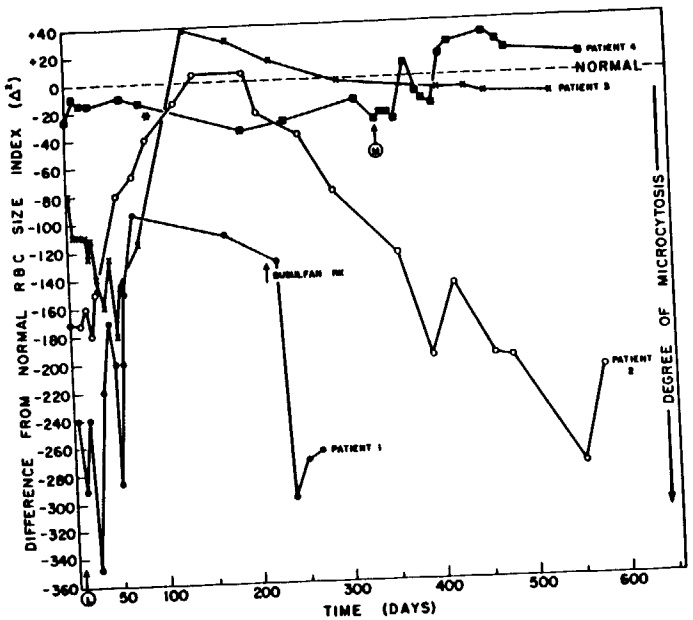

Fig. 36. Graph of changes in the red blood cell size Difference Index Δ^2 that followed TBI therapy of 250 R in three patients with polycythemia rubra vera, and the lack of changes in a patient with idiopathic thrombocytopenia (see text for explanation).

the known normal RBC distribution. As differences in RBC size distribution from normal increase, the size of this computed number increases progressively. Because we use percentage rather than the actual number of RBC/channel to make the determination less sensitive to minor fluctuations, the final computed number cannot be considered identical to the chi-square number. Accordingly, therefore, we have designated this computed number the Difference Index (Δ^2), affixing a minus sign or plus sign if the modal RBC is smaller or larger than that of normal human blood.

The manner in which the RBC size Difference Index (Δ^2) changes during the course of hematologic remission in patients with PRV is illustrated in Fig. 36. Patients 1, 2, and 3 had had PRV for many years. Patient 4 had idiopathic thrombocythemia (IT), a disease akin to PRV with abnormal platelet production, but with normal RBC kinetics and without expansion of the bone-marrow organ. In contrast with the Δ^2 values of Patient 1, 2, and 3, those of Patient 4 are near normal. The values -10 to -20 indicate a slightly abnormal RBC size distribution caused by slightly microcytic RBC possibly the result of a slight decrease in his iron stores from blood loss. The initial Δ^2 for Patient 1 was -240, Patient 2, -170, and Patient 3, -80 to -110; all these values

1027370

indicate extreme microcytosis and RBC volume distribution (RBCVD) profiles shifted far to the left of normal.

At zero time (L) all four patients received total-body irradiation therapy in the low-exposure-rate total-body irradiation facility (LETBI). The three PRV patients were exposed to 250 R over an 8- to 9-day period (about 30 R/day). The IT patient was exposed to 150 R in a 5-day period. During the first 30 days after exposure, the Δ^2 of RBC in all patients remained the same or worsened in parallel with their depression of leukocyte and thrombocyte values. Then the abnormal Δ^2 values of two PRV patients (Patients 1 and 2) began to change as larger RBC were made. In Patient 3, marrow depression was more pronounced than anticipated; an increase in thrombocyte values did not start until about the 45th postirradiation day. In parallel with recovery of leukocyte and platelet values his RBC Δ^2 began changing at about the same rate as in the other two patients. In Patient 4 no significant change occurred in RBC Δ^2 even though a satisfactory temporary remission in abnormal platelet production was obtained. Ninety days after exposure (see *) his platelets were sufficiently recovered for him to donate a transfusion to another patient. Approximately one year later he was again treated with 150 R of total-body irradiation at 30 R/day in 5 daily fractional exposures at 1.5 R/min in the ORAU medium-exposure-rate total-body irradiator (METBI). This exposure rate, about 60 times greater than that in LETBI, apparently produces more bone-marrow damage per unit of exposure than the slower rate, as evidenced by greater depressions in WBC and platelet counts. His bone marrow recovery from this exposure in this graph is attended by a shift to greater than normal size ($\sim +20\,\Delta^2$) persisting to the date of writing, about 10 months later.

The courses of the PRV patients have now been followed for almost 600 days. Good clinical remissions were obtained lasting about one year in Patient 2, and still present after 500 days in Patient 3. Examination of the Δ^2 values in these two patients show that both reached or exceeded normal RBC size about 120 days after therapy. In Patient 2, the RBCVD profile at this time could not be differentiated by eye from that of a normal person. Although he clinically was free of complaints for about the next 200 days, his RBC Δ^2 gradually increased (to -200 to -300) as other hematologic values (RBC count, MCV, Hgb, WBC, and platelet count) increased and his relapse progressed.

In Patient 1, the course of the Δ^2 values indicate that an actual remission was not obtained although the patient reported feeling better for about 3 months. About 8 months after the radiation therapy, busulfan therapy was required for control of thrombocytosis. This chemotherapy has not changed RBC production according to the Δ^2 values.

The ferrokinetics of typical PRV patients with and without therapy may explain these changes. According to some hematologists, a PRV patient in relapse apparently suffers in part from an iron deficiency in relation to the enormous demand for iron of his expanded, hyperactive bone-marrow organ. As a result, even though his total iron stores would be considered adequate for normal RBC production, they are inadequate for his rate of hemoglobin production and so microcytic RBC are produced. Therapy that decreases the number of bone-marrow stem cells or the mitotic rate of their progeny equates iron stores and pro-

duction so that normal-size cells are produced. Since the number of the small cells in a cohort that are destroyed daily (as they reach senility of 120 days of age) are more numerous than the new cells that are produced, RBC mass decreases as a new steady state of RBC production of a larger RBC is obtained. The Δ^2 values reported here indicate that this process took about 120 days in Patients 2 and 3, but appeared to be cut short in Patient 1 in less than 2 months. According to the Δ^2 values and RBC kinetic theory, a new steady state of RBC production was obtained in this patient also, but attainment of a normal size distribution was prevented by a concomitant true (as opposed to relative) iron deficiency, probably secondary to blood loss in the past.

Using electronic RBCVI and the Difference Index (Δ^2) we are measuring postirradiation effects on RBC production and size in all patients treated with total-body irradiation. Elsewhere in this report we describe similar studies of in-bred mouse strains undergoing continuous and fractionated exposures to determine the tolerable (repairable) level of daily radiation exposure of a model RBC stem-cell system.

1027371

RADIOPHARMACEUTICAL DEVELOPMENT

Gallium-67 as a Tumor-Scanning Agent

During the past year a major portion of the work in development of radiopharmaceuticals has been devoted to the study of gallium-67 as a tumor-scanning agent (R. L. Hayes, B. L. Byrd, J. E. Carlton, and J. J. Rafter). Recent observations in our clinical program (8) have indicated that radionuclides of gallium may have considerable potential as scanning agents for detecting nonosseous as well as osseous tumors. Scans of unusually good contrast have been obtained with ^{67}Ga in a number of patients afflicted with different types of malignancies (see page 99). Gallium-67 has a 3.3-day half-life and decays by electron capture emitting gamma rays of moderate energy suitable for camera imaging as well as rectilinear scanning. The radiation dose is low, permitting the use of millicurie-range doses.

Animal studies are being carried out concurrent with the clinical investigations to identify factors that underlie deposition of ^{67}Ga in tumors. We have found that various nonosseous tumors in mice and rats will concentrate ^{67}Ga: ESR-586 preputial gland carcinoma, P-1798 lymphosarcoma, C3H/HeJ mammary tumor, AKR/J thymic lymphoma, R-3259 giant cell sarcoma, Walker-256 carcinosarcoma, CA-755 adenocarcinoma, and a new transplantable neoplasm of rats (RFT) (Science 167, 289, 1970). This last tumor showed the greatest affinity for gallium and has been adopted as a model for further study. The RFT tumor arose from the skin or subjacent tissues of the thigh of a Fischer-344 rat surviving total-body gamma irradiation; it is slow-growing, is readily transplanted, and can metastasize to the lung, adrenal, and lymph nodes. Figure 37 shows a rectilinear ^{67}Ga scan of a rat transplanted with RFT tumor. Recently Adenovirus 31 and SV-40 tumors in hamsters have been studied in collaboration with the Molecular Anatomy Group at Oak Ridge National Laboratory; good absolute and relative ^{67}Ga tumor localizations were obtained.

As background for the clinical use of ^{67}Ga we have investigated the effects of various conditions on localization of ^{67}Ga in animal tumors. The initial human studies carrier-free ^{67}Ga was given as citrate with arbitrary level of 7 mg of citrate per kg of body weight. Results with the Fischer-344 RFT tumor indicate that variations in the amount citrate, in the range of 7.0 to 0.07 mg/kg body weight, do not affect deposition of ^{67}Ga in tumor tissue nor its relative concentration with respect to other tissues. Various other chelating agents can be used without changing the distribution in the test animal, i.e., nitriloacetate (NTA) or salicylate (Table 18). With strong chelating agents, hydroxyethylethylenediaminetriacetate (HEDTA) and ethylenediaminetetracetate (EDTA), the concentration in tumor tissue decreases rapidly, but the ratio to other normal tissues remains approximately the same, the main effect being to increase urinary excretion. These re-

sults suggest that the active agent involved in the localization process is an ionic form of gallium.

The distribution of ^{67}Ga with time in the RFT tumor rat is shown in Fig. 38. After 24 hr the tumor uptake is essentially complete remaining constant through a period of six days. A similar behavior has been observed in man.

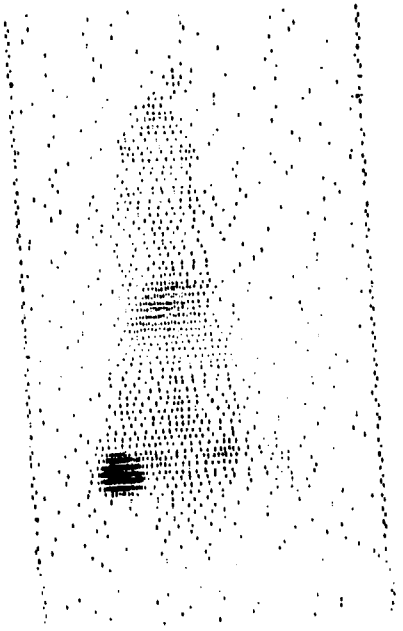

Fig. 37. Scan of an RFT tumor rat three days after intravenous ^{67}Ga administration The tumor on the left thigh comprised only 1% of the rat's body weight but retained approximately 30% of the injected dose.

Table 19 shows the distribution of ^{67}Ga in rats bearing RFT tumors of different implant ages. To avoid effects of age and sex in this study we used male animals only with a maximum difference in age of only 2 weeks (all groups were about 5 months old at termination of study). Rather dramatic differences between early (3-week) and older (5- and 9-week) implants were observed in two studies. This difference may be the result of a better blood supply in the younger implants, leading to more effective competition with other gallium-fixing tissues such as bone, liver, and spleen (see Fig. 38). On the other hand, death of tumor cells owing to inadequate blood supply without grossly visible necrosis could be the major explanation. Where massive necrosis has been present in the different tumor types, the assay of ^{67}Ga in grossly viable tissue has always been much higher than that in the necrotic

1027372

TABLE 18

EFFECT OF VARIOUS CHELATES ON THE DISTRIBUTION OF ^{67}GA IN THE RFT TUMOR RAT (24 HOURS)

Chelate	Citrate	NTA	Salicylate	HEDTA	EDTA
Concentration In Tumor *	3.7	3.5	3.3	0.23	0.07
Ratio Tumor Concentration To:					
Blood	19	20	13	15	20.
Muscle	19	14	16	13	13
Liver	4.1	3.1	2.5	2.8	3.6
Femur	2.7	2.3	2.5	2.1	1.8
Number of Animals	8	2	2	2	2

* Percent administered dose per gram tissue normalized to 250 g body weight.

TABLE 19

EFFECT OF TUMOR AGE ON THE DISTRIBUTION OF ^{67}GA IN THE RFT TUMOR RAT (24 HOURS)

	Days After Implantation		
	23	46	62
Tumor Concentration *	9.9 ± 0.8†	3.3 ± 0.1	3.5 ± 0.6
Tumor Weight (g)	0.5 ± 0.1	4.6 ± 0.2	8.2 ± 1.20
Ratio Tumor Concentration To:			
Blood	32 ± 1	15 ± 1	22 ± 4
Muscle	77 ± 12	23 ± 2	44 ± 14
Liver	7.7 ± 0.7	3.8 ± 0.3	3.8 ± 0.4
Femur	10 ± 1	3.1 ± 0.1	3.3 ± 0.5
Number of Animals	5	5	5

* Percent administered dose per gram tissue normalized to 250 g body weight.

† Standard deviation of the mean.

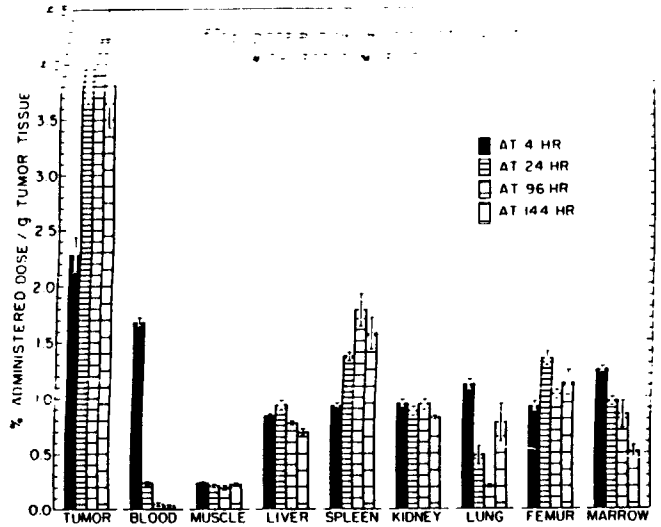

Fig. 38. Histogram showing the concentration of ^{67}Ga in the RFT tumor and various normal tissues at time intervals from 4 hr through 6 days.

portion (as much as 30-fold but usually approximately 5). Gross and microscopic autoradiograms also indicate that ^{67}Ga is mainly associated with viable tumor tissue.

Studies of the effect of stable gallium on deposition of ^{67}Ga in tumors indicate that gallium "binding sites" are saturable. Table 20 shows the results of one such study; the carrier distinctly decreased the amount of gallium-67 in tumor. The decrease in tumor concentration was greater than that in other soft tissues except for muscle; a decrease in tumor:bone ratio, also seen, was to be expected, since stable gallium at these levels enhances the concentration of gallium in bone (USAEC Report ORAU-107, p. 125, 1968). In another study, stable gallium at lower levels, between 0.05 and 0.35 mg/kg, caused no decrease in tumor:soft-tissue ratios. At levels above 0.05 mg absolute concentrations in tumor decreased (Fig. 39). At higher levels of gallium (5 to 20 mg/kg) we found a saturation level of about 20 μg Ga/g tumor tissue. This saturation level will undoubtedly vary with the type of tumor and its general viability. Clearly, in the clinical use of ^{67}Ga the presence of appreciable carrier (stable) gallium will probably be detrimental to the diagnostic procedure.

Comparison with Other Tumor-Scanning Agents

From time to time various radiopharmaceuticals have been proposed as general tumor-scanning agents. Among the more successful have been ^{131}I-albumin, ^{75}Se-selenomethionine, and ^{197}Hg, ^{203}Hg-

1027373

EFFECT ... IN THE RFT TUMOR RAT (24 HOURS)

	Stable Gallium (mg/kg)		
	0.0	0.5	1.0
Tumor Concentration *	3.9 ± 0.5†	1.7 ± 0.1	1.4 ± 0.3
Ratio Tumor Concentration To:			
Blood	20	6	7
Muscle	23	30	37
Liver	5	2	3
Bone	5	1	1
Number of Animals	4	4	4

* Percent administered dose per gram tissue normalized to 250 g body weight.

† Standard deviation of the mean.

chlormerodrin. Table 21 shows a comparison of ^{67}Ga with these three agents. The data show that ^{67}Ga is superior to all in absolute tumor concentration and in ratio of tumor to normal tissue concentration. The true test of the relative merits of various tumor-scanning agents will of course require comparison in patients.

Since indium is chemically similar to gallium and also has a plasma-protein binding pattern resembling that of gallium (Fed Proc 27, 838, 1968) we compared the distribution of high specific activity ^{114m}In with that of ^{67}Ga. In absolute and relative tumor localization ^{67}Ga was superior to ^{114m}In at both 1 and 4 days. Recently Hunter and deKock (J Nucl Med 10, 323, 1969) have proposed carrier-free ^{111}In ($T_{\frac{1}{2}} = 2.8$ days) as a tumor-scanning agent. Table 22 shows a comparison of this radionuclide with ^{67}Ga in a recent study using the RFT rat tumor; ^{67}Ga was again superior. Gallium-67 has also given much better tumor localization than ^{114m}In in mice bearing transplanted P-1798 lymphosarcoma, CA-755 adenocarcinoma, and ESR-586 preputial gland tumors.

Enhancement of Uptake

It would obviously be highly desirable to find some means by which the affinity of tumor tissue for ^{67}Ga could be increased, or failing this, to at least enhance localization in tumors relative to that in normal tissue. In either situation if an enhancement could be achieved early after the dose (hours), possibly the positron-emitting radionuclide ^{66}Ga ($T_{\frac{1}{2}} = 9$ hr) and even ^{68}Ga ($T_{\frac{1}{2}} = 68$ min) might be of diagnostic use,

TABLE 21

COMPARISON OF ^{67}GA WITH OTHER TUMOR-SCANNING AGENTS IN RFT TUMOR RATS

Days After Dose:	^{67}Ga Citrate 1	^{75}Se Selenomethionine 1	^{203}Hg Chlormerodrin 1	^{125}I-Albumin 1	^{125}I-Albumin 3
Tumor Concentration *	4.9 ± 0.4†	0.63 ± 0.07	0.013 ± 0.005	0.32 ± 0.04	0.11 ± 0.01
Ratio Tumor Concentration To:					
Blood	16 ± 1	1.2 ± 0.1	1.6 ± 0.5	0.2 ± 0.0	0.3 ± 0.0
Muscle	24 ± 3	3.4 ± 0.3	7.1 ± 2.2	2.5 ± 0.3	3.8 ± 0.6
Liver	4.7 ± 0.5	0.5 ± 0.0	0.3 ± 0.1	1.3 ± 0.1	1.0 ± 0.1
Femur	3.9 ± 0.4	3.1 ± 0.2	3.7 ± 1.0	2.9 ± 0.2	4.0 ± 0.5
Lung	13 ± 2	1.0 ± 0.1	0.6 ± 0.2	0.3 ± 0.0	0.6 ± 0.1
Marrow	4.6 ± 0.1	0.8 ± 0.1	1.6 ± 0.6	0.7 ± 0.1	1.2 ± 0.1
Number of Animals	4	4	4	4	4

* Percent administered dose per gram tissue normalized to 250 g body weight.
† Standard deviation of the mean.

adding the advantage of tomographic coincidence detection. Even radionuclide therapy might be worth consideration if localization were sufficiently rapid and specific. If the mechanism of localization in tumor tissue is found, we will have new leads for these prospects.

One approach to both enhancing relative concentration of ^{67}Ga in tumor tissue and also increasing the rate of clearance from nontumor tissue is the use of scandium as a nontumor "blocking" agent. In previous studies (USAEC Report ORAU-107, p. 130, 1968) we showed that low levels of scandium (0.5 mg Sc/kg) increase the deposition of gallium radionuclides in bone with a dramatic early clearance of nonosseous tissues, similar to that produced by much higher levels of stable gallium. In the RFT tumor rat, unlike stable gallium (Table 20), scandium with ^{67}Ga does not reduce the concentration of ^{67}Ga in tumor tissue, but it does increase the rate of clearance from nonosseous tissues (Table 23). High relative concentrations of ^{67}Ga in tumor tissue are achieved within 2 to 4 hr persisting through 24 hr. Whether this effect of scandium is a general one has yet to be determined by studies of other tumor types. By in vitro studies using gel filtration and ultrafiltration we have established that, as with gallium (15), scandium is bound by blood serum proteins. Furthermore scandium competes for gallium serum-protein binding-sites. Presumably a similar competition accounts for the scandium-induced decrease in deposition of gallium in normal nonosseous tissues.

TABLE 22

COMPARISON OF THE DISTRIBUTION OF ^{67}GA WITH THAT OF ^{111}IN IN RFT TUMOR RATS (3 DAYS)

	^{67}Ga	^{111}In
Tumor Concentration *	4.8 ± 0.3†	0.67 ± 0.07
Ratio Tumor Concentration To:		
Blood	110 ± 7	3.9 ± 0.3
Muscle	33 ± 3	3.2 ± 0.3
Liver	6.6 ± 0.5	0.47 ± 0.03
Bone	5.9 ± 0.3	1.5 ± 0.1
Lung	25 ± 2	1.0 ± 0.1
Marrow	6.1 ± 0.6	0.38 ± 0.02
Number of Animals	4	4

* Percent administered dose per gram tissue normalized to 250 g body weight.
† Standard deviation of the mean.

1027374

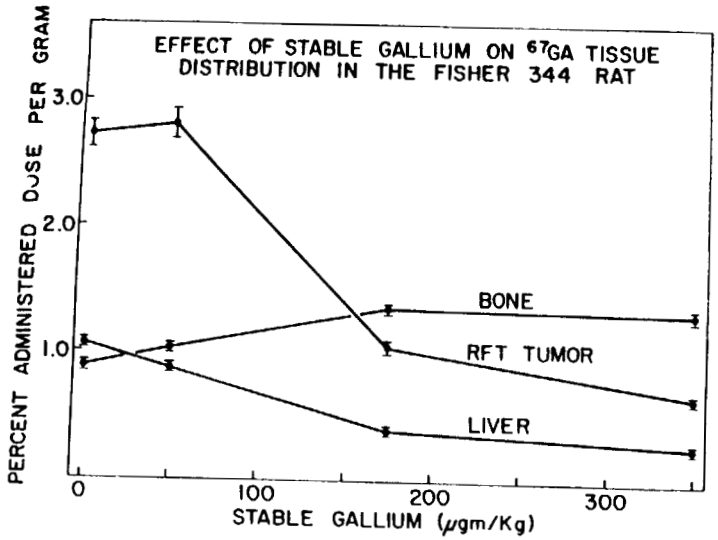

Fig. 39. Effect of simultaneous administration of stable gallium on the distribution of ^{67}Ga in selected tissues of the RFT tumor rat.

Mechanism

The mechanism of gallium uptake is an important question. As mentioned in the foregoing, ^{67}Ga appears mainly in viable rather than necrotic tumor; its distribution is intracellular and little ^{67}Ga is found associated with the nuclei. It is not merely a diffusion phenomenon such as occurs with brain-scanning agents, since its deposition in tumor tissue does not change with time (days) after maximum concentration is attained (24 hr). The greater perfusion afforded by hypervascularity might provide a heightened uptake of the radionuclide in tumor tissue, but the basic process appears to involve "binding" of the gallium in either a primary or secondary manner, i.e., direct binding in the tumor tissue or binding to some other agent which in turn is concentrated by the tumor.

Ultracentrifugation of homogenates of RFT tumor tissue indicates 80 to 90% of the ^{67}Ga present is associated with subcellular particulate components. Nuclei were shown by autoradiography and in another separation to be associated with scant ^{67}Ga. When we treated homogenates with Triton X-100 and n-butyl alcohol (agents used to extract lipid-bound enzymes), approximately 80% of the ^{67}Ga appeared in the supernatant after ultracentrifugation. We obtained similar results with biopsy tissue from a patient with malignant lymphoma. The activity in the supernatant from butyl alcohol and Triton-treated homogenates appears from dialysis and ultrafiltration studies to be mainly associated with macromolecular material. Treatment with 5% trichloroacetic acid renders the ^{67}Ga in the supernatant completely dialyzable.

1027375

These studies constitute only preliminary results in our investigation of the mechanism of ^{67}Ga localization in tumor tissue. Subcellular fractionation coupled with further ultrastructural studies, purification, and identification of the biochemical nature of the agent(s) will be required before we can form any detailed conjecture as to the exact process. However, at this point, because of the known affinity of blood sera proteins for gallium (15), we are tempted to believe that the binding agent is protein. Furthermore, the results with scandium as a blocking agent for nontumor tissues (Table 23) suggest that the binding agent is specific and perhaps present in tumor tissue itself rather than of secondary origin.

Effect of Age on Gallium Distribution

Recently we have examined the effect of age on gallium distribution in both osseous and nonosseous tissues in the rat (R. L. Hayes, B. L. Byrd, and J. E. Carlton). Although Dudley and Friedman (Science 115: 146-147, 1952) had reported that age had little effect on the localization in rat bone, our previous data suggested the existence of such an effect. We examined the effect of age on both carrier-free (^{67}Ga)

TABLE 23

EFFECT OF SCANDIUM ON THE EARLY DISTRIBUTION OF ^{67}GA IN THE RFT TUMOR RAT

	Time(Hr) - Sc(mg/kg)		
	4 - 0.0	4 - 0.5	2 - 0.5
Tumor Concentration *	2.82 ± 0.27†	2.83 ± 0.16	1.89 ± 0.15
Ratio Tumor Concentration To:			
Blood	1.4 ± 0.1	11.6 ± 1.1	9.9 ± 0.8
Muscle	9.8 ± 0.9	96.0 ± 18.0	35.0 ± 0.6
Liver	2.7 ± 0.2	18.4 ± 0.5	15.8 ± 1.2
Femur	2.5 ± 0.2	1.7 ± 0.1	1.4 ± 0.2
Marrow	1.8 ± 0.2	20.0 ± 4.5	18.9 ± 2.1
Number of Animals	4	8	6

* Percent administered dose per gram tissue normalized to 250 g body weight.

† Standard deviation of the mean.

and stable gallium distribution, at the time also comparing the distribution of ^{85}Sr in rats drawn from the same populations.

Table 24 shows a portion of the results; tissue distribution was measured at 2 and 24 hr. Values for bone are the average of the rib, femur, and calvaria. Owing to the differences in the weights of the age groups (5 animals each) we normalized these values to body weights of 250 g. A perhaps fairer test of differences in tissue distribution is the use of concentration ratios, also shown in Table 24 for blood, muscle, and liver. The bone: blood and bone: liver ratios differed significantly between these two age groups. The trend is similar for carrier-free and stable gallium, both at 2 hr and at 24 hr. Table 25 shows with increased age the decreasing uptake in bone of ^{85}Sr at an early time after the dose, similar to the interval that might be used in clinical tests with both short-lived ^{87m}Sr ($T_{\frac{1}{2}}$ = 2.8 hr) and

TABLE 24

EFFECT OF AGE ON THE DISTRIBUTION OF ^{67}GA IN THE RAT

	Carrier Free		5 mg Ga/kg *	
Age (weeks)	5	20	5	20
	2-HOUR DISTRIBUTION			
Bone (%/g)†	1.2 ± 0.1‡	0.57 ± 0.05	3.0 ± 0.1	1.3 ± 0.02
Ratio Bone Concentration to:				
Blood	0.89 ± 0.09	0.28 ± 0.02	55 ± 13	13 ± 2
Muscle	5.7 ± 1.0	3.2 ± 0.3	190 ± 32	120 ± 12
Liver	2.2 ± 0.2	1.1 ± 0.1	71 ± 7	17 ± 1
Number of Animals	5	5	5	5
	24-HOUR DISTRIBUTION			
Bone (%/g)	2.2 ± 0.2	1.1 ± 0.03	2.0 ± 0.1	0.85 ± 0.06
Ratio Bone Concentration to:				
Blood	35 ± 7	2.4 ± 0.2	46 ± 4	20 ± 3
Muscle	22 ± 6	15 ± 1	120 ± 30	140 ± 12
Liver	4.7 ± 0.9	1.1 ± 0.01	18 ± 2	10 ± 1
Number of Animals	5	5	5	5

* Administered as citrate in a molar ratio of 3:1, citrate:Ga.

† Percent administered dose normalized to 250 g body weight.

‡ Standard deviation of the mean.

1027376

TABLE 25

EFFECT OF AGE ON THE 2-HOUR DISTRIBUTION OF ^{85}SR IN THE RAT

	^{85}Sr	^{85}Sr	^{85}Sr	^{67}Ga
Age (weeks)	8	20	28	8
Bone (%/g)†	4.0 ± 0.1‡	3.0 ± 0.1	2.7 ± 0.1	2.2 ± 0.1
Ratio Bone Concentration to:				
Blood	45 ± 2	16 ± 1	9.5 ± 0.5	40 ± 9
Muscle	78 ± 11	40 ± 2	24 ± 2	200 ± 37
Liver	120 ± 4	47 ± 2	29 ± 1	43 ± 5
Number of Animals	5	5	5	5

* Administered 5 mg Ga/kg as citrate; 3:1 molar ratio of citrate to Ga.

† Percent administered dose per gram normalized to 250 g body weight.

‡ Standard deviation of the mean.

^{68}Ga ($T_{\frac{1}{2}}$ = 68 min). The effect of age on ^{85}Sr distribution similar to that for gallium is apparent; for comparison data in column 4 of Table 25 show the distribution of stable gallium in 8-week-old rats. The ^{85}Sr data in column 2 of Table 25 can also be compared with the 2-hr distribution data for stable gallium in Table 24.

Separation of ^{68}Ga from EDTA

We have devised a rapid and efficient ion exchange method to separate ^{68}Ga from EDTA (J. E. Carlton and R. L. Hayes). Despite its 68-min half-life ^{68}Ga may be of use as a tumor-scanning agent if we find how to promote the rapid clearance of gallium from nontumor tissues. The positron decay mode of ^{68}Ga would provide for tomographic scanning by coincidence-detection techniques. Gallium-68 also effectively labels hydrous ferric oxide colloid prepared by heat hydrolysis for liver and bone-marrow scanning.

It is readily available from its ^{68}Ge parent, which has a 280-day half-life, a long useful life for this generator system. Gallium-68 is readily separated from parent ^{68}Ge absorbed on an alumina support by eluting with 0.005 M sodium ethylenediametetraacetate (EDTA) adjusted to pH 7 (Int J Appl Radiat Isotop 12, 62, 1961). But to make it an effective agent for scanning tumor or the reticuloendothelial system we must separate it from the EDTA. Although this can be

accomplished efficiently by a solvent extraction technique, a less time-consuming method is desirable.

To separate the ^{68}Ga from EDTA and any trace of dissolved aluminum that occurs on prolonged contact with EDTA the eluant (~20 ml) is mixed with an equal volume of concentrated HCl and rapidly passed through a column of 50 to 100 mesh Dowex 1-X2 anion exchange resin in the chloride form with the use of the apparatus shown in Fig. 40.

Column heights as short as 2 cm have performed satisfactorily with flow rates as high as 15 ml/min; recoveries have been approximately 98%. Higher cross linkage resins may be used, but with 10% cross linkage (X10) recovery drops to 85%. Analytical determinations indicate that the product (~5 ml) from any one separation run will contain less than 0.5 μg EDTA and no more than 3 μg of aluminum.

Rare Earths as Bone-Scanning Agents

The rare earths are bone seekers and, with proper manipulation of the dosage form, several of their radionuclides may prove to be useful scanning agents. We have recently made preliminary studies of the radionuclide pair, ^{140}Nd-^{140}Pr (B. L. Byrd and R. L. Hayes).

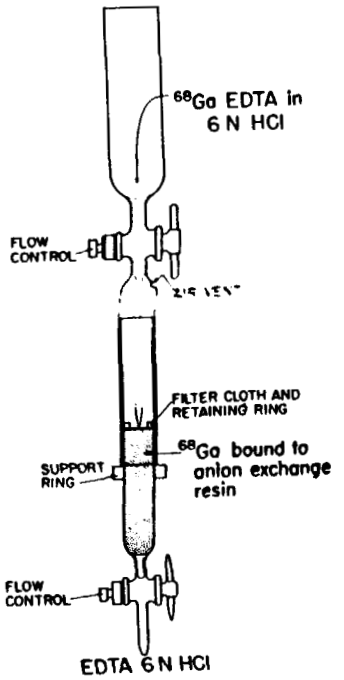

Fig. 40. Artist's drawing of apparatus used in the rapid separation of ^{68}Ga from EDTA.

1027377

Most of the bone-scanning agents now in use suffer either from lack of ready availability, long half-life that limits the administered dose thereby handicapping scanning resolution, high photon energies unsuitable for camera visualization, or a combination of these faults. Radionuclides with reasonably short half-lives and moderate-energy photon emissions are available among the rare-earth elements. We have previously reported animal distribution studies related to the potential use of one member of this group, ^{157}Dy (USAEC Report ORAU-107, p. 133, 1968). Dysprosium-157 decays by electron capture, has a half-life of only 8.1 hr, and emits approximately one 327 keV photon per disintegration, providing a low enough radiation dose for multimillicurie administration. When administered to the rat with an excess of nitrilotriacetate (NTA) good bone localization and high bone-to-soft-tissue concentration ratios are obtained within a few hours. Neodymium-140, another potentially useful member of the rare-earth group, has a half-life of 3.3 days and decays by electron capture to ^{140}Pr, which in turn decays ($T_{\frac{1}{2}}$ = 3.4 min) by both electron capture (50%) and positron emission (50%). The gamma emissions from this parent-daughter pair are almost entirely 511 keV annihilation photons and consequently, like ^{18}F, could be useful in coincidence detection techniques. With conventional rectilinear scanning ^{140}Nd would provide initially three times as many photons as ^{85}Sr for equivalent radiation doses to the bone. Carrier-free ^{140}Nd is readily produced in high yield by a p,2n interaction with ^{141}Pr (100% abundant) and separated by high pressure ion exchange from the target (R. E. Lewis, Oak Ridge National Laboratory, personal communication).

As with the other rare earths, the chelate form will determine the distribution of ^{140}Nd. Table 26 shows that the tissue distribution of ^{140}Nd-^{140}Pr administered intravenously to the rat varies widely depending on its chemical form. Unlike dysprosium, for which NTA was judged the best agent to provide bone localization, neodymium localizes best with HETA. At 3 days the concentration of ^{140}Nd in bone drops to 65% (disregarding decay) of that at 3 hr (Table 26) while the bone:soft-tissue ratios increase. The results with diethylenetriamine-pentaacetate (DTPA) are of interest since it could be potentially a scanning agent for both brain and kidney; on whole-body counts at 3 hr the animals had excreted an average of 96% of the dose.

Radiation Dosimetry of Gallium Isotopes

Because of our continuing interest in the use of gallium isotopes for scanning, the internal radiation doses from ^{66}Ga, ^{67}Ga, ^{68}Ga, ^{72}Ga, and ^{73}Ga have been compared (Evelyn E. Watson). Table 27 lists the half-lives and major radiations from these five radioisotopes. All have relatively short half-lives, varying from 68 min for ^{68}Ga to 3¼ days for ^{67}Ga.

The absorbed fractions for the energies shown in Table 27 were calculated from the data of Brownell, et al. (J Nucl Med Supplement No. 1, Pamphlet No. 3, Feb 1968) and Walter S. Snyder, et al. (J Nucl Med, Supplement No. 3, Pamphlet No. 5, Aug 1969) for the Medical Internal Radiation Dose Committee (MIRD). The results were used in calculating the mean dose to the whole body for three different circumstances: (1) uniform distribution of the radioisotope in the body;

TABLE 26

EFFECT OF VARIOUS CHELATES ON THE 3-HOUR DISTRIBUTION OF ^{140}ND IN THE RAT

	CHELATE *					
	Citrate	NTA	HEDTA	EDTA	DTPA
Bone (%/g)†	0.87 ± 0.07‡	2.4 ± 0.03	2.4 ± 0.1	2.1 ± 0.1	0.019 ± 0.005
Ratio Bone Concentration to:					
Blood	2.2 ± 0.6	130 ± 9	490 ± 160	240 ± 16	63
Muscle	33 ± 4	200 ± 32	> 1000	490 ± 130	24
Liver	0.17 ± 0.02	1.9 ± 0.2	8.0 ± 1.4	5.4 ± 0.5	2.1
Kidney	0.57 ± 0.33	3.1 ± 0.4	8.3 ± 1.0	5.5 ± 0.4	0.13
Lung	2.4 ± 0.5	12 ± 1	65 ± 9	33 ± 3	3.8
Number of Animals	4	4	4	4	4

* All agents administered at a level of 40 μmol/kg body weight.

† Percent administered dose/g of tissue normalized to 250 g body weight.

‡ Standard deviation of the mean.

1027378

TABLE 27

Half-lives, Major* Radiations,
Energies, and Intensities for Gallium Isotopes

Radio-isotope	Half-life	β^- Maximum Energy (MeV)	β^- Intensity (%)	β^+ Maximum Energy (MeV)	β^+ Intensity (%)	γ Energy (MeV)	γ Intensity (%)
^{66}Ga	9.4 hr			4.15	57	0.511	114
						1.04	35
						2.75	25
^{67}Ga	78 hr					0.093	40
						0.184	23
						0.296	21
^{68}Ga	68 min			1.90	87	0.511	176
^{72}Ga	14.1 hr	0.660	15			0.630	27
		0.670	22			0.835	96
		0.960	30			0.894	10
						2.20	26
						2.50	21
^{73}Ga	4.8 hr	1.19	86			0.0533	17
						0.296	87
						0.325	12

*Emitted from at least 10% of decays

TABLE 28

Mean Dose from Gallium Isotopes
(rads/millicurie)

	^{66}Ga	^{67}Ga	^{68}Ga	^{72}Ga	^{73}Ga
Whole body - uniform distribution	0.79	0.34	0.053	0.82	0.13
Whole body - 100% of isotope in 5-cm tumor in center of body	0.45	0.31	0.034	0.72	0.042
Whole body - 100% of isotope in 2-cm tumor in neck	0.45	0.32	0.026	0.70	0.047
Tumor dose - 5-cm tumor in center of body - 100% uptake of isotope	570	180	40	430	110
Tumor dose - 2-cm tumor in neck - 100% uptake of isotope	8200	2400	580	5200	1600

(2) 100% of the radioisotope uniformly distributed in a tumor (5-cm diameter) in the center of the body; and (3) 100% of the radioisotope uniformly distributed in a tumor (2-cm diameter) in the neck. In each of these calculations, the radioisotope was assumed to remain in the body without any loss by excretion; only physical decay was taken into account. Table 28 presents the results of these calculations.

The mean dose to the whole body is smaller when the radioisotope is localized in a tumor because the nonpenetrating radiations (beta particles and low-energy photons) are absorbed in the tumor tissue. The location and size of the tumor seem to have little effect on the whole-body dose.

A comparison of the mean dose to a 5-cm diameter tumor in the center of the body and to a 2-cm diameter tumor in the neck is also presented in Table 28. For each of the gallium radioisotopes, the smaller tumor receives a radiation dose approximately 13 times higher than the larger tumor.

Radiation Dose to Fetus from Radiopharmaceuticals

The dose to the fetus from gamma emitters present in the bladder has been estimated by the Radiation Safety group and collaborators. (Roger J. Cloutier, Walter S. Snyder*, Gordon G. Warner*, and Sarah A. Smith†). We modified the standard-man model developed by Fisher and Snyder (Proc First International Congress of Radiation Protection, Vol. 2, pp. 1473-1486, Pergamon Press, 1968) for the Monte Carlo calculation of absorbed dose to various organs from gamma emitters to provide a standard-female model. The female model, in addition to having the standard organs described in the standard-man model, has a uterus of size and shape that change during various stages of pregnancy. This permits the calculation of the radiation dose to the uterus and the developing fetus as pregnancy progresses.

Because the uterus during pregnancy assumes the general shape outlined in Fig. 41, the model selected for the uterus is a cone with a hemispherical cap, Fig. 42. The length of the cone and the radius of the cap are varied to approximate the size of the uterus during pregnancy.

Ideally it would be desirable to define the position of the developing fetus in the uterus and to calculate the energy absorbed by various organs of the fetus. This is not possible because the fetus is free, within limits, to move somewhat. For this preliminary study, we

* Oak Ridge National Laboratory, Oak Ridge, Tennessee.

† Florence State University, Florence, Alabama.

1027379

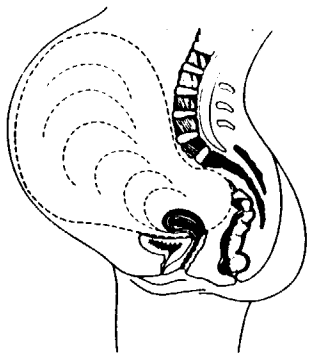

Anatomical Diagram of Uterus Growth During Pregnancy.

Fig. 41.

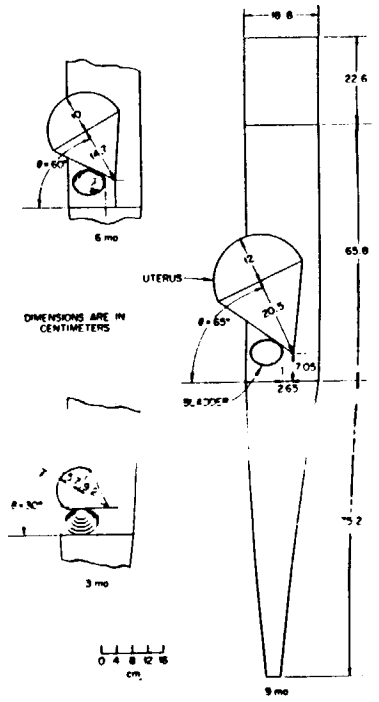

Model of Pregnant Woman.

Fig. 42.

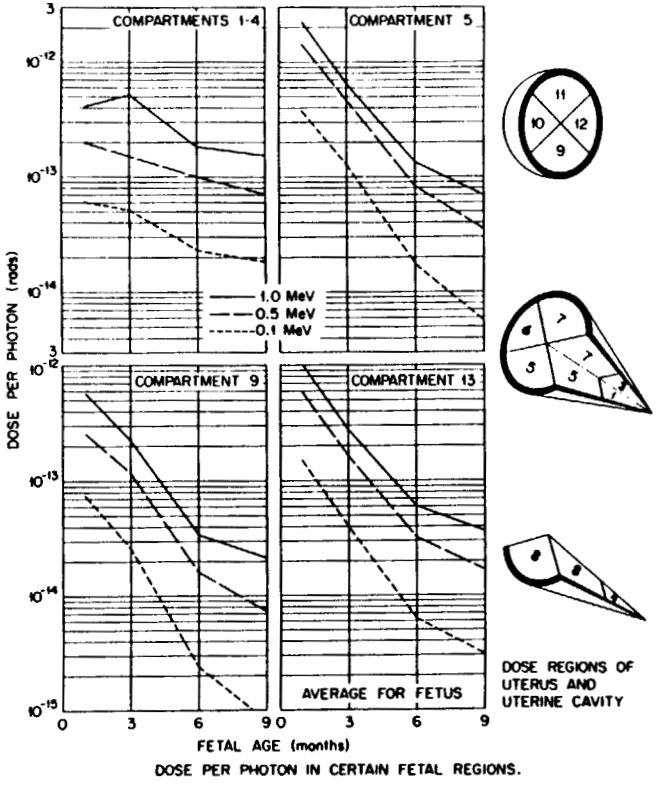

DOSE PER PHOTON IN CERTAIN FETAL REGIONS.

Fig. 43.

considered the fetus as occupying the entire cavity of the uterus and calculated the rad dose to various parts of this volume, Fig. 43

This first study involves the absorbed dose to the uterus and the fetus from gamma emitters located in the bladder of the mother. Because of the closeness of the bladder to the uterus and fetus, this model should be useful in calculating the radiation dose to the uterus and fetus from radioisotopes that are excreted in the urine.

1027380

CLINICAL INVESTIGATIONS IN NUCLEAR MEDICINE

Radioactive Gallium Uptake in Tumors

The observation that radioactive gallium concentrates in a variety of human neoplasms has proved of great interest to clinicians and investigators, and possibly is the most significant recent development in nuclear medicine. Not only can ^{67}Ga assist the clinician in locating tumors otherwise difficult to find but its unique relation with neoplastic growth provides investigators with a previously unknown metabolic factor for studying tumor genesis.

After our initial clinical observation in a patient with Hodgkin's disease, we have now studied 101 sets of scans of 78 patients with at least 20 different neoplasms (C. L. Edwards, R. L. Hayes, Bill Nelson, and N. Tehranian). Table 29 lists the results of the scans by

TABLE 29

PATIENTS SCANNED WITH GALLIUM-67 FOR TUMOR LOCALIZATION

Diagnoses	Positive	Negative
Hodgkin's disease	8[b]	5
Reticulum cell sarcoma	5	0
Lymphoblastic lymphoma	4	0
Lymphocytic lymphosarcoma	0	5[*,*,*]
Mixed or unspecified lymphoma	0	2
Lymphocytic leukemia	0	4
Plasma cell myeloma		
Lung, squamous cell	4	0
" adenocarcinoma	1	2[*]
" poorly differentiated	2	3[*]
" unspecified	2[*]	0
Tumors of-		
Breast	3[b,b]	2
Kidney	2[a]	0
Ovary	0	2[*]
Thyroid, medullary	0	2
" papillary	0	1
" poorly differentiated	1[a,a]	0
Bowel, large	0	1
Malignant tumor (paraganglioma?)	1[c]	0
Ewing's sarcoma	1[b]	0
Histiocytoma	0	1[*]
Glioblastoma	0	1
Adenocarcinoma, metastatic	2[b,b]	0
Squamous cell carcinoma, metastatic	1[b]	0
Undifferentiated neoplasm, metastatic	2[b]	1
No tumor	0	2

[*] Uncertain tumor at time of scan.
a Pulmonary metastases.
b Bone metastases.
c Scan interpreted as positive after surgical exploration.

the type of tumors. Although the procedure was limited to patients believed to have neoplasms, two patients with negative scans later were found not to have had a malignant neoplasm at the time of the scan. There is doubt about how much residual tumor was present at the time of the scan in seven other patients with negative scans; although none was thought to have had all the tumor removed at surgery, each has had a benign course.

The poorly differentiated lymphomas, reticulum cell sarcoma and lymphoblastic lymphosarcoma (see cover) have concentrated gallium consistently and most avidly. In these patients we have seen tumor concentrations of as much as 50% of the dose per kilogram of tumor, more than 100 times that in blood or muscle and 10 times that in the liver. Consistent but less intense concentration has been observed in patients with bronchogenic squamous cell carcinoma, and a variety of poorly differentiated adenocarcinomas.

Eight of 13 patients with Hodgkin's disease had positive scans

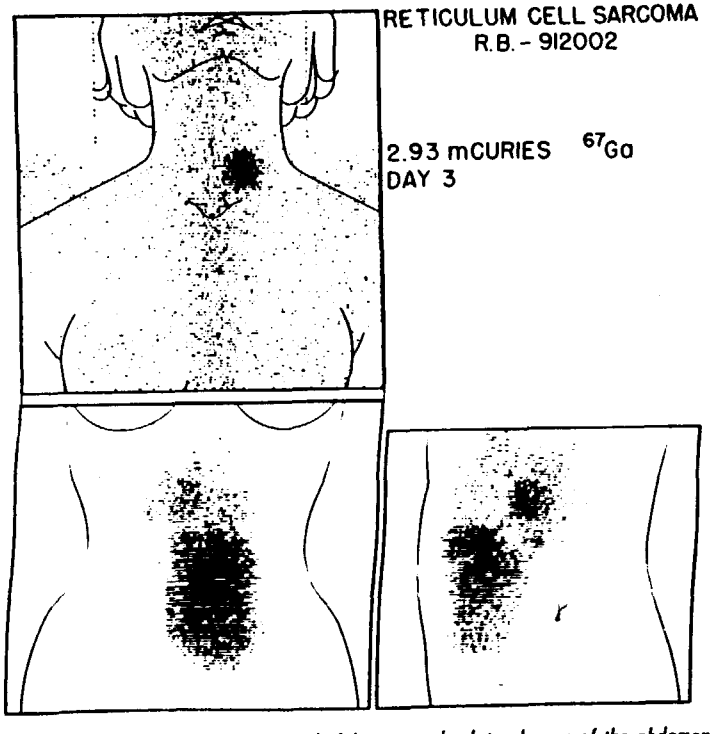

Fig. 44. Anterior scans of the chest and abdomen, and a lateral scan of the abdomen of a 45-year-old woman with reticulum cell sarcoma involving the mesenteric and left supraclavicular lymph nodes. The supraclavicular lesion had escaped the attention of the patient and a number of examiners.

1027381

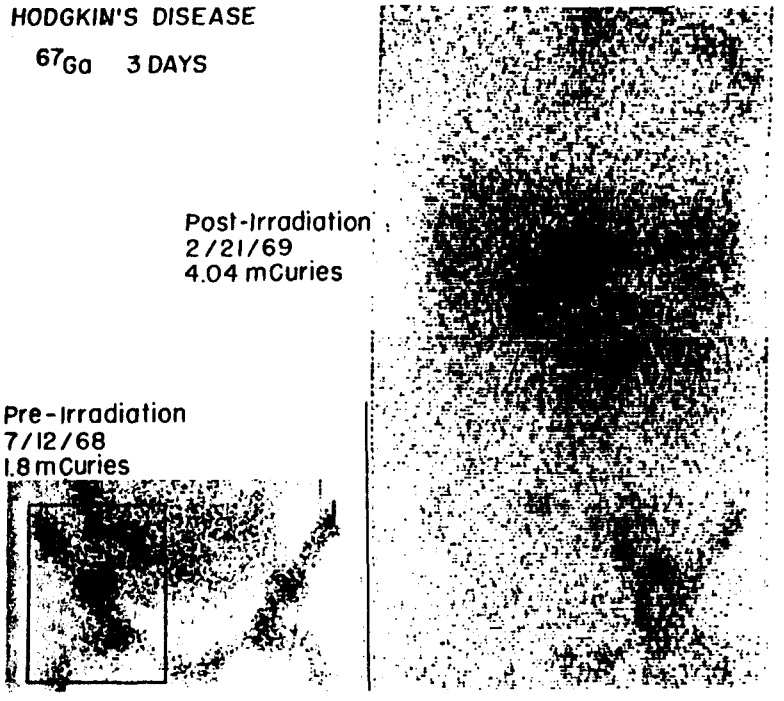

Fig. 45. (Left) Anterior scan of the pelvis of a patient with Hodgkin's disease, showing gallium-67 localized in tumor of the right inguinal and iliac lymph nodes. (Right) A composite of anterior chest and pelvic scans 7 months after radiotherapy shows gallium-67 in tumor of the left pelvic and axillary lymph nodes, the mediastinum, and a large tumor in the epigastrium.

initially. All eight had Hodgkin's granuloma, Luke's mixed type. The five patients with negative scans all had disease previously proved by biopsy and lymphangiogram. One of these was of the nodular sclerosing type; the others were Luke's mixed type. Well-differentiated lymphomas (lymphocytic lymphosarcoma, lymphocytic leukemia), plasma cell myelomas, and medullary thyroid carcinomas have given negative scans consistently. Scanning with gallium-67 has been of greatest clinical assistance in demonstrating lesions deep in the epigastrium where they are not readily demonstrated by other techniques (Figs. 44 and 45). A possible future use may be to distinguish malignant from benign lesions found by X ray or palpation, but our experience until now with benign tumors, granulomas, and abscesses has been too narrow to allow such distinction.

The mechanism of the tumor concentration remains obscure. The well-known bone-seeking properties of gallium may account for some of the lesions seen (Table 29). Histologic and autoradiographic studies

indicate that the localization occurs in the viable tumor rather than in necrotic or fibrotic tissue. Effective cancer chemotherapy and radiation prevent the concentration in tumor. The uptake of gallium in normal structures within the field of radiation therapy is also greatly decreased (Fig. 45).

When carrier-free gallium citrate is injected intravenously, much of it is bound by plasma protein, especially transferrin. It leaves the blood rather slowly (Fig. 46); 5% of the dose is still in the blood at 41 hr (48 hr for patients without tumor localization and 30 hr for those with good tumor localization). In addition to the deposition in tumors, liver, spleen, and skeleton (including marrow) considerable amounts of gallium are found in the lungs, kidneys, adrenals, and epidermis of patients examined at autopsy. The average whole-body retention is 66% at 8 days by whole-body counting (Fig. 47). This value correlates well with the average urinary excretion of 25.7% at 7 days (Fig. 48), and the average excretion in the stool, 9% at 7 days.

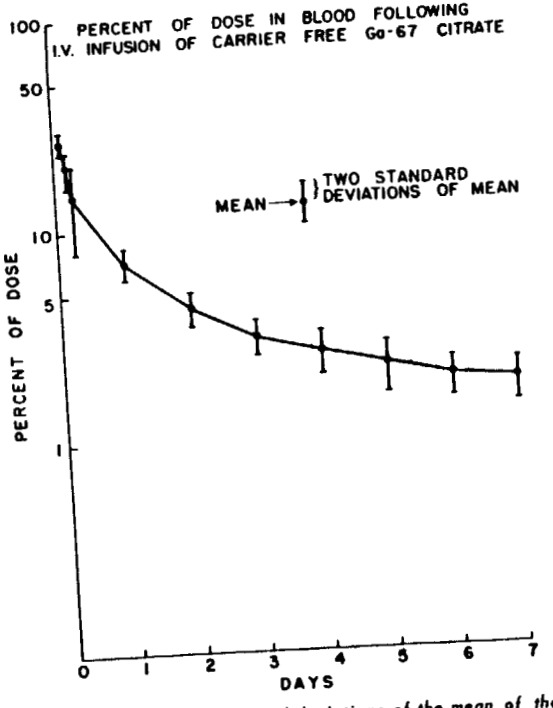

Fig. 46. (a) The average and two standard deviations of the mean of the percentage of the dose remaining in the estimated blood volume (7% of body weight) for 36 doses of carrier-free gallium-67 citrate administered by intravenous infusion.

1027382

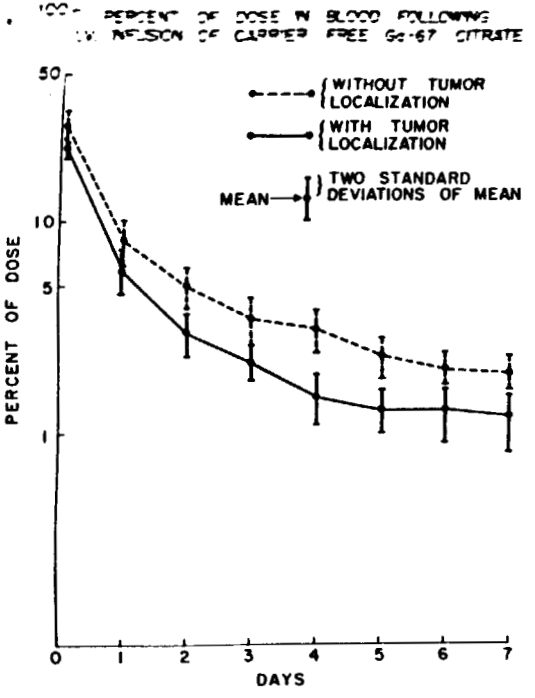

Fig. 46. (b) The average percentage of the dose remaining in the blood of patients who showed good tumor localization of gallium compared with those who show no or very little tumor localization; there was more rapid clearance from the blood in the former group.

Hoping for better visualization of abdominal tumors, we are exploring possible ways of delivering the gallium at higher concentrations to the tumor. These methods include intralymphatic and intraarterial systems, which may also decrease the excretion into the bowel thereby enhancing the contrast between abdominal tumors and the normal structures.

Differentiating Primary Myelofibrosis with Radioisotopes

Primary or idiopathic myelofibrosis, a myeloproliferative disorder, is characterized by marrow fibrosis and extramedullary hemopoiesis. To determine whether radioisotopic tests are useful in differentiating primary myelofibrosis from other similar diseases we collected and reviewed various laboratory data in our 44 patients who had one or more disorders of the syndrome (Francis A. Goswitz, Helen Vodopick, M. Francine Pennington, and Martha L. Clevenger). Radioisotopic data of value in addition to the radiocolloid total-body scans were the blood

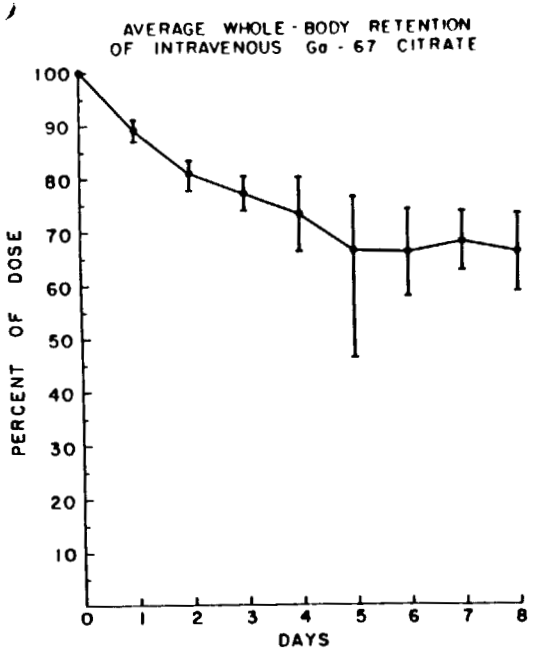

Fig. 47. The average whole-body retention after 39 intravenously administered doses of carrier-free gallium-67 citrate. The whole-body retention was measured with the ORAU high-level whole-body counter and the linear scanner.

volume, and external monitoring of the liver, spleen, and marrow on days 1 and 5 after the intravenous injection of ^{59}Fe.

Of four patients who had total-body scans, three were typical of the myelofibrosis pattern (radioactivity concentrated in the liver and spleen with little or no radioactivity in the skeleton). In one patient the radioactivity besides that in the liver and spleen was considered possibly due to the presence of an associated disease, disseminated lupus erythematosis.

Blood volumes determined directly by ^{131}I or ^{125}I serum albumin to measure plasma volume and ^{51}Cr-labeled erythrocytes to quantify red-cell mass were studied in four patients and in two patients twice. All six results showed elevated plasma volumes (above 40 ml/kg) and blood volumes (above 70 ml/kg). Figure 49 graphs the results of the studies performed in patients with primary and secondary myelofibrosis. Note in primary myelofibrosis that the red-cell mass is normal to elevated; thus this finding cannot be used in distinguishing a patient with this disorder from one with polycythemia vera.

To detect extramedullary erythropoiesis by external counting, an index was calculated by dividing the day 1 ^{59}Fe activity of the liver or

1027383

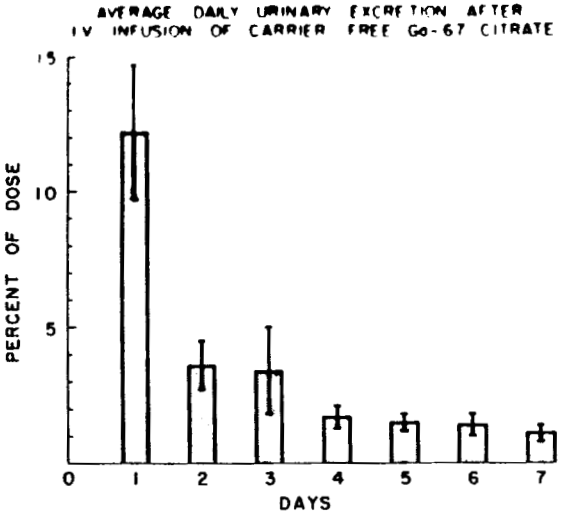

Fig. 48. Urinary excretion after intravenously administered carrier-free gallium-67 citrate in 17 patients. The average cumulative urinary excretion after 7 days was 25.7% of the doses.

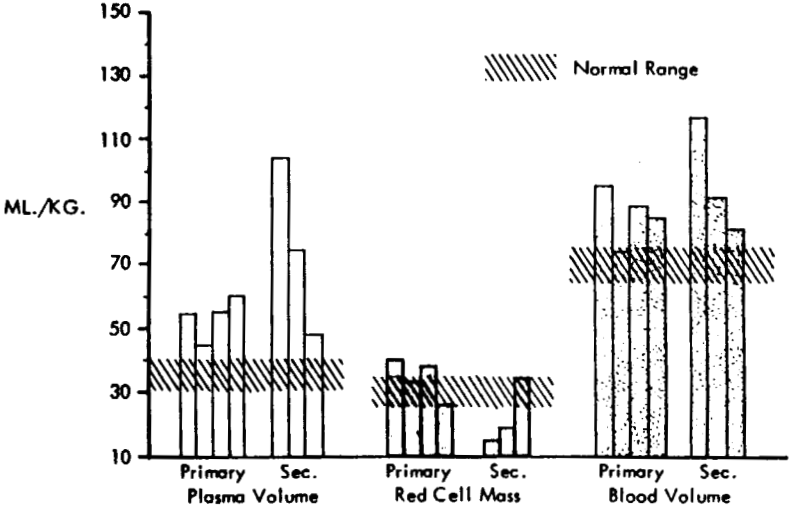

Fig. 49. Results of true blood volume studies performed in four patients with primary and three patients with secondary myelofibrosis.

TABLE 30

EXTERNAL MONITORING

INDICES IN EXTRAMEDULLARY ERYTHROPOIESIS

Patient	Disorder	Day 1 Index Organ/Heart	Gardner's Spleen	Index* Marrow (Sacrum)
A	Primary myelofibrosis	1.82	0.98	1.00
B	Primary myelofibrosis	2.09	1.07	1.22
C	Primary myelofibrosis	2.50	2.19	0.85
D	PRV, secondary myelofibrosis	2.63	1.72	0.92
E	PRV, secondary myelofibrosis	2.34	1.38	2.09
F	Refractory anemia	0.76	0.70	1.63
G	Rheumatoid disease, iron-def.	1.19	0.90	2.51
	INDEX FOR ERYTHROPOIESIS	>1.75	>2	>2

*Ratio of counts on day 1: day 5 over same organ

spleen over that of the heart. If this ratio is greater than 1.75, extramedullary erythropoiesis was presumed to exist. The ratio must decrease after day 1 unless iron storage is present. The ratio is based on the principle that ^{59}Fe activity will reach its peak on day 1 since iron must first be incorporated into hemoglobin within the erythrons. The counting rate will progressively decrease over the organ as the ^{59}Fe now within the mature erythrocytes is released into the circulation. We compared this index with that of Gardner and Nathan's "Effective Erythropoietic Index" (New Engl J Med 274, 420, 1966) in our three patients with histologically proven at autopsy to be primary myelofibrosis. The results are reported in Table 30. For these three cases Gardner's index appears too conservative. One advantage of our index is that detection of erythropoiesis can be made on day 1 rather than at 5 days.

In summary, a combination of the following radioisotopic findings suggests primary myelofibrosis: a radiocolloid total-body scan with all the radioactivity concentrated in the liver and spleen; increased plasma and blood volumes; ^{59}Fe counting index over the liver or spleen compared to the heart on day 1 consistent with erythropoiesis.

WHOLE-BODY COUNTING

Throughout the country the clinical use of whole-body counters and isotope retention studies has remained restricted largely to clinical and animal metabolic research. The numerous diagnostic procedures that

1027384

can be performed with this modality compete unfavorably with other laboratory tests that require usually less than one day to perform and report. In addition, low background, high-sensitivity whole-body counters are unusually expensive for ordinary general hospitals where high equipment cost must be offset by a large volume of relatively inexpensive test procedures that can be billed to the patient at a profit. The short-term potential for the widespread use of such counters is, therefore, small. Their long-term potential appears to some of us, however, to be substantial.

The use of whole-body counters does not require focusing of the sensors, fecal and urinary collections, any handling of the ambulatory patient, or changing techniques for quantitation of different isotopes as most other isotope procedures do; thus relatively untrained personnel can make many precise measurements of isotope retention in large numbers of persons. Assay times as short as 3 min or less are possible with present technology so that one counter can make about 100 assays per 8-hr shift where population pressures demand large scale automated diagnosis and screening for disease. The resulting measurements are easily and rapidly converted by automated computations into clinically meaningful numbers in context with other laboratory procedures. The growing shortage of physicians in relation to the growing population will soon require development of routine diagnostic testing procedures, like whole-body counting, that can be performed by paramedical personnel. These tests can categorize patients and their complaints and save physicians' time in handling minor problems or problems best attached in another clinic. Until that time, however, diagnostic whole-body counting techniques will be used chiefly by a hospital staff that has one and is dedicated to using it. Other uses will be for detection, measurement, and identification of radioactive contamination in occupational medicine and for metabolic research involving chemical substances that can be traced with isotopes.

In this chapter we report on our use of the whole-body counter in clinical thyroid disease, and in experimental metabolic research directed toward defining the etiologic agent or agents responsible for the high incidence of thyroid disease in the ORAU Marmoset Research Colony. In the clinical study, we show for the first time with a sufficiently large number of patients that the whole-body counting technique for measuring iodide binding correlates so well with the usual collimated crystal measurement that either technique can be reliably used to obtain the same clinically desired information. This study is basic to our relying on the use of whole-body counting for measuring iodide metabolism in small animals where thyroid gland activity cannot be measured by a collimated crystal because of its size, variable location, or permissible dose.

Radioiodine Whole-Body Retention

We have continued our study of whole-body ^{131}I retention as a quantitative measure of thyroid function (Harold D. Hodges, C. L. Edwards, C. C. Lushbaugh, and W. D. Gibbs). Oral or intravenous ^{131}I has been shown to be a universally applicable means of determining the functional level of thyroid metabolism in laboratory animals of all

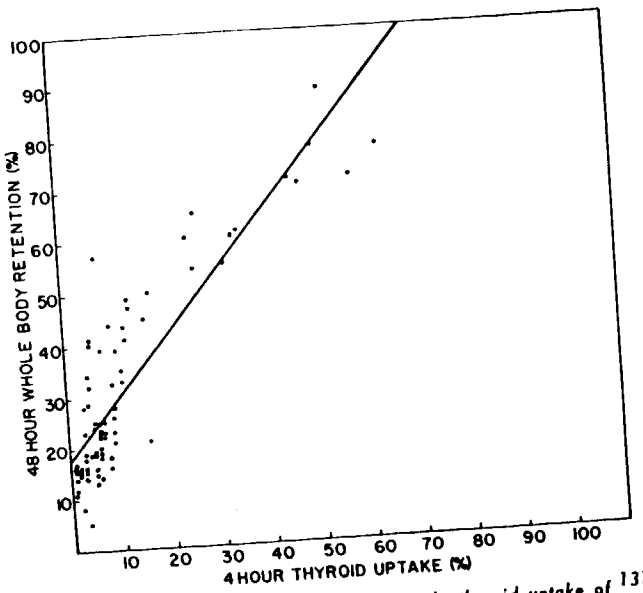

Fig. 52. Plot of 48-hr whole-body retention and 4-hr thyroid uptake of ^{131}I in 109 patients. Coefficient of correlation is 0.882.

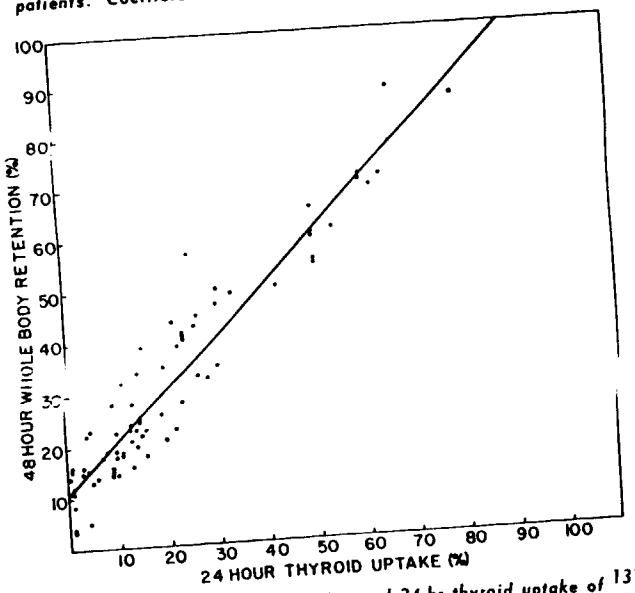

Fig. 53. Plot of 48-hr whole-body retention and 24-hr thyroid uptake of ^{131}I in 109 patients. Coefficient of correlation is 0.954.

1027386

hr whole-body retention were compared, the coefficient of correlation was +0.954 and the regression equation:

$$\% \text{ thyroid uptake} = \frac{\% \text{ whole-body retention} - 10.90}{1.00}$$

In patients with impaired renal function or cardiac problems, excretion of unbound ^{131}I can be delayed. If the period of retarded renal clearance extends beyond 48 hr, this method of measuring thyroid uptake could possibly give falsely high results. However, in the series of 109 patients this error was not observed.

Whole-body counting can serve as a substitute for the standard thyroid uptake method when exceedingly small doses of ^{131}I are required. With a low background whole-body counter, the dose administered to patients can be as low as 30 to 50 nanocuries. It also eliminates the errors encountered with an enlarged or abnormally located gland.

A high- or medium-level whole-body counter also can be used to monitor the uptake of therapeutic doses that are difficult to measure with equipment used for tracer studies. The clinician can then be alerted early to any inadvertent loss of the therapeutic dose as can happen when the patient receives some exogenous iodine or goitrogen before receiving the treatment. The technique also allows one to more accurately estimate the actual radiation dose delivered to the thyroid.

Iodine Metabolism in Marmosets

In our previous research report on finding a fatal thyroid disease in perinatal and adult marmosets, we suggested that the hyperplastic and degenerative aspects of this disease implied that some environmental goitrogenic substance was involved. Two studies were undertaken to try to approach this etiologic problem by nondestructive methods: (1) cobalt turnover or retention study in cobalt-sensitive and nonsensitive animals; and (2) iodine metabolism study to determine whether abnormal iodine turnover kinetics were actually present in the colony as histologic appearance of thyroid gland suggested and as would be expected if a goitrogen were present (Harold D. Hodges, W. D. Gibbs, Thomas A. Smith, C. C. Lushbaugh, and N. Gengozian). Elsewhere in this report we have summarized the whole-body cobalt retention studies that were done because cobalt, a well-known goitrogen for some animals, is present in the commercial diet of the marmosets at a level of 0.25 ppm. We report here the parallel study of whole-body iodine retention kinetics in selected adult marmosets thought by the animal caretaking staff to be clinically normal.

Twelve marmosets were given a dose of carrier-free ^{131}I intraperitoneally (0.3-0.4 microcuries each) and whole-body counts were obtained immediately after the dose and at 1, 2, 5, 6, 7, 8, and 9 days. Four animals were counted initially in the clinical low-level whole-body counter to test the feasibility of using this technique with these small delicate animals. Eight additional animals were subsequently studied with a small whole-body counter built at the Marmoset Research Center especially for this experiment using the geometry-insensitive configuration developed by Gibbs. It consists mainly of two opposing NaI crystals arranged to sense a constant volume in which the location of a

sizes and shapes, and obviates the need for collimated detection (Lushbaugh, Nature 198 (4883): 862-864, 1963; Gibbs, et al., In Second Annual Oak Ridge Radioisotope Conference, USAEC Report TID-7689, pp. 20-21, 1964). Furthermore, because the low-level whole-body counter is more sensitive than the usual small collimated NaI crystal detector, dose reduction of 10- to 100-fold can be obtained. The method, however, is slower than the present clinical technique; it requires up to a week to establish the turnover rate of the bound iodine compartment, but provides additional useful information about daily bound iodide utilization rates.

To determine the degree of correlation between the two techniques in man, we have studied parallel ^{131}I thyroid uptake and whole-body ^{131}I retention in 109 patients. As shown in Fig. 50, we have found an excellent correlation between the thyroid uptake and whole-body retention of ^{131}I as early as 48 hr after the dose and as late as 10 days. Each patient was counted in our low-level whole-body counter each time a thyroid uptake measurement was made for periods up to 10 days. Correlation of thyroid uptake with whole-body retention was also made with the 4-hr measurements and with daily measurements up to 10 days. Our results show that 48 hr is the earliest time the coefficient of correlation between simultaneous measurement of thyroid uptake and whole-body retention exceeds 0.950. This linear correlation observed at 48 hr allows quantitative extrapolation of thyroid uptake from the 48-hr whole-body ^{131}I retention assay with the use of the regression equation:

$$\% \text{ thyroid uptake} = \frac{\% \text{ whole-body retention} - 9.45}{1.07}$$

This equation is derived from the linear regression line relating the values for the 48-hr thyroid uptake and the 48-hr whole-body retention assay, as shown in Fig. 51. The coefficient of correlation between 48-hr thyroid uptake and 48-hr whole-body retention is 0.962.

We also investigated the relation of the 48-hr whole-body retention to thyroid uptake at 4 hr and 24 hr. Figures 52 and 53 show the plots of these regression lines. The coefficient of correlation between 4-hr thyroid uptake and 48-hr whole-body retention was +0.882 and the regression equation:

$$\% \text{ thyroid uptake} = \frac{\% \text{ whole-body retention} - 17.82}{1.17}$$

The correlation coefficient +0.882 indicates that the 48-hr whole retention is not a good estimator of 4-hr thyroid uptake as might be expected or that the 4-hr thyroid uptake is not related quantitatively to the eventual uptake. However, when the 24-hr thyroid uptake and 48-

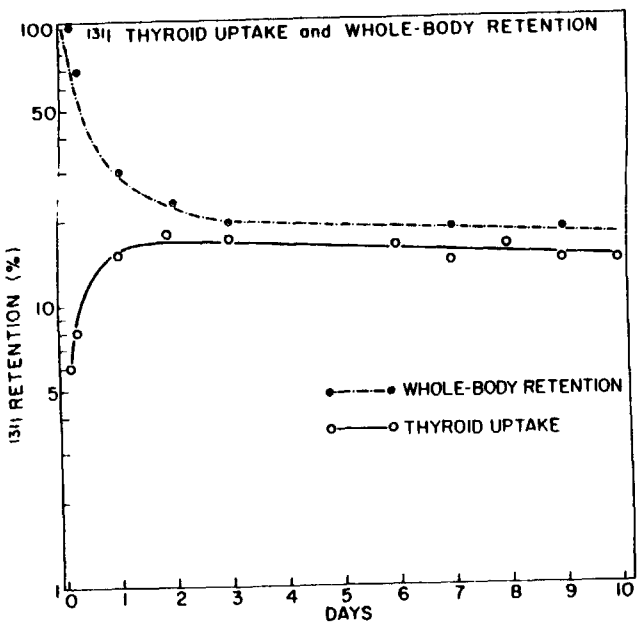

Fig. 50. Whole-body retention and thyroid uptake of ^{131}I in a normal patient. Note that slopes of whole-body retention and thyroid uptake curves are nearly parallel after 48 hours.

1027385

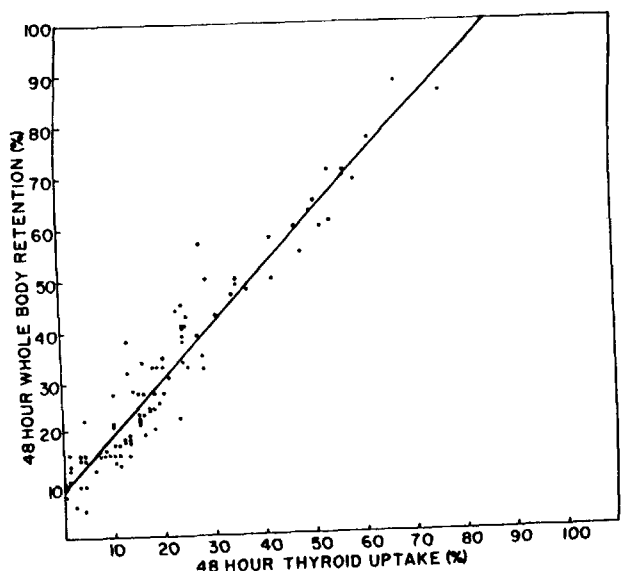

Fig. 51. Plot of 48-hr whole-body retention and 48-hr thyroid uptake of ^{131}I in 109 patients. Coefficient of correlation is 0.962.

Gibbs, Harold D. Hodges, Mildred Bailey, Larry Papiez*, and C. C. Lushbaugh). The metabolic importance of cobalt is relatively unknown other than the minute amounts needed for vitamin B_{12} synthesis and consequently for erythropoiesis. It is also required in greater than trace amounts, independent of its content in vitamin B_{12} for red-cell production in some species like swine. Large amounts of it, which do not seem to be required at all for normal bone-marrow function, can, however, produce erythrocytosis in rats and man. Even though it is now well known that RBC produced under cobalt ion influence are ineffective in relieving the anoxia of anemia because such hemoglobin has a decreased oxygen dissociation rate, cobalt formerly was prescribed as a chloride salt in many shotgun remedies for correction of anemias of unknown cause. Such empirical use is found in animal husbandry where it is still included in many synthetic commercial diets for almost all laboratory animals.

The fatal human myocarditis and thyroid destruction caused by cobalt incorporated into a Canadian beer to improve its foaming characteristics and its goitrogenic effect in some anemic children suggest that cobalt should be considered a toxic metal for man when consumed in greater than true trace amounts. In our search for possible goitrogens that might be implicated in the hyperplastic goitrous thyroid disease in our marmoset colony, we were not surprised to find that our commercially obtained diet contained added cobalt chloride (0.25 ppm). A literature search, however, failed to reveal whether this amount might be damaging to the thyroid glands of New World primates. Cobalt's known harmful effect on the gland varies with species; mice, rats, and rabbits apparently are not susceptible but guinea pigs and man are. Individual sensitivity is highly variable in man suggesting that other factors such as intestinal absorption of orally ingested cobalt salts may play a role in determining toxicity; average intestinal absorption for man is thought to be 10% of the daily intake but highly variable for unknown reasons.

The direct approach to this problem would be a study of the cobalt metabolism of marmosets. We deferred this study because of the present expense and scarcity of this animal, and because there is no means to determine deleterious effects without destroying the animals. We therefore undertook first an interspecies study of more commonly used laboratory animals to determine a possible basis for the species-specific effect.

In the initial experiments, reported here, we tested one obvious possibility that variations in rate of turnover of injected cobalt might underlie species sensitivity. We determined the turnover rate of cobalt chloride (tagged with ^{60}Co) by whole-body counting of mice, rats, guinea pigs, and rabbits after intraperitoneal injection of the salt, counting the animals daily for 30 days (except for weekends). Mice

* Summer Student from Washington State University, Pullman, Washington.

1027388

were counted in groups of five; the others were counted individually. The doses were 1.6 microcuries/mouse, 3.3 microcuries/rat, 5.0 microcuries/rabbit or guinea pig. The specific activity of the cobalt chloride was 400 curies/gram, so the tag was a true tracer of the animal's own cobalt present at the time of injection. The results are shown in Fig. 54 as the mean retention curves for the four species for 30 days. These curves were fitted best by the well-known exponential equation used in compartmental analysis where

$$R_{(t)} = U_{(o)}e^{-\lambda t} + B'_{(o)}e^{-\lambda t} + B''_{(o)}e^{-\lambda t}$$ and R = Retention;

U = unbound fraction; B' and B'' are bound fractions; $\lambda = \frac{.639}{T_{50}}$

and T_{50} = the time required for excretion of 50% of the tracer located in compartments U, B', or B'' at zero time. The parameters of this model for the four species are shown in Table 32.

From these data the theoretical rate of accumulation of cobalt was determined, with the assumption of uniform daily intake. The leveling off of these accumulation curves occurs when input balances output and environmental equilibrium is established. The resulting cobalt accumulation values (Table 33 and Fig. 55) show that the mouse, rat, and rabbit establish their equilibrium of the body burden of cobalt in about 201, 278, 134 days respectively, while the guinea pig requires

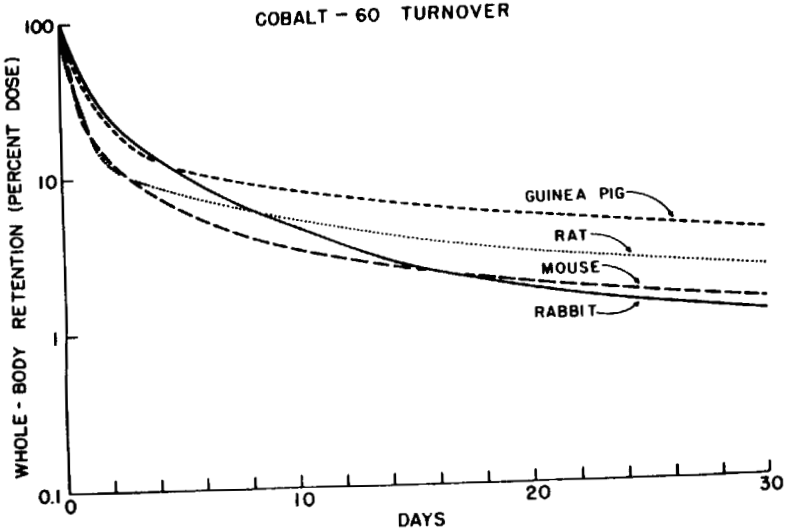

Fig. 54. Averaged whole-body retention curves for ^{60}Co chloride (injected I.P.) in four different animal species. Note that the highest retention over the 30-day study occurred in the guinea pigs that are the most sensitive of these species to cobalt thyroidal intoxication.

point source or a diffuse mass of radioactivity has little or no effect upon the counts per microcurie measurement. Only one or two animals were counted over each two-week period to avoid upsetting animal care routine and provide time for training personnel in the technique.

A sample of blood was drawn immediately before administration of ^{131}I for thyroxine determination (T_4). Whole-body retention kinetics for each animal was calculated and plotted graphically. These curves were analyzed as the sum of two exponentially excreting processes. The more rapidly disappearing portion of the tracer probably represents renal excretion of unbound iodide and the more slowly excreted portion the turnover of bound iodine. The magnitude of the two compartmental fractions of the dose and their turnover half-times were estimated by graphic analysis of the retention curves and by an analog computer program using a model representing the sum of two exponentially decaying compartments. These results are summarized in the table. Although the fits of the curves obtained with the analog computer are probably not unique, we could not obtain good fits by altering the parameters shown.

We discarded the results of 2 animals because an uncontrollable shift in counting sensitivity occurred during the early phase of this study that was subsequently corrected. The 10 animals studied could be classified on the basis of the turnover times (T_{50}) of their second or bound-iodide compartment: four animals had a greater than 25-day T_{50} and six animals had a less than 25-day T_{50}: the mean T_{50} for each group was 34.4 and 15.2 days. The differences between the means and ranges of values of the other parameters of the metabolic iodide model were not significant in these two classes. The mean percentage of iodide bound was 15.8 in Class I animals, and 13.3 in Class II animals. This 3% difference is in the logical direction, however, for this division of the animals. The serum thyroxine values (performed in the clinical chemistry laboratory by Allen Webb) vary widely and do not seem to correlate with any of the parameters of the individual or grouped whole-body retention curves. This variability in T_4 assay was found occasionally when the same animals were assayed three times or more during the year. For example, in one animal T_4 assays of 4.0, 4.6, and 7.5 were found at 3-month intervals. In other animals, however, either consistently low (2.4 μg/100 ml) or normal (3.6 - 4.2 μg/100 ml) values were obtained repeatedly and made us feel that the test is reliable. Its variability and lack of correlation with the whole-body retention-curve parameters, therefore, mean to us that these animals are not in a steady state of thyroxine production, storage, and utilization. This interpretation is also supported by the 2-fold difference in the T_{50} values of the bound-iodide compartment that led us to divide the animals into two classes. Since both man and the Rhesus monkey normally have long bound-iodide T_{50} values (90 and 65 days) the assumption that other long-lived slow-growing primates such as the marmoset would normally have prolonged bound-iodide turnovers seems reasonable. We suggest, therefore, that the four Class I marmosets in Table 31 are normal. If so, the bound-iodide T_{50} values of the second class must be considered abnormally rapid owing to partial thyroid blockade. This interpretation supports our contention that these animals are or have been in contact with some still unknown goitrogen.

1027387

TABLE 31

Two-Exponential Compartmental Model for ^{131}I Whole-Body Retention in Marmosets.

Class	Animal No.	Compartment: Unbound Iodide U_o	T_{50}	Bound Iodide B_o	T_{50}	Serum Thyroxine T_4
I		(%)	(hrs)	(%)	(days)	(μg/100 ml)
Normal ? $B_{T_{50}}$ = >25.0	1	85.0	7.5	15.0	37.5	7.5
	2	85.0	12.0	15.0	31.5	3.8
	3	77.0	10.0	23.0	41.0	4.0
	4	90.0	9.2	10.0	27.7	2.8
Mean		84.3	9.7	15.8	34.4	
II						
Blocked ? $B_{t_{50}}$ = <25.0	1	88.0	14.5	12.0	17.3	0.5
	2	84.0	10.0	16.0	18.0	4.8
	3	90.0	6.5	10.0	15.0	4.2
	4	87.0	8.5	13.0	15.0	3.0
	5	91.0	10.0	9.0	15.0	3.4
	6	87.0	8.0	13.0	12.0	2.4
Mean		86.7	10.0	13.3	15.2	

Since all the animals in both classes were considered clinically normal, the thyroid metabolic system of Class I animals may be considered compensated and that of Class II recently decompensated or compensating. To test this hypothesis, we obviously need more animals and some that are definitely ill. We are expanding this study, therefore, to include clinically sick, newly arrived animals and others that have been in the colony for a long time but have recently begun appearing unhealthy. In another section of this report we describe the continuing occurrence of hyperplastic thyroid disease in the colony.

Cobalt Retention in Several Species

Because of the findings of a thyroid disorder in marmosets implicating cobalt as a possible factor, we have studied variations in whole-body cobalt retention in sensitive and non-sensitive species (W. D.

hepatic, and renal-vascular diseases all exist in the colony-bred and imported marmosets. In light of this whole-body counting study, these diseases might enable toxic levels of cobalt ion retention in an otherwise resistant species. We are attempting also to determine the morphologic or functional identity, if any, of compartments B' and B". In light of what is known about tissue responses to cobalt poisoning, one is tempted to guess that bone-marrow and thyroid binding is represented by compartment B" kinetics.

When more marmosets become available for research, we plan to test in them the hypothesis suggested by the present study that cobalt sensitivity of a species can be predicted from the size and turnover kinetics of compartment B".

INSTRUMENTATION AND COMPUTER TECHNOLOGY

Computer Development

The Division relies heavily on complicated electronic instrumentation. We see the development and testing of new tools to be an essential integral part of our program. Elsewhere in this report are entries that describe improvement in physiologic monitoring apparatus for studying radiosensitivity in man.

For some years we have realized that computers can yield important benefits in biomedical research, and sensing this trend, we embarked on an effort to develop, around an IBM 1800 computer, a resource for our various activities. Scientists and administrators alike in the Division have had to make major shifts in attitudes. We had to build capabilities and recruit a computer staff, and we had to accumulate first-hand experience. At times there were setbacks but, persuaded that the computer is an essential tool, we have persisted and are now beginning to see the fruits of our investment. During 1969 we saw significant achievements and foresee in 1970 additional contributions to our collection, storage, and analysis of data by our computer group (Howard Harmon, Earl McDow, Jr., Paulette Aaron, R. F. Queener, and Mona Smith).

Major efforts in 1969 were devoted to engineering studies required to expand the computer. The eight-thousand word "K" memory of the central processor was increased to 16-K; an additional tape drive doubled tape handling; and two additional disk drives greatly increased the random access storage. The initial configuration of the IBM 1800 computer had been severely limited to printer output; however, a new Calcomp X-Y plotter and two typewriter printers are recently operational. A display scope will be installed during the first quarter of 1970. The additional output devices with high efficiency will rapidly display research data, thereby dramatically reducing the time from data-collection to data-reduction and display. We have expanded terminal input-output sections to avoid a developing critical bottleneck. Special engineering studies have been completed in the use of the terminals in computer-instrument connections. Systems engineering was done under some pressure to meet delivery schedules of new components. Each schedule was successfully met, and updated software systems were available for immediate use. As each new device went into operation, earlier programs with many links essential for the 8-K processor, had to be reworked to achieve maximum use of the expanded computer.

1027390

The data bank for the NASA-AEC project of all known clinical cases of total-body irradiation now numbers more than 3,000 cases. These cases, each complete with all available recorded clinical data, requires that analyses must be done on a large computer. The CDC computer at ORNL was used initially, but in 1969, the bank had to be transferred to a 360-computer system. During the transfer, the data bank was also updated into a less massive tape system for more efficient use of advanced capabilities available on the 360 system. Routine analyses are again in progress, including an updated analysis of nurses' notes for correlating anorexia, nausea, vomiting with dose levels, and portal irradiation responses.

We have developed an administrative manual for the computer operation and established libraries and handling procedures for program and data card decks, program documents, print-outs, and tapes. To assure an orderly, efficient operation we had to design and test work forms. We also had to write a program for a daily, weekly, monthly, and annual summary of computer time expended on each computer application; it now is proving to be valuable in providing accounting information.

The Medical Division had a number of linked programs operational on the limited computer configuration. Other programs in various states of completion were dormant, pending installation of the additional equipment; part of them have been activated and others are in the process of being completed. We rewrote or completed a number of programs for on-line, time-sharing procedures. The on-line operation, in a time-sharing mode, for monitoring remotely located liquid scintillation counters has received additional sophistication. We now can present the analyzed data either in histogram form on the printer, or as an analog curve with the X-Y plotter. The program for analyzing data from the whole-body counter on the "scatter-window" technique was adapted for other whole-body counting facilities. (The program requires a very large central processor and final analyses are done at the K-25 Computer Center.) Additionally, we modified the program for statistically analyzing the electronic erythrocyte-size distributions to accept multichannel analysis data from paper tapes; a small data bank was started for this project. We then expanded the program to add new data, retrieve, and analyze group or individual data on humans or research animals.

We delinked an existing bone-marrow report program. A generalized program has been written that selects information according to specified criteria so that the data can be used for any probit analysis. We also delinked the program for power spectrum analysis of the pulmonary impedences from patients in the low-exposure total-body irradiator (LETBI). One of the more dramatic uses of the IBM 1800

TABLE 32

Parameters for Exponential Compartmental Analysis of Cobalt Chloride Whole-Body Retention in Four Rodent Species After IP Administration.

Species	"Compartment" Unbound U_o	T_{50}	Bound B_o'	T_{50}	B_o''	T_{50}	E_t *
Nonsusceptible	%		%		%		
Mouse	76	0.17	20	1.8	4	18.5	1.49
Rat	79	0.33	15	2.5	6	22.3	2.37
Rabbit	60	0.40	34	2.3	6	12.7	2.09
Susceptible							
Guinea pig	72	0.50	18	2.1	10	20.7	3.63

* Body burden in daily dose units.

TABLE 33

Environmental Cobalt Equilibration Times

Species	Level 50%	95%	99%	~100%	Final Level % of Daily Intake
	(Days)				
Mouse	27	80	122	201	1.49
Rabbit	18	55	84	134	2.09
Rat	32	96	145	278	2.37
Guinea Pig	30	89	137	248	3.63

248 days. However, the mouse then has retained only about 1.5 times its daily dose while the rat has 2.4, the rabbit 2.1, and the guinea pig 3.6 times their daily dose. At the time of environmental equilibrium only bodily compartment B" contains a significant amount of the metal in all species. The "resistant" species (mouse, rat, and rabbit) appear to retain less cobalt and turn it over more rapidly than the "sensitive" guinea pig. The time for more than 10% of the original dose to remain in the "bound" compartments B' and B" was found to be for the mouse 2.5 days, rat 4.5 days, rabbit 6.0 days, and guinea pig

1027389

7.0 days. The most rapidly excreting compartment U can be assumed to represent direct renal clearance and urinary excretion; compartments B' and B" represent systems that compete for the injected cobalt and bind it in some fashion that requires enzymatic work before it is released and then excreted. On the basis of these assumptions these data imply that cobalt toxicity results from slow initial renal absorption and urinary excretion that allows increased cobalt binding by other organs where retention of the metal is prolonged. Cobalt toxicity in man and other species may, therefore, be enhanced by the presence of diseases causing decreased renal function, and diseases such as hepatitis where enzymatic detoxification of metalic-protein complexes is reduced. Inborn genetic differences in absorption and binding capabilities in various species may also play a role.

Studies are in progress to determine the daily percentage of absorption of trace and "therapeutic" oral doses of cobalt in these species. These additional data are needed to determine whether variations in total-body turnover rates are related to variation in gastrointestinal absorbability and dietary concentrations. Our parallel histopathologic studies of marmoset diseases have shown that intestinal,

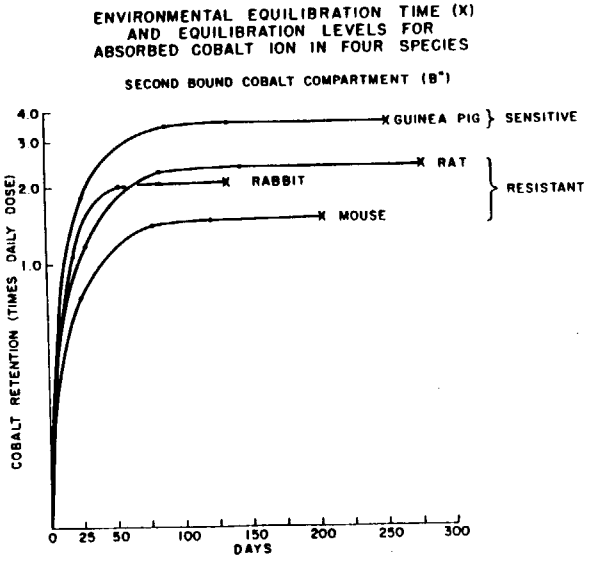

Fig. 55. Graph of the theoretical total-body accumulation curves of cobalt in the four species. The times when constant daily intake reaches equilibrium with the amount excreted is shown by the (X) that terminates each curve. After this time the curves are flat and body burden is not increased unless intake is increased. These equilibration levels or body burdens are scaled in terms of dose.

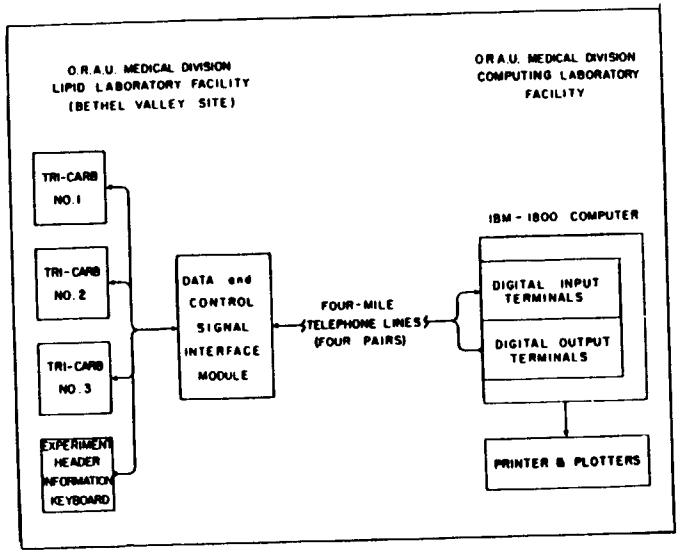

Fig. 56. Block diagram of Tri-Carb interfacing system.

signals, the cardiac R-R interval signals (analyzed into frequency histograms over 4-min sampling periods) and power spectrum analysis of pulmonary impedance waveforms. Using these systems we are able to reduce to the most salient facts the large volumes of data produced by monitoring a patient during treatment that often lasts and produces data for a week or more.

Our early success in interfacing has led us recently to attempt a similar connection to the Nuclear-Chicago Pho-Gamma III scintillation camera offering considerable advantage in the analysis of the camera's signals, and in plotting the patterns on the computer's readout devices. This design has proved to be taxing to the engineers because the camera's complex timing functions are easily desynchronized. Our circuits must also delay the camera's action by a standard interval of 218 microseconds so that the X and Y coordinate voltages for each gamma event can be accurately analyzed and stored in the computer. Our most recent efforts are directed toward making the computer read the X and Y coordinate signals properly, and improving the electronic circuits to prevent desynchronization and to achieve a minimum dead time for each pulse analysis.

The Profile Scanner for Retention Studies

Work has continued on developing our means for locating and determining the precise amounts of radioactivity in patients (W. D. Gibbs, C. L. Edwards, Danny McFadden, and Y. Tateno*). The

* Damon Runyon Fellow from Chiba University, Chiba, Japan.

1027392

profile scanner is potentially useful in gathering whole-body retention data for internally administered radionuclides in tracer and therapeutic dose ranges. Further it could provide data on the retention by specific body sections (organs) from which we could determine turnover rates and biologic half-lives and also detect abnormal localization of a nuclide as an indicator of disease.

To use the profile scanner for these quantitative measurements, major modifications were introduced last year (USAEC Report ORAU-107). Since then the single channel analyzer section in the multichannel analyzer has been found to be unstable. This deficiency has been corrected by adding an external amplifier and a single channel analyzer to the system.

After all the changes in instrumentation, it was necessary to redetermine such basic performance factors as the range in which the increase in observed count is linear with respect to radioactivity

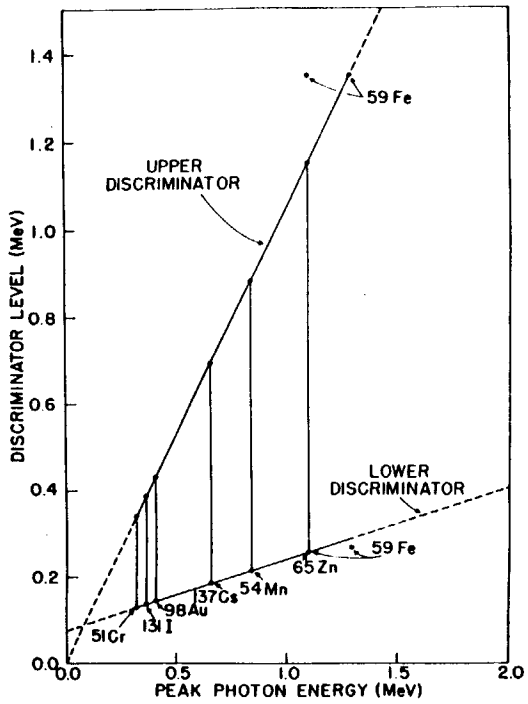

Fig. 57. Optimum windows determined for several radioisotopes showing the linear relation of upper and lower bounds to gamma-ray energy.

computer is the on-line monitoring and analysis of physiologic signals from patients undergoing protracted treatment in LETBI. We developed a program using Duncan's Multiple Range Test for analyzing the RR interval data for these patients.

Programs have been written for the receipt and analysis of clinical data such as scans, whole-body counts and their identifying data.

We anticipate that the new X-Y plotter and display scope will be of use in the collaborative work on scan analysis with the Oak Ridge National Laboratory Medical Instruments Group. These initial programs have long-range promise and are essential for developing a more adequate way to analyze the voluminous data from clinical research.

Preliminary engineering studies showed much promise for interfacing the Nuclear Chicago Pho-Gamma Camera to the IBM 1800 for contrast enhancement of scans. Preliminary test programs for this study are now completed.

Another programming task makes a detailed monthly analysis of operating costs comparing them with previously projected expenditures for the fiscal year; it provides quick reference indices indicating deviations from projected monthly and accumulated expenditures.

Interfacing of Instruments to Computer

The instrumentation department has continued to devise interfacings of the Medical Division's research instruments to the IBM 1800 computer: Packard Tri-Carbs, Beckman Analytrol, LETBI physiologic monitor, and the Nuclear-Chicago Pho-Gamma III Camera (T. R. Barclay and A. C. Morris, Jr.) The computer has an on-line capability whereby a remote research or clinical instrument, needing to transmit its data, may interrupt the normal off-line operation. When such a signal is received the computer automatically stops any operations in progress and transfers into memory storage (from its disk location) the program to service that particular interrupt. It then signals the instrument to send its data over interconnecting transmission lines, and on completion a signal indicating the finish of data exchange is sent to the originating instrument; the computer than reverts to its original work. The major types of computer functions used in interfacing a remote instrument are:

1. Digital Inputs (Switch contact closures or voltage pulses that act to signal the computer.)
2. Digital Outputs (Signals produced by the computer to affect an external control.)
3. Analog Inputs (Time-varying voltages and currents whose information content is carried by the amplitude, phase, or frequency components in the signal.)
4. Analog Outputs (Time-varying signals generated by the computer for the purpose of calibration, automatic standardization, comparison, proportional control, etc.)

Our objective has been to learn how to use these various functions to control and read data from remote equipment.

1027391

Last year we reported the first device that we interfaced -- a Beckman Analytrol film densitometer -- used for particle-size determinations with films from a research ultracentrifuge.

More recently we have worked on an interfacing system for the three Packard Tri-Carb liquid scintillation counters used in the lipid project at our Bethel Valley site 4 miles east of the computer facility. Our first attempts to complete the interface failed because the Data Set connection provided by the telephone company did not supply any means for delaying a Tri-Carb's readout sequence until our computer programs were ready. We are now driving four pairs of telephone lines, 4 miles long, directly between Bethel Valley and the computer. As each counter finishes a count it closes a relay contact producing a digital input closure to the computer. Simultaneously the interface provides an electrical "lock-out" preventing the other two counters from sending data until the first is through. A digital output signal from the computer starts the data transmission sequence. All digital input and output signals are released when the data transmission is completed so the computer can begin taking information from one of the other Tri-Carbs, or return to its off-line programming. The lock-out circuitry we designed, to assure that only one Tri-Carb can be sending data at a time, is fairly cumbersome so we do not plan to expand beyond a 4-machine capacity with this arrangement.

Thunderstorms last summer caused spurious interrupt signals to be generated in our long telephone-line link and destroyed some of the diodes in our matrix boards. We now avoid these difficulties with two approaches. First, we have replaced the 1N446 switching diodes in the matrix boards with 1N2484 power-type diodes that have better survival capabilities during lightning discharges. Second, we have installed 48-volt zener diodes from each telephone line wire to ground at both ends of our transmission line to limit the absolute value of voltage that can be induced. These measures have proved effective in reducing spurious interrupts and failures of components during thunderstorms. We have completed numerous successful runs with this interfacing design, many covering long sample runs with more than one scintillation counter operating.

Recently our staff has designed and begun constructing a faster version of the Tri-Carb interface using solid-state components. New circuits have been developed that use transistor switches, mercury relays, and diode-matrix information boards; moreover, solid-state circuits will automatically transmit the sample number and other experiment information. Our operating interface unit can transmit data from a Tri-Carb in 15 seconds. The new solid-state version will reduce this time to about 4 seconds -- the maximum speed being determined by how fast the long telephone lines can be made to respond to our pulse signals. Figure 56 shows a block diagram of the solid-state system.

This year we improved the system for interfacing physiologic monitor signals from the LETBI control room to the computer. We now can transmit signals both on-line, while the patient is being treated, and off-line with the use of data stored on 10½-in. reels of magnetic tape. At present we are able to automatically analyze two physiologic

Improving a Preamplifier

An improved red-cell-sizing preamplifier has been constructed for use in the Division's studies on normal and abnormal blood cell characteristics (A. C. Morris, Jr. and T. R. Barclay). This design marks the first time our engineers have used solid-state integrated circuits in a new development project. Two RCA type CA3030A operational amplifiers produce gain functions for the two stages of preamplification. The first stage is driven directly from the aperture electrodes and uses a noninverting circuit to give a gain $A_1 = 10$. This kind of circuit successfully removes the adverse effects of source impedance loading that are troublesome in some commercial versions. The second stage inverts the cell signals with a gain $A_2 = -10$. The combination of stages connected in cascade produces a gain $A_t = -100$ to drive a commercial amplifier and multichannel-analyzer system. Provisions are made for a pulser input on the pre-amplifier's front panel with a selection of three precalibrated pulse amplitudes. The operator can use these pulses to quickly assure proper equipment function before daily cell-sizing experiments begin. The operator can also use these precision pulses to check the overall linearity, zero-intercept, and amplification of the electronics system.

Our circuitry includes a constant-current supply providing a continuous range of aperture currents from 10 microamperes to more than 10 milliamperes. Such a wide span of currents lets us use large experimental changes in sizing-orifice geometry and variations in electrical field strength at the aperture. Two digital voltmeters mounted on the preamplifier instrument case (Fig. 59) give continuous indications of aperture current and voltage.

The electronic circuits for the new preamplifier, constant-current supply, and the aperture assembly are enclosed in a steel case of $\frac{1}{4}$-in. thickness, which serves as a magnetic shield to reduce 60-Hz interference from nearby transformers, motors, fluorescent lamps, and laboratory power-line circuits. Layers of Conetic and Netic* foils, has been glued to the interior of the preamplifier compartments to achieve a greater interference reduction for these more sensitive circuits. Access to the electrode assembly is through a hinged, $\frac{1}{4}$-in. steel door (Fig. 59). This door remains closed, completing the magnetic shield, when cell-sizing operations are under way.

One of our summer employees, Mr. Eugene Culver, a mechanical engineering student from Georgia Tech, worked this past summer toward modifying the electrode assembly and installing it in the instrument case. He also worked to produce a better vacuum and plumbing system for use with this equipment. His work was instrumental in bringing this cell-sizing preamplifier system to completion.

Our current evaluation of this new instrument includes electronic tests for linearity, zero-intercept, noise, resolution, stability, and interference reduction. Additional studies are being made with both fresh and chemically fixed red cells from animals and human sources.

---

* Perfection Mica Co., Bensenville, Ill.

1027394

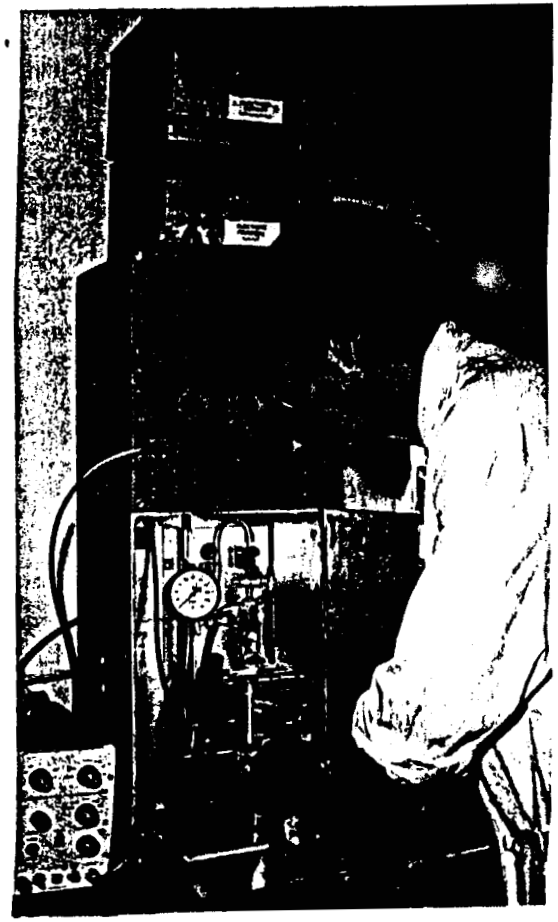

Fig. 59. Integrated-circuit preamplifier for cell-sizing studies in operation.

An evaluation of these data is being expedited with the use of analytical programs in the IBM 1800 computer.

Whole-Body Counter for Animals

Several years ago a small instrument was constructed for counting mice, rats, and for radioassaying gross biologic tissue samples. More recently the need has developed for a similar counter, only larger, for such animals as rabbits, small dogs, guinea pigs, etc., and we have designed and built a suitable instrument for this purpose (A. C. Morris, Jr.). We used two 12.5 cm diameter x 5 cm thick

and the isoresponse pattern of the detector system. Experiments were conducted with point sources of ^{131}I and ^{137}Cs and we found that observed count was linear with respect to activity up to 300,000 counts/min. Above this rate the response rapidly departs from linear, and at a counting rate of 10^6 counts/min the counting loss is 20%. If all 12 detectors are used, even with minimum collimator openings (0.5 cm), the maximum counting rate constraint would not allow profile scanning of patients with more than 2 to 5 millicuries of radioactivity (depending on distribution and the decay scheme of the radionuclide). Consequently we measured the isoresponse pattern of the instrument using only the two outer detectors of both the upper and lower sets and compared it to the isoresponse pattern with all 12 detectors. The uniformity of response was not significantly altered. There was a 5% decrease in counts at a distance of 30 cm off the midline laterally, and a 5% increase 15 cm off the midline vertically. Thus, the sensitivity can be reduced by a factor of 3 without significantly altering the geometric response, thereby extending the linear response range to allow scanning doses of 6 to 15 millicuries. We have determined that most accurate quantitation is achieved in whole-body counting by counting a band in the gamma-ray spectrum other than the photopeak band (USAEC Report ORAU-107). The experimental procedures for determining the "minimum error window" (MEW) for whole-body counting were repeated for the profile scanner to determine the MEW for ^{51}Cr, ^{131}I, ^{198}Au, ^{137}Cs, ^{54}Mn, ^{65}Zn, and ^{59}Fe. Figure 57 shows the results obtained for this instrument. The pattern of upper and lower discriminator settings is similar to that obtained with the low-level whole-body counter. For monoenergetic or nearly monoenergetic gamma-ray emitters there is a linear relation between gamma-ray energy and discriminator settings. All MEW's include the photopeak plus some scattered radiation. Experiments now under way suggest that the resolution of the profile scan will be satisfactory even when the MEW is used, despite the scattered radiation.

A system for computer storage and retrieval of digital scan data and patient identification has been developed. The storage program places on magnetic tape patient identification, anatomic landmarks, radionuclide, size of dose, date and hour of dose, and the digital data for each scan. Subsequently all data on a patient may be retrieved and analyzed to compute the whole-body retention or the retention in selected body sections. The computer analysis program will plot the activity profile scan as a histogram with the computer printer. Figure 58 shows a histogram (A) and the usual photographic record (B) for comparison.

1027393

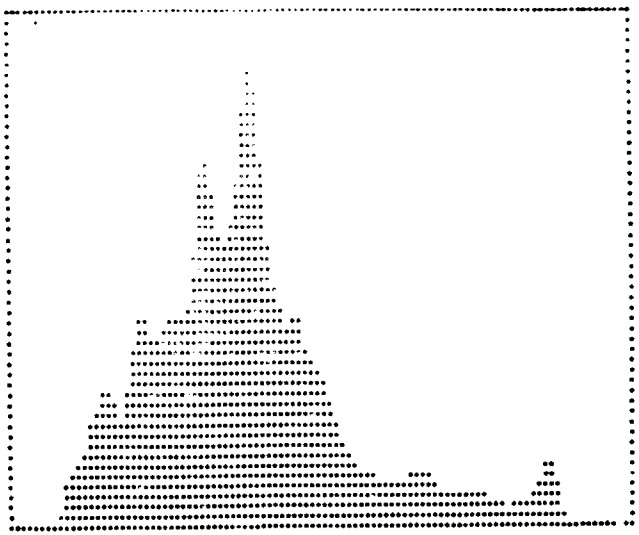

Fig. 58. (A) Computer print-out of linear scan of a patient 24 hr after administration of ^{67}Ga.

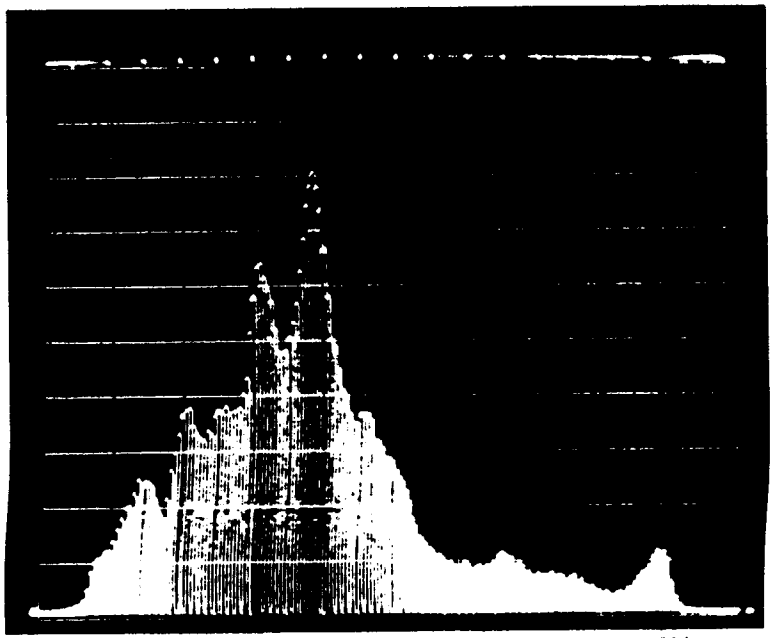

Fig. 58. (B) Photographic record of linear scan shown in Fig. 58A.

BASIC STUDIES RELATED TO RADIATION, NEOPLASIA, AND METABOLISM

BIOLOGICAL CHEMISTRY

During 1969, the biological chemistry research program dealt primarily with lipid characteristics of neoplastic and normal cells, metabolic studies of ether-linked lipids, and biochemical features of membranes.

Our efforts in these areas of research reflect not only those of individuals from our own group (M. L. Blank, E. Cress, P-O Hagen, R. D. Harlow, K. Healy, T-c Lee, B. Malone, A. Moehl, F. Snyder, J. Soodsma, N. Stephens, R. Wood, and R. Wykle) but also collaborative studies with staff members of Oak Ridge National Laboratory and several universities. (See publications list and list of consultants.)

This chapter includes brief reports of some of our published studies done during 1969 and not adequately covered in last year's report; summaries of the "in press" articles are not included. No attempt has been made to relate our findings to the publications of others outside our organization in these areas of research. The details of the rationale, results, and conclusions discussed and how they relate to other published work can be obtained from the published and in press references cited.

Auxiliary research projects included developments in lipid methodology (chromatography and liquid scintillation spectrometry) (3, 5, 2, 25, 33, 39, 40, and 45), studies on the lipids of insects (14, 43), research on the minor lipids of Clostridium butyricum (a species rich in plasmalogens) (108), and correlative biochemical and morphological studies of inclusion bodies found in mitochondria (92). Moreover, a number of reviews dealing with these areas of research have been written during the past year on ether-linked lipids (54, 95, 91), on the biochemistry of lipids in neoplastic cells (111), and on radiochromatography (28, 96, and 94).

Our group's interest in the ether-linked lipids began in 1962 when we first found "free" glyceryl ethers in irradiated bone marrow (Radiation Res 19, 129, 1963). At that time, the possible significance of these "free" glyceryl ethers in marrow was thought to be related to their radioprotective effects since Brohult (Acta Radiol Suppl 223, 99p, 1963) and others had reported that glyceryl ethers administered to humans and animals exposed to irradiation prevented the leukopenia that normally occurs under such conditions. At about the same time in related studies, we had also discovered a class of lipids in human and animal tumor cells that had identical chromatographic properties to those of diacyl glyceryl ethers. Further work with these compounds led to their complete characterization and to the elucidation of their biosynthetic pathway.

The role that ether-linked lipids play in living cells is not known, although those that exist as phospholipids appear to be important

1027396

structural components of membranes. On the other hand, the high levels of diacyl glyceryl ethers in neoplastic cells might simply reflect the extreme "reductive" state of tumor cells since the formation of fatty alcohols (from fatty acids) and of glyceryl ethers requires hydrogen transfer reactions via nicotinamide adenine diphosphate (NADPH). Such reactions provide a mechanism for oxidizing NADPH at the substrate level.

Lipid Characteristics of Neoplastic Cells

Glyceryl ethers appear to be closely associated with neoplasia and cell transformation. Our continuing studies (55, 30, 35, 46, 44, 42, 1, 112, 29, and 83) of lipids in a wide variety of normal and neoplastic cells have demonstrated high levels of ether lipids, primarily diacyl glyceryl ethers, in many spontaneous and transplantable tumors (including those of viral origin and some chemically induced). There does not appear to be any accumulation of the diacyl glyceryl ethers during rapid cellular proliferation (pouch granulomas, regenerating liver, or embryonic tissues), or in normal tissues.

The alkyl and alk-1-enyl hydrocarbon chains linked to glycerol by an ether bond have a characteristic pattern in all lipid classes of the neoplasms examined and differ significantly from the acyl chains. Both the O-alkyl and O-alk-1-enyl moieties of normal and neoplastic cells consisted mainly of 16:0, 18:0, and 18:1 O-hydrocarbon chains. Fibroblasts (L-M cells) tend to accumulate ether-linked lipids when grown in suspension cultures and these systems appear useful for investigating regulatory factors in the distribution of acyl, alkyl, and alk-1-enyl moieties in glycerolipids. During the course of our experiments with ether-linked lipids, we found an inverse relation of cholesteryl esters and triglycerides in the blood of tumor-bearing animals (106) that suggests that neoplastic growth in some way alters the biosynthesis of low-density lipoproteins in host livers. Some experiments were carried out to identify species of cholesteryl esters (major acyl moieties 16:0, 18:1, 18:2, 20:4, and 22:6) in Ehrlich ascites cells (104).

The structure of rat liver phosphoglycerides has been analyzed (Randall Wood and R. D. Harlow). The distribution of fatty acids esterified at each position of glycerol in phosphatidyl serine (PS), phosphatidyl inositol (PI), and diphosphatidyl glycerol (DPG) and the composition of sphingomyelin (SPH), lysophosphatidyl choline, and free ceramides isolated from rat liver was determined. The carbon number distribution of the diglyceride acetates derived from each of the phosphoglycerides and of the ceramide trimethylsilyl ether derivatives was also determined. The rat liver SPH contained a high percentage of long-chain saturated and monounsaturated acids. The carbon number distribution of free ceramides and those derived from SPH was similar.

Each of the phosphatides exhibited a characteristic acyl distribution and diglyceride carbon-number distribution. The 1-position of PS and PI contained almost exclusively (> 90%) stearic acid. Unlike the other phosphatides, DPG contained primarily C-18 acids and a high percentage of the major acid, 18:2, was esterified at the 1-position. The di-

NaI (T1) crystals spaced 220 cm apart and shielded with lead plates 3.2 cm thick. Our design has the axis of the crystals horizontal, letting each half-section of the lead shield expand toward the central counting chamber (Fig. 60). A $\frac{1}{2}$-in. thick steel plate supports and helps distribute the weight of the 3,000 pound shield. Short steel sheets around the sides and top give scatter compensation. This arrangement provides a sample-counting volume measuring 40 cm high by 25 cm wide by 55 cm deep in the center of the shield (Fig. 61). High voltage power for the detectors comes from a single regulated supply run through a voltage-division network so the gain of each photomultiplier assembly may be independently peaked. Pulses from both detectors are combined in one preamplifier and are then processed by a spectrometer system. An evaluation of the geometric response within the sample-counting volume and determinations of proper spectrometer window settings for an isotropic counting response are now under way for radionuclides in common use.

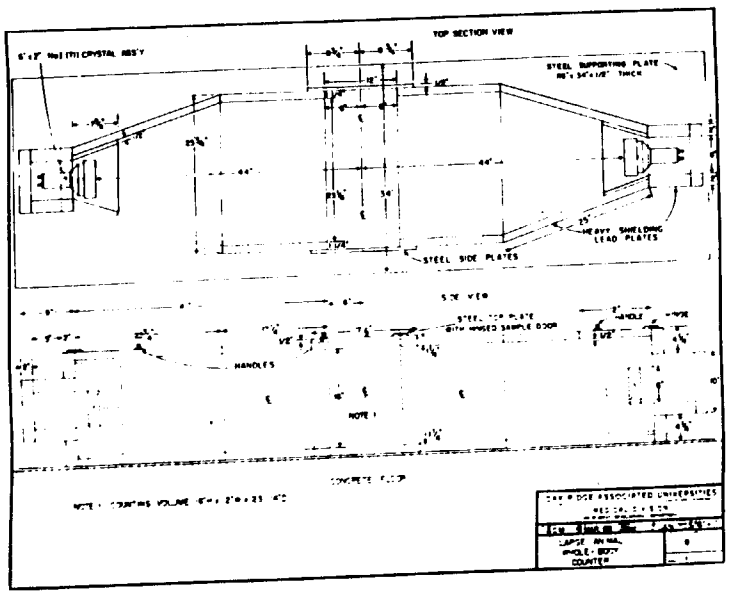

Fig. 60. Design of shield for the large animal whole-body counter.

1027395

Fig. 61. Animal being introduced into sample compartment of whole-body counter.

glycerides derived from PI and DPG had or approached a 1-random-2-random distribution, whereas those of PS showed pairing of certain acids. The data indicate that selectivity of diglyceride species characterizing each phosphoglyceride class occurs in rat liver. None of the carbon-number distributions of the diglycerides derived from each of the phosphoglycerides resembled the 1,2-diglycerides obtained from rat liver triglycerides. (See Reference 112).

Metabolic Studies of Ether-Linked Lipids in Cell-Free Systems

In October 1968 we found a new microsomal enzyme system that synthesizes O-alkyl bonds (32), and which has since become the focus of our research effort (31, 99, 36, 47, 98, 97, 78, 100, 114, and 107). The sequence of reactions studied is depicted in Fig. 62. We have identified (97) labeled O-alkyldihydroxyacetone-P, O-alkyldihydroxyacetone, and O-alkyl-acyl-glycerophosphate (suggested as intermediates in this system in our initial studies). Although the exact nature of the initial reaction between fatty alcohols and the dihydroxyacetone-P is not known, we have not excluded that dihydroxyacetone-P is simply required for attachment to the enzyme, after which the aldehyde is formed for reaction with the fatty alcohol as we originally proposed. Other possible reaction mechanisms for the initial step include the formation of CoA intermediates (98). Kinetic data on the following factors have been obtained: time, CoA, Mg^{++}, ATP, protein, pH, and triose-P isomerase inhibitors (phosphate, and 1-hydroxy-3-chloro-2-propanone phosphate). This project is now concerned with elucidation of the precise enzymatic mechanisms responsible for the biosynthesis of alkyl and alk-1-enyl glyceryl ether lipids of normal and neoplastic cells. Our studies on the

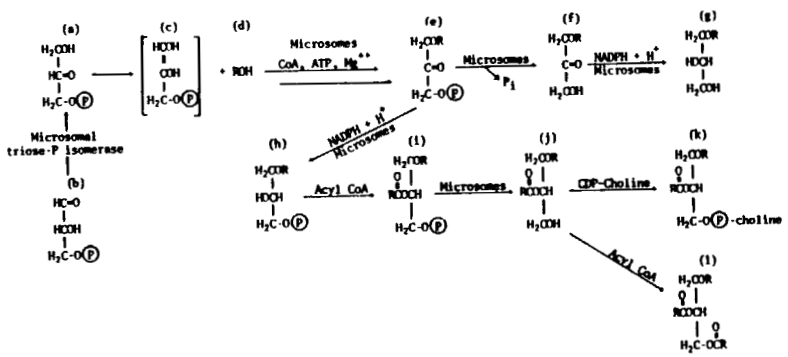

Fig. 62. Biosynthesis of O-alkyl lipids. The compounds depicted in the scheme are (a) dihydroxyacetone-P, (b) O-glyceraldehyde-3-P, (c) enol-form of compounds [(a) and (b)], (d) long-chain fatty alcohol, (e) O-alkyldihydroxyacetone-P, (f) O-alkyldihydroxyacetone, (g) O-alkylglycerol, (h) O-alkylglycerol-P, (i) O-alkyl analogue of phosphatidic acid, (j) 1-O-alkyl-2-acyl glycerol, (k) O-alkyl choline phosphoglyceride, and (l) diacyl glyceryl ether.

1027397

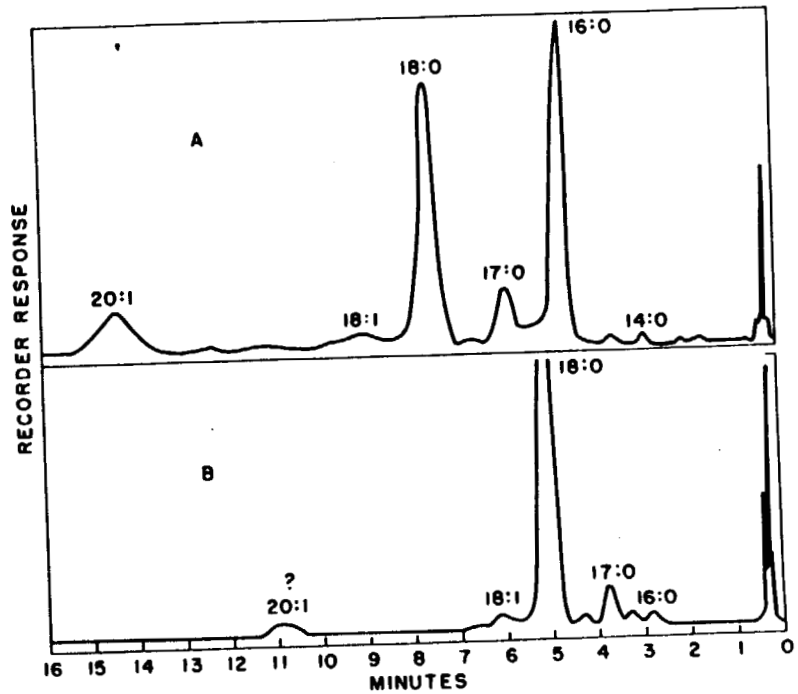

Fig. 63. Gas-liquid chromatograms showing the resolution of the isopropylidene derivatives of alkyl glyceryl ethers (upper tracing, A) and intact fatty aldehydes (bottom tracing, B) derived from alk-1-enyl glyceryl ethers. A liquid phase of EGSS-X was used to resolve the isopropylidene derivatives at 200°, and the intact aldehydes at 170°. Only the isopropylidene derivatives of the alkyl glyceryl ethers contained ^{14}C; two separate samples (90 and 180 min after incubations of the 16:0 fatty alcohol) chromatographed under these conditions had 92 and 90% of the activity associated with the isopropylidene derivative of the 16:0 glyceryl ether (chimyl alcohol). The glyceryl ethers used for these analyses were isolated from total lipids of microsomes of the digestive gland of the starfish.

biocleavage of O-alkylglycerols in neoplastic cells have indicated that such cells have lost their ability to metabolically break down the ether bond (93). The cancer cells seem to have lost the function of an essential component of the cleavage system through genetic aberration perhaps involving the loss of a specific enzyme protein.

We have also examined the biosynthesis of alkyl glyceryl ethers by microsomal enzymes of digestive glands and gonads of the starfish, Asterias forbesi (Fred Snyder, Boyd Malone, and M. L. Blank). A microsomal enzyme system that can synthesize alkyl ether linkages

in glycerolipids has been isolated from the digestive glands and gonads of the starfish Asterias forbesi. The total lipids of the microsomes from the digestive glands contain approximately 4.5% alkyl glyceryl ethers and 5.5% alk-1-enyl glyceryl ethers. Figure 63 shows that the chain lengths of alkyl moieties consist of 16:0 (31%), 18:0 (39%), and 20:1 (13%), whereas the chain lengths of the alk-1-enyl moieties consist mainly of 18:0 (79%).

The biosynthetic system for alkyl ethers utilizes long-chain fatty alcohols and glyceraldehyde-3-phosphate as substrates and ATP, CoA, and Mg^{++} as cofactors. The time course for the reaction is linear for at least 90 min (Fig. 64), and the products produced have chromatographic properties identical to those we have found in microsomes from neoplastic cells. No alk-1-enyl glyceryl ethers are formed in this

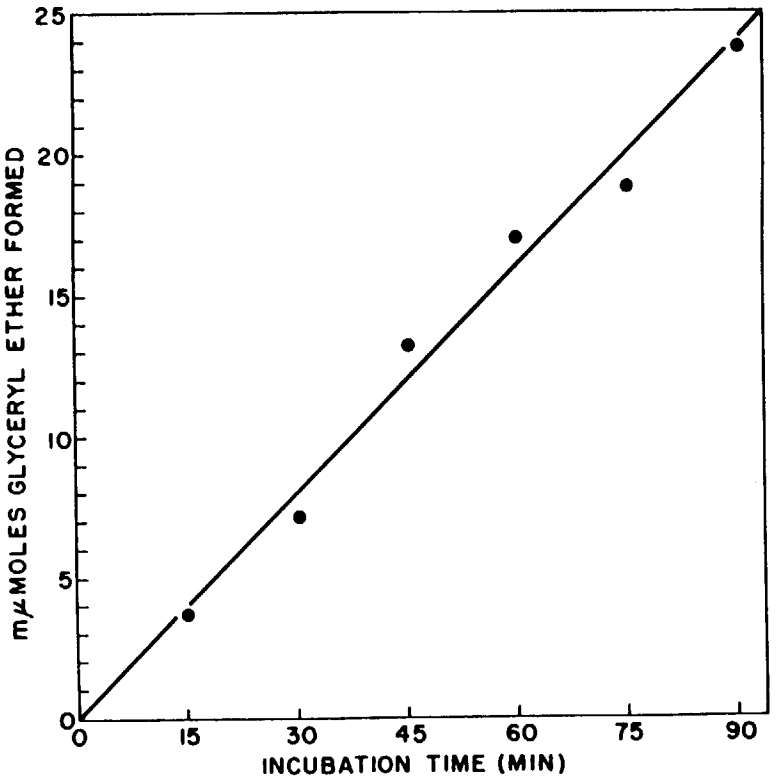

Fig. 64. Incorporation of [1-^{14}C]cetyl alcohol into O-alkylglycerols of total lipids (after $LiAlH_4$ reduction) by an ether synthesizing enzyme complex in microsomes from the digestive gland of starfish. Each value is the mean of duplicate incubations.

1027398

system, Gas-liquid chromatography of the ^{14}C-labeled O-alkylglycerol isopropylidene derivatives (prepared after $LiAlH_4$ reduction of total lipids) revealed that approximately 90% of the ^{14}C was associated with the $C_{16:0}$ glyceryl ether fraction after incubation of ^{14}C labeled $C_{16:0}$ fatty alcohol. The role of the cofactors in this reaction is not yet known. The initial reaction mechanism is poorly understood because of the presence of a microsomal triose isomerase in most preparations tested. (See Reference 31).

We have studied the source of glycerol for the biosynthesis of alkyl glyceryl ethers (Robert L. Wykle and Fred Snyder). In this work we used a specific inhibitor (1-hydroxy-3-chloro-2-propanone phosphate) to distinguish between glyceraldehyde-3-P and dihydroxyacetone-P as the glycerol source of alkyl glyceryl ethers. Only dihydroxyacetone-P reacted with fatty alcohols in the presence of the inhibitor and microsomes from preputial gland tumors to produce the O-alkyl linkage (CoA, ATP, and Mg^{++} are essential cofactors). The products formed have chromatographic properties consistent with the reaction sequence we proposed in an earlier paper.

The data in Fig. 65 (B and C) demonstrate the presence of triose-P isomerase and the absence of glycerophosphate dehydrogenase (Fig. 65-D) in microsomal preparations of the preputial gland tumors washed as many as three times. Figure 65-A illustrates similar measurements made on preparations of commercial triose-P isomerase and glycerophosphate dehydrogenase. The slight slope in the initial O.D. curves in parts C and D of Fig. 65 indicates that there is a slow oxidation of NADH by the microsomes unrelated to the reduction of dihydroxyacetone-P. Although glycerophosphate dehydrogenase was absent from the microsomes, we could not remove the isomerase by zonal centrifugation or by passing the microsomes through Sephadex G-200 columns. Both DL-glyceraldehyde-3-P and dihydroxyacetone-P served equally well as the glycerol source in the biosynthesis of alkyl glyceryl ethers in the microsomal preparations (Table 34).

The halogenated dihydroxyacetone-P (0.4 μmoles per vial) completely inhibited the triose-P isomerase activity (Fig. 65-C) in the microsomal preparations as originally documented by Hartman for triose-P isomerase isolated from rabbit muscle (Biochem Biophys Res Commun 33, 888, 1968). Our microsomal preparation containing added α-glycerophosphate dehydrogenase rapidly converted dihydroxyacetone-P to glycerophosphate in the presence of the inhibitor (Fig. 65-C), indicating that the inhibitor did not affect α-glycerophosphate dehydrogenase activity. The data in Table 34 show that both dihydroxyacetone-P and DL-glyceraldehyde-3-P, with ^{14}C-hexadecanol, produced alkyl glyceryl ethers in the presence of microsomes, CoA, ATP, and Mg^{++}, but only the dihydroxyacetone-P served as the glycerol source in the presence of the inhibitor. (See Reference 47).

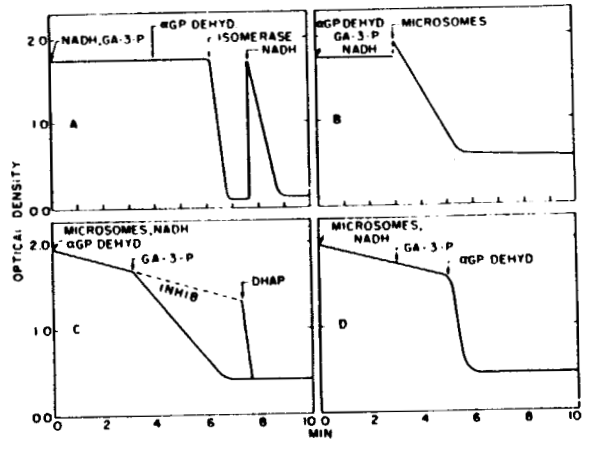

Fig. 65. The presence of triose-P isomerase in microsomes from preputial gland tumors. The components added to the assay mixture (3ml) were as follows: 5 μmoles DL-glyceraldehyde-3-P (GA-3-P); 5 μmoles dihydroxyacetone-P (DHAP); 1 μmole NADH; microsomes, washed 3 times, containing approximately 0.2 mg protein (similar results were obtained using microsomes washed 5 times); 300 μmoles potassium phosphate buffer, pH 7.1; 0.4 μmole 1-hydroxy-3-chloro-2-propanone phosphate (Inhib.); approximately 40 μg α-glycerophosphate dehydrogenase (αGP Dehyd.); and approximately 10 μg triose-P isomerase with commercially available enzymes. Part B demonstrates the presence of a microsomal triose-P isomerase. Part C demonstrates that the microsomes oxidize NADH at a slow rate in the absence of glyceraldehyde-3-P and that the chlorine derivative of dihydroxyacetone-P completely inhibits the microsomal triose-P isomerase. Part D shows that αGP dehydrogenase was absent from the washed microsomes and suggests that the triose-P isomerase in microsomes is not simply contamination from the soluble fraction.

Metabolic Studies of Ether-Linked Lipids in Intact Cells

Recent work with 1-^{14}C, 1-^{3}H-labeled hexadecanol revealed that alcohols were incorporated better than acids into the O-alkyl chains of various lipid classes in Ehrlich ascites cells (105). In addition, the data (105) also showed that radioactivity of the fatty alcohols was incorporated into plasmalogens with the appropriate loss of tritium from the doubly labeled fatty alcohol. Similar labeling patterns, but much higher rates of incorporation, were obtained with the doubly labeled hexadecanol in the ascites cells grown in suspension cultures (113). Additional in vivo data (107) obtained from Ehrlich ascites cells demonstrated that 1-^{14}C-alkyl-2-^{3}H-glyceryl ethers were directly converted to plasmalogens having a $^{14}C/^{3}H$ ratio identical to that of the glyceryl ether used as a precursor. In these studies, a glyceryl ether having a substituent

1027399

on the O-alkyl moiety was isolated. The nature of this O-alkyl substituted glyceryl ether is not yet fully characterized, but it forms derivatives similar to those of a chemically synthesized β-hydroxy-O-alkyl glyceryl ether. Other in vivo experiments have demonstrated that S-ether analogues of glyceryl ethers are completely different in behavior from the O-ethers; orally administered S-ethers are eliminated primarily in in the urine (34).

Biochemical Features of Membranes

Knowledge of the composition of mammalian cell membranes has been limited because of the difficulty in preparing pure material. Until the last decade, it was limited to data concerning myelin and the erythrocyte, which may be poor models for mammalian cells. We need better information in order to understand the mechanism of assembly and the dynamic function of membranes. Studies of model membranes and experiences with enzyme reconstitution have already illustrated the vital role and specificity of lipids in the functional properties of biomembranes. During 1969, our group investigated some aspects of the biochemistry of membranes isolated from cell surfaces (9) and from the endoplasmic reticulum (19). Our experiments have indicated that significant differences occur in the distribution of smooth and rough endoplasmic

TABLE 34

The Effect of 1-Hydroxy-3-Chloro-2-Propanone Phosphate on the Biosynthesis of Alkyl Ether Bonds in Lipids from Dihydroxyacetone Phosphate and DL-Glyceraldehyde-3-Phosphate by Microsomes of Preputial Gland Tumors

System	Glycerol Source: GA-3-P 5 μmoles	Glycerol Source: DHAP 5 μmoles	Inhibitor* 0.4 μmoles	Incorporation of 1-^{14}C-cetyl alcohol into O-alkylglycerols† % ^{14}C: Exp. 1	Exp. 2
1. Complete‡	+	-	-	23	30
2. Complete	-	+	-	24	30
3. Complete	+	-	+	3	3
4. Complete	-	+	+	25	28
5. Complete except microsomes were boiled 15 min	+	+	+	1	1

*Before adding other components of the complete system, each vial of microsomes was preincubated in the presence or absence of 1-hydroxy-3-chloro-2-propanone phosphate for 15 min at 37°C in 2 ml of 0.1 M phosphate buffer (pH 7.1). The complete system was then incubated for 1 hr at 37°C.

†O-Alkylglycerols were liberated from total lipid by $LiAlH_4$ reduction and verified by gas-liquid chromatography of the isopropylidene derivatives of the glyceryl ethers.

‡Each vial contained 30 μmoles ATP, 0.3 μmole CoA, 13 μmoles Mg^{++}, 1 mg microsomes (washed 3 times), and 100 mμmoles 1-^{14}C-cetyl alcohol in a final volume of 3 ml of 0.1 M phosphate buffer (pH 7.1).

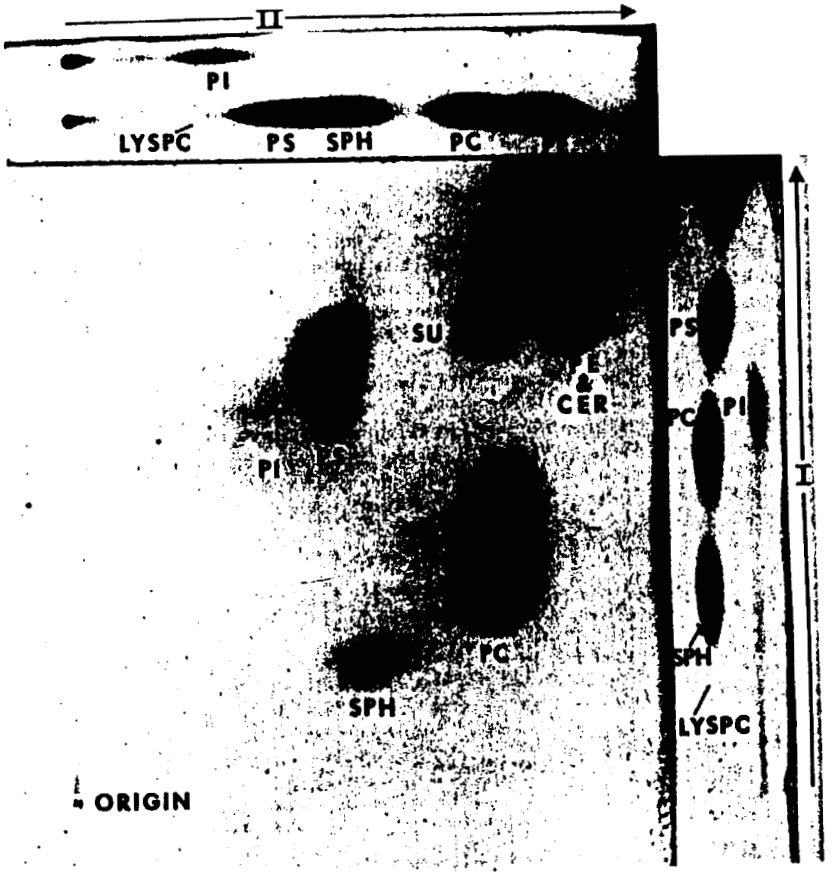

Fig. 66. Two-dimensional thin-layer chromatograms of total lipids from whole brain (above) and synaptic plasma membranes (next page). The abbreviations refer to the following lipid classes: PC, phosphatidylcholine; PE, phosphatidylethanolamine; PS, phosphatidylserine; SPH, sphingomyelin; LYSPC, lysophosphatidylcholine; CER, ceramide; SU, sulfatides; X_1 and X_2 are unidentified lipids. The solvent system for direction I was $CHCl_3$-MeOH-HAc-H_2O (50:25:8:4, v/v) and the solvent system for direction II was CH_3Cl_3-MeOH-NH_4OH (65:35:8; v/v). The 250-μ adsorbent layer was Silica Gel HR.

reticulum between normal and neoplastic cells (110). Enzymic function and structural components are being correlated with the type of endoplasmic reticulum (109).

1027400

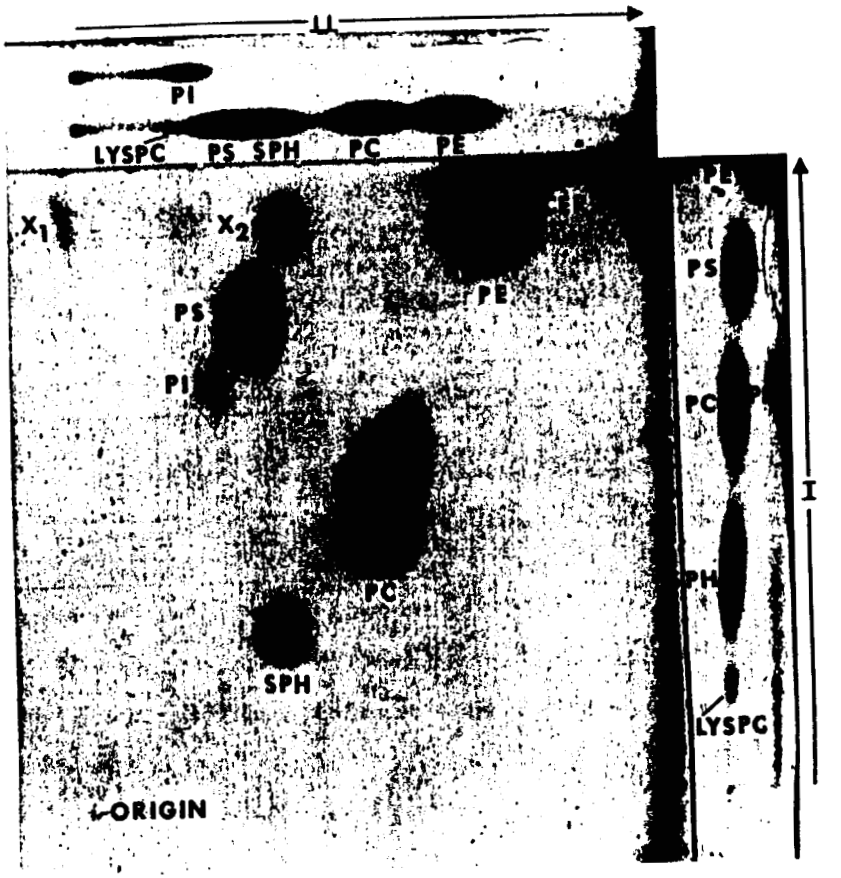

A plasma membrane fraction derived from rat-brain nerve endings or the synaptic plasma membrane fraction, isolated by zonal centrifugation, was analyzed for its lipid content and the composition of its lipid classes and their aliphatic moieties (Carl Cotman*, M. L. Blank, Anita Moehl, and Fred Snyder). With the exception of glycolipids and sphingomyelin, the lipid classes of synaptic plasma membrane are very similar to whole brain (Fig. 66). Phosphatidylcholine and phosphatidylethanolamine are the major lipids and make up 62% of the total membrane lipid. Cholesterol and ceramide make up the

* ORNL MAN Program.

major neutral lipids and 21% of total brain lipid. The synaptic plasma membranes contain lower quantities of glyceryl ethers in phosphatidylethanolamine and phosphatidylcholine fractions than in whole brain (Table 35). Certain distinctive features in fatty acid content were found (Table 36); synaptic plasma membranes contained much less 18:1 acyl moieties in phosphatidylethanolamine and phosphatidylserine

TABLE 35

Quantity of Glyceryl Ethers in PE and PC Lipid Fractions of Whole Brains and SPM of Rats.*

	Alk-1-enyl Glyceryl Ether		Alkyl Glyceryl Ether	
	SPM	Whole Brain	SPM	Whole Brain
PE	[illegible]	[illegible]	[illegible]	[illegible]
PC	[illegible]	[illegible]	[illegible]	[illegible]

* Expressed as weight percentage of each class based on the total alkyl and alk-1-enyl glyceryl ethers liberated by $LiAlH_4$ reduction (multiply each value by 2 for an approximation of percentage of intact phosphoglycerides).

TABLE 36

Composition of Acyl Chains (weight per cent) in Phospholipids of Synaptic Membranes and Whole Brain of Rats.

Designation of Side Chain	Acyl Moieties					
	Synaptosomes PE	Whole Brain PE	Synaptosomes PS + PI	Whole Brain PS + PI	Synaptosomes PC	Whole Brain PC
16:0	7.5	5.8	3.6	3.5	50.7	39.5
16:1	0.3	0.3	0.3	0.3	1.0	1.2
17:0	0.4	0.1	0.2	0.1	0.2	0.6
18:0	23.7	19.4	40.8	36.2	12.6	14.0
18:1	6.6	19.6	7.2	19.7	24.2	28.8
18:2	0.2	0.5	Trace	0.2	0.6	0.9
20:0	Trace	0.2	Trace	0.2	Trace	0.4
18:3	0.4	4.3	Trace	2.4	1.0	1.9
20:3	0.3	0.6	Trace	0.9	0.1	0.3
20:4	19.0	15.2	10.0	12.3	5.6	6.8
22:A*	5.4	[illegible]	3.9	2.5	0.9	0.4
22:B*	1.5	[illegible]	2.0	1.1	Trace	0.5
22:C*	Trace	Trace	Trace	Trace	Trace	Trace
22:6	32.9	25.7	32.2	19.6	3.4	4.6

* A, B, and C for the 22 carbon chain are thought to contain four, five, and five double bonds, on the basis of retention time and gas-liquid chromatography analysis of identical sample after hydrogenation. The values represent mean values of two separate brain preparations; the maximum range in variation observed between duplicate samples of the acyl moieties was 2%.

plus phosphatidylinositol than found in whole brain, whereas most other acyl moieties with the exception of the longer chain unsaturated fatty acids are similar. The 22:6 acyl chains in synaptic plasma membranes account for approximately 32% of the total fatty acids in phosphatidylethanolamine and phosphatidylserine plus phosphatidylinositol, but in whole brain the 22:6 fatty acids account for only about 26 and 20% of phosphatidylethanolamine and phosphatidylserine plus phosphatidylinositol, respectively. The alk-1-enyl moieties in phosphatidylethanolamine (Table 37) are restricted to 16:0, 18:0, and 18:1 chain lengths in both synaptic plasma membranes and whole brain. (See Reference 6.)

1027401

TABLE 37

Composition of Alkyl and Alk-1-enyl Glyceryl Ether Side Chains.

Designation of Side Chain	Alk-1-enyl Moieties*		Alkyl Moieties*	
	Synaptosomes (PE)	Whole Brain (PE)	Whole Brain (PC)	Whole Brain (PE)
16:0	29.8	22.6	52.5	37.0
16:1			1.5	0.5
17:0	1.0	1.0	0.8	0.8
18:0	54.2	51.2	13.3	29.7
18:1	15.5	24.9	32.9	32.0
18:2 + 19:0	0.6	0.2	1.5	Trace
20:0	0.4	0.2	Trace	Trace
18:3 + 20:1	0.5	0.2	Trace	Trace

* The values represent mean values of two separate brain preparations. The average variation between duplicate samples for the three major chain lengths was 3.1%. * The values represent an analysis on single samples of brain preparations.

A study of the microsomes of rat liver has been made with the zonal centrifuge and resolution of rough- and smooth-surfaced membranes has been achieved (Ten-ching Lee, D. C. Swartzendruber, and Fred Snyder). The microsomal fraction of rat liver consists of free ribosomes and smooth- and rough-surfaced vesicles that are derived from fragmentation of the endoplasmic reticulum. Two methods, based on differences in density and sedimentation rate, have been used to subfractionate microsomes from rat liver into predominantly smooth- and rough-surfaced fractions (Acta Path Microbiol Scand Suppl 166, 1, 1963). However, both methods have been hampered by the small capacities of commercially available high-speed centrifuge rotors, difficulties in maintaining gradient stability during acceleration and deceleration, and problems in loading the gradient and the sample. The development of the zonal ultracentrifuge system (Science 154, 103, 1966) has largely overcome these difficulties and we developed a zonal centrifugation procedure that separates the different elements of the microsomal fraction in a B-XXIX zonal rotor. The method is described in the published paper (94).

Results of a typical experiment in which the rat liver postmitochondrial supernatant was subjected to zonal centrifugation in a B-XXIX rotor for 2 hr at 25,000 rpm are shown in Fig. 67. This procedure separated the original supernatant into three protein fractions as indicated by the UV absorption peaks at 280 mμ. Electron microscopy disclosed that Fraction II contained mostly smooth-surfaced vesicles with some contamination of free ribosomes, whereas Fraction III consisted mainly of rough-surfaced vesicles. The majority of free ribosomes were found in the higher density region of the soluble phase

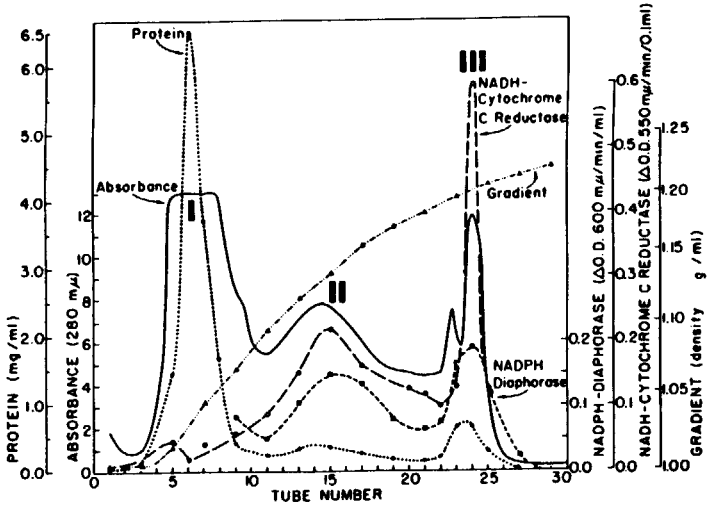

Fig. 67. Zonal profile of absorbance, density, protein, NADH-cytochrome c reductase, and NADPH diaphorase from rat liver postmitochondrial fraction. Centrifugation was to 5 x 10^{10} $\omega^2 t$ (25,000 rpm, 2 hr, B-XXIX rotor). Fraction I represents soluble proteins, Fraction II represents smooth microsomes, and Fraction III represents rough microsomes.

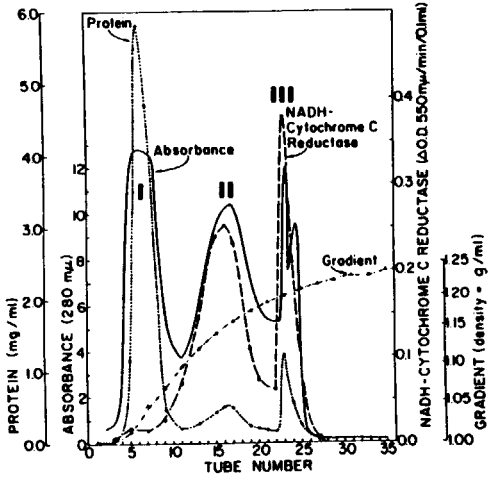

Fig. 68. Zonal profile of absorbance, density, protein, and NADH-cytochrome c reductase obtained for postmitochondrial fraction of liver from phenobarbital-treated rat. The experimental animals received daily intraperitoneal injections of 9 mg of sodium phenobarbital 100 g body weight for 2 days. Fraction I represents soluble proteins, Fraction II represents smooth microsomes, and Fraction III represents rough microsomes.

1027402

TABLE 38

PROTEIN, PHOSPHOLIPID, AND RNA CONTENT IN SUBMICROSOMAL FRACTIONS PREPARED BY ZONAL CENTRIFUGATION

	Smooth-Surfaced Microsomes	Rough-Surfaced Microsomes
Tube Number	11-21	22-27
Protein*	12.1	11.6
mg/g liver	(11.6, 12.1, 12.5)	(10.5, 11.5, 12.7)
RNA†	3.57	2.87
mg/g liver	(3.50, 3.64)	(2.67, 3.07)
mg/mg protein	0.29	0.24
Phospholipid†	4.65	3.26
mg/g liver	(4.72, 4.58)	(3.22, 3.30)
mg/mg protein	0.38	0.28

* Average of three experiments. Protein ratio of smooth-surfaced microsomal fraction to rough-surfaced microsomal fraction is 1.04.

† Average of two experiments.

whereas the ratio was 1.04 for the microsomal fractions derived from normal liver. Phenobarbital treatment causes the proliferation of smooth endoplasmic reticulum in rat liver (J Cell Biol 31, 243, 1966) and the zonal profile, Fig. 68, Fraction II, plainly reflects this fact.

Our experiments demonstrate that zonal centrifugation subfractionates the microsomal components of rat liver into smooth- and rough-surfaced forms. This system not only offers high capacity and good resolution, but also makes it possible to visualize the distribution of the elements present in the microsomal fraction of a cell as a continuous spectrum of subcellular particles. (See Reference 19.)

(Fraction I). The peaks consisting of smooth- and rough-surfaced vesicles were further characterized by NADH-cytochrome c reductase and NADPH diaphorase activities. The protein, phospholipid, and RNA contents of the two submicrosomal fractions are listed in Table 38. Protein was equally distributed in the two subfractions, but phospholipids were higher in the fraction containing smooth-surfaced vesicles. The high concentration of RNA in this fraction may be explained by the contamination with free ribosomes.

The zonal profile of the postmitochondrial fraction of livers from phenobarbital-treated rats is shown in Fig. 68. The protein ratio between smooth- and rough-surfaced membrane fractions was 1.46,

The Medical Division maintains one of the few research colonies of marmosets in the United States. This small New World primate of the family Callithricidae, has a high incidence of fraternal twinning and placental vascular anastomoses between the fetuses. Studies in our laboratory with colony-bred marmosets have shown hemopoietic chimerism in fraternal twins, as indicated by sex chromosome analysis of cultured lymphocytes and by the female-specific character, the drumstick, of the neutrophilic polymorph (9, 10). Further, skin transplants between chimeric co-twins have shown complete immunologic tolerance (26). This phenomenon of naturally occurring hemopoietic chimerism and its corollary of specific tolerance, unique in primates, dictates the potential usefulness of marmosets in transplantation immunology. In addition to immunologic experiments, we are devoting considerable effort to improving technology of the colony care and to defining the pathologic disorders of this species.

Skin Allograft Tolerance

In support of our previous studies demonstrating skin allograft tolerance among co-twins, it was necessary to establish the immunocompetence of marmosets to allografts from unrelated animals of the same species. Preliminary data indicated full immune capabilities to foreign skin grafts, yet allograft rejection times differed significantly depending on species relationships of donor and host. The genetic relationship of the many genera and species of marmosets is unknown; as an empirical tool, we followed an artificial taxonomic classification of one genus, Saguinus, as described by Philip Hershkovitz (Folia Primat 4, 381, 1966). For the present study of skin grafts we used two species of the hairy-faced white-lipped tamarins, S. nigricollis and S. fuscicollis ssp., one of the white-moustached tamarins, S. m. mystax, and one of the bare-faced tamarins, S. o. oedipus (Raymond P. Porter and N. Gengozian). We performed intra- and interspecies transplants among these forms, using a technique previously described (Proc Soc Exp Biol Med 127, 860, 1968). The last day postgrafting on which intact viable tissue could be identified visually was recorded as the last day of graft survival. Hair direction and skin pigment identified long-term surviving transplants.

The survival times of the intraspecies allografts are shown in Table 39. Among the four species tested, the mean survival time (MST) ranged from 38 days for S. fuscicollis to greater than 70 days for S. o. oedipus. With one exception (Pair No. 3, S. fuscicollis) second- and third-set grafts survived for significantly shorter times than first-set grafts. A few of the longer surviving allografts regrew hair before final rejection. Most grafts, however, underwent a chronic rejection; they remained dry and scaly, were pale and nonedematous, and often lost their pigment. Final rejection produced a tight, puckered, unpigmented scar. Figure 69 shows an excellent long-term surviving allograft in S. o. oedipus (Table 39, pair No. 3). In all respects the allograft resembled an autograft; the graft on its reciprocal partner was rejected in 65 days.

The survivals of grafts exchanged between S. fuscicollis and two

1027403

TABLE 39

Survival Time of Intraspecies Skin Grafts in the Genus *Saguinus* (Tamarins)

Species	Graft set	Pair No.	Sex[a]	1	2	3
S. fuscicollis (ssp. *illigeri*)	1	1.	M	64[b]	14	-
			F	64	19	-
		2.	M	63	10	9
			M	36	10	9
		3.	M	28	35	24
			M	15	13	12
		4.	(F) M	55	-	-
		5.	(F) F	24	-	-
		6.	(M) M	22	-	-
		7.	(F) M	13	-	-
		Mean survival time (MST)		38	17	13
S. nigricollis	1	1.	M	47[d]	-	
			F	31	-	
		2.	M	c	60[d]	
			M	160[d]	60[d]	
		3.	(M)[e]M	16		
		Mean survival time (MST)		64[g]		
S. mystax (ssp. *mystax*)	1	1.	M	44	11	8
			F	79	17	14
		2.	M	50[d]		
			F	50[d]		
		3.	(M) F	>38[f]		
		Mean survival time (MST)		53[g]	14	11
S. oedipus (ssp. *oedipus*)	1	1.	M	45	-	
			M	47		
		2.	M	69		
			F	>77[f]		
		3.	M	65		
			M	179[d]		
		4.	M	39[d]		
		5.	F	39[d]		
		Mean survival time (MST)		70[g]		

[a] M, male; F, female. Animals paired to denote reciprocal exchange partners.

[b] Graft survival time in days.

[c] Mechanical failure.

[d] Grafts surviving at time of manuscript submission.

[e] Letter in ( ) denotes sex of donor in a one-way graft exchange.

[f] Animals died with intact graft on day indicated.

[g] Minimal MST due to continuing survival of same grafts.

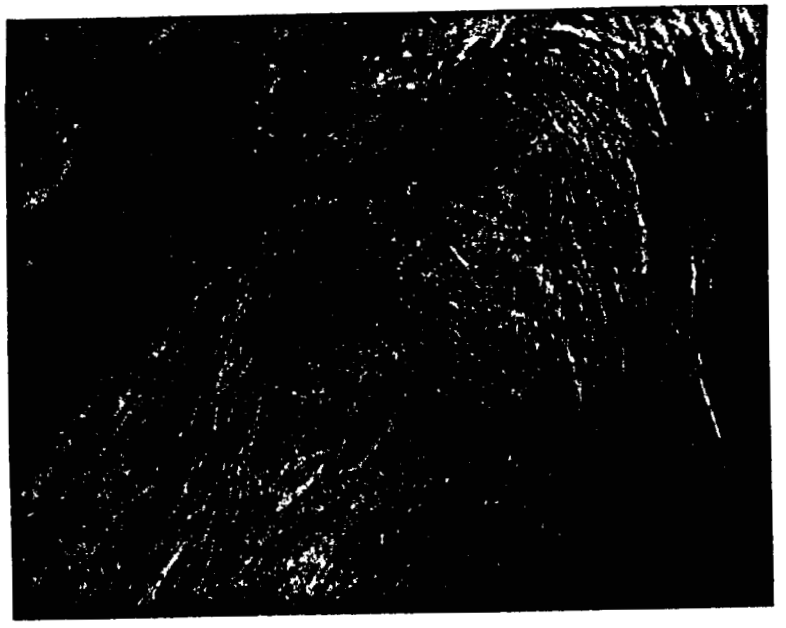

Fig. 69. Long-term surviving intraspecies allograft in S.o. oedipus (Table 1, pair No. 3, photograph 92 days posttransplant). Dash line demarcates pigmented graft and arrows indicate direction of hair growth.

other Saguinus species, S. mystax and S. oedipus contrast with the intraspecies series (Table 40). The MST for the first-set response of these xenografts ranged from 14 to 23 days. The second-set response in most experiments was also greater with interspecies grafts. White-graft rejection, indicating a vigorous reaction of the host, of third grafts was often recorded.

The intervals between the multiple foreign grafts in the foregoing series ranged from 16 to 118 days. There was no apparent correlation with the intervals between transplantation attempts and survival time of second- or third-set grafts. The sex of donor and host did not affect allograft or xenograft survival.

Postgraft erythroagglutinating antibody specific for donor antigens was uniformly absent in all graft series with one exception. An incomplete antibody, $\log_2$ titer of 7 (detected with a rabbit anti-marmoset serum Coombs reagent), appeared in the serum of an S. f. illigeri tamarin that had rejected its third-set graft from S. m. mystax (Pair No. 1, Table 40). Sera from this animal after the first- and second-set graft rejections were only weakly reactive ($\log_2$ titer of 2). The reciprocal exchange partner, S. m. mystax, did not form detectable erythroagglutinins even though a white-graft response occurred.

1027404

TABLE 40

Survival Time of Interspecies Skin Grafts in the Genus *Saguinus* (Tamarins)

	S. fuscicollis[a] vs. *S. mystax*[b,d]						*S. fuscicollis* vs. *S. oedipus*[c,d]					
Donor	*S. fuscicollis*			*S. mystax*			*S. fuscicollis*			*S. oedipus*		
Recipient	*S. mystax*			*S. fuscicollis*			*S. oedipus*			*S. fuscicollis*		
Graft set	1	2	3	1	2	3	1	2	2	1	2	3
Pair No.												
1.	19[e]	11	<5	32	12	8	13	9	<5	<7	7	<6
2.	18	8	-	13	9	-	16	11	-	31	9	-
3.	14	8	-	18	-	-	13	-	-	30	-	-
Mean Survival Time	17	9		21	10		14	10		<23	8	

[a] *S.f. illigeri* [b] *S.m. mystax* [c] *S.o. oedipus*

[d] Right and left column of each interspecies group correspond as reciprocal exchange partners.

[e] Graft survival time in days. Underlined numbers indicate white graft rejection.

The primary intraspecies (allo-) grafts among the four Saguinus species survived significantly longer than those among other mammalian and primate species. Two interdependent factors, biologic and geographic, may account for this. Biologically, the marmoset's natural hemopoietic chimerism provides each animal with two sets of transplantation antigens recognized as "self": its own and that of its co-twin. Such ubiquitous chimerism in a random-bred population increases the probability of shared major transplantation antigens and consequently of decreased incompatibility among its members. Geographically, the tamarins used in this study have evolved in fairly restricted areas and a finite pooling of genes for histocompatibility antigens is likely. For example, S. o. oedipus ranges through a small region of northern Colombia, bounded on two sides by populations of S. leucopus and S. o. geoffroyi, each separated from S. o. oedipus by large rivers. The relatively short survival times (13-64 days) obtained with intraspecies grafts of S. fuscicollis (ssp. illigeri) may reflect a greater heterogeneity within this subspecies. This correlates with Hershkovitz's suggestion that intergradation may occur between S. f. leucogenys, S. f. lagonotus, and S. f. illigeri because of their geographically intermediate areas.

Kidney Grafts

The natural hemopoietic chimerism of the marmoset may also convey tolerance to organs or tissues other than skin, if we assume that the requisite transplantation antigens of the grafted organ are completely expressed by their blood-forming cells. To extend, therefore, our information on allograft tolerance and rejection phenomena, a study on kidney grafting in unrelated and co-twin marmosets was undertaken (N. Gengozian, Sun Lee*, and Raymond P. Porter). Details of the technique used will not be given; however, we should realize that to remove the kidney from the donor we had to sacrifice the animal since a segment of the aorta and vena cava are taken with the renal vessels and kidney. The vessel incisions and final relocation of the transplanted kidney in the recipient by end-to-side anastomoses between the aorta and aorta, and vena cava and vena cava are diagramed in Fig. 70. Inset B of Fig. 70 shows how the ureter was anastomosed in fish-mouth fashion to the bladder. Figure 71 shows the donated kidney sutured in place just before the clamp on the aorta was released to permit blood flow into the organ.

For the experiment, three male-female co-twin marmosets, each with known blood cell chimerism, were chosen. In one pair, reciprocal skin-graft tolerance had already been demonstrated and the recipient was bearing a successful, tolerated skin graft at the time of the operation. For reasons noted, reciprocal kidney exchanges between the co-twins could not be performed and tolerance could be tested in only one direction. Each twin received one kidney from its co-twin after bilateral nephrectomy so that its survival depended upon successful functioning of the transplant. As a control to evaluate the normal kidney allograft rejection process, a similar kidney transplant was performed between two unrelated marmosets. Although Dr. Lee had never worked with marmosets before (indeed had never seen one until his visit), all operations proceeded without any difficulties.

The animal receiving the kidney from an unrelated marmoset died at 9 days. Its blood urea nitrogen (BUN) 2 days before death was 360 mg/100 ml, in contrast to 37 mg/100 ml recorded immediately before the operation. (The BUN levels of five normal animals, tested during a period of 5 weeks, have ranged from 17 mg/100 ml to 43 mg/100 ml. Histologic examination of the nonrelated kidney graft by Dr. C. C. Lushbaugh revealed a florid host-versus-graft lymphoid reaction superimposed on a subsiding granulocytic exudative response that presumably occurred immediately after transplantation. The lymphoid infiltration was interstitial and concentrated around the arcuate vasculature, penetrating the cortex from large foci of small and medium-sized lymphocytes. Of the three twins grafted, one died 61 days after the transplant. The BUN of this animal on day 48 was 59 mg/100 ml, slightly above normal, and then gradually increased until 1 day before death it was 220

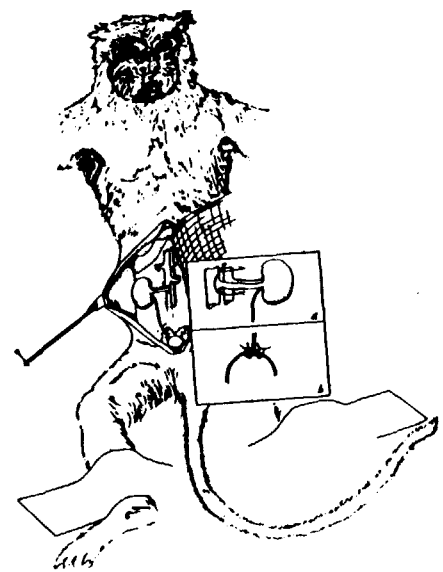

Fig. 70. Diagram showing transplanted kidney with end-to-side anastomoses of aorta and vena cava. Inset (a) demonstrates cutting of aorta and vena cava in removing kidney from donor. Inset (b) shows fish-mouth method of anastomosing ureter to recipient's bladder.

* Dr. Sun Lee, a surgeon from Scripps Clinic and Research Foundation, La Jolla, California, has perfected several microsurgical techniques on organ transplants in rats; he visited our laboratory as a consultant to perform the operations.

1027405

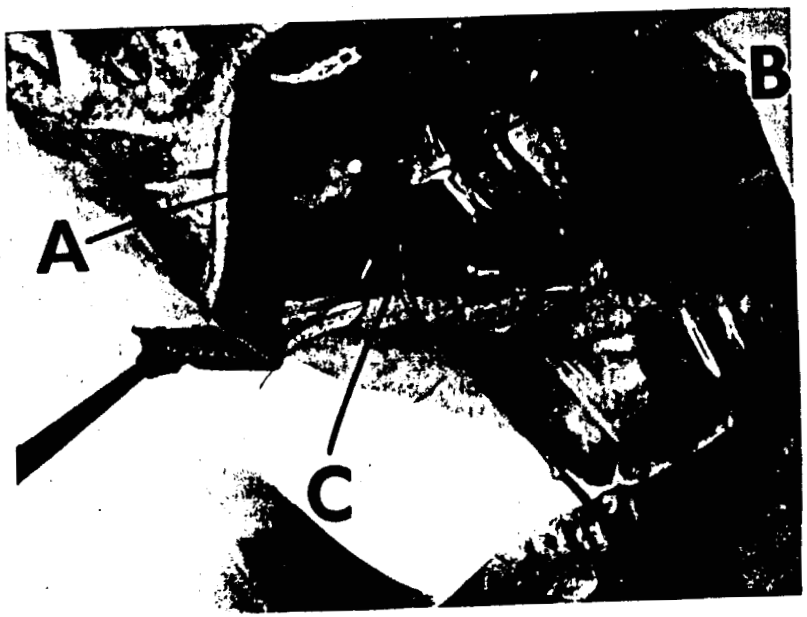

Fig. 71. Photograph showing transplanted kidney immediately before releasing clamp on aorta and vena cava. (A), kidney; (B) clamp on aorta and vena cava; (C) ureter.

mg/100 ml. The lymphoid response in this chimeric kidney was much less extensive than that in the acutely rejected kidney, yet appeared to be typical of a mild chronic host-versus-graft reaction. Two animals are still alive approximately 5 months postgrafting, and as indicated by weekly BUN determinations their chimeric kidneys are functioning normally.

The results of this initial organ transplant suggest that the blood chimerism extends tolerance to tissues other than skin. However, the death of one of the twins after renal failure raises the possibility that in some animals split tolerance may occur; i.e., acceptance of one allogeneic system (hemopoietic) but not of another (kidney). An analogous situation has been reported by Stone, et al. (Science 148, 1335, 1965) in cattle chimeras where chronic rejection of skin allografts has occurred in the face of an existing stable population of chimeric blood-forming cells. Relevant to this, the blood chimeric status of the marmosets did not change during the kidney postgraft period, even in the twin that died with renal failure attributed to a subacute HvG reaction. Also, sometime before the kidney operation, this latter animal had received a skin graft from its co-twin that was intact at the time of death. Several more kidney transplant attempts among both related and unrelated marmosets are needed to delineate more accurately the immune

1027406

rejection processes associated with this organ and to substantiate the possibility of split tolerance in these animals.

Twinning Frequency and its Origin

Breeding of the marmoset in our laboratory the past 5 years has yielded sufficient data to determine the twinning frequency and to evaluate its monozygotic or dizygotic origin. In 261 recorded deliveries, there have been 77% twins, 5% triplets, and 18% single births. Further, the sexes of the twins approximate that expected for fraternal twinning, i.e., 1 (mm): 2 (mf): 1 (ff). Cytogenetic analysis of blood-forming tissues from these animals suggests that co-twin vascular anastomosis occurs consistently during prenatal development: in 52 of 52 heterosexual pairs tested we found hemopoietic cell chimerism by sex chromosome identification. Of interest also, however, we detected heterosexual chimerism in 3 of 47 isosexual twin pairs and in 3 of 19 single-born animals. Three possible pathways may account for such chimerism in the latter groups: (a) exchange of cells from one fetus to another (or another pair) followed by death and resorption of one fetus, (b) transplacental passage of hemopoietic cells from the maternal to the fetal system, or (c) early aggregation of the blastomeres of twins culminating in a single-born chimeric young. We obtained evidence for chimerism induction by the first mechanism in both presumptive "twins" and "single-born" young (Fig. 72). The frequency of heterosexual chimerism found in isosexual twins (6%) compares to the frequency of triplets observed in our breeding program. However, the frequency of heterosexual chimerism among the single-born animals (3/19) was smaller than that expected (50% or 9/19) if we assume that all single births result from death and resorption of one fetus of a pair. The question may be asked, therefore, whether any of the single born are in fact true nonchimeras (i.e., nonisosexual hemopoietic chimeras), representing fertilization and development of a single ovum.

On the basis of the preceding information, we must assume that all marmosets, even single born, have a high probability of being hemopoietic chimeras. In certain experimental situations, however, it would be desirable and indeed perhaps necessary to have an "abnormal" marmoset, that is, one that is not a blood chimera. A method of procuring a nonchimera, single young was suggested by an early report of Hill and Hill (Assoc des Anatomistes Comptes Rendus 22, 264, 1927) who had noted that in two sets of presomite twins the ovulation was biovarian, i.e., each ovary had a single corpus luteum. This was later confirmed by Wislocki (Amer J Anat 64, 445, 1939) in an examination of an additional seven sets of ovaries. These observations raised the possibility that the development of a single zygote, and therefore a potential nonchimera, could be achieved by removal of one ovary.

Effect of Unilateral Ovariectomy on Twinning

Unilateral (left) ovariectomies were performed on six Saguinus fuscicollis marmosets and the results of breeding these animals over a 3-year period are shown in Table 41. (N. Gengozian and C. Merritt*)

* Present address: National Institutes of Health, Bethesda, Md.

TABLE 41

Breeding Produced by Hermosera after Unilateral Ovariectomy.

Female No.	Date of Ovariectomy	Breeding Results: Date of delivery, number and sex of offspring			
1	7/15/66	5/16/67	5/20/68	2/22/69	10/9/69
		2- M, F	2- M, F	2- F, F	3- M, M, F
2	7/18/66	12/29/66	7/10/67	3/31/69	
		2- M, F	2- M, F	1- M*	
3	8/23/66	7/2/67	12/30/68		
		1- ?†	1- ?†		
4	7/19/66	7/5/67			
		1- ?‡			
5§	11/25/66	9/22/67	4/21/68	12/25/68	7/11/69
		2- M, F	2- M, M	2- M, F	2- F, F¶
6§	11/25/66	-			

* This single born male is chimeric for female cells as revealed by sex chromosome analysis.

† Pregnancy terminated in abortion; only one embryo, sex unknown, could be found. Two yolk sacs were found with placenta of 7/2/67 abortion.

‡ Pregnancy terminated in abortion and only one embryo, sex unknown, could be found. The female died shortly after delivery.

§ Females had delivered twins sometime before operation, No. 5 three times, and No. 6 once.

¶ Both young were full-term stillborn.

Fourteen pregnancies were recorded in five of the six females. Three terminated in early abortion, and in each, only a single embryo was found. However, in one placenta, two yolk sacs could be identified. Of the 11 pregnancies carried to term, only one yielded a single young. This animal, a male, was, however, a blood chimera carrying female cells by chromosome analysis. One pregnancy yielded triplets, two males and a female. Finally, of the nine twins delivered, six were heterosexual pairs.

The twinning frequency and sexes recorded from this small group of animals compares to that observed in our colony for a much larger group of nonovariectomized breeding females. Tentatively, we may therefore conclude that removal of one ovary does not interfere with the normal breeding pattern; these results are perhaps not surprising in view of the compensatory hypertrophy in one ovary after complete (Brit J Exp Biol 5, 19, 1928) or partial removal of the other, described

1027407

by Lipschutz (Brit J Exp Biol 2, 331, 1925). In many species unilateral ovariectomy leads to an increase in the number of mature follicles in the remaining ovary, so that the number of corpora lutea formed does not differ significantly from that of nonovariectomized females. The mechanism of this phenomenon, referred to as the "law of follicular constancy", is still not known. However, two hormonal pathways have been suggested: (a) removal of one ovary results in an increase in the release of pituitary gonadotrophins, which then leads to the hypertrophic condition; or (b) removal of one ovary exposes the remaining ovary to greater amounts of gonadotrophins without an in-

Fig. 72. Products of conception showing two fetuses and one embryo, which was undergoing resorption at time of abortion. If pregnancy had continued to term, and if evidence for the existence of the additional embryo had been lost, this birth might have been recorded as twins. Heterosexual chimerism in such isosexual "twins" has been found.

creased release from the pituitary. Apparently the marmoset also exhibits some trophic response following unilateral ovariectomy. "True" single young, therefore, may be attained by a relocation, rather than a removal of one ovary, with the vascular network and consequently any pituitary-ovary hormonal feedback mechanism not altered.

Twin Chimerism Index

Although procuring a marmoset with only one known genetic population of cells is not yet possible, the degree of heterosexual chimerism may range from less than 2% to more than 98%. Information obtained previously (10) on a limited number of co-twin pairs allowed us to speculate that if cell mixing during embryonic development is complete, the proportion of cells with female and male chromosomes should be the same in each member of a twin pair. That is, the proportion of chimerism in one member should be the complement of that in the other; the sum of the proportions should therefore equal 1.00. The extent to which this occurs is included in Table 42 for 28 sets of male-female twins and has been called the Twin Chimerism Index (TCI), simply the sum of the two proportions of chimerism (N. Gengozian, J. S. Batson, and C. T. Greene). Of the 28 pairs, 19 had similar proportions of male and female cells, i.e., the TCI approached 1.00. Nine pairs differed significantly from 1.00 (pr <.05). Note that a 50:50 mixture of male and female cells occurred infrequently. Pair 5 showed the extreme ranges in percentage of chimerism, 1% in the male and 97% in the female.

In the data of Table 42, it appeared that in general more male than female cells were present among the marmosets of both sexes. To verify this, we determined the absolute numbers of male and female cells scored in the 28 co-twins. In the males, of 2379 cells scored, 1441 were male (60.6%), giving an M/F ratio of 1.54. In the females, 1334 cells of 2430 were male (54.9%), giving an M/F ratio of 1.22. In each sex the M/F ratio was significantly greater than 1 (pr <0.05), and the ratio for the males was greater than that of the females (pr <0.05).

Among imported and laboratory-bred marmosets, 45% of 187 males were chimeric for female cells while 56% of 169 females were chimeric for male cells. More significantly, however, 77% of the male chimeras had less than 50% chimerism for female cells and only one of 85 had greater than 76% female-cell chimerism. Conversely, among the female chimeras, 19% had greater than 76% male-cell chimerism and 46% had less than 50% male-cell chimerism. This difference in the distribution of chimerism in the males and females was found to be statistically significant (X^2 32.6m pr <.01). This skewing toward predominance of the male cell, more pronounced among the male animals, is shown in Fig. 73.

The high rate of fraternal twinning, the consistent chimerism in heterosexual pairs, and the finding that single-born animals may be chimeras support the concept of universal chimerism in the marmoset. Until markers other than those based on sex are available, all marmosets, even single born, must be presumed to be hemopoietic chimeras. The correlation in the proportion of male and female cells in the co-twins

1027408

TABLE 42

HETEROSEXUAL LYMPHOCYTE CHIMERISM IN MARMOSET CO-TWINS

Pair No.	Sex	Age (mos) When tested	Lymphocyte Chimerism Cells scored[1]	%	Twin Chimerism Index (TCI) (% chimerism, M + F)[2] / 100
1	M	1	26/100	26	1.04
	F	1	78/100	78	
2	M	1	25/54	46	0.82[3]
	F	1	36/100	36	
3	M	1	63/100	63	0.96
	F	1	33/100	33	
4	M	1	54/100	54	1.09
	F	1	55/100	55	
5	M	1	1/100	1	0.98
	F	1	97/100	97	
6	M	3	29/100	29	0.88
	F	3	59/100	59	
7	M	4	45/50	90	1.10
	F	4	10/50	20	
8	M	6	16/50	32	0.92
	F	6	30/50	60	
9	M	6	26/50	52	1.24[3]
	F	6	36/50	72	
10	M	6	52/100	52	0.66[3]
	F	6	7/50	14	
11	M	6	19/50	38	0.82[3]
	F	6	44/100	44	
12	M	6	49/100	49	0.94
	F	6	43/95	45	
13	M	6	59/100	59	0.87
	F	6	28/100	28	
14	M	20	81/100	81	1.14
	F	6	17/52	33	
15	M	8	17/100	17	0.78[3]
	F	8	52/85	61	
16	M	8	33/100	33	1.00
	F	8	67/100	67	
17	M	8	40/100	40	1.17[3]
	F	11	43/56	77	
18	M	9	35/100	35	0.96
	F	9	43/71	61	
19	M	10	42/100	42	0.80[3]
	F	10	20/53	38	
20	M	11	60/88	68	0.90
	F	11	22/100	22	
21	M	12	6/100	6	0.96
	F	12	90/100	90	
22	M	12	26/100	26	0.91
	F	12	65/100	65	
23	M	14	30/64	47	1.00
	F	14	53/100	53	
24	M	14	18/67	27	0.86[3]
	F	14	118/200	59	
25	M	15	20/100	20	0.90
	F	15	70/100	70	
26	M	16	30/81	37	0.90
	F	17	53/100	53	
27	M	18	8/52	15	0.72[3]
	F	17	29/51	57	
28	M	18	28/73	38	0.92
	F	18	36/67	54	

[1] Numerator indicates the number of opposite sex cells found by sex chromosome analysis in each twin; denominator indicates the total number of cells analyzed.

[2] Twin Chimerism Index gives a measure of the identity of the cell population (M and F) in co-twins. Thus, a value of 1.00 indicates the proportion of male and female cells is the same in each twin, e.g., twin pairs 16 and 23. [Statistical development of TCI given in (6).]

[3] TCI is significantly different from 1.00 at 5% level.

and the infrequency of 50:50 mixtures parallels the situation observed in cattle twins with erythrocyte and leucocyte chimerism. This similarity in proportions between co-twins and yet displacement of cell proportions suggests that a common placental circulation develops early with an almost equally early domination of one cell population. In marmosets, the male cell line appears to have some selective advantage during establishment of any common "hemopoietic pool." We analyzed the sex chromosome data in cattle chimeras reported by several investigators; they suggest a similar situation. Thus, in 36 males, 1030 cells of 1849 scored were male, giving an M/F ratio of 1.26; in 39 females, 1007 cells of 1868 scored were male, giving an M/F ratio of 1.17. Male cells were in the majority in 38 of the 56 marmosets listed in Table 41. In the cattle data, 45 of 72 also showed more male cells (3 had equal numbers of each sex). In both marmosets and cattle, those with more male cells were almost equally divided among the two sexes. Although in both marmoset and cattle chimeras individuals with a high proportion of female cells are sometimes found, it appears significant that male cells usually constitute the majority in both sexes. The reason for this prevalence of male cells is unknown: whether there is a hormonal influence favoring male cell hemopoiesis,

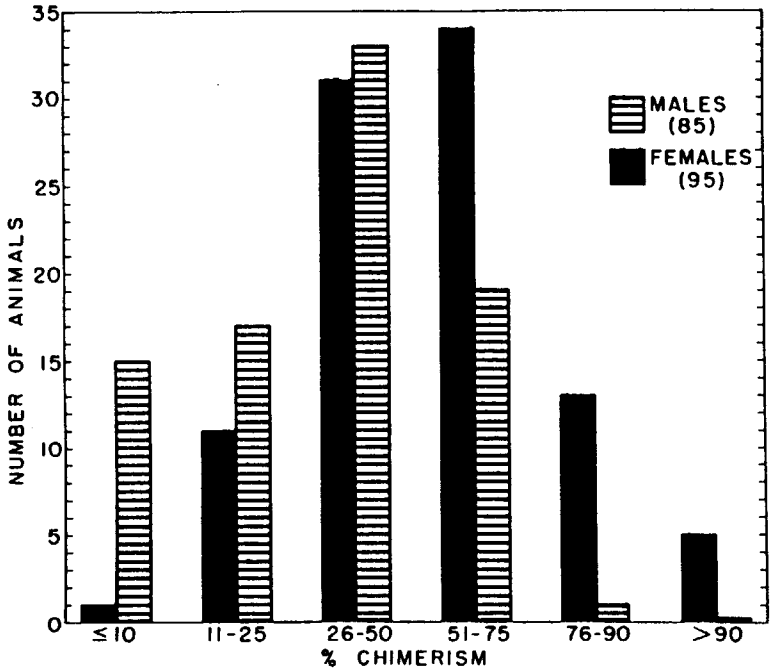

Fig. 73. Distribution of percentage of heterosexual chimerism in male and female marmosets.

1027409

or whether a cell bearing a Y chromosome has some physiologic advantage over a 2n-XX cell.

Marmoset Diseases

We have continued to enlarge the ORAU Marmoset Pathology Collection (C. C. Lushbaugh, Gretchen Humason, and N. Gengozian). During 1969 the histology study material reached 440 specimens, most of which represent complete necropsies comprising 25 or more tissues. These are stained routinely by the PAS stain for mucopolysaccharides and similar substances such as thyroid colloid; the Prussian blue reaction for iron; and the Romanofsky stains for hematopoietic tissue differentiation. After being screened as an individual clinical case for infectious and other diseases important to day-to-day colony control, the histologic slides of a necropsy are filed by organ and animal age for developmental studies and for pathologic studies on the effects of disease upon various organs and systems. Using this modus operandi, we have previously described the normal development of the gonads, lungs, liver, erythroblasts, and thyroid gland. These organs and cellular systems were singled out because an understanding of their development was basic to defining pathologic developmental states and perinatal diseases. Early it became apparent that human adult and neonatal pathology was not a complete basis for defining all causes of death in our colony; we needed a long-range systematic study to define the various ways, such peculiarities of the marmoset as, for example, natural intrauterine blood and tissue chimerism altered a disease process. Previously, we have reported diseases like human erythroblastosis fetalis, hyperplastic thyroid disease (and goiter) and intrauterine Chagas' disease. Many animals die, however, in which we are not able to define their cause of death precisely or to equate the relative importance of the multiple disease processes that we find. To continue improving our marmoset animal husbandry we need to define the causes of all deaths precisely; then we can design etiologic studies that will ultimately allow these diseases to be controlled, if not completely eliminated.

The thyroid disease problem still occupies our interest. During 1969, 67 out of 118 marmosets came to necropsy with evidence that severe acute thyroid disease is still a common occurrence. The acute hyperplastic and exhaustive forms of the disease were found in occasional adult animals that had been in the colony for as many as four years, but appeared most commonly in recently imported animals not yet acclimated to colony life. The continued finding of abnormalities of thyroid development and thyroid disease in stillborn and infant marmosets strengthens the probability that maternal thyroid function during pregnancy is abnormal in many instances (Table 43). The thyroid glands, attached to their tracheas, of three stillborn marmosets are shown in Fig. 74. The central one is normal while that on the left is abnormally small and that on the right abnormally large, a colloid goiter. All these stillbirths were 9.5 cm CR in length, near full-term size, and had surviving twins. We believe the abnormally small gland represents an additional end stage in the pathogenic schema we previously proposed, a hypoplastic gland representing retarded rate

TABLE 43

Incidence and Type of Thyroid Abnormality in Marmoset Necropsies in 1969.

Thyroid Status	Stillbirths (1969) < 6 cm CR		>6 cm CR		Liveborn (1969)*		Adults and Liveborn 1968 or Before		Total Thyroid Types	
	No.	%	No.	%	No.	%	No.	%	No.	%
Normal	11	100	0	0	0	0	17	28	28	24
Deformed (normal)	0	0	4	16	7	33	12	20	23	20
Exhaustive Degeneration	0	0	13	52	7	33	17	28	37	31
Hyperplasia and Resorption	0	0	8	32	7	33	15	24	30	25
Group Totals	11	100	25	100	21	100	61	100	118	100

* About 61 newborn survived in 1969.

of development. Two other instances of this condition are included in the "deformed" group in the Table.

Searching for clues to the etiology of this process, this year we studied adrenal cortical development and looked for instances of acute adrenal cortical necrosis. Others have reported that in the rabbit and some other species, frightening experiences such as caging, can cause adrenal cortical damage in a wild animal. This damage can lead to hormonal imbalance and thyroidal stimulation. The developmental aspect of this study is sufficiently complete to report that we have been unable to detect any developmental abnormality in the adrenal. Acute focal necroses of the adrenal gland cortex were found, however, in some postnatal and adult animals, located most commonly in the fascicular and reticular zones. Easily overlooked because of their minute size, they consist of one to about four eosinophilic pyknotic cells or small spaces containing granulocytic leukocytes and debris. Although their occurrence seems to correlate with the hyperplastic but not degenerative stage of marmoset thyroid disease, we cannot be certain that they are etiologically related. Their minute mass in relation to the remaining normal appearing (but lipid depleted) cortex would not lead one to suspect that a lethal level of adrenal cortical insufficiency was present but suggests that whenever possible, assays for adrenocortical steroids should be done to determine the clinical importance of this finding. This lesion was also found in some animals that died in the skin transplant experiment during the time when plaster of Paris jackets were used to protect the grafts. The fact that some of these transplant animals could be revived from a shock-like state by saline infusions may or may not be important here.

Elsewhere in this report, in the chapter on Whole-Body Counting we describe two metabolic studies that were undertaken this year to determine whether metabolic evidence for thyroid disease could be found in support of these pathologic findings.

1027410

A major new focus this year was upon the lympho- and hematopoietic system of marmosets dying from "natural" causes. This study was stimulated by the deaths of three colony-bred animals that were in the immunologic study concerned with natural and indirect chimerism. All three animals had histopathologic evidence for an acute and chronic hemolytic disease. We have found that the erythrophagocytosis and widespread hemosiderosis that we considered typical of an immune reaction in these cases is also present in animals not stimulated by any injections. In a recent small epidemic within the colony, six healthy animals died after a short illness. They included both colony-bred and imported marmosets; all were well acclimated in the colony for a long time. Hypertrophic lymph nodes were the only common gross abnormality, but microscopically there was severe hemosiderosis of spleen, liver, bone marrow, lungs, lymph nodes, and intestinal lymphatic tissues. We saw erythrophagocytosis and heavy iron deposits in the histiocytes of the peripheral and interfollicular sinuses of the lymph nodes and in the splenic red pulp. The lymphoid follicles contained toxic reaction centers; foci of lymphoid hyperplasia, while confined to the node, obliterated a portion of follicular and sinusoidal structures. This lymphoid hyperplasia suggests that these deaths were due to an epidemic virus infection although we have no other evidence to support this conjecture. The pathologic findings in this small epidemic are reported in this context, however, because they suggest that the high instance of this erythrophagocytic disease (about 20 to 30% of all adult deaths) reflects an altered defense reaction to a wide variety of stimuli not necessarily causing RBC trauma directly. Figures 75 and 76 show examples of this erythrophagocytosis by sinu-

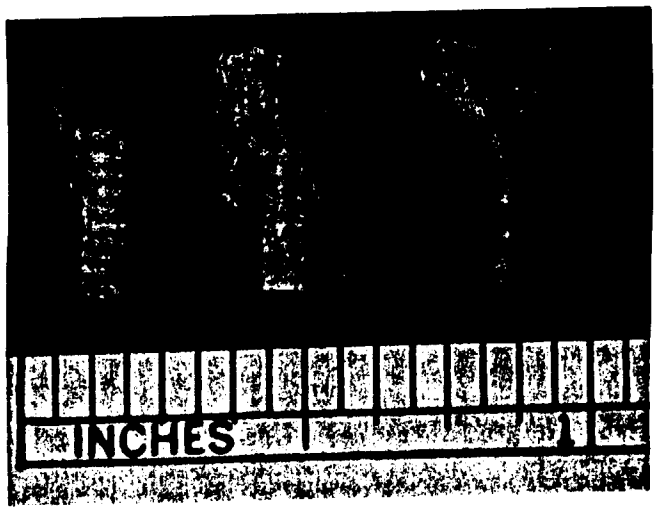

Fig. 74. Thyroid glands of three full-term stillborn marmosets; the middle one is normal; note hypoplasia (left) and hyperplasia (right).

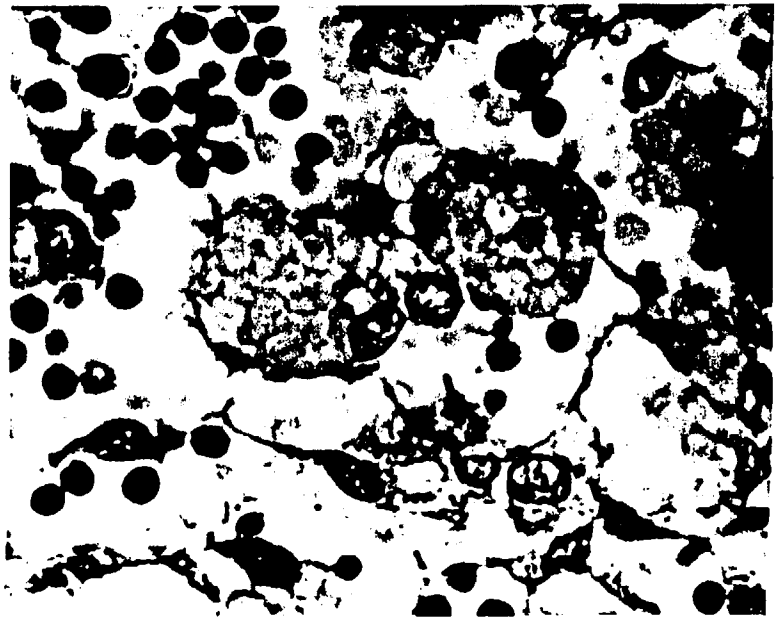

Fig. 75. Photomicrograph (X300) of marmoset lymph-node sinus showing histiocytic macrophages of the reticulum engorged with phagocytosed erythrocytes (hematoxylin and PAS stain).

soidal phagocytes in marmoset lymph nodes. Figure 76 is a photomicrograph of a specific histochemical stain for hemoglobin, Buffalo Black, which we used to be certain that the intracellular objects are RBC. Jandl, et al. (Science 158, 1582-1585, 1967) have reported that this pathologic appearance is associated with coating of RBC by 7S antibody not necessarily specific for the RBC antigens present. Fluorescent antibody microscopy might, therefore, identify those deaths in which erythrophagocytosis is due to antibody rather than direct RBC trauma. Criteria need to be developed to determine more objectively what role this hemodestructive process has played in individual deaths in any group of animals under study. Although immunologic identification of responsible antigens is not possible at present in these unexpected and often unattended deaths, some such approach is needed to define the etiology of this disease process.

Until Gengozian and his group and Hershkovitz developed criteria for identifying the subspecies of Saguinus fuscicollis used in these experiments, there was always the implication that the diseases we are trying to identify were not natural, owing to intersubspecies breeding that would not be expected to occur in the wild. Our necropsy experience during the last two years does not support this contention, since

1027411

the incidence or severity of diseases with possible immunologic causes does not correlate with the subspecies classification of each animal and his parentage now always known. Moreover, an increased incidence of auto-immune-like disease has been obtained in the imported adult animals protected by long residence in our colony from death due to reinfection and superinfections typical of their natural, heavily parasitized status. The decrease in deaths from parasitism parallels also an increase in pathologic processes that may represent genetic errors of metabolism. For example, during our search for marmoset hematopoietic abnormalities we found a lesion marked by numerous mucopolysaccharide rich, lipohistiocytes in the bone marrow, lungs, and some connective tissue (paricardial) loci. The abnormal cell resembles most closely the large histiocyte of human mucopolysaccharidosis whose genetic origins are only now being elucidated (Fig. 77). As far as we can determine such a condition has not been described in experimental animals previously. Obviously there is much yet to be learned about the nature of marmoset diseases.

In the course of investigation of diseases affecting marmosets, we have carried out a cooperative study on a highly specialized arthro-

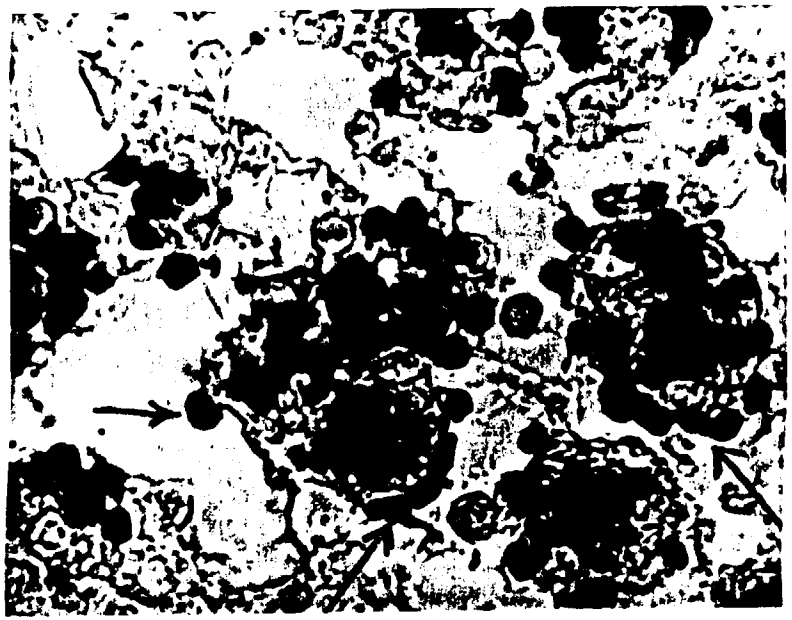

Fig. 76. Photomicrograph (X750) of marmoset lymph-node sinus stained with Buffalo Black to identify hemoglobin containing RBC within macrophages and agglutinated to their surfaces (arrows).

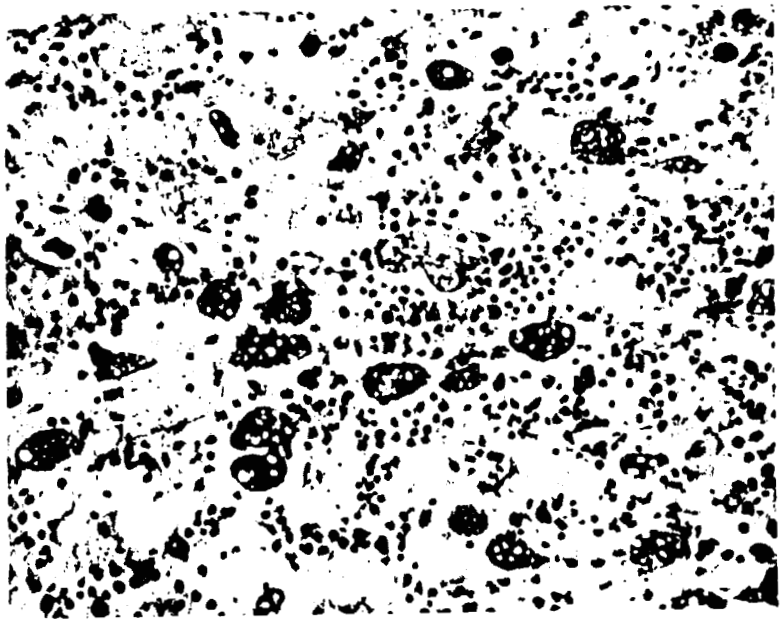

Fig. 77. Photomicrograph (X300) bone marrow of adult marmoset, dead from unknown cause. Note large lipohistiocytes staining positively for mucopolysaccharides (hematoxylin and PAS stain).

pod, Porocephalus clavatus (B. Nelson, G. E. Cosgrove*, J. T. Self†, and N. Gengozian). Immature forms are conspicuous among the many exotic parasites found in the imported marmosets. Although most arthropods are free-living, this kin of insects and spiders lacks eyes and has no respiratory or circulatory organs. It is adapted to parasitism even more than are its tiny cousins, the mites, and belongs to a separate small group of endoparasites known as Pentastomes or Linguatulids.

We found encysted arthropod nymphs at autopsy in 29% of marmosets in the ORAU colony (Lab Animal Care 18, 654, 1968) ranging up to 36 with an average of four; they occurred in many tissues, but the most common sites were lungs (13% of all necropsies), liver (8%), and serosal surfaces (4%). Histologically the cysts, containing viable nymphs, were lined by a thin, smooth homogeneous acellular membrane with an adherent, slightly compressed zone of host tissue rarely

* Oak Ridge National Laboratory

† University of Oklahoma, Norman, Oklahoma.

1027412

showing inflammatory reaction. In contrast, cysts containing dead nymphs were surrounded by an intense chronic inflammatory reaction with phagocytes, foreign-body giant cells, old blood, leukocytes of all types, and varying stages of fibrosis. The identity of the nymphs was established by feeding cysts to boa constrictors raised in the laboratory. A year later the snakes were killed and Self and Cosgrove found adult Pentastomes in the lungs, which proved to be Porocephalus clavatus, a species common in tropical New World snakes (J Parasitol 54, 696, 1968) that have a diet of mammals known to contain encysted nymphs.

Porocephalus clavatus in the Saguinus marmosets seems to be a well-adapted parasite, eliciting minimal host response as long as it is alive and able to maintain the integrity of the cyst membrane. Serial infections may be associated with mild systemic immune phenomena, but in the imported marmosets seen here the nymphs have not been shown to impair health. As yet, we do not know how long encysted nymphs can remain viable. Cysts were about as common in marmosets surviving a year or more in the colony as in those dying shortly after importation. Some marmosets in the colony for nearly 3 years contained nymphs presumed to have survived since importation because the snake-monkey cycle of transmission is precluded. We can be confident that marmosets born in our colony will be free from this parasite and associated reactions that might interfere with immunologic studies related to chimerism and tissue transplantation.

ULTRASTRUCTURAL STUDIES OF TUMORS

Virus-Cell Interaction

The electron microscopy project has continued work on the virus-cell interaction related to malignancy (D. C. Swartzendruber). Experimental studies of many disease processes, such as leukemogenesis, are possible only in laboratory animals. Several model systems are now available to study the development of leukemia, either in animals with spontaneous leukemia or in susceptible animals after the injection of potent viral preparations. One of the unsolved problems associated with virus induction of leukemia in model systems is identity of the initial sites of the virus-cell interaction that leads to malignancy. While at Michigan we reported, with Murphy and Ma*, in 1967 (Proc Soc Exp Biol Med 126, 731, 1967) that lymphatic tissue germinal centers of high-leukemia C58 mice contain large numbers of C-type murine leukemia viruses for many months before recognizable signs of disease emerge. Recently we have studied by electron microscopy two strains of mice, AKR/J mice with a high incidence of spontaneous leukemia of thymic origin and BALB/c mice with a low incidence of natural leukemia. Lymphatic tissue germinal centers of nonleukemic AKR/J and BALB/c mice contained characteristic C-type particles; fewer particles were

* University of Michigan, Ann Arbor, Michigan.

Fig. 78. Electron micrograph of 3-month-old AKR/J mouse spleen germinal center showing two C-type virus particles in an electron-dense, extracellular material.

detected in BALB/c mice (2nd International Conference on Germinal Centers of Lymphatic Tissue, Plenum Press, N. Y., 1969, p. 203). Subsequently virus-like particles similar in ultrastructure to C-type particles in mouse leukemias were found selectively localized in the lymphoid germinal centers of 2- to 6-month-old normal guinea pigs of Hartley stock. A second type of virus-like particle with a diameter of about 70 mμ and dense central core of 30 mμ was also found in germinal centers (23).

Characteristic C-type virus particles are abundant in splenic secondary follicles or germinal centers of AKR mice between 1 and 6 months of age. Most of the particles are mature C-type found in an electron-dense material believed to be extracellular (Fig. 78). "Budding" C-type

1027413

particles and cylindrical structures protruding into the basement membrane areas underlying endothelial cells are prominent in the central arterioles of splenic white pulp at about 5 months of age (Fig. 79). In older AKR mice, numerous mature C-type particles occur in expanded subendothelial spaces of these arterioles. How these findings relate to leukemogenesis in AKR mice is as yet unknown. Germinal centers and areas surrounding follicular arterioles are sites of cellular proliferation and interaction in immunologic phenomena; therefore the localization of many C-type viruses in these areas in leukemic mice may have particular relevance as yet unknown immunologic mechanisms affecting AKR leukemogenesis (23).

Gallium Localization in Leukemic Mice

Gallium-67 citrate preferentially localizes in certain tissues of leukemic mice (101). Gallium-67 concentrations were studied in AKR/J mice that develop lymphatic leukemia spontaneously and in BALB/c mice with disease induced by Rauscher leukemia virus. At 24 hr signifi-

Fig. 79. Electron micrograph of 5-month-old AKR/J mouse spleen white pulp showing the numerous virus-like particles in a portion of the central arteriole.

cantly higher concentrations localized in the thymus and involved lymph nodes of leukemic AKR/J mice than in nonleukemic AKR/J mice (Table 44). The radionuclide localized more in thymic tissue of young (7 weeks) AKR/J mice than in older (3 to 10 months) nonleukemic AKR/J mice (Table 45).

TABLE 44

Comparison of ^{67}Ga concentration in tissues of 8- to 10-month-old leukemic and nonleukemic AKR/J mice.

Mice (No.)	Thymus Weight	% administered dose/g*								
		Thymus	Spleen	Liver	Kidney	Lung	Muscle	Femur	Blood	Lymph Node
Nonleukemic (20)	0.071 g ±0.009†	2.28 ±0.27	2.70 ±0.24	4.36 ±0.48	8.87 ±1.38	4.28 ±0.92	0.45 ±0.04	6.13 ±0.38	1.71 ±0.18	1.83 ±0.20
Leukemic (17)	0.434 g ±0.079†	16.94 ±1.44	2.41 ±0.43	2.91 ±0.37	3.80 ±0.52	3.78 ±0.66	1.10 ±0.33	4.89 ±0.49	1.29 ±0.22	8.55 ±1.34

*Average values
†Standard error

TABLE 45

—Comparison of ^{67}Ga concentration in tissues of 7-week-old and 13-week-old AKR/J mice.

Mice (No.)	Thymus Weight	% administered dose/g*							
		Thymus	Spleen	Liver	Kidney	Lung	Muscle	Femur	Blood
7 weeks (9)	0.087 g ±0.006†	6.56 ±0.49	3.73 ±0.76	2.97 ±0.25	3.39 ±0.29	2.75 ±0.77	0.42 ±0.03	14.90 ±0.35	0.86 ±0.10
13 weeks (9)	0.088 g ±0.016†	2.05 ±0.35	1.48 ±0.18	2.34 ±0.23	3.28 ±0.26	4.89 ±0.90	0.33 ±0.02	9.67 ±0.35	0.81 ±0.13

*Average values
†Standard error

TABLE 46

Comparison of ^{67}Ga concentration in tissues of 7- to 8-week-old BLV infected and control BALB/c mice.

Mice (No.)	Spleen Weight	% administered dose/g*							
		Thymus	Spleen	Liver	Kidney	Lung	Muscle	Femur	Blood
Controls (10)	0.095 g ±0.003†	4.20 ±0.34	3.19 ±0.52	4.44 ±0.38	3.49 ±0.17	3.99 ±0.86	0.59 ±0.05	15.88 ±0.86	1.00 ±0.14
Leukemic (10)	1.709 g ±0.248†	2.47 ±0.16	6.75 ±0.56	8.77 ±0.53	3.49 ±0.23	8.26 ±0.86	0.75 ±0.06	8.13 ±1.08	4.40 ±0.57

*Average values
†Standard error

1027414

Although spleens of leukemic AKR/J mice often contained histologically typical lymphoma cells, the ^{67}Ga concentration did not increase with leukemic change in this organ. Concentrations of the radionuclide were increased in blood, spleen, liver, and lung of BALB/c mice with leukemia induced by Rauscher virus (Table 46).

Fig. 80. Electron microscopic autoradiogram of leukemic AKR/J mesenteric lymph node. Note silver grains indicating ^{67}Ga localization over cytoplasmic dense bodies.

Electron Microscopic Autoradiography of Gallium

With the recent finding of the preferential localization of ^{67}Ga in leukemic mouse tissues, we have a basis for a new approach to the study of murine leukemia. The technique of electron microscopic autoradiography has been used to identify the sites of ^{67}Ga localization in cells of AKR/J mouse tissues. With this technique (D. C. Swartzendruber and G. A. Wolfe), ^{67}Ga is shown to be associated with electron-dense, cytoplasmic inclusions in cells of spleen, thymus, lymph node, liver, and kidney. They are tentatively identified as lysosomes or microbodies. These subcellular components are abundant in phagocytic cells, in liver parenchymal cells, and in cells of the proximal convoluted tubules of kidneys. The majority of silver grains are found over these electron-dense cytoplasmic bodies (Figs. 80 and 81) suggesting that ^{67}Ga is associated with the lysosomes or microbodies of both normal and malignant tissues. Further experiments are required to determine the biochemical basis for ^{67}Ga association with these cytoplasmic particles in virus-induced murine leukemia.

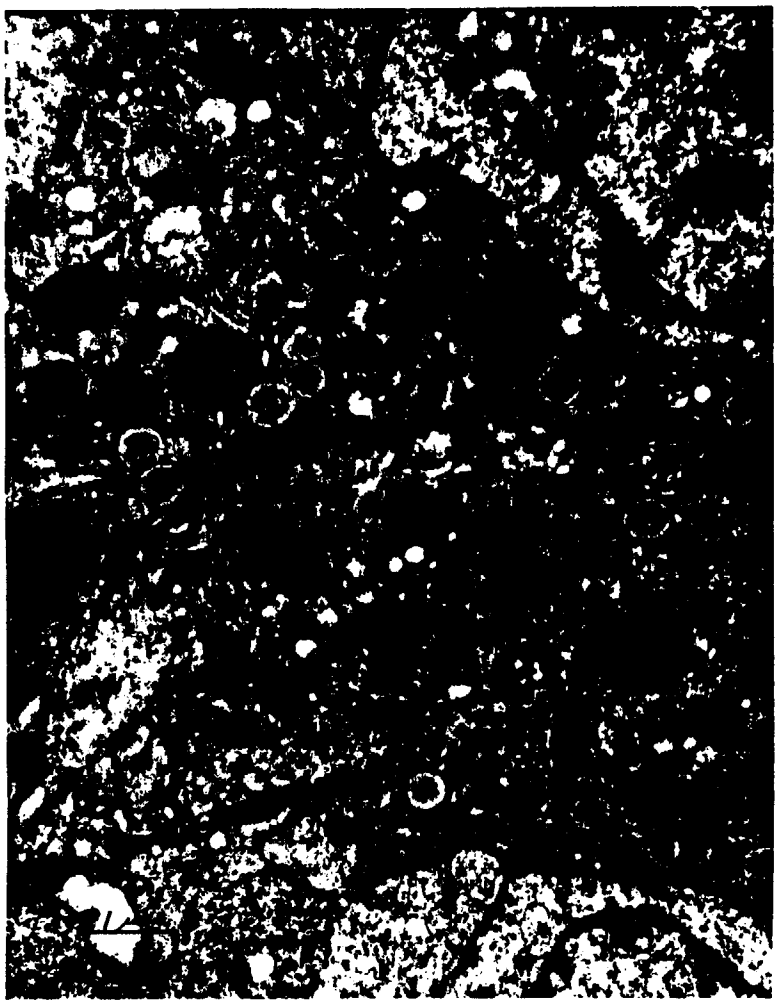

Fig. 81. Electron microscopic autoradiogram of leukemic AKR/J thymus. Note ^{67}Ga localization indicated by silver grains over cytoplasmic dense bodies.

1027415

INDUCED CYTOGENETIC ABNORMALITIES

The Cytogenetics group for its main goals has been attempting to characterize induced chromosomal abnormalities in leukocytes; we are seeking the mechanism of their induction, the methods of their removal, and the possible clinical implications of increased numbers of abnormal metaphases in the bone marrow or cultured from the blood.

Chromosome Changes After Radiation Accident

Chromosomal abnormalities have persisted in the peripheral blood leukocytes 126 months after accidental total-body irradiation (Kong-oo Goh and Eugene Joiner). In 1958, a group of eight men were accidentally exposed to total-body irradiation from fast neutrons and gamma rays. Chromosomal aberrations were found $2\frac{1}{2}$ years, $3\frac{1}{2}$ years (Bender, M. A. and Gooch, P. C. Radiat Res 18, 389, 1963), and 7 years (Goh, K. O. Radiat Res 35, 155, 1968) after the accident. We now report the chromosomal analyses of the cultured peripheral blood leukocytes of six of these men 126 months after the accident. The cultures were coded with 30 other cultures and analyzed blindly.

The modal chromosomal number was 46 which was seen in 75.6% of the 441 metaphases analyzed. Seventy-eight (17.9%) of these cells were abnormal and 50 (11.3%) were X_1 cells. Dicentric chromosomes were found in patients E and F and translocations in patients C, D, E, and F. Only patient E had 3 ring chromosomes. The smaller G chromosome, morphologically similar to the Ph^1 chromosome of chronic granulocytic leukemia, was found in patients B, C, and F. There were also many chromosomal breakages involving a G chromosome; clinically there is no evidence that any of these patients has chronic granulocytic leukemia. No correlation was found between the radiation exposure and the frequency of chromosomal aberrations. These findings indicate again that radiation can cause chromosomal breaks in human somatic cells and that it has a long-lasting effect.

Chromosomal breakages can be found in normal leukocytes cultured with the plasma or serum of patients 126 months after accidental total-body irradiation (Kong-oo Goh and Eugene Joiner). Metaphases with abnormal chromosomes and acentric fragments have persisted for years after the original radiation exposure. The explanation that has been given for this observation is that these cells were injured in the

predeoxyribonucleic acid synthesis (G_1) phase of their cell cycle at the time of the original irradiation and that they remained in this stage for a period of years and underwent mitosis in vitro after being stimulated by phytohemagglutinin (PHA) or other mitogenic substances. This suggestion could not explain several observations made in the cultures of the patients 7 years after total-body irradiation. Thus the possibility arose that a substance capable of affecting the chromosome for an extended time was produced or activated by total-body irradiation. In work reported earlier we tested this hypothesis by performing experiments in which normal leukocytes were cultured with autologous or homologous plasma and with plasma from the patients who had been irradiated (Radiat Res 35, 171, 1968). The results indicated that the plasma from the irradiated patients could induce chromosomal breakage in normal leukocytes. We have now completed chromosomal analyses of normal donors' leukocytes cultured in duplicate with the plasma and serum of the patients, 126 months after the accidental radiation exposure. Six (normal controls) cultures were made from the blood leukocytes of four women and one man with homolgous plasma. Twenty-four (experimental) cultures were also made from the leukocytes of these donors with the irradiated patients' plasma or serum obtained from freshly clotted blood. The cultures were coded and the metaphases were analyzed blindly. There were 28 (5.1%) abnormal metaphases of the 550 from the control cultures. The abnormalities were in the form of chromosomal breakages; no dicentrics, translocations, or ring chromosomes were seen. Since irradiated serum and irradiated plasma gave the same frequencies of chromosomal breakages in normal cells, these results were pooled. There were 248 (10.9%) abnormal metaphases in the 2275 analyzed, including 14 dicentrics, 11 translocations, 1 ring, and 15 small G chromosomes.

These findings support our original observations that the plasma of the accidentally irradiated men is capable of causing chromosomal breakages in normal cells 7 years after the accident. The factor causing the chromosomal breakage is also present in the serum and it has a long-lasting effect. Preliminary studies indicate that its effect is lost after storage at 0 to 5° C for 3 days and that it has no effect on chromosomes of cultured skin fibroblasts. An alternate view could be that irradiation produced an inhibitor to the healing process of normal lymphocyte chromosomes. This view would lead to the hypothesis that chromosomal breakages and healings are normal processes of lymphocytes in adapting to environmental changes or antigenic stimulation.

The results of chromosomal analyses have been completed in 14 patients with leukemia, polycythemia vera, or lymphoma treated with total-body irradiation (Kong-oo Goh and Margo Steinman). The dosages were from 50 R to 353 R and the dose rate was between 1.4 and 2.0 R/min. Four patients had acute leukemia (AL); two, polycythemia vera (PV); two, chronic granulocytic leukemia (CGL); three, lymphosarcoma (LSA); one, chronic lymphocytic leukemia (CLL); one, reticulum cell sarcoma (RCS); and one, multiple myeloma (MM). The youngest was a 6-year-old boy with AL and the oldest, an 88-year-old man with CGL. Eight patients did not receive any anticancer treatment before the chromosomal studies.

1027416

The phytohemagglutinin-stimulated blood leukocytes were cultured before and at various intervals after total-body irradiation. Colcemide was added during the last hour of incubation to arrest mitosis at metaphase. The cells were exposed to hypotonic solution, fixed, and prepared for chromosomal analyses. When possible, 100 metaphases per culture were analyzed. The results of these studies were obtained from the analyses of 4724 metaphases from 74 cultures. Increased chromosomal breakages were found in eight previously untreated patients after total-body irradiation. Of six previously treated patients, three did not have increased chromosomal breakages after total-body irradiation. These three patients had chronic myeloproliferative disorders (two, PV; one, CGL). They had been treated with ^{32}P, total-body irradiation, busulfan or combinations of these. A further increase of chromosomal breakages was found after total-body irradiation in three other previously treated patients who had been given a combination of local irradiation, Prednisone, Methotrexate, vincristine, and Alkeran. Two of these patients have AL and one has MM.

Blood leukocytes were cultured 30 min after total-body irradiation in six patients; in three, increased chromosomal breakages were seen. However, in the other three no mitoses were found in one culture, only seven metaphases in another, and no increase in chromosomal breakages in the third. In this small series no direct correlation was found between the dosages of total-body irradiation and the frequency of chromosomal breakages. The frequencies of chromosomal breakages in this group of patients apparently depend on the patient's primary disease, his previous treatment, and the dose of irradiation.

We have been able to study the chromosomes of a child who has presumably an induced congenital hypothyroidism from ^{131}I therapy given to his mother (Kong-oo Goh and Eugene Joiner). Blood was drawn from the child on two occasions, at age $5\frac{1}{2}$ and 7 for chromosomal and autoradiographic studies. The mother's peripheral blood leukocytes were also cultured for chromosomal studies. The boy has had thyroid replacement therapy since the diagnosis of hypothyroidism at the age of 8 months. As in other reports we found abnormal chromosomes and chromosomal breakages (12%) in the metaphases from the mother who when pregnant received 99 millicuries of ^{131}I for the treatment of thyroid carcinoma. Occasionally similar chromosomal abnormalities were found in the peripheral blood of the child; we also found a D chromosome that had a longer short-arm than any chromosomes of its group in all the metaphases that were karyotyped (Fig. 82).

After terminal labeling of the culture with tritiated thymidine, the silver-grain pattern of the long arm of this abnormal D is similar to that of a normal chromosome 15 (Table 47). Although the origin of the additional chromatin in the short arm of this abnormal chromosome remains undetermined, it could be the result of a reciprocal translocation from any of the chromosomes of a metaphase or an additional duplication of the short arm of a 15 chromosome. Either of these mechanisms could produce a heavily labeled silver-grain pattern with the short arm of this abnormal chromosome found in several metaphases. Furthermore, either of these mechanisms could be the result of the intra-uterine irradiation by ^{131}I.

TABLE 47

Silver-Grain Patterns* of Chromosome 13, 14, 15, from the Abnormal D Chromosome in Terminal-Labeled Metaphases Exposed in Utero to ^{131}I

Metaphases	13		14		15		Abnormal†
1	3+	3+	2+	2+	+		+
2‡	2+	2+	+	+	+		+
3	3+	3+	2+	2+	+		0
4	3+	3+	3+	3+	2+		2+
5	3+	3+	3+	3+	+		+
6	3+	3+	2+	2+	+		+
7‡	2+	2+	+	+	+		+
8	3+	3+	2+	2+	+		+
9	3+	3+	2+	2+	+		+
10	3+	3+	2+	2+	+		+
11	3+	3+	2+	2+	+	+	+§
12	3+	3+	2+	2+	2+		+
13	3+	3+	2+	2+	0		+

* The labeling patterns are scored as 3+ (total chromosome heavily labeled), 2+ (segment heavily labeled or total chromosome moderately labeled), and + (slightly segmentally labeled).
† The labeled patterns of the short arm are excluded from the scoring.
‡ Chromosomes 14 and 15 have the same labeling patterns.
§ This is a 47-chromosome trisomy D metaphase.

Chromosomes in Reticulum Cell Sarcoma

The cytogenetics group has continued its work on chromosomal abnormalities in human neoplasms. Chromosomal abnormalities may be found in metaphases from certain human cancer tissue, and the evidence suggests that these metaphases may represent the cancer cells. If so, we should be able, using these abnormal chromosomes as markers, to study the distribution of the cancer cells. We have studied the chromosomal patterns of the lymph node, bone marrow, and peripheral blood leukocytes of two untreated patients with reticulum cell sarcoma (Kong-oo Goh and Eugene Joiner). The metaphases were obtained from direct preparations or cultured cells. Table 48 summarizes the results of the chromosomal analyses of these two patients. An abnormally large acrocentric chromosome was found in 128 (80.5%) of the 159 metaphases obtained from direct preparations of lymph node of one patient and in 113 (88%) of the 128 metaphases of the other. No abnormal chromosomes were found in a second lymph node biopsy of the first patient, a normal lymph node. In the direct bone-marrow preparations, one metaphase that has the abnormal chromosome was found in the first patient, and none in the second. One metaphase that had the abnormal chromosome was found in peripheral blood cultures from each patient. The blood leukocytes

1027417

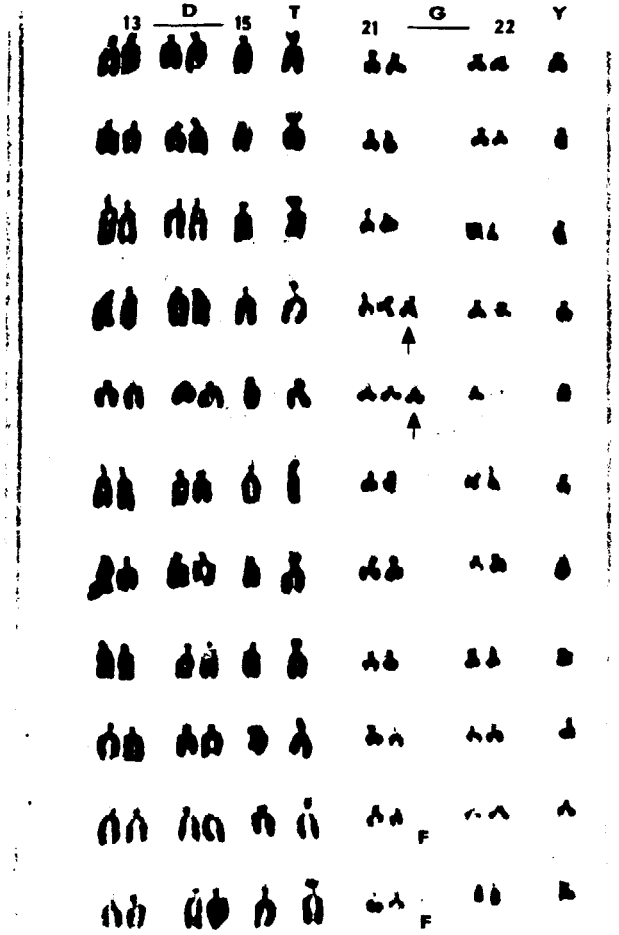

Fig. 82. Partial karyotypes of 11 metaphases from a child exposed in utero to ^{131}I showing D, G, abnormal D (T) and the Y chromosomes. Two of these metaphases have an additional G chromosome (arrowed) and two have a small fragment (F).

were cultured in the presence of phytohemagglutinin (PHA). The frequency of the abnormal chromosome decreased in the lymph-node cultures in the presence of the PHA. In the second patient no metaphase containing the abnormal chromosome was found after 6 days of in vitro incubation of lymph-node cells in the presence of PHA. These findings lead us to conclude: (1) not all cells in the reticulum cell sarcoma lymph node are diseased cells; (2) the disease does

indeed originate in the lymph node; (3) not all the lymph nodes are diseased; and (4) PHA may suppress the proliferation of the diseased cells in vitro besides stimulating the proliferation of normal lymphocytes.

Chromosomes in Women Taking Oral Contraceptives

The study of chromosome breaks in women taking oral contraceptives is well under way (Gayle Littlefield, Kong-oo Goh, and Mary Beth Klepper). Numerous physical, chemical, and biologic agents are known to produce chromosome breakage in vivo, in vitro, or both. A pilot study conducted by Goh suggested that the number of aberrant lymphocyte chromosomes is increased in women who are taking various types of oral contraceptive medications. A protocol has been designed to determine the range and variation in frequency of abnormal chromosomes in a larger group of oral contraceptive users, and in a larger group of female and male control subjects. Heparinized blood samples have been obtained from women who are taking oral contraceptives and from female and male control subjects at regular intervals of 4 to 5 weeks. Three-day lymphocyte cultures are done on each blood sample and 100 well-spread metaphases are counted and analyzed from each coded culture. All metaphases are examined for the following lesions: (1) chromatid/isochromatid gaps-achromatic lesions of one or both chromatids without displacement of the distal chromatin segment; (2) chromatid/isochromatid breaks -- achromatic lesions of one or both chromatids with displacement of the distal chromatin segment (Fig. 83-A); (3) fragments -- acentric chromosomal pieces that are not directly associated with the parent chromosome (Fig. 83-B); (4) translocated chromosomes (Fig. 84-A); (5) chromosomes with deletions (including the smaller G chromosome) (Fig. 84-A); (6) multicentric chromosomes (Fig. 84-B); (7) pulverized chromosomes (Fig. 84-B); and (8) ring chromosomes. Any metaphase having one or more defined chromosomal lesions with the exception of the chromatid/isochromatid gap is considered abnormal. Any metaphase having an aberration indicating that the cell is in its first generation post injury is designated as an X_1 cell. (All questionable metaphases are re-evaluated, either by reference to photographic enlargements, or by karyotypic analysis.)

To date, we have cultured lymphocytes from 245 blood samples, and microscopically analyzed over 19,000 metaphases. We have performed preliminary statistical evaluation of data from the first 123 completed cultures in this series. Of the 123 cultures, 34 were obtained from six female controls, 40 from seven male controls, and 49 from eight women who are taking oral contraceptive medications. All data were decoded and placed in one of three groups, i.e., male controls, female controls, or female subjects taking oral contraceptive medications. Data were pooled for each group. At this stage of the study no attempt has been made to correlate the type, dosage, or duration of treatment on breakage frequencies in women who are taking oral contraceptives, nor have we evaluated the effects of recorded illnesses on chromosome breakage in specific cultures. These considerations are obviously important and will be pursued after sufficient numbers of samples have been collected from each subject

1027118

TABLE 48

Distribution of Abnormal Chromosomes in Two Cases of Reticulum Cell Sarcoma

	<45		45		46		47		>47		Abn. *		Pseudo.*		Somal Break*	
	No.	%	No.	%	No.	%	No.	%	No.	%	Total No.	%	No.	%	No.	%
Case 1																
First Lymph Node																
Direct †							14.5				159	128	80.5		-	
Culture (45D) ‡	4	0		8	32		0		135	52	25	3	12		-	2 8
Bone Marrow																
Direct	1	1	1.4	63	89	3	4.2	3	4.2		71	1	1.4	9	14.3	1 1.4
Culture + PHA ‖ (3D)	1	3	5	54	90	1	1.7	1	1.7		60	0		1	1.7	1 1.7
Peripheral Blood + (3D)	1	4	7.1	49	87	1	1.8	1	1.8		56	1	1.8	0		3 5.4
Second Lymph Node																
Direct	0	1		14	87	1		0			16	0		0		2 14.3
Case 2																
Lymph Node																
Direct	4	4	3.1	21	16	90	70	9	7		128	113	88	6	29	22 17
Culture + PHA (3D)	7	3	8.1	13	35	12	32	2	5.4		37	15	40	2	15	5 13.5
Culture (3D)											19	18	95			
Culture + PHA (6D)	5	4	8.0	38	76	1	2	2	4.0		50	0		1	2.6	8 16
Peripheral Blood																
Culture + PHA (3D)	4	2	6.0	27	82	0		0	-		33	1	3	3	9	5 15
Culture + PHA (6D)	3	1	4.5	22	79	1		1	-		28	0		1	4.5	1 3.5
Bone Marrow																
Direct	1	1	4.8	12	57	-		7	33		21	0		2	16	0
Culture + PHA (3D)	2	4	18.0	13	59	1		1			22	0		3	13.5	0
Culture + PHA (6D)	3	1	4.2	19	80	1		0			24	0		1	5	1 5

Abn = Metaphases with abnormally large acrocentric chromosome
Pseudo. = Metaphases with a diploid chromosomal number, but, with one or more missing or additional chromosomes or both, in one or more of the seven major chromosomal groups.
Somal Break = Chromosomal break

† Reported previously
‡ (45D) = 45-day culture, etc.
§ Ten of these metaphases are tetraploid.
‖ Phytohemagglutinin was added in the culture medium.

to allow for meaningful subgrouping of cultures. Two criteria were used in the data evaluations: the total number of abnormal cells (cells that contain one or more abnormal chromosomes), and the total number of X_1 cells (cells that contain fragments). Detailed evaluation of specific chromosomal lesions and the frequency of breakage in

Fig. 83. A. Metaphase and karyotype from an oral contraceptive user. Note the isochromatid break of the long arms of a Group C chromosome.
B. Metaphase and karyotype from an oral contraceptive user. Shown are an extra submetacentric chromosome and a fragment, which were probably derived from the missing number 2 chromosome.

1027419

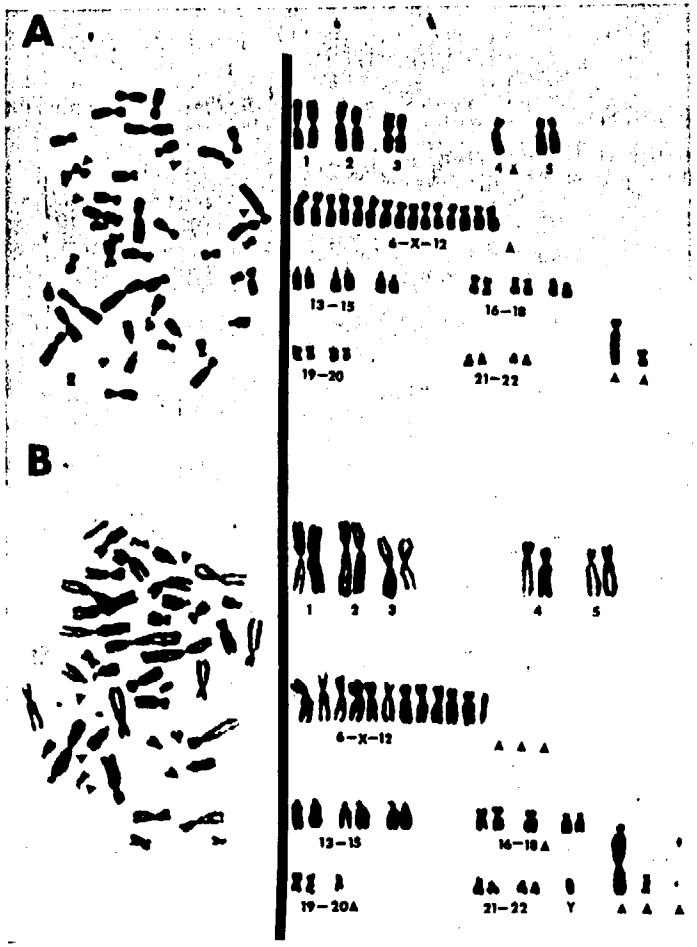

Fig. 84. A. Metaphase and karyotype from an oral-contraceptive user. A number 4 chromosome and a chromosome from Group C are missing. The two abnormal chromosomes shown at the bottom of the karyotype were probably formed as the result of a deletion of a portion of the long arms of the C chromosome, and a translocation of this segment to the long arms of the B chromosome.
B. A heavily damaged metaphase from a male control. Three Group C chromosomes, one Group E, and one Group F are missing. Two dicentric chromosomes and one pulverized chromosome are shown. Each dicentric chromosome was presumably formed by the breakage and rejoining of two of the four missing chromosomes. The fifth missing chromosome is probably represented in part by the pulverized chromatin material at the far right of the karyotype.

TABLE 49

Preliminary Data Based on Total Abnormal Metaphases Compared with Data Based on X_1 Cells Only

	Female Control		Male Control†		Experimental	
Number of cultures studied	34		36		49	
Number of metaphases analyzed	3,400		3,600		4,900	
Number of abnormal metaphases	201	(154)*	200	(159)	428	(371)
Range of abnormal metaphases	2-20	(1-11)	1-12	(1-10)	1-23	(1-19)
Mean of abnormal metaphases	5.91	(4.52)	5.55	(4.44)	8.73	(7.57)
Standard deviation from mean	3.66	(2.83)	2.89	(2.44)	4.69	(4.06)
Standard error of mean	0.62	(0.48)	0.48	(0.40)	0.67	(0.58)

* Numbers in parentheses refer to data based on X_1 cells only.
† Four cultures from one male control not included because of questionable marker chromosome.

specific groups of chromosomes will be performed later. The data are presented in Table 49.

Several observations are pertinent. The women taking oral contraceptives display a rather high standard deviation from the mean, reflecting possibly a significant variability in the response of specific individuals to the medication. In five the average percentage of abnormal cells was greater than 8%, while the highest control value was 7.5% abnormal cells. However in series of cultures from two women taking oral contraceptives, the average percentage of abnormal cells was 6.1% and 6.7%. These values were within the range of the higher control values. The breakage frequencies in cultures from male controls exceed those normally obtained in our laboratory. Our methods of obtaining samples at specific intervals do not allow us to exclude subjects who have recently had infections or inoculations. Health reports are remitted by each control and experimental subject at the time of blood collection. These reports will be essential in the final data analyses as we consider increased breakages on specific culture dates. Since each participant enrolled in this project will be

1027420

studied for approximately 24 months, we hope to obtain important information about the variations in chromosome breakage in both normal persons and women who are taking oral contraceptives.

RAPID EFFECTS OF INSULIN ON THE HYPOTHALAMIC SATIETY CENTER

Gold thioglucose administered intraperitoneally to mice results in necrosis of a portion of the hypothalamus. It is generally believed that the affected area of the hypothalamus controls feeding because obesity, caused by hyperphagia, occurs after gold thioglucose administration. The affected area has been called the "satiety center." In previous studies we established that in diabetic mice gold thioglucose does not produce necrosis of the satiety center (Amer J Physiol 214, 652, 1968).

This past year we collaborated with Dr. Albert F. Debons and his group* to investigate the sensitivity of the hypothalamic satiety center to gold thioglucose when the blood insulin levels were varied (Roger J. Cloutier, Evelyn E. Watson, and Albert F. Debons). Changes in insulin levels were produced with anti-insulin serum and by inducing diabetes with alloxan. The experiments showed that the sensitivity of the satiety center to gold thioglucose damage, even in diabetic mice, can be rapidly restored by the injection of insulin just before the gold thioglucose injection (Fig. 85). The satiety center was less sensitive

* State University of New York, Downstate Medical Center, Brooklyn, New York.

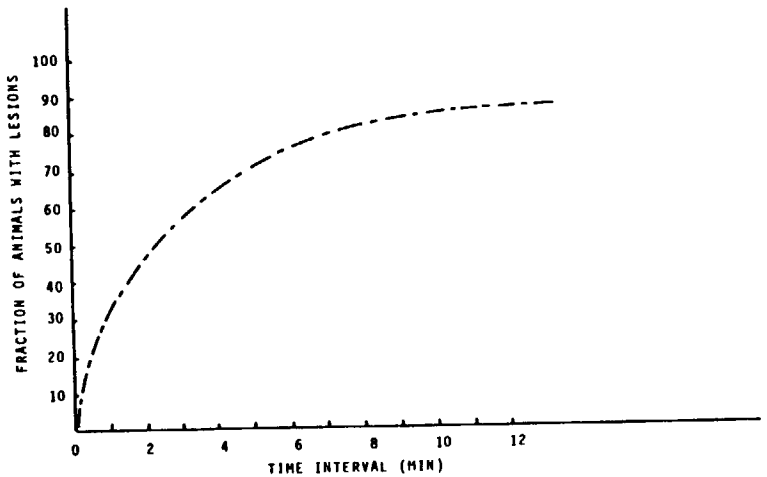

Fig. 85. Time interval between injection of insulin and gold thioglucose into diabetic mice.

to damage when the gold thioglucose injection preceded the insulin injection (7).

These studies are possible because neutron activation analysis permits the detection of the small quantities of gold (fractions of micrograms) in the hypothalamus. However, to prevent damage of the tissues an irradiation facility is required where the irradiation is performed at approximately room temperature. The Low Intensity Test Reactor (LITR) at Oak Ridge National Laboratory (ORNL) was used with satisfactory results for several years until it was closed down in 1968. Since that time the tissues have been irradiated in the ORNL Bulk Shielding Reactor. The relatively short half-life of the radioactive gold-198 (2.7 days) necessitates rapid analysis of the samples. Because the Medical Division is near the ORNL reactors and has the trained personnel and the equipment to analyze the radioactive samples, we have collaborated with Dr. Debons on these studies since 1964.

HEMODIALYSIS CANCER THERAPY–COLLABORATIVE PROJECT WITH ORNL

During the last six months of 1969 the Medical Division had Dr. Jere M. Bauer as a visiting investigator who was on sabbatical from the University of Michigan, where he is an Associate Professor in the Department of Internal Medicine. Working with Dr. Bauer as research associate was Mr. Frank Nakamura, who is also from the University of Michigan.

Their work was on hemodialysis against specific enzymes with the objective of creating a deficiency of a specific amino acid. Since most enzymes are large molecules, they do not pass into the blood, but the amino acids move through the membrane and are broken down; thus a sump effect is created for the amino acid. The major initial objective is to try to inhibit certain tumors by depriving them of a nutritional element known to be specifically needed for their growth. This project originated in the work of Dr. Stanfield Rogers, of the Biology Division of Oak Ridge National Laboratory, who requested that the Medical Division pursue this work with an aim to developing it for human trials. Dr. Bauer's work involved additional collaboration with Drs. James Regan and Conrad Richter of the Biology Division, and help and support from the administrative staff of ORNL.

Asparaginase was selected as the enzyme for first study, since it is known to inhibit growth of some neoplasms. It might also illustrate the value of this approach in that when it is injected directly into patients it sometimes causes serious toxic reactions.

Certain technical problems in dialyzing dogs and rats were solved. With the small-sized artificial kidney available, it was possible to achieve only slight reduction of blood asparagine levels in the dog. There was ample evidence that significant quantities of the amino acid were being removed, but presumably homeostatic mechanisms caused increased synthesis, which tended to compensate for removal. The

1027421

asparaginase preparation available also had glutamase activity resulting in some removal of glutamine from the blood.

Conclusions at this stage are as follows:

1) Work to date with hemodialysis against L-asparaginase indicates that the enzyme will completely destroy all asparagine (and glutamine) entering the dialysis bath.

2) The creation of such an infinite concentration gradient between plasma and dialyzate for a particular amino acid establishes the conditions for continued removal of a selected amino acid.

3) The advantage of this closed-circuit hemodialysis system lies in the selective nature of amino acid removal as opposed to the loss of all amino acids (including essential ones) in the conventional single-pass hemodialysis system. By limiting the amino acid loss to a single, non-essential amino acid, the stimulus to general mobilization of amino acids from tissue stores is avoided. Under these circumstances it may be easier to defeat the de novo synthesis and other homeostatic mechanisms that maintain the plasma level of a given amino acid.

4) Ultimate success in decreasing the plasma level of L-asparagine by this method will depend on increasing the absolute amount of L-asparagine passing from plasma into the dialysis bath. This can be done by enlarging the membrane surface area and increasing the rate of blood flow through the dialyzer.

5) Hemodialysis in the rat is feasible, but requires great care in placement of the arterial and venous catheters and in preventing excessive loss of body water through ultrafiltration.

1027422

PUBLICATIONS

From the Medical Division
Oak Ridge Associated Universities
1969

Reprints from the open literature and additional information on publications can be obtained by writing Mrs. Edward H. Anderson, Technical Editor, Medical Division, Oak Ridge Associated Universities, P. O. Box 117, Oak Ridge, Tennessee 37830. Complete lists of Medical Division publications are available.

PUBLICATIONS IN JOURNALS

1. Anderson, R. E., Cumming, R. B., Walton, M., and Snyder, F. Lipid metabolism in cells grown in tissue culture: O-alkyl, O-alk-1-enyl, and acyl moieties of L-M cells. Biochim Biophys Acta 176, 491-501, 1969.

2. Anderson, R. E., Garrett, R. D., Blank, M. L., and Snyder, F. The quantitative production of aldehydes from O-alk-1-enyl glycerols. Lipids 4, 327-330, 1969.

3. Anderson, R. E. and Snyder, F. Quantitative collection of $^{14}CO_2$ in the presence of labeled short-chain acids. Anal Biochem 27, 311-314, 1969.

4. Arimizu, N. and Morris, A. C., Jr. Quantitative measurement of radioactivity in internal organs by area scanning. J Nucl Med 10, 265-269, 1969.

5. Blank, M. L. and Snyder, F. The preparation of alkyl-1, 2 diols and their chromatographic behavior in relation to O-alkyl-glycerols. Biochim Biophys Acta 187, 154-156, 1969.

6. Cotman, C., Blank, M. L., Moehl, A., and Snyder, F. Lipid composition of synaptic plasma membranes isolated from rat brain by zonal centrifugation. Biochemistry 8, 4606-4612, 1969.

7. Debons, A. F., Krimsky, I., From, A., and Cloutier, R. J. Rapid effects of insulin on the hypothalmic satiety center. Amer J Physiol 217, 1114-1118, 1969.

8. Edwards, C. L. and Hayes, R. L. Tumor scanning with ^{67}Ga citrate. J Nucl Med 10, 103-105, 1969.

9. Gengozian, N. Marmosets: Their potential in experimental medicine. Ann N Y Acad Sci 162, No. 1, 336-362, 1969.

10. Gengozian, N., Batson, J. S., Greene, C. T., and Goslee, D. G. Hemopoietic chimerism in imported and laboratory-bred marmosets. Transplantation 8, 633-652, 1969.

11. Gengozian, N., Carlson, D. E., and Allen, E. M. Transplantation of allogeneic and xenogeneic (rat) marrow in irradiated mice as affected by radiation exposure rates. Transplantation 7, 259-273, 1969.

12. Gengozian, N. and Congdon, C. C. Effect of syngeneic anti-lymphocyte serum on rat-mouse radiation chimeras. Transplant Proc 1, 34-38, 1969.

13. Goh, K. O. Exogenous deoxyribonucleoside triphosphates: Their effect on pulverized human chromosomes at the G_2 phase. Proc Soc Exp Biol Med 131, 942-946, 1969.

14. Harlow, R. D., Lumb, R. H., and Wood, R. Insect lipids: Carbon number distribution of triglycerides in five species. Comp Biochem Physiol 30, 761-769, 1969.

15. Hartman, R. E. and Hayes, R. L. The binding of gallium by blood serum. J Pharmacol Exp Therap 168, 193-198, 1969.

16. Hübner, K. F. and Gengozian, N. Critical variables of the Jerne plaque technique as applied to rodent antibody-forming systems responding to heterologous red cell antigens. J Immunol 102, 155-167, 1969.

17. Humason, G. L. and Lushbaugh, C. C. Sirius supra blue FGL-CF; Superior to analine blue in the combined elastin, reticulum, and collagen stain. Stain Technol 44, 105-106, 1969.

18. Kniseley, R. M., Andrews, G. A., Edwards, C. L., and Hayes, R. L. Bone-marrow and skeletal scanning. Radiol Clin N Amer 7, 265-280, 1969.

19. Lee, T-c., Swartzendruber, D. C., and Snyder, F. Zonal centrifugation of microsomes from rat liver: Resolution of rough-and-smooth-surfaced membranes. Biochem Biophys Res Commun 36, 748-755, 1969.

20. Lozzio, B. B. and Comas, F. V. Biological effects of pokeweed mitogen. Int Arch Allergy 36, 266-281, 1969.

21. Lushbaugh, C. C., Haines, E. L., Davis, H. T., and Bibler, D. S. Power spectrum of the impedance pneumograph: A data reduction system producing an analytical parameter of potential clinical usefulness. Aerospace Med 40, 425-429, 1969.

22. Lushbaugh, C. C., Humason, G., and Gengozian, N. Intra-uterine death from congenital Chagas' disease in laboratory-bred marmosets (Saguinus fuscicollis lagonatus). Amer J Trop Med Hyg 18, 662-665, 1969.

23. Ma, B. I., Swartzendruber, D. C., and Murphy, W. H. Detection of virus-like particles in germinal centers of normal guinea pigs. Proc Soc Exp Biol Med 130, 586-590, 1969.

24. Mardon, D. N. and Balish, E. Modifications in a French pressure cell-laboratory press system. Appl Microbiol 17, 777, 1969.

25. Piantadosi, C., Snyder, F., and Wood, R. Synthesis of ^{35}S- and ^{14}C-labeled glyceryl thioethers. J Pharm Sci 58, 1028-1029, 1969.

26. Porter, R. P. and Gengozian, N. Immunological tolerance and rejection of skin allografts in the marmoset. Transplantation 8, 653-665, 1969.

27. Regan, J. D., Vodopick, H., Takeda, S., Lee, W. H., and Faulcon, F. M. Serine requirement in leukemic and normal blood cells. Science 163, 1452-1453, 1969.

28. Snyder, F. L. A review of instrumentation and procedures for ^{14}C and ^{3}H radioassay by thin-layer and gas-liquid chromatography. Isotop Radiat Technol 6, 381-400, 1969.

29. Snyder, F. and Blank, M. L. Relationships of chain lengths and double bond locations in O-alkyl, O-alk-1-enyl, acyl, and fatty alcohol moieties in preputial glands of mice. Arch Biochem Biophys 130, 101-110, 1969.

30. Snyder, F., Blank, M. L., and Morris, H. P. Occurrence and nature of O-alkyl and O-alk-1-enyl moieties of glycerol in lipids of Morris transplanted hepatomas and normal rat liver. Biochim Biophys Acta 176, 502-510, 1969.

31. Snyder, F., Malone, B., and Blank, M. L. The biosynthesis of alkyl glyceryl ethers by microsomal enzymes of digestive glands and gonads of the Starfish, Asterias forbesi. Biochim Biophys Acta 187, 302-306, 1969.

32. Snyder, F., Malone, B., and Wykle, R. L. The biosynthesis of alkyl ether bonds in lipids by a cell-free system. Biochem Biophys Res Commun 34, 40-47, 1969.

33. Snyder, F. and Moehl, A. Use of liquid scintillation quenching to quantitate lipid mass. Anal Biochem 28, 503-509, 1969.

34. Snyder, F., Piantadosi, C., and Wood, R. The metabolism of glyceryl thioethers. Proc Soc Exp Biol Med 130, 1170-1174, 1969.

1027423

35. Snyder, F. and Wood, R. Alkyl and alk-1-enyl ethers of glycerol in lipids from normal and neoplastic tumor tissues. Cancer Res 29, 251-257, 1969.

36. Snyder, F., Wykle, R. L., and Malone, B. A new metabolic pathway: Biosynthesis of alkyl ether bonds from glyceraldehyde-3-phosphate and fatty alcohols by microsomal enzymes. Biochem Biophys Res Commun 34, 315-321, 1969.

37. Vodopick, H. A., Rupp, E. M., and Gengozian, N. The bidirectional in vitro mixed leukocyte reaction: A mutual inhibitory phenomenon? Transplantation 7, 155-164, 1969.

38. Watson, E. E., Cloutier, R. J., and Berger, J. D. Tritium concentrations in neutron generator pump oil. Health Physics 17, 739-740, 1969.

39. Wood, R., Baumann, W. J., Snyder, F., and Mangold, H. K. Gas-liquid chromatography of dialkyl, alkyl acyl, and diacyl derivatives of glycerol. J Lipid Res 10, 128-131, 1969.

40. Wood, R. and Harlow, R. Gas-liquid chromatographic analysis of free long-chain aldehydes. J Lipid Res 10, 463-465, 1969.

41. Wood, R. and Harlow, R. D. Structural analyses of rat liver phosphoglycerides. Arch Biochem Biophys 135, 272-281, 1969.

42. Wood, R. and Harlow, R. D. Structural studies of neutral glycerides and phosphoglycerides of rat liver. Arch Biochem Biophys 131, 495-501, 1969.

43. Wood, R., Harlow, R. D., and Lambremont, E. N. GLC analysis of Heliothis virescens triglycerides at various metamorphic stages. Lipids 4, 159-162, 1969.

44. Wood, R., Harlow, R. D., and Snyder, F. Alkyl and alk-1-enyl glyceryl ethers derived from various rat tissue phospholipids. Biochim Biophys Acta 176, 641-643, 1969.

45. Wood, R., Piantadosi, C., and Snyder, F. Quantitative analysis and comparison of the physical properties of O-alkyl and S-alkyl ethers of glycerol. J Lipid Res 10, 370-373, 1969.

46. Wood, R. and Snyder, F. Tumor lipids: Metabolic relationships derived from structural analyses of acyl, alkyl, and alk-1-enyl moieties of neutral glycerides and phosphoglycerides. Arch Biochem Biophys 131, 478-494, 1969.

47. Wykle, R. L. and Snyder, F. The glycerol source for the biosynthesis of alkyl glyceryl ethers. Biochem Biophys Res Commun 37, 658-662, 1969.

1027424

GOVERNMENT DOCUMENTS

48. Kakehi, H., Gibbs, W. D., and Hayes, R. L. Counting characteristics of a medium-level whole-body counter. USAEC Report ORAU-108, August 1969, 29 pp.

CHAPTERS IN BOOKS AND SYMPOSIUM PROCEEDINGS

49. Andrews, G. A., Balish, E., Edwards, C. L., Kniseley, R. M., and Lushbaugh, C. C. Possibilities for improved treatment of persons exposed in radiation accidents. In: Handling of Radiation Accidents, International Atomic Energy Agency, Vienna, 1969, pp. 119-135.

50. Arimizu, N., Kakehi, H., and Morris, A. C., Jr. Area scanning for quantitative measurement of radioactivity in internal organs. In: Medical Radioisotope Scintigraphy, Vol. I., Vienna, International Atomic Energy Agency, 1969, pp. 653-663.

51. Gibbs, W. D. and Lushbaugh, C. C. Whole-body counter systems. In: Handbook of Radioactive Nuclides. Yen Wang, ed. Cleveland, Ohio, Chemical Rubber Co., 1969, pp. 134-140.

52. Lushbaugh, C. C. Reflections on some recent progress in radiation biology. In: Advances in Radiation Biology, Vol. 3, New York, Academic Press, 1969, pp. 277-313.

53. Lushbaugh, C. C. Theoretical and practical aspects of models explaining "gastrointestinal death" and other lethal radiation syndromes. In: Comparative Cellular and Species Radiosensitivity. V. P. Bond and T. Sugaharo, eds. Tokyo, Igaku Shoin, Ltd., 1969, pp. 288-297.

54. Snyder, F. The biochemistry of lipids containing ether bonds. In: Progress in the Chemistry of Fats and Other Lipids. Vol. 10, Part 3. Ralph T. Holman, ed. Oxford and New York, Pergamon Press, 1969, pp. 287-335.

55. Snyder, F. Ether-linked lipids in neoplasms of man and animals: Methods of measurement and the occurrence and nature of alkyl and alk-1-enyl moieties. In: Advances in Experimental Medicine and Biology. Vol. 4, Drugs Affecting Lipid Metabolism. New York, Plenum Press, 1969, pp. 609-621.

56. Swartzendruber, D. C. Localization of C-type viruses in preleukemic AKR mouse spleen. In: Proceedings 27th Annual Meeting, Electron Microscopy Society of America. Claude J. Arceneaux, ed. Baton Rouge, La., Claitor's Publishing Division, 1969, pp. 386-387.

57. Swartzendruber, D. C., Ma, B. I., and Murphy, W. H. Detection of virus particles in lymphatic tissue germinal centers. In: Second International Conference on Germinal Centers of Lymphatic Tissue, Plenum Press, N. Y., 1969, pp. 203-210.

PUBLISHED ABSTRACTS

58. Balish, E. and Pearson, T. A. Studies on the bacterial flora of three men accidentally exposed to total-body irradiation. Radiat Res 39, 525-526, 1969, abstr. Fb-1.

59. Barclay, T. R. and Morris, A. C., Jr. On-line computer interfacing of an analytrol film reader for measuring size of radioactive colloid particles. J Nucl Med 10, 387, 1969.

60. Blank, M. L. and Snyder, F. The occurrence of fatty alcohols in normal tissues and neoplasms. J Amer Oil Chem Soc 46, 1969. Program of Meeting, abstr. 139.

61. Carlson, D. E. The radiation exposure-rate effect: Action upon the immune response in mice. Diss abstr 29, 4040B, 1969.

62. Comas, F. V., Andrews, G. A., and Edwards, C. L. Changes in leucocyte values in patients with chronic granulocytic leukemia receiving spleen irradiation. Radiat Res 39, 491, 1969, abstr. De-1.

63. Edwards, C. L. and Hayes, R. L. Scanning tumors of soft tissue and bone with ^{67}Ga-citrate. J Nucl Med 10, 332, 1969.

64. Gibbs, W. D., Hodges, H. D., Queener, R. F., and Lushbaugh, C. C. Improvement in accuracy of whole-body radioisotope quantitation by the scatter-window method. J Nucl Med 10, 335, 1969.

65. Goswitz, F. A., Vodopick, H., and Clevenger, M. Blood lymphocyte kinetics in patients with chronic lymphocytic leukemia (CLL). J Nucl Med 10, 404, 1969.

65 a. Goswitz, F. A., Edwards, C. L., Wright, M. F., and Clevenger, M.: Value of radioisotopic tests in primary myelofibrosis. Southern Med J 62, 1431, 1969.

65 b. Goswitz, F. A., Vodopick, H., and Clevenger, M: The need to measure red-cell mass and plasma volume independently in patients with hematologic disorders. Southern Med J 62, 1431-1432, 1969.

10274 25

66. Hayes, R. L., Byrd, B. L., Carlton, J. E., Nelson, B., and Swartzendruber, D. C. Studies of the concentration of gallium in soft-tissue tumors. S Med J 62, 1432, 1969.

67. Hayes, R. L., Carlton, J. E., and Byrd, B. L. Localization of ^{67}Ga in soft-tissue tumors in experimental animals. J Nucl Med 10, 406, 1969.

68. Hodges, H. D., Edwards, C. L., Lushbaugh, C. C., and Gibbs, W. D. Whole-body ^{131}I retention as a quantitative measure of thyroid function. J Nucl Med 10, 459, 1969.

69. Lushbaugh, C. C. and Auxier, J. Reestimation of human LD_{50} radiation levels at Hiroshima and Nagasaki. Radiat Res 39, 526, 1969, abstr. Fb-2.

70. Snyder, F. Enzymic pathways for the biosynthesis and biocleavage of alkyl glyceryl ethers. J Amer Oil Chem Soc 46, 1969. Program of Meeting, abstr. 115.

71. Snyder, F., Blank, M. L., Soodsma, J., and Morris, H. P. Occurrence and enzymatic cleavage of glyceryl ethers in Morris transplanted hepatomas and normal rat liver. Proc Amer Ass Cancer Res 10, 84, 1969.

72. Snyder, F., Malone, B., and Soodsma, J. Metabolism of long-chain fatty alcohols: Formation of waxes and glyceryl ethers. J Amer Oil Chem Soc 46, 1969. Program of Meeting, abstr. 9.

73. Snyder, F., Wykle, R. L., and Malone, B. The biosynthesis of alkyl ether bonds in lipids from glyceraldehyde-3-phosphate and fatty alcohols by microsomal enzymes. Fed Proc 28, 595, 1969.

74. Vodopick, H., Rupp, E. M., Comas, F. V., Goswitz, F. A., and Edwards, C. L. ^{32}P-DFP leukokinetic study of the mechanisms of splenic irradiation in CGL. J Nucl Med 10, 449, 1969.

75. Wood, R. and Harlow, R. D. Metabolic relations derived from structural analyses of neutral glycerides and phosphoglycerides. J Amer Oil Chem Soc 46, 1969, Program of Meeting, abstr. 116.

76. Wood, R. and Harlow, R. D. Rat liver lipids: Metabolic relationships derived from structural analyses of neutral glycerides and phosphoglycerides. J Amer Oil Chem Soc 46, 1969. Program of Meeting, abstr. 7.

77. Wood, R. and Snyder, F. Tumor lipids: Metabolic relationships derived from structural analyses of acyl, alkyl, and

alk-1-enyl moieties of neutral glycerides and phosphoglycerides. J Amer Oil Chem Soc 46, 1969, Program of Meeting, abstr. 8.

78. Wykle, R. L. and Snyder, F. The biosynthesis of alkyl glyceryl ethers by a microsomal enzyme system from Ehrlich ascites cells: Kinetics and structural studies. J Amer Oil Chem Soc 46, 1969. Program of Meeting, abstr. 109.

MISCELLANEOUS

79. Berger, J. D. Book Review: Code of Practice for the Protection of Persons Exposed to Ionizing Radiations in Research and Teaching, 2nd Ed. London, Her Majesty's Stationery Office, 1968. Nuclear Safety 10, 521, 1969.

80. Cloutier, R. J. Book Review: Atlas of Radiation Dose Distribution, Vol. III. Moving Field Isodose Charts. IAEA. New York, International Publications, 1967. Health Physics 16, 815, 1969.

81. Kniseley, R. M. Book Review: Progress in Atomic Medicine, Vol. 2. John H. Lawrence, ed. New York, Grune and Stratton, 1968. Amer J Clin Path 52, 484, 1969.

IN PRESS

82. Andrews, G. A., Kniseley, R. M., Vodopick, H., Bergner, P-E. E., and Lushbaugh, C. C. Hematologic responses to total-body irradiation. Gesellschaft fflr Nuclearmedizin.

83. Blank, M. L. and Snyder, F. Long-chain fatty alcohols in normal and neoplastic tissues. Lipids.

84. Cloutier, R. J. Health physics education and training: Past, present, and future. Proceedings of Health Physics Mid-Year Symposium, January 1969.

85. Comas, F. V., Edwards, C. L., and Vodopick, H. Changes in leukocyte values in patients with chronic granulocytic leukemia. Radiat Res.

86. Gengozian, N. Male and female cell populations in the chimeric marmoset. In: Proceedings of the Second Conference on Experimental Medicine and Surgery in Primates.

1027426

87. Gengozian, N. and Porter, R. P. Transplantation immunology in the marmoset. In: Proceedings of the Second Conference on Experimental Medicine and Surgery in Primates.

88. Goh, K. O. Inner chromosomal structures of human leukemic cells: A light microscopic observation. Cytologia.

89. Hayes, R. L., Nelson, B., Swartzendruber, D. C., Carlton, J. E., and Byrd, B. L. Gallium-67 localization in experimental animal tumors. Science.

90. Nelson, B. and Kniseley, R. M. Marrow fibrosis in myeloproliferative disorders. In: Proceedings of the Symposium on Myeloproliferative Disorders of Animals and Man, Richland, Washington, May 22, 1968. AEC Symposium Series No. 15, CONF-680529, 1970.

91. Piantadosi, C. and Snyder, F. A review of plasmalogens and related derivatives: Their chemistry and metabolism. J Pharm Sci.

92. Sansone, G., Swartzendruber, D. C., and Snyder, F. Inclusions in mitochondria of preputial glands from mice. A combined biochemical and morphologic study. Biochim Biophys Acta.

93. Soodsma, J. F., Piantadosi, C., and Snyder, F. The biocleavage of alkyl glyceryl ethers in Morris hepatomas and other transplantable neoplasms. Cancer Res.

94. Snyder, F. Liquid scintillation radioassay of thin-layer chromatograms. Proceedings of the International Symposium on the Current Status of Liquid Scintillation Counting. New York, Grune and Stratton.

95. Snyder, F. The chemistry, physical properties, and chromatography of lipids containing ether bonds. In: Progress in Thin-Layer Chromatography and Related Methods. Ann Arbor Science Publishers, Ann Arbor, Michigan.

96. Snyder, F. Thin-layer radiochromatography and related procedures. In: Progress in Thin-Layer Chromatography. Ann Arbor Science Publishers, Ann Arbor, Michigan.

97. Snyder, F., Blank, M. L., Malone, B., and Wykle, R. L. Identification of O-alkyldihydroxyacetone phosphate, O-alkyldihydroxyacetone, and diacyl glyceryl ethers after enzymic synthesis. J Biol Chem.

98. Snyder, F., Malone, B., and Blank, M. L. Enzymic synthesis of O-alkyl bonds in glycerolipids. J Biol Chem.

99. Snyder, F., Malone, B., and Cumming, R. B. Synthesis of glyceryl ethers by microsomal enzymes derived from fibroblasts (L-M cells) grown in suspension cultures. Can J Biochem.

100. Snyder, F., Piantadosi, C., and Malone, B. The participation of 1- and 2-isomers of O-alkylglycerols as acyl acceptors in a cell-free system. Biochim Biophys Acta.

101. Swartzendruber, D. C., Byrd, B. L., Hayes, R. L., Nelson, B., and Tyndale, R. L. Gallium-67 distribution in tissues of leukemic and nonleukemic mice. J Nat Cancer Inst.

102. Upton, A. C. and Lushbaugh, C. C. The pathological anatomy of total-body irradiation. In: Atomic Medicine E. R. King and J. W. J. Carpender, eds.

103. Vodopick, H., Rupp, E. M., and Gengozian, N. An in vitro histocompatibility test in a search for tumor antigens. IAEA, Vienna.

104. Wood, R. Tumor lipids: Identification of sterol ester species in Ehrlich ascites cells. Cancer Res.

105. Wood, R. and Healy, K. Tumor lipids: Biosynthesis of plasmalogens. Biochem Biophys Res Commun.

105a. Medical Radionuclides: Radiation Dose and Effects. Proceedings of a symposium held at the Oak Ridge Associated Universities December 8-11, 1969. Edited by Roger J. Cloutier, C. Lowell Edwards, and Walter S. Snyder. AEC Symposium Series CONF-691212.

MISCELLANEOUS (IN PRESS)

106. Blank, M. L. and Snyder, F. (Abstract). Inverse relation in levels of cholesteryl esters and triglycerides in whole blood of tumor-bearing animals. In: Program for the 1969 Annual Meeting of the Society for Experimental Biology and Medicine, p. 2, Charleston, South Carolina.

107. Blank, M. L., Wykle, R. L., Piantadosi, C., and Snyder, F. (Abstract). Biosynthesis of O-alkyl and O-alk-1-enyl ether-linked lipids in neoplastic cells. In: Proceedings of the American Association for Cancer Research, 61st Annual Meeting (in press).

108. Hagen, P-O and Blank, M. L. (Abstract). Minor lipid components of Clostridium butyricum. J Amer Oil Chemists' Soc (in press).

1027427

109. Lee, T-c (Abstract). The metabolism of lipids in smooth- and rough-surfaced membranes of rat liver microsomes. To be presented at the Federation of American Societies for Experimental Biology to be held April 12-17, 1970, at Atlantic City, New Jersey.

110. Lee, T-c, Swartzendruber, D. C., Morris, H. P., and Snyder, F. (Abstract). Zonal centrifugation profiles of smooth- and rough-surfaced microsomes from normal and neoplastic tissues. To be presented by T-c Lee at the Xth International Cancer Congress, May 23-28, 1970, Houston, Texas.

111. Snyder, F. Glycerolipids in the neoplastic cell: Methodology, metabolism, and composition. In: Methods in Cancer Research, H. Busch, ed., Academic Press, Inc., New York (in press).

112. Wood, R., Walton, M., Healy, K., and Cumming, R. B. (Abstract). Plasmalogen biosynthesis in Ehrlich ascites cells grown in tissue culture. J Amer Oil Chemists' Soc (in press).

113. Wykle, R. L., Blank, M. L., Piantadosi, C., and Snyder, F. (Abstract). Identification of intermediates in the biosynthesis of O-alkyl lipids. Federation Proc (in press).

MEDICAL DIVISION CONFERENCES — 1969

January 7: Radiation safety in Latin America. Roger Cloutier, Division staff.

January 14: Single dose spleen irradiation in chronic granulocytic leukemia. F. Comas, Division staff.

January 21: Clinical applications of a new, rapid electrophoresis procedure employing pulse power in gradient gel. Robert Allen, ORTEC.

January 28: Stem cell number and radiosensitivity. L. H. Smith, ORNL Biology Division.

February 4: A new approach to greater precision in whole-body counting. W. D. Gibbs, Division staff.

February 11: Chromosome damage induced by plasma of X-rayed patients. Gayle Littlefield, Division staff.

February 18: Lymphocyte kinetics. Francis Goswitz, Division staff.

February 25: Localization of gallium in nonosseous tumors. R. L. Hayes, Division staff.

March 4: The radiation exposure rate effect: Action upon the immune response in mice. Donald E. Carlson, Postdoctoral Fellow.

March 18: Thyroid disease in the marmoset. C. C. Lushbaugh, Division staff.

March 25: Methods for processing radioisotope scans by digital computer. W. J. McClain, ORNL Instruments Development Group.

April 1: Relation of cell formation to organ formation: A botanical approach to a basic problem in morphogenesis. Don Foard, ORNL.

April 8: An apparently nonimmunologic effect of thymic cells. Joan Goodman, ORNL Biology Division.

April 15: Which lymphoproliferative disease? Bill Nelson, Division staff.

April 22: Morphologic studies of AKR mouse lymphoid tissues. Donald C. Swartzendruber, Division staff.

April 29: A new metabolic pathway: Biosynthesis of alkyl ether bonds from glyceraldehyde-3-phosphate and fatty alcohols by microsomal enzymes. Fred Snyder, Division staff.

May 6: Cross protection between traumatic shock and radiation adaptation. Lydia Corrill, Division staff.

May 13: Elucidation of body function by high resolution analyses of body fluids (effects of ionizing irradiation). Charles Scott, ORNL.

May 20: Further studies on the structural analyses of rat liver phosphoglycerides. Randall Wood, Division staff.

May 27: Nutritional aspects of blood neoplasia. James D. Regan, ORNL Biology Division.

June 3: Report on Vienna Symposium on Handling of Radiation Accidents. Gould A. Andrews, Division staff.

June 10: Microbiological studies of 'protected environment' units for patients. Gerald P. Bodey, University of Texas, M.D. Anderson Hospital, Houston, Texas.

June 17: Internal radiation dosimetry. Roger Cloutier, Division staff.

June 24: The radiosensitivity of rat bone-marrow cells. F. Comas, Division staff.

1027428

July 1: Trip report: Japan/U.S. seminar on experimental carcinoma of the glandular stomach, Hakone, Japan, June 7-13, 1969. C. C. Lushbaugh, Division staff.

July 8: Theory of quantitative radiation response time data. Per-Erik E. Bergner, Division staff.

July 15: Report on bone-marrow conference in Paris, June 16-17, 1969. N. Gengozian, Division staff.

July 22: Chemotherapy of malignant disease. Francis Goswitz, Division staff.

July 29: Additional studies of human chromosomal breakages. Kong-oo Goh, Division staff.

August 5: Radiation biology research at the University of Tennessee Agricultural Research Laboratory. Tom Noonan, UT-AEC.

August 12: Effects of prenatal radiation on large animals. R. L. Murphree, UT-AEC.

August 19: The use of radioprotectants in experimental tumor therapy. John Yuhas, ORNL Biology Division.

August 20: Summer Student Scientific Program

Human cytogenetic technique - Elizabeth Booker; Lipids of Spherophorus ridiculosis - Pamela High; The relation of cobalt turnover rate to thyroid function in some mammals - Larry Papiez; A search for virus particles in megakaryocytes - Elmo Rosario; Preparative ultracentrifuge techniques - Harley Schultz; Methionine biosynthesis in Candida species - Margaret Wilusz.

August 26: Studies of concentration of gallium in nonosseous tumors. R. L. Hayes, Division staff.

September 2: Equilibration of some biological systems to protracted gamma irradiation. Lydia Corrill, Division staff.

September 9: Monitoring physiologic responses during total-body irradiation therapy. A. C. Morris, Jr., Division staff.

September 9: Report on 2nd International Conference on Medical Physics. A. C. Morris, Jr., Division staff.

September 16: Postmortem studies of the distribution of radionuclides. Bill Nelson, Division staff.

September 23: Suppression and recovery of immunologic competence. Paul Nettesheim, ORNL Biology Division.

September 30: The resolution of rough- and smooth-surfaced microsomes by zonal centrifugation. Ten-ching Lee, Division staff

October 7: Tissue distribution of gallium-67 in murine leukemia. Donald C. Swartzendruber, Division staff

October 14: Metabolism of ethanolamine lipids in the brain. G. B. Ansell, Department of Experimental Neuropharmacology, The Medical School, University of Birmingham, England.

October 21: Hemoglobin biosynthesis in the mouse. Lorraine Kraus, Department of Biochemistry, U. T. Medical School, Memphis, Tenn.

October 28: Report on the IAEA Symposium, In Vitro Procedures with Radioisotopes in Clinical Medicine and Research, held in Vienna, Austria, September 6-14, 1969. Helen Vodopick, Division staff

November 4: Control of cell growth and division in bacteria. Howard Adler, ORNL Biology Division.

November 18: Relationship between bactericidal and metabolic activities in leucocytes. Anthony Sbarra, Tufts University Medical School, Boston, Mass.

November 25: Radiation dose from radioisotopes in the blood. Roger Cloutier, Division staff.

December 2: Megakaryocyte and platelet development and regulation. T. T. Odell, Jr., ORNL Biology Division.

December 16: Science-based management for research and development organizations. C. C. Congdon, ORNL Biology Division.

December 23: The linear scanner. W. D. Gibbs, Division staff.

December 30: Mutational studies of mammalian cells in culture. E. H. Y. Chu, ORNL Biology Division.

LIPID SEMINARS—1969

January 15: Round-table discussion of program plans in lipid research.

January 29: Catalytic properties, biological roles, and regulation of synthetic activities of microsomal glucose-6-phosphatase. Robert Nordlie, Department of Biochemistry, University of North Dakota, Grand Forks.

February 5: Determination of double-bond position in unsaturated fatty acids. Also, a report on the International Gas Chromatography meeting, Las Vegas, Nevada. Randall Wood, Division staff.

1027429

February 19: Phospholipids and phospholipid fatty acids of human platelets in three populations. James Iacono, Cincinnati General Hospital, University of Cincinnati.

March 12: The separation of microsomal fraction by zonal centrifugation. Ten-ching Lee, Division staff.

April 9: Lipids of Clostridium butyricum. Per-Otto Hagen, Division staff.

April 30: Glyceryl ether biosynthesis by microsomal enzymes in Ehrlich ascites cells. Robert Wykle, AEC Predoctoral Fellow.

May 20: Further studies on the structural analyses of rat liver phosphoglycerides. Randall Wood, Division staff.

May 21: Liquid scintillation spectrometry and recent developments. Ed Henry, Southeastern District Manager, Packard Instrument Company, Atlanta, Georgia.

June 24: Reports on the following meetings: American Oil Chemists' Society Symposium on Subcellular Particulates: Medical and Biochemical Application and Gordon Research Conference on Lipid Metabolism. Ten-ching Lee, PHS Fellow, and Per-Otto Hagen, Visiting Scientist, Division staff.

July 16: Lipids of plasma membranes, and plasmalogens: Biosynthetic approaches. Fred Snyder, Division staff.

July 30: Synthesis of compounds of interest to lipid chemists. Henry Rakoff, Summer Research Participant, Parsons College, Fairfield, Iowa.

REGIONAL LIPID MEETING

May 8 - 9, 1969

Speaker - Affiliation	Title of Talk
Bernard W. Agranoff Department of Biological Chemistry University of Michigan Ann Arbor, Michigan	Biosynthesis of some acidic phospholipids
A. K. Hajra Mental Health Research Institute University of Michigan Ann Arbor, Michigan	Identification and chemical synthesis of acyl dihydroxyacetone phosphate

Speaker - Affiliation	Title of Talk
Roy Vagelos School of Medicine Washington University St. Louis, Missouri	Studies on the biosynthesis and biological function of fatty acids

Attendance included 36 participants from 8 institutions. Brief talks were given by 18 participants in addition to the three main speakers.

FELLOWSHIPS AND TERM APPOINTMENTS

Visiting Clinical Scientist:
Jere Bauer, M.D.
On sabbatical from
University of Michigan

Visiting Scientist in Lipid Research:
Per-Otto Hagen, Ph.D.

Postdoctoral Appointment in Lipid Research:
Robert E. Anderson, Ph.D.
Gail Sansone, Ph.D.

Public Health Service Fellows:
Donald Carlson, Ph.D.
Ten-Ching Lu Lee, Ph.D.
David N. Mardon, Ph.D.

Postresident Assistants in Clinical Investigation:
E. Gifford Ammermann, M.D.
Steven Ominsky, M.D.
Nasser Tehranian, M.D.

UT Graduate Students:
Nancy Basford, B.S.
Charles Gottlieb, B.S.
John Kateley, M.S.
Mike Yurconic, B.S.

AEC Postdoctoral Fellow:
James Soodsma, Ph.D.

AEC Predoctoral Fellow:
Robert Wykle, M.S.

Damon Runyon Fellow:
Yukio Tateno, M.D.
University of Chiba Hospital

Student Fellows in Nuclear Medicine:
Coy Foster, University of Texas Medical Branch at Galveston
Bill S. Schnall, Cornell Medical Center
Edward George Kuehnel, State University of New York College of Medicine, Brooklyn

RESEARCH PARTICIPANTS — 1969

Surinder Datta
University of Wisconsin
Kenosha, Wisconsin

Henry Rakoff
Parsons College
Fairfield, Iowa

1027430

Robert C. Ricks
Arkansas State College
State University, Arkansas

Ram Tewari
Rutgers University
New Brunswick, New Jersey

STUDENT TRAINEES — 1969

Elizabeth S. Booker
University of Richmond
(Westhampton College)
Richmond, Virginia

Pamela High
Mercer University
Macon, Georgia

Larry Papiez
St. Martin's College
Olympia, Washington

Elmo Rosario
New Mexico State
Las Cruces, New Mexico

Harley S. Schultz
Cornell University
Ithaca, New York

Margaret M. Wilusz
Chestnut Hill College
Philadelphia, Pennsylvania

ORAU MEDICAL DIVISION ADVISORY COMMITTEE

1968-1969

William C. Moloney (Chairman)
Peter Bent Brigham Hospital

Rupert E. Billingham
University of Pennsylvania
School of Medicine

Frederick J. Bonte
The University of Texas
Southwestern Medical School

E. Richard King
Medical College of Virginia
Virginia Commonwealth University

Wright H. Langham
Los Alamos Scientific Laboratory

Donald B. Zilversmit
Cornell University

1969-1970

William C. Moloney (Chairman
Peter Bent Brigham Hospital

Rupert E. Billingham
University of Pennsylvania
School of Medicine

John Coniglio
Vanderbilt University

Robert Greenlaw
University of Kentucky
Medical Center

Wright Langham
Los Alamos Scientific Laborat

Shields Warren
Cancer Research Institute
New England Deaconess Hospit

MEDICAL COMMITTEE, ORAU COUNCIL

Oscar Touster (Chairman)
Vanderbilt University

Gail D. Adams
University of Oklahoma
Medical Center

E. A. Daigneault
Louisiana State University
Medical Center

Richard B. Escue
North Texas State University

Edward G. High
Meharry Medical College

John L. McCarthy
Southern Methodist University

Horace N. Marvin
University of Arkansas
Medical Center

Walter J. Peterson
North Carolina State University

Howard H. Vogel
University of Tennessee
College of Medicine

MEDICAL DIVISION EMPLOYEES

Scientific Staff

Paulette Aaron, B. S.
*Elizabeth M. Allen, B. S.
*Robert Anderson, Ph.D.
Gould A. Andrews, M.D.
*Norma Asbury
Mildred Bailey
*Edward Balish, Ph.D.
Thomas R. Barclay, B. S.
Jerre Batson, B. S.
William L. Beck, Jr., B.S.
*Per-Erik E. Bergner, M.D.
Merle Blank, B. S.
Billy L. Byrd, B.S.
Eddie Ruth Capshaw
James E. Carlton, B.S.
Stuart J. Chaskes, M.S.
Martha Clevenger, B.S.
Shirley B. Colyer, B.S.
*Frank V. Comas, M.D.
Lydia Corrill, M.S.
*Kathryn S. Craft, B.A.
Edgar Cress, B.S.
Rachel Dixon
C. Lowell Edwards, M.D.
Elizabeth Edwards
William Fishback
Nazareth Gengozian, Ph.D.
William D. Gibbs, B.S.
Thomas Gilman, B.S.
*Kong-oo Goh, M.D.
Francis A. Goswitz, M.D.
Charles T. Greene, B.A.
Per-Otto Hagen, Ph.D.
Fred Hamilton
Robert Harlow, B.S.
Raymond L. Hayes, Ph.D.
Kathleen Healy, B.S.
Harold D. Hodges, B.S.
Elizabeth Holloway
Karl F. Hübner, M.D.
Gretchen Humason, M.A.
Kathryn Hurst, B.S.
Eugene E. Joiner, M.S.
John R. Kateley, B.A.
Mary Beth Klepper, M.S.
Ralph M. Kniseley, M.D.

1027431

Gayle Littlefield, Ph.D.
Kathryn Lore, B.S.
C. C. Lushbaugh, M.D., Ph.D.
Dorothy Lushbaugh, B.S.
Boyd Malone, B.S.
Brenda Joan Marks, B.S.
J. E. McCarter
Sallie McCaskill
Alvis Earl McDow, Jr., B.S.E.E.
Daniel A. McFaddin
Jean P. McIntyre, B.S.
Anita Moehl, B.S.
A. C. Morris, Jr., M.S.E.
Frank T. Nakamura, B.S.
Bill M. Nelson, M.D.
Ted A. Pearson, M.S.
Francine Pennington, B.S.
William T. Pope
R. P. Porter, Ph.D.
Brenda Pritchard, B.S.
Richard F. Queener
John J. Rafter, B.S.
*Donald Reynolds
Robert C. Ricks, Ph.D.
Mack Ruffner
Elizabeth M. Rupp, B.A.
Ann Sipe
Mona Smith
Thomas A. Smith
Vivian Ann Smith, B.S.
Mary P. Smyser, B.S.
Fred L. Snyder, Ph.D.
Jerry Steele
Margo Steinman, M.S.
Nelson Stephens, B.S.
Tom Randall Stokes
Donald C. Swartzendruber, Ph.D.
Ryosaku Tanida, M.D.
Mary W. Thomas, B.S.
Van Upton
Helen A. Vodopick, M.D.
J. Ruth Walker
Allen M. Webb, B.S.
James O. White
Sandra Wilson
Randall Wood, Ph.D.
Gary Wolfe, B.S.

Nursing and Patient Care

*Margaret Blackburn, R.N.
Helen Brinker, R.N.
James Cozart
Mary Nell Craig, R.N.
John Dean
Thelma Eden, R.N.
Mable Helton, R.N.
Rita Holt, R.N.
Earl Jacobs
Sandra Landry, R.N.
*Martha Laxton, R.N.
Marilyn Mackley, R.N.
Bedford Mayott
Beuna Pack
Garfield Porter
Mary Rogers, R.N.
Lillie P. Simmons
*Elaine Stoetzel, R.N.
Mary E. Sutliff, R.N.
Naomi P. Wilson, R.N.
Eria Winters, R.N.
Lillie I. Woods

*Terminated during 1969

Administrative, Editorial,
Medical Records, and Secretarial

Elizabeth B. Anderson, M.S.
Becky S. Bailey
Frances Banner
*Kenneth L. Burton, M.S.
Blanche Carden
Carole J. Carter, B.S.
*Robert W. Cooper
John T. Crockett, Jr., B.S.
*Frances Darr
Laura P. Edwards
J. Howard Harmon
*Wanda Hodge
*Carolyn Hutchins
Mary Lee Johnson
Jane C. Kimbro, B.S.
Willa Fae Loveday
Mary McKeethan
Iris McPeters
*Ruth C. Paire
Jane Rogers
Nancy Sheehan, B.A.
Vernelle Stock
*Katherine Stubbs, B.F.A.
Dorothy Vola
*Patsy White
Florence C. Zenni

Custodial and Animal Care

Willie Barnett
Mark Brewer
Willie J. Brooks
*Clarence Buckley
Isaiah Caldwell
*Carroll Cline
Grace E. Foster
Charles Gaylor
James Graham
Renfro Henderson
Charlie Hunter
Rufus Jackson
James Kline
James Rather
J. R. Stevens
William Walker
Floyd Weaver
Alfred Webster
Jerry White
Johnnie Williams

*Terminated during 1969

CONSULTANTS AND COLLABORATORS — 1969

Norman G. Anderson, Ph.D.
Molecular Anatomy (MAN)
Program
Oak Ridge National Laboratory

Edmund B. Andrews, M.D.
Medical Arts Building
Knoxville

John A. Auxier, M.S.
Health Physics Division
Oak Ridge National Laboratory

Fritz H. Bach, Ph.D.
University of Wisconsin
Madison

Robert P. Ball, M.D.
Radiology Department
Oak Ridge Hospital

Jere M. Bauer, M.D.
University of Michigan
School of Medicine, Ann Arbor

1027432

RESEARCH REPO

ASSOCIATED UNIVERSI

ORAU-

Oak Ridge Institute for Science and Education, Medical Sciences Division

REPOSITORY

Oak Ridge Associated Universities. Annual Research Reports, Medical and Health Sciences Division

COLLECTION

Stone Road Facility; Room

BOX No.

No Folder title

Document No: ORAU 30002 Pg 5 of 6

FOLDER

1027433

10214 3h

ON THE COVER: *A molecular model (left) of a glyceryl ether diester. This lipid class has been found to occur in neoplasms at significantly higher concentrations than in normal tissues. The Medical Division's lipid research project has established the first known metabolic pathway for ether-linked lipids of this type. (See pages 161, 168, and 181 of this report.) Chromatogram (right) shows a total lipid extract from Ehrlich ascites carcinoma cells. The lipid class of glyceryl ether diesters is indicated by the arrow.*

ORAU-107
BIOLOGY AND MEDICINE
(TID-4500)

RESEARCH REPORT – MEDICAL DIVISION
Oak Ridge Associated Universities

FOR THE YEAR ENDING DECEMBER 31, 1968

OPERATING UNDER CONTRACT WITH
THE UNITED STATES ATOMIC ENERGY COMMISSION

Studies on the Microflora of Patients Exposed to 250-R Total-Body Irradiation in the LETBI Facility, 1.5 R/hr. *Edward Balish and Ted A. Pearson* 46
Studies on the Microflora of Three Men Accidentally Exposed to Total-Body Irradiation. *Edward Balish and Ted A. Pearson* . . . 52
The Influence of Total-Body Irradiation on Bacterial Agglutinins in Human Serum. *Edward Balish and Ted A. Pearson* 59
The Influence of Total-Body Irradiation on the Bactericidal Activity of Human Serum. *Edward Balish and Ted A. Pearson* . . 61
Studies on the Microflora of Two Patients Exposed to Partial-Body Irradiation. *Edward Balish and Ted A. Pearson* 65
Studies on the Microflora of Rats Exposed to 1400 rads Total-Body Irradiation. *Edward Balish, Ted A. Pearson, and Frank V. Comas* 68
Isolation of a Sphaerophorus-type Microorganism from the Stool of Two Patients. *Ted A. Pearson and Edward Balish* 71
Effects of Sulfur-Containing Nitrogen Sources on the Growth and Morphology of Candida albicans. *David N. Mardon, Edward Balish, Dallas C. Hilden, and Kathryn Hurst* 74
Methionine Biosynthesis in Candida albicans. *Edward Balish and David N. Mardon* 76
Influence of Glycine on Methionine Biosynthesis in Candida albicans. *David N. Mardon and Edward Balish* 78
Induction of Small-Colony Variants and Auxotrophs of Candida albicans by Ultraviolet Light and Chemical Mutagens. *Edward Balish and Norman Savage* 81
Accumulation of S-Adenosylmethionine by Auxotrophs of Candida albicans. *Norman Savage and Edward Balish* 84
Rapid Identification of Candida albicans in a Defined Liquid Culture Medium. *David N. Mardon, Edward Balish, Brenda Joan Marks, and Kathryn Hurst* 85
Modifications in a French Pressure-Cell – Laboratory-Press System. *David N. Mardon and Edward Balish* 89
Large Abnormal Acrocentric Chromosome Associated with Human Malignancies. *Kong-oo Goh* 91
The Effect of Deoxyribonucleoside Triphosphates on Pulverized Human Chromosomes at G_2. *Kong-oo Goh* 95
Autoradiographic Studies of the Abnormal Chromosome in Human Malignancies. *Kong-oo Goh and Eugene Joiner* 99
The Effect of Total-Body Irradiation on the Bone-Marrow Lymphocytes. *Kong-oo Goh* 102
Pseudodiploidy in Klippel-Feil Syndrome. *Kong-oo Goh* 105
Chloramphenicol and Acute Leukemia. *Kong-oo Goh* 108

1027436

Semistatistical Computer Analysis of Electronic Erythrocyte-Size Determination: A rapid laboratory method of detecting RBC disease. *C. C. Lushbaugh, R. C. Lushbaugh, and Dorothy H. Lushbaugh* 112
Evaluation of Therapeutic Response with Change in Electronic RBC Size Distribution. *C. C. Lushbaugh, Dorothy H. Lushbaugh, and C. L. Edwards* 116

MEDICAL RADIOISOTOPES 119
Tumor Scanning with Gallium-67. *C. L. Edwards and R. L. Hayes* 119
Experimental Animal Studies with Gallium-67. *R. L. Hayes, J. E. Carlton, B. L. Byrd, and J. J. Rafter* 125
The Effect of Scandium on the Tissue Distribution of Gallium and Indium in the Rat. *R. L. Hayes, B. L. Byrd, J. J. Rafter, and J. E. Carlton* 130
Rare Earths as Possible Bone-Scanning Agents. *R. L. Hayes, B. L. Byrd, and J. E. Carlton* 133
Assessment of Erythropoiesis by Ferrokinetics and Radiocolloid Bone-Marrow Scanning. *Francis A. Goswitz, C. L. Edwards, and Helen Vodopick* 136
Nonerythropoietic Iron Turnover Rate (NER) and Its Use as an Index to Quantitate Iron Stores. *Francis A. Goswitz, Helen Vodopick, and Bill Nelson* 138
Value of Plasma Iron-59 Disappearance in Determining Iron-Deficient Erythropoiesis. *Francis A. Goswitz* 140
Blood Volume in Myelofibrosis. *Francis A. Goswitz and Martha L. Clevenger* 142
Advantage of Measuring Blood Volume with Three Radioisotopes *Francis A. Goswitz* 144
Current Value of ^{131}I-Triolein for Evaluation of Malabsorption. *Francis A. Goswitz and Nelson Stephens* 146
Transistorized Electronic Circuits for the Miniaturized Surgical Probe. *A. C. Morris, Jr., T. R. Barclay, and J. V. Nemcek* . . . 148
Quantitative Measurement of Radioactivity in Internal Organs by Area Scanning. *Noboru Arimizu and A. C. Morris, Jr.* 151

LIPID METABOLISM 157
The Biosynthesis of Alkyl Ether Bonds in Lipids by a Cell-free System. *Fred Snyder, Boyd Malone, and Robert L. Wykle* 161
A New Metabolic Pathway: Biosynthesis of Alkyl Ether Bonds from Glyceraldehyde-3-Phosphate and Fatty Alcohols by Microsomal Enzymes. *Fred Snyder, Robert L. Wykle, and Boyd Malone* 168

IMMUNOLOGIC STUDIES AND THE DEVELOPMENT OF THE MARMOSET AS A LABORATORY PRIMATE 259

Further Observations on the Role of Acute Exposure Rates on Immune Suppression of Irradiated Mice. *Donald E. Carlson and N. Gengozian* 260

Critical Variables of the Jerne Plaque Technique as Applied to Rodent Antibody-Forming Systems Responding to Heterologous Red-Cell Antigens. *Karl F. Hübner and N. Gengozian* 264

Effect of Cell Concentration on the In Vitro Test for Mixed-Leukocyte Cultures. *Helen Vodopick, Elizabeth M. Rupp, and N. Gengozian* 268

Neutrophil and Lymphocyte Chimerism in the Imported and Laboratory-Bred Marmoset. *N. Gengozian, J. S. Batson, and C. T. Greene* 270

Blood Group Specificities on Marmoset Red Cells. *S. P. Datta and N. Gengozian* 275

Response to First-Set Skin Allografts in the Marmoset. *Raymond P. Porter and N. Gengozian* 278

Normal Development of the Thyroid and Parathyroid Glands in Marmosets. *Gretchen Humason, R. M. Kniseley, N. Gengozian, R. Cooper, and C. C. Lushbaugh* 282

Occurrence of a Thyroid Disease in Stillborn, Neonatal, and Young Marmosets. *C. C. Lushbaugh, Gretchen Humason, R. M. Kniseley, and N. Gengozian* 284

Intra-uterine Death from Congenital Chagas' Disease in Laboratory-Bred Marmosets (Saguinus fuscicollis lagonotus). *C. C. Lushbaugh, Gretchen Humason, and N. Gengozian* 287

COMPUTER TECHNOLOGY 291

Summary of Developments in Computer Methodology. *J. Howard Harmon* 291

Computer-Assisted Measurements of Colloid Particle-Size Distributions. *R. L. Hayes, J. E. Carlton, and Earl McDow, Jr.* 293

Development of an Electronic Interface between a Beckman Analytrol Film Densitometer and the On-Line IBM 1800 Computer. *T. R. Barclay and A. C. Morris, Jr.* 295

PUBLICATIONS 297

MEDICAL DIVISION CONFERENCES – 1968 304

LIPID SEMINARS – 1968 308

REGIONAL LIPID MEETING, 1968 309

1027438

FELLOWSHIPS AND TERM APPOINTMENTS 310

RESEARCH PARTICIPANTS – 1968 310

STUDENT TRAINEES – 1968 310

MEDICAL COMMITTEE, ORAU COUNCIL 311

ORAU MEDICAL DIVISION ADVISORY COMMITTEE 311

MEDICAL DIVISION EMPLOYEES 312

CONSULTANTS AND COLLABORATORS – 1968 314

1027439

INTRODUCTION

The Medical Division carries out one of the major biomedical programs devoted to both clinical studies and related research in basic sciences. It is supported by the United States Atomic Energy Commission. The major research objectives are (1) to delineate mechanisms of radiation injury, especially in the human being, and to devise improved methods of treating radiation injury; (2) to advance the beneficial applications of radiation for diagnosis and therapy; (3) to pursue selected basic studies, particularly ones related to cancer, that arise out of the ongoing program; and (4) to provide training in research for students, scientists, and physicians. The Division feels an obligation to contribute to the pool, not only of research scientists, but of physicians with knowledge of nuclear medicine.

The research accomplishments are covered in the body of the report, which is divided into six sections. The introductions to these sections provide further perspective on the goals and current activities in the Medical Division program. This introduction will deal mainly with staff, physical facilities, trainees, and relations with other organizations.

On July 1 Dr. Donald Swartzendruber arrived to head the ultrastructural anatomy effort and moved into the newly completed electron microscope facility. This addition is a significant strengthening to the Division program and provides a resource that had been acutely needed for several years. Dr. Francis Goswitz, who had been devoting half time to medical courses given by the Special Training Division of ORAU, transferred to full time Medical Division staff status where he shares in the clinical research and has expanded his studies in experimental hematology. To our regret, Dr. Edward Bird resigned to accept an appointment as Associate Professor of Medicine at Bowman Gray School of Medicine. We are pleased that he has been able to continue collaboration with our staff members on endocrinologic problems, particularly involving use of the whole-body counter. Dr. Raymond Porter completed his Ph.D., having done his thesis work under Dr. Gengozian in the immunology program, and joined this research group as a regular staff member. Dr. Surinder Datta, immunogeneticist who had been associated with the marmoset research project, accepted a position as Assistant Professor in the Department of Biology at the University of Wisconsin.

Our physical resources continue to grow. The outstanding event in 1968 was the completion of the Marmoset Research Center located on the property owned by ORAU near the technical library. This unit, housing well-equipped laboratories and a colony that will accommodate approximately 400 primates, was occupied in May. The initial cost, in excess of $375,000, was borne by ORAU. Also noteworthy, an AEC plant project, was the completion of the laminar-flow sterile-patient facility, which provides for the first time an environment that will reduce the threat of exogenous infections in patients who have been immunologically depressed by heavy doses of chemotherapy or exposure to radiation. It will be an important resource in the event of any future radiation accident, allowing victims to be carried through a period of bone-marrow depression in a sterile environment. Plans are to fully explore the use of this unit in providing improved ways for delivery of more intensive anticancer therapy. The research studies must await

additional financial support that will be required for extensive microbiological studies and sterile nursing care. During the year a proposal was developed for the purchase of the IBM 1800 computer that has been the central item of rental equipment in the development of the Medical Division's computer resource, and early in 1969 approval for purchase of this item was granted by the Atomic Energy Commission.

Training activities have continued to develop. We are pleased that Dr. Donald E. Carlson was awarded a Ph.D. at the University of Tennessee, having performed his thesis under the direction of Dr. Gengozian; subsequently he was awarded a Public Health Service Postdoctoral Fellowship to continue work here in immunology. Two other PHS Postdoctoral Fellowships were awarded, one to Ten-Ching Lu Lee, Ph.D., in the lipid project, and one to David N. Mardon, Ph.D., in the microbiological project. Dr. James Soodsma, Ph.D., of the lipid project, holds an AEC Postdoctoral Fellowship. Special postdoctoral appointments in the lipid program, supported by the American Cancer Society, are held by Dr. Robert E. Anderson and Dr. Gail Sansome, and Dr. Per-Otto Hagen is a visiting scientist under the same auspices. The Division also is host to four graduate students in the immunology laboratory, Nancy Basford, Charles Gottlieb, John Kateley, and Mike Yurconic; one in lipid research, Ahmed Mohamed; and an AEC Predoctor Fellow, Robert Wykle, in the lipid project. Dr. H. K. Speed, III, completed his one-year appointment as Postresident Assistant in December and returned to a post at the University of Oklahoma Medical School, one of the ORAU member schools. Dr. Romulo Mora, an exchange visitor from Manila, completed his one-year Assistantship in Clinical Investigation July 1, and returned to Buffalo. Dr. Guillermo Castaneda, assigned to the Medical Division on an International Atomic Energy Agency Fellowship, returned to his post with the Mexican National Nuclear Energy Commission in Mexico City, after a six-month tour for the purpose of studying radiation accidents, the acute radiation syndrome, and its management. In addition, there were six Medical Student Fellows in Nuclear Medicine, including four who came from member schools of ORAU. This program was supported in 1968 by Neisler Radiopharmaceuticals, Mallinckrodt Nuclear Company, and Abbott Laboratories. The AEC training programs administered by the University Participation Office of ORAU made it possible to have four Research Participants from the faculties of colleges and universities during the summer quarter. At the same time and under the same support ten undergraduate college students were assigned to the Division laboratories in the college training program.

This year, for the first time in several years, the Medical Division did not sponsor a major symposium on nuclear medicine. Plans are being made to resume these symposia in the fall or winter of 1969, with a meeting that will deal with dosimetry of radiation from internal radionuclides. During 1968 a third annual regional meeting on lipids was sponsored by the Division. More information about this very successful meeting is to be found on page 309 of this report.

As a part of our general training effort, approximately 35 lectures were given on campuses or at seminars or courses throughout the country. Approximately 28 papers were presented at regional or national meetings, and staff members attended more than 60 meetings during the year. In addition, a number of the senior staff have served

1027440

on ad hoc committees or advisory committees involving approximately 25 trips. We were also represented at a number of international meetings. The Division Chairman presented an invited paper in September at the Gesellschaft für Nuclearmedizin, Wiesbaden, Germany, and during this trip consulted at the International Atomic Energy Agency in Vienna. Earlier in the year he presented an invited paper to the Mexican Society of Nuclear Medicine. Roger Cloutier, as part of the Special Training Division's activity in the AEC Atoms in Action program, made two trips to Latin America, one to Argentina, and one to Caracas and Panama where he presented lectures in training programs. At the request of the United States Atomic Energy Commission, Dr. Frank Comas presented a paper in Mexico City at a symposium sponsored by the National Nuclear Energy Commission of Mexico. Dr. C. C. Lushbaugh visited Japan to participate in the United States - Japan Conference on Comparative Species Radiosensitivity, and consulted with staff members of the Atomic Bomb Casualty Commission in Hiroshima. He was also requested to consult with authorities in Buenos Aires about a radiation accident victim who received a massive local exposure to a cobalt-60 industrial source. Dr. Fred Snyder, in February, presented four lectures at a conference on liquid scintillation radioassay at the Istituto di Ricerche Farmacologiche in Milan, Italy. In September he returned to Milan to present a paper at the International Symposium on Drugs Affecting Lipid Metabolism, and to chair a session at the meeting. During this trip he also visited Rotterdam to attend the 9th Congress of International Society for Fat Research. Dr. Randall Wood attended and presented a paper at the 12th International Conference on the Biochemistry of Lipids in Loughborough, England, attended the 9th Congress of the International Society for Fat Research in Rotterdam, and visited with Dr. Ossi Renkonen at the University of Helsinki. Dr. Per-Erik E. Bergner, while on a personal trip to Europe, was able to include professional visits in Paris and Glasgow where he presented seminars and consulted on research results with colleagues there.

Dr. Gengozian continues in his appointment to a Ford Foundation Professorship in the Department of Zoology at the University of Tennessee in Knoxville. Dr. Comas, who holds a faculty appointment at the U. T. Research Center, spends one day a week teaching principles of radiotherapy to the resident staff. Dr. Fred Snyder continues in his appointment as Associate Professor of Biochemistry at the University of Tennessee Medical School, presenting a series of lectures there during the winter quarter. He also holds the title of Professor of Medicinal Chemistry at the University of North Carolina, at Chapel Hill. The Division continues to encourage the strengthening of cooperative bonds with the Oak Ridge National Laboratory and other institutions, as well as interdepartmental collaboration. It can be noted from the listings of research titles that healthy interaction among the various staff members is in evidence.

The Medical Division was honored this year by the announcement at the 1968 Spring Meeting of the American Oil Chemists' Society that our staff member, Dr. Randall Wood, was the recipient of the Bond Award. This award, which includes a gold medal, is given to the scientist who is judged to have presented the best research report at the previous year's meeting.

We take pride in the numerous professional activities that involve

senior staff members. We would also call attention to national recognition given to staff members for their professional activities. Dr. Lushbaugh has been appointed to the Editorial Board of Radiation Research and continues to serve on important national advisory committees including the Space Science Board of the National Academy of Sciences/National Research Council, the US-NASA ad hoc Committee on Electron Therapy, the Advisory Committee to the National Plutonium Registry, the Biomedical Advisory Committee to the Battelle-Northwest Laboratory. Dr. Snyder was appointed to the American Cancer Society Advisory Committee on Research, and is a member of the Editorial Board of the Journal of Lipid Research. The Division Chairman is a member of the Board of Trustees of the Society of Nuclear Medicine, and serves on the Editorial Board of the Journal of Nuclear Medicine, the Advisory Editorial Board to Minerva Nucleare, and is an editorial consultant in nuclear medicine to The New Physician. He also serves on the US-NASA ad hoc Committee on Electron Therapy. The Associate Chairman served as Chairman of the Council on Radioisotopes of the American Society of Clinical Pathologists during 1968, and continues as a member of the Pathology B Study Section of the National Institutes of Health. Staff members also have been active in regional and local professional activities, including the Health Physics Society, the Southeastern Sectional Society for Experimental Biology and Medicine, the Southeastern Chapter of the Society of Nuclear Medicine, the Tennessee Blood Club, and the local Medical Society.

The support for Medical Division activities continues to broaden. We operate under the ORAU contract with the Atomic Energy Commission, receiving our basic funding from the Division of Biology and Medicine, U. S. AEC. Projects are funded from other sources, both by direct grants and through interagency agreements. The NASA project, "Radiosensitivity in Man," under the direction of Dr. Lushbaugh, is in its 5th year. "A Study of Infections in Irradiated Patients" is supported by the U. S. Army, Medical Research and Development Command, with Dr. Balish as principal investigator. He also holds an NIH grant entitled "Studies on the Morphogenesis and Pathogenicity of Candida albicans." At the marmoset research center, Dr. Gengozian continues to direct the NIH grant, "Immunology of Hematopoietic Chimerism in Tamarins." Dr. Snyder, heading the lipid project, receives support from the American Cancer Society on "The Occurrence, Metabolism, and Function of Glyceryl Ethers in Neoplasms" and also collaborates in an NIH grant to the University of North Carolina (Dr. Claude Piantadosi) on "Basic Studies on Alkenyloxy Glycerol Ethers and Function of Glycerol Ethers in Neoplasms." This year, NIH agreed to support a new project, "Chromosomal Breaks in Women Taking Oral Contraceptives." This work will be done by the cytogenetics group under Dr. Goh's direction.

We are indebted perennially to Betty Anderson, technical editor, for her dedication to Medical Division publication problems. We also wish to thank Katherine Stubbs, staff illustrator, Rush King, ORAU photographer, Frances Banner, who typed the manuscript, and the staff of the ORAU Information Services Department for their important contributions to this report.

Gould A. Andrews
Chairman

1027441

STUDIES IN RADIATION AND RELATED TOPICS

The Medical Division devotes a major share of its resources to problems related to radiation. Not only do we seek to improve therapeutic uses of radiation, but we also search for better ways to manage unwanted radiation injury. Thus our mission includes both elucidation of mechanisms of radiation injury and its treatment. In pursuit of these objectives, we perform research in hematology, experimental radiotherapy, immunology, cytogenetics, pathology, and ultrastructural anatomy. We continue to assess the effects of total-body irradiation on patients with a variety of diseases, not only with the medium-exposure-rate total-body irradiator but also with the newer low-exposure-rate irradiator. We have treated patients with leukemia, lymphoma, idiopathic thrombocythemia, and polycythemia vera, and have had opportunities to evaluate the data on several additional radiation accident victims. Quantitative dose-response relations based upon hematologic values have been difficult to establish in patients with diseased blood-forming systems. Although mathematical normalization tends to minimize the apparent variability of such data, patients with the same disease have a large variance in response to the same dose of radiation; different diseases are associated with significantly different degrees of radiation sensitivity. Any dose-response relation derived from patients would not allow direct extrapolation to normal man. These data may be useful, however, to define levels of acute radiation damage to sensitive hematopoietic systems. There is no evidence for any increased resistance to radiation damage in any of these diseases, but there is evidence of increased sensitivity in leukemic states. Thus any estimates of normal human tolerance for radiation that are made on patients would err on the side of conservatism. These observations are important as the uses of atomic energy broaden throughout the world. They also are providing information of value to the program of the National Aeronautics and Space Administration.

We are not urging the widespread adoption of total-body radiation as suppressive therapy for blood disorders. Our studies at the medium-dose-rate showed no special benefits that could not be achieved by other methods. Our low-dose-rate studies are too preliminary for an overall evaluation. We believe that these studies are producing valuable information on human radiobiology. The threat of serious infection caused by suppressed leukocyte levels and depressed immune response has not been adequately studied in the human being. Our microbiologic project is developing information that will help prevent or control the infections that will follow radiation exposures resulting from accidental exposure of industrial or military personnel, or that might be a consequence of nuclear warfare. Therefore, we are carrying out complete microbiologic studies in patients who have received radiation. In another special aspect of the microbiology program, studies are under way in the morphogenesis and pathogenicity of Candida albicans; studies emphasize the biochemical basis for a relation between morphogenesis and pathogenicity. This fungus is a serious opportunistic pathogen in debilitated patients, especially those whose

immune response is impaired by therapy for cancer or leukemia. We may find an improved groundwork for prophylaxis and therapy of this organism, which is becoming also an increasingly important clinical problem in the complications of indiscriminate or prolonged antibiotic therapy.

A long-range goal is to develop techniques that will allow treatment of radiation injury by hematopoietic grafts. For this reason, animal studies are supported that have bearing on homograft problems and the management of complications of homologous disease. Part of the work related to this objective is covered in the section on immunologic studies.

Acknowledgements should be made to the enormous amount of support given to these projects by talented technological assistance and dedicated nursing service. We especially wish to acknowledge the careful hematologic work that has been performed meticulously by Mrs. Joyce Hewins, Mrs. Kathryn Lore, and Mrs. Mary Thomas of the hematologic laboratory, and the detailed plotting of data by Mrs. Mary Smyser.

Especially noteworthy is the continuing obligation felt by staff members who are supplied with specimens from human sources. The physicians from the clinical services and the pathology department, assisted by nurses and technicians, contribute a great deal of time and skill in obtaining bone-marrow samples, blood, body fluids, and tissue specimens. In a significant way these make possible the work in projects such as microbiology, cytogenetics, and ultrastructural anatomy.

Responses in Chronic Granulocytic Leukemia to Total-Body Irradiation*

G. A. Andrews, R. M. Kniseley, Helen Vodopick, Per-Erik E. Bergner, and C. C. Lushbaugh

The data have been analyzed on all our patients with chronic granulocytic leukemia given 50 R or 100 R total-body irradiation at 1.5 R/min in the ^{137}Cs medium-exposure-rate facility. Short-term evaluation of clinical response observed during the first 6 weeks after treatment of 13 patients who received these doses showed that the spleen remained palpable and unchanged in size in eight, slightly smaller in one, and distinctly smaller in another. In the other three the spleen was not palpable before or after treatment.

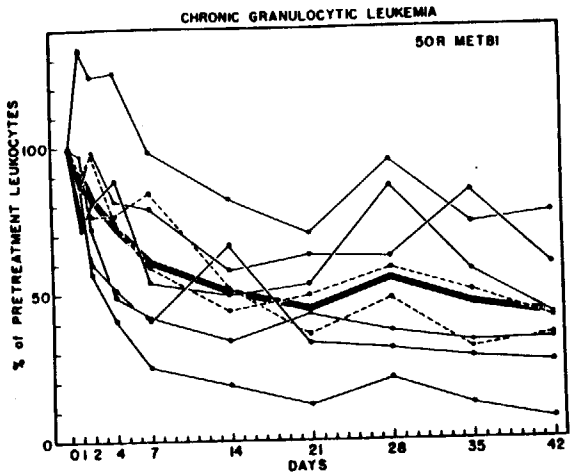

Fig. 1. The effect of 50 R total-body irradiation at 1.5 R/min upon blood granulocytes in in patients with chronic granulocytic leukemia. Individual variations in absolute numbers require the use of percentage of pretreatment values for purposes of comparison.

A definite decrease in liver size was recorded in only one patient. The general feeling of well being was unchanged in two, poorer in one, and some degree of improvement was recorded in 10, eight of whom were moderately or greatly improved. Figure 1 shows the effect of 50 R on leukocyte counts. All patients had high initial counts, predominantly of mature granulocytes, and the nongranulocytic elements are so few that the curves can be taken as representing mainly the numbers of granulocytes. They begin to decrease promptly at these low doses, and the count appears to be more responsive to radiation than that of normal patients. The depression of granulocytes in the leukemic patients is usually more persistent than in normals.

Only four patients were given 100 R. These showed a pattern similar to that of the 50 R group, but the degree of depression was greater; by day 21, three of the four had granulocyte levels below 20% of pretreatment levels. On the basis of the data now available, the dose of 100 R apparently produces a significantly greater depression in leukocytes than does the 50 R dose. This is in contrast to chronic lymphocytic leukemia in which the response of the leukemic cells to the two doses was the same.

The thrombocytes showed a moderate but definite increase during the first 2 weeks after treatment with either dose. The patients with chronic granulocytic leukemia were the only clinical group in which this increase was seen, although an earlier, more transient increase in platelets has been seen in some normal persons after higher doses. The posttreatment platelet increase in granulocytic leukemia may reflect in some way the fact that the platelets appear to be involved

* Presented in part at the Gesellschaft für Nuclearmedizin, Wiesbaden, Germany, September, 1968.

1021442

in the disease process. After the first 2 weeks thrombocytes showed a moderate, distinct depression, to below pretreatment values, which still persisted at the end of the 6-week period. The radiation-induced depression of abnormally elevated platelets in this disease tended to continue for weeks or months.

Mean hemoglobin values increased slightly during the latter part of the 6-week period and the increase was somewhat greater after the larger dose.

Responses to Total-Body Irradiation in Chronic Lymphocytic Leukemia and Lymphoma*

G. A. Andrews, R. M. Kniseley, Helen Vodopick, Per-Erik E. Bergner, and C. C. Lushbaugh

During 1968, the data were plotted and analyzed on all patients with chronic lymphocytic leukemia and lymphoma exposed to 50 R and 100 R total-body irradiation in the medium-exposure-rate total-body irradiator (METBI).

Chronic Lymphocytic Leukemia

Treatment exposures of 100 R were given to 20 patients, and of 50 R to 15 patients. These are not strictly comparable groups, but we believe after examining the cases that it is unlikely that differences in pretreatment status account for the differences in response to the two doses.

Examination was made of the records for clinical changes during the first 6 weeks after therapy in 35 patient treatments of either 50 R or 100 R. The lymph nodes became smaller in 20 and remained unchanged in 12. Of the palpable spleens, 10 were smaller after treatment, seven remained unchanged but palpable, and seven enlarged during the same interval. Similar changes occurred in the liver size.

Twelve patients recorded gain in weight, 13 lost weight, and eight were unchanged. The feeling of general well being improved to some degree in 21, remained unchanged in 12, and decreased in two. We could not demonstrate with any of these clinical responses that the effect of 100 R was greater than that of 50 R, although the small numbers of patients make this comparison inconclusive.

---

* Presented in part at the Gesellschaft für Nuclearmedizin, Wiesbaden, Germany, September, 1968.

1027443

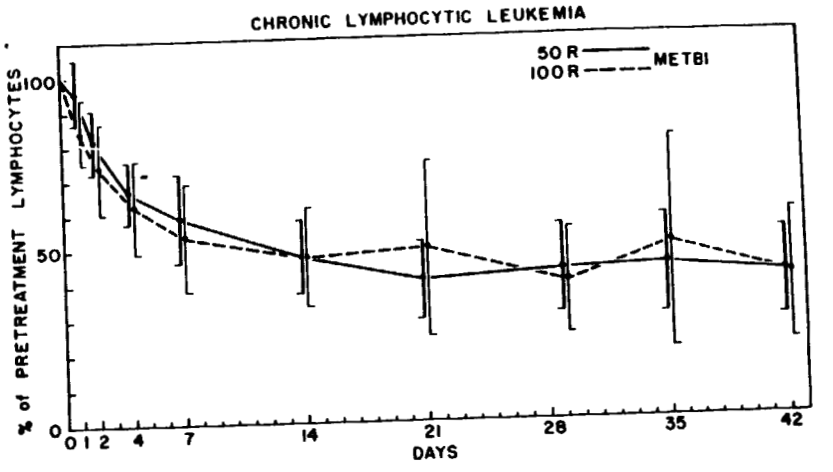

Fig. 2. Mean lymphocyte values in chronic lymphocytic leukemia after total-body irradiation expressed in percentage of pretreatment values (average of day -4 and day 0 values). Note remarkable similarity in responses to 50 R and 100 R exposure at 1.5 R/min.

Figure 2 shows the mean changes in blood lymphocytes after 50 R and 100 R exposures. There was no statistically significant differences in the degree of lymphocyte depression caused by these two doses. The leukemic lymphocyte responses to 50 R are greater than expected for normal lymphocytes. Although the most rapid fall occurs in the first week, the nadir is not reached until 3 or 4 weeks after exposure.

A striking difference is seen in the effect of the two doses on the thrombocyte levels, a much more pronounced depression being seen after the larger dose, as shown in Fig. 3. Furthermore, the variation in response of individual patients within the group is much greater at the lower dose, and suggests that recovery mechanism may be affected to a more variable degree with the lower dose, but that they are more completely suppressed by the higher dose.

Hemoglobin values tend to remain stable in those patients not anemic before treatment, and in those that were anemic there was usually no improvement during the 6 weeks following irradiation. In a small number of patients who had been requiring transfusions before treatment, the 100 R exposure apparently increased the number of transfusions needed, while 50 R did not.

Malignant Lymphoma

This group of 21 patients included six who were given 50 R; they are not reported here in detail but some information about them is given in Table 1. Twenty-two treatments of 100 R were given to 15

patients. These included 14 treatments to patients with lymphosarcoma and eight for other types of malignant lymphoma; none had Hodgkin's disease.

Evaluation of clinical response during the first 6 weeks after treatment showed no clear difference between the 50 R and 100 R groups.

Of 28 treatments with 50 R or 100 R, 24 of 28 showed some degree of shrinkage of lymph nodes; 17 showed a moderate or pronounced response while in three the nodes remained unchanged and in one they increased in size after therapy. Of the eight patients with palpable spleens, only two had definite regression of splenic size, while four showed continued enlargement, and in one the size remained unchanged. Of the palpable livers, 10 showed some regression in size while eight remained unchanged or became larger. There is no clear, consistent pattern of body weight change. The general feeling of well-being remained poor or unchanged in 17, but 11 expressed some degree of improvement in this subjective symptom.

Hematologic studies showed that most of these patients had at least a few atypical lymphocytes in the blood and we were not able to separate clearly those that should be considered as having a "leukemic" form of lymphosarcoma except for two who had larger numbers of abnormal cells and responded differently. All of the main group had pretreatment leukocyte counts of less than 15,000/cu mm and the numbers of lymphoid cells were less than 11,000/cu mm. The degree of depression in lymphocytes after therapy was not very great (lowest value was about 60% of pretreatment levels, reached at 7 days), and the failure to show a further drop after 7 days resembles the response of normal persons more than that of patients with chronic lymphocytic leukemia. By contrast the two patients with high numbers of abnormal lymphoid cells before treatment (16,000 and 26,800 cu mm) showed a very rapid and pronounced fall after 100 R, as shown in Fig. 4. Thus these patients with leukemic lymphosarcoma responded quite differently from patients with lymphocytic leukemia.

Thrombocyte values for the 100 R group showed a pattern almost identical with that of the patients with chronic lymphocytic leukemia given the same dose.

Hemoglobin values in this group of patients showed no significant change during the 6 weeks after exposure to either 50 R or 100 R.

Table 1 summarizes the minimum mean blood values observed after irradiation in three diseases. It again emphasizes the greater effectiveness of 100 R over 50 R upon the leukocytes of chronic granulocytic leukemia that is not found in chronic lymphocytic leukemia. Platelets are always more affected by the higher dose. Our patients with malignant lymphoma generally had lymphoid cells that were more resistant to radiation than those of patients with chronic lymphocytic leukemia, but two patients with leukemic lymphosarcoma, by contrast, showed a pronounced fall in lymphocytes after exposure.

We have had nine opportunities to treat a given patient with chronic lymphocytic leukemia or lymphosarcoma more than once with total-

1027444

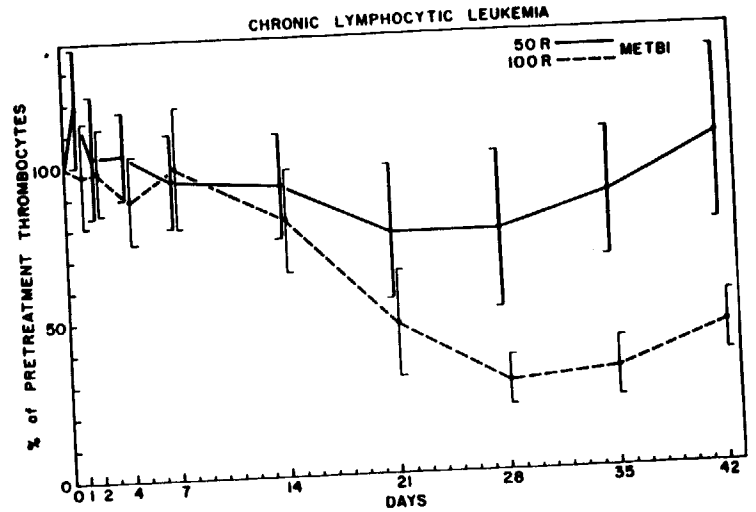

Fig. 3. Mean platelet responses expressed in percentage of pretreatment values in patients with chronic lymphocytic leukemia exposed to 50 R and 100 R total-body irradiation at 1.5 R/min. Note the significantly greater depression after the higher dose.

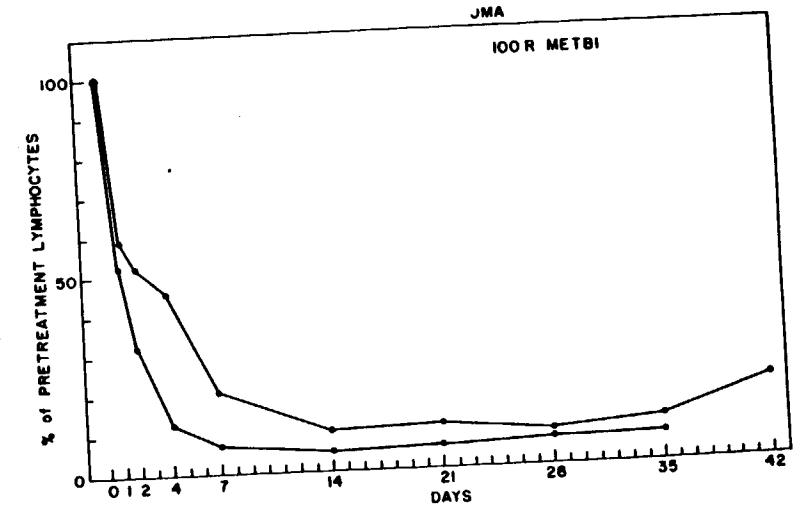

Fig. 4. Lymphocyte response to 100 R total-body irradiation at 1.5 R/min in two cases of lymphoma with leukemic manifestations. There is a rapid and pronounced fall in blood lymphoid cells sharply contrasting with the lesser response seen in the other patients with lymphoma.

body irradiation, and we have not been impressed with any significant change in radiosensitivity as a result of the previous dose. Usually many months intervened between successive doses.

Lymphocytes

The lymphocyte levels in chronic lymphocytic leukemia are certainly very sensitive to 50 R, probably more so than those in normal persons; data on the latter at this dose level are scanty. If we make a comparison with the Marshallese normals on Rongerik (Group III) who were estimated to have been exposed to 78 R, we find that their lymphocyte levels did not fall as much as leukemic lymphocytes would be expected to, from such a dose. Schrek has reported that some patients with chronic lymphocytic leukemia and lymphosarcoma have radioresistant lymphocytes as shown by an in vitro test. We saw variations in degree of lymphocyte depression after radiation in both groups, and less sensitivity in general in malignant lymphoma, but no clear separation of a resistant group in either diagnostic category.

TABLE 1

Minimum Mean Values During 6 Weeks after Total-Body Irradiation Expressed as Percentage of Pretreatment Level

	50 R	100 R
Total WBC		
Chronic lymphocytic leukemia	42%	36%
Chronic granulocytic leukemia	42	20
Malignant lymphoma	66	53
Lymphocytes		
Chronic lymphocytic leukemia	42%	42%
Chronic granulocytic leukemia	58	46
Malignant lymphoma	66	53
Platelets		
Chronic lymphocytic leukemia	80%	30%
Chronic granulocytic leukemia	73	53
Malignant lymphoma	70	32

Therapeutic Experience with the Low-Exposure-Rate Total-Body Irradiator (LETBI)

C. L. Edwards, C. C. Lushbaugh, Frank V. Comas, G. A. Andrews, and R. M. Kniseley

Total-body irradiation at the relatively low dose rate of 1.5 R/hr is proving to be an effective therapeutic approach to the control of

1027445

some blood dyscrasias. During the past year eight patients were treated in the LETBI facility bringing our total to 16 treatments. This experience with the LETBI facility has been summarized in Table 2.

TABLE 2

Summary of Low-Exposure-Rate Total-Body Irradiation Therapy

Pt. No.	Sex	Age	Exposure (R)	Residence (Hours)	Exposure (Hours)	Rad Dose	GI Effect	Change in Well-being	Tumor Reduction-Hematologic Improvement
A. Chronic lymphatic leukemia.									
1	M	76	100	73	67	52	0	0	+
2	M	77	100	80	66	52	0	0	+
B. Chronic granulocytic leukemia.									
1	M	12	100	74	67	52	0*	0	0†
2	F	45	100	79	67	52	0*	0	0†
3	F	55	100	77	70	52	0*	-	-
4	F	66	100	79	69	52	0**	-	0†
5	F	83	100	79	69	52	0**	0	0†
C. Lymphosarcoma									
1	M	79	100	76	67	52	0	+	+
2	M	62	250	202	170	130	0	++	+†
3	F	59	250	208	166	130	0	+++	++
D. Primary hemorrhagic thrombocythemia.									
1	M	61	150	116	100	78	0	+	++
2	M	62	150	119	103	78	0	+	++
E. Polycythemia rubra vera.									
1	M	60	100	80	66	52	0***	0	+
2	F	59	230	177	154	120	0	(++)	+++
3	M	61	250	204	172	130	0	++	+++
4	M	75	250	208	169	130	0	+++	+++

* Preexposure nausea that recurred at random intervals.
** Had transient bout of nausea during gastric wash for bacteriologic studies.
*** Had CVA with vomiting on last day after showing clinical improvement.
† Hematologic effects transient; other therapy required <6 weeks.

The lengths of time each patient resided in the facility and was exposed to the gamma radiation flux are also shown along with the resulting upper abdominal compartment dose in rads. Our dosimetry studies described elsewhere in this report have shown that "central" body radiation absorption is significantly lower in an omnidirectional flux like that of LETBI than in a single directional beam. The body apparently acts as an absorbent shield to all sites of interest, so that the exposure is attenuated and the dose is reduced to 52 to 54% of the free field measurement, much lower than the 65 to 67% estimate we were working with. This dose reduction in LETBI makes the degree of hematologic response obtained per dose unit quite comparable with that obtained at the higher flux; it prevents the conclusion that the low dose rate is any less efficient therapeutically than the higher one, except perhaps in patients with chronic granulocytic leukemia.

Even though patients must reside in the LETBI facility continuously for as long as 9 days to receive doses in the therapeutic range, their acceptance of this procedure is high, chiefly because this dose rate does not cause gastrointestinal distress or interfere with their

feeling of well-being. In our preliminary trials, although we were uncertain about untoward responses, we limited exposures to 100 R over 3 days. The lack of unpleasant symptoms was obvious, but clinical status improved little during or after the exposure period. With the length of exposure increased this year to about 9 days (a total residence time of about 200 hours; total exposure time, about 170 hours) clinical improvement often became obvious to the patients themselves before their residence in LETBI was ended. Three of five patients who received about 250 R exposure experienced an improvement in appetite during the therapy. Two were bedridden and became able to move about and care for themselves; each remarked spontaneously about his improvement. Although this improvement was not permanent, in two instances it lasted up to 240 days before it dissipated. In contrast, our experience with patients treated in the medium-exposure total-body irradiator (METBI) at higher exposure rate (1.5 R/min) is that even at lower total doses than the 250 R being used now in LETBI, the incidence of untoward symptoms of gastrointestinal distress typical of the radiation-induced prodromal syndrome has been high. These observations appear to demonstrate that exposure rates higher than 1.5 R/hr are required to trigger the

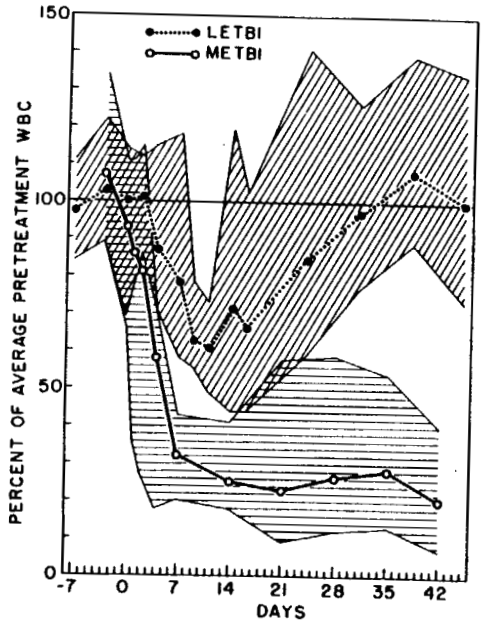

Fig. 5. This graph shows the average and the range of the total white blood cell count in five patients with chronic granulocytic leukemia treated with 100 R exposures in LETBI, and compares them with five patients treated with 100 R in METBI.

1027446

physiologic responses of nausea and vomiting in man; obversely, that man can repair gastrointestinal physiologic systems during exposure to this low dose rate.

Improvement in clinical well-being has been accompanied by desirable changes in the peripheral blood picture in patients with

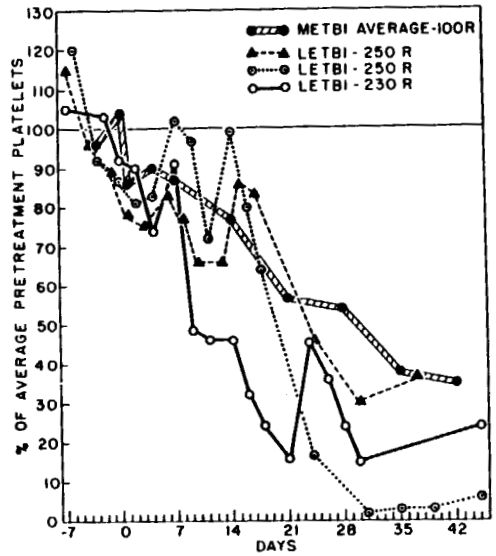

Fig. 6. This graph shows the response of the platelet count in three patients with polycythemia vera to exposure in LETBI comparing them with the average response of eight patients exposed to 100 R in METBI.

neoplastic blood diseases. In the patients where radiation exposure has been ineffective in producing a favorable hematologic response, clinical status has changed only a little or not at all. None of the five patients with chronic granulocytic leukemia, for example, treated with 100 R exposure in LETBI experienced clinical or hematologic amelioration of their disease to the same degree as those patients treated with 100 R in METBI (Fig. 5).

The best long-lasting hematologic responses have been obtained in therapy of the thrombocytosis of polycythemia rubra vera and idiopathic hemorrhagic thrombocythemia. In patients with polycythemia vera, this reduction in peripheral thrombocytosis has been accompanied by a decrease in headache, itching, and muscle cramps, and a return of the red blood cell volume profile toward normal as described in another paper in this report. Figure 6 shows the response of the platelet count in patients with polycythemia vera treated with 250 R

exposure in LETBI compared with the average response of eight patients treated with 100 R in METBI. One patient suffered a cerebral vascular accident during the LETBI treatment; interruption of the exposure was necessary after about 230 R. In addition to the amelioration of symptoms attributed to the blood disorders, two patients claimed improvement in their arthritic symptoms.

Three patients with malignant lymphomas were treated with about 250 R exposure. Each experienced at least temporary symptomatic improvement with some decrease in the size of the tumor masses. In one patient a massive abdominal tumor had incapacitated her to such an extent that she was barely able to sit up. After the radiation the tumor decreased sufficiently to allow her to become fully ambulatory, return home, and do light housekeeping. Subsequently she was given chemotherapy to effect further reduction in size of the tumor. She probably would have tolerated a longer initial exposure or an early reexposure, but these were not in our present protocol.

Patient acceptance of this form of treatment has been very good largely because of the lack of unpleasant gastrointestinal symptoms; the proven effectiveness encourages us to extend this treatment to more patients, some of whom will receive higher doses.

Theory of Quantitative Radiation-Response Data

Per-Erik E. Bergner

After a single dose of total-body gamma irradiation to patients with chronic lymphocytic leukemia, the white cell counts and platelet counts were recorded over a period of 42 days (see elsewhere in this volume). The patients were divided into two groups: one was given 50 R, and the other 100 R. The question then arose, Is there any difference in the response mechanism between the two dose levels? One thing that makes the question important is that, if there is any such difference, we must take it into account when trying to predict the effects of low doses; e.g., in connection with space flights or the very low doses encountered in occupational exposures.

Existing theories are usually designed for 0.1 response ("quantal response") whereas our data consisted of the response as a function of time. Moreover, the theories are essentially quantitative (they demand the estimation of one or several parameters) while the statistics of our data was poor enough to make such an analysis meaningless. In other words, the standard deviation was too large.

I have therefore tried to construct a new theory that would be meaningfully applicable to our data. In terms of the theory one calculates as a function of time not only the average response but the standard deviation as well. Hence, the spread in response (the

1027447

biologic variation) enters into the picture not as a merely annoying phendmenon but as an information-containing factor.

The basic principle of the approach is that the observed response is assumed to be the difference with time between a nondecreasing effect and a repair which may increase with time; both functions may stay constant, the important point being that they never decrease. The purpose of the data analysis is, in terms of this theory, to find out how the effect and repair are related to each other. The theory does not allow for definite conclusions, merely for possibilities, but this is as it should be because the theory is especially designed for substantially uncertain data.

White Cells

There is no significant difference between the two groups in the average response: the average count drops during the first 14 days and after then it remains constant. However, the standard deviation increases all the time, and I have interpreted this to mean that after the average response has reached its constant value effect and repair are still increasing, but they are increasing at about the same rate; according to this hypothesis one would expect an increasing standard deviation and, consequently, that the uncertainty in the prognosis of the system increases with time.

Of particular interest is the fact that the standard deviation of the 100 R group is constantly above that of the 50 R group. Hence, 100 R gives a less certain response than does a dose of 50 R. This surprising result can be understood in terms of elementary statistics.

Platelets

Doses of 100 R and 50 R give quite different average response: 50 R gives significantly less response than 100 R. On the other hand, the geometric shape of the two curves is remarkably similar, because the average counts start to decrease and then to increase (recover) at about the same points in time. On this basis it would be tempting to say that, although there are quantitative differences, the two groups are qualitatively similar - they have similar response mechanisms. However, the standard deviation for the 50 R group increases all the time, whereas for the 100 R group it first increases and then drops substantially until it starts to increase again; but the curve is still far below the 50 R curve. The final increase begins at the same time (day 28) as the average response starts to decrease. My interpretation of these findings is that the repair process becomes significant much earlier at a dose of 50 R than at 100 R. There is then a possibility that both 50 R and 100 R give effects of similar magnitude, but that 50 R gives less visible response simply because the repair starts earlier.

There are many reasons to believe that, compared with the white-cell response, the platelet response in these patients is close to what one would see in healthy people. Hence, if there is any truth whatsoever in the hypothesis of the previous paragraph, attempts in extra-

polation to low doses might give too optimistic results. Phrased differently, the hypothesis is that irradiation activates not only an effect but a repair process as well, and that when the dose decreases the repair starts earlier. In these terms, when the dose decreases, it is possible that the observed response (effect minus repair) drops more rapidly than the effect itself, significant parts of which may remain as so-called lasting effects[1] that do not show up until later.

REFERENCE

1. Sacher, G. A. and Trucco, E. The stochastic theory of mortality. Ann N Y Acad Sci 96, 985-1007, 1962, see p. 1000.

Study of the Mechanism of Splenic Irradiation in Chronic Granulocytic Leukemia

Helen Vodopick, Elizabeth M. Rupp, Frank V. Comas, Per-Erik E. Bergner, Francis A. Goswitz, and C. L. Edwards

The mechanism by which splenic irradiation can effectively lower the blood leukocyte count in chronic granulocytic leukemia (CGL) is unknown. Several possibilities exist: the destruction of cells passing through the spleen during the time of its irradiation or some indirect effect upon the bone marrow or a combination of both these effects.

To investigate this problem, leukokinetic studies using ^{32}P diisopropyl fluorophosphate (DFP) to label leukocytes under in vitro conditions have been performed on patients with CGL. Each patient served as his own control; pretreatment leukocyte disappearance curves were compared with those obtained after splenic irradiation. The leukokinetic studies done in association with the splenic irradiation were divided into two groups depending upon the temporal relation of the infusion of labeled cells to the splenic irradiation. In both instances, the blood to be labeled with ^{32}P-DFP was removed before the splenic irradiation was given. The in vitro tagged cells were given back to the patient either before or after the completion of a single dose of ^{60}Co splenic irradiation.

The amount of splenic irradiation to be given was calculated according to the following formula:

$$\text{Volume of tissue to be irradiated in cm}^3 \times \text{rads} = 1.6 \times 10^6$$
$$[\text{Length} \times \text{Width} \times \text{Depth of Spleen}] \qquad \text{(constant)}$$

Since the volume of tissue to be irradiated and the constant (product of volume x rads) were known factors, the rads could be varied to

1027448

give in one treatment a comparable dose from patient to patient.

Pretreatment control studies and leukokinetic studies started immediately after splenic irradiation (Studies I) have been completed in six patients with CGL (Table 3). An illustrative example is shown in Fig. 7. In addition two of these patients have had leukokinetic studies commenced just before splenic irradiation (Studies II) and completed after it.

The control studies in these patients showed a prolonged half-disappearance time of the labeled cells, as compared with normal persons. The leukokinetic studies done immediately after the completion of splenic irradiation revealed survival curves different from those done pretreatment.

The curves were seen to have three phases. Phase one was short as compared to the rest of the survival curve ($t_{1/2}$ range

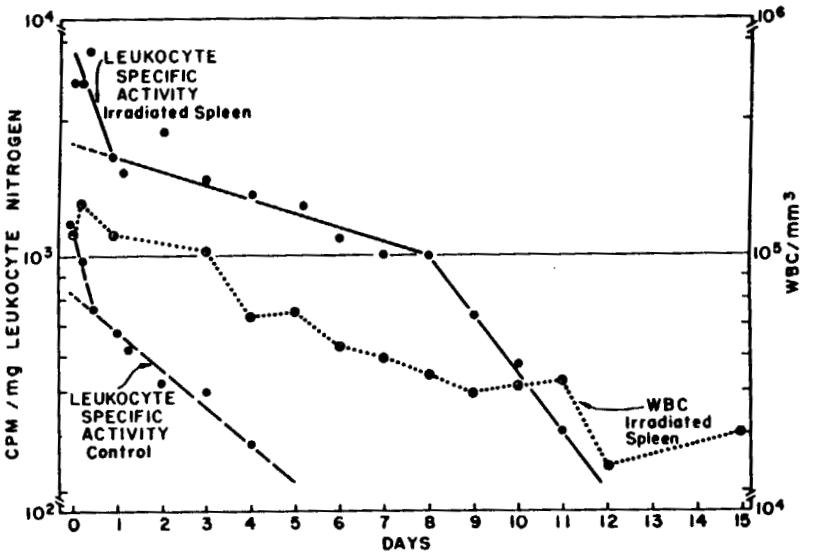

Fig. 7. Leukokinetic studies using ^{32}P-DFP in CGL in relapse. "Leukocyte specific activity" refers to leukocyte specific activity in the leukokinetic studies. All three curves were obtained on the same patient (Pt. 1). The lower curve represents the control pretreatment leukocyte survival study. The WBC count remained stable during this study. The upper two curves done at the same time show the changes after splenic irradiation. The falling WBC count in the circulation (middle curve) is accompanied by an apparently more sustained leukocyte survival of labeled granulocytes (upper curve).

TABLE 3

Comparison Studies of Granulocyte Survival in Patients with CGL

Patient	Phase	Control		Study I		Study II	
		T-1/2	Duration	T-1/2	Duration	T-1/2	Duration
1	1	3 hr		4 hr			
	2	96		192	192		
	3	-		56			
2	1	2-½		9		9	
	2	88		-	192	-	120
	3	-		91		72	
3	1	64		6			
	2			83	120		
	3			50			
4	1	11		3		6	
	2	-	72	-	120	92	120
	3	51		80		50	
5	1	12		2			
	2	61		104	120		
	3	-		50			
6	1	9		3			
	2	78		34			
	3	-		-			

2 to 9 hr); phase two was longer and showed further prolongation after splenic radiation; a third phase not present on four of the control studies became apparent after irradiation of the spleen.

Although these data have been incompletely analyzed, a tentative interpretation can be made. The rapid first phase is similar to that found in the control studies and represents either the rapid removal of injured cells, disappearance of a different granulocytic population, or recirculation of initially sequestered cells. The increased duration or survival of labeled cells during phase two suggests a diminished feed-in of unlabeled cells or a reduced production of cells. The specific activity of these labeled leukocytes is expressed as counts per minute per milligram of leukocyte nitrogen. This proposition is supported by the fact that specific activity of leukocytes given after splenic irradiation remains higher than the control specific activity in spite of the associated drop in the white blood cell count that occurred with the former group. Phase three indicates an accelerated destruction of cells or a dilution of the labeled pool with unlabeled granulocytes.

At this time a decreased production of granulocytes appears to be at least one of the main mechanisms accounting for the drop in the circulating white blood cells after splenic irradiation. However, we cannot exclude some abscopal effect. Revisions of these interpretations may be made after future study.

1027449

Leukokinetic Studies Using ^{32}P-DFP in Chronic Granulocytic Leukemia

Helen Vodopick, Elizabeth M. Rupp, Francis A. Goswitz, and C. L. Edwards

A previous report[1] on leukokinetics with the use of ^{32}P-diisopropyl fluorophosphate (^{32}P-DFP) to label cells in vitro has shown that the half-disappearance time of normal granulocytes in the circulation of man is 7 hr (normal range $t_{1/2}$ = 4 to 10 hr). These granulocytes disappear at an exponential rate implying a random destruction of cells rather than a death by senescence.

When this same technique of in vitro cell labeling is used in patients with chronic granulocytic leukemia (CGL) in relapse, cell disappearance rates differ from those found in normal persons (Fig. 8). The half-disappearance time of these leukemic cells ($t_{1/2}$ range = 25 to 96 hr) is prolonged. The disappearance curve does not always follow a single exponential rate; quite often a biphasic curve, and at times a slurred changing curve, has been observed.[2]

We have studied six patients with CGL in relapse. Unlike this previous report,[2] all except one of these patients had biphasic or triphasic disappearance curves (Table 4). When the second phase of each of these curves was extrapolated back to t_0 and then subtracted from the observed first phase, the actual half-disappearance time of Phase I was found to range from 2.5 to 12 hr. The second phase was long, 61 to 96 hr. In the only patient with a triphasic curve, Case 4, the second phase was expressed as a duration time, since a different, faster third rate of cell loss occurred before the second phase had reached a half-time value.

The finding of a short Phase I with a half-disappearance time in the range of normal would suggest the faster destruction of another group of cells. Whether cells damaged by in vitro handling or cells of a different population cause this faster removal rate is unknown. However, damaged cells are removed at an accelerated rate since the body recognized them as abnormal. In the present study Phase I ranged from 2.5 to as long as 12 hr. The latter figure suggests that this Phase I rate was not due to cell damage since this value exceeds that expected for even normal granulocyte removal. The most likely explanation for the Phase I curve is a removal of the mature granulocytes much as one would find in the leukocyte survival curve of normal persons who have only mature granulocytes.

The prolonged disappearance time of leukocytes found in patients with CGL in relapse has been ascribed to the presence of immature cells capable of dividing in the circulation. These labeled immature cells would produce labeled progeny which would in turn maintain the number of labeled circulating cells over a longer period than if only mature granulocytes are labeled as happens in normal persons.

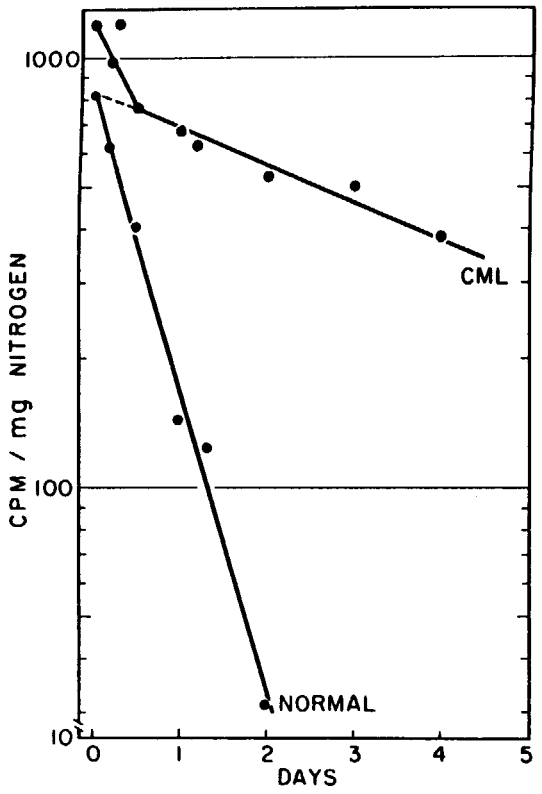

Fig. 8. Leukocyte survival curves of granulocytes labeled with ^{32}P-DFP. Lower curve shows the leukocyte survival of normal granulocytes with a half-disappearance time of 10 hr. Upper curve illustrates the prolonged biphasic curve found in CGL.

To carry out their functions, i.e., phagocytosis, granulocytes must mature and therefore are not used up until they do so.

These studies of leukocyte survival in CGL will serve as a base line for comparison with other studies in these patients under different clinical and therapeutic conditions.

REFERENCES

1. Mauer, A. M., Athens, J. W., Ashenbrucker, H., Cartwright, G. E., and Wintrobe, M. M. Leukokinetic studies. II. A method for labeling granulocytes in vitro with radioactive diisopropyl-fluorophosphate (DFP^{32}). J Clin Invest 39, 1481-1486, 1960.

2. Athens, J. W., Raab, S. O., Haab, O. P., Boggs, D. R., Ashenbrucker, H., Cartwright, G. E., and Wintrobe, M. M. Leukokinetic studies. X. Blood granulocyte kinetics in chronic myelocytic leukemia. J Clin Invest 44, 765-777, 1965.

1027450

TABLE 4

Leukocyte Half-Disappearance Time of Patients with CGL in Relapse

Patients with CGL in Relapse	Phase I Hours	Phase II Hours	Phase III Hours
1	3	96	--
2	2 1/2	88	--
3	64	--	--
4	11	72*	51
5	12	61	--
6	9	78	--

*Value given represents duration time since the half-disappearance time was not reached before Phase III began.

Cyclic Leukocytosis and Thrombocytosis in Chronic Granulocytic Leukemia

Helen Vodopick, C. L. Edwards, and Francis A. Goswitz

Spontaneous fluctuation of the leukocyte count in chronic granulocytic leukemia (CGL) has been recently reported by Morley and coworkers.[1] We report here our observation of a patient with a similar changing blood picture.

A 48-year-old woman was diagnosed as having chronic granulocytic leukemia in 1965. Initial therapy consisted of ^{60}Co splenic irradiation, 10 fractionated doses (1,480 R) in June, 1965; ^{60}Co

liver irradiation, 10 fractionated doses (1,480 R) in May, 1966; and ^{60}Co splenic irradiation, 1 dose (785 R) in March, 1967. In June, 1967 we noted for the first time that her leukocyte count dropped without any specific therapy from 58,000/cu mm to 22,000/cu mm over a period of 21 days. Subsequently frequent blood counts revealed a cyclic fluctuation of both the leukocyte and the platelet counts, which were in phase (Fig. 9).

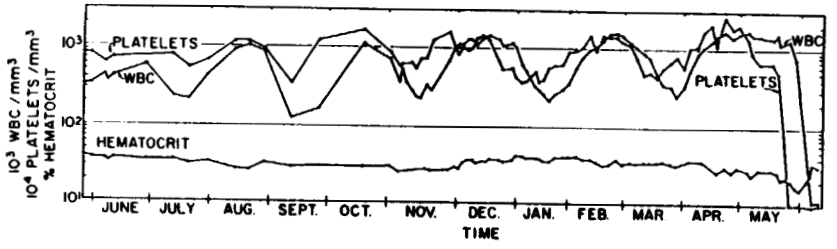

Fig. 9. Spontaneous cyclic leukocytosis and thrombocytosis during a 10-month period in a patient with chronic granulocytic leukemia. The precipitous drop of leukocyte and platelet values at the end of the fifth cycle was caused by drug therapy.

Four such cyclic changes were observed, each of which lasted 66 days. The fall in leukocyte count ranged from peaks of 100,000 to 150,000/cu mm to nadirs of 12,000 to 25,000/cu mm. The hematocrit varied only slightly, except for one episode of anemia for which she received two units of blood. The differential count of the blood showed no increase in blast forms during this period.

A bone-marrow aspirate obtained at the nadir of the first recognized cycle was morphologically consistent with the diagnosis of chronic granulocytic leukemia, but cytogenetically showed pulverization of the chromosomes. This latter finding was suggestive of an impending blastic crisis, which occurred 8 months later. Leukokinetic studies of her granulocytes labeled with ^{32}P-diisopropyl fluorophosphate showed a normal half-disappearance time of 10 hr, which is found in patients whose CGL is in control. This study was performed when her leukocyte count was 12,000/cu mm.

This phenomenon of cyclic leukocytosis and thrombocytosis may be more prevalent than is currently reported and may represent partial retention of a control mechanism shared in common over granulopoiesis and thrombopoiesis in such patients.

REFERENCE

1. Morley, A. A., Baikie, A. G., and Galton, D. A. G. Cyclic leucocytosis as evidence for retention of normal homoeostatic control in chronic granulocytic leukaemia. Lancet 2, 1320-1322, 1967.

1027451

Automated Determination of Muramidase Activity

Allen M. Webb, C. L. Edwards, and M. Francine Wright

The enzyme muramidase arises from a variety of cells and has been demonstrated in several biologic fluids including urine, milk, tears, saliva, and blood serum. Certain cells, particularly granulocytes and monocytes, are extremely rich in the enzyme. Alteration or degradation of enzyme-rich cells leads to increased activity in the serum and extracellular fluids. The enzyme is a low-molecular-weight protein probably involved in intracellular processes. However, no natural substrate has been found, and its specific function is unknown. In the study of leukemia, the measurement of enzyme activity has been used to aid in the differential diagnosis and to follow the course of the disease under treatment.

Difficulties are encountered in manual methods of assay. Turbidimetric methods require the measurement of a change in transmittance at an exact time after adding sample to reagent. When multiple samples are involved, manual methods are time consuming and tedious. Our automated method provides exact mixture of sample and reagent, a suspension of killed Micrococcus lysodeikticus.* This reagent is in 0.9% sodium chloride diluted to a concentration of 20 milligrams per 100 milliliters with distilled water. Lysis of the bacterial suspension produces a change in transmittance that is recorded at an exact-time-delayed interval and is reproducible for repeated samples and standards.

Our method of analysis uses standard autoanalyzer equipment consisting of Sampler II, pump, 630 mμ f/c colorimeter and recorder. The method manifold is constructed as shown in Fig. 10.

With the reagent and sample lines in distilled water, the recorder is set to give 100% transmission at a wavelength of 630 mμ. The reagent line is then placed in the bacterial suspension, and a base line of approximately 65% transmission is established. Standards, samples, and controls are analyzed at a rate of 40/hr, but alternate cups should contain distilled water to insure adequate wash.

The bacteriolytic activity of the enzyme produces an increase in light transmission that is recorded and is proportional to the enzyme concentration up to 16 micrograms per milliliter. Because a poor relation between enzyme activity and percentage of transmission exists at higher concentrations, all serum samples with 16 micrograms per milliliter or greater activity, were retested with dilution sufficient to reduce the activity to less than that level.

Enzyme activity is expressed as micrograms per milliliter by reference to a standard curve prepared with chicken egg white lyso-

* Worthington Biochemical Corp., Freehold, New Jersey

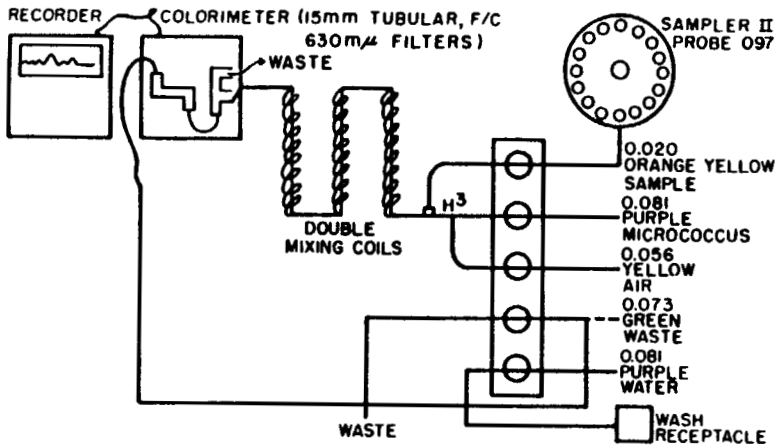

Fig. 10. Flow diagram of method.

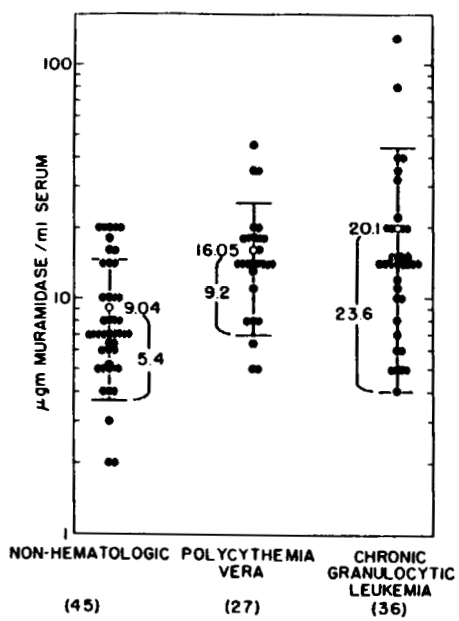

Fig. 11. Serum muramidase results for control group, polycythemia vera, and chronic granulocytic leukemia.

1027452

zyme in commercial control or pooled human serum of low enzyme activity. Stock muramidase standard (40 micrograms per milliliter) is prepared by adding 10 milliliters of commercial or pooled serum to a 400-microgram vial of chicken egg white lysozyme. Working standards of 4, 8, 12, 16, and 20 micrograms per milliliter are prepared by diluting 0.2, 0.4, 0.6, 0.8, and 1.0 milliliter of stock standard to a volume of 2.0 milliliter with commercial or pooled serum.

Our results show a mean enzyme activity value in a group of patients without hematologic disease to be 9.0 micrograms per milliliter. Perillie et al.,[1,2] using a turbidimetric method, reported a mean value of 8.2 micrograms per milliliter. Our findings in patients with hematologic diseases were no different from those previously reported.[3-5] That is, values for patients with granulocytic leukemia and polycythemia vera are greater than for patients with nonhematologic disorders (Fig. 11), and our values for one patient with monocytic leukemia were significantly greater than those for the granulocytic leukemia group.

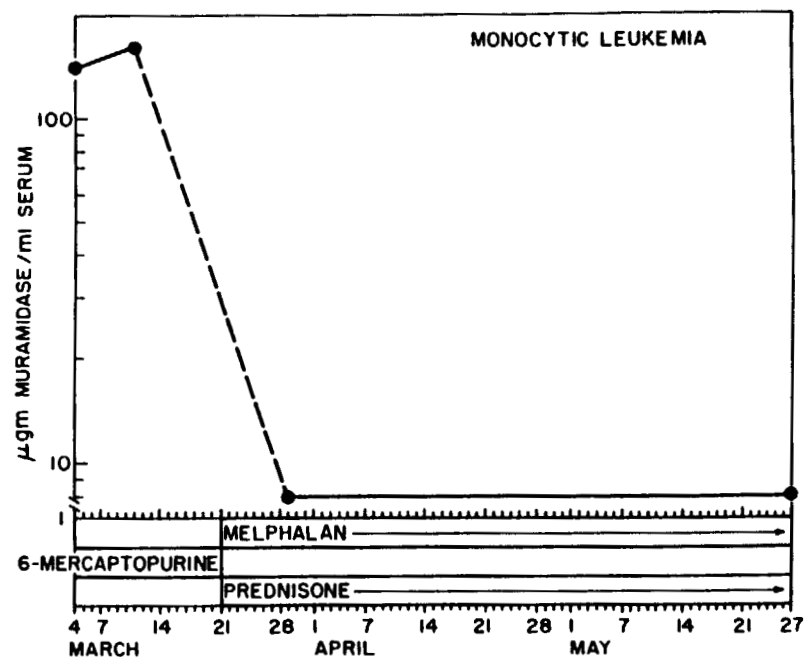

Fig. 12. Serum muramidase results in a monocytic leukemia patient during treatment.

In our studies we noted no difference between the lymphocytic leukemias and nonhematologic groups.

The high serum muramidase value in our case of monocytic leukemia returned to normal as remission was attained after appropriate therapy (Fig. 12). With this improved technique this measurement of muramidase activity may prove to be of practical value in the management of patients with leukemia undergoing chemotherapy and of patients who have received therapeutic or accidental irradiation.

REFERENCES

1. Perillie, P. E., Kaplan, S. S., and Finch, S. C. Significance of changes in serum muramidase activity in megaloblastic anemia. New Engl J Med 277, 10-12, 1967.

2. Perillie, P. E., Kaplan, S. S., Lefkowitz, E., Rogaway, W., and Finch, S. C. Studies of muramidase (lysozyme) in leukemia. JAMA 203, 317-322, 1968.

3. Inai, S., Hirao, F., Kishimoto, S., and Takahashi, H. Serum lysozyme. II. Lysozyme activity in normal human serum and in serum of patients with various diseases. Med J Osaka Univ 9, 33-43, 1958.

4. Osserman, E. F. and Lawlor, D. P. Serum and urinary lysozyme (muramidase) in monocytic and monomyelocytic leukemia. J Exp Med 124, 921-952, 1966.

5. Flanagan, P. and Lionetti, F. Lysozyme distribution in blood. Blood 10, 497-501, 1955.

Marrow Fibrosis in Myeloproliferative Disorders

Bill Nelson and R. M. Kniseley

Reticular and collagen fibers in the marrow were evaluated in autopsies of 90 patients who had presented with idiopathic myelofibrosis, polycythemia vera, thrombocythemia, and acute or chronic granulocytic leukemia. The series includes all autopsies of patients seen here for these diseases, except for a few dying shortly after the inception of the Medical Division in 1950. The salient criteria for classification based on findings at the time of first presentation are given in Table 5.

Histologic sections of the spleen, liver, and lymph nodes were

1027453

reviewed to determine the presence and severity of extramedullary hemopoiesis and of leukemic infiltrations. All the autopsies included several samples of marrow and most had labeled samples of vertebral bodies (T_6, T_{10}, L_1, and L_5), sternum, ribs, ilium, pubis, femur, patella, and tibia. Paraffin blocks representative of marrow from the trunk and femoral shaft were selected for additional sections and stains; bones in the fields of local radiotherapy and those with incidental lesions were excluded. Marrow of the femoral shaft was considered indicative of the extension of hemopoiesis to the

TABLE 5. Classification of 90 Patients with Myeloproliferative Disorders

Initial Diagnoses	Distinguishing Criteria	Autopsies	Final State of Marrow*			
			Blastic	Fibrotic	Both	Neither
Idiopathic myelofibrosis	Anemia, splenomegaly, and fibrosis of marrow	6		6		
Polycythemia rubra vera	Erythrocytosis, other causes excluded	7	2	2	2	1
Thrombocythemia	Great excess of platelets in blood, without erythrocytosis or leukocytosis	2	1			1
Chronic granulocytic leukemia	Great excess of mature granulocytes, fewer than 5% blasts in the blood	25	11	3	11	
Acute granulocytic leukemia	Great excess of primitive cells of the granulocytic series in the marrow	50	46		4	

*Blastic= Clinical or autopsy evidence of acute leukemic state; no more than slight or focal marrow fibrosis.
Fibrotic= More than slight increase in reticulum without acute leukemic state.
Both= Acute leukemic state and more than slight fibrosis.
Neither= No clinical or autopsy evidence of acute leukemic state, no more than slight or focal fibrosis.

extremities. Wright-stained smears and touch preparations from many of the autopsies were useful in the detection of slight extramedullary erythropoiesis or an early blastic state. Sections from all the representative blocks were stained with hematoxylin-eosin, hematoxylin-eosin-azure, Hutchinson's stain for iron, and the Humason-Lushbaugh method for reticular fibers, collagen, and elastica. (For optimal black and white photographic contrast of the argyrophilic fibers only the first steps of the Humason-Lushbaugh procedure were used, as in Figs. 13 and 14.)

The sections of marrow were evaluated without reference to the diagnoses, previous descriptions, or clinical information. Samples were graded for abundance and coarseness of reticular (argyrophilic) fibers relative to the cellularity, as indicated with Fig. 14. Because the quantity of reticular fibers was estimated in relation to the cellularity, hypercellular marrows graded as normal (N) often contained

more fibers than the marrow of healthy adults with the usual degree of adiposity of the hemopoietic tissue.

Collagen, identified with the Aniline Blue of the Humason-Lushbaugh method, was quantitated in a similar way; that in osseous tissue and blood vessels was disregarded in estimating the quantity.

Fig. 13. Marrow representative of idiopathic myelofibrosis, having a severe increase in reticulum, with irregular masses of bone containing coarse collagenous fibers that extend into the relatively cellular marrow. The large gaping sinuses are typical. (Silver impregnation with gold-toning; in the section reticulum is black, collagen and bone are brown, 200 X).

The fibrosis in patients presenting with idiopathic myelofibrosis was pronounced and always accompanied by abnormal ossification (Fig. 13). The histology of this fretwork of "fibre bone" has often been illustrated and described. We have not been able to differentiate it clearly from lesser bony abnormalities in one patient with polycythemia vera nor from rare foci in three patients with chronic granulocytic leukemia. Similar proliferations of bone have been reported with severe fibrosis of the marrow in patients with acute granulocytic leukemia, monocytic leukemia, and undifferentiated leukemia. In our series the abnormal medullary bone formation was conspicuous only in the six patients we had classed as having idiopathic

1027454

myelofibrosis and was the major morphologic feature distinguishing them from the others.

We join others in failing to recognize a role of necrosis or necrobiosis in the development of generalized myelofibrosis. Frank necrosis and reparative ossification do not adequately explain the diffuse marrow fibrosis or bony abnormality seen with myeloproliferative disease. Speculations concerning toxic or autoimmune factors in the genesis of marrow fibrosis are neither supported nor refuted by our experience.

The categories with the most marrow fibrosis (idiopathic myelo-

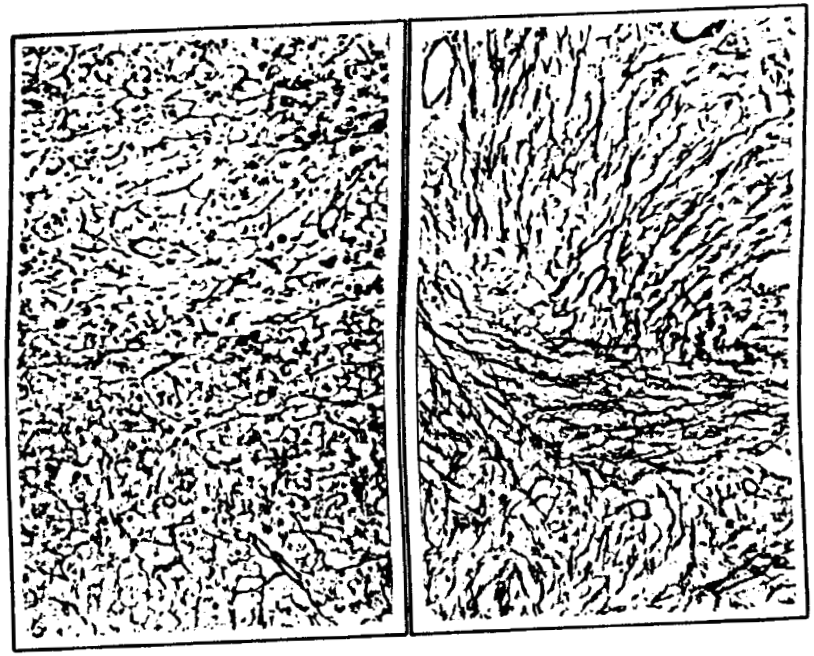

Fig. 14. Photographs of silver impregnations of marrow sections representative of two grades of increases in reticular fibers.
Left: Marrow reticulum moderately increased (2+). The argyrophilic fibers are more numerous than normal and some are longer and more coarse. (Acute granulocytic leukemia, 200X).
Right: Marrow reticulum increased severely (4+). This is the most pronounced degree, with greatly increased numbers of argyrophilic fibers, many of which are long, coarse, and arranged in bundles. Fibrosis is plainly evident by the arrangement of cells in hematoxylineosin stains, in which reticular fibers are scarcely visible. The waviness of some fibers is characteristic of the presence of collagen, confirmed by the Aniline Blue stain. (Chronic granulocytic leukemia, 200 X)

fibrosis and polycythemia vera) had the most extramedullary hemapoiesis, but within each category the severity of marrow fibrosis had little relation to extramedullary hemopoiesis or hepatosplenomegaly. Patients who had lived longer often had received more treatment, and many had marrow fibrosis, but the fibrosis could not be ascribed to radiation or chemotherapy.

The study supports the contention that the myeloproliferative disorders include several distinct diseases with certain features in common. We sought explanation for such clinical impressions as the poor prognosis of patients with "chronic" myeloproliferative disease who develop "secondary" myelofibrosis. One factor is apparent in Table 5: most of the 14 patients with chronic granulocytic leukemia having marrow fibrosis had also entered a blastic phase, which always ran a short course. Another factor lies in the frequent finding of at least slight marrow fibrosis and in a cumulative progression of the fibrosis that seems to occur in some patients. After the initial diagnosis of polycythemia vera or chronic granulocytic leukemia, marrow aspiration may not be required for several years. Thus the ominous portent of an unsatisfactory aspirate ("dry tap") may sometimes be an illusion, merely reflecting the fact that the need to examine the marrow signifies a deterioration of the clinical state. The fibrosis has obviously been present for some time; its presence may be incidental, and the finding should not preclude a search for other conditions, such as a blastic transformation, an infection, or toxicity from treatment.

Whatever the explanation, dry taps of leukemic and "late" polycythemic patients were most common in the last few months of life. Survival after diagnosis of secondary myelofibrosis was short compared to idiopathic myelofibrosis, although in our series none of the patients with idiopathic myelofibrosis had the longevity that is occasionally reported. The average survival after diagnosis in these six was only 19 months, and none lived longer than 40 months after the demonstration of fibrosis of the marrow. Other authors have also reported a prognosis comparable to that of patients with chronic granulocytic leukemia, half of whom in this series lived more than 41 months after diagnosis.

The selection of cases was affected by factors related to referral, and the circumstances of death tended to weight the series with patients having aggressive disease or complications of therapy. Patients with a more benign course, especially those with polycythemia vera and idiopathic myelofibrosis, were often seen briefly and returned to the care of referring physicians. Many patients with myeloproliferative disorders admitted to this hospital before the last autopsy in this series (February 1968) are still living, and some of these have fibrosis of the marrow. The overall incidence of fibrosis in these diseases may be lower than in the autopsied cases, but the likelihood of the development of significant marrow fibrosis warrants a prospective study with serial marrow biopsies in groups of patients with "agnogenic myeloid metaplasia," polycythemia vera, and chronic granulocytic leukemia.

1027455

Electron Microscopic Study of a Malignant Lymphoma

D. C. Swartzendruber and Bill Nelson

The classification of lymphatic tissue diseases is complicated by the labile organization of components, especially the lymphatic nodules. The constituent cells of lymphatic tissue are still not precisely defined, partly because of transitional and intermediate forms. The electron microscope can contribute to a better understanding of lymphatic tissue and its diseases by permitting more precise criteria for the identification of cells than tinctorial differences. Systematic ultrastructural studies require careful selection and orientation of the necessarily small tissue samples and correlation with histopathologic study. Malignant cells arranged in nodules corresponding to germinal centers were of special interest in this study.

The diagnosis of nodular malignant lymphoma of mixed histiocytic and lymphocytic type was based on biopsy of a cervical lymph node of a 59-year-old woman. A portion of this node was fixed in paraformaldehyde and gluteraldehyde, postfixed in OsO_4 and embedded in Epon 812. Lymphatic nodules seen in paraffin sections and in "thick" Epon sections

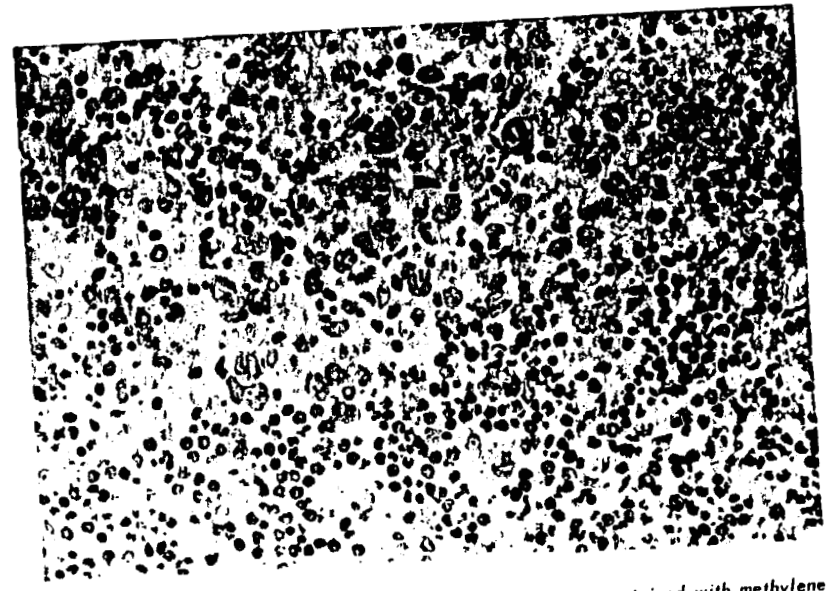

Fig. 15. Photomicrograph of a thick (~½ micron) Epon section stained with methylene blue. Such sections are used to orient adjacent thin sections for electron microscopy. Note the pale-staining germinal center and surrounding darker "cuff" of lymphocytes. All succeeding electron micrographs are from thin sections of this block. 400 X.

(Fig. 15) contained pale-staining central areas with features characteristic of germinal centers.

Many of the lymphocytes found within germinal centers and comprising the "cuff" around germinal centers had numerous expansions[1] of the nuclear membrane (Fig. 16). Cells (Fig. 17) in the germinal centers corresponding to large tissue lymphocytes or hemocytoblasts[2] had abnormally lobular nuclei. Nucleoli were enlarged in some of these cells but not in others. Clusters of ribosomes were present but they were less prominent than in typical hemocytoblasts.

Two other types of cells described as "light" and "dark" reticular cells (Fig. 18) were seen in the germinal centers. Desmosomes (Fig. 18

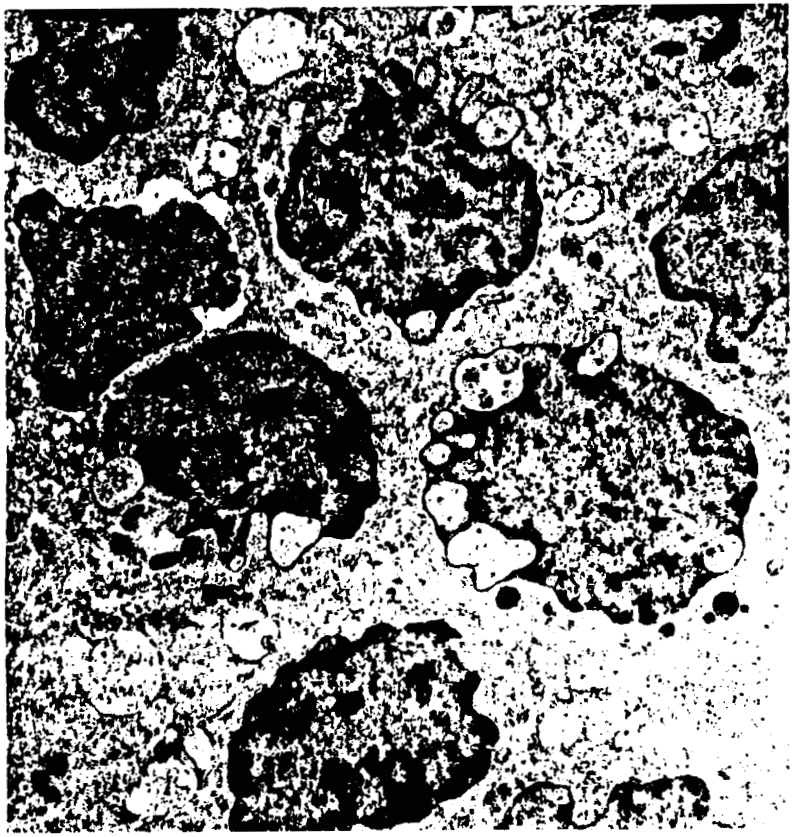

Fig. 16. Electron micrograph of lymphocytes adjacent to the germinal center. Note the bleb-like expansions of the nuclear membranes of three cells. 12,000 X.

1027456

Fig. 17. Electron micrograph of a large cell from the germinal center. The nucleus, N, appears highly lobulated in this plane of section. Note the centriole, C, and clusters of ribosomes in the cytoplasm. 12,000X.

inset) were observed frequently on the surfaces of opposed cell membranes. Despite the claim that the presence of desmosomes in lymph nodes indicates metastasis of an epithelial malignancy,[3] the clinical and histologic findings in this patient are clearly diagnostic of malignant lymphoma. Moreover, desmosomes have been demonstrated in benign lymphoid tissue.[4]

Ultrastructural studies can contribute valuable information about cellular abnormalities in malignancy. Although its primary use is not as a diagnostic tool, the electron microscope can demonstrate cellular structures that may be useful in supplementing the histopatholo-

Fig. 18. Electron micrograph of reticular cells in the germinal center. The small "dark" nucleus in the upper right belongs to a cell with narrow cytoplasmic strands (arrows) extending between and around other cells in this section. The large clear nucleus, N, with a prominent nucleolus belongs to an adjacent reticular cell. 13,000 X. Inset shows a desmosome of the macula adherens type found in the germinal center. 90,000X

1027457

gic diagnosis of certain neoplasms. The present study, however, emphasizes the need for further knowledge of the ultrastructure of normal lymphoid tissues and the changes induced by inflammation and other benign states.

REFERENCES

1. Bessis, M. Ultrastructure of normal and leukemic granulocytes. In: Proceedings of the International Conference on Leukemia-Lymphoma. C. J. D. Zarafonetis, editor, Lea and Febiger, 1965, pp. 281-303.

2. Fagraeus, A. Nomenclature of immunologically competent cells. In: Ciba Foundation Symposium on Cellular Aspects of Immunity. G. E. W. Wolstenholme and M. O'Connor, eds. Boston, Little, Brown and Co., 1960, pp. 3-4.

3. Bernhard, W. and Lepus, R. Fine Structure of the Normal and Malignant Human Lymph Node. Gauthier-Villars, Paris, 1964, p. 23-24, plate 94.

4. Swartzendruber, D. C. Desmosomes in germinal centers of mouse spleen. Exp Cell Res 40, 429-432, 1965.

Techniques for Enhanced TLD Reliability

W. L. Beck

In less than five years thermoluminescent dosimetry (TLD) has grown from an experimental laboratory technique to a widely used clinical method. Some of the superior characteristics that have brought about its acceptance are (1) accuracy, (2) wide sensitivity range, (3) tissue equivalence, (4) energy independence, (5) small size, and (6) reusability. Of these characteristics, accuracy and reusability are very dependent upon the techniques used for calibration and annealing. Since TLD is not an absolute method (that is, the quantity measured is not directly related to the exposure or the absorbed dose) calibration is necessary. We have developed improved methods for calibration and annealing in our TLD system.[1]

To determine the reproducibility and the reusability of extruded LiF dosimeters,* new ones were put through several cycles of annealing,

---

* Extruded dosimeters (1.4 x 1.4 x 7 mm rods) of lithium fluoride were obtained from the Harshaw Chemical Co., Cleveland, Ohio.

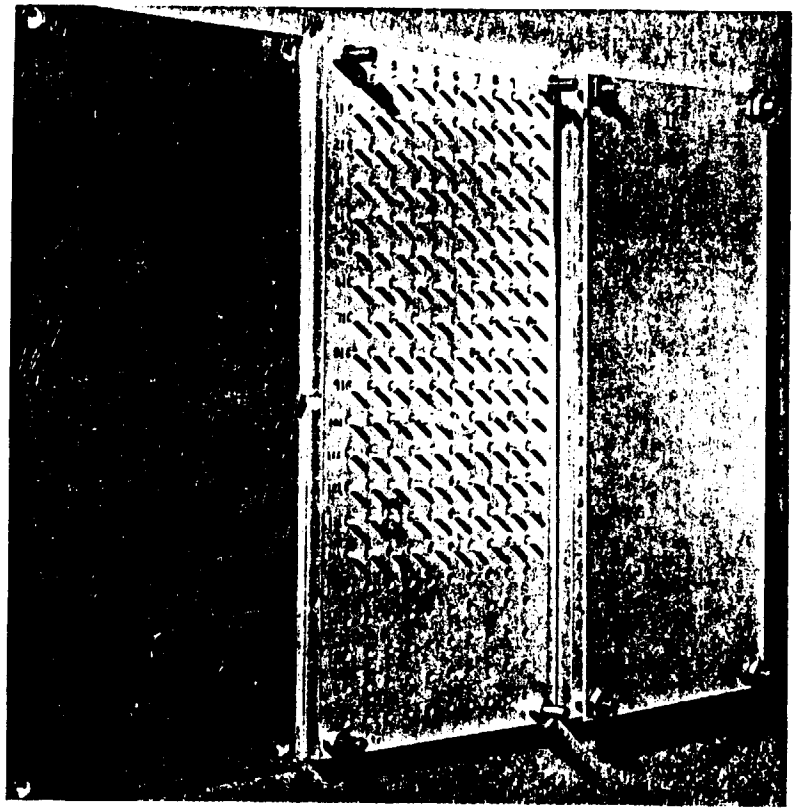

Fig. 19. Aluminum holders for annealing extruded dosimeters.

exposure to 100 R, and readout. We observed that (1) there were large differences in sensitivity (counts per roentgen) among those of the same batch; (2) changes in sensitivity of 15% or more resulted from changes in the annealing method; and (3) these annealing-induced changes were approximately equal for all dosimeters. To prevent condition 1 from producing errors in our measurements it was necessary to calibrate them individually. Condition 2 required that the sensitivity change between each use be determined. Condition 3 indicated, however, that the change in sensitivity between uses for all dosimeters could be estimated accurately if the change for a few dosimeters was measured.

On the basis of these findings, we developed the following calibration and annealing techniques. New dosimeters were first annealed for 1 hr at 400° C in specially designed aluminum holders (Fig. 19), which provided an environment of uniform heat during annealing and a convenient means of handling large numbers between annealing, exposure, and

1027458

readout. After the initial annealing, the dosimeters were then given a sensitizing exposure of 100 R and reannealed by a three-step process: (1) 400° C for 15 min, followed by cooling to room temperature in 20 to 30 min; (2) 100° C for 2 hr; and (3) a postexposure annealing of 100° C for 15 min.

An identification number was then lettered onto each dosimeter to facilitate individual calibration. They were exposed to 100 R and read out. The first 10% were designated as "reference dosimeters," and their average response was calculated. The response of each of the other dosimeters, the "working dosimeters," was then divided by the average response of the reference dosimeters. These quotients were taken as the working dosimeters' individual calibration factors. When a working dosimeter's response is divided by its calibration factor, the sensitivity of that dosimeter is adjusted to be equivalent to that of the reference dosimeters. The sensitivity of the reference dosimeters is determined by exposure to known doses each time the working dosimeters are used. Thus to determine the exposure that a working dosimeter has been given, its response (counts) is divided by its calibration factor (a constant) to adjust its sensitivity to be equivalent to that of the reference dosimeters; that quotient is divided by the sensitivity factor (counts per roentgen) of the reference dosimeters.

Laboratory exposures were generally measured with standard deviations of approximately 1%; measurements made by several different dosimeters at the same position on a patient rarely disagreed by as much as 5% and usually agreed to within 2%.

REFERENCES

1. Beck, W. L., Callis, E. L., and Cloutier, R. J. Phantom depth-dose measurements with extruded LiF in a low-exposure-rate total-body irradiator. In Proceedings of the Second International Conference on Luminescence Dosimetry, September 23-26, 1968. J. A. Auxier, K. Becker, and E. M. Robinson, eds. USAEC Report CONF-680920, 1968, pp. 976-989.

Patient Dosimetry for the Low-Exposure-Rate Total-Body Irradiator

W. L. Beck, Roger J. Cloutier, Frank V. Comas, C. C. Lushbaugh, and Tom R. Stokes

One can express the "dose" a patient receives from a total-body irradiation in many ways; but generally one chooses a single dose expression for a given analysis of dose versus specific biological response. The response studied often dictates the volume or site where the dose must be measured. The basic cause and effect concept, as discussed

in target-organ theory, suggests that specific biological regions, called target organs, control certain biological responses. The degree of response is directly related to the radiation dose that the target organ receives. Some simple examples include the relation of skin erythema to skin dose and of cataract formation to the dose to the lens of the eye. More complex are the relations involving the location of the target organs and responses such as nausea, vomiting, hematologic change, and lethality. For these responses the target-organ volume is generally indefinite and often obscure and must be deduced from analysis of the relations between the reaction and the doses to several possible target-organ regions. Since many responses and many possible target organs are of interest, we concluded that the most practical approach to this dosimetry problem was to determine as completely as possible the depth-dose distribution in a patient, so that the absorbed dose to any specific region assumed to be a target organ could be calculated with acceptable accuracy.

Obviously, the numerous depth-dose measurements required to satisfy our needs could not be made within a patient, so we used the analogue method of phantom dosimetry. The depth dose and the surface exposure were determined with a man-like phantom and a patient's depth-dose was assumed equal to the phantom's if there was good correlation between the surface exposure values measured on patient and phantom. Surface exposure measurements were made in the same nine positions on both patient and phantom for this comparison. The validity of this dosimetry technique depends upon two factors: how well the phantom represents the patient and the accuracy of the dosimetry measurements.

We used an Alderson Rando phantom[1] consisting of a head and trunk to resemble an average man that would be 5 ft 8 in. tall and weigh 162 lb if complete with arms and legs. The phantom is constructed of an isocyanate rubber that simulates human tissue both chemically and physically. The effective atomic number ($Z = 7.30 \pm 1\ 1/4\%$) and the specific gravity ($0.985 \pm 1\ 1/4\%$) have been adjusted to be the equivalent of tissue with respect to interactions with X and gamma radiation. Molded within the phantom is a human skeleton and a set of density-adjusted lungs (specific gravity = $0.30 \pm .01$). The phantom is sliced transversely into sections 2.5 cm thick. Each section is drilled with 5-mm diameter holes in a 3 x 3 cm grid to provide uniform positions to hold small dosimeters. These holes are filled with removable plugs of tissue-equivalent material when not in use as dosimeter sites.

All dosimetry measurements on the patients and phantom were made by thermoluminescence dosimetry (See p. 37). Small lithium fluoride dosimeters were placed in plastic pouches, which were taped to the patient's chest, waist, wrists, and ankles just before therapy. The dosimeters were not removed until the treatment was completed.

Phantom measurements were then made to determine the depth-dose distribution (Fig. 20). Lithium fluoride dosimeters were placed within the phantom and at surface positions just as on a patient. The phantom was exposed in different positions (sitting, standing, lying) and in several places within the 16 x 16 ft treatment room to simulate the patient's

1027459

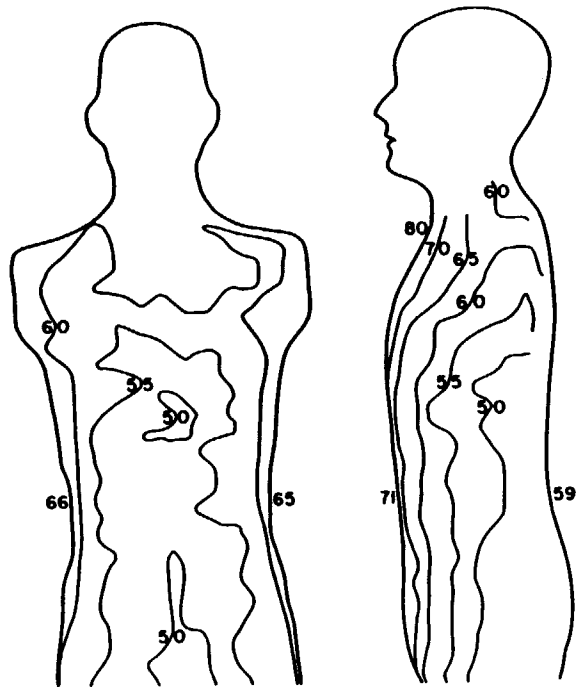

Fig. 20. Depth-dose distributions in the midlongitudinal and midsagittal planes as measured in the Alderson Rando phantom irradiated in the LETBI facility. The numbers are the rad dose when the exposure at the center of the treatment room is 100 R.

movements during therapy.

Figure 20 shows the isodose lines measured in the midsagittal and midlongitudinal planes. The midlongitudinal depth-dose distribution within the phantom is quite symmetrical; however, the midsagittal distribution is nonsymmetrical. We attribute the decrease in depth dose toward the back of the patient to the presence of the backbone and because in the lying and sitting positions there is shielding material (furniture) against the patient's back. Average target organ doses calculated from complete depth-dose distribution measurements are tabulated in Table 6. The average target organ dose is defined as the average dose measured within the volume in which the target organ is thought to reside.

REFERENCE

1. Alderson, S. W. The role of phantoms in radiology: Macklett-Alderson phantom systems. Cathode Press 23, 2-35, 1966.

TABLE 6

The Average Target Organ Dose in Rads Resulting From an Exposure of 100 R at the Center of the LETBI Treatment Room

ORGAN	AVERAGE TARGET ORGAN DOSE (Rads)
Cerebellum	71
Cerebrum	74
Heart	63
Lenses of Eyes	88
Spleen	62
Thyroid	80
Liver	68
Lungs	64
Vertebral Bones	59
Kidneys	60

The Radiosensitivity of Rat Bone-Marrow Cells, Irradiated In Vitro

Frank V. Comas

This study complements a series of experiments reported in the research report for 1967,[1] in which the radiosensitivity of rat bone-marrow cells was determined, after irradiating them in vivo.

A survival curve has been obtained for rat bone-marrow cells irradiated in vitro. Fischer-334 rats were used as recipients as well as cell donors. The bone-marrow cells were obtained from the femoral cavity and suspended in Hank's solution. The suspension was irradiated at melting ice temperature, with ^{137}Cs radiation, at a dose rate of 3.5 rads/min. These cells were then injected intravenously into recipient rats that had previously been given 1400 rads total-body irradiation. The recipients were killed 12 days after irradiation and bone-marrow infusion, and the number of spleen colonies was counted. Only colonies measuring more than 1 mm in diameter were scored.

The data were analyzed by a maximum likelihood method developed

1027460

by E. Frome at ORAU.[2] The results (Table 7 and Fig. 21) are very close to those obtained by irradiating the bone-marrow cells in vivo. The amount of radiation required to decrease survival to 37% (D_0), in the linear part of the curve, is 98 rads. The most interesting finding is that the extrapolation number is relatively high, when compared to the mouse,[3] the only other species for which similar data have been obtained. The difference in extrapolation number between mouse and rat bone-marrow cells probably signifies that the latter are better able to repair intracellular radiation damage. Rat bone-marrow cells would need to accumulate larger amounts of radiation before cell killing actually takes place. Beyond that point, however, the effectiveness of radiation in killing cells is about the same for the rat and the mouse: (about equal D_0 for both species).

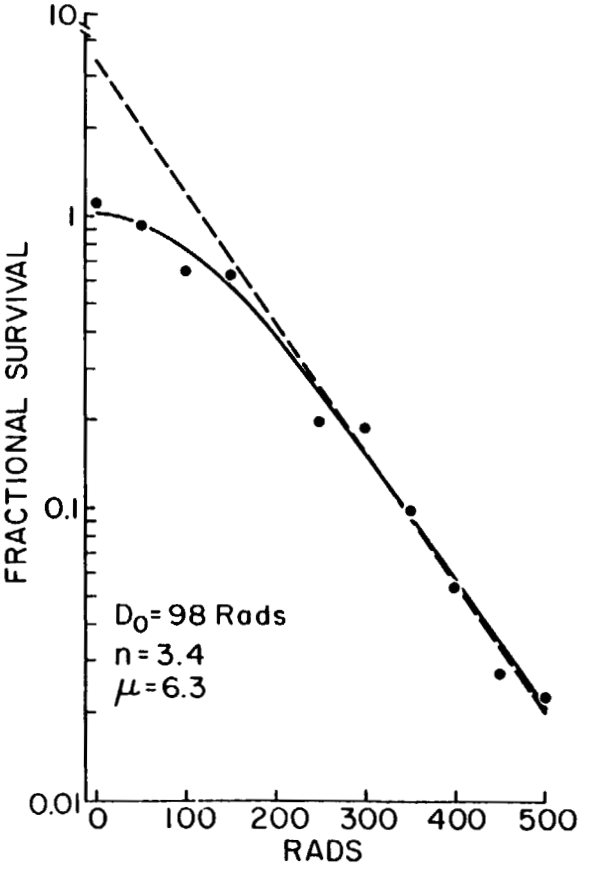

Fig. 21. Survival curve of rat bone-marrow cells, irradiated.

TABLE 7

Survival Curve Parameters of Rat Bone-Marrow Cells Irradiated In Vitro

Average No. of Spleen Colonies per 10^5 Cells (No irradiation)	D_0 (rads)	Extrapolation Number
6.3 (5.5-7.0)*	98 (92-105)	3.4 (2.2-4.6)

* Figures in parentheses are 95% confidence limits.

REFERENCES

1. Comas, F. V. The radiosensitivity of rat bone-marrow cells. In: USAEC Report ORAU-106, 1967, pp. 64-66.

2. Frome, E. L. and Beauchamp, J. J. Maximum likelihood estimation of survival curve parameters. Biometrics 24, 595-605, 1968.

3. Till, J. E. and McCulloch, E. A. A direct measurement of the radiation sensitivity of normal mouse bone marrow cells. Radiat Res 14, 213-222, 1961.

Biological Effects of Pokeweed Mitogen

*Frank V. Comas and Bismarck Lozzio**

A group of substances with mitogenic properties offers promise as useful drugs in the treatment of some bone-marrow diseases characterized by lack of production of blood cells. Among these drugs, phytohemagglutinin has been given to patients with aplastic anemias; the results have been encouraging, but many patients failed to respond. Pokeweed mitogen (PWM), an extract of Phytolacca americana has been recently found to have similar mitogenic properties in vitro,[1] and we decided to study the effects in vivo.

The drug was injected intraperitoneally to C3H mice in doses

* University of Tennessee Memorial Research Center, Knoxville, Tenn.

1027461

ranging from 20 to 55 mg/kg. These doses gave little evidence of toxicity, no mortality, and little or no weight loss. Several effects were studied:

Immunology

The PWM injected 3 days before injection of sheep red cells produced a reduction in the hemolysin and hemoagglutinin titers. If the drug was given 1 day before the antigen, however, no effect was noted on the production of antibodies.

Reticuloendothelial Function

This was studied by determining the clearance of carbon particles. The clearance was prolonged at 1 day after PWM injection but was increased by the third day. Thereafter it returned to normal.

Lymphatic System

An early action of PWM was to induce a hypoplasia of the thymus. Three days after injection the size of lymph nodes and spleen increased notably. Microscopically the germinal centers were enlarged and blast cells were observed in the spleen.

TABLE 8

Number of 10-Day Endogenous Spleen Colonies in 800 Rads Total-Body Irradiated Mice Receiving Pokeweed (PWM)

GROUP	No. of Mice	PWM (mg/100 g body wt.)	SPLEEN WEIGHT (% of body wt.)	SPLEEN COLONIES/SPLEEN
CONTROL*†	30	Saline	0.126±0.004‡	3.5±0.7
PWM*	10	2.0	0.165±0.007	3.5±1.2
PWM†	10	2.0	0.244±0.026	26.4±3.9
PWM†	10	4.0	0.286±0.037	33.8±5.0

* Five days after irradiation

† Two days before irradiation

‡ Mean ± one S.E.

Differences between control and experimental groups are significant (p.<.001)

Blood

The early effects (within 24 hr after PWM injection) consisted of lowering of the hemoglobin and the appearance of great numbers of large hypersegmented granulocytes. These changes are thought to be due to agglutination of red cells by PWM, and a direct toxic

effect on circulating granulocytes. From the first to the third day the hemoglobin went back to normal values. The absolute granulocyte count did not change appreciably during the 12 days of observation, except for a fleeting increase in the first 24 hr; this increase was probably due to a pyrogen because it was also observed in control mice. The number of lymphocytes first decreased, and later increased, peaked on the third day, and then slowly returned to normal values. From the third day onward abnormal cells were found in the blood; these cells constituted about 5% of all white cells. They resembled immature plasma cells and blast cells.

Spleen Colonies

Mice given PWM 2 days before a sublethal dose of total-body irradiation (800 rads) developed about 10 times as many hemopoietic endogenous spleen colonies as control animals that were also irradiated but given only a saline injection. If the drug was given after irradiation, no effect was noted (Table 8).

These results are interpreted as indicating that PWM, like phytohemagglutinin and other plant extracts, induces resting cells to mitosis. Resting cells, in this context, means cells that normally do not divide, like lymphocytes and noncycling bone-marrow stem cells. Apparently the type of cell that responds most to the drug is determined by the physiologic status of the animal. In the sublethally irradiated mouse it is the bone-marrow cells, whereas in the nonirradiated animals the major changes are found in the lymphatic system, probably because the main stress in a normal environment is an antigenic one.

REFERENCE

1. Farnes, P., Barker, B. E., Brownhill, L. E., and Fanger, H. Mitogenic activity in Phytolacca americana (Pokeweed). Lancet 2, 1100-1101, 1964.

Studies on the Microflora of Patients Exposed to 250-R Total-Body Irradiation in the LETBI Facility, 1.5 R/hr.

Edward Balish and Ted A. Pearson

Two patients, exposed to 250 R total-body irradiation at an exposure rate of 1.5 R/hr, have been studied. The first of these patients was a 61-year-old man with polycythemia vera. The blood leukocyte count was reduced to 25% of preirradiation values 24 days after exposure.

Staphylococcus albus and diphtheroids predominated in the nares of this patient before and after irradiation. Neisseria sp. and alpha hemolytic streptococci were consistently predominant in sputum before and after total-body irradiation; Staphylococcus aureus, diphtheroids, Klebsiella-Aerobacter, Escherichia coli, Candida sp. and beta streptococci (not group A) were also isolated before and after the exposure, but no overgrowth by any of the latter microorganisms was observed. The throat had a microflora similar to that described for the sputum except that no coliforms were isolated.

Gastric washings (Table 9) also contained a variety of microorganisms and resembled the microflora of the throat and sputum except for a more consistent presence of Candida sp. and the appearance of E. coli after irradiation. The pH of the gastric washings remained constant at 6.5 throughout the period of study (Table 9).

Rectal swabs showed a predominance of E. coli, Klebsiella-Aerobacter, and fecal streptococci before and after total-body irradiation. Proteus sp. were consistently present throughout the study period. Escherichia coli, Klebsiella-Aerobacter, and fecal streptococci were the major aerobic components in the stool (Table 10); S. albus was present before and for 17 days after irradiation. Table 10 also demonstrates that the numbers of Proteus mirabilis increased and remained as a major component in the stool between 14 and 50 days after the irradiation. Candida sp. were isolated on two occasions; once before and once again 31 days after total-body irradiation. A variety of anaerobic bacteria also were found in the microflora of this patient's stool (Table 10). Anaerobic Lactobacillus spp., Clostridium spp. and Bacteroides spp. were all present before irradiation. At nine days gram-positive beta hemolytic (double zone) anaerobes increased in numbers and persisted in the flora. When Clostridium perfringens became consistently prominent in the stool, the Bacteroides spp. and other Clostridium spp. decreased (Table 10). At fifty days Bacteroides melaninogenicus appeared (Table 10).

Urine specimens cultured after total-body irradiation contained S. albus, S. aureus, and diphtheroids.

The second patient, a 62-year-old man with a reticulum cell carcinoma was treated with 250 R total-body irradiation. White blood cell counts decreased to about 30% of preirradiation values within 36 days after exposure. Staphylococcus aureus, Streptococcus mitis, and Proteus sp. were the most prevalent microorganisms in the nares before total-body irradiation, but after irradiation, diphtheroids and Neisseria sp. were more consistently isolated. Even though Proteus sp. were present they never assumed a predominant role. The throat microflora consisted predominantly of Neisseria and alpha hemolytic streptococci. Proteus sp. were also consistently isolated after irradiation. Beta hemolytic streptococci were also isolated from the throat on days 14 and 17 after total-body irradiation. Diphtheroids were also isolated before and after the exposure to irradiation. The microorganisms in sputum were similar to those isolated from the throat; Neisseria sp. and alpha hemolytic streptococci predominated.

Gastric washings contained no viable microorganisms before and

1027462

10271463

TABLE 9

Microorganisms Isolated from Gastric Washings Collected from a Patient Before, During, and After 250 R Total-Body Irradiation (1.5 R/Hr)

Time	No. Microorganisms/ml Gastric Washing							
(DAYS)	*Neisseria*	*S. mitis*	*S. salivarius*	*S. aureus*	*Candida* sp.	*E. coli*	OTHERS	pH
-5	1.0×10^5	5.0×10^5		1.0×10^5	3.0×10^3		*S. albus* 1.0×10^4; *Proteus* sp. 1.0×10^2	6.5
-1	5.0×10^5	1.0×10^5	1.0×10^5	5.0×10^5	9.0×10^2		β streptococci(not A) 5.0×10^5	6.5
+2(250 R TBI 1.5 R/HR)	5.0×10^5	5.0×10^5		1.0×10^5	2.0×10^2		Enterococci 5.0×10^5; *Diphtheroids* 3.0×10^5	6.5
+7	5.0×10^5	5.0×10^5	4.0×10^3	1.0×10^5		1.0×10^5	*Klebsiella-Aerobacter* 1.6×10^3; *Proteus* sp. 1.0×10^2	6.5
+9	1.0×10^5		4.0×10^3	5.0×10^5	4.0×10^2	1.0×10^5	β streptococci(not A) 5.0×10^5	6.5 6.5
+14	5.0×10^5	5.0×10^5	2.0×10^4	5.0×10^4	1.5×10^3			6.5
+16	5.0×10^5	5.0×10^5		1.7×10^4	6.0×10^2	1.0×10^5	Enterococci 4.0×10^5	6.5
+24	5.0×10^5	5.0×10^5	4.2×10^3	5.0×10^5	1.0×10^5	1.2×10^4		6.5
+37	5.0×10^5	5.0×10^5		3.0×10^5	1.0×10^4	1.2×10^3	*Klebsiella-Aerobacter* 1.0×10^3	6.5

Patient D., male, 61, polycythemia vera

TABLE 10

Fecal Microbial Profile of a Patient Before, During, and After 250 R Total-Body Irradiation (1.5 R/Hr)

TIME	*E. coli*	*Klebsiella-Aerobacter*	Fecal streptococci	*Lactobacillus* sp	*Bacteroides* spp	*Clostridium* spp	*S. albus*	*Lactobacillus bifidis*	*Cl. perfringens*	*Proteus mirabilis*	OTHER
(DAYS)											
-1	4.1×10^9	1.6×10^6	4.1×10^6	4.9×10^6	4.1×10^9	4.1×10^8	8.1×10^4				*Candida sp.* 4.1×10^4
+9) 250RTBI (1.5R/HR)	1.1×10^9		7.0×10^5	4.2×10^5	8.3×10^8	7.0×10^8	8.4×10^5	3.5×10^8	3.5×10^8		
+14	1.4×10^{10}	9.6×10^7	1.0×10^9	2.9×10^8	4.8×10^9	9.6×10^5	9.6×10^5		9.6×10^5	1.9×10^9	
+17	2.6×10^8	1.3×10^8	5.1×10^7		8.6×10^7		4.3×10^4	4.3×10^7	8.6×10^7	4.3×10^5	
+25	2.7×10^9	1.2×10^9		1.1×10^8					3.9×10^6	5.5×10^7	
+31	3.9×10^{10}	2.2×10^9	1.0×10^9	6.1×10^8				7.7×10^7	6.9×10^6		*Candida sp.* 2.3×10^5
+50	1.5×10^{10}	3.8×10^7	7.7×10^7	1.7×10^8	6.4×10^7				1.2×10^5	1.1×10^8	*Bacteroides melaninogenicus* 6.4×10^6

Patient D., male, 61, polycythemia vera

TABLE 11

Microorganisms Isolated From Gastric Washings Collected From a Patient Before, During, and After 250 R Total-Body Irradiation (1.5 R/Hr)

Time (Days)	No. Microorganisms/ml Gastric Washings	pH
-5	NO GROWTH	2.0
+3) 250 R TBI	NO GROWTH	6.5
+7) (1.5 R/hr)	*S. mitis* 1.0×10^5, *E. coli* 1.2×10^3, *Klebsiella-Aerobacter* 1.0×10^5, *Proteus* sp. 1.0×10^5	6.5
+10	NO GROWTH	6.5
+17	*S. mitis* 5.0×10^5, *S. salivarius* 5.0×10^5, *Neisseria* 1.0×10^5 diphtheroids 7.0×10^2, *E. coli* 5.0×10^3, *Proteus* sp. 8.0×10^3	6.0

Patient B., male 62, reticulum cell sarcoma

3 days after the treatment (Table 11). However, a variety of microorganisms was found on days 7 and 17 (Table 11).

Escherichia coli predominated before and after irradiation in rectal swabs. Klebsiella-Aerobacter appeared to replace the Proteus sp. after the treatment. Diphtheroids, fecal streptococci and S. albus were also consistently isolated from rectal swabs before and after the irradiation. Pseudomonas aeruginosa was isolated from rectal swabs on one occasion at 3 days. The stool of this patient had consistently high populations of E. coli, Klebsiella-Aerobacter, Proteus sp. and fecal streptococci before and after irradiation; anaerobic Lactobacillus spp. was the major anaerobic component (Table 12). Bacteroides spp. and anaerobic diphtheroids became more numerous at 17 and 21 days (Table 12). The number of microorganisms in the urine increased after irradiation.

1027464

TABLE 12

Fecal Microbial Profile of a Patient During and After 250 R Total-Body Irradiation (1.5 R/Hr)

No. Microorganisms/g Stool (Dry Wt.)

Time (DAYS)	*E. coli*	*Klebsiella-Aerobacter*	*Proteus* sp.	Fecal streptococci	*S. salivarius*	*Lactobacillus* spp.	*Clostridium* spp.	Others
+3) 250R TBI +7) (1.5 R/hr) +10	6.2×10^9	4.6×10^6	7.7×10^5	6.9×10^7	1.5×10^7	4.6×10^8	7.7×10^6	
	2.6×10^7	2.1×10^9	5.5×10^7	5.5×10^5		1.6×10^6	5.5×10^5	
	6.4×10^9	6.4×10^6	3.8×10^8	1.3×10^8		7.7×10^9		*S. albus* 3.2×10^7 *Cl. perfringens* 6.4×10^5
+14	8.4×10^9		9.6×10^7	3.3×10^8	4.8×10^8	9.2×10^9	9.6×10^4	*S. albus* 2.0×10^6
+17	3.6×10^9	9.6×10^6	9.6×10^6	9.6×10^4	2.9×10^5	9.6×10^6		*Bacteroides* spp. 5.4×10^9 diphtheroids Aerobic 5.2×10^6 Anaerobic 1.2×10^9
+21	3.9×10^9	3.8×10^6	3.2×10^6			9.6×10^6		*Bacteroides* spp. 4.8×10^9 *S. albus* 9.6×10^4 diphtheroids Anaerobic 9.6×10^9

Patient B, male 62, reticulum cell sarcoma

Studies on the Microflora of Three Men Accidentally Exposed to Total-Body Irradiation

Edward Balish and Ted A. Pearson

On October 4, 1967, three men were exposed to high levels of X irradiation generated by a Van de Graaff accelerator near Pittsburgh, Pennsylvania. Studies thus far indicate that the energy of the X rays was from 500 to 800 kev and the exposure rates at film body height (42 in. above the floor) were approximately 40 R/min at 36 in. from the target and 300 R/min at 18 in. from the target. Total-body dose estimates for two of the men are 500 to 600 R and 100 to 200 R for the third. The dose to their extremities was higher. The contributing neutron dose is thought to be less than one rad. The three men were taken to Western Pennsylvania Hospital, Pittsburgh.

Dr. Michael Gilberti, to whom we are indebted for the information on the symptoms of the three patients throughout their hospitalization, was in charge of their care and management. Dr. Neil Wald, Dr. Abraham Braude, and Dr. Ken Brown, University of Pittsburgh, were active in the study and management.

Studies on the microbial flora of nose, throat, skin, urine, and stool specimens were started 12 days after the exposure.

The three exposed persons were hospitalized in an improvised "clean" room into which were placed two laminar-flow clean benches. Personnel entering the patients' room had to enter a clean anteroom where there they scrubbed and put on sterile clothing. Exits were made through a "dirty room" i.e., sterile garb was discarded. Several air samplings from the patients' room revealed that it was cleaner (but by no means sterile) than the outside corridor and other rooms not having the laminar-flow benches.

Antibiotic Treatment of the Patients

The two high-dose patients were given heavy antibiotic therapy when their total WBC count fell below 1000, and it was stopped when their WBC counts rose above the 2000 mark.

Low-Dose Patient Z, Male, 29 (100 to 200 R)

Nasal cultures from low-dose patient Z contained Klebsiella-Aerobacter and Staphylococcus albus. The application of Bacitracin ointment to the nares was probably responsible for the predominance of Klebsiella-Aerobacter. Two episodes of mild pharyngitis occurred, the first 13 to 16 days after exposure. The throat flora consistently showed alpha hemolytic streptococci, Neisseria sp., and diphtheroids during this period along with Staphylococcus aureus. The second episode coincided with the appearance of Escherichia coli in the throat. Escherichia coli was not detected in throat swabs taken in the first 20 days. Although E. coli persisted through day 36, it was not detected in the throat at 90 days. Staphylococcus aureus and S. albus were repeatedly isolated from the abdominal skin of this patient. (Phisohex was used for washing by all three subjects throughout their isolation period.)

Stool specimens of patient Z were fairly constant in their content of E. coli, Klebsiella-Aerobacter, Clostridium spp., Bacteroides spp. and fecal streptococci. The only substantially different microorganisms, present from day 26 through day 35, were diphtheroid-like microorganisms. They were not detected 90 days after the exposure. All urine specimens cultured throughout this 90-day period were sterile.

High-Dose Patient M (~550 R)

The bacterial flora of the nose, throat, and skin of this patient are shown in Table 13. This patient had S. aureus and S. albus in his nares for about 21 days after exposure. During this period (7 to 21 days) Bacitracin ointment was applied to both nares. At about 22 days a triple antibiotic ointment (Polymyxin, Neomycin, and Bacitracin) was applied. During this time (25 to 42 days after exposure) antibiotics were given per os, to sterilize the G. I. tract. Several nasal swabs taken during this period had no viable microorganisms.

Throat swabs contained a normal flora most of the time. However, throat swabs (Table 13) at 12 days transiently contained pneumococci, and these were not detected again until day 49. Pharyngitis and tonsillar exudates were manifest during the period of heavy antibiotic therapy, and Klebsiella-Aerobacter and Candida albicans were isolated (Table 13) from throat cultures.

Although many skin swabs (from the abdomen) did not contain microorganisms, probably because of phisohex washes, several were positive for S. aureus. After the heavy antibiotic therapy, diphtheroids, Bacillus sp., and Klebsiella-Aerobacter were isolated from the skin swabs (Table 13). Urine specimens throughout the period of observation (12 to 44 days) were sterile.

The microorganisms isolated from the stool are shown in Table 14. The aerobic microflora consisted of E. coli, Klebsiella-Aerobacter, and fecal streptococci. The anaerobes, the major components of the bacterial microflora, consisted of Bacteroides spp. and Clostridium spp. The time of heavy antibiotic therapy is obvious in Table 14. During this period stained fecal specimens revealed numerous bacteria and very often yeasts. Candida albicans was cultured once during this time. Another interesting feature is the fact that Streptococcus salivarius was cultured in fairly large numbers from day 19 to 23 after the exposure. Streptococcus salivarius is normally associated with the throat flora. After the period of antibiotic therapy Proteus sp. became a major component. The Bacteriology Laboratory at Western Pennsylvania Hospital began to isolate Proteus sp. from the stool soon after the antibiotics were withdrawn and it persisted in the stools for 90 days after the exposure.

1027465

10274666

TABLE 13

Microorganisms Isolated From Nose, Throat, Skin, and Urine After Accidental Exposure to Total-Body Irradiation (~ 550 R)

Days after Exposure		Nose*	Throat	Skin (Used Phisohex to Wash)
12	Bacitracin to Nares	*S. aureus, S. albus*	α streptococci, pneumococci, micrococci, *Neisseria*, β streptococci	*S. albus*
13		*S. aureus, S. albus*	α streptococci, micrococci, *Neisseria*, β streptococci	*S. albus*
14		No growth	α streptococci, *Neisseria*	No growth
15		*S. albus* (β)**	α streptococci *Neisseria*	*S. albus*
16		*S. albus*	α streptococci *Neisseria*	*S. albus*
17		*S. aureus*	α streptococci	No growth
19		*S. albus*	α streptococci, *Neisseria*, β streptococci	No growth No growth
20		*S. albus*	α streptococci, *Neisseria*, diphtheroids	No growth
21		*S. aureus*	α streptococci	No growth
22	Triple Antibiotics to Nares	No growth	α streptococci, *Klebsiella-Aerobacter*	No growth
27		No growth	α streptococci, *Neisseria*	No growth
28		No growth	α streptococci *Neisseria*	No growth
29		No growth	α streptococci	No growth
34		No growth	α streptococci	*S. albus*
35		No growth	α streptococci, β streptococci, *Candida*	No growth
41		No growth	α streptococci, β streptococci, *Candida*	No growth
42		No growth	α streptococci β streptococci	No growth
43		No growth	α streptococci	
44		No growth	α streptococci, *Neisseria*, diphtheroids micrococci	*S. albus*, diphtheroids
47		No growth	α streptococci, micrococci, diphtheroids	No growth
49		*S. albus*	α streptococci, β streptococci, pneumococci, micrococci, *Neisseria*	*S. albus*, *Bacillus* sp.
51		No growth	α streptococci, β streptococci, pneumococci, *Neisseria*	*S. albus*, *Bacillus* sp.
54		*S. albus*, micrococci	α streptococci, *Neisseria*, micrococci	*Klebsiella-Aerobacter*
56		*S. albus*	α streptococci, *Neisseria*, micrococci	*S. albus*
57		DISCHARGED FROM HOSPITAL		
90		*S. albus* (β)	α streptococci, *Neisseria*, *S. albus* (β) diphtheroids	

Tonsillar exudates Pharyngitis — Gingivitis

Patient M, male 31, ~ 550 rem

*Days 7 to 22 Bacitracin to nares 2 times a day; Day 22 to 51, Bacitracin, Neomycin, Polymyxin to nares 2 times a day.
**Beta hemolytic
No microorganisms were cultured from urine specimens throughout the entire period of study.

TABLE 14

Fecal Microbial Profile After Accidental Exposure to Total-Body Irradiation (~550 R)

No. Microorganisms/gram Stool (Dry Wt.)

Days After Exposure	*E. coli*	*Klebsiella-Aerobacter*	*Proteus* sp.	Fecal streptococci	*Lactobacillus*	*Bacteroides*	*Clostridium* spp.	*Cl. perfringens*	*Clostridium* sp. (pleo)	*S. salivarius*
12	8.5×10^6			1.3×10^6 (β)		1.5×10^{10}	1.1×10^9	8.5×10^4		
14	4.1×10^7	6.3×10^5		1.1×10^8		1.3×10^8	1.3×10^8			
15	9.2×10^7	2.3×10^5		2.1×10^6	3.1×10^5	4.6×10^9	2.7×10^9			
19	5.3×10^6	1.4×10^5		3.5×10^6	4.8×10^4	7.7×10^9			1.2×10^9	2.4×10^6
21	8.9×10^6			1.5×10^6		4.2×10^9	1.6×10^9			3.9×10^5
22	8.2×10^6	1.6×10^5		2.2×10^6		5.5×10^9	5.5×10^8		8.8×10^8	1.9×10^7
23	9.6×10^6	2.9×10^6		8.7×10^5		9.6×10^7			3.3×10^8	5.8×10^5
26/ Started Antibiotics										
28			(NO GROWTH							
29			(NO GROWTH							
30			(NO GROWTH							
35			(NO GROWTH							
36			(							
39			(*C. albicans*							
40			(NO GROWTH							
41			(NO GROWTH							
90	3.2×10^7		2.3×10^7	4.0×10^6	2.0×10^6		5.0×10^8			9.0×10^5

Oxacillin Nystatin Neomycin

Patient M, male 31

High-Dose Patient C (~550 R)

Findings are summarized in Table 15. Again while Bacitracin ointment was applied to the nares Klebsiella-Aerobacter was consistently isolated. When the nasal ointment was changed to a triple antibiotic preparation (Polymyxin, Neomycin, Bacitracin), several nasal swabs did not manifest viable microorganisms. Candida albicans was isolated on one occasion during the treatment with triple antibiotic ointment (Table 15).

No episodes of pharyngitis occurred in Patient C. Klebsiella-Aerobacter, Candida albicans, and pneumococci were cultured from the throat 12, 37, and 47 days, respectively, after exposure (Table 15).

Table 15 also shows that although S. aureus and S. albus were occasionally isolated from skin during isolation, many such specimens did not show any cultivable microorganisms; the phisohex wash was probably responsible.

Table 16 shows when the heavy oral antibiotic therapy began. After the antibiotic therapy was stopped Proteus sp. and Citrobacter freundeii appeared as new additional major components of the stool.

Patient C also had many positive urine cultures. Staphylococcus aureus, S. albus (β) and Klebsiella-Aerobacter were isolated before antibiotic therapy, and Klebsiella-Aerobacter was isolated on one occasion during heavy oral antibiotic therapy. Patient C was the only one who consistently showed positive urines.

Other Bacteriology

Patient C had extremely severe radiation injury to both hands and during his confinement S. aureus was isolated from them. After he was taken out of the laminar-flow isolation rooms Pseudomonas sp. and C. albicans were isolated from his hands. He also had an ear infection with Pseudomonas sp. during the time that he was in the "clean" room. All blood cultures taken during the leukopenic state were negative for microbial growth.

Summary of Studies on the Microflora

No pronounced alterations of the microbial profile of these men were evident except as follows: the low-dose victim (100 to 200 R) had a pharyngitis, which corresponded with the appearance of E. coli in throat cultures; Klebsiella-Aerobacter was also in the nares, probably as the result of the Bacitracin ointment applied daily after exposure. The stool of the low-dose victim had large numbers of anaerobic diphtheroids about 26 days after exposure. The increased diphtheroid population has also been observed in some of the patients we have studied after therapeutic total-body irradiation. However, we did not notice, as we have observed in our patients on several occasions, any dramatic increase in Clostridium perfringens in the accident victims. The two high-dose victims maintained a consistent microflora after exposure and before the use of oral antibiotics. During antibiotic therapy one

1027467

TABLE 15

Microorganisms Isolated From Nose, Throat, and Skin After Accidental Exposure to Total-Body Irradiation (~ 550 R)

Days After Exposure	Nares*	Throat	Skin	
				Phisohex Wash
12	*S. aureus, S. albus*	α streptococci, *Neisseria, Klebsiella-Aerobacter*	*S. aureus, S. albus*	
13	*Klebsiella-Aerobacter*	α streptococci, *Neisseria*, micrococci	*S. aureus, S. albus* (β)	
14	*Klebsiella-Aerobacter*	α streptococci, *Neisseria*	*S. albus* (β)	
15	*Klebsiella-Aerobacter*	α streptococci, *Neisseria*	*S. albus* (β)	
	S. aureus			
16	*Klebsiella-Aerobacter*	(α streptococci, diphtheroids	*S. aureus, S. albus*	
	S. albus	(		
17	*Klebsiella-Aerobacter*	(α streptococci, *Neisseria*	*S. albus*	
	S. albus	(		
		Antibiotics per os		
19	*Klebsiella-Aerobacter*	(α streptococci, diphtheroids	No growth	
21	*Klebsiella-Aerobacter*	(α streptococci, diphtheroids	No growth	
22	*Klebsiella-Aerobacter*	(α streptococci, diphtheroids	No growth	
23	*Klebsiella-Aerobacter*	(α streptococci, *Neisseria, S. albus*	No growth	
	E. coli			
29	*S. albus*	α streptococci, *Neisseria*	*S. albus*	
30	No growth	α streptococci	*S. albus*	
35	No growth	α streptococci, micrococci	No growth	
36	*S. aureus, S. albus*	α streptococci	No growth	
	Candida albicans			
37	No growth	*Neisseria, Candida albicans*	No growth	
41	No growth	α streptococci, *Neisseria*	No growth	
42	*S. aureus*	α streptococci, diphtheroids	*S. aureus*	
44	*S. aureus*	α streptococci, *Neisseria*, diphtheroids, micrococci, *S. aureus*	*S. aureus*	
47	*S. albus*	α streptococci, β streptococci, micrococci	*S. aureus*	
48	*S. albus*	α streptococci, micrococci	*S. aureus, S. albus*	
49	*S. aureus, S. albus*	α streptococci, β streptococci, pneumococci, diphtheroids, micrococci	*S. aureus, S. albus* (β)	
54	*S. aureus*	α streptococci, micrococci	*S. albus*	
56	*S. albus*	α streptococci, β streptococci, micrococci		
58	*S. aureus*, micrococci	α streptococci, β streptococci, micrococci	*S. aureus* (β), *S. albus*	
63	*S. albus* (β), *S. aureus*	α streptococci, *Neisseria*, diphtheroids, β streptococci, *S. albus* (β), *S. albus*		
		S. aureus		
90	*S. aureus, S. albus*	α streptococci, *Neisseria*, diphtheroids		

Patient C, male 39
*Day 7 to 22 Bacitracin to nares 2 times a day; Day 22 to 41, Bacitracin, Neomycin, Polymyxin to nares 2 times a day.

TABLE 16

Fecal Microbial Profile After Accidental Exposure to Total-Body Irradiation (~550 R)

Days After Exposure	*E. coli*	*Klebsiella-Aerobacter*	*Bacteroides* spp.	Fecal streptococci	*Clostridium* spp.	*Clostridium* sp. (pleo)	*Clostridium* sp. (B)	*Lactobacillus* spp.	*Proteus* sp.	*Citrobacter freundeii*
12	8.5×10^6	1.3×10^7	2.7×10^9	2.7×10^7 (B)	5.4×10^7					
16	1.4×10^6	2.5×10^6	1.3×10^9	6.8×10^6 (B)	4.3×10^8	1.7×10^{10}				
19			NO GROWTH)	Antibiotics Administered Days 16–29						
20			NO GROWTH)	Oxacillin						
21			NO GROWTH)	Nydramin						
22			NO GROWTH)	Neomycin						
28			S. albus)	Streptomycin I.V. Days 16–24						
35	3.1×10^8	1.9×10^8	1.2×10^9	Lincomycin substituted for oxacillin	3.0×10^7	6.2×10^8	7.7×10^6	9.6×10^6		1.9×10^8
38										
41	2.9×10^9	7.7×10^8	3.2×10^9	5.9×10^7	9.8×10^7		6.8×10^9	3.4×10^5		1.0×10^7
63	8.9×10^8	2.9×10^9	1.6×10^9	6.4×10^8	7.1×10^8		9.6×10^6		4.5×10^8	
90	3.0×10^8		2.0×10^8	4.0×10^8	5.0×10^8		6.0×10^6		1.0×10^6	

Patient C., male 39

high-dose victim had gingivitis and pharyngitis. Candida albicans was isolated from the gums and throat during that period. Nystatin appeared to prevent any serious C. albicans overgrowth. After discontinuing oral antibiotic treatment the microorganisms in the microflora of the two high-dose victims resembled those observed before antibiotic therapy except that Proteus sp. and Citrobacter freundeii were added to the major components of the stool microflora. Only the highest dose victim consistently had viable bacteria in his urine during the 30 days after irradiation.

An important observation was that no drastic alterations in the microflora occurred, possibly because of the "laminar flow" equipment. The clean environment may have "locked the microflora" and prevented any exogenous microorganisms from gaining entrance to the G. I. tract. Studies on patients housed in our own laminar-flow facilities should contribute more information in this area. A sterile environment along with antibiotic sterilization of the gut during severe leukopenia may prove to be important factors in preventing infections that occur before hematologic recovery.

The Influence of Total-Body Irradiation on Bacterial Agglutinins in Human Serum

Edward Balish and Ted A. Pearson

On the basis of our studies at the Medical Division total-body irradiation apparently did not influence the capacity of serum to agglutinate bacteria isolated from the patients' microflora. However, a study of the bacterial agglutination titers of the three accident victims (see previous abstract) revealed some interesting information. The victim who was exposed to the highest dose had the lowest agglutination titers, and the low-dose victim (100 R) had the higher agglutination titers. Bacteria isolated from each patient were used to measure the presence of agglutinating antibodies in their sera.

Low-dose victim Z (100 to 200 R) manifested a good agglutination reaction to microorganisms present in his nose and stool (Table 17). The Klebsiella-Aerobacter isolated from the patient's nose was agglutinated more than the Klebsiella-Aerobacter isolated from the patient's stool. The titer against Escherichia coli (from stool) increased for 25 days after the irradiation (Table 17). Sera collected from high-dose victim M (~550 R) also had agglutinating antibodies against bacteria isolated from his stool (Table 18). The titers were highest against a strain of E. coli isolated from a stool specimen 16 days after exposure (Table 18). Another E. coli isolated from the stool 12 days after irradiation, was not agglutinated by the patient's serum as well as the strain isolated on day 16. Agglutination titers against Klebsiella-

1027468

TABLE 17

Agglutination Titers of Sera Collected From Patient Z After Exposure to Total-Body Irradiation (~ 100 R)

Days After Exposure	Microorganisms Isolated From Patient		
	Klebsiella-Aerobacter (Nose)	*E. coli* (Stool)	*Klebsiella-Aerobacter* (Stool)
	Titer		
9	1024	256	1024
16	1024	256	512
25	1024	512	512
31	1024	512	512

TABLE 18

Agglutination Titers of Sera Collected From Patient M After His Exposure to Total-Body Irradiation (~ 550 R)

Days After Exposure	Microorganisms Isolated From Patient		
	E. coli (Stool) day 12	*Klebsiella-Aerobacter* (Stool)	*E. coli* (Stool) day 16
	Titer		
9	64	32	512
12	32	64	512
13	64	64	512
19	64	128	512
20	64	128	512
22	64	64	128
26	64	64	256
31	128	64	512
35	64	64	256

1027469

TABLE 19

Agglutination Titers of Sera Collected From Patient C After His Exposure to Total-Body Irradiation (~ 550 R)

Days After Exposure	Microorganisms Isolated From Patient		
	Klebsiella-Aerobacter (Stool)	*E. coli* (Stool)	*Pseudomonas* (Ear)
	Titer		
9	32	8	4
12	64	4	2
13	64	8	2
19	128	8	2
20	128	4	2
22	64	2	2
26	64	4	2
31	64	2	2
35	64	2	2

Aerobacter also increased within 19 days after the accidental exposure of patient M to total-body irradiation.

Sera from high-dose victim C (~550 R) had very low agglutinating activity against E. coli, (stool) and a strain of Pseudomonas isolated from his ear (Table 19). A good agglutinating response was evident with a strain of Klebsiella-Aerobacter isolated from his stool. The latter titer also appeared to increase within 20 days after the accidental exposure (Table 19).

The Influence of Total-Body Irradiation on the Bactericidal Activity of Human Serum

Edward Balish and Ted A. Pearson

In last year's research report we indicated that total-body irradiation may affect the bactericidal capacity of serum.[1]

Sera from the three radiation accident victims (see page 52) was used in studies on the influence of total-body exposure on the bactericidal effects of their serum. Serum from low-dose victim Z (100 to

200 R) did not have any capacity to kill Klebsiella-Aerobacter, and Escherichia coli (isolated from his stool) or the strain of Klebsiella-Aerobacter isolated from his nose. In some instances the serum caused a longer lag phase in growth of cultures. However, by 3 hr good microbial growth was evident in sera collected 9, 16, 25, and 31 days after exposure.

Serum from high-dose victim M (~550 R) also did not have the capacity to kill E. coli or Klebsiella-Aerobacter isolated from his stool, although the serum was perhaps more bacteriostatic on days 9 and 12 than on days 18, 19, and 20. The serum from patient M had an increased bacteriostatic effect against a strain of E. coli isolated from his stool at 19 days (Fig. 22). A killing effect appeared even within the first hour of incubation with sera collected then. The bactericidal effects of serum became more evident by 30 days. Heavy oral antibiotic therapy was being given at 25 to 42 days after exposure, and this calls for some reservation about an increased serum reaction against bacteria. However, Neomycin, the oral antibiotic that would have affected E. coli, is not absorbed to any great extent and no effect was evident on two other gram negative rods isolated from this patient's stool.

Serum from high-dose patient C (~550 R) also lost and then regained the capacity to kill bacteria after the accident. Some bactericidal activity was present against E. coli (from his stool) at 6 days

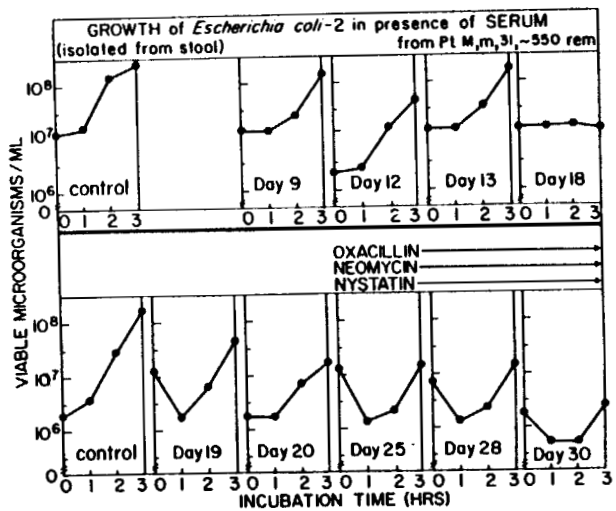

Fig. 22. Effect of sera from patient M, collected after accidental exposure to total-body irradiation, on the growth of Escherichia coli isolated from his stool.

1027470

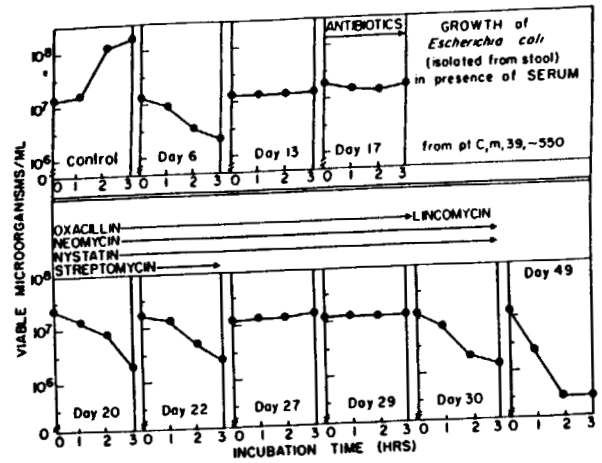

Fig. 23. Effect of sera from patient C, collected after accidental exposure to total-body irradiation, on the growth of Escherichia coli isolated from his stool.

(Fig. 23). However, the bactericidal effect was lost by day 13 where a bacteriostatic effect was observed (Fig. 23). On days 20 and 22 a bactericidal effect was evident; however, this was probably due to intravenous streptomycin (Fig. 23). On days 27 and 29 only the oral antibiotics were being given and a bacteriostatic effect was observed again. By day 30 a good bactericidal effect of the serum was present and persisted until day 49 (Fig. 23). No antibiotics were being administered during the latter period (days 30 to 49).

Klebsiella-Aerobacter, isolated from the nares of patient C, was also used in serum bactericidal studies. No bactericidal effect was present at 6 days after exposure, about the time that Bacitracin was applied to the nares. On days 13 and 17 after exposure the bacteriostatic effect against Klebsiella-Aerobacter was evident. The effect on days 20 and 22 was probably due to intravenous streptomycin. When it was no longer being administered, a bacteriostatic effect was demonstrated on days 27 and 29. It is also evident (Fig. 24) that a good bactericidal effect was present on days 30 and 49, when no antibiotics were being administered.

Figure 25 shows the effect of serum from patient C on a strain of Pseudomonas isolated from an ear infection. The ear inflammation was observed during the time of strict patient isolation in a "laminar-flow" room. A good bactericidal effect was evident on day 6; there appeared to be a bacteriostatic effect on day 13. Serum from days 17, 20, and 22 were bactericidal, probably because of intravenous streptomycin. Serum from days 27 and 29 had some bactericidal activity for

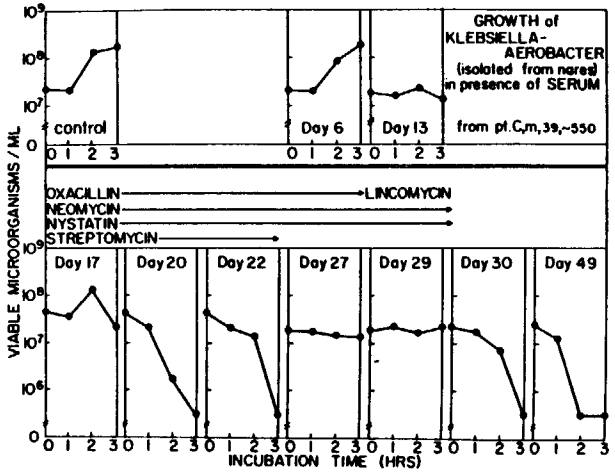

Fig. 24. Effect of sera from patient C, collected after accidental exposure to total-body irradiation, on the growth of Klebsiella-Aerobacter isolated from his stool.

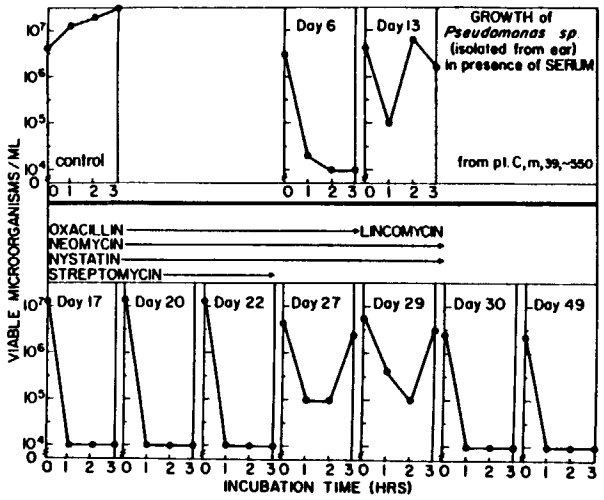

Fig. 25. Effect of sera from patient C, collected after his accidental exposure to total-body irradiation, on the growth of a Pseudomonas sp. isolated from his ear.

1027471

the first 2 hr of incubation; however, active growth was present within 3 hr. By days 30 to 49 the bactericidal effect observed on day 6 had returned to the serum (Fig. 25).

REFERENCE

1. Balish, E., Pearson, T. A., Tanida, R., and Mora, R. J. A study of infections in irradiated patients. In: USAEC Report ORAU-106, pp. 38-44.

Studies on the Microflora of Two Patients Exposed to Partial-Body Irradiation

Edward Balish and Ted A. Pearson

Soon after a patient was treated with 4800 rads (partial-body irradiation to hip and shoulder over a period of 17 days) high fever developed. During the period of high fever the microflora of the nose, throat, sputum, and rectum was determined. The only unusual finding in the specimens was a Candida sp. (not C. albicans) in the sputum. Urines had no microbial growth; rectum, throat, and nares had a "normal" flora. The sputum consistently contained Candida sp. Blood cultures taken every 6 hr during this period failed to show any microbial growth. Antibiotic therapy was initiated and as is evident, Candida sp. soon predominated in rectal and stool cultures (Table 20). Mycostatin

TABLE 20

Fecal Microbial Profile After Exposure of a Patient To 4800 R Partial-Body Irradiation

Time (Days)	No. Microorganisms / g Stool (Dry Wt.)						
	E. coli	*Klebsiella-Aerobacter*	*Lactobacillus* spp.	Fecal streptococci	*Clostridium* spp.	*Bacteroides* spp.	*Candida* sp.
0	NO SPECIMEN						
4	1.3×10^8	7.0×10^2	7.6×10^8	6.0×10^9	1.4×10^7		
5	2.9×10^9	2.9×10^8	7.1×10^7	1.9×10^9	2.9×10^9		
7	6.0×10^9	1.4×10^9		6.0×10^9	3.3×10^9	2.7×10^{11}	
12*	2.0×10^{10}		1.1×10^7	1.4×10^{10}		4.3×10^{10}	
28*	$< 10^4$	$< 10^4$	$< 10^4$	$< 10^4$	$< 10^4$	$< 10^4$	4.6×10^7

* Antibiotic Therapy - Achromycin, Tetracycline, Streptomycin, Prostaphlin, Mycostatin after *Candida* overgrowth

Patient O.S., female 39, chronic granulocytic leukemia and multiple myeloma

was then given and this suppressed the Candida. Gastric washings also contained Candida sp. Alpha hemolytic streptococci, Neisseria sp., and Lactobacillus sp. were consistently isolated from gastric washings and most microbial growth was present when the pH of gastric contents was not very acidic (Table 21). Candida sp. were not isolated from stool specimens until antibiotic therapy was started. Then the numbers increased dramatically. This patient died several weeks later, but the patient did not die of infection since blood cultures continued to be negative and autopsy did not demonstrate any invasion by bacteria or yeast.

Another patient, a 55-year-old man with chronic granulocytic leukemia was treated with 242 rads of splenic irradiation. His nares had a predominance of S. albus before and after the treatment. Proteus sp. and Escherichia coli were isolated from the nares on one occasion but did not persist there. The throat microflora consisted predominantly of the alpha hemolytic streptococci, Neisseria sp. Staphylococcus albus and diphtheroids before and after splenic irradiation. Klebsiella-Aerobacter, predominant in the sputum before exposure, appeared to be eliminated from the sputum microflora after the spleen was irradiated. Neisseria sp., diphtheroids and Staphylococcus albus were also isolated from the sputum cultures before and after irradiation. Candida sp. were present in the sputum on two occasions when the patient was receiving therapy with penicillin. Gastric washings were positive for a variety of microorganisms before and after splenic irradiation (Table 22). Except for a more consistent presence of Candida sp. the microflora of the gastric washings resembled that of the throat and sputum. Only one gastric specimen had a low pH and from this one no microorganisms were isolated (Table 22).

Six days after irradiation E. coli replaced Klebsiella-Aerobacter as

TABLE 21

Microorganisms Present in Gastric Washings Collected From a Patient After 4800 R Partial-Body Irradiation

Time	No. Microorganisms/ml Gastric Washing					
(Days)	α hemolytic streptococci	*Neisseria* sp.	*Candida* sp.	*Lactobacillus* spp.	Other	pH
0	1.0×10^6				enterococci 2.0×10^5	3.5
5	1.1×10^6	1.6×10^6	1.0×10^3	4.0×10^2		5.5
7	2.5×10^5	3.0×10^5	5.0×10^2			5.5
12*	1.0×10^5	1.0×10^5	8.0×10^2	1.0×10^2		7.0
28*	1.0×10^5		9.7×10^3			6.5
41	1.0×10^5	1.0×10^5	2.9×10^4	1.6×10^4	*S. albus* 5.0×10^3	6.8

* Antibiotics: Achromycin, Tetracycline, Streptomycin, Prostaphlin Mycostatin when *Candida* overgrowth occurred.

Patient O S., female 39, chronic granulocytic leukemia and multiple myeloma

1027472

TABLE 22

Microorganisms Isolated From Gastric Washings Before and After a Partial-Body Exposure of 242 R (Spleen)

Time	No. Microorganisms/ml Gastric Washings					
(Days)	α hemolytic streptococci	*Neisseria* sp.	*S. albus*	*Candida* sp.	Others	pH
-4	2.0×10^5	1.0×10^5	1.0×10^3	1.4×10^3		5.0
-2	2.0×10^5	1.0×10^5	1.2×10^3	1.0×10^4		6.0
0 (242 R Spleen)	2.0×10^5	1.0×10^5	1.0×10^3	1.0×10^4		6.0
+4	1.0×10^6	1.0×10^5	2.0×10^3	1.2×10^4		6.0
+6	2.0×10^5		2.6×10^3	1.3×10^3	enterococci 1.0×10^5	6.0
+10*	2.0×10^5	1.0×10^5	4.0×10^2	1.0×10^2	*Klebsiella-Aerobacter* 1.0×10^2	6.0
+12*		NO GROWTH				2.0
+14*	8.7×10^5	4.6×10^5	2.0×10^3		enterococci 9.5×10^5 *Lactobacillus* spp. 2.0×10^3 diphtheroids 1.0×10^5	6.5

Patient E.L., male 55, CGL and multiple myeloma

*Penicillin - 60,000 units 2 times a day

TABLE 23

Fecal Microbial Profile of a Patient Before and After 242 R. Partial-Body Irradiation to the Spleen

Time	No. Microorganisms/g (Dry Wt.)								
(DAYS)	*E. coli*	*Klebsiella-Aerobacter*	Fecal streptococci	*Lactobacillus* spp.	diphtheroids	*Cl. perfringens*	*Bacteroides* spp.	*Sphaerophorus* sp.	OTHERS
-4		4.9×10^7	1.4×10^6	2.1×10^6	2.1×10^7	4.9×10^6			
0(242R spleen)	1.5×10^5	3.1×10^5	2.3×10^7	6.2×10^5		1.2×10^7	5.0×10^{10}	1.1×10^9	*S. albus* 2.3×10^5
+4		5.9×10^5	2.4×10^8	1.2×10^6	4.1×10^6				*Candida* sp. 5.9×10^4 *S. salivarius* 1.2×10^7
+6	1.5×10^6		7.7×10^8	7.7×10^7		1.3×10^9	6.4×10^{10}	6.1×10^{10}	*Candida* sp. 5.0×10^4 *S. salivarius* 7.7×10^8 *Clostridium* spp. 2.6×10^7
+10*	8.5×10^6		1.3×10^6	8.5×10^5	8.5×10^5	2.6×10^5	1.1×10^{10}		*S. salivarius* 9.4×10^6
+12*	1.2×10^8	2.3×10^6	6.2×10^6	1.5×10^7		3.1×10^6	1.3×10^7	3.1×10^6	
+14*	6.9×10^7	5.4×10^6	5.4×10^7	1.5×10^7		7.7×10^4	1.2×10^{10}	1.9×10^{10}	
+23*	1.2×10^6	3.8×10^5	1.6×10^8	1.1×10^9			2.7×10^9	2.6×10^9	*Clostridium* sp. 1.1×10^{10}

Patient E.L., male, 55, CGL and multiple myeloma.

*Penicillin, 60,000 units 2 times a day

the predominant aerobic microorganism isolated from rectal swabs. Fecal streptococci and S. albus were also isolated consistently whereas Candida sp. were only isolated from rectal swabs on one occasion 6 days after partial-body irradiation. E. coli, Klebsiella-Aerobacter, and fecal streptococci were the predominant aerobic microorganisms in the stool (Table 23). The anaerobic components of the stool consisted of Lactobacillus spp., diphtheroids, Clostridium perfringens, Bacteroides spp., and Sphaerophorus sp. (Table 23). Bacteroides spp. and Sphaerophorus sp. were the most numerous bacteria present. Candida sp. were isolated from the stool on two occasions after irradiation. Except for the inability to recover anaerobic diphtheroids, the penicillin therapy after splenic irradiation did not cause any drastic alterations in the fecal microflora. Urine specimens from this patient contained small numbers of Staphylococcus aureus.

These preliminary results indicate that studies on the microflora of patients exposed to therapeutic partial-body irradiation will provide useful information for our overall program on radiation and infection in human patients.

Studies on the Microflora of Rats Exposed to 1400 rads Total-Body Irradiation

Edward Balish, Ted A. Pearson, and Frank V. Comas

Although many studies have been carried out on the increased susceptibility of irradiated animals to infections by their endogenous bacterial flora very few have dealt with changes in the bacterial flora after total-body irradiation at lethal and sublethal levels. Vincent et al.[1] showed that within 7 days the Lactobacillus population of the small intestine of rats decreased (~4-fold) after total-body irradiation in the LD_{50} range (600 R). Pseudomonas sp. increased during that interval by as much as 1000-fold. Klainer et al.[2] found increased populations of coliforms, streptococci, and fungi after midlethal exposures to X irradiation in those animals that later died. Furth et al.[3] also observed a rise in coliform populations in the feces of dogs exposed to 450 R total-body irradiation. Kent, Osborne, and Wende,[4] in a recent study, did not show any great shift in the bacterial content of the small intestine 3 days after 800 R; but even at that early interval they observed pronounced increases in the coliform and enterococci content after 1400 R.

In the present experiments Fischer-334 rats were given 1400 rads total-body irradiation and the gastric and intestinal flora was studied at 6 and 12 days after irradiation. Usually the contents from two or three animals were combined into one sample and analyzed. Significant alterations in the microflora of stomach contents occurred at 12 days. Control rats and 6 of 9 irradiated rats had a predominance of

1027473

TABLE 24

Bacterial Profile of the Stomach of Rats 6 and 12 Days After Exposure to 1400 R Total-Body Irradiation

Dose (rads)	No. Bacteria/g Stomach Contents, 6 days after TBI: *Proteus* sp.	*Lactobacillus* spp.	Fecal streptococci
0 (3)	-	1.0×10^7	3.0×10^4
1400 (9)*	1.0×10^3	1.2×10^7	2.0×10^4

	12 days after TBI: *Pseudomonas aeruginosa*	*Lactobacillus* spp.	Fecal streptococci	*Enterobacter* sp.
0 (3)	-	2.5×10^6	2.5×10^6	-
1400 (4)	4.2×10^4	4.3×10^5	1.6×10^4	2.5×10^3

* Total number of rats assayed at indicated dose level. Stomach contents from two to three animals were combined and analyzed for microbial content.

TABLE 25

Bacterial Profile of the Small Intestine of Rats 6 and 12 Days After Exposure to 1400 R Total-Body Irradiation

Dose (rads)	No. Bacteria/g of Intestinal Contents (dry wt.), 6 days after TBI: *Lactobacillus* spp.	Fecal streptococci
0 (3)*	1.0×10^7	3.0×10^4
1400 (9)	5.2×10^6	1.6×10^4

	12 days after TBI: *Enterobacter* sp.	*Lactobacillus* spp.	Fecal streptococci	*Pseudomonas aeruginosa*
0 (3)		1.0×10^7	3.0×10^4	
1400 (6)	1.6×10^4	1.5×10^6	2.0×10^6	2.0×10^6

* Total number of rats assayed at indicated dose level. Small intestine contents from two to three rats were combined and assayed for microbial content.

TABLE 26

Bacterial Profile of Colon Contents from Rats 6 and 12 Days After Exposure to 1400 R Total-Body Irradiation

Dose (rads)	*Enterobacter*	Fecal streptococci	*Proteus* sp.	*Pseudomonas aeruginosa*	*Lactobacillus* spp.
		No. Bacteria/g Colon Contents			
		6 days after TBI			
0 (3)*	6.0×10^4	3.3×10^5		2.0×10^4	1.0×10^7
1400 (8)	1.5×10^5	1.0×10^5	4.0×10^3	1.0×10^5	1.0×10^7
		12 days after TBI			
0 (3)	7.0×10^3	1.0×10^5		1.0×10^4	5.0×10^6
1400 (4)	7.0×10^4	3.5×10^5	3.0×10^3	3.2×10^5	2.4×10^6

* Total number of rats assayed at indicated dose level. Colon contents from two to three rats were combined and assayed for microbial content.

lactobacilli and fecal streptococci at 6 days (Table 24). However, by 12 days Pseudomonas aeruginosa and Enterobacter sp. were consistently present. Similar findings were observed in the bacterial counts of the small intestine contents (Table 25). Colon contents (Table 26) did not show any noticeable changes in bacterial composition. Pseudomonas aeruginosa was present in the colon of control and irradiated rats; however, it was detected only in the stomach and small intestine of irradiated rats. Apparently mechanisms are operating to eliminate Pseudomonas aeruginosa from the stomach and small intestine because coprophagy is common in rat colonies. However, after irradiation the rats were not able to prevent Pseudomonas aeruginosa and Enterobacter sp. from becoming established in the stomach and small intestine. No obvious decrease in the Lactobacillus populations were evident.

REFERENCES

1. Vincent, J. G., Veomett, R. C., and Riley, R. F. Relation of the indigenous flora of the small intestine of the rat to post-irradiation bacteremia. J Bacteriol 69, 38-44, 1965.

2. Klainer, A. S., Gorbach, S., and Weinstein, L. Studies of intestinal microflora VI. Effect of X irradiation on the fecal microflora of the rat. J Bacteriol 94, 378-382, 1967.

3. Furth, F. W., Coulter, M. P., and Howland, J. W. Bacteriologic studies of the X-radiated dog. Amer J Pathol 28, 171-183, 1952.

4. Kent, T. H., Osborne, J. W., and Wende, C. M. Intestinal flora in whole-body and intestinal X-irradiated rats. Radiat Res 35, 635-651, 1968.

1027474

Isolation of a Sphaerophorus-type Microorganism from the Stool of Two Patients

Ted A. Pearson and Edward Balish

A Sphaerophorus-type microorganism was isolated from feces of two cancer patients who had received cobalt radiation therapy. The fecal microflora of these two patients are shown in Tables 27 and 28. In patient "L" (Table 27), the Sphaerophorus sp. was present at 10^6 to 10^{10} viable cells per gram of feces (dry weight). The organism was the predominant component along with the Bacteroides sp. throughout the entire study period. In patient "P" (Table 28) the Sphaerophorus sp. were also present in high numbers but disappeared (or dropped below 10^4 cells/g) the second week after radiation exposure (the Bacteroides spp. also disappeared).

Initial isolation of this Sphaerophorus-type organism was on blood agar with 5% defibrinated sheep blood. The colonies were 2 to 4 mm in diameter, brownish gray and nonhemolytic after 4 days incubation at 37° C in a BBL Gaspak Anaerobe Jar. However, after the cultures were kept at room temperature for 48 hr, beta hemolysis was observed around the colonies. A gram stain of the colonies from the blood plate showed nothing but amorphous gram negative material. A wet mount from the colony was observed under phase microscopy. The morphology of this microorganism is shown in Figs. 26 and 27. Large spheroids, with and without appendages, long rods, and short regular rods are seen

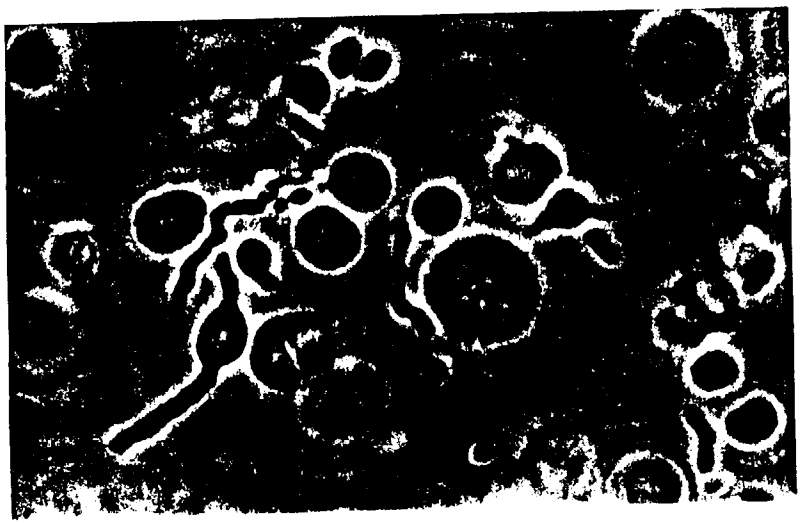

Fig. 26. Pleomorphism exhibited by Sphaerophorus isolate 6-13-68. Phase contrast 1,000 X.

TABLE 27

Anaerobic Fecal Microflora of Patient "L" Before and After 242 R Partial-Body Irradiation to the Spleen

Time (Days)	No. Microorganisms/g Stool (dry wt.) *Clostridium perfringens*	*Bacteroides* spp.	*Sphaerophorus* sp.
-4	4.9×10^6		
0	1.2×10^7	5.0×10^{10}	1.1×10^9
+4			
+6	1.3×10^9	6.4×10^{10}	6.1×10^{10}
+10	2.6×10^5	1.1×10^{10}	
+12	3.1×10^6	1.3×10^7	3.1×10^6
+14	7.7×10^4	1.2×10^{10}	1.9×10^{10}
+23		2.7×10^9	2.6×10^9

TABLE 28

Anaerobic Fecal Microflora of Patient "P" Before and After Exposure to Total-Body Irradiation (150 R - 1.5 R/hr)

Time (Days)	No. Microorganisms/g Stool (dry wt.) *Lactobacillus bifidis*	*Bacteroides* spp.	*Sphaerophorus* sp.	*Clostridium perfringens*
-3		8.5×10^9	2.3×10^9	7.7×10^7
0 (150 R TBI)		1.7×10^8		2.4×10^8
+3		1.3×10^8	8.3×10^8	1.6×10^9
+8		4.8×10^9	7.7×10^9	
+10	1.1×10^7	2.6×10^9	8.5×10^5	
+18	2.6×10^8			6.4×10^4
+24	4.7×10^7			
+31	2.8×10^8			
+45	1.0×10^5			

1027475

Fig. 27. Growth of Sphaerophorous isolate 6-13-68 in short rod form. Phase contrast, 1,000 X.

in Fig. 26. Figure 27 shows a pure culture of the same microorganism growing in the form of short rods before the development of spheroids.

The organism was an obligately anaerobic, gram negative, pleomorphic rod and was, therefore, tentatively identified as a member of the genus Sphaerophorus. The cultural characteristics of four representative species of Sphaerophorus, taken from Prevot[1] were compared to those of isolate 6-13-68. Prevot lists 17 species and most of these differed from our isolate because of their inability to produce gas in culture media and their requirements for serum or ascitic fluid for growth. Our Sphaerophorus isolate 6-13-68 did not correspond with any of the described species.

The sugar fermentation patterns of the four Sphaerophorus species and isolate 6-13-68 were compared. Isolate 6-13-68 did not fit any of the four described species as to acid production from lactose, arabinose, xylose, salicin, melibiose, cellobiose, and raffinose. Acid production was determined by growing the cells in a modified thioglycollate broth with cysteine and a 1% (w/v) concentration of each carbohydrate. The final pH of the culture was determined with a pH meter and compared with that of a control growth tube without any fermentable carbohydrate.

These results are preliminary but possibly the isolate of 6-13-68 may be a new species of Sphaerophorus. Further immunologic charac-

terization with known species of Sphaerophorus is necessary to completely identify this microorganism.

Members of the genus Sphaerophorus are commonly found as commensals in the alimentary tract of man and other animals. These anaerobic bacteria are also known to be important pathogens for animals, and, when looked for with proper techniques, have been isolated from infections in man. To more fully understand the role of this potentially important group of microorganisms, more research is needed on methods of isolation, identification, and characterization.

REFERENCE

1. Prevot, A. R. Manual for the Classification and Determination of the Anaerobic Bacteria, 1st ed., Lea and Febiger, Philadelphia, 1966.

Effects of Sulfur-Containing Nitrogen Sources on the Growth and Morphology of Candida albicans

David N. Mardon, Edward Balish, Dallas C. Hilden, and Kathryn Hurst

Previously we have reported that carbon dioxide and methionine can initiate filamentous growth of a yeast-like strain of Candida albicans.[1,2] Nickerson and his coworkers[3] demonstrated that cysteine promoted yeast-like growth of a filamentous mutant of C. albicans. The latter investigators also mentioned that cysteine inhibited the growth of the filamentous strain, prompting us to investigate whether other sulfur-containing nitrogen sources affected the growth and morphology of 6 strains of C. albicans.

Table 29 summarizes the results. Strains 10231-C, 10231-Y, 10261 and Y-5 grow predominantly as yeast-like cells in the defined minimal culture medium. Conversely, strains 10231-F and 10259 which are mycelial mutants, grew predominantly as filamentous forms in the minimal medium. All media, except the control, which contained no nitrogen source, and the cysteine-supplemented medium, contained 0.3 g nitrogen per liter of medium. With L-cysteine, 0.05 g nitrogen per liter of medium was used in an attempt to reduce toxicity; however, L-cysteine was still toxic at 0.05 g of nitrogen per liter of medium.

L-Methionine and L-methionine sulfoxide induced a predominance of filamentous forms with strain 10231-C. With yeast-like strains 10231-Y and 10261 only L-methionine and S-methyl cysteine initiated substantial amounts of filamentous growth. Methyl cysteine and oxidized glutathione promoted yeast-like growth in the normally filamentous 10231-F strain.

1027476

TABLE 29

Effects of Sulfur-Containing Nitrogen Sources on the Growth and Morphology of Six Strains of *Candida albicans*.

Nitrogen Source	Predominant Morphology of *C. albicans**					
	10231-C	10231-Y	10231-F	10261	10259	Y-5
None	(Y) N.G	(Y) N.G.	(Y) N.G.	(Y) N.G.	(F) N.G.	(Y) N.G.
NH_4Cl	Y**	Y	F	Y	F	Y
L-Methionine	F	F	F	F	F	Y
L-Methionine sulfoxide	F	Y	F	Y	F	Y
DL-Methyl methionine	Y	Y	F	Y	F	Y
S Methyl L-cysteine	Y	F	Y	F	F	Y
S-Ethyl-L-cysteine	F	Y	F	Y	F	Y
L-Cysteine	(Y) N.G.	(Y) N.G.	(Y) N.G.	(Y) N.G.	(Y) N.G.	(Y) N.G.
L-Ethionine	(Y) N.G.	(Y) N.G.	(Y) N.G.	(Y) N.G.	(Y) N.G.	(Y) N.G.
L-Glutathione oxidized	(Y)	(Y)	(Y)	(Y)	(F)	(Y)
L-Glutathione reduced	N.G.	N.G.	N.G.	N.G.	N.G.	N.G.

* At 16 hr in glucose-salts-biotin medium + the indicated nitrogen source.

** Y = yeast-like form predominant
F = filamentous form predominant
N.G. = no appreciable growth with the indicated nitrogen source

Only L-cysteine and L-ethionine induced a yeast-like morphology of filamentous strain 10259. However, no appreciable growth took place when cysteine or ethionine was used as the sole nitrogen source. The Y-5 yeast strain appears to be very stable and none of the nitrogen compounds tested were able to convert it to the filamentous form.

As shown in Table 29 we now have strains of C. albicans that remain as yeast forms and filamentous forms under a variety of nutritional conditions. We also have several strains that can be readily converted from yeast-like cells into filamentous cells and vice-versa. By studying the metabolism of the sulfur-containing

amino acids in these strains under selected nutritional conditions, we hope to uncover the biochemical basis for morphogenesis and pathogenicity of C. albicans.

REFERENCES

1. Mardon, D. N. and Phillips, A. W. Effect of carbon dioxide and oxygen on morphogenesis in Candida albicans. Bacteriol Proc 1965, p. 16, abstr.

2. Mardon, D. N. and Phillips, A. W. Effects of amino acids on morphogenesis in Candida albicans. Bacteriol Proc 1968, p. 31, abstr.

3. Nickerson, W. J. and Van Rij, N. J. W. The effect of sulfhydryl compounds, penicillin, and cobalt on the cell division mechanism of yeasts. Biochim Biophys Acta 3, 461-475, 1949.

Methionine Biosynthesis in Candida albicans

Edward Balish and David N. Mardon

Although certain sulfur-containing amino acids play a key role in controlling the cellular form of Candida albicans[1] and cysteine increases the pathogenicity of C. albicans,[2] the enzymic pathway responsible for the production of methionine in this dimorphic pathogen is unknown. Balish and Svihla[3] demonstrated that both yeast-like and filamentous forms of C. albicans can accumulate and store large amounts of S-adenosylmethionine. However, the filamentous cells had a greater capacity to accumulate this compound than did those in the yeast-like phase. S-Adenosylmethionine participates in a methyltransferase reaction that results in the formation of methionine from homocysteine.[4,5] Since C. albicans can accumulate the methyl donor S-adenosylmethionine, we decided to ascertain whether the methyl transferase enzyme was present in cell-free extracts from yeast-like and filamentous forms of C. albicans.

Cell-free extracts were prepared from cultures that had been allowed to grow for 48 hr at 37° C. The cells were then ruptured by passage through a French Pressure Cell. Table 30 shows that cell-free extracts from yeast (ATCC 10231 and 10261) and those from filamentous (ATCC 10259) cells of C. albicans can form methionine from homocysteine via the enzyme S-adenosylmethionine (or methyl methionine): homocysteine methyl transferase (EC 2.1.1.e). In this reaction a radioactive methyl group is transferred from the methyl donor, S-adenosylmethionine, to homocysteine forming labeled

1027477

TABLE 30

Adenosylmethionine (or methylmethionine) homocysteine: methyltransferase activity of cell-free extracts from yeast and mycelial strains of *Candida albicans* at 30°C and 37°C.

Organism Used	Methyl Donor			
	Adenosylmethionine		Methylmethionine	
	30°C	37°C	30°C	37°C
C. albicans (10231)	22*	44	24	122
C. albicans (10261)	70	155	78	336
C. albicans (10259)	110	790	193	1680

*Millimicromoles methionine/mg protein/hour.

methionine (Reaction 1). Methylmethionine may also serve as the methyl donor in this reaction (Reaction 2).

Reaction 1. S-adenosylmethionine $\xrightarrow[\text{homocysteine}]{\text{enzyme}}$ Methionine and S-adenosyl-homocysteine

Reaction 2. Methylmethionine $\xrightarrow[\text{homocysteine}]{\text{enzyme}}$ 2 methionine

In their tracer analysis Shapiro and Yphantis[6] using methyl donors, with radioactive methyl groups estimated methionine production in these initial studies. Passing 0.1 ml of the reaction mixture through a Dowex 50 column in the Li+ form allows the radioactive methionine formed to pass through the column whereas the methyl donors are retained on the column. On the basis of the specific activity of the methyl donor, the amount of methionine produced in the reaction can be calculated from the radioactivity passing through the Dowex 50 column. The production of methionine in the reaction is verified by thin-layer chromatography and paper chromatography.

Table 30 shows that 37° C is better for methionine production than 30° C, and that methyl methionine appears to be a more efficient methyl donor than S-adenosylmethionine. This may be due to the presence in the yeast-like and mycelial forms of C. albicans of enzymes that can split S-adenosylmethionine as well as demethylate

it. The S-adenosylmethionine appears to be split enzymically to methylthioribose and adenine.

REFERENCES

1. Nickerson, W. J. Symposium on biochemical basis of morphogenesis in fungi. IV. Molecular bases of form in yeasts. Bacteriol Rev 27, 303-324, 1963.

2. Winsten, S. and Murray, T. J. Virulence enhancement of a filamentous strain of Candida albicans after growth on media containing cysteine. J Bacteriol 71, 738, 1956.

3. Balish, E. and Svihla, G. Ultraviolet microscopy of Candida albicans. J Bacteriol 92, 1812-1820, 1966.

4. Balish, E. and Shapiro, S. K. Methionine biosynthesis in Escherichia coli; Induction and repression of methylmethionine (or adenosylmethionine): Homocysteine methyltransferase. Arch Biochem Biophys 119, 62-68, 1967.

5. Shapiro, S. K., Yphantis, D. A., and Almenas, A. Biosynthesis of methionine in Saubaromyces cerevisiae. J Biol Chem 239, 1551-1556, 1964.

6. Shapiro, S. K. and Yphantis, D. A. Assay of S-methylmethionine and S-adenosylmethionine homocysteine transmethylases. Biochim Biophys Acta 36, 241-244, 1959.

Influence of Glycine on Methionine Biosynthesis in Candida albicans

David N. Mardon and Edward Balish

We have shown that Candida albicans can form methionine from homocysteine via the enzyme S-adenosylmethionine or methylmethionine homocysteine methyltransferase (EC 2.1.1.e). A primary goal is to determine whether there are qualitative and quantitative differences in the enzyme involved in sulfur amino acid metabolism of yeast-like and filamentous forms. Further evidence that the level of homocysteine methyltransferase may be critical to dimorphism in C. albicans is provided by the studies of Mardon and Phillips[1] and Chattaway, Holmes, and Barlow,[2] who independently demonstrated that walls from filamentous cells had lower levels of methionine than did those from yeast-like cells. However, Balish and Svihla[3] reported much higher levels of adenosylmethionine in the vacuoles of filamentous cells of C. albicans than in those of the yeast-like form. Thus filamentous cells may have important defects in either the synthesis or utilization of methionine.

1027478

Six strains of C. albicans were cultivated for 16 hr at 37° C in a glucose-salts-biotin medium containing glycine as the sole nitrogen source. Glycine is one of the nitrogen sources not containing sulfur that inducts a predominance of filamentous growth with strains 10231-C, and 10231-F, but has no influence on the morphology of strains 10231-Y, 10261, 10259, or Y-5. Glycine was used in order to compare the levels of homocysteine-methltransferase in cell-free extracts from yeast-like and filamentous cells grown in the presence of a nitrogen source with no sulfur.

In this culture medium (Table 31) predominantly yeast-like growth was obtained with strains 10231-Y, 10261 and Y-5 and filamentous growth with the other three strains (10231-C, 10231-F and 10259). Cell-free extracts were obtained with a French pressure-cell-Carver-press system. One-half milliliter of enzyme substrate reaction mixtures were incubated for 2 hr at 37° C. Then 0.2 ml of the reaction mixture was passed through a Dowex 50W-X8 Na+ column. The components in the reaction mixtures can be separated on the sodium column as shown in Fig. 28. The Na+ column chromatography procedure is a modification of the procedure used by Shapiro and Ehninger[4] to separate S-adenosylmethionine and S-adenosylhomocysteine. This column allowed the complete separation of the radioactive methyl donor (^{14}C-L-methylmethionine or ^{14}C-S-adenosyl-L-methionine) and the product of the methyltransferase reaction (EC 2.1.1.e), ^{14}C-methionine.

The relative quantities of methionine formed by cell-free extracts of each strain are shown in Table 31. The three filamentous strains produced less methionine with either methyl donor than did the three yeast-like strains. L-Homocysteine thiolactone, L-homocysteine, and under certain conditions, L-cystathionine could substitute for L-homocysteine as the methyl acceptor in this reaction. L-Cystine, L-cysteine, dithiothreitol, and reduced or oxidized glutathione could not accept the labeled methyl group. Further studies indicated that methionine inhibits the methyltransferase reaction whereas methionine analogues, such as L-ethionine, N-formyl methionine, S-methyl-L-cysteine, or hydroxymethylmercaptobutyrate did not significantly inhibit the methyl-group transfer. These studies provide additional data on the importance of sulfur amino acid metabolism in the control of the cellular form of C. albicans. At present in further studies we are using cell-free extracts from yeast-like and filamentous forms of C. albicans cultured under conditions that can initiate changes in their morphology. The experimental systems used allow us to study several other enzymes that may be associated with sulfur amino acid metabolism in C. albicans.

In our initial studies on the methyltransferase enzyme (previous paper in this report) the filamentous form (strain 10259) apparently had a higher specific activity for the methyltransferase enzyme than did yeast-like cells of strains 10231 and 10261. Our current data reveal that yeast-phase cells have a greater capacity to form methionine. A full explanation of this discrepancy is not available now. However, the data

TABLE 31

Influence of Glycine on Methionine Biosynthesis in *Candida albicans*

Strain	Predominant Morphology	Methyl Donor	
		L-Methyl-Methionine	S-Adenosyl-L-Methionine
10231-C	F	108*	155
10231-Y	Y	159	245
10231-F	F	140	151
10261	Y	227	230
10259	F	125	80
Y-5	Y	183	246

*Millimicromoles of methyl groups transferred to homocysteine/mg protein/hr.

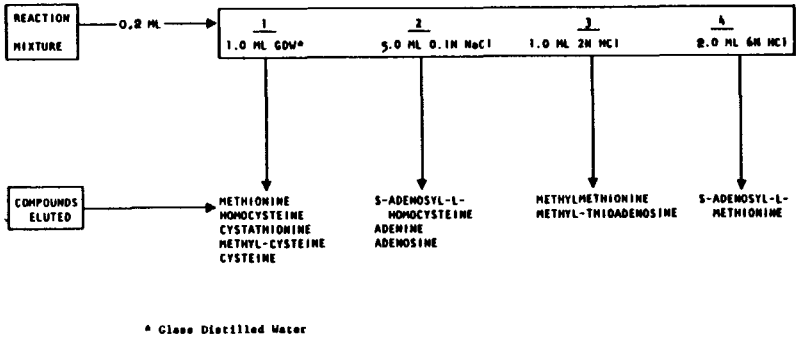

Fig. 28. Tracer assay for methionine with the Dowex 50W-X8 sodium column.

in the previous paper were derived from extracts prepared from much older cultures (48 hr) in a different medium.

REFERENCES

1. Mardon, D. N. and Phillips, A. W. Effects of amino acids on morphogenesis in Candida albicans. Bacteriol Proc p. 31, 1968, abstr.

2. Chattaway, F. W., Holmes, M. R., and Barlow, A. J. E. Cell wall composition of the mycelial and blastospore forms of Candida albicans. J Gen Microbiol 51, 367-376, 1968.

3. Balish, E. and Svihla, G. Ultraviolet microscopy of Candida albicans. J Bacteriol 92, 1812-1820, 1966.

4. Shapiro, S. K. and Ehninger, D. J. Methods for the analysis and preparation of adenosylmethionine and adenosylhomocysteine. Anal Biochem 15, 323-333, 1966.

1027479

Induction of Small-Colony Variants and Auxotrophs of Candida albicans by Ultraviolet Light and Chemical Mutagens

Edward Balish and Norman Savage

In our studies of the biochemical basis for the morphogenesis and pathogenicity of Candida albicans we attempted to isolate and characterize sulfur amino acid auxotrophs. Such mutants could allow us to ascertain whether the deletion of specific enzymes involved in biosynthesis of the sulfur-containing amino acids has any influence on morphogenesis and pathogenicity.

Table 32 is a summary of the mutagens used. We found that N-methyl-N'-Nitro-Nitrosoguanidine, N-Nitroso-N-Methylurethane, and ultraviolet light treatment produced small-colony variants (petites) and several biochemical auxotrophs. Nitrous acid and hydroxylamine hydrochloride also induced small-colony variants but not biochemical auxotrophs.

In these studies it was difficult to obtain biochemical auxotrophs with ultraviolet light; only three were isolated in 10 attempts.

Table 33 shows the response of small-colony variants to successive ultraviolet irradiations. In these experiments a small colony variant thai survived 60 sec UV exposure was subcultured in Sabouraud dextrose broth and the resultant population was then reexposed to ultraviolet irradiation. There was no large increase in resistance of these colonies to a 60-second ultraviolet light exposure nor was there any increase in biochemical auxotrophs. Similar experiments with large (normal) colonies showed some tendency for an increased resistance to ultraviolet irradiation in the first 30 sec., but no increased incidence of biochemical auxotrophs was observed (Table 34).

Culture conditions after the 60-sec exposure to UV irradiation were extremely important to survival of C. albicans and the development of

TABLE 32

The Effect of Selected Mutagens on the

Induction of Small-Colony Variants and Auxotrophs of *Candida albicans*

Mutagen	Exposure Time (min)	Trial No.	% Survival	% Small Colonies	Number of Mutants/10^3 Survivors	Types of Auxotrophs
Nitrous Acid (0.03M)	50		<0.1	46	0.0	0.0
Hydroxylamine Hydrochloride (0.1M)	30		1.0	10	0.0	0.0
N-Methyl-N'-Nitro-Nitrosoguanidine (0.01M)	60	(1)	9.00	9	1.8	Adenine, Guanine, Histidine, Leucine, Lysine, and Tryptophane
		(2)	2.00	27	1.1	
		(3)	0.03	10	4.1	
N-Nitroso-N-Methylurethane (0.001M)	60	(1)	13.00	13	0.0	Adenine, Guanine, Histidine, Leucine, Methionine, Tryptophane, Isoleucine, and Arginine
		(2)	4.00	30	6.6	
		(3)	1.00	50	10.7	
		(4)	.08	-	10.0	
Ultraviolet Light	60 (sec)	(1)	5.00	33	1.1	Guanine, Histidine, and Tryptophane
		(2)	.03	-	3.6	

TABLE 33

The Effect of Successive Ultraviolet Irradiation on the

Survival of Small-Colony Variants of *Candida albicans*

Response of small colonies to successive ultraviolet irradiation.

	0*	1	2	3	4	5
Exposure Time (Seconds)	% Survival	% Survival	% Survival	% Survival	% Survival	% Survival
0	100	100	100	100	100	100
10	100	100	100	100	100	100
20	90	82	83	87	82	93
30	66	52	44	60	-	-
45	26	19	11	22	-	-
60	11	15	2	4	5	11

* 0, 1-2-3-4-5 represent the number of previous UV exposures.

1027480

TABLE 34

Effect of Successive Ultraviolet Irradiation on the

Survival of Large (Normal) Candida albicans Colonies

Response to successive Ultraviolet irradiations.

	0*	1	2	3
Exposure Time (Seconds)	% Survival	% Survival	% Survival	% Survival
0	100	100	100	100
10	100	100	100	100
20	90	100	100	100
30	66	79	83	84
45	26	-	39	27
60	11	19	4	3

* 0, 1, 2, 3 represent the number of previous ultraviolet exposures.

TABLE 35

The Effect of Cultural Conditions on Survival and Small

Colony Development of *Candida albicans* After Ultraviolet Irradiation

Duration of Exposure (Seconds)	I* % Survival	I* % Small Colonies	II* % Survival	II* % Small Colonies	III* % Survival	III* % Small Colonies
0	100	<1	100	<1	100	<1
15	100	3-4	100	3-4	100	3-4
30	62	12	78	12	95	15
45	20	22	30	15	58	34
60	6	33	11	25	34	43

I* Grown on Sabouraud agar at 37°C; pre- and postirradiation.

II* Grown on defined medium before UV exposure and Sabouraud agar after exposure; both at 37°C.

III* Grown on Sabouraud agar at 37°C before UV; 25° after UV.

small-colony variants. Table 35 shows that growth on Sabouraud agar at 37° C before irradiation and at 25° C after irradiation resulted in more survivors.

Only one potential methionine-requiring mutant of C. albicans was isolated in the initial studies with chemical mutagens. However, this auxotroph appears to also have a leucine requirement and further work will be necessary to completely characterize the specific deficiency (ies).

Accumulation of S-Adenosylmethionine by Auxotrophs of Candida albicans

Norman Savage and Edward Balish

A filamentous mutant of Candida albicans accumulates much more S-adenosylmethionine than does the parent yeast-like strain.[1] We isolated several adenine-requiring mutants of C. albicans as well as one that requires methionine. Since adenine and methionine are two of the three basic components of S-adenosylmethionine, we decided to determine whether the auxotrophs could accumulate as much S-adenosylmethionine in their vacuoles as the parent strain.

Table 36 shows that strain W-3 (the prototroph) accumulated about 15 micromoles of S-adenosylmethionine per gram dry weight of cells with both adenine and methionine in the culture medium. Typical yeast-like morphology and good growth was maintained throughout the experiment.

A red, adenine-requiring mutant of C. albicans (1-NMU-5) demonstrated a comparable growth rate and slightly higher S-adenosylmethionine levels than did the prototroph. Another adenine deficient mutant (1-NMU-4) did not manifest an adequate growth rate; however, unusually high levels of S-adenosylmethionine were observed in cells of this auxotroph harvested at 20 hr. Another adenine-deficient mutant (V-NG-45) did not accumulate large amounts of S-adenosylmethionine. The two adenine-requiring mutants with the slowest growth rates (11-NMU-4 and V-NG-45) transformed to a filamentous cellular form. Only one methionine-requiring mutant (V11-NMU-1) has been isolated to date; it may also have a requirement for leucine. It had a fair growth rate, and transformed into a filamentous cellular form, but did not accumulate large quantities of S-adenosylmethionine when cultured in the methionine supplemented medium.

REFERENCE

1. Balish, E. and Svihla, G. Ultraviolet microscopy of Candida albicans. J Bacteriol 92, 1812-1820, 1966.

1027481

TABLE 36

Growth, Morphology, and S-Adenosylmethionine Content of Prototrophic and Auxotrophic *Candida albicans**

Organism All C. albicans	Culture age (Hr)	Cellular Morphology**	S-adenosylmethionine Micromoles/g Cells (dry wt.)	Dry wt. of Culture (mg)
W-3 Prototroph	0	Y	4.5	2.5
	12	Y	14.9	170.0
	20	Y	14.7	273.2
1-NMU-5 Red, adenine deficient	0	Y	18.7	3.8
	12	Y	18.3	122.8
	20	Y	16.8	259.0
11-NMU-4 Adenine deficient	0	Y	3.3	3.4
	12	F	9.4	31.8
	20	F	40.4	4.2
V-NG-45 Adenine deficient	0	Y	4.1	2.1
	12	F	7.5	49.8
	20	F	7.1	97.3
V11-NMU-1 Methionine deficient	0	Y	3.5	4.1
	12	F	11.6	10.0
	20	F	4.9	136.4

*Cultures were grown in a glucose-salts-Biotin medium, supplemented with adenine and methionine, at 37°C on a rotary shake machine. Mutant V11-NMU-1 was supplemented with methionine only.

**Y = Yeast-like cells; F = Filamentous cells.

Rapid Identification of Candida albicans in a Defined Liquid Culture Medium

David N. Mardon, Edward Balish, Brenda Joan Marks, and Kathryn Hurst

Germ-tube formation by Candida albicans has been observed within 4 hr after inoculation into mammalian serum,[1,2,3] or serum substitutes such as Versatrol,[1] tissue culture media,[2] or plasma.[3] Germ-tube formation has subsequently been proposed as a rapid means for identification of C. albicans.

Observations such as those described have led to speculation

about what component (s) in serum and other complex media are required for germ-tube formation[4,5,6] and some comments about whether this phenomenon is restricted to C. albicans.[2,7] However, in regard to the latter problem most investigators agree that only Candida stellatoidea seriously interferes with this diagnostic test. However, C. albicans and C. stellatoidea may not be truly different species.

We are unaware of any reports describing the formation of germ tubes by C. albicans in culture media that did not contain a variety of nitrogen sources. This report describes the production of germ tubes by C. albicans in a minimal glucose-salts-biotin medium containing a single nitrogen source.

Nine strains of C. albicans that produced chlamydospores on cornmeal agar and gave typical C. albicans reactions to sugar fermentation tests were used. Inocula were washed from 24 hr Sabouraud dextrose agar slants and diluted with glass-distilled water so that approximately 3 x 10^6 cells/ml were present in 0.5 ml of the experimental medium. Greater than 87% yeast-like cells were present in all cultures at the time of inoculation, and germ-tube formation was carried out at 37° C for 3 hr.

Germ-tube formation was similar in normal human serum, serum

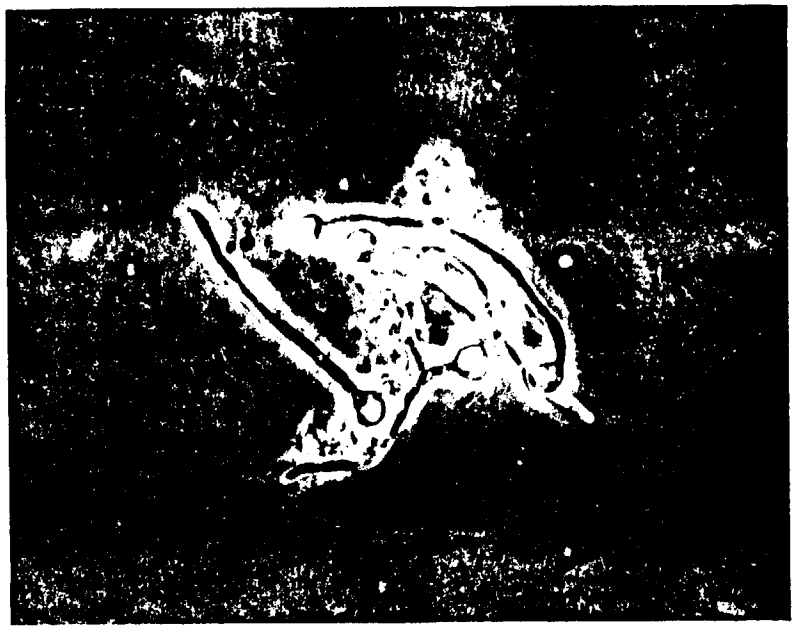

Fig. 29. Germ tubes formed by Candida albicans in serum, 3 hr at 37°C

1027482

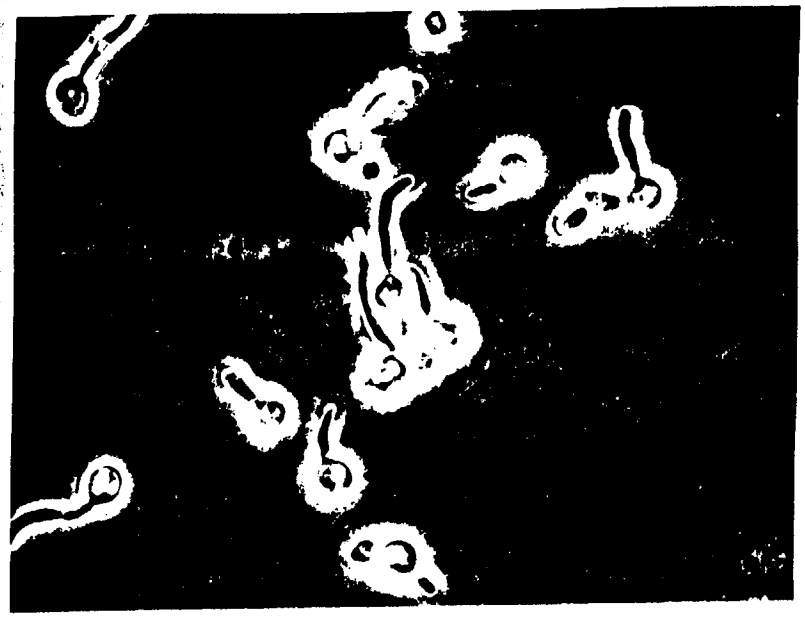

Fig. 30. Germ tubes formed by Candida albicans in a Glucose-Salts-Biotin medium with alpha-amino butyrate as the nitrogen source, 3 hr at 37°C.

from leukemic patients, and in glucose-salts-biotin media containing alpha-amino butyrate as the nitrogen source (Table 37). When the basal medium containing no alpha-amino butyrate was used only a filamentous mutant (10231-F) showed substantial germ-tube formation. The similar appearance of the tubes found in sera (Fig. 29) and those in the amino butyrate medium (Fig. 30) also indicates that this phenomenon is not unique to serum and other complex media. However, germ tubes formed faster (2 to 2.5 hr) in serum than in the defined culture medium.

Although greater numbers of germ tubes were found in serum and in the defined medium containing alpha-amino butyrate, some germ-tube formation was also obtained with the nine strains of C. albicans listed in Table 37, when ammonium chloride, L-methionine or S-ethyl-L-cysteine was the nitrogen source.

We are now investigating the effects of serum and the glucose-salts-biotin medium with alpha-amino-butyrate on seven other species of Candida.

In summary, we have been able to initiate germ tubes of C. albicans within 3 hr in a simple, defined culture medium. Apparently germ-tube production in both serum and the defined culture medium is characteristic of C. albicans and possibly C. stellatoidea and not of the other Candida species encountered in the clinical laboratory.

TABLE 37

Germ-Tube Formation by Nine Strains of *Candida albicans* in Sera and Defined Culture Medium

C. albicans Strain	% Germ-Tube Formation within 3 hr at 37°C			
	Serum		G-S-B Medium** + alpha-amino butyrate	G-S-B Medium
	Normal	Leukemic		
10231-Y	93	92	94	8
10231-F	97	66	98	37*
10261	100	73	78	5
Y-5	96	84	75	0
792	100	85	63	0
B-311	74	47	69	13*
39	96	87	64	0
8	78	97	49	0
AM-T	89	95	69	11

* The inocula contained the following percentages of filamentous cells with these strains: 10231-F, 13%, B-311, 10%; all others were > 98% yeast-like.

** Glucose-Salts-Biotin Medium.

REFERENCES

1. Taschdjian, C. L., Burchall, J. J., and Kozinn, P. J. Rapid identification of Candida albicans by filamentation on serum and serum substitutes. J Dis Child 99, 212-215, 1960.

2. MacKenzie, D. W. R. Serum tube identification of Candida albicans. J Clin Path 15, 563-565, 1962.

3. Bonfante, R. and Barroeta, S. Development and evaluation of a rapid identification test for Candida albicans. Mycopath Mycolog Appl 34, 33-39, 1968.

4. Landau, J. W., Dabrowa, N., Newcomer, V. D., and Rowe, J. R. The relationship of serum transferrin and iron to the rapid formation of germ tubes by Candida albicans. J Invest Dermatol 43, 473-482, 1964.

5. Landau, J. W., Dabrowa, N., and Newcomer, V. D. The rapid formation in serum of filaments by Candida albicans. J Invest Dermatol 44, 171-179, 1965.

1027483

6. Esterly, N. B., Brammer, S. R., and Crounse, R. G. The relation of transferrin and iron to serum inhibition of Candida albicans. J Invest Dermatol 49, 437-442, 1967.

7. Griffin, E. R. The value of the germ tube production test in the rapid identification of Candida albicans. J Med Lab Technol 21, 298-301, 1964.

Modifications in a French Pressure-Cell—Laboratory-Press System

David N. Mardon and Edward Balish

The French Pressure-Cell-Laboratory-Press system is an efficient method for obtaining cell-free extracts from yeasts[1,2] and filamentous fungi.[3] The basic system used in our laboratory consists of a French Pressure Cell (American Instrument Company, Inc., Silver Springs, Md.) and a Carver Laboratory Press (Fred S. Carver Inc., Hydraulic Equipment, Summit, N. J.)

Inherent in the use of such a cell-disruption system is the possi-

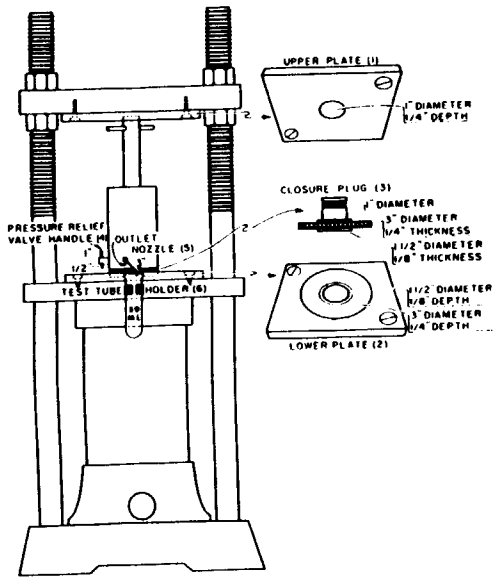

Fig. 31. French Pressure-Cell-Laboratory-Press System.

bility that the pressure cell may be improperly positioned in the press. This could result in its ejection from the press as pressure is applied. Therefore we designed removable steel plates (upper and lower) for the laboratory press. The upper plate contains a 1/4-inch deep by 1-inch diameter insert hole, which receives the top of the pressure-cell piston (Fig. 31-1); the lower plate has an insert hole 1/2-in. deep and 3-in. in diameter (Fig. 31-2) to receive the closure plug of the pressure cell (Fig. 31-3). These changes facilitate correct positioning of the pressure cell in the press and virtually eliminate the possibility that the pressure cell can be forced out under pressure. Addition of the removable steel plates to the laboratory press made it necessary to shorten one side of the pressure-relief valve handle 1/2 in. (Fig. 31-4). This modification was necessary to maintain sufficient clearance between the handle of the pressure-relief valve and the added bottom plate.

Other modifications included lengthening the outlet nozzle to 3 in. (Fig. 31-5) and attachment of a test tube holder to the base plate of the laboratory press (Fig. 31-6). These alterations aided in the collection of disrupted cells and cell extracts directly into the centrifuge tube. The addition of the test-tube holder also allowed the centrifuge tube to remain immersed in crushed ice while the disrupted cellular material was being collected.

These modifications have proved useful in safety and convenience for studies of methionine biosynthesis in cell-free extracts from yeast-like and filamentous cells of Candida albicans.

REFERENCES

1. Middlebrook, J. B. and Bowman, R. O. Preparation of axenic cultures of algae by use of a French Press. Appl Microbiol 12, 44-45, 1964.

2. Walters, J. R. and Stahly, D. P. Modification of the valve of the French Pressure Cell. Appl Microbiol 16, 1605, 1968.

3. Stine, G. J., Strickland, W. N., and Barratt, R. W. Methods of protein extraction from Neurospora crassa. Can J Microbiol 10, 29-35, 1964.

1027484

Large Abnormal Acrocentric Chromosome Associated with Human Malignancies*

Kong-oo Goh

From the cytogenetic finding of a giant abnormal acrocentric chromosome in each of a group of patients with an acute transformation of chronic myelocytic leukemia,[1] I proposed that this abnormal chromosome may in some way be associated with the malignant nature of the acute transformation.

A similar morphologic abnormal chromosome (Fig. 32) was found in six patients with four different malignancies: reticulum-cell sarcoma

* Published in Arch Intern Med 122, 241-248, 1968.

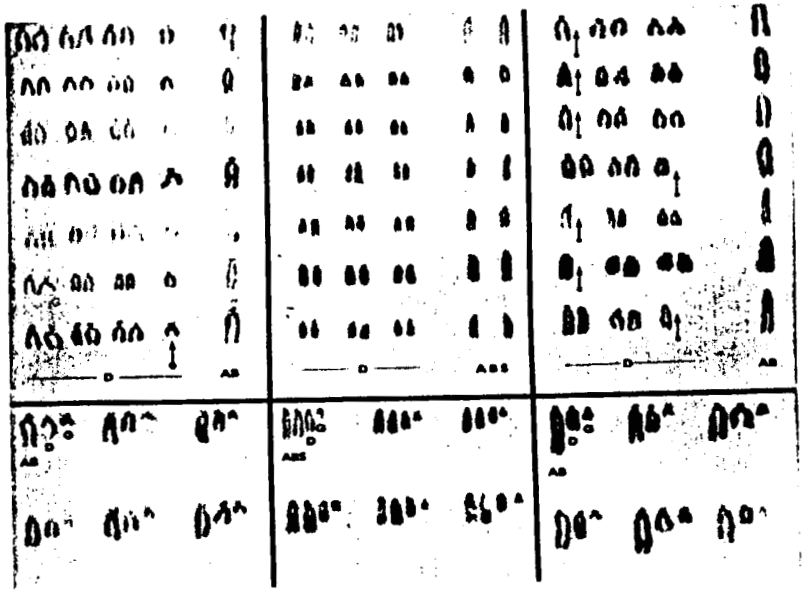

Fig. 32. Top: Normal D and abnormal chromosomes of a patient with reticulum-cell sarcoma (left), with malignant melanoma (middle), and leukolymphosarcoma (right). Abnormal chromosomes are in columns AB or ABS. Arrow with dark circle indicates additional and with white circle indicates the spaces of the missing chromosomes. Bottom: abnormal and normal D and G chromosomes. Note inconsistency in size of the abnormal chromosome compared to the normal D or G chromosome of its metaphase.

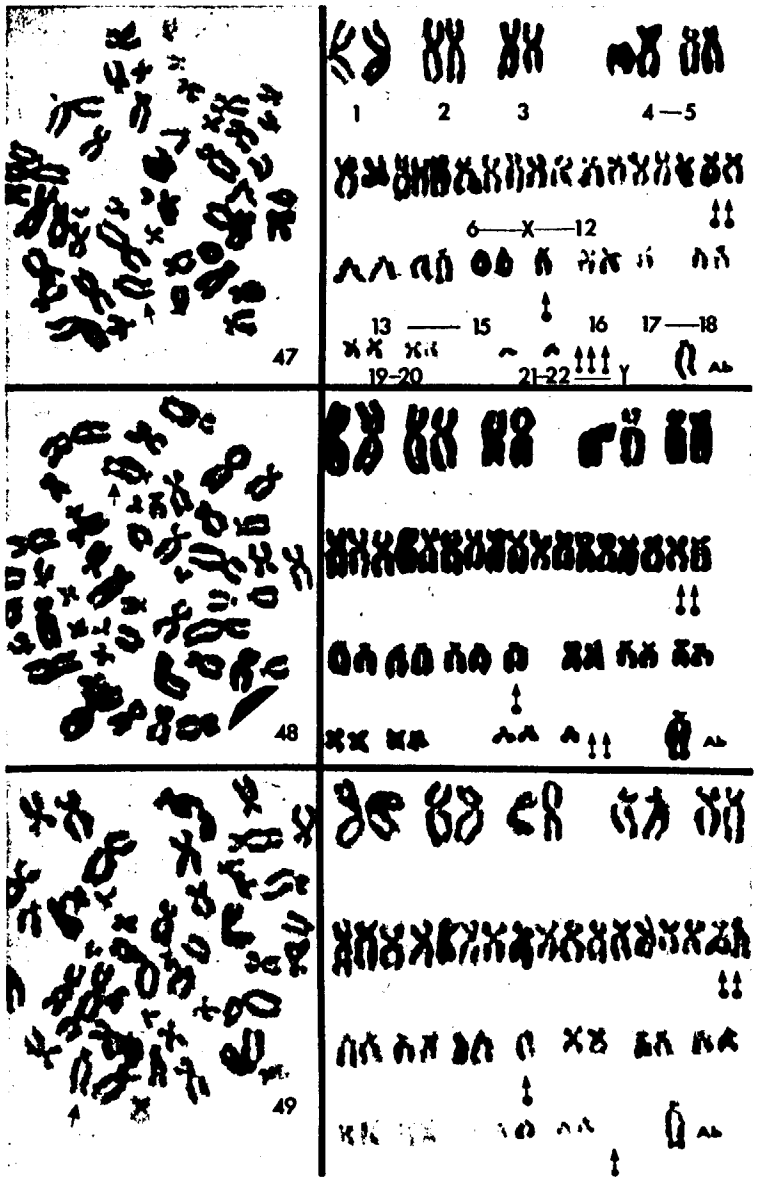

Fig. 33. Three metaphases and karyotypes of a patient with reticulum-cell sarcoma showing similarity except for a different number of missing G chromosomes. Abnormal chromosomes are marked AB in karyotypes, arrowed in metaphases.

1027485

(one); malignant melanoma (three); leukolymphosarcoma (one); and an early acute transformation of chronic myelocytic leukemia (one). Its frequency varied (Table 38); the highest incidence was found in metaphases obtained from direct tumor preparations and the lowest in the bone-marrow and peripheral-blood leukocyte cultures of patients with malignant melanoma. These findings give support to the possibility that this abnormal chromosome is in some way related to the malignant process. Its presence in the metaphases of the bone marrow and peripheral blood in patients with malignant melanoma confirms the clinical and autopsy findings of the widespread extension of the malignant disease.

Several clones of cells were found in the direct lymph-node preparation of a patient with reticulum-cell sarcoma (Fig. 33 and Table 39). Seventeen (24%) of the 70 detailed karyotyped metaphases in this patient had one or more acentric fragments (Fig. 34), suggesting that chromosomal breaks may be the original abnormality, which was followed by a translocation and led to a nondisjunction in a G chromosome (Fig. 35).

Although the present findings suggest a correlation between abnormal chromosomes and malignancy, occasional metaphases with similar abnormal chromosomes have been seen in persons without evidence of malignant diseases. Hence it was concluded that for the abnormal or mutant cell to become established in vivo, and to result in cancer, an explanation other than mutant-cell theory is necessary, such as impairment of the self-defense mechanism.

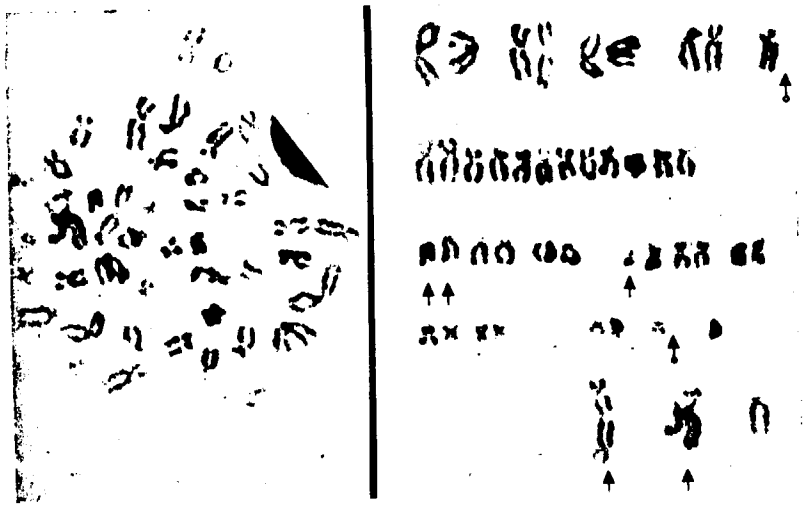

Fig. 34. Metaphase and karyotype in a direct preparation from a lymph node with reticulum-cell sarcoma showing simple chromosomal breaks (arrowed) and two translocating chromosomes (lower row). Arrow (white circle) indicates position of missing homolog chromosome.

TABLE 38

Cytogenetic Analyses of Six Patients
With Four Different Unrelated Types of Malignancies

Case	Material*	Days in Culture	Diploid No (%)	Aneuploid No (%)	Total Metaphases	Abnormal† No (%)
1	DLN	0	23 (14.5)	136 (85.5)	159	128 (80.5)
2	DTT	0	0	14 (100)	14	28 (200)‡
	CTT	3	0	43 (100)	43	86 (200)
	CTT	7	0	25 (100)	25	50 (200)
3	CBM	3	9 (75)	3 (25)	12	3 (25)
	CPB	3	17 (71)	7 (29)	24	1 (4)
4	CBM	3	42 (84)	8 (16)	50	6 (12)
5	DBM	0	2	1	3	1
	CBM	3	47 (68)	22 (32)	69	47 (68)
	CPB	3	23 (34)	45 (65)	68	61 (90)
6	DBM	0	2 (18)	9 (82)	11	4 (36)
	CBM	2	2 (10)	18 (90)	20	5 (25)

* DLN=Direct lymph node preparation; DTT=Direct tumor tissue; CTT=Cultured tumor tissue; CBM=Cultured bone marrow; CPB=Cultured peripheral blood; DBM=Direct bone marrow.
‡ A very large acrocentric chromosome.
† Each metaphase has two abnormal chromosomes.

TABLE 39

Chromosomal Distribution of 70 Detailed Karyotyped Metaphases
From Direct Lymph Node Preparations of Case 1

Chromosomal Number		36	45	46	47	48	49	50
Normal Chromosomal Group	1 A2 3	-1			-1 +1	-1 -1		
	B							
	C	-2	+1	+2 +2 +1 +1	+2 +1 +2 +1 +1 +2 +1	+2 +1 +1 +1 +2 +2 +1 +3	+2 +3 +2 +1 +1	+2 +3 +1
	D		-1	+1 +1	+1 +1 +1	+1 +1 +1 +1 +1 +1 +1	+1 +1 +1 +1 +2	+1 +1 +1
	E	-2			+1 -1			
	F	-3				+1		
	G	-3	-1 -2	-4 -3 -2 -3	-3 -2 -2 -1 -2 -1 -2	-2 -2 -1 -1 -2 -3 -1 -2	-1 -2 -2 -1 -2	-1
Abnormal Group	1*	+1	+1	+1 +1 +1 +1	+1 +1 +1 +1 +1	+1 +1 +1 +1 +1 +1 +1	+1 +1 +1 +1 +1	+1 +1 +1
	2†				+1 +1 +1	+1 +1 +1	+1 +1 +1	+1
Metaphases Having Fragments		1	1 1 1	1 1 1 1	1 1 1 1	2 2 1 1 1	1	
Number of Metaphases		1	1 1 1	3 1 1 1 1	2 4 1 1 1 1 1	19 6 2 2 1 1 2 1	5 3 1 1 1	2 1 1
% of Total				4.3	5.7	27 8.5	7.1 4.3	

* A very large acrocentric chromosome
† A very large submetacentric chromosome

REFERENCE

1. Goh, K. O. Cytogenetic studies in blastic crisis of chronic myelocytic leukemia. Arch Intern Med 120, 315-320, 1967.

1027486

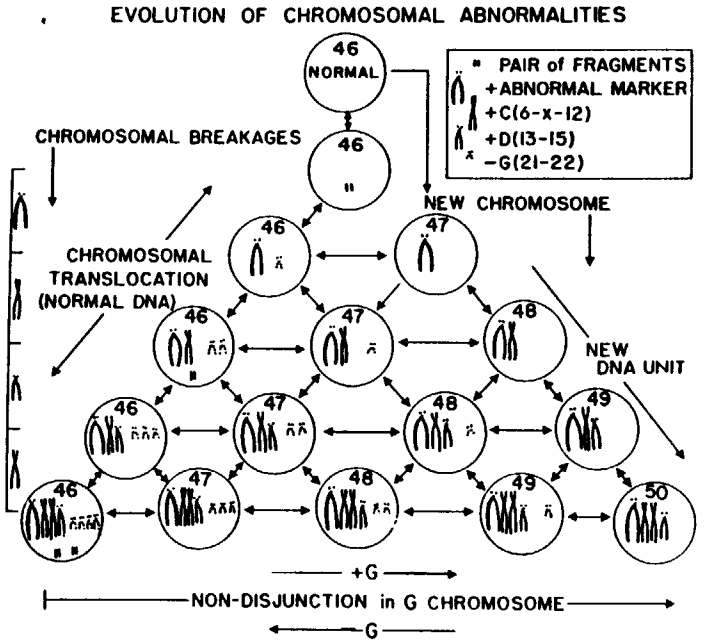

Fig. 35. Proposed evolution of clones of cells in one patient with reticulum-cell sarcoma. Chromosomal breaks are followed by translocation, then nondisjunction of G chromosomes.

The Effect of Deoxyribonucleoside Triphosphates on Pulverized Human Chromosomes at G_2*

Kong-oo Goh

Pulverization, a term adopted for extreme fragmentation of chromosomes (Fig. 36) has been found in patients who have virus infections or have been vaccinated. The mechanism of its production is unknown. We have designed experiments on the assumption that these chromosomal breakages are due to the weakness of the chromosomal DNA backbone.

From a patient who had been accidentally irradiated in 1958, 16 peripheral leukocyte cultures were made on November 7, 1966, a week

* Published in part in Clin Res 16, 42, 1968 and presented at the 7th Conference of Mammalian Cytology and Somatic Cell Genetics meetings October 23-26, 1968, at Gatlinburg, Tennessee.

after he had been vaccinated with polyvalent killed influenza virus. Two cultures were made from a normal person. To 15 cultures, deoxyribonucleotides were added alone and in combinations 4 hr before termination of the cultures (Table 40). The normal person had a normal chromosomal pattern. Seventy-one of the 100 control metaphases of the 16th culture (without added deoxyribonucleotides) and seven (0.5%) of the 1451 experimental metaphases were pulverized. Various (1 to 7%) frequencies of smaller G (Gq -) were found in the experimental cultures. The mitotic rate was 1.17% in the control and 1.82% (range 1.42 to 2.68%) in the experimental cultures.

Ahnström and Natarajan[1] have proposed that the chromosomal damage may be caused by an enzyme, DNA polymerase, which in time and space coincides with the duplication of chromosomal material and that this enzyme actively removes nucleotides from already formed chromosomal DNA. The chromosomal breakages seen in cytogenetic studies would thus be the result of the weakness of DNA backbone. This weakness could be prevented by adding deoxyribonucleotide triphosphates to the culture medium during the G_2 phase of the mitotic cycle to upset the equilibrium between them and the pyrophosphates; this upset could thus force the reaction toward the DNA polymers and prevent the removal of the already formed chromosomal DNA. The present findings suggest that the deoxyribonucleoside triphosphates

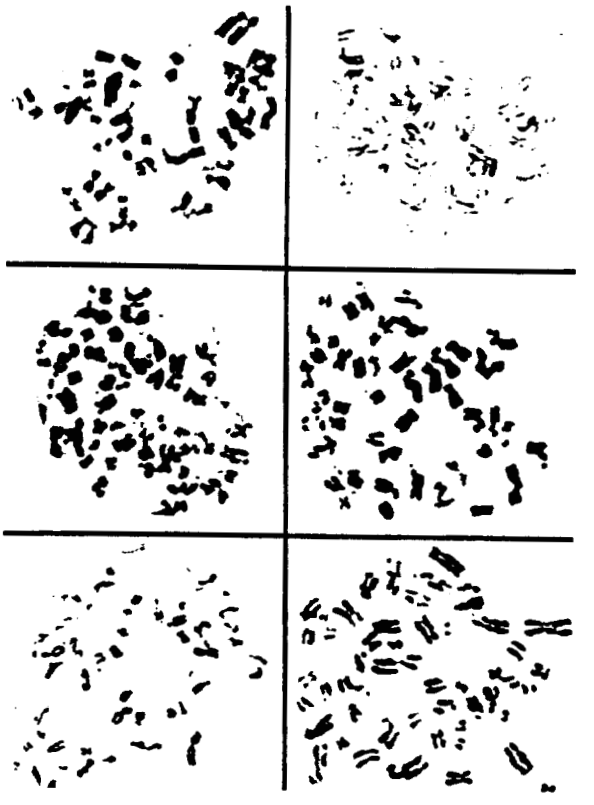

Fig. 36. Six metaphases from the patient's control culture without deoxyribonucleotides showing partial pulverization of chromosomes.

TABLE 40

Cytogenetic Analyses of the Control and Deoxyribonucleotides Added at G_2 Cultures

Culture	DNA bases*	Total metaphases	% 2N†	% Pulverized metaphases‡	X_1 cells§	Other abnormal cells‖	Smaller G¶	Mitotic Rate**
1	dATP	100	93	0	7	10	5	1.68
2	dGTP	100	89	2	15	12	5	1.63
3	dCTP	100	85	0	12	9	4	2.02
4	dTTP	100	85	0	12	13	5	2.27
5	dATP+dGTP	100	84	0	10	10	6	1.80
6	dGTP+dCTP	100	82	0	8	19	7	1.75
7	dCTP+dTTP	65††	88	0	7.7	12.3	3.1	2.19
8	dGTP+dTTP	100	85	0	8	14	2	2.68
9	dATP+dCTP	100	79	0	9	13	3	1.60
10	dATP+dTTP	100	80	0	8	7	1	1.40
11	dATP+dGTP+dCTP	100	86	0	8	11	4	1.67
12	dATP+dGTP+dTTP	100	90	0	15	10	4	1.94
13	dATP+dCTP+dTTP	100	88	0	10	15	5	1.69
14	dGTP+dCTP+dTTP	100	68	4	15	18	2	1.62
15	dATP+dGTP+dCTP+dTTP	86††	81	1	10	10	5.8	1.42
		1451	87	0.5	10.4	12.3	4.1	1.82
16	Control	100	?	71	5	2	?	1.17

* Deoxyadenosin 5'triphosphate (Na)=dATP; Deoxyguanosine 5'triphosphate (Na)=dGTP
Deoxycytidine 5'triphosphate (Na)=dCTP; Thymidine 5 triphosphate (Trisodium)=dTTP

† Percentage of metaphases having chromosomal number of 46 (normal diploid)

‡ Metaphases with pulverized chromosomes

§ Metaphases with direct terminal chromosomal breakages or acentric fragments

‖ Metaphases having abnormal chromosomal aberrations (translocations, dicentrics, rings, deletion)

¶ Deleted long arm of a G (Gq-) chromosome having the morphologic appearance of a Ph^1 chromosome

** Mitotic figures per 100 interphase nuclei

†† All the available well-spread metaphases

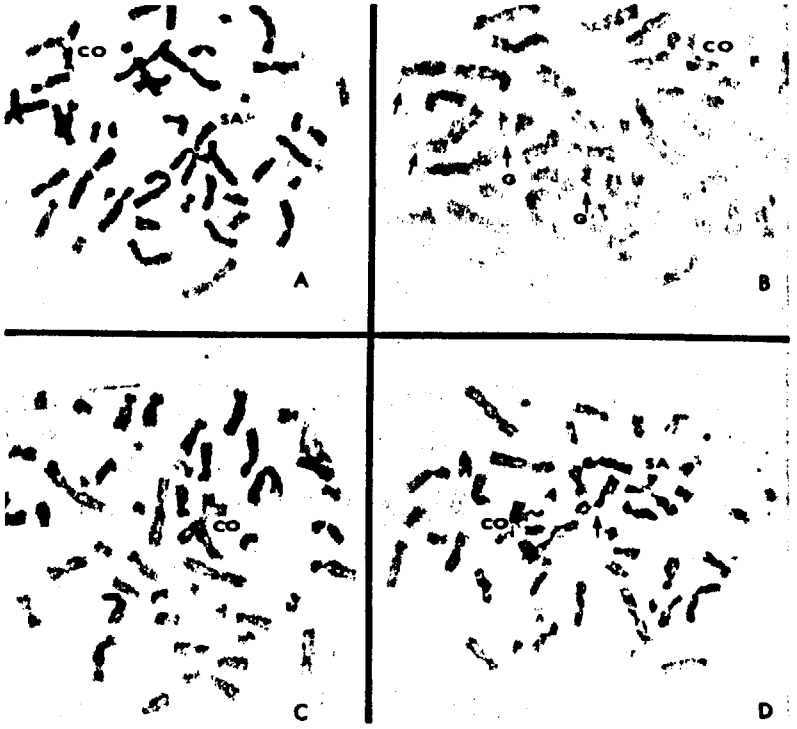

Fig. 37. Four metaphases from the experimental cultures where dGTP, dCTP, and dTTP were added during the G_2 period. CO = crossover; SA = satellite association and F = acentric fragment.

either prevent or heal the pulverized chromosomes. The finding of frequent other chromosomal abnormalities (Fig. 37) in the experimental cultures favors the latter possibility.

REFERENCE

1. Ahnström, G. and Natarajan, A. T. Mechanism of chromosomal breakage - A new theory. Hereditas 54, 379-388, 1966.

1027488

Autoradiographic Studies of the Abnormal Chromosome in Human Malignancies

Kong-oo Goh and Eugene Joiner

Several reports of an abnormally large acrocentric chromosome in human malignancies have stimulated great interest in the possibility that this chromosome is associated with the malignant process.[1] Such an abnormal chromosome has been reported from this laboratory in six different types of human malignancies.[1-4] The highest incidence was found in direct tumor preparations and the lowest in peripheral-blood and bone-marrow cultures.[1] This finding gave supportive evidence that metaphases with the abnormal chromosome represent malignant or mutant cells.

We raised the possibility that the abnormal chromosome could represent a group of different abnormalities, all with the same morphology, rather than a specific change. The great variation in size, as seen either in the same or different patients, suggested that the mechanism involved[1] could be (1) a translocation of a fragment to a normal D (13-15) or G (21-22) chromosome; (2) an inversion of one of the arms of any one of the B (4-5) or C (6-X-12) chromosomes; (3) a deletion of an arm of the A (1-3), B, or C chromosomes; or (4) an entirely new chromosomal DNA unit.

Fig. 38. Nine partial autoradiographic metaphases from a patient with reticulum-cell sarcoma. Shown are the different labeling patterns of the abnormal chromosomes and the absence of one or more of the normal D chromosomes in each of the metaphases.

Fig. 39. Metaphases and karyotype from a patient with reticulum-cell sarcoma showing the labeling of the terminal segment of the abnormal chromosome.

To investigate the mechanism by which this abnormal chromosome is produced, we used terminal autoradiographic labeling techniques[5] in direct tumor preparations. Different labeling patterns of the abnormal chromosome were found (Figs. 38-40). These findings suggest that this abnormal chromosome probably evolved from different normal chromosomes.

A common condition for the first three suggested mechanisms is chromosomal breakage. Chromosomal breakages are being seen in direct tumor preparations before anticancer treatment. They can be produced in vitro by agents known to produce experimental malignancy. However, not all agents that produce chromosomal breakages produce malignancies. Furthermore, breakages and morphologically similar abnormal chromosomes are seen occasionally in "normal" persons.[1] Thus, although the metaphases with this abnormal chromosome may represent abnormal or mutant cells, the abnormal chromosome can not be the sole cause of human malignancy as suggested.[6] An extension of

1027489

Fig. 40. Metaphase and karyotype from the same patient as Fig. 2 showing the centromere labeling of the abnormal chromosome.

Boveri's original view would be that a defect in the self-defense mechanism exists in cancer patients or that the internal environment of these patients favors the abnormal cells. A mutant cell (whatever the cause: spontaneous, induced by radiation, chemical agents, or virus) is therefore able to proliferate in such an environment. This continuous proliferation of the mutant cells would result in malignancy.[1]

REFERENCES

1. Goh, K. O. Large abnormal acrocentric chromosome associated with human malignancies: Possible mechanism of establishing clone of cells. Arch Intern Med 122, 241-248, 1968.

2. Goh, K. O., Swisher, S. N., and Rosenberg, C. A. Cytogenetic studies in eosinophilic leukemia: The relationship of eosinophilic leukemia and chronic myelocytic leukemia. Ann Intern Med 62, 80-86, 1965.

3. Goh, K. O. Pseudodiploid chromosomal pattern in chronic lymphocytic leukemia. J Lab Clin Med 69, 938-949, 1967.

4. Goh, K. O. Cytogenetic studies in blastic crisis of chronic myelocytic leukemia. Arch Intern Med 120, 315-320, 1967.

5. Goh, K. O. Autoradiographic studies in chronic myelocytic leukemia. In: Radioisotopes in Medicine: In Vitro Studies. R. L. Hayes, F. A. Goswitz, and B. E. P. Murphy, eds. AEC Symposium Series No. 13, CONF-671111, Oak Ridge, Tenn., June, 1968, pp. 695-715.

6. Boveri, T. The origin of malignant tumors, M. Boveri (trans.), Baltimore: Williams and Wilkins Co., 1929.

The Effect of Total-Body Irradiation on the Bone-Marrow Lymphocytes*

Kong-oo Goh

Chromosomal aberrations were found in the peripheral-blood leukocytes cultured with phytohemagglutinin seven years after total-body irradiation. These abnormalities were also found in the direct bone-marrow preparation of this group of patients.[1] The dividing cells of the human peripheral-blood leukocytes in the cultures stimulated by phytohemagglutinin (PHA) are thought to be small lymphocytes. The dividing cells in the direct bone-marrow preparations are thought to be myeloid cells. These findings confirmed observations of others that total-body irradiation caused chromosomal aberration in peripheral-blood lymphocytes. It also showed that total-body irradiation caused chromosomal aberration in the myeloid cells and that the chromosomal damaging effect appeared to be long lasting. The present communication reports the cytogenetic observations of the bone-marrow lymphocytes, seven years after total-body irradiation.

Bone-marrow specimens were cultured with and without PHA and were terminated after 4 and 7 days of incubation. Table 41 summarizes the cytogenetic analyses of the bone-marrow specimens cultured with PHA for 4 and 7 days. Table 42 shows the distribution of the chromosomal analyses of the bone-marrow specimens cultured without PHA.

The frequencies of chromosomal breaks, the abnormal cells, the

* Part of this report was published in Clin Res 16, 42, 1968.

1027490

TABLE 41

Cytogenetic Analysis of Metaphases Obtained from 4 and 7 Days of In vitro Cultured Bone-Marrow Materials with Phytohemagglutinin

Days / Code	Total Metaphases	%2N	Abnormal Cells* No.	Abnormal Cells* (%)[II]	X_1 Cells† No.	X_1 Cells† (%)	Chromosomal Breaks No. (%)	Chromosomal Breaks A/C[¶]	Fragments No. (%)	Dicentrics No. (%)	Translocation No. (%)	Rings No. (%)	Smaller G No. (%)
4 Days													
A	100	88	19		7		28	1.5	17	3	3	0	0
B	100	76	16		4		28	1.8	4	9	2	0	2
C	125	84	15	(12)	4	(3.2)	22(17.5)	1.5	5(4)	1(0.8)	5(4)	0	5(4)
D	100	94	16		8		25	1.5	10	2	2	1	3
E	100	93	19		7		29	1.5	20	0	1	1	5
F	200	92	22	(11)	10	(5)	33(16.5)	1.5	15(7.5)	5(2.5)	2(1)	0	2(1)
Total	725	88	107	(14.8)	40	(5.5)	165(22.8)	1.54	71(9.8)	20(2.8)	15(2.1)	2(0.3)	17(2.3)
7 Days													
A	37	92	3	(8.1)	1	(2.7)	4(10.8)	1.3	2(5.4)	0	1(2.7)	0	0
B	100	85	7		4		10	1.4	5	1	1	0	1
C	Not analyzable												
D	100	88	18		10		32	1.8	10	4	2	1	3
E	100	96	10		3		14	1.4	7	0	1	0	5
F	119	91	16	(13.5)	9	(7.5)	22(18.5)	1.4	11(9.3)	3(2.5)	0	0	3(2.5)
Total	456	90	54	(11.8)	27	(5.8)	82(18)	1.5	35(7.7)	8(1.8)	5(1.1)	1(0.2)	12(2.6)

types of chromosomal aberrations, and the chromosomal breaks per abnormal cell in the PHA-stimulated bone-marrow cultures are similar to those found in the cultured peripheral-blood leukocytes.[1] In the absence of PHA, fewer mitoses were seen in the cultures. These findings suggest that total-body irradiation also caused chromosomal breaks in the bone-marrow lymphocytes and that this effect may persist for a long time. An extension of this view would be that the bone-marrow lymphocyte pool is in constant exchange with the peripheral-blood lymphocyte pool.

REFERENCE

1. Goh, K. O. Total-body irradiation and human chromosomes: Cytogenetic studies of the peripheral blood and bone marrow leukocytes seven years after total-body irradiation. Radiat Res 35, 155–170, 1968.

Pseudodiploidy in Klippel-Feil Syndrome

Kong-oo Goh

The Klippel-Feil syndrome has been reported in 505 patients.[1] This rare congenital syndrome consists of short neck, low occipital hairline, and decreased mobility of the head. Normal cytogenetic studies have been reported in three cases.[1,2] In the course of our cytogenetic survey of congenital abnormalities, we examined an 8-year-old girl with this syndrome. She also had cleft palate and agenesis of the left kidney. The family history was not remarkable and the pedigree is summarized in Fig. 41.

The metaphases were obtained from standard peripheral-blood leukocyte cultures, which were terminated after 2, 3, and 4 days of incubation. The results of the cytogenetic analyses are summarized in Table 43. The high frequency of pseudodiploid metaphases represents at least four stem-cell lines as summarized in Table 44.

The pseudodiploid chromosomal pattern in this patient may be present in only a small fraction of patients with this rare syndrome. However, we also found a similar pattern in the karyotypes of photographed metaphases* of cases 1 and 2 reported[1] (Table 43 and Fig. 42).

* The negatives of the photographed metaphases were kindly supplied by Mr. Dante Picciano of Children's Hospital of the District of Columbia, Washington, D. C.

TABLE 42

Cytogenetic Analysis of Metaphases Obtained from 4 and 7 Days of In Vitro Cultured Bone-Marrow Materials without Phytohemagglutinin

4 Days Code†	Total Metaphases	2N‡	Abnormal Cells‡* No.	(%)¶	X-Cells† No.	(%)	Chromosomal Breaks No.	(%)	A/C#	Fragments No.	(%)	Dicentrics No.	(%)	Translocation No.	(%)	Rings No.	(%)	Smaller G No.	(%)
A	24	75	1	(4.2)	1	(4.2)	2	(8.4)	2.0	2	(8.4)	0		0		0		0	
B	49	80	7	(14)	5	(10)	9	(18)	1.3	7	(14)	0		0		0		3	(6.1)
C	1	--	0		0		0			0		0		0		0		0	
D	100	89	10	(10)	4	(4)	14		1.4	6		0		1		1		4	
E	52	94	3	(5.8)	1	(1.9)	3	(5.8)	1	1	(1.9)	0		0		0		3	(5.8)
F	---No Mitosis Seen---																		
Total	226	86	21	(9.3)	11	(4.9)	28	(12.4)	1.3	16	(7.1)	0		1	(0.4)	0		10	(4.4)
7 Days																			
A	---No Mitosis Seen---																		
B	5	0			0		0			0		0		0		0		0	
C	1	0			0		0			0		0		0		0		0	
D	100	3			0		3		1.0	0		0		0		0		3	
E	9	0			0		0			0		0		0		0		0	
F	3	0			0		0			0		0		0		0		0	
Total	118	3			0		3	(2.6)	1.0	0		0		0		0		3	(2.6)

† Cells having chromosomal aberrations
‡ Presumably first-generation cells with chromosomal aberrations and fragments
§ The coding of these patients is the same as those reported previously.
¶ Percentage of cells having diploid (46) chromosomal numbers.

The number inside the parentheses is the percentage of abnormalities per 100 metaphases. Without parentheses, the number of abnormalities is the same as the percentage.

* A/C: Chromosomal breaks per abnormal cell.

1027491

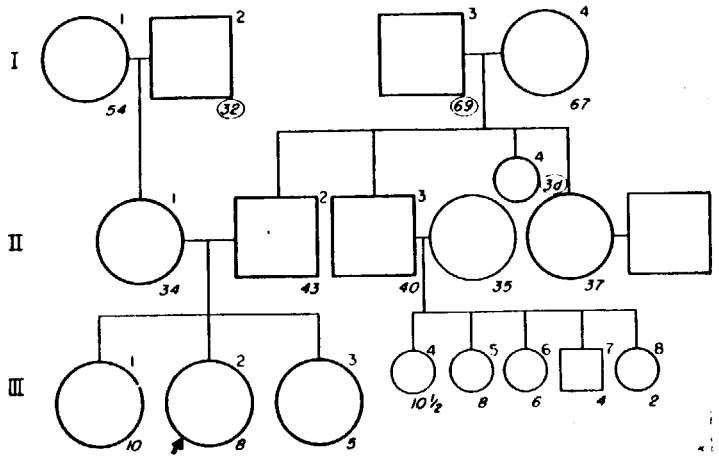

Fig. 41. Pedigree of present case (arrowed). The circled numbers in the lower right of the symbols indicate the age at which the person died.

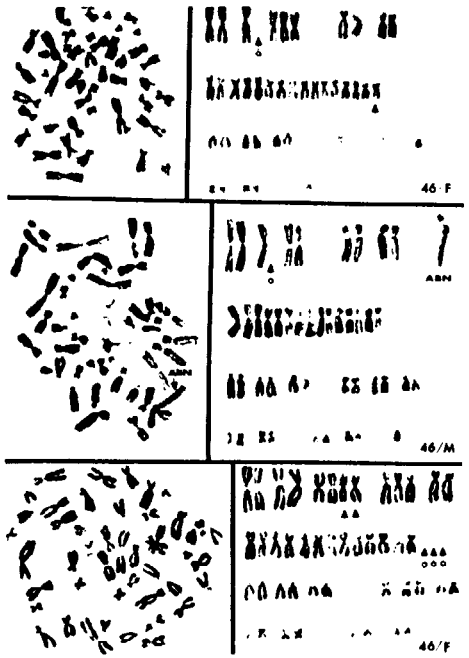

Fig. 42. Three pseudodiploid metaphases and their karyotypes of the present patient (upper), case 1 (middle) and case 2 (lower) reported by others [1]

1021492

TABLE 43

Cytogenetic Analyses of Three Cases of Klippel-Feil Syndrome[a]

Present patient	Chromosome number <45	45	46	47	>47	Total	%2N[†]	X Cell[‡] No. (%)	Pseudodiploidy No. (%)
	No. of metaphases								
2[§]	11	2	29	2	0	44	66	3 (6.8)	5 (11.3)
3	8	9	58	1	1	77	75	2 (2.6)	18[‖] (23.3)
4	11	0	40	0	2	53	76	7 (13.2)	3 (5.7)
Case 1	0	2	18	1	0	21	86	0	4 (20)
Case 2	2	0	16	1	0	19	84	0	6 (31.6)

[a] Cases 1 and 2 were reported by Morrison et al.[1]

[†] Percentage of cells having normal diploid chromosomal number (46).

[‡] Metaphases having chromosomal break.

[§] Days of in vitro incubation.

[‖] Detail summarized in Table 44.

TABLE 44

Distribution of the Missing and Additional Chromosomes of Eighteen Pseudodiploid Metaphases of the Present Patient

Chromosomal Group																								Abnormal Chromosome	Total Metaphases
	A			B		C			D			E		F		G			Y						
1	2		3	4-5		6-X-12			13-15			16-18		19-20		21-22									
+1			-1																						2
-1			+1																						3
			-1			+1																			4
				-1		+1																			2
	-1		+1	-1		+1																			1
			+1	+1		-1			-1																1
									-1															Medium size Acrocentric	1
						+1			+1			-1		-1											1
	-1			+1																					1
						-1								+1											1
-1				-1		+2																			1

The mechanism of the production of these pseudodiploid metaphases is unknown. However, from the finding of high frequency of chromosomal breakages in our patient, we are tempted to conclude that the pseudodiploid metaphases are probably the result of abnormal chromosomal healing. We rule out the possibility of a nondisjunction as the cause of the pseudodiploidy because several morphologically abnormal chromosomes were found in each of these three patients.

REFERENCES

1. Morrison, S. G., Perry, L. W., and Scott, L. P. Congenital brevicolis (Klippel-Feil syndrome) and cardiovascular anomalies. Amer J Dis Child 115, 614-620, 1968.

2. Cohney, B. C. The association of cleft palate with the Klippel-Feil syndrome. Plast Reconstr Surg 31, 179-187, 1963.

Chloramphenicol and Acute Leukemia

Kong-oo Goh

Chloramphenicol, a powerful broad-spectrum antibiotic, has been thought to be the cause of some cases of aplastic anemia.[1-3] The mechanism responsible is believed to be its toxic effect on the bone-marrow cells but does not explain the cases in which bone-marrow failure develops after the drug has been stopped, nor the persistence of the nuclear and cytoplasmic vacuolization of bone-marrow cells in some patients previously treated with it.

Chromosomal vacuolizations (Fig. 43), dissociations (Fig. 44), breakages (Fig. 45), and translocation (Fig. 45) were found in direct bone-marrow preparations of a patient with acute myeloblastic leukemia, thought possibly to be the result of chloramphenicol-induced aplastic anemia. Table 45 summarizes the chromosomal analyses. The direct bone-marrow preparations and the bone marrow cultured without phytohemagglutinin (PHA) had a lower frequency (61.0%) of diploid metaphases than bone marrow cultured with PHA (76.5%). Most of the aneuploid metaphases were hypodiploid with a normal G missing in 14 of the 31 metaphases with 45 chromosomes (Fig. 43). Chromosomal vacuoles were seen in metaphases obtained from direct bone marrow and cultured bone marrow in the absence of PHA, but they were not seen in bone marrow cultured with PHA. A high frequency of chromosomal breakages and pseudodiploid metaphases was found. Fifteen (40%) of the 37 pseudodiploid metaphases had at least one abnormally large acrocentric chromosome (Fig. 45).

Chemically, chromosomes consist of DNA, RNA, protein, and

1027493

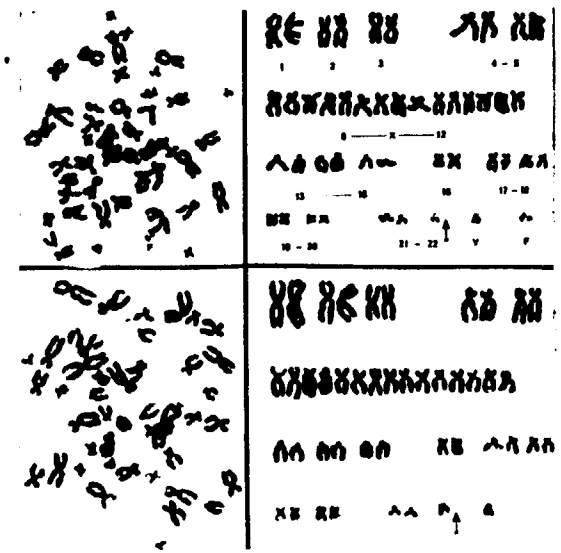

Fig. 43. Two 45-chromosome metaphases and karyotypes from 1967 (upper) and 1968 (lower) direct bone-marrow preparations. Note vacuoles of chromosomes and the position of the missing G chromosomes (arrows with white circle). A fragment (F) is also seen in the upper metaphase.

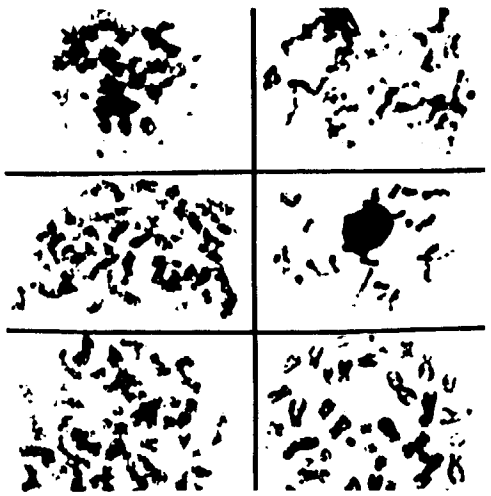

Fig. 44. Six metaphases showing the dissociation and vacuolization of chromosomes from direct bone-marrow preparations.

TABLE 45

CYTOGENETIC STUDIES OF THE BONE MARROW METAPHASES

Specimen*	Chromosomal Number No. of Metaphases <45	45	46	47	>47	Total	‡2N	Vacuoles	Dissociation	Breaks-ages	Pseudo-diploid
Sept. 13, 1967											
DBM	9	3(2)†	19	1	0	32	60	7	2	2	6(3)†
BMC + PHA	18	7(1)	91	0	4	120	76	0	0	6	9(5)
BMC	19	4(4)	22	0	1	46	48	2	1	1	2(2)
April 23, 1968											
DBM	18	8(4)	65	1	4§	96	68	3	9	4	9(2)
BMC + PHA	11	9(3)	77	1	2¶	100	77	0	7	8	11(3)
Total	75	31(14)	274	3	11	394				21	37(15)

* DBM = Direct bone marrow; BMC + PHA = Bone marrow culture with phytohemagglutinin
BMC = Bone marrow culture without phytohemagglutinin.

† The number inside the parentheses is the number of metaphases missing one G (21-22) chromosome.

‡ The number inside the parentheses is the number of metaphases having an abnormally large acrocentric chromosome.

§ Three tetraploid.

¶ Endoreduplication.

Fig. 45. Left: Two partial metaphases showing fragment (F), crossover (CO), translocation (T), chromosomal (SB) and chromatid (TB) breakages. Right: Partial karyotypes showing the normal 13-15 and the abnormal (Abns) chromosomes of four metaphases. Positions of the missing chromosomes are marked with white-circled arrows.

histone. Chloramphenicol, an inhibitor of protein synthesis, could cause deficiency of chromosomal protein, which might result in vacuolization as seen in the present patient and in a patient with pancytopenia.[4] These vacuoles could then lead to chromosomal "weakness" and resulting breakages. However, vacuoles were not seen in the metaphases obtained from the bone-marrow cultures stimulated by PHA in this patient. Thus it is hypothesized that a defect may have been already present in the myeloblasts of patients who develop the hematologic toxicities following chloramphenicol treatment, analogous to the glucose-6-phosphate dehydrogenase deficiency in which the defect is not expressed phenotypically as hemolytic anemia until other agents have been introduced.

REFERENCES

1. Wilson, L. E., Harris, M. S., Henstell, H. H., Witherbee, O. O., and Kahn, J. Aplastic anemia following prolonged administration of chloramphenicol. JAMA 149, 231-234, 1952.

2. Smiley, R. K., Cartwright, G. E., and Wintrobe, M. M.

1027494

Fatal aplastic anemia following chloramphenicol (chloromycetin) administration. JAMA 149, 914-918, 1952.

3. Rheingold, J. J. and Spurling, C. L. Chloramphenicol and aplastic anemia. JAMA 149, 1301-1304, 1952.

4. Castoldi, G. and Mitus, W. J. Chromosome vacuolization and breakage. Arch Intern Med 121, 177-179, 1968.

Semistatistical Computer Analysis of Electronic Erythrocyte-Size Determination: A rapid laboratory method of detecting RBC disease

C. C. Lushbaugh, R. C. Lushbaugh, and Dorothy H. Lushbaugh*

Erythrocyte (RBC) size can be used as a clinical determinant of RBC disease and electronic determination of size by the Coulter counter affords a means of producing RBC volume distributions (RBCVD) rapidly. Previously we have shown how this method, combined with a multichannel pulse-height analyzer (PHA) system, produces frequency distribution histograms that can be displayed on an oscilloscope and photographed. Our previous attempts to compare a patient's RBCVD with that of a normal person in quantitative rather than visual qualitative terms have involved computation of the modal and weighted mean cell volumes from the PHA data. These numerical values are averages similar to the mean corpuscular volume (MCV) commonly derived from RBC count and hematocrit and do not use all the information present in the electronic RBCVD. For example, mean cell sizes can be identical even when the histograms being compared have one or two modes signifying the presence in one of two subpopulations of cells and only one population in the other. On the other hand, the 100-channel PHA histogram representing the size distribution of the measurements of 100,000 individual RBC contains more information than is required for making mathematical comparisons. Following the suggestions of Edward Frome† and Robert Beaver‡ that quantile probability analysis could be used here as a data reduction system, we found that the 100 channel

* University of Florida, Gainesville.

† Formerly ORAU Data Processing statistician; present address: Marketing Research Department, Coca-Cola Company, Atlanta, Ga.

‡ Statistician, University of Florida, Gainesville.

1021495

RBCVD polygon could be reduced to decile channel divisions (see asterisks in Table 46) as in Fig. 46. The vertical dash lines in Fig. 46 demarcate the number of PHA channels that hold successively 10% (10,000 sized RBC) of the area (100,000 cells) under the curve drawn through the histogram of RBC sizes of a normal person's blood. These decile probabilities (~10%) are considered in our analysis as the number of cells that should be expected to fall within these channel boundaries if the blood being tested is normal. As shown in Table 46, this number is E_i and that observed for the patient is O_i. Using Pearson's Statistic as commonly employed to determine the chi-square of the difference between two or more numbers, we then can calculate a weighted squared-difference with the formula shown in Table 46. One of us (RCL) then developed a system for computer analysis of the RBCVD and programmed it for our IBM 1800 computer.

The digital data contained in the PHA memory is now read out by typewriter and punched onto cards following a prescribed format. The data on the punch cards from the RBCVD of a patient are fed into the computer along with those of the normal person to be used as reference and a single value (we call it the squared-difference index, Δ^2) is computed and printed out. If preparation time for the punch card

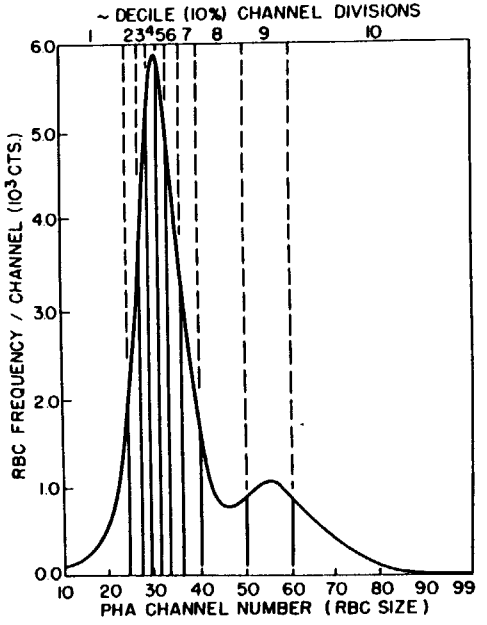

Fig. 46. Graph showing by dashed lines how the 100 PHA channels of the RBCVD polygon are divided into 10 groups so that each group (a decile) will normally contain 10% of the 100,000 cells that are sized.

TABLE 46

RBCVD ANALYSIS

0. Initial Determination of Decile Channel Divisions.*

I. Daily Data Collection: Normal and patient blood; Coulter RBC size distributions (#RBC/PHA Ch).

II. Data Reduction by Computer -

1. Normalization: percentage of RBC/Ch (10-99)

2. Decile Distribution: percentage of RBC/decile*

a) normal reference blood for day (E_i)
b) patient's blood...(O_i)

3. Calculation: Squared-Difference Index (Δ^2)

$$\Delta^2 = \sum_{i=1}^{10} \frac{(O_i - E_i)^2}{E_i}$$

$\Delta^2 \leq 4.0$ = normal RBCVD

$\Delta^2 > 4.0$ = abnormal RBCVD

* See text for explanation of this term.

data can be discounted (since it would not exist if our PHA was interfaced directly with the computer) the total time required from obtaining blood by finger puncture to the Δ^2 index number would be less than 2 min per patient. Under existing conditions the entire procedure takes 14 min but only 0.5 min of this is technician time.

Using this method, we then determined the day-to-day variation in the Δ^2indices of RBCVD of the blood of one normal person obtained repeatedly over about eight months. These values are graphed sequentially against time in Fig. 47 and as a frequency distribution in Fig. 48. In Fig. 47, the effect of occasionally noisy electronics on the accuracy of the method can be seen. Without this problem that requires constant correction in most electronic systems, the measurements are remarkably reproducible (2.5 ± 0.7). Their variance can be seen in Fig. 48 to be quite small, less than 5% being greater than the theoretical 95% fiducial upper limit for this data distribution. For purposes of clinical evaluations as indicated in Table 46, we have chosen, therefore, a Δ^2 index greater than 4.0 as the index that a person's RBCVD is different from the normal. We are now determining the validity of using this boundary for clinical appraisal by computing the Δ^2 of the

1027496

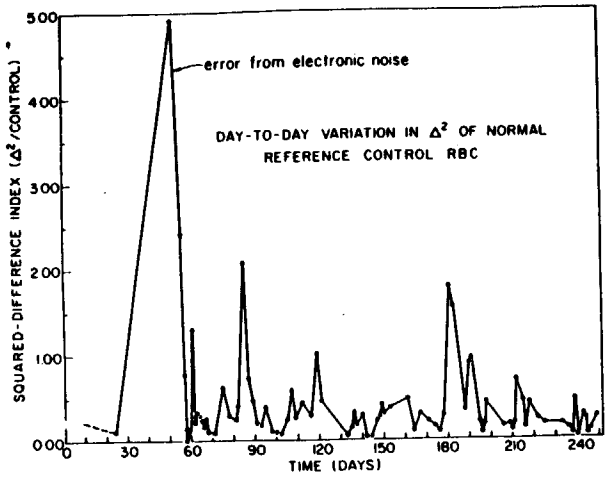

Fig. 47. Sequential changes in the squared-difference index (Δ^2) of RBCVD of one normal person determined at various intervals over eight months. All are compared arbitrarily to one RBCVD done on day 179. The occurrence of the deviation caused by electronic problems was successively avoided by control of 60 cycle ground loops.

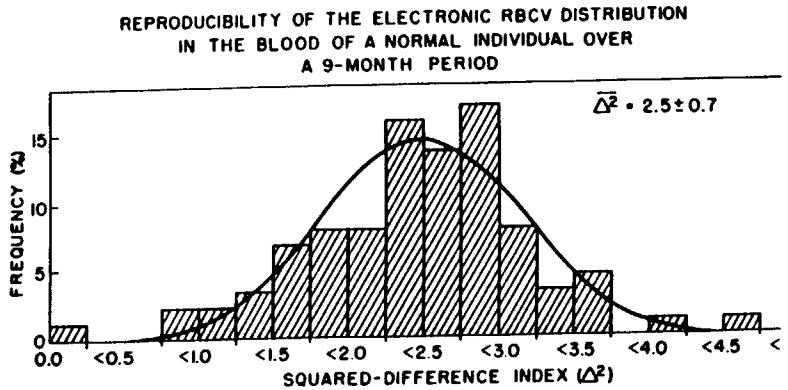

Fig. 48. This frequency distribution of squared-difference indices of RBCVD from one person indicates the remarkable reproducibility of this method of RBC size evaluation that permits its use in detection of abnormal RBC formation.

blood of a group of presumedly normal persons. As shown in the accompanying paper, patients with various neoplastic blood dyscrasias have Δ^2 indices far beyond this >4.0 boundary of normality and the Δ^2 index is proving to be an objective means of gauging improvement in RBC kinetics.

Evaluation of Therapeutic Response with Change in Electronic RBC Size Distribution

C. C. Lushbaugh, Dorothy H. Lushbaugh, and C. L. Edwards

In normal persons, electronically determined RBC size distribution is constant and reflects a steady state of RBC production and loss. Perturbation of the system by acute or chronic hemorrhage, nutritional deficiencies, or hemolysins results in changed RBC size distribution patterns that are often diagnostic. Patterns typical of microcytic, macrocytic, and hemolytic anemia have been determined and reported previously. These abnormal patterns are constant in untreated patients whose compensatory mechanisms have established a new but pathologic steady state in erythrokinetics. Therapy, if appropriate, acts as a perturbation to production of abnormal RBC and changes the previously existing RBC distribution pattern. "Successful" treatment is seen by this method as progressive changes that reestablish the RBC volume distribution (RBCVD) typical of the normal human in the normal steady state. Persistence of uncorrected pathologic conditions of erythrocyte production or nonsenescent RBC loss is revealed by failure of the RBC distribution pattern to return to normal. This kind of evaluation can be made visually by comparing the patient's current RBCVD patterns with those obtained earlier on himself, with a normal RBCVD pattern established for "man," or with a RBCVD determined for a normal subject on the same day the patient's sample is taken. We have found that, because of day-to-day "drift" in the electronic pulse-height analyzer system, it is best to compare with the RBCVD obtained daily from a person known to be free from medical problems in general and particularly from blood loss and other hematologic abnormalities. As shown in the preceding report, we have found that the RBCVD of a normal person does not vary greatly from day to day over long periods of repeated bleedings if less than 2 ml/wk is lost. Fresh blood from the same normal person can be used therefore not only to compare with many patients as a reference standard but also to "peak" the analyzer system so modal RBC size is always located in the same PHA channel. When this procedure is followed, almost identical RBCV patterns are obtainable from day to day for the normal control unless electronic failures occur or the system becomes "noisy."

In the preceding report our observations show that visual evalu-

1027497

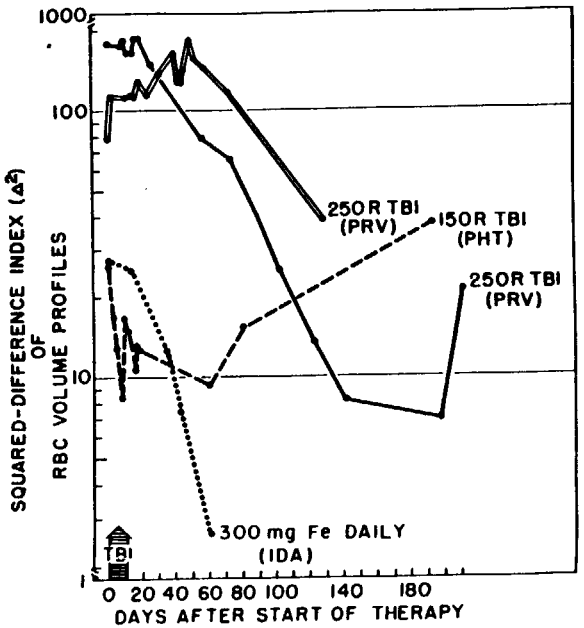

Fig. 49. Progressive changes in the Squared-Difference Indices of RBCVD patterns of four patients. In the patient with iron deficient anemia (IDA) treated with oral iron, the index returned to normal (normal Δ^2 is <4.0) within two months. Prolonged but temporary improvement after 250 R TBI was shown by decreasing indices in two patients (PRV), while a gradual increase in the index occurred in a patient with primary hemorrhagic thrombocythemia (PHT) after a short-lived clinical improvement following TBI therapy (150 R).

ations of degree of change in RBCVD can be replaced by using the Squared-Difference Index (Δ^2).

Determination of this index of RBCVD conformity for individual patients from day to day is proving to be a rapid means of data reduction, producing a single number whose size seems related to degree of dissimilarity between the patients and the normal control person's blood. Applying its use to our studies of the blood of patients undergoing treatment in the LETBI facility, we have found as shown in Figs. 49 and 50 that progressive decreases in the Δ^2 of RBCVD occur in some irradiated patients - for example those with polycythemia rubra vera (PRV) - when TBI alters the course of their disease temporarily. As shown in Fig. 49, this index changed for the better over the course of 200 days in one patient with PRV; over a period of about 80 days in another patient with this disease after a 60-day period during which his marrow was suppressed by his radiation exposure; and during about 60 days in an irradiated man

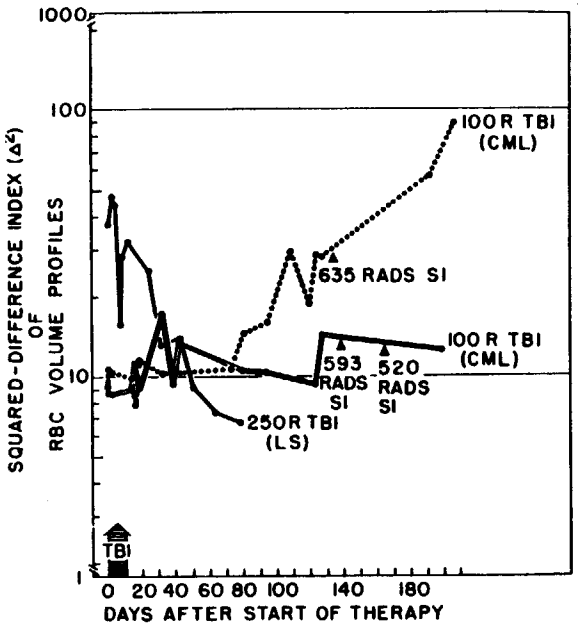

Fig. 50. The course of changes in the squared-difference index (Δ^2) of RBCVD patterns in three patients treated with TBI and in two instances also with local splenic irradiation (SI) at the times shown by the solid delta. The 250 R TBI of the patient with disseminated lymphoma (LS) produced a partial clinical remission that was accompanied by a progressive decrease in Δ^2. In the two cases of chronic granulocytic leukemia (CGL) treated with 100 R, no improvement occurred clinically or in the Δ^2 index. Splenic irradiation in both produced clinical improvements and lowered peripheral blood leukocyte counts but no alteration in the trend of the changes in the Δ^2 index.

with primary hemorrhagic thrombocythemia (PHT) following which the index worsened as the effect of the radiation therapy dissipated. The changes in this index in the irradiated patients shown in Figs. 49 and 50 are contrasted with its rapid return to normal in an unirradiated woman treated orally with an iron compound for iron deficiency anemia (IDA). In Fig. 50 the improvement of this index during a successful amelioration of a lymphosarcoma (LS) by 250 R TBI is shown in contrast with the changes in this index in two patients with chronic granulocytic leukemia where 100 R TBI was unsuccessful. Local irradiation to the spleen (SI) failed to alter the trend of the progressive worsening of this index of RBC abnormality.

1027498

MEDICAL RADIOISOTOPES

The Division devotes an important segment of its resources to the beneficial applications of radiation in diagnosis and therapy, the principal objectives being (1) to apply radioisotopic test compounds in the detection of tumors, (2) to measure functional disorders, and (3) to diagnose metabolic defects. This effort requires not only the skills of several staff members, particularly in organic chemistry, pharmacology, and instrumentation, but demands the careful judgment of physicians who first try a new test material in patients. After animal studies have been completed to demonstrate not only efficacy but safety of the material, the final step of the sequence involves administration of the materials to patients in the Medical Division's research hospital.

The radiopharmaceutical development project has focused mostly on the development of new tumor-detecting agents, both for soft-tissue neoplasms and lesions in bone. Work has continued on exploration of colloidal preparations that have superiority over those previously available for bone-marrow scanning.

Because of our major interest in both hematologic disorders and radiation damage to hematopoietic tissue, we have performed studies with radioactive iron in the assessment of red blood cell production and also studies of blood volume in hematopoietic disorders; they are included in this portion of the report.

A key resource in the advancement of beneficial applications lies in the support we receive from the instrumentation group who constantly are refining our equipment and devising new instruments that detect and assess radioactivity within patients. With the availability of the IBM 1800 computer, we are entering into a new phase of instrument development that will exploit as fully as possible the capabilities of this device. Much work is required in interfacing the electronic radiation-detection equipment with the computer. (See Section F on Computer Technology.)

Tumor Scanning with Gallium-67

C. L. Edwards and R. L. Hayes

The need for a good tumor-specific scanning agent has promoted a wide search for such materials. Others have investigated ^{197}Hg chlormerodrin, ^{131}I albumin, ^{131}I fibrinogen, ^{99m}Tc, ^{32}P, ^{75}Se, and ^{75}Se methionine, each with limited success. Except for intracranial lesions and differentiated thyroid carcinoma, tumor scanning has not had wide clinical application. Recently we observed an unusual affinity of certain extracranial soft-tissue tumors for carrier-free

11	Hodgkin's		wall lesion, iliac, and mediastinal nodes.	25	Carcinoma of cervix with abdominal metastases	-	Patient reported to have retroperitoneal metastases that were not visualized.
12	Bronchial carcinoma	+	Visualization of unsuspected pericardial metastases.	26	Bronchial carcinoma	↔	Recurrent disease visualized.

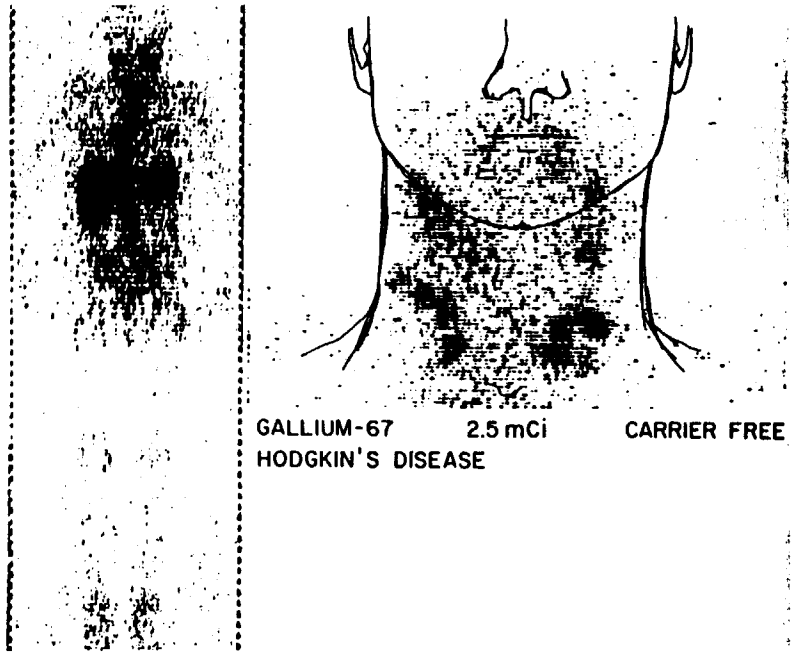

Fig. 51. Case 2. Posterior whole-body photoscan at 6 days after 2.5 millicuries of ^{67}Ga citrate. The scan was made with the ORAU whole-body scanner, which has a 5 1/4 x 3 in. NaI crystal and an 88-hole focusing collimator (left). Anterior photoscan of the neck area at 72 hr after the ^{67}Ga citrate, made with a Picker 5-in. Magnascanner with a 265-hole fine-focusing collimator (right). No contrast enhancement was used in either scan.

cell malignant lymphoma for two and a half years, was being treated with prednisone for a falling hemoglobin and enlarging peripheral lymph nodes. He did poorly, however, and died 2 weeks after the scan (Fig. 52). Permission for a complete autopsy was refused but consent for multiple needle biopsies was obtained. These specimens were assayed for ^{67}Ga and compared with blood obtained after his death as shown in Table 48. The relative concentration in the cervical lymph nodes, liver, and blood correspond to the good contrast on the scan.

Twelve patients with nonlymphomatous tumors were also scanned. Four patients (Cases 12, 22, 23, and 26) were thought to have residual or recurrent bronchial carcinoma. The scans showed activity concentrated in the area of the suspected carcinoma, except for Case 26. He had a pulmonary shadow on the chest X ray with a pleural abscess draining through the lobectomy incision. A recurrence was suspected but not shown. Scans were falsely negative in two patients with recurrent medullary carcinoma of the thyroid (Cases 14 and 24); in the

1027500

patient with metastatic poorly differentiated carcinoma of the thyroid (Case 7), however, the gallium localized in the tumor as well as or better than in any other patient (Fig. 53). The two patients with multiple myeloma showed no localization of the gallium at the sites of known osteolytic lesions, but many bone lesions were demonstrated in the patient with Ewing's sarcoma (Case 15) and in a patient with Hodgkin's disease in or adjacent to bone (Case 5).

The mechanism responsible for the localization of this radionuclide in soft-tissue neoplasms is unknown. The fact that gallium is readily bound to plasma proteins may suggest that protein binding is somehow responsible. However, early studies with ^{113m}In, another metal known to be bound to plasma proteins, have not demonstrated similar tumor localization.

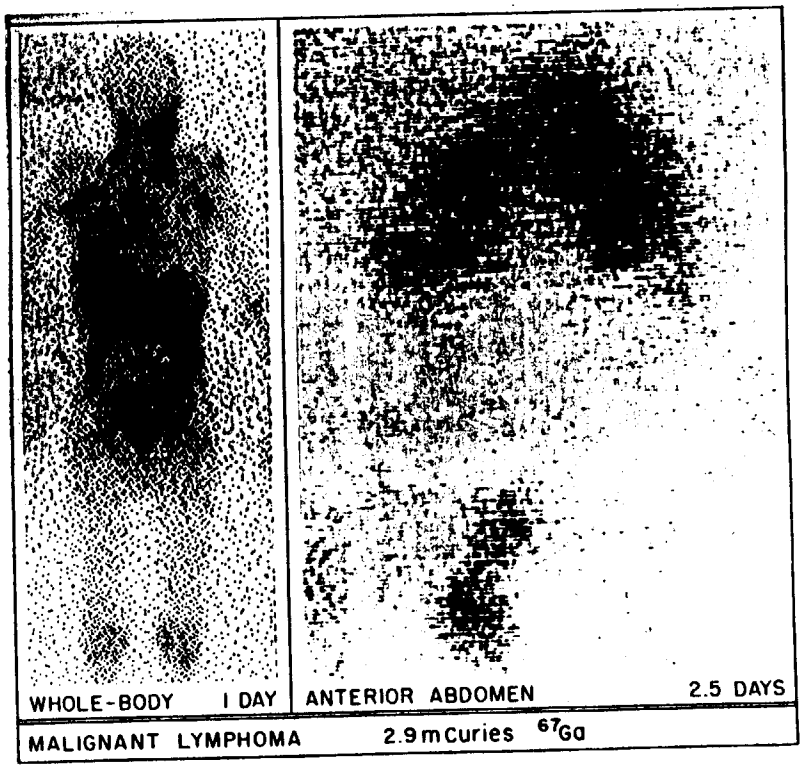

Fig. 52. Posterior whole-body photoscan 1 day after 2.9 millicuries of ^{67}Ga citrate. The scan was made with the ORAU whole-body scanner (left). Anterior photoscan of the patient's abdomen at 2.5 days, made with the 5-in. Picker Magnascanner (right). Note the large abdominal lymph nodes in the epigastrium on both scans. No contrast enhancement was used in either scan.

TABLE 48

Tissue Assay for Gallium-67 (Case 19) in Patient with Lymphoma

	Net Counts per Gram	Ratio to Blood
Blood, postmortem	173	1.0
Plasma, 2 days antemortem	128	0.7
Liver	1618	9.4
Spleen	872	5.0
Sternal marrow	617	3.6
Muscle	99	0.6
Thyroid	222	1.3
Kidney	523	3.0
Lung, left	1151	6.7
Lung, right	2098	7.5
Lymph node, cervical, tumor	19120	111.0
Lymph node, cervical, tumor	12837	74.0
Lymph node, axillary, tumor	9200	53.0

Fig. 53. Case 7. Posterior photoscan of upper torso made on ORAU whole-body scanner at 19 hr after 2.5 millicuries of ^{67}Ga citrate (left). No contrast enhancement was used. A P-A chest X ray at the time of the scan (right).

1027501

REFERENCES

1. Hayes, R. L. Radioisotopes of gallium. In Radioactive Pharmaceuticals, Proceedings of a Symposium, Oak Ridge Associated Universities, November 1965, G. A. Andrews, R. M. Kniseley, and H. N. Wagner, Jr., eds, AEC Symposium Series No. 6, CONF-651111, 1966, pp. 603-618.

2. Hayes, R. L., Carlton, J. E., and Byrd, B. L. Bone scanning with gallium-68: A carrier effect. J Nucl Med 6, 605-609, 1965.

3. Hayes, R. L., Byrd, B. L., and Carlton, J. E. Distribution of gallium in the rat as a function of time and dose. (in preparation)

Experimental Animal Studies with Gallium-67

R. L. Hayes, J. E. Carlton, B. L. Byrd, and J. J. Rafter

Previous work has shown that generator-produced gallium-68 ($T_{1/2}$, 68 min) in the citrate form can be used as a bone-scanning agent if sufficient stable gallium is administered to saturate gallium-binding sites on plasma proteins. This early dramatic effect of stable gallium on gallium distribution in the rat is shown in Fig. 54.

Although ^{68}Ga has been successfully used as a bone-scanning agent, its half-life is unduly short, and the collimation and shielding required because of its 0.511 Mev annihilation gamma emissions restricts the type of scanning equipment that can be used. Further it appears desirable to seek some appropriate means of eliminating or greatly minimizing the need to give stable gallium (see page 130). One obvious approach is the use of a longer lived gallium isotope to avoid carrier requirements during the early phase of gallium distribution. Gallium-67 with a 3.3 day half-life decays by electron capture emitting several moderate-energy gamma rays suitable for imaging with a scintillation camera (184 and 296 kev). In addition, its radiation dose is low and this permits the administration of millicurie amounts of activity. The ORAU Radiation Safety personnel have estimated the bone and whole-body radiation dose from ^{67}Ga are 2 rads and 0.3 rads respectively per millicurie administered, if we assume no excretion.

The one-day distribution of gallium in the rat at various levels of stable gallium is shown in Fig. 55. When compared with the data in Fig. 54, it is apparent that the effect of carrier gallium is far less dramatic at 24 hr than it is at the 2-hr period. However, considerable preferential bone deposition would result from the use of 0.5 to 1.0 mg Ga/kg. Studies at time periods through 10 days show an overall slow decrease in retention by most tissues with improvement

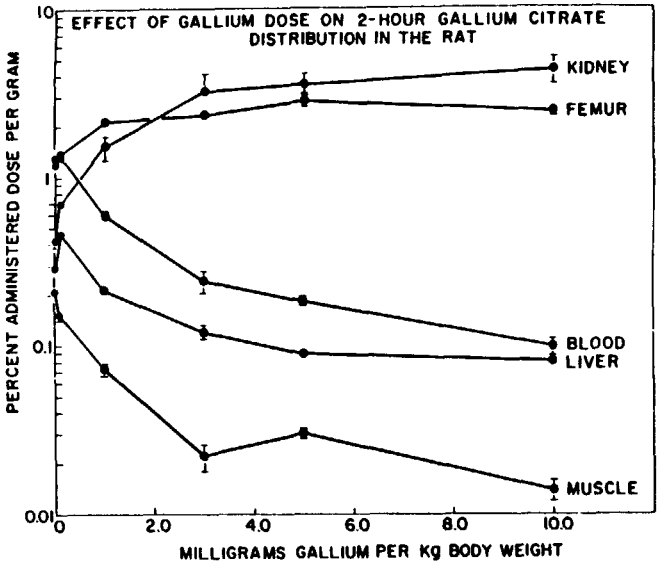

Fig. 54. Effect of gallium dose on the distribution of gallium in the rat 2 hr after administration.

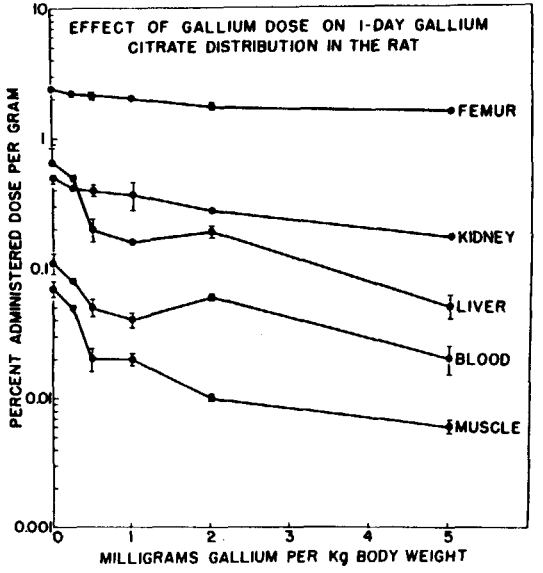

Fig. 55. Effect of gallium dose on the distribution of gallium in the rat 24 hr after administration

1027502

in the relative bone deposition; the spleen, however, shows a slight increase in absolute concentration.

The use of ^{67}Ga citrate as a bone-scanning agent in humans is now under investigation in the Division's clinical program. Recently we have observed that ^{67}Ga also concentrates in certain nonosseous soft-tissue tumors (see page 119). Scans of unusually good contrast have been obtained in a number of patients. These clinical findings have resulted in a new series of experimental animal studies aimed at determining the mechanism involved.

Localization of ^{67}Ga in tumor tissue has been observed in studies with a number of different mouse and rat tumor strains. There is often an associated change in the distribution in other tissues. In general the deposition in bone is depressed especially where tumors are large. Figure 56 shows a study of the distribution of carrier-free ^{67}Ga in the normal rat through 17 days (5 half-lives).

Table 49 shows the results of one study with a transplantable tumor developed by Dr. Frank Comas, the Medical Division's radiotherapist. Tumor uptake is high but bone deposition was not greatly altered in this study, possibly owing to the small size of the tumors (approximately 1 g). This particular tumor shows the highest ^{67}Ga concentration of those studied to date.

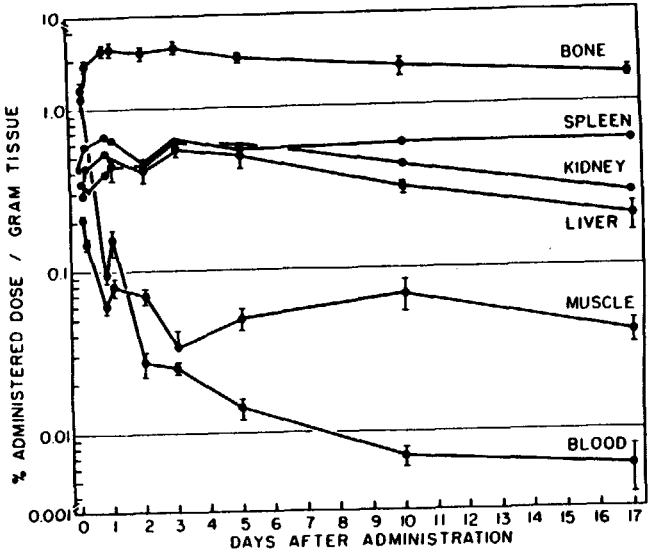

Fig. 56. Distribution of carrier-free ^{67}Ga in the rat as a function of time. Bone values are the averages of rib, femur, and calvaria.

TABLE 49

DEPOSITION OF GALLIUM-67 IN TRANSPLANTED POORLY DIFFERENTIATED RAT CARCINOMA

Tissue	% Administered Dose/g Tissue*
Liver	1.03 ± 0.04**
Spleen	1.48 ± 0.07
Femur	2.25 ± 0.09
Bone Marrow	1.19 ± 0.01
Tumor	8.20 ± 0.49
Ratio Tumor to:	
Blood	43
Muscle	31
Liver	8
Bone	5

* Killed 24 hr after administration of ^{67}Ga citrate

** Standard deviation of the mean

TABLE 50

EFFECT OF STABLE GALLIUM ON DISTRIBUTION OF GALLIUM-67 IN MICE WITH SPONTANEOUS MAMMARY CARCINOMA

Tissue	C.F.*	5 mg Ga/kg
	% Administered Dose/g Tissue	
Liver	8.82	1.14
Spleen	3.97	0.53
Femur	4.83	6.64
Blood	2.02	0.44
Tumor	3.11	0.65
Muscle	0.25	0.12

* Carrier free

1027503

TABLE 51

EFFECT OF INFECTION ON GALLIUM-67 DISTRIBUTION IN THE RAT

Tissue	Intramuscular S. aureus Injection			
	Control	1.00* (24-24)	0.10 (22-24)	0.01 (6-24)
	% Administered Dose/g			
Liver	0.65	0.98	0.90	0.68
Spleen	0.41	1.7	2.3	0.97
Marrow	0.44	2.2	2.0	1.0
Femur	2.48	1.5	1.8	2.9
Muscle	0.13	0.11	0.09	0.17
Injected Foot	---	---	0.50	0.47
Control Foot	---	---	0.25	0.43
Back (abscess)	---	1.6	---	---

* 1.0: 1 ml S. aureus ($1x10^8$ organisms per ml); (24-24): ^{67}Ga administered 24 hr after S. aureus, killed 24 hr after ^{67}Ga.

We do not yet know why ^{67}Ga given as a carrier-free preparation deposits in human soft-tissue tumors. However, the data in Table 50, suggest that high levels of gallium carrier may decrease the affinity at least of this tumor for ^{67}Ga, although in this study concentrations decreased in most tissues when stable gallium was added to the preparation. On the other hand, the administration of 1 mg Ga/kg had no apparent effect on the deposition of ^{67}Ga in a transplanted mouse lymphosarcoma.

With the help of the Medical Division's Microbiology Group the Distribution of ^{67}Ga in rats experimentally infected with various microorganisms has been studied. Table 51 shows that localization of gallium occurred at subcutaneous injection sites in the foot and back when we used Staphylococcus aureus. The deposition in the bone was depressed while that in the liver, spleen, and bone marrow was increased. Similar results were obtained with Escherichia coli, a gram-negative microorganism. Escherichia coli endotoxin also produced this type of alteration in the tissue distribution of ^{67}Ga in rats.

The Effect of Scandium on the Tissue Distribution of Gallium and Indium in the Rat

R. L. Hayes, B. L. Byrd, J. J. Rafter, and J. E. Carlton

Previously we have shown that short-lived ^{68}Ga in the citrate form localizes preferentially in bone at time intervals that permit its use as a scanning agent if sufficient stable gallium is administered with the ^{68}Ga. Similar results were obtained with ^{113m}In when gallium was used as a pseudocarrier for indium.[1] (Figure 57 shows an extension of this study to the rabbit.) This report describes the effect of scandium as a pseudocarrier for gallium and indium.

In both the gallium and indium studies several milligrams of gallium per kilogram of body weight were required to achieve satisfactory differential deposition for scanning purposes. Even though no toxic effects attributable to stable gallium have been observed in clinical studies, it would be desirable to find some means of eliminating or greatly minimizing the need for the administration of stable gallium.

A number of different approaches have been tried. For example, the use of chelating agents other than citrate was unsuccessful. Although soft-tissue concentrations could be reduced with stronger agents, there was a parallel reduction of the deposition in bone. Attempts to block with smaller doses of stable gallium before the administration of the radionuclide were not successful. Administration of EDTA to promote clearance of soft tissues after prior administration of the radionuclide was not effective. Ferric iron, given to saturate transferrin, did alter the distribution of the carrier-free nuclides but less than with stable gallium. With the exception of trivalent scandium other metals chosen for their chemical similarity and ionic size were also ineffective. Scandium was found to be unusually effective in promoting the clearance of gallium and indium from blood and soft tissues; it provides a high preferential bone disposition at early times (hours) after administration.

Figure 58 shows in the rat a greatly enhanced differential bone deposition of ^{68}Ga with as little as 0.5 to 1.0 mg Sc/kg body weight at 2 hr. Figure 59 shows a composite 2-hr positron picture (Anger Camera) of a rabbit administrated a ^{68}Ga preparation containing scandium at a dose of 1 mg/kg.

The bone localization of ^{113m}In in the rat, like that of gallium, was also enhanced by the simultaneous administration of scandium, although the effect was less pronounced than that of scandium on gallium. Higher levels of scandium were required to achieve a distribution needed for effective scanning.

The reason for the effect of scandium on the distribution of both gallium and indium is unknown. As with the gallium carrier effect,

1027504

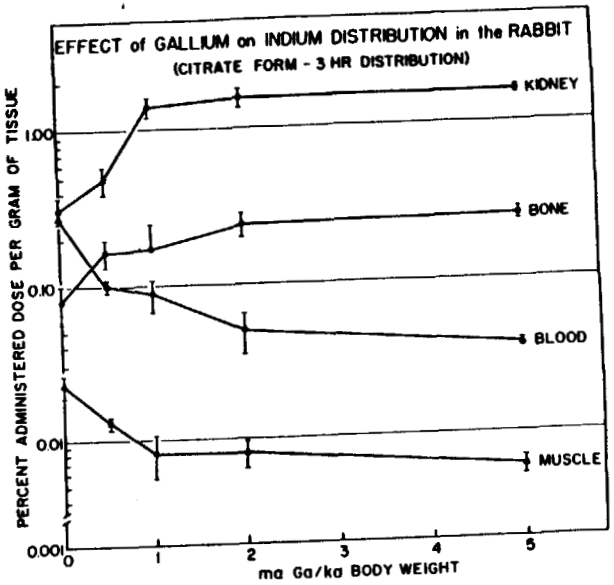

Fig. 57. Effect of simultaneous stable gallium administration (citrate form) on the distribution of high specific activity ^{114m}In (pseudo carrier-free) in the rabbit. Animals were killed at 3 hr. Bone values are the averages of rib, femur, and calvaria.

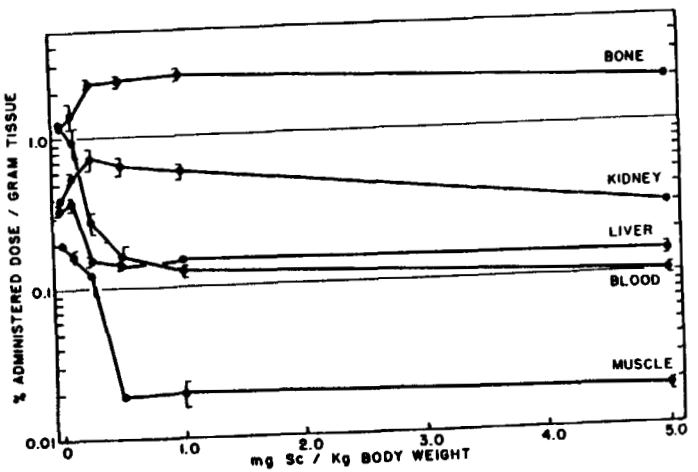

Fig. 58. Effect of scandium citrate on the distribution of gallium in the rat. Bone values are the averages of rib, femur, and calvaria.

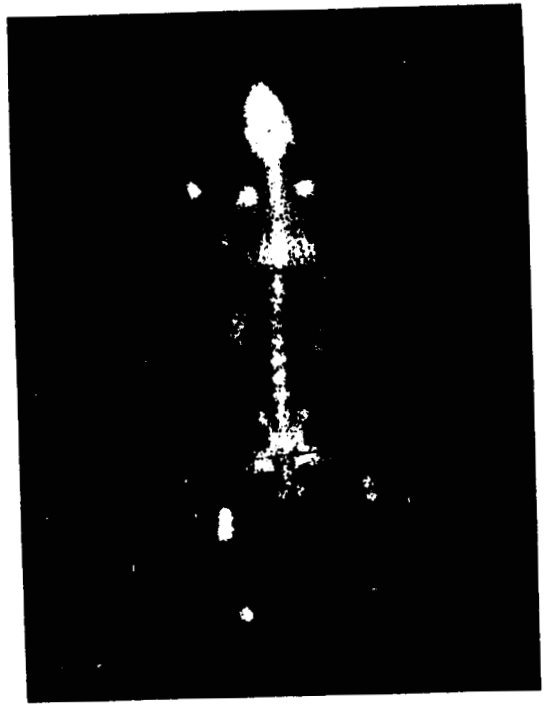

Fig. 59. Positron scintillation camera scan of the distribution of ^{68}Ga in a rabbit administered 1 mg Sc/kg (citrate). The animal was killed at 2 hr and the urinary bladder was removed before the scan.

a block or saturation of protein-binding sites by scandium may be involved. However, preliminary equilibrium dialysis studies have so far produced unclear results. On the other hand, Rosoff, et al.[2], in studies of the distribution of scandium in man, reported a binding of scandium by serum beta globulins. Scandium itself (administered as citrate) is only slowly excreted in both animals and humans; high blood levels persist for many hours after administration.

Application of the scandium effect in clinical bone-scanning procedures must await an evaluation of the toxicity of scandium, about which little is known. The acute intraperitoneal LD_{50} dose for scandium chloride has been reported to be approximately 30 mg Sc/kg of body weight in the mouse. Our preliminary investigations of the acute intravenous toxicity of scandium citrate in the rat and rabbit indicate a lethality approximately the same as that reported for the mouse. In another current study in rabbits weekly and twice-weekly intravenous injections of 5 mg/kg have been tolerated over a period of 10 weeks.

1027505

REFERENCES

1. Hayes, R. L., Byrd, B. L., and Carlton, J. E. Indium-113m as a kidney and bone scanning agent. In: USAEC Report ORAU-106, 1967, pp. 111-114.

2. Rosoff, B., Spencer, H., Cohn, S. H., and Gusmano, E. A. Metabolism of scandium-46 in man. Int J Appl Radiat Isotop 16, 479-485, 1965.

Rare Earths as Possible Bone-Scanning Agents

R. L. Hayes, B. L. Byrd, and J. E. Carlton

Radionuclides of the rare earths, particularly the higher atomic number members from terbium through lutetium, are avid bone seekers and as such are of interest as possible bone-scanning agents. These higher rare-earth elements show a greater affinity for the bone, have less liver deposition, and are excreted mainly in the urine.[1] Several have moderate-energy gamma emissions, which could be used for visualization with the Anger scintillation camera. Dysprosium-157 with an 8.1-hr half-life is of particular interest since it could be reactor-produced in a high yield with the use of separated ^{156}Dy. It decays to terbium-157 by electron capture emitting a 326 kev gamma ray. Terbium-157 has a 150-yr half-life but can be considered innocuous because it would be produced in such low yield from its short-lived parent. Furthermore it decays by electron capture with no associated gamma emission. The radiation dose in man from ^{157}Dy itself has been estimated by the ORAU Radiation Safety Office to be 0.34 rads to the bone and 0.06 rads to the whole body per millicurie administered, if we assume no excretion.

Because of its short half-life, rapid clearance of dysprosium from tissues other than the bone would be required if it were to be used as a scanning agent. Similar to reports in the literature, we found in a study of the early distribution of dysprosium citrate in the rat (^{159}Dy used as tracer) that there was a high concentration in liver. To decrease this objectionable deposition, various chelating agents were studied. Table 52 shows a comparison of the citrate results with those obtained with nitrilotriacetic acid (NTA), (2-hydroxyethylimino) diacetic acid (HEIDA), N- (carboxymethyl) -N′ -2-hydroxyethyl-N, N′-ethylene-diglycine (HEDTA), and ethylenediaminetetraacetic acid (EDTA). Although HEDTA was superior to NTA with respect to clearance from the liver, the deposition in bone was correspondingly decreased. On the basis of these preliminary findings we extended our investigation of the distribution of dysprosium nitrilotriacetate in the rat.

Figure 60 shows the effect of the dose of NTA on the 4-hr distri-

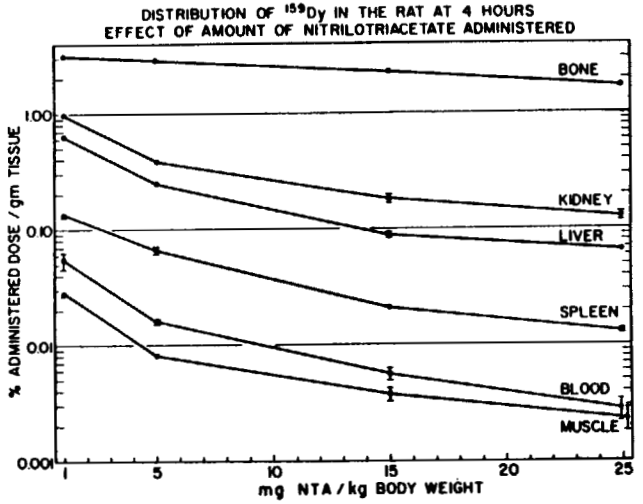

Fig. 60. Effect of administered dose of NTA on the distribution of ^{159}Dy (2 μg Dy/kg) in the rat. Animals were killed at 4 hr. Bone values are the averages of rib, femur, and calvaria.

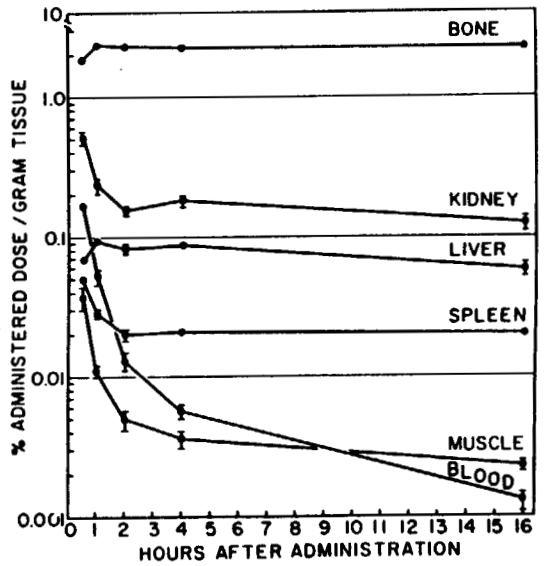

Fig. 61. Distribution of ^{159}Dy (2 μg Dy/kg) in the rat as a function of time. The NTA was administered at a level of 15 mg/kg. Bone values are the averages of the rib, femur, and calvaria.

1027506

TABLE 52

EFFECT OF VARIOUS AGENTS ON THE EARLY DISTRIBUTION OF DYSPROSIUM-159 IN THE RAT*

Tissue	Agent†				
	CITRATE	NTA	HEIDA	HEDTA	EDTA
	% Administered Dose/g				
Liver	2.1	0.61	0.80	0.24	0.16
Spleen	0.18	0.40	0.88	0.38	1.0
Kidney	1.8	0.44	0.81	0.28	0.26
Muscle	0.020	0.015	0.013	0.005	0.002
Avg. Bone	3.0	2.5	1.68	1.06	0.28
Blood	0.17	0.035	0.051	0.010	0.012

* 2 μg Dy/kg; killed at 4 hr

† Citrate 7 mg/kg; all other agents 4 mg/kg

bution of low levels of dysprosium (2 micrograms/kg) in the rat. A level of approximately 15 mg NTA/kg body weight appears to be optimum for differential bone deposition under these conditions. At this level the ratios of bone concentration to blood, muscle, and liver were 400:1, 600:1, and 26:1. The dose of stable dysprosium could be increased to 250 micrograms/kg, while maintaining the NTA level constant at 15 mg/kg, without any substantial change in these ratios. Figure 61 shows the distribution of dysprosium NTA in the rat through 16 hr (2 half-lives of ^{157}Dy). The ratios at this later period were 1700:1, 970:1, and 38:1 for blood, muscle, and liver. Clinical trials of this agent must await the determination of the toxicity of NTA. Dysprosium administered at the microgram per kilogram level should have no chemical toxicity.

REFERENCE

1. Durbin, P. W. Metabolic characteristics within a chemical family. Health Phys 2, 225-238, 1960.

Assessment of Erythropoiesis by Ferrokinetics and Radiocolloid Bone-Marrow Scanning

Francis A. Goswitz, C. L. Edwards, and Helen Vodopick

Ferrokinetic measurements quantitate erythropoiesis accurately but are relatively complex to perform. Radiocolloid bone-marrow scanning cannot quantitate erythropoiesis, but it is a simple procedure that will usually demonstrate the size and distribution of hemopoietic marrow. Seventeen patients with various erythropoietic disorders were studied to compare ferrokinetic data and the marrow pattern shown on the scan, and to determine whether the scan could be used to assess erythropoiesis or supplement the radioiron data.

Patients with effective erythropoiesis manifested by an increased plasma iron turnover rate (PITR) and an increased red-cell use of radioiron (percentage of ^{59}Fe used) in the ferrokinetic studies had total-body scans that demonstrated normal to increased marrow-distribution patterns; thus, the two types of studies correlated well. Figure 62 demonstrates two whole-body scans of a patient with chronic

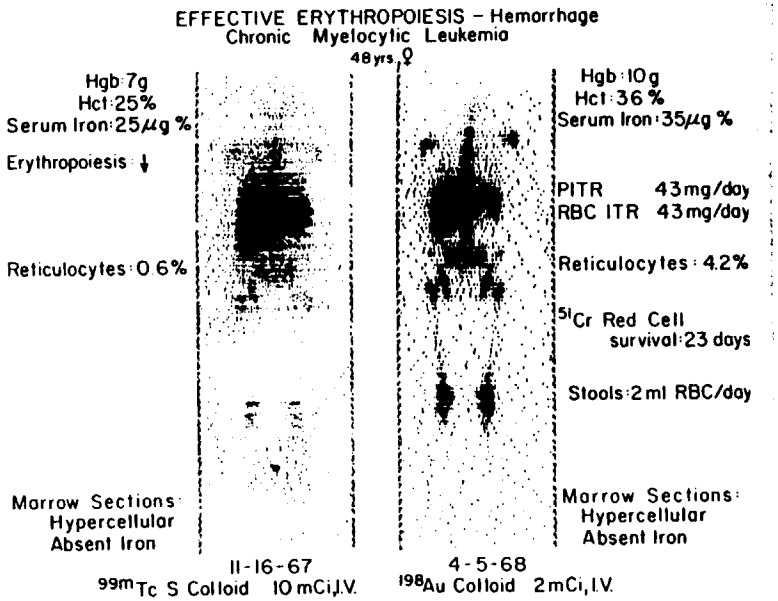

Fig. 62. Total-body scans, particularly the one of 4-5-68, showing pronounced expansion of the bone marrow with radioactivity extending into the proximal portions of the femur and tibia and the distal aspects of the femurs.

1027507

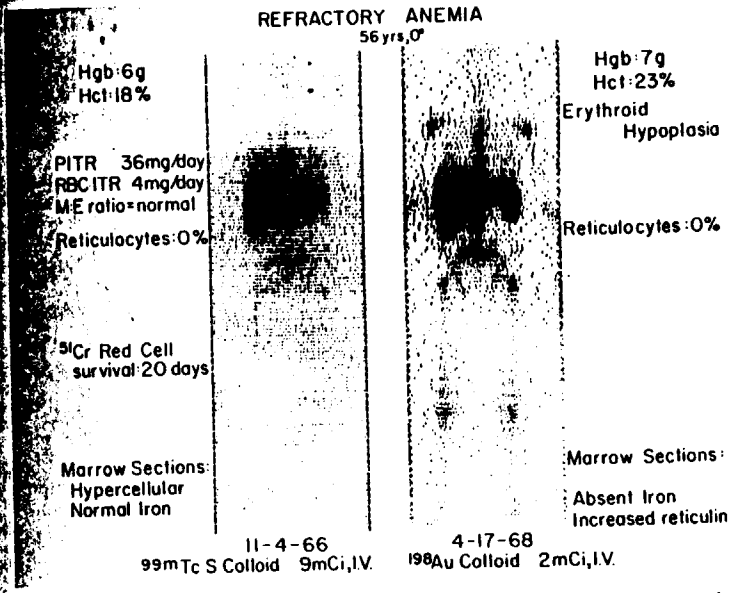

Fig. 63. Note a discrepancy between the bone-marrow scan of 11-4-66 and that of 4-17-68. The earlier scan had little, if any, visualization of the extremities, but the later scan demonstrated excellent visualization including feet and proximal legs.

granulocytic leukemia and iron-deficiency anemia. She had an increased plasma and red-cell iron-turnover rate (RBC ITR) when the second scan was performed with ^{198}Au colloid. Various scan patterns were seen in patients with ineffective erythropoiesis (intramarrow cell death) and with an increased PITR and decreased percentage of ^{59}Fe used. Patients with myelofibrosis and ferrokinetic data consistent with ineffective erythropoiesis presented a characteristic scan with almost all the radiocolloid in the liver and spleen, both organs usually large, and none or extremely little of the radioactivity in the bone marrow. Anemic patients with nonproliferative bone-marrow disorders, such as infections or red-cell hypoplasia, had a decreased PITR and decreased ^{59}Fe used for red-cell formation but their scans had a normal to increased pattern. This contrast of data from the two types of study was particularly prominent in patients with infection in whom augmented phagocytic activity caused increased radiocolloid in the bone marrow. Figure 63 is an example of a poor relation between the degree of erythroid cellularity and the extent of radiocolloid concentrated in the bone marrow demonstrated by two total-body scans.

Although the radiocolloid bone-marrow scan cannot yield quantitative data on erythropoiesis, it adds information about disorders of red-cell production when correlated with radioiron and other hematologic studies.

Nonerythropoietic Iron Turnover Rate (NER) and Its Use as an Index to Quantitate Iron Stores

Francis A. Goswitz, Helen Vodopick, and Bill Nelson

The most direct method of assessing the iron stores is the examination of marrow particles for stainable iron.[1] Although this is the method most commonly used in clinical medicine today, it is only a quantitative estimate of nonhemoglobin iron.

The plasma or serum iron concentration may also be useful in evaluating iron stores. If the plasma iron is high, the amount of iron in the stores is expected to be increased. If the plasma iron is low, the amount of iron in the stores is reduced or absent, except that patients with chronic infection, chronic renal disease, or malignant disease with anemia may have a low plasma iron despite excessive iron stores. Patients with chronic infection have an impairment in the release of iron from the reticuloendothelial (RE) cells, which supply most of the iron to the plasma. Furthermore, the plasma iron is subject to fluctuations, such as the diurnal variation, that complicate the evaluation of iron stores.

External monitoring of ^{59}Fe can contribute to the evaluation of iron-storage, showing various rates of accumulation in the liver, spleen, or sacral marrow after intravenous injection, although the absolute amounts of ^{59}Fe cannot be measured. Recently we have studied another use of ferrokinetics in the evaluation of iron stores, examining the premise that the stainable iron in marrow sections depends on the difference between the rate of removal of iron from the plasma and the rate of incorporation of iron into hemoglobin. This difference between the plasma iron turnover rate and the red-cell iron turnover rate is the nonerythropoietic iron turnover rate (NER). The NER represents the rate that iron enters nonerythropoietic sites, especially RE cells in the marrow, liver, and spleen and to a lesser degree other tissues such as muscle.

Twenty patients with various hematologic disorders were studied. All had marrow sampled by aspiration, needle biopsy, or autopsy after the ^{59}Fe studies. Stainable iron in the marrow sections was independently graded by each of us as absent, reduced (only a few histiocytes contained hemosiderin), normal, or increased 1+ to 3+ (Fig. 64).

In 15 of the 20 patients the NER correlated fairly well with the amount of marrow hemosiderin and was a good index of body iron stores (Fig. 64). Discrepancies between the marrow hemosiderin and the NER were observed in four patients with myelofibrosis who had little or no stainable iron and elevated NER values, ranging from 21 to 33 mg/day. Presumably the iron was being stored in extramedullary sites of erythropoiesis, the spleen and liver, rather than the marrow. One patient with a compensated hemolytic anemia had

1027508

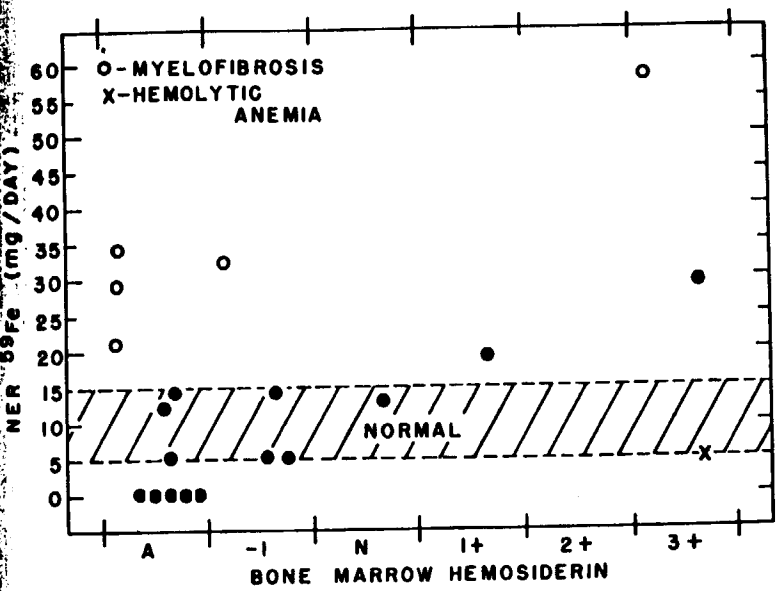

Fig. 64. Correlation of the nonerythropoietic iron turnover rate (NER) with the amount of marrow hemosiderin graded as absent (A), reduced (-1), normal (N), and either a slight (1+), a moderate (2+), or a massive (3+) increase. Five patients with myelofibrosis (open circles) and one patient with hemolytic anemia (X) are included. The 14 solid circles are data from patients with other hematologic disorders.

an NER of only 5 mg/day despite a massive increase (3+) of stainable iron in the marrow. The explanation for the discrepancy is that he used 95% of the ^{59}Fe injected for red-cell formation; hence the low NER despite the increase in hemosiderin caused by the destruction of red cells.

The NER provides quantitative information about the rate of entry of iron into the body stores. In many hematologic disorders the NER is proportional to the marrow hemosiderin; exceptions are myelofibrosis (and possibly other conditions of ineffective erythropoiesis) and hemolytic anemia; these are readily explained.

REFERENCE

1. Bothwell, T. H. and Finch, C. A. Iron Metabolism. Little, Brown and Company. Boston, Mass. 1962, p. 286.

Value of Plasma Iron-59 Disappearance in Determining Iron-Deficient Erythropoiesis

Francis A. Goswitz

In a separate report (page 138) the nonerythropoietic iron turnover rate was described as a useful index to evaluate the rate at which iron enters the tissue stores. The plasma ^{59}Fe clearance is proving to be useful in detecting iron-deficient erythropoiesis manifested by an absence of iron from the marrow.

Eleven patients with no stainable marrow iron, including three with myelofibrosis, received an intravenous injection of approximately 0.1 microcurie of ^{59}Fe/kg body weight. Ten had plasma disappearance curves for ^{59}Fe with half-times of less than 1 hr (Fig. 65). Normal persons clear half the radioactive iron from their plasma in 1 to 2 hr. Most of this ^{59}Fe leaves the plasma for the bone marrow, the normal

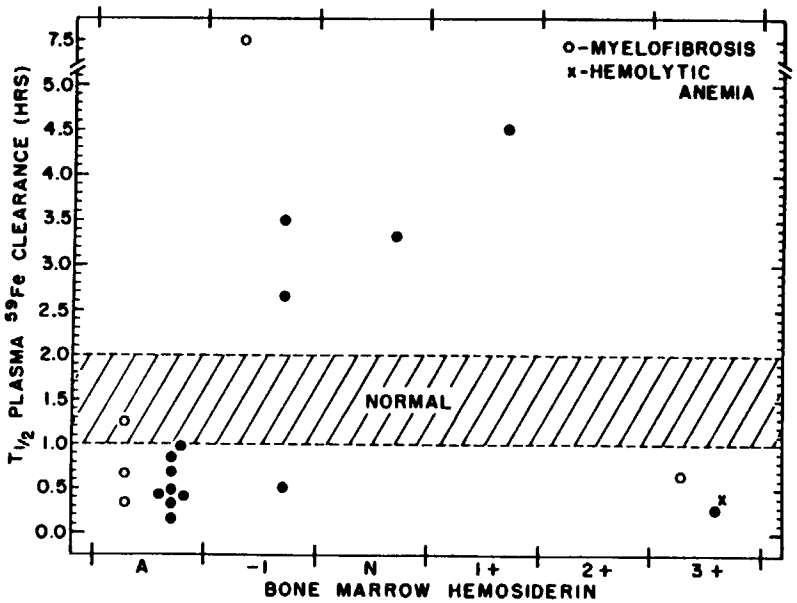

Fig. 65. Relation of $T_{1/2}$ plasma ^{59}Fe clearance values to the amount of bone-marrow hemosiderin determined by evaluating marrow sections for stainable iron. The solid circles represent patients with a variety of other hematologic disorders. Note that 10 of 11 patients with absent (A) bone-marrow hemosiderin had results below normal for $T_{1/2}$ plasma ^{59}Fe clearance.

1027509

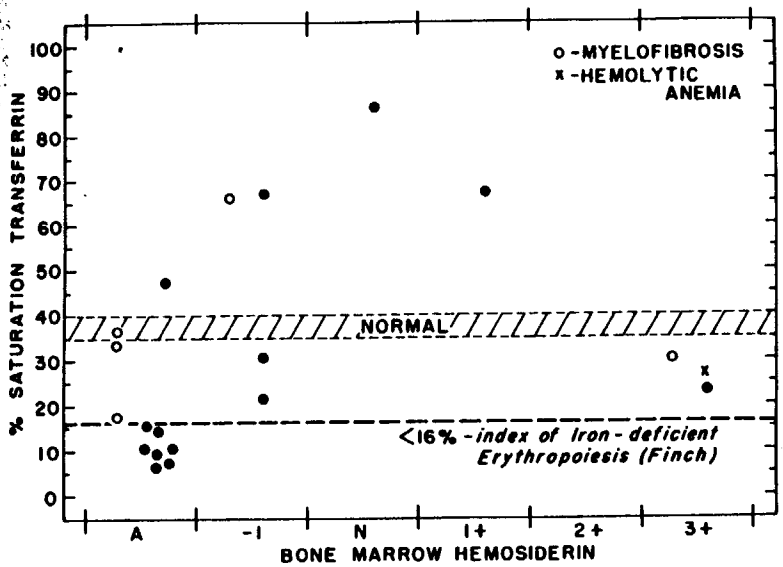

Fig. 66. Correlation of data between the percentage of saturated transferrin and the bone-marrow hemosiderin. The solid circles represent patients with a variety of other hematologic disorders. Nine of 11 patients with absent (A) stainable marrow iron had less than 35% of their serum transferrin saturated with iron.

site of hemoglobin production and erythropoiesis. If the bone marrow is depleted of iron, the ^{59}Fe will clear the plasma at a more rapid rate to enter the sites of hemoglobin production. If the bone marrow contains an excess of iron, the ^{59}Fe will clear the plasma at a slow rate since sufficient iron is already present in the bone marrow for hemoglobin synthesis.

Cook and Finch state that the best single criterion of iron-deficient erythropoiesis is a transferrin saturation of less than 16%.[1] Figure 66 compares the percentage of saturated transferrin to the absence of bone-marrow hemosiderin in these same 11 patients. In this group 9 of 11 patients had below normal values for percentage of saturated transferrin but only 7 of the 11 had a transferrin saturation of less than 16%.

Additional studies are indicated for a more accurate statistical comparison between the plasma ^{59}Fe clearance and the percentage of saturated transferrin as methods of detecting the iron-deficient state. A rapid plasma ^{59}Fe disappearance is certainly useful in confirming the presence of the iron-deficient state in a patient with absence of stored marrow iron.

REFERENCE

1. Cook, J. D. and Finch, C. A. Iron-binding globulin. In: Radioisotopes in Medicine: In Vitro Studies. R. L. Hayes, F. A. Goswitz, and B. E. P. Murphy, Eds. AEC Symposium Series No. 13, CONF-671111, June 1968, pp. 351-363.

Blood Volume in Myelofibrosis

Francis A. Goswitz and Martha L. Clevenger

To specifically diagnose a myeloproliferative disorder (polycythemia vera, acute or chronic granulocytic leukemia, primary or secondary myelofibrosis) may pose a difficult problem for the clinician. Some laboratory measurements such as the blood or plasma volume or the red-cell mass may help him to distinguish these disorders. In polycythemia vera the patient must have an increased red-cell mass; patients with granulocytic leukemia have usually a decreased but rarely an elevated red-cell mass. The red-cell mass and plasma volume have not been extensively studied in patients with myelofibrosis.

In typical cases the diagnosis of myelofibrosis is simple when an elderly patient presents with the triad of anemia, splenomegaly, and bone-marrow fibrosis. Since massive enlargement of the spleen is a common feature of this disease, the spleen, by containing many more erythrocytes than normal, would contribute to the patient's anemia as manifested by a decreased venous hematocrit (HCT_V). In normal healthy adults the spleen weighs 150 g and contains 50 ml blood of which 40 ml is red cells since the hematocrit of splenic blood is 80%.[1] In myelofibrosis the spleen may weigh 4000 g and would have 1333 ml blood if 33% of the organ's weight is blood. Furthermore, if the hematocrit of this blood is 80%, the spleen would contain 1066 ml red cells.

The normal 70-kg man has approximately a blood volume (BV) of 5000 ml, a red-cell mass (RCM) of 2000 ml, and a plasma volume (PV) of 3000 ml. Dividing the red-cell mass by the total blood volume gives a body hematocrit (HCT_O) of 40. This HCT_O is normally 0.9 of the HCT_V.

This study included six patients with myelofibrosis - four with the primary form or "agnogenic myeloid metaplasia" and two with secondary myelofibrosis (Table 53). The plasma volume was determined after the intravenous administration of radioiodinated human serum albumin labeled with iodine-125 ($R^{125}ISA$), and the red-cell mass was measured after the intravenous injection of ^{51}Cr-tagged red cells.

On the basis of their body weight, the plasma volume (normal: 40 ml/kg) and the blood volume (normal: 70 ml/kg) were elevated in all six patients with myelofibrosis (Table 53). Three of four patients with primary myelofibrosis had an increased red-cell mass (normal: 30 ml/kg); one patient had a slightly reduced red-cell mass (25 ml/kg). In contrast to the primary myelofibrosis group, the red-cell mass was reduced in the two patients with secondary myelofibrosis.

All six patients had a low venous hematocrit. All four patients with primary myelofibrosis had an elevated HCT_O/HCT_V ratio. The two patients with secondary myelofibrosis had a decreased HCT_O/HCT_V ratio (Table 53).

TABLE 53

BLOOD VOLUME DATA IN PATIENTS WITH PRIMARY (A THRU D) AND SECONDARY (E AND F) MYELOFIBROSIS

PATIENT	BODY WEIGHT kg	PLASMA VOLUME ML	RED CELL MASS ML	BLOOD VOLUME ML	BODY HCT HCT_O	VENOUS HCT HCT_V	HCT_O / HCT_V RATIO	PLASMA VOLUME ML/KG	RED CELL MASS ML/KG	BLOOD VOLUME ML/KG
A	71	3854	2850	6704	43	31	1.3	54	40	94
B	67	2900	2210	5110	43	35	1.23	43	33	76
C	72	3928	2617	6545	40	36	1.1	55	36	91
D	65	3827	1600	5427	30	32	0.94	59	25	84
MEAN ± S.D.	69 3	3627 403	2319 803	5946 1370	39 5	34 4	1.16 0.16	52 6	33 5	86 7
E	80	8270	1046	9316	11	21	0.52	103	13	116
F	45	3350	785	4135	19	26	0.73	74	18	92

The four patients with primary myelofibrosis had significant splenomegaly (spleens palpable at least 10 cm below lower costal margin). The spleen of patient E was not palpable, but palpation of this organ was difficult because he had generalized edema from prolonged steroid therapy. This patient had a primary diagnosis of refractory anemia of undetermined etiology. The spleen of patient F, who had chronic granulocytic leukemia, was palpable 6 cm below the lower costal margin.

The results demonstrate that blood-volume measurements may be useful in differentiating primary myelofibrosis from other similar disorders. The low venous hematocrit in this condition is partially due to the increased plasma volume and massive splenomegaly besides being caused primarily by ineffective crythropoiesis. The HCT_O/HCT_V ratio is also raised to or above unity with the rise being somewhat proportional to the degree of splenomegaly.

REFERENCE

1. Albert, S. N. Blood Volume. Charles C Thomas, Springfield, Illinois, 1963, p. 30.

1027510

Advantage of Measuring Blood Volume with Three Radioisotopes

Francis A. Goswitz

Blood volume determinations are commonly used to estimate the need for blood transfusions or to acquire knowledge of cytokinetics. The ideal requirements of any radiopharmaceutical to measure the blood volume are (1) uniform distribution, (2) nontoxicity, (3) entrance into no metabolic pool, (4) confinement to the pool measured, and (5) an excretory pathway limited to the urinary tract.

Too often physicians determine the red cell (RBC) mass indirectly by measuring only the plasma volume and the venous hematocrit (HCT_V); similarly, the plasma volume is estimated indirectly from measurement of only the RBC mass and the HCT_V, and the calculations assume that the body hematocrit equals 0.9 of the venous hematocrit. The following equations are used:

$$\text{RBC mass} = \text{plasma volume} \left(\frac{100}{100 - HCT_V\,(0.9)} - 1 \right)$$

$$\text{plasma volume} = \text{RBC mass} \left(\frac{100}{HCT_V \times 0.9} - 1 \right)$$

We have chosen as have other investigators to measure the red-cell mass and plasma volume independently since this venous hematocrit/body hematocrit ratio of 0.9 is not constant, and varies considerably under pathologic or physiologic conditions.[1,2] Radioisotopes such as $R^{125}ISA$ (radioiodinated human serum albumin) and ^{59}Fe (ferrous citrate) to measure the plasma volume and ^{51}Cr (sodium chromate) to measure the red-cell mass are necessary.

Nine patients with various hematologic disorders received intravenous injections of three radioisotopes, one after each 15-min interval in the following doses: $R^{125}ISA$ (0.1 microcuries/kg), ^{51}Cr-labeled RBC (2.0 microcuries/kg) and then ^{59}Fe-labeled plasma (0.1 microcuries/kg). Before injection of the dose, venous blood samples were drawn from an arm site not previously used. After injection of the ^{59}Fe, heparinized blood samples were collected at 15, 30, and 45-min. An automatic well counter equipped with a pulse-height discriminator assayed the blood for ^{125}I, ^{51}Cr, or ^{59}Fe.

Table 54 compares the results of the direct ($R^{125}ISA$, ^{59}Fe) and indirect (^{51}Cr) measure of the plasma volume. The ^{59}Fe technique reported a greater value than the $R^{125}ISA$ method in six of nine patients; however, the $R^{125}ISA$ results were higher in seven of the nine studied than those determined indirectly by the ^{51}Cr-labeled red cells. Table 55 compares the data of the three radioisotopic

10275 11

TABLE 54

Comparison of the Direct ($R^{125}ISA$, ^{59}Fe) and Indirect (^{51}Cr) Measure of the Plasma Volume

Patient No.	HCT_V %	$R^{125}ISA$ ml, 100%	^{59}Fe ml	Difference: $R^{125}ISA$-^{59}Fe ml	%	^{51}Cr ml	Difference: $R^{125}ISA$-^{51}Cr ml	%
1	18	3030	3430	-380	-10	3445	-395	-11
2	21	7900	8270	-370	- 5	4507	+3407	+43
3	25	3280	3344	- 64	- 2	3137	+143	+ 4
4	26	3134	3163	- 29	- 1	2371	+763	+24
5	27	5000	4455	+545	+11	4770	+230	+ 5
6	36	3928	4030	-102	- 3	5234	-1306	-34
7	37	3800	4166	-366	-10	3519	+281	+ 7
8	52	3660	3180	+480	+13	2455	+1205	+33
9	53	1830	1660	+170	+ 9	1760	+670	+27

TABLE 55

Comparison of the Direct (^{51}Cr) and Indirect ($R^{125}ISA$, ^{59}Fe) Measure of the Red-Cell Mass

Patient No.	HCT_V %	^{51}Cr ml, 100%	$R^{125}ISA$ ml	Difference: ^{51}Cr-$R^{125}ISA$ ml	%	^{59}Fe ml	Difference: ^{51}Cr-^{59}Fe ml	%
1	18	657	630	+ 27	+ 4	670	- 13	- 2
2	21	1046	3200	-2154	-206	3400	-2354	-250
3	25	913	960	- 47	- 5	1056	-143	- 16
4	26	729	1546	-817	- 21	1616	-887	- 22
5	27	1530	1667	-137	- 9	1405	+125	+ 8
6	36	2617	1972	+645	+ 24	2020	+597	+ 23
7	37	1786	1900	-114	- 6	2064	-278	- 15
8	52	2125	2750	-625	- 29	2820	-695	- 32
9	53	1360	1690	-330	- 24	2597	-1237	- 91

studies for the RBC mass. The indirect measure obtained by the $R^{125}ISA$ and the ^{59}Fe studies overestimated the RBC mass in seven of nine patients.

Since some patients with a blood abnormality may also have a disorder affecting protein or albumin metabolism, the plasma volume should be calculated on the basis of both $R^{125}ISA$ and ^{59}Fe although usually the former is the better tracer to study plasma volume. Red-cell mass is ideally measured by the injection of saline-washed

erythrocytes labeled with ^{51}Cr since blood loss that might alter this result can also be determined by this method. This study shows the value of measuring the RBC mass and the plasma volume independently since the indirect determinations of either the RBC mass from a measure of the plasma volume and HCT_v or of the plasma volume from a measure of the RBC mass and HCT_v are frequently inaccurate. The primary reason for this inaccuracy is that the HCT_v is not constant or representative of the total-body hematocrit.

REFERENCES

1. Albert, S. N., Gravel, Y., Turmel, Y., and Albert, C. A. Pitfalls in blood volume measurement. Anesth Analg 44, 805-814, 1965.

2. Strumia, M. M., Strumia, P. V., and Dugan, A. Significance of measurement of plasma volume and of indirect estimation of red cell volume. Transfusion 8, 197-209, 1968.

Current Value of ^{131}I-Triolein for Evaluation of Malabsorption

Francis A. Goswitz and Nelson Stephens

The literature contains conflicting reports about the usefulness of the radioiodinated triolein and oleic acid absorption tests in the evaluation of fat absorption. Texter and co-workers believe that these isotopic methods serve a useful purpose because of their simplicity and the limited availability and expense of fecal-fat balance studies.[1] Tuna, Mangold, and Mosser reported that the ^{131}I-triolein absorption study should be interpreted with caution because the radiochemical purity of the commercially available preparations is uncertain.[2] In four patients with fat malabsorption they demonstrated absorption curves with commercial preparations that resembled normals but no appreciable absorption when the pure radioiodinated triglyceride was given. In all five healthy persons without fat malabsorption, a smaller percentage of the purified ^{131}I-triolein was absorbed than of the commercial preparation.

Unfortunately the commercially prepared ^{131}I and ^{125}I-triglyceride is still impure. We found only 60 to 73% of the total radioiodine associated with the triglyceride fraction on thin-layer chromatograms; the remainder was distributed primarily among free fatty acids, diglycerides, cholesterol esters, and presumably, some phospholipids. All the ^{131}I-triolein samples were purified by preparative thin-layer chromatography; 98 to 100% of the ^{131}I in the purified samples was associated with the triolein. None of the ^{125}I-triolein samples were purified.

1027512

The purified ^{131}I-triolein and the impure commercially prepared ^{125}I-triolein were administered simultaneously to five patients without malabsorption. The results of these studies are shown in Tables 56 and 57.

The fat absorption studies were normal in these five patients with various disorders. The results agree with Tuna et al. in that discrepancies between the purified and impure triolein fractions were found in the percentage of the dose absorbed. The variations,

TABLE 56

Absorption as Reflected in Percentage of Dose in the Blood*

Patient	Primary Disease	^{131}I-Triolein (Purified)	^{125}I-Triolein (Commercial)	$^{125}I/^{131}I$ Ratio
A	Acute Leukemia	9	19	2.1
B	Carcinoma Lung	6	18	3.0
C	Regional Enteritis	11	17	1.5
D	Acute Sinusitis	8	5	0.6
E	Carcinoma Lung	14	7	0.5

Normal: Greater than 5% dose absorbed

* Values listed represent the highest of blood samples collected at 1, 3, 5 or 7 hr. Blood volume was estimated on basis of height-weight basis and percentage of total dose in the blood calculated from radioassays of blood.

TABLE 57

Percentage of Dose Excreted (Stool)

Patient	Primary Disorder	^{131}I-Triolein (Purified)	^{125}I-Triolein (Commercial)	$^{125}I/^{131}I$ Ratio
A	Acute Leukemia	1	3	3.0
B	Carcinoma Lung	5	3	0.6
C	Regional Enteritis	5	4	0.8
D	Acute Sinusitis	2	2	1.0
E	Carcinoma Lung	1	2	2.0

Normal: Less than 5% dose excreted

however, were less significant in our patients, particularly in the percentage of the dose excreted (Table 57). In fact, from a clinical interpretation, the values were all normal. The purified radioiodinated triolein is difficult, time-consuming, and expensive to prepare; we need further studies to determine its advantages for routine clinical use. Measurements of both blood and fecal radioactivity are indicated in the performance of this malabsorption test since a major criticism of the study of the impure ^{131}I-triolein was the lack of sensitivity of the blood radioactivity determinations for the detection of mild steatorrhea.[1] Since Tuna and his colleagues did not assay stool samples, further comparison of these data after the simultaneous administration of both the impure and pure radioiodinated triolein is necessary.[2]

REFERENCES

1. Texter, E. C., Jr., Cooper, J. A. D., Vidinli, M., and Finlay, J. M. Laboratory procedures in the diagnosis of malabsorption. Med Clin N Amer 48, 117-136, 1964.

2. Tuna, N., Mangold, H. K., and Mosser, D. G. Re-evaluation of the I^{131}-triolein absorption test. J Lab Clin Med 61, 620-628, 1963.

Transistorized Electronic Circuits for the Miniaturized Surgical Probe

*A. C. Morris, Jr., T. R. Barclay, and J. V. Nemcek**

A miniaturized surgical probe unit was reported previously[1] for use in localizing minute or hidden pieces of gland or metastatic tissue during thyroid surgery. The present report is of the recently developed transistorized circuits for this probe. This small hand-held device detects beta and gamma rays coming from tissue where a previously administered radionuclide is concentrated. Iodine-131 is most commonly given as a source material, although ^{125}I can be used if the spectrometer is carefully calibrated for the 35-kev energy. An external removable platinum shield at the crystal end of the probe serves as a single-hole collimator to make a directional sensitivity possible. A 12-ft coaxial cable conducts pulses from the photomultiplier in the probe to remote electronic spectrometric and audio circuits.

* Summer Student from Claremont Men's College, Claremont, California.

1027513

Pulses pass from the detecting probe into a preamplifier, amplifier, high voltage, single-channel analyzer, and linear rate-meter system of modular commercial design (Fig. 67). Circuits in these basic modules were modified to suit our probe's characteristics. For example, the coaxial cable in this probe is wired to serve the dual function of conducting high voltage to the probe, and then transmitting pulses in the reverse direction back to the preamplifier. Our preamplifier is of a charge-sensitive design that makes the circuits less sensitive to the 180 picofarad capacitance of the cable. The time constant of the preamplifier was changed to 4 microseconds to match the light-decay constant of the CsI (Tl) crystal.

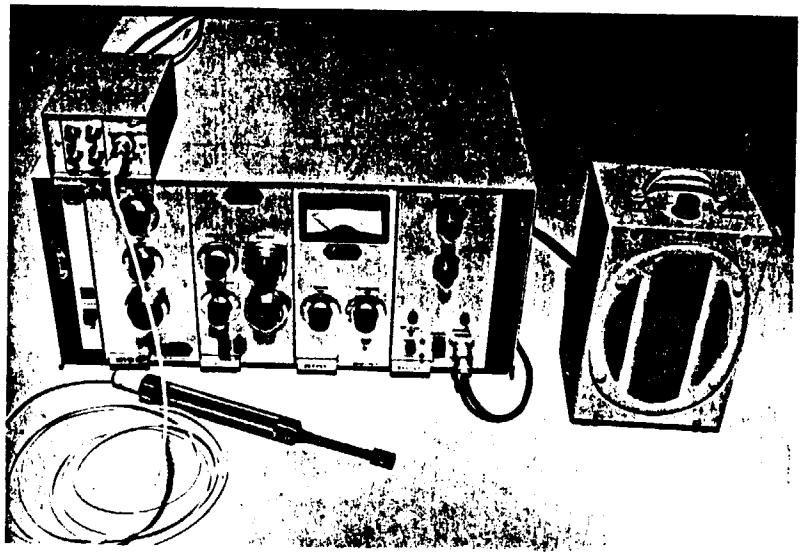

Fig. 67. Complete surgical probe system with hand-held probe unit, preamplifier, modular spectrometer system with special audio pitch-varying module, and loudspeaker box.

Signals from the spectrometer system drive a rate meter whose time-constant circuits are modified so the surgeon can hear the individual pulses at the lower counting rates. An analog signal is derived from the rate-meter output line for the special pitch-varying and audio circuits (Fig. 68). This circuitry, built into a blank module unit, consists of a differential amplifier, current amplifier, unijunction oscillator, audio amplifier, and loudspeaker. "Zeroing" and "range" adjustments are provided on the front panel for oscillator calibration purposes. These settings are made by first zeroing the output fre-

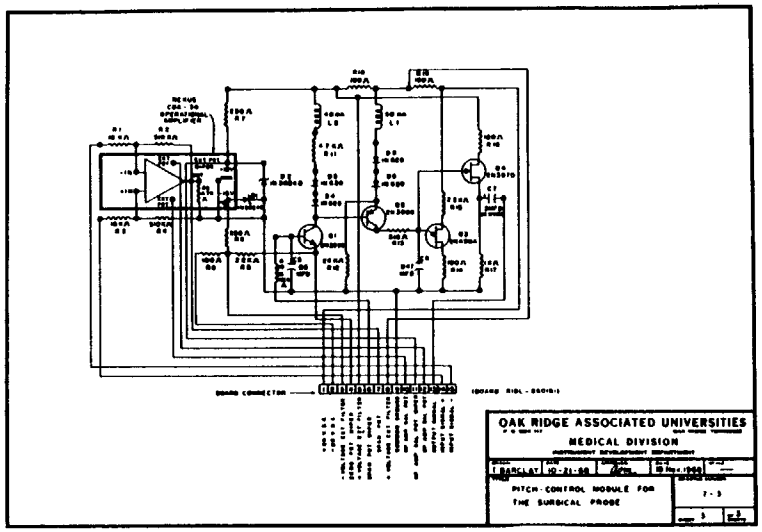

Fig. 68. Circuit diagram of the audio frequency unit. Signals from the linear rate meter serve as an input to this amplifier-oscillator circuit. Output signals drive a remote amplifier and loudspeaker.

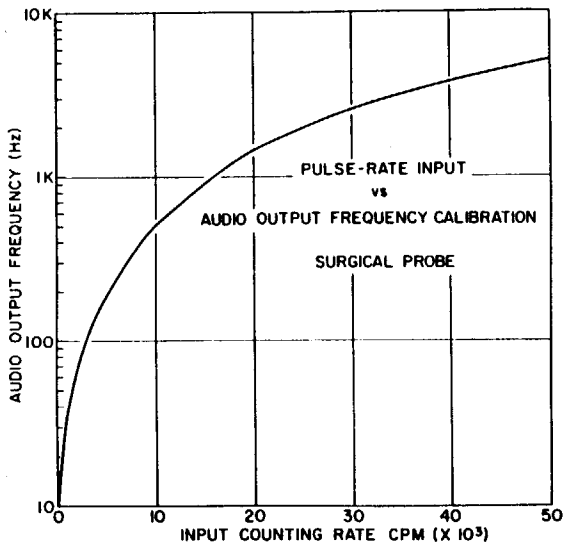

Fig. 69. Surgical probe output audio frequency vs. input counting rate. The input counting-rate range may be varied according to the surgical need, but the form of this output curve remains constant.

1027514

quency to about 10 pulses per second (pps) when no counts are received, and then setting the pulse rate with the range control to 5,000 pps when the rate meter gives a full-scale deflection. Figure 69 shows the frequency of the output audio signal versus the input counting rate to the rate meter. The circuits have been designed to give a rapid increase in audio pitch at low counting rates; the surgeon can thus hear a maximum rate change when he is seeking out some small elusive spot of activity.

We find the use of this surgical probe advantageous where a tumor or gland is able to take up radionuclide with good selectivity over the background tissue. An activity of 5 microcuries or more in a tumor the size of a pea is ample for good localization. This probe may be effectively used to help remove all of a primary tumor, and can be used to localize small metastases in later tracer scanning and operative efforts. Flexibility of the operating controls allows the equipment operator to follow the counting situation with an optimum electronic characteristic. The small size of this new probe permits easy manipulation in restricted surgical areas, an advantage that quickly becomes apparent when the surgeon is working in a small opening.

REFERENCE

1. Morris, A. C., Jr. An improved probe for detecting radioactivity at surgery. In: USAEC Report ORAU-101, 1966, pp. 156-158.

Quantitative Measurement of Radioactivity in Internal Organs by Area Scanning

Noboru Arimizu and A. C. Morris, Jr.*

Area scanning is a technique normally used to visualize the configuration of organs and tumors by a frequency distribution of dots or counts on a scan record. This record not only represents the patterns of distribution of radioactivity but also provides an approximate quantitation of radionuclide present.[1] The purpose of our study has been to see whether the information in a scan record can be used to assay the activity in internal organs. Our approach has been to find some method, empirical or direct, to calculate uptake from scan-record counts.

More than 850 area scans were performed in this series of experi-

* Work done while fellow in Radiological Research of the James Picker Foundation. Current address: Department of Radiology, Chiba University School of Medicine, Chiba, Japan.

ments to ascertain how the integrated area counts of scans vary with radionuclide geometry. Three different area scanners and five radionuclides (^{85}Sr, ^{68}Ga, ^{131}I, ^{113m}In, ^{99m}Tc) have been used. Point, plane, volume, and irregular source shapes have been scanned with focusing collimators[2] in air and in water phantoms to duplicate conceivable geometries for patients. Response data have been obtained by counting the number of recorded dots on the scan over the area of interest. Figure 70 illustrates a typical scan showing the dot patterns and the "summed areas" over which all the dots were counted. Figure 71 shows how these integrated dot counts vary with the diameter of the summed area and distance from the front face of the collimator for a 6-cm-diameter source in air. This experiment shows that if the summed area is made appropriately large, the integrated counts for all source distances will approach the same value.

Figure 72 is similar to Fig. 71 except that the counts were obtained with an ^{131}I source 10 cm deep in a water phantom. The dot summations were taken for the integral, peak, and scatter radiation bands. The "peak" counts in water had the same kind of summation plateau (Fig. 72) as the peak counts of Fig. 71 made in air. This fact indi-

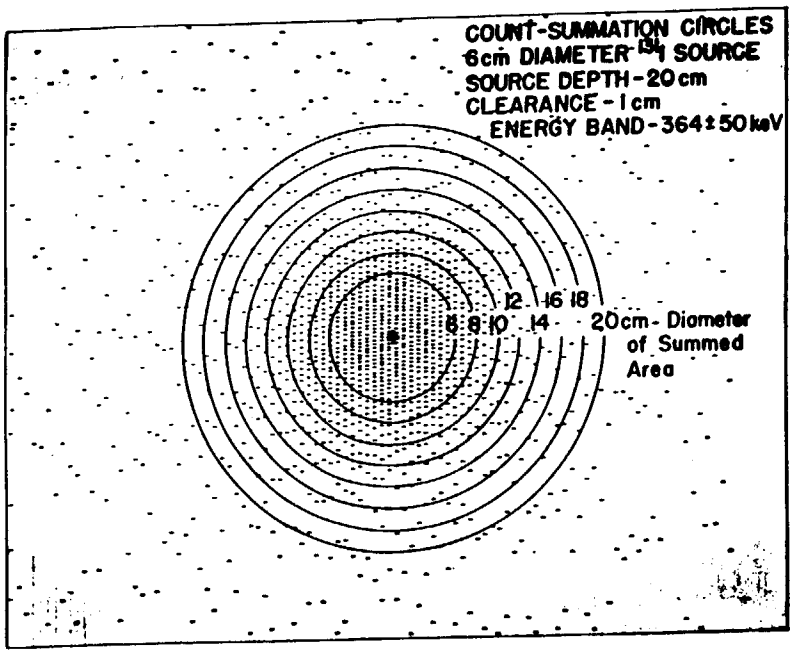

Fig. 70. Count-summation circles showing how the dots from an experimental area scan are integrated over increasing circular areas. Dot summations such as this are made to give the results shown in Fig. 2 and, when applied to clinical scan records, give needed data for uptake calculations.

10275 15

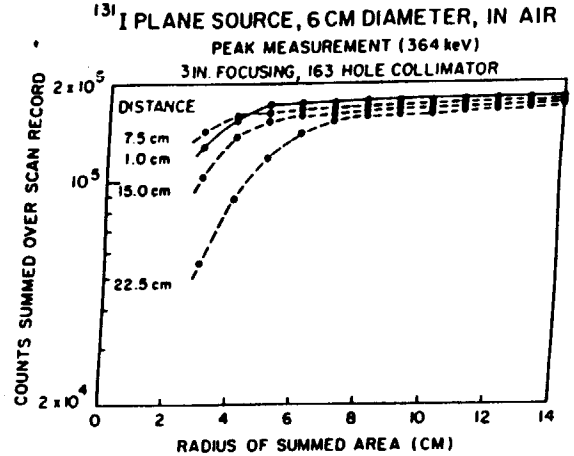

Fig. 71. Counts summed over increasing areas for a 6-cm-diameter plane source in air measured at several collimator-to-source distances. All curves approach the same value when the summation area is made large enough for the detector to fully scan the entire source.

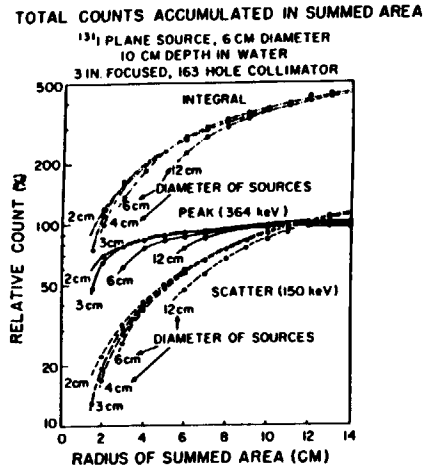

Fig. 72. Scanner response to plane sources of ^{131}I at a 10-cm water depth. All sources have equal total activity. Net counts are summed over circles of various diameters on the scan record with the highest peak count of the 364-kev curves taken as 100%. The summation curves for the peak counts level off, in this water phantom, in a manner similar to the curves of Fig. 71 made in air. Integral and scatter count summations, however, show a continuous increase with increasing area.

cates that if we select a proper area of summation on a scan record, and neglect attenuation, the counts recorded will relate directly to the activity present.

We then tried taking scans from both sides and performing uptake calculations from the dot-count summations to compensate for inverse-square and tissue-absorption effects. Figure 73 shows the results of calculations when both arithmetic [1/2(A+B)] and geometric ($\sqrt{A \times B}$) means from scan counts (A and B made from opposite sides of a water phantom) are used. The curves show the changes in calculated response for three different radionuclides when the source was moved from top to bottom. Further experiments showed that the average of the two means $C=1/2[1/2(A+B) + \sqrt{A \times B}]$ gave the best overall results for radionuclide quantitation.

The preliminary findings were then verified with a human-sized REMAB phantom.† Table 58 shows the results of these measurements with the three radionuclides. The plastic liver and spleen

† Alderson Research Laboratories, Inc., 48-14 33rd Street, Long Island City, 1, New York.

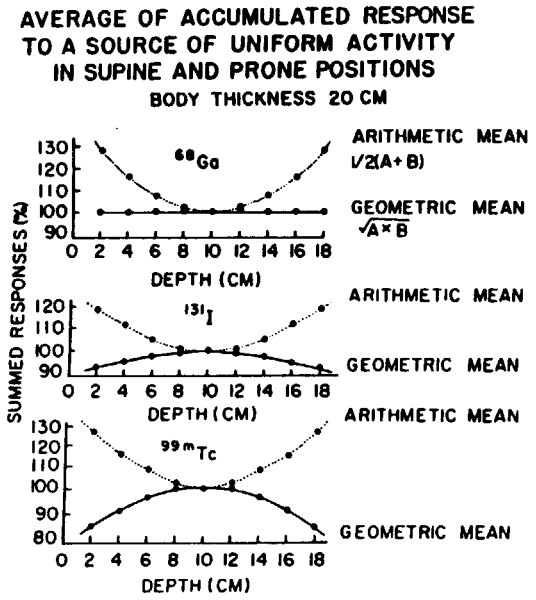

Fig. 73. Arithmetic and geometric means of summed counts for three radionuclides. Means are calculated from the scan dots taken in the prone (A) and (B) supine positions. Body thickness is 20 cm.

1027516

TABLE 58

LIVER AND SPLEEN SCAN UPTAKES OF MANIKIN "REMAB"

Organ	True Uptake	Calculation	^{99m}Tc with 3" Low-Energy 265-Hole Collimator	^{113m}In with 5" 86-Hole Collimator	^{68}Ga with 5" 86-Hole Collimator
LIVER	83%	$\frac{1}{2}(A+B)$	86%	82%	82%
		$\sqrt{A \times B}$	81%	78%	78%
		$\frac{1}{2}[\frac{1}{2}(A+B)+\sqrt{A \times B}]$	83%	80%	80%
SPLEEN	17%	$\frac{1}{2}(A+B)$	19%	19%	20%
		$\sqrt{A \times B}$	18%	19%	20%
		$\frac{1}{2}[\frac{1}{2}(A+B)+\sqrt{A \times B}]$	19%	19%	20%

models were filled with radioactive solution within the water-filled phantom, prone and supine scans were made, and the dot counts for each scan were obtained over an area chosen by inspection from the scan records. Additional scan dot counts have been made with the REMAB phantom to verify the accuracy of the quantitation results and, where sufficient activity was present, the experimental error was only 5% or less.

With access to a double-headed scanner and a computer[3] this technique offers the advantage of producing quantitative organ-uptake measurements along with diagnostic area scanning records.

REFERENCES

1. Brownell, G. L. Theory of radioisotope scanning. In: Medical Radioisotope Scanning, Proceedings of the Symposium on Medical Radioisotope Scanning, Athens, 1964, Vol. I, Vienna, International Atomic Energy Agency, 1964, pp. 3-34.

2. Harris, C. C., Bell, P. R., Satterfield, M. M., Ross, D. A., and Jordan, J. C. The design and performance of a large high-resolution focusing collimator. In: Medical Radioisotope Scanning, Proceedings of the Symposium on Medical Radioisotope Scanning, Athens, 1964, Vol. I, Vienna, International Atomic Energy Agency, 1964, pp. 193-208.

3. Tauxe, W. N., Chaapel, D. W., and Sprau, A. C. Contrast enhancement of scanning procedures by high-speed digital computer. J Nucl Med 7, 647-656, 1966.

1027517

LIPID METABOLISM

During the past year, the Lipid Research Group has focused its attention on the following:

(1) The biosynthesis and biocleavage of ether bonds in glycerolipids.
(2) Continuation of a general survey of the quantity and composition of ether-linked lipids and related lipid classes in neoplasms and other cells.
(3) Lipid composition and metabolism of cells grown in tissue culture.
(4) Lipids of plasma biomembranes (hepatic cells and synaptosomes), organelles, and viruses.
(5) Lipid methodology.

A major breakthrough in our work during 1968 was the isolation of a microsomal enzyme system that can synthesize O-alkyl ethers of glycerol from fatty alcohols and glyceraldehyde-3-phosphate. It is the first known pathway for the biosynthesis of the C-O-C bond in glycerolipids. Details of this system are described in two reports.

We have continued some collaborative work with the University of North Carolina (Dr. Claude Piantadosi); the University of Tennessee (Memphis) Graduate Teaching Program in Biochemistry (Dr. John Wood); University of Minnesota (Drs. Helmut K. Mangold and Wolfgang J. Baumann); the Molecular Anatomy Program (Drs. Norman Anderson and Carl Cotman); ORNL Biology Division (Drs. Neal Clapp, R. C. Cumming, and A. C. Upton); the National Institutes of Health, Biohazards Section (Dr. Alfred Hellman); Department of Biology, Western Carolina University (Dr. Roger Lumb); and the Department of Biochemistry, Howard University (Dr. H. P. Morris). Dr. Ronald Garrett (College of Pharmacy, University of Texas, Austin), a summer research participant, and Michelle Hughes (San Francisco College for Women), a summer research student, were affiliated with the lipid group during 1968. Graduate students included Robert L. Wykle (Department of Biochemistry, Memphis Medical Units, University of Tennessee) and Ahmed Mohamed (Department of Medicinal Chemistry, School of Pharmacy, University of North Carolina, Chapel Hill). Mr. Wykle was awarded an AEC predoctoral fellowship in January 1968. Postdoctoral fellows with our group during 1968 included Dr. James Soodsma (Department of Biochemistry, University of North Dakota, Grand Forks), awarded an AEC postdoctoral fellowship; Dr. Ten-ching Lee (Department of Medicine, Tulane University, New Orleans), awarded an NIH postdoctoral fellowship. Dr. Robert E. Anderson (Department of Biochemistry and Biophysics, Texas A&M University, College Station) and Dr. Gail Sansone (Department of Medicine, Tulane University, New Orleans) were with the lipid group on one-year postdoctoral trainee appointments supported by the American Cancer Society grant. Dr. P-O Hagen (Department of Surgical Research, University of Oslo, Norway) has recently joined the staff under support from the American Cancer Society and NIH.

Synopsis of Work in Progress

A. The Occurrence and Nature of Free and Bound Fatty Alcohols in Normal and Neoplastic Tissue

Our interest in investigating the occurrence of fatty alcohols in mammalian cells is related to our finding that fatty alcohols are direct precursors of glyceryl ethers. Fatty alcohols are present in most tissues in trace quantities (about 0.5% or less of total lipids). The chain lengths and degree of unsaturation are similar to those found in glyceryl ether moieties isolated from neutral- and phospho-glycerides.

B. The Lipid Composition of Influenza Virus Isolated from Humans by Zonal Centrifugation - in collaboration with Dr. N. G. Anderson, ORNL Molecular Anatomy Program

The lipids associated with myxoviruses (rich in lipids) are currently being studied. Thin-layer chromatography of the phospholipids present in influenza virus indicates that significant quantities of ceramides and glycolipids might be important in characterizing this virus; small amounts of glyceryl ethers are also present.

C. The Lipid Composition of Synaptic Plasma Membranes Isolated by Zonal Centrifugation - in collaboration with Dr. Carl Cotman, Department of Psychobiology, University of California at Irvine, and Dr. N. G. Anderson, ORNL Molecular Anatomy Program

Data indicate that the lipid composition of plasma membranes of synaptosomes is similar in many respects to that of plasma membranes isolated from rat liver (Fig. 74). The main difference in these two plasma membrane preparations appeared to be in the relative proportions of phosphatidyl ethanolamine and sphingomyelin. A comparison of the lipid composition of the synaptosome membranes with that of whole brain is given in Table 59.

D. Glyceryl Ether Content of Granulomas, Regenerating Liver, Embryonic Tissue, or Weanling Rats - a portion of this work is being done in collaboration with Dr. A. C. Upton, ORNL Biology Division

We have been unable to demonstrate any abnormal accumulation of glyceryl ethers in experimentally induced pouch granulomas, regenerating rat liver, or embryonic tissue from rats. However, this study has indicated that colostrum contains an abnormally high content of glyceryl ethers. Further investigation of the occurrence of glyceryl ethers in colostrums and in mammary cells is under way.

1027518

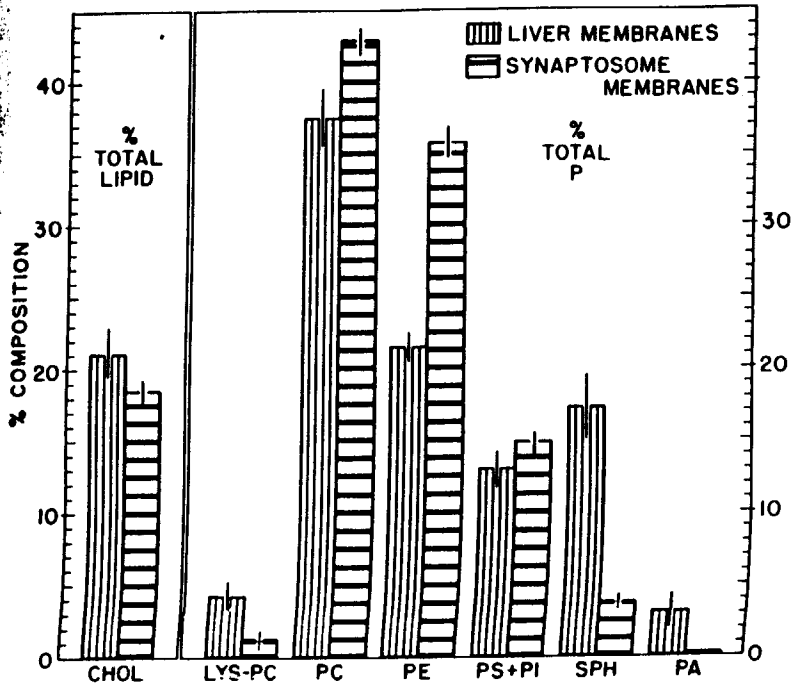

Fig. 74. Lipid classes of rat plasma membranes. The abbreviations designate: Cholesterol (CHOL), lysophosphatidyl choline (PC), phosphatidyl ethanolamine (PE), phosphatidyl serine (PS), sphingomyelin (SPH), and phosphatidic acid (PA).

E. Alkyl and Alk-1-enyl Content of Phosphatidylcholines and Phosphatidylethanolamines Isolated from a Wide Variety of Mammalian Tissues

This investigation indicates that choline-containing phosphoglycerides contain primarily alkyl glyceryl ethers, whereas ethanolamine-containing phosphoglycerides contain mostly the alk-1-enyl glyceryl ethers. The relation of alkyl- and alk-1-enyl-ethers in the two major phosphoglyceride classes appears to be characteristic of both normal and neoplastic tissues.

F. Metabolism of ^{14}C-Labeled Hydrocarbons in Normal and Neoplastic Tissue

Apparently long-chain aliphatic hydrocarbons are metabolized

TABLE 59

and Synaptic Plasma Membranes of Rats
Lipid Classes Present in Whole Brains

	Synaptosomes*	Whole Brain†
Cholesterol	18.6 % ± 1.2	19.4 % ± 1.3
Ceramide	1.6 % ± 0.3	1.5 % ± 0.35
Glycolipid (perhaps cerebroside)	0.9 % ± 0.15	9.6 % ± 0.5
Solvent front‡	0.87% ± 0.6	0.00
PE‡	28.2 % ± 1.3	30.5 % ± 0.7
PI + PS‡	11.8 % ± 0.6	8.69% ± 0.9
PC‡	33.9 % ± 0.6	28.8 % ± 0.7
Sphingomyelin‡	3.00% ± 0.3	1.39% ± 0.4
Lyso-PC‡	0.95% ± 0.7	Trace (not detected in P determination but something in this area on TLC)

*Average of 5 separate samples.

†Average of 3 separate samples.
The cholesterol, ceramide and cerebrosides are expressed as direct wt. % and the ‡phospholipids, based on phosphorus content, are expressed as % phosphorus of the remaining wt. %.

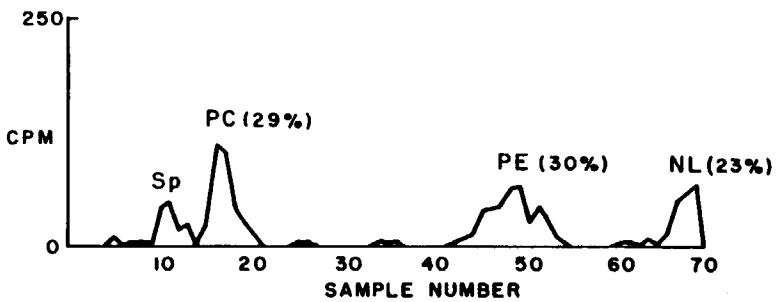

Fig. 75. Incorporation of radioactivity from hexadecane -1-^{14}C into lipids of Ehrlich ascites cells (Sp = sphingomyelin; PC = phosphatidyl ethanolamine; NL = neutral lipids). The hydrocarbon was administered intraperitoneally to mice bearing ascites cells.

1027519

to a greater extent by neoplastic cells than by healthy cells. Data indicate that oxidative enzymes in mammalian cells can oxidize hydrocarbons to a very slight extent (Fig. 75). Relatively high specific activities of alkyl and alk-1-enyl glyceryl ethers in lipids of Ehrlich ascites cells are obtained after the intraperitoneal administration of ^{14}C-labeled 18:0, 16:0, and 8:0 hydrocarbons to mice.

ABSTRACTS OF WORK COMPLETED

The Biosynthesis of Alkyl Ether Bonds in Lipids by a Cell-free System* †

Fred Snyder, Boyd Malone, and Robert L. Wykle

Investigators have found the biological significance and the biosynthetic pathways of ether-linked lipids containing glycerol difficult to determine.[1] Despite available knowledge concerning enzymes for the biocleavage,[2,3] deacylation,[4] acylation,[5,6] and phosphorylation[7] of glyceryl ethers, the biosynthesis of the ether bond in these compounds has not previously been demonstrated in a cell-free system.

This note describes an active enzyme complex capable of converting intact 1-^{14}C-labeled fatty alcohols into alkyl glyceryl ethers. The reaction has been demonstrated in whole homogenates and in microsomal-plus-supernatant fractions of transplantable preputial tumors in mice. These tumors are typical of neoplasms containing high quantities of alkyl ether linkages in both neutral- and phosphoglycerides.[8]

METHODS

The preputial tumors (ESR-586) used in our work were originally purchased from The Jackson Laboratory, Bar Harbor, Maine 04609. Our stock of tumors is maintained by transplanting small portions of minced tumor by subcutaneous injection on the back of C57BL/6 mice, with the use of a Lightwicz antrum trocar attached to a 10-ml syringe.

Animals were killed by decapitation approximately 14, 34-45, and 58 days after the tumors were transplanted. The entire tumor

* Supported in part by the American Cancer Society (Grant No. P-470).

† This is a reprint of an article appearing in Biochem Biophys Res Commun 34, 40-47, 1969.

was rapidly removed, trimmed of connective tissue, diced with scissors, and immediately placed in a beaker containing 20 ml ice cold 0.1 M potassium phosphate buffer at pH 7.0. All subsequent steps were carried out in crushed ice until incubation at 37° C was initiated. The tumors were homogenized in a Potter-Elvehjem homogenizer flask with four strokes of a Teflon pestle attached to a Lourdes homogenizing motor set at 50. All homogenates were centrifuged 4000 g min at 1° C in an International refrigerated centrifuge (Model PR-1) to remove the whole cells, nuclei, and other debris. In certain experiments, mitochondria (150,000 g min pellet), microsomes (6,000,000 g min pellet), and supernatant (6,000,000 g min supernatant) were prepared in a sucrose buffer with a Beckman Spinco centrifuge (Model L-65B) according to procedures previously described in detail.[3]

All preparations derived from the preputial tumor were incubated with various cofactors and ^{14}C-labeled substrates (0.4 microcuries per vial) in a final volume of 3.0 ml per glass vial in a Dubnoff metabolic shaking incubator at 37° C and 150 oscillations per min. The quantity of protein[9] incubated per vial was approximately 15 mg from the homogenates, 4 mg from the mitochondrial fraction, 1 mg from the microsomal fraction, and 7 mg from the supernatant fraction. The quantities of cofactors and substrates (per vial) used in this investigation were 30 μmoles ATP, 0.3 μmoles CoA, 12 μmoles $MgCl_2$ 3 μmoles NADP, 30 μmoles DL-α-glycerophosphate, 6 μmoles NADH, 78 mμmoles 1-^{14}C lauryl alcohol, 75 mμmoles 1-^{14}C cetyl alcohol, 40 mμmoles 1-^{14}C palmitic acid, 93 mμmoles 1-^{14}C myristic acid, 25 mμmoles 1-^{14}C octanoic acid, and 50 mμmoles 1-^{14}C palmitaldehyde. All ^{14}C-labeled substrates were purchased from New England Nuclear Corp., Inc. and purified by thin-layer chromatography (TLC) to >99% purity as determined by zonal profile scanning.[10,11] The exact combination of cofactors and substrates in each vial is described in the tables. The ATP, CoA, NADP, and NADH were purchased from P-L Biochemicals, Inc. The α-glycerophosphate was from Sigma Chemical Co. and the reagent grade $MgCl_2$ from Fisher Scientific Co.

Lipids were extracted from the incubation mixture by the procedure of Bligh and Dyer.[12] Aliquots of the total lipid extracts were chromatographed on Silica Gel G in solvent systems of hexane: diethyl ether:acetic acid (90:10:1 or 80:20:1, v/v) for resolving neutral lipids, or on Silica Gel HR in a solvent system of chloroform:methanol:acetic acid:saline (50:25:8:4, v/v) for resolving phospholipids. Aliquots of total lipids were reduced with $LiAlH_4$, and the products (fatty alcohols and the O-alkyl and O-alk-1-enyl glycerols) were resolved on Silica Gel G in a solvent system of diethyl ether saturated with water.[13] In some instances, the free glyceryl ethers were quantitatively eluted from the Silica Gel G with chloroform:methanol (2:1, v/v) and the isopropylidene derivatives of the glyceryl ethers were prepared.[14] The isopropylidene derivatives were chromatographed on Silica Gel G in a solvent system of hexane: diethyl ether (90:10 or 80:20, v/v). All chromatoplates were radioassayed by liquid scintillation area or zonal profile scans.[10,11] Gas-liquid chromatography (GLC) of the glyceryl ether isopropylidene derivatives was carried out as previously described.[15] Radioactivity was collected directly in a scintillation solvent[11] with aluminum tubing as the connecting link between the GLC detector and the counting vial containing the scintillation solvent.

1027520

RESULTS AND DISCUSSION

The biosynthesis of the ether bond in glyceryl ether lipids was demonstrated in homogenates and a microsomal-plus-supernatant fraction obtained from preparations of a transplantable preputial tumor in mice. The identification of newly synthesized O-alkylglycerols from 1-^{14}C-labeled fatty alcohols in a cell-free system was based on the TLC isolation of (a) ^{14}C-diacylglyceryl ethers (Fig. 76), (b) ^{14}C-O-alkylglycerols after $LiAlH_4$ reduction of total

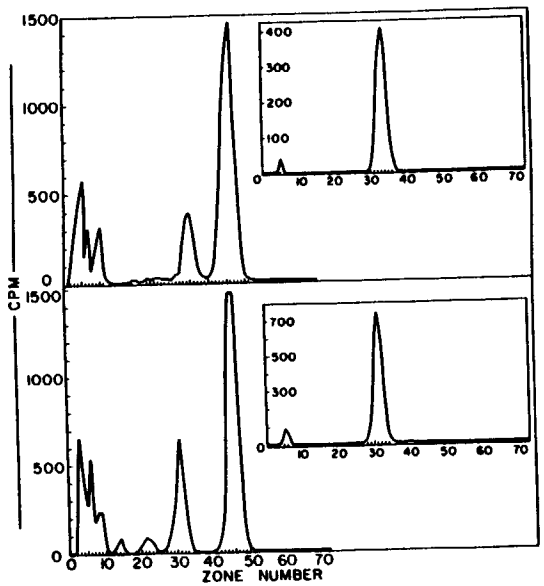

Fig. 76. Zonal profile scans of total lipid extract obtained after a 3-hr incubation of 1-^{14}C cetyl alcohol (upper scan) and 1-^{14}C lauryl alcohol (lower scan) with homogenates of preputial tumors and cofactors (ATP, CoA, NADP, and α-glycerophosphate). Peak identification of resolved components is according to zone number: free fatty acids (13-16), triglycerides (18-24), diacylglyceryl ethers (26-35), wax esters (40-50). The diacylglyceryl ethers were isolated by preparative TLC and reduced with $LiAlH_4$; about 75% of the ^{14}C in this fraction was associated with the O-alkylglycerols and the remainder with fatty alcohols derived from the acyl moieties. The zonal profile scans depicted in the insert were obtained by chromatography of the isopropylidene derivatives of the O-alkylglycerols liberated from total lipids by $LiAlH_4$ reduction (see text for details).

lipid extracts (Tables 60 and 61) and of purified glyceryl ether diesters (Fig. 76), and (c) isopropylidene derivatives of the O-alkylglycerols isolated after $LiAlH_4$ reduction (Fig. 76), and on the GLC isolation of isopropylidene derivatives of the ^{14}C-labeled O-alkylglycerols liberated from total lipids by $LiAlH_4$ reduction.

Figure 76 depicts zonal profile scans of thin-layer chromatograms of an extract obtained from the homogenates, which were incubated with $^{14}C_{12:0}$ and $^{14}C_{16:0}$ fatty alcohols and cofactors. The solvent system used resolves diacyl glyceryl ethers (zones 26-35) and triacylglycerols (zones 18-24). Glyceryl ether biosynthesis is relatively slow, but as much as 46% of 78 mμmoles 1-^{14}C lauryl alcohol was incorporated into ether linkage with glycerol during a 5-hr period. Gas-liquid chromatography of the ^{14}C-labeled O-alkylglycerol isopropylidene derivatives prepared from the homogenate samples revealed that 90% and 89% of the ^{14}C were associated with the $C_{12:0}$ and $C_{16:0}$ glyceryl ethers. Such data indicate that the $C_{12:0}$ and $C_{16:0}$ fatty alcohols were attached to the glycerol moiety intact and that neither degradation nor chain elongation occurred in our system.

Our experiments with the homogenates (Fig. 76) were also designed to rule out the presence of glyceryl ethers in neoplasms simply as the result of a reversibility of the ether-cleaving enzymes in rat liver.[2,3]

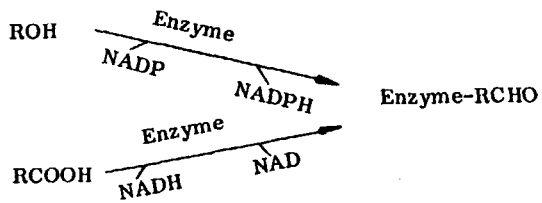

The enzyme aldehyde complex could react with a glycerol intermediate to form a hemiacetal structure that yields glyceryl ethers by dehydration.

However, we soon established that only 1-^{14}C fatty alcohols could be rapidly incorporated into O-alkylglycerols: 1-^{14}C-labeled $C_{8:0}$, $C_{14:0}$, or $C_{16:0}$ fatty acids (in the presence of NADH) and 1-^{14}C palmitaldehyde were not substrates. Although the free 1-^{14}C palmitaldehyde was not incorporated into O-alkylglycerols (Table 60), it did not rule out the possibility that a tightly bound aldehyde-enzyme complex resulting from the oxidation of alcohol to aldehyde could form the active enzyme complex. But when we found that NADP, a hydrogen acceptor necessary for the oxidation of an alcohol to an aldehyde,[3] inhibited the incorporation of the fatty alcohols into O-alkylglycerols (Table 61), it seemed that reversibility of the ether-cleaving enzyme system was not responsible for biosynthesis of glyceryl ethers.

The biosynthesis of glyceryl ethers was also studied in subcellular fractions incubated with 1-^{14}C-labeled fatty alcohols. The data in

1027521

Table 60 showed that the microsomes-plus-supernatant fraction was essential for the biosynthesis of ether bonds; neither microsomes nor supernatants alone were sufficient. Boiled supernatants added to microsomes and boiled microsomes added to supernatants were inactive, but a supernatant fraction obtained from rat liver was able to replace the active supernatant derived from the tumor. Biosynthesis of glyceryl ethers could not be demonstrated in preparations obtained from old tumors (58 days), which grossly appeared necrotic.

The cofactor requirements for maximum incorporation of 1-^{14}C fatty alcohols into glyceryl ethers were ATP, CoA, and Mg^{++} (Table 61). α-Glycerophosphate does not appear to be the glycerol source in this reaction. The results obtained from our experiments suggest

TABLE 60

BIOSYNTHESIS OF ALKYL ETHER BONDS OF LIPIDS IN HOMOGENATES AND SUBCELLULAR FRACTIONS OF PREPUTIAL TUMORS FROM MICE

Sample	Incorporation of 1-^{14}C fatty alcohols* into O-alkylglycerols†	
	Cetyl alcohol	
	mμmoles	% ^{14}C
1. Homogenate‡	10	13
2. Mitochondria	1	1
3. Microsomes	2	3
4. Supernatant	1	2
5. Mitochondria + supernatant	4	5
6. Microsomes + supernatant	11	15
7. Microsomes + boiled (15 min) supernatant	1	2
8. Boiled (15 min) microsomes + supernatant	1	2
9. Microsomes + supernatant from rat liver	11	15

*Incubated for 3 hr with ATP, CoA, and Mg^{++} as described in methods section.

†O-Alkylglycerols liberated from total lipids by $LiAlH_4$ reduction.

‡Essentially none of the radioactivity from 1-^{14}C palmitaldehyde, 1-^{14}C octanoic acid, or 1-^{14}C myristic acid (incubated under identical conditions) was incorporated into O-alkylglycerols.

TABLE 61

EFFECT OF COFACTORS AND SUBSTRATES ON THE BIOSYNTHESIS OF ALKYL ETHER BONDS OF LIPIDS IN A MICROSOME-PLUS-SUPERNATANT FRACTION OBTAINED FROM MOUSE PREPUTIAL TUMORS

Cofactor additions	Incorporation of ^{14}C into O-alkylglycerols*,†		
	Substrate	mμmoles	% ^{14}C
1. Complete system ‡	1-^{14}C cetyl alcohol	17	23
2. Complete system minus CoA	1-^{14}C cetyl alcohol	8	10
3. Complete system minus Mg^{++}	1-^{14}C cetyl alcohol	8	10
4. Complete system minus CoA and Mg^{++}	1-^{14}C cetyl alcohol	6	8
5. Complete system + NADP	1-^{14}C cetyl alcohol	8	11
6. Complete system + α-glycero-phosphate	1-^{14}C cetyl alcohol	13	17
7. Complete system + α-glycero-phosphate; microsomes + boiled (15 min) super-natant	1-^{14}C cetyl alcohol	2	2
8. No cofactors	1-^{14}C cetyl alcohol	1	1
9. Complete system + NADH	1-^{14}C palmitic acid	1	3

*Incubated for 3 hr as described in methods section.

†O-Alkylglycerols liberated from total lipids by $LiAlH_4$ reduction.

‡Each vial contained ATP, CoA, Mg^{++}, and microsomes-plus-supernatant in the amounts described in the methods section.

that, instead, an aldehydogenic glycerol derivative reacts with the fatty alcohols to form glyceryl ethers. This glycerol derivative could be thought of as a phosphorylated intermediate, since ATP and Mg^{++} are necessary as cofactors. The stimulatory effect of CoA is probably related to an enhanced utilization of the initial product in acylation reactions (also requiring ATP for thiokinase), a system that is active in this tumor.[6] Further investigation of the system to establish the identity of the glycerol moiety reacting with fatty alcohols is now under way.

REFERENCES

1. Snyder, F. The biochemistry of lipids containing ether bonds. In: Progress in the Chemistry of Fats and Other Lipids, Ralph T. Holman, ed., Pergamon Press, Ltd., Oxford, Vol. 10, pp. 287-335, 1969.

2. Tietz, A., Lindberg, M., and Kennedy, E. P. A new pteridine-requiring enzyme system for the oxidation of glyceryl ethers. J Biol Chem 239, 4081-4090, 1964.

3. Pfleger, R. C., Piantadosi, C., and Snyder, F. The biocleavage of isomeric glyceryl ethers by soluble liver enzymes in a variety of species. Biochim Biophys Acta 144, 633-648, 1967.

4. Snyder, F. and Piantadosi, C. Deacylation of isomeric diacyl [1-^{14}C] alkoxyglycerols by pancreatic lipase. Biochim Biophys Acta 152, 794-797, 1968.

5. Waku, K. and Lands, W. E. M. Acyl coenzyme A:1-alkenyl-glycero-3-phosphorylcholine acyltransferase action in plasmalogen biosynthesis. J Biol Chem 243, 2654-2659, 1968.

6. Snyder, F. and Piantadosi, C. Acylation and degradation of alkoxyglycerols in vitro. Fed Proc 27, 458, 1968, abstr. 1360.

7. Kiyasu, J. Y. and Kennedy, E. P. The enzymatic synthesis of plasmalogens. J Biol Chem 235, 2590-2594, 1960.

8. Snyder, F. and Wood, R. The occurrence and metabolism of alkyl and alk-1-enyl ethers of glycerol in transplantable rat and mouse tumors. Cancer Res 28, 972-978, 1968.

9. Lowry, O. H., Rosebrough, N. J., Farr, A. L., and Randall, R. J. Protein measurement with the folin phenol reagent. J Biol Chem 193, 265-275, 1951.

10. Snyder, F. and Kimble, H. An automatic zonal scraper and sample collector for radioassay of thin-layer chromatograms. Anal Biochem 11, 510-518, 1965.

11. Snyder, F. and Smith, D. An automated system for sample collection and computer analysis of thin-layer radiochromatograms. Separation Sci 1, 709-722, 1966.

12. Bligh, E. G. and Dyer, W. J. A rapid method of total lipid extraction and purification. Can J Biochem Physiol 37, 911-917, 1959.

13. Wood, R. and Snyder, F. Quantitative determination of alk-1-enyl- and alkyl-glyceryl ethers in neutral lipids and phospholipids. Lipids 3, 129-135, 1968.

14. Wood, R. GLC and TLC analysis of isopropylidene derivatives

of isomeric polyhydroxy acids derived from positional and geometrical isomers of unsaturated fatty acids. Lipids 2, 199-203, 1967.

15. Snyder, F. and Blank, M. Relationships of chain lengths and double bond locations in O-alkyl, O-alk-1-enyl, acyl, and fatty alcohol moieties in preputial glands of mice. Arch Biochem Biophys, in press.

A New Metabolic Pathway: Biosynthesis of Alkyl Ether Bonds from Glyceraldehyde-3-Phosphate and Fatty Alcohols by Microsomal Enzymes* †

Fred Snyder, Robert L. Wykle, and Boyd Malone

We have recently described in preputial gland tumors[1] a complex of microsomes (100,000 g pellet) plus soluble protein (100,000 g supernatant) that makes alkyl ether bonds in glycerolipids from 1-^{14}C-labeled long-chain fatty alcohols. It is the first cell-free system found to form glyceryl ethers. Cofactor requirements for maximum incorporation of the fatty alcohols into C-O-C bonds were ATP, CoA, and Mg^{++}. Fatty acids or fatty aldehydes did not serve as substitutes for the fatty alcohols in this system. Formation of the ether bond in the incubation mixture was documented by (a) isolation of diacyl glyceryl ethers; (b) isolation of ^{14}C-labeled alkylglycerols (free glyceryl ethers) by thin-layer chromatography (TLC) after $LiAlH_4$ reduction of diacyl glyceryl ethers and total lipids; and (c) gas-liquid chromatographic isolation of isopropylidene derivatives of the ^{14}C-labeled O-alkylglycerols (formed by $LiAlH_4$ reduction) having alkyl side chains identical to the fatty alcohol precursors incubated.

The facts that soluble proteins from rat liver could be substituted for the soluble protein fraction from the tumor in stimulating ether biosynthesis and that α-glycerophosphate had no effect on ether biosynthesis suggested to us that some other glycolytic product (perhaps an aldehydogenic glycerol derivative) was the glycerol acceptor in the formation of the alkyl ether bond.[1] We have just completed a series of experiments with a number of key compounds in the glycolytic pathway to determine the source of the glycerol moiety and the nature of the reaction responsible for the biosynthesis of glyceryl ethers.

* This work has been supported in part by the American Cancer Society (Grant No. P-470).

† This is a reprint of an article to be published in Biochem Biophys Res Commun 34, 315-321, 1969.

1027523

METHODS

The biological and analytical methods used were the same as those described in our original communication on this subject.[1] Microsomes (unwashed and washed three times) were prepared at 100,000 g in 0.1 M phosphate buffer containing 0.25 M sucrose.[1] Quantities of substrates and cofactors incubated per vial in a final volume of 3 ml (Tables 62 and 63) were 10 or 30 μmoles ATP, 10 or 30 μmoles ADP, 0.3 μmoles CoA, 12 μmoles Mg^{++}, 15 μmoles DL-glyceraldehyde-3-PO_4, 75 mμmoles 1-^{14}C-cetyl alcohol (0.4 μc added in 10 λ of 1% Tween 80), 3 μmoles NADP, 6 μmoles NADPH, 20 μmoles D-glucose-6-PO_4, 1 unit glucose-6-PO_4 dehydrogenase, and 125 μmoles NaF. The commercial sources of cofactors and substrates were the same as before.[1] The complete system referred to in the tables includes ≈1.3 mg microsomal protein, 15 μmoles DL-glyceraldehyde-3-PO_4, 30 μmoles ATP, 12 μmoles Mg^{++}, and 0.3 μmoles CoA per vial. All incubations were for 3 hr at 37° C in a Dubnoff shaker set at 150 oscillations/min unless otherwise stated. The NADPH generating system consisted of glucose-6-PO_4, glucose-6-PO_4 dehydrogenase, and NADP.

Glyceryl ether lipids were isolated by thin-layer chromatography before and after $LiAlH_4$ reduction of total lipids. The presence of glyceryl ethers in representative samples was confirmed by thin-layer and gas-liquid chromatography of their isopropylidene derivatives; 86-91% of the ^{14}C-activity was associated with 16:0 glyceryl ether peak (chimyl alcohol) after incubating cetyl alcohol.

RESULTS AND DISCUSSION

The results in Table 62 are typical, and conclusively demonstrate that a microsomal enzyme complex can form a C-O-C bond when long-chain fatty alcohols and glyceraldehyde-3-PO_4 are substrates; ATP, Mg^{++}, and CoA are essential cofactors. Ten μmoles of ATP had the same effect as the 30 μmoles generally used, and ADP can substitute for ATP but not on an equal molar basis at lower concentrations. NADPH is required at one of the stages before acylation can occur. Fatty acids, fatty aldehydes, or glycerophosphate did not participate as substrates. Nonspecific esterases, requiring no cofactors, incorporate a portion of the fatty alcohols into waxes during incubations.

Previous data obtained with homogenates, in the absence of an added glycerol source, indicated that the reaction for ether biosynthesis proceeded rather slowly,[1] and a number of the experiments reported here were also completed with 3-hr incubations. However, time curves for biosynthesis of ethers obtained recently with the specific microsomal system described in this paper have revealed that maximal incorporation of fatty alcohols occurs be-

TABLE 62

The Biosynthesis of C-O-C Bonds in Glycerolipids by Microsomes of Preputial Gland Tumors

System	% ^{14}C of 1-^{14}C-cetyl alcohol (75 mμmoles incubated) incorporated into O-alkylglycerols derived from total lipids after $LiAlH_4$ reduction*
1. Complete	31, 26, 19, 28
2. Complete minus ATP	0.9, 1.2
3. Complete minus CoA	1.0, 0.93
4. Complete minus Mg^{++}	1.0, 0.99
5. Complete minus glyceraldehyde-3-PO_4	1.9, 0.75
6. Complete except microsomes were boiled	1.9, 0.75
7. Microsomes and ^{14}C-cetyl alcohol alone	0.64, 2.3

Microsomes were washed 3 times; see text for details on cofactors, substrates, and other conditions.

*Values calculated for individual vials.

TABLE 63

The Effect of NADPH and NaF on the Formation of "Free" O-Alkylglycerols by an Ether-Synthesizing Enzyme Complex in Preputial Tumor Microsomes

System	"Free" glyceryl ethers before $LiAlH_4$ reduction	"Free" glyceryl ethers after $LiAlH_4$ reduction of total lipids
	% 1-^{14}C-cetyl alcohol (75 mμmoles) incorporated*	
†1. Complete	2.9, 1.6	31, 32
†2. Complete plus NADPH at beginning of incubation	1.3, 1.2	2.4, 3.1
†3. Complete; at end of 3 hr, NADPH was added and incubated for 1 more hr.	8.1, 8.1	31, 31
†4. Complete; at end of 3 hr, NADPH and soluble fraction were added and incubated for 1 more hr.	15, 13	33, 34
‡5. Complete; at end of 0.5 hr, NADPH generating system added and incubated for 0.5 hr.	19, 17	32, 31
‡6. Complete plus NaF; at end of 0.5 hr, NADPH generating system added and incubated for 0.5 hr.	1.3, 0.33	21, 20

*Values calculated for individual vials.

†Microsomes were washed 3 times; see text for details on cofactors, substrates, and other conditions.

‡Unwashed microsomes.

1027524

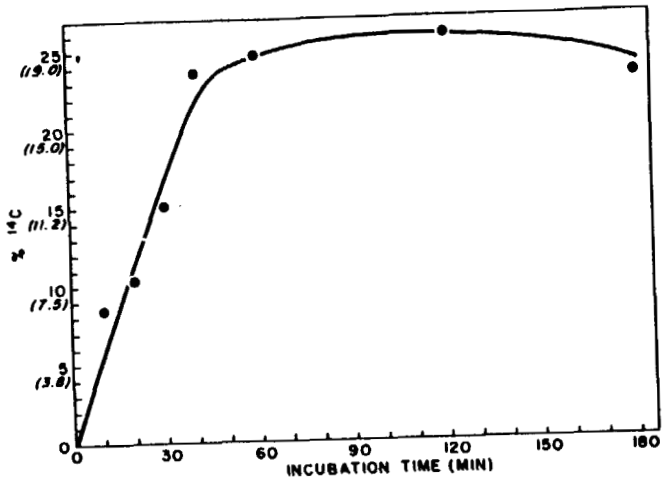

Fig. 77-1. Incorporation of 1-^{14}C-cetyl alcohol into O-alkylglycerols of total lipids (after $LiAlH_4$ reduction) by an ether-synthesizing enzyme complex in preputial tumor microsomes. Each value is the mean of duplicate incubations. The values in parentheses below the percentages refer to mμmoles of fatty alcohol incorporated. The complete system, as described in text, was used for this experiment.

tween 0.5 and 1 hr, and changes very little after this period (Fig. 77-1). The following reaction scheme is indicated by our incubation of substrates and cofactors (Tables 62 and 63), and by the chromatographic behavior (Fig. 77-2) of the labeled components found after incubations:

We believe that the first step (Fig. 77-3) is the formation of a hemiacetal (II) and that the keto form (IV) of the glyceryl ether phosphate from dehydration of the hemiacetal occurs, since there is no appreciable biosynthesis of free glyceryl ethers (Table 63) or diacyl glyceryl ethers in the absence of NADPH. Furthermore, the O-alkylglycerols isolated after $LiAlH_4$ reduction of samples incubated without NADPH would be expected if the keto form were present. Although NADPH is necessary for the reduction of the ketone intermediates (IV and VII) before acylation can occur, it cannot be added at the beginning of the reaction when reduction of the glyceraldehyde-3-PO_4 can also occur and prevent the formation of C-O-C bonds (Table 63). The enzymic reduction of the keto compounds (IV and VII) would also permit the proper stereochemical orientation of the hydroxyl group at position 2, since naturally occurring glyceryl ethers have the alkyl moiety at the 1-position of glycerol[2] (Hirschmann's nomenclature[3]). Indeed, the buildup of ^{14}C-labeled free glyceryl ethers (VI) present in the total lipids of samples incubated with NADPH (Table 63, Fig. 77-2) and the buildup of other ^{14}C-components, which we believe to be compounds IV and VII, in the absence of NADPH, support this conclusion (Fig. 77-2). These data are

compatible with the observation that phosphatidate hydrolase can attack lysophosphatidates.[4] Furthermore, NaF inhibited the release of phosphate and prevented the formation of free glyceryl ethers in the presence of NADPH. The enzyme responsible for reduction of the keto compounds appears to be in the supernatant fraction or only loosely bound to microsomes.

Four preparations of homogenates (4,000 g min supernatant) in this series formed diacyl glyceryl ethers (23% ^{14}C incorporated) when NADP was added to generate NADPH, confirming our earlier data[1] on the biosynthesis of the diacyl type. Reaction B (Fig. 77-3) provides the necessary acylation sequence[1] that yields the diacyl glyceryl ethers isolated from homogenates containing an NADPH source. This portion of the scheme resembles the pathway for the biosynthesis of glycerides.[5]

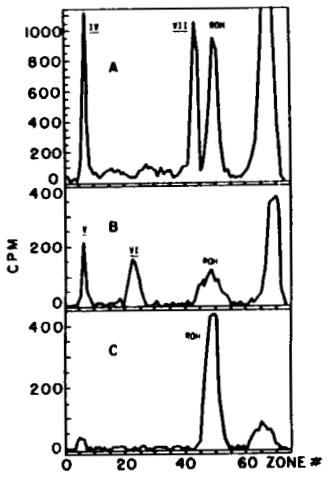

Fig. 77-2. Zonal profile scans (2-hr) of thin-layer chromatographic separations of total lipids isolated from the vials, described in Table 63, i.e., (A) no NADPH, (B) 6 μmoles NADPH added at end of 3 hr, and (C) 6 μmoles NADPH added at zero time. Numbers next to peaks are thought to be compounds depicted by same numbers in Fig. 77-1. The peak at solvent front (>zone 60) is other nonpolar lipids. The chromatogram was developed in diethyl ether:acetic acid, 100:0.5 (v/v). The isopropylidene derivative of the "free" glyceryl ethers (Chromatogram B, peak VI) was isolated by gas-liquid radiochromatography[1]; 88% of the ^{14}C was collected as the 16:0 glyceryl ether (chimyl alcohol).

1027525

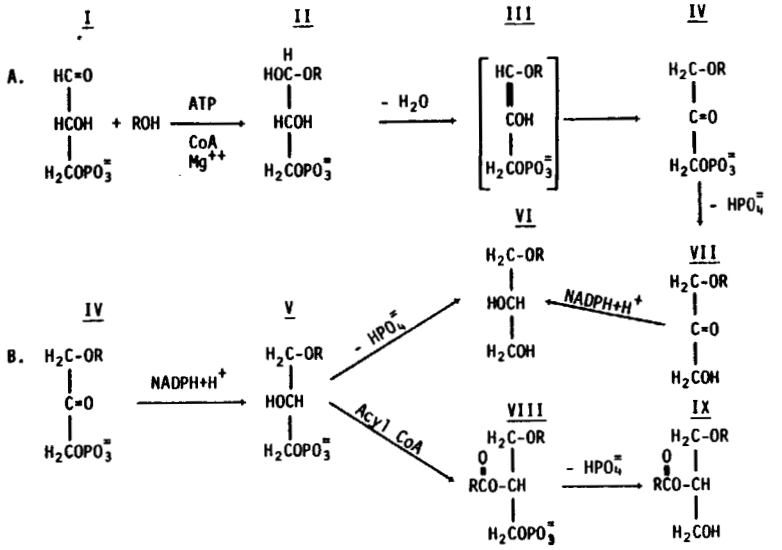

Fig. 77-3. Proposed biosynthetic pathway for alkyl glyceryl ethers.

The roles of CoA, ATP or ADP, and Mg^{++} in reaction A are not known although it is quite possible that the fatty alcohols require phosphorylation. Kinetic data of the various parameters involved are being accumulated by us while we study the isolation and characterization of intermediates in this new biosynthetic pathway. The direct precursor role of fatty alchols in the biosynthesis of glyceryl ethers was suggested by earlier data showing that the locations of double bonds in the hydrocarbon moieties of glyceryl ethers and fatty alcohols in normal preputial glands were nearly identical.[6]

REFERENCES

1. Snyder, F., Malone, B., and Wykle, R. L. The biosynthesis of alkyl ether bonds in lipids by a cell-free system. Biochem Biophys Res Commun, 34, 40-47, 1969.

2. Snyder, F. The biochemistry of lipids containing ether bonds. In: Progress in the Chemistry of Fats and Other Lipids, Ralph T. Holman, ed., Pergamon Press, Ltd., Oxford, Vol. 10, pp. 287-335, 1969.

3. Hirschmann, H. The nature of substrate asymmetry in stereoselective reactions. J Biol Chem 235, 2762-2767, 1960.

4. Ansell, G. B. and Hawthorne, J. N. Phospholipids.

Elsevier Publishing Co., New York, 1964, p. 168.

5. Weiss, S. B. and Kennedy, E. P. The enzymatic synthesis of triglycerides. J Am Chem Soc 78, 3550, 1968.

6. Snyder, F. and Blank, M. Relationships of chain lengths and double bond locations in O-alkyl, O-alk-1-enyl, acyl, and fatty alcohol moieties in preputial glands of mice. Arch Biochem Biophys (in press).

Ether-Linked Lipids in Neoplasms of Man and Animals: Methods of Measurement and the Occurrence and Nature of the Alkyl and Alk-1-Enyl Moieties*

Fred Snyder

Naturally occurring glycerolipids containing ether bonds can be classified according to two structural types: alkyl and alk-1-enyl. The two types of glyceryl ethers and their derivatives can be resolved from their corresponding acyl analogues by adsorption chromatography and then further subfractionated according to carbon number and degree of unsaturation by gas-liqud chromatography (GLC) and argentation thin-layer chromatography (TLC). These compounds contain the ether linkage in the α-position and have a D-configuration.[1-5] The alk-1-enyl linkage in both the neutral glycerides[5-7] and in the phosphoglycerides[3] is cis. Neutral glycerides contain most of the alkyl-type ethers and phosphoglycerides most of the alk-1-enyl type.[8,9] The ether-linked neutral glycerides show polymorphism.[10]

In spite of the widespread occurrence of ether lipids, the biochemical mechanism for the formation of the ether linkage and the interconversions of alkyl and alk-1-enyl types and their derivatives are still poorly understood.[11] The abnormally high levels of α-glyceryl ether diesters (GEDE), primarily the alkyl type, in a wide variety of neoplastic cells of man[9,12] and numerous transplantable tumors[12-15] have raised some intriguing questions about their possible function in cellular proliferation.

The paper published in the proceedings of the Milan meeting on "Drugs Affecting Lipid Metabolism" illustrates useful methods for the analysis of ether-linked lipids. This abstract summarizes data on the alkyl and alk-1-enyl content of GEDE, phosphatidyl choline (PC), and phosphatidyl ethanolamine (PE) fractions of Walker-256 carcinosarcoma (rat), taper liver tumor (mouse), and a lymphosarcoma (human); the nature of the alkyl and alk-1-enyl side chains of these lipids is also described.

Our earlier studies of the ether lipids in a wide variety of normal and neoplastic cells[8,9,15] reported only the total quantity of alkyl and alk-1-enyl glyceryl ethers in the neutral glyceride and phosphoglyceride fractions. The contribution of the ether linkage in individual lipid classes was not determined. In this investigation the exact contribution of ethers from three major lipid classes (GEDE, PE, and PC) was established for several tumors. In all tumors, the relative proportion of alkyl to alk-1-enyl ethers was highest in GEDE and PC fractions, which is opposite that found in PE (Table 64). Except in the lymphosarcoma sample, the ratio of ether types in PC and PE was relatively constant. Obviously the alkyl/alk-1-enyl ratio in the PC fraction more nearly approaches the value of this ratio for GEDE. The data suggest that a metabolic relation might exist between the PC ethers and GEDE.

The alkyl and alk-1-enyl hydrocarbon chains (Table 65) linked to glycerol by an ether bond were found to have a characteristic pattern for all lipid classes in the neoplasms examined and differed significantly from the acyl moieties. Both the alkyl and alk-1-enyl ether

TABLE 64

Alkyl and Alk-1-enyl Content† of Glyceryl Ether Diesters, Phosphatidyl Cholines, and Phosphatidyl Ethanolamines of Neoplastic Tissues

		TOTAL LIPIDS			GEDE		PC		PE	
Tissue	Species	% Dry Tissue	% NL	% PL	Alkyl	Alk-1-enyl	Alkyl	Alk-1-enyl	Alkyl	Alk-1-enyl
Walker-256 Tumor	CFN Rat	9.61	60	40	0.96	0.17	8.85	2.16	2.17	11.90
Taper Liver Tumor	HA/ICR Mice	14.29	78	22	1.16	0.27	8.94	1.48	3.17	14.45
Lympho-sarcoma	Man	22.21	85	15	0.77	0.55	1.73	1.39	1.49	18.30

† Expressed as weight percentage of total neutral glycerides for GEDE and total phosphoglycerides for PC and PE.

types contained 16:0, 18:0, and 18:1 as the main hydrocarbon moieties (Fig. 78). However, in all lipid classes the alkyl ethers contained larger quantities of 18:1 and lower quantities of 18:0 than the alk-1-enyl ethers. Linoleic and other fatty acids that are not normally synthesized de novo in mammalian cells are found only in minute quantities in ether linkages. On the other hand, fatty acid esters in GEDE, TG, PC, and PE fractions contain significant quantities of linoleic, arachidonic, and other long-chain polyunsaturated fatty

* Supported in part by the American Cancer Society (Grant No. P-470). Excerpts of a paper from Advances in Experimental Medicine and Biology, Vol. 2, Plenum Publishing Corp., New York (in press 1969). Presented at the Third International Symposium on Drugs Affecting Lipid Metabolism, Milan, Italy.

1027526

TABLE 65

Nature of Alkyl and Alk-1-enyl Chains in Glyceryl Ether Diesters, Phosphatidyl Cholines, and Phosphatidyl Ethanolamines of Neoplasms

Carbon Chain	Walker-256 Tumor			Taper Liver Tumor			Lymphosarcoma		
	GEDE	PC	PE	GEDE	PC	PE	GEDE	PC	PE
	Alkyl Type Ethers (%)								
14:0	--	0.8	t	t	0.7	t	--	--	--
14:1 (15:0)	--	t	t	t	--	--	--	--	--
16:0	39.2	54.4	37.5	36.2	42.7	34.1	32.1	45.6	36.2
16:1 (17:0)	t	t	t	t	t	t	1.1	1.1	1.7
18:0	18.7	15.8	30.6	19.5	12.2	28.0	42.4	16.0	38.7
18:1	38.2	26.4	28.4	39.5	41.9	35.9	24.4	37.3	23.4
18:2 (19:0)	1.9	1.0	1.4	2.5	2.5	2.0	--	--	--
20:0	2.0	1.6	2.1	2.3	t	t	--	--	--
	Alk-1-enyl Type Ethers (%)								
14:0	--	--	--	--	--	--	--	--	--
14:1 (15:0)	--	--	--	--	--	--	--	--	--
16:0	38.9	43.0	39.9	45.1	50.4	43.0	44.4	56.3	37.1
16:1 (17:0)	--	t	t	t	t	t	4.6	2.6	2.5
18:0	37.4	30.2	36.0	26.2	25.8	29.3	45.1	22.7	41.1
18:1	23.7	23.2	20.2	22.0	22.0	25.9	5.9	18.4	19.3
18:2 (19:0)	--	1.8	1.5	3.6	1.8	1.8	--	--	--
20:0	--	1.8	2.4	3.1	t	t	--	--	--

t indicates trace quantity.

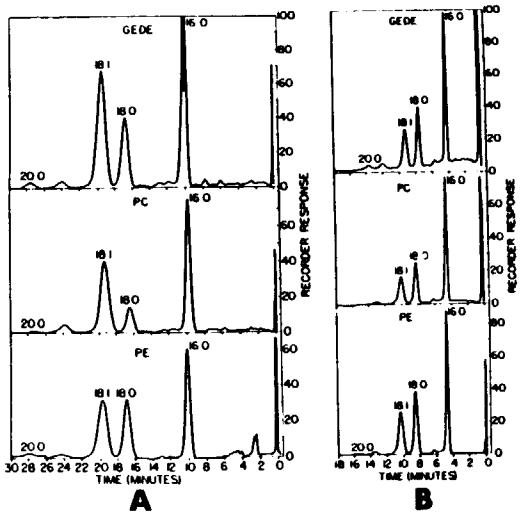

Fig. 78. A. A typical chromatogram showing the resolution of the isopropylidene derivatives of alkyl glyceryl ethers by gas-liquid chromatography according to the procedures described in the text. The alkyl glyceryl ethers were isolated from the GEDE, PC, and PE lipids found in the taper liver tumor. B. A typical chromatogram showing the resolution of intact fatty aldehydes by gas-liquid chromatography according to the procedures described in the text. The aldehydes were isolated from the GEDE, PC, and PE alk-1-enyl ethers found in the taper liver tumor.

1027527

acids. Possibly the alkyl and alk-1-enyl chains merely reflect the general fatty acid composition of the 1-position of glyceryl lipids. However, a more detailed positional analysis of the hydrocarbon chains in TG, GEDE, PC, and PE in Ehrlich ascites cells has demonstrated that this is probably not the reason.[16] Instead, the hydrocarbon moieties found in ether linkages are characteristic of fatty acids that can be synthesized de novo from acetyl-CoA and malonyl CoA.

REFERENCES

1. Baer, E. and Fischer, H. O. L. Studies on acetone-glyceraldehyde, and optically active glycerides. IX. Configuration of the natural batyl, chimyl, and selachyl alcohols. J Biol Chem 140, 397-410, 1941.

2. Baumann, W. J., Mahadevan, V., and Mangold, H. K. Optisch aktive, synthetische und natürliche O-Alkyl-glyceride. Z Physiol Chem 347, 52-58, 1966.

3. Cymerman-Craig, J., Hamon, D. P. G., Purushothaman, K. K., Roy, S. K., and Lands, W. E. M. Optical rotary dispersion and absolute configuration. V. Absolute configuration of natural plasmalogen. Tetrahedron 22, 175-178, 1966.

4. Schmid, H. H. O., Baumann, W. J. and Mangold, H. K. Alkoxy lipids. III. Naturally occurring D(+)-1-O-cis-alk-1-enyl diglycerides. Biochim Biophys Acta 144, 344-354, 1967.

5. Schmid, H. H. O., Baumann, W. J., and Mangold, H. K. The structure and configuration of "neutral plasmalogens". J Am Chem Soc 89, 4797-4798, 1967.

6. Norton, W. T., Gottfried, E. L., and Rapport, M. M. The structure of plasmalogens: VI. Configuration of the double bond in the α, β-unsaturated ether linkage of phosphatidyl choline. J Lipid Res 3, 456-459, 1962.

7. Warner, H. R. and Lands, W. E. M. The configuration of the double bond in naturally-occurring alkenyl ethers. J Am Chem Soc 85, 60-64, 1963.

8. Wood, R. and Snyder, F. Quantitative determination of the alk-1-enyl- and alkyl-glyceryl ethers in neutral lipids and phospholipids. Lipids 3, 129-135, 1968.

9. Snyder, F. and Wood, R. Alkyl and alk-1-enyl ethers of glycerol in a variety of normal and neoplastic tissues from humans. Cancer Res (in press).

10. Oswald, E. O., Piantadosi, C., Anderson, C. E., and Snyder, F.

Infrared spectra and polymorphism of glycerol ether derivatives. Chem Phys Lipids 1, 270-281, 1967.

11. Snyder, F. The biochemistry of lipids containing ether bonds. In: Progress in the Chemistry of Fats and Other Lipids, Ralph T. Holman, ed., Pergamon Press, Ltd., Oxford, Vol. 10, pp. 287-335, 1969.

12. Snyder, F., Cress, E. A., and Stephens, N. An unidentified lipid prevalent in tumors. Lipids 1, 381-386, 1966.

13. Cheng, S.-S., Piantadosi, C., and Snyder, F. Lipid droplets and glyceryl ether diesters in Ehrlich ascites cells grown in tissue culture. Lipids 2, 193-194, 1967.

14. Wood, R. and Snyder, F. Characterization and identification of glyceryl ether diesters present in tumor cells. J Lipid Res 8, 494-500, 1967.

15. Snyder, F. and Wood, R. The occurrence and metabolism of alkyl and alk-1-enyl ethers of glycerol in transplantable rat and mouse tumors. Cancer Res 28, 972-978, 1968.

16. Wood, R. and Snyder, F. Tumor Lipids: Metabolic relationships derived from structural analyses of acyl, alkyl, and alk-1-enyl moieties of neutral glycerides and phosphoglycerides. Arch Biochem Biophys (in press).

The Cleavage of Chimyl Alcohol by Homogenates of Rat Livers and Morris Hepatomas

James F. Soodsma and Fred Snyder

The cleavage of chimyl alcohol by homogenates of rat livers and transplantable Morris hepatomas was compared; the hepatomas were types 7777 and 7794A. Interest in the properties of these hepatomas arose because the 7794A resembles liver in that it has a low glyceryl ether content but the 7777 hepatoma is more deviated from liver and, like other neoplastic tissues, possesses a substantially higher glyceryl ether content. Other work has suggested that the ether-cleaving enzyme is low or absent in cells rich in glyceryl ethers.[1] It might be suggested on this basis that the cleavage system would be diminished or absent in the 7777 hepatomas and probably intermediate in activity in the 7794A. Table 66 shows the results of the experiment to test this hypothesis. The 7794A hepatoma exhibits a level of activity not statistically lower than that of normal or host animal livers, whereas the level in the 7777 hepatoma is significantly lower ($p<0.01$). Therefore, a lack of the cleavage

1027528

TABLE 66

CLEAVAGE OF CHIMYL ALCOHOL (^{14}C) BY VARIOUS TISSUES

	Cleavage Enzyme Activity*
Rat liver (4)†	7.26 ± 2.16
Minimal deviation hepatomas:	
7794A (4)	5.84 ± 1.77
7777 (4)	1.39 ± 0.66
Host liver (2)	5.77 ± 0.86
Rat liver vs. 7777	$p < 0.01$
7794A vs. 7777	$p < 0.01$
Rat liver vs. 7794A	$p > 0.05$

*Expressed as mμmoles chimyl alcohol cleaved per 20 min per mg protein.

†Figures in parentheses represent the number of tissues assayed in duplicate.

activity may account for a buildup of ether-linked lipids in this hepatoma; however, the high level of ether linkages could also be due to increased ether synthesis or a combination of the two effects.

REFERENCES

1. Pfleger, R. C., Piantadosi, C., and Snyder, F. The biocleavage of isomeric glyceryl ethers by soluble liver enzymes in a variety of species. Biochim Biophys Acta 144, 633-648, 1967.

Acylation and Degradation of Alkoxyglycerols in Vitro* †

Fred Snyder and Claude Piantadosi‡

Acylation and oxidative degradation of isomeric alkoxyglycerols has been investigated in whole homogenates and fractions of neoplastic cells, which contain high levels of alkyl and alk-1-enyl ethers of glycerol[1] and in those of several normal tissues. Recently we have demonstrated by means of zonal centrifugation and electron microscopy that the alkyl etherase complex in rat liver is a soluble protein.[2] Neoplastic cells were found to be lacking in this enzyme, but contained a system which readily acylated alkoxyglycerols in the presence of ATP and CoA. Acylation of the 1-isomeric alkoxyglycerols occurred primarily at the 3-position, producing 1,3-diglyceride analogues (Fig. 79). Enzymes for deacylation of glyceryl ether diesters were not present in neoplasms. The deacylation rates obtained with pancreatic lipase were essentially the same for diacylalkoxyglycerols and triacylglycerols.

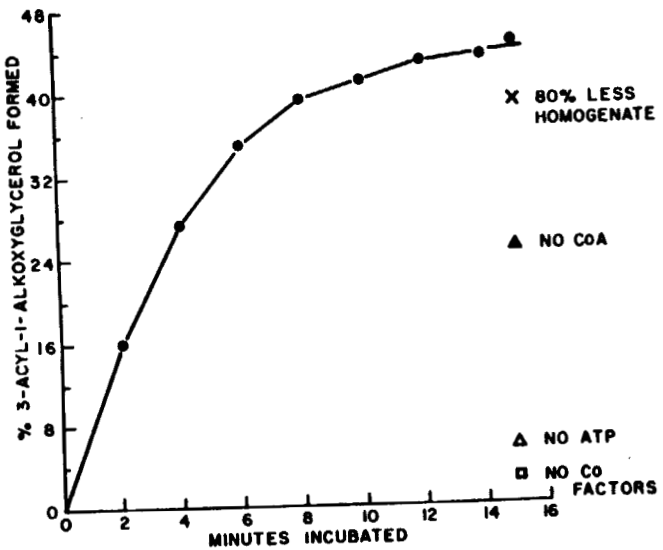

Fig. 79. Acylation of chimyl alcohol by a homogenate of preputial tumors.

* Supported in part by USAEC, NIH Grant GM 12562-04, and American Cancer Society Grant P-470.

† Presented at the annual meeting of the Federation of the American Societies of Experimental Biology, Atlantic City, New Jersey, April 15-20, 1968; published in Federation Proceedings 27, 458, 1968.

‡ University of North Carolina, Chapel Hill, North Carolina.

1027529

REFERENCES

1. Wood, R. and Snyder, F. Characterization and identification of glyceryl ether diesters present in tumor cells. J Lipid Res 8, 494-500, 1967.

2. Pfleger, R. C., Piantadosi, C., and Snyder, F. The biocleavage of isomeric glyceryl ethers by soluble liver enzymes in a variety of species. Biochim Biophys Acta 144, 633-648, 1967.

Tumor Lipids: Metabolic Relations Derived from Structural Analyses of Acyl, Alkyl, and Alk-1-Enyl Moieties of Neutral Glycerides and Phosphoglycerides* †

Randall Wood and Fred Snyder

The composition of the hydrocarbon moieties of the 1-, 2-, and 3-positions of triglycerides and glyceryl ether diesters (GEDE) and of the 1- and 2-positions of diacyl and alkyl acyl phosphatidyl cholines (PC) and diacyl, alkyl acyl, and alk-1-enyl acyl phosphatidyl ethanolamines (PE) from Ehrlich ascites cells (EAC) was determined. The carbon number percentage distribution of triglycerides, GEDE, and the diglyceride-type acetates derived from each class of PC and PE was also determined by gas-liquid chromatography analysis of the intact lipids.

The fatty acid compositions of the 1-, 2-, and 3-positions of the triglycerides are different and also differ from the composition of the corresponding positions of the GEDE, which are not the same.

* Synopsis of complete article accepted for publication in Arch Biochem Biophys.

† Presented at the 12th International Conference on the Biochemistry of Lipids, Loughborough, England, September 8, 1968.

Both triglycerides and GEDE exhibit a 1-random-2-random-3-random type of distribution (Table 67).

The choline-containing phosphatides consist of approximately 66% diacyl PC and 33% alkyl acyl PC. Ethanolamine-containing phosphatides are composed of 55% diacyl PE, 30% alkyl acyl PE, and 15% alk-1-enyl acyl PE. The carbon chain of the 1-position of each PC and PE class is predominantly saturated and the 2-position is dominated by polyunsaturated fatty acids. All PC and

TABLE 67

Comparison of determined and calculated carbon numbers of triglycerides and glyceryl ether diesters from Ehrlich ascites cells

Glyceride	% Carbon number[a]								
	46	48	50	52	54	56	58	60	62
TG (Determined)[†]	0.4	1.3	6.9	21.7	32.4	19.1	13.2	3.8	1.1
Calc. (1-, 2-, 3-random distr.)[‡]	0.2	1.6	8.6	24.7	33.4	16.8	9.2	3.4	0.8
Calc. (PC diacyl Ac. + 3 Pos. TG)	0.1	1.5	8.5	24.7	33.4	17.5	9.7	3.4	0.8
Calc. (Diglyceride Ac. + 3 Pos. TG)	0.2	1.6	8.3	22.4	31.6	19.0	11.0	4.2	1.2
Calc. (PE diacyl Ac. + 3 Pos. TG)	T	0.2	3.0	18.8	42.4	19.8	10.9	4.0	0.8
GEDE (Determined)[†]	0.8	6.3	18.2	24.4	20.1	17.6	9.2	2.5	1.1
Calc. (1-, 2-, 3-random distr.)[‡]	1.0	6.0	16.1	22.8	21.4	17.6	9.8	3.5	1.2
Calc. (PC alkyl acyl Ac. + 3 Pos. GEDE)	1.0	5.9	15.2	22.5	23.8	18.1	9.1	3.3	0.9
Calc. (Free alkyl acyl + 3 Pos. GEDE)	0.9	6.0	16.5	23.9	22.6	16.7	9.0	3.1	1.0
Calc. (PE alkyl acyl Ac. + 3 Pos. GEDE)	T	0.9	6.9	18.6	27.2	25.2	14.2	5.3	1.7
Calc. (PE alk-1-enyl acyl Ac. + 3 Pos. GEDE)	T	0.9	7.4	19.2	27.3	24.6	13.6	5.1	1.6

TG = Triglycerides; GEDE = Glyceryl ether diesters; Ac. = Acetate.

[a]Determined values represent the mean of 3 analyses.

[†]Analyzed intact by GLC.

[‡]The 1-random-2-random-3-random distribution was calculated from the determined composition of the 1, 2, and 3 position of the glyceride.

PE classes except the alk-1-enyl acyl PE show a 1-random-2-random distribution.

In EAC, randomly synthesized diglycerides are apparently used randomly for triglycerides and diacyl PC biosynthesis, and the biosynthesis of GEDE and alkyl acyl PC from an alkyl acyl intermediate also occurs without selectivity. These observations are supported by the close agreement between the determined carbon number percentages of the triglycerides and of the glyceryl ether diesters and the percentages calculated from the respective diglyceride types and the fatty acids of the 3-position (Table 67). In contrast, we have shown that selectivity of diglycerides for the biosynthesis of triglycerides, PC and PE occurs in rat liver (See pp. 183-185). The similarities in composition at both the 1- and 2-positions between triglycerides and diacyl PC and between GEDE and alkyl acyl PC suggest a loss of selectivity of acyl CoA: lysophosphatide acyl transferase enzymes, which are present in normal tissue. Metabolic relations derived from structural analyses of acyl, alkyl, and alk-1-enyl moieties of glycerides and phosphoglycerides and from established pathways for acylation reactions

10275530

led to the proposal of a metabolic pathway for the biosynthesis of lipids containing glyceryl ethers (Fig. 80) in EAC. The suggestion of the glyceraldehyde-3-phosphate is based on other recent evidence[1] obtained in our laboratory.

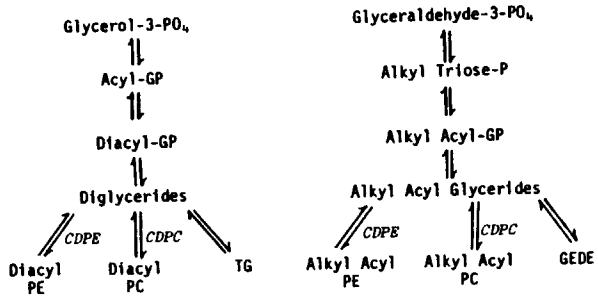

Fig. 80. Proposed metabolic pathway for the biosynthesis of glyceryl ether containing neutral glycerides and phosphoglycerides (right) and the established pathway for the biosynthesis of acyl glycerides (left).

REFERENCE

1. Snyder, F., Malone, B., and Wykle, R. L. The biosynthesis of alkyl ether bonds in lipids by a cell-free system. Biochem Biophys Res Commun 34, 40-47, 1969.

Rat Liver Lipids: Metabolic Relations Derived from Structural Analyses of Neutral Glycerides and Phosphoglycerides

Randall Wood and R. D. Harlow

The distribution of fatty acids esterified at each position of glycerol of the major lipid classes, triglycerides (TG), phosphatidyl choline (PC) and phosphatidyl ethanolamine (PE) of rat liver was determined. The carbon number distribution of triglycerides and diglyceride acetates derived from PC and PE was also determined (Fig. 81). Each of the triglyceride positions showed a distinct fatty acid distribution that was not arranged randomly, indicating pairing of some acids (Table 68). The composition of the fatty acids esterified at the 1-position of PC and PE was the same, but different from the 1-position of TG, and the composition of the 2-position was different in all three classes. The carbon number distribution of PC and PE diglyceride acetates was different and neither distribution agreed with the random distri-

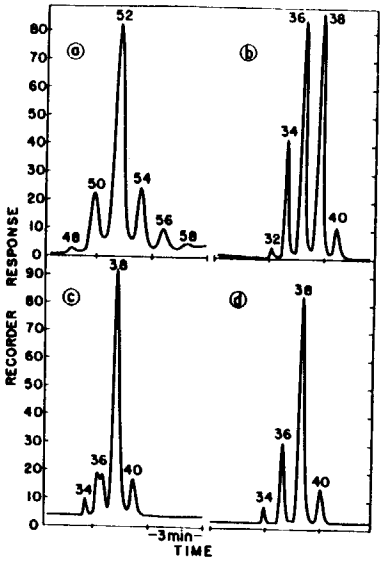

Fig. 81. Representative chromatograms (GLC) of triglycerides (a), hydrogenated PC diacyl acetates (b), unhydrogenated PE diacyl acetates (c), and hydrogenated PE diacyl acetates (d) of rat liver.

TABLE 68

STEREOSPECIFIC ANALYSIS OF RAT LIVER TRIGLYCERIDES[a]

Fatty Acid	Percentage and Std. Deviation 1-Position XI[†]	2-Position IX[‡]	3-Position XII[†]
14:0	1.8 ± 0.4	1.0 ± 0.3	0.4 ± 0.1
15:0	0.7 ± 0.2	0.1 ± 0.1	0.1 ± 0.1
16:0	57.2 ± 5.1	12.7 ± 5.6	12.1 ± 1.2
16:1	4.2 ± 0.1	2.9 ± 0.9	3.9 ± 0.4
17:0	0.8 ± 0.5	T	0.5 ± 0.1
17:1	0.3 ± 0.1	0.5 ± 0.1	0.6 ± 0.1
18:0	8.5 ± 1.3	3.5 ± 0.6	7.8 ± 0.5
18:1	21.9 ± 4.2	58.3 ± 6.9	60.9 ± 0.9
18:2	4.4 ± 1.2	19.2 ± 0.2	11.3 ± 1.6
20:1	T	0.5 ± 0.4	1.1 ± 0.7
20:4	--	0.9 ± 0.1	1.2 ± 0.3

[a] Means and standard deviations were calculated from duplicate analyses of three separate samples.

[†] Determined from 1,3-diglycerides

[‡] Determined from 1,2-diglycerides

1027531

bution values calculated from the determined compositions of the 1- and 2-positions of each class; this disagreement indicated pairing of some acids in these lipid classes also. The determined TG carbon number distribution did not agree with the distribution calculated from either PC or PE diglyceride acetates plus the 3-position of the TG which indicates selectivity of diglycerides used for the biosynthesis of either TG or phospholipids or both. These findings demonstrate a difference in lipid metabolism of tumor cells and normal tissue not reported previously: tumor cells do not show selectivity of diglycerides used for TG and PC biosynthesis, whereas rat liver does show diglyceride selectivity.

Preliminary Information Regarding the Occurrence of Ether-Linked Lipids in Tumors Induced by Diethylnitrosamine

N. K. Clapp and Fred Snyder*

In previous studies, most neoplasms of animal[1,2] and human[1,3] origin were shown to contain significant levels of alkyl and alk-1-enyl glyceryl ether diesters. Recent work indicated that ether-linked phosphoglycerides are also higher in neoplasms than in most normal cells.[2,3] So far, relatively high levels of ether lipids have been found in several nontransplantable spontaneous tumors and numerous transplantable tumors,[2] including those of viral origin. The purpose of this study was to determine the occurrence of glyceryl ethers in chemically induced tumors and to relate the findings to those from tumors previously studied.

Six male RF mice, which were given diethylnitrosamine (DEN) in the drinking water (6 mgm/kg body wt/day for 7 weeks), developed lung adenomas, liver hepatomas, and squamous cell carcinomas of the forestomach. These neoplasms were examined histologically and lipid analyses were performed as previously described.[1] Normal nontreated tissue and nontumorous tissues from mice given DEN were also analyzed by the same procedure. The tumors induced by DEN contained substantial quantities of ether-linked lipids in contrast to very low or undetectable amounts in control and treated nontumorous tissue. The ether-linked lipids in the neutral glyceride fraction of the stomach tumors appear as glyceryl ether diesters on thin-layer chromatograms. Stomach tumors that appeared more malignant histologically also contained higher amounts of glyceryl ether diesters. Lung and liver tumors were not large enough to yield adequate lipids for complete analysis. Further studies are in progress to confirm the impressions obtained in these preliminary results.

* Biology Division, Oak Ridge National Laboratory.

REFERENCES

1. Snyder, F., Cress, E. A., and Stephens, N. An unidentified lipid prevalent in tumors. Lipids 1, 381-386, 1966.

2. Snyder, F. and Wood, R. The occurrence and metabolism of alkyl and alk-1-enyl ethers of glycerol in transplantable rat and mouse tumors. Cancer Res 28, 972-978, 1968.

3. Snyder, F. and Wood, R. Alkyl and alk-1-enyl ethers of glycerol in a variety of normal and neoplastic tissues from humans. Cancer Res 29, 251-257, 1969.

Relations of Chain Lengths and Double Bond Locations in O-Alkyl, O-Alk-1-enyl, Acyl, and Fatty Alcohol Moieties in Preputial Glands of Mice*

Fred Snyder and M. L. Blank

Wax esters, glyceryl ether diesters, triglycerides, and sterol esters are the major lipid classes present in normal preputial glands of mice (Table 69). Small amounts of phosphatidyl choline (PC) and phosphatidyl ethanolamine (PE) were also found. Three-fourths of the PE fraction was comprised of alk-1-enyl ethers, whereas most of the PC fraction (≈90%) was present in the diacyl form. The ether linkage was found to be at the 1-position of glycerol.

The chain lengths of the alkyl and alk-1-enyl hydrocarbon moieties of glyceryl ether diesters, phosphatidyl choline, and phosphatidyl ethanolamine were similar to one another and to the alcohol moieties of the waxes. Principal hydrocarbon chains in ether linkage with glycerol were 14:0, 14:1, 16:0, and 16:1 (Table 70).

The location of double bonds in the acyl, alkyl, and alk-1-enyl hydrocarbon moieties of the various lipid classes was determined by gas-liquid chromatography of the aldehyde fragments produced by reductive-ozonolysis (Table 71). The 18:1 acyl moieties from the triglycerides and waxes consisted primarily of the Δ-9 isomer, but small amounts of the Δ-11 isomer were also found. The 16:1 acyl moieties of triglycerides were also mainly the Δ-9 isomer, whereas in waxes the 16:1 acyl moieties were equally divided between Δ-6 and Δ-9 isomers.

* Supported by the American Cancer Society (Grant No. P-470).

1027532

TABLE 69

Lipid Class Composition of Preputial Glands in Mice*

Lipid class	% of total lipids
Sterol esters	5
Waxes	48
Alk-1-enyl GEDE	8
Alkyl GEDE	6
Triglycerides	17
Free fatty acids	tr
Sterols + diglycerides	3
GEME†	1
Alk-1-enyl PE	2
Alkyl PE	tr }
Diacyl PE	tr } about 1%
Alk-1-enyl PC	tr }
Alkyl PC	tr }
Diacyl PC	6
Other phospholipids‡	3

*A duplicate analysis of a pooled sample (100 glands).

†Consisted of a ratio of 1.7 alk-1-enyl to alkyl glyceryl ethers, entirely 1-isomer.

‡Included traces of sphingomyelin, phosphatidyl serine, and phosphatidyl inositol.

TABLE 70

Percentage Composition (Wt. %) of Acyl, Alkyl, Alk-1-enyl, and Alcohol Hydrocarbon Moieties in Lipid Classes of Normal Preputial Glands of Mice

Lipid class chain	TG	WAX		GEDE			PC		PE	
	Acyl	Acyl*	Alcohol*	Alkyl	Alk-1-enyl	Acyl*	Alkyl + alk-1-enyl (hydrogenated)	Acyl	Alkyl + alk-1-enyl (hydrogenated)	Acyl
less than 14:0	3	6	tr	3	4	10	2	--	2	--
14:0	2	1	4	25	24	6	30	1	31	1
14:1	) 4	7	10	12	9	9	) 5	1	) 8	1
15:0		3	3	5	8	15†		tr		tr
16:0	23	11	69	48	43	28	57	37	50	14
16:1	5	22	9	7	10	12	--	13	--	7
17:0	2	6	tr	tr	tr	tr	tr	tr	3	tr
18:0	6	6‡	4	1	1	2	6	6	6	12
18:1	30	16	tr	tr	1	7	--	23	--	22
18:2	23	5	--	--	--	1	--	6	--	6
18:3	2	1	--	--	--	2	--	tr	--	tr
20:0	--	9	--	--	--	2	--	tr	--	tr
20:3	tr	) 7	--	--	--	1	--	1	--	4
20:4	tr		--	--	--	6	--	11	--	34
22:X	tr	tr	--	--	--	tr	--	tr	--	tr

*The retention times of certain acyl moieties in these fractions indicate the presence of branched-chain fatty acids.

†GLC analysis after argentation TLC indicated that the major proportion (13%) of this quantity was a 13:2 chain.

‡GLC analysis after argentation TLC indicated that the major proportion (4.5%) of this quantity was a 17:2 chain.

TABLE 71

Position of Double Bonds in Acyl, Alkyl, and Hydrocarbon Moieties in Triglycerides, Waxes, and Glyceryl Ether Diesters of Preputial Gland Lipids

		TG	WAXES		GEDE
		Acyl	Acyl	Alcohols	Alkyl
		Wt. %			
18:1	Δ 8	1	tr	Insufficient sample	
	Δ 9	91	92		
	Δ11	8	8		
16:1	Δ 5	--	2	4	tr
	Δ 6	--	42	67	57
	Δ 7	10	5	17	13
	Δ 8	8	1	tr	6
	Δ 9	80	49	12	24
	Δ10	tr	tr	--	--
	Δ11	3	--	--	--
14:1	Δ 4	Insufficient sample	4	tr	tr
	Δ 5		29	74	56
	Δ 6		41	26	37
	Δ 7		2	--	tr
	Δ 8		4	--	tr
	Δ 9		20	--	7

Location of double bonds in the 16:1 and 14:1 alcohol and acyl moieties of waxes and the alkyl moieties of glyceryl ether diesters was similar. The 16:1 fraction was comprised mainly of the Δ-6 isomer and smaller quantities of the Δ-7 and Δ-9 isomers. The Δ-5 and Δ-6 isomers accounted for more than 90% of the 14:1 chains in the fatty alcohols of waxes and in the alkyl moieties of glyceryl ether diesters; the acyl moieties of waxes contained approximately 70% of these isomers.

The data indicate that in preputial glands of mice the intermediary pathways or enzymatic sites responsible for the biosynthesis of fatty alcohol, and to some extent fatty acids, in the waxes must be identical to those pathways or sites responsible for the biosynthesis of the alkyl chains of glyceryl ether diesters. The similarities of alkyl and alk-1-enyl ether-linked hydrocarbon moieties suggest that these two classes of lipids can be interconverted enzymatically.

Lipid Composition and the Presence of Inclusion Bodies in Mitochondria of the Mouse Preputial Gland*

Gail Sansone, D. C. Swartzendruber, and Fred Snyder

Intramitochondrial inclusion bodies, characterized as electron-dense, round or globular, and extremely osmophilic, have been described in various tissues.[1,2] The composition of these bodies is unknown. This note describes similar inclusion bodies found in high concentrations in the mitochondria of preputial glands of mice.

* Supported in part by the American Cancer Society (Grant No. P-470).

1027533

Preputial glands were obtained from male and female ICR strain

Fig. 82. Electron micrographs of thin sections of mitochondrial pellets fixed in 2.5% gluteraldehyde buffered with 0.1 M sodium cacodylate, pH 7.2, postfixed in 1% OsO_4, pH 7.2, and embedded in Epon 812. Thin sections were first stained with aqueous uranyl acetate and then with lead citrate. A. Section of a mitochondrial pellet from mouse preputial glands. Note the dense, osmophilic intramitochondrial granules, ranging in size from approximately 100 mμ to 200 mμ. These granules do not appear to have a membrane, and their electron density is not appreciably affected by staining with lead citrate or uranyl acetate (40,400 x). B. Section of a mitochondrial pellet from preputial gland tumors illustrates the lack of dense granules (40,800 x).

TABLE 72

Lipid Composition of Mitochondria Isolated from Preputial Glands and Preputial Tumors

Lipid Fractions	% of Total Lipid Extracted	
	Gland	Tumor
TOTAL NEUTRAL LIPIDS*	25.4	16.7
Sterol esters	---	1.2 ± 0.5
Wax esters	10.4 ± 1.0	1.5 ± 0.7
Neutral plasmalogen	1.9 ± 0.8	---
Glyceryl ether diester	2.6 ± 0.3	---
Triglyceride	2.8 ± 0.2	2.6 ± 0.9
Fatty acid	0.2 ± 0.04	0.9 ± 0.06
Fatty alcohol	0.4 ± 0.03	---
Sterols	7.6 ± 0.9	10.2 ± 0.1
Unidentified	0.7	0.3
TOTAL POLAR LIPIDS†	74.6	83.3
Cardiolipin (phosphatidic acid area)	9.7	14.0
Phosphatidylethanolamine	25.4	26.7
Phosphatidylinositol + phosphatidylserine	4.3	4.0
Phosphatidylcholine	31.5	33.3
Unidentified	3.7	5.3

* Mean values of duplicate samples from 3 separate preparations. The ± values represent standard deviations.

† Based on a duplicate phosphorus determination of one mitochondrial preparation of each tissue.

mice (bred randomly) ranging in age from 2 to 8 weeks. Transplantable preputial tumors (ESR-586) were also examined. The mitochondrial pellets from the glands and the tumors were obtained by the procedure of O'Brien and Kalf.[3] The mitochondrial inclusion bodies occurred in high concentrations in the preputial glands of all mice tested. The tumor mitochondria contained very few intramitochondrial granules but were otherwise morphologically similar; therefore, preparations of the tumor were used for comparison with the preputial gland tissue with its plentiful granules. The extreme osmiphilia indicated that the inclusion bodies were lipid. The total lipids were extracted and thin-layer chromatography was used to resolve the lipid constituents of the mitochondrial fractions from both tissues. The various classes were quantitated by photodensitometry[4] and phosphorous analyses.[5]

The results given in Table 72 show that the preputial gland mitochondria contained 23% total lipids and the tumor contained 16% total lipids when calculated on a dry weight basis. The preputial mitochondria contained 26% neutral lipid, whereas the tumor mitochondria contained only 17%. The preputial gland mitochondria contained primarily waxes and smaller quantities of sterols, glyceryl ether diesters, and triglycerides. In contrast, the tumor mitochondria contained only minor amounts of neutral lipids except for free sterols, and the quantity of these was similar to that found in the gland mitochondria. The data suggest that the mitochondrial inclusion bodies in the preputial gland may be composed mainly of waxes, a major constituent of the gland. See Fig. 82.

1027534

REFERENCES

1. Setala, K., Merenmies, L., Niskanen, E. E., Nyholm, M., and Stjernvall, L. Mechanism of experimental tumorigenesis. VI. Ultrastructural alterations in mouse epidermis caused by locally applied carcinogen and dipole-type tumor promotor. J Nat Cancer Inst 25, 1155-1189, 1960.

2. Minick, O. T., Kent, G., Orfei, E., and Volini, F. I. Non-membrane enclosed intramitochondrial dense bodies. Exp Mol Pathol 4, 311-319, 1965.

3. O'Brien, T. W. and Kalf, G. F. Ribosomes from rat liver mitochondria. I. Isolation procedure and contamination studies. J Biol Chem 242, 2172-2179, 1967.

4. Privett, O. S. and Blank, M. L. Charring conditions for the quantitative analysis of mono-, di-, triglycerides by thin-layer chromatography. J Amer Oil Chem Soc 39, 520, 1962.

5. Rouser, G., Siakotos, A. N., and Fleischer, S. Quantitative analysis of phospholipids by thin-layer chromatography and phosphorus analysis of spots. Lipids 1, 85-86, 1966.

Lipid Class Composition of Several Rat and Mouse Tumors

Randall Wood and Fred Snyder

A number of transplantable rat and mouse tumors have been analyzed in this laboratory to determine the percentage of alkyl and alk-1-enyl glyceryl ethers present in the neutral and phospholipids.[1] The results showed that the neutral lipids contained higher percentages of alkyl glyceryl ethers than normal tissue.[2] The phospholipids of the various tumors also contained levels of alkyl and alk-1-enyl glyceryl ethers comparable to the values obtained for certain normal tissues that are rich in glyceryl ethers.[2] To determine the distribution of the ether-linked lipids among the various lipid classes, it was necessary to first determine the lipid class composition. This report compares the composition

of the major lipid classes of eleven transplantable rat and mouse tumors.

The rearing of the tumor-bearing animals, removal of the tumors, and the lipid extraction procedures have been described previously.[2] Quantitative photodensitometric thin-layer chromatography analysis of each lipid class was carried out as reported earlier.[3] Total lipid concentrations of the samples were determined gravimetrically with a microbalance.[2] Standards and samples were spotted alternately in quadruplets and developed in the appropriate solvent system. Neutral lipids were developed in a hexane:diethyl ether:acetic acid (80:20:1 v/v) solvent system, and phospholipids were developed in a chloroform:methanol:acetic acid:isotonic saline (75:25:8:4 v/v) solvent system. Percentages represent the mean of four determinations of a large composite sample.

The percentages of ten lipid classes of the eleven tumors are given in Table 73. The percent recovery column (Table 73) shows

TABLE 73

Comparison of Lipid Class Percentages of Several Rat and Mouse Tumors

Tumor	% Lipid Class*									
	Chol E.†	TG	FFA	Chol.	PC	PE	PS+ PI	Lyso PC	Sphingo.	% Recovery
Sarcoma 180	2	15	40	19	8	5	2	1	5	97
Melanoma B16	1	38	2	3	40	10	5		3	102
Carcinoma E0771	2	14	3	4	32	9	2	2	3	70
Sarcoma T-241	2	55	10	11	15	3	1	T	2	98
Taper liver tumor	1	5	3	5	61	11	1	2	2	93
Friends virus leukemia	2	2	4	6	54	20	2	2	3	94
KHZ mammary tumor	1	54	1	8	21	2	8	T	3	97
Ehrlich ascites carcinoma	4	10	1	8	34	12	3		8	79
Walker 256	1	8	2	4	46	12	8	3	3	87
Fischer R3259	1	20	5	7	62	3	3	4	2	106
Fibroadenoma after 800 R TBI	3	41	2	15	11	4	2	1	3	82

*Percentages represent the mean of four photodensitometric determinations.

†Chol. E. = cholesterol esters; TG = triglycerides; FFA = free fatty acids; Chol. = cholesterol; PC = phosphatidyl choline; PE = phosphatidyl ethanolamine; PS = phosphatidyl serine; PI = phosphatidyl inositol; Lyso PC = lysophosphatidyl choline; Sphingo. = sphingomyelin.

the percentage of the total lipids that the sum of the 10 classes analyzed represents. Some of the tumors contained up to 30% lipids belonging to other lipid classes than those analyzed, but for the most part the 10 classes represented more than 90% of the total lipids. Triglycerides, phosphatidyl choline, and phosphatidyl ethanolamine are the three major lipid classes that usually represent more than 60% of the total lipids. Cholesterol was the next largest lipid class

1027535

followed by the other classes that represented less than 10% of the total in most cases. Each tumor is characterized by a distinct lipid class composition (Table 73). No correlation appears among the compositions of a single tumor type. The origin of the tumor, rate of growth, loss of certain enzymes, etc., probably account for the observed heterogeneity of lipid class composition.

REFERENCES

1. Snyder, F. and Wood, R. The occurrence and metabolism of alkyl and alk-1-enyl ethers of glycerol in transplantable rat and mouse tumors. Cancer Res 28, 972-978, 1968.

2. Wood, R. and Snyder, F. Quantitative determination of alk-1-enyl- and alkyl-glyceryl ethers in neutral lipids and phospholipids. Lipids 3, 129-135, 1968.

3. Privett, O. S., Blank, M. L., Codding, D. W., and Nickell, E. C. Lipid analysis by quantitative thin-layer chromatography. J Amer Oil Chem Soc 42, 381-393, 1965.

Lipid Metabolism in Cells Grown in Tissue Culture: O-Alkyl, O-Alk-1-enyl, and Acyl Moieties of L-M Cells*

Robert E. Anderson, Robert B. Cumming†, Marva Walton†, and Fred Snyder

The lipid composition of L-M cells, a variant of L-cells, grown in a lipid-free, chemically defined medium and in this medium plus 10% horse serum has been determined (Table 74). The lipid classes of the L-M cells grown on horse serum are quantitatively similar to those of the L-M cells grown on the chemically defined medium; the lipid composition of the cells grown under both conditions is different from that of the horse serum. However, L-M cells utilize fatty acids from the serum since large levels of linoleic acid are found in the lipid classes of those cells grown on horse serum (Table 75).

The L-M cells and the tumors induced by injecting L-M cells

* Supported in part by the American Cancer Society (Grant No. P-470) and by USAEC under contract with the Union Carbide Corporation.

† Biology Division, Oak Ridge National Laboratory.

TABLE 74

GLYCERYL ETHER CONTENT OF LIPIDS OF HORSE SERUM AND L-M CELLS*

Lipid class	O-Alkyl glycerol %	O-Alk-1-enyl glycerol %	Total glyceryl ether %
a) Serum			
NL	nd†	nd	nd
PL	2.8	2.3	5.1
b) L-M cells grown with 10% serum			
NL	5.6	nd	5.6
PL	6.0	6.3	12.3
PC	2.4	t **	2.4
PE	7.7	8.8	16.5
c) L-M cells grown without serum‡			
NL	18.4 (17.0-19.7)	nd	18.4
PL	7.0 (5.4-8.5)	8.9 (8.7-9.0)	15.9
PC	4.0 (3.1-4.8)	nd	4.0
PE	5.7 (4.2-7.1)	10.4 (8.8-11.9)	16.1
d) L-M Tumor Male Mice§			
NL	5.7 ± 1.8 (8)	1.5 ± 0.3 (8)	7.2
PL	7.5 ± 2.4 (8)	6.6 ± 2.7 (8)	14.1
e) L-M Tumor Female Mice§			
NL	7.2 ± 5.1 (9)	1.8 ± 1.5 (9)	9.0
PL	9.0 ± 3.3 (9)	5.4 ± 4.8 (9)	14.4

* Average of duplicate analyses of $LiAlH_4$ reduction products (18), as described in text.

† nd means none was detectible; t represents trace (less than 0.1%).

‡ Average of two different cell harvests. Range given in parentheses.

§ The number in parentheses is the number of animals used. The values preceded by ± are standard deviation.

into mice are rich sources of glyceryl ethers. Glyceryl ether diesters are most abundant in the L-M cells grown on the chemically defined medium (20% of the neutral lipids), whereas the tumors contain approximately 8% glyceryl ether diesters in the neutral lipid fraction (Table 74). The phospholipids of L-M cells grown with and without serum and of L-M tumors contain near equal percentages of glyceryl ethers (12.3-15.9%). The hydro-

1027536

carbon side chains of O-alkyl and O-alk-1-enyl glycerols consist almost entirely of palmitic, stearic, and oleic acid analogues (Table 76).

TABLE 75

FATTY ACID COMPOSITION OF THE LIPID CLASSES OF L-M CELLS AND HORSE SERUM

	L-M Cells grown with horse serum					L-M Cells grown in chemically defined medium					Horse serum			
Fatty acid	TG	CEDE	FFA	PE	PC	TG	CEDE	FFA	PE	PC	CE	TG	FFA	PC
	Area %													
14:0	4.3	7.6	2.9	0.2	0.8	7.0	14.5	7.1	1.3	4.0	t	1.5	1.1	t
14:1+15:0	1.3	1.5	0.4	0.3	t	1.0	2.0	1.1	0.2	1.1	t	0.3	t	t
16:0	16.8	24.5	17.5	3.0	14.0	16.4	26.0	20.9	5.9	19.6	9.9	33.8	21.6	14.6
16:1	4.4	4.2	4.7	1.9	6.2	9.5	8.2	14.7	13.2	20.1	0.9	1.4	1.4	t
17:1	0.1	t	0.2	0.3	0.3	0.4	0.1	0.7	0.8	1.1	t	t	t	t
18:0	16.1	12.6	21.1	15.3	15.5	10.4	7.0	8.9	11.0	5.8	0.3	6.3	12.7	29.3
18:1	38.3	33.4	39.1	39.6	30.6	48.6	32.3	46.0	65.0	48.5	10.9	44.9	22.2	11.4
18:2	12.7	7.7	11.4	35.1	30.9	t	0.2	t	t	t	76.7	9.3	30.0	44.1
20:0	0.4	1.2	t	t	t	0.5	1.7	1.1	0.9	nd†	nd	2.4	9.0	0.4
18:3+20:1	1.5	1.5	1.8	1.7	0.8	1.3	1.2	t	1.1	t	nd	nd	nd	nd
20:2	0.2	0.2	0.4	0.4	0.6	t	t	nd	nd	nd	nd	nd	nd	nd
20:3	1.2	1.5	0.2	0.4	t	2.2	1.0	nd	nd	nd	nd	nd	nd	nd
20:4	0.7	0.7	0.5	1.6	0.5	0.2	0.5	nd	nd	nd	1.2	nd	nd	t
>20:4	2.0	3.5	nd	0.2	nd	3.4	6.0	nd	nd	nd	nd	nd	nd	nd
Total Saturates	37.6	45.9	41.5	18.5	30.3	34.3	49.2	38.0	19.1	29.4	10.2	44.0	44.4	44.4
Total Unsaturates	62.4	54.2	58.5	81.5	69.9	65.7	50.8	62.0	80.9	70.8	89.7	55.9	55.6	55.5

* t represents trace (less than 0.1%).

† nd means none was detectible.

TABLE 76

O-ALKYL AND O-ALK-1-ENYL SIDE-CHAIN COMPOSITION OF THE LIPID CLASSES OF HORSE SERUM AND L-M CELLS

Ether chain length	L-M Cells grown in chemically defined medium			L-M Cells grown with horse serum				Horse serum*	
	NL	PC O-Alkyl	PE O-Alkyl	PE O-Alk-1-enyl	NL	PC O-Alkyl	PE O-Alkyl	PE O-Alk-1-enyl	PC O-Alkyl	PE O-Alk-1-enyl
14:0	0.9	2.9	t†	1.4	t	4.2	t	t	7.6	0.7
15:0	0.2	0.7	t	t	nd‡	0.1	t	nd	2.4	0.2
16:0	29.1	41.6	22.7	36.3	25.3	40.8	25.2	48.8	59.2	59.2
16:1	0.2	5.1	t	t	t	2.0	t	t	2.1	8.1
17:0	t	t	t	0.3	nd	nd	t	t	t	t
17:1	t	t	nd	0.8	nd	t	t	t	t	t
18:0	20.3	5.5	17.9	12.1	30.4	11.8	37.5	26.7	3.3	13.8
18:1	49.2	44.4	59.4	48.7	41.5	40.7	37.3	24.6	23.1	11.4
18:2	nd	nd	t	nd	2.8	0.6	t	t	t	t

* A peak in the area of 16:0 br appeared in the serum O-alkyl and O-alk-1-enyl glycerols with an area percent of 2.3 and 6.7, respectively.

† t represents trace (less than 0.1%).

‡ nd means none was detectible.

Alkyl and Alk-1-enyl Glyceryl Ethers Derived from Various Rat Tissue Phospholipids

Randall Wood, R. D. Harlow, and Fred Snyder

The wide-spread occurrence of alkyl and alk-1-enyl glyceryl ethers in nature has been well documented. Recently, we described a method for the quantitative determination of alkyl and alk-1-enyl glyceryl ethers of neutral lipids and phospholipids in which it was demonstrated that the phospholipids of certain normal rat tissues contain substantial quantities of glyceryl ethers.[1] The alkyl and alk-1-enyl glyceryl ethers derived from the total phospholipids of five rat tissues (brain, heart, femoral muscle, spleen, and bone marrow) were examined in more detail with the use of a combination of gas-liquid chromatography (GLC) and thin-layer chromatography (TLC) analytical techniques.

Alkyl and alk-1-enyl glyceryl ether percentages of the total phospholipids of the five rat tissues examined here have previously been determined.[1] The percentage composition of the alkyl and alk-1-enyl glyceryl ethers derived from the total phospholipids of the various rat tissues is shown in Table 77. The 16:0, 18:0, and 18:1 hydrocarbon chains represent more than 95% of the total in both the alkyl and alk-1-enyl glyceryl ethers. In contrast to the fatty acid chain lengths found in the phospholipids of these tissues, only traces of glyceryl ethers with carbon chains longer than 18:1 were found. Analysis of the glyceryl ethers after hydrogenation showed the presence of the 19:0 glyceryl ether in approximately the same concentration as shown in Table 77 for the 18:2 + 19:0 column. The apparent absence of the 18:2 glyceryl ether indicates that the enzyme systems responsible for the biosynthesis of glyceryl ethers are restricted to saturated and monoenoic species.

Early investigations of alkyl glyceryl ethers found in elasmobranch fishes demonstrated that these compounds were 1-isomers. Since the early studies, many investigators have assumed without adequate proof that only the 1-isomer of the glyceryl ethers occurs in nature. Improved methods[2,3] now make it possible to determine isomeric form directly on small samples. In the present study the alkyl and alk-1-enyl glyceryl ethers of all five rat tissues studies were shown to be the 1-isomers.

The O-alkyl glyceryl ethers of the five tissues examined did not contain any detectable glyceryl thioethers. Analyses of the isopropylidene derivatives of the glyceryl ethers with the use of a gas chromatograph equipped with a flame photometric detector, capable of detecting nanogram quantities of sulfur, did not reveal the presence of any eluting sulfur compounds. Metabolic studies with ^{35}S and ^{14}C labeled glyceryl thioethers have revealed that S-ethers are also metabolized differently from O-ethers.[4] The present study indicates that the biosynthesis of glyceryl ethers

1027537

TABLE 77

Comparison of Percentage Composition of Alkyl and Alk-1-enyl Glyceryl Ethers Derived from Total Phospholipids of Various Rat Tissues

Tissue	Hydrocarbon Chain Length §* 14:0	15:0	16:0	16:1	17:0	17:1	18:0	18:1	18:2 19:0
Glyceryl Alkyl Ether Isopropylidenes†									
Muscle	T‡	T	53.0	T	T	0.5	24.1	22.0	T
Marrow	0.5	0.5	52.0	0.3	0.4	T	17.3	28.1	0.4
Spleen	0.7	2.2	51.3	0.5	0.4	0.3	20.1	23.7	0.6
Heart	0.3	0.6	40.0	0.3	0.3	T	16.3	41.8	0.6
Brain	0.3	T	41.4	T	T	T	26.0	32.4	T
Glyceryl Alk-1-enyl Ether Aldehydes§									
Muscle	T	1.8	48.0	0.6	2.1	1.0	25.0	21.6	0.4
Marrow	T	0.5	33.1	0.4	2.0	0.8	41.0	20.5	0.9
Spleen	T	0.7	38.5	T	2.4	1.0	30.3	25.7	0.8
Heart	T	0.4	40.1	1.2	1.9	0.7	32.6	22.2	0.6
Brain	T	T	23.3	T	1.2	T	42.6	32.7	T

* The agreement between duplicate determinations and between different samples was ± 5% for the major components and ± 10% for the minor components.

† Percentages represent the means of duplicate determinations on two different samples except marrow which represents the mean of duplicate determinations on a single sample.

‡ Trace represents less than 0.25%.

§ Percentages represent the means of duplicate determinations on three different samples except marrow, which represents the mean of duplicate analyses on two different samples.

in the rat is limited to the saturated and monoenoic species of O-alkyl 1-glyceryl ethers and O-alk-1-enyl 1-glyceryl ethers.

REFERENCES

1. Wood, R. and Snyder, F. Quantitative determination of alk-1-enyl- and alkyl-glyceryl ethers in neutral lipids and phospholipids. Lipids 3, 129-135, 1968.

2. Wood, R. and Snyder, F. Chemical and physical properties of isomeric glyceryl monoethers. Lipids 2, 161-171, 1967.

3. Wood, R. and Snyder, F. Gas-liquid chromatographic analysis of long chain isomeric glyceryl monoethers. Lipids 1, 62-72, 1966.

4. Snyder, F., Piantadosi, C., and Wood, R. The metabolism of glyceryl thioethers. Proc Soc Exp Biol Med (in press).

Insect Lipids: Triglyceride Carbon Number Distribution of Five Species

R. D. Harlow, Roger H. Lumb, and Randall Wood*

Gas-liquid chromatography (GLC) and thin-layer chromatography (TLC) have made it possible to examine in more detail the structure of triglycerides. Structural analyses of triglycerides isolated from normal and neoplastic tissues of mammals and from insects have been performed. The carbon number distribution of insect triglycerides was determined in an attempt to correlate changes in the triglyceride distribution with basic metamorphic changes. The carbon number distribution of triglycerides also gives some information on the biosynthesis of triglycerides. Insects are well suited to such studies because each metamorphic stage is well defined, development proceeds from one stage to the next in a relatively short time, and they synthesize large quantities of lipids.

The distribution of triglyceride carbon numbers and the triglyceride fatty acid composition of insects from four orders (Hymenoptera, Diptera, Lepidoptera, and Coleoptera) were determined. The experimental procedures have been described previously.[1]

The percentage of total lipids of the wet weight varied from 2.0 to 10.0% in the insects studied. The triglycerides usually represented more than 50% of the total lipids. The larvae, pupae, and adult stages of the blowfly (Phormia regina) and the flesh fly (Sarcophaga bullata) contained large percentages of palmitoleic acid (30 to 40%) but the other species contained small amounts of this acid. The adult bee (Apis mellifera) contained approximately 40% linolenic acid in contrast to the small percentage of this acid found in the larval stage. Oleic and palmitic acids were present in large amounts in all the insect triglycerides analyzed.

The triglyceride carbon number distribution of each species at various developmental stages is given in Table 78 along with the calculated random distribution values. (Equal distribution of each acid among all positions of the triglyceride is assumed in the random distribution calculations.) Carbon numbers ranged from 46 to 56 with 48, 50, and 52 usually predominating. In certain instances carbon number 48 increased from larva to adult and carbon number 52 decreased. The most drastic change in the carbon number distribution was observed between the larvae and adults of honey bees. The increase in carbon number 54 corresponds to an increase observed in the linolenic acid. The drastic difference in the carbon number distribution of Sarcophaga

* Department of Biology, Western Carolina University, Cullowhee, North Carolina

1027538

TABLE 78

Triglyceride Carbon Number Distribution of Various Insect Species

Insect			Carbon Number Percent[a]					
Scientific Name	Common Name	Stage	46	48	50	52	54	56
Apis mellifera	Honeybee	Larva		4.5	45.5	45.5	4.5	
Calc.[†]			*1.6*	*12.3*	*33.2*	*37.3*	*14.9*	
Apis mellifera	Honeybee	Adult			7.2	52.9	38.9	1.0
Calc.			*0.6*	*2.4*	*15.7*	*40.8*	*37.2*	
Sarcophaga bullata	Flesh fly	Larva	0.2	14.0	43.9	35.1	6.8	
Calc.			*1.6*	*16.6*	*38.1*	*32.7*	*9.7*	
Sarcophaga bullata	Flesh fly	Pupa	1.8	21.9	52.6	23.0	0.7	
Calc.			*3.2*	*20.1*	*37.6*	*27.8*	*7.1*	
Sarcophaga bullata	Flesh fly	Adult	3.0	29.7	46.2	20.0	1.1	
Calc.			*2.7*	*27.5*	*41.8*	*22.6*	*4.2*	
Phormia regina	Blowfly	Larva	2.1	28.7	55.3	13.9		
Calc.			*6.1*	*31.3*	*39.5*	*19.0*	*3.1*	
Phormia regina	Blowfly	Pupa	5.2	38.0	47.6	9.2		
Calc.			*8.4*	*36.2*	*36.9*	*14.3*	*1.9*	
Phormia regina	Blowfly	Adult	11.6	41.3	36.1	10.2	0.5	
Calc.			*11.2*	*28.6*	*32.3*	*16.4*	*3.1*	
Galleria sp	Waxmoth	Larva		0.4	32.6	56.6	10.1	0.3
Calc.			*0.2*	*7.9*	*29.0*	*36.5*	*15.5*	
Photinus pyralis	Firefly	Adult			1.1	20.7	67.7	10.5
Calc.				*0.4*	*3.6*	*22.5*	*67.9*	
Sarcophaga and *Phormia* Diet[‡]			6.3	8.6	11.2	9.2	4.2	

[a]Percentages represent the mean of duplicate analyses.

[†]Random distribution calculated from triglyceride fatty acid analyses.

[‡]60.5% of the diet triglycerides contained carbon numbers shorter than 46.

and Phormia at various stages on the same diet (Table 78, bottom row) shows that triglyceride biosynthesis in these two species is not influenced by dietary lipids. In general, the calculated random carbon number distribution does not agree with the determined percentages, suggesting selective esterification of fatty acids at specific positions of the triglyceride molecule.

These results show that each insect species is characterized by a particular fatty acid composition and a specific triglyceride carbon number distribution that changes with each metamorphic stage. The results further suggest that a nonrandom distribution of fatty acids occurs during biosynthesis of triglycerides in insects.

REFERENCE

1. Wood, R., Harlow, R. D., and Lambremont, E. N. GLC analysis of Heliothis virescens triglycerides at various metamorphic stages. Lipids (in press).

The Determination of the Position of Double Bonds in Naturally Occurring Alkyl Glyceryl Ethers* †

M. L. Blank and Fred Snyder

A method based on reductive ozonolysis[1] was adapted for locating double bond positions in the hydrocarbon moieties of intact glyceryl ethers. The procedure includes the preparation of isopropylidene derivatives of the alkyl glyceryl ethers and their resolution according to degree of unsaturation by argentation chromatography. After reductive ozonolysis of the isopropylidenes, the cleavage products are subsequently separated and identified by gas-liquid chromatography. The procedure has been applied to the analyses of commercially available selachyl (Δ9 octadecyl) alcohol isolated from ratfish liver and to alkyl glyceryl ethers isolated from preputial glands of mice. Mouse preputial glands contain unusually high quantities of alkyl glyceryl ether diesters, waxes, and triacylglycerols. The locations of the double bonds in the main alkyl ether side chains were 16:1 (Δ6,Δ7,Δ8,Δ9), and 14:1 (Δ5, Δ6,Δ9). The positions of double bonds and the chain lengths in fatty alcohols liberated from wax esters were similar to those of the alkyl ether chains, whereas the fatty acids liberated from triacylglycerols were strikingly different.

* Supported in part by the American Cancer Society (Grant No. P-470).

† Presented at the Annual Meeting of the American Oil Chemists' Society, New York, New York, October 21-23, 1968.

REFERENCE

1. Privett, O. S. and Nickell, E. C. Determination of structure of unsaturated fatty acids via reductive ozonolysis. J Amer Oil Chem Soc 39, 414-419, 1962.

1027539

Analysis of Dialkyl Glycerol Ethers and Related Glycerides by Gas-Liquid Chromatography

Randall Wood, W. J. Baumann, Fred Snyder, and H. K. Mangold**

Dialkyl ethers of glycerol are known to be constituents of various biological materials, in which they occur as phospholipids. Marinetti et al.[1] obtained evidence suggesting the presence of 1,2-dialkyl glycerol ethers in hydrolysates of hydrogenated bovine heart lipids, and Popović[2] detected the same compounds in human heart muscle. More recently, evidence for the occurrence of dialkyl glycerophosphatides in rat brain was reported.[3] Sehgal, et al.[4] isolated bis-dihydrophytyl glycerol ether from the lipids of Halobacterium cutirubrum where they occur as glycerophosphatides.[5,6] Except with the halophilic bacteria, the diethers have not been conclusively identified and characterized mainly because of inadequate analytical methods.

A series of dialkyl glyceryl ethers were synthesized at the Hormel Institute, Austin, Minnesota. Such a homologous series is ideally suited for studying the gas-chromatographic behavior of these compounds and for developing methods for their analysis. We examined the dialkyl glyceryl ethers and related partial glycerides and source of their derivatives by gas-liquid chromatography (GLC) and thin-layer chromatography (TLC) in an attempt to develop a method for the quantitative analysis of these compounds.

Dialkyl glycerol ethers, alkyl glycerol ethers, and glycol monoethers, which can be obtained from naturally occurring lipids by hydrolysis, or by reduction with lithium aluminum hydride, are well resolved from each other by adsorption chromatography. The thin-layer chromatogram (see Fig. 83) depicting the separation of disubstituted glycerols and related lipids demonstrates, however, that 1-alkyl, 2-acyl glycerols overlap with 1,3-diglycerides. The lipid classes isolated by TLC can be further resolved by GLC.

The trimethylsilyl ethers (TMS) and acetates of dialkyl, alkyl acyl, and diacyl glycerols were analyzed by GLC under conditions similar to those we have used for the analysis of triglycerides. When mixtures of derivatives of isomeric diacyl glycerols (1,2- and 1,3-diglycerides) were chromatographed, broadened or shouldered peaks were obtained, but complete resolutions could not be achieved. Mixtures of derivatives of 1,2- and 1,3-alkyl acyl glycerols behaved in an analogous manner. The TMS derivatives of dialkyl glycerol ethers have retention times identical to those of the diglyceride derivatives having two fewer methylene groups. The acetates of dialkyl glycerol ethers and diglycerides, however, can, as a rule, be

* The University of Minnesota, The Hormel Institute, Austin, Minn.

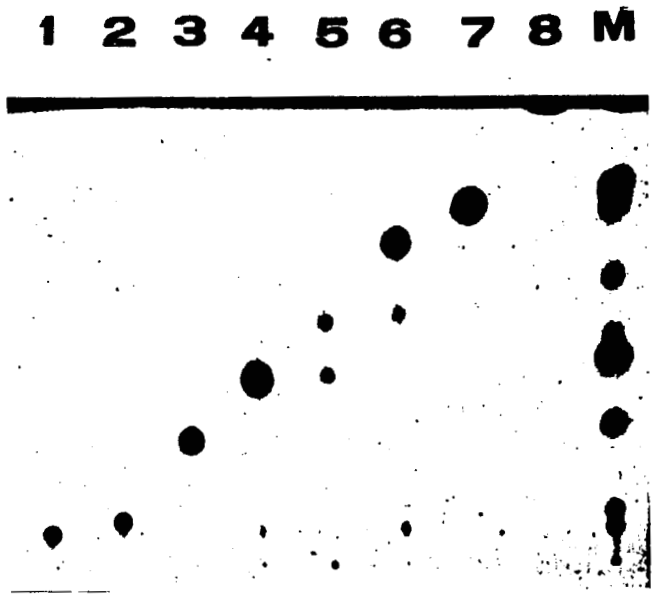

Fig. 83. Thin-layer chromatogram of dialkyl, alkyl acyl, and diacyl glycerols and related lipids: (1) 1-monopalmitin, (2) glycerol 1-hexadecyl ether, (3) glycol monomyristin, (4) tetradecyl glycol ether, (5) 1,2- and 1,3-dipalmitin (1,2-isomer is the lower spot), (6) 1-octadecyl-2- and 3-hexadecanoyl glycerols (1,2-isomer is the lower spot), (7) 1-octadecyl-2-hexadecyl glycerol ether, (8) tripalmitin, and (M) mixture of 1-8. For experimental conditions see text.

separated within each class and from each other. The TMS derivatives and acetates of alkyl acyl glycerols are eluted between those of the dialkyl glycerol ether of the same carbon number and the next higher homologue, and between the diglyceride of the same carbon number and the preceding homologue.

On the nonpolar stationary phase used in this investigation, the TMS derivatives and acetates of diglycerides have been similar retention times and cannot be separated from each other. However, the TMS derivatives of 1,2-dialkyl glycerol ethers are eluted ahead of the corresponding acetates despite the higher molecular weight of the TMS derivatives.

Gas chromatographic analyses of both TMS derivatives and acetates of 1,2-dialkyl glycerol ethers give accurate and reproducible results. As shown in Table 79 the "area percentages" found resemble more closely the weight percentages than mole percentages. The two derivatives are equally suitable for the quantification of alkyl acyl and diacyl glycerols.

1027540

TABLE 79

Quantitative determination of 1,2-dialkyl glycerol ethers as trimethylsilyl derivatives and acetates by gas-liquid chromatography*

Chain Length		Carbon Number	Trimethylsilyl Ethers			Acetates		
1-Position	2-Position		Weight %	Mole %	Found %†	Weight %	Mole %	Found %†
18	12	30	16.8	18.7	17.0	18.1	20.0	18.1
16	16	32	8.6	9.1	8.6	14.5	15.2	15.3
18	16	34	23.3	23.5	22.8	24.9	24.9	24.9
18	18	36	19.8	19.1	21.4	17.7	16.9	18.8
18	20	38	31.5	29.6	30.6	24.8	23.1	22.8

*Analyses were carried out on a Pyrex column packed with 1% OV-1. The temperature was programmed from 150-285°C at approximately 5°/min.

†Percentages found represent the mean of three determinations.

REFERENCES

1. Marinetti, G. V., Erbland, J., and Stotz, E. The structure of beef heart plasmalogens. J Amer Chem Soc 81, 861-864, 1959.

2. Popović, M. Über die glycerinäther des menschlichen herzmuskels. Z Physiol Chem 340, 18-23, 1965.

3. Horrocks, L. A. and Ansell, G. B. Studies on the phospholipids of rat brain which contain glyceryl ethers. Biochim Biophys Acta 137, 90-97, 1967.

4. Sehgal, S. N., Kates, M., and Gibbons, N. E. Lipids of Halobacterium cutirubrum. Can J Biochem Physiol 40, 69-81, 1962.

5. Kates, M., Sastry, P. S., and Yengoyan, L. S. Isolation and characterization of a diether analog of phosphatidyl glycerophosphate from Halobacterium cutirubrum. Biochim Biophys Acta 70, 705, 1963.

6. Faure, M., Marechal, J., and Troestler, J. Les phosphatides éther des bactéries halophiles. Sur la présence d'un acide pyrophosphatidylglycérophosphorique chez Halobacterium cutirubrum. Compt Rend 257, 2187-2190, 1963.

Gas-Liquid Chromatographic Analyses of 1,2- Ethanediol Monoethers and Monoesters

*Randall Wood and W. J. Baumann**

The occurrence of natural lipids in which the alcoholic moiety consists of short-chain diols, such as 1,2-ethanediol, propanediols, or butanediols instead of glycerol, has been recognized only very recently.[1] The separation of diol lipids from the bulk of lipid material is extremely difficult and their presence has been demonstrated by indirect means only. Intact individual classes or molecular species of diol lipids have not been isolated from natural sources. Analyses of the hydrolysis products from neutral or polar lipid fractions revealed that diol lipids occur in nature as monoesters (I), diesters (II), and alk-1-enyl monoether monoesters (III).

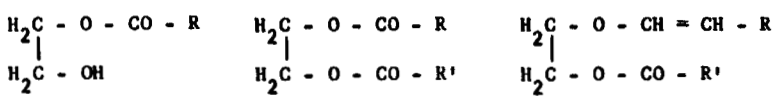

(I) (II) (III)

Because these lipids occur in nature but are overlooked owing to inadequate analytical methods, 1,2-ethanediol monoethers and monoesters were synthesized and then analyzed by gas-liquid chromatography (GLC). These homologous series served as model compounds for evaluating quantitatively various derivatives of these compounds by GLC.

Mixtures of trifluoroacetate (TFA) derivatives of glycol monoethers and glycol monoesters, ranging in chain length from C_{12} to C_{20}, are resolved completely by gas chromatography on both polar and nonpolar liquid phases (Fig. 84). The mono-unsaturated compounds of each class are well resolved from the corresponding saturated ones on the EGSS-X column, and are partially resolved on the SE-30 column. On either liquid phase the glycol ether trifluoroacetates are eluted ahead of the TFA derivatives of glycol esters of corresponding chain lengths, but the difference in elution time between ethers and esters is more pronounced on the polar phase.

The elution order of the trimethylsilyl (TMS) ether derivatives is similar to that of the TFA derivatives. On the SE-30 column, trimethylsilyl ethers of glycol esters are eluted midway between the glycol ether derivatives of the same chain lengths and the next higher homologues having two methylene groups more, while the TFA derivatives of the glycol esters are eluted immediately after the glycol ether of the same chain length (Fig. 84). The TMS derivatives of

* The University of Minnesota, The Hormel Institute, Austin, Minn.

1027541

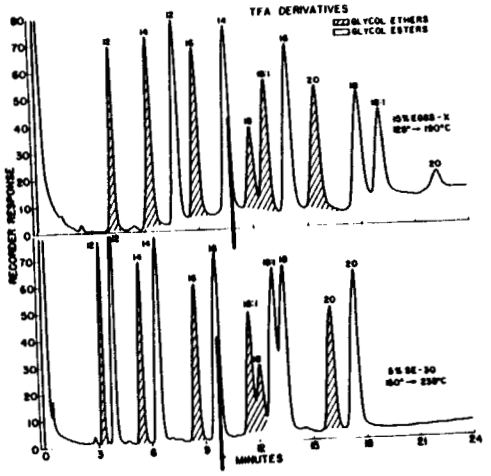

Fig. 84. Typical chromatograms of TFA derivatives of glycol monoethers and glycol monoesters obtained on polar and nonpolar columns. The approximate retention times of methyl stearate are indicated by vertical lines. Analytical conditions are given in Table 80.

saturated and of the corresponding unsaturated glycol esters were resolved on the polar liquid phase, but the glycol ethers were only partially resolved. Acetates can also be analyzed on both polar and nonpolar columns, but the EGSS-X column had to be operated at a higher temperature than for the TFA or TMS derivatives of the glycol esters to achieve elution in a reasonable length of time. Saturated and unsaturated glycol ethers and esters were completely resolved on the polar phase but were only partially resolved on the nonpolar liquid phase. The acetates of both the glycol ethers and esters gave unsymmetrical peaks on the SE-30 column; the glycol temperature failed to improve peak symmetry.

Expectedly, the trifluoroacetates, acetates, and trimethylsilyl ethers of glycol ethers are eluted ahead of the corresponding glycol esters on both liquid phases (Fig. 84). The elution order of the three derivatives relative to each other on EGSS-X liquid phase is TMS derivative before TFA derivative before acetate. The sequence of elution on the SE-30 liquid phase is TFA derivatives before TMS derivatives before acetates. The TMS derivatives are eluted immediately before, and the acetates are eluted with, the TFA derivatives having two methylene groups more. The approximate elution times of methyl stearate relative to the TFA derivatives for both the polar and nonpolar liquid phases are indicated in Fig. 84.

The gas chromatographic analyses of the trimethylsilyl ethers and acetates of glycol ethers and glycol esters give quantitative and reproducible results. Values determined by GLC on polar and nonpolar

TABLE 80

Comparison of Known and Experimentally Determined Values for TMS, Acetate, and TFA Derivatives of Glycol Ether and Ester Standard Mixtures Obtained by Gas Chromatography on Polar and Nonpolar Liquid Phases

Glycol Lipid	Carbon Chain	Standard Mixture		Found† for Standard Mixture on 5% SE-30‡			Found† for Standard Mixture on 15% EGSS-X§	
		Weight %	Mole %*	TMS	Acetate	TFA	TMS	Acetate
Monoether	12:0	13.4	16.8	15.7	14.9	15.5	14.6	14.6
	14:0	18.0	20.1	19.9	19.9	20.5	19.4	19.5
	16:0	19.5	19.7	20.2	20.5	21.1	20.1	19.8
	18:0	9.0	8.2	8.2	8.7	7.7	8.2	9.8
	18:1	19.2	17.8	17.7	17.4	16.7	18.1	17.0
	20:0	20.8	17.5	18.3	18.6	18.5	19.6	19.2
Monoester	12:0	13.2	16.5	14.8	14.3	16.4	14.1	14.2
	14:0	14.8	16.6	16.0	15.0	17.2	15.3	15.6
	16:0	16.3	16.6	16.8	16.3	17.2	16.4	17.0
	18:0	17.9	16.6	17.6	18.2	17.0	17.0	17.8
	18:1	17.4	16.3	16.7	16.7	16.6	17.5	16.0
	20:0	20.4	17.4	18.1	19.5	15.6	19.7	19.5

* Weight and mole percentages of the parent compounds.

† Area percentages were determined with a digital integrator and represent the mean of two determinations.

‡ Column temperature was programmed from 150-235°C at approximately 4°C/min.

§ Column temperature was programmed from 125-185°C at approximately 3°C/min when TMS derivatives were analyzed. Acetates were analyzed isothermally at 195°C.

liquid phases for both derivatives agree quite well with the known percentages of the standard mixtures except for the TFA derivatives as shown in Table 80.

REFERENCE

1. Bergelson, L. D. Diol lipids. In: Progress in the Chemistry of Fats and Other Lipids, Ralph T. Holman, ed., Pergamon Press, Ltd., Oxford, Vol. 10, pp. 239-286, 1969.

1027542

The Quantitative Production of Aldehydes from O-Alk-1-enyl Glycerols*

Robert E. Anderson, Ronald D. Garrett,† M. L. Blank, and Fred Snyder

Acid catalyzed hydrolysis of O-alk-1-enyl glycerols to produce alcohols and aldehydes is a well-known reaction (Eq. 1).

$$RCH_2\text{-}O\text{-}CH{=}CH\text{-}R' \xrightarrow{H_3O^+} RCH_2OH + R'CH_2CHO \qquad (I)$$

Schmid and Mangold[1] used this reaction to detect O-alk-1-enyl glycerols on chromatograms. The aldehydes liberated are separated from the reaction products and unreacted starting materials by two-dimensional thin-layer chromatography (TLC). Horrocks[2] also used this "separation-reaction-separation" technique to determine the O-alk-1-enyl content of phospholipids. He[2] concluded that the hydrolysis of O-alk-1-enyl glycerols was quantitative because the amount of lysophospholipids recovered as by-products agreed with the O-alk-1-enyl glycerol content of the original lipid sample as determined by iodine addition. Viswanathan et al[3] sprayed O-alk-1-enyl-containing lipids on Silica Gel HR with 15% methanolic HCl and recovered quantitative yields of dimethylacetals. They[4] later demonstrated that the O-alk-1-enyl moieties of beef heart glyceryl phosphoryl ethanolamine were quantitatively cleaved when exposed to HCl fumes and then to ammonia vapors on a TLC plate. Schmid and Mangold,[5] using neutral plasmalogens from human perinephric fat, demonstrated that aldehydes liberated with HCl fumes were identical in composition to the dimethylacetal derivative of aldehydes prepared with methanolic HCl.

We recently applied the procedure of Schmid and Mangold[1] to a mixture of radioactive lipids (containing O-alk-1-enyl glycerols) that had been reduced with lithium aluminum hydride.[6] Contrary to expectation, we observed that most of the radioactivity remained at the origin after chromatography on thin layers instead of migrating with alcohol and aldehyde standards. We, therefore, believed that an investigation of the quantitative release of aldehydes from O-alk-1-enyl glycerols by acid hydrolysis was mandatory. This paper describes the results of our study.

Octadecenal was prepared by oxidation of the tosylate derivative

* Supported in part by the American Cancer Society (Grant No. P-470).

† Present address: College of Pharmacy, University of Texas, Austin, Texas.

of octadecenol in dimethylsulfoxide and sodium bicarbonate according to the procedure of Mahadevan et al.[7] The 1-^{14}C-hexadecanal was made from 1-^{14}C hexadecanol by the same procedure.[7] Both aldehyde preparations were purified by preparative chromatography on 0.5 mm Silica Gel G thin layers in an equilibrated solvent system of hexane-ether (80:20, v/v).

Total lipids of rat brain were reduced with lithium aluminum hydride[6] and the resulting O-alk-1-enyl glycerols were obtained by preparative chromatography on 0.5-mm thin-layers of Silica Gel G in an equilibrated solvent system of ether-water (100:0.5, v/v). Solvents and other chemicals were reagent grade and used without further purification.

We evaluated the quantitative production of aldehydes liberated by the procedure of Schmid and Mangold[1] by pipetting an aliquot of 1-^{14}C-hexadecanal containing 50 micrograms octadecenal at the bottom of thin layers of Silica Gel G and exposing the adsorbent to HCl fumes according to their specifications.[1] After development in three separate solvent systems, the plates were subjected to zonal profile-scan analysis.[8] Exposure to fumes caused approximately one half the radioactivity to remain at the origin in each of the three solvent systems; similar data were obtained in repeated experiments in which we consistently found 50 to 85% of the radioactivity to be localized in regions other than that of the aldehyde. We cannot explain the erratic response since not all reaction products were identified. The procedure of Viswanathan et al[4] is similar to that of Schmid and Mangold,[1] except that the plate exposed to HCl fumes is neutralized by subsequent exposure to NH_3 vapor before chromatography. We treated 1-^{14}C hexadecanal and 50 micrograms octadecenal by the method of Viswanathan and co-workers[4] and found only 42% of the activity on the TLC plate to be in the aldehyde region.

The following procedure was developed in our laboratory for the production of aldehydes from lipid mixtures containing O-alk-1-enyl glycerols. A solution of O-alk-1-enyl glycerols (0.1 - 2 mg) in 1.5 ml ether was placed in a 1-dram vial and 1 ml of concentrated HCl was added. After vigorous shaking for 1 to 2 min, the ether layer was removed and the aqueous phase was extracted once with ether and once with hexane. The combined ether extracts were washed twice with distilled water to remove all traces of acid before they were evaporated to dryness under a stream of nitrogen. The reaction products were redissolved in a small amount of ether and the aldehydes were recovered by preparative TLC in an equilibrated system of hexane-ether (80:20, v/v). The reaction products recovered after a typical hydrolysis are shown in Fig. 85. The minor component (5% of total mass) on the chromatoplate appearing midway between the O-alk-1-enyl glycerols and liberated aldehydes is probably the cyclic acetal of the O-alk-1-enyl glycerols.

This procedure was also shown to be quantitative in terms of aldehyde recovery after shaking an ethereal solution of 1-^{14}C-hexadecanal and 150 micrograms O-alk-1-enyl glycerols with concentrated HCl

1027543

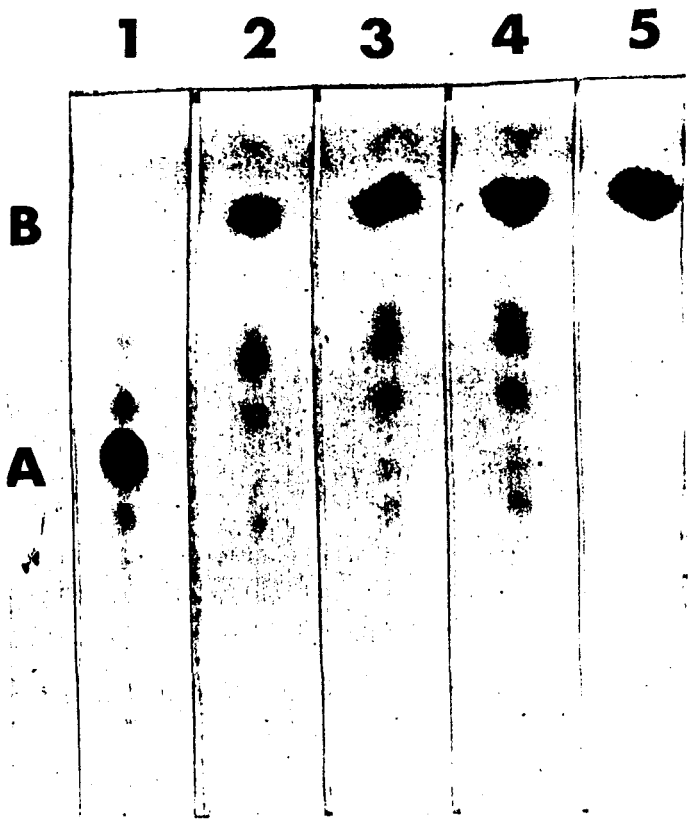

Fig. 85. Thin-layer chromatography of O-alk-1-enyl glycerols and their hydrolytic products after being shaken in ether with concentrated HCl for various periods of time. A, O-alk-1-enyl glycerols; B, aldehydes lane 1, O-alk-1-enyl glycerols; lanes 2, 3, and 4, reaction products after being shaken 1, 2, and 3 min with concentrated HCl; and lane 5, standard octadecenal. Developing solvent, ether-water (100:0.5 v/v).

for 1 min. Zonal profile scans indicated that the aldehydes were structurally unaltered by this procedure. Furthermore, results obtained in which the hydrolysis was carried out in the presence of 50 micrograms Silica Gel G indicate that O-alk-1-enyl glycerols separated by preparative TLC can be hydrolyzed directly to aldehydes in the presence of Silica Gel G, thereby eliminating the time-consuming elution and concentration step.

The composition of the aldehydes liberated from O-alk-1-enyl glycerols by the "separation-reaction-separation" procedure[1] and by shaking an ethereal solution of O-alk-1-enyl glycerols with con-

TABLE 81

Composition of Ether-Linked Hydrocarbons in O-Alk-1-enyl Glycerols Subjected to Various Treatments*

Sample	Acid†				
	16:0	17:0	18:0	18:1	Total 18
	Area %				
a) O-alk-1-enyl glycerols (Isopropylidene derivative after hydrogenation)	23.3	1.1	75.6		75.6
b) Aldehydes liberated with HCl fumes	22.2	1.1	42.9	33.8	76.7
c) Aldehydes liberated by HCl shake in the absence of silica gel	22.7	1.1	42.9	33.2	76.1
d) Aldehydes liberated by HCl shake in the presence of silica gel	22.2	1.1	42.7	34.0	76.7

* a) O-Alk-1-enyl glycerols were hydrogenated and then converted to isopropylidene derivatives for GLC, b) sample exposed to HCl fumes on a TLC plate, c) and d) samples shaken in ether with concentrated HCl. All procedures are described in the text.

† Only traces (<0.1%) of material with retention times longer than 18:1 were found.

centrated HCl in the presence and absence of silicic acid was determined by gas-liquid chromatography (Table 81). These data were compared to the composition of the isopropylidene derivatives of the O-alk-1-enyl glycerols that had been hydrogenated with platinum oxide catalyst. The C-16 and C-18 aldehydes produced by the two types of hydrolysis have identical compositions. However, the modified procedure outlined in this communication is essential for quantitative recovery of aldehydes, and it can be directly applied to the analysis of O-alk-1-enyl glycerols in the presence of silicic acid.

REFERENCES

1. Schmid, H. H. O. and Mangold, H. K. Alkoxylipids. II. "Neutral plasmalogens" in the liver oil of the ratfish (Hydrolagus colliei). Biochim Biophys Acta 125, 182-184, 1966.

2. Horrocks, L. A. The alk-1-enyl group content of mammalian myelin phosphoglycerides by quantitative two-dimensional thin-layer chromatography. J Lipid Res 9, 469-472, 1968.

3. Viswanathan, C. V., Basilio, M., Hoevet, S. P., and Lundberg, W. O. Reaction thin-layer chromatography in the analysis of mixtures of alkenyl acyl- and diacyl-phosphatides. J Chromatog 34, 241-245, 1968.

4. Viswanathan, C. V., Phillips, F., and Lundberg, W. O. Two-dimensional reaction thin-layer chromatography in the analysis of phosphatide plasmalogens. J Chromatog 35, 66-71, 1968.

5. Schmid, H. H. O. and Mangold, H. K. Neutrale plasmalogene und alkoxydiglyceride in menschlichem depotfett. Biochem Z 346, 13-25, 1966.

6. Wood, R. and Snyder, F. Quantitative determination of alk-1-enyl- and alkyl-glyceryl ethers in neutral lipids and phospholipids. Lipids 3, 129-135, 1968.

7. Mahadevan, V., Phillips, F., and Lundberg, W. O. Reactions of dimethyl sulfoxide with sulfonate esters of fatty alcohols. I. Synthesis of higher saturated and unsaturated fatty aldehydes. Lipids 1, 183-187, 1966.

8. Snyder, F. and Kimble, H. An automatic zonal scraper and sample collector for radioassay of thin-layer chromatograms. Anal Biochem 11, 510-518, 1965.

1027544

Deacylation of Phosphatidyl Choline and Phosphatidyl Ethanolamine by Crude Pancreatic Lipase Preparations* †

Robert L. Wykle and Fred Snyder

The hydrolysis of the 1-acyl group of phosphoglycerides[1] by pancreatic lipase can serve as the basis for the complete analysis of the hydrocarbon moieties in 1,2-diacyl, 1-O-alkyl-2-acyl, and 1-O-alk-1-enyl-2-acyl-phosphoglycerides. We investigated the possibility of using crude commercial lipase preparations in this reaction and analyzing the products by thin-layer chromatography and gas-liquid chromatography. The fatty acid pattern of lyso-glycero-3-phosphorylcholine released from egg lecithin by the pancreatic lipase preparations was similar to the fatty acid pattern of 1-acyl-glycero-3-phosphorylcholine released from egg lecithin by snake venom phos-

* Supported in part by the American Cancer Society (Grant No. P-470).

† Presented at the annual meeting of the Society for Experimental Biology and Medicine, Oak Ridge, Tennessee, November 12, 1968.

pholipase A. Analysis of the monoglycerides formed after phospholipase C hydrolysis of lysolecithin indicated that both the 1- and the 2-acyl groups had been removed by pancreatic lipase. The presence of the alk-1-enyl ether linkage in the lysocholinephosphoglyceride fraction from beef heart after the pancreatic lipase reaction also confirmed that 2-acyl groups were removed by pancreatic lipase. Our studies demonstrate that commercially available pancreatic lipase possesses a high level of phospholipase A activity, making it unsuitable for the selective cleavage of phosphoglycerides.

REFERENCE

1. De Haas, G. H., Sarda, L., and Roger, J. Positional specific hydrolysis of phospholipids by pancreatic lipase. Biochim Biophys Acta 106, 635-640, 1965.

The Quantitative Collection of $^{14}CO_2$ in the Presence of Labeled Short-Chain Acids*

Robert E. Anderson and Fred Snyder

In 1961 our laboratory described the collection of $^{14}CO_2$ for liquid scintillation counting.[1] This procedure was subsequently modified by Cuppy and Crevasse.[2] In the original communication,[1] it was emphasized that "volatile compounds in enzymatic studies might invalidate interpretations based on $^{14}CO_2$ collected in this manner..." This warning has gone essentially unheeded in numerous reports where labeled short-chain acids were used as substrates. In our experience with acetate, some ^{14}C will always be present in the $^{14}CO_2$ absorbent when the gas is liberated with mineral acid.

This report describes the collection of $^{14}CO_2$ in the presence of other volatile compounds. The basis for the separation is that at pH 6, below the pK_1 of carbonic acid (6.39), equilibrium favors the production of CO_2 and H_2O. On the other hand, at this pH, equilibrium favors the salt of short-chain acids.

The flask shown in Fig. 86 A is routinely used in this laboratory for enzymic incubations in which $^{14}CO_2$ is collected. It consists of a liquid scintillation vial with a rubber serum stopper inserted through a hole in the plastic cap that screws on the vial. The paper lining inside the cap is replaced by a rubber washer to assure an

* Supported by the American Cancer Society (Grant No. P-470).

1027545

air-tight fit. The top end of the spiral wire is bent and passed through the side of the serum stopper. The glass cup is the bottom portion of a half-dram vial. The entire assembly is similar to that of Cuppy and Crevasse,[2] except for the flask. We prefer the scintillation vials to Erlenmeyer flasks because it is easier to extract the lipids from incubations carried out in vials.

At a predetermined time, an enzymic incubation is terminated by injecting 1 ml of methanol through the rubber stopper. Five-tenths milliliter of Hyamine[3] is placed in the center well and 1 ml 1.0 M phosphate buffer is added to the incubation solution so that it has a final pH of approximately 6. The liberation of $^{14}CO_2$ is accomplished by shaking the vial at 37° C for 90 min. The pH of the phosphate buffer is determined before the incubation by adding the buffer at various pH's to a simulated incubation solution. It is not necessary to include the enzyme in this determination, and in reactions where the cofactors have a limited buffering capacity, the pH of the buffer may be calculated stoichiometrically.

To demonstrate that the buffered solution releases only $^{14}CO_2$ at pH 6, sodium bicarbonate- ^{14}C and sodium acetate-2- ^{14}C were incubated separately at this pH for various periods of time. The results are graphically shown in Fig. 86 A. At the end of 90 min, only traces of the acetate (0.05% of that incubated) could be found in the Hyamine. Conversely, no detectable ^{14}C from bicarbonate remained in the buffered solution.

In a separate series, the bicarbonate and acetate were incubated with boiled mitochondria. After shaking 1 hr at 37° C, the pH was adjusted to 6 and radioactivity was collected. Under these conditions, only 180 cpm of the 1.37×10^6 cpm of acetate used were found in the Hyamine; of the 1.52×10^5 cpm of bicarbonate incubated, only 240 cpm remained in the buffer.

Figure 86 B depicts the effect of pH on the release of formic, acetic, propionic, and octanoic acids from solution. The two low pH's were achieved by adding 6 N H_2SO_4 to the incubation solution. Phosphate buffer was used to adjust the incubation solution to pH 3 and 6. As seen in the figure, the mineral acid releases appreciable quantities of radioactive short-chain acids. Therefore, in experiments testing the capacity of a tissue to oxidize these short-chain acids, results could be misleading if the $^{14}CO_2$ were released with mineral acid.

From the data given in Fig. 86 B, apparently any pH between 3 and 6 should be adequate for quantitative release of $^{14}CO_2$ in the presence of other volatile compounds. However, for lipid work, neutral pH is preferred since acidic conditions may promote structural changes in the lipids.

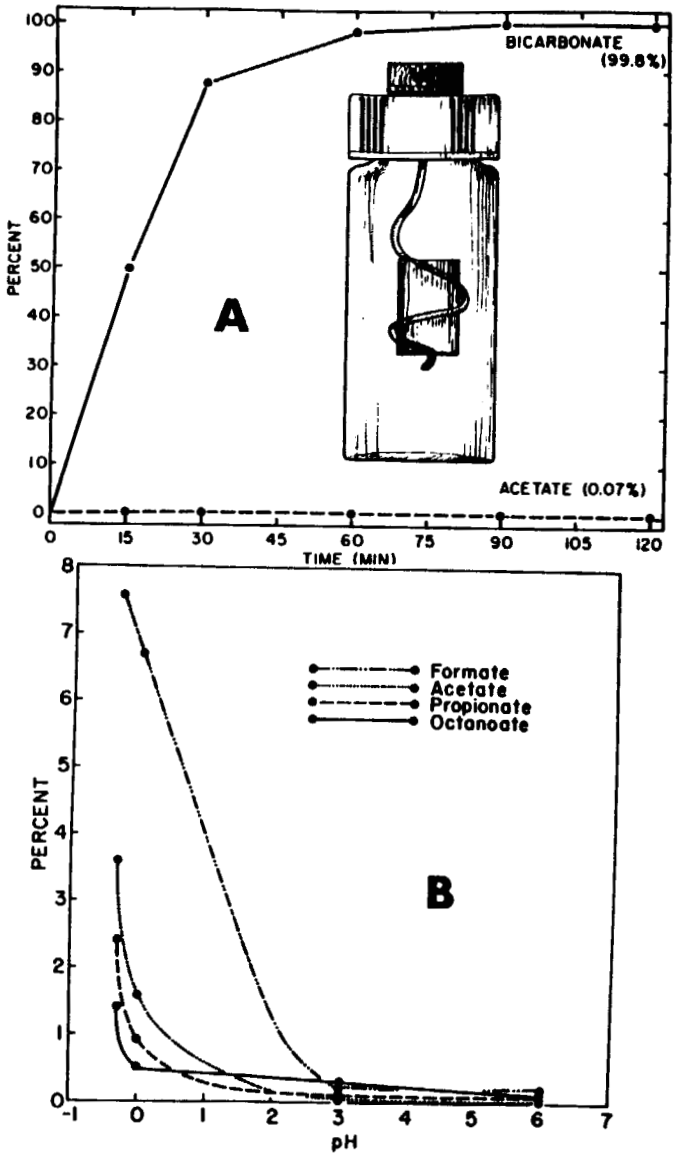

Fig. 86. A. Graph of the percentage of the radioactivity of $NaH^{14}CO_3$ and $NaO_2C^{14}CH_3$ collected in Hyamine as a function of time, at pH 6.0 and 37°C. Insert illustrates the modified scintillation vial used for incubations. B. Graph of the percentage of the radioactivity of sodium formate-^{14}C, sodium acetate-2-^{14}C, sodium propionate-2-^{14}C, and sodium octonoate-1-^{14}C collected in Hyamine as a function of pH, at 37°C and during a period of 90 min.

1027546

REFERENCES

1. Snyder, F. and Godfrey, P. Collecting $C^{14}O_2$ in a Warburg flask for subsequent scintillation counting. J Lipid Res 2, 195, 1961.

2. Cuppy, D. and Crevasse, L. An assembly for $C^{14}O_2$ collection in metabolic studies for liquid scintillation counting. Anal Biochem 5, 462-463, 1963.

3. Passmann, J. M., Radin, N. S., and Cooper, J. A. D. Liquid scintillation technique for measuring carbon-14-dioxide activity. Anal Chem 28, 484-486, 1956.

The Preparation of 1,2 Octadecane Diol and its Chromatographic Behavior*

M. L. Blank and Fred Snyder

A recent paper by Nikkari and Haahti[1] reported the isolation of diester waxes from skin surface lipids of the rat. α-Hydroxy fatty acids and long-chain 1,2-diols were found after hydrolysis of the wax fraction. They pointed out that both these components could be mistaken for alkyl glyceryl ethers if the total lipids had been subjected to $LiAlH_4$ reduction. Since our laboratory has been involved in the study of glyceryl ethers and many of our survey analyses are based upon $LiAlH_4$ reduction products, we decided to check some of our routine methods of identifying ether lipids with a sample of long-chain 1,2- diols to rule out their interference.

The 1,2- octadecane-diol produced by permanganate oxidation of 1-octadecene was isolated and purified by thin-layer chromatography (TLC). Various studies were then made between the 1,2-octadecane-diol and known alkyl glyceryl ethers.

Thin-layer chromatography of the diol and the alkyl glyceryl ethers provided poor resolution of these two lipid classes (Fig. 87), a confirmation of Nikkari and Haahti's[1] data. However, we applied three methods that easily distinguished the two similar lipid classes: (1) Infrared spectroscopy- The diol showed no major absorption band at 8.9 microns like that characteristic of C-O-C bonds. (2) Thin-layer chromatography- The isopropylidene derivative of the diol had a higher R_f value (Fig. 87) than the alkyl glyceryl ethers on thin layers of Silica Gel G developed in a solvent system of hexane:diethyl ether,

* Supported in part by the American Cancer Society (Grant No. P-470).

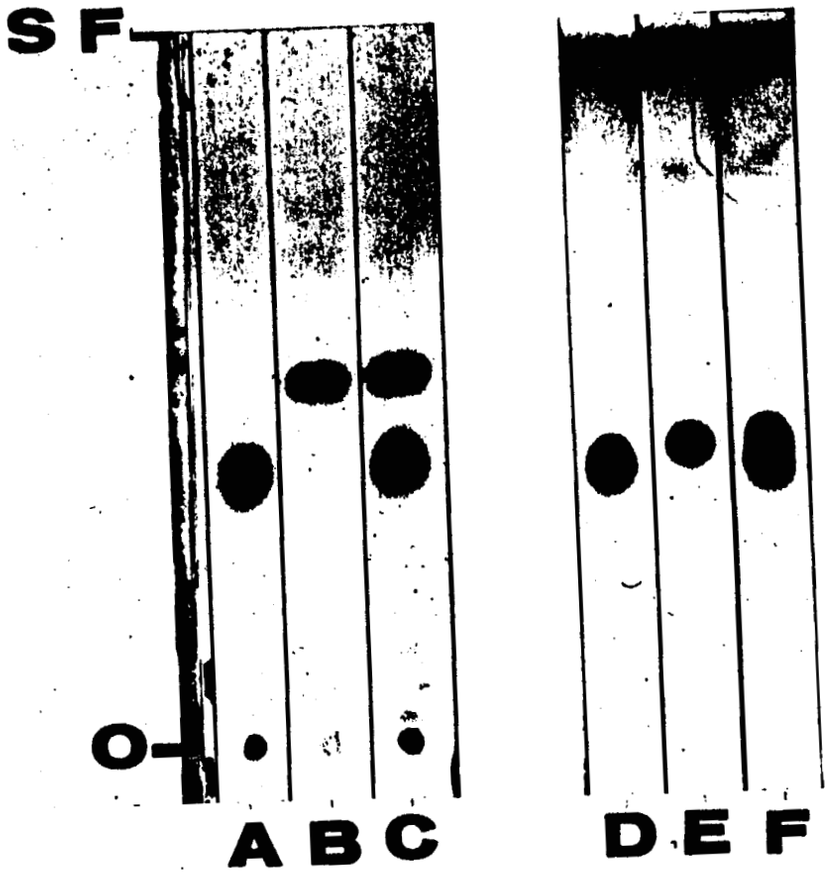

Fig. 87. Thin-layer chromatogram depicting the resolution of a mixture of 16:0, 18:0, and 18:1 glyceryl ethers (A,D), and a mixture (C,F) of the two lipid classes. Lanes A, B, C are chromatogram of the isopropylidene derivatives developed in hexane: diethyl ether 80:20 (v/v). Lanes D, E, and F represent a chromatogram of the original compounds developed in diethyl ether: water 100:0.5 (v/v). The adsorbent was Silica Gel G.

80:20 (v/v). (3) Gas-liquid chromatography- The isopropylidene derivative of the diol revealed that it had a shorter retention time on an EGSS-X column than the isopropylidene derivatives of naturally occurring glyceryl ethers (Fig. 88). Since most of our work with alkyl glyceryl ethers normally includes analyses by methods

1027547

2 and 3, it is unlikely that diols of this type would interfere with any of our results.

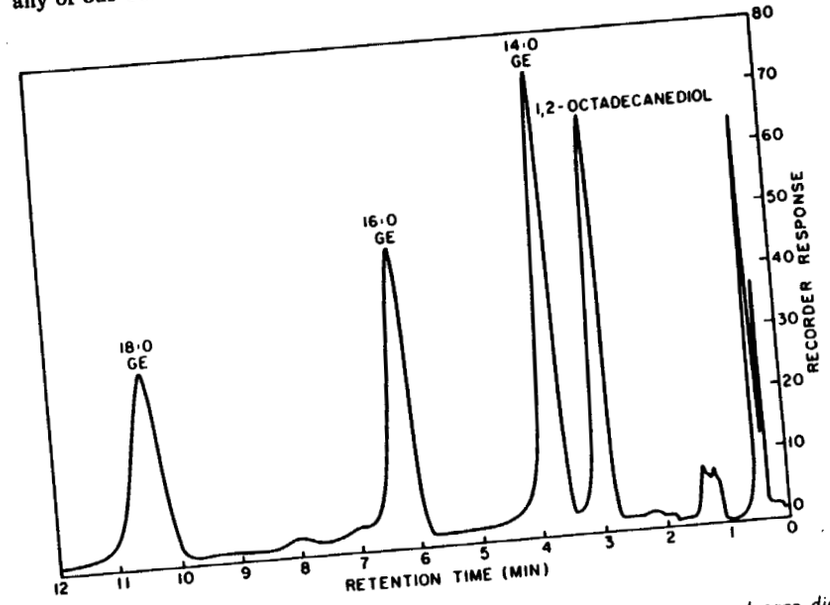

Fig. 88. Gas-liquid chromatogram of isopropylidene derivatives of 1,2 octadecane diol and 16:0, 18:0, and 18:1 glyceryl ethers. Samples were chromatographed on EGSS-X liquid phase at a temperature of 190°C.

REFERENCE

1. Nikkari, T. and Haahti, E. Isolation and analysis of two types of diester waxes from the skin surface lipids of the rat. Biochim Biophys Acta 164, 294-305, 1968.

1021548

THEORETICAL AND EXPERIMENTAL STUDIES IN METABOLISM AND DISTRIBUTION OF NUCLIDES

A broadening interest in science about theoretical aspects of life processes has brought the discipline of theoretical biology into its own. This development has led many researchers to reexamine old assumptions and to construct new hypotheses that may profoundly affect the nature of experimental design for many biomedical studies.

The objective of this aspect of our program is to quantitate patterns of absorption, distribution, and excretion of tracer metals, radionuclides of medical interest, and environmental and occupational contaminants. Our whole-body counting facility is a basic instrument with special applications in testing the hypotheses of the theorist who works in tracer methodology. As our whole-body counter has entered into routine use for biological measurements, refinements in instruments and data handling of electronic signals have continued; we believe that we are making a contribution to the methodology of whole-body counting. Thus schemes for reducing background, and counting in scatter regions to overcome geometric problems of nonhomogeneous and shifting radioactivity are two technical advances recorded in this section. This year clinical whole-body counting work not only has emphasized the trace elements of copper and zinc but also has pursued the important question of thyroxine metabolism in patients who are given therapy with thyroid hormone. This latter group includes patients in our long-term thyroid cancer study and patients who have become thyroid deficient after radioiodine treatment for hyperthyroidism. This study gives promise of clinical usefulness in relation to the best use of thyroid replacement therapy.

Ergodic Theory: Tracer Theory as a Special Case of Generalized Statistical Mechanics

Per-Erik E. Bergner

Previous work on tracer theory has given rise to a logical structure that in many respects is reminiscent of classic statistical mechanics.[1,2] It has, therefore, appeared natural to me to consider the original problems not as being specific for, say, nuclear medicine but rather as general physicomathematical ones. Those attempts have resulted in a statistical mechanics that can be considered as a generalized classic statistical mechanics, in the sense that concepts like volume and concentration are abandoned, which means that the theory is applicable also in the presence of unknown gradients (non-well-stirred

systems). Of particular interest is that, starting from general principles of physics, one obtains the tracer method as a logical consequence of those principles rather than as a specific experimental procedure resulting from the progress in nuclear technology.

The basic postulate is that the motion of a particle in the system S is a time-homogeneous Markovian process. We say that S is open when the total time the particle is expected to stay in S (mean-time of sojourn) is finite. Consider the situation where one particle enters S at time t=0, another at t=Δt, another at t=2Δt, and so on until t=nΔt. The expected number of particles in S converges to a definite, finite number when $n \to \infty$. This is true also for any subsystem of S, and in terms of particle distribution, one can then define a unique probability distribution - steady state - by letting $\Delta t \to 0$.

This distribution is thus generated according to a specific time rule. Consider now the expected motion of a single particle, and we have thereby defined a time-depending and transient (S is open) probability distribution that proves to be definitely related to the steady-state distribution. Such a relation is called ergodic: a relation between a time process and a time-independent structure. The transient distribution can be estimated by observing not only one particle but a large number of mutually independent particles, and this is exactly what is done in a tracer experiment.

The approach clearly demonstrates that, in a steady-state system, it does not matter whether all tracer is injected at the same time (a δ-injection) or whether the injection is prolonged. Moreover, many of the problems we have been considering in biology and medicine now appear much more general: It is thus not astonishing that in chemical engineering and geophysics basically the same equations are used as in medicine and biology.

On the basis of the outlined approach, it has been possible to define physically significant parameters that can be determined from whole-body retention data[2] (See page 221). In other words, the theory suggests a set of new parameters; the practical usefulness must be, however, tested by experiments. This is in perfect conformity with common experience: experiments imply theory that implies new experiments.

REFERENCES

1. Bergner, P-E. E. Ergodic Properties of the Tracer System. USAEC Report ORAU-103, 1967, 46 pp.

2. Bergner, P-E. E. Turnover Compartmentalization: A statistical tracer theory for analysis of whole-system retention data. USAEC Report ORAU-104, 1967, 29 pp.

1027549

Principal Problems in the Clinical Use of Whole-Body Counting

Per-Erik E. Bergner

Soon after World War II people started to build low-level whole-body counters for humans. To begin with, the sole purpose was to detect possible contaminations; in other words, the projects were parts of what today is called Health Physics. Later on, however, investigators realized that these expensive instruments could possibly serve as tools for clinical diagnosis and research, especially in studies of metabolic disorders, and I feel that, at present, the majority of new counters are built with those goals in mind. Still, after more than 20 years of experience, these instruments have found little clinical use as compared with less expensive radionuclear equipment like linear scanners. It is then natural to ask: Why is it so?

One of the main advantages of low-level whole-body counters is that the whole-body retention of injected radioisotopes can be followed without the messy procedure of collecting urine and stools. The retention curves obtained are commonly plotted on semilogarithmic paper and straight lines are fitted to the data; frequently the fits are reasonably good. The slopes of the lines constitute a set of parameters that are considered as characteristics of the observed metabolic system and, consequently, they should contain some valuable information for the clinician as well as for the researcher. Doubtless this is correct, and the "only" problem is to find out what kind of information the parameters contain.

We can easily show that, no matter how we define the physiologic state of a metabolic system, this state is in a very complicated way (actually, in an unknown way) related to the parameters described in the previous paragraph. Hence, we should expect the relation between these parameters and different metabolic disorders to be quite complex and, at a first glance, merely confusing.

There are essentially two ways out of this dilemma. Let the first one be called the phenomenologic approach, which mainly uses statistical methods, without ever asking for the meaning (in terms of physics) of the parameters: all we are interested in is whether there is any correlation between the set of parameters, or some mathematical combination of them, and the patient's physiologic condition.

Let the other method be called the physical approach: On the basis of elementary physical properties of particles (molecules, ions) we try to deduce parameters that can be determined from retention data. These parameters, which are likely to differ from those previously discussed, will then have precise physical significance and, hopefully, be easier to interpret. Some aspects of this approach are discussed elsewhere in this volume.

The phenomenologic approach has been used, for instance, by

Moore et al.[1] in the determination of what they call lean-body mass and total-body water. However, as a rule of thumb, every statistical method leads to conclusions that refer to a large population and, if the standard deviation is large, they do not tell much about the individual patient. And this seems to be true here.

We could try by trial and error to find out what factors affect the retention data and, by keeping some of them constant, we could decrease the standard deviation. Such studies, among pharmacologists referred to as "scanning," can usually be done only on animals, but surprisingly little has been published in that direction. In my own opinion, extensive animal studies are necessary but, in many countries, the trend is seemingly to work directly on humans; in England the regulations are such that it is often easier to obtain permission for experimentation on humans than on animals.

One factor, which we know influences retention data, is the diet. For instance, the common usage of iodinated quinolines in the treatment of intestinal amebiasis has caused some trouble in measurements of ^{131}I-uptake in the thyroid: the effects of the medications are irregular and may last for several months. Last year we did a series of ^{42}K-retention studies on rats[2] with the idea to see how the retention data were affected by an increased uptake of dietary potassium. The effects were irregular and nonconclusive. Actually, the seemingly only sure conclusion was that studies of this type must be done on a large scale and under observation and control of a large number of different variables; the experimental and theoretical implications are obvious and, perhaps, depressing.

Must we conclude that the use of retention data as tools in diagnosis and research is an unrealistic dream? Personally I believe the answer is "no" but that the situation is much more complicated than is usually anticipated: although the equipment for metabolic research is less expensive than that for, say, high-energy physics, the problems are equally complex and demanding. Hence, it seems to me that a low-level total-body counter requires a huge staff and must be followed up by extensive animal work. As it now is, metabolic research units are scattered all over the world, and an integrated multivariate analysis is practically impossible.

If we limit the goal to clinical diagnosis, short cuts may exist. Thus, most of the work has hitherto been with "proper tracers," i.e., materials that mimic the natural metabolites. However, a substantial progress in nuclear medicine has been achieved with the aid of artificial substances (colloids and high-molecular-weight substances); e.g., in the study of kidney and liver functions. Such substances usually participate in a much smaller number of physiologic processes than do natural metabolites, and they are therefore likely to be more directly dependent on specific metabolic functions and less dependent on variations in the diet; this last properly brings down the standard deviation, whereby the test becomes clinically more reliable. At this institution, studies with ^{52}Cr-labeled RBC seem to support this idea;[3] simultaneous recordings of whole-body retention and blood

activity appear to provide means for an early recognition of pathologic conditions in the RBC-system (including parts of the reticuloendothelial system.)

REFERENCES

1. Moore, F. D., Olesen, K. H., McMurrey, J. D., Parker, H. V., Ball, M. R., and Boyden, C. M. The body cell mass and its supporting environment. W. B. Saunders Company, Philadelphia, 1963.

2. Bergner, P.-E. E., Gibbs, W. D., and Yarbrough, M. C. Preliminary analysis of calcium and potassium retention data. In: USAEC Report ORAU-106, 1967, pp. 174-175.

3. Lushbaugh, C. C., Gibbs, W. D., Franz, W., and Bergner, P.-E. E. Analog computer analysis of human ^{51}Cr RBC survival and whole-body retention data. In: USAEC Report ORAU-101, 1966, pp. 106-111.

L-Thyroxine Turnover by Whole-Body Counting in Patients Receiving Exogenous Thyroid Hormone

E. D. Bird and W. D. Gibbs

The rate of L-thyroxine turnover is related to the basal metabolic rate. Ingbar and Freinkel[1] have shown that the rate of L-thyroxine turnover increases in patients with hyperthyroidism and decreases in hypothyroid ones.

L-Thyroxine is frequently given to obese patients to increase their metabolic rate. Although this may help at first, it loses its effect with time and as a result the amount of administered thyroxine may be increased. Many of these patients may finally be taking as much as 10 grains of desiccated thyroid daily and not losing weight or showing any of the clinical signs of excess circulating L-thyroxine. At the opposite end of the spectrum are some totally thyroidectomized patients who are maintained in a euthyroid state by 1-1/2 grains of thyroid, a dose that is usually considered to be one half the normal maintenance requirement for a totally thyroidectomized patient. Furthermore, when the dose of thyroxine is increased in such patients, they develop, at least temporarily, the symptoms of excess circulating L-thyroxine.

Since apparently both these groups of patients have an abnormal metabolism of L-thyroxine, we attempted to confirm this by giving

^{131}I L-thyroxine and measuring the turnover rate in a whole-body counter. In this study patients were given ^{131}I L-thyroxine intravenously in doses that ranged from 20 to 40 microcuries containing 0.6 to 1.2 micrograms of L-thyroxine. Whole-body counting was performed before we gave the dose to establish the normal body background, twice the first day, and daily thereafter for periods up to 30 days. Blood samples were collected and the rate of blood disappearance of ^{131}I L-thyroxine was measured in five patients. Daily neck counts were done by the standard thyroid-uptake method. The values shown in Table 82 were computed as described:

T-1/2 - the half-time of the exponential disappearance of the ^{131}I label from the body.

T_{50} - the time required for the first 50% of the ^{131}I label to leave the body. (In several patients T_{50} and T-1/2 are different because of a rapid elimination of ^{131}I during the first 24 hr. Early rapid excretion is probably due to free iodide in the dose material.)

T-1/2 Thyroid Corrected - daily monitoring of all patients for concentrations of ^{131}I in the neck with the use of the standard thyroid-uptake counting method.

In patients that concentrated more than 1% of the dose in the neck, the neck activity was subtracted from the whole-body radioactivity to obtain the extrathyroid radioactivity (Fig. 89). The resulting disappearance half-time is reported as T-1/2 thyroid corrected.

T-1/2 Blood - the time required for 50% reduction in blood radioactivity after 24 hr.

Three patients had their thyroid medication slowly changed toward what is usually considered normal and the ^{131}I-L-thyroid turnover study was repeated.

Table 82 lists the results of the ^{131}I-L-thyroxine whole-body half-time (T-1/2), the time taken for 50% of the ^{131}I L-thyroxine to be excreted (T_{50}), the ^{131}I-L-thyroxine half-time corrected for uptake in the thyroid, (T-1/2 corrected) and the half-time for ^{131}I L-thyroxine measured in the blood (T-1/2 blood). The amount of thyroid each patient was taking at the time the investigation was carried out is also listed.

The patients taking more than normal amounts of L-thyroxine (Group 1) had a shorter T-1/2, T_{50}, T-1/2 (corrected) and T-1/2 (blood) time. In all patients taking less than a normal replacement (Group 2), these values were increased. Patients in Group 3, who had multinodular goiters, were inconsistent in that two had an increased rate of turnover and two were normal. The patients in Group 4 were normal. One patient in this group was a euthyroid patient who had a normal intact thyroid and was not taking desiccated thyroid.

1027551

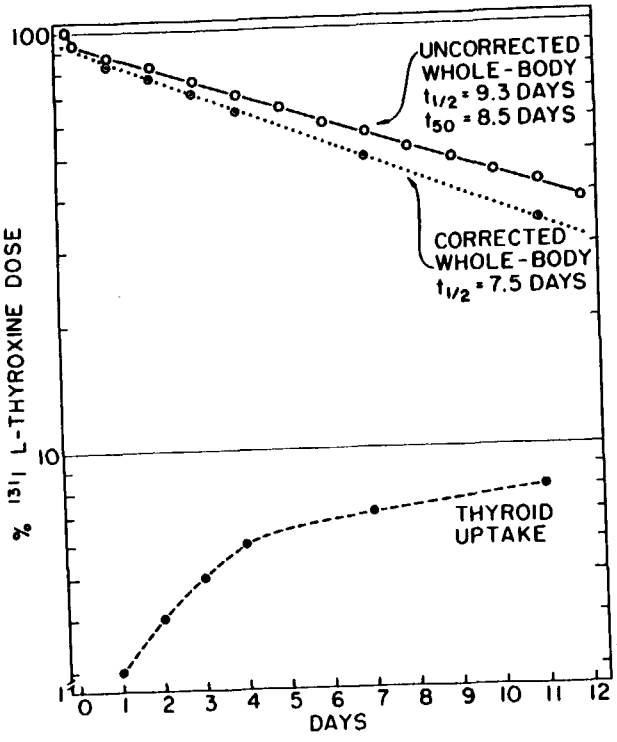

Fig. 89. Typical whole-body retention and thyroid uptake after intravenous ^{131}I-L-thyroxine in a patient with goiter. Note rapid excretion during first 6 hr. Corrected whole-body retention obtained by subtracting thyroid content from whole-body retention.

Although his whole-body T-1/2 of 131I thyroxine was longer than normal, the T-1/2 (thyroid corrected) came within the normal range.

Table 83 lists the results obtained in the one patient from Group 1 (patient B), and two patients from Group 2 (patients C and E) who had repeat ^{131}I-L-thyroxine studies after having their thyroid dose changed to "normal." The T-1/2 values indicate that, as the daily intake of desiccated thyroid approaches normal, the whole-body turnover rate also changes toward normal.

Few data are available on the whole-body retention of ^{131}I L-thyroxine. The data obtained by using the whole-body counter should give a much clearer picture of the true L-thyroxine turnover than can be determined by measurements of blood disappearance. Although we need more data on normal subjects, we have the impression that the whole-body half-time is longer than is reported by

TABLE 82

Results Obtained in Patients Receiving ^{131}I-L-Thyroxine

Patients	T-1/2	T_{50}	T-1/2 Thyroid Corrected	T-1/2 Blood	Daily Desiccated Thyroid (Grains)
Group 1 - taking excess thyroid					
A	5.0	4.7	5.0	4.5	10
B	2.4	2.0	2.4		12
Group 2 - taking less thyroid than normal yet euthyroid					
C	9.5	7.0	9.5		2
D	8.0	7.5	8.0		2
E	10.3	10.3	10.3	6.8	2
F	9.6	9.6	9.6	6.5	2
Group 3 - goiters but euthyroid					
G	12.0	10.8	8.3	7.8	none
H	9.5	8.5	7.5		1
I	7.5	7.5	5.3	4.3	none
J	8.3	7.3	5.3		none
Group 4 - normals					
K	5.8	5.8	5.8		3
L	5.7	5.2	5.7		3
M	5.5	5.5	5.5		3
N	6.5	6.5	6.5		3
O	8.2	7.3	6.8		none

All times computed in days.

TABLE 83

^{131}I-L-Thyroxine Whole-Body Half-Time Changes Related to Dose of Desiccated Thyroid

Patient	Daily Desiccated Thyroid (grains)	T-1/2 (days)
B	12	2.4
	3	4.5
C	2	9.5
	3	5.5
E	2	10.3
	4	5.3

1027552

others using the blood-disappearance curves. In the patients we studied who had simultaneous whole-body and blood determinations, the whole-body turnover rate was always slower than that of blood (Table 82).

The discrepancy between the whole-body turnover rate and blood turnover rates was much greater in the euthyroid patients taking a smaller dose of thyroid than would be considered normal. This indicates that the peripheral tissues are holding on to L-thyroxine for a much longer time than are the blood proteins.

Oddie has reported some data on whole-body retention of L-thyroxine and found that the half-time of blood and the whole body was the same.[2] The patients he reported were all given potassium iodide to prevent recycling of ^{131}I through the thyroid. Most of our patients were thyroidectomized; we did not administer potassium iodide. We have some preliminary evidence in animals that the administration of potassium iodide does have some extrathyroid effect on the whole-body half-time of L-thyroxine.

The data obtained in this study indicate the remarkable ability of the body to adjust the metabolism of L-thyroxine to its needs. Evidently little benefit is obtained from giving more than 3 grains of desiccated thyroid to patients regardless of the reason for the medication. A qualifying statement needs to be made here that, although 3 grains appears to be the amount required by most patients, few data are available that relate the L-thyroxine requirement to body size. We have some preliminary information (not included in this report) that the daily requirement of thyroid may be related to body size.

This study demonstrates that the old methods of measuring only the blood-protein iodide and the ^{131}I uptake in the thyroid gland provide only a limited amount of information and often a misleading conception of what is really going on in the thyroid gland and whole body. The very long half-time obtained in two of our patients with a goiter provides information that would never have been realized otherwise, since both these patients appeared clinically euthyroid and had normal protein-bound iodine and ^{131}I thyroid uptakes.

The whole-body counting method of measuring L-thyroxine turnover rate appears to be the most accurate way to obtain quantitative information.

REFERENCES

1. Ingbar, S. H. and Freinkel, N. Simultaneous estimation of rates of thyroxine degradation and thyroid hormone synthesis. J Clin Invest 34, 808-819, 1955.

2. Oddie, T. H., Fisher, D. A., and Rogers, C. Whole-body counting of I^{131}-labeled thyroxine. J Clin Endocrinol 24, 628-637, 1964.

Tracer and Treatment Discrepancy as a Problem of Radioiodine Therapy

C. L. Edwards, R. Tanida, and W. D. Gibbs

In a high percentage of cases the treatment of hyperthyroidism with ^{131}I results in hypothyroidism, an apparent overshooting of the desired goal of euthyroidism. However, even with the same dose, a sizable percentage of patients will require further treatment presumably because of an inadequate therapeutic dose. As expected, the higher the treatment dose, the greater the probability of hypothyroidism; but the smaller the dose, the greater the chance of needing a subsequent dose. No dose or dose schedule seems to be completely free of either undesired effect.

Therapeutic doses are usually prescribed on the basis of some formula that uses an estimate of gland weight and the uptake of a tracer dose. Inconsistent results have been blamed on poor estimates of the gland size and upon variations in radiosensitivity. Errors in the thyroid uptake of the tracer are rarely incriminated and the uptake of the treatment dose is seldom checked. The assumption that the therapeutic dose is handled in the same way as the tracer is based on sound principles of tracer dynamics, but only when all other factors remain constant, a condition not easily maintained in the clinical setting. We recently had an opportunity to study a patient with hyperthyroidism in whom the therapeutic dose of radioiodine was completely ineffective.

Case 1

This 46-year-old woman had had signs and symptoms of hyperthyroidism for three months. Her thyroid uptake of a tracer dose of ^{131}I was 66% in 24 hr and 67% in 48 hr. Eight days later she was given 8.5 millicuries of ^{131}I as therapy. One month later she returned with no apparent benefit. In reviewing the whole-body counting data after her therapeutic dose, we learned that she had retained only 7% of the dose, only 0.1 as much as we had assumed to have been assimilated into her thyroid gland alone. In retrospect, we were unable to account for this rapid excretion but the ineffectiveness of the dose was no longer a mystery. This experience caused us to look for similar discrepancies.

Since 1959, we have collected comparable whole-body retention data for 50 therapeutic doses of ^{131}I, before which an uptake of a tracer dose was determined within 10 days. The thyroid uptakes were measured according to the ORINS universally intercalibrated standard system at 24 and 48 hr. The tracer doses ranged from 25 to 100 microcuries. The therapeutic doses ranged from 4 to 20 millicuries. All doses were obtained from commercial sources of radiopharmaceuticals. Whole-body retention of the tracer doses was measured in the low-level whole-body counter or the linear scanner. Whole-body retention of the treatment doses was measured in the high-level whole-body counter. In each instance the count at

1027553

2 hr and before the first voiding was taken as the 100% value.

The relation between the whole-body retention and the thyroid uptake was first determined for 47 patients in whom both the whole-body retention and the thyroid-uptake data were measured for the same tracer dose at 24 hr, and for 11 patients at 48 hr. These values are plotted in Fig. 90 as solid dots. The average difference between the whole-body retention and the thyroid uptake (the extrathyroidal pool) is shown as a solid line for 24 and 48 hr (% whole-body retention at 24 hr = % thyroid uptake + 21.2% ± 8.7%; % whole-body retention at 48 hr = % thyroid uptake + 15.2% ± 8.5%). The two standard deviation limits for these means are shown as broken lines.

The whole-body retention of each treatment dose was then plotted against the thyroid uptake of the corresponding tracer dose (small open dots in Fig. 90) and compared with the mean obtained

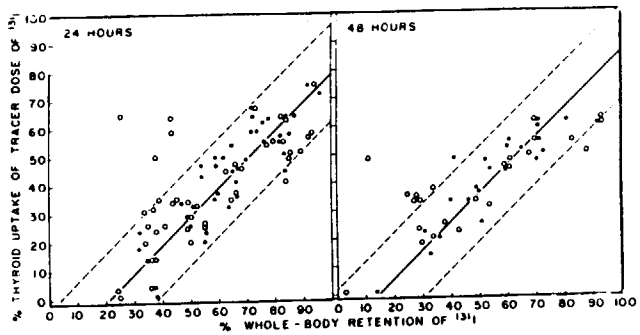

Fig. 90. Comparison of the whole-body retention of treatment doses of ^{131}I with the thyroid uptake of a preceding tracer dose; (°) the whole-body retention (%) of each therapeutic dose of ^{131}I is plotted against the thyroid uptake (%) of a tracer dose given within 10 days of the treatment dose; (•) the whole-body retention (%) of each tracer dose is compared with the thyroid uptake (%). The solid line is the mean for the tracer doses only while the broken line shows the two standard deviation limits for the mean.

for the tracer doses. In 12 instances these points fell outside the limits of two standard deviations from the mean. The whole-body retention was significantly more than expected in 2 patients and significantly less in 10. A review of the patients uncovered an explanation for the discrepancy in only one. He received some iodinated radiopaque media during the interval between the tracer and the treatment doses.

In 7 of 24 determinations the whole-body retention at 48 hr was significantly different from that expected from the tracer study. These differences point up a possible explanation for inconsistent

therapeutic results. None of these 7 could be explained even after reviewing the charts and would have gone undetected had not retention studies been done after the treatment doses. Thus any evaluation of a treatment schedule for ^{131}I may be misleading, if the results are not correlated with a direct measure of the thyroid uptake or fate of the treatment dose.

Effect of L-Thyroxine Administration on Whole-Body Retention of Iodine-131 L-Thyroxine in Rats

E. D. Bird, Everett D. Wilson, Jacques Baenziger, and W. D. Gibbs

Radioactive labeled thyroxine has become a very useful isotope in the investigation of thyroid disorders. The low concentrations of stable L-thyroxine in the serum makes direct measurement difficult. This hormone is secreted by the thyroid and is excreted in the bile and feces either unchanged or as a conjugated product.[1]

In hypothyroid rats the biliary excretion rate of thyroxine is reduced whereas in rats given desiccated thyroid the rate of thyroxine excretion increases.[2] An increased plasma disappearance of ^{131}I-L-thyroxine in patients with hyperthyroidism and a decreased disappearance of ^{131}I-L-thyroxine in patients with liver disease and hypothyroidism has been reported.[3] We confirmed these differences in humans and in addition noted that the whole-body retention of ^{131}I-L-thyroxine in patients with total thyroid ablation was related to the amount of their thyroid replacement.[4] (See page 223 of this report.) Potassium iodide is usually administered to block the recirculation of the ^{131}I released from ^{131}I-L-thyroxine. Since our patients had previously had total thyroid ablation, we did not administer potassium iodide when we measured the retention of ^{131}I-L-thyroxine.

The present study was undertaken to determine the effect of L-thyroxine on the half-time of ^{131}I-L-thyroxine turnover in thyroid-ablated rats.

Adult male rats of the Fischer strain weighing approximately 200 g were divided into four groups as indicated in Table 84. Animals in each of groups 2, 3, and 4 were given a single dose of 1 millicurie of ^{131}I 4 weeks before the administration of a tracer dose of 10 microcuries of ^{131}I thyroxine. This amount of ^{131}I produces thyroid ablation with minimal structural damage to other organs.[4] The whole-body retention of ^{131}I at the end of 4 weeks was less than 1% in all animals. A correction for this residual iodine was made throughout the tracer experiment.

1027554

Daily thyroxine replacement therapy was begun 10 days before the administration of the 10-microcurie tracer dose of thyroxine and continued throughout the experiment. The thyroxine solution was prepared fresh daily by dissolving sodium levothyroxine (synthroid) in physiologic saline. The L-thyroxine was injected intraperitoneally once daily in a volume of 0.25 milliliters. The rats were counted periodically in a low-level whole-body counter and corrections for background and physical decay were made. All rats were autopsied at 21 days after the tracer dose and selected tissues were assayed in a well scintillation counter (Table 84).

The whole-body retention of ^{131}I thyroxine is graphically displayed in Fig. 91, and the results indicate that ^{131}I-labeled thyroxine disappears from the body in a biphasic manner. The initial phase represents a rapid use of thyroxine and elimination of labeled degradation products from the body by way of the liver, bile, and feces.[1] The second phase probably reflects turnover of iodide in the extrathyroidal space in all groups as well as recycling of iodide in the controls.

Extrapolating a best-fit straight line of the slow phase back to zero time gives the initial activity of the slow phase, and we can determine from point-by-point subtraction the half-time of thyroxine turnover of this extrapolation.

The half-time for the hypothyroid rats (Group 1) was 28 hr. The

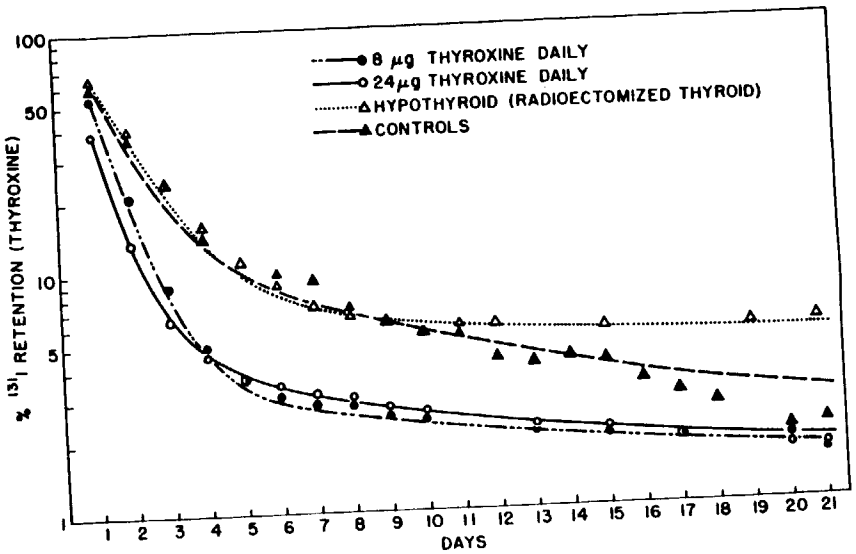

Fig. 91. Mean whole-body retention of ^{131}I-L-thyroxine in control, hypothyroid and treated rats. Each group consisted of 10 animals.

TABLE 84

Disappearance Half-times of ^{131}I-L-Thyroxine in Rats

Treatment Groups	Whole-Body T-1/2 in Hours
1 Controls	24
2 Thyroid destroyed with radioactivity	28
3 Thyroid destroyed with radioactivity and 8 micrograms thyroxine injected daily	20
4 Thyroid destroyed with radioactivity and 24 micrograms thyroxine injected daily	16

TABLE 85

Retention of ^{131}I Thyroxine (Percent Dose)

	Controls	Hypothyroid	8µg	24µg
Whole body	2.2	5.6	1.6	1.65
Thyroid*	1.2	.034	.017	.012
Liver*	.024	.018	.006	.003
Kidney*	.01	.022	.008	.004
Blood†	< .001	< .001	< .001	<.001
Fur‡	< .001	< .001	.056	.069

* % in total organ

† % per milliliter

‡ % per gram

thyroid-ablated rats that were treated with 8 and 24 micrograms of thyroxine had half-times of 20 and 16 hr. The half-time of the controls was 24 hr.

The concentration of thyroxine in various tissues 21 days after administration of the tracer dose can be seen in Table 85. With the

1027555

exception of the control group the label is widespread throughout the body. The fur has the greatest concentration of activity. As would be expected, the thyroids of the control group contained approximately 50% of the whole-body activity.

Evans et al.[5] reported that a dose of 0.5 micrograms of L-thyroxine was necessary to maintain body growth in a surgically thyroidectomized rat. To demonstrate the relation between L-thyroxine half-time and the amount of administered thyroxine, we used 8 micrograms, hoping to produce slight thyroid toxicity, and 24 micrograms to produce severe toxicity. The data support the finding that thyroidectomized patients who take large doses of thyroid have a very short half-time for ^{131}I-L-thyroxine.

We realize that, although the rats in groups 2, 3, and 4 were virtually thyroidectomized and did not require potassium iodide to block the recirculation of ^{131}I freed from the thyroxine, the control groups that had intact thyroid glands may have had some recirculation of ^{131}I; thus the true whole-body thyroxine half-time may be slightly shorter than we have noted.

These data, along with human data, (See page 223 in this report) demonstrate that in attempting to maintain normality the biological system has remarkable ability to adjust the metabolism of thyroxine to the amount present in the body within fairly wide limits.

REFERENCES

1. Taurog, A. Conjugation and excretion of the hormone. In: Biology Department. The Thyroid, Report of a Symposium, 1954. (Brookhaven Symposia in Biology p. 7) Upton, N. Y., U. S. Brookhaven National Laboratory, 1955, pp. 111-136.

2. Klitgaard, H. M. Biliary and urinary I^{131} excretion in euthyroid, hyper- and hypothyroid rats injected with labeled thyroxine. Proc Soc Exp Biol Med 82, 578-579, 1953.

3. Lennon, E. J., Engbring, N. H., and Engstrom, W. W. Studies of the rate of disappearance of labeled thyroxine from the intravascular compartment. J Clin Invest 40, 996-1005, 1961.

4. Watts, R. W. E. Metabolic rate changes following thyroid destruction by AT^{211} and I^{131} in the rat. Proc Soc Exp Biol Med 89, 220-222, 1955.

5. Evans, E. S., Rosenberg, L. L., and Simpson, M. E. Relative sensitivity of different biological responses to thyroxine. Endocrinology 66, 433-440, 1960.

Possible Copper Intoxication Following Ovulation-Suppressing Contraceptives

C. L. Edwards and E. D. Bird

Copper intoxication, although uncommon, is usually due to ingested copper salts. In the acute form it produces a gastrointestinal syndrome with nausea, vomiting, colic, and diarrhea. Also there may be severe headache, hemolytic anemia, jaundice, and even death. Chronic or subacute intoxication is a less well defined entity, but it may also produce serious gastrointestinal symptoms. We recently studied a patient with hypercupremia and refractory diarrhea, both of which subsided after she stopped taking oral contraceptive pills. This led us to postulate a causal relation between the estrogens, the hypercupremia, and the diarrhea.

Case Report

In January, 1968, a 42-year-old housewife was admitted with severe abdominal cramps and diarrhea for one month. Her stools had become increasingly frequent and the pains more severe despite antispasmodics and opiates. No blood, excessive mucus, or fat was visible in her stools.

For several years she had been anemic, thought to be from excessive menstrual blood loss. For 30 months she had been taking Ortho-Novum, 2 mg, an estrogen-progesterone contraceptive to regulate her periods and minimize her blood loss. In January 1967 she had been found to have splenomegaly, leukocytosis, and lymphadenopathy, and thus was suspected of having an early lymphocytic leukemia or a lymphoma, with infiltration of the bone marrow. No treatment was prescribed and she remained essentially free of symptoms until the onset of the abdominal complaints. There was no familial history of metabolic disorders and no known exposure to copper.

On physical examination her abdomen was soft but tender generally. Her spleen was palpable 5 cm below the costal margin and the liver edge was just palpable. There was no icterus or other discoloration. No lesions were seen by proctoscopy to 25 cm. The laboratory findings included a leukocytosis of WBC 14,800/cu mm and a mild hypochromic anemia. Liver function tests were also slightly abnormal. Alkaline phosphatase 5.6 units, SGOT 55 units, and cholesterol of only 125 mg/100 ml. The alpha$_2$ fraction of the serum globulins was also increased. No ova or parasites were seen in the stool examination, and no pathogens grew on culture. A barium enema showed an extremely irritable colon with extensive hypertrophic mucosal changes but no ulcerations. Both the upper GI series and small-bowel X rays were normal.

In the clinical chemistry laboratory the patient's serum was definitely green when compared with others. To find the

1027556

cause of the color, the serum ceruloplasmin was checked and the patient was asked to discontinue the Ortho-Novum. The ceruloplasmin level was 213 mg/100 ml, or approximately five times normal, so she was asked to resume the Ortho-Novum to permit further copper studies. However, after only a few days the cramping pain and diarrhea became much more severe. After 6 days she asked that the contraceptive be discontinued permanently. The serum copper was about four times normal and the 24-hr urinary excretion was 270 μg (Table 86). At this point we suspected that the hypercupremia

TABLE 86

Serum and Urine Copper and Serum Ceruloplasmin Values in Relation to Oral Contraceptive Medication.

	Serum Copper μg/100 ml	Serum Ceruloplasmin mg/100 ml	Urine Copper μg/24 hr
Normal	75 - 145	20 - 35	4 - 30
January 31		213	
Ortho-Novum omitted February 1-10			
February 12	368	110	270
" 14	456		76
" 16	364		
Ortho-Novum discontinued on February 16			
February 20	207	94	122
" 22		80	112*
" 26	198	70	43*
" 28		65	
April 16	135	58	
August 13	123	58	

* Urine collections February 22-23 and 24-25.

and estrogens were responsible for the diarrhea.

Until the contraceptive was discontinued permanently, such measures as diet restriction, opiates, antispasmodics, emollients, and absorbents were all ineffective in controlling the diarrhea or the colic. The patient had continued to lose weight, having lost more than 25 pounds and had had a serious problem of maintaining hydration and electrolyte balance. By 4 days after the Ortho-Novum was stopped, the serum copper had decreased to 207 μg/100 ml. Likewise, the ceruloplasmin had dropped to 94 mg/100 ml. After 1 month she was no longer having colic or diarrhea, and had regained 10 pounds. Unfortunately, at about this time she developed migratory polyarthritis. The latex fixation test for rheumatoid factor was positive. She was treated with aspirin. At 6 months her serum

copper was 123 μg/100 ml and ceruloplasmin 58 mg/100 ml; she had regained her former weight but continued to have some mild arthropathy.

Hypercupremia occurs normally in pregnancy as well as in a number of disease states, e.g., leukemia, lymphoma, especially Hodgkin's disease, other malignancies, chronic infections, liver disease - notably cirrhosis, and in rheumatoid arthritis. In addition, medications containing estrogens and possibly testosterone will increase the serum copper and ceruloplasmin. In 1966, Carruthers, et al.[1] reported hypercupremia in all of 23 healthy ambulatory women taking oral contraceptives. However, only four had copper values as high as 300 mg/100 ml, and none so high as in our patient. In addition to taking estrogens our patient is thought to have rheumatoid arthritis which is associated with hypercupremia. Perhaps the underlying disease enhances the effect of the estrogen.

The mechanism of the hypercupremia associated with estrogens is uncertain. The accompanying proportional increase in the serum ceruloplasmin that results from estrogens suggests that the increased copper is secondary to the increased ceruloplasmin analogous to the increased protein bound iodine and thyroxine-binding globulin also seen in response to estrogens. This is further supported by the fact that urinary copper is not usually increased in patients taking estrogens. However, our patient had significantly elevated urine copper (Table 86). Further, the concentration of copper in the liver biopsy specimen taken during the hypercupremia was only 8.5 μg/g compared to a normal of 25 to 40, in contrast to patients with cirrhoisis, lymphoma, and leukemia where copper usually is excessive in the liver and serum. This apparent depletion of liver copper may have serious implications of its own.

Since these observations were made, at least two patients have been reported as having severe diarrhea believed to be related to oral contraceptives. Vascular occlusions were thought to be the cause of the diarrhea, on the basis of the finding of thumb print indentations into the lumen of the spastic colon as seen on barium enema. These findings are said to be reversible and similar findings can be seen in our patient's colon X rays (Fig. 92). No notation of serum copper levels or discolored serum were included in those reports. Likewise, in none of the discussions of the hypercupremia of estrogens has there been any symptoms attributed to the excessive serum copper. The fact that our patient had higher levels may account for this difference. The increase in urinary excretion may also indicate that the copper was not as well bound to protein and, as is true with other metals, more toxic in the unbound form. The symptomatic improvement that our patient experienced after stopping the Ortho-Novum was so dramatic that it is difficult for us to believe the drug was not responsible. Although it is quite possible that our patient's diarrhea was not caused by the hypercupremia, we believe that the striking elevation in serum copper offers a possible alternative to the vascular occlusion explanation for the diarrhea, and that further attention should be given to the

1027557

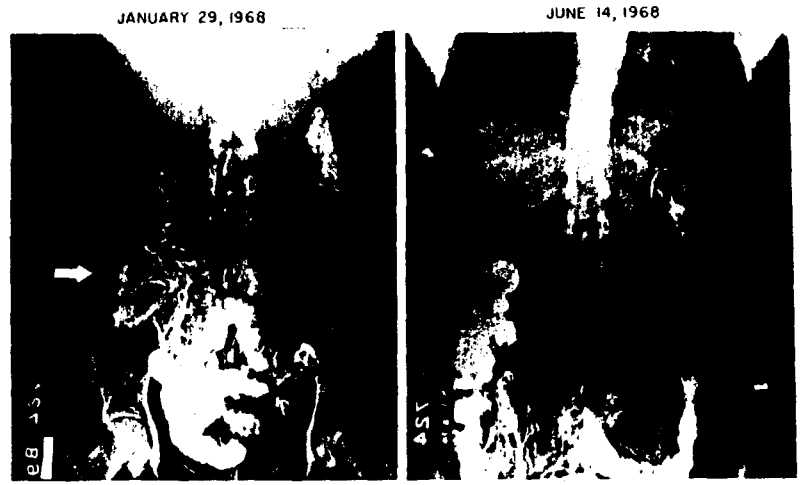

Fig. 92. Barium enema examination in January 1968, while the patient was taking Ortho-Novum, showing "thumb print" impressions on the barium shadow in the cecum. The absence of the indentions can be seen on the X ray to the right obtained after she had stopped the drug.

alterations of copper metabolism attending the use of oral contraceptives.

REFERENCE

1. Carruthers, M. E., Hobbs, M. E., and Warren, R. L. Raised serum copper and caeruloplasmin levels in subjects taking oral contraceptives. J Clin Path 19, 498-500, 1966.

Effect of Oral Contraceptives on Whole-Body Retention and Tissue Distribution of Copper-67 in Female Rats

E. D. Bird, David Mescher, Everett D. Wilson, and W. D. Gibbs

Oral contraceptives increase serum copper and ceruloplasmin concentrations in women.[1] A patient in the Medical Division had symptoms of heavy-metal intoxication and green serum that was subsequently found to contain concentrations of serum copper and ceruloplasmin that were four to five times normal. Copper concentration in urine was also increased. This patient had been taking a contraceptive, Ortho-Novum. After she discontinued the

drug, the copper concentrations in the serum and urine returned to normal. See page 234.

The increased serum copper after the administration of oral contraceptives may be the result of increased copper absorption, altered distribution, or decrease in copper excretion.

Ortho-Novum contains 2 mg of a progestational agent, norethindrone and 0.1 mg of an estrogen, mestranol. It has been suggested that the abnormal serum increases in copper are due solely to the estrogenic component in the oral contraceptives.[2]

To determine the effect of oral contraceptives on the distribution and retention of copper, the present study was designed with the use of radioactive copper-67 in rats.

Table 87 summarizes the experimental groups of adult female Charles River rats and their treatments. Each group consisted of 10 rats with group 1 as control. Rats in group 2 were given 5 micrograms of mestranol daily; those in group 3 were given 10 micrograms of mestranol daily; and group 4 received 5 micrograms of mestranol and 625 micrograms of norethindrone daily. All agents were given by intraperitoneal injection.

A single oral dose of 10 microcuries of carrier-free ^{67}Cu was given on the 21st day of the study and the whole-body retention was measured over the next 13 days in an animal whole-body counter. After 13 days all animals were killed, and tissue samples were assayed for ^{67}Cu.

The results in Table 88 are the means of 10 animals in each group expressed as the percentage of dose per gram of tissue. The most significant changes noted when mestranol was given alone were increased ^{67}Cu concentrations in the kidney and stomach whereas, when norethindrone was added to the regimen, ^{67}Cu concentration increased in the liver, spleen, and muscle.

Whole-body retention curves are depicted for each group in Figs. 93-96. During the first 3 days after administration of ^{67}Cu, all animals lost radioactivity at a half-time of about 9 days. The rate of loss after the first 3 days was also about the same in all groups. The only difference appeared to be a wider scatter of isotope retention about the mean in the treated groups as compared to the control; alterations in copper absorption were thus indicated.

The data in Table 88 indicate that distribution of copper in the body is also altered. The most significant increase in copper concentration after contraceptive administration was found in the liver. Ceruloplasmin, the protein that binds copper, is an alpha-2 globulin produced in the liver. Estrogens cause an increase in serum concentration of the alpha-2 globulins.

In the first 21 days retention apparently was not altered but

1027558

TABLE 87

Summary of Animal Groups and Treatments

Group*	Rx
I	Controls
II	5 micrograms mestranol daily, I.P.
III	10 micrograms mestranol daily, I.P.
IV	5 micrograms mestranol and 625 micrograms norethindrone daily, I.P.

* Each group consisted of 10 rats.

TABLE 88

Distribution of ^{67}Cu in Rats
(Percentage of dose per gram of tissue)

Specimen	Control	Mestranol 5 µg	Mestranol 10 µg	Mestranol, 5 µg Norethindrone, 625 µg
Blood	0.077	0.072	0.079	0.072
Spleen	0.060	0.051	0.060	0.085
Kidney	0.845	0.962	1.045	1.330
Liver	2.101	2.248	2.013	3.080
Stomach	0.171	0.201	0.200	0.256
Heart	0.263	0.209	0.216	0.305
Lungs	0.196	0.133	0.147	0.208
Thyroid	0.027	0	0.012	0.010
Muscle	0.023	0.030	0.035	0.042

All values in each group are mean of 10 rats.

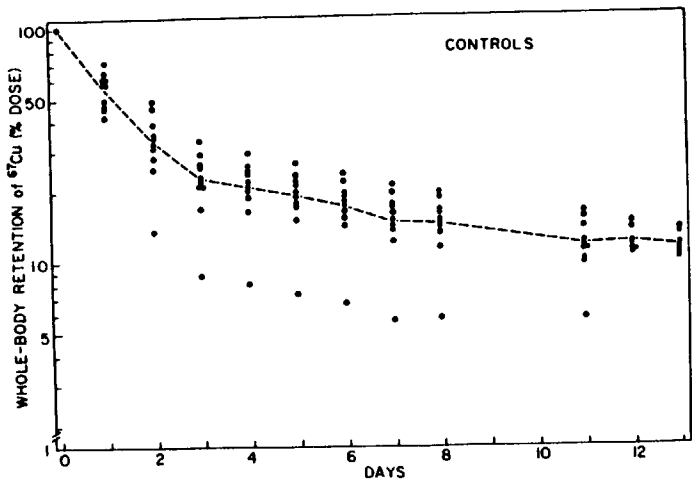

Fig. 93. Whole-body retention of orally administered ^{67}Cu in 10 control rats. The individual data and mean retention are shown.

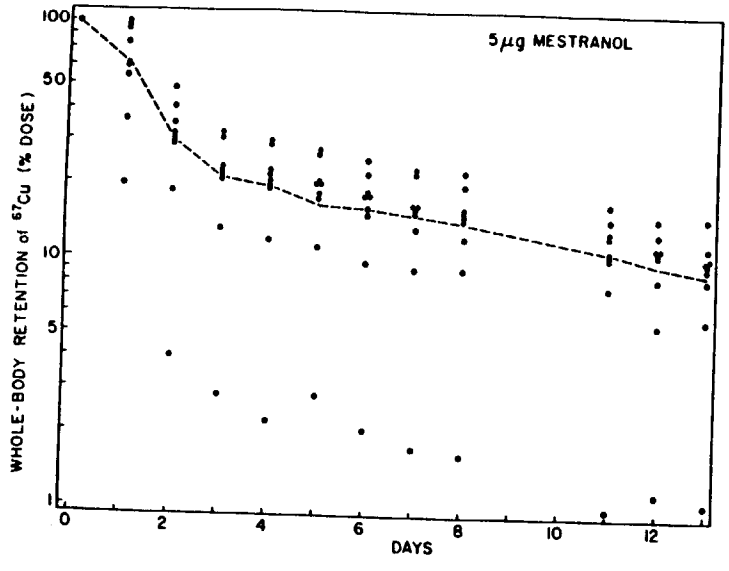

Fig. 94. Whole-body retention of orally administered ^{67}Cu in rats receiving 5 micrograms mestranol daily. Note wide variations among individual animals.

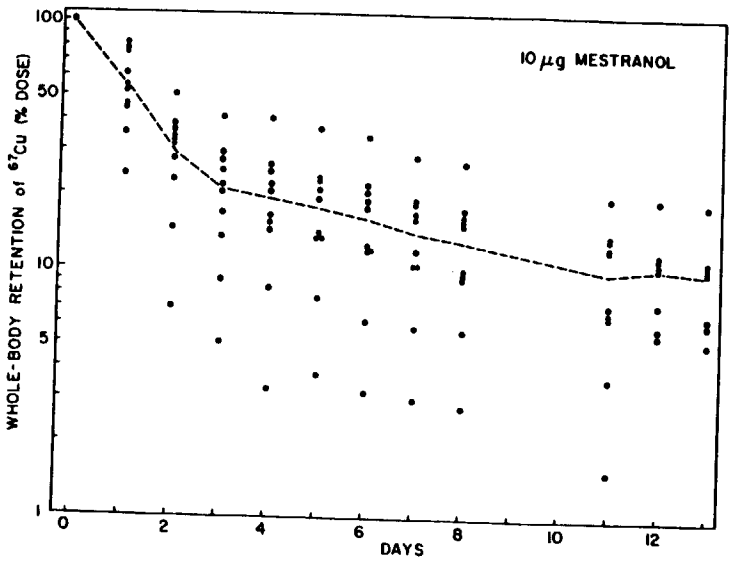

Fig. 95. Whole-body retention of orally administered ^{67}Cu in rats receiving 10 micrograms mestranol daily.

1027559

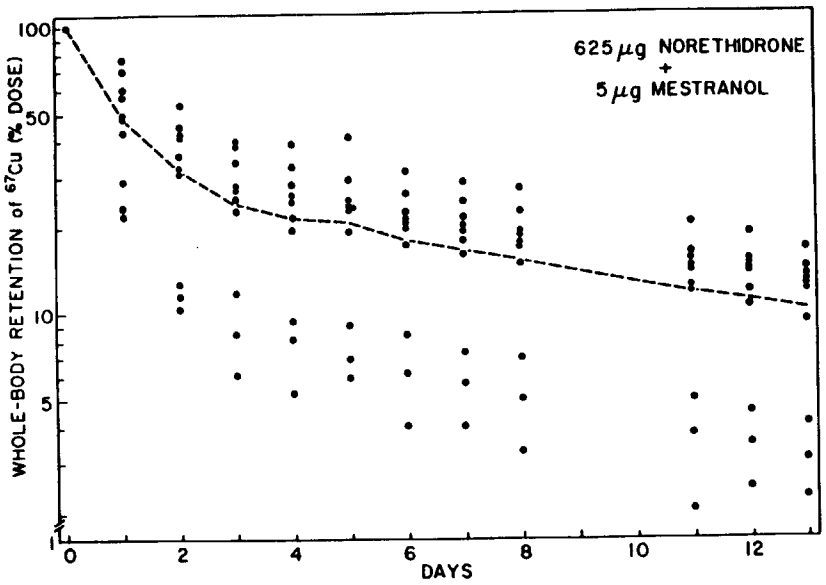

Fig. 96. Whole-body retention of orally administered ^{67}Cu in rats receiving 5 micrograms mestranol plus 625 micrograms norethidrone daily.

the distribution data indicate an increased amount of copper in the liver, spleen, and muscle. This suggests that the increased serum concentration of copper after administration of oral contraceptives results from the redistribution of copper with an increase in copper concentration in the liver during the early stages of treatment, presumably because the alpha-2 globulin (ceruloplasmin) increased or enhanced absorption of dietary copper.

REFERENCES

1. Carruthers, M. E., Hobbs, C. B. and Warren, R. L. Raised serum copper and caeruloplasmin levels in subjects taking oral contraceptives. J Clin Path 19, 498-500, 1966.

2. Clemetson, C. A. B. Caeruloplasmin and green plasma. Lancet 11, 1037, 1968.

Changes in Zinc-65 Partition Between Mother and Progeny During and After Pregnancy in Rats

E. D. Bird, Everett D. Wilson, David Mescher, Jacques Baenziger, and W. D. Gibbs

Zinc is an essential nutritional element for humans and animals.[1,2] Few clinical disorders related to it have been characterized to date; those that have been reported reflect the effect of zinc on growth and were recognized after the numerous animal studies showed that zinc deficiency produces growth failure.

One of the authors noted a typical zinc deficiency syndrome in two brothers, both of whom were born prematurely and ate a zinc deficient diet most of their lives. In addition, the mother ate a very poor diet during both pregnancies. Therefore, these boys probably had very low total-body zinc stores at birth and their diet never restored this deficiency.

This experiment investigated the metabolism of zinc in the prenatal and postnatal period by measuring whole-body retention of ^{65}Zn in normal and pregnant rats, and the subsequent transfer of ^{65}Zn through the milk to the young.

Adult nulliparous female Charles River rats were injected intraperitoneally with a single dose of 250 microcuries of ^{65}Zn. Whole-body counts were done daily for the first 14 days and periodically up to 84 days.

During this counting period the females were continuously exposed to males after 14 days in a ratio of 3 females to 1 male. Only one female of a group of 10 became pregnant; she delivered 13 young 41 days after the ^{65}Zn injection. The mother and young were counted for 21 days.

Figure 97 shows the whole-body retention of ^{65}Zn in the rat that became pregnant, the progeny of this rat, and the mean retention of nine rats that did not become pregnant. The 50% whole-body retention value for normal adult females was found to be 6 days. At birth the total litter had 1.1% of the original dose that had been given to the mother 41 days before parturition.

During gestation, the growing fetuses had between 15 and 24% of the original dose available to them. The amount of ^{65}Zn in the litter increased from 1.1% of the mother's original dose at birth to 4.0% at 21 days, the weaning date. This increase represents the amount of ^{65}Zn transferred to the young through the mother's milk. Apparently the mother's urinary and fecal excretion of ^{65}Zn decreases during lactation. The combined total percentage of activity in the mother and young at birth was 16.5% of the original dose. After 21 days the total activity in mother and young was 14.2%, a total loss of only

1027560

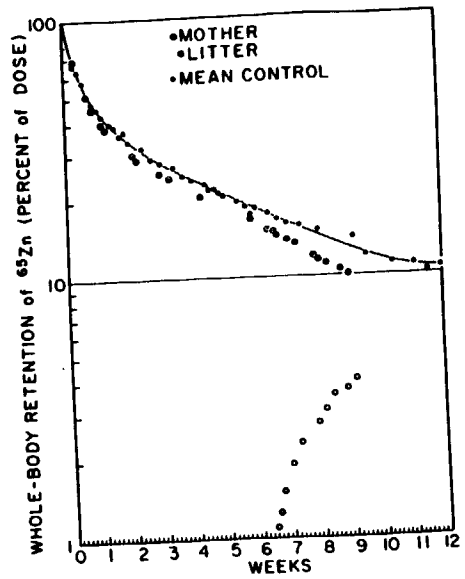

Fig. 97. Whole-body retention of ^{65}Zn in nine normal and one pregnant rat. Also shown is ^{65}Zn content of litter from birth through 19 days.

2.3% due to fecal excretion of young and mother. During this same period, the normal nonpregnant rats lost 6% of the original dose.

Figure 98 graphs the ^{65}Zn retention data on two mothers who received ^{65}Zn 10 and 23 days after delivery and that of the two litters. The 23-day-old litter received 5.5% of the maternal dose through the milk in the first 24 hr after ^{65}Zn administration. The 10-day-old young received 27% of the original maternal dose. The biological half-time of ^{65}Zn administered during lactation was only 1.5 days for the heavily lactating female as compared to 2.5 days for the female very near the end of the lactating period. Again, the maternal excretion rate by the feces is apparently reduced considerably in the heavily lactating female. By adding the activity of the litter and the mother, who was dosed when the litter was 10 days old, we found that the 50% fecal and urine excretion level was not reached until approximately 12 days, whereas the 50% excretion level in feces and urine was reached in approximately 3 days in the female given ^{65}Zn near the end of the lactating period.

Feaster et al.[3] reported that 56.3% of an initial oral dose of ^{65}Zn and zinc chloride was excreted in the feces within 45 hr in pregnant rats. This represents only 14% retention. The main reason for our much longer whole-body retention half-time of 6

days is probably intraperitoneal administration, or, alternatively, perhaps the ^{65}Zn given by Feaster et al. was not carrier free. The influence of dietary factors must always be taken into consideration when tracers are given orally. Bird and Dunavant (unpublished data) found that in humans a diet high in phytate would reduce the absorption of orally administered ^{65}Zn from 75% to 30%.

The data from this initial study in animals indicate that most of the transfer of zinc from mother to progeny occurs during lactation. A mother who is zinc deficient will no doubt produce offspring that are zinc deficient and they will remain so as long as they are breast fed.

Reduced fecal and urinary excretion of zinc during lactation is an interesting observation and probably represents a normal physiologic mechanism to supply a growth factor, zinc, to the young. The maternal milk probably contains a carrier protein for zinc that has a high binding coefficient.

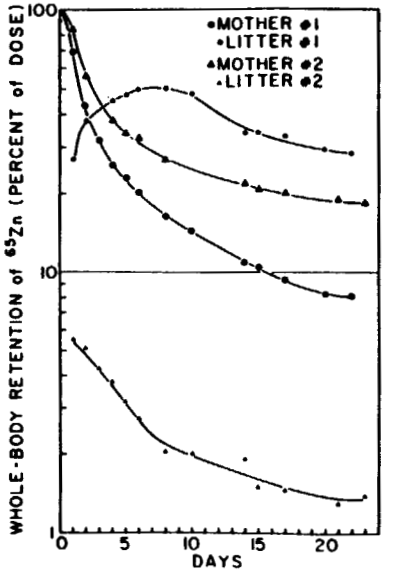

Fig. 98. Whole-body retention of ^{65}Zn in two mother rats given ^{65}Zn when litters were 10 days and 23 days old. Zinc-65 content of the litters is also shown.

REFERENCES

1. Todd, W. R., Elvehjem, C. A., and Hart, E. B. Zinc in the nutrition of the rat. Amer J Physiol 107, 146-156, 1934.

1027561

2. Prasad, A. S., Miale, A., Jr., Farid, Z., Sandstead, H. H., Schulert, A. R., and Darby, W. J. Biochemical studies on dwarfism, hypogonadism and anemia. Arch Int Med 111, 407-428, 1963.

3. Feaster, J. P., Hansard, S. L., McCall, J. T., and Davis, G. K. Absorption, deposition and placental transfer of zinc^{65} in the rat. Amer J Physiol 181, 287-290, 1955.

Antimony Pentoxide for Sodium Removal in Neutron Activated Brain*

E. D. Bird,† J. F. Emery,‡ S. B. Lupica,‡ and W. S. Lyon‡

Previous studies showed that a tranquilizing drug, phenothiazine, caused the concentration of manganese in the basal ganglia of the subhuman primate brain to increase significantly. This increase appeared to be associated with an augmented amount of pigment in the brain. Since this area of the brain has the propensity to concentrate a number of cations, we believed that it was important to measure other metals in the basal ganglia of primates after phenothiazine.

Copper as well as manganese is concentrated in biologic pigmented tissues, and the clinical effects of this metal on the brain resemble those of manganese. We, therefore, measured copper and manganese in the various nuclei of the brain of our phenothiazine-treated primates.

The amount of tissue available for analysis is quite small, and neutron activation analysis was therefore chosen for measurement of these cations. The high concentrations and good neutron cross section of sodium and chloride results in the production of 15-hr ^{24}Na and 37-min ^{38}Cl. The gamma-ray spectra of these nuclides obscure the peaks for copper and manganese. Girardi[1] has described a recent radiochemical separation using antimony pentoxide to remove sodium from activated samples. We used such a technique in our

* Research sponsored by the U. S. Atomic Energy Commission under contract with the Union Carbide Corporation, and National Institutes of Health, Grant No. AM12746-02.

† Present address: The Bowman Gray School of Medicine, Winston-Salem, N. C.

‡ Analytical Chemistry Division, Oak Ridge National Laboratory, Oak Ridge, Tenn.

procedure and were able to measure both copper and manganese simultaneously.

Macaca mulatta were given phenothiazine for variable times at gradually increasing amounts until 60 mg per day was given and then killed. Tissues were dissected with plastic instruments, dried in a vacuum oven in nonmetallic containers, and then transferred to plastic vials for neutron activation analysis in the Oak Ridge National Laboratory Research Reactor. Samples were irradiated for 2 min at a neutron flux of $1.5 \times 10^{13} n \cdot cm^{-2} \cdot sec^{-1}$. The tissue sample plus 0.1 mg each of copper and manganese carrier was then digested with fuming HNO_3 containing a few drops of H_2SO_4, and the mixture was heated to remove chlorine. After further nitric acid digestion, the samples were cooled and passed through a 0.5-gr column of Sb_2O_5 that had been preconditioned with 9 N HNO_3. The eluate was counted with a 3-in. x 3-in. NaI crystal in a 512-multichannel analyzer.

Typical gamma-ray spectra taken before and after the Sb_2O_5 separation are shown in Figs. 99 and 100.

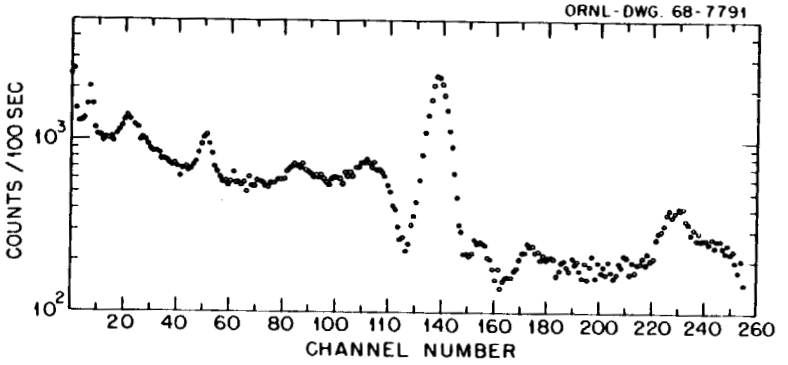

TISSUE BEFORE SEPARATION
~10 keV / channel

Fig. 99. Tissue Before Separation ~10 kev/channel

Total volume of sample plus 9 N HNO_3 washes passed through the Sb_2O_5 column was 7 ml. The eluates were collected and counted on a 3-in. x 3-in. NaI (Tl) detector equipped with a 512-channel analyzer. For ^{64}Cu the 0.51 Mev gamma-ray photopeak was integrated, and for ^{56}Mn the 0.84 Mev gamma-ray photopeak was used. After corrections for decay, the photopeak areas were compared with those of the standards, and the amount of copper and manganese present was calculated. Quantitative recovery of both copper and manganese activity was determined by

1027562

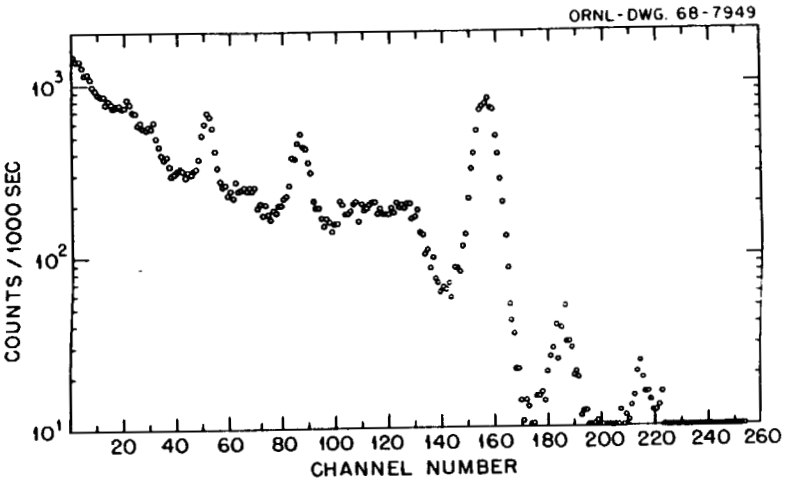

TISSUE AFTER SEPARATION
~10 keV / channel

Fig. 100. Tissue After Separation ~10 kev/channel

passing known amounts of ^{64}Cu and ^{56}Mn through the system in simulated experiments. Quantitative recovery was noted in a total passed through a volume of 6 ml.

Each tissue sample was done in duplicate. The average copper and manganese concentrations in the various nuclei of the basal ganglia from treated animals appears in Table 89. The average manganese concentration in basal ganglia of control animals is

TABLE 89

Copper and Manganese in Brain Tissue

Tissue	Treated			Controls
	Number of Samples	Copper* µg/g	Manganese* µg/g	Manganese* µg/g
Putamen	9	32.4 ± 5.4	2.05 ± 0.24	1.88 ± 0.31
Caudate	7	32.7 ± 3.7	2.05 ± 0.19	1.81 ± 0.08
Globus Pallidus	8	25.2 ± 7.5	2.05 ± 0.28	2.09 ± 0.23

*Dry Weight Basis

listed in Table 89 for comparison. We have not measured the copper concentration in control animals.

Although the manganese concentration of the basal ganglia in animals treated for 1 month increases significantly, the present results indicate no significant difference in manganese concentration when animals are treated for longer periods up to one year.

The use of the Sb_2O_5 technique provides a rapid and clean method for removal of sodium before the simultaneous measurement of copper and manganese.

REFERENCE

1. Girardi, F. and Sabbioni, E. Selective removal of radiosodium from neutron-activated materials by retention on hydrated antimony pentoxide. J Radio Anal Chem 1, 169-178, 1968.

Improvement in Accuracy of Whole-Body Radioisotope Quantitation by the Scatter-Window Method

W. D. Gibbs, Harold D. Hodges, R. F. Queener, and C. C. Lushbaugh

Accurate relative or absolute quantitation of the radioactive content of humans cannot be achieved with present methods if the radioisotope changes distribution with time.

An empirical approach to the solution of this problem and the results of a clinical test of the method have been described for ^{131}I in previous Medical Division Research Reports.[1,2] This approach is based on the assumption that for every radioisotope a "window" exists in which the variation in observed counts per minute per unit radioactivity is minimum with changes in source location or distribution.

The experimental procedure for determining the optimum window consists of counting a point source in 33 different locations in a humanoid water phantom in the whole-body counter. The gamma-ray spectrum with the source at each location is recorded on punched paper tape for input to a computer. The computer is programmed to determine the difference in the counts in every possible continuous window of 50 kev and wider for each source location from the counts obtained with the source in an arbitrarily chosen reference location (usually center of abdomen). The absolute values of the spectral differences are summed. The resulting differences are then printed out in order of magnitude.

1027563

The window with the smallest difference between the standard reference position and the 33 other locations then appears first on the printout and is where counting variations caused by changes in radioisotope distribution are minimum.

The optimum windows shown in Fig. 101 are not always those appearing at the head of the computer printout. In some instances the computer determines by this method a window that is unstable from the viewpoint of possible electronic drift or that is insensitive in terms of the number of counts observed per unit of radioactivity. However, all the windows shown in Fig. 101 appear in the computer printout among the first 10 in the listing.

Figure 101 shows a plot of optimum windows for ^{51}Cr, ^{131}I, ^{198}Au, ^{137}Cs, ^{54}Mn, ^{65}Zn, ^{59}Fe, and ^{60}Co versus gamma-ray energy. Except for ^{60}Co and ^{59}Fe, the optimum thresholds and window tops show a linear relationship to gamma-ray energy.

The conventionally used photopeak windows for all the radioisotopes we have studied are shown by this computer computational method to have large counting variations with changes in radioisotope distribution.

The optimum windows shown in Fig. 101 are all located in the scatter region of the spectrum. Every optimum window avoids all main photopeak counts; this is contrary to the conventional methods of gamma-ray spectrometry where only the photopeak counts are analyzed.

As noted earlier the ^{59}Fe and ^{60}Co optimum windows do not fit on the lines predicted by the optimal window locations for other radioisotopes (Fig. 101). The other radioisotopes are essentially monoenergetic emitters while ^{60}Co emits two gamma rays (1.17 Mev and 1.33 Mev) in cascade and ^{59}Fe emits two gamma rays (1.10 Mev and 1.29 Mev) with about equal frequency but not in cascade. For ^{60}Co the computer analysis selects the window threshold at 0.36 Mev, which is on the threshold line (Fig. 101), for the 1.33 Mev gamma ray. The window top determined by the computer analysis is at 1.11 Mev, which is on the window top line (Fig. 101) for the 1.17 Mev gamma ray. With ^{59}Fe the window top fits the line with respect to the 1.10 Mev gamma-ray, but the threshold does not fit at all. The reason for this exception is not understood.

The intersection of the threshold and window top lines at 100 kev indicates that for gamma rays of energy less than about 100 kev the "optimum scatter window" concept cannot be used (Fig. 101). This seems reasonable because in tissue there is a high probability that gamma-ray interactions will be photoelectric rather than Compton at energies in the region of about 100 kev and below. For energies below 100 kev the best approach for most accurate counting may be to collect all counts in the total spectrum from zero energy to just above the photopeak.

The optimum windows shown in Fig. 101 complicate the problems of quantitation of more than one radioisotope in the same person because the optimum windows for one radioisotope may

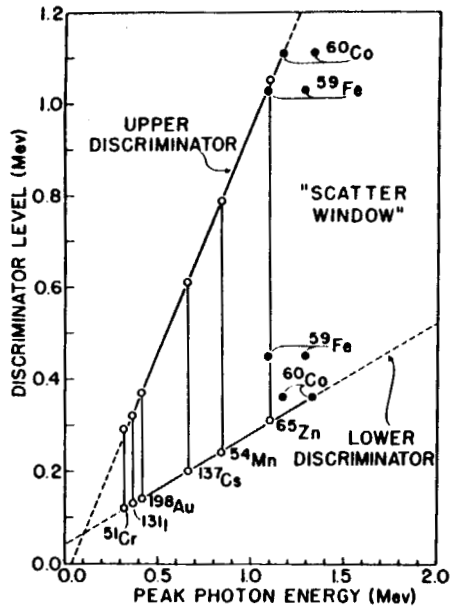

Fig. 101. Optimum windows determined for several radioisotopes and the linear relation of upper and lower bounds to gamma-ray energy.

overlap the photopeak of the other. As yet we have not resolved this complication and have restricted the "optimum scatter window" method to single radioisotope retention studies.

The "optimum scatter windows" that have been determined for one whole-body counter are most likely not the optimum windows for all other whole-body counters. Such factors as detector geometry, detector size, and shielding probably play significant roles. However, we do believe that, for every whole-body counter configuration, a set of optimum windows does exist and that they can be determined by the same empirical approach that is described here. Probably the window boundaries will have a linear relation to gamma-ray energy for monoenergetic emitters and the upper and lower bounds will intersect at about 100 kev. If this proves to be true, then one only needs to determine the optimum window for ^{51}Cr, ^{54}Mn, and ^{65}Zn and construct a graph similar to Fig. 101 from which optimum window for monoenergetic emitters of all energies can be read directly.

REFERENCES

1. Gibbs, W. D., Hodges, H. D., and Lushbaugh, C. C. Standardization and calibration of a whole-body counter for clinical research. In: USAEC Report ORINS-53, 1965, pp. 145-149.

2. Gibbs, W. D., Hodges, H. D., Bailey, M., and Lushbaugh, C. C. Test of an empirical system for correcting geometric error in whole-body counting of reportioning radioactive labels using iodine-131. In: USAEC Report ORAU-106, 1967, pp. 179-181.

1027564

Background Improvement for a Low-Level Whole-Body Counter

W. D. Gibbs, Harold D. Hodges, and Mildred Bailey

Constant effort is required to obtain a stable low background even in a well-protected multishielded whole-body counter like the one in the Medical Division. Extreme care in choice of construction materials prevents most but not all build-in radioactive contamination of the shield. Although most radioactive contaminants will decay in time and produce over the years a continuing improvement of background radioactivity, our experience shows that week-to-week and even day-to-day fluctuations occur that seriously interfere with low-level radioassays of man unless active control procedures are built into such counters to be used routinely.

Soon after our whole-body counter operation began (December 1964) background fluctuations were so variable that elaborate measurements were required to enable precise radioassays. Most of this instability was due to variable concentrations of radon daughter isotopes. One source was soon found to be the outside air that was being supplied to the plastic compartment where a patient resides during an assay. We installed a filter system and a tracheal duct leading directly to the inner plastic chamber (June 1965). Immediately our average background measurements decreased significantly. In about a month the background varied still less as shown by significant decrease in the extreme ranges of the counts (Fig. 102). The residual, continuing fluctuations have recently been found to be due to pulse-like releases of radon into the shielded room from the 0.25-in. lead liner inside the 5.0-in.-thick steel shield. This naturally radioactive lead is covered with 0.0625 in. stainless steel with resin-sealed seams that apparently are not impermeable to radon gas. Installation and constant operation of a vacuum pump connected by pipe to the gravel-filled (olivine) space between the outermost concrete shield and the 5.0-in. steel shield (November 1965) resulted (Fig. 102) in another major decrease in background radioactivity. Continued pumping lowered the average background counts asymptotically until early 1967. This relatively steady background

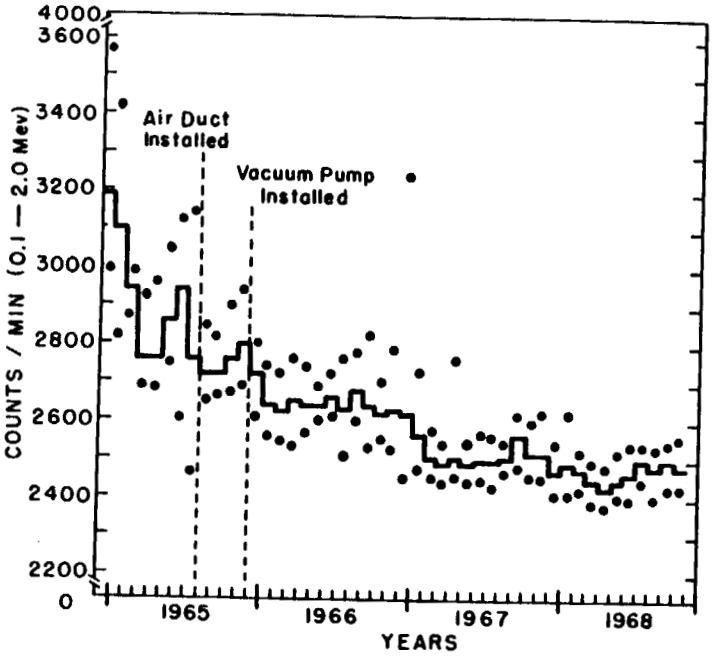

Fig. 102. Progressive improvement mean and extreme background counts each month (100 kev to 2.0 Mev) in relation to our installation of measures to combat the buildup of ^{226}Ra daughters.

is 78% of that obtained initially. A detailed examination of the initial (December 1964) and most recent (November 1968) background spectra (Fig. 103) shows a "difference" spectrum (also shown in the figure) that is an almost perfect fit for the combined spectra for the radon daughters ^{214}Pb and ^{214}Bi. The excess counts in the 0.510- and 0.610-kev peaks probably reflect the presence of ^{106}Ru (half-life = 1 year) inadvertently incorporated in the steel shield initially. Since this isotope has now decayed to about 6% of the amount initially present, only a very slight further decrease in these energy regions of the background spectrum can be expected.

A study of the frequency distribution (Fig. 104) of 334 daily background counts for the year 1967 shows that their mean was 2513 counts/min with a 2410-count minimum and a 2759-count maximum (extremes of -4% and +10%). Although this positively skewed distribution suggests that some improvement can still be obtained by better methods for confining all ^{226}Ra daughters behind the lead shield, our "true" or "best obtainable" background level probably lies between 2200 and 2400 counts/min. With the detector volume now in use (10,330 cm^3 NaI) such a background

1027565

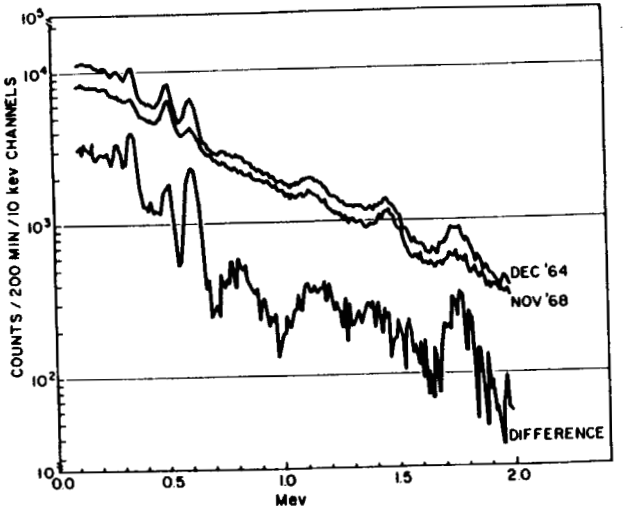

Fig. 103. The initial and present whole-body counter background spectra and their net difference spectra show that background improvement resulted chiefly from decay and removal of radon daughters.

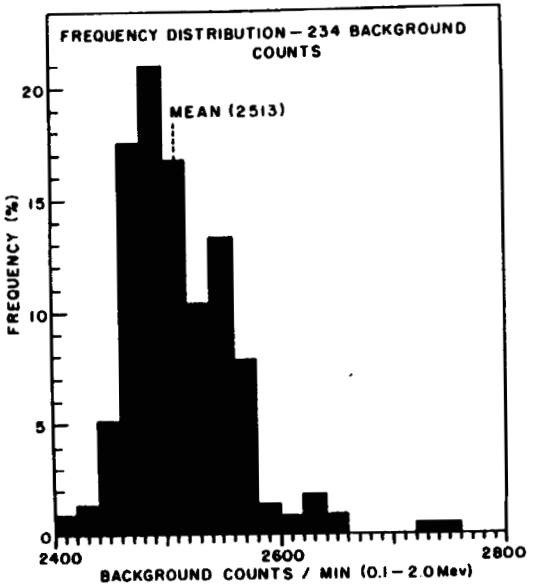

Fig. 104. Frequency distribution of 334 (year 1967) background counts showing skewness resulting from sporadic pumping failures that permitted ^{226}Ra daughter buildup over weekends and other unattended periods.

level would achieve for us a background index of 0.213–0.233 counts/min/cm^3, compared to our present index of 0.241 and the world's best of 0.214, at the Veterans Administration Hospital, Iowa City, as reported in the IAEA Directory of Whole-Body Radioactivity Monitors.

Improvements in Profile-Scanner Instrumentation

W. D. Gibbs, C. L. Edwards, and Harold D. Hodges

The profile scanner has been in use at the Medical Division for about 10 years. During this time it has been used extensively to measure the whole-body retention of diagnostic and therapeutic doses of radiopharmaceuticals. It has also been used to determine qualitatively the longitudinal distribution of several radionuclides.[1,2] We have hoped that this instrument could provide rapid quantitative information of the distribution of internal radionuclides. We have modified the instrumentation several times; for example, refining the readout of the original rate-meter, strip-chart profile, but until recently we had achieved no major advances toward the quantitation of radioactivity in body sections.

Recently the instrument has been modified to provide discrete numerical data collection with data output in the form of perforated tape that can be read and analyzed by computer. In addition, the activity profile is displayed on a cathode-ray (tube) screen for immediate visual analysis and may be recorded on Polaroid film.

The new instrumentation consists of a 400-channel pulse-height analyzer, a parallel-to-serial converter, a tape perforator, and a Polaroid camera mounted onto the multichannel analyzer cathode-ray display (Fig. 105). In practice the outputs of the twelve 2-in. x 2-in. NaI detectors[3] are summed in one preamplifier and the preamplifier output is connected to the multichannel analyzer. This analyzer is operated in multiscale mode with the window adjusted to accept counts only in the photopeak of the radioisotope under study. In multiscale operation the accumulated time per channel can be selected (0.75, 1,5, 3.0, 6.0, and 12.0 sec/channel). Speed of the table drive can also be selected. Speeds of 10.9, 15.5, 21.8 or 30.25 cm/min are provided. No changes have been made in collimation,[3] and the collimator opening can be varied between 0 and 10 cm. These variables allow a selection of combinations to meet the wide ranges of total radioactivity and distribution encountered in patients.

Quantitation of radioisotopes in body sections requires precise location and recording of anatomic landmarks. To facilitate correlation of anatomic landmarks with the activity profile, a fixed headboard and adjustable footboard have been added to the scan table.

1027566

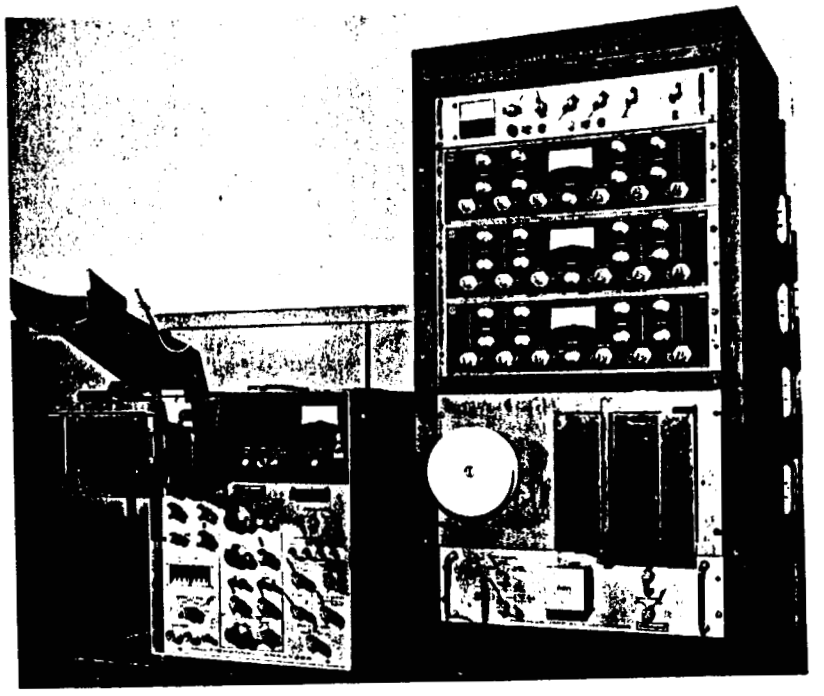

Fig. 105. Profile scanner instrumentation. Multichannel pulse-height analyzer with camera is shown at the left. At the right, detector high-voltage power supply and distribution system (top), tape perforator (center), and parallel-to-serial converter (bottom).

In addition, a centimeter scale on the side of the scan table and a moving pointer allow measurement of the distance of such landmarks as eyes, chin, sternal notch, xyphoid, etc., from an arbitrarily chosen starting point (Fig. 106). These data, along with the table speed and channel accumulated time, are punched into cards and read into the computer along with the counting data. The landmarks can then be related to a specific data channel in the activity profile. The table-drive motor is connected to the count switch of the multichannel analyzer so that table movement and multiscaling start simultaneously.

As the patient is being scanned we take a time-exposure Polaroid photograph of the activity profile which shows a white profile of the distribution of radioisotope on a black background (Fig. 107). The grid is obtained by briefly turning on its illumination light while the scan is being made.

This linear scanning system provides both immediate and permanent visual display of the profile, without rate-meter lag, and

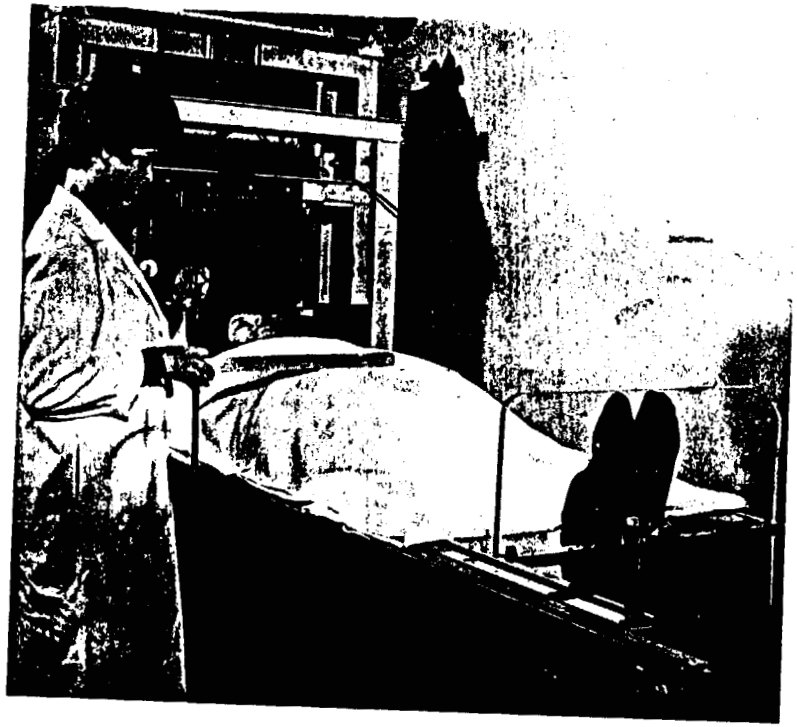

Fig. 106. Profile scanner bed with patient-positioning footboard and anatomic landmarking pointer.

numeric data in discrete form. The numeric data collection makes possible quantitative analyses of radioisotope concentration in any body section, the resolution of course being limited by collimation, table speed, and multiscale channel advance speed. The precise relations between these factors and the resolution obtainable are not yet known but are being determined.

REFERENCES

1. Pircher, F. J., Sitterson, B. W., and Andrews, G. A. The ORINS linear scanner in diagnosis and treatment of thyroid carcinoma with iodine131. J Nucl Med 1, 251-261, 1960.

2. Pircher, F. J., Brucer, M., Morris, A. C., Jr., and Black, R. The ORINS linear scanner in clinical diagnosis. J Nucl Med 3, 26-40, 1962.

3. Morris, A. C., Jr. A linear scanner for human radioisotope research. USAEC Report ORINS-33, March 1960, 26 pp.

1027567

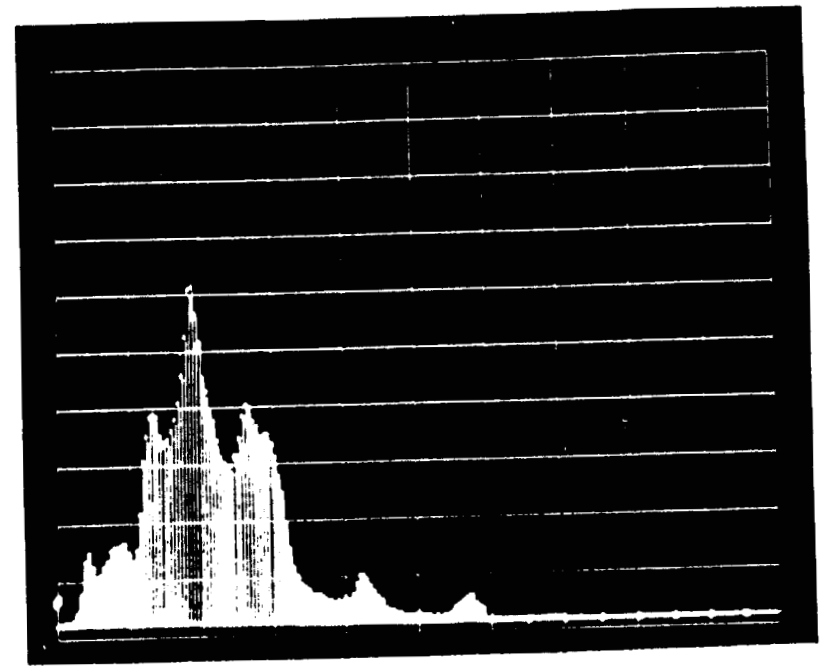

Fig. 107. Profile scan of ^{67}Ga in a patient. Head at left (channel 10) xyphoid at point of greatest activity (channel 38) and feet at channel 118.

1027568

IMMUNOLOGIC STUDIES AND THE DEVELOPMENT OF THE MARMOSET AS A LABORATORY PRIMATE

The immunology project has evolved out of the objective of obtaining marrow transplants, particularly as a means of sustaining persons who have been heavily irradiated. We are using two experimental models to better understand the genetics of tissue transplantation. One is the mouse radiation chimera in which cell chimerism is induced by injecting foreign bone marrow after the subject is exposed to lethal radiation. An immediate problem now under investigation is the effect of radiation exposure rates on immune suppression. Our previous studies showed that the immune response was depressed more when high rates were used; this phenomenon has played a major role in the success of foreign marrow grafts in mice. Further basic studies in attempting to define the mechanism of this rate effect are reported here. The use of the Jerne plaque technique to identify host-graft incompatibilities in the mouse radiation chimera was previously demonstrated in our laboratory. In continuing to pursue this aspect of the problem we reevaluated the technique itself with the surprising conclusion that each antigen-antibody system assayed may require a unique set of experimental conditions. Direct application of these findings to the foreign chimera problem is now possible. Studies in the mouse radiation chimera are being paralleled in the second experimental model, one in which hemopoietic cell chimerism occurs naturally, the marmoset. This primate, because of its unique reproductive physiology, is a chimera produced by nature. Yet, current studies have revealed that, unlike the mouse radiation chimera in which the hemopoietic system is invariably 100% of donor origin, the natural chimerism in the marmoset may range from less than 2% of the cell population to greater than 98%. The sole criterion for chimerism is now based on sex chromosome analysis of proliferating white blood cells and the "drumstick" sex indicator in mature neutrophilic cells; considerable emphasis is being placed on the development of suitable red-cell antigen markers with which to distinguish erythrocyte chimerism. The degree of white-blood-cell chimerism appears to be unrelated to induction of immunologic tolerance, in that exchange skin grafts between twin pairs have shown complete acceptance regardless of the percentage of foreign-cell chimerism. Skin homograft immunity is well expressed in this animal as revealed by rejection of grafts between unrelated marmosets. However, the rejection times of homografts have reflected the subspecies relation of donor and recipient; grafts exchanged between animals within one subspecies survive considerably longer than those exchanged between subspecies. Whether this indicates a gene pooling of an interbreeding population of wild animals or the consequence of the natural chimerism or both is not known. Continued breeding and development of the marmoset in our colony as a laboratory primate should in the future provide animals that may answer this and other questions related to the natural cell chimerism.

Further Observations on the Role of Acute Exposure Rates on Immune Suppression of Irradiated Mice

Donald E. Carlson, and N. Gengozian*

Previous work in this laboratory has established that suppression of antibody formation in sublethally irradiated mice depended upon the acute exposure rate used. After 600 R or 700 R, mice exposed at 72 R/min produced only 3 to 6% as much agglutinin as those exposed at 8 R/min.

In the present study these observations were extended (1) to investigate the effect of acute radiation exposure rate at various times either before or after antigen administration; (2) to establish that the exposure-rate dependence of antibody formation occurred at the cellular level; and (3) to compare the rate dependence of immune suppression to animal mortality.

Sheep erythrocyte antigen was injected into groups of 15 mice either 5, 1, or 1/2 days before, 2 hr, 1/2, 1, or 5 days after 700 R at 8 R/min, 40 R/min, or 72 R/min. Serum samples were collected at five weekly intervals after antigen injection. To determine the levels of circulating antibody, the test antigen was added to serial 2-fold dilutions of serum and saline; the reactions were then scored for macroscopic agglutination. Data for each experiment were expressed as titer as a function of time after antigen administration; titer is defined as the reciprocal of the highest dilution of serum where agglutination was detectable. The results of this study are shown in Fig. 108. Antibody responses were expressed as integral $\log_2$ titer units. Thus, each point on the figure represents five consecutive determinations for the 15 mice used in each experimental group.

Radiation given 5 days after injection of antigen produced no depression of antibody response. Three days or 1 day after antigen administration, 700 R at the three exposure rates caused rate-dependent suppression of antibody formation, although adjacent points (8 R/min and 40 R/min) were not statistically different. When antigen was given 12 hr before radiation exposure, however, responses of the two higher exposure-rate groups were sharply depressed. Under these conditions the difference between the 8 R/min and 40 R/min group responses was approximately 6 $\log_2$ titer units; this corresponds to a 64-fold depression of antibody production with a 5-fold increase of acute exposure rate.

The sharp decrease in titer of the 40 R/min and 72 R/min

* This investigation was supported in part by Public Health Service Training Grant GM 730 from the National Institute of General Medical Sciences, Public Health Service.

1027569

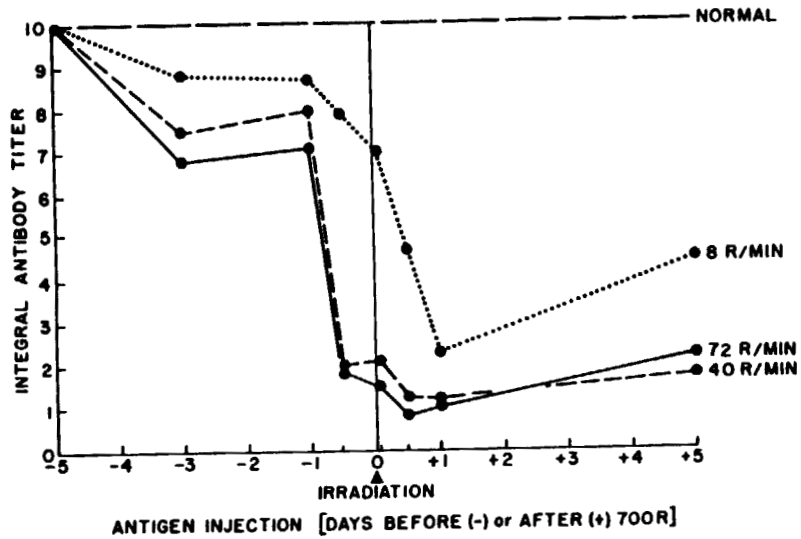

Fig. 108. The effect of exposure rate on antibody production as a function of time of antigen administration relative to irradiation at 700 R.

recipients when the period between initiation of antibody response (antigen injection) and radiation was shortened from 24 hr to 12 hr suggests that early steps in the process of antibody formation are highly sensitive to radiation delivered at 40 R/min or more. In contrast, the 8 R/min response was only slightly decreased over this time increment. Thus radiation delivered at different rates may differentially impair either the animal's ability to recognize and process foreign antigens or the ability of immunocompetent cells to undergo immune induction. Although differential cell killing cannot be ruled out, the difference in the -12 hr and -24 hr 40 R/min or 72 R/min group responses cannot be explained on the basis of cell division occurring during the additional 12-hr period.

When antigen was given after irradiation, responses of the two high-rate groups were similar; however, over the first 24 hr after irradiation the 8 R/min groups showed decreasing responses. The minimum total response occurred when antigen was injected 24 hr after radiation exposure. The slightly increased responses observed in all groups when antigen injection was delayed for 5 days were attributed to postirradiation recovery and repair.

To establish that the exposure-rate sensitivity of antibody formation resulted from differential damage to immune cells, and to rule out indirect effects resulting from the differentially irradiated cell environment, the following in vivo cell culture technique was used.

All recipient mice were exposed to 950 R at 150 R/min. Each

animal received intravenously a suspension of spleen cells from syngeneic donors exposed 2 hr previously to 300 R at either 4 R/min, 40 R/min, or 72 R/min, followed immediately by intraperitoneal injection of sheep erythrocyte antigen. Recipient mice were killed by exsanguination on the sixth day, and levels of circulating antibody were determined as described previously. Antibody production was attributed to the transferred cells since 950 R completely suppressed antibody formation in control animals given antigen alone.

Figure 109 shows the results of 300 R ^{60}Co gamma rays on donor spleen cells exposed at either 4 R/min, 40 R/min, or 72 R/min. A linear relation was obtained between the number of injected spleen cells and the resulting $\log_2$ antibody titers. Slopes of the regression lines were not statistically different; however, the levels of response for each exposure rate were significantly different ($P<0.01$). Additional experiments using different total exposures were qualitatively similar for both primary and secondary antibody responses. These experiments provide evidence that an exposure-rate dependence exists at the immunocyte level and suggest that rate-dependent suppression of antibody formation observed in intact mice also results from differential damage to the immunocytes themselves.

The effect of acute radiation exposure rate was compared for antibody formation and animal mortality at total exposures that gave maximum exposure-rate differences. Previous studies showed

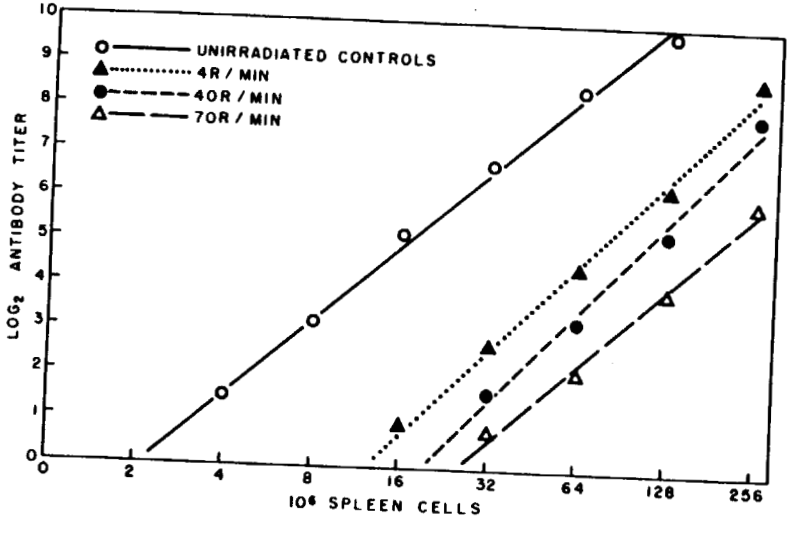

Fig. 109. The effect of exposure rate on primary antibody production of transferred spleen cells exposed to 300 R.

1027570

that maximum exposure-rate-dependent depression of antibody formation occurred in intact mice at 700 R. Radiation mortality studies established that 1000 R produced the maximum exposure-rate-dependent difference in 30-day survival.

Figure 110 presents antibody responses of groups of mice exposed at 700 R at exposure rates of from 4 R/min to 100 R/min,

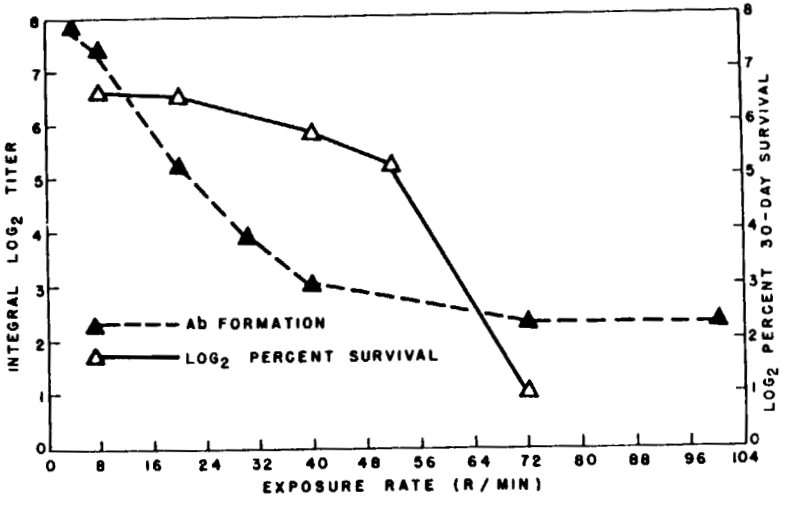

Fig. 110. Comparative effect of exposure rate upon mortality of irradiated mice and suppression of antibody formation, at exposures of maximum rate sensitivity for each end point (1000 R for mortality, and 700 R for immune suppression).

and $\log_2$% 30 day survival of mice irradiated between 8 R/min and 72 R/min to a total exposure of 1000 R. Thirty-day survival ranged from 100% after 8 R/min to 2% after 72 R/min. Survival data were plotted as $\log_2$% survival so that the shape of the resulting curve could be directly compared to antibody-formation data, also plotted as a $\log_2$ function. Antibody formation was sensitive to increased exposure rate from 4 R/min to 40 R/min; between 40 R/min and 72 R/min no additional depression ($P>0.05$) was observed. In contrast, animal survival was not sharply decreased from 8 R/min to 52 R/min. Between exposure rates of 52 R/min and 72 R/min, 30-day survival was decreased by a factor of 20 (40% to 2%).

The lack of parallelism of these two end points suggests that the exposure-rate sensitivity of the immune system is separate from systemic effects related to animal mortality and that radiation death is not a measure of immune incompetence. Although exposure-rate sensitivities have not been reported for the major organ systems involved in radiation mortality, it would be expected that different

cell types would possess different exposure-rate sensitivities just as different cell types exhibit different sensitivities to radiation given at standard dose rates. Thus the sharp drop in survival observed at 1000 R between 52 R/min and 72 R/min would be expected to reflect the range of maximum rate sensitivity for one or more cell systems required for survival of the animal.

Critical Variables of the Jerne Plaque Technique as Applied to Rodent Antibody-Forming Systems Responding to Heterologous Red-Cell Antigens

Karl F. Hübner and N. Gengozian

The Jerne technique was developed for the classical model of immune hemolysis: sheep erythrocytes, anti-sheep erythrocyte antibody, and guinea pig complement (C'). The Immunology group of ORAU was among the first to apply this technique to a system not using sheep red blood cells (RBC) as immunogen. The work of Gengozian et al.[1] indicated that this technique may reveal graft-vs-host and host-vs-graft activity of spleen cells of mouse-hamster radiation chimeras. But the same test, when applied to spleen cells of mice protected with rat bone marrow, gave no meaningful information. Difficulties encountered in these efforts induced us to investigate some variables pertinent to the Jerne technique.

Important factors in the hemolytic plaque technique are the agar, the medium used for its preparation, the Ca^{++} and Mg^{++} concentration, the source (species) of complement (C'), and the presence or absence of diethylaminoethyl (DEAE) dextran in the reacting system. A primary, yet heretofore unconsidered variable, is the species interrelations of different antigen-antibody systems. We studied the following combinations: mouse anti-sheep RBC, mouse anti-rat RBC, mouse anti-hamster RBC, rat anti-mouse RBC, and hamster anti-mouse RBC.

The effect of different C' and different concentrations of Ca^{++} and Mg^{++} on the hemolytic efficiency of day 5 and day 12 antisera was studied with a simple "hemolytic spot test." Drops of the heat-inactivated serum after serial 2-fold dilution were placed on agar plates containing target RBC. After addition of C' hemolytic spots became visible and were scored after 60 min with regard to the degree of hemolysis: complete, incomplete, partial, or no hemolysis. The results of the different spot tests gave us the optimal conditions for each system and are shown in Table 90.

These improved conditions were used in a final spot test comparing the efficiencies of the three C' in each of the species combinations. The activity of each C' could be increased and

1027571

TABLE 90

Optimal Ca^{++} and Mg^{++} concentration and dilution factors for different complements and for different antigen-antibody systems.

Species Antibody	Antigen (RBC)	Concentration of Ca^{++} and Mg^{++} in Elsen's medium			Dilution of Complement		
		Guinea Pig C'	Human C'	Rabbit C'	Guinea Pig C'	Human C'	Rabbit C'
Mouse	Sheep	B	D	C	1:10	1:4	1:4
Mouse	Rat	B	C	C	1:4	1:4	1:2
Mouse	Hamster	C	C	C	1:4	1:4	1:4
Rat	Mouse	D	C	C	1:10	1:2	1:2
Hamster	Mouse	B	C	C	1:4	1:2	1:2

* B: Ca^{++}, 1.5×10^{-4}M; Mg^{++}, 5×10^{-4}M

C: Ca^{++}, 0.75×10^{-4}M; M^{++}, 2.5×10^{-4}M

D: Ca^{++}, 0.375×10^{-4}M; Mg^{++}, 1.25×10^{-4}M

the results indicated that guinea pig C' and human C' are equally effective in the mouse anti-sheep system, that rabbit C' is most efficient in the mouse anti-rat combination, and that human C' brings about the highest degree of hemolysis with mouse anti-hamster serum as well as with rat and hamster antisera against mouse RBC.

To test these conclusions the improved conditions were used in the actual Jerne technique. The plaque-forming cell response (PFC) of the spleen cells of the different species was determined on 4 consecutive days starting 3.5 days after immunization with RBC. The results are presented in Fig. 111. The differential effectiveness of the various C's was found to be in agreement with the optimal conditions anticipated by the final spot-test. Guinea pig C' and human C' were equally efficient on mouse hemolytic antibody against sheep RBC, but rabbit C' was superior in the mouse anti-rat system and human C' yielded more hemolytic plaques in all the other systems. The similarity in the shapes of the curves in Fig. 111 indicates that the differences in the number of plaques are dependent on the type of C' used.

Different C's applied to one system not only result in different numbers of plaques but also produce plaques of different average size. The average plaque size was determined for each species combination and C'. The results (Fig. 112) demonstrate how the average plaque size changes with different C's. A comparison between the PFC responses and the corresponding average plaque size suggests the conclusion that a high PFC response is accompanied by a greater average plaque size. The relation between the number of antibody molecules and the number of C' molecules required to cause lysis may explain the differences in plaque size. But additionally the average plaque size varies according to the

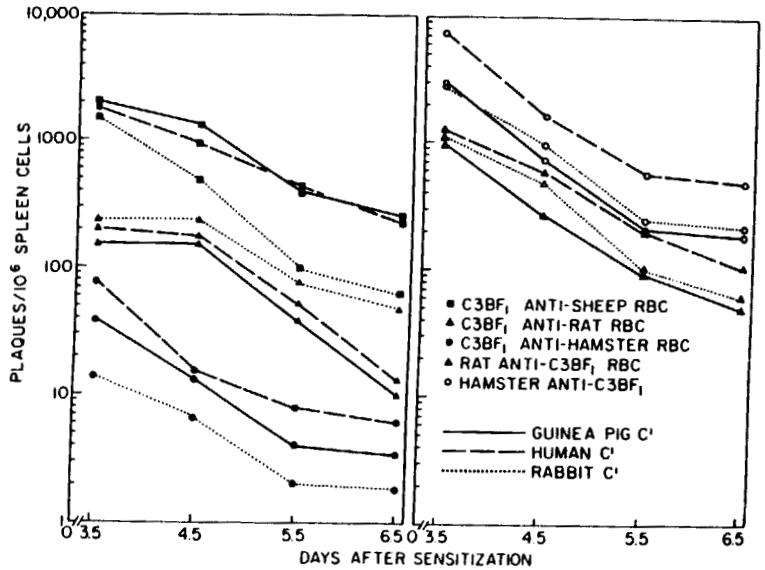

Fig. 111. PFC-response of rodents revealed by complement of three different species. Each point represents the mean of six animals. A statistical analysis using Duncan's "new multiple range test" at the 5% confidence level showed the most effective complement in each of these systems to be significantly different from the "poorest" C' throughout.

C' involved. The reason for this C'-dependent variation is not known. In view of these findings, the Jerne plaque technique may with further refinement serve as a model for studying the interrelations of hemolysins and C' necessary for cell lysis.

Finally we studied the role of the presence or absence of DEAE dextran in the agar. The PFC response was measured in the presence and absence of DEAE dextran with two kinds of agar: lonagar No. 2 and Difco Noble agar. Two different media, Eisen's medium and Hanks' solution, were also tested in this additional experiment. The results gave no indication that the absence of DEAE dextran in either agar increased the number of hemolytic plaques. The total number of plaques depended on whether the agar was prepared in Hanks' solution or Eisen's medium, the latter giving consistently better results in the presence of DEAE dextran (optimal concentration: 0.5 mg/ml of agar). If dextran was not added, agar dissolved in Eisen's medium failed to yield any plaques in contrast to the results obtained with Hanks' solution.

When agar is heated to a boil, sulfated polysaccharide bonds form with Ca^{++} ions possibly participating in the gelation. Sulfated polysaccharide inhibits plaque formation by viruses and

1027572

hemolysins. The polycation, DEAE dextran, eliminates this inhibition by binding at the polyanionic groups. Polycations probably compete with the Ca^{++} ions for that position forming the sulfate bond. Probably this is the mechanism by which DEAE dextran overcomes the anticomplimentary effect of agar. Our findings support this explanation, which was originally offered by Liebhaber and Takemoto.[2,3] Hanks' solution has an abundance of Ca^{++} and Mg^{++} to be bound to the sulfate saccharide and to be available in sufficient amounts for complement-dependent hemolysis. Therefore, we can still obtain a fair number of plaques even in the absence of DEAE dextran. On the other hand, Eisen's medium, containing only about one-half the amount of Mg^{++} and one-seventh the amount of Ca^{++}, will be deficient in these cations; hemolysis will be reduced or impossible unless DEAE dextran is added to counteract the indirect anticomplementary effect of agar.

Our studies indicate the need for caution in the interpretation of results obtained with the Jerne technique especially when it is applied to quantitate an immune response, either in regard to the total number of cells involved or, and particularly, when it is used to evaluate the amount of antibody produced by individual cells. Finally, the species interrelation of the antigen, the antibody forming system, and the source of complement are critical interdependent variables that must be determined to obtain the maximum response for any one system as assayed by the plaque-forming procedure.

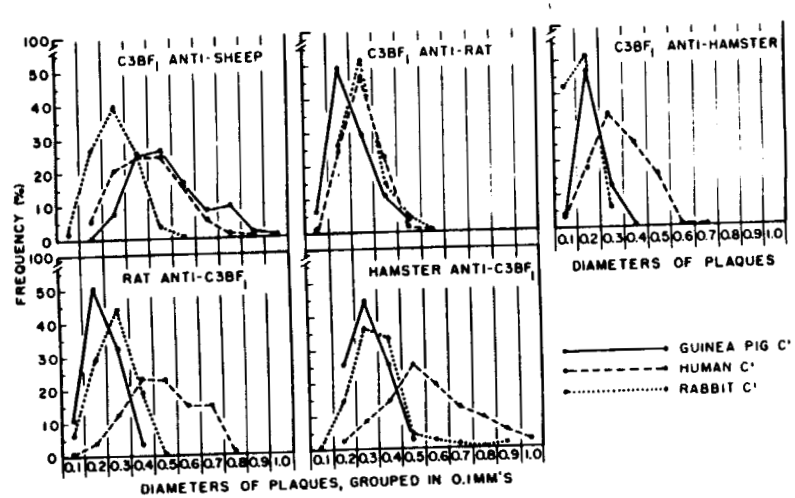

Fig. 112. Comparison of plaque size-distribution polygons obtained by using complements. For each system 130 to 150 plaques were measured.

REFERENCES

1. Gengozian, N., Gottlieb, C. F., and Allen, E. M. Demonstration of an early host-graft incompatibility reaction in radiation chimeras with the Jerne plaque technique. Proc Soc Exp Biol Med 126, 135-140, 1967.

2. Takemoto, K. K. and Liebhaber, H. Virus-polysaccharide interactions. I. An agar polysaccharide determining plaque morphology of EMC virus. Virology 14, 456-462, 1961.

3. Liebhaber, H. and Takemoto, K. K. Alteration of plaque morphology of EMC virus with polycations. Virology 14, 502-504, 1961.

Effect of Cell Concentration on the In Vitro Test for Mixed-Leukocyte Cultures

Helen Vodopick. Elizabeth M. Rupp. and N. Gengozian

Interest in histocompatibility testing has been generated by the increase in the number of transplantation operations being performed. Of the compatibility tests, the in vitro test for mixed leukocyte culture (MLC) is frequently used.

In this test lymphocytes from two different persons are reacted in vitro: the greater the incompatibility between these persons the greater the lymphocyte stimulation and blastic transformation. The end point used to measure response is the incorporation of ^{14}C thymidine into cells that have undergone blastic transformation and are thus capable of synthesizing DNA.

Many of the variables influencing this test are known. However, few data on the effect of variations of reacting cell numbers, that is, lymphocyte concentration, are available.

In a previous report[1] we recognized that the bidirectional MLC test, with both viable cell populations capable of responding and stimulating, gave reduced responses when compared to the unidirectional system in which one of the reacting populations was inhibited by the antibiotic, Mitomycin C.

Two questions to be answered were, What is the least number of stimulating cells that can be used to assess compatibility in a unidirectional system? What influence would varying the cell populations in a two-way system have on their maximal response?

A series of experiments was performed with the same two

1027573

persons as lymphocyte donors. In one set of experiments both lymphocyte populations were viable and uninhibited. A gradient of cells from each reacting population was used (Fig. 113) so that the total number of lymphocytes per milliliter of culture fluid remained constant. The usual concentration of lymphocytes for either the unidirectional or bidirectional system is 1 x 10[6] ml of culture medium. As can be seen in Fig. 113, the maximum reaction occurred on day 7 with similar but declining degree of response on the three succeeding days. The response obtained on day 7 was little different in tubes II to VI but the most consistent response on the following days was found in tube IV where a one-to-one ratio of cells was used.

In the unidirectional system, lymphocyte variation was done in the same manner as described before. However, after the

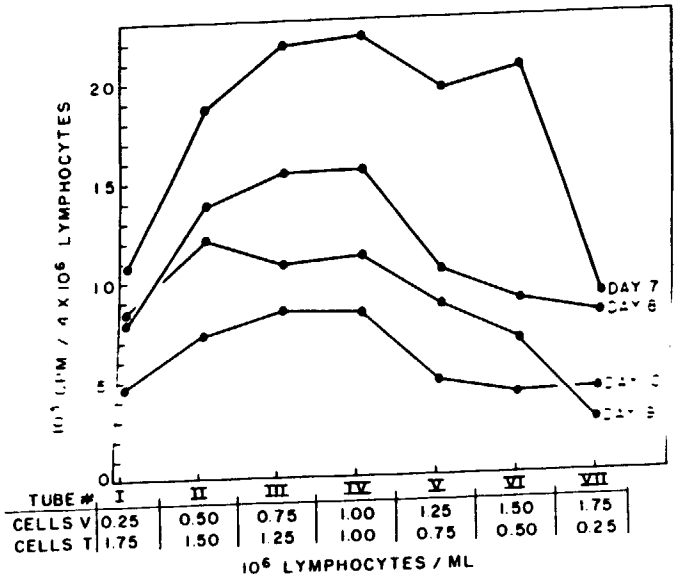

Fig. 113. Bidirectional mixed-leukocyte culture test:. Cell concentrations were varied so that the total number of cells per culture tube remained constant. Highest response was found on day 7 and one-to-one lymphocyte ratio produced the most consistent reaction compared to the other points on the respective curve.

maximum reaction occurred with a one-to-one ratio of stimulating-to-responding lymphocytes, incorporation of ^{14}C thymidine was not reduced so long as the number of stimulating cells remained greater than the number of responding cells present.

From these experiments we have shown that cell concentration

and duration of culture also play an important role in the test for mixed leukocyte cultures.

REFERENCE

1. Vodopick, H., Rupp, E. M., and Gengozian, N. The bi-directional in vitro mixed leukocyte culture reaction: A mutual inhibitory phenomenon? Transplantation, in press.

Neutrophil and Lymphocyte Chimerism in the Imported and Laboratory-Bred Marmoset

N. Gengozian, J. S. Batson, and C. T. Greene

We had previously demonstrated heterosexual hemopoietic chimerism in the marmoset by sex-chromosome analysis of cells obtained from blood, bone marrow, spleen, and lymph node, and also by the use of the sex-chromatin marker of the peripheral-blood neutrophils. This latter marker was used in a small group of randomly selected imported male and female marmosets and offered presumptive evidence for the consistency of fraternal twinning and prenatal vascular anastomoses by virtue of its decrease in incidence (sex-chromatin bearing neutrophils per 500 cells scored) in one half of the females and a corresponding increase in incidence in one half of the males. The study of heterosexual blood chimerism has heretofore been limited to imported adult animals of unknown sib relationships. Establishment of a breeding colony in our laboratory has permitted study of chimerism in known twin pairs. This report concerns parallel analyses of lymphocyte chimerism as determined by sex chromosomes and neutrophil chimerism with the use of the sex-chromatin "drumstick" marker in both laboratory-bred and imported adult marmosets.

On the basis of sex chromosome analyses of peripheral-blood lymphocytes, imported males and females were classified as being "chimeric" or "nonchimeric" for heterosexual cells. Blood smears for drumstick scoring of the neutrophils were obtained from 17 male and 17 female nonchimeric marmosets, and from 18 male and 18 female chimeric marmosets. The data for these two groups are given in Tables 91 and 92. Since these were unrelated imported marmosets and not heterosexual twin pairs, they were arbitrarily tabulated in order of their scoring for the neutrophil drumstick; i.e., in increasing order of frequency. The frequency of the drumstick-bearing neutrophils was found to be significantly greater in the nonchimeric females than in the nonchimeric males (Table 91, 1.85% vs 0.25% $pr<0.02$). Among the chimeric males and females (Table 92),

1027574

TABLE 91

Analysis for Sex Drumstick in Neutrophils of 17 Unrelated Male and Female Marmosets Nonchimeric for Lymphopoietic Cells*

Animal No.	Males		Females	
	Neutrophil Analysis			
	Cells Scored†	%	Cells Scored	%
1	0/500	0	3/379	0.79
2	0/500	0	5/500	1.00
3	0/500	0	5/500	1.00
4	0/500	0	6/500	1.20
5	0/439	0	5/368	1.36
6	0/326	0	7/500	1.40
7	0/134	0	8/500	1.60
8	1/500	0.20	8/500	1.60
9	1/500	0.20	9/500	1.80
10	1/500	0.20	10/500	2.00
11	1/500	0.20	10/500	2.00
12	1/336	0.30	12/500	2.40
13	2/500	0.40	12/500	2.40
14	1/217	0.46	12/500	2.40
15	1/213	0.47	13/500	2.60
16	4/500	0.80	14/500	2.80
17	5/500	1.00	9/242	3.72
Total	18/7165	0.25% (±0.06)‡	148/7989	1.85% (±0.15)

* Nonchimerism for lymphocytes determined by sex chromosome analyses of 50-100 cells obtained from peripheral blood.

† Numerator indicates number of neutrophils bearing sex drumstick; denominator indicates number of neutrophils scored.

‡ Standard error.

the drumstick marker appeared with equal frequency (0.87% vs 0.87%). For both sexes, the frequency of the drumstick-bearing neutrophil among the chimeras was significantly different from that of the nonchimeric marmosets ($pr<0.05$). Thus, this sex marker apparently offers a means of identifying heterosexual chimerism for cells of the neutrophilic series.

In Table 92, the percentage of heterosexual lymphocyte chimerism is also shown for each individual animal. This ranged from less than 2% (male No. 17) to 100% (female No. 6). The total number of cells scored for each sex was tabulated, and an average percentage chimerism was determined for males and females. As a group, the percentage of chimerism among females was significantly greater than the percentage of

TABLE 92

Analysis for Sex Drumstick in Neutrophils of 18 Unrelated Male and Female Marmosets Chimeric for Lymphopoietic Cells

Animal No.	Males				Females			
	Neutrophil analysis		Lymphocyte chimerism		Neutrophil analysis		Lymphocyte chimerism	
		%		%		%		%
1	0/500*	0	20/50†	40	0/117	0	18/50	36
2	0/500	0	31/50	62	0/500	0	59/65	91
3	1/500	0.20	8/50	16	1/500	0.20	27/90	30
4	1/500	0.20	33/50	66	1/500	0.20	24/50	48
5	2/500	0.40	19/50	38	1/500	0.20	16/32	50
6	2/500	0.40	9/100	9	1/500	0.20	50/50	100
7	3/500	0.60	21/63	33	2/500	0.40	41/50	82
8	3/500	0.60	6/50	12	4/500	0.80	31/100	31
9	3/500	0.60	32/50	64	4/500	0.80	32/50	64
10	3/500	0.50	23/50	46	3/348	0.86	26/50	52
11	3/500	0.60	9/50	18	5/500	1.00	21/50	42
12	4/500	0.80	26/50	52	4/365	1.10	47/60	78
13	5/500	1.00	14/50	28	4/349	1.15	32/50	64
14	8/500	1.60	8/50	16	6/500	1.20	34/50	68
15	9/500	1.80	30/50	60	8/500	1.60	10/64	16
16	7/358	1.95	16/52	31	9/500	1.80	29/50	58
17	10/500	2.00	4/65	(06)‡	9/500	1.80	15/50	30
18	13/500	2.60	17/25	68	9/500	1.80	3/17	18
Total	77/8858	0.87% (±0.10)§	326/955	34.1% (±1.5)	71/8179	0.87% (±0.10)	515/978	52.7% (±1.6)

* Numerator indicates number of neutrophils bearing sex drumstick; denominator indicates number of neutrophils scored.

† Numerator indicates number of opposite sex cells found by sex chromosome analysis; denominator indicates total number of cells analysed. All figures based on cells scored from one culture for each animal.

‡ This percentage chimerism obtained from culture of bone marrow cells. Culture of peripheral blood lymphocytes at the same time yielded a negative test for chimerism in scoring of 227 cells. A subsequent culture of peripheral blood lymphocytes 4 months later revealed 5 female cells of 100 scored. Thus, if the lymphocyte data is pooled, percentage chimerism would be 1.7%. This may not be justified since some animals have shown changes in chimerism with time (to be published).

§ Standard error.

chimerism among the males (52.7% vs 34.1%, pr<0.05). Statistical analyses showed no correlation between the degree of lymphocyte chimerism and the percentage of neutrophils bearing the sex chromatin material among the individual animals. Data from several animals in Table 92 may be cited to support this conclusion. For example, male No. 2 was negative for drumstick-bearing neutrophils, yet showed 62% chimerism for female lymphocytes. Male No. 17 showed less than 2% lymphocyte chimerism in analyses of more than 300 cells, yet had a neutrophil drumstick frequency of 2.0%, comparable to the nonchimeric female level.

To document further the sex specificity of the drumstick marker, neutrophils of marmoset twins of like sex and of known single births were scored. This was done for both male and female marmosets bred in the laboratory and known to be nonchimeric by sex-chromosome analysis of peripheral-blood

1027575

lymphocytes. Among 14 females, the neutrophil drumstick-bearing frequency was 1.54%, statistically comparable to that observed for the nonchimeric females of Table 91. Of 14 males, only two (co-twins) had neutrophils bearing drumstick-like appendages, giving a frequency of 0.05% among these animals. This frequency is in contrast to the data obtained in the imported group of nonchimeric (lymphocytes) male marmosets in which more than one half the animals showed a positive test for drumstick-bearing neutrophils (Table 91). The data suggest that the latter animals may have been chimeric for neutrophils while being nonchimeric for lymphocytes.

Analyses for blood chimerism were made in 10 sets of heterosexual twin pairs born in our colony. The data in Table 93 show that all animals were chimeric for peripheral-blood lymphocytes. Scoring for the neutrophil drumstick appendage in the co-twins revealed no positive correlation with the percentage of lymphocyte chimerism and supported the conclusion reached previously with data obtained from the unrelated, imported animals (Table 92). An interesting result was the close approximation of the frequency of the drumstick-bearing neutrophils among the co-twin pairs. We had previously reasoned that chimerism should result in (a) a diluting out, i.e. decrease in numbers of the drumstick-bearing neutrophils in females chimeric for male cells; and (b) the presence of these cells in males chimeric for female cells. With few exceptions, the data in Table 93 support this thesis. Of the 20 animals involved, only three (females of pairs 8 and 9, and the male twin of pair 7) failed to show the expected changes in the frequency of these cells as a consequence of heterosexual chimerism. The close correlation in the drumstick scoring between the co-twins recalls the almost identical percentages of this marker noted earlier for the imported male and female chimeric animals (Table 92). In a comparison of the frequency of the drumstick-bearing neutrophils as population percentages between the laboratory-bred (Table 93) and imported male and female chimeras (Table 92), no significant difference was found (pr<0.05).

Of primary interest was the correlation of lymphocyte chimerism between the co-twins (Table 93). We may introduce the hypothesis that if cell mixing during embryonic development is perfect, the proportion of cells with female (or male) sex chromosomes should be identical in each twin. That is, the proportion of chimerism in one twin should be the complement of the proportion of chimerism in the other, and the sum of the proportions should equal one when mixing is perfect. This has been noted in Table 93 as the Twin Chimerism Index (TCI), which is simply the sum of the two proportions of chimerism and gives a measure of identity of the cell populations (male and female) in the co-twins. Pairs 1,2,6,8,9, and 10 showed similar proportions of heterosexual cells, i.e., the TCI approached 1.00. The TCI for pair 3 was found to be significantly greater than 1, and the TCI for pairs 4,5, and 7 was significantly less than 1 (pr<0.05). To test on the basis of sex chromosome analysis

TABLE 93

Analysis for Blood Lymphocyte Chimerism and Sex-Drumstick Neutrophils in Laboratory-Bred Heterosexual Marmoset Twins

Pair No.	Sex	Neutrophil Scoring*	Lymphocyte Chimerismt	Twin Chimerism Index, (% Chimerism, F + M)‡ / 100
1	F	2/500	30/50 (60)	
	M	2/500	16/50 (32)	.92
2	F	5/500	10/50 (20)	
	M	4/500	45/50 (90)	1.10
3	F	0/500	36/50 (72)	
	M	2/500	26/50 (52)	1.24
4	F	4/500	7/50 (14)	
	M	3/500	52/100 (52)	.66
5	F	4/500	31/61 (51)	
	M	5/500	12/50 (24)	.75
6	F	6/500	27/51 (53)	
	M	7/500	35/100 (35)	.88
7	F	0/500	52/85 (61)	
	M	0/500	17/100 (17)	.78
8	F	13/500	67/100 (67)	
	M	9/500	33/100 (33)	1.00
9	F	10/500	43/95 (45)	
	M	10/500	49/100 (49)	.94
10	F	5/500	53/100 (53)	
	M	2/500	24/62 (39)	.92

* Numerator indicates number of neutrophils with sex drumstick material; denominator indicates number of cells scored.

† Numerator indicates the number of opposite sex cells found by sex chromosome analysis in each twin; denominator indicates the total number of cells analysed. Figures in parentheses indicate percent heterosexual chimerism.

‡ Twin Chimerism Index gives a measure of the identity of the cell population (M and F) in co-twins. Thus, a value of 1.00 indicates an equal proportion of male and female cells in each twin, e.g. twin pair 8.

this hypothesis that the proportion of cells of opposite sex is complementary for each pair, a chi-square test was made. Except for pair no. 9, we found that the heterosexual lymphocyte proportions were not complementary.

The present study with known iso- and heterosexual co-twins and single-birth animals have verified the sex specificity of the drumstick in the marmoset. The almost identical population

1027576

percentages for this marker in imported males and females known to be chimeric by sex chromosome (lymphocyte) analysis and their close correlation with data from known heterosexual co-twins are to be contrasted with the population percentages obtained with the nonchimeric (lymphocyte) imported groups, the isosexual co-twins, and single-birth animals. The data thus confirm the value of the drumstick neutrophil as offering presumptive evidence for chimerism but also indicate that the variability of the appearance of this marker and the lack of correlation with lymphocyte chimerism prevents its use in quantitative estimation of chimerism. Lymphocyte chimerism was found in all heterosexual co-twins and, analogous to the situation in cattle twins, the proportion of blood chimerism in one twin was the same as that of its co-twin.

Blood Group Specificities on Marmoset Red Cells

S. P. Datta and N. Gengozian

Eightly to ninety percent of marmosets are born as members of a twin pair. This twinning is invariably fraternal and is accompanied by placental vascular anastomoses. Cytogenetic analysis of blood lymphocytes, lymph-node, spleen, and bone-marrow cells has shown that each member of an unlike-sexed twin pair is chimeric; i.e., it contains a mixture of two kinds of cells - one cell type with two X chromosomes and the other with one X and one Y chromosome. It has been presumed that chimerism occurs in members of like-sexed twin pairs but evidence for this is still lacking. Thus, owing to the unavailability of additional genetic markers, we have been unable to make maximum use of this high incidence of naturally occurring cell chimerism. An ideal marker would have one or more of the following attributes: (a) it should be based upon easily accessible tissue; (b) it should not require costly and time-consuming technology for its identification; and (c) it could be used for separation of the two cell types. Since we can obtain blood samples from marmosets easily, at frequent intervals, and without adverse effects on the health of the animal, our efforts have been directed at possible genetic markers that are distinctive of various blood constituents. This report documents part of our current work on erythrocyte antigens.

In a series of experiments, erythrocytes from a panel of six marmosets and six humans were tested with three anti-human N reagents; two of these reagents were commercial sera prepared from rabbit anti-human erythrocyte antisera and the third reagent was a laboratory-prepared saline extract of Bauhinia purpurea seeds. The anti-N specificity of the Bauhinia extract had been assessed by tests with a panel of 20 type O blood samples from persons

of various M-N phenotypes. Results of these experiments are summarized in Table 94. One reagent of rabbit origin failed to agglutinate marmoset erythrocytes whereas the other rabbit reagent agglutinated erythrocytes of some marmosets. Absorption of this reagent with marmoset erythrocytes removed activity for all marmoset cells but had little effect on reactions against human N and MN cells. Since only a small amount of this serum was available, further work on the marmoset specificity detected by this serum was not done. This specificity may be unrelated to human N antigen or may represent a subfraction thereof.

TABLE 94

Cross Reaction Between Marmoset Erythrocytes and Various Anti-human N Reagents

Erythrocytes	Unabsorbed Reagents			Absorption of Reagent with			
	Rabbit (No. 1)	Rabbit (No. 2)	Bauhinia	Rabbit (No.2) Marmoset 30-3-2	Bauhinia Marmoset 30-3-2	Bauhinia M*	Bauhinia M†
Human O,M ‡	0	0	0	0	0	0	0
O,MN	++	++	++	++	0	0	+
O,N	++	++	+++	++	0	0	+
Marmoset 31-4-2 §	0	0	++++	0	0	++±	++++
30-3-2	0	+	++++	0	0	++±	++++

* N = Human AB,N

† M = Human AB, M

‡ Two samples of each phenotype

§ Six marmosets were tested, the two reported in the table represent the patterns that were observed.

The Bauhinia extract agglutinated erythrocytes from all marmosets. Results of parallel absorptions of the extract with equal volumes of various types of erythrocytes are also shown in Table 94. Absorption with marmoset erythrocytes removed activity for both the human and marmoset cells; human N cells removed activity for all human cells and slightly diminished the activity for marmoset cells; absorption with human M cells reduced the reaction against human N and MN cells but had little effect on activity against marmoset erythrocytes. Removal of anti-N specificity by M cells is known to occur with anti-N of rabbit origin also and is believed to be a consequence of immunochemical similarity between the M and N antigens. The removal of anti-N activity of the Bauhinia lectin by marmoset erythrocytes suggests that these cells also contain an immunochemical entity similar to that of human-N antigen. That this entity is antigenic is suggested by results of absorptions of a cattle anti-marmoset erythrocyte antiserum (Table 95). Absorption with human O, M cells does not remove reactions for human cells that contain A or N antigen; absorption with AB, M cells leaves behind antibodies that react with only those human cells that contain N antigen. This absorption suggests that the antiserum contains an anti-A like specificity and an anti-N like

1027577

TABLE 95

Analysis of Cattle Anti-Marmoset Erythrocyte Serum (No. 718): Cross Reaction Between Marmoset Erythrocytes for Human N antigen.

Type of Erythrocyte	Number of Individuals	Unabsorbed Antiserum	Antiserum absorbed with erythrocytes from Human O,M	Human AB,M	Human AB,N	Marmoset 34-2-2
Human O,M*	6	+	0	0	0	0
O,MN	4	+	+	+	0	0
O,N	6	+	+	+	0	0
A,M	4	+	+	0	0	0
B,M	1	+	0	0	0	0
AB,N	1	+	+	+	0	0
AB,M	1	+	+	0	0	0
Marmoset 34-2-2		++	++	++	++	0
30-5-2		++	++	++	++	++

* Complete blood types for these samples were available.

TABLE 96

Analysis of Cattle Anti-Marmoset Erythrocyte Serum (No. 718) for Individual Specificities.

Marmoset Red Cell (No.)	Unabsorbed Serum	Serum absorbed with cells: 38-2-2	41-1-3	38-1-4	34-2-2	Postulated antigen(s) on erythrocytes
30-5-2	+	+	+	+	+	ABCDE
38-2-2	+	0	+	+	+	ABCD
41-1-3	+	0	0	+	+	ABC
38-1-4	+	0	0	0	+	AB
34-2-2	+	0	0	0	0	A
Antibodies after Absorption	(ABCDE) +	E	DE	CDE -	BCDE	

antibody. This suggestion is strengthened by the observation that both these activities are removed by absorptions with the human AB, N cell. The preimmune serum did not contain these specificities and since both these antibodies can be removed by absorption with marmoset erythrocytes, it is reasonable to assume that these antibodies represent a specific response to entities on the marmoset erythrocytes. Like the Bauhinia lectin, the anti-N activity of this cattle serum could also be removed by absorption with human M

cells but the amount of M cells required for this purpose was almost four times the amount of N cells.

The previous studies, although demonstrating the presence of an N-like specificity on the marmoset red cell, did not provide genetic markers of individual specificity, which was the primary goal. The cattle anti-marmoset serum (No. 718) was therefore analyzed for the presence of antibodies directed against type-specific antigens of marmosets. As shown in Table 96, pilot absorptions with cells from four marmosets suggests that this antiserum contains a minimum of five specificities. Subsequent absorptions of this antiserum with selected marmoset cells have been done and have resulted in the preparation of 200 ml of a typing fluid, which presumably contains only the postulated specificities D and E (Table 96). The demonstrated capability of procuring individual specific reagents from immune cattle serum indicates a feasible approach to the use of blood-group markers for our marmoset chimerism studies.

Response to First-Set Skin Allografts in the Marmoset

Raymond P. Porter and N. Gengozian

The immunologic significance of natural blood-cell chimerism, known to be a consistent feature in the marmoset, has been under investigation in this laboratory. We showed that chimeric dizygotic marmoset co-twins that are subspecies hybrids tolerate their littermate's transplanted skin apparently permanently; these experiments on co-twin chimeragrafts are still in progress and now extend over 700 days.[1]

Immunologic tissue-tolerance data also require evidence of immunologic competence as shown by rejection of similar tissue when exchanged between individuals of the same species. Since marmosets are tolerant of their littermate's histocompatibility antigens and 80% of deliveries are biovular twins, marmosets might be expected to show partial tolerance to a broader spectum of family related antigens; i.e., histoantigens other than those of their specific phenotype. The recent artificial taxonomic classification of these South American primates[2] was applied to imported marmosets in our colony and permitted selection of marmosets with different degrees of genetic parity. To test a hypothesis that chimerism induces a degree of histocompatibility between related members of a natural population, three series of experiments were carried out.

In the first two series of experiments, two subspecies of one of the three "white-lipped" tamarin marmoset species Saguinus fuscicollis were used. Twenty-seven of these tamarins were skin

10275 78 278

grafted by a method previously described[3] in either an intra- or intersubspecies reciprocal exchange combination. In a third series, four "cotton-top" tamarins, Saguinus oedipus, were skin grafted in intraspecies combination.

Skin allograft survival time was used as a qualitative assay for histocompatibility; the results of three small series of first-set allografts are summarized in tabular form. Table 97 A shows the survival data of skin allografts reciprocally exchanged between 8 S.f. illigeri and 8 S.f. lagonotus. The intersubspecies graft mean survival times (MST) were 19 days and 24 days. These acute rejections were typical of allografts seen in humans. However, when first-set skin was exchanged between tamarins of the same subspecies (S.f. illigeri vs S.f. illigeri) survival was relatively long but skin was eventually rejected; three of these 11 intrasubspecies allografts survived for as long as 2 months; the MST was nearly 40 days (Table 97 B). When tamarins of another monospecific tamarin species (S. oedipus) were skin grafted, the rejection response time was also extended; the MST for four animals was greater than 58 days (Table 97 C).

TABLE 97
Survival Time (in days) of Marmoset First-set Allografts.

(A)	Pair No.*	Donor-Host Relationship: *S.f. lagonotus* vs *S.f. illigeri*	*S.f. illigeri* vs *S.f. lagonotus*
	1	14†	20
	2	14	26
	3	14	28
	4	18	(dead day 3 postgrafting)
	5	21	29
	6	22	33
	7	22	18
	8	26	14
MST‡		19	24
(B)		*S.f. illigeri* vs *S.f. illigeri*	*S.f. illigeri* vs *S.f. illigeri*
	9	64	64 - regrew hair
	10	63	36
	11	55	(not first set)
	12	24	(dead day 7 postgrafting)
	13	15	28
	14	13	(mechanical loss of graft after day 8 postgrafting)
MST		40	
(C)		*S. oedipus* vs *S. oedipus*	*S. oedipus* vs *S. oedipus*
	15	65 - Regrew hair	>77 - Graft surviving with good hair growth at time of death
	16	45	47
MST		>58	

* Columns are arranged so reciprocal partner's data are matched left to right.

† Last day postgrafting epidermis considered viable by gross observation.

‡ MST = Mean survival time

These data on the survival times of grafts show the immunologic competence of marmosets to respond to allotypic tissue antigens by promptly rejecting donor tissue. Acute rejection always occurred when animals did not share close genetic relationship, i.e., classified as different subspecies. When animals were closely related, however (same race of a multirace species, or same species of a monotypic species) individuals tolerated grafted tissue for a time greater than that expected for random-bred

Fig. 114. Chronic rejection of allograft. Biopsy section day 49 postgrafting. H and PAS stain; X

a. Ballooning of cells
b. PAS positive cytoplasmic granules
c. Keratohyalin granules.
d. Area of liquification necrosis.
e. Granulation tissue showing absence of round-cell infiltration (See text)

1027579

mammals.[4] These differences in survival time of grafts suggest that major and minor histocompatibilities exist between our artificially classified groups of naturally chimeric marmosets.

Although some grafted skins showed prolonged survival, histologic examination of biopsy material taken from these grafts showed that reconstruction of the epidermis did not progress normally. When allogeneic skins survived beyond 2 weeks, a reconstruction of a normal integument did not always occur. Rather than the usual hyperplastic sheet of epithelium that eventually regenerated skin accessories,[4] an abnormally thick epithelial-like tissue developed that alternated with thin epithelial-like tissue in irregular patterns. Pronounced ballooning and vacuolization of cells of the thickened epithelia was also observed. Some features characteristic of epithelium were, however, discernible in this tissue (Fig. 114). Hair regrowth in these grafts was not observed. The five grafts that survived beyond 60 days appeared equal to their control autographs throughout the period of observation until about the last week in situ when they underwent an abrupt rejection.

The relatively long-term survival of allografts in the series of more closely related tamarins can theoretically be the effect of at least two biologic principles: (a) gene pooling of an interbreeding population of wild animals; and (b) consequence of natural chimerism. Since single birth (nonchimeric) marmosets are a rarity, the first effect will be difficult to prove. The need for family studies is apparent. We hope that the ORAU Marmoset Research Center breeding program will supply the needed animals in the future.

REFERENCES

1. Porter, R. P. and Gengozian, N. Survival of skin transplants between marmoset co-twins. In: USAEC Report, ORAU-106, 1967, pp. 206-208.

2. Hershkovitz, P. Taxonomic notes on tamarins, genus Saguinus (Callithricidae, primates), with descriptions of four new forms. Folia Primat 4, 381-395, 1966.

3. Porter, R. P. and Gengozian, N. A technique for orthotopic, fitted skin grafts in the marmoset. In: USAEC Report, ORAU-101, 1966, pp. 62-65.

4. Billingham, R. E. and Silvers, W. K., eds. Transplantation of tissue and cells. Wistar Institute Press, Philadelphia, 1961.

Normal Development of the Thyroid and Parathyroid Glands in Marmosets

Gretchen Humason, R. M. Kniseley, N. Gengozian, R. Cooper, and C. C. Lushbaugh

A continuing high rate of abortion in the ORAU marmoset colony and the Primate Research Colony of the San Diego Zoological Society has nonintentionally provided embryonic and fetal specimens from which we are constructing the normal histogenesis of various organs.[1] Simultaneously we are attempting to find any pathologic conditions that might play a role in these reproductive failures,[2] Our attention this year was focused on the thyroid because of its well-known basic importance to growth processes and its vital role in pregnancy. This organ has not been studied systematically up to now in these species. Modern concepts of the interdependence of maternal and fetal thyroidal function in humans suggest that all primate fetuses must not only receive maternal thyroxine but must also develop in utero the capability of themselves producing increasing amounts of thyroxine in response to thyroid-stimulating hormone (TSH) from the fetal pituitary gland. Successful response to this feedback demand is demonstrated histologically by the orderly sequence of changes in gland morphology in relation to somatic growth (crown-rump length). This response has been previously described in great detail for man.

Using 191 Saguinus fuscicollis (S.f.) and 54 S. oedipus (S.o.) aborti, we were able to obtain 25 S.f. and 27 S.o. thyroid glands that were normal according to human histologic criteria. Merging these two sets of glands was necessary to obtain examples at all ages because 23 of the 25 S.f. glands were from animals smaller (younger) than 8.0 cm crown-rump (CR) and 21 of the 27 S.o. glands were from animals larger (older) than 8.0 cm CR. With the eight overlapping specimens, we were then able to construct a continuum of stages of thyroid and parathyroid development identical with that of man, if we ignored the difference in man's rate of somatic growth. Using some material Dr. Edith Potter* kindly loaned to us we also found three points of histologic correspondence between thyroid development in man and marmoset, as shown in Fig. 1: at ~2.0 cm in each, at 18.5 cm in man with 6.0 cm in marmoset, and at 35 cm in man with 10 cm in marmoset. These corresponding stages represent respectively the end of the embryonic period, the midpoint of pregnancy when viability is close to being established, and full term (10 lunar months in man and 5 lunar months in marmosets).

In Fig. 115 the disparity in somatic growth between man and

* Professor Emeritus of Obstetrical and Gynecologic Pathology, University of Chicago.

1027580

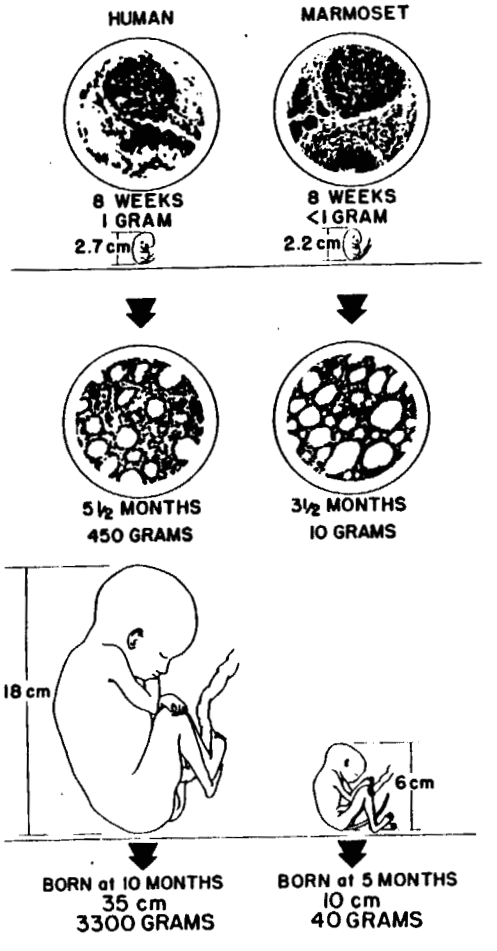

Fig. 115. Thyroid development in man and marmoset is shown at corresponding stages of development: at about 6 to 8 weeks in both (end of embryogenesis); at 12 weeks in marmoset and 22 weeks in man (stage of well-established function); and at full term at 20 weeks in marmoset and 40 weeks in man.

marmoset is shown at these three corresponding stages of thyroid development. At the 2-cm CR stage, the thyroid glands are poorly differentiated epithelialcords, but as shown in Fig. 115, the marmoset parathyroid gland is well-differentiated and probably already functional while at that size the human parathyroid gland does not yet show enlargement of cell cytoplasm.

In the marmoset of between 3 and 4 cm CR, embryonic thyroid organogenesis is completed and fetal epithelial growth and hormone production begin. These changes are revealed histologically in the appearance of minute acinar spaces in the epithelial cords that appear to pinch off and form follicles. In the rest of the fetal period the follicular cavities increase progressively in size. They are kept filled with typically homogenous colloid. The tall columnar epithelium of early fetal life gradually decreases in height and is low cuboidal at birth. Definition of these stages of thyroid growth in relation to CR length has enabled us to uncover an intra-uterine disease affecting marmoset thyroid development described elsewhere in this report.

REFERENCES

1. Humason, G. L., Lushbaugh, C. C., Gengozian, N., and Cooper, R. W. Pathologic observations on causes of fetal death in marmosets. In: USAEC Report ORAU-106, 1967, pp. 212-214.

2. Kniseley, R. M., Lushbaugh, C. C., Humason, G. L., and Gengozian, N. Embryology of marmoset gonads. In: USAEC Report ORAU-106, 1967, pp. 214-217.

Occurrence of A Thyroid Disease in Stillborn, Neonatal, and Young Marmosets

C. C. Lushbaugh, Gretchen Humason, R. M. Kniseley, and N. Gengozian

In attempting to define the stages of normal thyroid development of marmosets in relation to intrauterine size and neonatal size or age, we found that only 13% of the specimens could be considered completely normal, the rest showing a disease that is the subject of this report. Although some diseased thyroid glands were also found in stillborn cotton-top marmosets from the San Diego Zoo colony, and in stillborn squirrel monkeys obtained from the Department of Obstetrics, Vanderbilt University, these were not used in this report because greater numbers appeared in our colony including neonatal, adolescent, and adult animals. This complete range of ages in 166 specimens enabled us to construct a hypothetical schema of the pathogenesis of this disorder as shown in Fig. 116.

Since the disease is expressed morphologically as a hyperplastic epithelial process, it is easily confused with the normal hyperplastic-like appearance of the developing thyroid gland unless the relations of follicular size, epithelial height, and colloid content with one another and with somatic length or age are kept in mind. Two

1027581

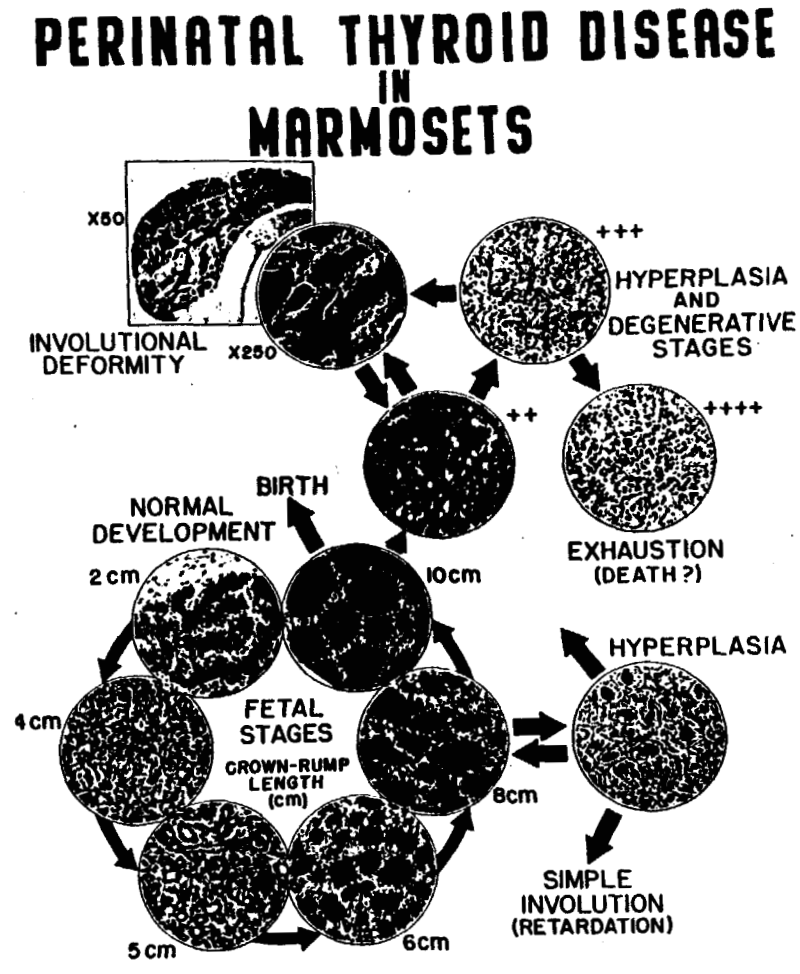

Fig. 116. Pathogenic schema hypothesized for a hyperplastic goitrogenic thyroid disease of unknown etiology found in laboratory-bred marmosets. The arrows indicate that in the latter half of fetal life some stress causes hyperplasia with and without glandular destruction. Simple hyperplasia leads to retardation of glandular development and colloid goiter. The degenerative process may lead to glandular exhaustion (?death) or, on recovery, to glandular deformity characterized by huge colloid-filled "lakes" instead of round follicles.

kinds of hyperplastic glands are found; one uncomplicated by degenerative cellular changes and the other containing all degrees of cellular degeneration and necrosis. We have designated these glands as simple hyperplasia and hyperplastic cellular exhaustion

(Table 98). In both kinds the amount of intrafollicular colloid seems to vary inversely with the apparent severity or stage of development of the pathologic process. The large number (102) of our 191 fetal or young marmosets showing the "exhaustive" variety of disease enabled us to arrange them in an apparent progression of severity. These changes have previously been described in dead human fetuses where they have been occasionally interpreted as postmortem autolytic changes. The preponderance of opinion, however, is that most of these autolytic degenerative changes are truly antemortem.

TABLE 98

Distribution of Thyroid Disease Among Dead Colony-Bred Progeny of Wild-Caught *Saguinus fuscicollis* Classed by Length of Survival and Viability.

A. Numbers

Disease Groups	Total Number	Length of Survival (Months)					Fetal Stage	
		0*	<1	>1<6	>6<12	>12	Previable CR Length <8cm	Viable CR Length >8cm
1. None	25	23	2	0	0	0	23	2
2. Hyperplasia (pure)	21	18	1	1	0	1	3	18
3. Hyperplasia exhaustive	102	66	5	13	10	8	27	75
4. Involution (simple)	10	4	6	0	0	0	1	9
5. Involution deformative	33	6	7	12	4	4	3	30
TOTAL	191	117	21	26	14	13	57	134

* Stillborn

In its extreme form (Group 3 ++++) the gland contains no colloid whatsoever, and the cohesiveness of the follicular epithelium has been lost so that the follicular spaces are filled with "loose" rounded-up cells in varying stages of parenchymatous degeneration. Some of these cells are remarkably well-preserved and a "new" cell is present among them. This cell may be an Ashkenazy or Hürthle-like cell, since the cytoplasm stains PAS-positive, and giant forms of it can be found. We believe that this extent of the disease is incompatible with life but that at lesser stages recovery can occur.

Our evidence for recovery is admittedly only deductive and quite incomplete on the basis of only 33 specimens (17% of our study material) that show a structural thyroid abnormality not previously described in any mammalian species and found only in ORAU colony-bred marmosets. Most of these animals (91%) had survived into late fetal or early neonatal life or adolescence. In this deformity the thyroid colloid is contained in irregularly shaped epithelium-lined spaces instead of round follicles. In some glands such spaces extend almost its entire length and have numerous connecting spaces giving a picture that resembles the map outline of a fresh water lake in the TVA system. No dead wild-caught marmoset adults have as yet shown this abnormality; we therefore suspect that it is

1027582

produced when the hyperplastic process develops during fetal thyroid development and the animal then recovers. As shown in the figure, we have labeled this kind of gland "deformed involution."

The etiology of this whole process is not known. Its hyperplastic and degenerative nature suggests that some goitrogenic substance is involved. Examination of the colony environment and the commercial diet used here has been begun for any substance with known goitrogenic potency. We find that cobalt, a known goitrogen for man, but not for the rat or rabbit, is slightly in excess of 0.81 ppm of the ORAU diet regimen. At this level, however, grown marmosets (approximate body weight 350 grams) would need to consume about four times the usual amount of this diet daily to approach comparable human whole-body toxic levels of cobalt (4 to 10 mg/70 kg).[1] Finding the true primary or a single etiologic agent may be complicated by unknown levels of malnutrition and iodine insufficiency, and by the presence of minute traces of pesticide residuals. All are possibly present in wild-caught monkey colonies and are capable of producing this disease themselves or potentiating any thyrotoxic effect of minute traces of dietary cobalt. A dietary, clinical biochemical, and ^{131}I tracer metabolic study is being undertaken to find the mechanism so this disease can be excluded from our colony.

REFERENCE

1. Roy, P. E., Bonenfant, J. L., and Turcot, L. Thyroid changes in cases of Quebec beer drinkers' myocardosis. Amer J Clin Path 50, 234-239, 1968.

Intra-uterine Death from Congenital Chagas' Disease in Laboratory-Bred Marmosets (Saguinus fuscicollis lagonotus)

C. C. Lushbaugh, Gretchen Humason, and N. Gengozian

Two abortions that occurred in the ORAU marmoset colony were of unusual interest because of a rare disease that was found. Since all parents were Saguinus fuscicollis lagonotus, neither abortion should have been the result of intra-uterine immunogenic attack by maternal antibodies. Microscopic examination of histologic sections to determine cause of death led to the discovery of a pathologic microorganism, the leishmanial form of Trypanosoma cruzi. These were found in the placenta of 0.5-mm crown-rump (CR) embryo and in the body tissues of the 6-cm-CR fetus.

Most of the parasitized cells in the placenta were fetal trophoblasts and endothelial cells of the trabecular vessels. Rare

questionably parasitic bodies were found in some maternal decidual cells and histiocytic cells. Many of the fetal blood vessels of the placenta were packed with free leishmanial forms (Fig. 117). Since all the tissues at autopsy had been subjected to chemical fixation, fresh tissue was not available for axenic testing in mice for biologic identification. The organisms were, however, tentatively identified by the presence of the typical nuclear body and rod-shaped kinetoplast. Our observations suggest that this embryonic death is a rare example of Chagas' placentitis, a disease well known in man but not previously known to cause reproductive failure in the marmoset.

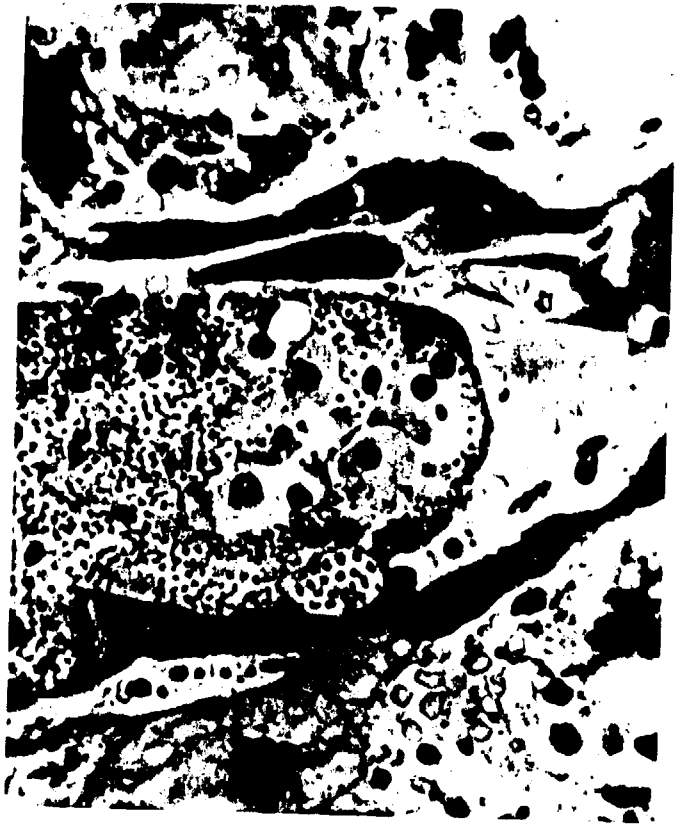

Fig. 117. Leishmanial forms appearing like granular debris packed between nucleated red blood cells in embryonic placental capillaries. The sharp separation of form from maternal blood by the endothelium and chorion suggests a degree of maternal immune resistance. (Photomicrograph X 750 of an iron hematoxylin stain of a thin-sectioned (~1 micron) plastic-embedded specimen.

1027583

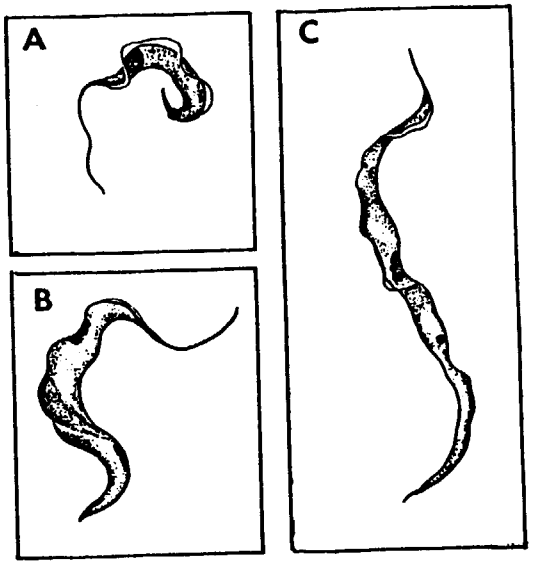

Fig. 118. Drawing of the types of circulating trypanosomes found in peripheral blood of the mother, (A) the father, (B) and other marmosets, (C) dead from unrelated causes. The trypanosome A is typical of T. cruzi; B, T. rangeli; and C, a T. rangeli-like organism partially autolyzed post-morten (all magnified about 3000 X).

To determine what Leishmania-like form was involved, smears of the mother's blood were searched for trypanosomes; twelve were found that could be positively identified as T. cruzi-like by anatomical measurements. They showed the characteristic "C" shape," small size, and extreme posterior position of the kinetoplast typical of T. cruzi organisms (Fig. 118).

The tissues of the 6-cm fetal abortus revealed leishmanial forms in the striated muscle of the skin, spinal column, and tail; in smooth muscle of the urinary bladder; in connective tissue phagocytes of the liver, heart, kidney, and adrenal gland; in myocardial muscle; and in parenchymal cells of the liver. This infection is an example of congenital Chagas' disease, a serious pediatric problem in Ecuador where our species of marmosets are obtained in the wild.

Examination of blood samples from 30 other animals and 77 adult hearts, 135 fetal and neonatal hearts, and 58 brains in the ORAU histology collection of S. fuscicollis autopsies, and 59 hearts from autopsies of S. oedipus loaned us by Dr. Cooper of the San Diego Zoological Society failed to turn up any other instances of T. cruzi-like parasitism.

There are numerous reports of human placental infection and high, but not necessarily fatal, neonatal and childhood incidence of Chagas' disease; but only two previous reports have been made of its occurrence in wild-caught marmosets. None have been reported in laboratory-bred marmosets before. Accidental infection of laboratory workers by T. cruzi from blood and excreta of other species of monkeys and from bug bites have occurred. The occurrence of this infection in the ORAU marmoset colony suggests, therefore, that precautions against possible human transmission must be maintained, even though results of hemagglutination tests done for us recently with the maternal serum by the Communicable Disease Center, USPH, Atlanta, Georgia, imply that this T. cruzi-like organism may be a nonhuman strain that has a low infectivity or virulence for man.

1027584

COMPUTER TECHNOLOGY

Summary of Developments in Computer Methodology

J. Howard Harmon

Computer technology has in recent years found increasing applications in biomedical research. The ORAU Medical Division has been using computer techniques for about six years. Since June 1966 the investigators have been using ORNL and K-25 computers and a rented IBM 1500 to test potential computer applications in several projects. The most notable application has been in the NASA-supported collection and analysis of the large data bank of 1400 patients and normals who received total-body irradiation. This report details recent efforts to develop techniques or to make existing programs more efficient and capable.

The Medical Division has been using the IBM 1800 computer to test the feasibility of on-line operation in a time-sharing mode for several separate projects simultaneously. The centralized computer has the ability to handle batch problems during free time while on-line with research instruments. The initial emphasis has been on the extension of research capabilities. It has been demonstrated, however, that economies in operation can be expected to accrue as investigators find increased research uses. We have been carrying out our basic studies using an 8-thousand "words" (K) memory core supplemented with the other Oak Ridge computers for large-batch problems. A proposal has been submitted to USAEC, Division of Biology and Medicine, for an additional 8-thousand memory core, one additional tape drive, and two additional disk drives.

With the limited 8-K core, the Medical Division has been able to develop and operate limited time-sharing techniques with the computer on-line to more than one research instrument. These basic techniques have been built so that high efficiencies might become possible soon after receiving the proposed additional equipment. Basic on-line programs have been written to operate the computer in the time-sharing mode.

The Division's most difficult on-line program uses a multiplexer to transmit digital data from three liquid scintillation counters in the lipid laboratory located about four miles from the computer. Upon signal the computer will interrupt a nonprocess program and pull from memory core the proper program for receiving data from a counter that has completed a sample count. In less than 5 sec the computer will receive and store a sample count and its identifying information. After completion of each transmission the computer returns to the nonprocess problem. This application has the potential of releasing approximately 15 man days of effort per week in the routine calculations of data from three liquid scintillation counters.

This rapid on-line capability may be extended to other research and clinical instruments such as radionuclide scanners, uptake counters, and multichannel analyzers.

The computer also has a demonstrated ability to monitor on a time-sharing basis, receive, and analyze an analog signal; the computer receives and samples an analog voltage at a rate of 40 times/sec. A densitometric reading of an exposed film from an ultracentrifuge can be read and analyzed in 3 min. This short time interval may be compared to the more than 4 hr previously required for the manual calculations. The analog input feature of the IBM 1800 computer can be used for any application that produces an analog voltage; e.g., (a) it can record data from radiation detectors in the low-exposure total-body irradiator (LETBI) which produce a voltage analogous to the radiation strength; (b) it can read and convert from analog to digital form, real time physiological vital signs from patients receiving total-body irradiation; (c) it can analyze any analog signal from research instruments such as a gas chromatograph.

Several research instruments in the Medical Division generate digital data that might be communicated to the computer in the on-line mode. However, as these data are produced, each instrument will make an output to a paper tape punch and then, at a convenient nonprime hour, the data will be read into the computer through a high-speed paper-tape reader and processed. Calculated results will be delivered to the investigator at the beginning of the following work day.

In the field of computer technology, as in other research areas, the ORAU Medical Division seeks opportunities to collaborate with personnel in the Oak Ridge National Laboratory. A system for recording, analyzing, and displaying radioisotope scan data has been developed by G. R. Dyer and M. M. Satterfield of the ORNL Medical Nuclear Instrumentation Group, and W. J. McClain of the K-25 Computing Technology Center. Picture-element counts received from a radioisotope scan are compressed logarithmically to six bits per count to be recorded on the magnetic tape. Control pulses originating from the rectilinear scanner store each compressed count on the tape, and generate direction pulses, end-of-line characters, and tape record gaps. After the recording of one or more scans, or other processing of a scan by digital computer, the taped data may be read to provide a fast and flexible two-dimensional map on a laboratory cathode-ray oscilloscope. Data of as many as 60 levels of magnitude are read in continuous mode from the magnetic-tape recorder and are displayed immediately on the cathode-ray oscilloscope. A given six-bit count representing the intensity at the corresponding picture element is converted to an analog signal to provide an unblanking level that controls the number of electrons striking the screen of the scope. Controls are available for providing plan views or isometric views in any desired orientation. Mr. McClain is working with ORAU programmers in the development of an IBM 1800 computer program to process and display scan data received from ORAU patients.

1027585

Computer-Assisted Measurements of Colloid Particle-Size Distributions

R. L. Hayes, J. E. Carlton, and Earl McDow, Jr.

When colloids are used as agents to assess the function of the reticuloendothelial system, it is highly desirable to use a colloid preparation that has a uniform particle size; otherwise the test results may be difficult to interpret. With bone-marrow scanning high residual blood levels may occur under some circumstances.

We have used sedimentation-velocity ultracentrifugal methods to measure particle size for developing new labeled colloids as bone-marrow scanning agents. A knowledge of the particle-size distribution as well as the average particle size is valuable in the interpretation of animal data, particularly when nonhomogeneity in the preparation, not apparent visually, has led to erroneous results that are otherwise inexplicable. It is quite time consuming to measure particle-size distribution if sedimentation-velocity boundaries are analyzed by the usual methods; it is impractical for routine monitoring of preparations. With on-line computer techniques we have been able to determine particle-size distributions on a routine basis with only a moderate expenditure of time.

Figure 119 shows a typical densitometer tracing from a cell photograph taken during a sedimentation-velocity run on an analyti-

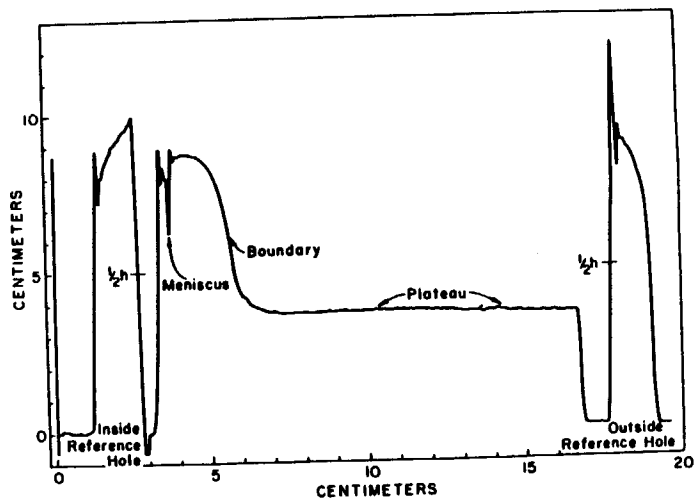

Fig. 119. Typical densitometer tracing of an analytical ultracentrifuge colloid sedimentation pattern.

cal ultracentrifuge. With the use of the computer, it is no longer necessary to make a laborious manual analysis of these data. Instead the voltage derived from a potentiometer connected to the servo-driven recorder of the densitometer is fed directly to the computer (see page 295). This signal is then monitored at the rate of 50 times/sec. The computer program detects the initial base line, recognizes the cell meniscus, the inside and outside cell reference holes, and relates elapsed time to the distance from the center of rotation. Using the heights on the boundary and that of the plateau together with a data smoothing routine, we determine the colloid concentration as a function of the distance from the center of rotation. Analysis of these data then provides a measure of the particle-size distribution. Computer-generated curves for the colloid concentration and particle-size distributions of a hydrous ferric oxide colloid preparation are shown in Fig. 120.

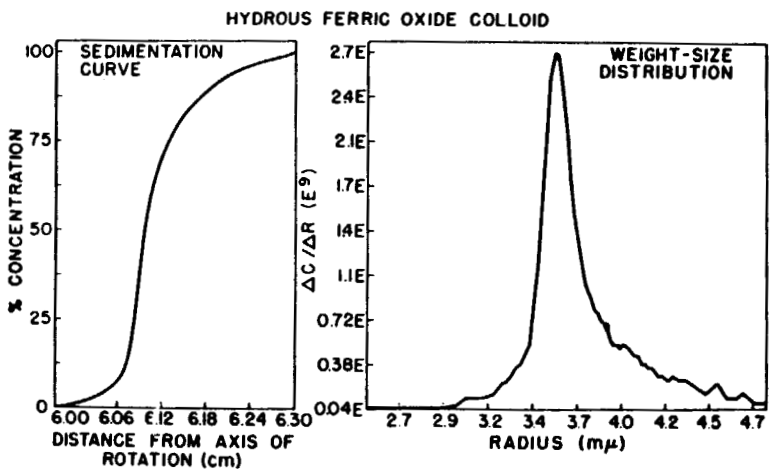

Fig. 120. Computer-generated curves for colloid sedimentation-boundary (left) and weight-size distribution (right) of a hydrous ferric oxide colloid preparation.

1027586

Development of an Electronic Interface between a Beckman Analytrol Film Densitometer and the On-Line IBM 1800 Computer

T. R. Barclay and A. C. Morris, Jr.

In developing our computer capabilities, we have demonstrated our ability to receive and process data from remote research instruments. This procedure makes use of the Time Shared Executive (TSX) features of the on-line IBM 1800 computer, whereby the receipt of a process interrupt (PIC) signal from a remote device causes the computer to cease any nonprocess program it might be doing, and to take data from the remote instrument under a process program. After receipt of the data, and its analysis and storage, the computer then reverts to its original nonprocess operation. Many external instruments can be connected to the computer simultaneously and these are serviced serially through a priority-interrupting feature of the system. A nonprocess program (such as an inventory calculation) in the computer may be interrupted many times, by external instruments submitting data for analysis, before being completed. Suitable programming prevents one program from interfering with the operation of others.

The Beckman Analytrol film densitometer is the first instrument we have used to demonstrate this operation (Fig. 121). At the Medical Division this instrument is mainly used for determinations of particle-

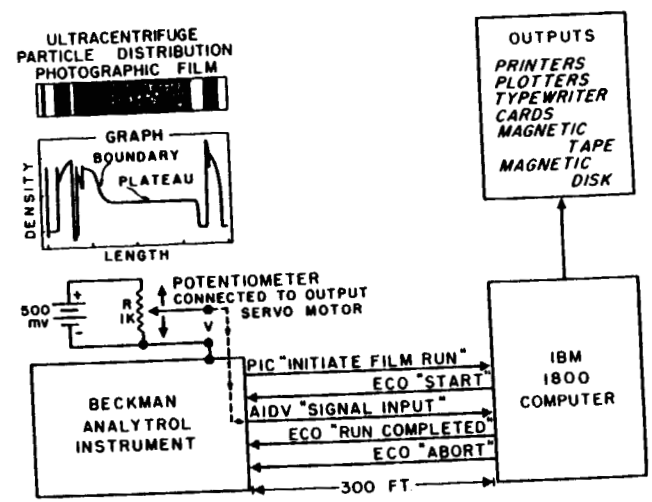

Fig. 121. Control circuits for interfacing the Beckman Analytrol to the on-line IBM-1800 computer.

size distribution with film exposures from a research ultracentrifuge (see page 293 of this report). The speed with which particles progress through the sample fluid under high-G fields permits us to calculate the average particle size. As shown in Fig. 121 we have connected a potentiometer to the servo-driven shaft of the Analytrol's recorder and a voltage derived from this circuit is transmitted to the analog input terminals (AIVD) of the computer. When the operator wants to send film data, a pushbutton activates a process-interrupt (PIC) circuit to the computer and causes the Analytrol program to be pulled in from a memory disk into the operating part of the computer's core. The computer signals that it is ready to receive data by closing an "electronic contact operate" (ECO) circuit (Fig. 121) to the Analytrol, thereby starting the film-drive motor. The computer then records analog signals (AIVD) from the Analytrol until the run is completed. Other ECO circuits signal to the operator the condition of the computer and indicate when the film run is over. Computations on the received data start immediately and results are usually being printed in 15 sec or less--a process that takes about 5 hr/film when carefully done by hand.

It is our purpose to extend this on-line TSX operation to other research instruments (e.g., clinical radionuclide scanners, liquid scintillation counters, etc.) where such operation is feasible.

1027587

PUBLICATIONS

From the Medical Division
Oak Ridge Associated Universities
1968

Reprints from the open literature and additional information on publications can be obtained by writing Mrs. Edward H. Anderson, Technical Editor, Medical Division, Oak Ridge Associated Universities, P. O. Box 117, Oak Ridge, Tennessee 37830. Complete lists of Medical Division publications are available.

PUBLICATIONS IN JOURNALS

Comas, F. V., Andrews, G. A., and Nelson, B. Spleen irradiation in secondary hypersplenism. Amer J Roentgenol 104, 668-673, 1968.

Cosgrove, G. E., Lushbaugh, W. B., Humason, G., and Anderson, M. G. Synhimantus (Nematoda) associated with gastric squamous tumors in muskrats. Bull Wildlife Disease Assoc 4, 54-57, 1968.

Cosgrove, G. E., Nelson, B., and Gengozian, N. Helminth parasites of the tamarin, Saguinus fuscicollis. Lab Animal Care 18, 654-656, 1968.

Debons, A. F., Krimsky, I., Likuski, H. J., From, A., and Cloutier, R. J. Gold thioglucose damage to the satiety center: inhibition in diabetes. Amer J Physiol 214, 652-658, 1968.

Frome, E. L. and Beauchamp, J. J. Maximum likelihood estimation of survival curve parameters. Biometrics 24, 595-605, 1968.

Gibbs, W. D., Hodges, H. D., and Lushbaugh, C. C. Precise geometry-independent radioassay of large biological samples. J Nucl Med 9, 264-266, 1968.

Goh, K. O. (Letter to the editor) Chromosomes in chronic lymphocytic leukaemia. The Lancet 2, 104, July 13, 1968.

Goh, K. O. Large abnormal acrocentric chromosome association with human malignancies. Possible mechanism of establishing clone of cells. Arch Intern Med 122, 241-248, 1968.

Goh, K. O. Smaller G(Gp-) and t(Gp-;Dp+) chromosomes. Amer J Dis Child 115, 732-738, 1968.

Goh, K. O. Total-body irradiation and human chromosomes: Cytogenetic studies of the peripheral blood and bone marrow leukocytes seven years after total-body irradiation. Radiat Res 35, 155-170, 1968.

Goh, K. O. and Sumner, H. Breaks in normal human chromosomes: Are they induced by a transferable substance in the plasma of persons exposed to total-body irradiation? Radiat Res 35, 171-181, 1968.

Lambremont, E. N. and Wood, R. Glyceryl ethers in insects: Identification of alkyl- and alk-1-enyl glyceryl ether phospholipids. Lipids 6, 503-510, 1968.

Pfannenstiel, P., Sitterson, B. W., and Andrews, G. A. ^{130}I for studying the effects of thyroid-stimulating hormone in patients with thyroid cancer. J Nucl Med 9, 90-95, 1968.

Pfleger, R. C., Anderson, N. G., and Snyder, F. Lipid class and fatty acid composition of rat liver plasma membranes isolated by zonal centrifugation. Biochemistry 7, 2826-2833, 1968.

Porter, R. P. and Gengozian, N. Transplantation in the marmoset (Callithricidae): A technique for orthotopic, fitted skin grafts. Proc Soc Exp Biol Med 127, 860-867, 1968.

Ross, D. A. and Morris, A. C., Jr. A stable, low-background whole-body counter designed for uniform detector geometry. Int J Appl Radiat Isotop 19, 731-739, 1968.

Snyder, F. Thin-layer chromatography radioassay: A review. Advance Tracer Method 4, 81-104, 1968.

Snyder, F. and Cress, E. A. Application of thin-layer chromatographic zonal ^{14}C-profile scans to the analysis of urinary constituents derived from lipids. Clin Chem 14, 529-534, 1968.

Snyder, F. and Wood, R. Deposition of triglycerides of increased carbon number in irradiated rat marrow. Radiat Res 33, 142-149, 1968.

Snyder, F. and Wood, R. The occurrence and metabolism of alkyl and alk-1-enyl ethers of glycerol in transplantable rat and mouse tumors. Cancer Res 28, 972-978, 1968.

Snyder, F. and Piantadosi, C. Deacylation of isomeric diacyl (1-^{14}C) alkoxyglycerols by pancreatic lipase. Biochim Biophys Acta 152, 794-797, 1968.

Van Woert, M. H. Reduced nicotinamide-adenine dinucleotide oxidation by melanin: Inhibition by phenothiazines. Proc Soc Exp Biol Med 129, 165-171, 1968.

1027588

Wood, R. Gas-liquid chromatographic analysis of long-chain fatty alcohols. J Gas Chromatog 6, 94-96, 1968.

Wood, R. and Baumann, W. J. Gas-liquid chromatographic analyses of 1,2-ethanediol monoethers and monoesters. J Lipid Res 9, 733-738, 1968.

Wood, R. and Snyder, F. Quantitative determination of alk-1-enyl- and alkyl-glyceryl ethers in neutral lipids and phospholipids. Lipids 3, 129-135, 1968.

GOVERNMENT DOCUMENTS

Radioisotopes in Medicine: In Vitro Studies. Proceedings of a symposium held at the Oak Ridge Associated Universities, November 13-16, 1967. R. L. Hayes, F. A. Goswitz, and B. E. P. Murphy, eds. USAEC Symposium Series No. 13, CONF-671111, June 1968, 753 pp.

CHAPTERS IN BOOKS AND SYMPOSIUM PROCEEDINGS

Andrews, G. A. The therapeutic use of bone-marrow transplantation. In: Proceedings of the International Conference on Leukemia-Lymphoma. Ann Arbor, 1967. Edited by Chris J. D. Zarafonetis, Philadelphia, Lea and Febiger, 1968, pp. 423-432.

Beck, W. L., Callis, E. L., and Cloutier, R. J. Phantom depth-dose measurement with extruded LiF in a low-exposure-rate total-body irradiator. In: Proceedings of the Second International Conference on Luminescence Dosimetry. Sept. 23-26, 1968. J. A. Auxier, K. Becker, and E. M. Robinson, eds. USAEC Report CONF-680920, 1968, pp. 976-989.

Berger, J. D., Watson, E. E., and Cloutier, R. J. Health Physics aspects of low-energy accelerators. In: The Use of Small Accelerators for Teaching and Research. Jerome L. Duggan, ed. USAEC Report CONF-680411, October 1968, pp. 112-137.

Cloutier, R. J. and Dalton, C. P. Radiation safety problems connected with the medical use of radioisotopes. In: Proceedings of the First International Congress of Radiation Protection, Rome, Sept. 5-10, 1966. W. S. Snyder, H. H. Abee, L. K. Burton, R. Maushart, A. Banco, F. Duhamel, and B. M. Wheatley, eds. London Pergamon Press, 1968, Vol. 2, pp. 1603-1613.

Comas, F. V. The time factor in fractionated irradiation of mouse skin. In: Dose Rate in Mammalian Radiation Biology. D. G. Brown, R. G. Cragle, and T. R. Noonan, eds. USAEC Report CONF-680410, 1968, pp. 18.1-18.12.

Gengozian, N., Carlson, D. E., and Gottlieb, C. F. Radiation exposure rates: Effects on the immune system. In: Dose Rate in Mammalian Radiation Biology. D. G. Brown, R. G. Cragle, and T. R. Noonan, eds. USAEC Report CONF-680410, 1968, pp. 16.1-16.23.

Goh, K. O. Autoradiographic studies in chronic myelocytic leukemia. In: Radioisotopes in Medicine: In Vitro Studies. R. L. Hayes, F. A. Goswitz, and B. E. P. Murphy, eds. AEC Symposium Series No. 13, CONF-671111, 1968, pp. 695-715.

Lushbaugh, C. C. Absence of electrolyte loss in the gastrointestinal syndrome. In: Bond, V. P., Round Table Discussion on Mechanism of Intestinal Radiation Death. Symposium on Gastrointestinal Radiation Injury, Richland, Washington, September 25-28, 1966. Excerpta Medica Foundation, 1968, pp. 356-362.

Lushbaugh, C. C. Recent progress in assessment of human resistance to total-body irradiation. In: Postattack Recovery from Nuclear War. Proceedings of the Symposium held at Fort Monroe, Virginia. Nov. 6-9, 1967. National Academy of Sciences, National Academy of Engineering, National Research Council, 1968, pp. 193-198.

Lushbaugh, C. C., Comas, F., Edwards, C. L., and Andrews, G. A. Clinical evidence of dose-rate effects in total-body irradiation in man. In: Dose Rate in Mammalian Radiation Biology. D. G. Brown, R. G. Cragle, and T. R. Noonan, eds. USAEC Report CONF-680410, 1968, pp. 17.1-17.23.

PUBLISHED ABSTRACTS

Anderson, R. E., Cumming, R. B., and Snyder, F. The lipid composition of L-M cells grown in suspension culture. J Amer Oil Chem Soc, program in Vol. 45, August 1968, abstr 129.

Blank, M. and Snyder, F. Determination of the position of double bonds in naturally occurring alkyl glyceryl ethers. J Amer Oil Chem Soc, program in Vol. 45, August 1968, abstr 121.

Carlson, D. and Gengozian, N. The radiation exposure-rate effect: Action upon the primary immune response in mice. Radiat Res 35, 572, 1968, abstr GD-11.

Edwards, C. L., Tanida, R., and Gibbs, W. D. Tracer and treatment discrepancy as a complication of radioiodine therapy. J Nucl Med 9, 367-368, 1968, abstr.

1027589

Edwards, C. L., Tanida, R., and Mora, R. Laminar scintiscans for determining depth of small metastases of thyroid carcinoma. J Nucl Med 9, 313-314, 1968, abstr.

Goh, K. O. Cytogenetic studies of bone-marrow lymphocytes after total-body irradiation. Clin Res 16, 42, 1968.

Goh, K. O. The effect of deoxyribonucleotide triphosphates on pulverized human chromosomes at G_2. Clin Res 16, 452, 1968.

Goswitz, F. A., Edwards, C. L., and Vodopick, H. Assessment of erythropoiesis by ferrokinetics and radiocolloid bone-marrow scanning. J Nucl Med 9, 319, 1968, abstr.

Hartman, R. E. and Hayes, R. L. Indium and gallium binding by blood serum. Fed Proc 27, 838, 1968, abstr 3520.

Hayes, R. L., Byrd, B. L., and Carlton, J. E. ^{113m}In as a possible bone scanning agent. J Nucl Med 9, 323, 1968, abstr.

Hodges, H. D., Lushbaugh, C. C., and Gibbs, W. D. Calibration of a whole-body counter for quantitating total potassium in human subjects. J Tenn Acad Sci 43, 49, 1968, abstr.

Lambremont, E. N. and Wood, R. Glyceryl ethers in insects: Identification of the alk-1-enyl and alkyl alkenyl ethers in the phospholipid fraction of three insect species. J Amer Oil Chem Soc 45, Program Addendum, 1968, abstr 157.

Lushbaugh, C. C., Comas, F. V. and Andrews, G. A. Radiation dose-response relations derived from clinical data. Health Physics 15, 165-166, 1968, abstr P/15.

Lushbaugh, C. C. and Lushbaugh, D. B. Evaluation of therapeutic response using change in electronically determined red blood cell size distribution. Amer J Clin Path 50, 627, 1968.

Porter, R. P. Chimerism and immunologic tolerance: A consequence of fraternal twinning in the marmoset. Diss abstr 27, 479-B, 1968.

Porter, R. P. and Gengozian, N. Immunologic tolerance of grafted skin exchanged between marmoset dizygotic co-twins. Fed Proc 27, 505, 1968, abstr 1627.

Snyder, F. Automated thin-layer chromatography. J Amer Oil Chem Soc 45, Program Addendum, 1968, abstr 143.

Snyder, F. and Piantadosi, C. Acylation and degradation of alkoxyglycerols in vitro. Fed Proc 27, 458, 1968, abstr 1360.

Snyder, F., Piantadosi, C., and Wood, R. The metabolism of glyceryl thioethers. J Amer Oil Chem Soc - program in Vol. 45, August 1968, abstr 84.

Webb, A. M., Edwards, C. L., and Wright, M. F. Automated determination of muramidase activity. Clin Chem 14, 820, 1968, abstr 81.

Wood, R. and Snyder, F. Analysis of glyceryl-alkyl and -alk-1-enyl ethers by gas-liquid chromatography and thin-layer chromatography. J Amer Oil Chem Soc 45, Program Addendum, 1968, abstr 175.

IN PRESS

Anderson, R. E. and Snyder, F. A simple procedure for the quantitative collection of $^{14}CO_2$ in the presence of ^{14}C-labeled short chain fatty acids. Anal Biochem

Andrews, G. A., Kniseley, R. M., Vodopick, H., Bergner, P-E. E., and Lushbaugh, C. C. Hematologic responses to total-body irradiation. Gesellschaft für Nuclearmedizin

Arimizu, N. and Morris, A. C., Jr. Quantitative measurement of radioactivity in internal organs by area scanning. J Nucl Med

Edwards, C. L. and Hayes, R. L. Tumor scanning with gallium-67 citrate. J Nucl Med

Gengozian, N. Marmosets: Their potential in experimental medicine. Ann N Y Acad Sci

Gibbs, W. D. and Lushbaugh, C. C. Whole-body counter system. In: Handbook of Radioisotopes.

Goh, K. O. The somatic metaphase chromosomal structures of rat kangaroo (Potorous tridactylis). Cytologia

Hübner, K. F. and Gengozian, N. Critical variables of the Jerne plaque technique as applied to rodent antibody-forming systems responding to heterologous red-cell antigens. J Immunol

Humason, G. and Lushbaugh, C. C. Sirius supra blue FGL-CF staining of collagen in the combined elastin, reticulum, and collagen stain. Stain Technol

Lushbaugh, C. C. Reflections on some recent progress in human radiobiology. In: Advances in Radiation Biology. M. R. Zelle, ed. New York, Academic Press

1027590

Lushbaugh, C. C. Theoretical and practical aspects of models explaining "gastrointestinal death" and other lethal radiation syndromes. Japan

Nelson, B. and Kniseley, R. M. Marrow fibrosis in myeloproliferative disorders. In: Proceedings of the Symposium on Myeloproliferative Disorders of Animals and Man, Richland, Washington, May 22, 1968. AEC Symposium Series

Snyder, F. The biochemistry of lipids containing ether bonds. In: Progress in the Chemistry of Fats and Other Lipids. Vol. X (R. T. Holman, ed.), Pergamon Press, Ltd. Oxford, 1969, pp. 287-335.

Snyder, F. Ether-linked lipids in neoplasms of man and animals: Methods of measurement and the occurrence and nature of the alkyl and alk-1-enyl moieties of neutral glycerides and phosphoglycerides. Advances in Experimental Medicine and Biology. Plenum Publishing Corp., New York

Snyder, F. A review of instrumentation and procedures for ^{14}C and ^{3}H radioassay by thin-layer and gas-liquid chromatography. Isotop Radiat Technol

Snyder, F. and Blank, M. L. Relationships of chain lengths and double bond locations in O-alkyl, O-alk-1-enyl, acyl, and fatty alcohol moieties in preputial glands of mice. Arch Biochem Biophys

Snyder, F., Malone, B., and Wykle, R. L. The biosynthesis of alkyl ether bonds in lipids by a cell-free system. Biochem Biophys Res Commun

Snyder, F. and Moehl, A. Use of liquid scintillation quenching to quantitate lipid mass. Anal Biochem

Snyder, F., Piantadosi, C., and Wood, R. The metabolism of glyceryl thioethers. Proc Soc Exp Biol Med

Snyder, F. and Wood, R. Alkyl and alk-1-enyl ethers of glycerol in lipids from normal and neoplastic human tissues. Cancer Res

Upton, A. C. and Lushbaugh, C. C. The pathological anatomy of total body irradiation. In: Atomic Medicine. E. R. King and J. W. J. Carpender, eds.

Ur, A. and Lushbaugh, C. C. Some effects of electrical fields on red blood cells, with remarks on electronic red blood cell sizing. Brit J Haematol

Vodopick, H. A., Rupp, E. M., and Gengozian, N. The bidirectional in vitro mixed leukocyte reaction: A mutual inhibitory phenomenon? Transplantation

Wood, R., Baumann, W. J., Snyder, F., and Mangold, H. K. Analysis of dialkyl glycerol ethers and related glycerides by gas-liquid chromatography. J Lipid Res

Wood, R. and Snyder, F. Tumor lipids: Metabolic relationships derived from structural analyses of acyl, alkyl, and alk-1-enyl moieties of neutral glycerides and phosphoglycerides. Arch Biochem Biophys

Wood, R., Harlow, R., and Lambremont, E. N. GLC analysis of Heliothis virescens triglycerides at various metamorphic stages. Annual Southeastern Meeting of the Society for Experimental Biology and Medicine Program, p. 12.

MEDICAL DIVISION CONFERENCES—1968

January 2: Vascular radiation effects in animals. Two motion picture films. Robert Moseley, University of Chicago, and Phyllis Stearner, Argonne National Laboratory.

January 9: Recent advances in photon spectroscopy with semiconductor detectors and their implications in biomedical research. John Walter, ORTEC.

January 16: The alkylating agents, dimethylnitrosamine (DMN) and diethylnitrosamine (DEN), and carcinogenesis. Neal K. Clapp, ORNL Biology Division.

January 30: Biochemical analysis of the recombination-mechanism of DNA strand of T.5. bacteriophage. Robert K. Fujimura, ORNL Biology Division.

February 6: Mutational studies of mammalian somatic cells in culture. E. H. Chu, ORNL Biology Division.

February 13: Neutron activation analysis of biological tissue with special reference to trace elements in the lung. Hamilton Smith, Western Regional Hospital Board, Glasgow, Scotland.

February 20: The biomedical graduate school. R. C. Fuller, Director, University of Tennessee - Oak Ridge Graduate School of Biomedical Sciences.

February 27: A report on the microbiological aspects of a recent radiation accident. Edward Balish, Division staff.

March 5: Power spectrum analysis of pulmonary impedance pneumograph. Edward Frome, Division staff.

March 12: Basic principles of tracer methods and applications. Per-Erik E. Bergner, Division staff.

1027591

March 19: Blood group studies in marmosets. S. P. Datta, Division staff.

March 26: The time factor in fractionated irradiation of mouse skin. F. Comas, Division staff.

April 2: Application of activation analysis to the study of effects of gold thioglucose on the satiety center. Roger Cloutier, Division staff.

April 9: The marmoset as a research primate. John Hampton, Institute for Dental Science, University of Texas, Houston, Texas.

April 16: Genetic continuity. Kong-oo Goh, Division staff.

April 23: Projection of Ph.D. research on the biosynthesis of the lipid ether bond. Robert L. Wykle, Division staff.

April 30: Pancreas and parathyroid scanning. E. James Potchen, Washington University School of Medicine, Division of Nuclear Medicine, St. Louis, Missouri.

May 7: Bone seekers as scanning agents. Raymond L. Hayes, Division staff.

May 14: Tissue transplantation between chimeric cattle twins. R. G. Cragle, UT-AEC Agricultural Research Laboratory.

May 21: Studies of antigen localization in spleen lymphatic germinal centers. Michael G. Hanna, Jr., ORNL Biology Division.

May 28: The information center concept. Francois Kertesz, Coordinator, ORNL Information Center.

June 4: Some applications of small computers in medical nuclear instrumentation. Ross Burrus and Paul Aebersold, Tennecomp Corporation.

June 11: Marrow fibrosis in myeloproliferative disorders. Bill Nelson, Division staff.

June 18: The occurrence and metabolism of glyceryl ethers in minimal deviation hepatomas (7777 and 7794A) and normal liver. Fred Snyder, Division staff.

June 25: Preliminary clinical studies with ^{67}Ga. C. L. Edwards, Division staff.

July 2: In vitro control of dimorphism of Candida albicans. David N. Mardon, Division staff.

July 9: Effects of radiation on chimerism in cattle. William H. Stone, Department of Genetics, University of Wisconsin, Madison, Wisconsin.

July 16: Cellular recovery and repair. Richard F. Kimball, Director of Biology Division, ORNL.

July 23: Antibodies to erythropoietin (with discussion of a case). Robert Lange, U. T. Memorial Research Center, Knoxville, Tennessee.

July 30: Statistical analysis of human chromosome data. Marvin Kastenbaum, ORNL.

August 6: Applications of electron microscopy to virus etiologic studies of leukemia. D. C. Swartzendruber, Division staff.

August 13: The use of thermoluminescent dosimetry at ORAU Medical Division. Roger Cloutier and W. L. Beck, Division staff.

August 19: Summer Student Scientific Program

Iodine-131 thyroxine distribution in rats - Jacques Baenziger; The ED_{50} for wet desquamation in fractionated irradiation - Eleanor Blakely; Empirical testing of an animal whole-body counter - Donna Dean; Effect of sulfur-containing amino acids on growth and morphology of Candida albicans - Dallas Hilden; Survey for glyceryl ethers - Michele Hughes; Histological quantitation of reticular and collagen fibers in the bone marrow of patients with chronic granulocytic leukemia - Sharon Krag; Effects of oral contraceptives on copper-67 distribution in rats - David Mescher; A review of the paper to be published on the miniaturized surgical probe - Joseph Nemcek; Detection of antibody-forming cells by the "cluster" technique - Connie Parker; Mouse anti-rat bone-marrow serum and mouse anti-rat neutrophil serum - Kirstan Schell.

August 20: The hematological effects of pokeweed mitogen in the mouse. F. V. Comas, Division staff.

August 27: Effect of prenatal radiation on growth. Polly G. Martin, UT-AEC Research Laboratory.

September 3: Possible copper intoxication associated with ovulatory suppressing contraceptives and related studies. C. L. Edwards, Division staff.

September 10: Autoradiographic studies of abnormal human chromosomes. Kong-oo Goh, Division staff.

1027592

September 17: Natural chimerism and skin transplantation studies in marmosets. R. P. Porter, Division staff.

September 17: (special seminar) Hemoglobinopathies. Prawase Wasi, Department of Medicine, Siriraj Hospital, Bangkok, Thailand.

September 24: Clinical evaluation of iron in tissue stores. Francis Goswitz, Division staff.

October 1: Experimental alteration of the tissue distribution of various bone-seeking elements. R. L. Hayes, Division staff.

October 8: Evaluation of the Jerne plaque technique. Karl F. Hübner, Division staff.

October 15: Ultrastructure of murine myxosarcomas associated with Rauscher virus transformation. Robert C. Brown, ORNL Biology Division.

October 22: A semi-statistical evaluation of therapeutic response in RBC size distribution by Coulter counting. C. C. Lushbaugh, Division staff.

October 29: On-line applications engineering for the IBM 1800 computer. A. C. Morris, Jr., Division staff.

November 5: Marrow fibrosis and epithelial cytomegaly after busulfan (myleran) treatment for chronic granulocytic leukemia. Bill Nelson, Division staff.

November 12: Lipid metabolism in cells grown in tissue culture: 0-alkyl, 0-alk-1-enyl, and acyl moieties of L-M cells. Robert E. Anderson, Division staff.

November 19: Leukokinetic studies using ^{32}P-DFP in chronic myelogenous leukemia. Helen Vodopick, Division staff.

November 26: Immune competence and aging. Takashi Makinodan, Biology Division, ORNL.

December 3: Tumor lipids; metabolic relationships derived from structural analyses of acyl, alkyl, and alk-1-enyl moieties of neutral glycerides and phosphoglycerides. Randall Wood, Division staff.

December 10: Recent scientific observations in Yugoslavia and Israel. Robert D. Lange, U. T. Memorial Research Center, Knoxville, Tennessee.

December 17: Reticular neoplasma in germ-free mice. H. E. Walburg, Jr., Oak Ridge National Laboratory.

LIPID SEMINARS — 1968

January 10: Projection of Ph.D. research on the biosynthesis of the lipid ether bond. Robert Wykle, Graduate Student from the University of Tennessee, Memphis.

February 7: Biology and biochemistry of the Chlomydia group of microorganisms. Howard M. Jenkin, The Hormel Institute, University of Minnesota, Austin.

February 28: Ehrlich ascites cell triglyceride, glyceryl ether diester, and lecithin interrelationships. Randall Wood, Division staff.

March 27: Diacyl glyceryl ethers: their synthesis and relationship to function in elasmobranch fishes. Donald C. Malins, Fish and Wildlife Service Bureau of Commercial Fisheries, Food Science Pioneer Research Laboratory, Seattle, Washington.

April 10: The cleavage of chimyl alcohol by a rat liver enzyme system. James F. Soodsma, AEC Postdoctoral Fellow.

April 24: The lipids of L-M cells. Robert E. Anderson, Postdoctoral Associate.

May 8: Alkylglycerols as acyl acceptors in normal and neoplastic tissues. Fred Snyder, Division staff.

May 29: Determination by reductive ozonolysis of double bond positions in glyceryl ethers, waxes, and their derivatives. Merle Blank, Division staff.

June 19: Isolation of the fraction of the ether-cleaving enzyme that produces fatty aldehydes and fatty alcohols. James F. Soodsma, AEC Postdoctoral Fellow.

June 26: Factors in mammalian cell cultures for biochemical studies. Robert Cumming, ORNL Biology Division.

July 17: Interactions of steroids with microbiological systems. Ronald Garrett, Summer Research Participant, University of Tennessee, Memphis.

July 31: Phosphonolipids. B. C. Pal, ORNL Biology Division.

August 20: Carbohydrate metabolism in neoplasms. Robert E. Anderson, Postdoctoral Associate.

October 2: Glyceryl ether and wax ester metabolism in the preputial gland. Gail Sansone, Postdoctoral Fellow.

October 16: The metabolism of glyceryl thioethers. Fred Snyder, Division staff.

1027593

October 16: The lipid composition of L-M cells grown in suspension culture. Robert E. Anderson, Postdoctoral Associate.

October 16: The determination of the position of double bonds in naturally occurring alkyl glyceryl ethers. Merle Blank, Division staff.

October 24: Membrane phospholipids and phospholipid fatty acid composition of the erythrocyte membrane. Gary Nelson, Lawrence Radiation Laboratory, Livermore, California.

November 20: Movies of HeLa cell cultures. Arthur Kretchmar, U. T. Memorial Research Hospital, Knoxville.

December 11: Lipase and triglyceride structure. Robert Jensen, University of Connecticut, College of Agriculture, Storrs.

Regional Lipid Meeting
March 7-8, 1968

Speaker - Affiliation	Title of Talk
Ossi Renkonen Department of Serology and Bacteriology University of Helsinki Helsinki, Finland	Analysis of Individual Molecular Species of Polar Lipids
Angelo Scanu Department of Medicine University of Chicago Chicago, Illinois	Advances in the Study of the Structure of Serum Lipoproteins

Attendance included about 50 participants from 10 institutions. Brief talks were given by 24 participants in addition to the two main speakers.

Fellowships and Term Appointments

Postdoctoral Appointment in Lipid Research:
Robert E. Anderson, Ph.D.
Gail Sansone, Ph.D.

Visiting Scientist in Lipid Research:
Per-Otto Hagen, Ph.D.

Public Health Service Fellows:
Donald Carlson, Ph.D.
Ten-Ching Lu Lee, Ph.D.
David N. Mardon, Ph.D.

Postresident Assistants in Clinical Investigation:
Romulo J. Mora, M.D.
Henry K. Speed, III, M.D.

IAEA Fellow:
Guillermo Castaneda, M.D.
Mexico City, Mexico

UT Graduate Students:
Nancy Basford, B.S.
Charles Gottlieb, B.S.
John Kateley, M.S.
Mike Yurconic, B.S.

University of North Carolina Graduate Student:
Ahmed Mahgoub Mohamed, M.S.

AEC Postdoctoral Fellow:
James Soodsma, Ph.D.

AEC Predoctoral Fellow:
Robert Wykle, M.S.

Student Fellows in Nuclear Medicine:
Peter Friedell, Chicago Medical School
DeVon Hale, University of Utah College of Medicine
Robert Hufft, Jr., University of Missouri Medical Center
Newell Pugh, Louisiana State University School of Medicine
Buford Rowe, West Virginia University School of Medicine
Jane Sanders, University of Mississippi School of Medicine

RESEARCH PARTICIPANTS — 1968

Ronald D. Garrett
University of Tennessee
Medical Units
Memphis, Tennessee

Norman Lee Savage
Southwest Texas State College
San Marcos, Texas

Sarah A. Smith
Florence State College
Florence, Alabama

Everett D. Wilson
Sam Houston State College
Huntsville, Texas

STUDENT TRAINEES — 1968

Jacques Baenziger
New College
Sarasota, Florida

Eleanor Alice Blakely
University of San Diego
College for Women
Alcala Park, San Diego, Cal.

Donna Joyce Dean
Berea College
Berea, Kentucky

Dallas Carolyn Hilden
Mercy College of Detroit
Detroit, Michigan

1027594

Michele Marie Hughes
San Francisco College
for Women
San Francisco, California

Sharon Krag
Texas Lutheran College
Sequin, Texas

David Anthony Mescher
Whittier College
Whittier, California

Joseph Nemcek
Claremont Men's College
Claremont, California

Connie Lou Parker
North Central College
Naperville, Illinois

Kirstan Lee Schell
New Mexico State University
University Park, New Mexico

MEDICAL COMMITTEE, ORAU COUNCIL

John L. McCarthy (Chairman)
Southern Methodist University

Gail D. Adams
University of Oklahoma
Medical Center

Roland H. Alden
University of Tennessee
Medical Units

Juan D. Curet
University of Puerto Rico

E. A. Daigneault
Louisiana State University
Medical Center

Edward G. High
Meharry Medical College

Howard L. Hunter
Clemson University

Horace N. Marvin
University of Arkansas
Medical Center

Oscar Touster
Vanderbilt University

ORAU MEDICAL DIVISION ADVISORY COMMITTEE

William C. Moloney (Chairman)
Peter Bent Brigham Hospital

Rupert E. Billingham
University of Pennsylvania
School of Medicine

Frederick J. Bonte
The University of Texas
Southwestern Medical School

E. Richard King
Medical College of Virginia

Wright H. Langham
Los Alamos Scientific Laboratory

Donald B. Zilversmit
Cornell University

MEDICAL DIVISION EMPLOYEES

Scientific Staff

Paulette Abee, B.S.
Elizabeth M. Allen, B.S.
Robert Anderson, Ph.D.
Gould A. Andrews, M.D.
Mildred Bailey
Edward Balish, Ph.D.
Thomas R. Barclay, B.S.
Jerre Batson, B.S.
Robert J. Beaver, M.S.
William L. Beck, Jr., B.S.
Edward D. Bird, M.D.
Per-Erik E. Bergner, M.D.
Merle Blank, B.S.
Linda T. Brown
Billy L. Byrd, B.S.
Ernest L. Callis, B.S.
Eddie Ruth Capshaw
James E. Carlton, B.S.
Stuart J. Chaskes, M.S.
Martha Clevenger, B.S.
Carroll Cline
Shirley B. Colyer, B.S.
Frank V. Comas, M.D.
Edgar Cress, B.S.
Evelyn B. Cunningham, B.A.
Surinder P. Datta, Ph.D.
Rachel Dixon
C. Lowell Edwards, M.D.
Elizabeth Edwards
William Fishback
Clarence Forney
Dorothy C. Gaither, M.S.
Nazareth Gengozian, Ph.D.
William D. Gibbs, B.S.
Thomas Gilman, B.S.
Kong-oo Goh, M.D.
Francis A. Goswitz, M.D.
Charles T. Greene, B.A.
Per-Otto Hagen, Ph.D.
Fred Hamilton
Robert Harlow, B.S.
Oliver Hawkins
Raymond L. Hayes, Ph.D.
Joyce Hewins, A.B.
Harold D. Hodges, B.S.
Elizabeth Holloway
Karl F. Hübner, M.D.
Gretchen Humason, M.A.
Kathryn Hurst, B.S.
Eugene E. Joiner, M.S.
Marjorie Ketelle, B.S.
Mary Beth Klepper, M.S.
Ralph M. Kniseley, M.D.
Ten-Ching Lu Lee, Ph.D.
Kathryn Lore, B.S.
C. C. Lushbaugh, M.D., Ph.D.
Dorothy H. Lushbaugh, B.S.
Boyd Malone, B.S.
David Mardon, Ph.D.
Brenda Joan Marks, B.S.
J. E. McCarter
Sallie McCaskill
Alvis Earl McDow, Jr., B.S.E.E.
Jean McIntyre, B.S.
Anita Moehl, B.S.
A. C. Morris, Jr., M.S.E.
Bill M. Nelson, M.D.
Etna Palmer, M.D.
Ted A. Pearson, M.S.
Charles Phipps, B.S.
William T. Pope
R. P. Porter, Ph.D.
Richard F. Queener
John J. Rafter, B.S.
Donald Reynolds
Mack Ruffner
Elizabeth M. Rupp, B.A.
Ann Sipe
Thomas A. Smith
Mary P. Smyser, B.S.
Fred L. Snyder, Ph.D.
Jerry Steele
Margo Steinman, M.S.
Nelson Stephens, B.S.
Tom Randall Stokes
Donald C. Swartzendruber, Ph.D.
Ryosaku Tanida, M.D.
Mary W. Thomas, B.S.
Helen A. Vodopick, M.D.
Mary Alyce Watkins, A.B.
Allen M. Webb, B.S.
James White
Sandra Wilson
Randall Wood, Ph.D.
Gary Wolfe, B.S.
Francine Wright, B.S.

1027595

Nursing and Patient Care

Margaret Blackburn, R.N.
Helen Brinker, R.N.
James Cozart
Mary Nell Craig, R.N.
John Dean
Thelma Eden, R.N.
Mable Helton, R.N.
Rita Holt, R.N.
Earl Jacobs
Martha Laxton, R.N.
Marilyn Mackley, R.N.
Bedford Mayott
Barbara Nance, R.N.
Beuna Pack
Garfield Porter
Mary Rogers, R.N.
Lillie P. Simmons
Elaine Stoetzel, R.N.
Mary E. Sutliff, R.N.
Naomi P. Wilson, R.N.
Eria Winters, R.N.
Lillie I. Woods

Administrative, Editorial, Medical Records, and Secretarial

Elizabeth B. Anderson, M.S.
Frances Banner
Kenneth L. Burton, M.S.
Blanche Carden
Carole J. Carter, B.S.
Frances Darr
Laura P. Edwards
J. Howard Harmon
Wanda Hodge
Carolyn Hutchins
Mildred A. Hyp
Mary Lee Johnson
Willa Fae Loveday
Judy Owens, B.A.
Ruth C. Paire
Emily Roemer
Jane Rogers
Nancy Sheehan, B.A.
Mona Smith
Katherine Stubbs, B.F.A.
Dorothy Vola
Patsy White
Florence C. Zenni

Custodial and Animal Care

Willie Barnett
Sam Bell, Jr.
Mark Brewer
Willie J. Brooks
Clarence Buckley
Isaiah Caldwell
Jerry Constance
Grace E. Foster
James Graham
Clarence Hamilton
William Hawkins
Renfro Henderson
Ernest Hickson
Rufus Jackson
James Kline
James Rather
J. R. Stevens
William Walker
Gene Warrington
Alfred Webster

CONSULTANTS AND COLLABORATORS — 1968

Norman G. Anderson, Ph.D.
Biology Division
Oak Ridge National Laboratory

Edmund B. Andrews, M.D.
Medical Arts Building
Knoxville

John A. Auxier, M.S.
Health Physics
Oak Ridge National Laboratory

Fritz H. Bach, Ph.D.
University of Wisconsin
Madison

Robert P. Ball, M.D.
Radiology Department
Oak Ridge Hospital

Jere M. Bauer, M.D.
University of Michigan
School of Medicine, Ann Arbor

W. J. Baumann, Ph.D.
University of Minnesota
Hormel Institute
Austin

M. A. Bender, Ph.D.
Biology Division
Oak Ridge National Laboratory

R. R. Bigelow, M.D.
Medical Arts Building
Oak Ridge

Edward Bird, M.D.
Bowman Gray School of
Medicine, Wake Forest
Winston-Salem, N. C.

B. B. Blevins, D.D.S.
Medical Arts Building
Oak Ridge

Matthew Block, M.D.
University of Colorado Medical
Center, Denver

Donald Brown, M.D.
University of Colorado Medical
Center, Denver

Louis Bryan, M.D.
Doctors Building
Oak Ridge

Edward Buonocore, M.D.
U. T. Memorial Research
Center Hospital, Knoxville

Amoz I. Chernoff, M.D.
U. T. Memorial Research Center
Knoxville

Kenneth W. Christenberry, M.D.
501 Church Avenue, SW
Knoxville

C. C. Congdon, M.D.
Biology Division
Oak Ridge National Laboratory

Robert Cooper, D.V.M.
Primate Research Colony
San Diego Zoological Society
San Diego, Calif.

G. E. Cosgrove, M.D.
Biology Division
Oak Ridge National Laboratory

Dexter Davis, M.D.
Medical Arts Building
Oak Ridge

Albert F. Debons, Ph.D.
Veterans Administration Hospital
Brooklyn, N. Y.

J. D. Egan, M.D.
Veterans Administration Hospital
Omaha, Neb.

Earl Eversole, Jr., M.D.
Medical Arts Building
Oak Ridge

1027596

Ben I. Friedman, M.D.
University of Tennessee
School of Medicine, Memphis

Warren Glaser, M.D.
Downstate Medical Center
Brooklyn, N. Y.

Douglas Grahn, Ph.D.
Argonne National Laboratory
Argonne, Ill.

Nathan S. Hall, Ph.D.
UT-AEC Agricultural Research
Laboratory, Oak Ridge

George T. Harrell, M.D.
Milton S. Hershey Medical
Center, Pennsylvania
State University, Hershey

C. Craig Harris, M.S.
Duke University Medical
Center, Durham, N. C.

Warren W. Harris, Ph.D.
Oak Ridge National Laboratory

Ernest L. Hendrix, M.D.
Medical Arts Building
Oak Ridge

Robert Heyssel, M.D.
Johns Hopkins Medical
Institutions, Baltimore, Md.

John U. Hidalgo, M.S.
Tulane University
Biomedical Computing System
New Orleans, La.

Perry M. Huggin, M.D.
East Tennessee Tuberculosis
Hospital, Knoxville

Melville L. Jacobs, M.D.
City of Hope Medical Center
Duarte, Calif.

Raymond A. Johnson, M.D.
Medical Arts Building
Oak Ridge

Marvin A. Kastenbaum, Ph.D.
Mathematics Division
Oak Ridge National Laboratory

Herbert D. Kerman, M.D.
Halifax District Hospital
Daytona Beach, Fla.

Avery P. King, M.D.
Medical Arts Building
Oak Ridge

Alfred P. Kraus, M.D.
University of Tennessee
College of Medicine, Memphis

Lorraine Kraus, M.D.
University of Tennessee
College of Medicine, Memphis

A. L. Kretchmar, M.D., Ph.D.
U. T. Memorial Research Center
and Hospital, Knoxville

William G. Laing, M.D.
1501 Clinch Avenue, SW
Knoxville

Edward N. Lambremont, Ph.D.
Louisiana Nuclear Science Center
Louisiana State University
Baton Rouge

Robert D. Lange, M.D.
U. T. Memorial Research Center
and Hospital, Knoxville

Wright Langham, Ph.D.
Los Alamos Scientific Laboratory
Albuquerque, N. M.

Robert A. Lewis, M.D.
608 Main Avenue, SW
Knoxville

James L. Liverman, Ph.D.
Oak Ridge National Laboratory

Bismarck B. Lozzio, Ph.D.
U. T. Memorial Hospital
and Research Center
Knoxville

Helmut Mangold, Ph.D.
University of Minnesota
Hormel Institute
Austin

Margaret Maynard, M.D.
Medical Arts Building
Knoxville

Christopher B. Merritt, M.D.
Johns Hopkins University
Hospital, Baltimore, Md.

Isadore Meschan, M.D.
Bowman Gray School of Medicine
Wake Forest College
Winston-Salem, N. C.

William O. Miller, M.D.
606 Main Avenue, SW
Knoxville

George R. Minor, M.D.
University of Virginia Hospital
Charlottesville

William C. Moloney, M.D.
Boston City Hospital

K. Z. Morgan, Ph.D.
Oak Ridge National Laboratory

Dana W. Nance, M.D.
Oak Ridge Hospital

Robert W. Newman, M.D.
Medical Arts Building
Knoxville

Thomas R. Noonan, M.D.
UT-AEC Agricultural Research
Laboratory, Oak Ridge

Robert Nordlie, Ph.D.
University of North Dakota
Grand Forks

Richard A. Obenour, M.D.
1501 Clinch Avenue, SW
Knoxville

Thomas H. Oddie, D.Sc.
University of Arkansas Medical
Center, Little Rock

T. T. Odell, Ph.D.
Biology Division
Oak Ridge National Laboratory

Charles Oderr, M.D.
Oak Ridge Hospital

Fearghus T. O'Foghludha, Ph.D.
Medical College of Virginia
Richmond

Claude Piantadosi, Ph.D.
University of North Carolina
Chapel Hill

Orville Privett, Ph.D.
University of Minnesota
Hormel Institute
Austin

W. W. Pugh, Jr., M.D.
Doctors Building
Oak Ridge

James D. Regan, Ph.D.
Biology Division
Oak Ridge National Laboratory

D. A. Ross, Ph.D., M.D.
Oak Ridge National Laboratory

Henry B. Ruley, M.D.
Medical Arts Building
Oak Ridge

Eugene L. Saenger, M.D.
General Hospital
Cincinnati, Ohio

H. H. O. Schmidt, Ph.D.
University of Minnesota
Hormel Institute
Austin

C. D. Scott, Ph.D.
Oak Ridge National Laboratory

C. W. Sensenbach, M.D.
Medical Arts Building
Oak Ridge

Leigh Simmons, D.V.M.
Biology Division
Oak Ridge National Laboratory

1027597

Norman Simon, M.D.
945 Fifth Avenue
New York

W. Eidson Smith, M.D.
Blount Professional Building
Knoxville

Walter S. Snyder, Ph.D.
Oak Ridge National Laboratory

Alan Solomon, M.D.
U. T. Memorial Research Center
Knoxville

Ben H. Spargo, M.D.
University of Chicago

Paul Spray, M.D.
Doctors Building
Oak Ridge

P. E. Steiner, M.D.
University of Pennsylvania
School of Medicine

George M. Stevens, III, M.D.
Doctors Building
Oak Ridge

W. N. Tauxe, M.D.
Mayo Clinic
Rochester

William M. Tipton, M.D.
522 West Church Street
Knoxville

Joe E. Tittle, M.D.
Doctors Building
Oak Ridge

V. R. R. Uppuluri, Ph.D.
Oak Ridge National Laboratory

A. C. Upton, M.D.
Biology Division
Oak Ridge National Laboratory

Henry N. Wagner, Jr., M.D.
Johns Hopkins Hospital
Baltimore

H. Stephen Weens, M.D.
Emory University School of Medicine
Atlanta

LEGAL NOTICE

This report was prepared as an account of Government sponsored work. Neither the United States, nor the Commission, nor any person acting on behalf of the commission

A. Makes any warranty or representation, expressed or implied, with respect to the accuracy, completeness, or usefulness of the information contained in this report, or that the use of any information, apparatus, method, or process disclosed in this report may not infringe privately owned rights; or

B. Assumes any liabilities with respect to the use of, or for damages resulting from the use of any information, apparatus, method, or process disclosed in this report

As used in the above, "person acting on behalf of the Commission" includes any employee or contractor of the Commission, or employee of such contractor, to the extent that such employee or contractor of the Commission, or employee of such contractor prepares, disseminates, or provides access to, any information pursuant to his employment or contract with the Commission, or his employment with such contractor.

ORAU-1(

RESEARCH REPORT 1967

MEDICAL DIVISION

REPOSITORY Oak Ridge Institute for Science and Education, Medical Sciences Division

COLLECTION Oak Ridge Associated Universities Annual Research Reports, Medical and Health Sciences Division

BOX No. Vance Road Facility, Room 202A
No folder title.

FOLDER Document no. ORAU-3000-2, Part 4 of 6

10217598

1027599

RESEARCH REPORT—MEDICAL DIVISION
Oak Ridge Associated Universities

For the Year Ending December 31, 1967

NOTICE

This report contains preliminary data and was prepared primarily to record the year's work, and is not intended as a substitute for publication in the open literature. It is subject to revision and does not represent a final report. Please do not quote from or refer to this work in open literature without permission from individual authors to reference the material as a personal communication.

Operating Under Contract With
The United States Atomic Energy Commission

ORAU–106

Single copies are available on request from:
Medical Division
Oak Ridge Associated Universities
Oak Ridge, Tenn. 37830

Printed in the United States of America
Price $3.00
Available from: Clearinghouse for Federal Scientific and Technical Information,
Springfield, Virginia 22151

ON THE COVER: Young Saguinus fuscicollis twins aged four weeks, bred in the Medical Division's primate colony; the marmoset is unique among primates in that twinning is normal (about 80% of pregnancies) and natural chimerism occurs. The colony is a major resource in the Division's immunology program under Dr. Nazareth Gengozian.

1027600

CONTENTS

ORGANIZATION OF RESEARCH viii

INTRODUCTION 1

STUDIES IN RADIATION AND RELATED TOPICS 5

Preliminary Comparison of Peripheral Blood Responses to Medium and Low-Exposure Rates of Therapeutic Total-Body Irradiation. C. L. Edwards, Frank V. Comas, G. A. Andrews, and C. C. Lushbaugh 5

Effect of Total-Body Irradiation Upon Plasma Iron and Erythrocyte Enzymes in Humans. C. L. Edwards, Allen M. Webb, and C. C. Lushbaugh 10

The Low-Exposure-Rate Total-Body Irradiation Facility (LETBI). G. A. Andrews, W. L. Beck, Roger J. Cloutier, A. C. Morris, Jr., T. R. Barclay, Frank V. Comas, C. L. Edwards, and C. C. Lushbaugh 13

Dosimetry for the Low-Exposure-Rate Total-Body Irradiation Facility. W. L. Beck, E. L. Callis, Patricia Dalton, and Roger J. Cloutier 19

Physiologic Monitoring in the Low-Exposure-Rate Total-Body Irradiation Facility. A. C. Morris, Jr., T. R. Barclay, and C. C. Lushbaugh 23

Interference Investigation of 60-Hertz Power Sources in the LETBI Facility. T. R. Barclay and A. C. Morris, Jr. 27

Power-Spectrum Analysis of Pulmonary Impedance Pneumograph. Edward L. Frome, C. C. Lushbaugh, Herbert T. Davis, III, and Donna S. Bibler . 33

R-Wave Detector for Use with Cardiac Waveforms from the Physiologic Monitor. T. R. Barclay and A. C. Morris, Jr. 37

A Study of Infections in Irradiated Patients. Edward Balish, Ted A. Pearson, R. Tanida, and Romulo J. Mora 38

Decreased Sodium-24 Excretion in Rat GI Syndrome After 1200-Rad Fission Neutron Exposure. C. C. Lushbaugh and W. D. Gibbs. 44

Autoradiographic Confirmation of Stimulated Lipid Metabolism in Radiation Damaged Rat Bone Marrow. Gretchen L. Humason, Fred Snyder, Edgar Cress, and C. C. Lushbaugh 46

Evaluation of Leukocyte Survival in vitro by Cytochemical Staining and Autoradiography. Jerry D. Hunter, Martha L. Clevenger, and Francis A. Goswitz 48

Effect of Prednisone on the Total Lipid Content of Leukemic Lymphocytes. Francis A. Goswitz, Fred Snyder, Martha L. Clevenger, and Nelson Stephens 53

Separation of Viable Lymphocytes from Normal Blood. Martha L. Clevenger and Francis A. Goswitz 54

Abnormal Lymphocyte Volume Distribution Typical of Chronic Lymphocytic Leukemia. Dorothy H. Lushbaugh, Francis A. Goswitz, Martha L. Clevenger, and C. C. Lushbaugh 56

Some Effects of Electrical Fields on Red Blood Cells. A. Ur, C. C. Lushbaugh, and Dorothy H. Lushbaugh 58

The Origin of Acid Resistant Erythrocytes in Prenatal Mice. Gretchen L. Humason and C. C. Lushbaugh 61

The Radiosensitivity of Rat Bone-Marrow Cells. *Frank V. Comas* 64
Effect of Phytohemagglutinin on Endogenous Spleen Colonies in Mice. *Frank V. Comas and Bismark Lozzio* 66
Maximum Likelihood Estimation of Survival-Curve Parameters. *Edward L. Frome, Frank V. Comas, and J. J. Beauchamp* 67
Stereologic Quantitation of the Components of Rabbit Marrow. *Margaret A. Slaughter, Y. Ito, Francis A. Goswitz, and Bill Nelson* 70
The Effect of Total-Body Irradiation on the Direct Bone-Marrow Metaphases. *Kong-oo Goh* 72
Breaks in Normal Human Chromosomes: Are They Induced by a Transferable Substance in the Plasma of Persons Exposed to Total-Body Irradiation? *Kong-oo Goh and H. Sumner* 77
Autoradiographic Studies in the Ph1 Chromosome. *Kong-oo Goh* 81
Cytogenetic Studies in Blastic Crisis of Chronic Myelocytic Leukemia. *Kong-oo Goh* 85
Partial G/D Translocation Associated With Mental Retardation in Two Members of a Family. *Kong-oo Goh and L. E. Tucker, Jr.* 91
Chromosomal Breaks in Women Taking Birth Control Pills. *Kong-oo Goh* 97

MEDICAL RADIOISOTOPES 105
Factors Affecting the Distribution of Hydrous Ferric Oxide Colloid. R. L. *Hayes, J. E. Carlton, B. L. Byrd, and J. J. Rafter* 105
Indium-113m as a Kidney and Bone Scanning Agent. R. L. *Hayes, B. L. Byrd, and J. E. Carlton* 111
Measurement of Hydrous Ferric Oxide Colloid Particle Size. R. L. *Hayes and J. E. Carlton* 115
Distribution of Gallium as a Function of Time and Stable Gallium Dose. R. L. *Hayes, B. L. Byrd, and J. E. Carlton* 117
The Binding of Gallium and Indium by Blood Serum Proteins. R. E. *Hartman and R. L. Hayes* 120
The Effect of Various Metals on the Distribution of Gallium and Indium. R. L. *Hayes and B. L. Byrd* 121
Scanning Technique for Determining Depth of Radioactive Foci. C. L. *Edwards, R. Tanida, and Romulo J. Mc:a* 122
Bronchiectasis Producing False-Positive Radioiodine Scan for Metastases of Thyroid Cancer. C. L. *Edwards, R. Tanida, and Bill Nelson* 124
Improvements in the Whole-Body Scanning System. A. C. *Morris, Jr., and William T. Pope* 127
Correlation of Erythropoiesis and Reticuloendothelial Function in Rabbits. Y. *Ito, Francis A. Goswitz, and Bill Nelson* 128
Red Cell Survival in Normal Ponies Measured with DFP (^{32}P). R. F. *Queener, M. C. Yarbrough, C. C. Lushbaugh, W. D. Gibbs, and Daniel G. Brown* 132

LIPID METABOLISM 135
Quantitative Determination of Alk-1-enyl- and Alkyl-Glyceryl Ethers in Neutral and Phospholipids. *Randall Wood and Fred Snyder* 136

1027601

Infrared Spectra and Polymorphism of Glycerol Ether Derivatives. *Edward O. Oswald, Claude Piantadosi, Carl E. Anderson, and Fred Snyder* . . . 139
Deacylation of Isomeric Diacyl-1-^{14}C-alkoxyglycerols by Pancreatic Lipase. *Fred Snyder and Claude Piantadosi* 140
Synthesis of Labeled Glyceryl Thiomonoethers. *Claude Piantadosi, Randall Wood and Fred Snyder* 141
Analysis and Characterization of Glyceryl Thiomonoethers. *Randall Wood, Claude Piantadosi and Fred Snyder* 142
Quantitative Analysis of Long-Chain Aldehydes. *Randall Wood and Robert Harlow* 144
Quantitative Analysis of Intact Triglycerides and Related High-Molecular-Weight Lipids. *Randall Wood and Robert Harlow* 146
Application of Thin-Layer Chromatographic Zonal ^{14}C-Profile Scans to the Analysis of Urinary Constituents Derived from Lipids. *Fred Snyder* . . 147
Automated Thin-Layer Chromatography. *Fred Snyder* 149
The Measurement of Chemical Mass by Liquid Scintillation Quenching. *Fred Snyder and Anita Moehl* 149
The Occurrence and Metabolism of Alkyl and Alk-1-enyl Ethers of Glycerol in Transplantable Rat and Mouse Tumors. *Fred Snyder and Randall Wood* 151
Occurrence of Glyceryl Ether Diesters in Human Tumors. *Fred Snyder, Randall Wood, Edgar Cress, and Nelson Stephens* 154
The Distribution and Metabolism of Glyceryl Ether Diesters in Disrupted Ehrlich Ascites Cells. *Fred Snyder and Randall Wood* 156
The Metabolism of Glyceryl Thioethers. *Fred Snyder, Claude Piantadosi, and Randall Wood* 159
Glyceryl Ethers in Insects: Identification of the Alkyl- and Alk-1-enyl-glyceryl Ethers in the Phospholipids of Three Insect Species. *Edward N. Lambremont and Randall Wood* 161
Metabolism of Long-Chain Fatty Alcohols in a Variety of Tissues: in vivo and in vitro. *Fred Snyder and Boyd Malone* 163
Lipid Class and Fatty Acid Composition of Rat Liver Plasma Membranes Isolated by Zonal Centrifugation. R. C. *Pfleger, Norman G. Anderson, and Fred Snyder* 165
Gas-Liquid Chromatographic Analysis of Heliothis virescens Triglyceride Composition at Various Metamorphic Stages. *Randall Wood, Robert Harlow, and Edward N. Lambremont* 169

THEORETICAL AND EXPERIMENTAL STUDIES IN METABOLISM AND DISTRIBUTION OF NUCLIDES 171
Fitting Models to Data: The Problem of Uniqueness. *Per-Erik E. Bergner and Warren Franz* 171
Preliminary Analysis of Calcium and Potassium Retention Data. *Per-Erik E. Bergner, W. D. Gibbs, and M. C. Yarbrough* 174

Cesium-137 and Potassium-40 in Patients and Normal Subjects. W. D. Gibbs, Harold D. Hodges, Linda C. Thompson, and C. C. Lushbaugh . . 175
Test of an Empirical System for Correcting Geometric Error in Whole-Body Counting of Reportioning Radioactive Labels Using Iodine-131. W. D. Gibbs, Harold D. Hodges, Mildred Bailey, and C. C. Lushbaugh 179
Zinc Retention in Rabbits Under Myelopoietic Stress. W. D. Gibbs, P. J. Sides, L. W. Anglin, M. C. Yarbrough, and C. C. Lushbaugh 181
Route of Iron-59 Loss in the Rabbit. R. F. Queener, P. J. Sides, and W. D. Gibbs 182
Toxic Effect of Chromium on Red Cell Survival. W. D. Gibbs, L. W. Anglin, P. J. Sides, and C. C. Lushbaugh 184
Gold Thioglucose Damage to the Satiety Center: Inhibition by Diabetes. A. F. Debons, Isidore Krimsky, H. J. Likuski, Annette From, and Roger J. Cloutier 186
Phenothiazine Inhibition of Reduced Nicotinamide Adenine Dinucleotide (NADH) Oxidation by Melanin. M. H. Van Woert 190

IMMUNOLOGIC STUDIES AND THE DEVELOPMENT OF THE MARMOSET AS A LABORATORY PRIMATE 194
Radiation Exposure-Rate Dependence of the Immune Response. Donald E. Carlson and N. Gengozian 194
Demonstration of an Early Host-Graft Incompatibility Reaction in Radiation Chimeras with the Jerne Plaque Technique. N. Gengozian, C. F. Gottlieb, and Elizabeth M. Allen 196
Graft-Versus-Host Reaction in Man Produced by Thoracic-Duct Lymphocytes. Helen Vodopick, C. C. Congdon, C. L. Edwards, N. Gengozian, Bill Nelson, Kong-oo Goh, and G. A. Andrews 198
Further Studies Using the in vitro Mixed Leukocyte Test. Helen Vodopick, Elizabeth M. Rupp, and N. Gengozian 201
Further Studies on Isohemagglutinins in the Marmoset. N. Gengozian . . . 203
Survival of Skin Transplants Between Marmoset Co-Twins. Raymond P. Porter and N. Gengozian 206
Survival of ^{51}Cr Labeled Red Cells in Marmosets. C. B. Merritt and N. Gengozian 208
Pathologic Observations on Causes of Fetal Death in Marmosets. Gretchen L. Humason and C. C. Lushbaugh with N. Gengozian and R. W. Cooper 212
Embryology of Marmoset Gonads. R. M. Kniseley, C. C. Lushbaugh, Gretchen L. Humason, and N. Gengozian 214
Parasites of the Imported Tamarin, Saguinus fuscicollis G. E. Cosgrove, Bill Nelson, and N. Gengozian 217

1027602

MISCELLANEOUS 221
An Interface Scanner for Automatic Data Processing of Liquid Scintillation Spectrometer Readout. H. Kimble and R. McKee 221
PUBLICATIONS 223
MEDICAL DIVISION CONFERENCES – 1967 229
LIPID SEMINARS – 1967 233
REGIONAL LIPID MEETING, 1967 234
FELLOWSHIPS AND TERM APPOINTMENTS 234
RESEARCH PARTICIPANTS – 1967 235
STUDENT TRAINEES – 1967 235
MEDICAL COMMITTEE, ORAU COUNCIL 236
ORAU MEDICAL DIVISION ADVISORY COMMITTEE 236
SYMPOSIUM 236
MEDICAL DIVISION EMPLOYEES 237
CONSULTANTS AND COLLABORATORS – 1967 239

INTRODUCTION

The Medical Division has three major research objectives: (1) to delineate mechanisms of radiation injury, especially in the human being, and to devise improved methods of treating radiation injury; (2) to advance the beneficial applications of radiation for diagnosis and therapy; and (3) to pursue selected basic studies, particularly ones related to cancer, that arise out of the ongoing program. Some research leads into areas not strictly within these categories but arising as logical developments from earlier studies. The Division considers that the provision of training opportunities is also an important goal and is attempting to increase the number of trainees in programs of one year or longer.

Since the research accomplishments are covered in the body of the report, this introduction deals with staff, physical facilities, trainees, and relations with other organizations.

Staff changes include the following: Dr. Lisbeth Kraft resigned after a relatively short affiliation. She has continued to serve as a consultant and has contributed in a significant way to efforts to improve standards of care for experimental animals. New staff members are Dr. Edward D. Bird, Dr. Karl Hübner, and Dr. S. P. Datta. Dr. Bird is a clinical endocrinologist particularly interested in the effects of drugs and trace elements on the basal ganglia. Dr. Hübner, a former trainee here, is a pediatrician who is devoting full time to research in immunology. Dr. Datta is an immunogeneticist particularly interested in genetics of blood-group antigens who has also joined Dr. N. Gengozian's immunology group. Dr. Melvin Van Woert served during part of the year as a temporary senior staff member; he worked effectively in the clinical program and in research.

A significant addition to the Medical Division's scientific resources has been undertaken and will become a reality in mid-1968. Dr. Donald Swartzendruber, now at the University of Michigan, has accepted a position on the senior staff, starting in July 1968, to direct a new program in electron microscopy. He formerly worked at the Biology Division of Oak Ridge National Laboratory and shares scientific interests with staff members there and at the Medical Division. The Division has sought for several years to initiate a research effort in electron microscopy, but the event that brought this close to reality was the acquisition, without significant cost, of a surplus, good quality electron microscope. This acquisition was made possible largely through the efforts of Dr. C. S. Shoup of AEC's Oak Ridge Operations office.

Physical facilities have continued to be augmented. The "Annex," purchased in 1966 from Abbott Laboratories, has been extensively remodeled particularly to provide office space needed for the computer program and to upgrade our animal quarters. A considerable portion of the building, including laboratories, is now in use. The low-

1027603

exposure-rate total-body irradiation facility (nicknamed LETBI) for human radiation studies has been completed and put into operation.

At year's end, the new marmoset building, which is being constructed through ORAU's corporate resources on ORAU property next to the library, was about half complete.

There has been some increase in the predoctoral and postdoctoral trainees at the Medical Division. Dr. Raymond C. Pfleger, working with the lipid group, completed his Ph.D. at the University of North Carolina and moved to the AEC project at the Lovelace Foundation. Dr. Raymond P. Porter, in the immunology program, has completed his Ph.D. at the University of Miami and will continue to work in the marmoset project. At the postdoctoral level, Dr. David Mardon has just joined the microbiology project, and Dr. James Soodsma will join the lipid project early next year. Others in active predoctoral training are Robert Wykle, lipids; Donald Carlson, immunology; and Charles Gottlieb, immunology.

In clinical research, a one-year postresidency program was completed by Dr. Amiram Ur, from Israel, and Dr. Milton Dunsky, from St. Louis University. Dr. Romulo J. Mora from Manila is in training as an Assistant in Clinical Investigation.

The Fellowship in Nuclear Medicine for medical students has been filled by five persons. It is supported by Neisler Radiopharmaceuticals, Mallinckrodt-Nuclear Company, and Abbott Laboratories.

The AEC training programs administered by the University Participation Office of ORAU made it possible to have five research participants from the faculties of colleges and universities at the Division during the summer of 1967. At the same time, and under the same support, eight promising undergraduate college students worked in Division laboratories.

During 1967 the Division has consciously sought to extend relations and cooperative activities with other institutions. Ties with the University of Tennessee Memorial Hospital have been made closer by joint research projects and plans are under way to establish a rotation of residents from that institution. Collaboration with the Biology Division of the Oak Ridge National Laboratory and with the University of Tennessee - AEC Agricultural Research Laboratory has continued. Recent joint work has been developed with the Molecular Anatomy Program of ORNL. Dr. Gengozian has just been appointed to a Ford Foundation professorship in the department of zoology at the University of Tennessee in Knoxville and he will spend one day each week at these duties. Dr. Frank Comas continues to spend one day per week teaching principles of radiotherapy as a visiting professor at the University of Tennessee Memorial Hospital in Knoxville.

The Medical Division continued to participate actively in the

1027604

courses for physicians given by the Special Training Division of ORAU under Dr. Francis Goswitz.

The annual symposium in medicine, held November 13-16, was titled, Radioisotopes in Medicine: In Vitro Studies. Coeditors of the proceedings are Dr. R. L. Hayes and Dr. Francis Goswitz of the Division staff, and Dr. Beverley Murphy of Montreal, Canada. More than 295 guests, participants, and speakers at the symposium represented the United States and nine other countries from Latin America, Asia, and Europe. The published proceedings will be available in the summer of 1968.

In February an informal work conference was held at the Medical Division on Dosimetry in Total-Body Irradiation from External Photon Beams. This meeting was supported by the National Aeronautics and Space Administration as a part of the project here being carried out under the direction of Dr. C. C. Lushbaugh. The participants included 12 invited experts and 7 members of the Medical Division staff. The proceedings have been edited by Roger J. Cloutier, F. T. O'Foghludha, and Frank V. Comas, and are available as U. S. AEC Report CONF-670219.

In March the Medical Division sponsored a Lipid Conference with more than 40 participants from five universities, all ORAU sponsoring institutions. There were two invited guest speakers and 25 papers were presented by the participants. These lipid meetings, originated by Dr. Fred Snyder, emphasize participation by graduate students and have proved highly successful.

Grant support from non-AEC sources has increased consistently in the past year. The work for NASA, "Radiosensitivity in Man," enters into the fourth year under the direction of Dr. Lushbaugh. Dr. Edward Balish is in his second year of work on "A Study of Infections in Irradiated Patients" supported by the U. S. Army Medical Research and Development Command. Dr. Balish has also received approval of an NIH grant entitled "Studies on the Morphogenesis and Pathogeneity of Candida albicans." An ongoing project supported by an NIH grant is "Immunology of Hematopoietic Chimerism in Tamarins" directed by Dr. Gengozian. Work was begun by Dr. Snyder in December on a sizable new project entitled "The Occurrence, Metabolism, and Function of Glyceryl Ethers in Neoplasms" supported by the American Cancer Society. "Basic Studies on Alkenyloxy Glycerol Ethers and Derivatives" is an NIH grant to the University of North Carolina (Dr. Claude Piantadosi) which includes support for collaborative work here under Dr. Snyder. Arrangements are being made to transfer an NIH grant held by Dr. Bird before he joined our staff, for the study of "Manganese and Dopamine in Brain after Phenothiazine." Additional proposals are under consideration.

We are indebted to Betty Anderson, technical editor, Katherine Stubbs, staff illustrator, Rush King, ORAU photographer, Frances

Banner, typist, and the staff of the ORAU Information Services Department - Donald W. Ulmer, Evelyn Bradford, Ethel Ayres, and T. F. X. McCarthy - for their important contributions to this report.

Gould A. Andrews
Chairman

1027605

STUDIES IN RADIATION AND RELATED TOPICS

The Medical Division devotes a major share of its resources to problems related to radiation. We seek not only for improved therapeutic uses of radiation, but also for better management of unwanted radiation injury. Our mission thus includes both mechanisms of radiation injury and its treatment. In pursuit of these objectives we carry out studies in hematology, experimental radiotherapy, immunology, cytogenetics, and pathology. These studies yield research results often extending beyond the subject area of the original objective.

The human total-body irradiation program this year has initiated radiation exposures in the new low-exposure-rate total-body irradiator (LETBI). The observations are adding to our knowledge of the role of dose rate in response to radiation and especially in the responses of patients with certain hematopoietic disorders. The observations are also providing information of importance to the program of the National Aeronautics and Space Administration.

Our interest in preventing or correcting damage caused by radiation includes studies on infections and hemorrhagic manifestations. A long-range goal is to develop techniques that allow treatment of radiation injury by hemopoietic grafts; for this reason animal studies are supported in the homograft problem and management of complications of homologous disease. Part of the work related to this objective is covered in Section V, Immunologic Studies.

Preliminary Comparison of Peripheral Blood Responses to Medium and Low-Exposure Rates of Therapeutic Total-Body Irradiation

C. L. Edwards, Frank V. Comas, G. A. Andrews, and C. C. Lushbaugh

The low-exposure-rate (1.5 R/hr) total-body irradiation facility (LETBI) described elsewhere in this report has been in clinical use for the past 6 months. During this period seven patients have received eight treatments (Table 1).

Patient acceptance of this form of treatment has been very good. The experimental nature of the treatment along with alternative options has been explained to each person. Isolation for as long as 5 days has been no problem from the standpoint of the attending personnel or the patients. The furnishings are such that the patients have not found their experience unpleasant. Few symptoms are expected from protracted exposures of 100 R and only mild

anorexia not clearly related to the exposure was reported by some of the patients.

Each patient is observed for at least 1 week for base-line hematologic, bacteriologic, and biochemical studies before irradiation, and for 6 weeks after irradiation. The hematologic data are complete for five treatments, allowing preliminary comparison with data obtained from patients exposed with the medium-exposure-rate (1.5 R/min) total-body irradiator (METBI).

Three of the patients had previously been treated in the METBI facility. Figure 1 compares the leukocyte and platelet counts in a

TABLE 1

Patients Treated in Low-Exposure-Rate Total-Body Irradiator

Patient	Diagnosis	Exposure (R)	Exposure (Hours)	Elapsed Time* (Hours)	Elapsed Time* (Days)
1	Primary Thrombocythemia	150	100	116.0	4.8
2	Lymphosarcoma	100	66.7	76.2	3.2
3	Chronic Lymphocytic Leukemia	100	66.7	73.1	3.0
3	Chronic Lymphocytic† Leukemia	100	65.8	79.6	3.3
4	Chronic Granulocytic Leukemia	100	66.7	74.4	3.1
5	Chronic Granulocytic Leukemia	100	66.7	78.7	3.3
6	Chronic Granulocytic Leukemia	100	70.2	76.8	3.2
7	Polycythemia Vera†	100	65.8	79.6	3.3

* The elapsed time is the interval over which the irradiation was given and exceeds the exposure time by the amount of "down" time, such as the time the patient spends out of the irradiating room or when attendants are in the room with him.

† The second treatment of patient No. 3 and the treatment of patient No. 7 were administered simultaneously.

1027606

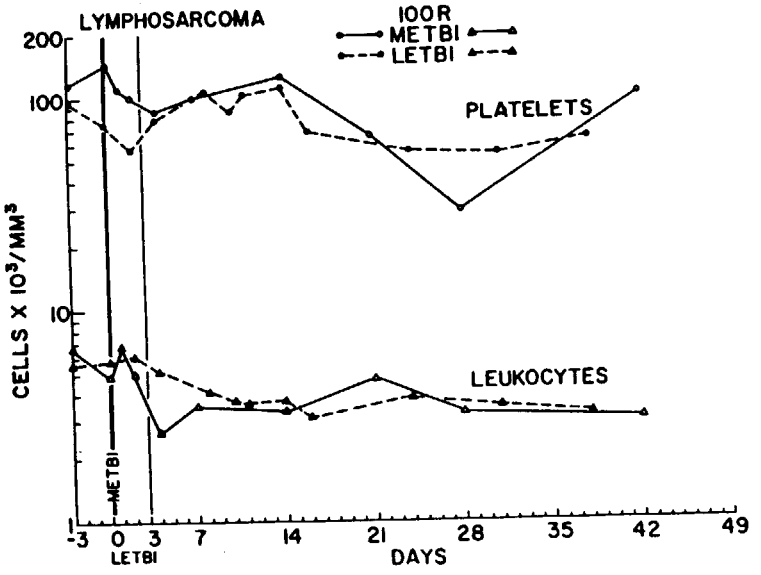

Fig. 1. Comparison of platelet and leukocyte values in a patient with lymphosarcoma given 100 R at two different dose rates.

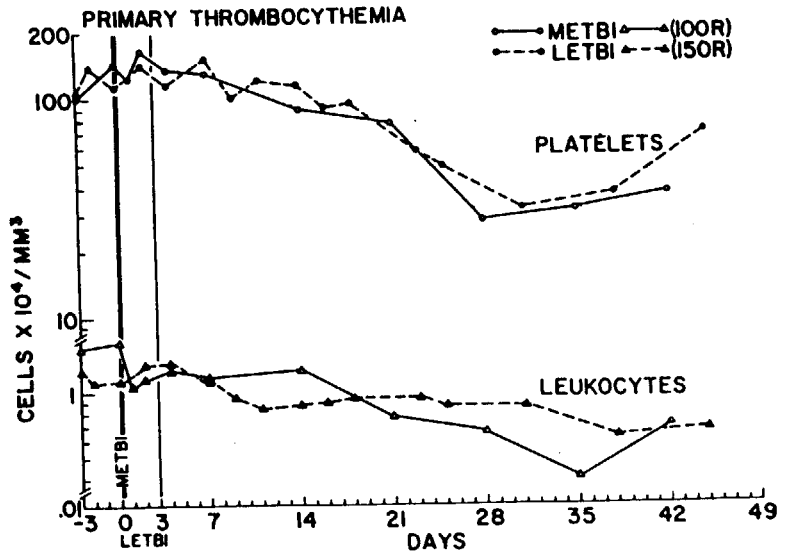

Fig. 2. Comparison of platelet and leukocyte values in a patient with primary thrombocythemia given total-body irradiation at two different dose rates.

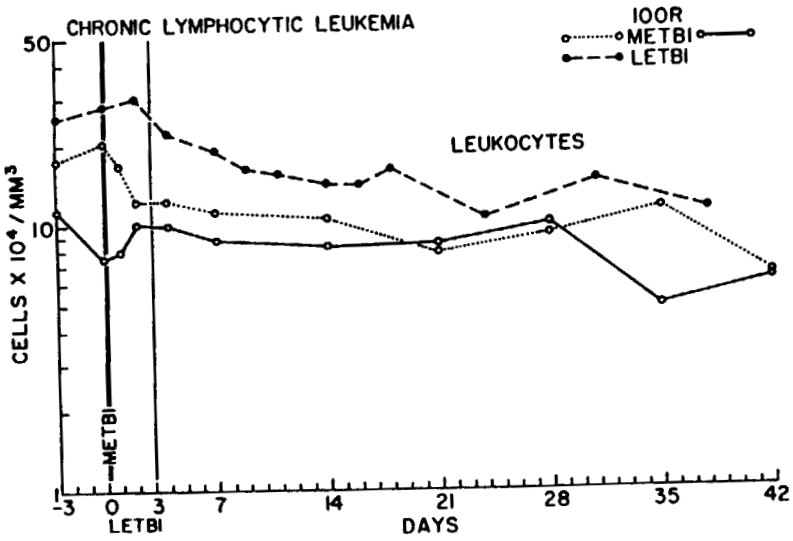

Fig. 3. Leukocyte values in a patient with chronic lymphocytic leukemia given total-body irradiation at two different dose rates.

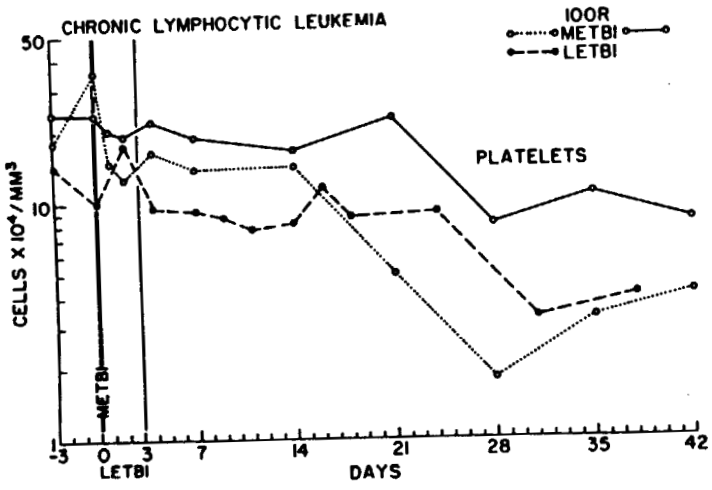

Fig. 4. Platelet values of patient shown in Fig. 3.

1027607

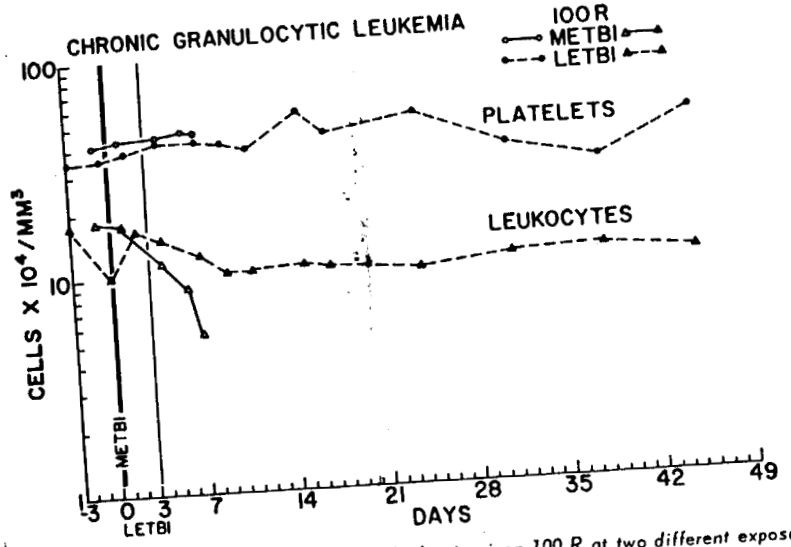

Fig. 5. Patient with chronic granulocytic leukemia given 100 R at two different exposure rates.

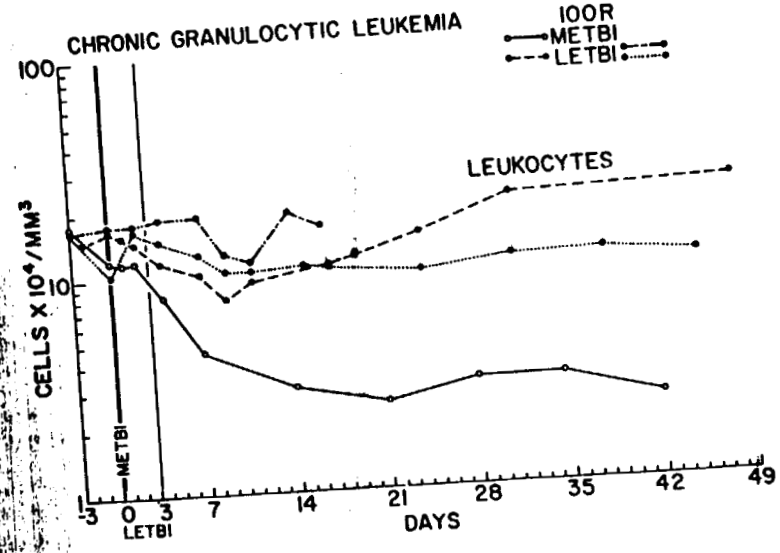

Fig. 6. Leukocyte response of three patients with chronic granulocytic leukemia exposed to 100 R at low exposure rate compared with average response of a group of similar patients treated at a higher dose rate.

patient with lymphosarcoma after 100 R of total-body irradiation at the two exposure rates. No great difference in the response to the two exposure rates is evident. A patient with primary thrombocythemia was exposed to 150 R in the LETBI facility. His leukocyte and platelet response to this treatment corresponds closely with that observed after an earlier exposure of 100 R in the METBI facility (Fig. 2). A patient with chronic lymphocytic leukemia had been treated on two previous occasions with 100 R at the medium exposure rate. Comparing the responses to the three treatments we find the effects of 100 R at the two exposure rates are similar (Figs. 3, 4).

One of the three patients with chronic granulocytic leukemia has subsequently received 100 R total-body irradiation in the METBI facility. Although these data are incomplete, the higher exposure rate seems to have produced a much greater decrease in the leukocyte count (Fig. 5). This observation is supported when the leukocyte response to 100 R in LETBI in each of the three patients with chronic granulocytic leukemia is compared with the mean response compiled from the patients with this disease previously treated in the METBI (Fig. 6).

These very preliminary observations indicate that total-body exposures of 100 R at the two exposure rates (1.5 R/hr and 1.5 R/min) produce similar effects upon the platelet and leukocyte counts in the patients with chronic lymphocytic leukemia and lymphosarcoma. The decrease in the platelet count after 100 R at 1/5 R/hr is significant in the patient with chronic lymphocytic leukemia, but hardly evident in the three patients with chronic granulocytic leukemia. The greatest disparity between the effects from the different exposure rates is seen in granulocytic leukemia where 100 R at 1.5 R/hr has had very little effect in three patients' leukocyte counts while the response to 100 R at 1.5 R/min is very prompt and therapeutically significant.

Further therapeutic studies at these and higher doses are planned.

Effect of Total-Body Irradiation Upon Plasma Iron and Erythrocyte Enzymes in Humans

C. L. Edwards, Allen M. Webb, and C. C. Lushbaugh

After total-body irradiation hematologic and biochemical changes may serve as indices of the time and dose of the radiation exposure. The drop in the number of circulating lymphocytes is perhaps the most rapid and best known change.

Erythrocyte production also decreases after total-body irradiation as is evident in the decreased utilization of radioiron and fewer circu-

1027608

lating reticulocytes. Reticulocytes normally constitute less than 1% of the total erythrocytes, and therefore it is difficult to obtain statistically reliable values. Radioiron utilization studies require injection of the radioisotope and obtaining subsequent blood samples over a week or 10 days to assess the incorporation of iron into hemoglobin at the time of injection. Less cumbersome parameters of arrest and recovery of hematopoiesis to assess this would be desirable. Plasma iron levels and red blood cell enzyme studies offer this possibility.

Plasma iron levels are largely dependent upon the erythrocyte destruction (hemoglobin catabolism) and production. The catabolism of hemoglobin releases ionic iron to the transport protein in plasma which delivers it to sites of erythrogenesis or iron stores. Anything that suspends hemopoiesis and interrupts the incorporation of iron into hemoglobin reduces the flux of iron from the plasma. Thus the plasma clearance time for iron is prolonged and elevated plasma iron levels develop unless the influx of iron from hemoglobin catabolism is also reduced.

Data have been obtained from 11 patients treated with 100 R total-body irradiation at the medium-exposure rate (approximately 1.5 R/min. The exposure extended over 3 days. Plasma iron determinations were obtained in the fasting state at the same time each morning to minimize diurnal fluctuations. At the higher exposure rate a mean elevation of 80% over the pretreatment average occurred by the second day after irradiation (Fig. 7). The mean then dropped to values less than the pretreatment average by the sixth day. Patients treated at the lower exposure rate also revealed an increase in plasma iron by the third day of irradiation. The values then decreased to below pretreatment levels by the seventh to fourteenth days (Fig 8). The magnitude of the elevation observed after the lower dose rate exposure has been less than at the higher dose rate. No changes in the iron binding capacity were observed at this dose.

It is not certain whether the rise in plasma iron is dose dependent and if so, through what ranges of doses. These data suggest that the rise is dose-rate dependent, although the range for each dose rate is quite wide and is itself probably dependent upon the state of erythropoiesis at the time of the irradiation. The greatest change has been in patients with polycythemia vera with brisk erythropoiesis, and low plasma iron levels before treatment. Similarly, the drop in plasma iron levels presumably corresponds to recovery of erythropoiesis, the magnitude of the drop being dependent upon the rate at which erythropoiesis is resumed and the state of the iron stores.

With the resumption of erythropoiesis, the reticulocyte count should rise and with it the level of erythrocyte glutamic oxalic transaminase (GOT). This enzyme is known to be present in higher concentrations in young erythrocytes.[1] Erythrocyte GOT and lactic acid dehydrogenase (LDH) have been measured in four patients exposed to 100 R at 1.5 R/hr. No significant change attributable to the

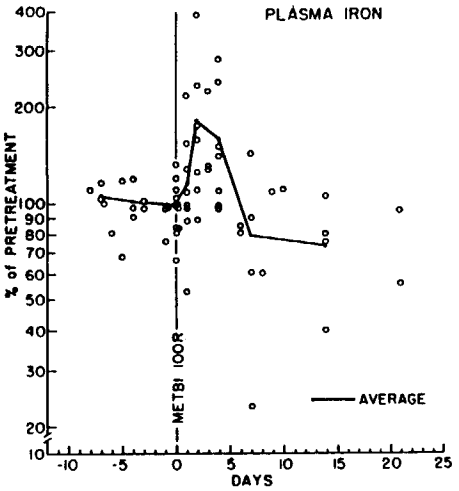

Fig. 7. Plasma iron determinations in 11 patients treated with 100 R total-body irradiation at 1.5 R/min.

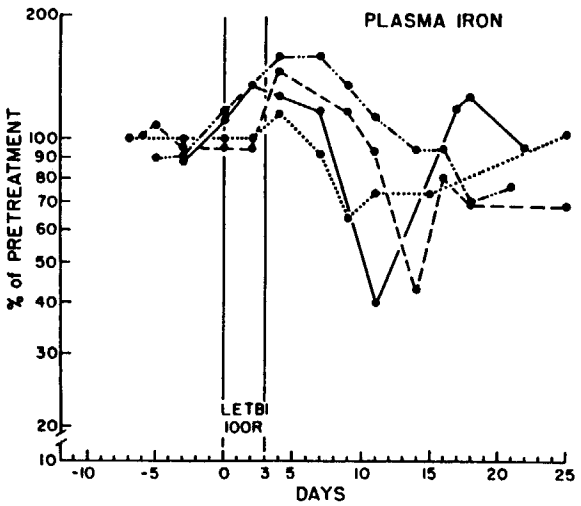

Fig. 8. Plasma iron determinations in four patients treated with 100 R total-body irradiation at 1.5 R/hr.

1027609

irradiation was seen in the erythrocyte enzymes of these patients. Further observations at different radiation doses are planned.

REFERENCE

1. Sass, M. D., Vorsanger, E., and Spear, P. W. Enzyme activity as an indicator of red cell age. Clin Chim Acta 10, 21-26, 1964.

The Low-Exposure-Rate Total-Body Irradiation Facility (LETBI)

G. A. Andrews, W. L. Beck, Roger J. Cloutier, A. C. Morris, Jr., T. R. Barclay, Frank V. Comas, C. L. Edwards, and C. C. Lushbaugh

A radiation exposure facility has been developed for investigating the therapeutic usefulness of total-body irradiation (TBI) at low-exposure rates. Previously we,[1] as well as others, have demonstrated the effectiveness of this form of radiation therapy in patients with chronic lymphocytic and other leukemias. The medium-exposure-rate total-body irradiator (METBI), previously described,[2] was used to expose patients to ^{137}Cs gamma radiation at about 1.5 R/min. Midline exposures of 50 to 100 R were given within 1.5 hours. Radiobiologic observations on dose fractionation and protraction in animals and man suggest that beneficial effects of TBI in chronic leukemia and other myeloproliferations may be augmented by low-exposure rates or dose fractionation. These observations provide the experimental and clinical rationale for this new low-exposure-rate facility.

The low-exposure-rate total-body irradiation facility (LETBI) diagramed in Fig. 9 consists primarily of a large concrete outer room in which a smaller inner exposure room is centrally positioned. Ten ^{60}Co sources located in the outer room, as shown, irradiate the inner room from all sides.[3]

The resulting radiation field enabled the inner room to be made sufficiently large (16 ft x 16 ft x 8 ft) for two patients to live, as in a two-bed ward, for an extended time (days) during their exposure to 1.5 R/hr (Fig. 10). The eight corner sources (Fig. 9) initially consisted of 26 curies each of ^{60}Co and the central ceiling and floor sources of 4 curies each. These sources are operated and monitored remotely from an instrument console (Fig. 11) located in an adjacent control room (Fig. 9C), that also contains closed circuit TV monitors, an intercommunication system for patient surveillance, and a physiologic monitoring system described elsewhere in this report. All these instruments, operational relays, safety interlock switches,

interrupt circuits are wired to an IBM 1800 computer in another adjacent room (Fig. 9D) for data storage and processing on a constant real-time basis during the facility's operation. Switches on the console permit the various interrupt levels in the IBM 1800 computer, located in the room below, to be activated so that prearranged programs for analysis of physiological signals can be called and executed. Figure 12 shows the signals that are now being fed into the computer. On the analog side, calibrated voltages in the + 10 millivolt range are being supplied from the conditioned physiologic monitor outputs. Other analog signals from the radiation monitor report on the operation of the individual sources. All these signals are recorded and analyzed by the computer programs. The computer is programed to check the values of all analog signals and to signal an alarm if any physiologic signals or radiation levels stray outside preset limits or source-containing

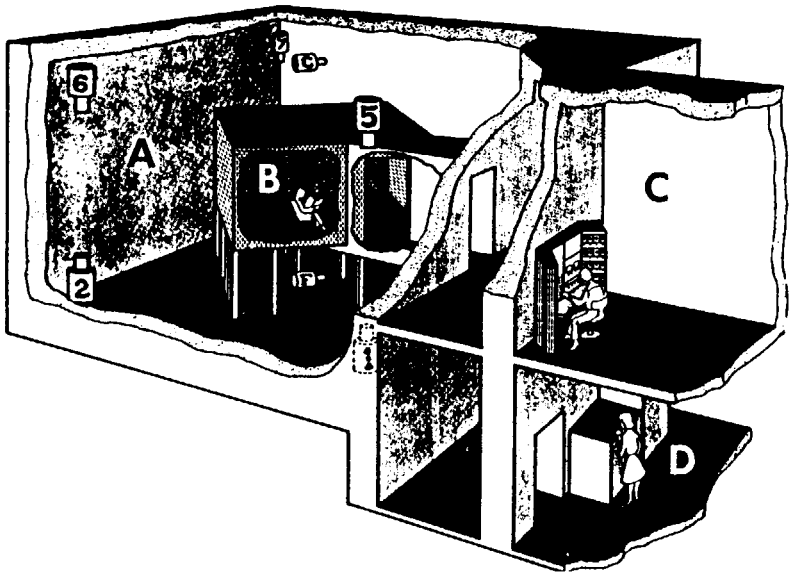

Fig. 9. Cutaway diagram of low-exposure-rate total-body irradiation facility (LETBI) showing:

A. Concrete shielded radiation containment room.

B. Centrally positioned radiation exposure living room.

C. The remote control room for operation of the ^{60}Co sources (only sources numbers 1, 2, 5, 6, 7, C, and F are shown), radiation exposure level supervision, nursing, and physiologic surveillance of the patient.

D. The on-line computer and data processing room.

1027610

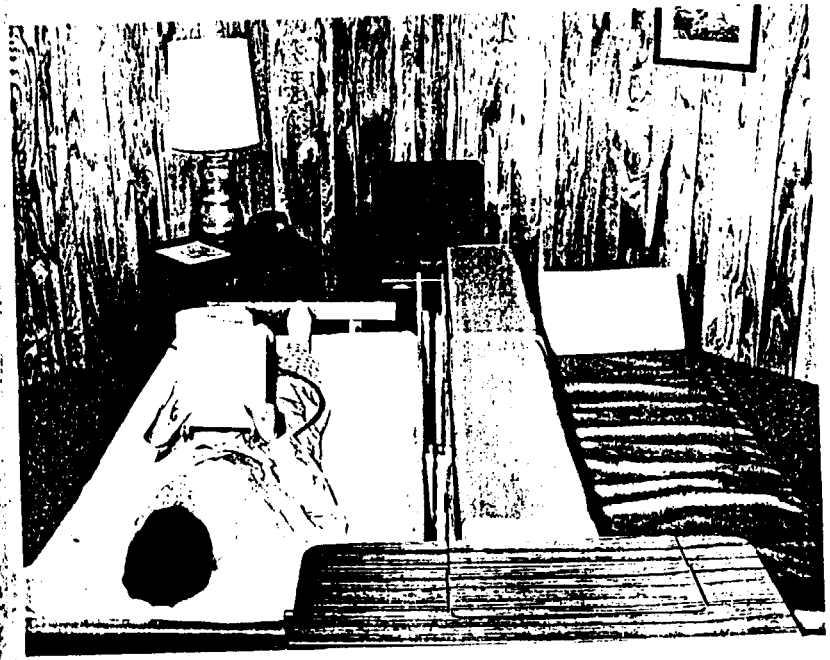

Fig. 10. A simulated closed-circuit TV view of a patient in the radiation exposure living room (Fig. 9, room B) showing the two centrally placed studio couches and other furnishings.

pistons fail to return to their shields on demand. Digital switch closure signals (Fig. 12) from the console enable the computer to record when the sources are raised and lowered and the reasons interruptions in exposure occurred.

When a patient is admitted to LETBI for radiation therapy, the radiation safety officer first determines that only the patient or patients are present within the confines of the interlocked area. All doors are then closed and the radiotherapist activates the facility by unlocking the master control switch, presses the "ON" button and prescribes the exposure level to be obtained in terms of accumulated exposure hours (e.g. 66.7 hr for ∿100 R TBI at ∿1.5 R/hr). Until this exposure time is accumulated on exposure meters controlled by radiation monitors, the unit is operated under the supervision of the nursing staff.

The radiation is turned off automatically whenever the patient leaves the treatment room or when anyone enters the interlock-controlled area. When the patient leaves to visit the bathroom located off the entrance hall to the treatment room but does not leave the

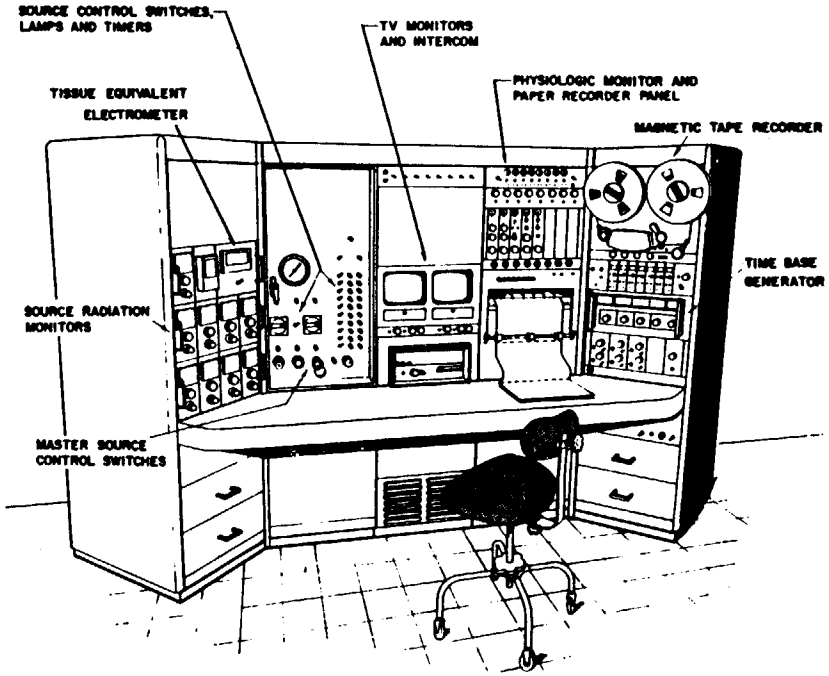

Fig. 11. Drawing of the LETBI console. The source controls and radiation monitors are located to the left, the TV monitor and intercom are in the center panel, and the physiologic monitoring and recording sections are located to the right.

controlled area itself, the radiation devices are turned on automatically upon his return to the treatment room. If the exposure is interrupted for nursing care, meals, and any other reason, the radiation devices must be turned on by the nurse who records the reason for the interruption. These events and exposure times are recorded by computer and the nursing and technical staff (Fig. 13) for use in retrospective studies of therapeutic effectiveness and evaluation of possible radiation-induced effects. Hematologic studies, and a system of dosimetry based on the use of tissue equivalent humanoid phantoms in LETBI are described elsewhere in this report.

REFERENCES

1. Andrews, G. A., Lushbaugh, C. C., Kniseley, R. M., White, D. A., and Friedman, B. I. Haematological effects of whole-body radiation in the human being. In IAEA Panel: Effects of Ionizing Radiations

1027611

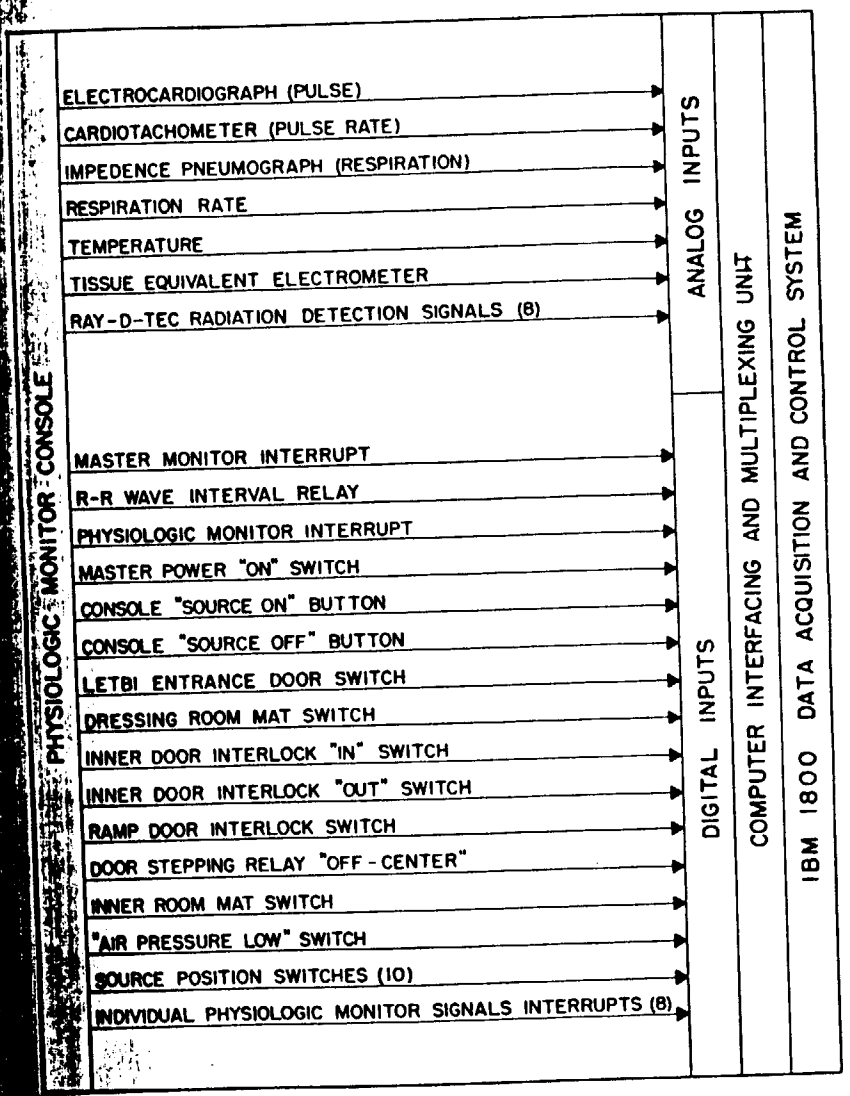

Fig. 12. Interfacing diagram showing the types of analog and digital signals flowing from the LETBI console to the IBM-1800 computer.

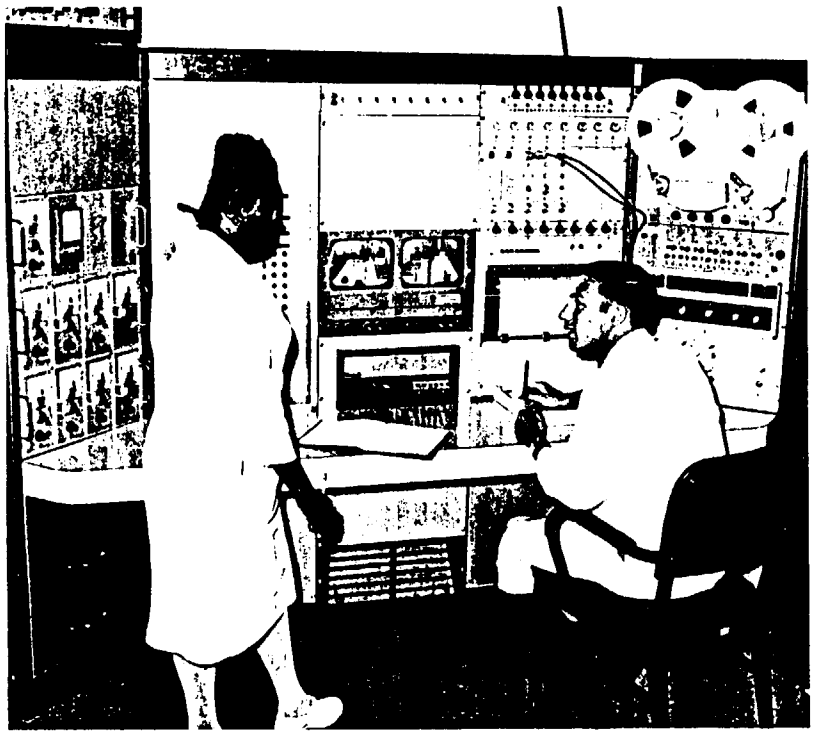

Fig. 13. LETBI console unit in operation. Progress of the patient's irradiation is being monitored by the operator and an attending nurse.

on the Haematopoietic Tissue, International Atomic Energy Agency, Vienna, 1967, pp. 75-83.

2. Brucer, M. A total-body irradiator. Int J Appl Radiat 10, 99-105, 1961.

3. Beck, W. L., Callis, E. L., Dalton, Patricia, and Cloutier, Roger J. Dosimetry for the low-exposure-rate total-body irradiation facility (this report).

1027612

Dosimetry for the Low-Exposure-Rate Total-Body Irradiation Facility

W. L. Beck, E. L. Callis, Patricia Dalton†, and Roger J. Cloutier*

The objectives of the low-exposure-rate total-body irradiator (LETBI) dosimetry study were to produce a large, uniform exposure field with an exposure rate of approximately 1 R/hr and to accurately determine a patient's absorbed dose.

The initial step in this study was an investigation of the various source arrangements that would provide the desired exposure field.[1] The basic requirements were that the field be uniform (± 5%) throughout a treatment volume large enough to provide two patients with comfortable living quarters for extended exposure periods.

The calculations made to find an optimum source configuration incorporated two major assumptions: that the sources could be considered "point" sources and that variations in the exposure rate are produced by the inverse square law. Attenuation or scattering were not taken into account. Calculations were done for a single source arrangement and several multiple-source configurations.

A configuration of 10 sources in a rectangular array was selected because the predicted exposure field was uniform within ± 5% throughout a treatment volume of 14' x 14' x 6'. This arrangement provided the greatest percentage of usable treatment volume per volume of shielding-superstructure and consequently proved to be the most economical structure to build.

Figure 14 compares the isodose or relative exposure lines predicted theoretically for the horizontal midplane of the volume to be occupied by the treatment room and the corresponding measured isodose lines. These results indicate that the horizontal variations in the field were predicted very well by theory. The measured vertical variation, however, was ± 15% compared to a predicted value of only ± 5%.

The source manipulators were designed to vary the exposure rate by changing the fraction of the 3 in.-long source positioned in the beam portal. Operating the manipulator with only a fraction of the source exposed was found to be the primary factor contributing to the vertical field gradient. The vertical gradient was reduced by positioning the entire source in the beam portal. The exposure rate was reduced

---

* Graduate student, physics department, University of Tennessee, Knoxville, Tenn.

† Present address: U. S. Food & Drug Administration, Dept. of Food Chemistry, Washington, D. C.

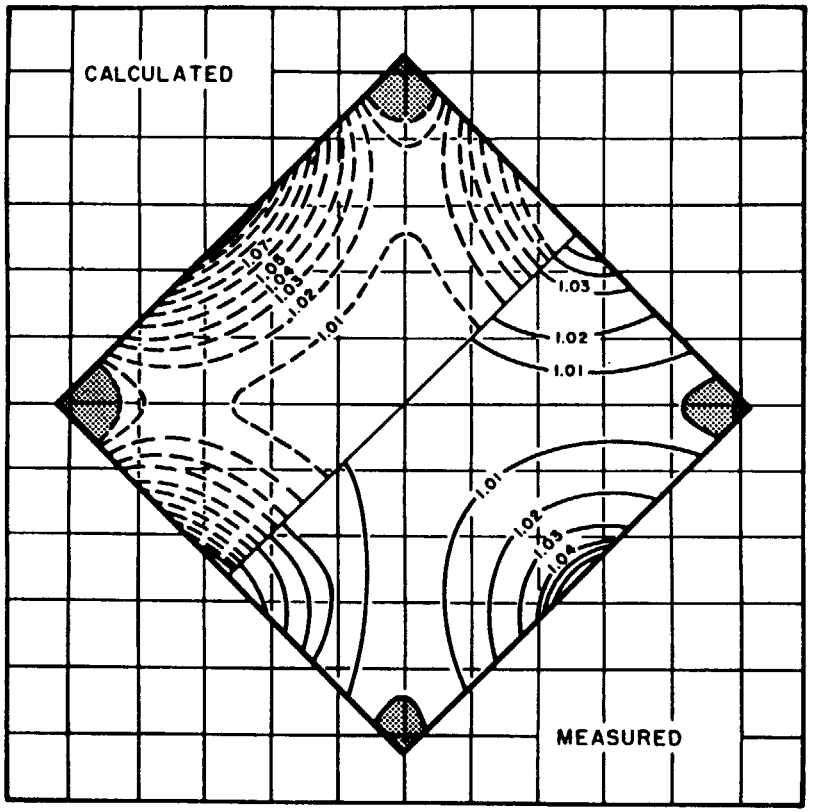

Fig. 14. Comparison of the relative exposure lines predicted theoretically (upper half) for the horizontal midplane of the volume to be occupied by the treatment room and the corresponding measured (lower half) isodose lines.

to the desired value by placing cylindrical lead attenuators over the beam portal.

The variation in the exposure field through the midplane of the completely furnished treatment room is shown in Fig. 15. Except for the small shaded areas, all measurements are between ± 5% and only one measurement in 289 varied by more than ± 10% of the exposure at the center of the room. Within 90% of the treatment volume the exposure rates varied by no more than ± 10%, and furniture placement restricts the patient from occupying most of these areas.

All the exposure measurements were made with a miniature Geiger detector with a selective shield,[2] chosen for its sensitivity, reproducibility, energy independence, and small size. This instrument was also desirable because it could be operated remotely from the control room.

1027613

Calibration was accomplished by measuring the exposure rate at the center of the room with a Victoreen condenser R-meter. On June 1, 1967, the exposure rate at the center of the treatment room was 1.50 R/hr. The exposure rate will be kept approximately constant by decreasing the thickness of the lead attenuators to compensate for the ^{60}Co decay.

Spectral measurements made with a NaI (Tl) detector at several

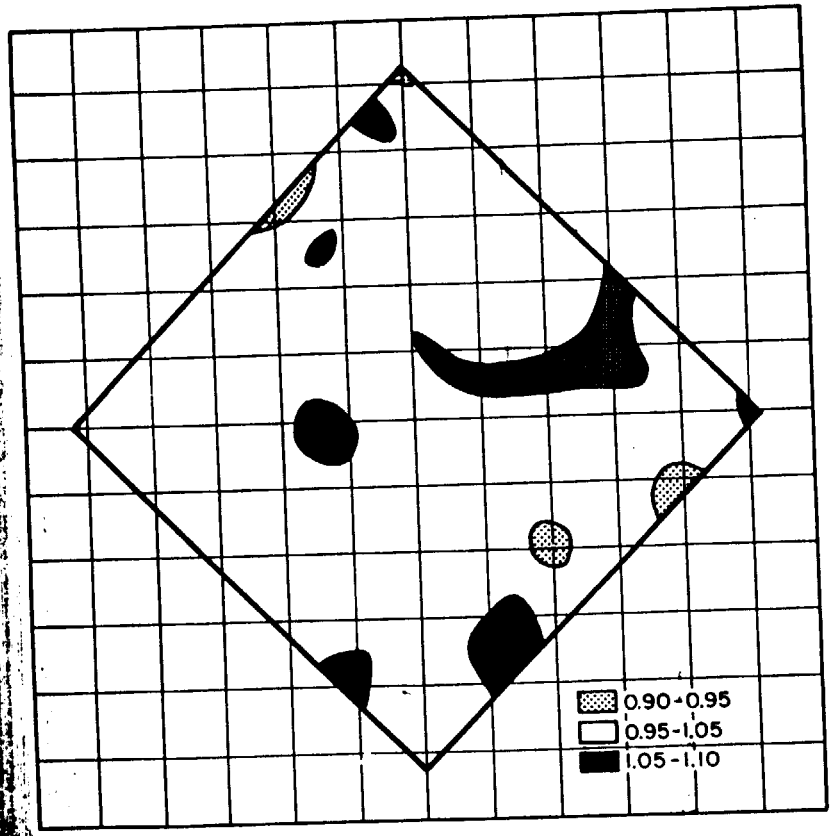

Fig. 15. Variation in the exposure field through the horizontal midplane of the completely furnished treatment room.

10276 14

TABLE 2

LETBI PATIENT DOSIMETRY

Relative Exposures

Position	Phantom	Pt #1	Pt #2	Pt #3	Pt #4	Pt #5	Pt #6	Pt #3*	Pt #7	Average	S.D.
Room Center	100	100	100	100	100	100	100	100	100	100	---
Chest	78	67	75	73	81	---	70	71	69	73.0	±4.75
Left Wrist	76	69	81	78	84	74	75	75	78	76.7	±4.30
Right Wrist	82	71	81	72	81	74	73	78	75	76.3	±4.24
Left Ankle	76	82	77	72	77	74	77	76	71	75.8	±3.23
Right Ankle	76	---	78	78	78	74	77	75	70	75.7	±2.15

*The second treatment of Patient No. 3 and the treatment of Patient No. 7 were administered simultaneously.

positions within the treatment volume showed no significant variations in energy distribution.

During patient treatment, thermoluminescent dosimeters are worn on the patient's wrists, ankles, and chest. The patient's absorbed dose is determined by correlating the measurements with surface-depth dose ratios obtained from phantom studies. Table 2 gives the surface exposures measured on the patients treated in the facility in 1967. The surface exposures are less than the exposure measured in the center of the room (100 R) due to attenuation by the patient's body.

REFERENCES

1. Dalton, P. and Cloutier, R. Source arrangement for a low-exposure-rate total-body irradiation facility for man. USAEC Report ORINS-52, 1967, 205 pp.
2. Wagner, E. B. and Hurst, G. S. A Geiger-Mueller γ-ray dosimeter with low neutron sensitivity. Health Physics 5, 20–26, 1961.

Physiologic Monitoring in the Low-Exposure-Rate Total-Body Irradiation Facility

A. C. Morris, Jr., T. R. Barclay, and C. C. Lushbaugh

A physiologic monitoring system has been developed for use in the low-exposure-rate total-body irradiation (LETBI) facility to study vital functions of patients undergoing radiation treatment. The basic monitoring system is illustrated in the block diagram of Fig. 16. The system has been initially developed to record the following six variables:

1. EKG waveform (frequency response: 0.01 to 250 Hz).
2. Heart or pulse rate (range: 0 to 200 beats/min).
3. Respiration waveform (frequency response: 0.01 to 10 Hz).
4. Respiration rate (range: 0 to 60 breaths/min).
5. Rectal temperature (range: 34° to 42° C).
6. Time base (from start of irradiation).

Shown in Fig. 17 signals from the patient are conducted through a

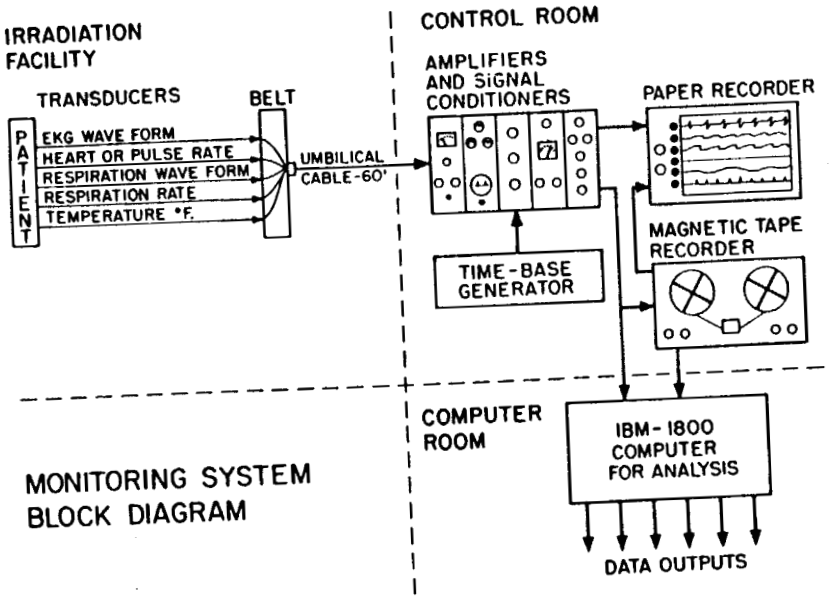

Fig. 16. Block diagram for the physiologic monitor in the LETBI facility.

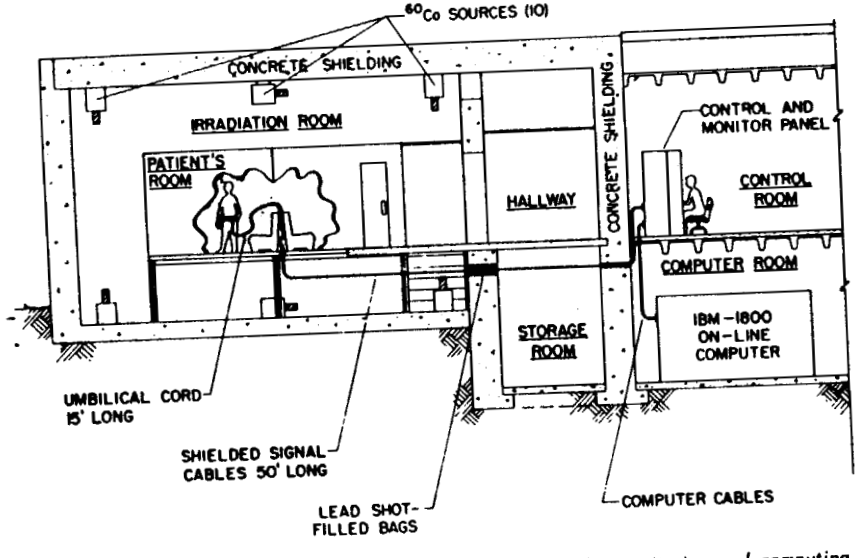

Fig. 17. Cutaway side view showing the arrangement of the monitoring and computing equipment for a radiation treatment.

1027615

flexible umbilical cable in the irradiation room and a 65-ft long signal cable running to the monitor console. The remote console location is necessary because of the gamma radiation field. Signals from the patient are conditioned by the monitor electronics and are then transmitted for recording and analysis through cables to the computer room located below the monitor. We investigated a number of electrode and sensor arrangements to obtain the most information with the least inconvenience to the patient. The configuration shown in Fig. 18 permits us to record the first four of the listed variables with the use of only three electrodes attached to the patient. The EKG waveform and pulse rate are obtained with the use of a differential amplifier and a cardiotachometer of standard manufacture. The respiration waveform and breathing rate are obtained, however, at a frequency of 50 khz so that the two types of information from the same set of electrodes will not mutually interfere. A rectal thermistor probe is used to sense the patient's temperature. Wiring for future monitoring of galvanic skin resistance (GSR) has been included in the cables.

One of the problems with using the monitor is that radiation treatments are planned to last a week or more. Difficulties have been experienced in getting the electrodes applied for minimum irritation, and in arranging the interconnecting belt and umbilical cord for least discomfort and restraint for an ambulatory patient. The electrode, belt, and cable arrangement shown in Fig. 19 overcame these problems.

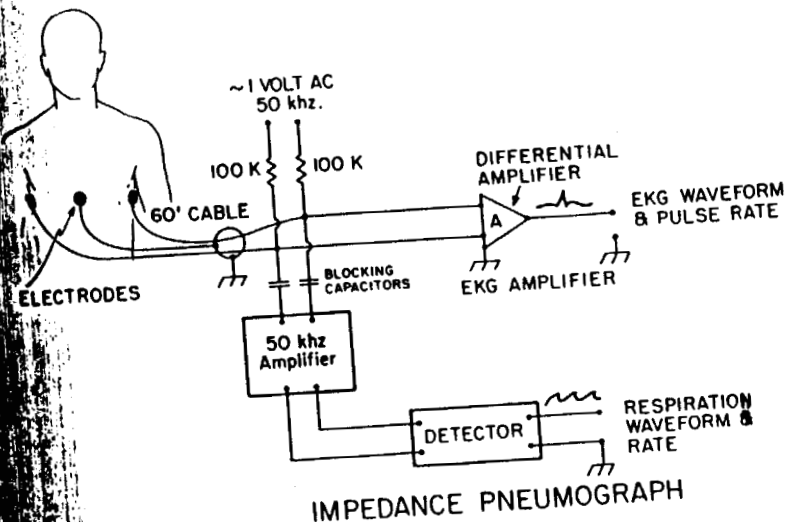

Fig. 18. Electrode and amplifier block diagram showing the method of obtaining cardiac and respiratory signals from the same set of applied electrodes.

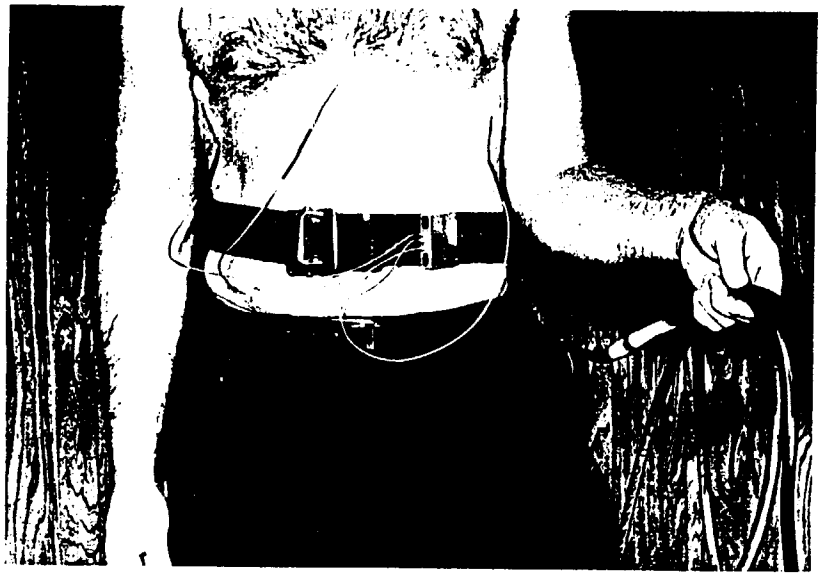

Fig. 19. Position of monitoring electrodes on a patient.

Fig. 20. Patient wearing the interconnecting webbed belt and the umbilical cord. The quick-disconnect assembly located about a foot down the umbilical cord permits the patient to use lavatory facilities in an adjacent room without having to remove his electrodes.

When the electrodes cause irritation to the skin they are moved to nearby locations. Usually the patient wears the belt over his hospital clothing as shown in Fig. 20, and guides the umbilical cord with his hands as he moves about the room. The umbilical cord has a set of quick-disconnect connectors near the belt so that the patient or attendant can uncouple and reestablish the monitoring circuits without the need for removing the electrodes.

This system for monitoring patients being irradiated has functioned well as have both magnetic and paper recorders; we plan, however, to make some circuit additions for a more flexible playback arrangement. Until the development of a final data reduction and analytical system, all the physiologic data from each irradiated patient are being stored on magnetic tapes for repeated analysis by various programs.

Interference Investigation of 60-Hertz Power Sources in the LETBI Facility

T. R. Barclay and A. C. Morris, Jr.

Power-frequency interference is a major problem confronting those making low-level biopotential measurements, and the physiologic measurements we are now making in the low-exposure-rate total-body irradiation (LETBI) facility are not exempt from this difficulty. The interference on our recording charts results from the fact that electric currents and voltages can be induced in a patient from nearby equipment powered from the commercial supply system. These artifacts show up most frequently in the EKG trace, and other traces derived from it, because the information frequency bandwidth for the EKG ranges from 0.01 to 250 Hz and the 60-Hz power-line frequency falls in the middle of this band. The respiration signals are derived from a 50-kHz, 100-microampere constant-current supply and are much less affected by signals at the power-line frequency. The temperature measurements are made with direct currents and are also negligibly affected.

The interference in the EKG trace is coupled to the patient in two ways, similar to the broadcast and reception of radio signals. The first mode is by electric flux coupling, where charges in the subject are set in motion by moving charges in wiring and nearby electrical devices. This type of coupling is illustrated in Fig. 21. In the upper portion of the figure a single-ended amplifier is shown with capacitive coupling to a patient from a fluorescent lamp. Interference occurs because an AC voltage is induced through the lower resistor R_E to ground. This is picked up by the amplifier at terminal A and produces an output voltage E_o heavily contaminated with the power-frequency component. The lower portion of Fig. 21 shows how this 60-Hz com-

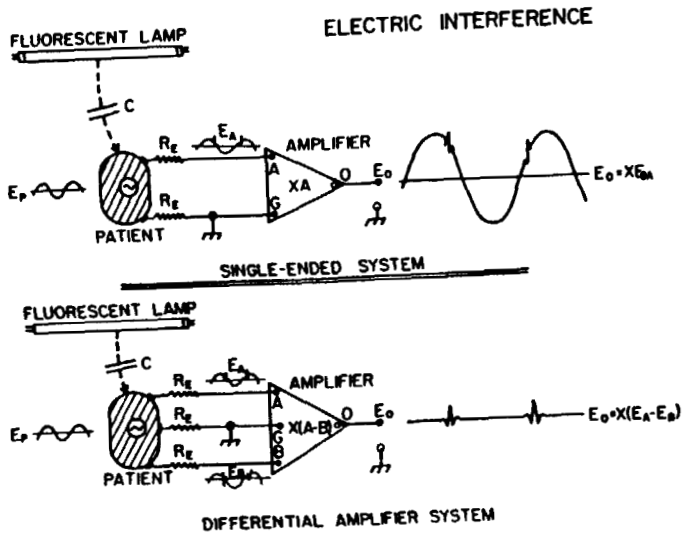

Fig. 21. Electric field interference schematic.

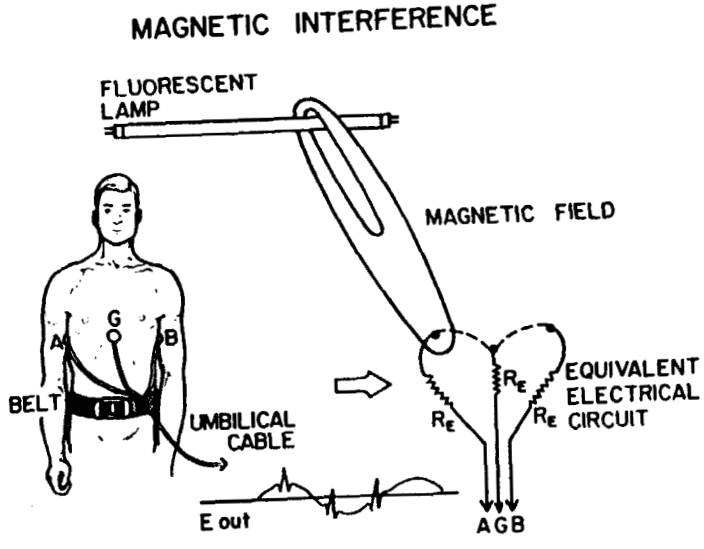

Fig. 22. Magnetic field interference schematic.

1027617

ponent can be greatly attenuated through the use of a differential amplifier. The common-mode 60-Hz voltage is cancelled out by the differential amplifier characteristic. At the same time the differential EKG voltage is amplified properly and the output voltage E_o is interference free. In operation, with the differential amplifier connected, we find that by making low resistance electrode connections, and positioning them carefully on the patient, good recordings can be obtained. Our interference-free recording of a 1-millivolt EKG voltage in the presence of a 60-Hz signal, many factors higher in magnitude, shows the efficacy of the differential amplifier circuit.

The second mode of interference transfer is by magnetic flux coupling, where currents are induced in the patient through a transformer-like action by currents and magnetic fluxes in nearby power wiring and electrical equipment. Figure 22 shows how our present three-electrode patient connections act as two, one-turn secondary loops of a transformer coil through the patient; an electrical device acts as the primary circuit and air is the transformer core. If there is an imbalance in the flux coupling between the source and the two patient loops, a differential current and voltage will exist at terminals A and B that will be detected and amplified. Because this kind of signal is not rejected by the differential amplifier circuit we have been particularly interested in locating and mapping the magnetic field sources and intensities in the LETBI facility.

To explore these magnetic fields a resonant probe was constructed as shown in Fig. 23. The probe consists of a coil wound on an iron core that is made resonant to 60 Hz with a parallel capacitor. An oscilloscope with a high-sensitivity preamplifier was used as a readout device (Fig. 24). The volume contained within the LETBI room was measured off in 2-ft increments and every electrical device was turned on to provide a "worst case" condition. Measurements were then made holding the probe axis vertical, and with the oscilloscope located in the outside hall with an interconnecting cable between the two. Values were recorded for planes parallel to the floor, ceiling, four walls, a vertical cross section 3-3/4 ft from the west wall, and a horizontal cross section 3 ft above the floor.

Figure 25 shows a flux map made on a plane 3 ft above the floor. The flux is concentrated near the color TV set, and near the wall corners and door where wiring is present. A magnetic flux map of the east wall (Fig. 26), showed two intense flux areas. One was located at the intercom and power switch panels, and the other (highest intensity recorded in the room, 50 millivolts) located in the door corner directly above some fluorescent-lighting ballast circuits. Figure 27 shows the flux pattern obtained in a vertical cross section taken directly beneath a row of fluorescent lamps. These lamp fixtures give off an appreciable amount of magnetic flux and, as seen in the figure, this field falls off with distance.

To determine the magnitude of the magnetic coupling, a two-loop wire

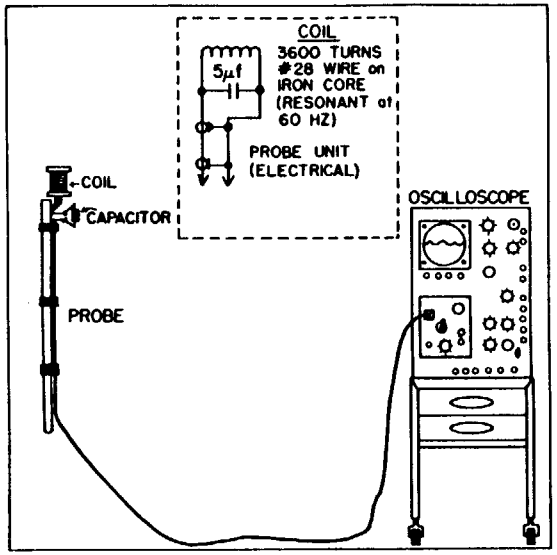

Fig. 23. Flux probe diagram for 60 Hz magnetic interference measurements in the LETBI facility.

Fig. 24. Magnetic field measurements being made in the irradiation room with the resonant flux probe.

1027618

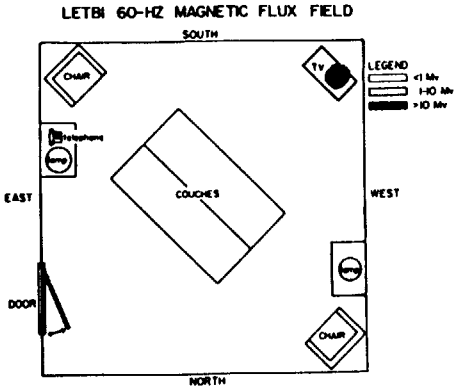

Fig. 25. Magnetic field intensity measured three feet above the room floor.

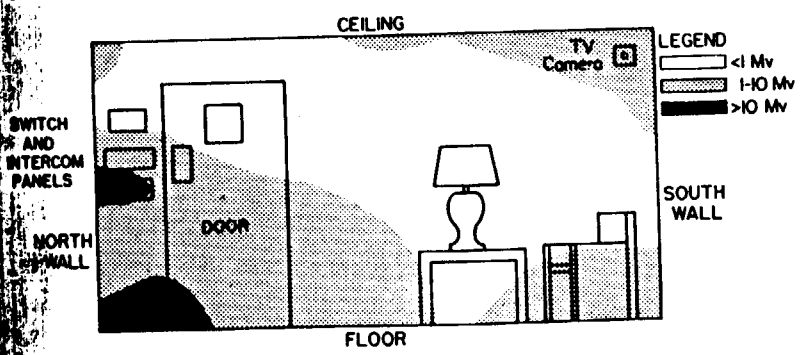

Fig. 26. Magnetic field intensity measured along the irradiation room's east wall.

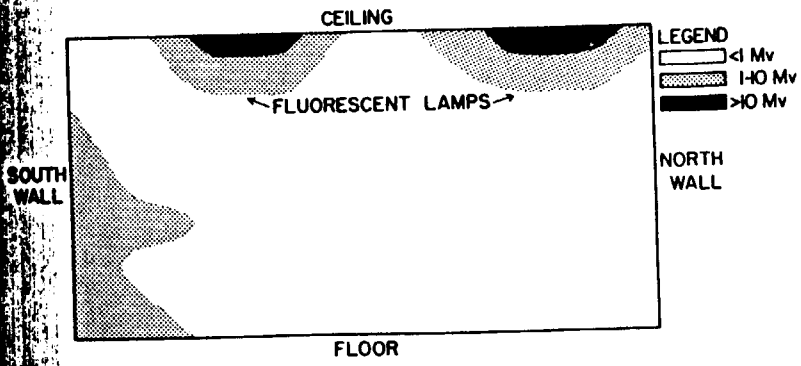

Fig. 27. Magnetic field intensity measured in a vertical cross section directly below a row of ceiling fluorescent lamps.

probe was constructed similar in shape to the equivalent circuit shown in Fig. 22. This probe was held near one of the fluorescent lamps on the ceiling, positioned with one loop toward the lamps and the other loop pointed away. The unequal flux coupling produced a differential voltage of 50 microvolts in our measuring instruments. Although this intensity of magnetically coupled voltage is not detrimental to our present EKG measurements, it would have serious effects on EEG or other low-level physiologic signals which we might attempt to record in the future.

In light of these flux and voltage values we experimented with some convenient shielding materials to reduce the magnetic fields. Our search probe was positioned inside a two-foot cubic box of fine copper screen. This gave no reduction in the probe signal, so a second box of galvanized hardware cloth was built over the first one. Even with this double-screen shield the probe signal was not reduced. We then placed the search probe in a canister of Conetic foil (a material having a high magnetic permeability) and again the signal was not reduced. We have concluded from these tests that any successful magnetic shielding of the room would involve covering all room surfaces with thick ferrous metal sheets— an impractical arrangement because of the needed gamma-ray exposure field coming through the room walls. A grounded screen shield would probably help reduce the electric field and might well be considered for future installation, but it would be ineffectual for the magnetic fields.

If the 60-Hz magnetic fields must be reduced for some future lower-level measurements, we would probably have to change all the appliances to use direct-current power. This would eliminate the troublesome alternating-current fields but would also restrict the type of appliances used.

During the course of these experiments we have found that electrode placement patterns for best signals and minimum power-line interference varies considerably with the condition of the patient. The patients to be irradiated and monitored in the facility frequently have enlarged abdominal organs that congest the thoracic cavity and change the cardiac electrical surface patterns. Usually preliminary care in securing a good, low-resistance sternal ground electrode connection, together with trying the two active electrodes at various chest test sites, give optimum results.

1027619

Power-Spectrum Analysis of Pulmonary Impedance Pneumograph

Richard L. Frome, C. C. Lushbaugh, Herbert T. Davis, III, and Donna S. Bibler*

Evaluation of the impedance pneumograph (Fig. 28) is usually by visual inspection, counting respiratory cycles, and comparing amplitudes and regularity. Continuous physiologic monitoring, however, produces a vast amount of analog recordings that overwhelms the analyst unless some form of automatic data reduction can be obtained that minimizes the interpretive work load. We have found that measurement of the power spectrum through spectral analysis of the pulmonary impedance wave form is a natural way to achieve meaningful data reduction that discloses abnormalities in respiration.

Respiration, as measured by the impedance pneumograph described on page 35 can be considered as a trace of length T from an arbitrary origin and designated $X_i(t)$ where i refers to the ith trace and t is time ($0 < t < T$). The classical harmonic analysis could be used to investigate the power in X (t). Jenkins[1] discusses the difference between this method of time series analysis, and the statistical approach used in this investigation.

If X (t) is a stationary time series and ave $\{X(t)\} = 0$, then

$$C(\tau) = \text{ave}\ \{X(t)\ X(t+\tau)\} \qquad (1)$$

the autocovariance function, and its Fourier transform

$$P(f) = \int_{-\infty}^{\infty} e^{-i2\pi f\tau}\, C(\tau)\, d\tau = \int_{-\infty}^{\infty} \cos(2\pi f\tau) c(\tau) d\tau \qquad (2)$$

the power spectrum of X (t).

Then, if $\tau = 0$ in eq 1

$$C(0) = \text{var}\ \{X(t)\} = 2\int_0^{\infty} P(f)df \qquad (3)$$

so that 2P (f) df represents the contribution to the variance[2] (or power) of the process from frequencies between f and (f + df), where only positive frequencies are considered.

The traces X_{it} were sampled at equally spaced intervals of time, Δt, and the discrete time series X_{it}, $t=1,\ldots n$ ($n = T/\Delta t$) were used to estimate the autocovariances and the power spectra. The value of Δt and T chosen depended primarily upon two factors[1]:

(1) The Nyquist frequency, $\omega_n = \pi/\Delta t$ radians/minute or $1/2\ \Delta t$ cycles per minute. All frequencies above ω_n will be aliased with those in the range $(0, \omega_n)$

* Department of Statistics, Johns Hopkins University, Baltimore, Md.

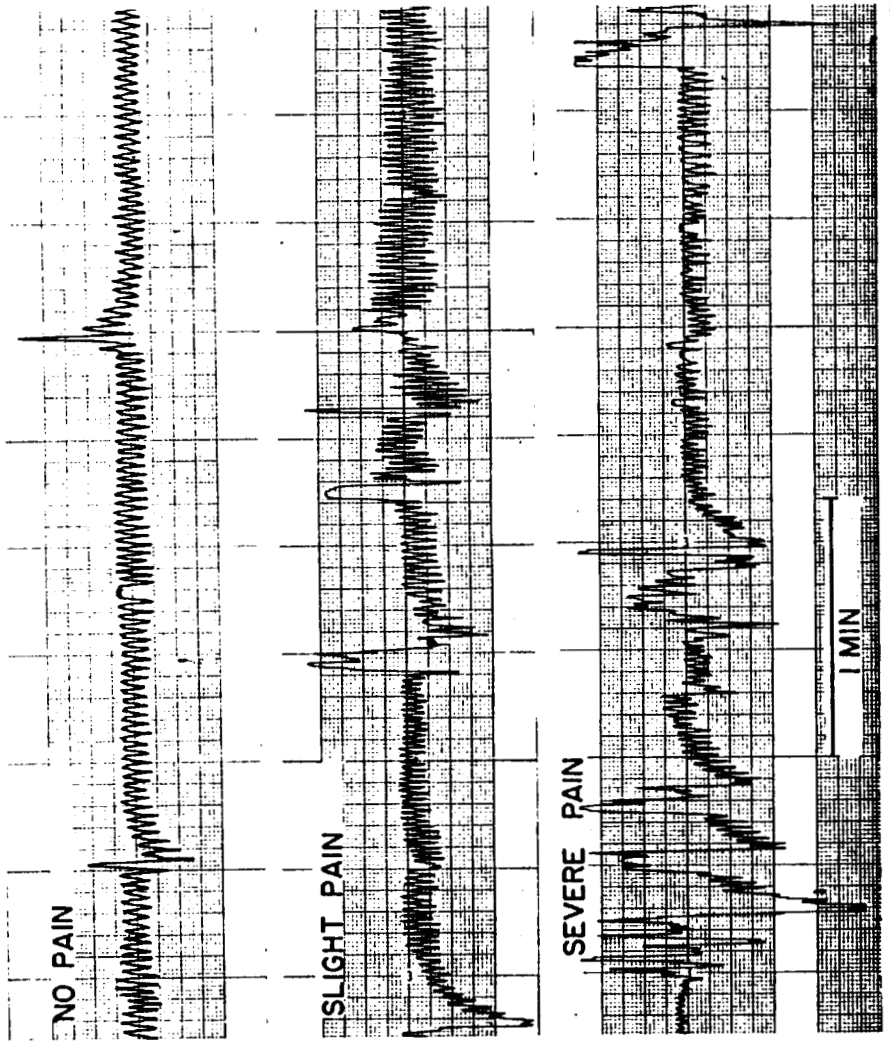

Fig. 28. Pulmonary impedance traces from patient experiencing different subjective degrees of pain.

1027620

(2) The resolution required in the estimated spectrum and the lowest frequencies of interest.

Our specific aim was to estimate the aliased spectrum for frequencies from 0 to 1/2 Δt cycles per minute. To obtain estimates that converge, a lag window in the time domain or the equivalent spectral window in the frequency domain was necessary. For this purpose, the Blackman-Tukey estimation procedure[3] with hamming was used.

Examples:

Figure 28 shows the pulmonary impedance traces produced while the patient was experiencing different subjective degrees of pain expressed as none, slight, and severe. The power spectra of these three traces are presented in Fig. 29. They indicate that more

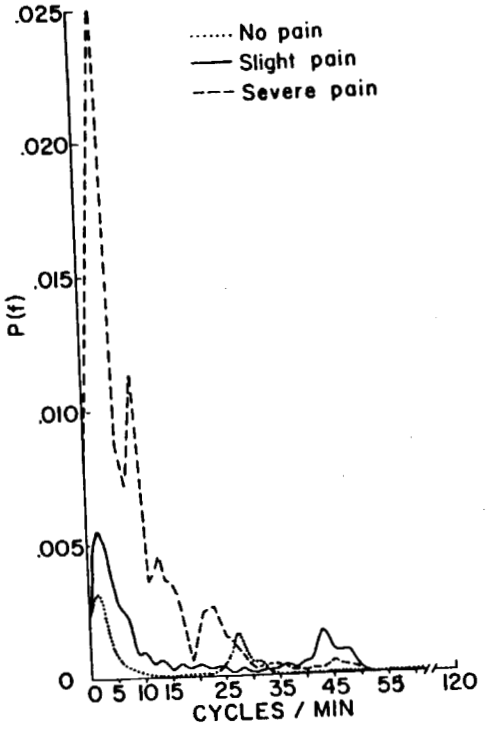

Fig. 29. Power spectra of pulmonary impedance traces from patient experiencing pa Each spectrum was estimated using the Blackman-Tukey procedure with n=96 Δt=.0416 minutes, T=4 minutes, and m=120 (m=number of lag terms.)

energy is expended in respiration as pain increases; and that low frequency cycles show a substantial increase.

These results may be compared with the power spectra of the respiratory traces obtained from a control subject during or immediately after three different levels of physical activity (Fig. 30). The spectrum "before exercise" indicates periodic breathing at approximately 15 breaths per minute, as expected from a system operating in a steady state condition. The "after exercise" spectrum reflects the increased respiratory response to a large demand for oxygen. Much more power is used to meet it. The "20-min after exercise" spectrum corresponds well with the "before exercise" spectrum, indicating that respiration has been adjusted back to the normal level.

Our studies so far show that changes occur in the power spectra of the pulmonary impedance pneumograph during clinical conditions such as normal exertion, pain, and gastrointestinal distress. They

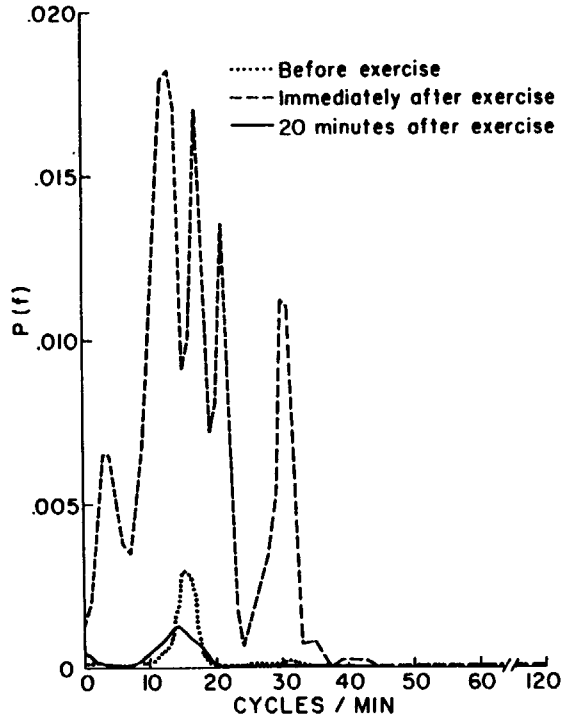

Fig. 30. Power spectra of pulmonary impedance traces from control. Each spectrum was estimated using the Blackman-Tukey procedure with n=960, Δt=.0416 minutes, T=4 minutes, and m=120 (m=number of log terms).

1027621

indicate that this kind of analysis may not produce spectra that are diagnostic of any one pathophysiologic condition, but such spectra will reflect the onset or abatement of undesirable clinical conditions. Differentiation between respiratory power utilization under normal and pathologic stress appears to depend upon an increased power contribution from low frequencies during pain.

1. Jenkins, C. M. General considerations in the analysis of spectra. Technometrics 3, 133-166, 1961.

2. Tukey, J. W. Discussion, emphasizing the connection between the analysis of variance and spectrum analysis. Technometrics 3, 191-219, 1961.

3. Blackman, R. B. and Tukey, J. W. The measurement of power spectra. Dover Publications, Inc., New York, N. Y., 1958.

R-Wave Detector for Use with Cardiac Waveforms from the Physiologic Monitor

T. R. Barclay and A. C. Morris, Jr.

One procedure used in clinical applications for detecting cardiac arrhythmias is the measurement of pulse interval (R-R, heart wave interval) variations from beat to beat. It is also used to study the function of a healthy heart while under stress conditions.

We have a need for a device that will communicate a signal, as a function of the R-wave spike, to the IBM-1800 Computer digital interrupt input. In addition to measuring the R-R interval, the signal to the interrupt input can be used for triggering other computer programs into action. Therefore we modified the input wiring of the heart-rate coupler on the physiologic monitor to provide common circuitry to the coupler through which on-line (live) and off-line (taped) recorded EKG signals are routed.

An output pulse is available from the heart-rate coupler, which is produced as a function of the input EKG signal R-wave voltage spike. The output pulse is routed to the input of the R-interval computer interface circuit (Fig. 31).

The input circuit differentiates the input signal to provide a short-duration positive pulse to the base of transistor Q_2. The positive spike

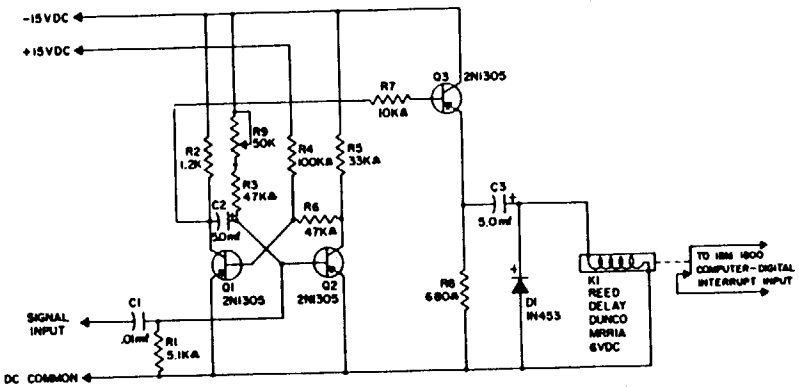

Fig. 31. R-Wave detector and relay circuit for the physiologic monitor.

turns Q_2 OFF, and turns Q_1 ON. The collector of Q_1 rises from a negative potential to a less negative potential, then back to the original negative potential as the single shot action of the monostable multivibrator moves through its cycle. The positive-going pulse from the collector of Q_1 turns Q_3 (relay driver) OFF. The change in potential on the emitter of the transistor Q_3 forces the capacitor C_3 of the D. C. clamp circuit to charge up through the diode D_1. The next change in potential on the emitter of Q_3 allows C_3 to discharge and actuates the relay. The relay closure completes a digital input interrupt circuit of the computer.

This action occurs with each R wave. Thus with each heartbeat a signal of the proper interval is recorded.

A Study of Infections in Irradiated Patients

Edward Balish, Ted A. Pearson, R. Tanida, and Romulo J. Mora

Studies are continuing on infection, the most serious complication of sublethal total-body irradiation. Our objective is to identify the species of microorganisms causing these infections, to determine their portals of entry, and the responses to therapy. It is important to ascertain whether changes in the natural bacterial flora occur after treatment with total-body or partial-body irradiation even when there is no clinical infection. Alterations in the flora could result in the overgrowth of more virulent species of microorganisms and

1027622

may be an important factor in the etiology of postirradiation infections.

Numerous reports in the literature indicate that the bacterial flora of normal human beings remains relatively stable for long periods of time.[1-4] Previously we reported that 100 R of total-body irradiation resulted in alterations of the nasal, gastric, and fecal bacterial flora. In addition to further studies on the microbial flora of a patient given total-body irradiation, this report includes some observations on the influence of such irradiation on the bactericidal effect of serum. No antibiotics were administered to these patients during the study.

Table 3 shows the populations of microorganisms isolated from fecal samples collected before and after a patient was exposed to 50 R TBI. It can be seen that the flora was not altered drastically by the irradiation. Of special interest (Table 3) are the anaerobic, spore-forming microorganisms. Although nonhemolytic, gram-positive, anaerobes were isolated before and after the exposure, β- hemolytic Clostridium perfringens began to increase in numbers within 2 weeks after the exposure. This increase in Cl. perfringens has not been encountered in our previous studies and its significance remains to be determined. Candida sp. were also isolated in fairly large numbers on one occasion following total-body irradiation but were not able to persist for any length of time.

Table 4 shows the bacterial microflora of gastric washings col-

TABLE 3

Fecal Microbial Profile of a Patient Before and After Exposures to 50 R Total-Body Irradiation

No. Microorganism/gm stool (dry wt)

Clostridium sp.	*Clostridium perfringens*	*Klebsiella-Aerobacter*	*Fecal Streptococci*	*E.coli*	*Candida sp.*
1.3×10^{9}		4.7×10^{10}	3.3×10^{9}		
5.0×10^{9}		1.3×10^{10}	8.3×10^{10}	2.8×10^{11}	
3.7×10^{8}		1.2×10^{9}	5.6×10^{9}	1.4×10^{11}	
3.7×10^{10}		2.6×10^{8}	3.1×10^{8}	8.9×10^{9}	
9.2×10^{8}	9.0×10^{5}	3.0×10^{8}	1.4×10^{8}	4.0×10^{8}	3×10^{6}
6.0×10^{10}		1.1×10^{10}	2.4×10^{8}	4.9×10^{8}	
3.1×10^{8}	4.6×10^{7}	7.7×10^{9}	3.1×10^{9}	7.7×10^{9}	
2.6×10^{10}	1.9×10^{7}	1.6×10^{10}	3.4×10^{10}	1.1×10^{11}	
1.7×10^{9}	8.3×10^{9}		9.2×10^{8}	2.6×10^{10}	

TABLE 4

Microorganisms Isolated from Gastric Washings Collected from a Patient Before and After Exposure to 50 R TBI

Time (Days)	No. Microorganisms/ml Gastric Washing						pH
	Streptococcus mitis	*Streptococcus salivarius*	*Pseudomonas sp.*	*Neisseria sp.*	α streptococci	*Staphylococcus aureus*	
-7	1.0×10^6	1.8×10^6	1.4×10^4				4.5
-3				6.0×10^4	5.8×10^4		3.5
0(Pre)	1.0×10^6	7.2×10^5	2.1×10^3	1.0×10^5		2.9×10^5	5.5
0(Post)	1.0×10^5	7.8×10^5	1.4×10^3	5.5×10^5		2.6×10^3	5.5
+1	3.2×10^4	1.5×10^4		8.4×10^5		1.2×10^4	4.1
+3	3.2×10^6	9.4×10^4	3.8×10^3	8.4×10^5		2.3×10^3	5.0
+7	NO GROWTH						1.3
+14	1.3×10^6	1.5×10^6	1.7×10^3	2.2×10^6		7×10^2	5.5
+21	1.2×10^5	6.0×10^4		3.4×10^5			4.6
+23	3.5×10^4	1.0×10^5		1.2×10^5			4.0
+28	2.5×10^6	2.9×10^5		5.0×10^6		1.0×10^4	5.5
+31	NO GROWTH						

[redacted] from this patient before and after he was exposed to 50 R TBI. [redacted] remarkable alterations occurred in the bacterial flora of the [redacted] gastric washings. Although Pseudomonas and Staphylococcus aureus [redacted] were present before exposure, no overgrowth or important shift in [redacted] populations was observed. It was also evident that the bactericidal [redacted] mechanisms operating in the small intestine were still functional, [redacted] since no viable Pseudomonas microorganisms were isolated from the [redacted] after total-body irradiation (Table 5). After exposure, Klebsiella-

TABLE 5

Microorganisms Isolated from Urine Samples Collected from a Patient Before and After Exposure to 50 R TBI

No. Microorganisms/ml Urine			
Klebsiella-Aerobacter	*Staphylococcus albus*	*Streptococcus faecalis*	*Diphtheroids*
1.0×10^5	4×10^2	2.9×10^4	
1.0×10^6		2.3×10^4	2.2×10^4
1.6×10^7			
6.0×10^7			
1.6×10^7			
1.6×10^8			
8.0×10^7			
7.2×10^7			
1.0×10^8			
1.5×10^8			
4.2×10^8			

[redacted] bacteria were isolated from this patient's urine before [redacted] total-body irradiation (Table 5). After exposure, Klebsiella-

[redacted] microorganisms were consistently isolated in pure culture [redacted] relatively large (clinically significant) numbers. However, [redacted] all manifestations of urinary-tract infection were evident [redacted] time. Two weeks after the last sampling time indicated

1027b23

in Table 5, no viable microorganisms were present in this patient's urine.

Staphylococcus aureus predominated in nasal cultures throughout the 31-day observation period. Small numbers of pneumococci were isolated from throat swabs before, but not after, the irradiation. The rest of the bacterial flora of the throat was consistently normal.

Several reports in the literature indicate that irradiation can interfere with the capacity of serum to kill bacteria.[5,6] We have explored this important aspect of host defense in patients exposed to 50 and 100 R TBI.

Figure 32 shows the comparative growth rate of Staphylococcus aureus (isolated from the patient's nose) when incubated with a 1/10 dilution of the patient's serum and in a growth medium without serum. Comparable growth rates were achieved with serum collected 6 days and 1 day before the exposure. Three days after the exposure some inhibition of S. aureus growth was evident. Serum collected 7 and 13 days after TBI inhibited the growth of S. aureus for the first 2 hr

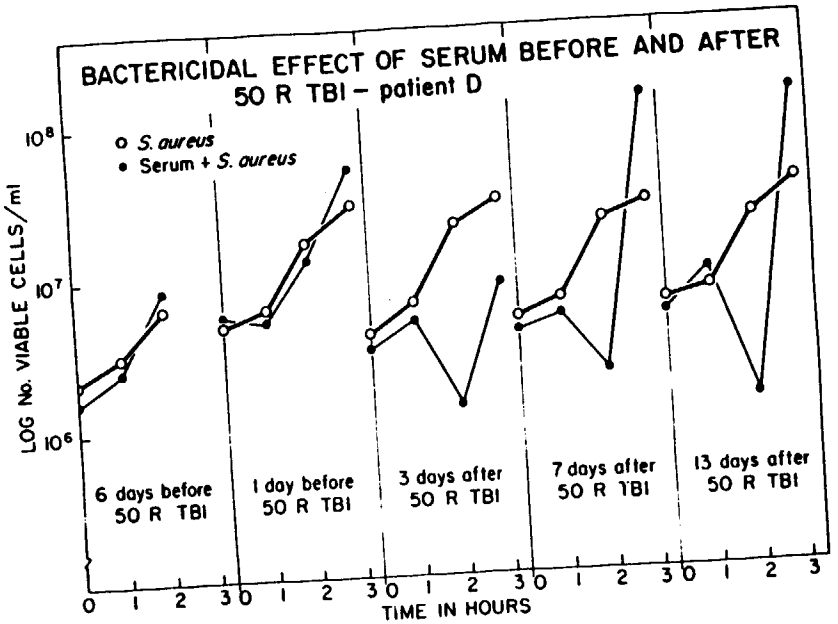

Fig. 32. The effect of serum, collected from a patient before and after he was exposed to 50 R total-body irradiation, on the growth of Staphylococcus aureus.

1027624

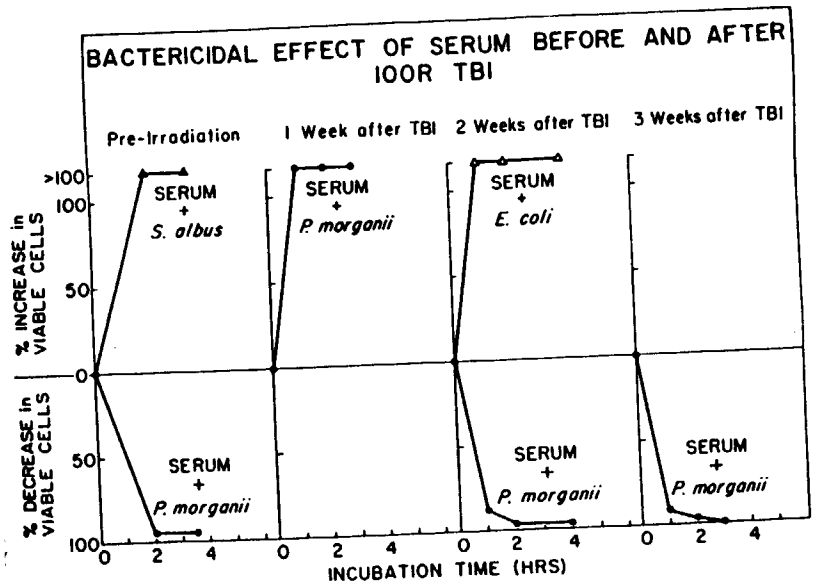

Fig. 33. The effect of serum, collected from a patient before and after his exposure to 100 R total-body irradiation, on the growth of Proteus morganii, Escherichia coli, and Staphylococcus aureus.

of incubation only, and a stimulatory effect was evident at 3 hr (Fig. 32).

Figure 33 shows the effect of 100 R TBI on the bactericidal effect of another patient's serum. Serum collected before the exposure had a pronounced bactericidal effect against Proteus morganii (isolated from the patient's urine). Serum collected 1 week after irradiation did not manifest any bactericidal effect against P. morganii, but activity against this organism was evident in serum collected in the second and third weeks after exposure. Escherichia coli, which was the predominant coliform in the patient's stool, was not inhibited by a serum sample that readily killed P. morganii.

These studies on a very few patients are preliminary. Many more patients, exposed to various doses of total-body irradiation, will have to be studied so that valid comparisons of radiation effects can be made. We anticipate that further studies on these important parameters will allow for a more meaningful explanation of, and prophylaxis for, postradiation infections.

During the year we had the opportunity to perform studies on

patients exposed in a radiation accident. These results will be reported later.

REFERENCES

1. Zubrzycki, L. and Spaulding, E. H. Studies on the stability of the normal human fecal flora. J Bacteriol 83, 968-974, 1962.

2. Wilson, G. S. and Miles, A. A. Topley and Wilson's Principles of Bacteriology and Immunity, Vol. 2. 5th ed. Williams and Wilkins Co., Baltimore, 1955, pp. 2464-2466.

3. Kraus, F. W. and Gaston, C. Individual constancy of numbers among oral flora. J Bacteriol 71, 703-707, 1956.

4. Sears, H. J., Brownlee, I., and Uchiyama, J. K. Persistence of individual strains of Escherichia coli in the intestinal tract of man. J Bacteriol 59: 293-301, 1950.

5. Fishman, M. and Shechmeister, I. L. The effect of ionizing radiation on phagocytosis and the bactericidal power of the blood. II. The effect of radiation on ingestion and digestion of bacteria. J Exp Med 101: 275-290, 1955.

6. Marcus, S. and Donaldson, D. M. Suppression of normal bactericidal action of rabbit serum following whole body X-irradiation. Proc Soc Exp Biol Med 83: 184-187, 1953.

Decreased Sodium-24 Excretion in Rat GI Syndrome After 1200-Rad Fission Neutron Exposure

C. C. Lushbaugh and W. D. Gibbs

Three groups of rats were exposed to fission neutrons from an unclad criticality assembly.* Two groups received 100 rads and one group 1200 rads. All rats exposed to 1200 rads (≈3600 rem?) died between 68 and 75 hr after exposure and had extensive mucosal denudation of the small intestine. One 100-rad group was allowed food and water ad lib while the other was pair fed with the 1200-rad group. The

* Exposures were made by John A. Auxier and John W. Poston, Health Physics Division, Oak Ridge National Laboratory.

1027625

rats in all groups were whole-body counted and individual retention curves were determined for neutron-activated ^{24}Na. When all 1200-rad rats were dead, the others were killed and residual ^{24}Na distribution in gastrointestinal tract, liver, and the rest of the body in all animals was assayed. No significantly different loss in body weight occurred in the 1200-rad rats in comparison with the 100-rad pair-fed controls.

Both these groups lost only 20% of their neutron-induced ^{24}Na activity while the 100-rad group fed ad lib lost 50%. Since there was no chance for any significant quantity of nonradioactive sodium to be excreted before equilibrium was reached ($^{24}Na/^{23}Na$ specific activity was instantly and uniformly determined by the neutron dose) death from the GI syndrome in these animals could not be attributed to electrolyte loss. Since previous studies by others point toward electrolyte loss as the mode of death in the GI syndrome, we attempted to resolve these discrepant results by studying the distribution of sodium in the organs of rats irradiated with 3000 rads of ^{60}Co.

Groups were killed at three successive daily intervals after radiation exposure, autopsied, and organ aliquots were then exposed to fission neutrons in the ORNL research reactor. The results of this experiment using neutron activation of tissue sodium show that remarkable shifts in interstitial electrolytes occur with time after a 3000-rad radiation dose. At the expected time of death with this dose (3+ days), most of the organs (Fig. 34) showed increase in sodium content while the heart,

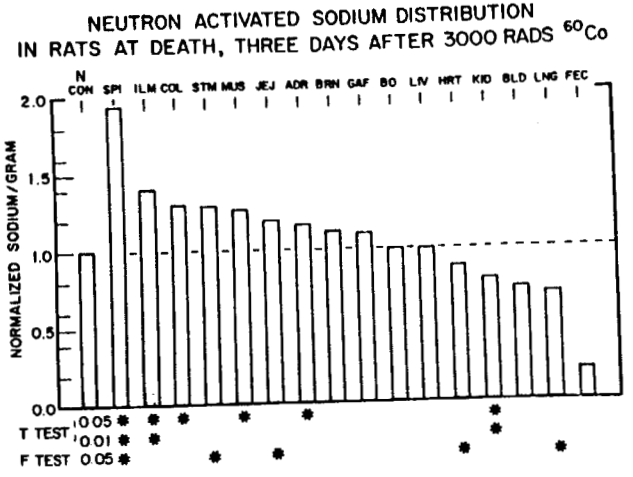

Fig. 34. Bar graph of the mean changes found in sodium content of all organs of all 3000-rad exposed rats, showing tests and levels of statistical significance of the data.

kidney, lungs, blood, and fecal fluid showed electrolyte loss. Since our previous studies show that no significant whole-body loss occurs, the loss from these organs and blood must be presumed to be a loss to these other organs resulting in interstitial and blood electrolyte levels incompatible with life.

Autoradiographic Confirmation of Stimulated Lipid Metabolism in Radiation Damaged Rat Bone Marrow

Gretchen L. Humason, Fred Snyder, Edgar Cress, and C. C. Lushbaugh

Radiation exposure causes such deleterious effects as mitotic arrest, atrophy, degeneration, and necrosis in radiosensitive tissues. At levels of exposure where repair occurs, histopathologic evidence of hyperplasia and regeneration is found among the cells damaged by the radiation. Compensatory regeneration, i.e., hyperplasia in a tissue undamaged by radiation exposure, to make up for the damage to another is not seen except in the response of irradiated fat cells to irradiation damage of the bone marrow.

In the normal rat few fat cells can be found histologically in the marrow of the femur, but immediately after irradiation, as the erythropoietic and myelopoietic cells decrease in number, fat cells appear and increase in size. They fill the spaces made available by loss of the hematopoietic tissue. At this time triglyceride biosynthesis becomes the main pathway for fatty acid metabolism in the marrow[1,2,3] and can be detected biochemically before replacement of hemopoietic cells by adipose cells becomes grossly evident.[4] The small adipose cells in irradiated marrow that undergo this change can be separated from large mature fat cells by sedimentation.[3] Their size suggests that they are new adipose cells arising from differentiation of precursor fat cells.[5]

Such cells in rat marrow might be identifiable microscopically when triglyceride synthesis is increased, and incorporation of ^{3}H-fatty acids into such cells would occur.

A total of 45 female and 15 male Carworth Farms Nelson-strain rats weighing approximately 200 grams were exposed to 800 R total-body irradiation (^{137}Cs) under conditions similar to those already described in detail.[4] Nine females and 3 males of the same strain served as controls. Animals were killed at various times after irradiation; 24 hr before killing, all rats were given either palmitic-9, 10, ^{-3}H acid (500 microcuries in corn oil), or stearic-9, 10, ^{-3}H acid (500 microcuries in corn oil) by oral intubation. Bone marrow, perirenal fat, and epididymal fat, removed immediately after killing the rats, were

1027b2b

placed in 10% formalin for histologic and autoradiographic study.

These studies to date show that both labeled fatty acids are actively incorporated into small cells recognizable as adipose cells because of stainable (oil red 0) fat content. Attempts to detect the origin of this cell with the use of the ^{3}H-fatty acid tracer, however, have not been successful. In irradiated marrows immediately after exposure, before microscopic evidence of damage is present, no cell contains sufficient ^{3}H to produce silver grains to mark it as the precursor cell. At this time only a few small cells are stainable for fat. As radiation atrophy proceeds, fat within cells becomes increasingly obvious. Figure 35 shows fat cells of different sizes that have developed in irradiated rat marrow by the seventh day. Large and small fat cells have an even, diffuse distribution of the label. No cells have a higher concentration than others indicating that at the individual cellular level fat synthesis from labeled fatty acid has been uniform over the observation period. The labeled fatty acids were not detected in the nonadipose tissue.

These studies confirm the observation that bone marrow irradiation

Fig. 35. *Photomicrograph (X1100) of autoradiogram (exposed 21 days) of a frozen section of rat bone marrow seven days after TBI of 900 R with 250 kvp X rays. The grains in the emulsion over the fat cells locate the incorporated ^{3}H-palmitic acid.*

results in intracellular fat synthesis in the marrow at a rapid, uniform rate. Further attempts are being made to recognize cells at earlier stages of this synthesis in order to locate and define the appearance of this quiescent, preadipose stage.

REFERENCES

1. Snyder, F. Triglyceride biosynthesis in irradiated bone marrow. Radiat Res 27, 375-383, 1966.

2. Snyder, F. and Wright, R. Effect of localized irradiation on the metabolism of bone marrow lipids. Radiat Res 25, 417-422, 1965.

3. Pfleger, R. C. and Snyder, F. Lipid turnover in an isolated population of irradiated bone marrow cells. Radiat Res 30, 325-328, 1967.

4. Snyder, F. and Cress, E. A. Bone marrow lipids in rats exposed to total-body irradiation. Radiat Res 19, 129-141, 1963.

5. Snyder, F. Scope and orientation of the lipid project. In: USAEC Report ORINS-53, 1965. pp. 9-12.

Evaluation of Leukocyte Survival in vitro by Cytochemical Staining and Autoradiography

Jerry D. Hunter, Martha L. Clevenger, and Francis A. Goswitz*

This study evaluated the use of cytochemical vital staining and autoradiography as indicators of cell viability after leukocytes were cultured in vitro. Hypothetically, a viable cell has normal membrane permeability and is able to exclude such vital dyes as trypan blue and nigrosin as well as trypan blue mixed with cytotoxic agents, eosin, or sodium desoxycholate (DOC). Thus, only "dead" cells become stained.[1]

Venous blood leukocytes were obtained from normal patients as well as those with chronic myelocytic leukemia (CML) and chronic lymphocytic leukemia (CLL). Leukocytes were isolated and incubated in Difco Culture Medium 199 with only penicillin-streptomycin added. At 24-hr intervals over a 3-day period, culture volumes were harvested by centrifugation and resuspended in 0.05 g of dye in 100 ml physiologic

* Research Participant, University of Texas, El Paso.

1027627

saline. Cells showing uptake of stain and "smudges," cells with disrupted plasma and nuclear membranes, were included in counting the total cells within the hemocytometer.

The percentage of stained cells of normal and CML cultures increas with time (Table 6). Trypan blue plus DOC increased the percentage of stained CML cells from an initial 24-hr average of 12% to a final averag at 72 hr of 60%. None of the vital stains showed any significant differen between the percentage stained of normal and CML leukocytes nor did stain intensity vary. In contrast, CLL leukocytes remained unchanged in the percentage stained. Cell smudging was especially characteristic of the 24- and 48-hr normal and CML cultures in trypan blue alone, yet these smudges did not usually stain. Sodium desoxycholate inhibited thi autolytic process, which theoretically is due to an increase in the permeability of the granulocytic lysosomes whose enzymes rapidly hydroly the cell contents.[2] Such rapid autolysis cannot occur in the bulk cultur because these total cell populations showed little decline over 72 hr while autolysis destroys most of the granulocytes in a hemocytometer within 10 to 12 min. Smudging in CLL lymphocytes over a 3-day period showed no remarkable increase, yet the smudges that were observed stained intensely (unlike the granulocytes) with trypan blue.

Lymphocytes of CLL in similar Medium 199 cultures were exposed to 600 R ^{137}Cs gamma irradiation, and their vital staining reactions were compared with nonirradiated (control) CLL cultures. Such treatment should lead to a decrease in survival of irradiated lymphocytes[3] and serve to test the hypothesis that vital stain exclusion can be used to evaluate viability. The irradiated culture population declined from an initial 24-hr postirradiation count of 2.25×10^6 cells/ml culture to 1.71×10^6 cells/ml 9 days after exposure, while the nonirradiated population did not significantly change during this time from 2.70×10^6 cells/ml (Table 7). Use of trypan blue and trypan blue with eosin or DOC indicated a moderate increase in the percentage of stained cells of the irradiated culture over a 9-day period while the controls were stable. If an increase in smudging of cells were used as the criterion of viability, a very significant increase with time was noted in the irradiated cultures especially with use of trypan blue plus eosin or DOC These smudges are further characterized by uptake of the trypan blue stain. Although a slight increase in smudging occurred in control cells this was significantly less than in the irradiated population. Morphologic deterioration evaluated by smudging was a more reliable standard for cell death than any staining reaction alone.

Incorporation of tritiated thymidine into leukocytes to evaluate DNA synthesis in CML, CLL, and normal cells, was assayed by use of liquid emulsion autoradiography. No ^3H-TdR uptake occurred in any culture from CLL or normal blood as expected (Table 8). In contrast, a very significant ^3H-TdR incorporation (2 to 7% of total) was noted in three of four CML cultures in the first 24 hr. Incorporation declined v increasing culture age until no uptake occurred in three of four patients after 72 hr. Although ^3H-TdR incorporation declined with age, a sig-

10216128

TABLE 6

Averages of % Stained Leucocytes and % Smudged
At Various Ages of In vitro Cultures Using Cytochemical Stains

Type of Vital Stain	Pathology	Culture Age at Time of Assays					
		24 hours		48 hours		72 hours	
		% Stained	%Smudged	% Stained	% Smudged	% Stained	%Smudged
Trypan Blue 0.05%	Normal*	10%	32%	16%	31%	27%	12%
	CML†	7	41	12	33	23	25
	CLL†	7	7	11	8	11	11
Nigrosin 0.05%	Normal	7	-	10	-	17	-
	CML	6	-	7	-	6	-
Eosin 0.05% + Trypan Blue 0.05%	Normal	14	-	14	-	27	-
	CML	6	-	15	-	17	-
DOC + Trypan Blue 0.05%	Normal	16	8	30	16	62	19
	CML	12	13	38	13	60	22
	CLL	13	7	14	10	10	17

*Average of 5 individuals in each stain.

†Average of 4 individuals in each stain.

TABLE 7

Effects of Cs^{137} Gamma Irradiation on the Average % Stained CLL Lymphocytes and Smudges/mm^3 Culture Volume at Selected Post-Irradiation Ages

Type of Vital Stain	Treatment	Culture Age - Days After Cs^{137} Exposure - 600R					
		1 Day		6 Days		9 Days	
		% Stained	Smudges	% Stained	Smudges	% Stained	Smudges
Trypan Blue	Irrad.	4%	320/mm^3	6%	480/mm^3	10%	1600/mm^3
	Control	3	320	4	800	5	640
Nigrosin	Irrad.	3	160	4	480	2	1120
	Control	2	0	3	640	3	320
Eosin and Trypan Blue	Irrad.	2	480	9	1920	8	2720
	Control	4	480	3	640	4	960
DOC and Trypan Blue	Irrad.	8	640	25	1440	15	1760
	Control	7	640	7	640	7	800
Population Count: Cells/ c.c. culture	Irrad.	2.25×10^6 cells/ml				1.7×10^6 cells/ml	
	Control	2.70×10^6 cells/ml				2.7×10^6 cells/ml	

TABLE 8

^{3}H-TdR Incorporation and % Smudging by CML and CLL Leukocytes Determined by Autoradiography on Short-Term Cultures, Medium 199 Only

Patient No.	Pathology	Culture Age and % WBC Labelled*		Culture Age and % of Total Cells Smudged	
		24 hours	72 hours	24 hours	72 hours
1	CML	7.0%	0%	1%	29%
2	CML	0%	0%	5%	28%
3	CML	2.0%	0%	2%	23%
4	CML	4.8%	3.2%	0%	6%
1	CLL	0%	0%	5%	3%
2	CLL	0%	0%	3%	0%
3	CLL	0%	0%	0%	4%
	Normal	0%	0%	9%	42%

*Total of 500 cells scored

nificant increase in cell smudging (from 0 to 5% of population at 24 hr to 6 to 29% at 72 hr) was observed. Both phenomena are independent, however, as percentage of smudging always increased regardless of the state of DNA synthesis. Thus, cell membrane deterioration again appears as a more consistent standard to evaluate cell death. Smudging can be induced by trauma involved in the smearing of cells; however, since this same disadvantage occurs at all times of cell harvest, the 6 to 29% increase in smudges of CML autoradiograms must be due to other factors than trauma alone.

In conclusion, the use of vital staining as an indicator of cell viability has definite limitations. Marked variations in percentage of stained cells were noted between the four vital stain preparations studied. There is little evidence to support the use of any one stain as a valid criterion for cell death, which is better evaluated by morphologic examination than by any cytochemical or autoradiographic technique.

REFERENCES

1. Lee, H. and Richards, V. Possible new approach to the evaluation of radiation injury of bone marrow. Nature 212, 1593-1595, 1966.

2. Epstein, L. B. and Stohlman, F., Jr. RNA synthesis in cultures of normal peripheral blood. Blood 24, 69-75, 1964.

3. Schrek, R. In vitro sensitivity of normal human lymphocytes to X-rays and radiomimetic agents. J Lab Clin Med 51, 904-915, 1958.

1027629

Effect of Prednisone on the Total Lipid Content of Leukemic Lymphocytes

Francis A. Goswitz, Fred Snyder, Martha L. Clevenger, and Nelson Stephens

The total lipid content of the blood lymphocyte in chronic lymphocytic leukemia is significantly less than that of normal lymphocytes as was reported last year.[1] Corticosteroids are frequently used in treating this disease as well as other diseases characterized by a proliferation of lymphocytes. Since prednisone usually exerts a lymphocytolytic action[1] in patients who are taking this drug, the changes in the total lipid content of the lymphocytes were investigated.[2]

Table 9 summarizes the data obtained to date. These results

TABLE 9

EFFECTS OF PREDNISONE ON MICROGRAMS TOTAL LIPID/10^7 LYMPHOCYTES

Patient	WBC X 10^3 / mm^3 blood	WBC % Lymphocytes	Before or off Prednisone	During or after Prednisone
A	256	100	80	60
	210	100		
B	21.4	96	130	80
	17.7	78		
C	29	98	120	20
	116	99.5		
D	80	85	150	110
	102	91		
E	138	96.5	220	10
	202	97.5		
			Mean 140 ± Standard Deviation 46	Mean 56 ± Standard Deviation 37

demonstrate that prednisone reduces the total lipid content of lymphocytes in patients with chronic lymphocytic leukemia. The mechanism of action on the lipid composition of these cells is now under investigation.

REFERENCES

1. Goswitz, F. and Snyder, F. Lipid composition of the blood lymphocyte in chronic lymphocytic leukemia. In: USAEC Report ORAU-101, 1966, pp. 5-8.

2. Dougherty, T. F., Berliner, M. L., and Berliner, D. L. Hormonal control of lymphocyte production and destruction. Progr Hemat 3, 155, 1962.

Separation of Viable Lymphocytes From Normal Blood

Martha L. Clevenger and Francis A. Goswitz

Since the lymphocyte in normal blood comprises only 0.06 to 0.1% of the total number of cells in the circulation, the problem in isolating these cells in pure quantities for biochemical analyses or in vitro studies is apparent. A simple and efficient method involving the basic techniques of filtration, centrifugation, and sedimentation for cell separation was developed in our laboratory for the collection of an almost pure population of viable human lymphocytes from venous blood.

After venipuncture 200 ml blood anticoagulated with sodium heparin (phenol free) is filtered through a sterile Leuko-Pak filter (Fenwal Laboratories, Morton Grove, Illinois).[1] It is important that all glassware used be washed in Microsolv (Microbiological Associate, Bethesda, Maryland). The following procedure is then performed upon the filtrate:

1) Centrifuge the filtrated blood at 850 rpm (150 g) for 15 min at 26° C.

2) Remove plasma, buffy coat, and top layer of red cells; mix these components well and centrifuge at 500 rpm (50 g) for 10 min.

3) Remove and save the plasma. Remove buffy coat with a small amount of plasma and mix well.

4) Transfer buffy coat to Wintrobe hematocrit tubes and sediment approximately 1 to 1½ hr at 37° C.

5) Centrifuge plasma from Step 3 at 500 rpm (50 g) for 10 min.

6) Remove and discard supernatant plasma. Transfer the remaining cells to Wintrobe tubes and sediment 1 to 1½ hr at 37° C.

7) Centrifuge all Wintrobe tubes at 500 rpm (50 g) for 10 min. To separate lymphocytes from some healthy persons, it may be necessary to combine buffy coats from each Wintrobe tube sedimenting an additional 30 min.

8) Remove and discard the supernatant plasma. Transfer WBC to 37° C culture medium (Eagle's). Determine the number of WBC and RBC/mm^3 medium. Make smear of WBC concentrate (Fig. 36) and perform a differential count. Calculate percentage of yield, percentage of RBC contamination, and percentage purity of all cells present in concentrate.[2]

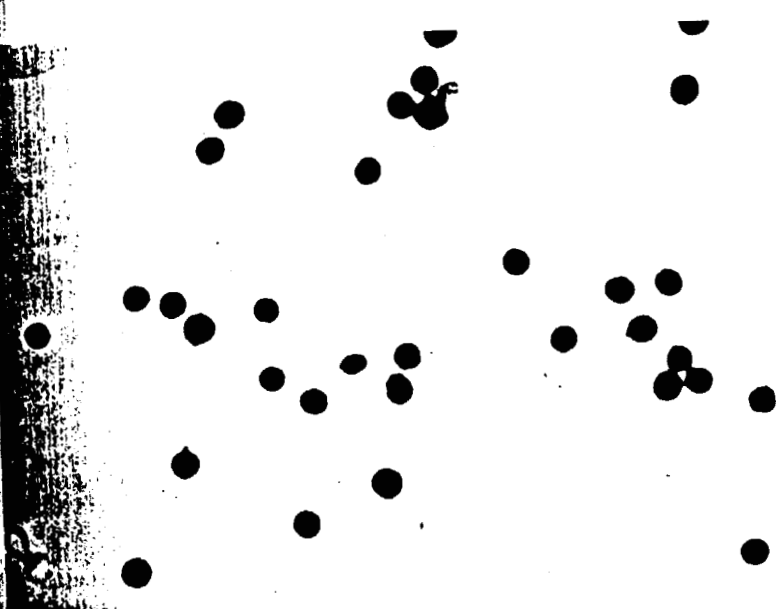

Fig. 36. *Photomicrograph of the lymphocyte layer smear. Magnification 400 x.*

1027630

The resulting lymphocyte suspension is platelet free with yields of approximately 15% and a purity of 85-90%. Granulocyte contamination is less than 1% and erythrocyte contamination is about 10%.

REFERENCES

1. Greenwalt, T. J., Gajewski, M., and McKenna, J. L. A new method for preparing buffy coat poor blood. Transfusion 2, 221-229, 1962.

2. Jago, M. A simple method for the separation of living lymphocytes from normal human blood. Brit J Haemat 2, 439-444, 1956.

Abnormal Lymphocyte Volume Distribution Typical of Chronic Lymphocytic Leukemia

Dorothy H. Lushbaugh, Francis A. Goswitz, Martha L. Clevenger, and C. C. Lushbaugh

The circulating lymphocyte of chronic lymphocytic leukemia is smaller than normal and remarkably uniform. Few explanations for this commonplace observation have been offered and none are generally accepted. The fact that most malignant cells are larger than their normal prototype or have increased nuclear to cytoplasmic ratios (usually because of increased nuclear volume) suggests that the typical small lymphocyte in CLL may not be malignant in the usual sense, but may be an incompetent cell incapable of functional development and, therefore, one that does not increase in size as it circulates.

In a previous preliminary report[1] we described an electronic method with a modified Coulter Counter apparatus for studying the volume distribution of lymphocytes from blood and lymph. We concluded from that study of normal human thoracic duct lymphocytes and CLL blood lymphocytes that the modal size of these two kinds of lymphocytes was not significantly different. Since then we have determined the cell volume distributions in concentrated samples of lymphocytes from the peripheral blood from 13 well persons and 15 patients with CLL and have found significant ($P>0.01$) differences in the circulating lymphocyte populations of these two groups of people, as shown in Table 10 and Fig. 37. Comparison of these results with those we have previously reported shows that the normal blood lymphocyte population has a larger modal and mean size than normal thoracic duct lymphocytes in man. We also found that when the number of leukemic lymphocytes in the peripheral blood is diminished by therapy, the volume distribution

1027631

TABLE 10

Comparison of Some Parameters of Normal and Leukemic Blood Lymphocyte Volumes

Population Parameter	Lymphocytes of Normal	CLL
	Channel #	Channel #
X Modal size	50.4 ± 2.2	41.3 ± 5.3
X Mean size	54.6 ± 2.5	47.0 ± 5.1
X Standard deviation	8.58± 0.83	8.20± 2.1*
X Skewness	0.093 ± 0.036	0.219± 0.097
	%	%
X Incidence of modal size F (max.)	3.76	6.73
X Coefficient of Variance	0.17 ± 0.01	0.20 ± 0.04*

*No significant difference by t test.

shifts toward the larger normal size. Since these 15 patients were in different stages of therapy, their modal and mean lymphocyte sizes varied more than these parameters in the normal persons. In Fig. 37 we compare the lymphocyte volume distribution polygons of the average of all normal blood samples with that of the patient whose blood smear was most typical microscopically of chronic lymphocytic leukemia (156,000 WBC/cmm; 97% lymphs). Although the normal and abnormal lymphocyte size distributions overlap because cells of almost all sizes are common to both, the difference in modal (or commonest) size is quite apparent (~ $170\mu^3$ vs. $245\mu^3$) because of its greater frequency. When these typical volumes are transposed to the geometric measurements of spherical cells of that size, the modal diameters would be 6.6 to 6.9 microns for the leukemic lymphocyte and 7.4 to 7.8 microns for the normal lymphocyte, numbers that agree well with those commonly accepted in hematology. Flattening and stretching these cells in preparation of blood films increase the measurements and their differences microscopically and make normal lymphocyte cytoplasm appear much more abundant than that of the leukemic cell. We are

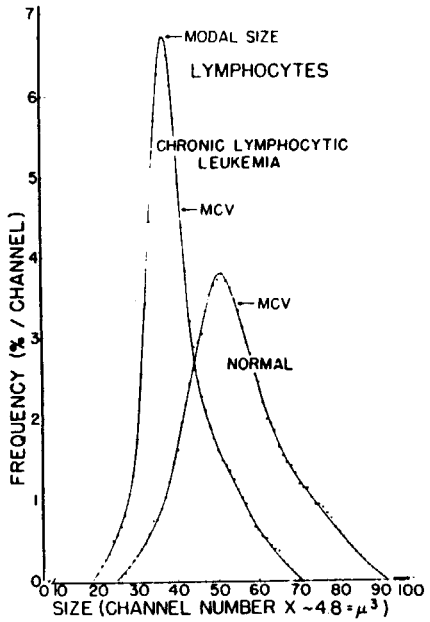

Fig. 37. Comparison of the lymphocyte volume distribution polygon of a typical chronic lymphatic leukemia with the average polygon for all normal samples studied.

now trying to quantitate this difference by removing the cytoplasm and then sizing the leukemic and normal lymphocytic nuclei.

REFERENCE

1. Lushbaugh, D. H., Edwards, C. L., and Lushbaugh, C. C. Absolute leukocyte differential counts by rapid electronic sizing. In: USAEC Report ORAU-101, 1966, pp. 158-160.

Some Effects of Electrical Fields on Red Blood Cells

A. Ur, C. C. Lushbaugh, and Dorothy H. Lushbaugh

When using the Coulter Counter in conjunction with a multichannel pulse-height analyzer, some investigators obtain a bimodal frequency distribution curve of red blood cells (RBC) while others obtain a uni-

1027632

modal one. This disagreement prompted an investigation of some physical factors that may affect RBC size in electronic particle-sizing systems to determine whether these factors could be responsible for the different kinds of size distributions of normal RBC. Three groups of experiments were done: in the first we studied the effect of intensity of aperture current, exposure time, and cell concentration upon the size distribution of normal RBC. In the second, we observed microscopically the effects of electrical fields on RBC morphology. In the third some of the parameters of electrical hemolysis were studied in the hemolyzometer previously described.[1-3]

The effects of various aperture currents upon the frequency distribution are shown in Fig. 38. Similar alterations in the curve

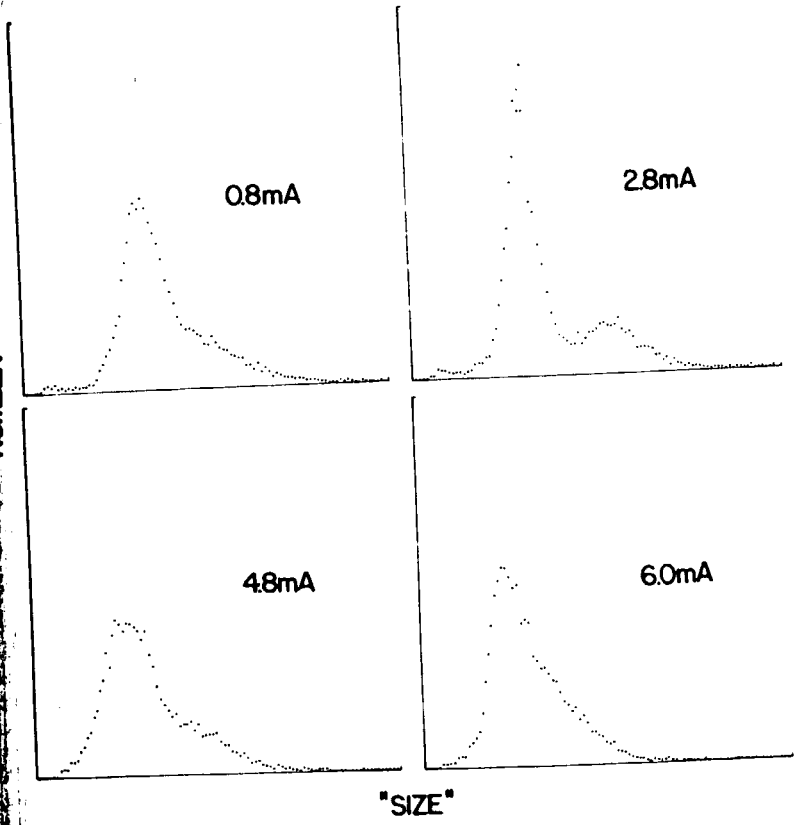

Fig. 38. Effects of various aperture currents upon the frequency distribution of red cell sizes.

could be produced by prolonged exposure (>30 min) to high aperture currents and by 10-fold increase in the RBC concentration being sized. Microscopically, RBC adjacent to the electrode showed changes that led to hemolysis after a latent period related in length to current intensity. Similarly the in vitro hemolyzometer experiments showed (Fig. 39) that, although hemolysis can be produced by electrical fields, large voltages are necessary. The latent period before hemolysis begins (-o-) and the time until hemolysis is complete (-x-) cannot be reduced even by extremely high currents to approximate the short time involved in determining size distribution curves electronically.

These experiments along with others on pH and chemical changes and physical factors, such as linear flow, velocity, coincident passage, etc., appear to explain the minor variations between the RBC frequency distributions obtained by different investigators and the variation obtained by repeated sizing of the same sample over long periods of time. The skewed bimodal RBC size distribution found with currents in the vicinity of 2.8 mA, however, could not be explained by these observations. Experiments, in progress, show that chemical fixation of the

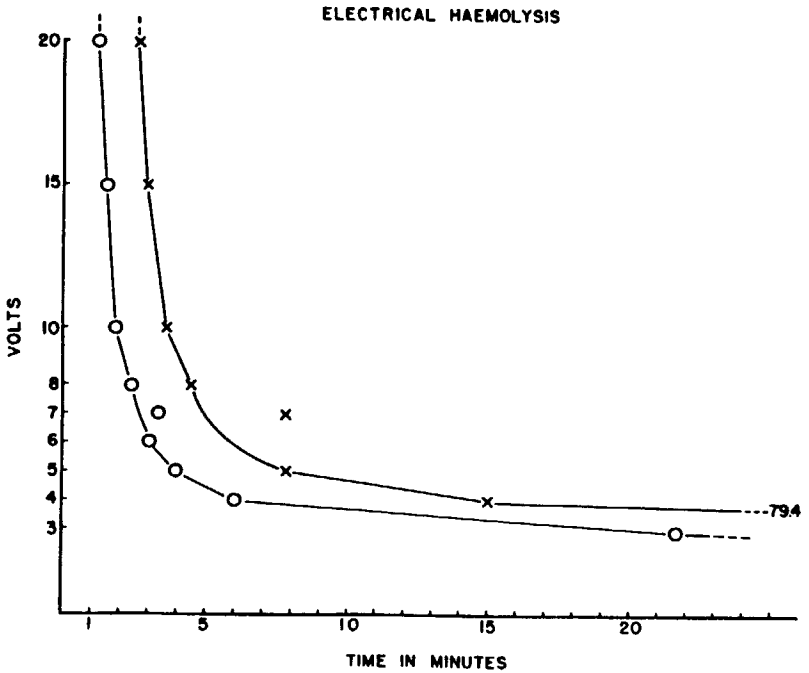

Fig. 39. Effects of time and voltage of red cell hemolysis. -O- represents beginning hemolysis; -X- represents completion of hemolysis.

1027633

RBC membrane can prevent the bimodal distribution even when electrical currents are used that usually cause it to appear. Clinical observations also show that, in some anemias resulting from erythroblastic failure, a bimodal RBC distribution cannot be obtained under any condition or setting. We believe, therefore, that the normal RBC vary among themselves in some structural or physiologic way, not necessarily size, that makes the bimodal distribution obtainable under rigidly controlled conditions of the electronic system. The use of aperture currents within the range that displays the bimodal distribution seems warranted in diagnostic practice because the bimodal RBC size distribution enhances the discrimination of the system for detection of different RBC populations.

REFERENCES

1. Morris, A. C., Jr., Lushbaugh, C. C., Lushbaugh, D. H., and Corley, R. H. A rapid electronic method for measuring red-cell fragility in hemolytic systems. In: USAEC Report ORINS-53, 1965, pp. 149-154.

2. Webb, A. M. and Lushbaugh, C. C. Automated RBC osmotic fragility measurements using a linear gradient device. In: USAEC Report ORAU-101, 1966, pp. 161-164.

3. Morris, A. C., Jr., and Lushbaugh, C. C. Micro osmotic fragility system for the nonautomated laboratory. In: USAEC Report ORAU-101, 1966, pp. 164-166.

The Origin of Acid Resistant Erythrocytes in Prenatal Mice

Gretchen L. Humason and C. C. Lushbaugh

Under certain pathologic conditions that stress RBC production, peripheral blood erythrocytes occur that are resistant to acid hemolysis. These RBC can be demonstrated as in Fig. 40 by protein staining using Betke's technique.[1] Because this resistance to elution by acid shows some correlation with the presence of a hemoglobin resistant to alkali denaturation and electrophoretically identical with fetal hemoglobin (Hb-F) this phenomenon has been assumed to be due to either (1) a reversion from hemoglobin A (Hb-A) to Hb-F production by adult erythroblasts receiving mRNA transcription of a part of the DNA molecule normally covered up; or (2) the release of a dormant population of fetal erythroblastic stem cells incapable of producing Hb-A.

In searching for an animal model to use to find experimental evidence to support one of these explanations of this poorly understood

Fig. 40. Photomicrograph (X1200) of blood smear from a patient with advanced Hodgkin's disease after elution with acid saline (3.5 pH) showing (arrow) an RBC that resisted hemolysis. Hemoglobin has been eluted by the acid from the other RBC to varying degrees. (Hematoxylin and eosin stain.)

phenomenon (often observed in human leukemia), we found that acid-resistant ("Betke positive") RBC were present in the blood of newborn mice even though, unlike man, the mouse does not produce Hb-F. These positive RBC are macrocytic and short-lived and are found only rarely in the blood of mice after the tenth postpartum day. Smears made, however, of the livers and yolk sacs of fetal mice, 10 to 18 days gestational age, revealed that mouse hepatic erythroblasts manufacture a hemoglobin that can be eluted by washing with saline buffered at 3.5 pH (typical of Hb-A) while yolk-sac megaloblasts contain a hemoglobin that reacts like Hb-F when we use Betke's technique as shown in Fig. 41. Others[2] have shown that at this time mouse blood contains "embryonic" hemoglobin ($Hb\text{-}E_{I, II, III}$) and Hb-A but no Hb-F. Russell[3] found embryonic hemoglobin in the nucleated cells of centrifuged blood of prenatal mice and assumed it was derived from the primitive yolk-sac blood islands. Our cytologic and histologic studies demonstrate the unequivocal yolk-sac origin of these nucleated megaloblastic RBC shown in Fig. 41, and show that Hb-F content is not necessary for so-called

1027634

Fig. 41. Photomicrograph (X1100) of blood of a 14-day-old prenatal mouse showing retention of hemoglobin by nucleated megaloblasts of yolk-sac origin, and loss of hemoglobin from erythrocytes (hepatic origin) after acid elution. (Ferric ferricyanide reduction stain.)

acid-resistant RBC as has been assumed up until now. Embryonic hemoglobin (Hb-E) also causes it.

These observations suggest a more tenable explanation for the Betke phenomenon: acid elution may be determined by the presence of beta chains as in Hb-A, so that, when beta chains are absent and gamma chains (Hb-F) and X, Y, or Z chains (Hb-E) are present, acid elution of such hemoglobin is prevented. Beta chains of globin might hypothetically be malproduced in disease and hemoglobin solubility so altered that the RBC react as though beta chains in Hb-A were not present. Such cells among RBC in leukemia might then be the result of abnormal beta-chain production due to mRNA error resulting from chromosome damage in the disease process or its chemotherapy. This explanation would not require the assumption of surviving embryonic and fetal erythroblastic clones that could be released in disease and produce abnormal hemoglobin. Such clones have not been demonstrated in normal adults, although

they do exist in fetal hemoglobin disease. Our suggested alternative explanation is being tested experimentally.

REFERENCES

1. Kleihauer, E., Braun, H., and Betke, K. Demonstration von fetalem Hamoglobin in den Erythrocyten eines Blutausstrichs. Klin Wchnschr 35, 637-638, 1957.

2. Fantoni, A., Bank, A., and Marks, P. A. Globin composition and synthesis of hemoglobins in developing fetal mice erythroid cells. Science 157, 1327-1329, 1967.

3. Craig, M. L. and Russell, E. S. A development change in hemoglobins correlated with an embryonic red cell population in the mouse. Develop Biol 10, 191-201, 1964.

The Radiosensitivity of Rat Bone-Marrow Cells

Frank V. Comas

The radiosensitivity of rat bone-marrow cells was determined by means of the spleen colony technique, which was developed for rats at ORAU last year.[1]

Groups of rats were given 1400 rads total-body irradiation and immediately injected intravenously with rat bone-marrow cells from irradiated donors. The donors received total-body irradiation doses ranging from 100 to 500 rads. The bone-marrow cells from the donor animals were obtained from the femora. The cells were suspended and diluted to a cell concentration ranging from 4 to 100 x 10^5 cells per 0.5 milliliter, depending upon the radiation dose given to the donor rats.

The recipient animals were killed 12 days after irradiation and bone-marrow injection, and the spleen colonies were counted. Only those colonies measuring over 1 mm in diameter were scored. For the computation of the survival curve parameters, the data were analyzed with the assumption that the relation between number of spleen colonies per 10^5 cells (Y), and radiation dose (X) is given by the expression $Y = \mu [1 - (1 - e^{-\beta X})^n]$ where μ is the number of spleen colonies for zero radiation dose, β is the slope of the exponential part of the curve, and n is the extrapolation number. (Details of these calculations are given by Edward Frome on page 67 of this report.)

1027635

Two separate experiments were performed that yielded similar results for the main parameter under investigation: D_o or $1/\beta$ (Table 11), that amount of radiation that reduces survival to 37% of the initial value. A graphic representation of Exp. 2 is shown in Fig. 42. Apparently the D_o of rat bone marrow is similar to that of

TABLE 11

Survival Curve Parameters

of Irradiated Rat Bone-Marrow Cells

	Spleen Colonies/ Spleen per 10^5 Cells (No irradiation)	D_o (rads)	Extrapolation Number
Experiment 1	4.0 (3.4-4.6) (a)	92 (94-97)	6.8 (3.0-10.7)
Experiment 2	5.4 (3.7-7.1)	100 (92-111)	3.3 (1.3-5.3)
Combined		96 (94-98)	

(a) Figures in parenthesis are 95% confidence limits

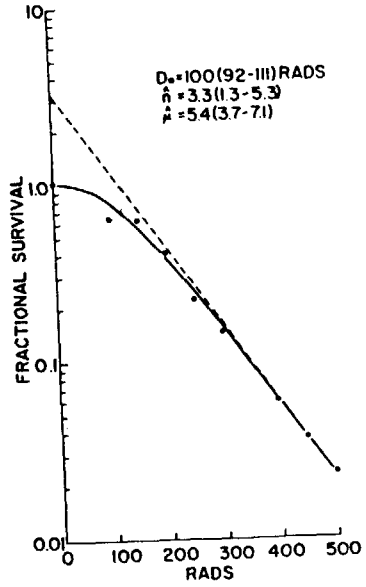

42. The radiosensitivity curve for rat bone-marrow cells: μ is the calculated number of spleen colonies per 10^5 cells in nonirradiated animals; n is the extrapolation number. Figures in parentheses are 95% confidence limits.

the mouse, but the extrapolation number is probably higher for rats than for mice.[2]

REFERENCES

1. Comas, F. V. and Byrd, B. L. Hemopoietic spleen colonies in the rat. Radiat Res 32, 355-365, 1967.

2. Till, J. E. and McCulloch, E. A. A direct measurement of the radiation sensitivity of normal mouse bone marrow cells. Radiat Res 14, 213-222, 1961.

Effect of Phytohemagglutinin on Endogenous Spleen Colonies in Mice

*Frank V. Comas and Bismark Lozzio**

Phytohemagglutinin (PHA) has a mitogenic effect on lymphoid cells and possibly on other types of cells as well. In this preliminary experiment, we tested the effects of the drug on the reproductive capabilities of hemopoietic cells in vivo.

Groups of C3H mice were given 800 rads total-body irradiation, with ^{137}Cs radiation at 3.5 rads/min. One group received PHA intraperitoneally 2 days before irradiation, and another group was injected 5 days after irradiation; the dose was 200 mg/kg body weight. The control animals were injected with saline. The surviving animals were killed 10 days after irradiation, and the spleen colonies were counted.

Mice injected with PHA before irradiation had many more spleen colonies than the controls, whereas such an increase was not found in mice receiving PHA 5 days after irradiation (Table 12). The spleen weights of these animals, however, were significantly greater than those of the controls. Histologically the spleen colonies were made up of primitive hemopoietic cells.

The provisional interpretation of these results is as follows: PHA given 5 days after irradiation may have added a further push

* University of Tennessee Memorial Hospital and Research Center, Knoxville, Tennessee.

1027636

TABLE 12

Spleen Weights and Number of Endogenous Spleen Colonies in Mice Given PHA Before and After 800 Rads Total-Body Irradiation

	Number of Mice	Spleen Colonies/Spleen	P (a)	Spleen Weight (mg)	P (a)
Controls	20	3.2	-----	33.8	------
PHA before irradiation	5	20.4	< 0.01	64.8	<0.01
PHA after irradiation	9	3.0	N. S.	42.4	<0.01

(a) Probability that differences between control and experimental groups are due to chance

to the already great mitotic activity of the hemopoietic cells in the spleen clones, as evidenced by the increased weight of the spleen. No new clones would necessarily develop, or if new colonies were formed they might be too small to be seen because only 5 days elapsed between the PHA injection and sacrifice.

The increased number of spleen colonies in animals given PHA before irradiation may also be due to the mitogenic effect of this drug, such that the cellular population at the time of irradiation was about six times greater than that of the controls. What cellular population is involved remains unknown. If only lymphoid cells responded to the drug, one could argue that lymphoid cells may be hemopoietic precursor cells in situations when the need to repopulate the hemopoietic organ is of great urgency, such as after sublethal doses of total-body irradiation.

Maximum Likelihood Estimation of Survival-Curve Parameters

*Edward L. Frome, Frank V. Comas, and J. J. Beauchamp**

In the quantitative investigation of cytologic damage resulting from ionizing radiation, the survival curve has been extensively used in attempting to establish relations between the radiation dose

* Mathematics Division, Oak Ridge National Laboratory.

(X) and the response of the biological system. When the spleen-colony counting method[1] is used to study the radiosensitivity of mammalian cells, the target model[2] provides a good description of cell survival data.[3] The expected number of colony-forming units per 10^5 bone-marrow cells surviving radiation dose X_i is given by

$$P_i = \mu \left[1-(1-e^{-\beta X_i})^{\nu}\right] \qquad (1)$$

where μ = expected number of colony-forming units when X = 0 (control), $\beta = 1/D_o$, and ν is the extrapolation number.

These parameters may be estimated using the maximum likelihood principle. The estimation procedure is based on the assumption that the number of colonies per spleen in the recipient animal will follow a Poisson distribution.

If
n_i = number of animals at dose X_i
m_{ij} = concentration of cells from the animal receiving dose X_i injected into the jth recipient animal
y_{ij} = number of colonies observed in the jth animal at dose X_i
then under the assumption that the y_{ij} are independent Poisson random variables, it follows that the likelihood function is

$$L = \prod_{i=1}^{N} \prod_{j=1}^{n_i} \frac{e^{-m_{ij}P_i} (m_{ij}P_i)^{y_{ij}}}{y_{ij}!} . \qquad (2)$$

Let $\theta_1 = \mu$, $\theta_2 = \beta$, $\theta_3 = \nu$, and $\underline{\theta}$ equal the vector of parameters, then the maximum likelihood estimator of $\underline{\theta}$ is given by the solution of the following system of equations

$$\frac{\partial \ln L}{\partial \underline{\theta}} = \left[\sum_i \frac{\partial P_i}{\partial \theta_\ell} \left\{\frac{Y_i}{P_i} - M_i\right\}\right]_{\ell = 1,2,3} = 0 \qquad (3)$$

where $Y_i = \sum_j y_{ij}$ and $M_i = \sum_i m_{ij}$. consider the following weighted sum of squares to be minimized:

$$\phi = \sum_{i=1}^{N} W_i(\underline{\theta}_0) \left(\bar{P}_i - P_i\right)^2 \qquad (4)$$

where $P_i = Y_i/M_i$, $W_i(\underline{\theta}_0) = M_i/P_i(\underline{\theta}_0)$, $P_i(\underline{\theta}_0)$ is equal to

1027637

P_i evaluated at $\underline{\theta}_0$, and $\underline{\theta}_0$ is a vector of initial estimates of the parameters. It can be demonstrated that the iterative weighted least squares procedure just described is equivalent to the solution of the maximum likelihood equations.

The asymptotic variance-covariance matrix of the estimators is given by the inverse of the matrix

$$\left[-E\left(\frac{\partial^2 \ln L}{\partial\theta_\ell \partial\theta_{\ell'}}\right)\right]_{\ell,\ell' = 1,2,3} . \qquad (5)$$

In practice, μ, β, and ν, which appear in the elements of this matrix, are replaced by their estimates in order to obtain estimates of the elements of this matrix.

When the assumption of Poisson variation and the form of the model as expressed by equation (1) are both correct, the statistic

$$\sum_{i=1}^{N} \sum_{j=1}^{n_i} (y_{ij} - m_{ij}\hat{P}_i)^2 / m_{ij}\hat{P}_i \qquad (6)$$

is distributed approximately as X^2 with $\left(\sum_{i=1}^{N} n_i\right) - 3$ degrees of freedom. For the case when m_{ij} is independent of j for each value of i, the X^2 statistic may be partitioned into two independent components to test for heterogeneity of variance and the goodness of fit of the data to the model. With the use of the asymptotic normality of maximum likelihood estimators approximate confidence intervals for the survival-curve parameters may be calculated. An application of this method to some experimental data by Frank V. Comas is found elsewhere in this report, page 67.

REFERENCES

1. Till, J. E. and McCulloch, E. A. A direct measurement of the radiation sensitivity of normal mouse bone marrow cells. Radiat Res 14, 213-222, 1961.

2. Atwood, K. C. and Norman, A. On the interpretation of multi-hit survival curves. Proc Nat Acad Sci 35, 696-709, 1949.

3. Krebs, J. S. The response of erythropoietic stem cells of mice to irradiation with fission neutrons. Radiat Res 31, 796-807, 1967.

Stereologic Quantitation of the Components of Rabbit Marrow

Margaret A. Slaughter, Y. Ito†, Francis A. Goswitz, and Bill Nelson*

A histologic study of rabbit marrow was undertaken in conjunction with a correlation of erythropoiesis and reticuloendothelial function. (See page 128 of this report.) The material studied consisted of 132 specimens of marrow, including particles aspirated through a large needle from the ilium of anesthetized rabbits and autopsy samples from the ilium and the upper, middle, and lower portions of the femur. Histologic sections from 32 specimens were considered to have adequate size and quality for quantitation. These 32 slides were labeled to conceal their identity before independent estimation (by MAS and BN) of the percentage by volume of granulocytes, red-cell precursors, megakaryocytes, miscellaneous cells, erythrocytes, "space," stroma, and fat cells. ("Space" included extracellular fluid and plasma. Stroma included vessel walls and connective tissue components.)

Stereologic quantitation was then applied to 15 of the 32 slides (by MAS), including samples from two untreated controls and from two rabbits before and after treatments to modify marrow function. The quantitation is based on microscopic identification of components at points uniformly distributed over the section, which is assumed to be a plane representative of the tissue.[1] At least 400 points were tallied to reduce statistical error. Artifacts from shrinkage and other distortions are presumed negligible and the percentage of points corresponding to each component is an expression of the volume of that component.

The results of this quantitation from the 15 slides are shown in Fig. 43. The percentage of fat cells in the iliac aspirates of the control rabbits ranged from 34 to 43%, and the other nucleated cells ranged from 20 to 32%. These figures probably are influenced by the aspiration of blood with the particles, and by the tendency for the particles so obtained to have more cohesive stroma and vasculature than the larger marrow samples available at autopsy. Whatever the explanation, the iliac aspirates from two control rabbits (one aspirated bilaterally) had more red cells, stroma, and "space" than did the larger samples of marrow taken from the femur at autopsy. The femoral marrow, especially that from the shaft, had more adiposity (52 to 80%), with other nucleated cells ranging from 15 to 25%.

---

* Student Trainee from Talladega College. Present address: Talladega College, Talladega, Ala.

† Damon Runyon Foundation Fellow from Japan. Present address: Department of Radiology; Research Institute for Tuberculosis, Leprosy, and Cancer; Tohoku University; 62 Kita 4 bancho; Sendai, Japan.

1027638

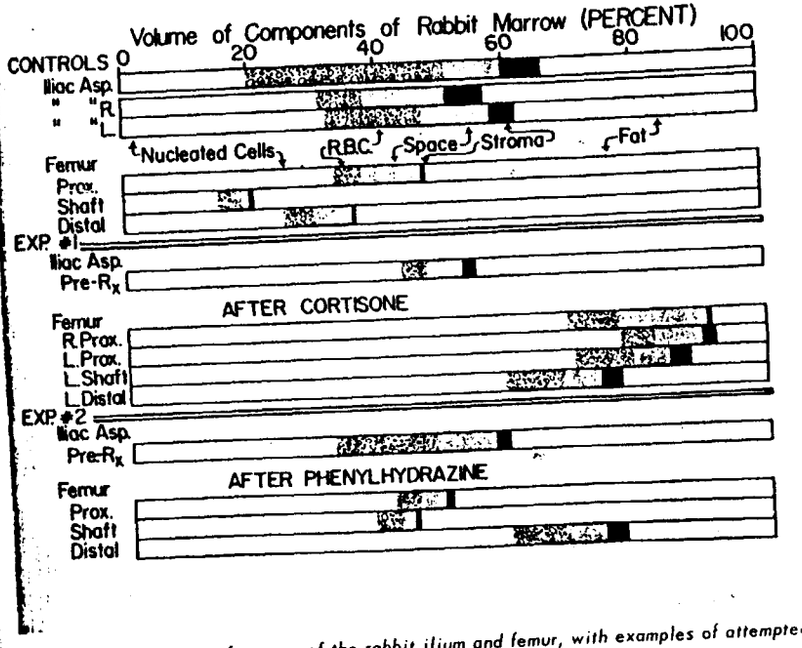

Fig. 43. Composition of marrow of the rabbit ilium and femur, with examples of attempte alteration by cortisone and phenylhydrazine.

The iliac aspirates from two other rabbits prior to treatment (Fig. 43, Exp. 1 and Exp. 2) had cellularity and adiposity similar to the control aspirates. Femoral marrow of one of these two rabbits showed a striking increase in cellularity after 3 weeks of treatment with cortisone. Phenylhydrazine in the doses given did not cause so much increase in cellularity, despite the induction of hemolytic anemia. For the sake of simplicity Fig. 43 does not show the differential counts of the nucleated cells (granulocytes, red-cell precursors, megakaryocytes, and miscellaneous cells) that are of interest in accounting for alterations in cellularity. Despite the difficulty of positive identification of the primitive cells in sections, mature forms predominate and granulocytic or erythropoietic hyperplasia could be quantitated in terms of the volume of the sample occupied by these components. The stereologic quantitation was compared with the two independent preliminary estimations, and a fairly good correlation was found. Inconsistencies were especially evident in the estimation of the volume of red-cell precursors, perhaps because of their uneven distribution (in "clones"), the small size of the cells, and the similarity of many of the cells to other small cells.

The stereologic quantitation requiring several hours per slide

gave considerable confidence in the reliability of the estimations that could be made in a few minutes. Altogether, this histologic study showed that marrow of the rabbit ilium and femur has considerable adiposity (in this respect resembling red marrow of man more than that of smaller laboratory animals such as the mouse, rat, guinea pig, or tamarin) and that quantitative changes in the components can be evaluated histologically. The magnitude of errors in this stereologic method has not yet been determined. Such problems as shrinkage of the marrow in preparation call for independent techniques of quantitation of marrow components.

REFERENCES

1. Nelson, B., Lothrop, Martha L., and Gengozian, N. Histologic changes in marrow after total-body irradiation of marmosets: a quantitative stereologic evaluation. In: USAEC Report ORAU-101, 1966, pp. 27-30.

The Effect of Total-Body Irradiation on the Direct Bone-Marrow Metaphases*

Kong-oo Goh

The effect of radiation on somatic chromosomes in man is well known. However, most results were obtained from the metaphases of the peripheral leukocytes after culturing with phytohemagglutinin (PHA) in vitro or from cell cultures. Here we report our observations of the chromosomal aberrations in direct bone marrow obtained from patients who had been accidentally exposed to total-body irradiation 7 years previously.

The metaphases for the cytogenetic studies were obtained from the direct bone-marrow preparations with the technique of Tjio and Whang, slightly modified. We obtained 227 well-spread metaphases from these patients as summarized in Table 13. Twenty-five (11%) abnormal and seven (3.1%) X_1 cells were encountered in this study. Table 14 shows the types and frequency of abnormal chromosomes. The most obvious contrast to the findings in peripheral leukocytes[1] is the absence of dicentric and ring chromosomes. The abnormal

* Part of these data will appear in Radiation Research (in press).

1027639

TABLE 13

Chromosome Number and Frequency of Abnormal Cells

Code	Chromosome Number <45	45	46	47	>47	Total	%2N*	Abnormal Cells No.	Abnormal Cells %	X_1 - Cells No.	X_1 - Cells %
	No. of Cells										
A	0	0	6	0	0	6	100	1	16.7	1	16.7
B	0	2	36	1	0	39	92	5	12.8	2	5.1
C	1	1	37	0	0	39	95	7	18.0	1	2.6
D	1	1	31	0	2+	35	89	4	11.4	1	2.9
E	0	1	46	0	0	47	98	4	3.5	2	4.3
F	0	1	59	0	1+	61	97	4	6.6	0	0
Total	2	6	215	1	3	227	95	25	11.0	7	3.1

* Percentage of cells having chromosome number of 46 (diploid)

\+ Tetraploid

TABLE 14

Types and Frequency of Abnormal Chromosomes

	Cells			Chromosomal Abnormalities									
	Analyzed	Abnormal Cells		Chromosomal Breaks			Fragments		Dicentrics	Translocation		Rings	Smaller G
		No.	%	No.	%*	A/C†	No.	%	No.	No.	%	No.	No.
A	6	1	16.7	1	17	1.0	1	16.7	0	0		0	0
B	39	5	12.8	5	13	1.0	2	5.1	0	0		0	2
C	39	7	18.4	8	20	1.1	1	2.6	0	1	2.6	0	1
D	35	4	11.8	4	11	1.0	1	2.9	0	0		0	2
E	47	4	8.5	4	9	1.0	2	4.3	0	0		0	2
F	61	4	6.6	4	7	1.0	0	---	0	1	1.6	0	1
Total	227	25	11.0	26	11	1.0	7		0	2		0	10

* Break per 100 metaphases

† Abnormality per abnormal cell

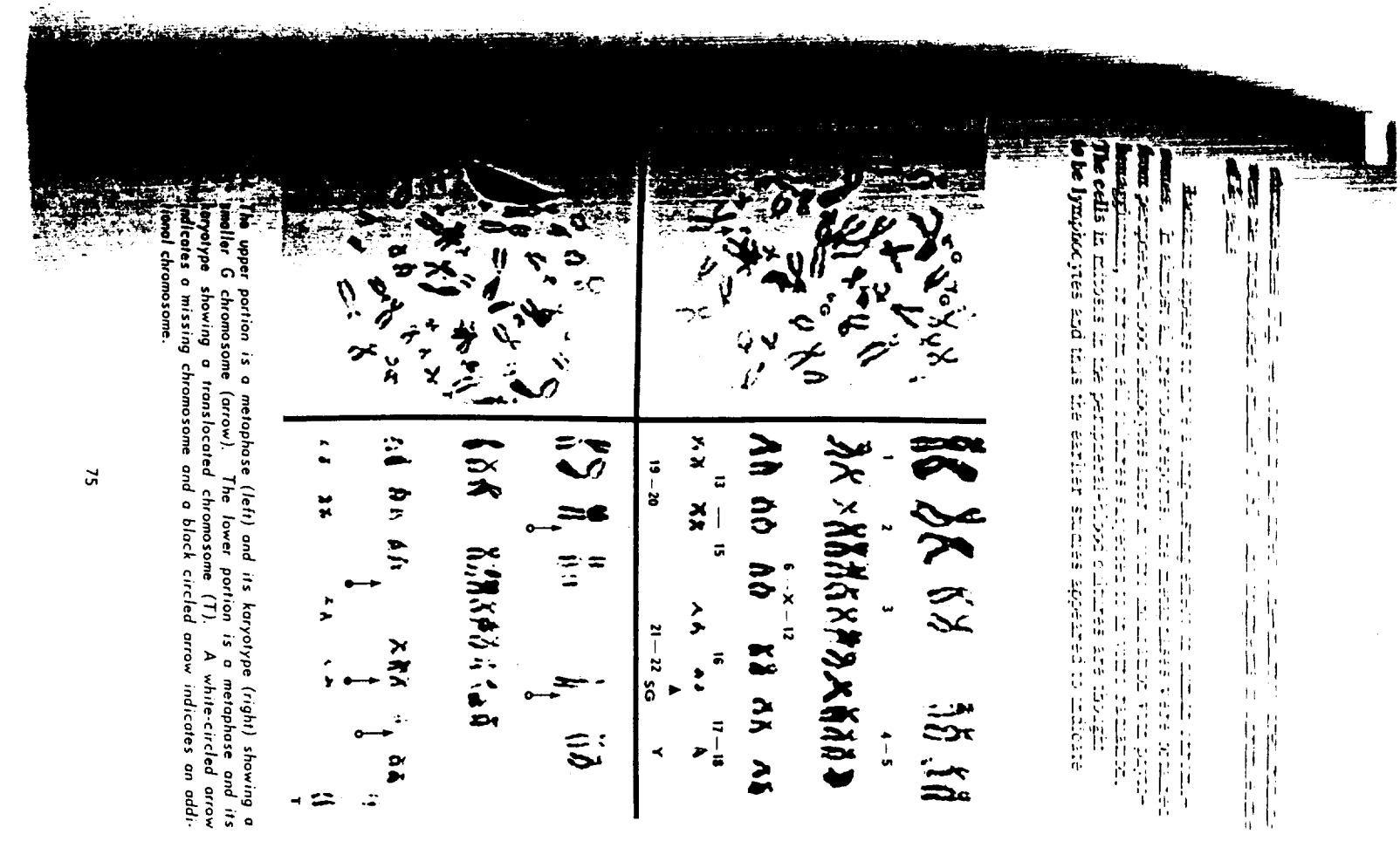

The upper portion is a metaphase (left) and its karyotype (right) showing a smaller G chromosome (arrow). The lower portion is a metaphase and its karyotype showing a translocated chromosome (T). A white-circled arrow indicates a missing chromosome and a black circled arrow indicates an additional chromosome.

that radiation causes chromosomal breaks in human lymphocytes and cultured cells.

The information obtained from the studies in patients with chronic myelocytic leukemia (CML) and the Ph^1 indicated that the metaphases obtained from the direct bone-marrow preparations are probably the cells giving rise to the myelocytes, erythrocytes, and possibly the megakaryocytes. Thus our findings indicate that radiation also injures the human myeloid cells of the bone marrow, although its effect is much less than that on the peripheral lymphocytes.

The SG chromosome having the morphologic appearance of Ph^1 chromosome could not have arisen in vitro, since the bone-marrow cells were prepared directly. In the few reports in which SG chromosomes were found in patients after radiation therapy for other diseases,[2,3] the patients had clinical evidence of CML at the time of cytogenetic studies. Here, no clinical or hematologic evidence of CML is found.

Although the SG had a similar morphologic appearance to the Ph^1 chromosome, in the present studies, the abnormal chromosome was found in the lymphoid[1] as well as myeloid cells. This is distinctly different from the Ph^1 chromosome which is found in myeloid cells but not in the lymphocytes of patients with CML. Also the incidence of almost 100% of the Ph^1 chromosome in the direct bone-marrow preparations of patients with CML is much higher than the 5.3% in the present patients.

Several possibilities could be considered in regard to the SG found here and the Ph^1 chromosome found in CML: (1) the Ph^1 chromosome in CML may be a coincident finding and have nothing to do with the pathogenesis of CML; (2) the SG chromosome found here may have a different pathophysiologic significance from the Ph^1 chromosome; and (3) the development of CML may depend on other factors that give advantage to the cells with an SG chromosome. It is not possible to say which is more likely from the present findings; perhaps the follow-up studies will eliminate some of these possibilities.

REFERENCES

1. Goh, K. O. The effect of total-body irradiation on human chromosomes: 1. Cytogenetic studies of the peripheral leukocytes seven years after total-body irradiation. In: USAEC Report ORAU-101, 1966, pp. 8-12.

2. Engel, E., Flexner, J. M., Engel-De Montmollin, M. L., and Frank, H. E. Blood and skin chromosomal alternations of a clonal type in a leukemic man previously irradiated for lung carcinoma. Cytogenetics 3, 228-251, 1964.

3. Gavosto, F., Pileri, A., Pegoraro, L. X-rays and Philadelphia chromosome. Lancet 1, 1336-1337, 1965.

1027641

Breaks in Normal Human Chromosomes: Are They Induced by a Transferable Substance in the Plasma of Persons Exposed to Total-Body Irradiation?*

Koog-oo Goh and H. Sumner†

Abnormal cells containing acentric fragments (X_1 cells) have been found in the cultured peripheral-blood leukocytes years after the original irradiation. The explanation for this finding has been that these cells were injured in the pre-deoxyribonucleic acid (DNA) synthesis (G_1) phase of their mitotic cycle at the time of the original irradiation. They remained in this stage for a period of years and underwent mitosis in vitro after being stimulated by phytohemagglutinin (PHA) or other mitogenic substances.[1] This interpretation, however, could not explain several observations such as an unstable-X_1 cell with a stable abnormal chromosome. Thus the possibility arises that a substance, capable of affecting the chromosomes for an extended time, was produced or activated by total-body irradiation.

To test this hypothesis on the possible mechanism of production of the X_1 chromosomal breaks found in patients 7 years after they had been exposed to total-body mixed gamma and neutron irradiation, we performed a series of experiments.

Normal Controls Peripheral-blood leukocytes from two normal men (Donors 1 and 2) and two normal women (Donors 3 and 4) were cultured with autologous plasma and with AB+ sera. No differences were found in the frequencies of chromosomal breaks either cultured with autologous plasma or in AB+ sera. Five (1%) chromosomal breaks were seen in 461 control metaphases.

Experimental Controls Eight cultures of normal leukocytes with normal plasma from nonirradiated donors were incubated as experimental controls. These cultures differed from the normal controls in that each plasma donor had at least one major red-cell antigen that was different from that of the leukocyte donor. Four of these cultures involved leukocyte and plasma of different sex. Six (1%) chromosomal breaks were seen in 643 metaphases analyzed.

---

* The patients are the same ones as reported in the direct bone-marrow studies (In press, Radiation Research).

† Present address: School of Medicine, Washington University, St. Louis, Mo. Summer Student Trainee from St. Edward University, Austin, Texas (1965) and temporary employee during summer 1966 and 1967.

Experimental Cultures (Irradiated Plasma) Nineteen cultures were made from the leukocytes of the normal controls and incubated with the plasma obtained from irradiated patients. There were 114 (8.7%) chromosomal breaks in the 1,318 metaphases analyzed. The types of breaks are shown in Figs. 45, 46, and 47. No male

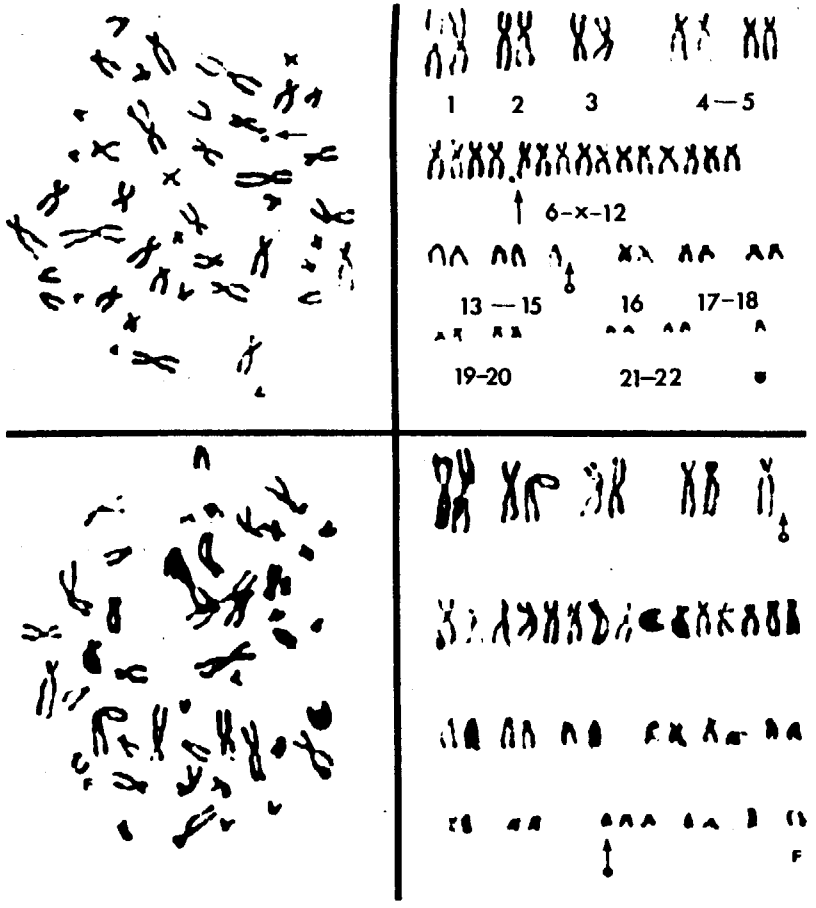

Fig. 45. Upper portion: A hypodiploid (45 chromosomes) obtained from the leukocytes of donor number 1 cultured with patient E's plasma. Shown are a missing chromosome D (arrowed with a white circle) and a chromosomal break in one of the 6-X-12 chromosomes (arrowed). Lower portion: A diploid metaphase and karyotype with a fragment (F) obtained from the leukocytes of donor number 2 cultured with patient B's plasma. Also shown are one missing chromosome in the 4-5 group (arrow with a white circle) and an additional one in the 21-22 group (arrow with a black circle).

1027642

Fig. 46. An abnormal metaphase and its karyotype obtained from the leukocytes of donor number 3 cultured with patient F's plasma. Shown are a missing chromosome number 2 (arrowed with a white circle), absence of two chromosomes (arrowed with a white circle), and a chromosomal break (arrowed) in the 6-XX-12 group, an unusual configuration chromosome (marked C.O.), probably a crossing over chromosome of German 2, and two abnormal chromosomes, probably the long arm (L.A.) and short arm (S.A.) of the missing chromosome number 2.

metaphases were found in any of the 579 metaphases obtained from the female donors' leukocytes (Donors 3 and 4) cultured with patients' (male) plasma.

These findings suggested strongly that the plasma of irradiated patients is capable of causing chromosomal breaks in normal leukocytes. The breaks in the normal leukocytes are the X_1 type. Although chromosomal breaks have been reported in association with virus, anticancer drugs, and other chemicals, the presence of a subclinical viremia in all these patients at the same time is highly unlikely. Also no other known causes of chromosomal breaks were obtained from clinical histories of these patients.

In studies with X-irradiated mice, Wald et al[3] have suggested a substance postulated as an activated virus. The X-irradiated mice developed chronic granulocytic leukemia. The cell-free filtrates of these leukemic mice could induce the same disease and with a specific abnormal chromosome in recipient mice. These findings indicate that radiation must have produced some substance that was capable of being transmitted through the cell-free filtrate. This hypothesis seems to agree with our observations. However, we are unable to say whether the substance in the plasma of these

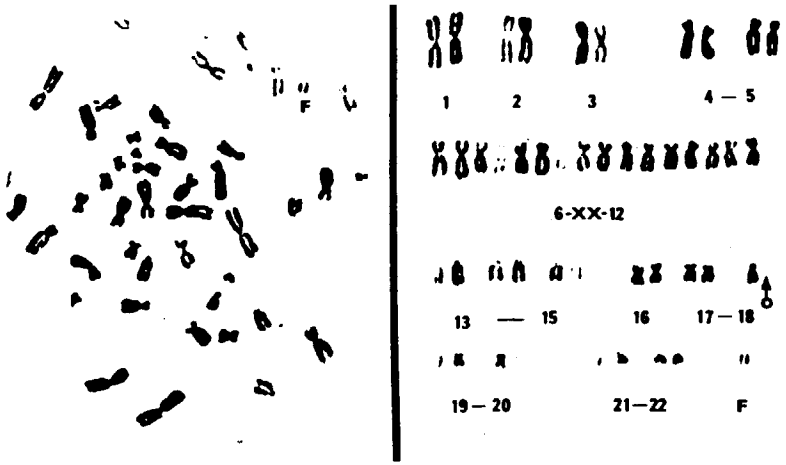

Fig. 47. A hypodiploid (45 chromosomes) metaphase and karyotype obtained from the leukocytes of donor number 4 cultured with patient E's plasma. Shown are a missing chromosome of 17-18 (arrow with a white circle) group and a fragment (F).

patients is a virus. Ahnström and Natarajan[4] have postulated, as another mechanism of chromosomal breakages, an enzyme that actively removes nucleotides from already formed DNA of the chromosome.

REFERENCES

1. Nowell, P. C. Unstable chromosome changes in tuberculin-stimulated leukocyte cultures from irradiated patients. Evidence from immunologically committed, long-lived lymphocytes in human blood. Blood 26, 798-804, 1965.

2. German, J. Cytological evidence for crossing-over in vitro in human lymphoid cells. Science 144, 298-301, 1964.

3. Wald, N., Upton, A. C., Jenkins, V. K., and Borges, W. H. Radiation-induced mouse leukemia, consistent occurrence of an extra and a maker chromosome. Science 143, 810-813, 1964.

4. Ahnström, G. and Natarajan, A. T. Mechanism of chromosome breakages - A new theory. Hereditas 54, 379-388, 1966.

1027643

Autoradiographic Studies in the Ph' Chromosome*

Kong oo Goh

The establishment of the correct human diploid chromosome number by Tjio and Levan in 1956 has stimulated great interest in studying human chromosomal complements in normal persons and in those with different diseases. In 1960 Nowell and Hungerford, using peripheral-blood leukocyte cultures, demonstrated a "cancer cell marker" in chronic myelocytic leukemia (CML). This abnormal chromosome appears to belong to the small acrocentric chromosomes in group G (21-22). However, whether it replaced a normal chromosome 21 or 22 is not known.

Morishima et al[1] showed that one pair of the human G chromosomes replicated their DNA late in the synthesis phase of the cell cycle and tentatively designated this pair of late replicating chromosomes as chromosome 21. Using this technique, we have attempted to study the DNA synthesizing pattern of the Ph^1 chromosome.

Table 15 summarizes the silver-grain patterns of 1, 3, X, D and G chromosomes of 20 normal female karyotypes and showed that in general a labeling pattern could be established. Using the centromere labeling pattern of chromosome 1 and the heavy labeling of one of the X chromosomes in the female as being indicative of terminally labeled metaphases (Fig. 48), we determined the labeling patterns of the Ph^1 chromosome. Table 16 summarizes the silver-grain patterns of G and Ph^1 chromosomes of 80 female CML karyotypes. Several labeling patterns were noted in the Ph^1 chromosome (Table 16).

The Ph^1 chromosome appeared more frequently as a member of a pair of G chromosomes that replicated their DNA late (Table 16). Less frequently, it was an early DNA replicating G chromosome. In a few late-labeling metaphases, the Ph^1 chromosome was the only labeled G chromosome and was heavily labeled (Fig. 49). These findings suggested that the Ph^1 chromosome found in CML could be derived from either a 21 or 22 chromosome, or from both in the same patient.

REFERENCE

1. Morishima, A., Grumbach, M. M., and Taylor, J. H. Asynchronous duplication of human chromosomes and the origin of sex chromatin. Proc Nat Acad Sci 48, 756-763, 1962.

---

* Presented at the Symposium on Radioisotopes in Medicine: In Vitro Studies, Oak Ridge, Tennessee, November 13-16, 1967. In: AEC Symposium Series CONF-671111 (in press).

TABLE 15

Silver-Grain Patterns* of 1, 3, X, D(13-15), and G(21-22) Chromosomes in 20 Terminal Labeled Metaphases of a Normal Female Peripheral-Blood Leukocyte Culture.

Metaphase	1†		3†		X‡	13		14		15		21		22	
1	2+	+	+	+	3+	3+	3+	2+	2+	+	0	+	+	0	0
2	2+	2+	+	2+	3+	3+	3+	2+	+	0	0	0	0	0	0
3	2+	2+	2+	2+	3+	3+	3+	2+	2+	0	+	2+	+	0	0
4	2+	+	+	0	3+	3+	3+	3+	2+	0	0	+	+	0	0
5	+	+	2+	2+	3+	3+	3+	2+	2+	0	0	0	0	0	0
6	+	2+	2+	+	3+	3+	3+	2+	2+	+	+	2+	+	0	0
7	2+	2+	+	+	3+	3+	3+	2+	2+	+	+	2+	+	+	+
8	+	+	2+	2+	3+	3+	3+	+	+	0	0	+	+	0	0
9	+	+	2+	0	3+	3+	3+	2+	0	+	0	+	+	0	0
10	2+	2+	2+	0	3+	3+	2+	2+	+	+	+	2+	+	0	0
11	+	+	2+	2+	3+	3+	3+	2+	2+	2+	0	+	+	+	+
12	2+	2+	+	+	3+	3+	3+	+	+	0	0	+	+	0	0
13	2+	+	2+	2+	3+	3+	3+	3+	2+	+	+	2+	2+	0	0
14	2+	2+	+	2+	3+	3+	3+	2+	2+	0	0	+	+	0	0
15	2+	2+	2+	2+	3+	3+	3+	2+	2+	0	0	0	0	0	0
16	2+	+	2+	+	3+	3+	3+	+	2+	0	0	+	+	+	+
17	2+	2+	+	+	3+	3+	2+	2+	0	0	0	0	0	0	0
18	2+	2+	2+	2+	3+	3+	3+	+	+	0	0	0	0	0	0
19	+	+	2+	2+	3+	3+	3+	2+	+	+	+	2+	0	0	0
20	+	+	2+	+	3+	3+	3+	3+	0	0	0	2+	2+	0	0

* The labeling patterns are scored as 3+ (total chromosome heavily labeled), 2+ (segmental heavy labeling or total chromosome moderately labeled), + (slightly segmentally labeled).

† Slight variation of homologs, but a persistant labeling of centromere.

‡ The most consistent pattern is the heavy label of X.

1027644

TABLE 16

Summaries of the Silver-Grain Patterns* of G(21-22) and the Ph^1 Chromosomes in 80 Terminal Labeled † Metaphases From Female Chronic Myelocytic Leukemia Patients.

CHROMOSOMES				METAPHASES	
21	22		Ph^1	No.	%
Labeling Patterns*					
+	0	0	+	29‡	36.2
0	0	0	0	19	23.8
+	0	0	0	11	13.7
+ +	0		0	5§	6.2
0	0	0	3+	4	5.0
0	0	0	+	1	
+	+	+	3+	4	5.0
+ +	0		+	1	
2+	0	0	2+	1‡	
2+	+	0	2+	1‡	
2+	0	0	0	1	
+	+	+	0	1	
3+	+	+	+	1	
2+	+	+	2+	1‡	

* The labeling patterns are scored as 3+ (total chromosome heavily labeled), 2+ (segmental heavy labeling or total chromosome moderate labeled), + (slightly segmentally labeled).

† The metaphases are considered terminally labeled only when the centromeres of chromosomes 1 and 3 are labeled and one of the X chromosomes is heavily labeled.

‡ Metaphases having the Ph^1 chromosome as a late replicating pair of G chromosomes.

§ Metaphases having the Ph^1 chromosome as an early replicating pair of G chromosomes.

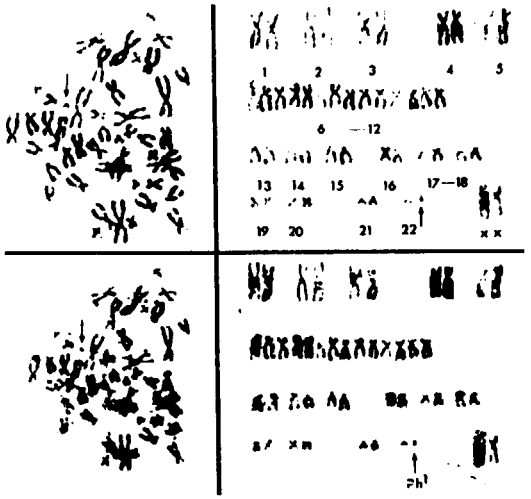

Fig. 48. A Ph-positive metaphase and its karyotype before autoradiography (upper portion) and the same metaphase and its karyotype after autoradiography (lower portion) showing the terminal-labeled pattern. The Ph^1 chromosome in this cell appears to replicate DNA early.

Fig. 49. A Ph^1-positive metaphase and its karyotype before autoradiography (upper portion) and the same metaphase and its karyotype after autoradiography (lower portion) showing the terminal-labeled pattern. The Ph^1 chromosome in this cell is the only G chromosome that replicated its DNA late.

1027645

Cytogenetic Studies in Blastic Crisis of Chronic Myelocytic Leukemia*†

Kong-oo Goh

Evidence is adequate that the Philadelphia (Ph^1) chromosome is present in all typical cases of chronic myelocytic leukemia (CML). In contrast to the chronic stage, few patients have been reported after their disease has been transformed into an acute stage. Furthermore, in some patients reported by others, no Ph^1 chromosome was found at this stage of the disease. In the course of our cytogenetic survey of CML, eight patients were studied during the acute stage of their disease. This paper reports our findings.

Table 17 summarizes the clinical course and the hematologic data of each patient. The results of the cytogenetic studies are summarized in Table 18. The modal chromosome number was 46 in all the patients with the exception of Patient 8. The average percentage of cells having a normal diploid chromosomal number was 62%. In Patient 8, 42 (84%) of the 50 metaphases were hyperdiploid. Four metaphases had 47, four had 45, 31 had 48, and three had 50 chromosomes. Only seven (14%) metaphases in this patient had a normal 46 chromosomes, and one was hypodiploid.

The Ph^1 chromosome was identified in each patient and was seen in 289 (83%) of the 347 metaphases analyzed. In Patient 8, diplo-Ph^1 (two Ph^1 chromosomes per cell) was seen in 28 (74%) of the 38 metaphases having more than 47 chromosomes as illustrated in the two lower metaphases of Fig. 50.

The missing chromosomes in the hypodiploid metaphases in this study are randomly distributed in different chromosomal groups. However, of the hyperdiploid metaphases, abnormal cell lines were established in two patients. In Patient 7, in eight metaphases having 48 chromosomes, the additional chromosomes were an extra C and F as shown in the upper metaphase of Fig. 50. In Patient 8, several abnormal cell lines were found among the hyperdiploid metaphases as shown in Table 19.

Other chromosomal abnormalities included a large submetacentric chromosome in four patients and a large acrocentric chromosome in all patients, as shown in Fig. 51. Although these abnormal chromosomes appeared morphologically similar in

---

* Part of this work was done while the author was associated with the University of Rochester School of Medicine, Rochester, N. Y.

† Published in Arch Intern Med 120, 315-320, 1967.

1027164

TABLE 17

Clinical and Hematologic Summaries of Acute Blastic Crisis

Patient	Sex	Age	Previous Treatments*	Hematocrit(%)	WBC X 10^3 per mm	%"Blasts"	Duration†	Interval‡
3	F	59	B,RT	28	90	33	24.5	2
4	M	42	B	18.5	47.3	60	8	8
6	M	24	B,CS,6MP	23	43	68	30	12
7	M	50	B,RT,6MP,CS	31	51	51	31	24
8	F	31	B,RT,6MP,CS	33	82	63	33	8
9	F	26	B,RT,6MP, ^{32}P,CS	43	13	58	76	3
10	F	60	B,RT,C,6MP,CS	30	121	27	36	3
11	M	68	B,RT,6MP,CS	27	201	60	36	6

* B=Busulfan; RT=Radiation Treatment; CS=Corticosteroids; 6MP=6-Mercaptopurine (Purinethol); C=Cyclophosphamide

† Original diagnosis of chronic myelocytic leukemia to death in months

‡ Interval between cytogenetic studies to death in weeks

TABLE 18

Chromosomal Analyses of Patients in Acute Blastic Stage of Chronic Myelocytic Leukemia

Patient	Specimen*	Chromosomal Number <45	45	46	47	>47 (No. of Cells)	Total	%2N†	%Hyper‡	Ph^1 Chromosome No.	Ph^1 Chromosome %	Abnormal Chromosomes No.	Abnormal Chromosomes %
3	DBM	----------0----------											
	PBC	0	1	31	9	3	44	70	25	19	43	1	2.3
4	DBM	5	2	36	1	0	44	82	2	41	93	4	9.1
6	DBM	----------0----------											
	PBC	1	1	34	3	5	44	77	18	40	91	3	6.8
7	IBM	4	1	21	3	8‖	37	57	30	36	97	5	13.5
8	IBM	1	0	7	4	38‖	50	14	84	49	98	1	2.0
9	PBC	3	3	28	0	1	35	80	3	14	40	8	22.8
10	DBM	9	2	34	4	1	50	68	10	48	96	1	2.0
11	DBM(Sternal)	2	1	9	3	6¶	21	44	24**	20	95	0	
	(Iliac)	0	2	14	3	3	22	64	27	22	100	2	9.1
	Grand Total	25	13	214	30	65	347	62	26**	289	83		

* DBM=Direct bone marrow; PBC=Peripheral-blood leukocyte culture; IBM=Incubated bone marrow (18-24 hours).

† Percentage of cells having 46 chromosomes.

‡ Percentage of cells having more than 46 chromosomes.

§ A large acrocentric or submetacentric chromosome as shown in Fig. 51.

‖ Detail analyses are presented in the text and shown in Fig. 50.

¶ Four of these metaphases have 92 chromosomes with two Philadelphia chromosomes.

** Exclude the four tetraploidy (presumably megakaryocytes).

102 1641

TABLE 19

Distribution of the Additional and Missing Chromosomes of the 49-Chromosome Metaphases in Patient 8

Chromosomal Group																								Metaphases	
A			B		C			D			E		F			G			Ph[1]				No.	%
1	2	3	4	5	6	X	12	13	14	15	16	18	19	20		21	22								
		+1											+1			-1			+2				10	33
					+1								+1			-1			+2				8	26
+1													+1			-1			+2				4	13
					+1								+1						+1				2	6
								+1					+1			-1			+2				1	
					+1			+1								-1			+2				1	
	-1	+1			+1								+1			-1			+2				1	
		+1			+1			+2								-1			+1				1	
					+1								+2			-1			+1				1	
		+1			+1			+1			-1		+1			-1			+1				1	
								+4					-1						0				1	
																		Total					31	

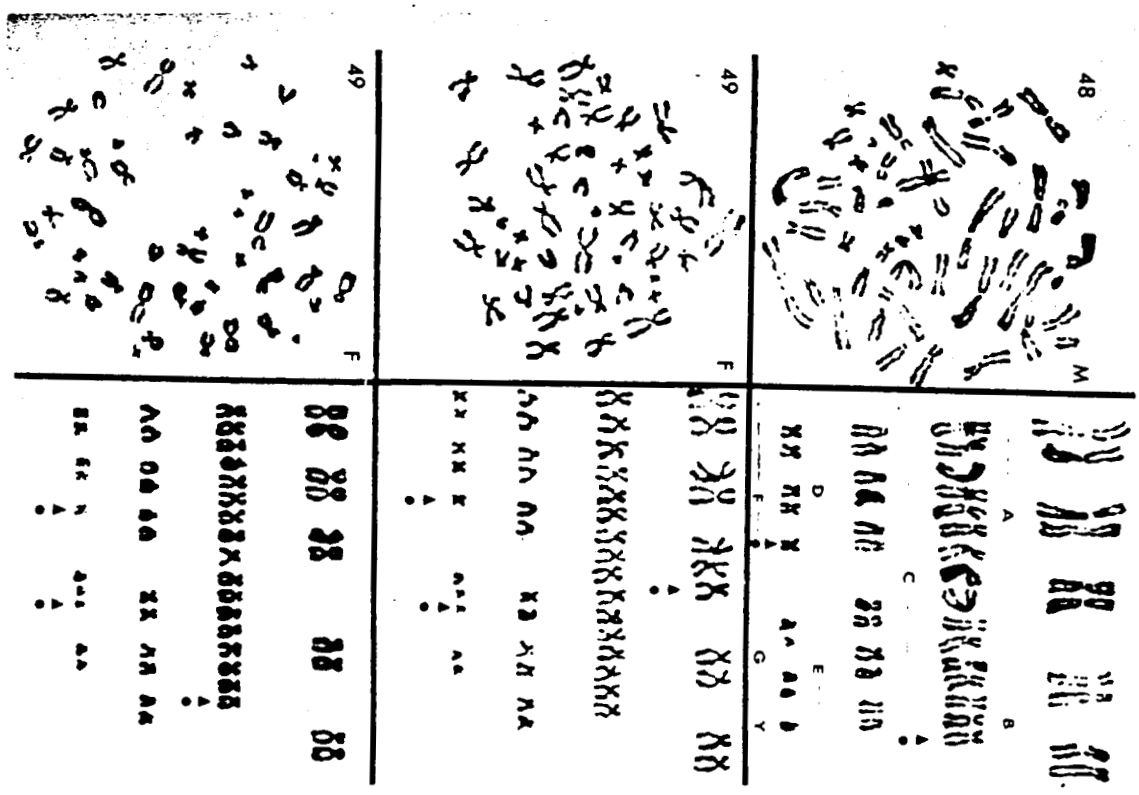

Fig. 50. Three metaphases and karyotypes were obtained from Patients 7 (upper) and 8 (middle and lower). The additional chromosomes are arrowed with a black circle. Note the similarity between the top and bottom karyotypes with the exception of a second Ph[1] in the bottom karyotype.

different metaphases, either from the same patient or from different patients, there was no evidence that the abnormal chromosome replaced a specific normal chromosome nor that it was an additional chromosome in each metaphase.

The present observations suggest (1) the Ph^1 chromosome is retained in the acute stage of CML; (2) occasionally there are diplo-Ph^1 chromosomal patterns; (3) the hyperdiploid metaphases seen are probably the acute leukemic cells although not all acute leukemic cells are hyperdiploid; (4) with the exception of a single hyperdiploid Ph^1 -negative cell, all the hyperdiploid cells have at least one Ph^1 chromosome indicating that the hyperdiploid cells probably arise from a cell or cells with a Ph^1 chromosome; (5) abnormal clones of cells, which were found in two patients, have some similarity in their abnormalities; and (6) perhaps the additional chromosomal abnormalities found in acute blastic crisis are associated with the transformation of CML into an acute stage.

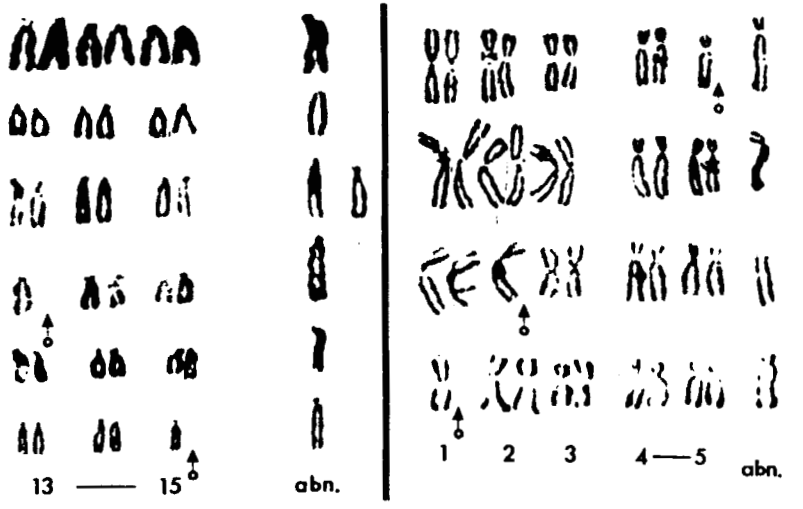

Fig. 51. Abstracts of ten metaphases were obtained from patients with acute transformation of CML. The left portion shows the normal D (13-15) chromosomes and the abnormally large acrocentric (marked abn.) chromosomes of six metaphases. (Rows 1 and 2, Patient 4; Row 3, Patient 6; Rows 4 and 5, Patient 7; and Row 6, Patient 9.) The right portion shows the normal A (1-3) and B (4-5) chromosomes. The abnormal chromosomes are in the right-hand column (marked abn.). (Rows 1 and 2, Patient 7; Rows 3 and 4, Patient 9.) The arrows with a white circle indicate a missing homologous chromosome.

1027648

Partial G/D Translocation Associated With Mental Retardation in Two Members of a Family

*Kong-oo Goh and L. E. Tucker, Jr.**

It is well known to cytogeneticists that in some metaphases there are satellite associations of the acrocentric chromosomes. In 1961 Ohno and associates[1] suggested that the material lost by a chromosomal break in a G chromosome would likely be translocated to a D chromosome. In the course of our cytogenetic survey in mentally retarded patients, a family with two mentally retarded members was studied. The pedigree of the members of this family is summarized in Fig. 52.

Cytogenetic studies of the cultured peripheral-blood leukocytes were performed in the available members of this family. The results are summarized in Table 20. A D chromosome was missing in the metaphases obtained from II_2 and II_4 (mentally retarded) patients. In each of these metaphases, an additional chromosome of the size of the C (6-X-12) chromosome was found. This additional chromosome was interpreted as a translocated D (13-15) chromosome (Figs. 53 and 54) in which a segment of a chromosome was added to the short arm of a normal D chromosome. But it was not possible to say from which chromosome this segment originated.

Cytogenetic studies of the peripheral-blood leukocytes of other members of this family are summarized in Fig. 52 and Table 20. A D chromosome was missing in the metaphases obtained from I_1 and II_3 and an additional chromosome, morphologically similar to the translocated chromosome of II_2 and II_4, was found. In addition, a smaller G (21 or 22) chromosome with a shorter long arm than any normal G chromosome was also found in these two phenotypical normal persons (Fig. 55). These findings suggested that the additional short arm of the translocated D chromosome originated from the long arm of a normal G chromosome.

The mechanism of the production of these two abnormal chromosomes must involve a break in the long arm of a normal G chromosome with the deleted segment being translocated to a normal D chromosome (Fig. 56). In the phenotypical normal members of this family, there is neither a gain nor a loss of any genetic material in their somatic cells. During meiosis, four gametes could be produced. In the mentally retarded members, the zygotes were formed by a normal and an abnormal gamete. The abnormal gametes have additional genetic material of part of the long arm of a G

---

* Abbott Student Fellow from Stanford University Medical School (1965).

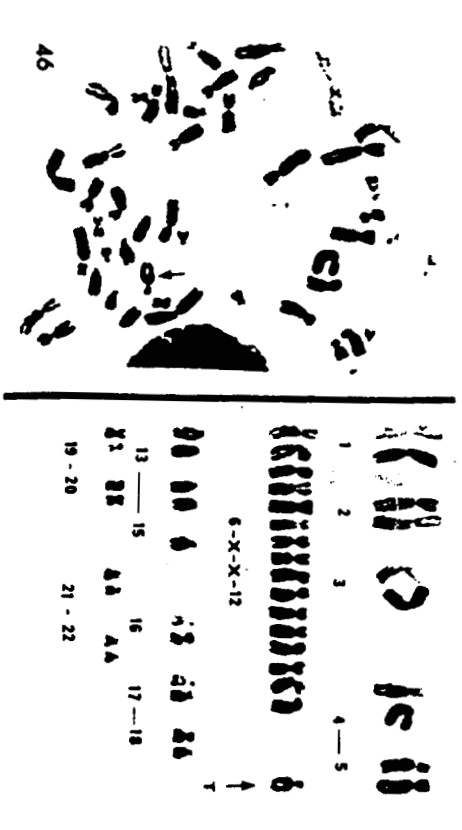

Fig. 53. Metaphase and karyotype of a cell obtained from II_4. A translocated D (13-15) chromosome is denoted by an arrow (T).

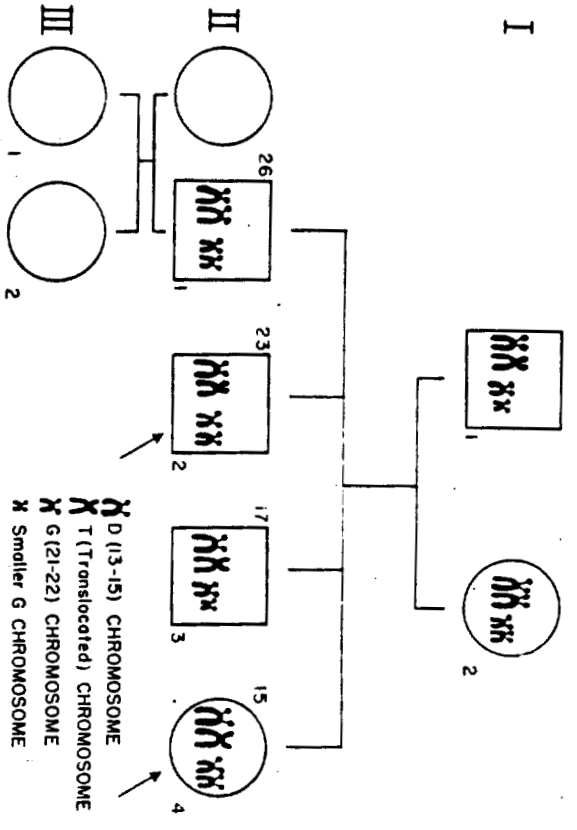

Fig. 52. Pedigree of the members of a family having two mentally retarded members (arrowed).

TABLE 20

Results of Cytogenetic Studies of a Family

With Two Mentally Retarded Members

	Chromosome Number							Abnormal Chromosomes			
								Smaller G*		Translocated D†	
	<45	45	46	47	>47	Total	% 2N	No.	%	No.	%
I_1	1	6	50	1	1	59	80	52	88	56	95
2	2	4	37	0	0	43	86	0		0	
II_1	3	9	33	2	0	47	70	0		0	
2‡	0	1	37	1	0	39	95	0		37	95
3	6	6	51	0	1	64	80	54	85	58	91
4‡	2	3	22	6	1	34	65	0		33	97

* Deleted long arm of a G chromosome.

† Translocation of the part of the long arm of a G to the short arm of a D chromosome.

‡ Mentally retarded members of the family.

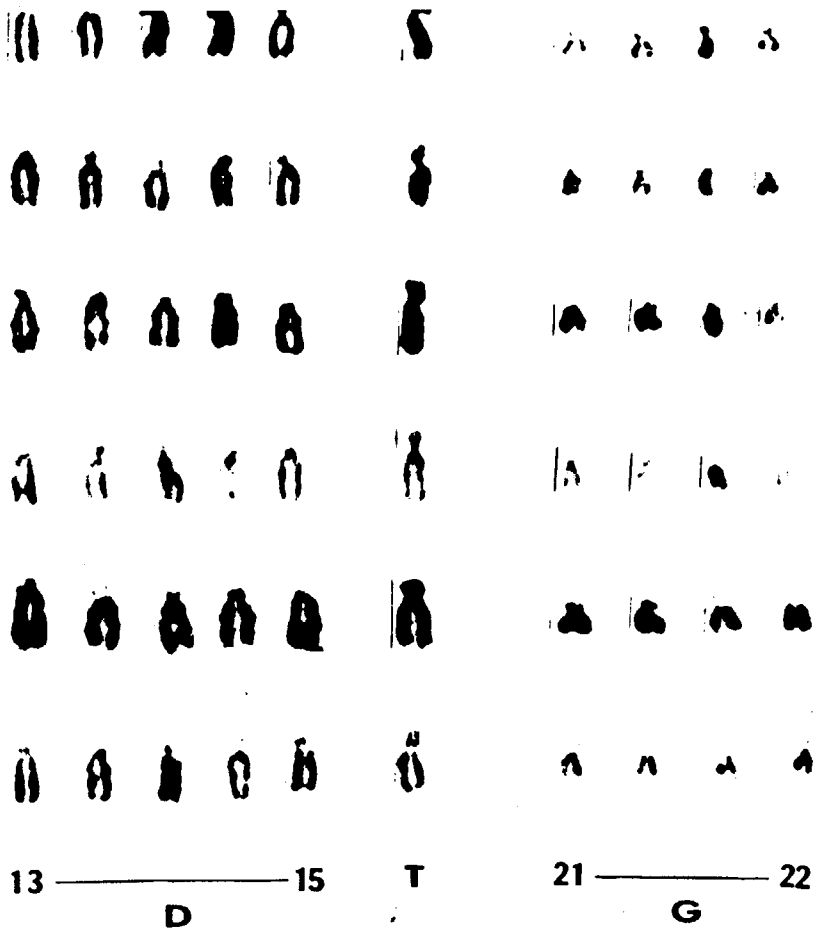

Fig. 54. Abstract of D (13-15) and G (21-22) chromosomes from six metaphases obtained from II_4. The translocated D chromosomes are shown in the 6th column marked with a T.

chromosome. Hence, these patients have partial trisomy of a G chromosome. In this family only three of the four possible gametes were able to form zygotes. Perhaps the gametes with only a smaller G chromosome are incapable of fertilizing an ovum or they are not able to survive.

The smaller G chromosome found in the metaphases of the cultured peripheral-blood leukocytes of I_1 and II_3 has a morpholo-

1027650

gical appearance of the Philadelphia (Ph^1) chromosome found in patients with chronic myelocytic leukemia.[2] The production of the Ph^1 chromosome may be analogous to the smaller G chromosome found in irradiated man.[3] The deleted long arm apparently is lost in the Ph^1 chromosome metaphases, since a translocation of the deleted part has been reported in only two metaphases with a Ph^1 chromosome.[1] This translocation, however, has not been seen in any of the more than 3,000 Ph^1 -positive metaphases analyzed in our laboratory. Hence, in the Ph^1 -positive metaphases of chronic myelocytic leukemia, there is a net loss of genetic material of the long arm of a G chromosome. In the present cases, however, the deleted long arm of a G chromosome, producing the smaller G chromosome, is translocated to the short arm of a D chromosome,

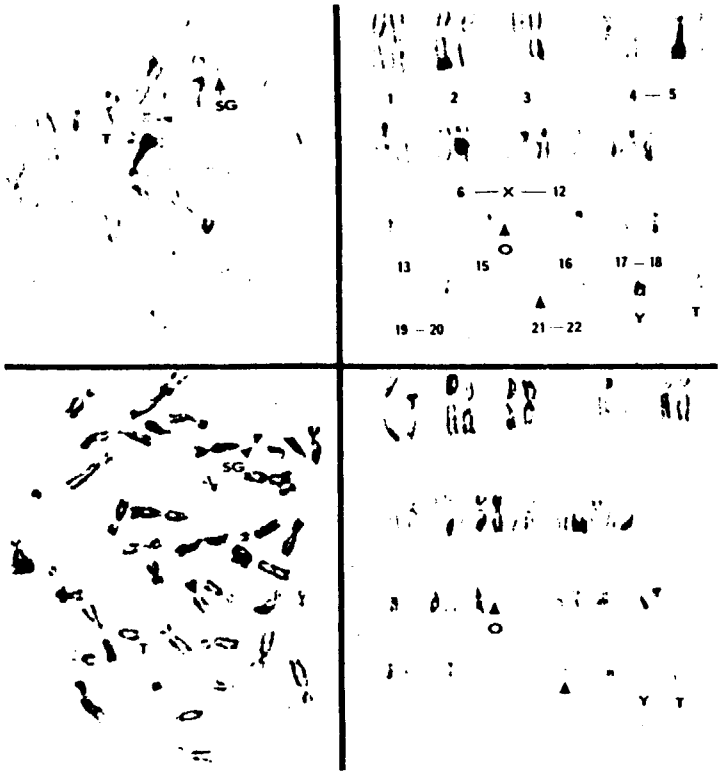

Fig. 55. Two metaphases (left) and their karyotypes (right) obtained from cultured peripheral-blood leukocytes of I_1 (upper portion) and II_3 (lower portion) of this family. A smaller G (21-22) and a translocated (T) chromosome were seen in each metaphase.

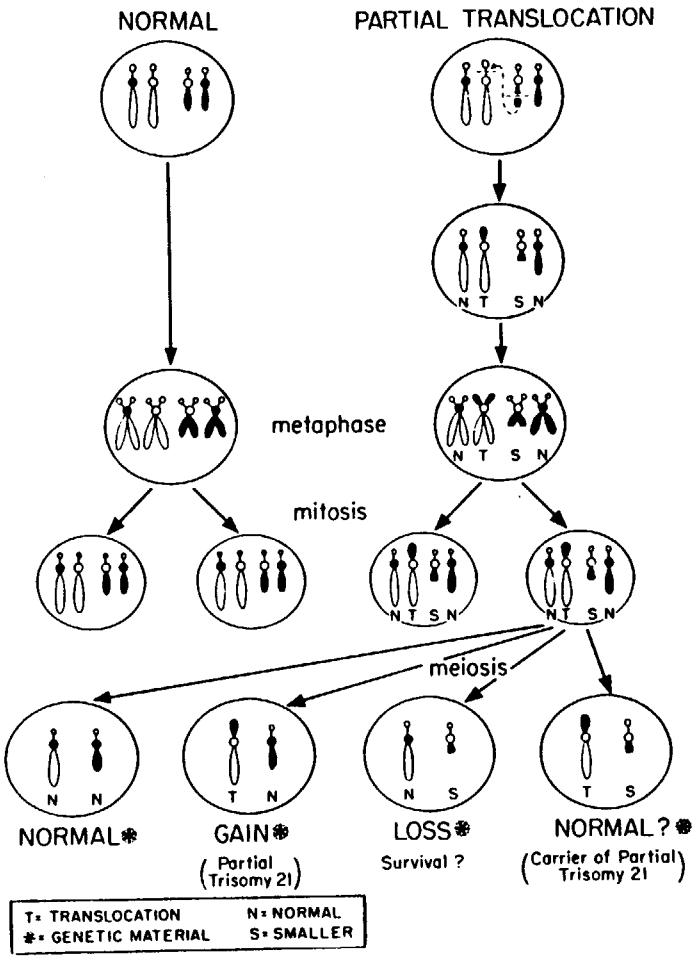

Fig. 56. The mechanism of the production of the translocated D (13-15) chromosome and the gametes possibly produced during meiosis.

hence there was neither a gain nor a loss of any genetic material. The possibility, however, remains that a small segment of the short arm of the 15 or the long arm of the 21 that produced these two abnormal chromosomes, undetected with the cytogenetic techniques now available, was lost during the translocation.

1027651

REFERENCES

1. Ohno, S., Trujillo, J. M., Kaplan, W. D., Kinosita, R., and Stenius, C. Nucleolus-organisers in the causation of chromosomal anomalies in man. Lancet 2, 123-126, 1961.

2. Nowell, P. C. and Hungerford, D. A. A minute chromosome in human chronic granulocytic leukemia. Science 132, 1497, 1960.

3. Goh, K. O. Smaller G chromosome in irradiated man. Lancet 1, 659-660, 1966.

Chromosomal Breaks in Women Taking Birth Control Pills

Kong-oo Goh

Chromosomal breaks have been reported in association with irradiation, virus, anticancer drugs, and certain chemicals. In the course of our studies in normal persons, we found persistent chromosomal breaks in a woman who had been taking birth control pills for 3 months (Table 21). In view of the possibility that the breaks were caused by the oral contraceptives, we studied four other women who were taking the drugs (Table 22) and also performed a series of experiments.

All metaphases were obtained from the peripheral-blood leukocytes cultured by our standard method. Crossed cultures were made of normal leukocytes incubated with the plasma obtained from women while taking and after they stopped taking the drugs. An abnormal cell was defined as any metaphase having one or more abnormal chromosomes without the acentric fragment (Fig. 57). An X_1 cell was defined as any metaphase containing one or more abnormal chromosomes accompanied by one or more acentric fragments (Figs. 58, 59).

Table 23 summarizes the results of the cytogenetic studies of the five women who had been taking the oral contraceptives for varying periods at the time of the cell cultures. The frequency of chromosomal breaks varied from 6% to 12% with an overall average of 9.9%, much higher than the 0.8% found in the normal controls (Table 24). The lowest incidence of breaks occurred in a woman who had taken the pills for only 6 weeks before the cytogenetic studies (Table 23, Case 2). The percentage of breaks returned almost to the normal range in Case 1 and to the normal range in Case 3, 6 and 12 weeks after the women had stopped taking the pills.

If the chromosomal breaks in these women were caused by the

1027652

TABLE 21

Results of Cytogenetic Studies of Case 1

Date	Chromosomal No. <45	45	46	47	>47	Total	%2N	Breaks Chromosomal No(%)	Breaks Chromatid No(%)	Abnormal Chromosomes Dicentrics No(%)	Abnormal Chromosomes Translocation No(%)	Abnormal Chromosomes S.G.* No(%)	Abnormal Cells X_1 No(%)	Abnormal Cells Others No(%)	Abnormal Cells Total No(%)
	——No. of Metaphases——														
Nov.19,1965§	6	18	75	1	0	100	75	12(12)	0	0	0	2(2)	12(12)	2(2)	14(14)
Mar.17,1966†	4	4	34	0	0	42	81	9(21)	0	0	0	1(2.4)	9(21)	1(2.4)	10(24)
Dec.16,1966	2	3	90	2	3‡	100	90	14(14)	5(5)	4	0	2(2)	12(12)	7(7)	19(19)
Dec.19,1966§	1	0	25	1	0	27	93	8(30)	1(3.7)	1(3.7)	0	0	7(26)	1(3.7)	8(30)
Jan.23,1967	1	6	93	0	0	100	93	11(11)	2(2)	2(2)	0	0	10(10)	2(2)	12(12)
Jan.23,1967	2	1	94	1	2‖	100	94	12(12)	2(2)	0	0	0	12(12)	2(2)	14(14)
Jan.30,1967	3	2	94	1	0	100	94	11(11)	3(3)	1(1)	0	1	11(11)	2(2)	13(13)
Mar.17,1967¶	2	3	94	1	0	100	94	3(3)	1(1)	1(1)	0	1	3(3)	3(3)	6(6)

* Smaller G chromosome, Figure 57

† Two weeks after mumps with complications

‡ One tetraploid

§ Three days after influenza vaccination

‖ One endoreduplication

¶ Six weeks after discontinuation of pills

TABLE 22

Type of Contraceptives Used by 5 Women

Case	Drugs (Trade Names)	Composition: Progestogen	Composition: Estrogen
1	Ortho Novum	Novethindrone, 2 mg	Mestranol, 0.1 mg
2	Oracon	Dimethisterone, 25 mg	Ethinyl estradiol
3	Ortho Novum	Novethindrone, 2 mg	Mestranol, 0.1 mg
4	Enovid (2 yrs)	Novethyndrel, 5 mg	Mestranol, 0.075 mg
	Ortho Novum (SQ) (2 yrs)		Mestranol, 0.08 mg
5	Ortho Novum (SQ)		Mestranol, 0.08 mg

1027653

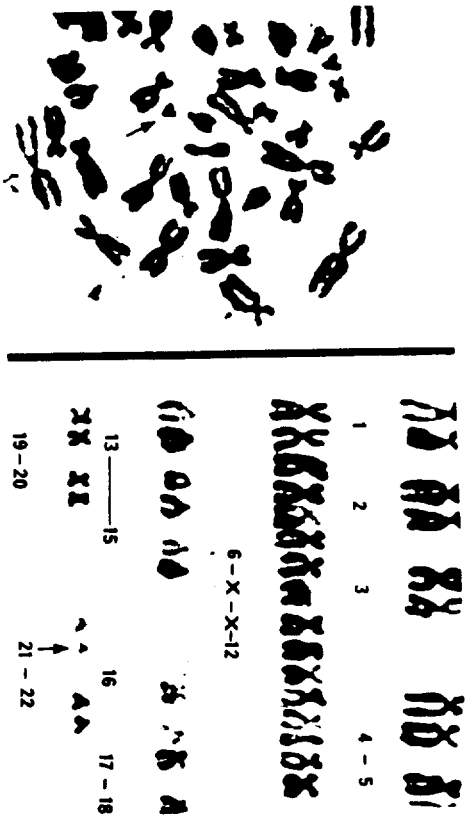

Fig. 57. A metaphase and its karyotype obtained from Case 1 showing a smaller G chromosome (arrowed). This is an abnormal cell and not an X_1 cell (no fragment found).

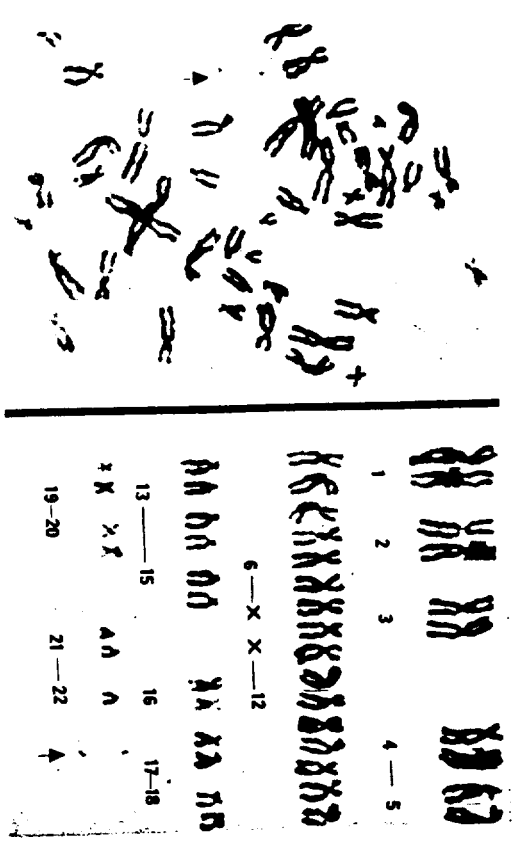

Fig. 58. A metaphase and its karyotype obtained from Case 3 showing a chromosomal break in a G chromosome. This cell is an X_1 abnormal cell.

TABLE 23

Results of Cytogenetic Studies of Five Women Taking Birth Control Pills

Case	Chromosomal No. <45	45	46	47	>47	Total	%2N	Breaks: Chromosomal No(%)	Breaks: Chromatid No(%)	Abnormal Chromosomes: Dicentrics No(%)	Abnormal Chromosomes: Translocation No(%)	Abnormal Chromosomes: S.G.* No(%)	Abnormal Chromosomes: Rings	Abnormal Cells: X_1 No(%)	Abnormal Cells: Others No(%)	Abnormal Cells: Total No(%)
	No. of Metaphases															
1†	14	30	446	5	5	500	89	60(12)	12(2.4)	7(1.4)	0	5(1)	0	57(11.4)	15(3)	72(14.4)
2(1 1/2)‡	0	7	87	2	3	99	88	6(6)	0	1(1)	3(3)	0	0	6(6)	4(4)	10(10)
3(24)	0	3	100	1	1	105	95	11§(10.5)	3(2.9)	1(1)	2(1.9)	3(2.9)	1(1)	11(10.5)	6(5.8)	17(16)
4(48)	2	0	98	0	0	100	98	8(8)	2(2)	0	2(2)	1(1)	0	8(8)	7(7)	15(15)
5(24) a	11	7	79	3	0	100	79	7(7)	3(3)	1(1)	0	1(1)	0	6(6)	3(3)	10(10)
b	5	10	85	0	0	100	85	7(7)	3(3)	0	0	0	0	7(7)	1(1)	8(8)
Total	32	57	895	11	9	1004	89	99(9.9)	23(2.3)	10(1)	7(0.7)	10(1)	1	95(9.5)	36(3.6)	132(13.2)

* Smaller G chromosome

† Summation of the Table21 (excluding March 17, 1966, December 19, 1966, and March 17, 1967)

‡ The parenthesized numbers indicate number of months patients have been taking pills

§ One had a direct chromosomal break of a G chromosome (Fig. 58)

1021654

TABLE 24

Results of Control Cytogenetic Studies of the Donors' Leukocytes

Leukocyte Donors	Chromosome Number: <45	45	46	47	>47	Total	% 2N	Breaks: Chromosome No.	Chromosome %	Chromatid No.	Chromatid %
	No. of Metaphases										
Aa	0	4	78	0	0	82	95	0		1	1.2
b	1	7	92	0	0	100	92	1	1	4	4
B	4	2	53	0	0	59	90	1	1.7	2	3.4
C	0	1	98	0	1	100	98	1	1	5	5
Total	5	14	321	0	1	341	94	3	0.8	12	3.5

TABLE 25

Results of the Cytogenetic Studies of Normal Leukocytes Cultured with Plasma Obtained from Women During and After Use of Birth Control Pills

Leukocyte Donors	Plasma Donors	Chromosomal No.: <45	45	46	47	>47	Total	%2N	Breaks: Chromosomal No(%)	Chromatid No(%)	Abnormal Chromosomes: Dicentrics No(%)	location No(%)	S.G.* No(%)	Abnormal Cells: X_1 No(%)	Others No(%)	Total No(%)
		No. of Metaphases														
During Use of Pills																
A	3	0	1	74	0	0	75	99	4†(5.3)	0	1†(1)	0	0	3(4)	0	3(4)
B	4	0	3	54	2	1	60	90	8(13)	0	0	1(1.7)	0	8(13)	2(3.3)	10(16.7)
C	4	1	4	95	0	0	100	95	12(12)	3(3)	0	2(2)	0	12(12)	2(2)	14(14)
Total		1	8	223	2	1	235	95	24(10.2)	3(1.3)	1	3(1.3)	0	23(10)	4(1.7)	27(11.5)
After Discontinuation of Pills																
B	1(12)‡	1	7	91	1	0	100	91	2(2)	2(2)	0	0	0	2(2)	0	2(2)
	3(8)‡	1	8	90	0	1§	100	90	1(1)	2(2)	0	0	0	1(1)	0	1(1)
Total		2	15	181	1	1	200	90	3(1.5)	4(2)	0	0	0	3(1.5)	0	3(1.5)

* Smaller G chromosome

† Two breaks in one metaphase with a dicentric chromosome (X_1) as shown in Figure 59

‡ The parenthesized numbers indicate weeks after discontinuation of pills

§ Endoreduplication

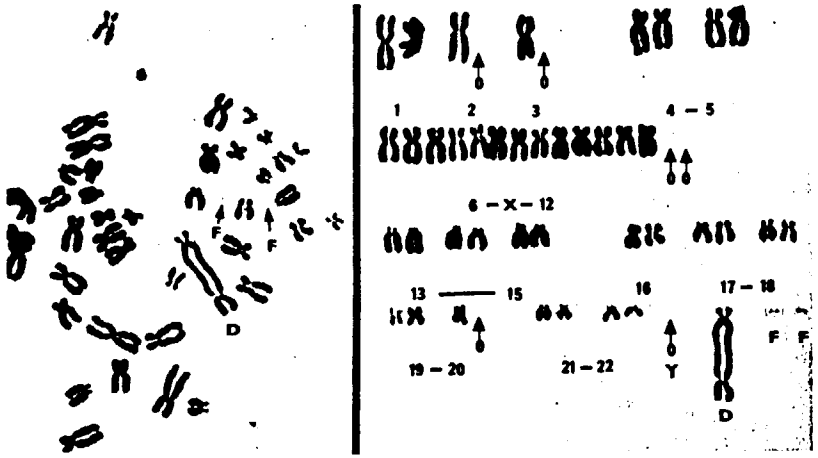

Fig. 59. A 41-chromosomes metaphase and its karyotype obtained from a crossed culture of normal leukocytes from Donor A incubated with the plasma obtained from a woman (Case 3) while she was taking contraceptives. Shown are a dicentric (D) chromosome and two pairs of fragments (F). The arrows with white circles indicate missing chromosomes. The small stained body in the metaphase at 12 o'clock was an artifact (not seen under direct microscopic examination). This cell is an XY abnormal cell.

imbalance of hormones in their blood, then cross experimental cultures should also cause chromosomal breaks in normal donors' leukocytes. Leukocytes from three normal men (Table 24) were cultured with the plasma from the women who were taking the pills. A frequency of 10.2% (range 5.3 - 13%) chromosomal breaks was found in these cultures as summarized in the upper portion of Table 25. A normal range of chromosomal breaks (lower portion of Table 25) was found in a normal man's leukocytes cultured with the plasma obtained from Cases 1 and 3, after they had stopped taking the pills. These preliminary findings suggest that birth control pills may cause chromosomal breaks as do some other drugs. The most interesting point of this observation is that the breaks returned to normal about 6 weeks after discontinuation of the drug. This indicates that these individuals are capable of removing the "mutant cells." Direct in vitro effects of the hormones, if any, on the human leukocyte chromosomes, and crossed experimental cultures with normal women's leukocytes are now being studied.

1027655

The objective of this aspect of the program is to apply radioisotopic test compounds in (1) detection of tumors, (2) measurement of functional disorders, and (3) diagnosis of metabolic defects. The agents are radioactive compounds already available, or ones newly synthesized and tested in animals. This effort requires the skills of a number of staff members, particularly in organic chemistry, pharmacology, and instrumentation, and it requires animal studies on the application of radiopharmaceuticals in human diagnostic procedures. The final step of the sequence involves the clinical trials in the Medical Division's research hospital. Because of our major interest in both hematologic disorders and radiation damage to hematopoietic tissue, we have during recent years sought for methods of scanning the bone marrow by radioactive agents. Our clinical experience has been enlarged during the past year, principally in the use of sulfur sol colloids of technetium-99m, but this preparation remains less than ideal for marrow scanning. Advances in animal work with ferric oxide colloids indicate that such compounds deserve clinical trial, and we plan to undertake them when adequate testing has been completed. Progress in scanning depends on support in new instrument design and scanning technology.

Factors Affecting the Distribution of Hydrous Ferric Oxide Colloid

R. L. Hayes, J. E. Carlton, B. L. Byrd, and J. J. Rafter

By virtue of its scavenger nature, hydrous ferric oxide can be labeled with a number of different radionuclides other than those of iron. Stable colloid preparations of these materials with varying particle sizes can readily be prepared. When administered intravenously these colloids are taken up by the reticuloendothelial cells in the bone marrow, liver, and spleen. In animals, such preparations administered at the milligram per kilogram level appear to be innocuous, the iron contained in the colloid dose eventually entering the iron pool. Because of these characteristics we believe that colloidal hydrous ferric oxide may have potential as an agent for bone-marrow scanning. Factors that affect the distribution of this material are being studied in animals with particular emphasis placed on enhancement of bone-marrow uptake. Factors under investigation are numbers of particles administered, particle size, stabilizer, and surface and charge effects.

One method of producing hydrous ferric oxide colloid is by the heat-hydrolysis of dilute solutions of ferric chloride. When radio-

nuclides of gallium are present during the hydrolysis, they are bound by the colloid particles, even though the final pH is less than 3. This is in contrast to other radionuclides so far tested. An advantage of this method of production is that the particle size of the colloid is rather uniform and can be varied by alterations in the heating rate and concentration of ferric chloride (see page of this report). Both ^{68}Ga ($T_{\frac{1}{2}}$ = 68 min) and ^{67}Ga ($T_{\frac{1}{2}}$ = 78 hr) have suitable characteristics for use as colloid labels for possible diagnostic procedures.

A heat-hydrolysis colloid preparation labeled with gallium and having a particle size of approximately 10 millimicrons has been studied extensively in the rabbit. Figure 60 shows the effect of numbers of particles (shown as milligrams of iron per kilogram) administered on its distribution. Clinical dextran (80 mg/kg body weight) was used as a stabilizer; the pH of the preparation was adjusted to 6 with sodium acetate after the addition of dextran. The volume of solution injected per kilogram of body weight was held constant except at the 4 mg Fe level where the volume was 1.4 that

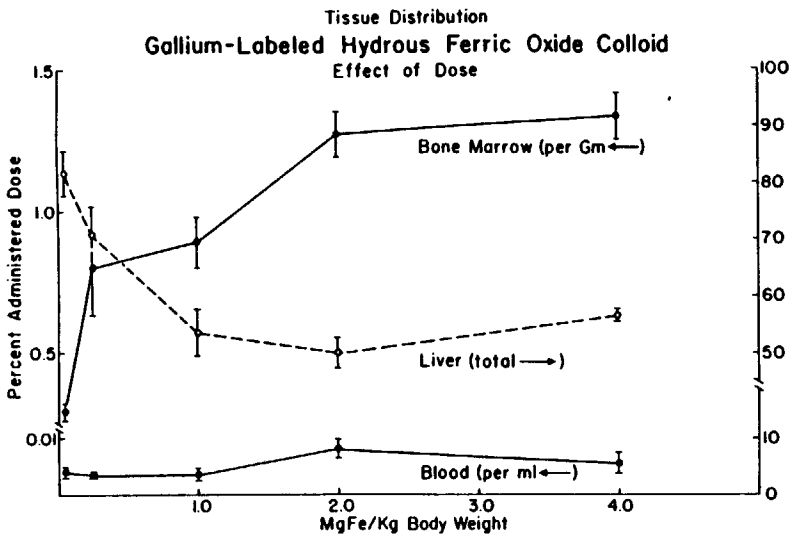

Fig. 60. The effect of numbers of colloid particles (mg Fe/kg) on the distribution of ^{72}Ga-labeled hydrous ferric oxide colloid in the rabbit (10 millimicron diameter). Stabilizer dextran (Abbott) was administered at the level of 80 mg/kg. The volume administered per kilogram body weight was held constant and the time of sacrifice was 1 hr except at the 4 mg level where there the volume was 1.4 times as great and the sacrifice time was 2 hr. All points are the averages for 4 or more animals. The vertical lines are the standard deviations of the means.

1027b5b

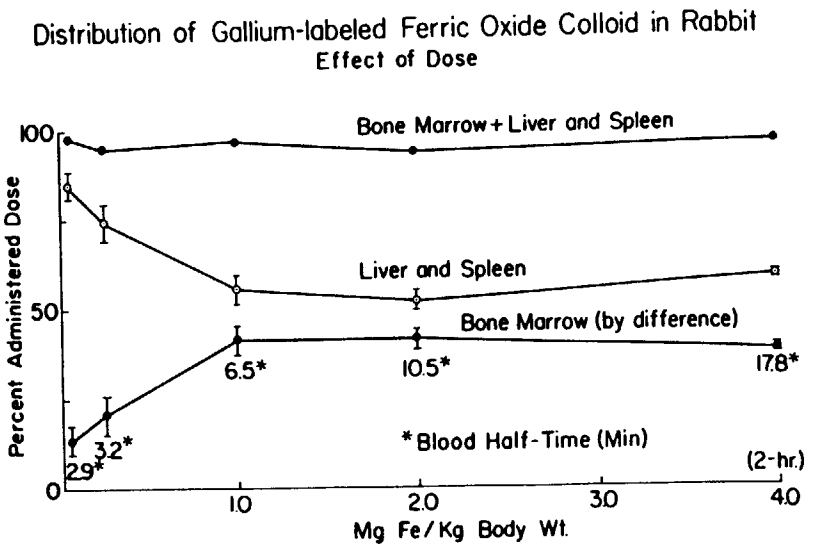

Fig. 61. The effect of numbers of colloid particles on the distribution of ^{72}Ga-labeled hydrous ferric oxide colloid in the rabbit. Data are from the studies shown in Fig. 60. The percentage of the dose in the total bone-marrow organ was estimated from the known amounts in the liver and spleen and an approximation of the percentage in the other tissues.

at the other levels. In keeping with the observations of others with other colloid preparations the blood disappearance half-time increased with an increase in the dose administered (see asterisks in Fig. 61). This was accompanied by a marked decrease in the deposition in the liver. The liver uptake was measured by both total-organ count and by multiple sampling. At low colloid doses, the concentration (%/g) in the liver was highly variable from site to site becoming uniform at the higher dose levels. To simplify the experimental procedure, the femur was the only bone-marrow site sampled; the total content was assayed, however. Accordingly, the dramatic increase seen in the concentration in the bone marrow does not necessarily represent the behavior of the bone-marrow organ as a whole. On the other hand, Fig. 61 does show a close parallel between the change in the estimated deposition in the total bone-marrow organ and the change observed in the concentration in the femur shown in Fig. 60.

The rate at which foreign colloidal material is removed from the blood can be greatly decreased by a sufficient increase in the total number of particles administered. Also the blood clearance of colloids at low dose levels is governed mainly by hepatic blood flow. These results suggest that in the rabbit the decrease in the clearance rate

with increasing colloid dose is responsible in part for the greater blood flow through the liver-spleen compartment compared to that through the bone-marrow compartment. This in turn results in an enhanced marrow deposition of the colloid. Similar results might be obtained in man, although not necessarily of the same magnitude. If this dose (particle number) enhancement of bone-marrow deposition is not diminished by a decrease in the particle size, a considerable reduction in the iron dose required to produce increased bone-marrow uptake may be possible. The effect of particle size on bone-marrow deposition is now under investigation.

The effects of the type of colloid stabilizer used on the deposition of gallium-labeled hydrous ferric oxide in the bone marrow are quite

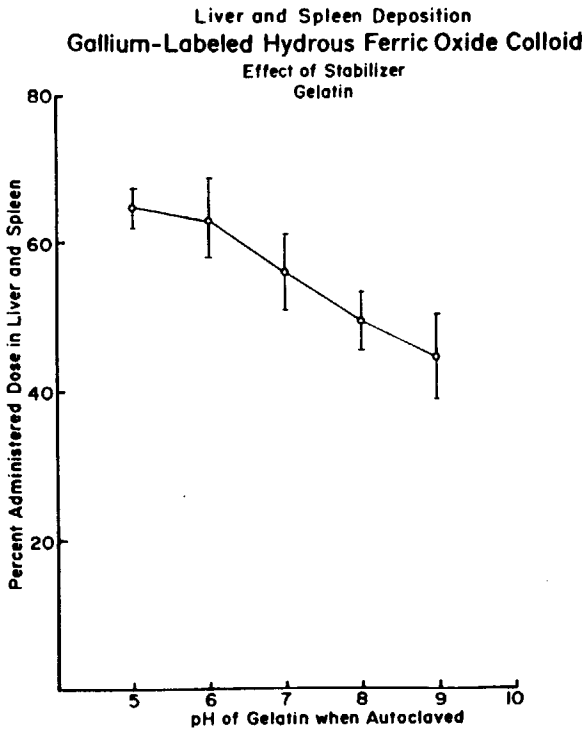

Fig. 62. The effect of pH adjustment of gelatin (Type A) before autoclaving (20 min) on the distribution of ^{72}Ga-labeled hydrous ferric oxide colloid (1 mg Fe. kg body wt; 10 millimicron diameter) in the rabbit. The gelatin preparations were administered at the level of 20 mg kg body weight. The vertical lines are the standard deviations of the means.

1027657

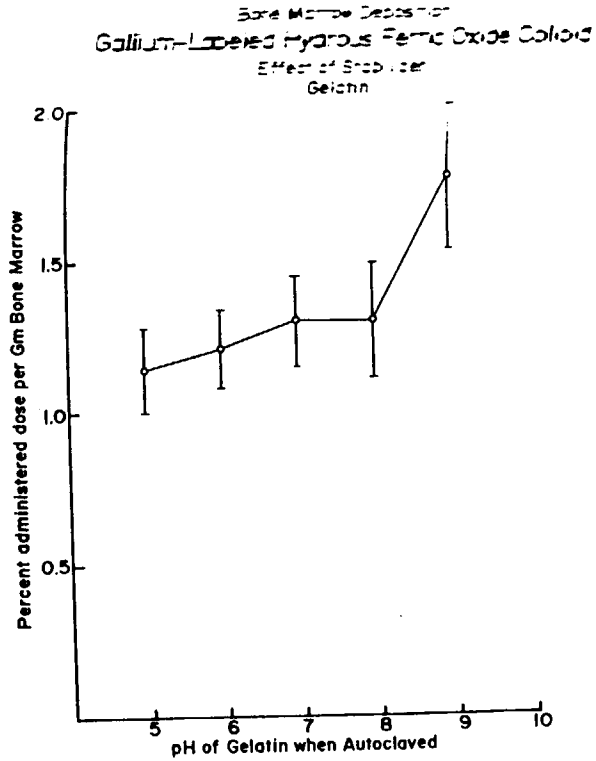

Fig. 63. Bone marrow data from the studies shown in Fig. 62.

varied. Previous studies have shown that in general bone-marrow uptake is increased by an initial increase in the dose per kilogram of dextran or gelatin stabilizer administered with the colloid. With increasing stabilizer dose the uptake plateaus and in some instances decreases. Gelatin is considerably more effective in enhancing bone-marrow deposition than is dextran. Effectiveness of different gelatin products also varies considerably. Type B gelatin produces higher uptakes than type A. Furthermore, the manner in which a gelatin product is processed may considerably change the preparation's effectiveness. Fig. 62 and Fig. 63 show the results of a study of the effect on distribution of gelatin pH when the gelatin stock solution was autoclaved for 20 min. The colloid dose was held at one milligram of iron per kilogram of body weight. The amount of gelatin and the volume of solution administered were also held constant. The decrease in the liver deposition (Fig. 62) and the associated increase in the femoral bone-marrow concentration (Fig.

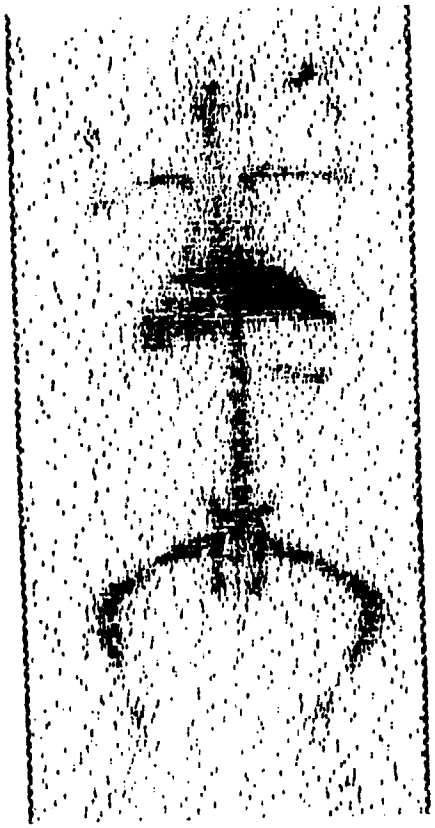

Fig. 64. Bone marrow scan of a rabbit given ^{68}Ga-labeled hydrous ferric oxide colloid (2 mg Fe/kg body weight; 10 millimicron diameter; gelatin autoclaved at pH 8 used as stabilizer).

63) as pH was increased is apparent. These changes in colloid distribution could be associated with changes in the isoelectric point and molecular weight of the gelatin preparations; however, these constants have not yet been evaluated.

Another approach to the preparation of labeled hydrous ferric oxide colloid is the use of base-induced hydrolysis (the use of sodium acetate, sodium carbonate, etc). A number of other radionuclides in addition to those of gallium can be used as labels with this method of preparation. In general, although excellent bone-marrow deposition has been obtained with this type of colloid, the results have been inferior to those obtained with the gallium-labeled heat-hydrolysis preparation.

1027658

The main difficulty has been in nonuniform particle size resulting in high residual blood levels, although the bone-marrow uptake was often excellent. Attempts to obtain monodispersed preparations are continuing.

Figure 64 illustrates the type of rabbit bone-marrow scan that can be obtained with a ^{68}Ga-labeled heat-hydrolysis colloid. The liver of this animal contained only 34% of the administered dose, the concentration in the femoral bone marrow was 1.6%/g, and the estimated content of the total bone-marrow organ was 55%.

Indium-113m as a Kidney and Bone Scanning Agent

R. L. Hayes, B. L. Byrd, and J. E. Carlton

The generator-produced radionuclide ^{113m}In is of considerable interest, as a radiopharmaceutical label. It has a 1.7-hr half-life, a main gamma emission of 390 kev and a parent (^{113m}Sn) half-life of 118 days.

Indium in the citrate form when administered intravenously in microgram quantities is diffusely distributed in animals, the blood having the highest organ content at periods up to 3 hr after administration. This behavior is due to the binding of indium by plasma proteins. (See page 120 of this report). As with gallium, the indium-binding protein sites can be saturated by administration of higher levels of indium with the excess of indium then depositing mainly in the kidneys and bone. However, this approach is not practical from a pharmaceutical standpoint since indium is quite toxic.

It has been found in in vitro studies that the protein-binding pattern for indium is similar to that of gallium. Accordingly, in vivo studies of the effect of gallium on the distribution of pseudo carrier-free levels of indium have been made with the use of high specific activity ^{114m}In ($T_{\frac{1}{2}}$ = 14h) for experimental convenience. Similar results have been obtained with ^{113m}In. The effect of gallium citrate on the distribution of ^{114m}In citrate is shown in Fig. 65. The remarkable and somewhat unexpected finding was that the presence of gallium, even at low levels, produced a quite dramatic deposition of indium in the kidney. Other studies indicate that this high level of kidney deposition persists for long periods of time. This is in marked contrast to the deposition of gallium in the kidney. Columns 1 and 2 of Table 26 show the results of a double-label experiment using ^{114m}In and ^{72}Ga. Column 3 contains the results of a previous study with ^{68}Ga for comparison. Note that the deposition of gallium in the kidney at this 3-hr period is considerably less than that for ^{114m}In.

These studies indicate that with this preparation ^{113m}In may be of use as a kidney-scanning agent. On the basis of an extrapolation from animal data, the radiation dose to the human kidney from ^{113m}In in this form is estimated by the ORAU Radiation Safety Office to be 0.3 rads per millicurie administered.

In addition to possible kidney scanning, Fig. 65 shows that ^{113m}In with added stable gallium may also have potential as a bone-scanning agent. For this purpose, it would be desirable to minimize the amount of gallium used. Other animal studies have indicated this might be accomplished by the use of chelating agents other than citrate. Table 27 shows a comparison of the distribution of citrate and nitrilotriacetic acid (NTA) preparations of ^{114m}In in the rat with the use of an added gallium level of 0.5 milligram Ga/Kg of body weight. In addition to a substantial increase in the bone-blood concentration ratio (2.5 vs 6.0) there was a marked decrease in the

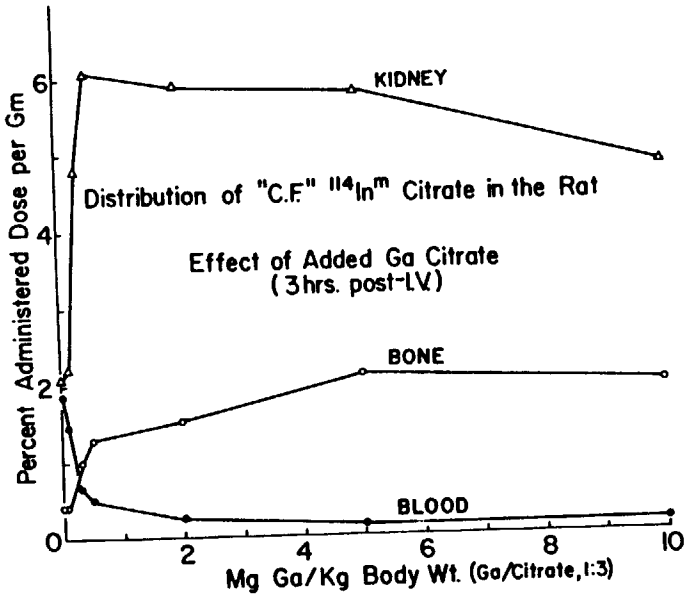

Fig. 65. The effect of added gallium citrate on the distribution of pseudo carrier-free ^{114m}In in the rat. Bone values are the averages of rib, femur, and calvaria values.

1027659

TABLE 26

Distribution of ^{114m}In, ^{72}Ga, and ^{68}Ga (Citrate) in the Rat as Influenced by Stable Gallium*

Tissue	^{114m}In		^{72}Ga		^{68}Ga
	Percent Inj. Dose/g				
Liver	0.27		0.04		0.07
Spleen	0.05		0.02		0.05
Kidney	5.78	(0.23)**	0.25		0.29
Lung	0.16		0.04		0.08
Muscle	0.03		0.01		0.02
Rib	3.11	(0.20)	3.12	(0.25)	4.04
Femur	1.90	(0.12)	1.92	(0.14)	2.55
Calvaria	1.31	(0.09)	1.47	(0.13)	1.42
Blood	0.14	(0.02)	0.05	(0.01)	0.16

*5 mg Ga/kg body wt.; 3:1 molar ratio citrate to Ga.: killed 3 hr after I.V. administration.
**Standard deviation of the mean.

TABLE 27

Effect of Gallium Citrate and Gallium NTA on the Distribution of ^{114m}In in the Rat

Tissue	Citrate		NTA	
	Percent Inj. Dose/g			
Kidney	6.10	(0.76)**	1.97	(0.14)
Rib	1.70	(0.14)	2.90	(0.26)
Femur	1.29	(0.07)	2.00	(0.18)
Calvaria	0.87	(0.04)	1.35	(0.12)
Blood	0.50	(0.06)	0.33	(0.04)

*0.5 mg Ga/kg body wt.; 3:1 molar ratio of chelate to Ga.; killed 3 hr after I. V. administration.
**Standard deviation of the mean.

deposition in the kidney with NTA, a desirable effect that would tend to decrease the radiation dose to the kidneys if ^{113m}In were used as a bone-scanning agent in this form. This potential use of ^{113m}In is undergoing further investigation.

Figure 66 shows a ^{113m}In bone scan of a rabbit made 3 hr after administration of an NTA preparation with an added gallium level of 1 mg Ga/Kg body weight.

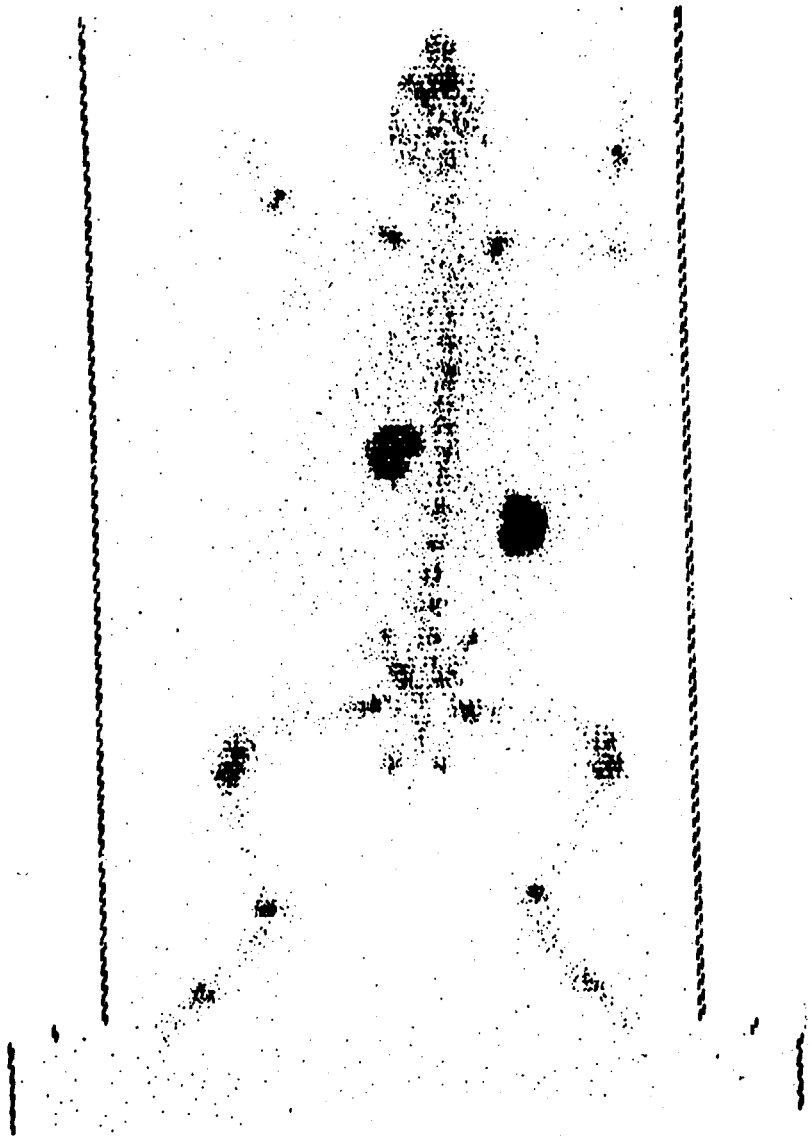

Fig. 66. Bone scan of a rabbit given 113m/n nitrilotriacetic acid (NTA) with added gallium NTA at a level of 1 mg Ga. kg body weight. Scan 3 hr after administration.

1027660

Measurement of Hydrous Ferric Oxide Colloid Particle Size

R. L. Hayes and J. E. Carlton

When colloids are used as agents for the study of hepatic blood flow or to assess the function of the reticuloendothelial system (RES), it is highly desirable to use a colloid preparation that has a reasonably uniform particle size. If this type of preparation is not used, the test results will be difficult to interpret. With bone-marrow scanning, high residual blood levels may occur. Ultracentrifugal methods have been used to measure particle size in developmental studies of labeled hydrous ferric oxide colloid as a bone-marrow scanning agent.

Hydrous ferric oxide colloids prepared by base hydrolysis of ferric

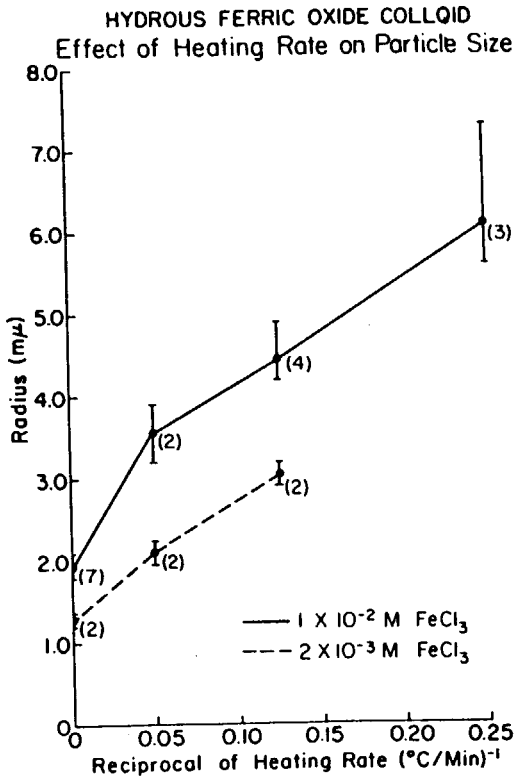

Fig. 67. Effect of concentration and heating rate on the particle size of hydrous ferric oxide colloid. Vertical lines represent the range. Numbers in parentheses are the runs made.

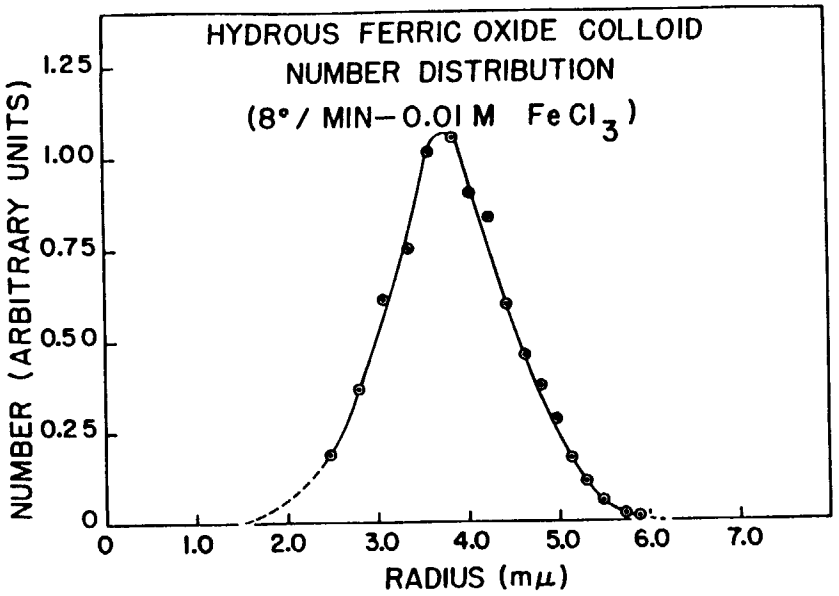

Fig. 68. Number distribution of particle size for a hydrous ferric oxide colloid preparation.

chloride usually have rather broad particle-size ranges. On the other hand, colloids prepared by heat-hydrolysis of dilute solutions of ferric chloride generally have a reasonably uniform size. Furthermore, the particle size of the colloid can be varied by alterations in the heating rate and the ferric chloride concentration. Figure 67 shows the results of a study of the weight average particle size of hydrous ferric oxide colloid as affected by concentration and heating rate. Although the particle size measurements shown in Fig. 67 cover only a size range of a factor of 5, the number of particles per unit mass (assuming no change in particle density) varies by a factor of 125. We believe that the colloids in the small particle size range may be of particular use in bone-marrow scanning, since this small size will necessitate using only a modest weight of iron to achieve an RES stressing dose (see page 105 of this report). An example of the uniformity of particle size in these preparations is shown in Fig. 68. This analysis was made with the sedimentation velocity method of Nichols et al.[1] Their method assumes that the diffusion of the particles can be neglected; this assumption has yet to be verified for the smaller size preparations, and possibly the smaller colloid sizes shown in Fig. 67 may be somewhat in error.

1027661

REFERENCE

1. Nichols, J. B., Kraemer, E. O., and Bailey, E. D. Particle size and constitution of colloidal ferric oxide. I. J Phys Chem 36, 326-339, 1932.

Distribution of Gallium as a Function of Time and Stable Gallium Dose

R. L. Hayes, B. L. Byrd, and J. E. Carlton

In the early 1950s ^{72}Ga ($T_{\frac{1}{2}}$ = 14 hr) in the citrate form was investigated clinically as a possible diagnostic and therapeutic agent for the detection and treatment of bone lesions. A major portion of this work was carried out at the Medical Division.

It was believed then that although gallium was an avid bone seeker, at least one or more days was required for adequate differential localization in the bone. In some preliminary studies with ^{67}Ga (a gallium radionuclide available in a carrier-free form) it was noted that the distribution of gallium was dose dependent. Recent animal studies aimed at exploring the possible diagnostic use of ^{68}Ga ($T_{\frac{1}{2}}$ = 68 min) have shown that gallium distribution during the first few hours after administration is highly dose dependent. Table 28 shows that the administration of an adequate dose of carrier gallium changes the diffuse "carrier-free" distribution pattern at 2 hr to one with localization primarily in the bone and kidney. This alteration of gallium distribution by carrier gallium has been the basis for a clinical investigation of ^{68}Ga as a bone-scanning agent.

Although ^{68}Ga has been successfully used as a bone-scanning agent, its half-life (68 min) is unduly short and the collimation and shielding required because of its high-energy gamma emissions places restrictions on the type of scanning equipment that can be used. Another isotope of gallium, ^{67}Ga, appears to be much more suitable for scanning and could be used for camera visualization as well. It has a half-life of 78 hr, decays by electron capture, and has gamma emissions of 93 (40%), 184 (24%), 296 (22%), and 388 (7%) kev. The radiation dose associated with its use as a bone-scanning agent is estimated by the ORAU Radiation Safety Office to be only approximately 2 rads per millicurie administered. The 184- and 206-kev gamma emissions could readily be used for camera visualization as well as in rectilinear (area) scanning.

To assess the potential of ^{67}Ga for bone scanning, the distribution of gallium over a 3-day period has been investigated with respect to the effect of carrier gallium. Table 29 shows the effect of gallium carrier on the distribution of high specific activity ^{72}Ga

TABLE 28

Effect of Gallium Carrier on the 2-Hr Distribution of Gallium Citrate in the Rat

Tissue	Mg Ga/Kg Body Wt.* "CF"	1.0	5.0
	Percent Inj. Dose/g		
Liver	0.39	0.21	0.09
Kidney	0.48	1.51	3.58
Muscle	0.20	0.07	0.03
Rib	1.60	2.96	4.30
Femur	1.03	2.15	2.85
Calvarium	0.57	1.28	1.47
Blood	1.62	0.59	0.18

* Molar ratio citrate to gallium 2:1

TABLE 29

Effect of Gallium Carrier on 24-Hr Distribution of Gallium Citrate in the Rat

Tissue	Carrier Ga mg/Kg Body Wt.* "CF"	0.25	0.5	1.0
	Percent Inj. Dose/g			
Liver	0.66	0.50	0.20	0.16
Spleen	0.44	0.32	0.12	0.10
Kidney	0.53	0.40	0.40	0.39
Lung	0.16	0.12	0.06	0.04
Muscle	0.07	0.05	0.02	0.02
Rib	3.28	2.91	3.13	2.91
Femur	2.42	2.40	2.13	2.00
Calvarium	1.31	1.25	1.40	1.27
Blood	0.11	0.08	0.05	0.04

* Molar ratio citrate to gallium 3:1

1027662

in the rat 24 hr after intravenous administration. With the pseudo carrier-free dose the bone uptake was excellent, but the soft tissues contained considerable activity. As the carrier gallium was increased the blood showed a further clearance and the concentration in the soft tissue decreased markedly. The 0.5 mg Ga/kg level localized in bone only slightly less than did the 1.0 mg Ga/kg level. Accordingly the distribution for the 0.5 level at 48 and 72 hr was studied. These results are shown in Table 30 together with the distribution

TABLE 30

Distribution of ^{72}Ga in the Rat with Time (0.5mg Ga/Kg Body Wt.)*

Tissue	Time after administration (hrs.) 2	24	48	72
	Percent Inj. Dose/g			
Liver	0.20	0.20	0.23	0.23
Kidney	0.54	0.40	0.32	0.28
Muscle	0.06	0.02	0.01	0.02
Rib	2.41	3.13	3.06	2.37
Femur	1.56	2.14	1.94	1.95
Calvarium	1.11	1.40	1.25	1.12
Blood	0.55	0.05	0.02	0.02

* Molar ratio citrate to gallium 3:1

at 2 and 24 hr. The distribution remained essentially constant from 24 to 72 hr. Although the liver (highest concentration of the soft tissues other than kidney) contained a somewhat higher level of activity than might be desired, the ratio of bone concentration to liver concentration was still greater than 10 to 1. On the other hand, the ratio of bone to blood and bone to muscle approached 100 to 1. Admittedly, the distribution of strontium is much more specific for bone and the concentration in soft tissue is considerably less than it is with gallium; however, no radioisotope of strontium has the desirable half-life and radiation characteristics of ^{67}Ga. Clinical trials of ^{67}Ga are planned in the near future.

The Binding of Gallium and Indium by Blood Serum Proteins

R. E. Hartman and R. L. Hayes*

Gallium-68 and ^{113m}In are of interest as radiopharmaceuticals because of their short half-lives (1.1 and 1.7 hr, respectively) and their availability from nuclide generators. Previous studies have shown that the effect of stable gallium on the in vivo distribution of ^{68}Ga can be attributed to the binding of gallium by serum proteins. The binding capacity can be saturated with higher levels of gallium carrier leading to the specific localization of the excess gallium in bone and kidneys. Using in vitro techniques, ^{113m}In has also been shown to have a saturable binding interaction with serum proteins. The protein-binding pattern is similar for both elements. Table 31 shows the results of a series of equilibrium dialysis measurements on human, rat, and bovine blood-protein fractions. Other studies have also been made on rabbit serum fractions. In general, the binding of gallium by transferrin was stronger than that observed with indium. On the other hand, indium binding to the other serum fractions was stronger than that for gallium. Dialysis of transferrin at pH 4.6 to remove transferrin iron resulted in transferrin preparations that bound both gallium and indium to a much greater degree.

---

* Research Participant, St. Bonaventure University, N. Y.

TABLE 31

Binding of Gallium and Indium by Human, Rat and Bovine Serum Fractions

Fraction	Gallium	Indium
	μ mol bound/mg protein	μ mol bound/mg protein
Human		
Serum	0.75	0.88
Albumin	0.04	0.18
II	0.04	0.10
III	0.73	0.70
IV	0.70	1.3
Transferrin	4.7	2.8
Rat		
Serum	0.89	1.0
II	0.07	0.11
III	0.27	0.62
IV	1.0	0.98
V	0.005	0.05
Bovine		
Serum	0.89	0.82
Albumin	0.06	0.20
II	0.04	0.10
III	1.22	0.65
IV	0.12	1.2
Transferrin	0.48	0.32

1027663

The Effect of Various Metals on the Distribution of Gallium and Indium

R. L. Hayes and B. L. Byrd

In the development of ^{113m}In and ^{68}Ga as bone-scanning agents, the effect of various metal citrates on the distribution of microgram (pseudo carrier-free) quantities of both indium and gallium has been studied in the rat. Indium distribution has been studied in the presence of gallium, aluminum, zirconium, yttrium, and iron. Gallium has been studied in the presence of calcium, aluminum, iron, cerium, and lanthanum. The dramatic effect of gallium on the distribution of indium has already been discussed. (See page 111 of this report.) The presence of aluminum produced a pronounced decrease in indium concentration in the soft tissues and blood but no change in the bone deposition. With gallium, aluminum produced some decrease in gallium concentration in the soft tissues except for the kidney. There was also a pronounced decrease in the blood level but no change in that of the bone. With the exception of iron, the other metals studied had little effect on the distribution of either indium or gallium. The remarkable effect of iron on the distribution of indium is shown in Table 32. Enhanced bone deposition and decreased blood level are probably due to the saturation of unsaturated iron binding sites on transferrin by the administered iron. Similar results have been obtained with gallium.

TABLE 32

Effect of Iron Citrate on the Distribution of Indium-114m in the Rat*

Tissue	Mg Fe/kg Body Wt. 0	0.8
	Percent Inj. Dose/g	
Liver	0.67	0.41
Kidney	2.10	10.50
Muscle	0.16	0.05
Rib	0.54	2.66
Femur	0.44	1.73
Calvarium	0.27	1.21
Blood	1.90	0.66

* Killed 3 hr after I.V. administration

Scanning Technique for Determining Depth of Radioactive Foci

C. L. Edwards, R. Tanida, and Romulo J. Mora

Laminography has proved to be a valuable technique in diagnostic radiography. Similarly it is expected that depth information would frequently be a help in radioisotope scanning. This is particularly true where precise localization is needed and where scanning from both the lateral and anterior-posterior directions is not feasible.

The fine-focusing collimator lends itself to this application when the object is a small source. Repeat scans with the focal point of the collimator at different planes will readily demonstrate the depth of the radioactive source, provided the distance of the collimator to surface is known, the focal length of the collimator is known, and the same scanning techniques (spectrometer setting, speed, etc.) are used. When the focal plane of the collimator is at the level of the radioactive source, the projected image will have minimum diameter and maximum density (counts per square centimeter, Fig. 69).

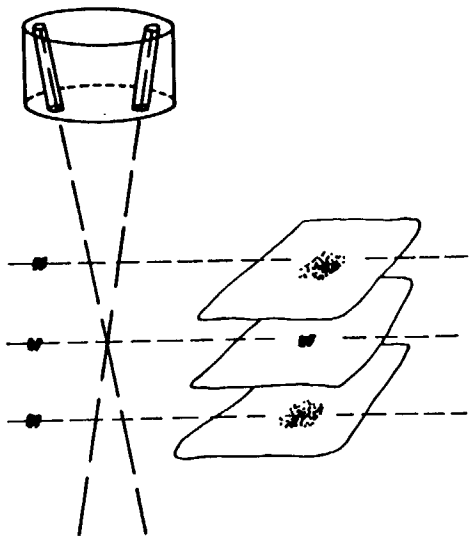

Fig. 69. Diagram showing the effect upon the image of scanning above, at, and below the plane of the collimator's focal point.

We have found this simple technique quite useful in locating resectable metastatic thyroid carcinoma (Fig. 70), and other small foci of radioactivity. After an abnormal focus of radioactivity is found, re-

1027664

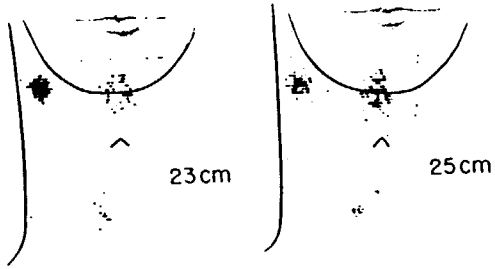

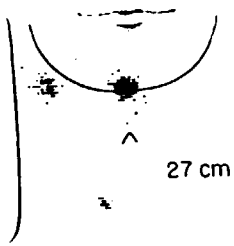

Fig. 70. Scans made five days after a dose of 100 millicuries of 131I in a patient with three small remnants of thyroid carcinoma. The lesions are in three distant planes. The distances indicate the distance of the collimator from the scanning table.

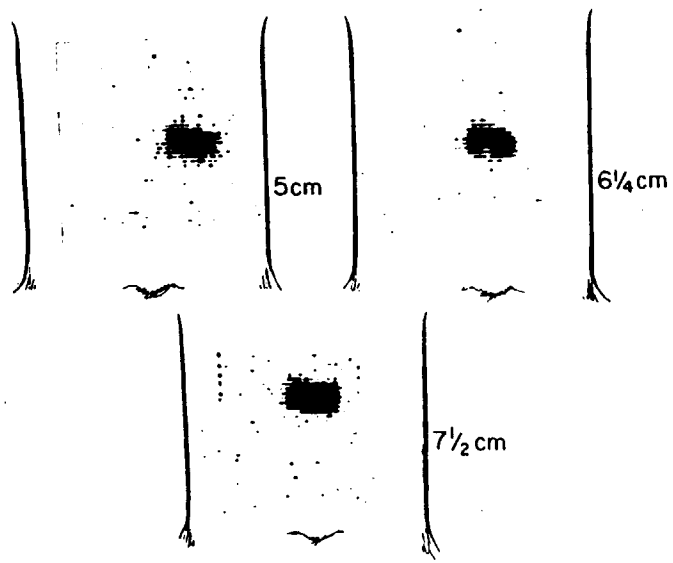

Fig. 71. Scans made five days after a dose of 100 millicuries of 131I in a patient with residual thyroid carcinoma. At surgery two small adjacent lesions were found as indicated in the scan made with the collimator 6.5 cm above the skin.

peated small scans are made over the area with the patient in the same position. The skin (or some other anatomic reference) to collimator distance is measured and recorded.

Changing the depth of focus is accomplished by merely raising or lowering the detector. The precise focal length of the collimator needs to be determined as our "5-inch fine-focusing collimator" has a focal distance of 14 cm or approximately 5-3/4 in.

The picture obtained with the focal plane passing through the object is actually the picture with the most precise representation of the shape of the object also. In one patient with residual carcinoma of the thyroid, scans had revealed a single small focus of radioactivity, which was presumed to be a small focus of residual carcinoma with only fair concentration of the isotope. Laminar scans revealed the focus to be two very small discrete foci more superficial than they had been thought to be (Fig. 71). They were subsequently resected.

Bronchiectasis Producing False-Positive Radioiodine Scan for Metastases of Thyroid Cancer

C. L. Edwards, R. Tanida, and Bill Nelson

Extra thyroidal localization of radioiodine is easily demonstrated after the thyroid gland is removed or ablated with radioiodine. These sites of accumulated radioiodine must be distinguished from foci of metastatic thyroid carcinoma especially when resection of the metastatic lesions is contemplated. Among the usual sites where radioiodine is detected upon scanning an athyrotic patient are salivary glands, saliva-stained tooth, mammary tissue, gastric mucosa, intestinal contents, urinary bladder, and ovaries.

In addition to these locations, we have found discrete foci of radioactivity at the end of the nose in one patient and in the perineum of another. The reason for the activity at these sites is unknown to us, but neither patient gives other evidence to make us suspect that the lesions are metastatic thyroid carcinoma. We were recently confronted with a localized accumulation of radioiodine in a bronchiectatic lesion of the lung, which upon scanning simulated metastatic thyroid carcinoma.

The patient is a 52-year-old woman who was found to have a papillary adenocarcinoma of the thyroid in 1962. A total thyroidectomy was attempted in two stages before her transfer to Oak Ridge. There was no evidence of lymph node or other metastases.

1027665

After a 5-millicurie dose of ^{131}I, a scan revealed several foci of radioactivity in the thyroid bed. These were excised and found to be remnants of normal thyroid tissue. After two doses of 100 millicuries of radioiodine, no further accumulation of radioiodine was seen other than the salivary glands, mouth, stomach, bowel, and urinary bladder. She was subsequently followed periodically with no evidence of further neoplastic disease until August 1967. After a 5-millicurie dose of ^{131}I, a focus of radioactivity was detected in the right lower lung field. In retrospect there was some evidence of it a year before (Figs. 72 and 73).

Localizing procedures revealed the lesion to be far anterior and near the cardiophrenic angle. X-ray laminagrams failed to demonstrate the lesion. A dose of 100 millicuries of ^{131}I was administered

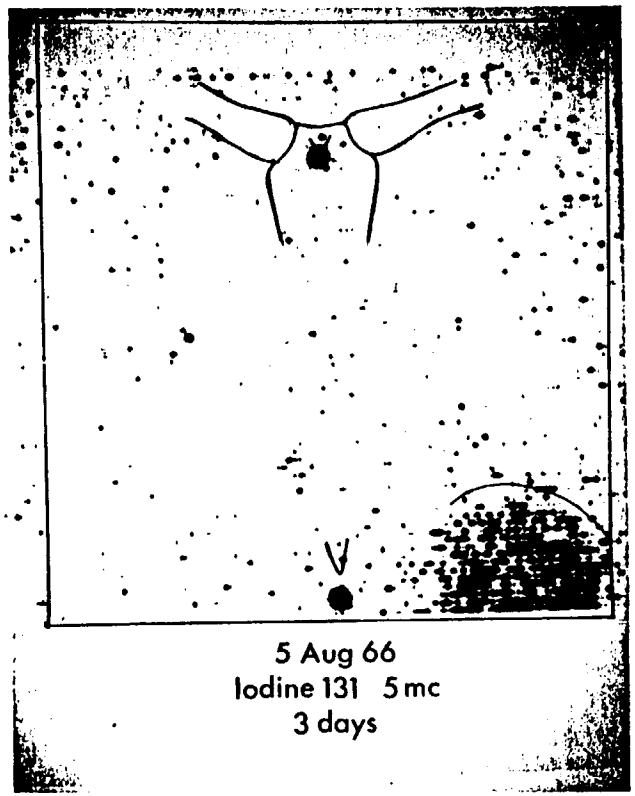

72. *Scan of the chest three days after a dose of 5 millicuries of 131I. Note the small cluster of dots to the right and above the xyphoid.*

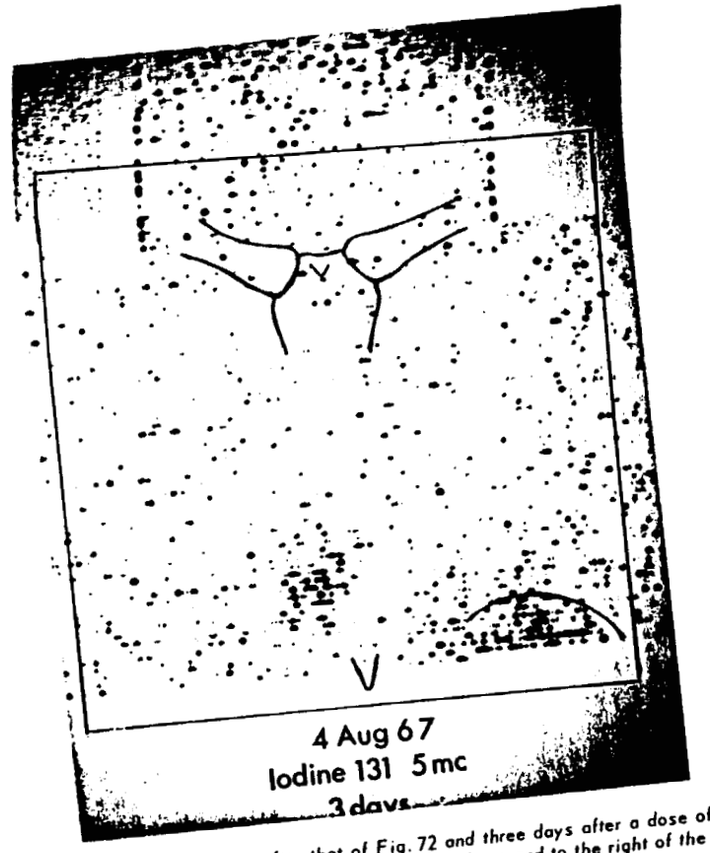

Fig. 73. Scan made one year after that of Fig. 72 and three days after a dose of 5 millicuries of 131I. Note the focus of activity above and to the right of the xyphoid.

to increase the activity within the lesion to a level that could be detected by the surgical probe detector. At thoracotomy a small nodular lesion was palpable in the tip of the median segment of the right middle lobe. The surgical probe detector confirmed this to be the site of the radioactivity. After excision, pathologic examination revealed tubular bronchiectasis. Assay of the secretions within the dilated bronchus revealed the presence of 131I, which accounted for the abnormal scan. No thyroid carcinoma or other neoplasia was found.

1027bbb

Improvements in the Whole-Body Scanning System

A. C. Morris, Jr., and William T. Pope

The Medical Division needs a radioisotope scanner that will produce whole-body scans in relatively short scanning times. This need has been filled for the past few years by a whole-body scanner whose basic framework was obtained commercially and was then modified by our mechanical and electronic shops for our applications. With the increased activity of our radionuclide development program, and our clinical use of such short-lived radioisotopes as ^{99m}Tc and ^{68}Ga, the need for a more flexible and rapid scanning system has become evident.

An extensive redesign and rebuilding of this scanner was therefore undertaken this year (Fig. 74). The original sweep speed of 40 in./min has been increased to 100 in./min with additional switch-selected speeds of 50, 25, and 10 in./min. We have standardized on five step spacings of 1/16, 1/8, 1/4, 1/2, and 1 in., also switch selected from the control panel of the scanner. To reduce the whole-body scan to a convenient size we have used, in the past, two recording ratios of 1 to 1 and 5 to 1. We found this to be an inadequate

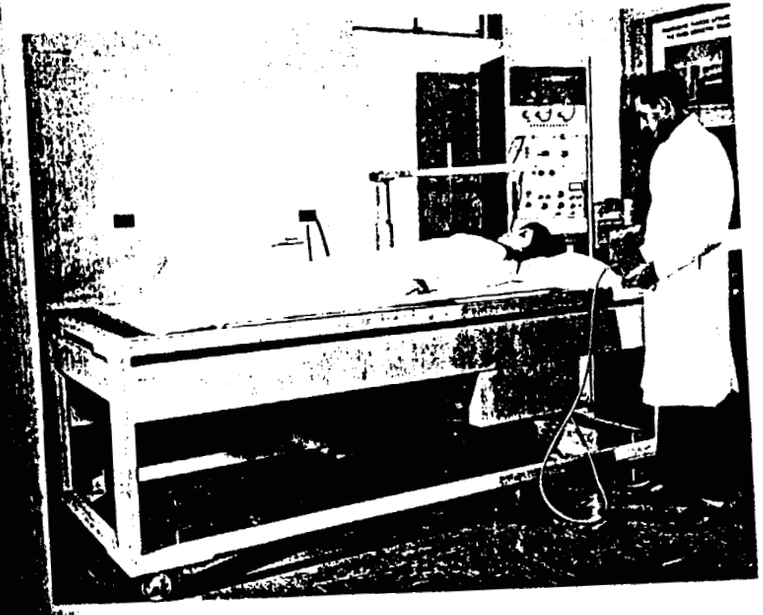

74. Photograph of patient being scanned on the rebuilt whole-body scanner.

selection, and the new recording system includes 1, 2, 5, and 8 to 1 ratios by panel selection. The scanner width control has also been improved to give a continuous variation of widths from 2 in. to the maximum of 21 in., and a remote indicator of the width has been placed on the operator's hand set-up switch box.

Other changes have been made to reduce the noise level of the drive mechanism and to increase the reliability of the scanner's operation. The rebuilt scanning system has now been returned to operation and initial results with it are promising.

Correlation of Erythropoiesis and Reticuloendothelial Function in Rabbits

Y. Ito, Francis A. Goswitz, and Bill Nelson*

In most medical centers ^{52}Fe is unobtainable and intravenous injections of radiocolloids must be used for bone-marrow scanning. Suitable colloidal particles are rapidly removed from the blood by phagocytic cells of the reticuloendothelial (RE) system present in red marrow and other tissues, especially the liver. The main clinical interest in red marrow concerns its production of blood cells, and the RE function is incidental aside from utility in providing scans to demonstrate the distribution and activity of hemopoietic marrow. To help in the interpretation of these scans, we designed experiments to detect (1) changes in erythropoiesis after administration of drugs reported to alter RE function, and (2) effects of stimulation and depression of erythropoiesis on the localization in the marrow of intravenously administered radiocolloids.

Colloidal ^{198}Au was injected intravenously into rabbits before and after specific drugs had been administered to produce the desired experimental effects. The distribution of the radiocolloid was assessed by scanning, external counts with the detector over the sacrum, and radioassay of tissue. Erythropoietic activity was determined from marrow smears and histologic sections obtained by needle aspiration and at autopsy.

The erythropoietic responses to agents reported to influence RE activity are depicted in Fig. 75, with normalization to control values.

* Damon Runyon Foundation Fellow from Japan. Present address: Department of Radiology; Research Institute for Tuberculosis, Leprosy, and Cancer; Tohoku University; 62 Kita 4 bancho; Sendai, Japan.

1027667

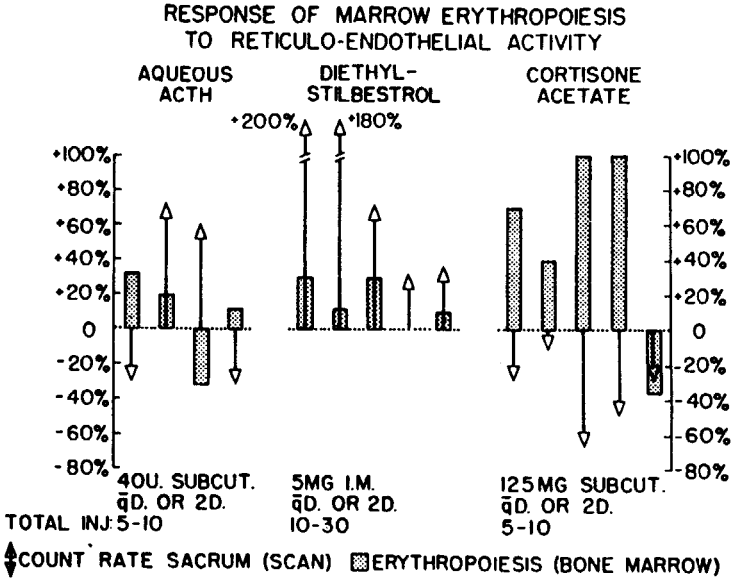

Fig. 75. Percentage changes from pretreatment values in sacral counting rate during marrow scan and in erythropoiesis determined by evaluation of red-cell precursors in New Zealand rabbits treated with ACTH, diethylstilbestrol, or cortisone.

The estrogen-treated rabbits all had increased marrow concentrations of ^{198}Au and increased erythropoiesis. Three of four rabbits given adrenocorticotropic hormone (ACTH) had opposite changes in the sacral counting rate and the number of red-cell precursors. Cortisone acetate suppressed the localization of ^{198}Au in the marrow of five rabbits, but only one had a reduction in the number of erythroid precursors in the marrow. The scans before and after cortisone treatment of one of these rabbits are shown in Fig. 76. Despite the decrease in concentration of radiogold in the marrow, red-cell precursors in this animal increased (Table 33).

A summary of the data comparing marrow erythropoiesis and RE cell activity is shown in Table 34. Of the 33 animals in the experimental groups, good correlation between the marrow ^{198}Au concentration and the number of red-cell precursors was found in 18 rabbits and fair correlation in 5 rabbits. In 10 animals, or 30% of the total, the correlation was "poor" (changes in ^{198}Au concentration were opposite to the increase or decrease in red-cell precursors). Four rabbits that received no treatment showed no effects from

TABLE 33

"RE Hypoplasia" ... Effects of Cortisone

(Data from representative rabbit, scans of which are shown in Fig. 76)

		Before R_X	R_X: Three Weeks
LOCALIZATION OF COLLOIDAL GOLD-198 IN MARROW	External Counts over Sacrum (cpm)	650	250
ERYTHROPOIESIS	Red-cell precursors (Volume in marrow sections)	48%	66%
	Ratio of red-cell precursors to granulocytes (marrow smears)	0.9	2.0

TABLE 34

Correlation of Erythropoiesis and Marrow Localization of I.V. Radiogold Colloid in Rabbits Treated to Alter Red-Cell Production or Phagocytosis

	Number of Rabbits	Good Correlation	Fair Correlation	"Poor" Correlation
RE Stimulation (ACTH, Estrogen)	7	4	2	1
RE Depression (ACTH, Cortisone)	7	1	2	4
Erythroid Hyperplasia (Phenylhydrazine, Testosterone, Phlebotomy)	12	10	1	1
Erythroid Hypoplasia (Chloramphenicol, Total-Body Irradiation, Protein-Free Diet)	7	3	0	4
Total	33	18	5	10

Control (Nontreated) Rabbits Studied = 4

Good or Fair Correlation = 70%
"Poor" Correlation = 30%

1027668

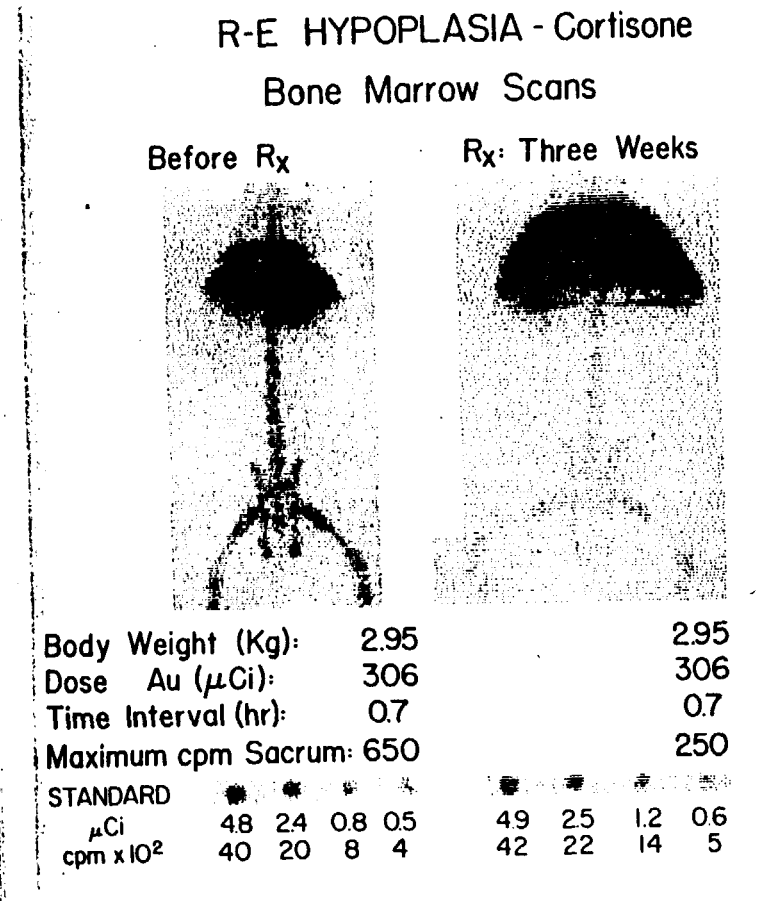

Fig. 76. Bone-marrow scans performed before and after three weeks of therapy with cortisone. Dose standards of 1 milliliter volume in plastic capsules scanned at same times to relate density of dots recorded by scanner to amount of radioactivity present.

the repeated doses of colloidal ^{198}Au, marrow aspirates, and phlebotomies.

A direct quantitative relationship between erythropoiesis and radiocolloid scans of marrow was not anticipated nor obtained, and the apparent discrepancies are not simply a matter of disparity between these marrow functions. Hepatic RE cells rapidly remove most of the radiogold from the blood (71 to 93% in these rabbits, depending on the treatment), and minor changes in hepatic blood

flow or Kupffer-cell function will obscure changes in marrow phagocytosis. These studies demonstrate that any assessment of erythropoiesis by radiocolloid bone-marrow scanning must be cautiously interpreted, and that direct quantitation is not feasible with this technique. The radiocolloid scan, however, is useful in showing the distribution of hemopoietic marrow as previously reported by others.[1,2]

REFERENCES

1. Kniseley, R. M., Andrews, G. A., Edwards, C. L., and Tanida, R. Scanning of bone marrow in hematopoietic disorders. In: Medical Radioisotope Scanning, Vol. II. Vienna, International Atomic Energy Agency, pp. 207-220, discussion 220-225, 1964.

2. Edwards, C. L., Andrews, G. A., Sitterson, B. W., and Kniseley, R. M. Clinical bone marrow scanning with radioisotopes. Blood 23, 741-756, 1964.

Red Cell Survival in Normal Ponies Measured with DFP (^{32}P)

*R. F. Queener, M. C. Yarbrough, C. C. Lushbaugh, W. D. Gibbs, and Daniel G. Brown**

The large blood volume, large veins, and greater than 120-day RBC survival time of the horse would make this animal ideal for study of RBC kinetics if it were not for his size and attendant handling difficulties. However, only two studies have been published on RBC survival in horses: two thoroughbreds that had RBC labeled with glycine-2-C^{14} [1] and 10 crossbred Percheron draft horses that had RBC labeled with d-isopropyl-phosphorofluoridate ^{32}P (^{32}P-DFP).[2] Red-cell survival was found to range between 137 and 162 days and have a mean life span of 147.2 ± 8.2 days.

The availability, technology, and ease in handling the pony[3] suggested that this animal might be even better suited than the horse to erythrokinetic and RBC-survival studies, and provide a means of overcoming the technical problems we have faced unsuccessfully so far in using ^{32}P-DFP as an RBC label in man.

Four ponies (~300 pounds each) were given 0.6 millicuries (2 mg), dissolved in propylene glycol and diluted to 20 ml, by injection into the jugular vein by catheter. Blood samples were obtained 30 min and 1 and 6 hr later, three times daily for the first week, twice weekly for 3 weeks, and weekly up to 50 days after labeling in two ponies. The second pair was studied by this schedule for only 2 weeks. Whole-blood and plasma ^{32}P activities were assayed in the 4 π beta counter for 2 ml whole blood specimens described previously.[4] Net percentage of ^{32}P activity per milliliter of whole RBC was computed and graphed on linear coordinates (Fig. 77).

The results of this study show that the intravenous labeling procedure used here produces RBC and plasma-protein labels that change much more rapidly during the first week than previous reports led us to expect. Plasma activity decreased to 50% of initial activity by 2 hr (t_{50} = 2 hrs) and then decreased exponentially with a t_{50} = 9 days. This persistent plasma activity was thus a major source of error for 3 weeks and required rigid control. During the first 3 days, unknown (biological?) causes seemed to produce daily unpredictable variations as large as 5% in plasma and net RBC activity. Contrary to previous descriptions of the tenacity of ^{32}P-DFP RBC label, we

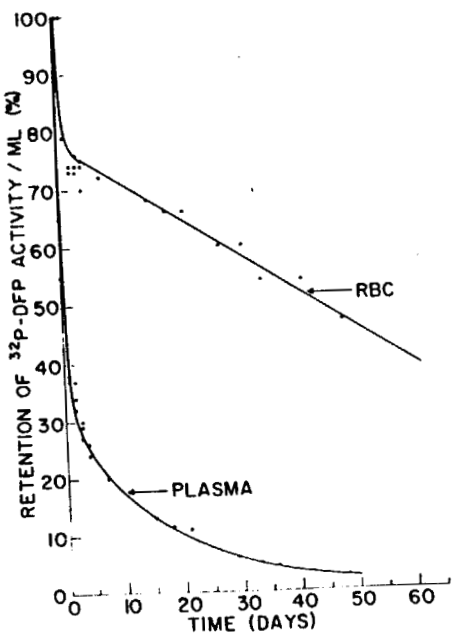

Fig. 77. Graph of retention of the 32P-DFP label on red blood cells and plasma proteins of a pony studied for 50 days.

* UT-AEC Agricultural Research Laboratory, Oak Ridge, Tenn.

1027669

found a rapid rate loss of the RBC label over the first 1 to 4 days. This observation might be explained as the result of our rapid injection of a large dose of drug so that only a small fraction of the circulating RBC mass became labeled, and a proportion of the DFP was only temporarily bound at sites that subsequently released it. As a result of this phenomenon, the RBC-survival curves became truly linear only after the first 5 to 7 days. The RBC life span was estimated graphically to be 123 and 164 days in the two ponies studied for 50 days and 100 and 103 days in the two studied for only 2 weeks. These underestimates are most likely due to the insufficiently long observation period.

These studies are being continued and fortify our opinion that considerably more experimental research is needed before DFP can be considered a routine RBC label in clinical hematology.

REFERENCES

1. Cornelius, C. E., Kaneko, J. J., Benson, D. C., and Wheat, J.D. Erythrocyte survival studies in the horse, using glycine-2-C^{14}. Amer J Vet Res 21, 1123-1124, 1960.

2. Marcilese, N. A., Figueiras, H. D., Kremenchuzky, S., Valsecchi, R. M., Camberos, H. R., and Varela, J. E. Red cell survival time in the horse, determined with di-isopropyl-phosphorofluoridate-P^{32}. Amer J Physiol 211, 281-282, 1966.

3. Brown, D. G., personal communication, UT-AEC Agricultural Research Laboratory, Oak Ridge, Tenn.

4. Gibbs, W. D. and Pope, W. T. A 4π ^{32}P-labeled diisopropyl-fluorophosphate (DFP) in blood. In: USAEC Report ORAU-101, 1966, pp. 168-170.

1027670

LIPID METABOLISM

The lipid program conducted at ORAU is concerned primarily with the chemistry, analysis, biological distribution, and metabolism of O-alkyl and O-alk-1-enyl ethers of glycerol (Fig. 78). These lipids contain ether bonds and exist in both neutral lipid and phospholipid fractions of mammalian cells; the biochemical mechanisms for their biosynthesis and biocleavage are still poorly understood and nothing is known about their function in cells. Biochemical and analytical studies have also been extended to related compounds, which include S-ethers of glycerol, fatty alcohols, and fatty aldehydes. Of particular interest in our research program have been the high levels of glyceryl ether diesters found in the neutral lipid fraction of human and animal tumors.

Development of new analytical techniques and novel approaches to the analysis and synthesis of lipids and their derived products are an important and integral part of the lipid program which makes it pos-

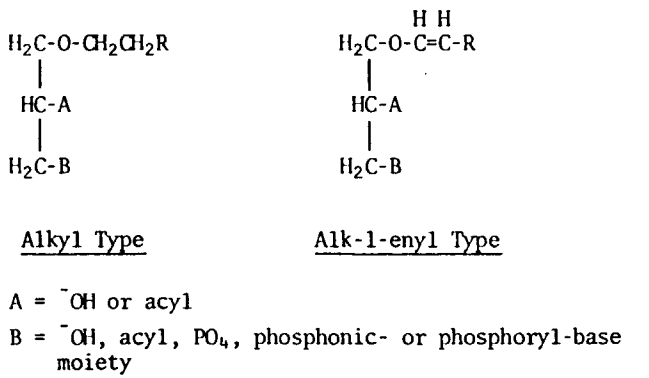

Fig. 78. Lipids found in nature that contain ether bonds can be classified according to the two structural types (alkyl or alk-1-enyl) depicted in Fig. 78. The other carbon positions (A and B) of the glycerol molecule can be occupied by hydroxyl, acyl, phosphorus, phosphoryl- or phosphonic-nitrogenous bases or even additional ether-linked hydrocarbon chains. Alkyl and alk-1-enyl are used to describe the α,β carbon bond adjacent to the O-ether linkage of the hydrocarbon chain attached to the 1-position of glycerol in lipids. Alkyl ethers refer to those compounds that do not have α,β unsaturation in the hydrocarbon chain but they may have unsaturation farther out along the chain. Alk-1-enyl ethers refer to those compounds that have α,β unsaturation (vinylic ethers, plasmalogen type) but may or may not have unsaturation farther out along the chain.

Metabolic studies in the lipid program have centered on the biocleavage and biosynthesis of lipids containing ether bonds. The thioethers of glycerol have been looked at as possible model compounds for studying the biochemical mechanism of glyceryl ether cleavage, and the oxidation of fatty alcohols, products of glyceryl ether cleavage, has been investigated. Identification of glyceryl ether diesters in several tumors has initiated a much broader investigation of the occurrence of glyceryl ethers in a spectrum of tumors and normal tissues from animals and humans. In addition, a segment of our program has been concerned with alterations in lipid metabolism in animals exposed to ionizing irradiation. The following abstracts summarize portions of the lipid studies completed during 1967.

In addition to the financial support by Atomic Energy Commission funds, certain projects have been financed by grants from the National Institute of General Medical Sciences (Grant # GM 12562-04) and the American Cancer Society (Grant # P-470). Collaborative research has been carried out with the University of North Carolina (Department of Medicinal Chemistry), the University of Minnesota (The Hormel Institute), the University of Tennessee (Department of Biochemistry, Memphis), and ORNL (Biophysical Separation Laboratory).

We are especially indebted to the valuable exchange with research participants who have spent time in our group: Dr. Edward N. Lambremont (Louisiana Nuclear Science Center, Louisiana State University, Baton Rouge, La.); Dr. Raul N. De Gasperi (Department of Physiology, University of Miami, Miami, Fla.); Dr. Alfred P. Morgan (Peter Bent Brigham Hospital, Boston, Mass.); and Miss Cristina Zepeda (a summer student participant from Our Lady of the Lake College, San Antonio, Texas).

Quantitative Determination of Alk-1-enyl-and Alkyl-Glyceryl Ethers in Neutral and Phospholipids

Randall Wood and Fred Snyder

We have developed a quantitative method for the simultaneous determination of alk-1-enyl- and alkyl-glyceryl ethers. Complete

1027671

resolution of the alk-1-enyl- and alkyl-glyceryl ethers. The specificity of this method can also be extended when used in conjunction with GLC, ion-complexing TLC, zonal scanning, and autoradiography to study composition, isomeric form, and the biosynthesis of glyceryl ethers in neutral and phospholipids.

The percentages of alk-1-enyl- and alkyl-glyceryl ethers in both the neutral and phospholipids of various rat tissues determined

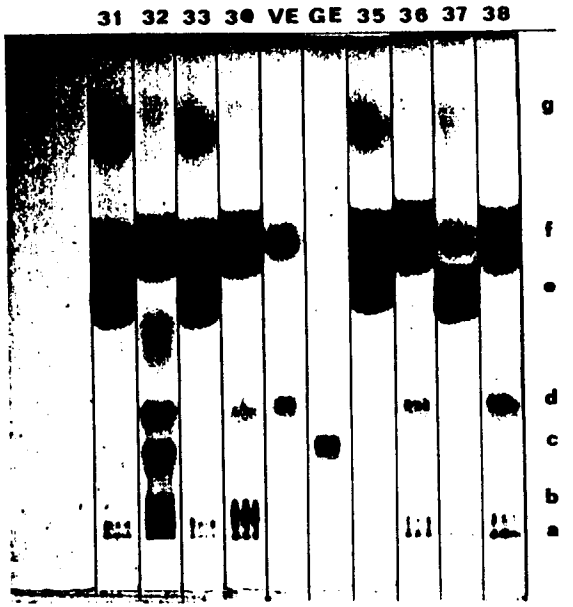

Fig. 79. *Chromatoplate depicting alk-1-enyl- (region d) and alkyl-glyceryl (region c) ethers of several different rat tissues. Odd and consecutive even-numbered lanes represent neutral and phospholipids of spleen 31-32, kidney 33-34, heart 35-36, and brain 37-38 tissues. Alk-1-enyl- and alkyl-glyceryl ether standards are represented by VE and GE. Regions a, b, and g represent unidentified reduction products. Sterols and long-chain alcohols are represented by e and f respectively. The solvent system was diethyl ether-30% aqueous ammonium hydroxide 100:0.25 (v/v).*

by the described method are shown in Table 35. Glyceryl ether glycerides represent 0.3 - 1.2% of the total neutral lipids, whereas the glyceryl ether phosphatides of brain, heart, marrow, muscle, and spleen represent 4.5 - 12.0% of their total phospholipids. Higher concentrations of glyceryl alkyl than of alk-1-enyl ethers were found in the neutral lipids, whereas the glyceryl alk-1-enyl ethers were found to predominate in the phospholipids.

TABLE 35

*Alk-1-enyl- and Alkyl-glyceryl Ether Concentrations Present in Neutral and Phospholipids of Various Rat Tissues**

Sample No.	Tissue†	Lipid Type‡	Percent Neutral and Phospho-lipid	Percent of N or P Lipid Fractions		
				Glyceryl Alk-1-enyl ether§	Glyceryl Alkyl Ether‖	Total Ether
21	Plasma	N	58.3	T¶	0.2	0.2
22	Plasma	P	41.7	0.2	0.2	0.4
23	Perirenal	N	99.7	T	0.4	0.4
24	Perirenal	P	0.3	0.9	0.2	1.1
25	Muscle (femoral)	N	52.3	T	0.2	0.2
26	Muscle (femoral)	P	47.7	2.4	0.4	2.8
27	Marrow (femoral)	N	37.2	0.1	0.4	0.5
28	Marrow (femoral)	P	62.8	2.2	2.0	4.2
29	Liver	N	39.5	0.1	0.2	0.3
30	Liver	P	60.5	0.2	0.4	0.6
31	Spleen	N	26.0	0.1	0.3	0.4
32	Spleen	P	74.0	1.6	1.3	2.9
33	Kidney	N	23.0	0.1	0.2	0.3
34	Kidney	P	77.0	0.5	0.1	0.6
35	Heart	N	26.5	0.1	0.3	0.4
36	Heart	P	73.5	1.3	0.3	1.6
37	Brain	N	23.2	0.2	0.1	0.3
38**	Brain (5 samples)	P	76.8	2.4±.22	0.59±.02	3.0
38A**	Brain (6 samples)	P	----	2.5±.33	0.61±.09	3.1

* Each value represents the mean of duplicate determinations.

† Tissue lipids from samples no. 21 to 30 were obtained from 130 to 160 g female rats and those from 31 to 36 were obtained from young adult female rats. Samples no. 37 to 38A were obtained from old adult male rats.

‡ N - Denotes neutral lipid, and P - Denotes phospholipid.

§ Commonly referred to as vinyl ethers.

‖ Includes glyceryl ethers with unsaturation in the hydrocarbon chain other than the one position.

¶ T - Represents less than 0.1%.

** Brain phospholipids were separated from neutral lipids by silicic acid chromatography at room temperature for sample no. 38 and below 5C for sample no. 38A.

1027672

Infrared Spectra and Polymorphism of Glycerol Ether Derivatives*

Edward O. Oswald,† Claude Piantadosi,‡ Carl E. Anderson,§ and Fred Snyder

The infrared spectra and the polymorphic forms of the α- and β-glycerol ethers, glycerol ether monoesters, and glycerol ether diesters were investigated. It was concluded from these studies that the α-ethers exist in at least two different crystalline forms, whereas the β-ethers exist in only one form. The stable A form of both isomers of the ethers probably has hexagonal packing of the side chains; however, the B form of the α- ethers may have triclinic packed chains. The α- monoester β-ethers and the β-monoester α- ethers also exist in at least two crystalline forms. The lower melting form B of the β-monoester α-ether does not correspond in crystalline structure to the lower melting form B of the α-monoester β-ether. The results indicate that there are at least three or possibly four crystalline forms of dipalmitoyl-α-batyl alcohol. The data imply that form D of dipalmitoyl-α-batyl alcohol is converted to form A and also that form B is converted to form A. The β-ether diesters are stable at room temperature in probably an orthorhombic arrangement, whereas the α-ether diesters are stable only in a triclinic or hexagonal arrangement. A comparison of the polymorphic forms of glycerides and glycerol ether derivatives demonstrated that both classes of compounds exist in a large number of similar crystalline forms; however, the glycerol ether derivatives may also exist in forms that have not yet been reported for the glycerides.

---

* Abstract of article published in Chem Phys Lipids, 1, 270-281, 1967. This investigation was supported by Public Health Research Grants GM 12562-01 and GM 12562-02 from the National Institute of General Medical Sciences, National Institutes of Health.

† Palms of Pasadena Hospital, Pathology Dept., St. Petersburg, Fla.

‡ Department of Medicinal Chemistry, University of North Carolina, Chapel Hill, N. C.

§ Department of Biochemistry, University of North Carolina, Chapel Hill, N. C.

Deacylation of Isomeric Diacyl-1-^{14}C-alkoxyglycerols by Pancreatic Lipase*

Fred Snyder and Claude Piantadosi†

Pancreatic lipase was used to compare the deacylation rates of ^{14}C-labeled α- and β-isomeric glyceryl alkyl ether diesters to those of ^{14}C-labeled triolein. The calculated half-time of the reaction rates for the initial deacylation step was approximately 8 min for both classes of lipids. Thin-layer chromatography of the lipolytic products was used to determine structural asymmetry of the labeled glyceryl ether diesters isolated; the lipase reaction can also be used to determine the point of attachment of acyl groupin in diacyl glyceryl ethers and to prepare monoacylalkoxyglycerols in bulk quantities (Fig. 80).

* Abstract of article accepted for publication in Biochim Biophys Acta.

† From the Department of Medicinal Chemistry, University of North Carolina, Chapel Hill, N. C.

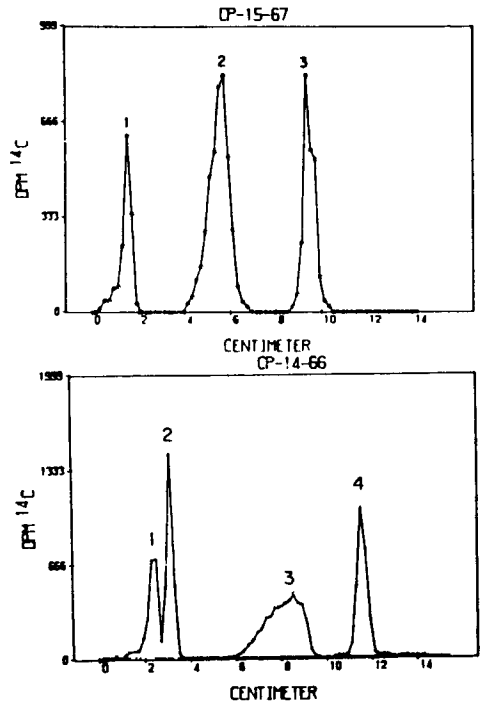

Fig. 80. Zonal ^{14}C-profile scans of lipolytic products formed during the pancreatic lipase reaction (15 min) in which diacyl-^{14}C glyceryl ethers were the substrate. Upper curve – (1) α-monoester-β-monoether, (2) fatty acid, (3) glyceryl ether diester. Lower curve – (1) α-monoether-β-monoester, (2) α-monoether-α'-monoester, (3) free fatty acids, (4) glyceryl ether diesters.

1027673

Synthesis of Labeled Glyceryl Thiomonoethers*

Claude Piantadosi,† Randall Wood and Fred Snyder

Labeled glyceryl thiomonoethers (S-ethers) were prepared in orde to compare their metabolic fate with that of naturally occurring glyceryl monoethers (O-ethers). Synthesis used in the preparation of the glyceryl thioethers was based on the Williamson reaction for the synthesis of ethers in general. We have used a modification of this reaction as have others[1] for the preparation of unlabeled 1-glyceryl thiomonoethers.

Optimum synthesis conditions were determined by making several unlabeled 1-glyceryl thioethers. Synthesis of 1-glyceryl 1-^{14}C hexadecyl thioether was carried out as follows: 1-thioglycerol (172 mg) was added to a 30-ml flask equipped with a stirrer containing 2.0 ml of dioxane and 2.0 ml of 1 N sodium hydroxide. Labeled hexadecyl-1-^{14}C bromide (69.4 mg) and unlabeled hexadecyl bromide (174.7 mg) dissolved in dioxane were added to the reaction flask and heated at 80 to 85° C for 3 hr under an atmosphere of nitrogen. The reaction mixture was cooled and 15 ml of distilled water was added. The resulting precipitate was filtered and washed with 50 ml of cold water. The white precipitate was dried over phosphorus pentaoxide for 12 to 18 hr and purified by silicic acid chromatography. The product (264.82 mg) was found to be 99% pure by thin-layer chromatography (TLC) and had a melting point of 75 to 76.5° C. Elemental carbon, hydrogen, sulfur, and oxygen values were in close agreement with the calculated values for the predicted empirical formula $C_{19}H_{40}SO_2$.

* Research supported in part by Research Grant GM-12562-04 from the Department of Health, Education and Welfare, National Institute of General Medical Services.

† Department of Medicinal Chemistry, School of Pharmacy, University of North Carolina, Chapel Hill, N. C.

One-glyceryl 1-^{14}C-octadecyl thioether was prepared in an analogous manner and was also found to be 99% pure by TLC. Its melting point was 74 to 74.7° C. Elemental carbon, hydrogen, sulfur, and oxygen values were found to be in close agreement with the calculated values for the predicted empirical formula $C_{21}H_{44}SO_2$. The specific activity of the labeled thioethers was 1.21 mc/mM.

REFERENCE

1. Lawson, D. D., Getz, H. R., and Miller, D. A. Synthesis of the sulfur analogs of batyl and chimyl alcohols. J Org Chem, 26, 615-616, 1961.

Analysis and Characterization of Glyceryl Thiomonoethers*

Randall Wood, Claude Piantadosi † and Fred Snyder

Thin-layer- and gas-liquid-chromatography (TLC) (GLC) and nuclear magnetic resonance- (NMR) and infrared (IR) spectroscopy have been used to analyze and characterize a series of saturated 1-glyceryl thiomonoethers ranging in chain length from C_{10} to C_{18}. Chromatographic and spectrographic behavior of the 1-glyceryl thioethers (S-ethers) and the 1-glyceryl ethers (O-ethers) are compared. Resolution of O-ethers and S-ethers by TLC is possible, but a mixture differing in chain lengths causes spot elongation and overlapping, making such a class separation impractical. Thioethers are easily distinguished from O-ethers by either NMR or IR spectra. The IR spectra of S-ethers are characterized by strong absorption at 9.68 and 11.4μ, regions of little or no O-ether absorption. Resonance of the S-ether protons adjacent to the carbon to sulfur bonds appears at approximately 2.5 ppm (center of triplet) while the same protons resonate down field approximately 1.0 ppm in the O-ether spectrum. Glyceryl S-ether isopropylidene derivatives can be quantitatively analyzed by GLC as shown in Fig. 81 and Table 36, but require higher column temperatures than the corresponding O-ethers. We have been unable to separate mixtures of both O-ether

* Research supported in part by Research Grant GM-12562-04 from the Department of Health, Education and Welfare, National Institute of General Medical Services.

† Department of Medicinal Chemistry, School of Pharmacy, University of North Carolina, Chapel Hill, N. C.

1027674

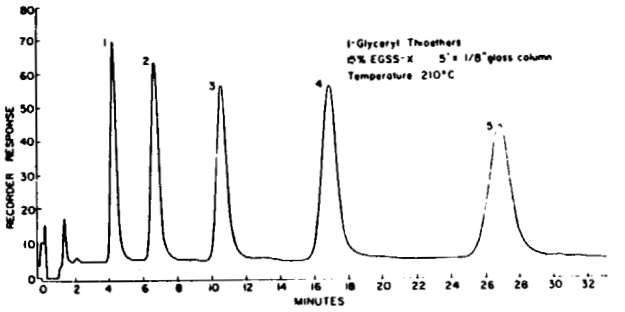

Fig. 81. Gas-liquid chromatographic tracing of 1-glyceryl thioether isopropylidene derivative standard mixture. Chromatographic conditions are given in the margin of the figure. Numbered peaks represent a homologous series of increasing hydrocarbon chain length of two carbon units starting at C_{10} for peak 1.

and S-ether isopropylidene derivatives on a number of polar liquid phases examined; however, preliminary results with nonpolar liquid phases look promising. The underlying interest in the analysis and characterization of synthetic glyceryl thiomonoethers is that they will allow us to determine whether these compounds occur in biological samples, and if so, allow something to be learned of their function.

TABLE 36

*Quantitation of Standard Mixtures of Glyceryl Ether Isopropylidene Derivatives by GLC**

Hydrocarbon Chain Length	O-ethers†			S-ethers†		
	Area % Found	Known Weight %	Known Mole %	Area % Found	Known Weight %	Known Mole %
10	14.7‡	12.24	15.49	13.1‡	11.2	14.1
12	17.5	16.35	18.47	14.3	14.0	15.9
14	20.3	19.87	20.26	17.7	18.1	18.6
16	22.5	23.39	21.76	26.0	26.6	25.2
18	25.0	28.14	24.01	28.9	30.1	26.2

* Analyses were carried out on 5' x 1/8" glass columns packed with 15% EGSS-X.

† Analyses of O-ethers were carried out at 200°C while S-ethers were analyzed at 210°C.

‡ Area percentages represent the mean of three determinations.

Quantitative Analysis of Long-Chain Aldehydes

Randall Wood and Robert Harlow

Quantitative gas-liquid chromatography (GLC) analysis of long-chain fatty aldehydes was achieved without derivitization. Myristyl, palmityl, stearyl, and oleyl aldehydes used in the quantitation mixture were synthesized and purified according to the procedure of Mahadevan et al.[1] Analyses were carried out on glass columns (5' x 1/8") containing 15% ethylene glycol succinate methyl silicone polymer (EGSS-X) temperature programed from 135 to 180° C at approximately 2° C/min. A chromatogram depicting the resolution of the aldehyde mixture is shown in Fig. 82. In contrast to aldehyde derivatives (dimethyl acetals) that undergo degradation during GLC analysis,[2,3] free aldehydes did not show any decomposition under our analysis conditions. The lack of decomposition is supported by the close agreement between experimentally determined values and known percentages shown in Table 37. Despite a common belief that free aldehydes are unstable and decompose, polymerize, etc., rapidly, no detectable change has been observed in the aldehyde mixture after 4 months of storage at -20° C in carbon disulfide. Possibly the antioxidant properties of the carbon disulfide solvent make possible the storage and quantitative GLC analysis of long-chain aldehydes without decomposition. The method is currently being used to determine glyceryl alk-1-enyl ether composition by GLC analysis of the aldehydes released after hydrolysis.

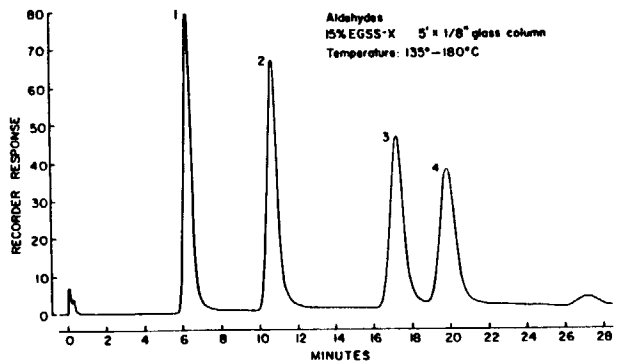

Fig. 82. The chromatogram tracing depicts the analysis of a fatty aldehyde mixture without derivitization. The numbered aldehyde peaks are (1) myristyl; (2) palmityl; (3) stearyl; and (4) oleyl.

1027675

TABLE 37

Quantitation of Aldehyde Standard Mixture by GLC of Free Aldehydes*

Aldehyde	Area % Found †	Known Mole %	Known Weight %
Tetradecanal	24.1	23.9	20.6
Hexadecanal	26.4	27.7	27.0
Octadecanal	25.7	26.1	28.3
Cis-9-octadecenal	23.8	22.4	24.1

* Analyses carried out on 5' x 1/8" glass column packed with 15% EGSS-X and temperature programmed from 135 to 180° C.

† Each of the percentages represent the mean of three determinations.

REFERENCES

1. Mahadevan, V., Phillips, F., and Lundberg, W. O. Reactions of dimethyl sulfoxide with sulfonate esters of fatty alcohols. I. Synthesis of higher saturated and unsaturated fatty aldehydes. Lipids 1, 183-187, 1966.

2. Stein, R. A. and Slawson, V. A model for fatty aldehyde dimethyl acetal gas-liquid chromatography. The conversion of octadecanal dimethyl acetal to methyl 1-octadecenyl ether. J Chromatog 25, 204-212, 1966.

3. Mahadevan, V., Viswanathan, C. V., and Phillips, F. Conversion of fatty aldehyde dimethyl acetals to the corresponding alk-1-enyl methyl ethers (substituted vinyl ethers) during gas-liquid chromatography. J Lipid Res 8, 2-6, 1967.

Quantitative Analysis of Intact Triglycerides and Related High-Molecular-Weight Lipids

Randall Wood and Robert Harlow

A satisfactory and reliable high-temperature chromatographic system for the quantitative gas-liquid chromatography (GLC) of intact triglyceride and related high molecular weight lipids isolated from biological sources has been developed. Progress in this area was accomplished after considerable modification of an Aerograph Model 204 gas chromatograph. The column oven and flash heater were modified to accept a 4 mm O.D. glass column fitted with Kovar Pyrex to metal seals described by Radin[1] and Litchfield et al.[2] Extension of the column through the flash heater at the entrance and beyond the Kovar seal at the column exit allows on-column injection and chromatography of samples without exposure to metal surfaces that cause decomposition. Unpacked columns were installed while being heated to the softening point to prevent breakage. Gas pressure and vacuum are used to pack and unpack the column without removal from the instrument. Detector sensitivity was improved by the installation of a ceramic flame tip (0.03 inch I.D.), and oxygen and hydrogen gas preheaters and regulators. Spurious peaks and excessive base-line drift were eliminated by preconditioning septums at 300+°C under vacuum for 4 hr. Figure 83 shows a chromatogram obtained with the described system on a triglyceride and a glyceryl ether diester (GEDE) mixture isolated from neoplastic tissue. The GEDE, differing in molecular weight by only 14 units, is eluted ahead of the corresponding triglyceride. In addition to triglycerides and GEDE, intact high molecular weight compounds such as waxes, hydrocarbons, cholesterol esters, neutral plasmalogens, diglycerides, and diethers have been analyzed.

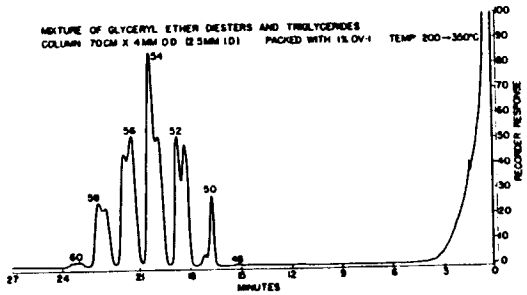

Fig. 83. A chromatogram obtained with the described system on a triglyceride and a glyceryl ether diester mixture isolated from a neoplastic tissue. Peak numbers represent the sum of the number of carbon atoms in the hydrocarbon chains. Chromatographic conditions are given in the margin of the figure.

1027676

REFERENCES

1. Radin, N. S. The use of Kovar seals in high temperature gas chromatography with glass columns. J Chromatog 20, 392-394. 1965.

2. Litchfield, C., Harlow, R. D., and Reiser, R. Gas-liquid chromatography of triglyceride mixtures containing both odd and even carbon number fatty acids. Lipids 2, 363-370, 1967.

Application of Thin-Layer Chromatographic Zonal ^{14}C-Profile Scans to the Analysis of Urinary Constituents Derived from Lipids*

Fred Snyder

Thin-layer chromatography (TLC) has been a useful tool in the analysis of numerous urinary constituents such as steroids, amino acids, and bile acids. As in most applications of adsorption TLC, it is best used in conjunction with other chromatographic processes such as gas-liquid partition and ion exchange.

Our interest in the metabolism of ester- and ether-linked lipids has led us to investigate the use of TLC for resolving ^{14}C-labeled urinary products derived from lipids. Our data show good resolution of short-chain acids and glycerol on 250-μ layers of Silica Gel G. A major urinary nonlipid ^{14}C-product of the metabolism of glyceryl 1-^{14}C hexadecyl thioether was isolated as a single component on 250-μ Silica Gel G layers in a solvent system of ethanol: ammonium hydroxide: water (80:4:16 v/v/v). Ion-exchange chromatography resolved this single ^{14}C-component into two major and three minor ^{14}C-fractions.

Automated equipment for fraction collection[1] and computerized analysis[2] of thin-layer chromatograms has been used in this investigation. The complete system, with recent modifications, will be described in detail. Figure 84 depicts a typical separation for a standard ^{14}C-mixture of citric acid, formic acid, acetic acid, propionic acid, and glycerol.

---

* Presented at ORNL Symposium on Urinary Constituents of Low Molecular Weight, November 30 - December 1, 1967.

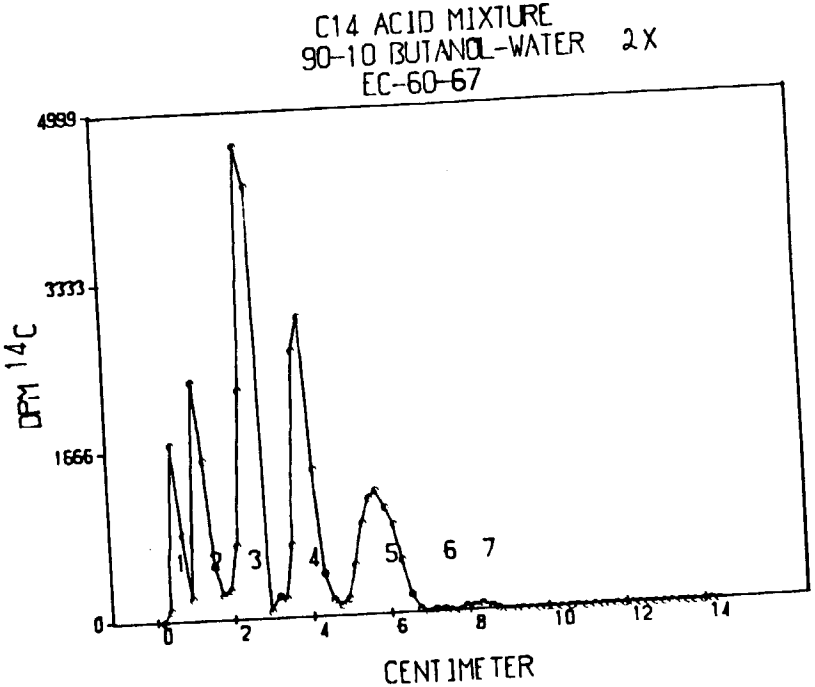

Fig. 84. A zonal 14C-profile scan of a standard mixture of 14C compounds resolved on 250-micron layers of Silica Gel G. Solvent development was carried out twice in a solvent system of butanol: water (90:10 v/v). The peak numbers refer to (1) citric acid, (2) acetic acid, (3) formic acid, (4) propionic acid, and (5) glycerol.

REFERENCES

1. Snyder, F. and Kimble, H. An automatic zonal scraper and sample collector for radioassay of thin-layer chromatograms. Anal Biochem 11, 510-518, 1965.

2. Snyder, F. and Smith, D. An automated system for sample collection and computer analysis of thin-layer radiochromatograms. Separation Sci 1, 709-722, 1966.

1027677

Automated Thin-Layer Chromatography*

Fred Snyder

Two scraping devices (manual and automatic models) for collection of thin-layer chromatographic (TLC) zones have recently been modified to accept conventional TLC end plates. The instruments permit the collection of TLC zones in a manner analogous to the collection of fractions from silicic acid columns. High-resolution curves for both radioactive and colorimetric quantitative analyses can now be obtained from adjacent lanes on the same TLC plate, and other lanes can be used for visualization by carbonization. The system uses a pipetting device having a sample holder compatible with the turntable of the zonal scraper. This device automatically dispenses reagents for radiometric or colorimetric assay in appropriate volumes. Plottings and calculations of the results are included in the computerized system. Special emphasis will be given to a new liquid scintillation-quenching technique for quantitation of chemical mass and to an automatic plate-coating device. Data obtained with this system will be shown with reference to its application in organic chemistry and biochemistry.

---

* Presented at a symposium on Practical Applications of Chromatography in Lipid Analysis, spring meeting of the American Oil Chemists' Society, Washington, D. C., March 31 - April 5, 1968.

The Measurement of Chemical Mass by Liquid Scintillation Quenching

Fred Snyder and Anita Moehl

We have developed a procedure for quantitatively measuring the chemical mass of lipids in a liquid scintillation spectrometer by taking advantage of colored quenching phenomena in such systems. An H_2SO_4-lipid reaction was carried out in a scintillation vial at 200° C. The reaction is based on that originally described by Marsh and Weinstein[1]; a "charred" solution that has a very broad absorption band in the near ultraviolet region is produced under these conditions.

A glass tube (Fig. 85) containing a mixture of a plastic scintillator and a β-emitter (^{14}C, ^{137}Cs, ^{99}Tc, ^{3}H), attached to a plastic holder, is inserted into the "charred" solutions for radioassay in a scintillation spectrometer. The counting rate of the plastic source is decreased by the color intensity of the "charred" solution. The linearity for the

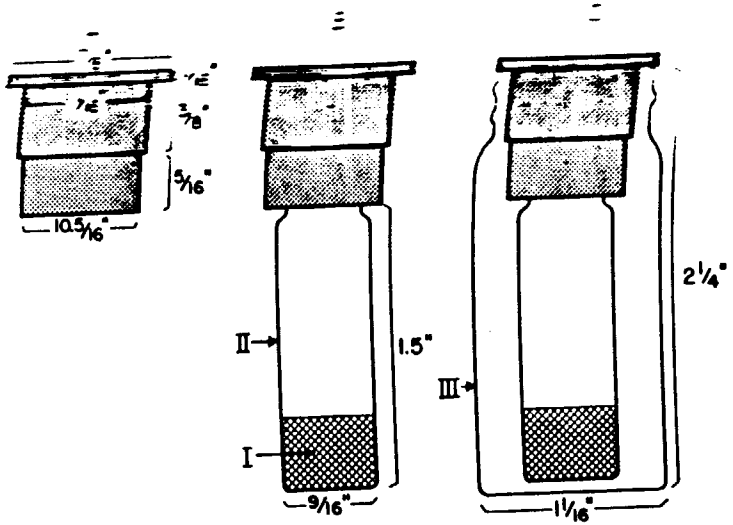

Fig. 85. Drawings of component parts for arrangement of plastic scintillation source used to determine lipid mass by liquid scintillation quenching. Plastic cap (A) holds tube (B-II) that contains plastic scintillator mixed with beta emitter (B-I). The special assembly (B) fits on regular commercially available liquid scintillation vial (III) as shown in sketch (C).

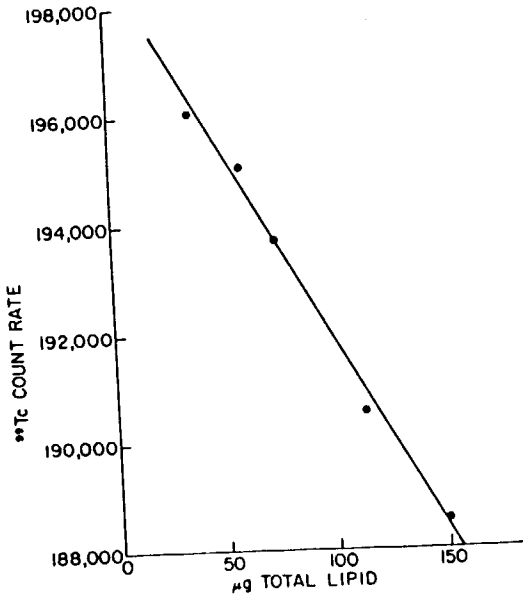

Fig 86 A typical curve obtained for the determination of lipid mass by liquid scintillation quenching of ^{99}Tc mixed with Pilot B plastic scintillation beads.

1027678

[illegible] source is shown in Fig. 85. The method is simple and quantitative. Furthermore, it is adaptable to the computerized system now operational for measuring the quantitative distribution of low-energy betas along a thin-layer chromatographic lane.

REFERENCES

1. Marsh, J. B. and Weinstein, D. B. Simple charring method for determination of lipids. J Lipid Res 7, 574-576, 1966.

2. Snyder, F. and Smith, D. An automated system for sample collection and computer analysis of thin-layer radiochromatograms. Separation Sci 1, 709-722, 1966.

The Occurrence and Metabolism of Alkyl and Alk-1-enyl Ethers of Glycerol in Transplantable Rat and Mouse Tumors

Fred Snyder and Randall Wood

Thirteen transplantable animal tumors have been quantitatively analyzed for their glyceryl alkyl and alk-1-enyl ethers in the neutral lipid and phospholipid fractions. Our data demonstrate that the quantity of glyceryl ethers in the neutral lipid fraction of tumors is significantly higher than that found in normal tissues. The glyceryl ether content of the tumor phospholipids is also high, but certain normal tissues (marrow and brain) also contain similarly high levels of glyceryl ethers in the phosphatides (Table 38).

Metabolic studies on the incorporation of palmitic-1-^{14}C acid into the glyceryl ether diesters isolated from Ehrlich ascites cells revealed that ^{14}C was incorporated into both the ether hydrocarbon chain (13 to 25% of the total glyceryl ether diester activity) and the esterified fatty acids of this fraction. Labeling of the glyceryl ether diesters did not occur when lipid precursors (e.g., acetate) or $^{3}H_2O$ were administered to mice bearing the ascites cells. The specific activity of the triglyceride fraction was always higher than that of the glyceryl ether diesters found in Ehrlich ascites cells. After five daily injections of labeled palmitic acid to animals bearing eight different tumor types, the specific activities of the alk-1-enyl ethers were always higher than the alkyl ethers in the neutral lipid fraction (Table 39). The specific activities of the alkyl and alk-1-enyl ethers of the phospholipid fraction isolated in these experiments were usually about the same.

1027179

TABLE 38

Glyceryl Ether Content of Neutral and Phospholipid Fractions of Transplantable Tumors in Mice and Rats*

TUMOR	Total lipids of tumor %	Lipid fraction	Lipid in fraction %	Glyceryl alk-1-enyl ether %	Glyceryl alkyl ether %	Alkyl / alk-1-enyl ratio	Total glyceryl ethers in fraction %	Total glyceryl ethers of total lipids %
Mouse (ICR Strain) Sarcoma 180	10.9	NL	70.4	0.16	0.77	4.8	0.93	1.05
		PL	29.6	0.41	0.95	2.3	1.36	
Mouse (C57/BL6 Strain) Melanoma B16	9.0	NL	26.6	0.12	0.83	6.9	0.95	2.05
		PL	73.4	0.87	1.59	1.8	2.46	
Mouse Adeno-carcinoma E0771	10.6	NL	57.7	0.11	0.86	7.8	0.97	1.97
		PL	42.3	1.75	1.57	0.9	3.32	
Mouse (C57/BL6 Strain) Sarcoma T241	10.2	NL	53.5	0.61	2.29	3.7	2.90	3.79
		PL	46.5	1.60	3.22	2.0	4.82	
Mouse (ICR Strain) Taper liver tumor	15.7	NL	60.0	0.15	1.11	7.4	1.26	2.59
		PL	39.9	2.11	2.48	1.2	4.59	
Mouse (DBA/2 Strain) Friends virus leukemia	7.3	NL	20.8	0.25	1.55	6.2	1.80	1.73
		PL	78.1	0.70	1.04	1.5	1.74	
Rat (Charles River Dawly Strain) Walker 256	9.8	NL	51.1	0.70	1.56	2.2	2.26	2.96
		PL	48.8	1.76	1.95	1.1	3.71	
Rat (Fischer Strain) R3259	10.6	NL	68.9	0.12	0.42	3.5	0.54	2.12
		PL	31.1	3.70	1.94	0.5	5.64	
Mouse Ehrlich ascites carcinoma	8.5	NL	19.3	0.28	1.02	3.6	1.30	1.84
		PL	80.7	0.30	2.10	7.0	2.40	
Mouse Carcinoma C1025	7.7	NL	66.9	0.86	1.31	1.5	2.17	1.26
		PL	33.1	2.33	1.48	0.6	3.81	
Mouse KHZ mammary tumor	14.9	NL	51.5	0.20	0.30	1.5	0.50	1.42
		PL	48.5	1.49	0.92	0.6	2.41	
Mouse Ridgway osteogenic sarcoma	6.2	NL	51.4	0.34	0.48	1.4	0.82	1.77
		PL	48.6	2.05	0.75	0.4	2.80	
Mouse Mecca lymphosarcoma	8.1	NL	68.9	0.23	0.50	2.2	0.73	1.88
		PL	31.1	2.55	1.76	0.7	4.31	

* All percentages are expressed as free alkoxyglycerols; each value should be multiplied by 3 to express percentages in terms of their diacyl or phospholipid types.

TABLE 39

*Specific Activity of Glyceryl Alk-1-enyl and Alkyl Ethers Isolated from Rat and Mouse Tumors after Administration of Potassium ^{14}C-1-Palmitate**

Tumor type	Total glyceryl ethers of total lipids % †	Radioactivity in ether-containing lipids % ‡	Lipid fraction	Specific activity of N or P lipid fractions: Glyceryl alk-1-enyl ethers CPM/mg X10^3	Specific activity of N or P lipid fractions: Glyceryl alkyl ethers CPM/mg X10^3
Walker 256	2.97	7.37	N	14.1	12.3
			P	10.3	10.8
Fischer R3259	2.12	4.17	N	19.0	5.1
			P	6.1	7.5
Sarcoma 180	1.05	3.97	N	57.8	29.0
			P	75.6	70.4
Melanoma B16	2.05	5.86	N	54.4	23.3
			P	36.5	28.7
Adenocarcinoma E0771	1.97	4.00	N	32.4	16.0
			P	38.4	25.4
Sarcoma T241	3.79	5.90	N	54.6	25.0
			P	62.8	40.6
Taper liver tumor	2.59	4.34	N	54.3	23.9
			P	54.5	50.6
Friends virus leukemia	1.73	5.43	N	117.5	47.4
			P	84.2	55.9

N refers to neutral lipid fraction and P refers to phospholipid fraction.

* All tumor-bearing animals were injected intraperitoneally each day with 20 microcuries of potassium-1-^{14}C palmitate (specific activity 36.4 μc/mg) for a period of 5 days. The animals were killed and the tumors were removed for lipid analyses 6 hr (mice) or 24 hr (rats) after the last ^{14}C injection.

† All percentages are expressed as free alkoxyglycerols: each value should be multiplied by 3 to express percentages in terms of their diacyl or phospholipid types.

‡ Expressed as percentage of total lipid ^{14}C.

Occurrence of Glyceryl Ether Diesters in Human Tumors

Fred Snyder, Randall Wood, Edgar Cress, and Nelson Stephens

We have made a quantitative study of the alkyl and alk-1-enyl ethers of glycerol in the neutral and phospholipid fractions isolated from a variety of human neoplasms (Table 40) available from the National Institutes of Health tumor-bank program. Nonmalignant human tissues from patients have also been examined for their glyceryl ether content. Thin-layer chromatograms (TLC) of the human tumor lipids indicated that the intact glyceryl ether diesters are found at relatively high levels in human tumors, whereas TLC patterns of the total lipids of a number of nonmalignant tissues obtained from a 14-year-old boy who died suddenly of bilateral lobar hemorrhagic pneumonitis and tissues from a 17-year-old boy who died instantaneously of cyanide poisoning did not show significant spots in the glyceryl ether diester area.

The alkyl and alk-1-enyl composition of glyceryl ethers isolated from the neutral and phospholipid fractions of the human tumors and nonmalignant tissues (after $LiAlH_4$ hydrogenolysis) is shown in Table 40. All values are expressed in terms of the deacylated glyceryl monoethers as percentage of the lipid fraction analyzed. Each value should be multiplied by 3 to obtain approximate values for the corresponding quantities of glyceryl ethers expressed as diesters or phosphatides.

The total glyceryl ether content of the human tumors investigated in this study ranged from 0.42 to 4.73% of the neutral lipid fraction and from 1.61 to 12.5% of the phospholipid fraction. The relative quantities of neutral and phospholipids varied with tumor type although the ratio of alkyl to alk-1-enyl ethers in the human tumors was higher in the neutral lipid fractions than in the phospholipid fraction. The percentage of glyceryl ethers in the neutral lipid fraction of some typical nonmalignant human tissues was much lower than that found in the tumors (Table 41).

1027680

TABLE 40

Glyceryl Ether Content[a] of Neutral and Phospholipid Fractions of Human Tumors

Tumor	Lipid Fraction	Lipid in Fraction %	Glyceryl Alk-1-enyl Ether %	Glyceryl Alkyl Ether %	Alkyl / Alk-1-enyl Ratio
Metastatic adenocarcinoma	NL	81.90	0.30	0.72	2.40
	PL	18.10	0.93	0.76	0.82
Neurofibrosarcoma	NL	77.19	0.22	0.35	1.59
	PL	22.81	8.58	3.97	0.46
Squamous cell carcinoma	NL	38.66	0.50	0.50	1.00
	PL	61.34	2.21	1.08	0.49
Adenocarcinoma	NL	68.81	0.19	0.45	2.37
	PL	31.19	2.58	1.51	0.58
Adenoma	NL	36.49	0.36	0.86	2.39
	PL	63.51	6.17	2.62	0.42
Metastatic undiffer. carcinoma	NL	47.55	0.22	0.49	2.45
	PL	52.45	1.78	1.42	0.80
Metastatic embryonal carcinoma	NL	37.50	1.51	1.66	1.03
	PL	62.50	1.27	0.41	0.32
Metastatic liposarcoma	NL	75.00	0.12	0.92	7.67
	PL	25.00	1.17	0.44	0.38
Metastatic poorly differ. carcinoma	NL	90.51	0.18	0.31	1.72
	PL	9.49	3.14	0.69	0.22
Metastatic poorly differ. adenocarcinoma	NL	30.40	0.72	1.14	1.30
	PL	69.60	3.33	1.89	0.57
Metastatic poorly diff. transitional cell carcinoma	NL	30.92	0.91	1.70	1.87
	PL	69.08	1.18	0.85	0.72
Chronic myelocytic leukemia	NL	70.74	0.08	0.34	4.25
	PL	29.26	1.45	0.45	0.31
Adenocarcinoma	NL	91.64	0.23	0.35	1.52
	PL	8.36	1.59	0.95	0.81
Astrocytoma	NL	33.54	0.56	0.79	1.41
	PL	66.46	2.37	1.07	0.45
Metastatic squamous cell carcinoma	NL	88.70	0.18	0.33	1.83
	PL	11.30	4.28	1.82	0.43
Squamous cell carcinoma	NL	66.91	0.38	0.58	1.53
	PL	33.09	2.65	0.87	0.33
Undiff. carcinoma	NL	78.50	0.71	1.31	1.85
	PL	21.50	2.35	0.91	0.39

[a] All percentages are expressed as free alkoxyglycerols; each value should be multiplied by 3 to express percentages in terms of their diacyl or phospholipid types.

TABLE 41

*Glyceryl Ether Content of Neutral and Phospholipid Fractions of Normal Human Tissues**

Tissue	Lipid Fraction	Lipid in Fraction %	Glyceryl Alk-1-enyl Ether %	Glyceryl Alkyl Ether %	Alkyl / Alk-1-enyl Ratio
Pancreas	NL	84.86	0.03	0.18	6.0
	PL	15.14	1.17	0.30	0.2
Testicle	NL	50.21	Trace	Trace	---
	PL	49.79	1.39	0.92	0.7
Spleen	NL	30.07	0.07	0.22	3.14
	PL	69.93	1.57	0.84	0.54
Perirenal Fat	NL	93.27	0.07	0.29	4.14
	PL	6.73	Trace	Trace	---
Liver	NL	50.21	Trace	Trace	---
	PL	49.79	0.50	0.32	0.64

* Freshly-frozen specimens obtained from a 14-year-old boy (Colorado Specimen No. 301-66) who was apparently well until he died suddenly of bilateral lobar hemorrhagic pneumonitis.

The Distribution and Metabolism of Glyceryl Ether Diesters in Disrupted Ehrlich Ascites Cells*

Fred Snyder and Randall Wood

Total lipids from Ehrlich ascites carcinoma cells contain approximately 2% glyceryl ether diesters (Table 42). Carcinoma cells were disrupted in a French pressure cell, and centrifuged fractions were examined for glyceryl ether diester and triglyceride content by thin-layer chromatography and gas-liquid chromatography. The highest

* Presented at the American Oil Chemists' Society fall meeting, October, 1967, Chicago, Illinois.

1027681

TABLE 42

Lipid Composition of Ehrlich Ascites Cells

Lipid Classs	% Total Lipids* Batch 6	Batch 7
Cholesteryl Esters	12.	11.
Glyceryl Ether Diesters	1.9	1.5
Triglycerides	18.	14.
Free Fatty Acids	1.4	1.0
Cholesterol	9.6	11.
Phosphatidyl Choline	22.	22.
Phosphatidyl Ethanolamine	21.	19.
Sphingomyelin	12.	12.

* Total extractable lipids were 8.3 ± 2.3% of the cellular dry weight of EAC grown for 5 days in the peritoneal cavities of white Swiss mice.

TABLE 43

*Distribution of Diacylalkoxyglycerols in Ehrlich Ascites Cells**

Cell Fraction	Diacylalkoxy-glycerols	Alkyl/Alk-1-enyl Ratio: Neutral Lipids	Phospholipids
15,000 x g (10 min)	2.95 ± 0.55	5.5	2.8
34,000 x g (3 hr)	0.70 ± 0.16	2.6	2.6
Supernate	1.09 ± 0.1	2.9	1.1

* Based on 7 batches of cells.

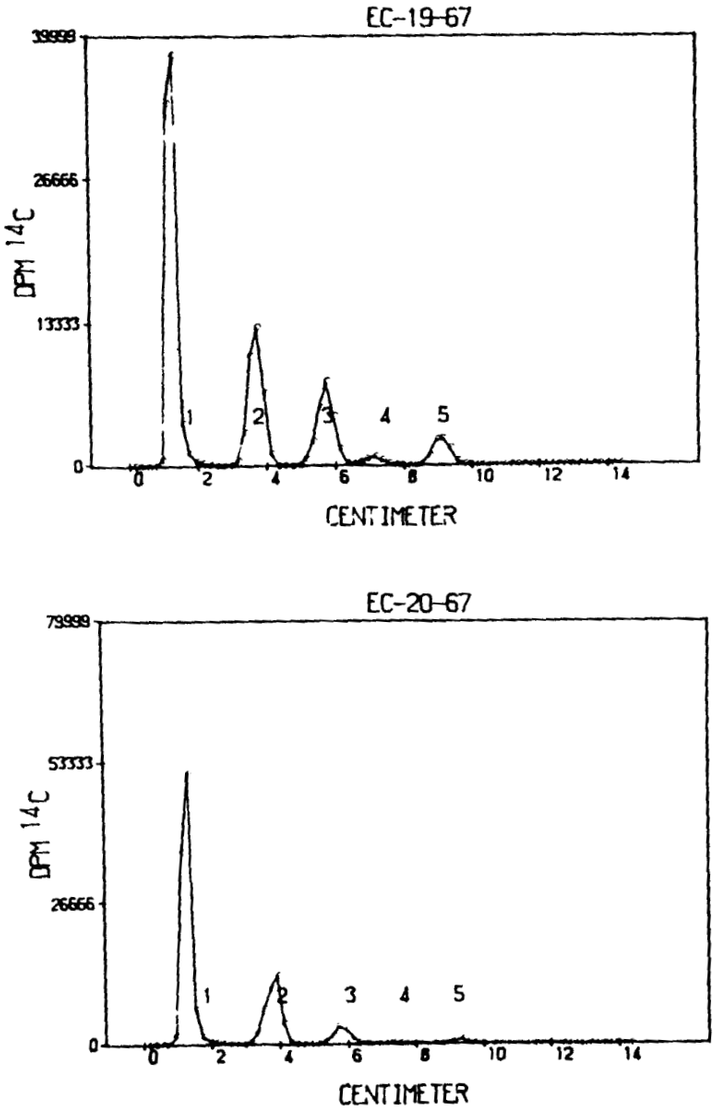

Fig. 87. Carbon-14 distribution in lipid classes in centrifuged fraction of disrupted Ehrlich ascites cells. Upper TLC ^{14}C profile scan (EC-19-67) is from 15,000 g (10 min) fraction and lower TLC ^{14}C profile scan (EC-20-67) is 34,000 g (3 hr) fraction. Identification of peaks: (1) phospholipids, (2) free fatty acids, (3) triglycerides, (4) glyceryl ether diesters, and (5) cholesteryl esters.

1027682

proportion of the neutral lipid ether ... s fo ... the ... 00 g ... min) fraction and the least amount in the 34,000 g (3 hr) fraction (Table 43). After the mice bearing the tumor were given five daily injections of palmitic-1-^{14}C acid, only the 15,000 g fraction had a significant peak of radioactivity in the glyceryl ether diesters as detected by zonal ^{14}C profile scans (Fig. 87).

The Metabolism of Glyceryl Thioethers

Fred Snyder, Claude Piantadosi, and Randall Wood

The O-ethers of glycerol (alkyl[1,2] and alk-1-enyl[3,4]) are readily cleaved by mammalian enzymes. Recently, our group has shown that the "etherase" complex in rat liver can be solubilized. Studies to elucidate the mechanism of the hydroxylation step and that of the reduction-oxidation of the initial detectable product (aldehyde) are planned. We felt that the glyceryl thioethers would be valuable model compounds to use in these studies since it would be possible to label the three critical parts of the glyceryl ether (the ether linkage, the hydrocarbon chain, and the glyceryl moiety).

Initial evaluation of 1-^{14}C-labeled glyceryl thioethers ($C_{16:0}$ and $C_{18:0}$) was carried out in feeding experiments with rats. These studies revealed that the glyceryl S-ethers are metabolized different from the glyceryl O-ethers. A very high percentage of the ^{14}C from the S-ethers was found in the urine during the first day after administration (Table 44) and essentially none of the label appeared as $^{14}CO_2$ (Fig. 88). Small quantities of ^{14}C were found in tissue lipids primarily distributed in the phospholipid components. The data indicate that the S-ethers of glycerol are not suitable as model compounds for examining the biochemical mechanism of ether cleavage. On the other hand, the marked difference in the biological behavior of the O- and S-ether bond has raised some interesting questions on the biochemistry of ether bonds. The question of the occurrence of S-ethers of glycerol in nature remains to be answered.

* Department of Medicinal Chemistry, School of Pharmacy, University of North Carolina, Chapel Hill, N. C.

REFERENCES

1. Tietz, A., Lindberg, M., and Kennedy, E. P. A new pteridine-requiring enzyme system for the oxidation of glyceryl ethers. J Biol Chem 239, 4081-4090, 1964.

TABLE 44

*Urinary Excretion of ^{14}C After Feeding Glyceryl O and S Ethers to Rats**

Compound	^{14}C Excreted (% of injected ^{14}C dose)
18:0-1 (S-ether)	87
16:0-1 (S-ether)	45
16:0-1 (O-ether)	5
16:0-2 (O-ether)	3

* 24 to 27 hr urine collection after oral intubation of ^{14}C glyceryl ethers. Only 0.8% of ^{14}C was found in urine 24 hr after feeding 1-$^{14}C_{16:0}$ acid.

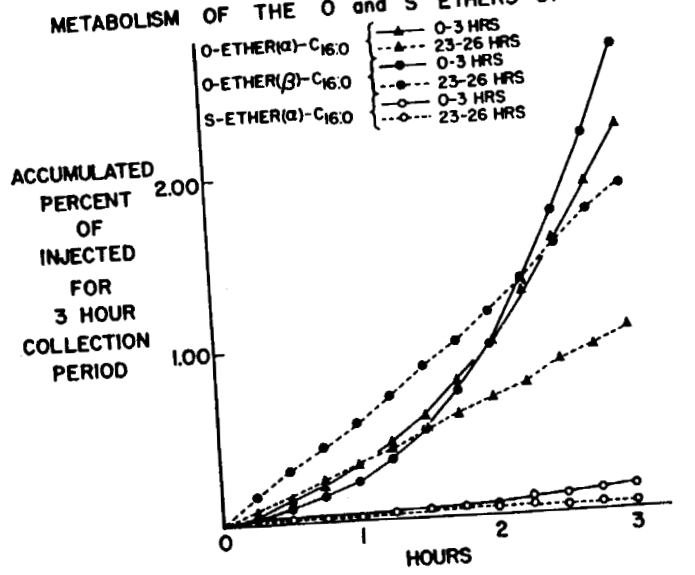

Fig. 88.

1027683

2. Pfleger, R. C., Piantadosi, C., and Snyder, F. The biocleavage of isomeric glyceryl ethers by soluble liver enzymes in a variety of species. Biochim Biophys Acta 144, 633-648, 1967.

3. Warner, H. R. and Lands, W. E. M. The metabolism of plasmalogen: enzymatic hydrolysis of the vinyl ether. J Biol Chem, 236, 2404-2409, 1961.

4. Ansell, G. B. and Spanner, S. The magnesium ion-dependent cleavage of the vinyl ether linkage of brain ethanolamine plasmalogen. Biochem J 94, 252-258, 1965.

Glyceryl Ethers in Insects: Identification of the Alkyl- and Alk-1-enyl-glyceryl Ethers in the Phospholipids of Three Insect Species

Edward N. Lambremont and Randall Wood*

The neutral lipid and phospholipid fractions obtained from adult American cockroach (Periplaneta americana) and larvae, pupae and adult boll weevil (Anthonomus grandis) and tobacco budworm (Heliothis virescens) were quantitatively analyzed for alkyl- and alk-1-enyl-glyceryl ethers by a procedure developed in this laboratory.[1] Both the alkyl- and alk-1-enyl-glyceryl ethers were found almost exclusively in the phospholipid fractions. The glyceryl alk-1-enyl ethers were found to predominate at all metamorphic stages in Heliothis virescens while higher concentrations of the alkyl glyceryl ethers were found in Periplaneta americana and Anthonomus grandis. The alkyl- and alk-1-enyl-glyceryl ethers of Heliothis larvae and Periplaneta adults were isolated by preparative thin-layer chromatography (TLC) for further characterization by gas-liquid chromatography (GLC), TLC, and chemical behavior. A thin-layer chromatoplate of Periplaneta (A) and Heliothis (B) alkyl-, alk-1-enyl-, hydrogenated alk-1-enyl-, and isopropylidene alkyl-glyceryl ethers is shown in Fig. 89 along with synthetic standards. The alk-1-enyl ethers of both species and the alkyl ethers of Periplaneta were found to be the 1-isomer by TLC on arsenite impregnated layers, a method previously shown to separate isomeric glyceryl ethers[2]; however, Heliothis alkyl glyceryl ethers were found to contain both the 1- and 2-isomers. This is the first reported 2-isomer found in nature. Heliothis and Periplaneta percentage composition of both the alkyl- and alk-1-enyl-glyceryl ethers obtained

* Research Participant, Louisiana State University, Baton Rouge, La.

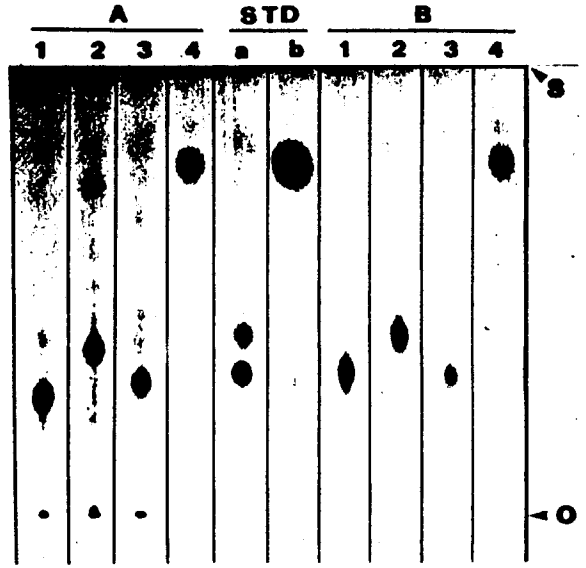

Fig. 89. A thin-layer chromatoplate of Periplaneta (A) and Heliothis (B) glyceryl ethers and derivatives. The numbered lanes represent: (1) alkyl-; (2) alk-1-enyl-; (3) hydrogenated alk-1-enyl-; and (4) isopropylidene alkyl-glyceryl ethers. Alkyl- (bottom spot) and alk-1-enyl-glyceryl ether (lane a) and isopropylidene alkyl glyceryl ether (lane b) standards appear at the center of the chromatoplate. The origin and solvent front are marked by O and S.

by GLC analysis of the alkyl isopropylidene derivatives and alk-1-enyl aldehydes are shown in Table 45. The alkyl and alk-1-enyl ethers of the same species have similar composition but the composition between the two species is quite different.

In addition to previously mentioned contributions of this investigation, it has also served to illustrate that glyceryl ethers are not confined to the higher animals and that this class of lipids appears to be ubiquitous in nature.

REFERENCES

1. Wood, R. and Snyder, F. Quantitative determination of alk-1-enyl and alkyl-glyceryl ethers in neutral lipids and phospholipids. Lipids, in press, 1967.

2. Wood, R., and Snyder, F. Chemical and physical properties of isomeric glyceryl monoethers, Lipids 2, 161-171, 1967.

1027684

TABLE 45

*GLC Analysis of Glyceryl Alkyl Ether Isopropylidene Derivatives and Glyceryl Alk-1-enyl Ether Aldehydes of Two Insect Species**

Hydrocarbon Chain Length†	% Glyceryl Alkyl Ether		% Glyceryl Alk-1-enyl Ether	
	Heliothis‡	*Periplaneta*	*Heliothis*	*Periplaneta*
16:0	8.2	2.5	15.9	5.4
17:0	T	T	0.9	5.6
18:0	43.5	79.4	34.6	67.3
18:1	T	8.0	2.1	19.5
19:0	2.4	6.4	2.8	2.1
20:0	31.2	3.6	35.8	---
20:1	7.2	---	---	---
21:0	---	---	4.6	---
22:0	T	---	1.9	---
Unknown	7.7	---	1.4	---

* Analyses were made on 5 ft. x 1/8 in. glass column packed with 15% EGSS-X. Isopropylidene derivatives were analyzed at 210°C and aldehydes were chromatographed at 160°C.

† Identification of even-numbered carbon chains up to C_{20} are based on co-chromatography with known standards at two or more temperatures and log. plots of retention time versus carbon number. Identification of odd carbon numbered chains are based on log. plots of retention times versus carbon number and is therefore considered tentative.

‡ The glyceryl alkyl ether values are for the 1-isomer since only the 1-isomer forms isopropylidene derivatives.

Metabolism of Long-Chain Fatty Alcohols in a Variety of Tissues: in vivo and in vitro

Fred Snyder and Boyd Malone

Fatty alcohols, produced during the cleavage of alkoxyglycerols, are formed by the reduction of fatty aldehydes in the presence of NADPH.[1] Recently, Friedberg and Greene[2] described an enzyme system in mammalian and dogfish livers that esterifies the fatty

alcohols with waxes. We have examined the oxidation and esterification of 1-^{14}C fatty alcohols in a number of tissues, in vivo and in vitro.

The lipid class distribution of ^{14}C found 3 hr after intravenous administrations of 1-^{14}C labeled $C_{16:0}$ and $C_{18:0}$ long-chain alcohols is given in Table 46 for liver and spleen from rats. These data demonstrate that oxidation of the alcohol to the fatty acid and subsequent acylation with glycerol is the major metabolic route in both liver and spleen, but it is also obvious that direct esterification with fatty acids to form waxes can also occur under these conditions. The soluble protein fraction (34,000 g supernate) of cells appears to contain the active enzymes for these conversions (Table 47). The liver fraction formed more wax than analogous fractions from kidneys, spleens, lungs, or bone marrow; similar results were obtained for both the $C_{16:0}$ and $C_{18:0}$ alcohols. Oxidation of the fatty alcohols to fatty acids was highest in the livers and kidneys and the $C_{16:0}$ alcohol was the most active substrate.

REFERENCES

1. Pfleger, R. C., Piantadosi, C., and Snyder, F. The biocleavage of isomeric glyceryl ethers by soluble liver enzymes in a variety of species. Biochim Biophys Acta, 144, 633-648, 1967.

2. Friedberg, S. J. and Greene, R. C. The enzymatic synthesis of wax in liver. J Biol Chem 242, 234-237, 1967.

TABLE 46

Distribution of ^{14}C in Rat Tissue Lipids 3 hrs after Intravenous Injection of 1-^{14}C in $C_{16:0}$ and $C_{18:0}$ Alcohols

Tissue	Fatty Alcohol Administered	% of ^{14}C in Lipid Classes				
		Phospho-lipids	Fatty Alcohols	Fatty Acids	Tri-glycerides	Wax
Liver	$C_{16:0}$	56.60	2.26	1.75	32.41	6.14
Liver	$C_{18:0}$	75.67	2.48	0.30	11.95	4.56
Spleen	$C_{16:0}$	69.41	5.23	0.06	13.49	12.89
Spleen	$C_{18:0}$	59.86	5.89	9.08	1.67	2.75

1027685

TABLE 47

Distribution of ^{14}C in Soluble Fraction of Rat Tissue Lipids after Incubation for 1 hr at 37°C

Tissue -- Substrate	% ^{14}C in Lipid Classes				
	Phospho-lipids	Fatty Alcohols	Fatty Acids	Tri-glycerides	Wax
Liver - $C_{16:0}$ Alcohol	0.74	67.97	12.70	1.42	13.80
Liver - $C_{18:0}$ Alcohol	0.76	67.18	7.50	1.02	17.35
Kidney - $C_{16:0}$ Alcohol	0.95	72.84	15.99	2.15	6.44
Kidney - $C_{18:0}$ Alcohol	0.93	83.29	4.69	2.00	4.51
Spleen - $C_{16:0}$ Alcohol	1.18	92.22	0.54	0.19	4.02
Spleen - $C_{18:0}$ Alcohol	0.34	88.33	2.88	0.91	4.70
Lung - $C_{16:0}$ Alcohol	1.01	89.08	0.46	0.33	7.73
Lung - $C_{18:0}$ Alcohol	0.00	85.55	2.72	1.07	6.17
Bone Marrow - $C_{16:0}$ Alcohol	0.85	85.11	0.78	0.87	11.80
Bone Marrow - $C_{18:0}$ Alcohol	0.66	80.49	3.75	1.19	7.43

Lipid Class and Fatty Acid Composition of Rat Liver Plasma Membranes Isolated by Zonal Centrifugation

R. C. Pfleger, Norman G. Anderson,† and Fred Snyder*

Plasma membranes of rat liver, exclusive of endoplasmic reticulum, were isolated by zonal centrifugation for analysis of lipid classes and fatty acid composition. The plasma membranes yielded 880 μg protein and 390 μg total lipid per gram of liver. Neutral lipids, amounting to 27% of the total extractable lipids,

* Present address: Lovelace Foundation for Medical Education and Research, Albuquerque, N. M.

† Biology Division, Oak Ridge National Laboratory.

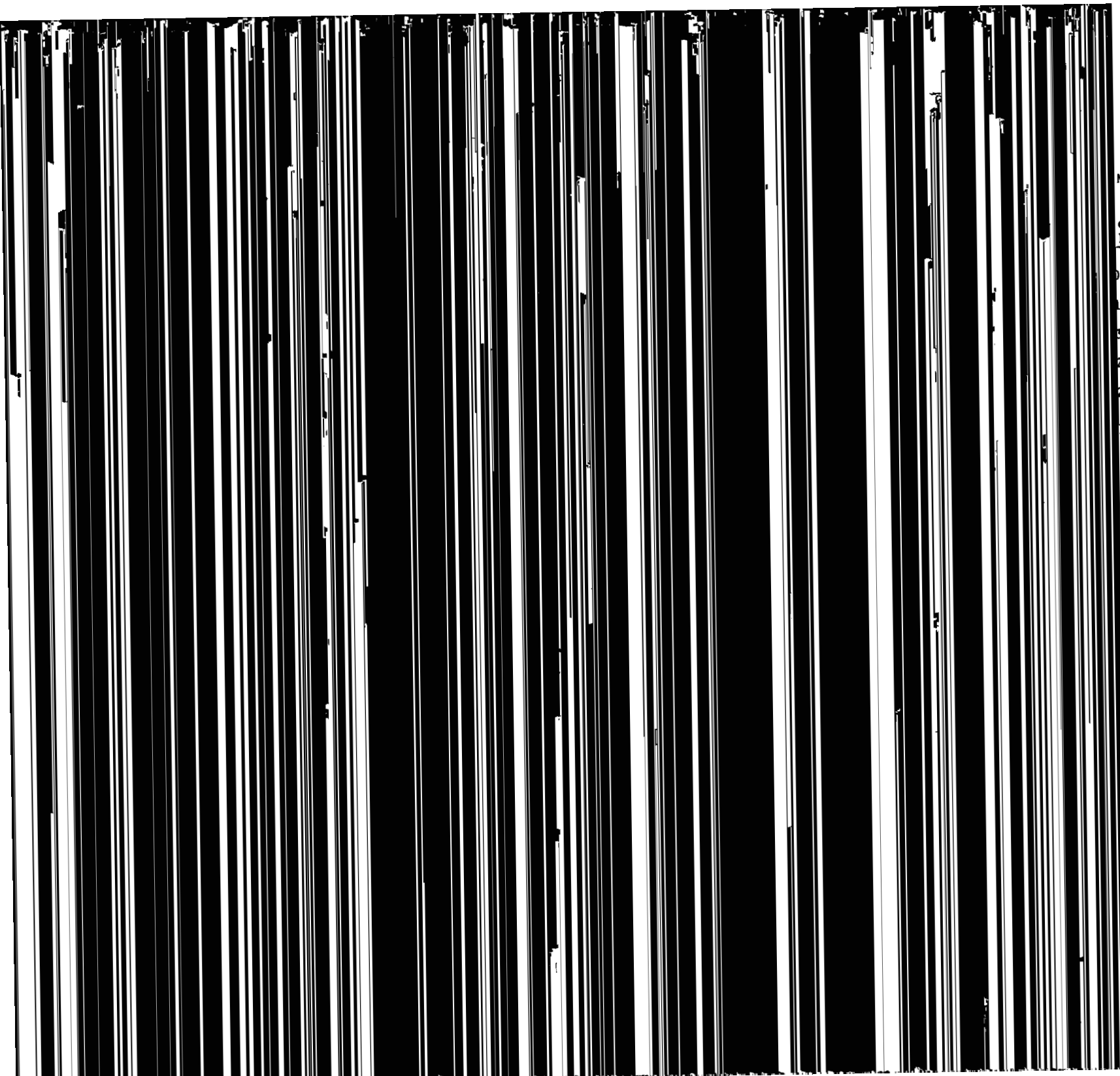

MEMBRANES

of Total Extracted*
) ± 6.3
19 ± 1.23
31 ± 0.87
2 ± 3.4
28 ± 0.72
1 ± 7.4
15 ± 0.98
2 ± 4.6
96 ± 1.34
89 ± 1.20
01 ± 1.17
70 ± 0.54
9 ± 3.6
1 ± 10.9

) different membrane

ferent membrane preparations
alkyl ethers accounted for
counted for 0.24 ± 0.06%.

rus content and assuming
for each lipid class
Table 49

ement using sphingomyelin

TABLE 49

FATTY ACID COMPOSITION OF THE MAJOR LIPID CLASSES OF RAT LIVER PLASMA MEMBRANES

Fatty Acids*	LPC	SPHI	PC	PS+PI	PE	PA	PGP	Unknown	TG	FFA
<14:0	+	+	0.1	+	+	+	+	+	+	+
14:0	0.2	0.2	0.5	+	0.2	1.4	1.2	+	1.66	2.93
15:0	1.0	0.2	0.5	+	0.6	0.4	+	+	+	+
16:0	33.4	18.7	30.2	12.1	26.0	26.3	23.8	32	35.7	31.6
16:1	0.1	0.1	0.8	0.5	0.3	+	0.9	+	3.50	3.07
17:0	3.4	0.1	+	+	1.5	0.9	+	+	1.43	
18:0	45.7	39.2	29.8	49.2	31.9	30.0	28.3	48	3.64	21.9
18:1	4.0	3.7	9.6	4.6	6.5	13.0	15.3	10	32.3	19.0
18:2	3.7	4.2	15.3	5.2	12.4	16.8	16.3	10	21.8	13.2
A		3.5	1.7	2.0	4.1	+	+		+	+
20:4 B	5.9	12.8 17.2	11.6 +	26.4 +	15.4 +	12.1 +	16.9	+		6.26 +

* The number before the colon represents the number of carbon atoms, and the number after the colon represents the number of double bonds.

A = Total percentage of minor peaks occurring between 18:2 and 20:4.

B = Total percentage of minor peaks occurring after 20:4

All values expressed as percentage of total fatty acids

LPC (lysophosphatidylcholine); SPHI (sphingomyelin); PC (phosphatidylcholine); PS (phosphatidyl serine); PI (phosphatidyl inositol); PE (phosphatidylethanolamine); PA (phosphatidic acid); PGP (polyglycerol-phosphatides); TG (triglyceride); FFA (free fatty acids).

1027681

Gas-Liquid Chromatographic Analysis of Heliothis virescens Triglyceride Composition at Various Metamorphic Stages

*Randall Wood, Robert Harlow, and Edward N. Lambremont**

Heliothis virescens, the tobacco budworm, was reared from egg to the desired stage singly in plastic vials containing a semi-defined diet. The lipids were extracted, weighed, and the triglyceride was isolated by preparative thin-layer chromatography (TLC). The triglyceride carbon number distribution was determined by gas-liquid chromatography (GLC) of the intact triglycerides according to a procedure described elsewhere (see page 146 of this report). Fatty acid methyl ester composition was also determined for each fraction by conventional analytical GLC.

The percentage lipid of the various metamorphic stages is shown in the second column of Table 50. The lipid content reaches its maximum at late-larva to early-pupa stage, which decreases to a value in the mid-age pupae that remains constant until early adult, at which time the lipid content decreases with age. The carbon number distribution of mature larvae and 11-day-old adult triglycerides is shown for comparison in Fig. 90. The carbon

* Research Participant, Louisiana State University, Baton Rouge, La.

Fig. 90. The GLC analysis Heliothis virescens intact triglycerides of mature larvae 11-day-old adults. Peak numbers represent the sum of triglyceride fatty carbon atoms.

TABLE 50

Comparison of Heliothis virescens *Triglyceride Composition at Various Stages of Development*

Metamorphic Stage	% Lipid Dry Wt.	% Carbon Number*					
		48	50	52	54	56	58
Young larvae	15.2	0.9+	17.9	64.3	16.5	0.5	
Mature larvae	14.2	2.6	33.6	56.6	7.2		
Young pupae	43.3	2.3	31.7	58.6	7.4		
Mid-age pupae	26.5	2.5	35.2	51.4	10.4	0.5	
Old pupae	26.4	2.0	35.8	54.8	8.3	T	
Adults	29.8	2.3	36.2	54.4	7.2		
4-Day old adults	27.4	0.8	21.6	62.2	15.4		
7-Day old adults	15.0	1.2	23.3	55.3	19.9	0.2	
11-Day old adults	9.4	0.8	20.2	53.5	25.3	0.2	
Diet Triglycerides	2.6	0.4	7.9	39.2	48.2	3.6	0.6

* The carbon number represents the sum of the number of carbon atoms in the hydrocarbon chains.

\+ Represents the mean of two determinations.

distribution percentage of triglycerides obtained from nine different development stages and the diet is given in Table 50. The triglyceride distribution is very narrow (48 to 56) at all stages of development with carbon numbers 50, 52, and 54 representing more than 95% of the total. Carbon number 50 percentage decreased with increased age, while carbon number 54 increased but also showed pulsating increases, which coincided with the basic metamorphic changes from larvae to pupae to adult. Carbon number 52 showed the least variation. Fatty acid methyl esters ranged in chain length from $C_{14:0}$ to $C_{20:4}$, but the C_{16} and C_{18} fatty acids represented more than 95% of the total at all developmental stages. Oleic and palmitoleic acids showed the least change. Palmitic acid decreased with increased age, the same as observed for triglyceride carbon number 50, and linoleic acid showed a pulsating increase similar to that observed for triglyceride carbon number 54. The observed changes in specific triglyceride carbon numbers with a corresponding simultaneous change in specific triglyceride fatty acids indicate a nonrandom fatty acid distribution and suggest triglyceride carbon number or molecular species specificity.

1027688

THEORETICAL AND EXPERIMENTAL STUDIES IN METABOLISM AND DISTRIBUTION OF NUCLIDES

Our objective is to quantitate patterns of absorption, distribution, and excretion of tracer metals, radionuclides of medical interest, and environmental and occupational contaminants. Where possible the work is done in patients with whole-body counting, combined with chemical and radioassay data. Selected questions arising out of the major objective have led to interesting results in animals. Some of the experiments reported here were done by college students on the ORAU Student Trainee Program working with members of the Medical Division staff. Also included in this section is a collaborative project involving neutron activation for analysis of gold thioglucose, carried out in cooperation between Roger J. Cloutier of ORAU and Dr. A. F. Debons' group at Downstate Medical Center, New York. The paper on phenothiazine inhibition of NADH oxidation by melanin represents work done by Dr. Melvin Van Woert while he was here as a temporary staff member before he joined the faculty at Yale University. It is a preview of work in the area of phenothiazine toxicity, manganese toxicity, and Parkinson's disease which is being initiated by Dr. Edward Bird, who recently has joined our clinical staff from the University of Florida Medical School. He will also pursue related studies in endocrinology and metabolism.

Fitting Models to Data: The Problem of Uniqueness

*Per-Erik E. Bergner and Warren Franz**

A common situation today is where one has an equation containing a number of parameters, the numerical values of which one tries to estimate by fitting the equation to a set of experimental data. The dominating philosophy has been that one accepts the set of parameter values that gives the best fit, e.g., that minimizes the sum of the distances between the experimental data points and the curve generated by the equation with the parameter values inserted. Most often the so-called least-square method is used.

When doing a thing like this, it is necessary first to postulate that a "correct" set of parameter values actually exists; otherwise, the

* Department of Chemical Engineering, University of Tennessee, Knoxville.

whole procedure would be meaningless. But this immediately generates a quite fundamental question: Why should the correct parameter values give the best fit? One answer is given by the idea of maximum likelihood, i.e., by choosing the proper measure of goodness of fit, the parameter values giving the best fit also gives maximum probability to the experimental data. In addition to being philosophically obscure, this approach is often of little practical value because to find the "proper" measure of fitness, one must know the underlying statistics of the experimental data, and this knowledge is usually not available.

A more playboy-like viewpoint is to accept a specific fitting procedure simply as a rule of the game: "This is how we select our parameter values." The scientific validation of the method is then solely based upon the practical success, i.e., whether or not the results make sense and give valuable information with respect to some outside data. For instance, one might ask whether the obtained parameters simplify the diagnosis of certain diseases or whether they make it possible to localize changes in an otherwise nonaccessible system.

However, no matter which viewpoint one prefers, there is at the end a pure mathematical problem that seems hard to overcome: Existing curve-fitting procedures frequently give nonunique results. That is, for a given set of experimental data one can obtain completely different sets of parameter values all of which give equally good fit. Although the problem is mentioned in the literature, no one seems hitherto to have been able to formulate any satisfactory solution.

We have recently faced this problem in our attempts to fit a specific model for the metabolism of chromium-labeled RBC.[1] First we used an analog computer, which of course is a rather subjective method: The goodness of fit was judged simply upon visual inspection. Nevertheless, although the spread in the parameter values was substantial, the overall result appeared to make biological sense.[1] The annoying spread in the parameters could be due to several factors, like the necessary errors in the experimental data points and the semiquantitative clinical grouping of the patients. Another possible factor is the model itself (when considered as an approximation of the "real" system).

However, we felt that the analog method, subjective as it is, could be a main source of the scatter and that, therefore, it would be worthwhile to make the curve fitting on a digital computer. A random-vector method was used. This program (called MINIMI) has the following advantages: Upper and lower limits of the parameters can be read into the program, it provides a function map when a minimum is obtained showing the effect of small variations in each of the parameters, and many different measures of goodness of fit can be used. The program is slower but does not seem to have the stability problems that the standard least-square minimization programs have when searching for a minimum.

The results were depressing. The computer was able to localize

1027689

minima for widely different sets of parameter values: The scatter was larger than what we obtained with the analog computer. However, the model contains seven parameters, two of which can be determined graphically, and we could therefore reduce it to a five-parameter problem for the computer. This improved the results: The variation between the computer-estimated set of parameter values, for a given set of experimental data, decreased. It became eventually possible to select a definite set of parameters for each patient.

When these results were compared with those obtained with the analog computer, the following could be observed: The scatter in the parameters within the different clinical groups was still about the same; so from this viewpoint, the digital method did not imply any substantial improvement. But what was really disappointing was that the kind of clinical sense, which could be recognized in the parameters determined by the analog computer,[1] had to some extent disappeared. Moreover, the values given by the digital computer to one of the parameters appeared definitely unphysiological.

We feel that the results of this investigation give a good illustration to the problems formulated at the beginning of this report: When working with models of different kinds, one must remember that the mere fact that a model fits data means little if anything. Moreover, when the model contains several parameters, the fit is probably not unique. A lot of fundamental research is needed on the theory of "curve fitting." Although fitting of a model is a quite common situation today, the fundamental problems of the underlying theory are surprisingly neglected.

In the present context, a specific question is why the analog-computer fit gave seemingly more sensible results. One possible answer is, of course, that the results are simply incidental. Another of many possible answers is that in this particular case, the analog method was the more appropriate one. The reason for suggesting this is that the experimental data points were occasionally quite scattered and a "data smoothing" became necessary. When working with the analog computer, the investigator had to do the smoothing under the restrictions of the model; hence, if the model has, as we believe, a reasonable correlation with reality, this means that the data smoothing had to be done under the restrictions implied by the actual physiology. When working with the digital computer, we lacked any theory giving rules for how the smoothing should be done, and, therefore, chose simply to fit smooth curves by eye and from these curves read the data into the computer: we may thereby have introduced an "unphysiological bias."

REFERENCE

1. Lushbaugh, C. C., Gibbs, W. D., Franz, W., and Bergner, P.-E. E. Analog computer analysis of human ^{51}Cr RBC Survival and whole-body retention data. In: USAEC Report ORAU-101, 1966, pp. 106-111.

Preliminary Analysis of Calcium and Potassium Retention Data

Per-Erik E. Bergner, W. D. Gibbs, and M. C. Yarbrough

A new theory (turnover compartmentalization) for evaluation of whole-body retention data has previously been reported.[1,2] In a recent paper[3] the theory has been applied to ^{45}Ca-retention data obtained on a parathyroidectomized cow. The results indicate that, although the new concepts are yet not completely understood, they do provide a tool for some physiologically meaningful interpretations of data. Thus, from the ^{45}Ca-retention curve alone (observation time: 9 days) it was possible to conclude that parathyroid extract causes an increase in the serum and fecal calcium, whereas there is a decrease in the turnover of bone-calcium. These results agree with what has been commonly believed and suggest, therefore, that the theory can serve as a practically useful basis for whole-body retention studies. However, it is also made obvious by the theory that to obtain information about the metabolism one has to study the system under different conditions, which agrees with what has been observed in other fields: to obtain information of the "normal" system one has to study the effects of perturbations. An example of this is the relaxation theory in chemical kinetics.

To this end we are now conducting an experiment on ^{42}K-retention in rats. The reason for selecting rats is that their metabolism is fast enough to allow for a reasonable portion of the retention curve to be observed during the time period set by the physical half-life of ^{42}K. We have equipment available that can serve as whole-body counters for these small animals: the retention can be observed for up to 6 days, and during this time 60 to 70% of the initial dose is excreted. The corresponding time period for a normal human is about 3 days, during which only 6 to 10% of the initial dose is excreted. In principle the animals have received a tracer injection at the beginning of each week. During the first week they were kept on a normal diet but received then extra potassium (potassium chloride was added to the drinking water).

Although the experiment is not completed yet some conclusions can be made. It has been assumed that in man the potassium system is well stirred,[4] which would imply a single exponential retention curve. For our rats this is definitely not so: the first part of the curves looks somewhat exponential, but after about 2 days they rather appear linear. The response to the extra potassium intake is obvious and consistent. The retention decreases in all the animals when they receive the KCl in the water. We had, however, expected that the rats would gradually build up a new steady state; instead, the rats show a periodic response: whereas the retention is always less than when the animals are on normal diet, it increases one week, decreases the next week, and then up again.

In terms of turnover-compartment theory, the results mean the following: Let us consider the amount of potassium that under steady-state conditions would stay in the animal between 0 and 6 days. We also consider the turnover of this particular compartment, i.e., the amount of such "short-lived" potassium that leaves the organism per unit of time. Then, the data indicate (they are still not completely processed) that the size and the turnover of this 0 to 6 day compartment increase when the animal receives extra potassium in the diet. However, these increases vary up and down from one week to another, a phenomenon that, as far as we know, has not been reported before. Hopefully we shall eventually be able to obtain, on the basis of this type of studies, a better understanding of the physiologic mechanisms controlling the potassium retention.

1027690

REFERENCES

1. Bergner, P.-E. E. Turnover compartmentalization. In: USAEC Report ORAU-101, 1966, pp. 103-105.

2. Bergner, P.-E. E. Turnover compartmentalization: A Statistical tracer theory for analysis of whole-system retention data. USAEC Report ORAU-104, 1967, 29 pp.

3. Bergner, P.-E. E. (1967) Paper presented at the third international symposium on quantitative biology of metabolism, Helgoland, West Germany (in press).

4. Moore, F. D. Discussion, p. 40. In: Compartments, Pools, and Spaces in Medical Physiology. Edited by Per-Erik E. Bergner and C. C. Lushbaugh. AEC Symposium Series No. 11, CONF-661010, August 1967.

Cesium-137 and Potassium-40 in Patients and Normal Subjects

W. D. Gibbs, Harold D. Hodges, Linda C. Thompson, and C. C. Lushbaugh

Cesium-137 and potassium-40 are the principal radioactive elements contributing "natural" gamma radioactivity to the human body, thereby establishing the natural background level of gamma-ray activity and its spectrum in the subjects in whom the metabolism of other radionuclides are being studied in the whole-body counting research facility. Previously we reported an initial whole-body counting survey of normal persons to determine the ^{137}Cs body burden and ^{40}K content in relation to total-body weight.[1] A remarkable variability was found that forbade our use of normalized standards and required individualized direct determinations of lean-body mass, ^{40}K content, and $^{137}Cs/K$ ratios for precise assay of

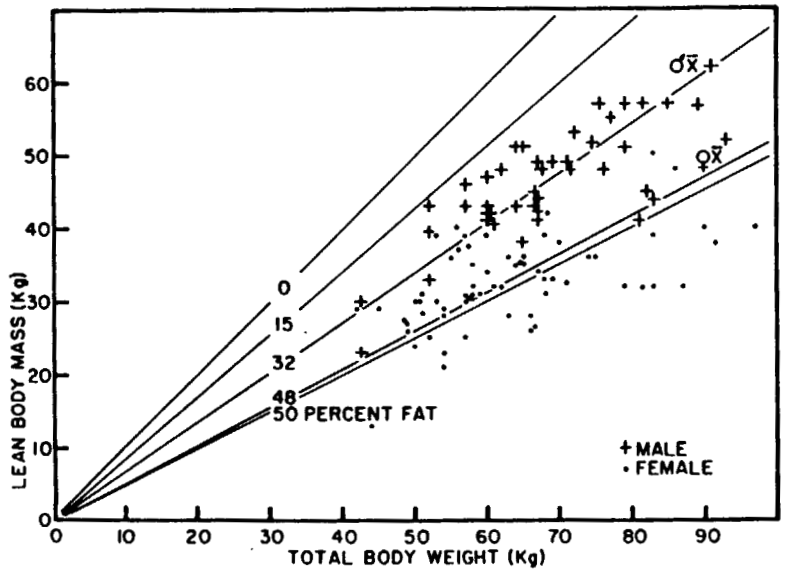

Fig. 91. Lean body mass (based on ^{40}K values) and total weight in 134 patients.

an unknown or purposefully introduced radionuclide in the whole body. We have extended these observations now to include such measurements in 134 patients selected only because they had undetectable body burdens (less than 0.5 nanocuries) of diagnostic or therapeutically administered isotopes at the time they were admitted to the hospital and counted in the low-level whole-body counter as an admission routine. No effort has been made to divide the patients into diagnostic groups because the numbers in any such group would be too small for statistical purposes. The influence of the high incidence of thyroid disease known to be present among the women patients can be seen, however, in the study of lean body mass by sex, as shown in Fig. 91. Comparison of these data (Fig. 91) with those reported previously for 416 normal subjects reveals that the average patient in our patient population has a smaller lean body mass (7% lower in male and 15% in female patients), but a greater proportion of fat. This change is most obvious among the female patients where almost half exceed the 50% fat level, which was the upper bound among our normal subjects.

Tables 51 and 52 compare the ^{137}Cs content and Cs/K ratios of normal subjects and the recent yearly changes in these parameters in our patient population. The reasons for the obviously larger total amount of ^{137}Cs and higher $^{137}Cs/K$ ratio in normal persons are not known but must reflect either dietary differences or a more rapid than normal turnover and loss of cesium in ill patients. Two

1027691

TABLE 51

Patients

	1965	1966	1967
Males			
Number of Subjects	11	29	8
Mean Total - ^{137}Cs*	8.26 ± 3.13	6.76 ± 3.23	4.23 ± 1.24
Mean $^{137}Cs/kg$*	0.12 ± 0.05	0.10 ± 0.04	0.06 ± 0.01
$^{137}Cs/K$†	0.068	0.055	0.032
Mean Wt (kg)	65.81	68.65	71.15
Females			
Number of Subjects	12	37	37
Mean Total - ^{137}Cs*	6.02 ± 3.09	4.09 ± 1.48	3.37 ± 1.70
Mean $^{137}Cs/kg$*	0.10 ± 0.05	0.07 ± 0.02	0.05 ± 0.02
$^{137}Cs/K$†	0.078	0.047	0.037
Mean Wt (kg)	60.85	61.59	63.31

* All ^{137}Cs values are in nanocuries ± 1 standard deviation.

† Values are nanocuries of $^{137}Cs/kg$ potassium.

TABLE 52

Cesium-137 in Normal Persons

	1965	1966
Males		
Mean Total - ^{137}Cs	15.55 ± 6.01	9.57 ± 3.65
Mean ^{137}Cs/kg	0.21 ± 0.10	0.13 ± 0.05
^{137}Cs/K	0.109	0.066
Mean Wt (kg)	72.04	75.52
Females		
Mean Total - ^{137}Cs	7.12 ± 2.22	5.53 ± 1.60
Mean ^{137}Cs/kg	0.13 ± 0.04	0.09 ± 0.03
^{137}Cs/K	0.079	0.059
Mean Wt (kg)	55.7	57.4

patients in 1966 and one in 1967 were found to contain less than 1.5 nanocuries of cesium suggesting that an altered metabolism of cesium may be the more likely explanation for this phenomenon, since all three of these patients manifested difficulties in maintaining normal electrolyte balance.

REFERENCE

1. Gibbs, W. D., Hodges, H. D., Lushbaugh, C. C., and Quarles, J. F. A two-year study of cesium-137 and potassium in normal subjects. In: USAEC Report ORAU-101, 1966, pp. 117-119.

1027692

Test of an Empirical System for Correcting Geometric Error in Whole-Body Counting of Reportioning Radioactive Labels Using Iodine-131

W. D. Gibbs, Harold D. Hodges, Mildred Bailey, and C. C. Lushbaugh

The accurate quantitation of the radioactive content of an object as large and variably shaped as the human body cannot be achieved with present methods if the radioisotopic label changes location with time. Except for evenly distributed electrolytes such as sodium, potassium, and cesium, most noncolloidal radioisotopes introduced into the body undergo a series of changes in spatial distribution and location during whole-body retention studies. This phenomenon is commonly seen with ^{131}I, ^{59}Fe, radioactive-labeled vitamins, and many other tracers.

A new approach to the solution of this problem is described here. Whole-body retention measurements are used as an example of how a system of scatter counting was developed that enables direct quantitation of the ^{131}I content in any distribution in any size human subject.

A point source of ^{131}I was counted at 33 different locations in a water phantom (Fig. 92). The spectrum of the source at each

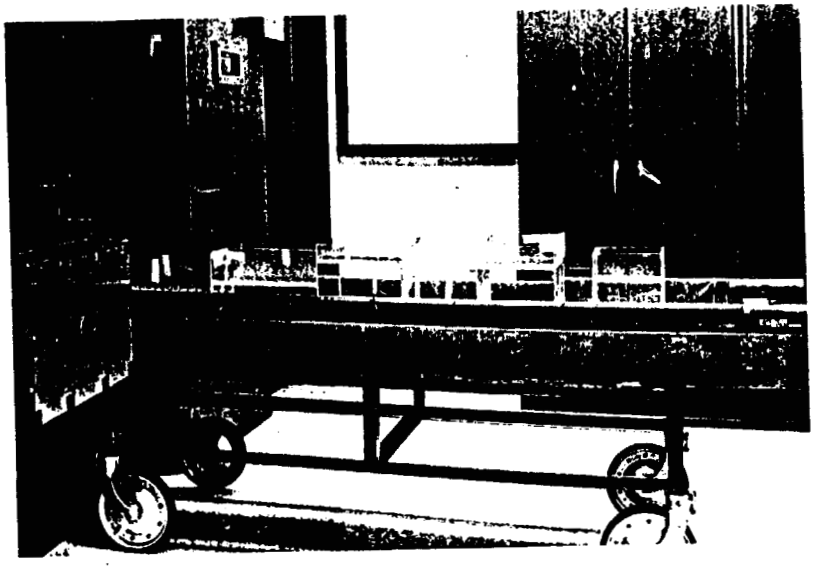

Fig. 92. Multicompartmented water phantom.

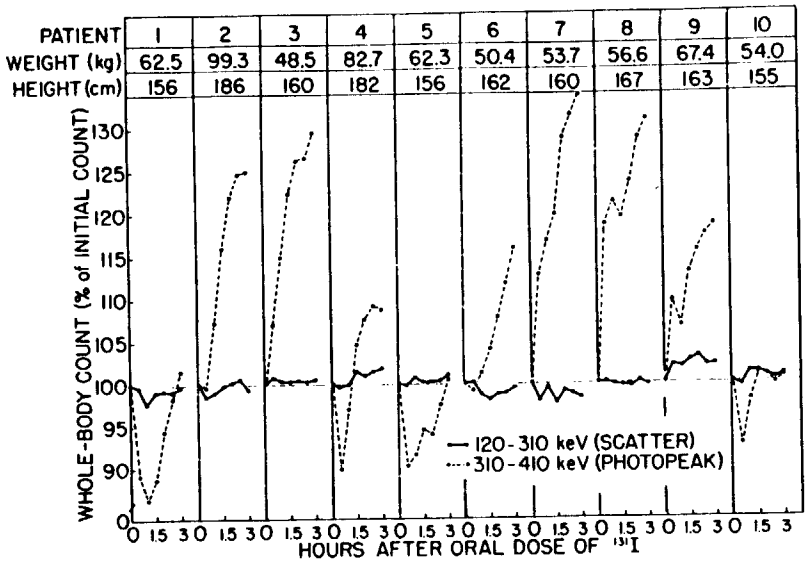

Fig. 93. Variations in whole-body count during first 3 hr after oral doses of ^{131}I. Values are shown for ten patients each counted with the two different techniques.

location was stored in a multichannel pulse-height analyzer. The data of the 33 spectra were punched into paper tape to enable convenient computer input. The computer was programmed so that the counts obtained in every possible continuous window of 50 kev and wider for each source location were compared with the counts obtained with an arbitrarily chosen source location (center of the abdomen). The absolute values of the differences observed were then summed. The window in which the sum of the differences was the smallest is the window in which counting errors caused by changes in distribution of ^{131}I are minimum. The minimum error window for ^{131}I determined by this analysis was 120 to 310 kev.

The accuracy of the computer analysis was tested with 10 patients given oral doses of ^{131}I in capsule form. Each patient was counted immediately after administration of the dose and at 30-min intervals thereafter for 3 hr (7 counts). The whole-body content of ^{131}I present in each patient was kept constant except for physical decay by having them refrain from voiding during the 3-hr period.

Figure 93 shows the results obtained when the photopeak counts

1027693

(310 to 410 kev) and the scatter window counts (120 to 310 kev) are expressed as percentage of the initial count. Errors as large as +35% were obtained when the photopeak window was used, but maximum observed error was less than +3% with the "minimum error" or "scatter window."

Zinc Retention in Rabbits Under Myelopoietic Stress

W. D. Gibbs, P. J. Sides, L. W. Anglin,* M. C. Yarbrough,† and C. C. Lushbaugh*

This research was stimulated by an observation we made in a child with subacute myelogenous leukemia an abnormally high absorption of ^{65}Zn and an exceedingly slow rate of zinc excretion. Prepatory to trying to determine whether zinc metabolism may be altered by leukemic bone-marrow stress or the inanition that frequently accompanies this disease and its therapy, we studied ^{65}Zn retention (20 microcuries $^{65}ZnCl$ intravenously) in normal rabbits and others with a leukocytosis induced by Freund's adjuvant (1.25 ml/kg body weight injected subcutaneously). The leukocyte levels (11 to 12,000/cu mm; 80% lymphs) doubled within one week after the injection and remained steady at this new steady state over the 3-month study period of zinc retention. No significant changes occurred in their differential counts.

The results of this study using four normal and four stressed rabbits showed no difference in the zinc turnover rates in the two groups. Figure 94 shows the average percentage of retention of ^{65}Zn in all rabbits plotted linearly and semilogarithmically over the 90-day study period. At the end of this time all the rabbits were killed and their organs, blood, and carcasses were assayed for residual ^{65}Zn content. Figure 94 diagrams the fact that 95% of the 90-day residual ^{65}Zn label was in the carcass; 80% in the bone; 10 to 15% in muscle; 5 to 10% in the other organs and bone marrow. The linear graph appears to predict that the large amount of zinc incorporated in the bone will be turned over slowly so that this metabolic compartment will finally dominate and be the determinent of body and environmental zinc equilibrium level. If so, zinc re-

* Summer Student Trainee, University Participation Office, ORAU.

† Present address: General Clinical Research Center, University of Oregon Medical School, Portland, Oregon.

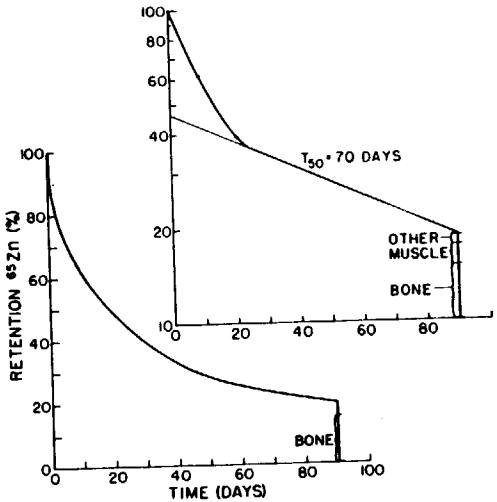

Fig. 94. Shows linear and semilogarithmic plots of average per cent retention of ^{65}Zn in rabbits showing that after 90 days the majority of the zinc is in the skeleton and muscle.

tention in young growing animals or adult animals with bone disease would be expected to be high and retention prolonged. Similarly zinc dietary deprivation in childhood would also be expected to augment retention of ^{65}Zn and restrict its rate of excretion. The kinetics of zinc metabolism might be expected, therefore, to resemble that of calcium more than any other dietary mineral constituent.

These observations would seem to depreciate the importance of any zinc involved in myeloproliferation in contrast to its role in skeletal development.

Route of Iron-59 Loss in the Rabbit

R. F. Queener, P. J. Sides, and W. D. Gibbs*

The rabbit is commonly used in studying alterations in peripheral blood morphology because it can be bled easily. Little attention, however, is usually paid to its "abnormal" erythrokinetics even though RBC loss rate in normal animals of this species is complicated by random

* Summer Student Trainee, University Participation Office, ORAU.

1027694

RBC "death."[1] Our studies[2] of the loss of ^{51}Cr and ^{59}Fe labeled RBC in this animal confirmed the presence of random RBC loss, but our whole-body counting assays showed that this could not be random death or destruction since the ^{59}Fe was being lost from the body. Iron-59 (given intravenously as ferrous citrate) was so rapidly incorporated into the circulating RBC mass (>98% within 2 days) that the animals must have had (at the time of labeling) severely depleted iron stores as though from chronic hemorrhage. Our study of ^{59}Fe whole-body retention in the rabbit disclosed a ^{59}Fe excretion rate measured as a T_{50} of ~100 days (5 to 7 times faster than that of normal man). Rapid intestinal mucosal loss of partially absorbed iron was ruled out as an explanation by our use of intravenous injection of the iron that was rapidly incorporated into the circulating RBC mass.

Hemorrhage was, therefore, the only plausible explanation for this phenomenon, but no evidence for this could be found on examination of the animals or their cages. When, however, we assayed separately the urinary and fecal excretions of rabbits labeled intravenously with 40 microcuries of ^{59}Fe citrate, we found as shown in

TABLE 53

	Percent Dose			
Rabbit #1	0-6 days	7-14 days	14-19 days	Total
Feces	4.32	2.21	0.86	7.39
Urine	0.12	0.43*	0.01	0.56
Rabbit #2				
Feces	2.34	2.70	0.94	5.98
Urine	0.05	0.02	0.01	0.08

*Urine sample contaminated with feces.

Table 53 that fecal loss of the ^{59}Fe RBC label was present at the levels expected from our previous whole-body counting studies. In the studies reported here, measured excretion and whole-body retention summed to greater than 93% of the administered dose. The 7% discrepancy occurred because fecal collection was not completely quantitative and chemical elution of the label by urine occurred in the metabolic cages. The values for fecal content of the original dose in the table should, therefore, be corrected upwards.

These data suggest that the random loss of ^{59}Fe-labeled RBC that is superimposed on the expected loss from RBC senescent death

in the normal rabbit results from chronic gastrointestinal RBC loss. The cause for this loss is unknown to us, since we could find no mucosal lesions that might predispose the animals to hemorrhage.

REFERENCES

1. Burwell, E. L., Brickley, B. A., and Finch, C. A. Erythrocyte life span in small animals. Comparison of two methods employing radioiron. Amer J Physiol 172, 718-724, 1953.

2. Opdyke, D. F., Franz, W., Gibbs, W. D., Bergner, P.-E. E., and Lushbaugh, C. C. Effect of chromium on rabbit red blood cell survival. In: USAEC Report ORAU-101, 1966, pp. 111-115.

Toxic Effect of Chromium on Red Cell Survival

W. D. Gibbs, L. W. Anglin, P. J. Sides,* and C. C. Lushbaugh*

Previously we tested in rabbits the hypothesis that chromium RBC labeling produces RBC damage and leads to random RBC death. We used increasing amounts of nonradioactive chromium in the labeling procedures[1] to show that RBC sequestration by the reticuloendothelial system was increased by increasing amounts of carrier chromium. Because our lowest carrier level (10 micrograms per milliliter RBC) was considered by some to be higher than that ever used clinically, we studied the effect of 2.0 and 8.0 micrograms under identical conditions. Whole-body counting and peripheral blood assays were done at weekly intervals for 11 weeks to determine whether altered ^{51}Cr chromium blood clearance and whole-body retention occurred. All blood ^{51}Cr activity was gone before 80 days when all the rabbits were killed and their organs were assayed for residual ^{51}Cr activity.

Our results show (Table 54) that 2.0 and 8.0 micrograms per milliliter RBC cause a more rapid loss of the labeled cells from the peripheral blood while increasing the whole-body retention of the label. That this discrepancy is caused by reticuloendothelial sequestration is shown by the data in Table 55 where the ^{51}Cr activity per gram of spleen and bone marrow is expressed as multiples of ^{51}Cr activity per gram of kidney. Significantly enhanced splenic sequestration is

* Summer Student Trainee, University Participation Office, ORAU.

1027695

TABLE 54

Blood and Whole Body ^{51}Cr Retention 10 and 20 Days After RBC Labeling

	Carrier Chromium Added (µg/ml RBC) 0.0	2.0	8.0
	(%)	(%)	(%)
Blood			
10 days	60	50	50
	60	50	50
	70	60	50
20 days	30	26	30
	28	35	30
	50	38	30
Whole Body			
10 days	70	75	88
	72	75	80
	76	74	84
20 days	54	58	62
	60	60	68
	60	58	70

TABLE 55

$$\frac{^{51}Cr \text{ Activity/Gram of Organ}}{^{51}Cr \text{ Activity/Gram of Kidney}}$$

(80 Days After ^{51}Cr Labeling)

Organ	Carrier Chromium (µg/ml RBC) 0.0	2.0	8.0
Spleen	5.7	15.1	31.7
	2.6	4.8	22.3
	24.0	20.0	--
Bone Marrow	1.6	1.7	8.3
	1.1	2.2	1.1
	4.9	1.6	--

shown when 8 micrograms are used, but the level of splenic sequestration seen without any carrier makes the effect with 2.0 micrograms questionably larger than "normal." Indeed any chromium may enhance random RBC destruction and sequestration under certain conditions as described previously.[1]

REFERENCE

1. Opdyke, D. F., Franz, W., Gibbs, W. D., Bergner, P.-E. E., and Lushbaugh, C. C. Effect of chromium on rabbit red blood cell survival. In: USAEC Report ORAU-101, 1966, pp. 111-115.

Gold Thioglucose Damage to the Satiety Center: Inhibition by Diabetes*†

A. F. Debons,‡ Isidore Krimsky,‡ H. J. Likuski,‡ Annette From,‡ and Roger J. Cloutier

The administration of gold thioglucose to mice brings about hyperphagia and obesity. The selective affinity of certain cells in the hypothalamic area for gold thioglucose is thought responsible for the change since these cells accumulate gold and are subsequently destroyed. The region of the hypothalamus suffering damage is known as the satiety center.[1,2] A recent study by us demonstrated that glucose antimetabolites inhibit gold deposition and prevent hyperphagia and obesity.[3] Experimental evidence for the effect of blood glucose levels on gold thioglucose uptake by the satiety center remains fragmentary and, to some extent, contradictory.[4-6] Experiments were conducted to evaluate the influence of the gold thioglucose-hyperglycemia relation on satiety center function. Mice with induced diabetes mellitus were injected with gold thioglucose and were studied for (1) the development of hyperphagia and obesity and (2) accumulation of gold and development of lesions in the satiety center.

Diabetes mellitus was induced in CBA mice by the administration

---

* In press, American Journal of Physiology

† This work was supported, in part, by Public Health Service Grants AM-07037 and AM-08667 to the Downstate Medical Center, New York.

‡ Radioisotope Service, Veterans Administration Hospital, and State University of New York, Downstate Medical Center, Brooklyn, New York.

1027696

of 100 mg/kg of alloxan[7] or guinea pig anti-insulin serum. Gold thioglucose, 800 mg/kg, was administered in a single intraperitoneal injection. The amount of gold in the satiety center and in the blood was measured by neutron activation analysis. Samples were activated in the ORNL Low Intensity Test Reactor. Gold deposits were localized in the satiety center by autoradiography after neutron activation.

Mice given gold thioglucose exhibited hyperphagia and obesity and showed gold deposits and lesions in the satiety center (Figs. 95C and 96C). Gold thioglucose-treated animals with alloxan-induced diabetes showed a decreased deposition of gold (Table 56) and fewer lesions (Figs. 95D and 96D). Despite the pronounced decrease in the amount of gold in the satiety center of diabetic animals, no correlation was shown between the degree of hyperglycemia and the amount of gold deposited. The administration of gold thioglucose to alloxan-diabetic mice did not alter the existing hyperphagia nor bring about obesity. Mice made diabetic by the administration of guinea pig anti-insulin serum were also resistant to gold thioglucose-induced lesions of the satiety center.

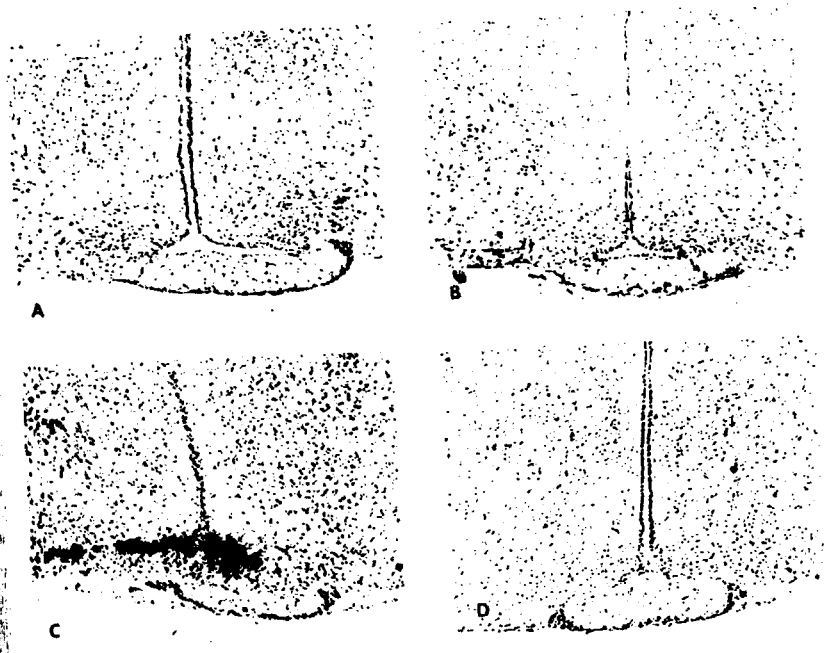

Fig. 95. *Typical autoradiograms of sections through the hypothalamus illustrating gold localization in (a) untreated, (b) diabetic untreated, (c) gold thioglucose treated, and (d) diabetic gold thioglucose treated mice.*

1027697

TABLE 56

Gold content of the satiety center for mice given gold thioglucose

Treatment	No. of Animals	Blood Glucose* mg/100 ml	Gold Content Micrograms/mg dry weight Cortex	Satiety Center
Gold thioglucose treated	26	168† (100-200)	0.0027† (0.0018-0.0044)	0.0907† (0.0621-0.1391)
Diabetic gold thioglucose treated	12	433 (320-520)	0.0017 (0.0007-0.0028)	0.0131 (0.0011-0.0333)

* Blood glucose values at time of gold thioglucose administration

† Values represent mean and range observations

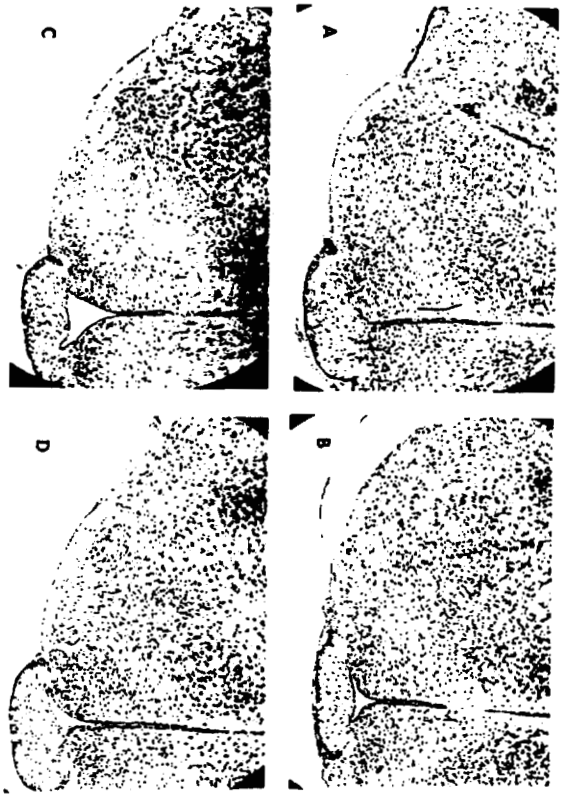

Fig. 96. Transverse sections through the median eminence demonstrating typical appea ance of the satiety center is (a) untreated, (b) diabetic untreated, (c) gold thic glucose treated, and (d) diabetic gold thioglucose treated mice. Note presenc of lesions in gold thioglucose treated and absence in diabetic gold thioglucos treated and untreated diabetic mice.

REFERENCES

1. Marshall, N. B., Barrnett, R. J., and Mayer, J. Hypothalamic lesions in gold thioglucose injected mice. Proc Soc Exp Biol Med 90, 240-244, 1955.

2. Mayer, J. and Marshall, N. B. Specificity of gold thioglucose for ventromedial hypothalamic lesions and hyperphagia. Nature 178, 1399-1400, 1956.

3. Likuski, H. J., Debons, A. F., and Cloutier, R. J. Inhibition of gold thioglucose induced hypothalamic obesity by glucose analogues. Amer J Physiol 212, 669-676, 1967.

4. Edelman, P. M., Schwartz, I. L., Cronkite, E. P., Brecher, G., and Livingston, L. The effect of hyperglycemia on hypothalamic gold uptake and hyperphagia in gold thioglucose-treated mice. J Exp Med 121, 403-413, 1965.

5. Mayer, J. (In Discussion following J. Mayer) The hypothalamic control of gastric hunger contractions as a component of the

mechanism of regulation of food intake. Amer J Clin Nutr 8, 547-561, 1960.

6. Mayer, J. and Marshall, N. B. Mode d'action de l'aurothiogluctose et régulation glucostatique de la nutrition. Compt Rend Acad Sci 242, 169-171, 1956.

7. Tocus, E. C. and Cavallo, M. Production of diabetes mellitus in mice with alloxan. Fed Proc 20, 192, 1961 (abstract).

Phenothiazine Inhibition of Reduced Nicotinamide Adenine Dinucleotide (NADH) Oxidation by Melanin

*M. H. Van Woert**

Melanins are pigments of high molecular weight formed by the enzymatic oxidation of polyphenols. The polymer melanin has been demonstrated to be a stable-free radical and theoretically should have exceptional electron-acceptor properties.[1] Since the melanin granules almost completely replace the mitochondria in the melanocyte of the amphibian, Amphiuma tridactylum,[2] the ability of melanin to substitute for mitochondria in oxidizing the coenzyme reduced nicotinamide adenine dinucleotide (NADH) was investigated.[3]

A double-beam spectrophotometer and a Warburg apparatus were used to measure the rate of oxidation of NADH by melanin. Both synthetic melanin prepared from L-dihydroxyphenylalanine (dopa) by tyrosinase and melanin granules isolated from the Amphiuma liver were investigated.

Figure 97 shows the rate of oxidation of NADH by dopa melanin at various pH's. The optimal pH for the reaction was 7.2. One atom of oxygen was consumed per mole of coenzyme oxidized. Electron paramagnetic resonance spectroscopy revealed a decrease in the amplitude of the melanin-free radical signal after the addition of NADH, presumably due to the formation of reduced melanin. Amphiuma melanin granules also oxidized NADH but at a lower rate (Fig. 98).

Chlorpromazine has been shown to accumulate preferentially in

* Present address: Yale University School of Medicine, New Haven, Conn.

1027698

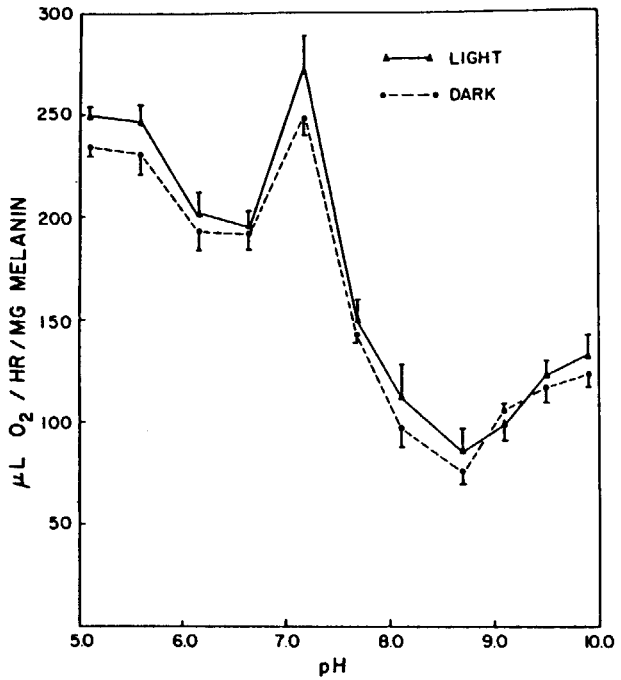

Fig. 97. Rate of oxidation of NADH (13μ moles) by dopa melanin (1 mg) versus pH. Points and perpendicular lines are the mean of 4 to 7 determinations ± SEM. The reaction was run in the dark (dotted line) and in the presence of visible light (solid line).

melanin-containing tissues of animals and man. In vitro chlorpromazine quenches the melanin-free radical by forming a charge-transfer complex.[4] As shown in Table 57, chlorpromazine as well as other phenothiazines inhibited the NADH oxidation by melanin.[5] This phenothiazine inhibition is prevented by the prior addition of chloroquine (Table 57), another melanin-binding drug. The chemical interaction of melanin and phenothiazines may be relevant to some of the metabolic effects of these drugs.

REFERENCES

1. Pullman, A. and Pullman, B. The band structure of melanins. Biochim Biophys Acta 54, 384-385, 1961.

2. Van Woert, M. H., Nicholson, A. and Cotzias, G. C. Mito-

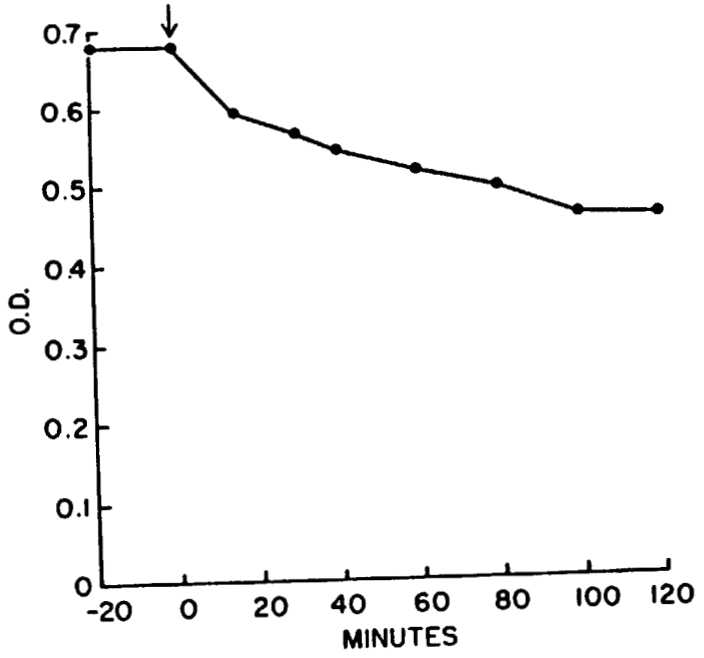

Fig. 98. Oxidation of 0.39 µM NADH in the presence of 0.9 mg Amphiuma melanin granules at pH 7.2 measured at 340 mµ in a Carey 14 double-beam recording spectrophotometer. The arrow indicates the addition of melanin to both the sample and blank cuvettes.

chondrial functions of polymelanosomes. Comp Biochem Physiol 22, 477-485, 1967.

3. Van Woert, M. H. Oxidation of reduced nicotinamide adenine dinucleotide by melanin. Life Sci 6, 2605-2612, 1967.

4. Forrest, I. S., Gutmann, F., and Keyzer, H. In vitro interaction of chlorpromazine and melanin. Aggressologie (Paris) 7, 147-153, 1966.

5. Van Woert, M. H. Phenothiazine inhibition of reduced nicotinamide adenine dinucleotide (NADH) oxidation by melanin. Clin Res 15, 472, 1967 (Abstract).

1027699

TABLE 57

PER CENT INHIBITION OF MELANIN OXIDATION OF NADH

	pH7.4	---- pH 8.5 ----		
	1.0mM	1.5mM	1.0mM	0.5mM
Trifluoperazine (Stelazine)	67.4	53.4 (1.4)	46.0 (2.4)	23.7 (3.4)
Chlorpromazine (Thorazine)	60.3	48.7 (1.8)	44.9 (5.2)	18.3 (8.8)
Promethazine (Phenergan)	53.2	65.7 (3.7)	41.7 (4.3)	21.7 (5.8)
Promazine (Sparine)	51.5	63.8 (2.5)	54.9 (3.6)	30.1 (2.4)
Ethopromazine (Parsidol)	26.2	7.2 (3.0)	9.9 (9.1)	10.4 (7.3)
Chloroquine	19.3		15.6 (5.6)	
Chloroquine + Trifluoperazine			19.0 (3.6)	

Percentage inhibition of melanin oxidation of NADH. Numbers in parentheses are the SEM of 3 to 5 determinations.

IMMUNOLOGIC STUDIES AND THE DEVELOPMENT OF THE MARMOSET AS A LABORATORY PRIMATE

The program in immunology has evolved out of the objective of obtaining marrow transplants, particularly as a means of sustaining persons who have been heavily irradiated. Because of the difficulties in achieving successful grafts in man as well as the obstacle of secondary or homologous disease (well demonstrated in experimental animals) the marmoset was chosen as an experimental tool. When natural chimerism was discovered in the species, interest in its immunologic and genetic usefulness broadened and we embarked on a major effort to develop an additional laboratory primate with certain unique features. Data collected in this project have been grouped under a single heading along with immunologic studies devoted to effects of exposure rate and investigations of graft-host incompatibility.

Radiation Exposure-Rate Dependence of the Immune Response

Donald E. Carlson and N. Gengozian*

Previous work in this laboratory[1,2] has shown the importance of radiation exposure rate in suppressing the immune response of lethally irradiated mice in order to achieve prolonged bone-marrow grafts. It was noted that as the exposure rate was increased (1) a higher proportion of grafted animals survived, (2) a higher proportion of surviving mice possessed functional erythropoietic and granulopoietic tissue of donor origin, and (3) fewer of the mice that lacked functional grafted elements synthesized antibody against antigens of donor specificity.

We extended these observations to determine the exposure range over which an effect of exposure rate was exerted on humoral antibody formation. Preliminary studies were necessary to determine the effect of exposure rate on radiation lethality to establish 30-day mortality levels for each exposure rate, to determine the best route of antigen administration, and to find the type of antigen that best showed an exposure-rate dependence. In the study reported here, intravenously administered sheep erythrocytes were used.

Adult mice were exposed to total-body ^{60}Co gamma radiation of 200 R, 400 R, 600 R, 700 R, 800 R; exposure rates of 8 R/min, 40 R/min, and 72 R/min were used at each exposure level. Studies were also performed at the maximum sublethal level ($LD_{0/30}$) and at the 25% lethal range ($LD_{25/30}$) for the three different exposure rates. Within 2 hr after exposure each mouse (20 to 30 per group) was injected with 1/2 ml of a 2% suspension of sheep erythrocytes, and weekly blood samples obtained to determine the level of circulating serum agglutinin. This was done by serial 2-fold dilution of the serum in saline; a standard volume of the appropriate erythrocyte suspension was added and the samples were incubated, centrifuged, and read by macroscopic agglutination. The endpoint for each sample was taken as the last dilution in which detectable agglutination occurred. Data were expressed as titer (the $\log_2$ of the reciprocal of the highest dilution in which agglutination was seen) plotted against time through 35 days for each exposure level and exposure rate. The area under each curve was determined for points between days 7 and 35 and was designated the integral titer.

Figure 99 shows data for the agglutinin response to sheep erythro-

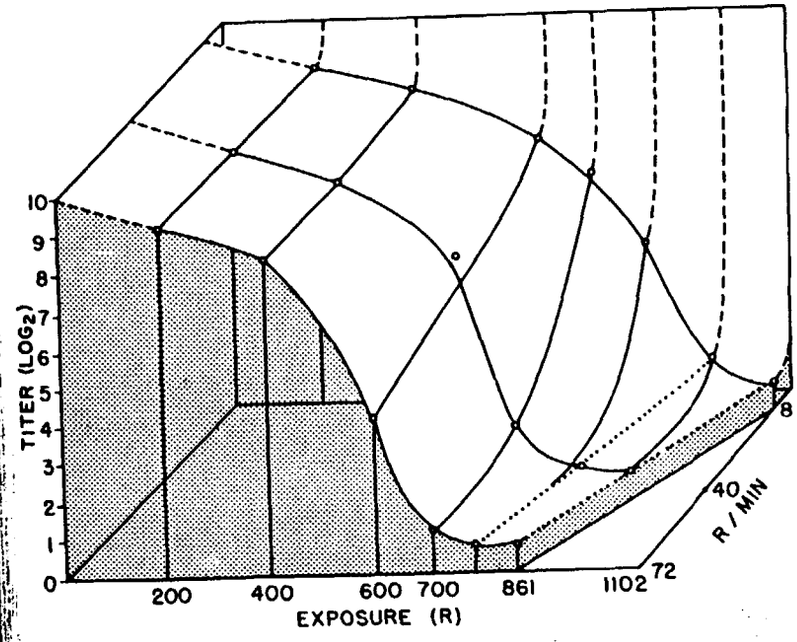

Fig. 99. Integral titer as a function of exposure and exposure rate. Dashed lines represent the expected values in regions where data have not yet been obtained. The two dotted lines connect data points for exposure levels representing the maximum $LD_{0,30}$ and the LD_{25} respectively.

* Public Health Service Fellow

cytes, in which the exposure, exposure rate, and integral titers are plotted. Production of agglutinin fell more sharply with increasing exposure level when the exposure rate was increased from 8 R/min to 40 R/min; raising the exposure rate from 40 R/min to 72 R/min resulted in an even sharper decline as the radiation exposure was increased. No exposure-rate dependence existed at 200 R and 400 R, where the exposure level was insufficient to suppress antibody formation even for the highest exposure-rate group. Also, only slight differences in integral titers were apparent between exposure-rate groups that received the highest radiation doses; here suppression of antibody formation was nearly complete after exposure at the lowest rate. However, between 400 R and 800 R a striking difference was seen in integral titers between exposure-rate groups, which reached a maximum at 700 R. At this exposure level the difference in agglutinin levels between mice that received exposures of 8 R/min and 72 R/min was 5-1/2 titer units, or a 45-fold difference in serum antibody concentration.

Studies are now under way to determine the immunologic mechanisms operating in this system.

REFERENCES

1. Gengozian, N. Transplantation of rat bone marrow in irradiated mice: Effect of exposure rate. Science 146: 663-664, 1964.

2. Gengozian, N. and Carlson, D. Consideration of radiation exposure rates in transplantation of xenogeneic and allogeneic bone marrow in irradiated mice. Third International Congress of Radiation Research, Book of Abstracts, abstr. 356, p. 90, 1966.

Demonstration of an Early Host-Graft Incompatibility Reaction in Radiation Chimeras with the Jerne Plaque Technique

N. Gengozian, C. F. Gottlieb, and Elizabeth M. Allen*

It is well documented that mice can be protected from lethal total-body irradiation by injection of isogeneic, allogeneic, and xenogeneic bone marrow shortly after exposure. With foreign-marrow treatment, a major complication in the subsequent recovery of the animal has been the secondary disease syndrome, attributed to an immunologic incompatibility reaction between host and donor tissue.

* University of Tennessee Graduate Fellow.

1027101

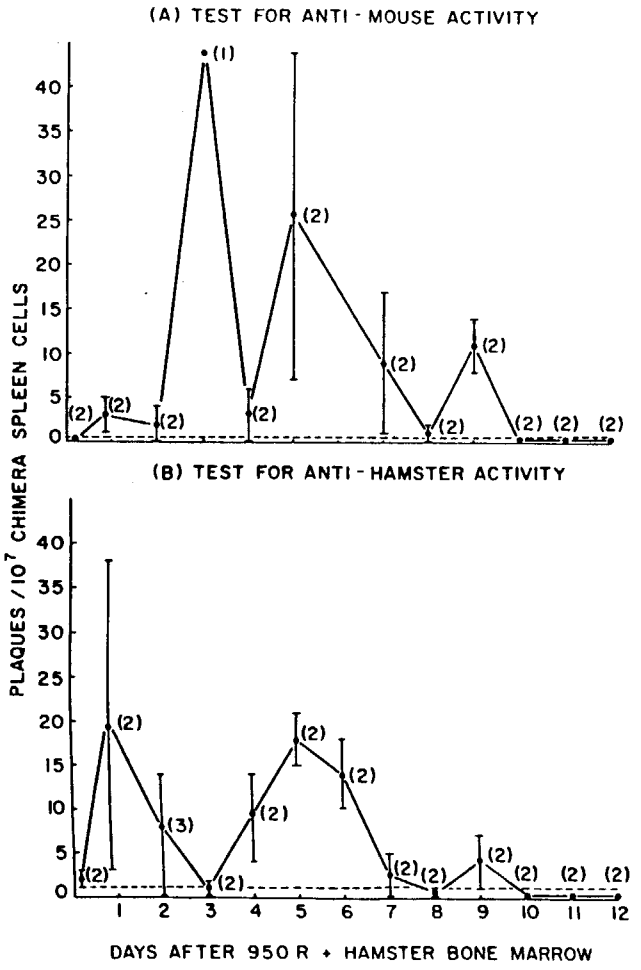

Fig. 100. *Plaque formation as a function of time in lethally irradiated mice treated with hamster bone marrow. A. Target cells in agar plates were mouse (host) red blood cells, plaque formation therefore indicating the presence of anti-mouse activity in the chimera spleens. B. Target cells in agar plates were hamster (donor) red blood cells, plaque formation therefore indicating the presence of anti-hamster activity in the chimera spleens. Numbers in parentheses indicate number of spleen cell pools (3-5 spleens per pool) tested at the various time intervals. Each point represents the mean number of plaques obtained from each pool and longitudinal bars indicate the spread in number of plaques counted. Horizontal dashed lines represent the mean background number of plaques obtained from normal spleens of hamsters (A) and mice (B) for the reciprocal target red blood cells.*

Evidence points strongly to a graft-vs-host etiology although some host reaction to the graft has not been ruled out. It was reasoned that if a graft-vs-host mechanism is the primary factor, the reaction should begin almost immediately after infusion of the donor's immunologically competent cells. They should react promptly against the host environment far earlier than the recognized clinical manifestations of secondary disease that occur 3 to 4 weeks after irradiation and marrow treatment. To test this hypothesis, spleens of lethally (950 R) irradiated mice treated with either rat or hamster bone marrow were removed at 24-hr intervals for a period of 14 days after marrow infusion. Tests for immunologic activity of the spleen cells against either host or donor red blood cells were made with the Jerne plaque technique, a localized hemolytic test in agar. Evidence for both host and graft activity, i.e. anti-host and anti-graft reactions, was obtained with spleen cells of mice that had been treated with hamster bone marrow. The responses obtained were of low magnitude and variable, and were evident primarily through the first 6 days post-treatment (Fig. 100).

The significance of these findings relative to the etiology of secondary disease in foreign radiation marrow chimeras can only be speculated upon at present. Of immediate relevance to the present concept of an "early" host reaction are factors previously known to be important in establishing chimerism yet having ill-defined mechanisms: (1) larger amounts of foreign marrow are required to establish a radiation chimera when compared to syngeneic systems; (2) the greater the total-body radiation (usually supralethal) to the host, the greater the probability of establishing a foreign-marrow graft; and (3) the "take" of foreign marrow is related to the phylogenetic distance between host and donor. These factors are affected by or can affect the "early" host reaction. Similarly, the early graft-vs-host reaction could also result in an increase of antibody-forming cells occurring at the expense of proliferation of precursors for the hemopoietic cells necessary to promote recovery. In view of these considerations, this early reaction concept suggests a cause and effect phenomenon that may be implicated in the subsequent recovery of the xenogeneic chimera leading to the secondary disease syndrome.

Graft-Versus-Host Reaction in Man Produced by Thoracic-Duct Lymphocytes

Helen Vodopick, C. C Congdon, C. L. Edwards, N. Gengozian, Bill Nelson, Kong-oo Goh, and G. A. Andrews*

The graft-vs-host reaction has been reported to occur in man after allogeneic bone-marrow transplantation.[1,2] We have observed

* Biology Division, Oak Ridge National Laboratory.

1027702

a similar phenomenon in a man after the intravenous infusion of thoracic-duct lymphocytes in an attempt at immunotherapy of a patient with malignant melanoma (Fig. 101).

Metastatic tumor involving lymph nodes were excised, irradiated with 20,000 R, and injected into a normal volunteer. Four weeks later the thoracic duct of the donor was cannulated for collection of lymph, from which lymphocytes were removed and given intravenously to the patient. Altogether 22 x 10^{10} lymphocytes were given over a 4-day period. In the 2 days preceding the infusions of lymphocytes, the patient received two doses of nitrogen mustard totaling 0.4 mg/kg.

On the second day of the infusions, the patient had fever, chills, and anorexia, which continued intermittently until death 6 days later. Diarrhea, diffuse erythematous skin rash, and swollen knees developed.

The absolute lymphocyte count fell rapidly after the first day of infusion and reached a nadir of 65 lymphocytes per cubic millimeter on the fifth day, which was earlier and faster than is expected when nitrogen mustard is given alone.[3] No eosinophilia was observed. The hematocrit of 35% remained stable until the day before death when it dropped to 29% and then to 21% on the day of death. Concomitant with this drop the serum bilirubin rose to 5 milligrams percent. The direct Coombs test was negative. Serum gamma globulin rose from a preinfusion value of 12% to 25% on the day of death. The protein immunoelectrophoresis showed no abnormality. A skin biopsy on the day before death showed infiltrations of lymphocytes, pyknotic nuclei, and nuclear fragments in the dermis and epidermis. At autopsy focal necrosis was seen in the spleen, liver, lymph nodes, and adrenals. Depletion of lymphocytes from lymphopoietic organs was striking.

Despite the brief interval from infusion to death, we believe this patient had a graft-vs-host reaction due to transfusions of thoracic-duct lymphocytes obtained from a donor who had been "sensitized" to his malignant melanoma. Cytogenetic studies on the patient's blood 2 days before his death showed more than half the circulating lymphocytes were female. The clinical manifestations of fever, chills, anorexia, diarrhea, and diffuse erythematous skin rash are similar to the graft-vs-host reaction that follows allogeneic bone marrow and leukocyte transfusions.[1,2,4] The lymphopenia, a 2-fold rise in the gamma globulin level, the lymphocytic infiltration of the skin, focal necrosis of the spleen, and lymphoid aplasia support this diagnosis.[5,6]

REFERENCES

1. Mathé, G. Secondary Syndrome: A stumbling block in the treatment of leukemia by whole-body irradiation and transfusion of allogeneic haemopoietic cells. In: Diagnosis and Treatment of

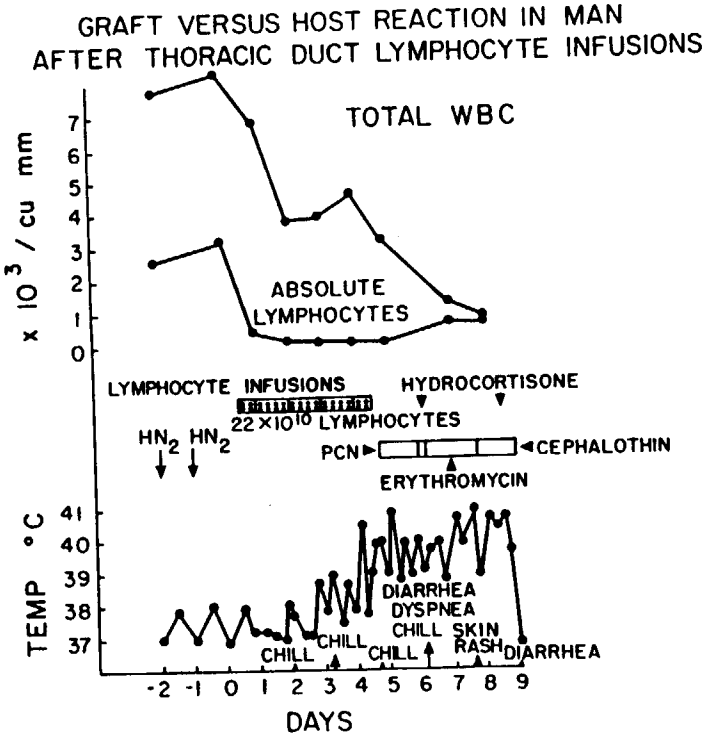

Fig. 101. The clinical, hematologic, and therapeutic changes occurring in a man who developed graft-vs-host reaction after receiving 22 x 10^{10} allogeneic thoracic-duct lymphocytes.

Acute Radiation Injury. Proceedings of a Scientific Meeting Jointly Sponsored by the International Atomic Energy Agency and the World Health Organization, Geneva, 1960, New York, International Documents Service, 1961, pp. 191-223.

2. Mathé, G., Amiel, J. L., Schwarzenberg, L., Cattan, A., Schneider, M., de Vries, M. J., Tubiana, M., Lalanne, C., Binet, J. L., Papiernik, M., Seman, G., Matsukura, M., Mery, A. M., Schwarzmann, V., and Flaisler, A. Successful allogeneic bone marrow transplantation in man: Chimerism, induced specific tolerance and possible anti-leukemic effects. Blood 25, 179-196, 1965.

3. Smiley, R. K., Martin-Villar, J., and Belanger, L. F. Effect of autologous bone marrow on the cytopenias induced by nitrogen mustard. Can Med Ass J 84, 1230-1234, 1961.

4. Schwarzenberg, L., Mathé, G., de Grouchy, J., de Nava, C., de Vries, M. J., Amiel, J. L., Cattan, A., Schneider, M., and Schlumberger, J. R. White blood cell transfusions. Israel J Med Sci 1, 925-956, 1965.

5. de Vries, M. J. and Vos, O. Delayed mortality of radiation chimeras: A pathological and hematological study. J Nat Cancer Inst 23, 1403-1439, 1959.

6. Congdon, C. C. and Urso, I. S. Homologous bone marrow in the treatment of radiation injury in mice. Amer J Path 33, 749-767, 1957.

1027703

Further Studies Using the in vitro Mixed Leukocyte Test

Helen Vodopick, Elizabeth M. Rupp, and N. Gengozian

In assessing the antigenic-stimulating and the immune-responding capabilities of lymphocytes as measured by the in vitro mixed leukocyte culture technic,[1] we were impressed by the finding that the 23 out of 30 reciprocal unidirectional reactions (one viable uninhibited population of lymphocytes vs another viable population inhibited with Mitomycin C) equalled or exceeded their bidirectional counterpart (both populations viable and uninhibited). Mitomycin C is an antibiotic capable of inhibiting DNA synthesis and cell division while preserving cell viability and antigenicity.[2] One typical set of curves is illustrated in Fig. 102.

In the bidirectional system, 2 x 10^6 lymphocytes are mixed with an equal number of lymphocytes from a normal unrelated donor, both of which are capable of stimulating as well as responding to each other. The response of homologous lymphocytes to one another is manifested by blastic transformation and by commencement of synthesis of DNA, which can be measured by incorporation of labeled thymidine. In a unidirectional reaction, the type of response is the same; however, only the uninhibited lymphocytes are able to respond.

Certain possibilities were investigated to explain these discrepancies: (1) Nutrient depletion of culture media. Renewal of culture media daily to bidirectional stimulated cells did little to augment their peak response and did not extend their survival. (2) Incomplete inhibition of cells by Mitomycin C. Negligible activity was obtained when two inhibited cell populations were cultivated together. (3) Alteration of cell antigenicity by Mitomycin C. Studies with lymphocytes from identical twins in uni-

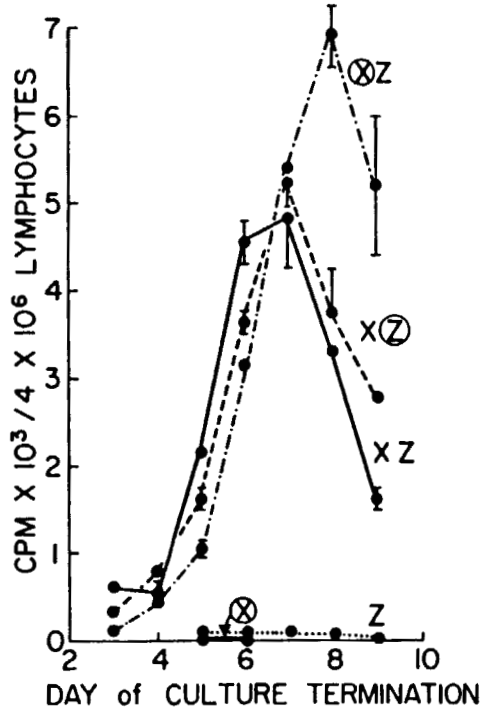

Fig. 102. A time study in the comparison of bidirectional and the reciprocal unidirectional reactions of mixed leukocyte cultures. Encircled letters indicate that cell population had been treated with Mitomycin C.

directional and bidirectional reaction systems showed the former system to give the same results after Mitomycin C treatment, thus ruling out the possibility of new or different antigenicity conferred on lymphocytes by such treatment. (4) Blood groups and sex. Analysis of the data suggested these factors did not influence either the unidirectional or bidirectional system.

Thus we conclude that in a unidirectional system, inhibition of one cell line allows the other uninhibited population to react maximally to the antigenic stimulus, while in the bidirectional test a mutual inhibition as well as stimulation decreases the immunologic capabilities of both cell populations.

These findings dictate that some caution must be exercised in comparing the bidirectional vs the unidirectional reaction as a measure of histoincompatibility between two persons.

1027704

REFERENCES

1. Bain, B., Vas, M. R., and Lowenstein, L. The development of large immature mononuclear cells in mixed leukocyte cultures. Blood 23, 108-116, 1964.

2. Szybalski, W. and Iyer, V. N. Crosslinking of DNA by enzymatically or chemically activated mitomycins and profiromycins, bifunctionally "alkylating" antibiotics. Fed Proc 23, 946-957, 1964.

Further Studies on Isohemagglutinins in the Marmoset

N. Gengozian

The ORAU marmoset colony consists primarily of the hairy-faced white-lipped members of the Saguinus nigricollis group. As classified by P. Hershkovitz, there are three species: S. graellsi, S. nigricollis, and S. fuscicollis. The first two are monotypic, while S. fuscicollis is considered to be composed of no less than 13 subspecies. Our colony is made up primarily of members of this latter diversified group; four have been identified: S. f. illigeri, S. f. lagonotus, S. f. leucogenys, and S. f. nigrifrons.

Tests for naturally occurring isohemagglutinins, complete or incomplete between the four subspecies have been negative. Although we have not attempted cross immunizations in all 12 possible combinations, we have sufficient data to indicate that blood-group differences do exist among and within these four subspecies. Thus, reciprocal immunizations between S. f. lagonotus and S. f. illigeri have produced consistent antibody formation. Generally, four kinds of antibody are formed as revealed by absorption, elution, and density gradient centrifugation: a complete agglutinin, reactive in saline at room temperature, which sedimented as a macroglobulin (19S); an incomplete antibody detectable with a Coombs reagent (rabbit anti-tamarin serum), which sedimented as a light (7S) protein; a cold agglutinin (19S); and a cold autoagglutinin (19S). Only the incomplete antibody, however, is formed with consistency the others appearing quite variably after either a primary, secondary, or tertiary stimulation. An isohemagglutin curve showing the response to primary and secondary immunizations of an S. f. lagonotus tamarin with S. f. illigeri red cells is shown in Fig. 103. Successful isoimmunization within one subspecies, S. f. illigeri, has also been obtained with the formation of only an incomplete antibody, but this has been considerably more difficult to evoke than the inter-subspecies immunizations.

Of the four agglutinins formed, only the incomplete antibody has proved to be satisfactory for discriminating blood-group differences. Table 58 shows a schematic scoring with three isoimmune reagents for

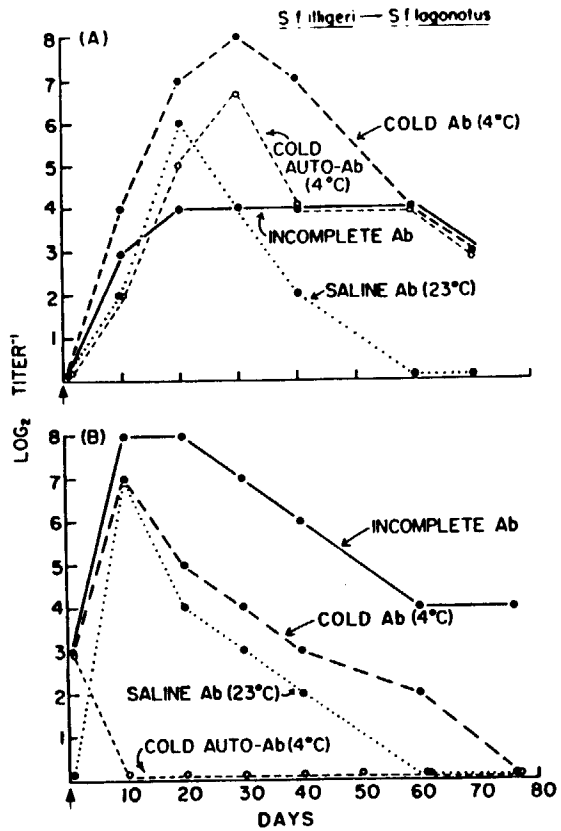

Fig. 103. Isohemagglutinin response of S.f. lagonotus tamarin immunized with red cells of S.f. illigeri. A. Primary response. B. Secondary response. Incomplete antibody (Ab) detected with a rabbit anti-tamarin serum antiserum.

a panel of red cells from the four different subspecies. Note that there are distinguishing red cell antigenic specificities among these groups. Thus, with the first reagent, S. f. lagonotus anti-S. f. illigeri, the red cells of two subspecies, S. f. nigrifrons and S. f. lagonotus, were essentially nonreactive, while S. f. illigeri and S. f. leucogenys cells showed strong and comparable reactivity. With the second reagent, obtained by the reciprocal immunization scheme of the first, only S. f. lagonotus cells were reactive; but this reagent showed distinct variation in reactivity with different members of this subspecies, indicating intrasubspecies specificity. Similarly, with the third reagent shown (S. f. illigeri anti-S. f. illigeri), although reactivity was apparent

1027705

TABLE 58

Red Cell Specificity in *Saguinus fuscicollis* ssp. as Revealed by Three Isoimmune Reagents

Subspecies Red Cells	Isoimmune Reagent* 1. *S.f. lagonotus* anti- *S.f. illigeri*	2. *S.f. illigeri* anti- *S.f. lagonotus*	3. *S.f. illigeri* anti- *S.f. illigeri*
1. *S.f. illigeri*	+	-	-
2. "	+	-	+
3. "	+	-	+
4. *S.f. leucogenys*	+	-	-
5. "	+	-	+
6. "	+	-	+
7. *S.f. nigrifrons*	-	-	-
8. "	-	-	-
9. "	-	-	±
10. *S.f. lagonotus*	-	+	-
11. "	-	+	+
12. "	-	-	+

*Reagents contained incomplete antibodies detectable with a rabbit anti-tamarin serum antiserum. The + and - scoring system indicates clear distinctions can be made between the individuals tested with the various reagents. No cross correlation between the reagents and their reactivit for any one particular subspecies of *Saguinus fuscicollis* is intended.

TABLE 59

Tests of Red Blood Cells of "Hybrid" Offspring from Mating of Two Subspecies of *Saguinus fuscicollis*

Red Cells	Titration of Isoimmune Serum ($\log_2$)$^{-1}$ 2	3	4	5	6	7	8	9
	Reaction*							
Paternal *(S.f. lagonotus)*	1±	-	-					
Maternal *(S.f. illigeri)*	4	4	4	4	4	4	3	1±
Twin offspring								
A	4	4	4	4	4±	3	1	1±
B	4	4	4	4	4±	3	1	1±

*Reactions scored from - (no agglutination) to 4+ (agglutination of all cell Isoimmune serum contained incomplete antibody detected with rabbit anti-tamarin serum antiserum.

with cells of all four subspecies, individual specificity was detected within each subspecies.

In view of the chimerism that is presumed to exist in all tamarins (and therefore in all red-cell donors, immunized recipients, and panel test cells), extensive cross absorptions are needed for more definitive information on this point. The evidence for individual specificity will provide a means now of pursuing the initial question of red-cell chimerism.

The isoimmune reagents may also be used to study the genetic inheritance of blood-group antigens. Intersubspecies breeding between S. f. lagonotus and S. f. illigeri in our colony has provided the opportunity to test red-cell specificity of the offspring from such matings. As shown in Table 59, red cells of both twins, A and B, showed the same degree of reactivity with the isoimmune reagent, S. f. lagonotus anti-S. f. illigeri, as obtained with the maternal cells, S. f. illigeri. Unfortunately, the S f. lagonotus father of these offspring died before we had obtained reagents capable of reacting with cells of this subspecies.

Survival of Skin Transplants Between Marmoset Co-Twins

Raymond P. Porter and N. Gengozian

The marmosets, small New World primates (Platyrrhine), have in their reproductive physiology three features that make them unique among mammals: (1) a greater than 80% frequency of twinning occurs; (2) the twinning is considered to be almost always dizygotic; and (3) placental vascular anastomosis is consistently noted between the fetal twins. A natural, apparently inclusive, hematopoietic chimerism resulting from the biologic interaction of these three reproductive qualities has been demonstrated. To the transplantation immunologist, therefore, the marmoset offers a unique biologic tool for the study of cellular immunologic tolerance. Natural chimerism, occurring early in embryologic development, suggests that a state of immunologic tolerance must exist between the two genetically determined, different blood-forming systems and probably between other tissues of such twins as well.

One of the three species of white-lipped tamarins, Saguinus fuscicollis ssp., members of the marmoset family Callithricidae, was used in this study. Six twin pairs of tamarins born in our primate colony were available for these experiments. Chest skin, 9 mm in diameter, was orthotopically transplanted from each individual to its littermate to challenge naturally induced tolerance in these adults. In the histocompatibility assay each co-twin received exchanged tissue, as well as control autografts. All exchanged skins are surviving, support a normal hair growth, and are grossly comparable to control autografts

1027706

Fig. 104. Skin graft from female onto male co-twin in whom blood cell chimerism has been demonstrated. Photograph taken on day 44 postgrafting. Note deep pigmentation of graft. Hair growth was equal in onset and quality to that of host and control autograft (not visible).

(Fig. 104). The survival time of such chimeragrafts* for six co-twin pairs is shown in Table 60. Note that four pairs were heterosexual litter mates. These were shown to be 2a XX/XY lymphocyte chimeras. The other two were isosexual twins and chimerism therefore could not be detected by sex-chromosome analysis.

Skin chimeragrafts, autografts, and nongrafted chest skin biopsies, taken 41 to 153 days postgrafting, were histologically indistinguishable. Unrelated tamarins were also skin grafted to establish the immunologic competence of this species. The first-set skin allograft mean survival time varied from 2 to 7 weeks. Second- and third-set skin allografts showed accelerated rejections including "white graft" response.

---

* Transplanted tissue between co-twins.

TABLE 60

Survival of *Saguinus fuscicollis* Co-twin Chimeragrafts

Twin Pair No. & Sex		Lymphopoietic Chimerism (%)	Days Survival*
1.	M	-	367
	M	-	
2.	M	17%	324
	F	76%	
3.	M	74%	289
	F	36%	
4.	M	62%	253
	F	34%	
5.	M	35%	214
	F	53%	
6.	M	-	21
	M	-	

*As of December 1, 1967.

Survival of ^{51}Cr Labeled Red Cells in Marmosets

C. B. Merritt and N. Gengozian*

Marmosets, because of their natural hemopoietic chimerism, are uniquely well-suited for studies of the immunologic mechanisms of tolerance and of the potential development of autoimmunity after the spontaneous or artificial breaking of tolerance. Shortened red-cell survival is often seen with autoimmune disorders. Since our previous studies had shown the marmosets to have both human A- and B-like red-cell antigens, the possibility was considered that immunization of marmosets with the human antigens may induce an autoimmune reaction as revealed by a decrease in survival of autologous red blood

* Summer Student Trainee from Tulane University School of Medicine, New Orleans, La. Present address: Johns Hopkins Hospital, Baltimore, Md.

1027707

cells. In this study, the following groups of animals were tested for the survival of either autologous or homologous ^{51}Cr labeled red blood cells (RBC): (1) normal, adult marmosets (autologous RBC); (2) adult marmosets previously immunized with human A (Rh+) cells (autologous RBC); (3) adult marmosets previously immunized with human B (Rh+) cells (autologous RBC); (4) female marmosets that had been mated with "compatible" males (based on isohemagglutinin studies) and produced viable young (homologous RBC male); (5) female marmosets that had been mated with "incompatible" males (based on isohemagglutinin studies) and whose pregnancies always terminated in abortion or infant death (homologous male RBC); and (6) one marmoset, which after extensive isoimmunizations, developed an apparent autoimmune hemolytic anemia with cold autoagglutinins and a direct positive Coombs reaction (autologous RBC).

Red-cell survival values were calculated according to the method of Lindsey et al.[1] For each marmoset, three parameters of red-cell survival were calculated: 'k', the slope of the isotope disappearance curve, EDR, the erythrocyte destruction rate, and t_{50}, the half-life of the red cells. The value 'k' is defined as the slope of the line obtained when $\text{Log}\frac{(\text{Counts/ unit hemoglobin on day t})}{(\text{Counts/ unit hemoglobin on day 0})}$ is plotted against time. Thus, if k denotes the slope of the curve on day t, then $k \triangleq (\text{Log}_{10} Y_t)/t$ where $Y_t = \frac{(\text{Counts/ unit hemoglobin on day t})}{(\text{Counts/ unit hemoglobin on day 0})}$, and the antilog of k represents the fraction of the previous day's activity remaining. The t_{50} value may be expressed as the value of t at the point where $Y_t = 0.5$; hence $t_{50} = \text{Log}_{10}(0.5)/k$. All calculations were done in terms of the values obtained by measuring the cpm/mg hemoglobin. Statistical analysis of the data was performed by the "New Multiple Range Test" proposed by Duncan[2] and modified by Kramer[3] to compare the slopes of the isotope disappearance curve. This is a multiple decision procedure that allows us to group the slopes into ordered sets, where the slopes in each set are significantly different from each other.

Table 61 shows the survival values (t_{50}, k, EDR) for each of the groups. The red-cell half-life (t_{50}) in the normal adult marmosets (Group 1) was found to be 15.9 days, with an isotope disappearance slope (k) of -0.019. Those marmosets previously immunized with either human A or B-like antigens (Groups 2 and 3) and subsequently challenged with autologous red cells, showed red-cell survival values not significantly different from the control group, suggesting lack of any autoimmune induction. In Group 4 injection of homologous male red cells into "compatible" females showed a significantly shorter survival time when compared to the normal autologous control group. Most interesting, however, was Group 5, in which the survival time (t_{50}) of homologous male cells in "incompatible" females was reduced to 10.6 days, significantly greater than that in the homologous "compatible" pairs. Finally, the greatest reduction in red-cell survival time (t_{50} = 8.2 days) in this study was obtained after injection of autologous red cells in a marmoset that had developed autoimmune hemolytic anemia following a course of red-cell isoimmunization (Group 6). The isotope

TABLE 61

Survival of Autologous and Homologous ^{51}Cr-labelled Red Cells in Marmosets

Survival value*	Group Results:*					
	A			B	C	D
	1‡	2	3	4	5	6
t_{50}	15.9	16.5	16.3	13.8	10.6	8.2
k	-0.019	-0.018	-0.019	-0.023	-0.029	-0.037
EDR	4.34	4.17	4.33	4.94	6.59	8.17
n	14	4	4	3	3	1

* Using the "New Multiple Range Test" [2,3] the slopes (k) are grouped in ordered sets, where the slopes in each set are not significantly different from each other. For an approximate 5% level of significance, the ordering from left to right is set A>B>C>D.

* t_{50}, red cell half-life, k, slope of isotope disappearance curve; EDR, erythrocyte destruction rate (%); n, number of animals in each group.

‡ Group 1, normal adult (autologous RBC; Group 2, immunized with human A RBC (autologous RBC); Group 4, compatible mating pair (homologous male RBC); Group 5, incompatible mating pair (homologous male RBC); Group 6, isoimmunized marmoset with autoimmune hemolytic anemia (autologous RBC) (see text also).

disappearance curve for this animal and four representative control animals (Group 1) is shown in Fig. 105.

Although the numbers of animals in this study for each of the experimental conditions considered were limited, several interesting facts are evident. First, red-cell survival studies in the marmosets appear to be sensitive enough to detect natural and induced autoimmunity in these animals. The differences in survival time of homologous male RBC in the "compatible" and "incompatible" groups of females are suggestive of an erythroblastosis fetalis-like situation in the latter group, in agreement with our earlier recording of this disease in marmosets.[4] Furthermore, the difference in survival times of homologous and autologous red cells suggests this technique may be useful in detecting the subtle genetic differences manifested by the different subspecies in our colony.

REFERENCES

1. Lindsey, E. S., Donaldson, G. W. K., and Woodruff, M. F. A. Erythrocyte survival in normal mice and in mice with autoimmune hemolytic anemia. Clin Exp Immunol 1, 85-98, 1966.

2. Duncan, D. B. Multiple range and multiple F tests. Biometrics 11, 1-42, 1955.

3. Kramer, C. Y. Extension of multiple range tests to group means with unequal numbers of replications. Biometrics 12, 307-310, 1956.

4. Gengozian, N., Lushbaugh, C. C., Humason, G. L., and Kniseley, R. M. 'Erythroblastosis foetalis' in the primate, Tamarinus nigricollis. Nature 209, 731-732, 1966.

1027708

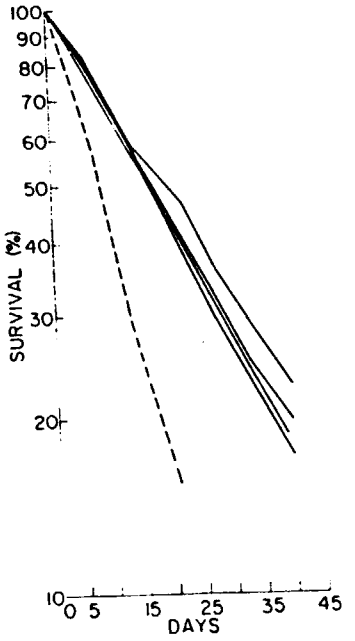

Fig. 105. Survival of autologous red cells in marmosets. Solid lines: normal, adult marmosets; dash line: marmoset with autoimmune hemolytic anemia.

Pathologic Observations on Causes of Fetal Death in Marmosets

*Gretchen L. Humason and C. C. Lushbaugh with N. Gengozian and R. W. Cooper**

The extraordinarily large number of abortions, premature leliveries, and perinatal deaths in marmoset colonies is only partially explainable and requires pathologic study. The determination of causes of death, however, can be made only if the course of organic differentiation and growth is well known so that hypoplasias, developmental anomalies, and other defects peculiar o the intrauterine environment can be detected and any acquired liseases defined. The dead concepti of the Saguinus oedipus (R. W. Cooper, San Diego Zoo N.C.1., Primate Research Colony) and Saguinus fuscicollis (N. Gengozian, Medical Division Marmoset Research Program) are under study for this purpose. Because of he different nature of the two colonies and the different species involved, the two groups of material are being studied separately so hat any interspecies differences can be detected. To date 48 S. oedipus and 147 S. fuscicollis concepti have been examined grossly ind microscopically.

Examination of the cumulative histograms of crown-rump size listribution of the concepti shows three striking facts: (1) No live etuses seem to occur before 9 cm CR or longer; (2) Three "peak" size incidences of death seem to occur; (3) The incidence of prenatal leaths truncates between 10.5 and 11.5 cm.

These observations have led us to the following hypotheses that re being tested by histopathologic study: (1) The period of viable prematurity begins about 9 cm as previously conjectured by Wislocki rom his observations on marmoset placentae; (2) The major causes f death are divisible into three classes related to age (size): (a) ess than 6 cm CR - decidual, placental, and individual embryonic ailures, (b) between 6 and 9 cm CR - circulatory placental problems nd previable births caused by twinning, and (c) greater than 9 cm - rematurity, early delivery resulting from complications of twinning, erinatal injuries, and acquired hemolytic diseases resulting from himerism and maternal - fetal incompatibilities; and (3) The maximum" CR size of the newborn marmoset is about 11 cm but arly birth induced by multiple concepti lowers the "normal" birth ize to about 10 cm.

So far these hypotheses are supported by the following observations: lthough the pulmonary capillaries lose their epithelial covering between - and 8.5-cm CR so that pulmonary aerability is established then, the placental capillaries are the major loci of erythroblastic tissue until 9 cm CR. Hepatic erythropoiesis is largely suppressed until the 9 cm stage. Erythropoietic development in the bone marrow is insignificant until about 10 cm. These peculiarities of erythroblast development probably determine 9 cm to be the viability bound. Infants of less than 9 cm would be expected to suffer from anemia of prematurity until bone-marrow erythropoiesis became adequately established after birth.

1027709

---

* Primate Research Colony, Zoological Society of San Diego.

Placental "infarcts", intervillous thrombosis and leukocytic exudate as well as early intrauterine death of one twin seem to support the thesis that decidual abnormalities are present during the "up to 6 cm period." No gross or microscopic basis, however, for the embryonal malformation thesis has been found so far.

The occurrence of a large and a small twin characterized by hypoplasia of the organs of the small twin seems to imply that the large twin has obtained the major oxygen and nutritional benefit of the placental blood. More detailed study of fresh placentae and their circulatory configuration is needed to determine whether this inequality is functional or due to umbilical vascular patterns. About half the time both umbilical cords are attached primarily to the same placenta. Whether this condition or that of the two cords emanating from the different placentae is associated with "robust twin disease" is not known.

Gross and microscopic proof has been found for fatal "transfusion syndrome" in the perinatal period. Here one twin is found "bloodless" while the other has a huge dark red liver that may have "blood blisters" on it or is associated with abdominal hemorrhage. The exact mechanism for this accident is unknown but it may be associated with the intrauterine retention of one placenta so that uterine contractions milk the blood of one twin into that of the other.

Intracranial hemorrhage along the cerebral commissure as well as in the posterior fossa is not an uncommon finding. This finding is common in those premature neonates that were born alive but then died soon afterwards. Whether this intranatal birth injury underlies some cases of "maternal rejection" should be considered.

The iron staining of the S. oedipus liver collection is different from that of the S. fuscicollis collection[1] where about 40% showed the hepatic parenchymal iron staining of hemolytic anemia or hepatic injury. In S. oedipus only five unequivocal instances of heavy hepatic parenchymal iron staining were found. Even so these instances suggest that maternal - fetal blood incompatibilities are present in this species if not to the same degree as in S. fuscicollis.[2]

Other developmental studies are in progress concerning the ovary (page 214 of this report), the erythroblast, lymphopoiesis in the thymus, spleen, and lymph nodes, bone-marrow production, cerebral myelinization, and adrenal cortical atrophy.

REFERENCES:

1. Lushbaugh, C. C., Humason, G., Kniseley, R. M., and Gengozian, N. Normal and pathologic intrauterine development of marmosets (Saguinus fuscicollis). In: USAEC Report ORAU-101, 1966, pp. 65-68.

2. Gengozian, N., Lushbaugh, C. C., Humason, G. L., and Kniseley, R. M. 'Erythroblastosis foetalis' in the primate, Tamarinus nigricollis. Nature 209, 731-732, 1966.

Embryology of Marmoset Gonads

R. M. Kniseley, C. C. Lushbaugh, Gretchen L. Humason, and N. Gengozian

As part of the program to develop the marmoset as a laboratory primate, we are studying the embryology of the gonads of this species to determine the course of its sexual development. The material in this report was obtained from 126 embryos, fetuses, and perinatal newborns that delivered spontaneously. The ORAU Medical Division colony of Saguinus fuscicollis provided 86 specimens (42 females, 44 males); Dr. Robert Cooper, Director of the Primate Research Colony of the San Diego Zoological Society, contributed 40 specimens (18 females, 22 males) of another marmoset species, Saguinus oedipus, the cotton-topped marmoset. Because gestational lifetime of these spontaneously aborted fetuses is known only approximately, we use the crown-rump length (CR) of each fetus to represent its age.

Ovary. The earliest ovary available for study was from an embryo of 2.8 cm CR. The organ has undifferentiated cords of cells with dark-staining oval nuclei and compact cytoplasm with scattered foci of oogonia. At 3.4 cm CR length early clusters of oogonia are beginning to differentiate. By 5.6 cm CR length the cortex is clearly defined by primitive lobules of oogonia, and miotic division has begun. The medulla has cords of dark-staining epithelial cells with elongate nuclei arranged in connective tissue. At 6.4 cm CR length, in the Saguinus fuscicollis, cells with rather voluminous cytoplasm and containing PAS-positive granules appear in the medulla singly and in small groups. These cells, glandular interstitial cells, are subsequently found in most ovaries throughout fetal life (Fig. 106). They become more sparse as term approaches, and with the exception of one specimen, have disappeared in the neonatal period. In contrast, the 18 specimens of Saguinus oedipus failed to contain examples of these cells. At 7.1 cm CR (Fig. 106) oocytes begin to appear in the inner cortex and primordial follicles, consisting of oocytes with a rim of medullary cells, and become distinct at 7.8 cm CR. The active

1027710

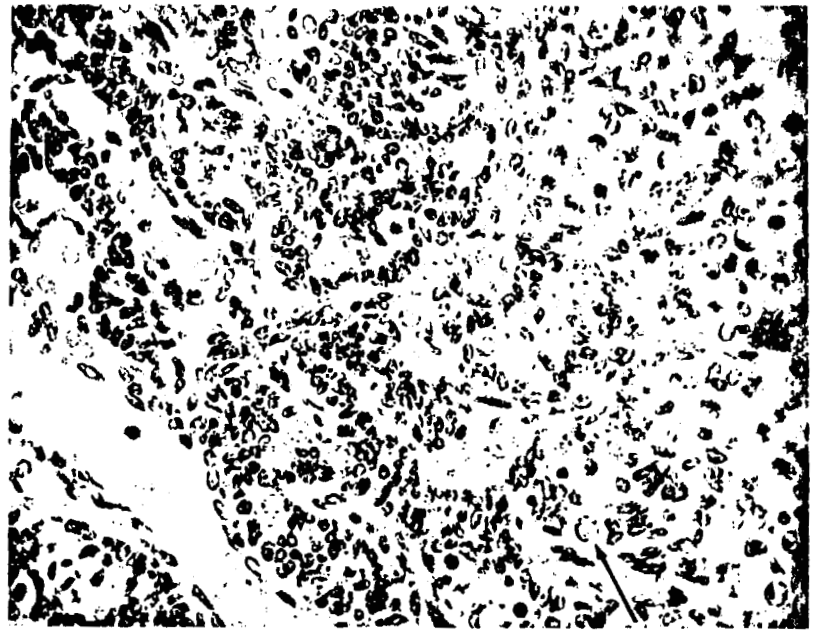

Fig. 106. Marmoset ovary at 7.1 cm CR length showing the cortico-medullary region. Among the epithelial cords of the medulla are glandular interstitial cells singly and in small clumps. Active miosis in the primitive lobules is present and scattered larger oocytes are appearing in the cortico-medullary margins (arrow).

miotic activity in the primitive lobules continues as the fetuses grow. Primordial follicles increase in number so that by 9.5 cm CR the primordial follicles have supplanted the primitive lobules in the inner half of the cortex. In the neonatal period the primordial follicles predominate, but oogenesis still continues peripherally till about 2 months when it ceases.

Testes. The earliest testes available for study were in a 3.0 cm CR fetus. Differentiation was much further advanced than in the ovary at this age and the organ was significantly larger. Glandular interstitial cells predominate, and tubules are distinct from the tunica albuginea. Even at this age there are a few larger cells, judged to be spermatogonia, placed among the sustentacular cells. The prominence of glandular interstitial cells persists throughout most of fetal life constituting between one-half and three-fourths of the tissue, but at about 8.5 cm CR the glandular interstitial cells dwindle in size and number making up usually only one-tenth of the gonad just before full term. At 1 month of age glandular interstitial cells

have almost completely regressed. Granulocytopoiesis surprisingly was detected in the earliest of the testes (3.0 cm CR) before it was established in the bones. It is present almost without exception in the testes throughout the gestation period but not in the ovaries. There is considerable variability in the degree but between 6.0 cm CR and 9.0 CR lengths the greatest activity is observed (Fig. 107). Megakaryocytes were found in a few instances in the interstitial tissue.

These data raise a number of interesting questions: Why does granulocytopoiesis appear in the fetal testes but not in the ovary? Does this granulopoietic activity have a significant role in the development of the hemopoietic organ? If so, there should be its counterpart in the ovary. Also, we must speculate about the relation of the phenomenon to the natural chimerism of this primate. The occurrence of glandular interstitial cells in the ovary poses a similar question. Presumably their appearance and regression regression reflect the same changes in gonadotrophic levels that determine these same events for the interstitial cells of the testes.

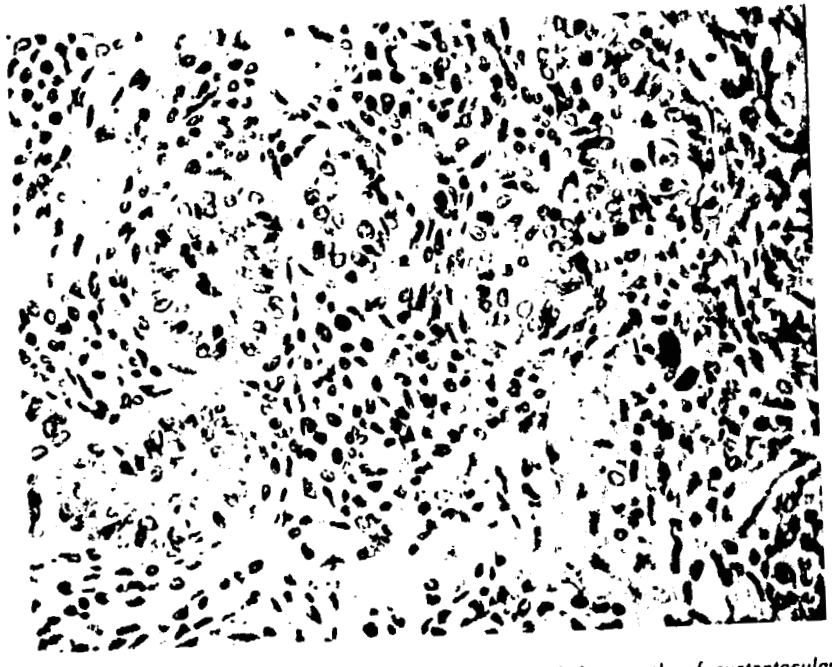

Fig. 107. Marmoset testes at 8.8 CR length showing tubules mostly of sustentacular cells widely separated by interstitial tissue that contains many glandular interstitial cells and active granulopoietic tissue. The dark nuclei are interpreted as megakaryocytes, one of which is in mitosis (x 425).

1027111

The reason for their development or their possible later function is unknown.

In summary, the gonads in general develop in a sequence similar to that described for man and Macaca mulatta,[1] but several unique features are found in this material not described in man or Macaca mulatta: (1) Granulopoiesis is a consistent and usual event in the male gonadal connective tissue of the marmoset. (2) No comparable phenomenon occurs in the embryological development of the ovaries of the marmosets. (3) In the ovary, glandular interstitial cells are frequently seen during the mid and third portions of gestation in Saguinus fuscicollis but not in Saguinus oedipus.

REFERENCE

1. van Wagenen, G. and Simpson, M. E. Embryology of the ovary and testis, Homo sapiens and Macaca mulatta. New Haven, Yale University Press, 1965.

Parasites of the Imported Tamarin, Saguinus fuscicollis

G. E. Cosgrove, Bill Nelson, and N. Gengozian*

Saguinus fuscicollis and some Saguinus nigricollis are in use as laboratory animals at the Medical Division of the Oak Ridge Associated Universities. All tamarins killed or dying have been necropsied, and the pathologic findings in the imported animals have been reported.[1] (In that report these small primates were called Tamarinus nigricollis; we are now using the classification of Hershkovitz.[2]) The principal findings of parasitologic examinations in 455 necropsies are presented in Table 62, which lists 20 species. Five of these have been described as new species; several others have not been fully identified. About 20 other species of parasites were encountered on rare occasions or are under separate taxonomic study. Altogether we have found more than 40 parasitic species in this host, greatly extending the list of parasites of Saguinus (=Leontocebus) presented by Yamashita.[3]

Widely differing periods of survival in the colony afforded a chance to study the persistence of certain parasites under colony conditions (Table 63). The findings suggest that some parasites have considerable longevity and persist even when the intermediate hosts necessary for their transmission are not available. Two of these may cause serious

* Biology Division, Oak Ridge National Laboratory.

TABLE 62

The Principal Parasites of Saguinus

Parasite		Incidence (%)	Location	Number Found Range	Number Found Av.
* Platynosomum amazonensis	Trematoda: Dicrocoeliidae	8	Gallbladder, bile ducts	1-12	3
* Platynosomum marmoseti	Trematoda: Dicrocoeliidae	0.4	Gallbladder, bile ducts	9-64	37
Athesmia foxi	Trematoda: Dicrocoeliidae	8	Gallbladder, bile ducts	1-25	6
Phaneropsolus sp.	Trematoda: Lecithodendridae	4	Small intestine	1-13	3
* Neodiplostomum tamarini	Trematoda: Diplostomatidae	2	Small intestine	1-14	4
Paratriotaenia sp. (=Oochoristica sp.)	Cestoda: Anoplocephalidae	26	Small intestine	1-26	6
Sparganum	Cestoda: Diphyllobothriidae	0.4	Subcutaneous	1-2	1
Prosthenorchis elegans	Acanthocephala: Oligacanthorhynchidae	74	Small intestine, cecum	1-60	9
Strongyloides sp.	Nematoda: Strongyloididae	9	Small intestine	1-10	3
Trypanoxyuris tamarini	Nematoda: Oxyuridae	22	Cecum, colon	1-150	7
Primasubulura jacchi	Nematoda: Subuluridae	15	Small intestine, colon	1-17	3
Filaroides sp.	Nematoda: Filaroididae	18	Lung	1-17	2
Molineus vexillarius	Nematoda: Trichostrongylidae	78	Small intestine	1-114	14
Longistriata sp.	Nematoda: Heligmosomatidae	26	Small intestine	1-85	9
* Spirura tamarini	Nematoda: Spiruridae	44	Esophagus	1-107	7
Dipetalonema gracile	Nematoda: Dipetalonematidae	20	Peritoneal cavity	1-24	5
"Spirurid"	Nematoda: ?	5	Pancreas	1-3	1
Fonsecaiges saimirii	Acarina: Psoroptidae	?	Hair	?	?
* Listrocarpus cosgrovei	Acarina: Listrophoridae	?	Hair	?	?
Porocephalus clavatus	Pentastomida: Porocephalidae	29	Tissue cysts	1-30	4

*New species described from the colony.

1027712

TABLE 63

Relationship of the Incidence of Selected Parasites of Saguinus fuscicollis to Time in the Colony

Days in Colony:	0 - 7	31 - 60	365 - 828	Intermediate Host
No. of Necropsies:*	46	40	37	Required
INCIDENCE:	%	%	%	
Increased				
Sarcocystis	11	5	27	?
Unchanged				
Trypanoxyuris	33	27	35	No
Filaroides	17	8	11	Yes
Porocephalus	33	52	43	Yes
Decreased				
Cestodes	46	25	5	Yes
Prosthenorchis	95	85	32	Yes
Molineus	95	85	47	No
Longistriata	26	50	11	No
Spirura	50	48	11	Yes
Dipetalonema	30	27	14	Yes
Uncertain				
Trematodes	†	†	†	Yes

*This table was prepared by analysis of data from several shipments having a wide range of survival.

†Too few for analysis but a tamarin surviving 689 days had Asthesmia foxi in the bile ducts, and two surviving 430 and 498 days had Phaneropsolus species in the small intestines.

illness long after importation: Prosthenorchis elegans always provokes secondary inflammation at the site of attachment in the small intestine, and often fatal abscesses, peritonitis, or septicemia. Dipetalonema gracile occasionally causes a chronic peritonitis with adhesions, fibrosis, and splenomegaly. Treatment for both these worms is unsatisfactory, and it is fortunate that the arthopods required for transmission of these two infections can be excluded from the colony. The cycle of infection by other species of parasites is direct and reinfection could have occurred; fortunately the parasites transmissible by direct infection are generally of low pathogenicity for this host. A similar listing of the parasites in another colony of marmosets and tamarins was published recently.[4] We plan to present a more detailed account of the parasites found in our colony in a future publication.

REFERENCES

1. Nelson, B., Cosgrove, G. E., and Gengozian, N. Diseases of an imported primate Tamarinus nigricollis. Lab Animal Care 16, 255-275, 1966.

2. Hershkovitz, P. Taxonomic notes on tamarins, genus Saguinus (Callithricidae, Primates), with descriptions of four new forms. Folia Primat 4, 381-395, 1966.

3. Yamashita, J. Ecological relationships between parasites and primates. I. Helminth parasites and primates. Primates 4, 1-96, 1963.

4. Deinhardt, F., Holmes, A. W., Devine, J., and Deinhardt, J. Marmosets as laboratory animals. IV. The microbiology of laboratory kept marmosets. Lab Animal Care 17, 48-70, 1967.

1027713

MISCELLANEOUS

An Interface Scanner for Automatic Data Processing of Liquid Scintillation Spectrometer Readout

H. Kimble and R. McKee**

Automatic transmission of research data from a number of liquid-scintillation spectrometers to a remote data processing center has been accomplished by the use of an automatic interface scanner and a single data-phone system. Digital output data from the liquid scintillation spectrometers and precoded digital information is automatically transmitted to an automatic card punch or directly to an electronic computer.

Although the interface scanner described in this report was designed specifically for use on liquid-scintillation spectrometers, the system is compatible with other instruments having progressive digital readouts. Also, the number of input devices that may be interfaced to the data-phone system is limited only by the practical limitation imposed by the total elapsed time of the data readout for all input devices.

Circuit drawings will be included in USAEC Report ORAU-105 (in preparation).

Continuous sequential scanning of the operating mode of the several input devices is done by a motor-driven scan switch. The scan switch consists of a number of magnetic reed switches equal to the number of input devices. A small combination clutch-brake-gear motor drives a bar magnet sequentially over the reed switches. A contact closure is given on each switch every six seconds. Higher scan rates may be desirable for other installations, but the motor speed should be held within the limitation of the motor brake to ensure closure of the reed switch when the scan motor is stopped.

Each of the input devices is modified with the addition of an end-of-count relay and a readout relay. Contact closure of the end-of-count relay and its respective scanner switch completes the circuit to the set coil of a twin-coil latching relay. Operation of the set coil of the latching relay stops the scan motor, closes the ringing circuit of the data-phone, closes one contact to the readout relay and

* ORAU Technical Services Department

turns on the indicator lamp of the input device ready to read out.

When a "ready" condition is established by the data-phone system and the card punch or computer is ready to receive data, the data-receive relay closes the second contact to complete the circuit to the readout relay and to the respective motor-driven cam timer in the unit.

Stopping of the scan motor locks out all other input devices. Also, since the scan is sequential, a simultaneous end-of-count closure by two or more devices will result in a readout of each instrument according to its place on the scan switch.

The motor-driven cam timers are the type having a single-cycle clutch which is magnetically started and mechanically held for one complete revolution.

The first cam on the timer closes a tee-bar relay, which completes the circuit from the data solenoid driver to the digit relays in the interface scanner. The digit relays in the interface scanner are wired in parallel through connectors with their respective digit solenoid in the readout of each input device. The tee-bar relays prevent feedback of the signal from one input device to other input devices. When data from the input device are completed, the tee-bar relay is dropped out. The second cam on the timer momentarily completes the circuit to the digit relay corresponding to the number of the readout device transmitting the data. The third cam completes the circuit to the "End of Transmission" relay, which opens the telephone circuit and drops out the data-receive relay. The fourth cam completes the circuit to the reset coil of the latching relay and places the unit back in the scanning mode.

The data-phone system used is the AT&T number 401A transmitter and 401J receiver and was modified by the local telephone company for automatic unattended operation.

Also, manual operation of the digit relays allows transmission of coded digital information before automatic transmission from the input devices. A simple push-button switch for each digit relay allows manual operation. Placing the automatic manual switch in manual position will operate the data-phone ringing circuit and a "line ready" lamp illuminates when the card punch or computer is ready to receive data.

Further description of the use of the interface scanner described here is contained in the 1966 Research Report.[1]

REFERENCE

1. Snyder, F. and Bibler, Donna. An automated system for sample collection and computer analysis of thin-layer radiochromatograms. In: USAEC Report ORAU-101, 1966, pp. 154-155.

1027714

PUBLICATIONS

From the Medical Division Oak Ridge Associated Universities 1967

Reprints from the open literature and additional information on publications can be obtained by writing Mrs. Edward H. Anderson, Technical Editor, Medical Division, Oak Ridge Associated Universities, P. O. Box 117, Oak Ridge, Tennessee 37830. Complete lists of Medical Division publications are available.

PUBLICATIONS IN JOURNALS

Andrews, G. A. Radiation accidents and their management. Radiat Res Suppl 7, 390-397, 1967.

Cheng, S.-S., Piantadosi, C., and Snyder, F. Lipid droplets and glyceryl ether diesters in Ehrlich ascites cells grown in tissue culture. Lipids 2, 193-194, 1967.

Cloutier, R. J. and Watson, E. E. Measuring plutonium in wounds: Advantages of using the americium gamma ray. Health Physics 13, 811-813, 1967.

Comas, F. V. and Byrd, B. L. Hemopoietic spleen colonies in the rat. Radiat Res 32, 355-365, 1967.

Fanger, F. and Lushbaugh, C. C. Radiation death from cardiovascular shock following a criticality accident. Arch Path 83, 446-460, 1967.

Gengozian, N. and Batson, J. S. Effects of whole-body irradiation on a small South American primate Saguinus fuscicollis. Int J Radiat Biol 11, 539-551, 1966. (Publication became available in 1967.)

Gengozian, N., Batson, J. S., and Nelson, B. M. Bone-marrow grafting attempts in marmosets after whole-body irradiation. Int J Radiat Biol 11, 553-561, 1966. (Publication became available in 1967.)

Gengozian, N., Gottlieb, C. F., and Allen, E. M. Demonstration of an early host-graft incompatibility reaction in radiation chimeras with the Jerne plaque technique. Proc Soc Exp Biol Med 126, 135-140, 1967.

Gengozian, N. and Hübner, K. F. Effect of phytohemagglutinin (PHA) on an antibody-forming system. J Immunol 99, 184-190, 1967.

Goh, K. O. Cytogenetic studies in blastic crisis of chronic myelocytic leukemia. Arch Intern Med 120, 315-320, 1967.

Goh, K. O. Pseudodiploid chromosomal pattern in chronic lymphocytic leukemia. J Lab Clin Med 69, 938-949, 1967.

Goh, K. O., Swisher, S. N., and Herman, E. C. Chronic myelocytic leukemia and identical twins: Additional evidence of the Philadelphia chromosome as a postzygotic abnormality. Arch Intern Med 120, 214-219, 1967.

Likuski, H. J., Debons, A. F., and Cloutier, R. J. Inhibition of gold thioglucose-induced hypothalamic obesity by glucose analogues. Amer J Physiol 212, 669-676, 1967.

Lim, J., Piantadosi, C., and Snyder, F. A comparison of phospholipid biosynthesis in irradiated bone marrow and liver. Proc Soc Exp Biol Med 124, 1158-1161, 1967.

Lushbaugh, C. C., Comas, F., and Hofstra, R. Clinical studies of radiation effects in man. A preliminary report of a retrospective search for dose-relationships in the prodromal syndrome. Radiat Res Suppl 7, 398-412, 1967.

Lushbaugh, C. C., Cloutier, R. J., Humason, G., Langham, J., and Guzak, S. Histopathologic study of intradermal plutonium metal deposits: Their conjectured fate. Ann N Y Acad Sci 145, 791-797, 1967.

Oswald, E. O., Piantadosi, C., Anderson, C. E., and Snyder, F. Infrared spectra and polymorphism of glycerol ether derivatives. Chem Phys Lipids 1, 270-281, 1967.

Pfleger, R. C., Piantadosi, C., and Snyder, F. The biocleavage of isomeric glyceryl ethers by soluble liver enzymes in a variety of species. Biochim Biophys Acta 144, 633-648, 1967.

Pfleger, R. C. and Snyder, F. Lipid turnover in an isolated population of irradiated bone marrow cells. Radiat Res 30, 325-328, 1967.

Snyder, F. Thin-layer chromatography radioassay: A review. Advances in Tracer Methodology 4, 81-104, 1967.

Uchiyama, G., Hitchcock, A. A. C., and Morris, A. C., Jr. Clinical results with a color-recording rescanner. J Nucl Med 8, 437-443, 1967.

Wood, R. GLC and TLC analysis of isopropylidene derivatives of isomeric polyhydroxy acids derived from positional and geometrical isomers of unsaturated fatty acids. Lipids 2, 199-203, 1967.

Wood, R. and Snyder, F. Characterization and identification of glyceryl ether diesters present in tumor cells. J Lipid Res 8, 494-500, 1967.

1027715

Wood, R. and Snyder, F. Chemical and physical properties of isomeric glyceryl monoethers. Lipids 2, 161-171, 1967.

GOVERNMENT DOCUMENTS

Bergner, P.-E. E. Ergodic properties of the tracer system. USAEC Report ORAU-103, August 1967, 46 pp.

Bergner, P.-E. E. Turnover compartmentalization: A statistical tracer theory for analysis of whole-system retention data. USAEC Report ORAU-104, May 1967, 29 pp.

Cloutier, R. J., O'Foghludha, F., and Comas, F. V. Conference on dosimetry of total-body irradiation by external photon beams. USAEC Report CONF-670219, 1967, 32 pp.

Compartments, Pools, and Spaces in Medical Physiology. Proceedings of a symposium held at the Oak Ridge Institute of Nuclear Studies, an operating unit of Oak Ridge Associated Universities, October 24-27, 1966. Edited by Per-Erik E. Bergner and C. C. Lushbaugh, AEC Symposium Series No. 11, CONF-661010, 1967.

Dalton, P. and Cloutier, R. Preliminary design of a low-level total-body irradiation facility for man. USAEC Report ORINS-52, May 1967, 205 pp.

CHAPTERS

Andrews, G. A. Ethical considerations in human experimentation. In: Proceedings of the 12th Annual Bio-Assay and Analytical Chemistry Meeting, USAEC Report CONF-661018, October 13-14, 1966, pp. 208-212.

Andrews, G. A. Total-body irradiation in the human being. In: Proceedings of the XIth International Congress of Radiology, Rome, September 1965, Excerpta Medica International Congress Series No. 105, 1967, pp. 1583-1589.

Andrews, G. A., Lushbaugh, C. C., Kniseley, R. M., White, D. A., and Friedman, B. I. Haematological effects of whole-body radiation in the human being. In: IAEA Panel: Effects of Ionizing Radiations on the Haematopoietic Tissue. International Atomic Energy Agency, Vienna, 1967, pp. 75-83.

Bergner, P.-E. E. The concepts of mass, volume, and concentration. In: Compartments, Pools, and Spaces in Medical Physiology. Edited by P.-E. E. Bergner and C. C. Lushbaugh. AEC Symposium Series No. 11, CONF-661010, 1967, pp. 21-37.

Kniseley, R. M. The bone marrow. In: Principles of Nuclear Medicine, Henry N. Wagner, Jr. (Ed.), Philadelphia, W. B. Saunders, 1967, pp. 404-412.

Lushbaugh, C. C. Some biological end points of dosimetric value derived from clinical data. In: Proceedings of the 1st International Symposium on Biological Interpretation of Dose from Accelerator-Produced Radiation. USAEC Report CONF-670305, 1967, pp. 94-113.

PUBLISHED ABSTRACTS

Arimizu, N. and Morris, A. C., Jr. Area scanning for quantitative measurement of radioactivity in internal organs. J Nucl Med 8, 312, 1967. Abstr. 0-3.

Bergner, P.-E. E. Turnover compartmentalization theory. J Nucl Med 8, 327, 1967. Abstr. S-6.

Bergner, P.-E. E., Lushbaugh, C. C., Gibbs, W. D., and Franz, W. Analogue computer analysis of human chromium-51 RBC survival and whole-body retention data. J Nucl Med 8, 292-293, 1967. Abstr. I-5.

Dalton, C. P. and Cloutier, R. J. An arrangement of radioactive sources for a low exposure rate total-body irradiation facility. Phys Med Biol 12, 116, 1967. Abstr.

Hartman, R. E. and Hayes, R. L. Gallium binding by blood serum. Fed Proc 26, 780, 1967. Abstr. 2918.

Hayes, R. L., Carlton, J. E., and Byrd, B. L. Preliminary note: Bone scanning with gallium-68: A carrier effect. In: The Year Book of Nuclear Medicine, Vol. 2. Edited by James L. Quinn, III, Chicago, Year Book Medical Publishers, 1967, pp. 363-364, Abstr.

Hayes, R. L., Carlton, J. E., Byrd, B. L., and Rafter, J. J. Factors influencing the distribution of labeled hydrous ferric oxide colloid. J Nucl Med 8, 203, 1967. Abstr. L-3.

Lushbaugh, C. C. and Gibbs, W. D. Decreased ^{24}Na excretion in rat GI syndrome after 1200-rad fission neutron exposures. Radiat Res 31, 593-594, 1967. Abstr. D 6-12.

Snyder, Fred. Cleavage of the 1- and 2-isomers of ^{14}C-labeled glyceryl ethers by a soluble multienzyme system of rat liver. Seventh International Congress of Biochemistry Abstracts IV, p. 734, 1967. Abstr. E-56.

Snyder, Fred and Arrington, J. Radioprotective and metabolic studies of alkenyl and alkyl ethers of glycerol and glycol. Abstracts of Papers for the 15th Annual Meeting of the Radiation Research Society, San Juan, Puerto Rico, p. 35, May 1967. Abstr.

Snyder, F. and Wood, R. The subcellular distribution and metabolism of glyceryl ether diesters in Ehrlich ascites cells. J Amer Oil Chem Soc 44, 381A, 1967. Abstr. 72.

1027716

Wood, Randall. Gas-liquid chromatographic analysis of hydroxy fatty acids and partial glycerides. AOCS Short Course Handbook on Quantitative Gas-Liquid Chromatography, July 30-August 4, 1967, p. 28, Rice University, Houston, Texas. Abstr.

Wood, R. and Snyder, F. Quantitative determination of glyceryl alk-1-enyl and alkyl-alkenyl ethers in neutral and phospholipids. J Amer Oil Chem Soc 44, 380A-381A, 1967. Abstr. 71.

BOOKS

Humason, Gretchen L. Animal Tissue Techniques, 2nd ed. W. H. Freeman and Co., San Francisco, 1967, 569 pp.

PH.D. THESES

Pfleger, Raymond D. The enzymatic cleavage of the ether bond of alkoxyglycerols by a soluble protein fraction of liver and other tissues. (University of North Carolina).

Porter, Raymond P. Chimerism and immunologic tolerance: A consequence of fraternal twinning in the marmoset. (University of Miami).

MISCELLANEOUS

Lushbaugh, C. C. Editorial: Radiation and shock. JAMA 200, 181, 1967.

Gibbs, W. D., Hodges, H. D., and Lushbaugh, C. C. Letter to the editor: Another method for correcting the whole-body count in iron-59 absorption studies in anemia. Blood 29, 934-935, 1967.

Kniseley, R. M. Book Review: Clinical Capillary Microscopy. Edited by Eli Davis, Springfield, Illinois, Charles C Thomas, 1966, 231 pp., Amer J Clin Path 48, 199, 1967.

Snyder, F. Book Review: Advances in Chromatography, Vol. 2 Edited by J. C. Giddings and Roy A. Keller, Marcel Dekker, Inc. 1966. J Amer Oil Chem Soc 44, 464A, 1967.

Snyder, F. Book Review: Advances in Chromatography, Vol. 3. Edited by J. C. Giddings and Roy A. Keller, Marcel Dekker, Inc. 1966. J Amer Oil Chem Soc 44, 464A-465A, 1967.

IN PRESS

Andrews, G. A. Book Review: Progress in Medical Radioisotope Scanning, Vol. II, IAEA, Vienna, 1964. Health Physics.

Andrews, G. A. Bone-marrow transplantation in the treatment of leukemia-lymphoma. In: Proceedings of the International Leukemia-

Lymphoma Conference, Ann Arbor, Michigan, 1967. Lea and Febiger.

Andrews, G. A., Congdon, C. C, Edwards, C. L., Gengozian, N., Nelson, B., and Vodopick, H. Preliminary trials of clinical immunotherapy. Cancer Res

Bergner, P.-E. E. Turnover compartmentalization: In: An Approach to Analysis of Whole-Body Retention Data. 3rd International Symposium on Quantitative Biology of Metabolism, Helgoland, West Germany.

Comas, F. V., Andrews, G. A., and Nelson, B. Spleen irradiation in secondary hypersplenism. Amer J Roentgenol

Cloutier, R. J. and Dalton, C. P. Radiation safety problems with the medical use of radioisotopes. In: Proceedings of the 1st International Congress of the International Radiation Protection Association, Rome, September 5-10, 1966. Pergamon Press.

Debons, A. F., Krimsky, I., Likuski, H. J., From, A., and Cloutier, R. J. Gold thioglucose damage to the satiety center: Inhibition in diabetes. Amer J Physiol

Gengozian, N. Marmosets: Their potential in experimental medicine. Ann N Y Acad Sci

Gibbs, W. D., Hodges, H. D., and Lushbaugh, C. C. A method for precise geometry-independent radioassay of large biological samples. J Nucl Med

Goh, K. O. Smaller G-D/partial G^2 translocation in acute leukemia. Amer J Dis Child

Goh, K. O. The somatic metaphase chromosomal structures of rat kangaroo (Potorous tridactylis). Cytologia

Goh, K. O. Total-body irradiation and human chromosomes: Cytogenetic studies of the peripheral-blood and bone-marrow leukocytes seven years after total-body irradiation. Radiat Res

Goh, K. O. and Sumner, H. Breaks in normal human chromosomes: Are they induced by a transferable substance in the plasma of persons exposed to total-body irradiation? Radiat Res

Lushbaugh, C. C. Absence of electrolyte loss in gastrointestinal syndrome. In: Bond, V. P., Round Table Discussion on Mechanism of Intestinal Radiation Death. Symposium on Gastrointestinal Radiation Injury, Richland, Washington, September 25-28, 1967.

Pfannenstiel, P., Sitterson, B. W., and Andrews, G. A. The use of iodine-130 to study the effect of thyroid stimulatory hormone in patients with thyroid cancer. J Nucl Med

1027717

Porter, R. P. and Gengozian, N. Transplantation in the marmoset (Primate): A technique for orthotopic fitted skin grafts. Proc Soc Exp Biol Med

Snyder, F. The biochemistry of lipids containing ether bonds. Progress in the Chemistry of Fats and Other Lipids.

Snyder, F. and Wood, R. Deposition of triglycerides of increased carbon number in irradiated rat marrow. Radiat Res

Snyder, F. and Wood, R. The occurrence and metabolism of alkyl and alk-1-enyl ethers of glycerol in a variety of human and animal tumors. Cancer Res

Van Woert, M. H. Oxidation of reduced nicotinamide adenine dinucleotide by melanin. Life Sciences

Wood, R. Gas-liquid chromatographic analysis of long-chain fatty alcohols. J Gas Chromatog

Wood, R. and Snyder, F. Quantitative determination of alk-1-enyl- and alkyl-glyceryl ethers in neutral lipids and phospholipids. Lipids

Medical Division Conferences — 1967

January 3: A Search for Tumor Antigens Using the In Vitro Histocompatibility Test - Helen Vodopick Goswitz, Division staff.

January 10: Principles and Applications of Gas-Liquid Chromatography - Randall Wood, Division staff.

January 17: Heart and Lung Evaluation from Regional Photoelectric Signals (Using X ray as Constant External Source of Radiation) - Charles Oderr, Radiologist, Oak Ridge Hospital of the Methodist Church.

January 24: A Review of Radiation and Infection - Edward Balish, Division staff.

January 31: Turnover Compartmentalization - Per-Erik E. Bergner, Division staff.

February 7: Delayed Irradiation Effects on Laboratory Mice - Gerald E. Cosgrove, Biology Division, ORNL.

February 14: The Radiosensitivity of Rat Bone-Marrow Cells Measured by the Spleen Colony Technique - Frank Comas, Division staff.

February 21: Isotopic Effects in Amino Acid Chromatography - Peter Klein, Division of Biological and Medical Research, Argonne National Laboratory.

February 21: The Present and Future Clinical Applications of Rectilinear Scanners - Albert Gilson, Head of Nuclear Medicine, University of Miami School of Medicine, Miami, Florida.

February 28: The Acute Effects of Neutron Irradiation on the Burro - M. H. Wykoff, UT-AEC Agricultural Research Laboratory.

March 7: The Effect of Total-Body Irradiation on Human Chromosomes - Kong-oo Goh, Division staff.

March 14: The Advantages of ^{99m}Tc as a Clinical Tracer Element - Paul Harper, Head, Section on Nuclear Medicine, University of Chicago, Chicago, Illinois.

March 21: Colloids for Scanning the Reticuloendothelial System - Raymond Hayes, Division staff.

March 21: Electron Microscopic Studies of Human and Murine Leukemias - D. C. Swartzendruber, University of Michigan.

March 28: Studies on Isologous Mouse Macroglobulin - W. D. Fisher and M. G. Hanna, ORNL Biology Division.

April 4: The Medical Division Computer: Its Capabilities and Possible Application Areas at ORAU - Fred Brown, Systems Engineer for IBM.

April 11: The Role of Vascular Damage in Lethal Radiation Syndromes - C. C. Lushbaugh, Division staff.

April 18: Computer Handling of Scanning Matrices - W. N. Tauxe, Chief, Section on Nuclear Medicine, Mayo Clinic.

April 25: Animal Toxicity Studies of a Ferric Oxide Colloid Suitable for Marrow Scanning - Bill Nelson, Division staff.

May 2: Fatty Alcohols: Enzymatic Acylation and Oxidative Reactions - Fred Snyder, Division staff.

May 9: Melanin Pigment as Related to Parkinson's Disease - Melvin Van Woert, Division staff.

May 16: Rate Studies of ^{14}C Thymidine Incorporation Using In Vitro Mixed Leukocyte Cultures - Helen Vodopick, Division staff.

May 23: Quantitative Determination of Glyceryl Alk-1-enyl and Alkyl-Alkenyl Ethers in Neutral and Phospholipids of Normal and Tumor Tissues - Randall Wood, Division staff.

May 30: Radiation Effects on Human Testis - E. F. Oakberg, Biology Division, ORNL.

1027118

June 6: Some Preliminary Data on the Study of Radiation and Infection in Human Patients - Edward Balish, Division staff.

June 13: Red Blood Cell Survival Studies - Per-Erik E. Bergner, Division staff.

June 20: The Hemopoietic "Stem Cell" - C. W. Gurney, Professor an Chairman, Department of Medicine, Rutgers Medical School, New Brunswick, New Jersey.

June 27: Angiographic Studies in the Diagnosis of Tumors - Edward Buonocore, U. T. Memorial Hospital, Knoxville, Tennessee.

July 11: Preliminary Report on the First Patient Treated with LETBI C. L. Edwards, Division staff.

July 17: Does Ionizing Radiation Produce Nonspecific Life-Shortening in Man? (Special Lecture) - P. R. J. Burch, Medical Research Council, Environmental Radiation Research Unit, Department of Medical Physics, The University of Leeds, The General Infirmary, Leeds, England.

July 18: Isohemagglutinins in the Marmoset - N. Gengozian, Division staff.

July 25: Human Chromosome Breakages - Kong-oo Goh, Division staff.

August 1: Clinical Role of Radiocolloid Bone-Marrow Scanning in Assessing the Pathogenesis of Erythrocyte Disorders - Francis A. Goswitz, Division staff.

August 8: Radiobiological Research at UT-AEC Agricultural Research Laboratory - Thomas R. Noonan, Director, Animal Research Progr

August 15: Binding of Gallium by Blood Sera - Ronald E. Hartman (Research Participant), St. Bonaventure University, St. Bonaventure New York.

August 22: Report of Research Projects by Summer Student Trainees: Effects of Nausea and Vomiting on Human EKG and Pulmonary Impedance Signals - Larry W. Anglin; The Skin Response of Mice After Fractionated Irradiation - Patricia E. Bigini; Radiation Dosimetry - Measurement and Plots - Robert J. Carpenter, Jr.; ASLS (Analog Simulations of Logical Systems) - Philip J. Pichotta; The Route of Chronic Iron Loss in the Rabbit - Paul J. Sides; Stereologic Quantitation of the Components of Rabbit Marrow - Margaret A. Slaughter; Lipids of Subcellular Fractions Isolated from Ehrlich Ascites Cells - Maria C. Zepeda.

August 29: Remarks on Electronic RBC Sizings - Amiram Ur, Division staff.

September 5: Sixty-Hertz Interference Problems in the LETBI Facility - A. C. Morris, Jr. and T. R. Barclay, Division staff.

September 12: Quantitation of Components of Rabbit Bone Marrow - Bill M. Nelson, Division staff.

September 19: A Report on Trip to Europe, the Mid-East, and Asia - Fred Snyder, Division staff.

September 26: Focusing and Nonfocusing Collimators - C. Craig Harris, Duke University Medical Center, Durham, North Carolina.

October 3: Clinical Applications of the Radioimmunoassay Method - Roger Unger, Veterans Administration Hospital, Dallas, Texas.

October 10: High-Resolution Automated Analysis of Body Fluids for Molecular Constituents - Charles D. Scott, Body Fluid Analysis Group, Chemical Technology Division, ORNL.

October 17: Atoms in Action in Latin America - Roger Cloutier, Division staff.

October 24: Radionuclide Development Program at the Isotopes Development Center, Oak Ridge National Laboratory - Homer Hupf, ORNL.

October 31: Handling Radiation Accidents - Gould A. Andrews, Division staff.

November 2: Ferremic Paradox in Hematologic Disorders with Discussion of Iron Metabolism - Matthew Block, Head, Division of Hematology, University of Colorado, Medical Center, Denver, Colorado.

November 7: Application of Turnover Compartmentalization to Calcium Metabolism - Per-Erik E. Bergner, Division staff.

November 21: An Abnormal Chromosome Associated with Human Malignancies - Kong-oo Goh, Division staff.

November 28: Isolation and Characterization of Transplantation Antigens - Raymond Popp, Biology Division, ORNL.

December 5: Neutron Activation Analysis of Brain Tissue from Rhesus Monkeys Following Phenothiazine - Edward D. Bird, Division staff.

December 12: Radiation Exposure Associated with Medical Diagnostic Studies - K. Z. Morgan, Director, ORNL, Health Physics Division.

December 14: Effect of Cholesterol and Dietary Fat on Atherosclerosis - Raymond Reiser, President of the American Oil Chemists' Society, Professor of Biochemistry, Department of Biochemistry and Biophysics, Texas A and M University, College Station, Texas. (Special Seminar).

December 19: Blockade of the Reticuloendothelial System - Thomas J Saba, Department of Physiology and Biophysics, U. T. Medical School, Memphis, Tennessee.

1027719

Lipid Seminars — 1967

January 25: Gas-Liquid Chromatography Analysis of Triglycerides and Other Related High Molecular Weight Compounds - Randall Wood, Medical Division, ORAU.

February 8: Lipid Accumulation in C. albicans - Edward Balish, Medical Division, ORAU.

February 20: Synthesis and Excretion of Bile Pigments - Peter Klein, Argonne National Laboratory, Argonne, Illinois.

March 27: Industrial Applications of Thin-Layer Chromatography - Merle L. Blank, National Dairy Institute, Glenview, Illinois.

May 19: Studies on Rat Kidney Glucose-6-Phosphatase - James F. Soodsma, Department of Biochemistry, University of North Dakota.

May 24: Lipids of Plasma Membranes of Hepatic Cells - Raymond C. Pfleger, Medical Division, ORAU.

June 5: The Gas-Liquid Chromatography of Intact Triglycerides - Robert Harlow, Medical Division, ORAU.

June 21: Lipid Metabolism of Insects - Edward Lambremont, Summer Research Participant.

July 12: Acetyl Transport Mechanisms - Ademeo F. D'Adamo, Albert Einstein College of Medicine, Yeshiva University, Bronx, New York.

July 19: The Alpha-Oxidation Route for Fatty Acid Degradation - Norman S. Radin, Mental Health Research Institute, University of Michigan, Ann Arbor, Michigan.

July 26: Fatty Acid Composition of the Phospholipids from Rat Liver Cytoplasmic Membranes - Raymond C. Pfleger, Medical Division, ORAU.

August 30: Travelogue and Assorted Information for Europe-Asia trip - Fred Snyder, Medical Division, ORAU.

September 13: Factors Determining the Chain Length of Synthesizing Fatty Acids. GLC Analysis of Triglycerides - Raymond Dils, Biochemistry Department, University of Birmingham, Birmingham, England.

October 25: Review of Long Chain Fatty Aldehyde Metabolism - Robert Wykle, Medical Division, ORAU.

November 15: Principles of Nuclear Magnetic Resonance Spectroscopy - B. M. Benjamin, ORNL, Organic Chemistry Division.

November 29: Practical Applications of Nuclear Magnetic Resonance Spectroscopy - B. M. Benjamin, ORNL, Organic Chemistry Division.

December 20: Lipids in Surgical Disease - Alfred P. Morgan, Peter Bent Brigham Hospital, Boston, Massachusetts.

Regional Lipid Meeting
March 2-3, 1967

Speaker - Affiliation	Title of Talk
Alan Hofmann Department of Gastroenterology Mayo Clinic Rochester, Minnesota	Transport of Lipids by Bile Salt Micelles
Guy A. Thompson, Jr. Department of Biochemistry University of Washington Seattle, Washington	The Biochemistry of Ether-Containing Lipids

Fellowships and Term Appointments

Resident Physicians:
- A. Julian Ahler, M. D.
- Deloris Rissling, M. D.

Postresident Assistants in Clinical Investigation:
- Milton H. Dunsky, M. D.
- Amiram Ur, M. D.
- Romulo J. Mora, M. D.

Picker Foundation Fellow:
- Noboru Arimizu, M. D.

Damon Runyon Fellow:
- Yasuhiko Ito, M. D.

AEC Predoctoral Fellow:
- Raymond P. Porter, M. S.

1027120

Student Fellows in Nuclear Medicine:
- George McCarl
- William Doyle
- Dwight Short
- Everett McKissic
- Arlene Gwon
- Anice Peters

PHS Fellow:
- Donald Carlson, M. S.

UT Graduate Fellow:
- Charles Gottlieb, M. S.

Visiting Scientist:
- Raul De Gasperi, M. D.

Research Participants — 1967

Ronald E. Hartman
St. Bonaventure University
St. Bonaventure, New York

Jerry D. Hunter
University of Texas
El Paso, Texas

Edward N. Lambremont
Louisiana State University
Baton Rouge, Louisiana

Robert C. Ricks
Arkansas State College
State College, Arkansas

Norman L. Savage
Southwest Texas State College
San Marcos, Texas

Student Trainees — 1967

Larry W. Anglin
Francis T. Nicholls State College
Houma, Louisiana

Carol E. Barth
Beaver College
Glenside, Pennsylvania

Patricia Bigini
St. Joseph's College for Women
Long Island, New York

Robert Carpenter
Hardin-Simmons University
Abilene, Texas

Philip J. Pichotta
Wisconsin State University
Platteville, Wisconsin

Paul J. Sides
Centre College of Kentucky
Danville, Kentucky

Margaret A. Slaughter
Talladega College
Talladega, Alabama

Maria C. Zepeda
Our Lady of the Lake College
San Antonio, Texas

Medical Committee, ORAU Council

John L. McCarthy (Chairman)
Southern Methodist University

Gail D. Adams
University of Oklahoma
Medical Center

Roland H. Alden
University of Tennessee
Medical Units

Juan D. Curet
University of Puerto Rico

E. A. Daigneault
Louisiana State University
Medical Center

Edward G. High
Meharry Medical College

Howard L. Hunter
Clemson University

Horace N. Marvin
University of Arkansas
Medical Center

Oscar Touster
Vanderbilt University

ORAU Medical Division Advisory Committee

William C. Moloney (Chairman)
Peter Bent Brigham Hospital

Rupert E. Billingham
University of Pennsylvania
School of Medicine

Frederick J. Bonte
The University of Texas
Southwestern Medical School

E. Richard King
Medical College of Virginia

Wright H. Langham
Los Alamos Scientific
Laboratory

Donald B. Zilversmit
Cornell University

Symposium

Symposium November 13-16, 1967, Radioisotopes in Medicine: In Vitro Studies

Edited by: Francis A. Goswitz, Raymond L. Hayes, and Beverley Murphy

Elizabeth B. Anderson, Technical Editor

In press, AEC Symposium Series CONF-671111

1027721

Medical Division Employees

Scientific Staff

Elizabeth M. Allen, B. S.
Gould A. Andrews, M. D.
Mildred Bailey
Edward Balish, Ph.D.
Thomas R. Barclay, B. S.
Margaret Bateman, B. S.
Jerre Batson, B. S.
William L. Beck, Jr., B. S.
Edward D. Bird, M. D.
Per-Erik E. Bergner, M. D.
Billy L. Byrd, B. S.
Ernest L. Callis, B. S.
James E. Carlton, B. S.
Sarah Cecil
Kay Clayton, B. S.
Martha Clevenger, B. S.
Roger J. Cloutier, M. S.
Frank V. Comas, M. D.
Edgar Cress, B. S.
Evelyn B. Cunningham, B. A.
Surinder P. Datta, Ph.D.
Rachel Dixon
C. Lowell Edwards, M. D.
Elizabeth Edwards
William Fishback
Clarence Forney
Dorothy C. Gaither, M. S.
Nazareth Gengozian, Ph.D.
William D. Gibbs, B. S.
Thomas Gilman, B. S.
Kong-oo Goh, M. D.
Francis A. Goswitz, M. D.
Charles T. Greene, B. A.
Brenda Joan Hall, B. S.
Robert Harlow, B. S.
Oliver Hawkins
Raymond L. Hayes, Ph.D.
Joyce Hewins, A. B.
Harold D. Hodges, B. S.
Elizabeth Holloway
Karl F. Hübner, M. D.
Gretchen Humason, M. A.
Eugene E. Joiner, M. S.
Marjorie Ketelle, B. S.
Ralph M. Kniseley, M. D.
Lisbeth Kraft, D. V. M.
Dorothy Litton
Kathryn Lore, B. S.
C. C. Lushbaugh, M. D., Ph.D.
Dorothy H. Lushbaugh, B. S.
Boyd Malone, B. S.
David Mardon, Ph.D.
J. E. McCarter
Sallie McCaskill
Anita Moehl, B. S.
A. C. Morris, Jr., M. S. E.
Bill M. Nelson, M. D.
Etna Palmer, M. D.
Ted A. Pearson, M. S.
Charles Phipps, B. S.
Raymond C. Pfleger, Ph.D.
William T. Pope
Richard F. Queener
John J. Rafter, B. S.
Evalyn Repplinger, M. B.
Mack Ruffner
Elizabeth M. Rupp, B. A.
Thomas A. Smith
Mary Smyser, B. S.
Fred L. Snyder, Ph.D.
Margo Steinman, M. S.
Nelson Stephens, B. S.
Ryosaku Tanida, M. D.
Mary Thomas, B. S.
Melvin Van Woert, M. D.
Helen Vodopick, M. D.
Mary Alyce Watkins, A. B.
Allen M. Webb, B. S.
James White
Randall Wood, Ph.D.
Francine Wright, B. S.
Robert Wykle, M. S.
Martin C. Yarbrough, B. S.

Nursing and Patient Care

Lucy Amburn
Margie Bagley, R. N.
Margaret Blackburn, R. N.
Ervin Bobo
Helen Brinker, R. N.
James Cozart
Mary Nell Craig, R. N.
John Dean
Thelma Eden, R. N.
Mable Helton, R. N.
Rita Holt, R. N.
Marilyn Mackley, R. N.
Bedford Mayott
Barbara Nance, R. N.
Beuna Pack
Garfield Porter
Naomi Presnell, R. N.
Mary Rogers, R. N.
Lillie P. Simmons
Elaine Stoetzel, R. N.
Mary E. Sutliff, R. N.
Eria Winters, R. N.
Lillie I. Woods

Administrative, Editorial, Medical Records, and Secretarial

Elizabeth B. Anderson, M. S.
Frances Banner
Kenneth L. Burton, B. S.
Blanche Carden
Carole J. Carter, B. S.
Frances Darr
Laura P. Edwards
J. Howard Harmon
Mary Lynn Christiansen
Wanda Hodge
Julia Hopper
Mildred Hyp
Ann Lake, B. S.
Willa Fae Loveday
Kathryn McCulloch, B. S.
Maryrose McGown
Barbara Messenger
Judy Owens, B. A.
Ruth C. Paire
Emily Roemer
Evelyn Sipe
Mona Smith
Tom Stokes
Katherine Stubbs, B. A.
Lana Toburen
Dorothy Vola
Patsy White
Florence C. Zenni

Custodial and Animal Care

Willie Barnett
Mark Brewer
Willie J. Brooks
Clarence Buckley
Isaiah Caldwell
Jerry Constance
Grace E. Foster
James Graham
Clarence Hamilton
Fred Hamilton
Renfro Henderson
Eugene Hickson
James Kline
Carlos McGhee
James Rather
Jerry Steele
J. R. Stevens
William Walker

1027722

Consultants and Collaborators — 1967

Norman G. Anderson, Ph.D.
Biology Division
Oak Ridge National Laboratory

Edmund B. Andrews, M. D.
Medical Arts Building
Knoxville

John A. Auxier, M. S.
Health Physics
Oak Ridge National Laboratory

Fritz H. Bach, Ph. D.
Laboratory of Genetics
University of Wisconsin
Madison

Robert P. Ball, M. D.
Radiology Department
Oak Ridge Hospital

Jere M. Bauer, M. D.
University of Michigan School of Medicine
Ann Arbor

W. J. Baumann, Ph.D.
University of Minnesota
Hormel Institute
Austin

M. A. Bender, Ph.D.
Biology Division
Oak Ridge National Laboratory

R. R. Bigelow, M. D.
Medical Arts Building
Oak Ridge

B. B. Blevins, D.D.S.
Medical Arts Building
Oak Ridge

Matthew Block, M. D.
Division of Hematology
University of Colorado Medical Center
Denver

Donald Brown, M. D.
Department of Radiology
University of Colorado Medical Center
Denver

Louis Bryan, M. D.
Doctors Building
Oak Ridge

Edward Buonocore, M. D.
U. T. Memorial Research Center Hospital
Knoxville

Amoz I. Chernoff, M. D.
Director of Research
U. T. Memorial Research Center
Knoxville

Kenneth W. Christenberry, M. D.
501 Church Ave., SW
Knoxville

Lowell T. Coggeshall, M. D.
Route 3
Foley, Ala.

C. C Congdon, M. D.
Biology Division
Oak Ridge National Laboratory

Robert Cooper, D.V.M.
Director, Primate Research Colony
San Diego Zoological Society
San Diego

G. E. Cosgrove, M. D.
Biology Division
Oak Ridge National Laboratory

Dexter Davis, M. D.
Medical Arts Building
Oak Ridge

Albert F. Debons, Ph.D.
Department of Surgery and Physiology
Veterans Administration Hospital
Brooklyn, N. Y.

Earl Eversole, Jr., M. D.
Medical Arts Building
Oak Ridge

Warren L. Franz, M. S.
Department of Chemical Engineering
University of Tennessee
Knoxville

Ben I. Friedman, M. D.
University of Cincinnati School of Medicine
Cincinnati, Ohio

Warren Glaser, M. D.
Department of Medicine
State University of New York College of Medicine
Downstate Medical Center
Brooklyn, N. Y.

Douglas Grahn, Ph.D.
Division of Biological and Medical Research
Argonne National Laboratory
Argonne, Ill.

Nathan S. Hall, Ph.D.
Laboratory Director
UT-AEC Agricultural Research Laboratory
Oak Ridge

George T. Harrell, M. D.
Milton S. Hershey Medical Center
Pennsylvania State University
Hershey

C. Craig Harris, M. S.
Division of Nuclear Medicine
Department of Radiology
Duke University Medical Center
Durham, N. C.

Warren W. Harris, Ph.D.
Biophysics Separations Laboratory
Oak Ridge National Laboratory

Ernest L. Hendrix, M. D.
Medical Arts Building
Oak Ridge

Robert Heyssel, M. D.
Vanderbilt University
Nashville

John U. Hidalgo, M. S.
Tulane University
Bio-Medical Computing System
New Orleans, La.

Perry M. Huggin, M. D.
East Tennessee Tuberculosis Hospital
Knoxville

Melville L. Jacobs, M. D.
City of Hope Medical Center
Duarte, Calif.

Raymond A. Johnson, M. D.
Medical Arts Building
Oak Ridge

Marvin A. Kastenbaum, Ph.D.
Mathematics Division
Oak Ridge National Laboratory

Herbert D. Kerman, M. D.
Halifax District Hospital
Daytona Beach, Fla.

Avery P. King, M. D.
Medical Arts Building
Oak Ridge

Alfred P. Kraus, M. D.
University of Tennessee College of Medicine
Memphis

Lorraine Kraus, M. D.
University of Tennessee College of Medicine
Memphis

1027723

A. L. Kretchmar, M. D., Ph.D.
U. T. Memorial Research Center and Hospital
Knoxville

William G. Laing, M. D.
1501 Clinch Ave., SW
Knoxville

Edward N. Lambremont, Ph.D.
Louisiana Nuclear Science Center
Louisiana State University
Baton Rouge, La.

Robert D. Lange, M. D.
U. T. Memorial Research Center
Knoxville

Wright Langham, Ph.D.
Los Alamos Scientific Laboratory
Albuquerque, N. M.

Robert A. Lewis, M. D.
608 Main Ave., SW
Knoxville

Henry J. Likusky, Ph.D.
Downstate Medical Center
New York City

Stuart W. Lippincott, M. D.
Department of Radiation Biology
Medical College of Virginia
Richmond, Va.

James L. Liverman, Ph.D.
Assistant Director
Oak Ridge National Laboratory

Bismarck B. Lozzio, Ph.D.
U. T. Memorial Hospital and Research Center
Knoxville

Helmut Mangold, Ph.D.
University of Minnesota
Hormel Institute
Austin

Margaret Maynard, M. D.
Dermatologist
Medical Arts Building
Knoxville

Christopher B. Merritt, M. D.
Johns Hopkins University Hospital
Baltimore, Md.

Isadore Meschan, M. D.
Department of Radiology
Bowman Gray School of Medicin
Wake Forest College
Winston-Salem, N. C.

William O. Miller, M. D.
Urologist
606 Main Ave., SW
Knoxville

George R. Minor, M. D.
Department of Surgery
University of Virginia Hospital
Charlottesville

William C. Moloney, M. D.
Director
Hematology Laboratory
Boston City Hospital
Boston, Mass.

K. Z. Morgan, Ph.D.
Health Physics Division
Oak Ridge National Laboratory

Dana W. Nance, M. D.
Oak Ridge Hospital

Robert W. Newman, M. D.
Medical Arts Building
Knoxville

Thomas R. Noonan, M. D.
Associate Director
UT-AEC Agricultural Research Laboratory
Oak Ridge

Robert Nordlie, Ph.D.
Department of Biochemistry
University of North Dakota
Grand Forks

Richard A. Obenour, M. D.
1501 Clinch Ave., SW
Knoxville

Thomas H. Oddie, D.Sc.
Department of Radiology
University of Arkansas Medical Center
Little Rock

T. T. Odell, Ph.D.
Biology Division
Oak Ridge National Laboratory

Charles Oderr, M. D.
Oak Ridge Hospital

Fearghus T. O'Foghludha, Ph.D.
Division of Radiation Physics
Medical College of Virginia
Richmond

James P. OKunewick, Ph.D.
Experimental Pathology Department
Armed Forces Radiobiology Research Institute
National Naval Medical Center
Bethesda, Md.

Stanley W. Olson, M. D.
Director
Tennessee Mid-South Regional Medical Program
Vanderbilt University
Box 95, Station 17
Nashville, Tenn.

Claude Plantadosi, Ph.D.
Department of Medicinal Chemistry
University of North Carolina
Chapel Hill

Orville Privett, Ph.D.
University of Minnesota
Hormel Institute
Austin

W. W. Pugh, Jr., M. D.
Doctors Building
Oak Ridge

D. A. Ross, Ph.D., M. D.
Medical Nuclear Instrumentation Group
Oak Ridge National Laboratory

Henry B. Ruley, M. D.
Medical Arts Building
Oak Ridge

Eugene L. Saenger, M. D.
Radioisotope Laboratory
General Hospital
Cincinnati, Ohio

H. H. O. Schmidt, Ph.D.
University of Minnesota
Hormel Institute
Austin

N. G. Scott, Ph.D.
Chemical Technology Division
Oak Ridge National Laboratory

C. W. Sensenbach, M. D.
Medical Arts Building
Oak Ridge

Leigh Simmons, D.V.M.
Biology Division
Oak Ridge National Laboratory

Norman Simon, M. D.
945 Fifth Avenue
New York, N. Y.

W. Eidson Smith, M. D.
Blount Professional Building
Knoxville

1027724

Walter S. Snyder, Ph.D.
Health Physics Division
Oak Ridge National Laboratory

Alan Solomon, M. D.
U. T. Memorial Research Center
Knoxville

Ben H. Spargo, M. D.
Department of Pathology
University of Chicago
Chicago, Ill.

Paul Spray, M. D.
Doctors Building
Oak Ridge

P. E. Steiner, M. D.
Department of Pathology
University of Pennsylvania School of Medicine
Philadelphia

George M. Stevens, III, M. D.
Doctors Building
Oak Ridge

W. N. Tauxe, M. D.
Section of Clinical Pathology
Mayo Clinic
Rochester, Minn.

William M. Tipton, M. D.
522 West Church Street
Knoxville

Joe E. Tittle, M. D.
Doctors Building
Oak Ridge

V. R. R. Uppuluri, Ph.D.
Mathematics Division
Oak Ridge National Laboratory

A. C. Upton, M. D.
Biology Division
Oak Ridge National Laboratory

Henry N. Wagner, Jr., M. D.
Division of Nuclear Medicine
Johns Hopkins Hospital
Baltimore, Md.

H. Stephen Weens, M. D.
Emory University School of Medicine
Atlanta, Ga.

Trevor Williams, Ph.D.
Head, Biomathematics Division
International Agency for Research on Cancer
16, Avenue Marechal Foch
69, Lyon, France

Mr. Richard D. Wittrup
Administrator
University of Kentucky Medical C
Lexington, Ky.

LEGAL NOTICE

This report was prepared as an account of Government sponsored work. Neither the United States, nor the Commission, nor acting on behalf of the commission:

A. Makes any warranty or representation, expressed or implied, with respect to the accuracy, completeness, or useful information contained in this report, or that the use of any information, apparatus, method, or process disclosed in this rep infringe privately owned rights; or

B. Assumes any liabilities with respect to the use of, or for damages resulting from the use of any information, apparat or process disclosed in this report.

As used in the above, "person acting on behalf of the Commission" includes any employee or contractor of the Com employee of such contractor, to the extent that such employee or contractor of the Commission, or employee of such con pares, disseminates, or provides access to, any information pursuant to his employment or contract with the Commission, or ment with such contractor.

Research Report

MEDICAL DIVISION
Oak Ridge Institute of Nuclear Studies

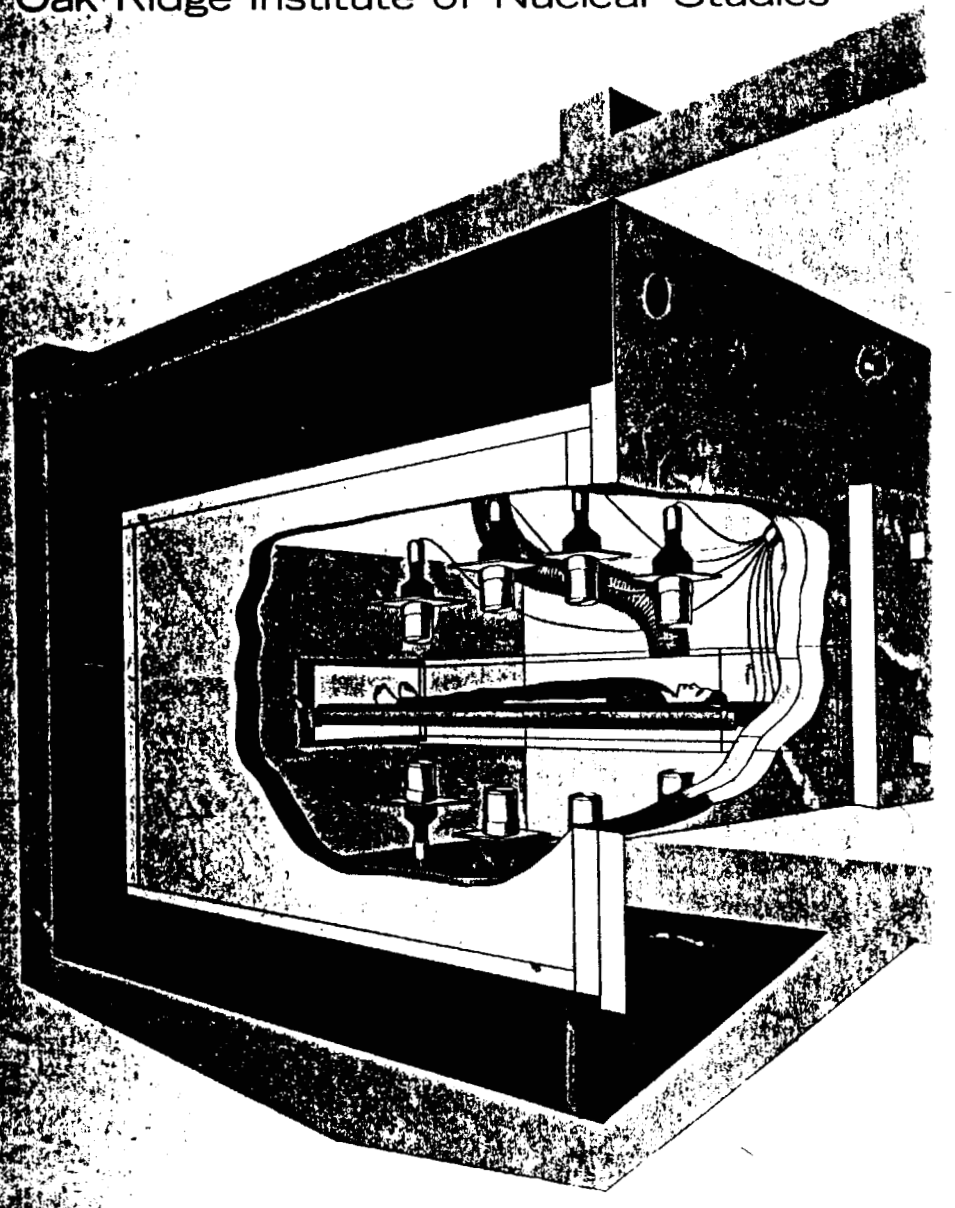

An Operating Unit of Oak Ridge Associated Universities

REPOSITORY Oak Ridge Institute for Science and Education, Medical Sciences Division

COLLECTION Oak Ridge Associated Universities Annual Research Reports, Medical and Health Sciences Division

BOX No. No Folder Title.

FOLDER Document No.: ORAU-30002, Part 2 of 6

Vance Road Facility, ~~Room~~ Room 202A

1027725

COVER: Cutaway view of the low-background, whole-body counter now in operation at the Medical Division. Unusual measures were taken to obtain materials throughout that would contain minimal amounts of natural and fallout radioactivity. The light green represents the outer concrete shield, a mix of specially selected cement and marble aggregates. The dark green is crushed magnesium and iron orthosilicate ore (olivine), which forms the next attenuating layer. Blue indicates the 5-inch thick shield fabricated from pre-World War II, low-activity steel. In this steel box are located the detectors and the plastic enclosure for the patient and stretcher. The duct indicated in orange supplies filtered air to the patient being measured. The patient first showers to remove any external traces of radioactivity before dressing in the clean hospital scrub suit (coded bright blue to avoid even the slightest contamination from regular hospital laundry), thus lowering chances for carrying small amounts of contaminating radioactivity into the counter. The electrical conduits, shown in orange, from the eight balanced crystal-phototube assemblies exit through the top right of the steel shield and tie into a multichannel analyzer (not shown) for spectral identification of radioisotopes and quantitative measurements of radioactivity in patients. Illustration by Jeanne Simmons.

1027726

RESEARCH REPORT – MEDICAL DIVISION
Oak Ridge Institute of Nuclear Studies

FOR THE YEAR ENDING DECEMBER 31, 1965

Operating Under Contract With
The United States Atomic Energy Commission

ORINS-53

Single copies are available on request from:
Medical Division
Oak Ridge Institute of Nuclear Studies
Oak Ridge, Tenn. 37830

Printed in the United States of America
Price $3.00
Available from: Clearinghouse for Federal Scientific and Technical Information, Springfield, Virginia 22151

1027727

Contents

	Page
ORGANIZATION OF RESEARCH	viii
INTRODUCTION	1
MECHANISMS OF RADIATION INJURY	5
Autopsy Findings after Therapeutic Total-body Irradiation. *B. Nelson.*	5
Strongyloidiasis and Malignant Lymphoma. *W. A. Rogers, Jr.* and *B. Nelson.*	7
Scope and Orientation of the Lipid Project. *F. Snyder.*	9
In Vitro Incorporation of Palmitic-1-^{14}C Acid Into Irradiated Bone-marrow Cells. *R. Pfleger, F. Snyder,* and *C. Piantadosi.*	12
Phospholipid Biosynthesis in Irradiated Tissues. *J. Lim, F. Snyder,* and *C. Piantadosi.*	15
Turnover of Fatty Acids in the Triglycerides of Irradiated Bone Marrow. *J. N. Bollinger.*	18
The Deposition and Metabolism of Batyl Alcohol-1-^{14}C in the Rat. *F. Snyder, C. Piantadosi,* and *E. Oswald.*	19
Lipids Present in the Walker-256 Tumor. *J. N. Bollinger.*	21
Thin-layer Chromatographic Analysis of Lipids Isolated from Ehrlich Ascites Carcinoma Cells. *S. Cheng, C. Piantadosi,* and *F. Snyder.*	23
STUDIES RELATED TO TREATMENT OF RADIATION INJURY	26
Human A- and B-like Antigens and Antibodies in Marmoset Serum. *N. Gengozian* and *C. Merritt.*	26
Formation of Isohemagglutinins in the Marmoset, *Tamarinus nigricollis. N. Gengozian.*	28
Erythroblastosis Foetalis in the Primate, *Tamarinus nigricollis. N. Gengozian, C. C. Lushbaugh, G. L. Humason,* and *R. M. Kniseley.*	31
Diseases of an Imported Primate, *Tamarinus nigricollis. B. Nelson, G. E. Cosgrove,* and *N. Gengozian.*	34
Consideration of Radiation Exposure Rates in Transplantation of Xenogeneic and Allogeneic Bone Marrow in Irradiated Mice. *N. Gengozian, D. Carlson,* and *E. Allen.*	35

Abnormal Immune Mechanism in Allogeneic Radiation Chimeras. *N. Gengozian, B. Rabette,* and *C. C. Congdon.* 38
A Model of Hemopoiesis for Mammalian Recovery Experiments. *A. L. Kretchmar.* 41
Reduced Erythropoietic Capacity in Lethally Irradiated Mice Treated with Isologous or Homologous Bone-marrow Cells. *A. L. Kretchmar* and *E. Rupp.* 47
Secondary Mortality and Body Weight Loss in Lethally Irradiated Mice Given Small Doses of Isologous Bone-marrow Cells. *A. L. Kretchmar* and *W. R. Conover.* 50
Serine-3-^{14}C Metabolism in Mice as Determined by Respiration Pattern Analysis. *A. L. Kretchmar* and *C. E. Phipps.* 51
The Radiosensitivity of Bone-marrow Cells Made Hypoxic by Vascular Occlusion. *F. Comas.* 53
Cytogenetic Interrelation of the Myeloproliferative Disorders. *K. O. Goh.* 55
Smaller G Chromosome in Irradiated Man. *K. O. Goh.* 56
Intermittent Corticosteroid Therapy in the Malignant Lymphocytic Diseases. *D. A. White.* 60

METALS METABOLISM AND MEDICAL RADIOISOTOPE DEVELOPMENT 64

Basic Studies of Gallium Distribution. *R. L. Hayes, B. L. Byrd,* and *J. E. Carlton.* 64
Colloidal Hydrous Ferric Oxide as an Agent for Scanning of the Reticuloendothelial System. *R. L. Hayes, J. E. Carlton,* and *B. L. Byrd.* 67
The Laboratory Evaluation of Rats Progressing Through a Fatty-liver Cycle Caused by Cerium. *G. C. Kyker, J. J. Rafter, V. Z. Holten, A. Webb, B. Chastain,* and *M. K. Ballenger.* 67
Production of Lanthanide Radioisotopes for Clinical Use. *G. C. Kyker* and *J. J. Rafter.* 71
Effects of Lanthanide Chlorides on Selected Enzymes. *V. Z. Holten, G. C. Kyker,* and *M. Pulliam.* 72
The Effect of Glucose Inhibitors on Gold-Thioglucose-induced Hypothalamic Obesity in Mice. *H. J. Likuski, A. F. Debons,* and *R. J. Cloutier.* 73

1027128

THERAPY WITH RADIATION 75
Total-body Irradiation Program. *D. A. White, C. L. Edwards, F. V. Comas, G. A. Andrews,* and *R. M. Kniseley.* 75
Variations in Leukocyte Alkaline Phosphatase Scores After Radiation Therapy in Some Blood Dyscrasias. *G. L. Humason, C. C. Lushbaugh,* and *F. Comas.* 79
Immunotherapy of Acute Leukemia: An Experimental Approach. *C. L. Edwards, C. C. Congdon, N. Gengozian, H. Vodopick,* and *G. A. Andrews.* 81
Lipid Embolism to the Brain After Lymphography. *B. Nelson, E. A. Rush, M. Takasugi,* and *J. Wittenberg.* 83

RADIOISOTOPES IN DIAGNOSIS 85
Gallium-68 Citrate in Bone Scanning. *J. Ahumada, R. L. Hayes, R. Tanida,* and *C. L. Edwards.* 85
Clinical Bone-marrow Scanning. *R. M. Kniseley, G. A. Andrews, R. Tanida, C. L. Edwards,* and *G. C. Kyker.* 90
Whole-body Scans After Absorption of ^{131}I-Fatty Acids in a Patient with Chylothorax. *E. A. Rush* and *F. Snyder.* 98
^{131}I-Fibrinogen Plasma Disappearance and Evaluation as a Scanning Agent. *E. A. Rush.* 101
On the Ergodic Properties of the Tracer System. *P.-E. E. Bergner.* 102
Exchangeable Mass: Determination Without Assumption of Isotopic Equilibrium. *P.-E. E. Bergner.* 103
On Stationary and Nonstationary Red-cell Survival Curves. *P.-E. E. Bergner.* 105
Determination of Red-cell Destruction From DF ^{32}P-Data. *P.-E. E. Bergner* and *J. D. Lawson.* 105
A Mathematical Description of the Discrepancy Between Whole-body Peripheral Blood Retention of ^{51}Cr in Red Cell Label. *J. D. Lawson, P.-E. E. Bergner, C. C. Lushbaugh, W. D. Gibbs,* and *D. H. Lushbaugh.* 107
Feasibility of Using *In Vivo* DF ^{32}P and Whole-body Counting in Red-cell Survival Studies. *C. C. Lushbaugh, W. L. Scott, M. C. Yarbrough, R. Queener,* and *W. D. Gibbs.* 112
An *In Vitro* Method for DF ^{32}P Labeling of Red Cells for Intravenous Administration. *C. C. Lushbaugh, R. Queener,* and *W. D. Gibbs.* 115

A Test of the Extravascular Concept of the Dynamics of Rose Bengal Blood Clearance in the Rat. *C. C. Lushbaugh, M. L. Davis,* and *W. D. Gibbs.* 117

BIOLOGICALLY IMPORTANT RADIOISOTOPIC MATERIALS: ABSORPTION, WHOLE-BODY RETENTION, AND DEPOSITION IN SPECIFIC ORGANS. 120

Clinical Evaluation of the ORINS Medium-level Whole-body Counter. *M. Takasugi, C. C. Lushbaugh, C. L. Edwards,* and *W. D. Gibbs.* 120

The Possibility that Tobacco Contributes to Human Radioactive Body Burdens. *W. D. Gibbs, C. C. Lushbaugh,* and *H. D. Hodges.* 125

Whole-body Retention and Distribution of Manganese-54 Chloride in the Rat. *W. D. Gibbs, A. Hendrix,* and *H. D. Hodges.* 128

Aestival Variation of Thyroid Function in the Box Turtle. *C. C. Lushbaugh, G. L. Humason, M. C. Yarbrough, R. Queener,* and *W. D. Gibbs.* 133

NASA STUDY ON RADIATION EFFECTS 138

Human Radiosensitivity as Measured by Study of Clinical Data from Therapeutic Total-body Irradiation. *C. C. Lushbaugh, G. A. Andrews, R. Hofstra,* and *F. Comas.* 139

INSTRUMENT DEVELOPMENT AND METHODOLOGY 143

Color and Contrast Enhancing Rescanner. *G. Uchiyama, A. A. C. Hitchcock,* and *A. C. Morris, Jr.* 143

Standardization and Calibration of a Whole-body Counter for Clinical Research. *W. D. Gibbs, H. D. Hodges,* and *C. C. Lushbaugh.* 145

A Rapid Electronic Method for Measuring Red-cell Fragility in Hemolytic Systems. *A. C. Morris, Jr., C. C. Lushbaugh, D. H. Lushbaugh,* and *R. H. Corley.* 149

Measurement of Plutonium in Wounds: Self-absorption by Plutonium. *R. J. Cloutier* and *E. E. Watson.* 154

Gas-liquid Chromatography Analysis of Long Chain Isomeric Glyceryl Ethers. *R. Wood* and *F. Snyder.* 157

1027729

Modified Silver Ion Thin-layer Chromatography. *R. Wood* and *F. Snyder.* 158

A Modified Applicator for the Uniform Coating of Thin-layer Plates. *R. Wood* and *F. Snyder.* 159

A Comparison of Zonal Scans, Strip Scans, and Autoradiographic Scans of Thin-layer Chromatograms. *F. Snyder.* 160

PUBLICATIONS 163

ACKNOWLEDGEMENTS 167

AUTHOR INDEX 168

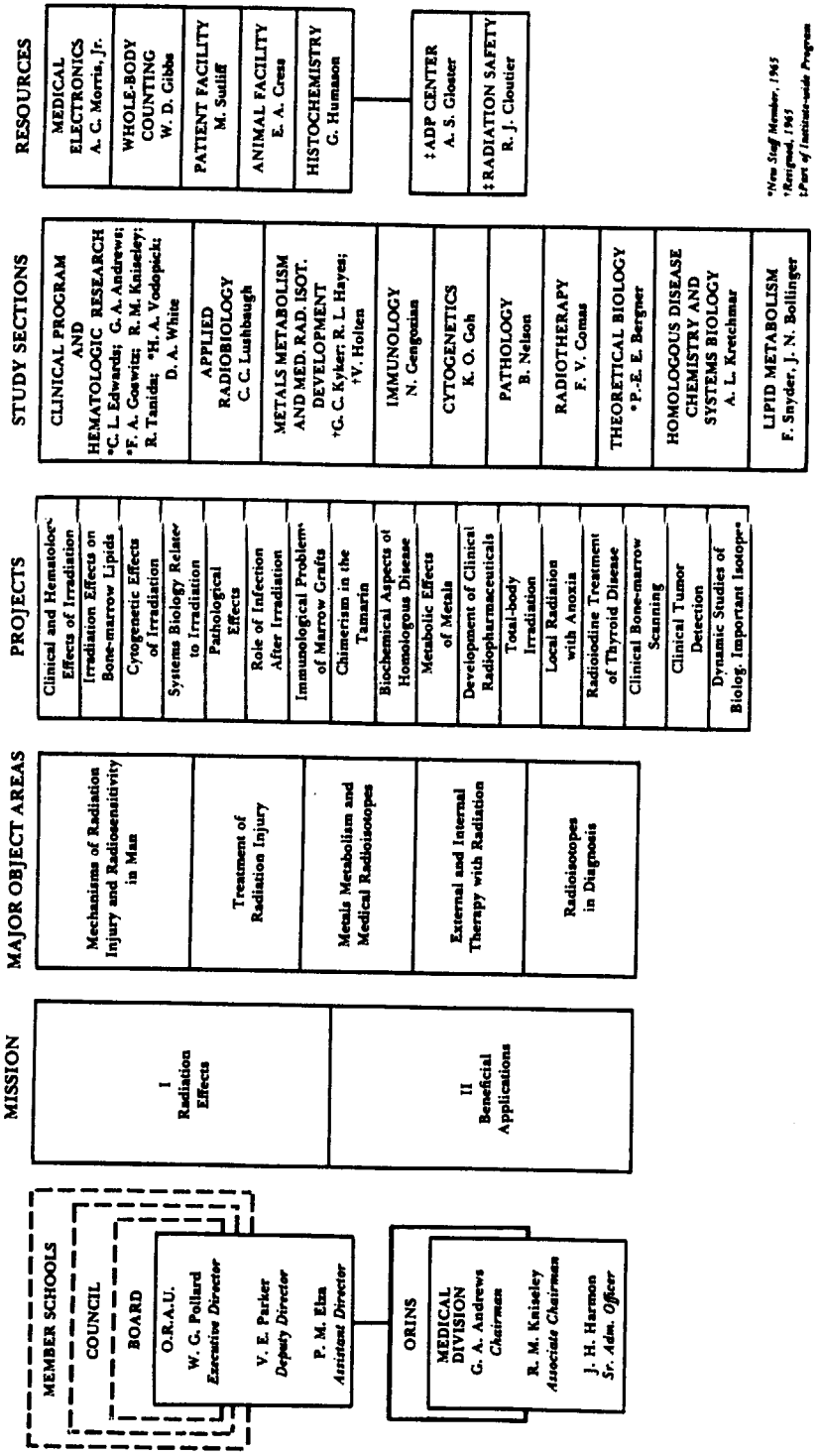

Introduction

The Medical Division is a clinical and laboratory research unit, one of the major "on site" biomedical investigational laboratories supported by the U. S. Atomic Energy Commission through its Division of Biology and Medicine. Additional support comes from the National Aeronautics and Space Administration; this work is an integral part of the Atomic Energy Commission program on radiation effects and funds are channeled through the Atomic Energy Commission. The tamarin project is supported in large part by the National Institutes of Health. A new program about to be initiated, on infections associated with marrow depression, will be supported by the Department of Army, Research and Development Command, through the Armed Forces Epidemiological Board.

A 30-bed hospital offers appropriate space and equipment for studies upon selected patients; laboratories provide for animal experiments and a variety of biological investigations. Special facilities make it possible to give total-body irradiation to patients and to assay whole-body radioactivity with a wide range of sensitivities. The major objectives of the program are to obtain information on radiation effects and the treatment of radiation damage, especially as related to total-body irradiation in the human being, and certain uses of radioisotopes in clinical medicine. The outline on Page viii gives some relationships of the program, its objectives, organization, and staff.

Effective January 1966, the corporate name of the Oak Ridge Institute of Nuclear Studies will be changed to Oak Ridge Associated Universities. The new name was established because it more accurately describes the actual corporate status of the organization and makes clear the role of the universities. The Oak Ridge Institute of Nuclear Studies, of which the Medical Division is a part, will remain an operating unit of Oak Ridge Associated Universities.

Late in 1965, the Division lost a valued staff member, Dr. Granvil C. Kyker, who was appointed head of the Fellowship Office of Oak Ridge Associated Universities. Dr. Virginia Holten, a recent addition to the staff who was working with Dr. Kyker, resigned to take another position. The Division feels the loss of these valued staff members. Dr. Kyker's contribution to the Division over the years has been very large. He made significant advances in understanding the biological effects of rare-earth elements, contributed notably to the biological effects of rare-earth elements, contributed notably to the development of younger investigators, and developed special facilities

for the Division. He has always supported strongly the over-all objectives of the program, and on many occasions has characteristically put the needs of the whole group above his personal interests.

New additions to the staff include Dr. C. Lowell Edwards, Chief of Clinical Services, who assumed his duties early this year. Dr. Per-Erik E. Bergner, a theoretical biologist from Sweden who has been with us on a temporary appointment, recently joined the regular staff. Dr. Frank Goswitz and his wife, Dr. Helen Vodopick, internists with special training in hematology who were at the Division earlier as trainees, have returned to the Institute as senior staff members. Dr. Goswitz is on the staff of the Special Training Division, in charge of medical courses, and will have his research activity at the Medical Division. Dr. Vodopick is part of the Medical Division clinical staff, working chiefly in hematologic research. Dr. Ralph Kniseley, formerly Assistant Chairman, has become Associate Chairman of the Division.

Two staff members were assigned for extended periods to other laboratories for collaborative work. Dr. Frank Comas spent nine months in the radiotherapy department of Dr. Henry Kaplan at Stanford University, working on radiosensitivity and anoxia. During most of Dr. Comas's absence we were fortunate in having as a temporary staff member, Dr. Kazuko Bill, who worked very effectively in radiology and radiotherapy. Dr. Fred Snyder spent five months at the University of North Carolina in the department of pharmacology with Dr. Claude Piantadosi, principally engaged in ^{14}C labeling of lipid compounds. Both Dr. Snyder and Dr. Arthur Kretchmar have participated in the collaborative program initiated with the department of biochemistry at the University of Tennessee's Medical School, and have given series of lectures to graduate students at the Memphis campus.

An important trend this year has been enhancement of the areas of cooperation between the Medical Division and the Biology Division of Oak Ridge National Laboratory. Joint interests have also developed with the research program at the University of Tennessee Memorial Research Hospital in Knoxville.

Trainees and visiting scientists continue to play a major role in the Medical Division's activities. Dr. Douglas Lawson, a temporary staff member from Waterloo University (Canada), working in mathematics with Dr. Kretchmar and Dr. Bergner, completed his planned stay during the year. Dr. B. V. Suryanarayana, Mysore, India, has worked in the clinical program as assistant clinician. Dr. Masayuki Takasugi, Fukuoka, Japan, a trainee in clinical investigation, has worked with the clinical program, and has done research with the medium level

1027731

whole-body counter. Dr. Jaime Ahumada, Bogota, Colombia, supported in part by an ICETEX Fellowship (Colombian Fellowship Organization), has also been a part of the clinical program and his work has included research with ^{68}Ga. Dr. Noboru Arimizu, Chiba, Japan, has been on a Picker Fellowship working with external counting techniques. Dr. Randall Wood, an AEC postdoctoral fellow, has worked in lipid investigations. Two men doing thesis work for their doctorates are Donald Carlson, immunology, and Raymond Pfleger, the lipid program.

In early November a symposium on radiopharmaceuticals was held in Oak Ridge under sponsorship of the Medical Division. Dr. Henry Wagner, Jr., of Johns Hopkins, joined with Dr. Kniseley and me in planning the program and in editing the proceedings which are soon to be published. Speakers included 37 from the United States and five from overseas. Participants who came to Oak Ridge numbered 151; this did not include members of our own staff and other area scientists. Special financial support for the symposium came from the Division of Technical Information and the Division of Nuclear Education and Training, U. S. Atomic Energy Commission.

The Medical Division's continuing interest in computer technology as a biomedical research tool was advanced in 1965 with the establishment of an Institute data processing center headed by A. S. Gloster, Jr. The center is providing professional programming services to key medical research projects and performs routine card processing. Necessary computer services are currently being obtained from the Oak Ridge National Laboratory mathematics panel and the K-25 computer center.

As 1965 draws to a close the Medical Division feels an acute need for additional laboratory space and various efforts are being made to fill this need. The National Aeronautics and Space Administration program in radiation effects has moved forward well and work is beginning on a new, low-dose-rate human radiation facility to be supported jointly by the Atomic Energy Commission and the National Aeronautics and Space Administration.

I would like to call attention to the acknowledgements on Page 166. This does not record all those who have helped in substantial ways to make this program possible.

The reports that follow represent a major portion of the research results of the year, but do not cover all aspects of the ongoing long-range program or all of the collaborative work done. Most of these

reports represent briefer versions of articles recently published, in press, or planned for publication.

The staff is again indebted to Betty Anderson, technical editor; Jeanne Simmons, technical illustrator; and Rush King, photographer, in preparing this report.

GOULD A. ANDREWS
Chairman

1027732

Mechanisms of Radiation Injury

The work of the Division on mechanisms of radiation injury places most emphasis on acute effects. Hematologic, biochemical, immunologic, and cytogenetic changes are investigated with the view to (1) better management of unwanted radiation injury and (2) improved therapeutic use of radiation. Although much of the work is done on experimental animals, there is a constant effort to correlate the results with experience in the human being.

Autopsy Findings after Therapeutic Total-body Irradiation

B. Nelson

Subsequent to the preparation of the Research Report for 1964, 13 patients have died after treatment with total-body irradiation (TBI). Authorization for autopsy was refused only once. The 12 autopsies were thorough, with particular attention to the primary disease and to radiosensitive tissues, especially the hemopoietic and lymphatic systems. *Table 1* outlines the autopsy experience. The nine cases in the 100 R category are arranged by the length of survival after irradiation; three of these had previous total-body irradiation.

All these patients survived past the period of acute irradiation injury with the exception of the boy who died 24 days after 300 R (Case 12). In this instance, severe pancytopenia was present before TBI, probably as a manifestation of the disease rather than previous chemotherapy: marrow aspirates at the time of TBI were very hypercellular and blastic; autopsy showed atrophic fatty marrow predominating, with some foci of hypercellularity. Megakaryocytes, granulocytes, and red cell precursors were relatively more numerous than before TBI, but most cells were still leukemic blasts.

The man who lived 2½ months after 200 R was also pancytopenic before TBI. His death was probably due to pneumonia and uremia from renal complications of multiple myeloma.

The elderly man with chronic lymphocytic leukemia (Case 2), surviving 2½ months after 100 R, had a dramatic reduction in circulating lymphocytes, but severe lymphocytosis had recurred without complete remission. Indirectly, TBI may have contributed to his death

from overwhelming strongyloidiasis and bacteremia. *(See pp. 7–9).*

In all other cases, survival was longer and deleterious residual effects of TBI were not detected.

In summary it can be said that nearly all these patients died from infection or hemorrhage related to the persistence or recurrence of the disease for which they were treated. One exception (Case 9) is of special interest in several respects. Autopsy was of value in showing that death was caused neither by lymphosarcoma nor therapy but by an unsuspected gastric carcinoma. The relatively high incidence of co-existence of malignant lymphoma and other malignancies is well known; two such cases were found in earlier patients. The interval between therapy and death was too short to consider irradiation as a cause of any of these coexisting neoplasms.

The transition of a malignant lymphoma of a small-cell type to a more ominous reticulum-cell sarcoma is considered a feature of the neoplasm, although therapy may have played a role in suppressing the lymphocytic component (Case 10; also discussed elsewhere, pp. 83–84). It should also be mentioned that these patients were treated with agents such as adrenocorticosteroids and conventional chemotherapeutic drugs before therapy, after therapy, or both. Most, having survived the period of danger and benefit from irradiation, were being treated with other means at the time of death. Accordingly, we must be cautious in attributing autopsy findings to TBI.

Our continuing experience serves to emphasize that total-body radiation in sublethal doses does not produce distinctive persistent morphologic changes easily recognizable by even the most careful standard histologic techniques applied to the individual patient. (Studies of the lens of the eye were not done in these patients.) The presence of underlying hematologic diseases in most of our patients and the therapy for these diseases further complicate the evaluation, especially of the hematopoietic and lymphatic tissues.

Although one gains some measure of reassurance about the ill effects of irradiation from these studies, it must be emphasized that significant chromosomal changes are not detected by routine techniques and that a large series of patients uncomplicated by preexisting disease would be needed to clearly evaluate subtle contributions to aging and carcinogenesis; these latter effects have no histologic earmarks proving their relation to radiation and only a controlled study of their incidence can show such a relation.

1027733

TABLE I

	Patient	(age)	Diagnosis	TBI (R)	Interval from treatment to death
1.	Man	49	Lymphosarcoma	50	3 years
2.	Man	71	Chronic lymphocytic leukemia	100	2½ months
3.	Man	46	Lymphosarcoma	100	4 months
4.	Man	76	Chronic lymphocytic leukemia	100	4 months
5.	Woman	51	Subacute granulocytic leukemia	100	9 months
6.	Boy	7	Acute lymphocytic leukemia	100	10 months
7.	Woman	66	Reticulum cell sarcoma	100	1½ years
8.	Woman	41	Lymphosarcoma	100	2½ years
9.	Woman	71	Lymphosarcoma (died from gastric adenocarcinoma)	100	3 years
10.	Woman	54	Lymphosarcoma	100	3 years
11.	Man	43	Multiple myeloma	200	2½ months
12.	Boy	8	Acute leukemia	300	24 days

Strongyloidiasis and Malignant Lymphoma*

W. A. Rogers, Jr.† and B. Nelson

In the application of radiation or chemotherapy to treatment of malignant diseases, the evaluation of results is often complicated by intercurrent infections. The following data were collected from the series of patients treated in the Division's radiation program. Recently, two men treated for malignant lymphoma died unexpectedly from bacterial infections and at autopsy were found to have severe enterocolitis caused by *Strongyloides stercoralis*, with migration of the larvae to the lungs and other tissues. This parasite differs from other nematodes in having the capacity to reproduce indefinitely within a susceptible host, sometimes resulting in the death of a debilitated person from invasion

*In press, JAMA.

†Present address: West Virginia University Hospital, Morgantown, W. Va. Work done while an Abbott Student Fellow, supported by Abbott Laboratories.

by hordes of larvae. Strongyloidiasis is endemic in Southern Appalachia, but usually symptoms are mild or absent.

"Opportunistic infections" with organisms of low pathogenicity are often reported with malignant lymphoma, although nematodes have not previously been implicated. These two cases suggest that, in addition to the recognized factors of cachexia and constipation, impairment of immunologic responses may predispose to overwhelming strongyloidiasis. This speculation is supported by the report of increasing resistance to repeated infections in healthy animals. Depression of cellular

Fig. 1. Remnants of larvae of Strongyloides stercoralis (arrows) in multinucleated giant cells in abdominal lymph node from Case 2 (hematoxylin and eosin). Note the typical inflammatory reaction, despite the treatment of chronic lymphocytic leukemia with 100 R total-body irradiation and adrenocorticosteroids.

1027734

inflammatory reactions may not be involved in this predisposition; at least in these cases characteristic inflammatory reactions were seen (*Fig. 1*).

Whatever the reason for decreased host resistance, we can add *Strongyloides stercoralis* to the long list of organisms that cause relatively little harm to healthy persons but can cause serious disease in patients treated for malignant lymphoma. The term "opportunistic infection" has been used especially with certain fungi, but may include disease caused by many bacteria and a few viruses. It has recently been applied to another organism occasionally seen in Division autopsies, *Pneumocystis carinii*, presumably a protozoan. If these organisms can be called "opportunistic," surely the term can be applied to a parasitic worm aggressively invading a weakened host.

Scope and Orientation of the Lipid Project

F. Snyder

The Lipid Program at the Institute during 1965 has been concerned with three primary problems:

1. The biochemical mechanism of fat-cell formation in irradiated bone marrow.
2. The intermediary metabolism of the alkoxy glyceryl ethers.
3. The interrelations of lipid metabolism in tumors and host tissues.

Data from our laboratory indicate that the diglyceride intermediary pathway *(Fig. 2 and Fig. 3-A)* common to phospholipid and triglyceride biosynthesis in liver is also present in bone marrow. Data obtained have shown that the formation of increased numbers of fat cells occurs only in bone-marrow areas exposed directly to the irradiation field[1] and that the new fat cells originate from a fraction of a marrow-cell suspension that had been separated from floating mature fat cells by centrifugation.[2] Biochemical evidence has also demonstrated that ionizing irradiation can severely inhibit fatty acid oxidation,[3] phospholipid biosynthesis, and triglyceride turnover.[2] Our *in vitro* experiments on fatty acid incorporation have shown that the overall rate of conversion of radioactive fatty acids into triglyceride via

the diglyceride pathway is not elevated (*Fig. 3-B*) in an isolated population of irradiated marrow cells, but instead is about the same as that found in controls (at 1 and 2 days after 800 R). Therefore, under these conditions, one should expect an accumulation of diglyceride when phospholipid biosynthesis is blocked in this system *(Fig. 3-C)*. However, labeled diglycerides do not increase appreciably: this could occur if a critical level of diglyceride were capable of activating the triglyceride forming enzymes of *potential* fat cells thereby using the larger pool of diglyceride available *(Fig. 3-D)*.

Our interest in the alkoxy glyceryl ethers stems from the bone marrow project. The glyceryl ethers are found in bone marrow, and they have been reported to have hemopoietic and radioprotective actions. We are investigating their presence (including isomeric forms) in tissues and the metabolism of the ether bond by liver, spleen, and marrow. The biosynthesis of glyceryl ether phosphatides and the cleavage of the alkoxy ether bond by liver is being investigated *in vivo* and *in vitro*. Related methodology in this area has been the development of a rapid gas-liquid chromatography technique for the quantitative analysis of isomeric glyceryl ethers as their trifluoroacetate derivatives.

The tumor project has been concerned with elucidating the chemical structure of a relatively nonpolar lipid component that we have routinely found in all tumor extracts. Studies have also been made by comparing the metabolic uptake of labeled lipids of normal host cells and tumor cells to biosynthetic mechanisms operating in isolated cell

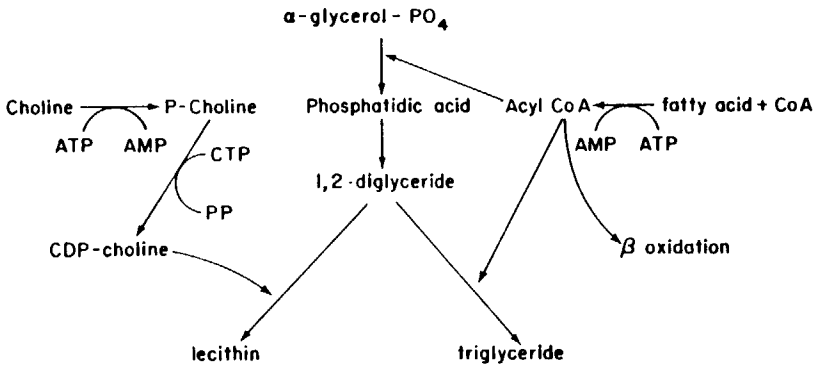

Fig. 2. Metabolic pathway of biosynthesis of phospholipids and triglycerides having a diglyceride as the common intermediate. CoA = coenzyme A; ATP = adenosine triphosphate; AMP = adenosine monophosphate; PP = pyrophosphate; CTP = cytidine triphosphate; CDP = cytidine diphosphate.

1027135

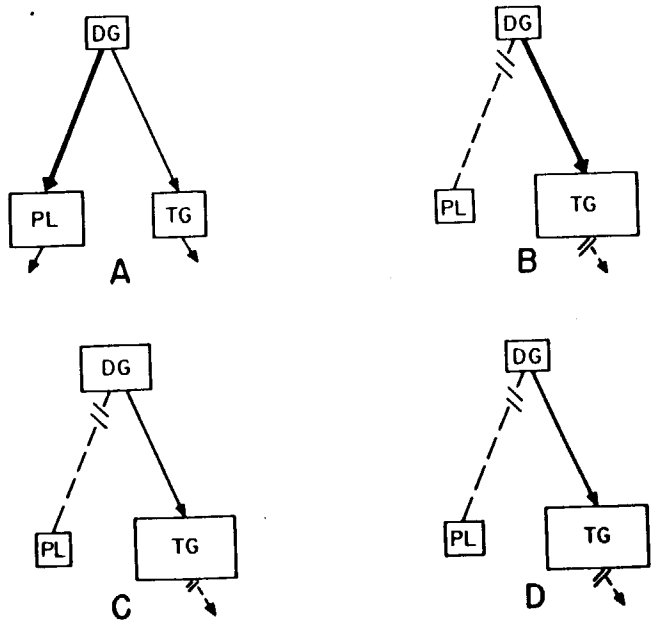

Fig. 3. Theoretical biochemical model, developed to show how irradiation of marrow may cause increased formation of fat cells. The symbols refer to the following lipids: diglycerides (DG), triglycerides (TG), and phospholipids (PL). Solid arrows have thickness proportional to rate of ^{14}C-fatty acid incorporation, broken lines represent inhibition or block caused by radiation, and sizes of the rectangles are proportional to amounts present (pool sizes). A represents normal marrow. B and C represent possible explanations for radiation effect which must be rejected as improbable. In B there is an increased rate of conversion of diglycerides to triglycerides. This concept is incompatible with in vitro results that show the per cent of radioactivity from labeled fatty acids incorporated into triglycerides is about normal. In C the pool of diglyceride greatly increases because of the blockage of synthesis of phospholipids. However, it is known that no important increase in diglyceride occurs. In D is seen the situation which occurs in vitro: i.e., the per cent of radioactivity incorporated into triglyceride is the same as normal. Since there is in fact increased triglyceride in irradiated marrow, it is suggested that there is a diluting effect on the radioactive label entering the triglycerides. Although the diglyceride level does not increase, C, such a diluting effect could also be brought about by the combination of phospholipid breakdown and activation of potential fat cells capable of using up resulting diglycerides.

systems. A portion of this latter problem has dealt with the formation of lipid granules in older Ehrlich ascites cells grown in tissue culture.

The subsequent abstracts through page 25 report some of the year's research activities. In addition, we collaborated with staff members of the School of Pharmacy and Department of Biochemistry at the University of North Carolina on a project on the chemical synthesis of ^{11}C and ^{3}H glyceryl ethers.

REFERENCES

1. Snyder, F. and Wright, R. Effect of localized irradiation on the metabolism of bone marrow lipids. Radiat Res 25, 417–422, 1965.
2. Snyder, F. Triglyceride biosynthesis in irradiated bone marrow. Radiat Res, in press, 1965.
3. Snyder, F. Fatty acid oxidation in irradiated bone marrow cells. Nature 206, 733, 1965.

In Vitro Incorporation of Palmitic-1-^{14}C Acid Into Irradiated Bone-marrow Cells*

R. Pflegert, F. Snyder, and C. Piantadosi‡

Earlier work in this laboratory demonstrated that fatty acid esterification into triglycerides is increased in irradiated bone marrow.[1] Within one week after total-body irradiation (800 R), the triglycerides of femoral marrow increase from 5% to as high as 50% of the wet weight.[2] This research led to the *in vitro* experiments reported in this paper for marrow cells incubated with ^{14}C-labeled palmitic acid.

K-Palmitate-1-^{14}C (specific activity = 0.14 μc/3.6 mg/flask) was incubated at 37°C from 0.5–5h in 1 ml of Tyrode's solution containing approximately 150 mg of normal or irradiated (800 R) bone marrow. The femoral bone marrow was obtained from female rats (165–200 g) killed 1, 2, 3, 4, and 5 days after 800 R total-body irradiation. After incubation, lipid extracts were prepared. Thin-layer chromatograms and zonal scans of these extracts were used to determine the degree and type of incorporation for the labeled fatty acid.

Incorporation of palmitic acid into triglycerides and phospholipids

*Material presented at the 1965 Annual Meeting of the Tennessee Academy of Science.
†An Oak Ridge Graduate Fellow from the University of North Carolina.
‡At the University of North Carolina, school of pharmacy and department of biochemistry. chemistry.

1027136

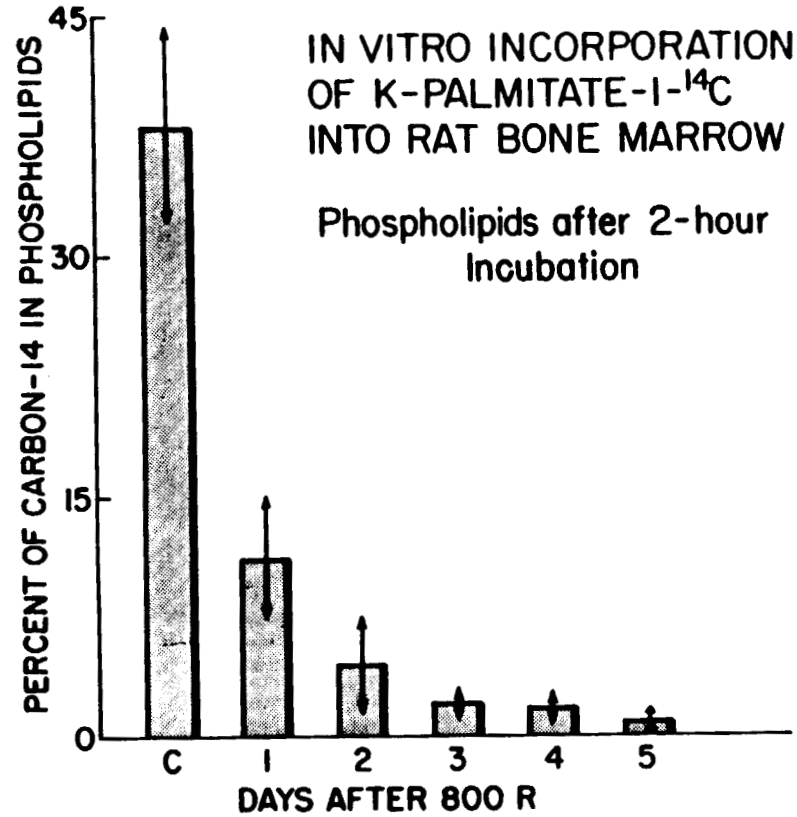

Fig. 4. The incorporation of palmitic-1-^{14}C acid into phospholipids of irradiated bone marrow, in vitro.

of femoral marrows reached a maximum after 2 hr of incubation. As seen in *Fig. 4*, at intervals of one day or more after total-body irradiation there was a significant inhibition of the esterification of fatty acids into phospholipids (primarily lecithin). Triglyceride biosynthesis continued in the irradiated marrow at the same rate as in the control for the first two days after 800 R, after which it too was inhibited by ionizing irradiation *(Fig. 5)*. The data suggest that triglyceride-synthesizing enzymes are more resistant to ionizing irradiation than the enzymes responsible for phosphatide synthesis. The block in phospholipid biosynthesis caused by irradiation has helped explain increased fatty acid esterification into triglycerides of irradiated marrow,

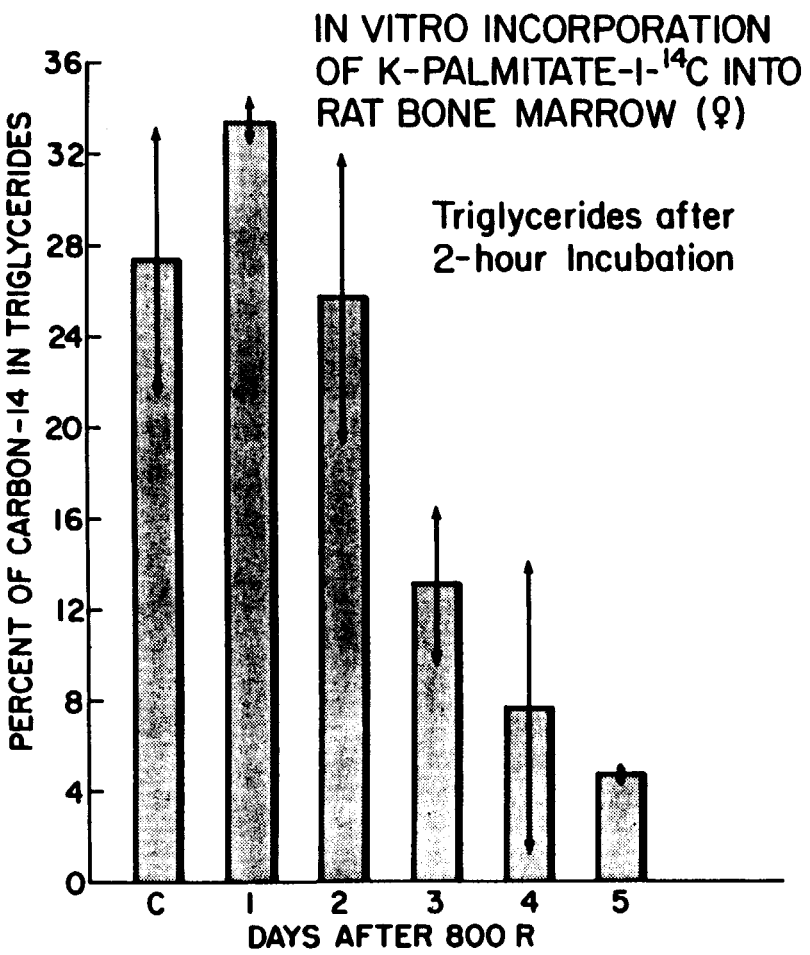

Fig. 5. The incorporation of palmitic-1-^{14}C acid into triglycerides of irradiated bone marrow, in vitro.

on the basis of a possible control mechanism of the diglyceride pathway that is common to both triglyceride and phospholipid in biosynthesis.

REFERENCES

1. Snyder, F. and Wright, R. Effect of localized irradiation on the metabolism of bone-marrow lipids. Radiat Res 25, 417–422, 1965.
2. Snyder, F. and Cress, E. A. Bone-marrow lipids in rats exposed to total-body irradiation. Radiat Res 19, 129–141, 1963.

1027137

Phospholipid Biosynthesis in Irradiated Tissues*

J. Lim,† F. Snyder, and C. Piantadosi‡

We investigated the effect of gamma irradiation on phospholipid biosynthesis in liver, serum, and marrow. The incorporation rates of palmitic-1-^{14}C and oleic-1-^{14}C acids, and $^{32}PO_4$ into the various phosphatides were studied at 2, 4, 6, and 12 hr.

Figure 6 shows three typical chromatoplates of phospholipid sepa-

Fig. 6. Plate A: left lane = PL standards; middle and right lanes = total liver lipids of a control animal 2 hr after oral 1-^{14}C palmitic acid. Plate B: middle lane = PL standards; left and right lanes = serum lipids of two different control animals 12 hr after 1-^{14}C palmitic acid. Plate C: middle lane = PL standards; left and right lanes = marrow lipids of two different irradiated animals 2 hr after oral 1-^{14}C oleic acid. Zones 1, lysolecithin; 2, sphingomyelin; 3, lecithin; 4, phosphatidyl serine; 5, cephalin; and 6, neutral lipids, and possibly polyglycerol phosphatides, phosphatidic acid, and cardiolipin.

*This investigation was supported in part by Public Health Service grants GM-123562-01 and GM-123562-02 from the National Institute of General Medical Sciences to the University of North Carolina.

†Guest scientist from the University of North Carolina at the Medical Division, June-October, 1965.

‡At the University of North Carolina, School of Pharmacy, and department of biochemistry.

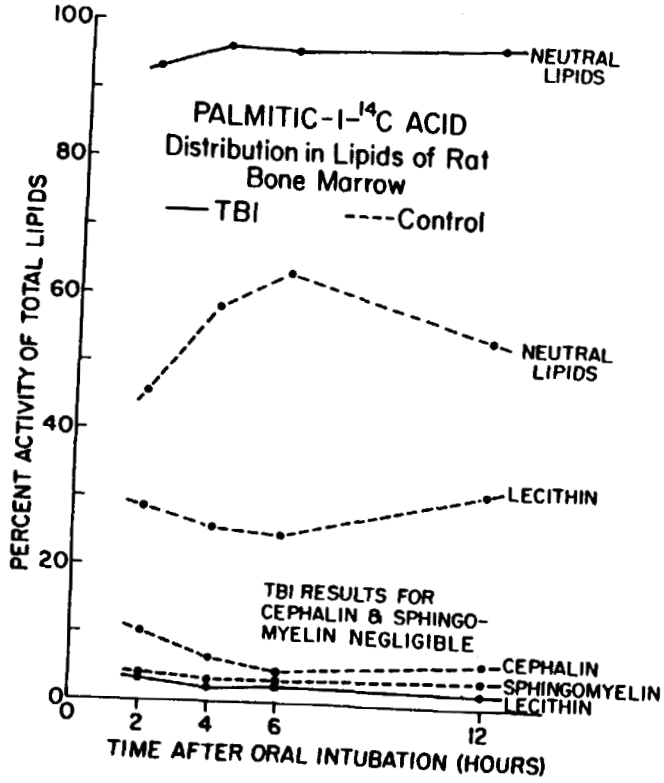

Fig. 7. Incorporation of palmitic-1-^{14}C acid (in vivo) into phospholipids of irradiated bone marrow.

rations prepared for densitometric analysis by the sulfuric acid-charring procedure. Zones 1 to 6 of similar chromatograms, but visualized by iodine vapor, were scraped off and collected separately for quantitative radioactivity analysis. The liver lipids (Plate A) show comparatively significant proportions of cephalin in contrast to those of the serum (Plate B) and the marrow lipids of irradiated animals (Plate C).

Experiments measuring the incorporation of 1-^{14}C palmitic acid into various lipid classes of blood serum, liver, and marrow of normal and irradiated animals revealed that the distribution of radioactivity was greatest in the neutral lipid fraction of irradiated bone marrow

1027738

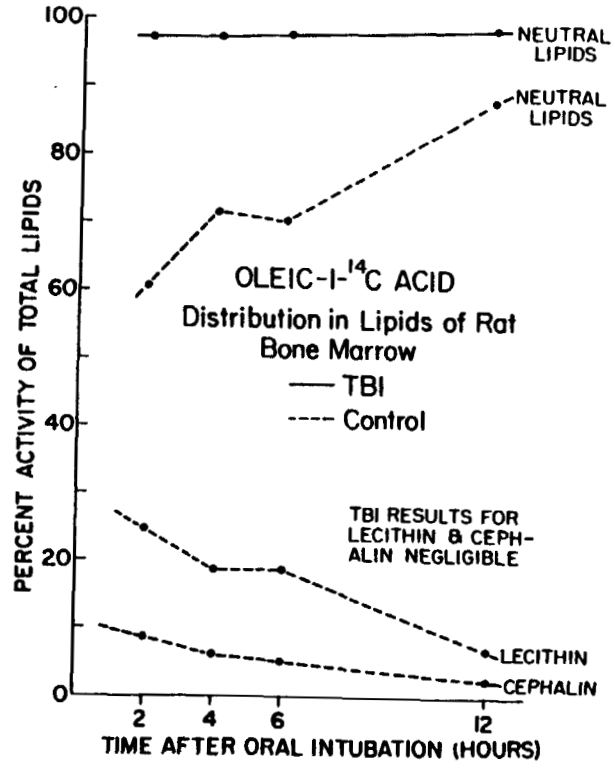

Fig. 8. Incorporation of oleic-1-^{14}C acid (in vivo) into phospholipids of irradiated bone marrow.

when triglyceride formation was extremely active. Lecithin followed by cephalin were the major phospholipids incorporating radioactivity in all tissues. Total-body irradiation did not appear to exert any appreciable effect on the specific activities of these phospholipids in all tissues studied. Although radioactivity distribution studies showed little change in liver and serum, both palmitic-1-^{14}C (*Fig. 7*) and oleic-1-^{14}C (*Fig. 8*) acid incorporation into bone-marrow phospholipids was decreased significantly by the effects of irradiation. The general plateauing, or slight decrease, in specific activities occurs with the phospholipids of all tissues in both control and irradiated at around 4 to 6 hr after the oral administration of 1-^{14}C-palmitic acid.

Turnover of Fatty Acids in the Triglycerides of Irradiated Bone Marrow*

J. N. Bollinger

Snyder and Wright[1] have shown that irradiation of a single femur of the rat produces a localized increase in fatty acid esterification by triggering an increased biosynthesis of marrow triglycerides. A previous report[2] has shown that dietary fat significantly changes the fatty acid composition of the bone-marrow triglycerides of the irradiated rat by readily supplying fatty acids to the sites of increased synthesis.

Recent studies have shown that the increased synthesis of triglycerides of the irradiated marrow was not followed by an essentially inactive "fatty-marrow" state. Within one week after feeding a 20% safflower oil diet the percentage of linoleic acid in the marrow increased to a level of 53%. In contrast to the results of continued safflower-oil feeding (linoleic acid remained at this elevated level for four weeks), the percentage of linoleic acid dropped to 37% one week after switching to a coconut oil diet. Confirming the turnover of the triglycerides at a time when the total marrow-lipid level remained above normal was the finding of a 6.5 fold increase in short chain acids two weeks after being switched to the coconut oil diet *(Fig. 9)*.

*In press, Radiat Res.

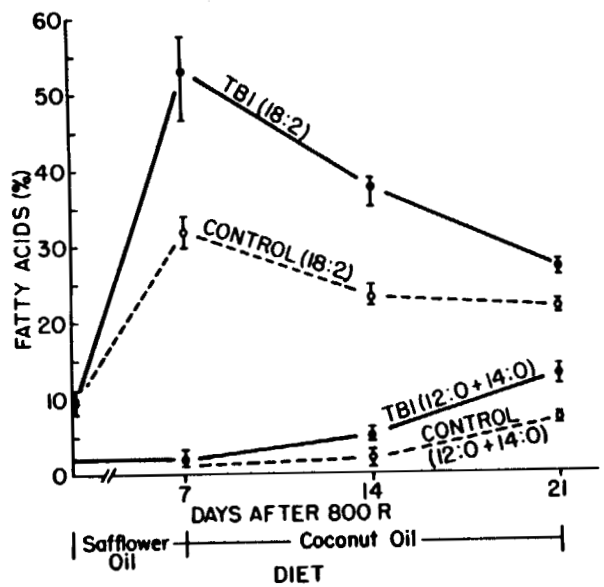

Fig. 9. Turnover of linoleic acid in rats fed a 20% safflower oil diet for one week after irradiation and then switched to a 20% coconut oil diet for two more weeks. The TBI rats received 800 R total-body irradiation. The closed (TBI) and open (control) circles represent the mean GLC values and the vertical lines represent the range of three groups of four pooled femurs each.

1027139

REFERENCES

1. Snyder, F. and Wright, R. Effect of localized irradiation on the metabolism of bone-marrow lipids. Radiat Res 25, 417–422, 1965.
2. Bollinger, J. N. Effect of dietary fat and total-body irradiation on the fatty acid composition of bone-marrow lipids. USAEC Report ORINS-49, 31–33, 1964.

The Deposition and Metabolism of Batyl Alcohol-1-^{14}C in the Rat*

F. Snyder, C. Piantadosi† and E. Oswald†

The distribution, metabolism, and excretion of batyl alcohol occurring 6 hr after oral administration of the radioactive glyceryl ether were used to determine the degree and type of metabolic changes in the lipid fraction of various tissues. Under the conditions of this experiment, most of the ingested label was found in the intestines but 11% was found in the liver. Other tissues contained less than 0.3% of the administered dose.

Thin-layer chromatography scans of the lipids found in intestinal contents and cells showed that significant cleavage of the ether bond occurred in this location: labeled di- and mono-ethers, free fatty acids, and fatty alcohols were found in addition to the original glyceryl ether.

*Presented at the American Oil Chemists' Society Fall Meeting, October 10–13, 1965, Cincinnati, Ohio. This investigation was supported in part by Public Health Service grants GM-123562-01 and GM-123562-02 from the National Institute of General Medical Sciences to the University of North Carolina.

†At the University of North Carolina, school of pharmacy, and department of biochemistry.

The lipids isolated from the intestinal tract only, also contained labeled triglycerides and phospholipids. Approximately 30 and 24% of the lipid label found in the contents and tract, respectively, was as the unchanged batyl-1-^{14}C alcohol.

The major portion of the radioactive plasma lipids contained the ^{14}C label as glyceryl ether diesters (53%) and phospholipids (25%). In the liver (*Fig. 10*), 70% of the ^{14}C was in the phospholipids (58% in the lecithin and 26% in the cephalin fractions).

The authors are indebted to Edgar Cress and Nelson Stephens for expert technical assistance in this study.

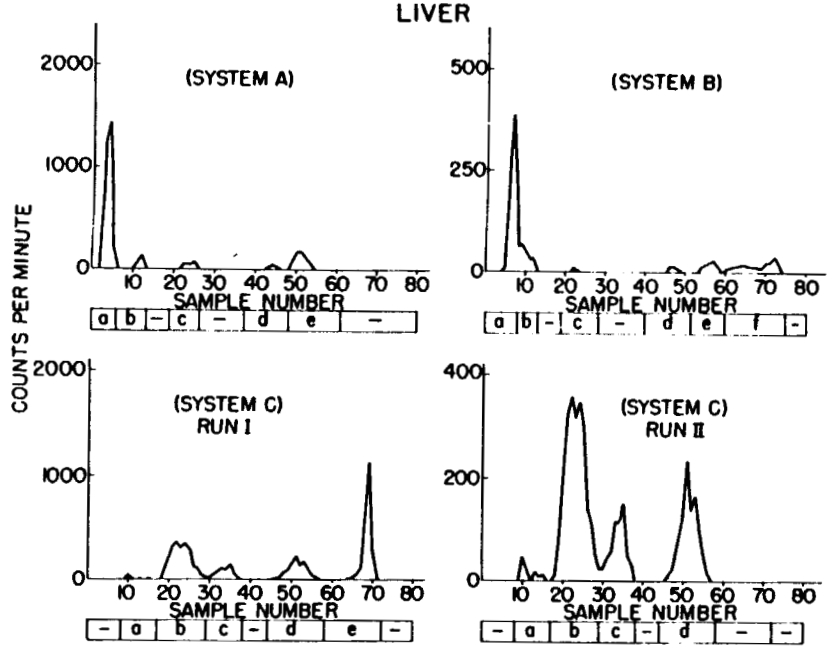

Fig. 10. Zonal scans of thin-layer chromatograms of total lipids extracted from liver. Solvent System A: a. phospholipids, b. glyceryl ether monoesters and diglycerides, c. free fatty acids, d. triglycerides, e. glyceryl ether diesters. Solvent System B: a and b. phospholipids, c, d, e, and f. Other neutral lipids represented in Solvent System A. Solvent System C: Run I: b. sphingomyelin; c. lecithin, d. cephalin, e. neutral lipids. Solvent System C: Run II; containing only the labeled phospholipids: b. sphingomyelin, c. lecithin, d. cephalin.

1027140

Lipids Present in the Walker-256 Tumor

J. N. Bollinger

Thin-layer chromatography of Walker-256 tumor lipids has revealed the presence of an unusually high (1 to 3%) quantity of a lipid component not normally found in mammalian tissue *(Fig. 11)*. Lipids isolated from plasma, liver, bone marrow, heart, kidney, spleen, and adipose tissue taken from rats bearing the tumor implant did not contain this component in readily detectable amounts. Data show that the Fisher rat tumor, spontaneous tumors occurring after total-body irradiation of rats, and Ehrlich ascites tumor cells from mice also contain relatively high levels of this unknown lipid component.

Several milligrams of the unknown material were isolated from the lipids of Walker-256 tumor tissue by preparative thin-layer chro-

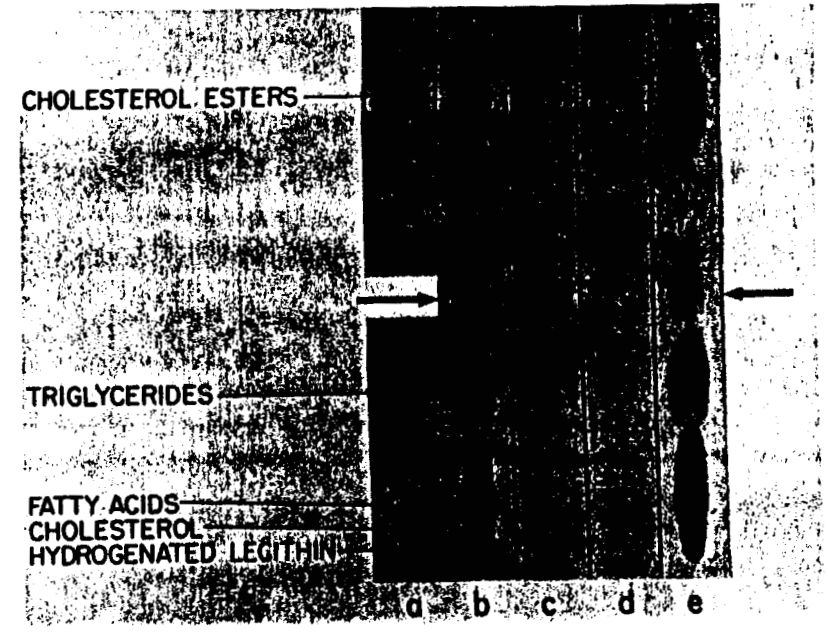

Fig. 11. Thin-layer chromatographic plate. (a) Standard lipid mixture; (b) total tumor lipids; (c) batyl dipalmitate; (d) methyl oleate; (e) tumor neutral lipids. Arrows indicate the unknown tumor lipid component.

matography. Infrared spectra suggest that the component is an ester of long-chain polyunsaturated acids *(Fig. 12)*. Thin-layer chromatography and gas-liquid chromatography have indicated that the unknown is not a methyl ester, triglyceride, or a glyceryl ether diester although it has a polarity similar to these lipids. Saponification and methylation of the saponifiable fraction confirmed that fatty acids (C^{12}-C^{22}) are part of the molecule *(Fig. 13)*. Attempts to identify the molecule to which the fatty acids are esterified have been unsuccessful.

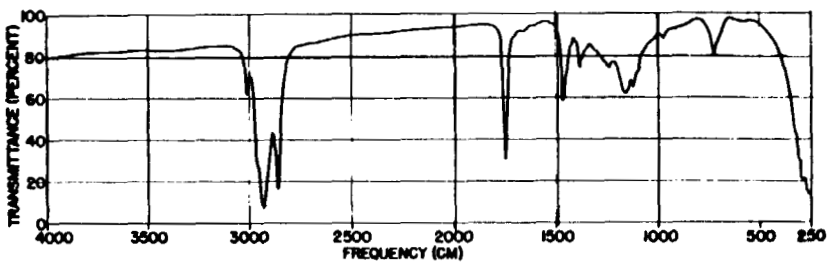

Fig. 12. Infrared spectra of unknown tumor lipid.

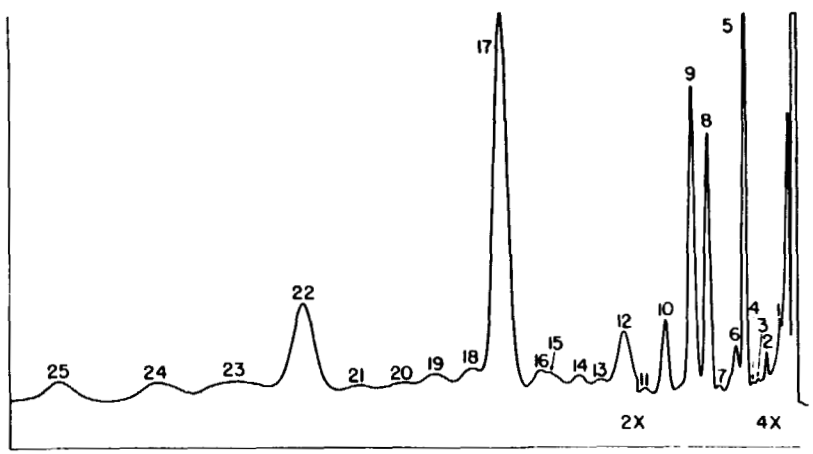

Fig. 13. Gas-liquid chromatography of fatty acid methyl esters from the unknown tumor lipid. (1) laurate; (2) myristate; (5) palmitate; (8) stearate; (9) oleate; (10) linoleate; (17) arachidonate. Other components have not been conclusively identified.

1027141

Thin-layer Chromatographic Analysis of Lipids Isolated From Ehrlich Ascites Carcinoma Cells*

S. Cheng,† *C. Piantadosi*,‡ *and F. Snyder*§

Earlier work by DiPaolo and co-workers' demonstrated that Ehrlich ascites cells possess refractile lipoid granules as determined by phase contrast microscopy. These workers noted that the number of granules in each cell increased as the ascites tumor cells grew in the

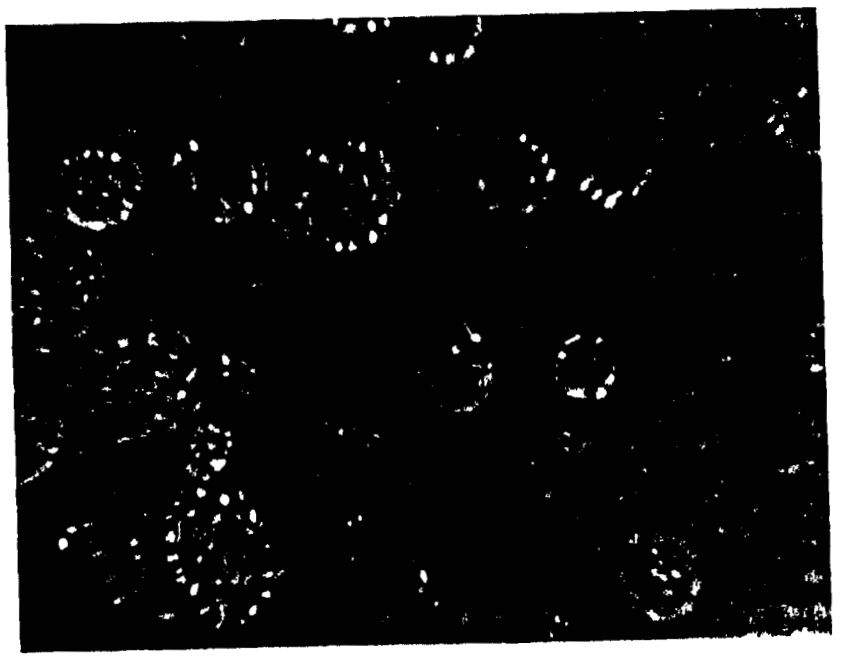

Fig. 14. Ehrlich ascites carcinoma cells after incubating for four days in medium 199 containing 10% calf serum. The lipid granules show up as light circles within the cells and are stainable with oil red O.

*Material, in part, presented at the American Oil Chemists' Society Spring Meeting, Los Angeles, 1966.

†Research Participant from the University of North Carolina, School of Pharmacy, Chapel Hill, N. C.
‡From the University of North Carolina, School of Pharmacy, Chapel Hill, N. C.
§Medical Division, Oak Ridge Institute of Nuclear Studies, Oak Ridge, Tenn.

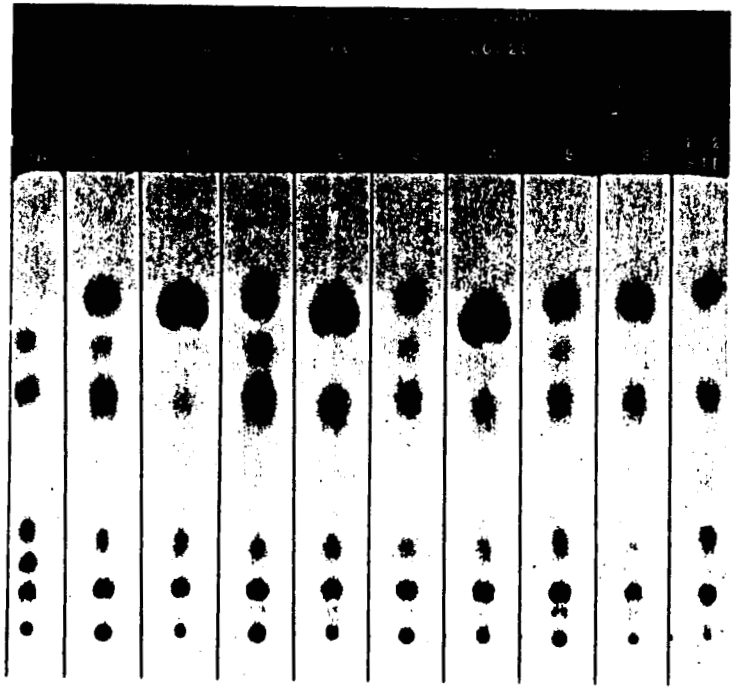

Fig. 15. Thin-layer chromatogram of lipids extracted from Ehrlich ascites carcinoma cells and media. Lipids from carcinoma cells are shown in columns 109, 111, 113, 115. Lipids from the extracellular fluid that contained the tumor cells are shown in columns 110, 112, 114, and 116.

peritoneum of the mouse. Our data confirm their observation and further show that Ehrlich ascites cells grown in tissue culture also develop increased numbers of lipoid granules as the incubation period extends *(Fig. 14)*. DiPaolo *et al.*[1] used only silicic acid column chromatography to analyze lipid classes in the cells. We thought it would be worthwhile to reinvestigate the lipid composition of the Ehrlich ascites cells with the use of thin-layer chromatography and to relate our findings to the occurrence of intracellular lipid granules.

The lipid composition of ascites cells grown *in vivo* and *in vitro* was found to be similar. A typical example of the major lipid classes present in the ascites cells and the extracellular fluid containing the cells is shown in *Fig. 15*. The triglycerides and sterol esters are present in approximately equal quantities within the cells; phospholipids, cholesterol, and free fatty acids were also found in the cells, but to a lesser extent. The most significant observation was the occurrence of an unknown spot on thin-layer chromatography plates directly above the triglycerides in all lipid extracts from the Ehrlich ascites cells. The unidentified spot was not present in the extracts of the extracellular fluid. The R_f of this unknown class of lipid is identical to an unidentified compound also found in other tumors [Walker-256 (rat), Fisher (rat), spontaneous (rat), and human]. The polarity of this compound is similar to that of a glyceryl ether diester, but no definitive proof of structure is available at this time.

These findings have led to an investigation on the incorporation of acetate-1-^{14}C, palmitic-1-^{14}C acid, linoleic-1-^{14}C acid, and batyl-1-^{14}C alcohol into the lipids of Ehrlich ascites carcinoma cells *(in vivo* and *in vitro)*. We hope that these experiments will elucidate whether biosynthesis of the unidentified tumor component occurs in the ascites cells.

1027742

REFERENCE

1. DiPaolo, J. A., Heining, A., and Carruthers, C. Isolation and lipid analysis of lipoid granules from Ehrlich ascites tumor cells. Proc Soc Exp Biol Med 113, 68–70, 1963.

Studies Related to the Treatment of Radiation Injury

The objective is to prevent or correct the damage caused by radiation; to a large extent the effort is focused on the infections and hemorrhagic manifestations of total-body irradiation. Since a major method of treatment is the use of hematopoietic grafts, we are greatly concerned with animal studies on the prevention, mechanisms, and treatment of the complications of "secondary" or homologous disease. Clinical studies with irradiated patients elucidate mechanisms of marrow depression, and some blood diseases characterized by severe bone marrow depression are also of interest because they simulate the irradiated state. Immunologic studies in patients have been limited but will probably assume greater importance in the future.

Human A- and B-like Antigens and Antibodies in Marmoset Serum*

N. Gengozian and C. Merritt†

Previous studies in our laboratories and by others[1-3] have shown that, like most New World monkeys, the marmosets have a B-like antigen on their red cells. More recent studies have revealed the presence of an A-like antigen on their cells also.[1,3] Corollary tests on marmoset saliva have shown the presence of an A-like antigen but the complete absence of any B-like substance.[1,2] In contrast to the cellular antigens, most marmoset sera contain a natural anti-B antibody but no anti-A.[1,2] As an approach to determining the relation of the cellular and body fluid antigens, tests were made for the presence of A- and B-like antigens in marmoset serum. Selected marmosets were also immunized with either human A or B cells to determine the feasibility of inducing an immune response in animals already bearing these antigenic substances on their cells and in their saliva.

*Supported by Public Health Service Research Grant No. R 01 AM09289-01 AIB, from the National Institutes of Health.

†Tulane University School of Medicine, temporarily at the Medical Division to work on this project.

Inhibition tests using human anti-A and anti-B reagents were performed to detect the presence of A- and B-like antigens in marmoset sera. Serum samples were collected from both young (10 weeks old) and adult (age unknown) marmosets for testing. As shown in *Table 2*, the inhibition tests strongly suggest the presence of an A-like antigen in the sera of the young marmosets. Thus, of 15 samples tested, 10 showed a partial, yet significant, inhibition of the human anti-A test system. More striking was the fact that the agglutinates formed in the presence of marmoset serum had a high degree of dissociation on standing at room temperature for 10 min. This is to be compared to the control system where maximum agglutination was retained. The inhibition tests with the adult sera, on the other hand, suggested considerably less activity for the A antigen, although 5 of the 10 sera tested yielded some dissociation of the agglutinates on standing for 10 min. The inhibition tests for the B-like antigen in the sera from young animals were essentially negative, there being only a slight dissociation on standing. The tests with the adult sera showed no activity for the B antigen in either of the two reaction times studied (data not shown).

Immunization with human A and B red cells resulted in antibody formation in both systems with no real difference between the two. Immunization with cell type A resulted in the formation of antibody reactive with B cells also. The reciprocal was true where immunization with B cells also resulted in antibody reactive with A cells. More important, however, was the observation that such immunization procedures did not have any adverse affect on the animals. Thus, there appears to be a definite dissimilarity between the antigens present on the cells and in the tissue fluids of the animals and the antibody formed in response to injection with the human antigens, emphasizing also the nonidentity of the marmoset blood group antigens with that of the human.

The presence of the A-like but not a B-like substance in the marmoset sera agrees with the finding that these animals are secretors of A substance but not B substance in their saliva. It is tentatively suggested that in young animals the A substance may be produced and released into the serum, and as the animal matures, becomes attached to the red cells. Verification of this will be possible when a suitable anti-A reagent capable of reacting with the marmoset cells is obtained.

1027743

TABLE 2

Inhibition Tests for A Antigen in Marmoset Serum*

Animal Age	No. Animals	Reaction Time (min)	Log$_2$ Serum Dilution 0	1	2	3	4	5	6	Saline Control
10 Weeks	10	2	2+	2+	2+	3+	4+	4+	4+	4+
		10	−	−	−	−	1+	3+	4+	4+
	5	2	4±	4±	4±	4+	4+	4+	4+	
		10	−	−	−	±	±	3+	4+	
Adult	5	2	4+	4+	4+	4+	4+ →			
		10	−	±	1+	3+	4+ →			
	5	2	4+	4+ →						
		10	2+	4± →						

*Reaction System: Human anti-A plus A red cells.

REFERENCES

1. Gengozian, N. Human A- and B-like antigens on red cells of marmosets. Proc Soc Exp Biol Med 117, 858–861, 1964.
2. Wiener, A. S., Moor-Jankowski, J., and Gordon E. B. Blood groups of apes and monkeys. V. Studies on the human blood group factors A, B, H, and Le. Amer J Phys Anthrop 22, 175–188, 1964.
3. Merritt, C. B. and Hampton, J. K. Human blood groups in the cotton-top marmoset, *Oedipomidas oedipus*. Fed Proc 24, 631, 1965.

Formation of Isohemagglutinins in the Marmoset, *Tamarinus nigricollis**†

N. Gengozian

The small South American primates of the Hapalidae family, the marmosets, are unique in that twin births are an almost consistent occurrence. This twinning phenomenon is further unusual in that all twins appear to be fraternal and placental vascular anastomoses result in hematopoietic chimerism of the young. Thus, sex chromosome analyses of blood, lymph-node, spleen, and bone-marrow cells have revealed a complete hematopoietic chimerism to exist in these animals. Erythrocyte chimerism, although presumed to exist, has not yet been demonstrated, owing to the unavailability of blood grouping reagents in this species of primates. Tests for naturally occurring isohemagglutinins in these animals have thus far been negative.

The natural blood chimerism would appear to preclude or make exceedingly difficult successful red-cell isoimmunizations since both donor and recipient could conceivably have two (or more) major genetically distinct blood-group antigens. One approach for the isoimmunization procedure would be to use animals in which the degree of chimerism (as determined by sex-chromosome analysis) is low, which would then permit immunization with one major population of red cells. This procedure was followed by isoimmunizing marmosets with red cells placed in complete Freund's adjuvant, giving multiple injections over a period of 10 days. Successful isohemagglutinin formation was obtained in several animals; however, several unexpected developments occurred. As shown in *Table 3* for representative sera, the agglutinins formed were extremely labile when stored at 4°C. Freezing of the sera usually prevented loss of this activity although in some sera even freezing did not completely prevent loss of agglutinin activity. One animal yielded the most interesting immune serum in that it formed (a) labile agglutinins active at room temperature, (b) cold agglutinins stable on storage at 4°C, (c) an incomplete antibody detected only with a Coombs reagent, and (d) a cold autoagglutinin later in the immunization period. Appropriate absorption procedures permitted identification and isolation of the four different antibodies formed. Ultracentrifugation studies in sucrose density gradients permitted separation of the incomplete antibody from the cold agglutinins and the labile room temperature reactive agglutinins as shown in *Fig. 16*. Thus, the incomplete antibody was in the slowly sedimentating fractions, presumably of the 7S variety, and the cold and labile agglutinins in the more rapidly sedimentating fractions, most likely 19S proteins. Treatment of the serum with 2-mercaptoethanol substantiated this interpretation, as the incomplete antibody was not affected by this treatment while the cold and labile room-temperature-reacting agglutinins were destroyed.

The results obtained thus far indicate the existence of major anti-

*In press, Nature (London).

†Supported by Public Health Service Research Grant No. R 01 AM09289-01 AIB, from the National Institutes of Health.

1027744

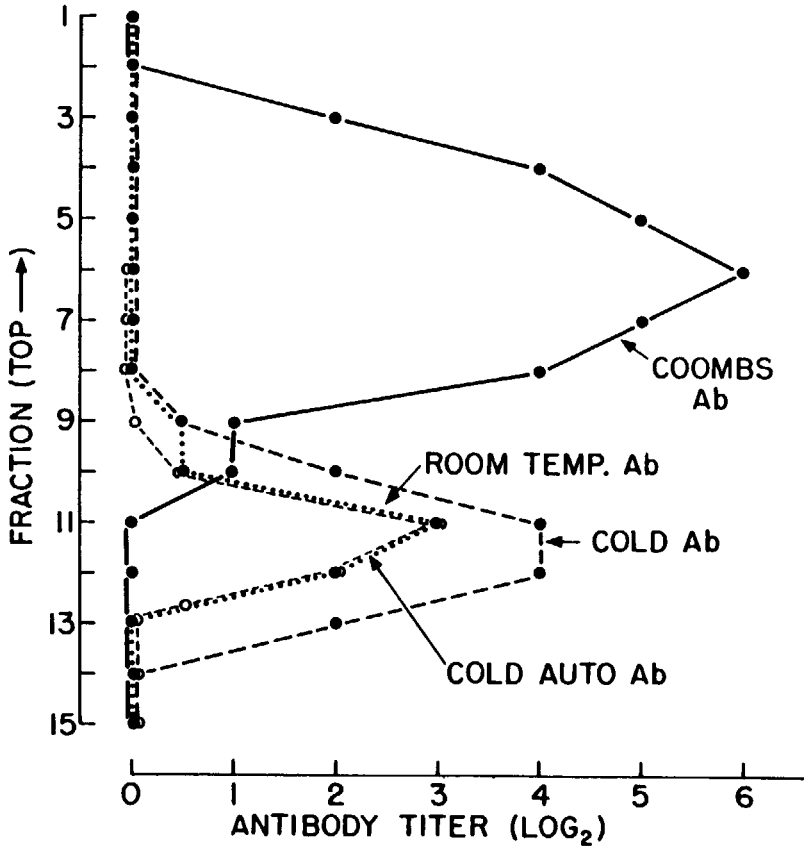

Fig. 16. Gradient fractionation of marmoset immune serum containing four different antibodies.

genic blood groups among the marmosets and show the feasibility of obtaining reagents capable of delineating animals by their red-cell antigens. The determination of red blood cell chimerism will then be possible and should afford an important adjunct to our hematopoietic chimerism studies. More interesting and perhaps more germane to the phenomenon of hematopoietic chimerism in these animals is that isoimmunization among animals that are already blood chimeras will lead to problems in auto-immunization and immunologic tolerance.

1027745

TABLE 3

Lability of Marmoset Isohemagglutinins

Antiserum	Days kept at 4°C	Titer (log_2) 1	2	3	4	5	6	7
"A"	0	4	4	4	3	1	—	
	7	—	—	—				
"B"	0	4	4	3	2	1	—	
	7	—	—	—	—			
"C"	0	4	4	3	2	1	±	—
	1	3	2	2	1	—		
	3	2	1	—	—			
	6	—	—	—				

Erythroblastosis Foetalis in the Primate, *Tamarinus nigricollis**

N. Gengozian, C. C. Lushbaugh, G. L. Humason, R. M. Kniseley

Foetal and neonatal hemolytic anemia, erythroblastosis foetalis, occurs naturally in man and is a major cause of human intrauterine and postpartum death. To our knowledge it has not been reported heretofore as occurring naturally or experimentally in primates other than man. The present report concerns both histopathologic and serologic evidence suggesting isoimmunization during pregnancy in the New World primate, *T. nigricollis*.

Although breeding of this marmoset in our laboratory has been successful, many pregnancies have been terminating in spontaneous abortion, stillbirths, and premature deliveries. These misfortunes were attributed entirely to unknown inadequacies of the laboratory environment until after a recent delivery of a stillborn foetus and its twin that lived for 16 days. Pathologic examination suggested that a disease similar to erythroblastosis foetalis was present in both. Similar histologic evidence of the disease was obtained in twins that died near

*Supported by Public Health Service Research Grant No. R 01 AM09289-01 AIB, from the National Institutes of Health.

term *in utero* after the traumatic death of their mother. Typical histopathologic findings in these cases were erythroblastic cellular foci in lungs, adrenal, placenta, liver, and bone marrow; hepatic parenchymal atrophy and hemosiderosis; thymic medullary lymphorrhexis with thymic cortical preservation; and generalized lymphorrhexis and lymph-node atrophy.

Independent serologic studies in both deliveries served to substantiate the pathologic interpretation of hemolytic disease in these animals. In the first case, after the death of the second twin, the mother's serum was tested for antibody to the paternal cells. As shown in *Table 4*, both saline and Coombs reactive antibodies were found. In the second case, the cells of both foetuses showed a Coombs positive reaction on direct test, one showing a definite 1+ agglutination, the other a 2+ reaction. The maternal serum also yielded a positive Coombs reaction when tested with the paternal cells. This agglutination, however, as shown in *Table 4*, was only weakly positive (1+) over a series of serum dilutions. In view of the blood chimerism known to exist in these animals, this finding may be interpreted as being due to the existence of two genetically different populations of red cells in the father, only one of which is reacting with the maternal antibody. This interpretation may also apply to the reactions observed with the direct Coombs test of the foetal cells noted previously.

Fig. 17. Photomicrographs (X900) of dilated fetal (F) placental capillaries containing hemocytoblasts, erythroblasts, and normoblasts, separated from maternal (M) blood by the typically thin trabeculum of the primate.

The natural occurrence of hemolytic disease of the newborn in this species is of particular interest in view of the nature of twinning among these primates. Thus the marmosets are unique in that (a) fraternal twin births are an almost consistent occurrence, and (b) placental vascular anastomoses result in foetal hematopoietic chimerism. The trabecular, rather than villous, structure of these placentae also affords many areas of intimate contact of maternal and foetal tissues that could potentiate isoimmunization of the mother. This is demonstrated clearly in the placenta obtained from the second case discussed in this report *(Fig. 17)*. This anatomical structure, combined with consistent fraternal twinning and blood chimerism, would seem to improve the chances for this disease to occur naturally. This primate, therefore, offers many experimental approaches to the study of the prevention and cure of this disease. Also, one obvious way to promote a successful breeding program would be the selection of suitable male-female pairings for mating.

TABLE 4

Detection of Maternal Antibodies to Paternal Cells In Two Cases of Hemolytic Disease of the Newborn

		Serum dilution (log_2)								
	Agglutinin type	2	3	4	5	6	7	8	9	10
Case 1	Saline	3+	3+	3+	1+	—	—	—		
	Incomplete*	4+	3+	3+	3+	2+	2+	2±	1+	—
Case 2	Saline	—	—	—						
	Incomplete	1+	1+	1+	1+	1±	±	—	—	—

*Detected by Coombs test with rabbit-anti-marmoset immune serum.

1027746

Diseases of an Imported Primate, *Tamarinus nigricollis**†

B. Nelson, G. E. Cosgrove,‡ and N. Gengozian

The findings have been analyzed in more than 500 necropsies of the New World monkey *Tamarinus nigricollis* kept for experimental use at the Division. Parasites were usually found and some were responsible for much morbidity and mortality. An acanthocephalan, *Prosthenorchis,* was the most common and most serious pathogen. This worm caused lesions in the ileum that were secondarily infected, sometimes with fatal consequences. Other helminths, including a new species of *Spirura,*[1] were also common but seldom incriminated as a cause of disease. The endoparasitic nymph of a linguatulid arthropod was often innocuously encysted in the lungs, liver, and other tissues.

Various bacterial infections, especially peritonitis and pneumonia, seemed less important than *Prosthenorchis* as a primary cause of disease, but were the most common immediate cause of death. Rarely, fungi caused disease. Protozan infections were present, but not shown to be pathogenic. Sarcocystis was seen as innocuous intramuscular bodies; to our knowledge this organism has not previously been reported from New World monkeys.

Neoplasms in monkeys have rarely been reported and the finding of a malignant lymphoma of the small-cell type is of special interest *(Fig. 18).* This was the only neoplasm found in the series.

A disorder of bone, probably osteomalacia from vitamin D deficiency, was until recently a serious problem in tamarins living many months in the colony. The morbidity and mortality from most other causes was much greater for new arrivals in the colony. The necropsy experience reflects the rigors of procurement, and the advantage gained by selection of a better source of supply and by air shipment. Knowledge of the diseases found will be useful in the planning and analysis of experimental studies using these small primates.

Tom Smith assisted in the care of the tamarins and James O. White prepared most of the histologic sections.

*In press, Lab Animal Care.

†The work has been supported in part by U. S. Air Force Contract No. AF41(657)-398 and by the National Institutes of Health Contract No. AM 09289-01 AIB.

‡Biology Division, Oak Ridge National Laboratory.

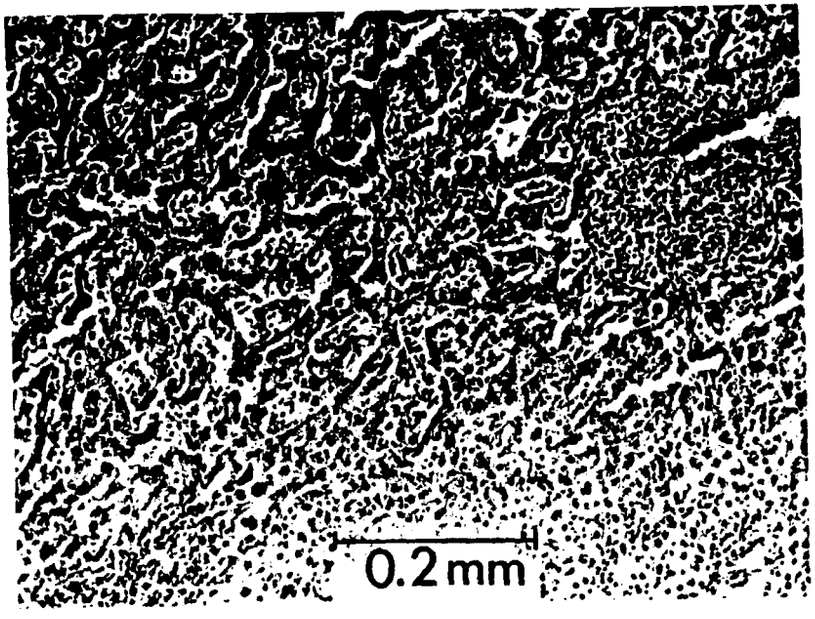

Fig. 18. Liver of Tamarinus nigricollis showing massive infiltration by small round cells. The fact that excessive numbers of lymphocytes were seen in blood vessels suggests that the neoplasm be classified as lymphocytic leukemia rather than lymphosarcoma. To our knowledge this is the first neoplasm reported in a tamarin.

1027747

REFERENCE

1. Cosgrove, G. E., Nelson, Bill M., and Jones, A. W. *Spirura tamarini* Sp. N. (Newatoda: Spiruridae) from an Amazonia primate, *Tamarinus nigricollis* (Spix, 1823). J Parasitol 49 (6), 1010–1013, 1963.

Consideration of Radiation Exposure Rates in Transplantation of Xenogeneic and Allogeneic Bone Marrow in Irradiated Mice

N. Gengozian, D. Carlson, and E. Allen*

Previous studies in this laboratory have shown that the success of foreign-marrow transplantation in irradiated mice was dependent upon the rate of radiation exposure given the animal. Thus, at a dose

*Research visitor at the Medical Division, Predoctoral trainee U.S.P.H.S. in Institute of Radiation Biology, University of Tennessee.

of 900 R, transplantation of xenogeneic (rat) bone marrow was not effected when the radiation was given at 3.75 R/min or 19.8 R/min. The higher exposure rates of 39.7 R/min and 53.4 R/min were sufficient to permit transplantation of the rat marrow, but in only a small proportion of the animals thus treated.

It was also shown that this "take" or "nontake" of the graft was a reflection of the degree of suppression and rate of recovery of the immune mechanism at the different exposure rates. At the lower exposure rates, immunologic recovery of the irradiated animal resulted in only temporary takes and the subsequent formation of antibody directed against the foreign marrow. This effect is not simply a reflection of the widely recognized decreased biologic effectiveness of radiation given at lower dose rates, but suggests a more complex, qualitatively different response. The present study was designed to investigate whether a similar phenomenon was operating at a higher total radiation dose and also its effect on transplantation of allogeneic (homologous) bone marrow.

Mice were given 900 R or 1200 R total-body irradiation at varying exposure rates with either the ^{137}Cs total-body irradiator designed for the treatment of patients or a ^{60}Co therapy unit. Within 2 hr after irradiation, groups of mice from each exposure rate received intravenously nucleated xenogeneic (rat) or allogeneic bone-marrow cells. Of the mice receiving 900 R and allogeneic marrow, it was found that this treatment did not increase the survival above the radiation controls when the animals were exposed to radiation at a rate of 3.75 R/min or 19.8 R/min. Mice receiving radiation at 39.7 R/min and 53.4 R/min, and subsequently treated with allogeneic marrow, showed increased 30-day survival when compared to the irradiation controls. Most interesting, however, was the fact that a donor graft could not be detected in the 30-day survivors of mice in any of the four radiation exposure-rate groups. These data are shown in *Fig. 19.* In those mice receiving 1200 R and allogeneic marrow, increased survival above the radiation controls was obtained for the three different exposure rates studied, 3.75 R/min, 39.7 R/min, and 53.4 R/min. Only in the two higher exposure-rate groups, however, was a permanent transplant of donor marrow effected *(Fig. 20).*

In both studies involving allogeneic marrow, it was not possible to demonstrate the presence of antibody directed against the foreign graft in animals that tested negative for a transplant. Mice receiving 1200 R at varying exposure rates followed by rat bone-marrow treatment showed essentially the same results as in the allogeneic group;

1027148

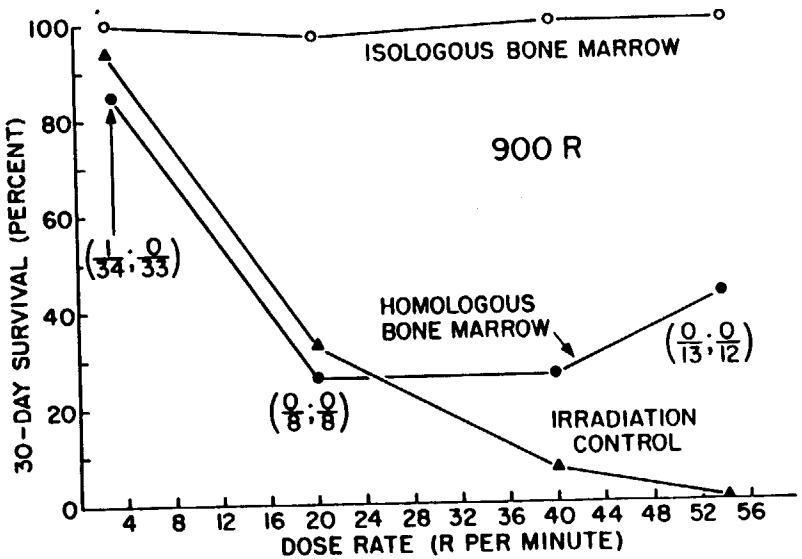

Fig. 19. Survival after 900 R at varying exposure rates and allogeneic (homologous) bone marrow. (Numbers in parentheses indicate number of animals having a donor graft over number tested. First set test on day 30; second on day 60.)

i.e., the absence of a permanent graft in the lowest exposure-rate group, 3.75 R/min. Here, however, it was possible to demonstrate the subsequent formation of antibody against rat cells, indicating that a rejection process had taken place in these animals irradiated at a low exposure rate (data not shown).

The results obtained verify our conclusions on the existence of an exposure-rate-dependent immune mechanism. Although antibody formation could not be demonstrated in those treated with allogeneic marrow, this is considered to be due to the insensitivity of the method attempted; i.e., detection of humoral antibody reactive with donor red cells. More sensitive methods, such as skin-graft rejections, may be able to detect immunologic reactions between two closely related antigenic systems. In any event, it is apparent that the effect of the allogeneic marrow at the different exposure rates was to provide a "tiding-over" effect; i.e., a protection from hematopoietic death until their own hematopoietic systems recovered from the radiation-induced damage. This was most evident in the 900 R group. Moreover, the exposure-rate-dependent immune mechanism was operating at a level of radiation (1200 R) that was lethal to 95 to 100% of the animals treated.

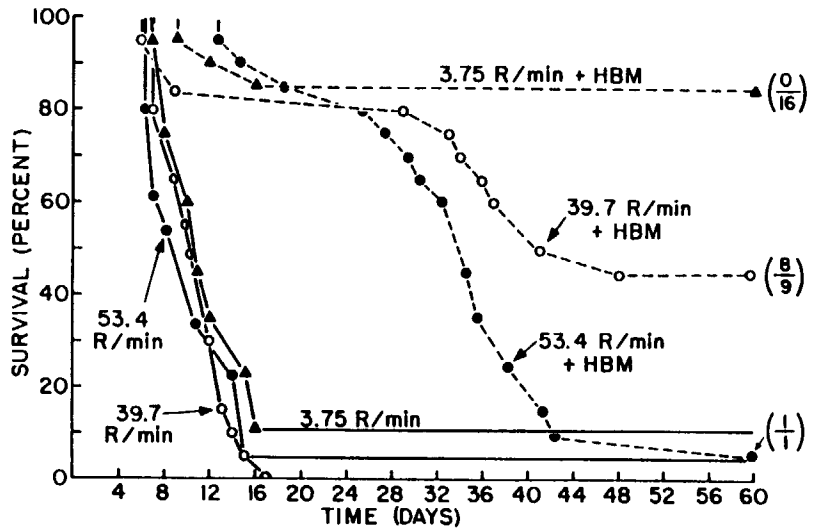

Fig. 20. Survival after 1200 R at varying exposure rates and allogeneic (homologous) bone marrow. (Numbers in parentheses indicate number of animals having a donor graft over number tested at that time.)

Abnormal Immune Mechanism in Allogeneic Radiation Chimeras*

N. Gengozian, B. Rabette, and C. C. Congdon†

The immune response following antigen injection in many species of animals consists of the sequential formation of two major molecular forms of antibody: the 19S macroglobulins and the 7S γ-globulins. Depending on the species of animal and the type and dosage of antigen, the antibody formed during the first and second weeks after antigenic stimulation is usually the 19S variety, and it is then replaced during the subsequent weeks by 7S molecules. Furthermore, treatment *in vitro* of antibody with 2-mercaptoethanol (2-ME) has been shown to result in dissociation and inactivation of 19S molecules without affecting 7S

*Full paper published in Science 149, 645–647, Aug. 6, 1965.
†Biology Division, Oak Ridge National Laboratory.

1027749

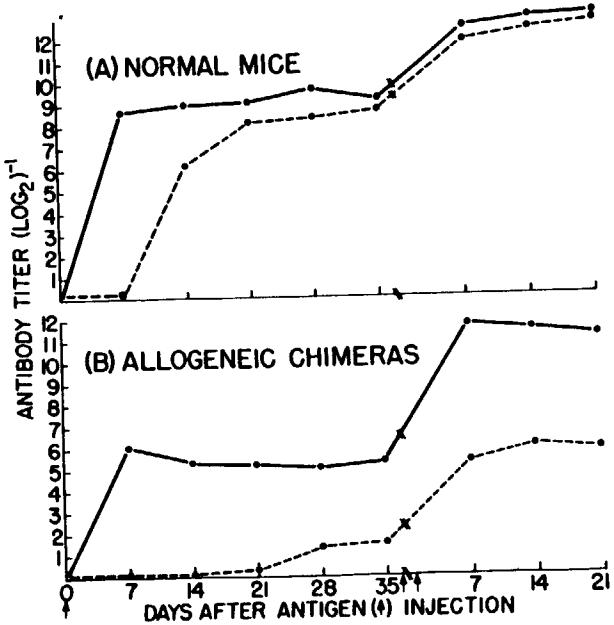

Fig. 21. Agglutinin response to Salmonella typhi flagellar antigen in (A) normal unirradiated mice and (B) allogeneic radiation chimeras after a primary (first) and tertiary (third) antigen injection. Titration before (solid lines) and after (broken lines) 2-mercaptoethanol treatment of the serum samples.

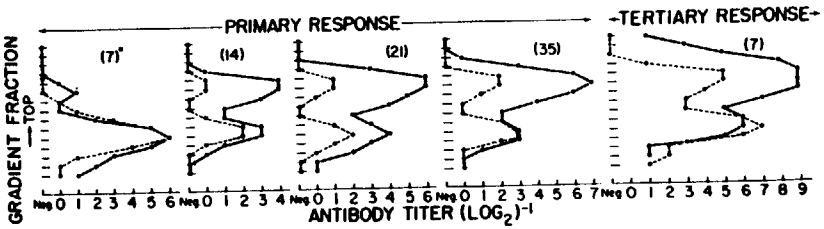

Fig. 22. Titration for antibody in sucrose gradient fractions of immune serum obtained form normal, unirradiated mice (solid lines) and allogeneic radiation chimeras (broken lines) according to the immunization scheme shown in Fig. 21. Numbers in parentheses indicate days after immunization.

antibody proteins. This provides another means of classification of antibody, that is, 2-ME resistant and 2-ME sensitive. Since this change in the type of antibody produced is a key qualitative feature of the "normal" immune response, it was possible that any impairment of immune competence in allogeneic radiation chimeras would be reflected in impaired conversion from "large-antibody" to "small-antibody" synthesis. Therefore, the ability of allogeneic chimeras to show the sequential development in 2-ME-sensitive (large) and 2-ME-resistant (small) antibodies was determined.

Allogeneic and isogeneic radiation chimeras were injected with *S. typhi* antigen six to eight months after radiation and bone-marrow treatment. The animals were bled weekly for five weeks, reinjected with the antigen six and 10 weeks after the first injection, and bled at weekly intervals for three weeks after the third injection. The individual sera were titrated for *S. typhi* flagellar (H) agglutinins before and after treatment with 2-ME. After the titrations, the remaining portions of the serum for each day were pooled for ultracentrifugation in sucrose density gradients and the fractions were titrated for antibody.

Figure 21 (A and B) shows the results of the first and third antigenic stimuli on antibody formation in normal mice and in allogeneic chimeras. (The response of the isogeneic chimeras resembled the normal and are therefore not presented.) In the normal group, the antibody formed during the first week was 2-ME-sensitive, but from the 14th through the 35th day, the presence of 2-ME-resistant antibody is evident. The tertiary response resulted in the appearance of predominantly 2-ME-resistant antibody. In contrast, the allogeneic radiation chimeras showed a lower primary response consisting primarily of 2-ME-sensitive antibody. The tertiary response was excellent and comparable to the normal group, but *Fig. 21B* shows that this response also consisted predominantly of 2-ME-sensitive antibody.

The ultracentrifugation studies *(Fig. 22)* showed the presence of almost entirely "large" antibody, that is, rapidly sedimentating type, in the 7-day sample of the primary response in normal mice. The synthesis of "small" antibody, that is, more slowly sedimentating type, is well under way in the second week and predominates throughout the 35-day period. In the allogeneic chimeras, there was a significant difference from the normal control in the proportions of "small" and "large" antibody formed throughout the 35-day period. This impaired conversion to "small" antibody synthesis among the allogeneic mice is evident mainly after the third antigen injection, where the response consisted predominately of the rapidly sedimentating "large" antibody.

Thus, allogeneic chimeras possess an abnormal mechanism for the production of humoral antibody. Additional studies have revealed that this defect is present in varying degrees among such mice. Whether this variability is related to the status of the immunologic tolerance between host and graft tissues in these animals is not known. Such chimeras may be used as models for the study of the sequential conversion of synthesis of larger antibody to that of the smaller type; the physiology of this process in normal animals is not yet clearly understood.

1027750

A Model of Hemopoiesis for Mammalian Recovery Experiments

A. L. Kretchmar

I have previously reported on work with a model of erythropoiesis that can be programmed for study with an analog computer.[1] Osgood's concept, that the hemopoietic system can be considered as an ecological system, is introduced by assuming that the dividing stem cells compete with other dividing marrow cells for essential nutrients and space. The assumption appears in the equation for the stem-cell population as a competition parameter, small a, and results in a birth rate among stem cells that decreases with increasing numbers of stem cells, and of dividing but differentiated cells. Since the latter are assumed to originate from the stem-cell pool by differentiation and division, there is a time lag between any change in the size of the stem-cell pool and a corresponding change in the number of dividing differentiated cells. As a consequence, when the size of the stem-cell pool is reduced and the system is allowed to recover, there is overshoot and oscillation in the stem cell and dividing differentiated cell populations, and the extent of the overshoot and number of oscillations depends upon what values are arbitrarily assigned to the unknown competition parameters, *Fig. 23*. It was shown that when the model was used to simulate mammalian recovery experiments, recovery in the model was consistent with data in the literature from animal experiments. *Figure 24* shows some more recent results demonstrating this.

A prediction of the model was that after irradiation and injection of bone marrow, complete recovery could occur in peripheral red-cell

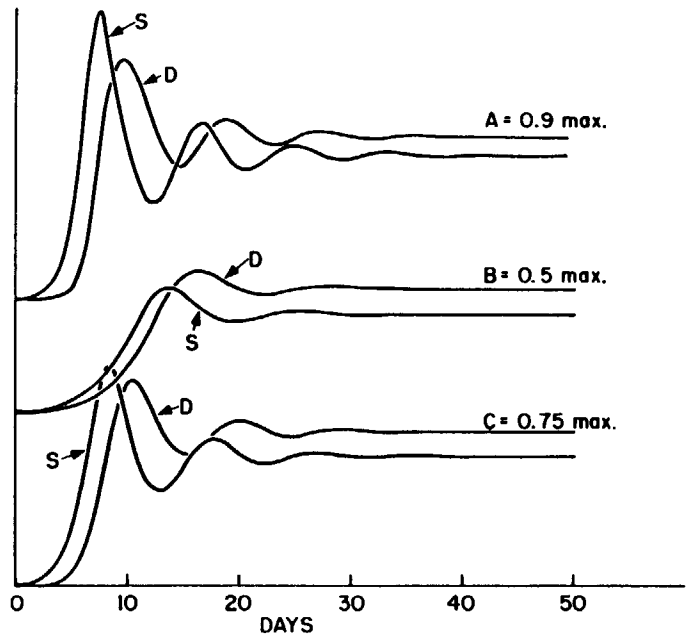

Fig. 23. Analog computer analysis of recovery in the stem-cell, S, and dividing-differentiated cell, D, populations; A, B, C, are plotted on the same time scale but A and B are offset on the ordinate to show the effect of the three different arbitrary choices (A,B,C) for the competition parameters in the equation for the stem-cell population. The effect on rate of recovery, degree of overshoot, and number of oscillations is illustrated.

parameters without corresponding complete recovery of the stem-cell pool. This prediction was tested in animal experiments, and was verified. In addition, we found that there is a secondary reduction of the stem-cell pool of homologous chimeras at 20 to 40 days.

A prediction of the model that has not yet been tested in animal experiments, but leads to interesting though highly speculative discussion, is based on data summarized in *Table 5*. The experiments of Urso and Congdon[2] were simulated in the computer. When the time to half recovery in the model is compared with that from the Urso and Congdon data shown in columns 1 and 2, recovery in the model is roughly comparable to that in animals when the stem-cell pool of the model begins with about 1/10 the number of bone-marrow cells that were injected in the animal experiments. This raises the interesting

1027751

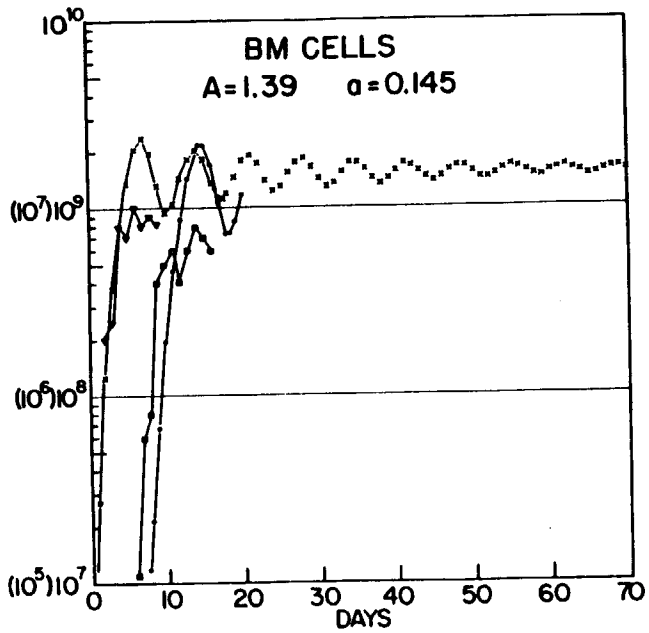

Fig. 24. Comparison of recovery in a model of hemopoiesis with data taken from the literature (Urso and Congdon, 1957) of recovery in lethally-irradiated mice given isologous bone-marrow cells. The dots and crosses show results from the computer starting from two different stem-cell population sizes. The open triangles and squares show recovery in femoral bone-marrow cells of mice given 2.4×10^8 and 1.0×10^6 isologous cells respectively.

possibility that the marrow cells used in Urso's and Congdon's experiments contained about 10% undifferentiated progenitor cells; but if 10% of the total marrow population of nucleated cells are undifferentiated progenitor cells then only about 20% of these will be in cycle, the remaining 80% are presumably in prolonged G_1 or, as suggested by Lajtha, in a resting or G_0 state. Becker *et al.*[3] recently published results that support this prediction. They have shown that only a small fraction of colony-forming units can be killed with brief exposure to tritiated thymidine of very high specific activity. Most of the cells responsible for spleen-colony formation are therefore not in S.

Figure 25 shows recovery in a stem-cell population in which the length of G_1 is allowed to vary from a minimum of 3 hr to a maximum of about 53 hr, depending on the size of the population. The variable

G_1 avoids the assumption of a separate G_0 state. At time 0 we begin with 10^7 cells all in G_1, they rapidly enter S, and the population begins to grow. During the first few days 2/3 of the population are stem cells in S. When recovery is complete, however, only about 1/4 of the population is in S, 70% are in G_1 and the remainder are in G_2 or mitosis. If it is assumed (1) that erythropoietin "effectively penetrates" the stem cells during G_1 but can be metabolized or otherwise rendered ineffective if G_1 is prolonged; and (2) that erythropoietin must be present in the S phase (discussed later) of the stem-cell cycle, then it can be seen that during early recovery when G_1 is very short and most of the population is in S, sensitivity to erythropoietin would be minimal. However, at about five days, as the fraction of the population in G_1 goes to 50% or more and G_1 lengthens, sensitivity to erythropoietin would rapidly increase. This was the result in Fried's experiments,[4] i.e.,

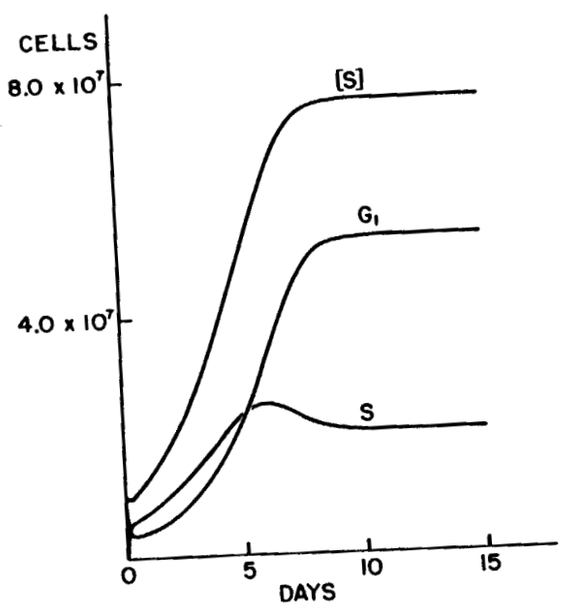

Fig. 25. Analog computer tracing of recovery in stem-cell population, [S]. The number of these stem-cells that are in the G_1 and S phase of cell cycle are shown by the curves marked G_1 and S. The curves showing G_2 cells and mitoses are not included to maintain graphic simplicity. They are respectively 1/7 and and 1/14 of the cells in S.

1027752

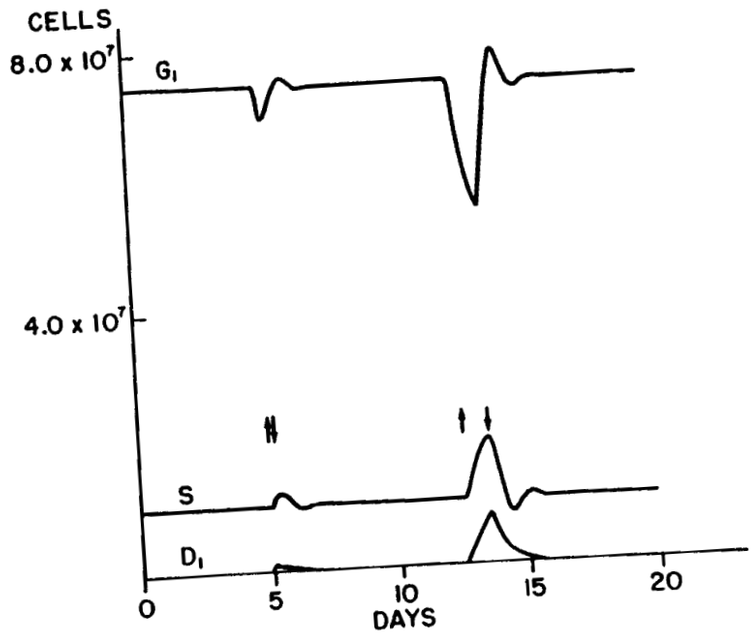

Fig. 26. Analog computer tracing illustrating a "recruitment phenomenon" in the action of erythropoietin on a model of a stem-cell population; G_1 and S as in Fig. 25; D_1 traces the earliest erythroblast population. Curves of the total stem-cell population and the G_2 and mitosing cells are not shown, as in Fig. 25.

recovery in stem-cell pool size was more rapid than recovery in erythropoietin sensitivity but when the latter began to recover at about four to five days it was very rapid.

An interesting "recruitment phenomenon" is observed in the response of this stem-cell population to erythropoietin as shown in *Fig. 26*. It is assumed that erythropoietin acts on stem cells by a process similar to enzyme induction and that, as shown by Pardee[5] for bacteria, the inductive process occurs during replication of the relevant genes; that is, it is assumed that stem cells are triggered during S. The D_1 curve shows the earliest erythroblast population. There is no red cell production as in a hypertransfused animal and the D_1 population is

zero. A few stem cells are in S but nearly all are in G_1. Erythropoietin is assumed to trigger cells out of S beginning at the first upward pointing arrow, but acting for only 2 hr. The small reduction in the stem-cell population is "felt" and G_1 cells move into S. The erythropoietin action is for such a short time that very little increase in the D_1 population occurs and most of the S cells stay in the stem-cell pool. With more prolonged erythropoietin action, however (second upward arrow), and recruitment of G_1 cells into S potentiates the action of the hormone and there is a rapid increase in D_1 cells. Note that a "recruitment phenomenon" of this kind is almost ideally suited to control of erythropoiesis; at first it potentiates the action of erythropoietin, but then as the fraction of G_1 cells is reduced and G_1 is shortened, the stem-cell population becomes progressively less sensitive to erythropoietin.

TABLE 5

Comparison of Recovery in Irradiated Mice Given Isologous Bone-marrow Cells With Recovery In a Model of Hemopoiesis

IBM Cell Dose*	Time to 1/2 Recovery* Days	Model "Stem-Cell" Dose
0.6×10^6	13	
	—	10^5
10^6	9	
	—	10^6
1.28×10^7	6¼	
6.4×10^7	5½	
10^8	5	10^7
2.4×10^8	4	

*Urso and Congdon, 1957 (Ref. 2).

REFERENCES

1. Kretchmar, A. L. Analog computer model of the erythropoietic system, Exper Hematol 7, 70, 1965.
2. Urso, P. and Congdon, C. C. The effect of the amount of isologous bone marrow injected on the recovery of hematopoietic organs, survival and body weight after lethal irradiation injury in mice, Blood 12, 251–260, 1957.
3. Becker, A. J., McCulloch, E. A., Siminovitch, L., and Till, J. E. The effect of differing demands for blood cell production on DNA synthesis by hemopoietic colony-forming cells in mice, Blood 26, 296–308, 1965.
4. Fried, W. A comparison of the rate of recovery of erythropoietin sensitive cells and of colony forming units after X-irradiation, Exper Hematol (in press).
5. Pardee, A. B. and Klahu, R. A model for periodic oscillations in bacteria, Fed Proc (in press).

1027753

Reduced Erythropoietic Capacity in Lethally Irradiated Mice Treated with Isologous or Homologous Bone-marrow Cells*

A. L. Kretchmar and E. Rupp

In studying a model of the erythropoietic system from the point of view of mammalian recovery after total-body irradiation and the injection of bone-marrow cells, we realized that a normal peripheral blood picture would be possible even though complete recovery in the immature ("stem cell") cellular pools had not taken place. It was only necessary to change the relative probabilities of differentiation from and proliferation in the "stem-cell" pool to obtain complete peripheral recovery with an incompletely regenerated marrow population. This possibility was investigated in the experiments summarized here.

Radiation chimeras were produced in the usual way by injecting 20 to 40 $\times 10^6$ homologous bone-marrow cells into lethally irradiated mice.

The bone-marrow cell donors were normal unirradiated mice (isologous or homologous). Irradiated mice given similar numbers of isologous bone-marrow cells and normal untreated mice were controls. All animals were bled from the ocular sinus in a standard way. Hematocrit, hemoglobin, serum iron, and reticulocyte percentage were determined on each animal with the use of standard hematologic techniques. One half milliliter of blood was drawn into a heparinized Pasteur pipette from each animal at each bleeding. Bleeding was at three- and four-day intervals (alternating) for five bleedings, beginning on the days indicated in *Table 6*.

Table 6 presents a summary of the data. Removal of blood at this rate (approximately 1/3 of the total blood volume twice a week) constitutes a strong stimulus to erythrocytic differentiation and normal mice can maintain a daily production of new red cells that keeps a reticulocyte volume of 7 to 11% of the whole blood volume. Despite this elevated production of red cells, fully normal hemoglobin and hematocrit levels cannot be maintained and the values fall to 13–14.5 g/100 ml and 45 to 48% respectively from 16 to 17 and 48 to 52, which are the prebleeding levels in normal mice. The schedule, therefore, constitutes a maximal stimulus to erythropoiesis without unduly depressing peripheral red blood cell levels.

*Work done in collaboration with C. C. Congdon, Biology Division, Oak Ridge National Laboratory.

In irradiated mice given isologous bone marrow, the hematocrit and hemoglobin levels before bleeding were within normal limits at all times tested (7 to 132 days after irradiation and bone marrow). The response to bleeding was good but slightly subnormal. It is noteworthy that when 20 to 40 $\times 10^6$ cells are injected on the day of irradiation, regeneration of the marrow reaches a plateau by day 7 and does not show significant improvement even as long as 132 days after irradiation. Thus the marrow does not fully recover when this dose of isologous bone-marrow cells is used.

When the same number of homologous cells is given the response to bleeding is not so good as in the isologous marrow-treated groups. There is rapid initial recovery of the marrow with a secondary loss in erythropoietic capacity in the 20- to 40-day interval and not until 212 days after irradiation and bone-marrow treatment does the erythropoietic response of homologous chimeras equal that of mice treated with isologous bone-marrow cells.

Since one-third of the blood volume is removed at the first and each subsequent bleeding, the fact that host red blood cells are still circulating at seven days after irradiation does not interfere with the evaluation of erythropoietic response capacity because any new red cell formation must come from the proliferating graft. The progressive decline or plateau in values at low levels that occurs in the chimeras at the third, fourth, and fifth bleedings even with maximal (though subnormal) reticulocyte response indicates that erythropoietic capacity is less than that of isologous marrow-treated mice and is severely reduced at 22 and 37 days.

Serum iron levels were reduced in all groups to 1 to 2 gamma/ml from the prebleeding levels of 2 to 3 gamma/ml. Supplementary iron feeding by addition of ferrous sulfate to the drinking water did not alter the results. In general levels were higher in chimeras than in normal mice at the third and fourth bleeding with the levels for irradiated mice given isologous cells intermediate. Thus the serum iron levels were lowest in normal mice with greatest erythropoietic capacity and highest in the chimeras where erythropoietic capacity was reduced.

Irradiated mice given isologous or homologous bone-marrow cells do not have completely regenerated marrow-cell populations even though they may show complete recovery to normal values in hematocrit, hemoglobin, reticulocyte, and serum-iron determinations.

Approximately 200 days are required for chimeras to achieve a bone-marrow cell population with as great an erythropoietic capacity

1027754

as irradiated mice given isologous cells. Recovery in mice given isologous cells is rapid but not complete even at 132 days after irradiation. The erythropoietic capacity of chimeras shows a marked secondary reduction at the 20- to 40-day interval.

TABLE 6

Response of Radiation Chimeras to Bleeding*

Factor	Group	Time after X ray and bone marrow 7	22	37	76	132	176	212
Hematocrit	Normal	46	45	45	47	48	—	45
	IBM	44	44	41	44	40	—	—
	HBM	38	24	21	37	—	34	40
Hemoglobin	Normal	14	13.5	13	14.5	13.5	—	13
	IBM	13	12.5	12.5	13.5	11.5	—	—
	HBM	11	7.5	6	11	—	10	11.3
Reticulocyte Response†	Normal	6.7	9	7	9.5	11	—	11
	IBM	8.5	5.5	6	9.2	10.2	—	—
	HBM	6.7	2.5	2.0	7.5	—	7.1	11

*The data are the average of the values determined at the third and fourth bleeding when the response was more or less stabilized. The prebleeding values were normal, 48 to 52, 16 to 17, 0.5 to 1.0; Isologous bone marrow, 48 to 54, 16 to 17, 1 to 2; Homologous bone marrow, 46 to 54, 13 to 17, 1 to 2.

†The value shown is an indication of the absolute reticulocyte response and is obtained by multiplying the hematocrit by the fraction of the circulating red blood cells that are reticulocytes, as determined from a cresyl blue stained blood smear.

Secondary Mortality and Body Weight Loss in Lethally-Irradiated Mice Given Small Doses of Isologous Bone-marrow Cells*

A. L. Kretchmar and W. R. Conover

Barnes *et al.* have described "secondary disease" in lethally-irradiated mice given isologous bone-marrow cells and believe that the syndrome is related to lymphoid aplasia. We have been interested in their work because of the possible connection between their observations and the disease of radiation chimeras believed to be related to a graft-host immunologic incompatibility.

Mice were given 950 R total-body irradiation 250 keV at 15 milliamperes at 160 R/min and then given either 1×10^5, 1.5×10^5, or 1×10^6 isologous bone-marrow cells intravenously. The animals were then weighed periodically and a record was made of the date of death if mortality occurred.

The results are summarized in *Table 7*. Secondary mortality (30 to 100 days after treatment) was usually below 13% in our experiments. In only two groups, was the mortality comparable to that reported by Barnes *et al.*, 33% compared to 43% observed by the English group. In four of our experiments there was no mortality at all after 30 days. Pathologic data are being collected to ascertain the cause of death in these animals.

In other experiments we have observed that at 70 to 96 days after treatment lethally-irradiated mice given 1.5×10^5 isologous cells show anemia, subnormal erythropoietic capacity, and a reduction to 8.5 from a normal 15.3 spleen colony forming units per 10^5 marrow cells. It is, therefore, apparent that hemopoietic recovery in these animals is poor.

We conclude on the basis of work thus far that "secondary disease" in lethally-irradiated mice given small numbers of isologous bone-marrow cells is not prominent and that hemopoietic recovery requires more than 1×10^6 isologous marrow cells in mice given 950 R total-body irradiation.

*Work done in cooperation with C. C. Congdon, Biology Division, Oak Ridge National Laboratory.

REFERENCE

1. Barnes, D. W. H., Loutit, J. F., and Micklem, H. S. "Secondary disease" of radiation chimeras: A syndrome due to lymphoid aplasia. Ann N Y Acad Sci 99, 374-385, 1962.

1027755

TABLE 7

Mortality in Lethally-Irradiated Mice Given Isologous Bone-marrow Cells

Group	No. Mice	Bone Marrow Cell Dose and Day of Death						
		X ray only	1×10^5		1.5×10^5		1×10^6	
		0–30	0–30	31–100	0–30	31–100	0–30	31–100
		%	%	%	%	%	%	%
K-20, 15	55	100	27	13	7	13	0	0
K-21, 16	53	100	23	7	21	7	0	10
K-22, 17	55	100	33	0	7	13	20	0
K-23, 13	55	100	20	0	13	0	0	0
K-24, 14	55	100	73	0	13	7	0	0
K-25	34	100	40	33	—	—	0	0
K-26	35	100	33	33	—	—	0	0
	Average	100	35.6	12.3	12.2	8.0	3.0	1.5

Serine-3-^{14}C Metabolism in Mice as Determined by Respiration Pattern Analysis

A. L. Kretchmar and C. E. Phipps

We have previously reported data that indicate[1] significant alteration in serine metabolism of radiation chimeras. To study further the metabolism of this amino acid in chimeras by an *in vivo* technique we turned to respiration pattern analysis.

Normal mice were used in the studies summarized in *Fig. 27*. Our objective was to determine whether the respiratory pattern of $^{14}CO_2$ excretion could be influenced by injecting, simultaneously with the serine-3-^{14}C, certain unlabeled compounds. The compounds chosen were (1) glucose, since carbohydrate is known to have a "nitrogen sparing effect" on amino acid metabolism and might be expected to reduce the amount of ^{14}C recovered in 1 hr; (2) glycine, since glycine and serine are known from *in vitro* experiments to be in equilibrium

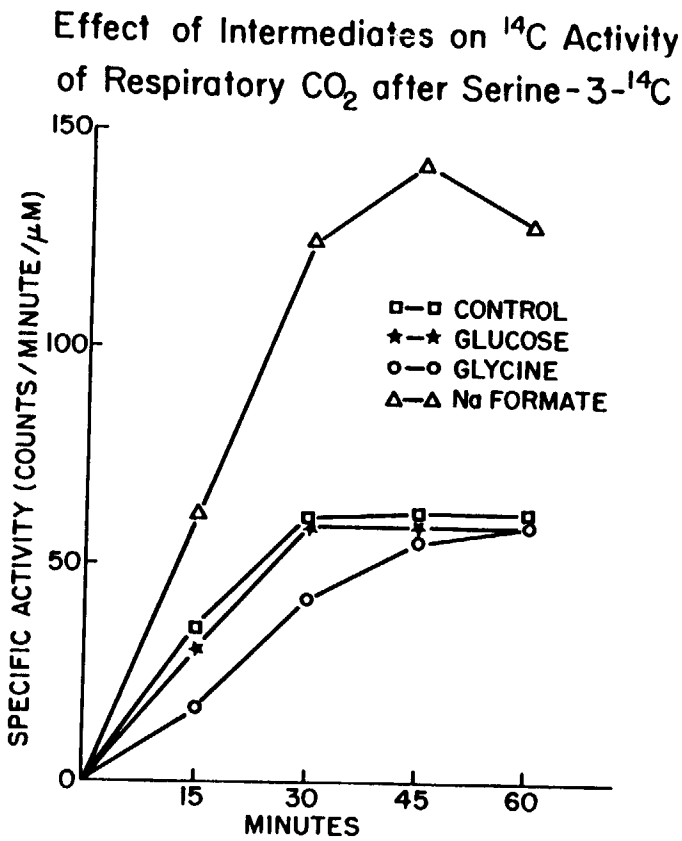

Fig. 27. The effect of unlabeled compounds when injected simultaneously with serine-3-^{14}C on the loss of ^{14}C into the respiratory CO_2 of mice.

over a reaction involving a derivative of formic acid bound to folic acid; and (3) formate, the other reactant with glycine. The labeled serine (DL ^{14}C-3-serine) was injected intraperitoneally in Tyrode's solution (control) or in solution with either glucose, glycine, or ammonium formate, and respiratory CO_2 was collected for 1 hr. The total CO_2 was measured by the Van Slyke-Neil manometric technique and the ^{14}C activity by dissolving the CO_2 in Hyamin and counting in an automatic liquid scintillation counter.

The results show that in normal mice the glycine-serine exchange pathway is functional *in vivo*. Thus, in the presence of exogenous glycine, the specific activity of respiratory CO_2 is lower for 45 min, indicating decreased metabolism of the 3-carbon of serine to formate and CO_2. The administration of exogenous formate, on the other hand, traps the 3-carbon that is metabolized via the hydroxymethyl-tetrahydrofolic acid in an expanded formate pool which is rapidly oxidized to CO_2.

We conclude that studies of this type are useful for *in vivo* analysis of serine metabolism of radiation chimeras.

1027756

REFERENCE

1. Kretchmar, A. L. and Congdon, C. C. The levels of free aspartic acid, glycine, and serine in tissues of bone marrow chimeras. Transplantation 1, 298–305, 1963.

The Radiosensitivity of Bone-marrow Cells Made Hypoxic by Vascular Occlusion*

F. Comas

An experiment was performed to test the degree of radiation protection achieved by irradiating femoral bone marrow of mice when the blood supply to the femur was interrupted. The hypothesis tested was that by interrupting blood flow, the bone marrow would be rendered anoxic, and thereby less radiosensitive than bone marrow irradiated under normal conditions of blood flow. Radiosensitivity was measured by injecting the irradiated marrows into lethally irradiated recipient mice and counting the number of hemapoietic clones developing in the spleens of these recipient animals. In this fashion one obtains a survival curve for bone-marrow stem cells.

The survival curve for normally oxygenated bone-marrow cells had a D_0 of 121 ± 12 rads (95% confidence limits), where D_0 is the radiation dose required to reduce survival to 37% of the initial value, in the exponential part of the survival curve. The extrapolation number was 0.92 ± 0.18, indicating that the survival curve was exponential all the way through without any initial shoulder. The survival curve for bone marrow irradiated while its blood flow was interrupted had a

*Work done in part while a visiting scientist at the Department of Radiology, Stanford University, in collaboration with R. F. Kallman.

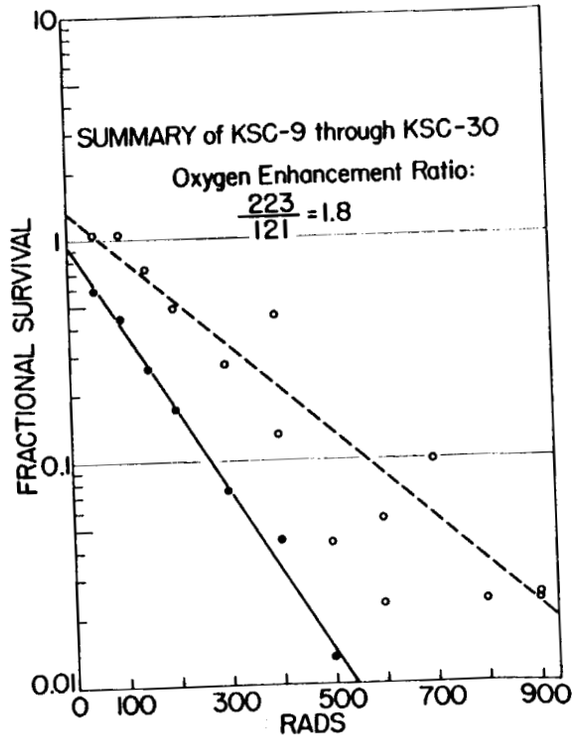

Fig. 28. Survival curves for bone-marrow stem-cells irradiated in vivo under normal conditions of oxygenation and under vascular hypoxia.

D_0 of 223 ± 78 rads, and an extrapolation number of 1.3 ± 0.3. The oxygen enhancement factor was, therefore, (223/121) 1.85.

The oxygen enhancement ratio found in this experiment is close to that determined in a previous experiment[1] in which the experimental animal was the rat, and the end point was the duration of inhibition of DNA synthesis after irradiation. That figure was 2.06. The present experiment, however, points out a new interesting finding, the great variability encountered in the radiosensitivity of the hypoxic bone marrow *(Fig. 28)*. This variability is not likely to be due to experimental artifacts because the survival curve for the well-oxygenated bone marrow shows none of this variability. The most likely explanation is that the attempted occlusion of the left common iliac artery during irradiation did not completely stop the blood flow, or that vascular collaterals might have existed between aorta and femoral arteries resulting in a reduced but still significant blood flow through the animal's leg. Thus we may have been dealing with tissue hypoxia instead of tissue anoxia. The significance of this observation relates to the possible clinical application of irradiation of human tumors under anoxia. For this to be effective, it is necessary that the irradiated tissues be rendered completely anoxic. From the present experiment it appears that anoxia cannot be obtained by simply occluding the main artery supplying the area to be irradiated, unless care is taken to obstruct all possible routes of collateral circulation.

1027757

REFERENCE

1. Comas, F. V. Comparative changes in radiosensitivity between bone marrow and a rat tumor irradiated under anoxia. Radiology 83, 528–533, 1964.

Cytogenetic Interrelation of the Myeloproliferative Disorders*

K. O. Goh

Cytogenetic studies in 50 patients with various types of myeloproliferative disorders (MPD) have been analyzed. The Ph¹ chromosome was identified either in bone marrow or in peripheral leukocyte cultures in every patient with chronic myelocytic leukemia (CML), whether it was in the typical chronic, myelofibrotic, or acute stage. No Ph¹ chromosome or other consistent chromosomal abnormality was seen in other types of MPD. However, nonconsistent chromosomal abnormalities have been seen in occasional patients with other types of chronic or acute MPD. No correlation was found between the acuteness of the clinical course of the disease and the fraction of cells with chromosomal abnormalities.

The results indicate that the Ph¹ chromosome signifies CML and is found in the immature cells of the myelocytic series. Cells with nonconsistent chromosomal abnormalities and the Ph¹ chromosome are found in patients with an acute transformation of CML. The non-

*Part of this work was done at the University of Rochester School of Medicine and Dentistry, Rochester, New York. Published in Clin. Res. 13:273, 1965.

consistent chromosomal abnormalities suggest the acute transformation; and the Ph[1] chromosome indicates the preexisting CML. Thus it is possible that the cytogenetic transformation of the CML pattern into the acute leukemic pattern might involve a mechanism similar to that of spontaneous acute leukemia or other types of the MPD.

Smaller G Chromosome in Irradiated Man*

K. O. Goh

In 1958, a criticality accident in Oak Ridge involved eight workers[1] who received total-body exposures of mixed neutron and gamma irradiation ranging from 68.5 to 339 rads. Cytogenetic studies have been part of a detailed clinical and laboratory follow-up of these men.

Cytogenetic analyses completed in three of the eight men have revealed a new observation. The metaphases were obtained from the bone marrow and peripheral blood leukocyte cultures which were terminated at different intervals after *in vitro* incubation with phytohemagglutinin (PHA). See *Table 8*. In 18 (2.5%) metaphases, a smaller G chromosome was observed (*Fig. 29*). Furthermore, chromatid and chromosomal breakages were seen in 30 and 105 chromosomes respectively. Of these, a chromosomal or chromatid break involving one of the G chromosomes was seen in six (4.4%) chromosomes as shown in *Fig. 30*, suggesting that metaphases with the small G chromosome found in these patients probably evolved from the metaphases with a chromatid or chromosomal break as shown diagrammatically in *Fig. 31*. The modal chromosome number was 46 which was seen in 83% of the metaphases analyzed.

A smaller G chromosome, known as the Philadelphia chromosome (Ph[1]), was first described in patients with chronic myelocytic leukemia (CML) in 1960.[2] The mechanism of its production has been thought to be a deletion of the long arms of one of the G chromosomes (21 or 22). This postulation is supported by a recent microspectrophotometric analysis that demonstrated a 40% decrease of DNA content in this abnormal chromosome as compared with the other chromosomes of this group.[3] The actual morphologic breakage of a G chromosome has

*In press, Lancet

1027758

TABLE 8

Cytogenetic Analyses in Patients Having Accidental Total-body Irradiation

Case	Doses*	Materials†	Chromosome Count							Smaller G		Breakage			
			<45	45	46	47	>47	Total	%M‡	No.	%	Chromosomal No.	%	Chromatid No.	%
Control		P.B.C. (3D)	0	1	98	0	0	99	99	0		0		1	1.0
		B.M.C. (3D)	8	11	78	3	0	100	78	0		0		3	3.0
B	270	P.B.C. (4D)	2	1	14	0	0	17	82	1	6.0	0		0	
		P.B.C. (7D)	2	4	51	0	0	57	90	0	0	8	14.0	2	3.5
		B.M.C. (3D)	1	9	89	1	0	100	89	1	1.0	14	14.0	2	2.0
		B.M.C. (7D)	4	16	76	2	1§	99	76	3	3.0	16	16.2	5	5.0
C	339	P.B.C. (3D)	9	8	91	3	2§	111	82	4	3.6	15	13.5	5	4.5
		B.M.C. (4D)	4	13	106	1	1¶	125	85	5	4.0	18	14.4	5	4.0
F	68.5	B.M.C. (3D)	9	12	76	1	2**	100	76	3	3.0	25	25.0	7	7.0
		B.M.C. (7D)	1	11	85	2	1	100	85	1	1.0	9	9.0	4	4.0

*Dose in rads.
†P.B.C. (3D) = Peripheral leukocytes cultured 3 days. The number stands for days *in vitro* culture.
B.M.C. = Bone-marrow cultures.
‡Percentage of cells having modal chromosome number of 46.
§Polyploid cell
¶Endoreduplication
**One of each, endoreduplication and polyploid.

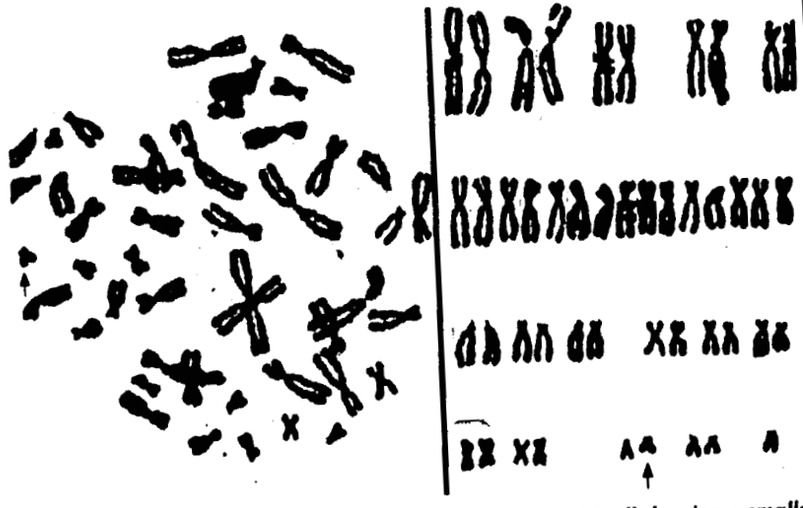

Fig. 29. Metaphase (left) and karyotype (right) of a diploid cell showing a smaller G chromosome (arrow).

Fig. 30. Metaphase (left) and karyotype (right) of a hypodiploid (45 chromosomes) cell showing chromatid break of a G (21-22) chromosome (small arrow). in the karyotype, the arrow with a white circle indicates a missing chromosome and the arrow with a dark circle indicates an additional chromosome. The long arrowed chromosomes are abnormal chromosomes.

1027759

not been reported in patients with CML. The present result leads us to speculate that the Ph¹ chromosome found in patients with CML could be the result, in an analogous fashion, of a chromosomal or chromatid break of a G chromosome.

In spite of a similar morphologic appearance of the smaller G chromosome reported here and the Ph¹ chromosome associated with CML, the present patients show no evidence of CML. Thus, this smaller G chromosome may not have the pathophysiology of the Ph¹ chromosome. Moreover, the incidence of the smaller G chromosome in

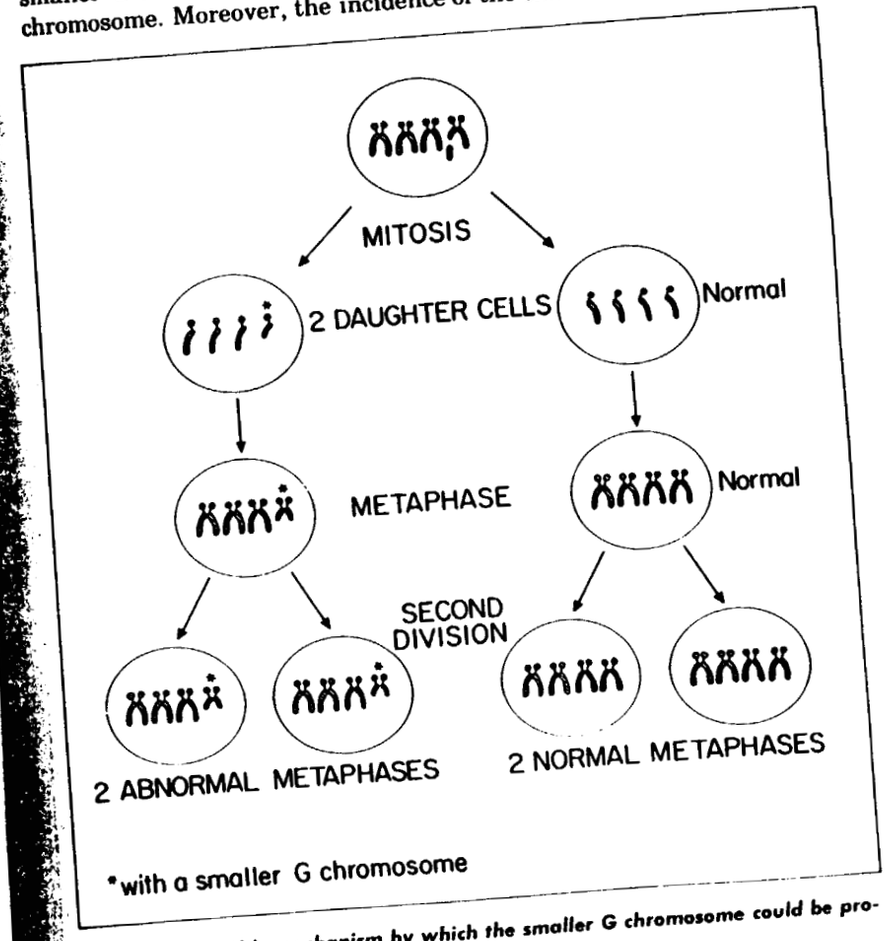

Fig. 31. A possible mechanism by which the smaller G chromosome could be produced.

these patients is much lower than that in CML. In these two ways, the present reported smaller G chromosome contrasts with the Ph' chromosome.

Bender and Gooch have observed radiation-induced chromosomal aberrations in the present patients 29[4], 42[5], and 60[6] months after the accident. But a smaller G chromosome was not seen in these studies.[6] It is possible that some of the present observations were induced during *in vitro* incubation, since many chromatid deletions were also seen in these patients. However, no induced smaller G chromosome had been seen in this laboratory in normals or patients without CML. Furthermore, a smaller G chromosome was also seen in the direct bone-marrow preparations of these men. Thus it is unlikely that the smaller G chromosomes seen in these patients were induced during *in vitro* incubation.

The comments and suggestions of Drs. T. C. Hsu and M. A Bender are greatly appreciated.

REFERENCES

1. Accidental Radiation Excursion at Y-12 Plant, June 16, 1958. U. S. Atomic Energy Commission Report Y-1234, Office of Technical Services, U. S. Department of Commerce, Washington, D. C., 1958.
2. Nowell, P. C. and Hungerford, D. A. A minute chromosome in human chronic granulocytic leukemia. Science 132, 1497, 1960.
3. Rudkin, G. T., Hungerford, D. A., and Nowell, P. C. DNA contents of chromosome Ph and chromosome 21 in human chronic granulocytic leukemia. Science 144, 1229–1231, 1964.
4. Bender, M. A and Gooch, P. C. Persistent chromosome aberrations in irradiated human subjects. Radiat Res 16, 44–53, 1962.
5. Bender, M. A and Gooch, P. C. Persistent chromosome aberrations in irradiated human subjects. II. Three and one-half year investigation. Radiat Res 18, 389–96, 1963.
6. Bender, M. A Personal communication.

Intermittent Corticosteroid Therapy in the Malignant Lymphocytic Diseases

D. A. White

Most patients with chronic lymphocytic leukemia or lymphosarcoma respond well to the various forms of radiation therapy and to certain of the alkylating agents. There appears to be little need for corticosteroid therapy in most patients with early and uncomplicated malignant lymphocytic disease. However, far-advanced chronic lymphocytic leukemia and lymphosarcoma may be unsuitable for treatment with radiation therapy, or myelosuppressive chemotherapeutic compounds. The corticosteroids frequently produce excellent subjective and objective improvement and are particularly useful in the presence of associated cytopenias, whether due to hypersplenism, ineffective hematopoiesis, or a previous treatment. Unfortunately, the complications of therapy with the corticosteroid drugs often preclude their long-term use in the dosage required.

A practical solution to the problem of prolonged corticosteroid therapy in far-advanced malignant lymphocytic diseases was reported in 1962 by Khuri, *et al.*[1] They administered large daily doses of a glucocorticoid for two to four weeks. The steroid then was rapidly reduced and discontinued. One week later the original daily dose was given one day a week or on two consecutive days a week.

This new approach to long-term corticosteroid therapy appeared to be appropriate for certain of our patients. During a period of 25 months, six patients with chronic lymphocytic leukemia and four with lymphosarcoma were treated with intermittent prednisone therapy. Their ages ranged from 41 years to 72 years. Four were women and six were men. Two different therapeutic regimens were used. Three patients with chronic lymphocytic leukemia and one with lymphosarcoma initially received 125 or 150 mg of prednisone daily. Three patients with chronic lymphocytic leukemia and three with lymphosarcoma were placed at once on prednisone every other day, or on two days a week, but not on consecutive days. After 25 months, the eight patients remaining in the study were on the following intermittent doses of prednisone: 150 mg on each of two successive days a week (1); 100 mg two days a week(2); 40 to 100 mg every other day (5).

Criteria were established for evaluating therapeutic results. The treatment was ineffectual in one patient with chronic lymphocytic leukemia who died one month after being placed on large daily doses of prednisone. All other patients had both objective and subjective improvement *(Table 9)*. One patient with chronic lymphocytic leukemia had an excellent response for one year and a good response during the remaining 13 months of the study. Previously he had an unsatisfactory response to a short course of prednisone in daily doses of 30 to 40 mg daily. His hematologic findings are illustrated in *Fig. 32*. Three leukemic patients and two with lymphosarcoma had good responses. A satisfactory response was observed in one patient with chronic lymphocytic leukemia and two with lymphosarcoma. Inter-

1027760

mittent steroid therapy was stopped in one leukemic patient with a good response because of nausea that did not respond to antacid therapy.

The incidence and severity of side effects (nervousness, insomnia, acneiform skin eruptions, moon face, and fluid retention) were appreciably less than would have been expected with comparable daily doses of prednisone. A few complications of corticosteroid therapy were observed. The most significant were posterior capsular cataracts and osteoporosis. Each complication was observed once during the 25 months of the study. During the following year another patient developed early posterior cataracts. All patients who have been on intermittent corticosteroid therapy for at least two years have developed some degree of osteoporosis. In two patients this has been associated with one or more pathologic fractures. We have not observed diabetes, peptic ulcers, or an increased incidence of infections.

Equally good results were obtained whether the patients were

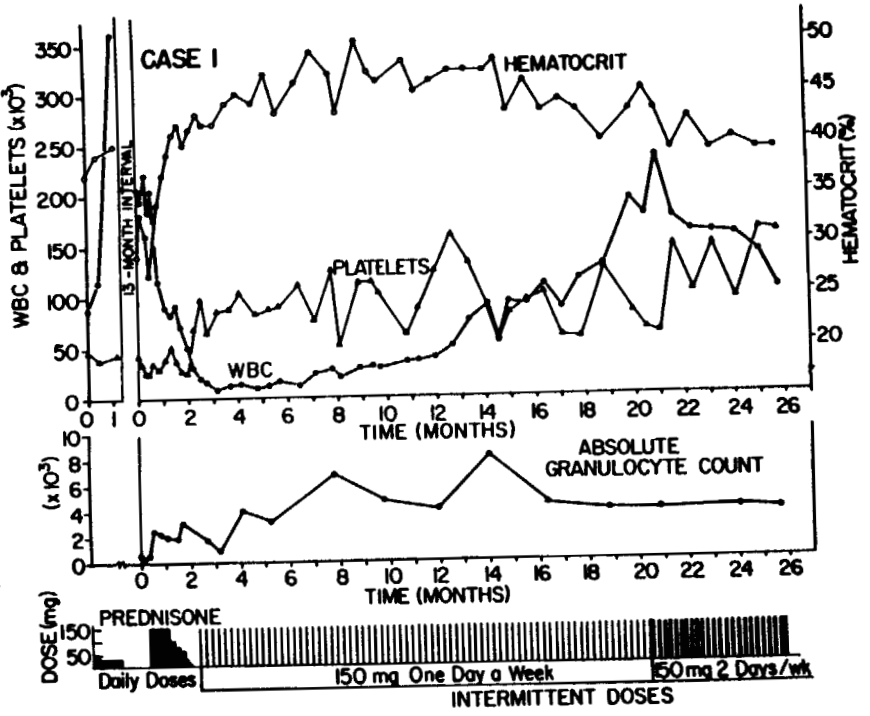

Fig. 32. Hematologic response to intermittent corticosteroid therapy given to a patient with chronic lymphocytic leukemia.

given large daily doses of prednisone or were started at once on an intermittent regimen. Most patients had greater subjective improvement when taking prednisone every other day than with longer intervals between doses. Since some side effects and complications occur, we believe that long-term intermittent corticosteroid therapy should be reserved for far-advanced cases of malignant lymphocytic disease no longer amenable to more conventional forms of treatment.

TABLE 9

Response to Intermittent Corticosteroid Therapy

	Excellent	Good	Satisfactory	None
Chronic Lymphocytic Leukemia	1	3	1	1
Lymphosarcoma		2	2	
	1	5	3	1

REFERENCE

1. Khuri, P. D., Harrington, W. J., Brown, E. B., Restrepo, A., and Pugh, R. P. Long term management of lymphocytic lymphomas and leukemias with intermittent glucocorticoid therapy. Presented at IX Congress of the International Society of Hematology, Mexico City, 1962.

19LL201

Metals Metabolism and Medical Radioisotope Development

These studies have the combined objectives of (1) developing improved radioactive materials for medical diagnosis and therapy and (2) elucidating mechanisms of certain toxic effects of lanthanons. During the year, the work with ^{68}Ga has progressed rapidly and this nuclide has shown great promise as a practical diagnostic agent. It appears that with different chemical forms it may prove useful in several different diagnostic applications. The work so far has been mainly on its deposition in bone; work on a colloid for studies of the reticuloendothelial system has been initiated also.

The lanthanon work has included an enzyme approach and new studies using disc electrophoresis to clarify the effect of these elements, in stable form, on serum proteins. All this is part of the work on characterization of the rare-earth-induced fatty liver.

The study by Likuski, Debons, and Cloutier, entitled *The Effect of Glucose Inhibitors on gold-thioglucose-induced Hypothalmic Obesity in Mice*, differs from most of the reports in this book in that most of the work on it was not done at the Medical Division. However, Roger Cloutier, of our Medical Physics group, has played a significant role in this, and it is an example of collaborative work in the Division.

Basic Studies of Gallium Distribution

R. L. Hayes, B. L. Byrd, and J. E. Carlton

An intensive basic study of the use of ^{68}Ga as a diagnostic agent for the detection of bone lesions has been carried out during the past year. This study was prompted by a recent observation that gallium given in the citrate form not only deposits very rapidly in active bone but at the same time clears readily within a few hours from other tissues when an adequate amount of gallium is administered. Gallium-68 has several properties that recommend it as a diagnostic agent. It has a short half-life (68 min.), decays by positron emission, and more important is obtained as the daughter of a long-lived parent radionuclide (^{68}Ge; $t_{1/2}$ = 280 days). Gallium-68 is readily separated from ^{68}Ge with the use of a Brookhaven type generator.

In our past work with ^{67}Ga we showed that a pronounced effect on tissue distribution was produced by the amount of stable carrier administered. This effect has been reinvestigated at time intervals after administration suitable to the use of ^{68}Ga (1 to 2 hr.). The results of this study are indicated in *Fig. 33*. With sufficient carrier gallium, the ratio of bone to blood and bone to muscle approaches 25:1 and 100:1. As the dose administered approaches the carrier-free level, the distribution of gallium becomes diffuse. The distribution is not affected by the amount of excess citrate administered. The same diffuse, relatively uniform pattern of tissue concentrations is also obtained when carrier-free ^{68}Ga is administered in the chloride form.

The gallium concentration at various times after administration at a level of 5 mg/kg is shown in *Fig. 34* for selected tissues. The bone deposition reaches a maximum value within 1 hr while the other tissues continue to clear.

Gallium-68 administered in the ethylenediaminetetra-acetic acid (EDTA) form is rapidly excreted in the urine; deposition in bone and tissues other than the kidneys and urinary bladder is insignificant.

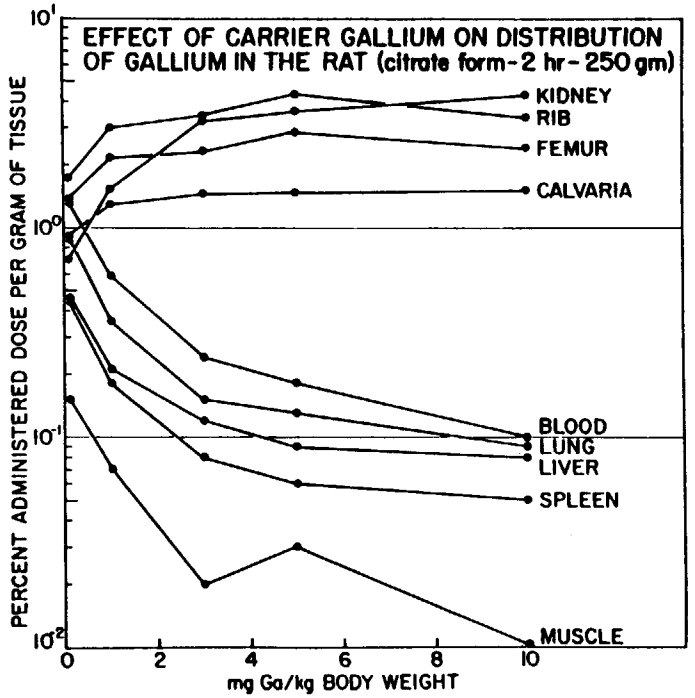

Fig. 33. Effect of carrier gallium on distribution of gallium citrate 2 hr after administration in 250 g rats.

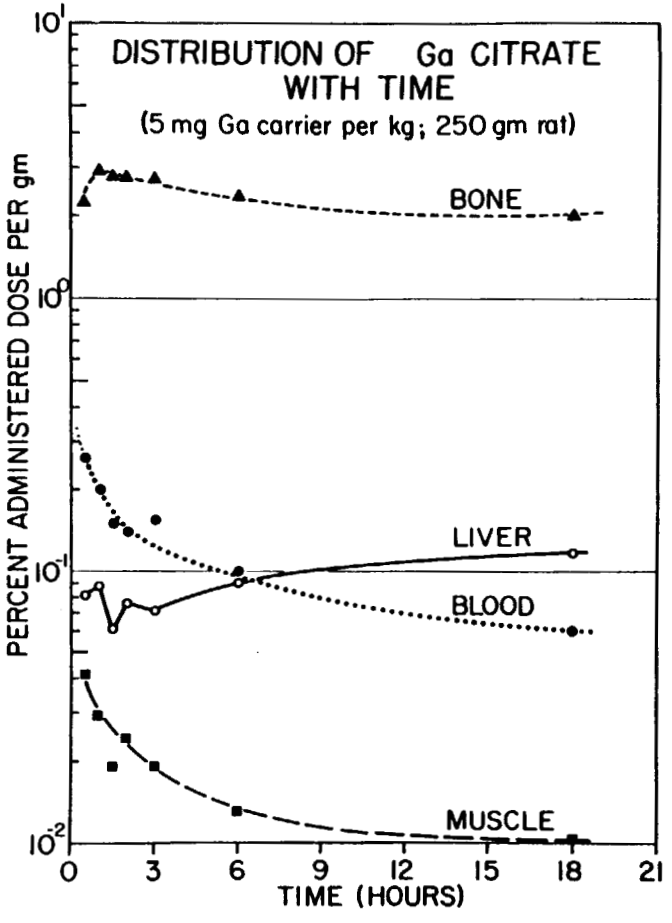

Fig. 34. Distribution of gallium citrate (5 mg Ga/kg) in the rat with time.

Gallium-68 in the EDTA form is now being investigated as a diagnostic agent for kidney studies.

Since the deposition of gallium in bone is dependent on its availability in the ionic form, generator-produced ^{68}Ga (EDTA form) must be converted into the citrate or another suitable form before use in bone scans. Animal studies have shown that this is readily accomplished by exchange when sufficient ionic carrier gallium is added to mask the presence of EDTA. The exchange must be promoted by heat and low pH, however.

1027763

Colloidal Hydrous Ferric Oxide as an Agent for Scanning of the Reticuloendothelial System

R. L. Hayes, J. E. Carlton, and B. L. Byrd

The precipitation of ferric hydroxide in the presence of other substances that would normally be soluble often results in a partial or complete removal of such substances from solution through a process of adsorption and coprecipitation. For this reason, such a precipitation procedure is often used in radiochemical separations; ferric hydroxide acts as a scavenger. Ferric hydroxide colloids are quite stable and are easily and rapidly prepared by hydrolysis of dilute solutions of ferric salts through heating. It seemed possible that use might be made of these properties to produce radionuclide preparations for the scanning of bone marrow, liver, and spleen. If a short half-lived radionuclide is used its long-term retention by the colloid is not of importance beyond its useful decay period. Initial tests in animals of a ^{68}Ga-labeled hydrous ferric oxide colloid preparation have given very favorable results. The use of other radionuclides in such preparations is being investigated, since the technique may have rather broad applications.

Figure 35 shows a scan of a rabbit made with a ^{68}Ga-labeled colloid. The liver, spleen, and bone marrow are quite clearly defined. Tissue assay studies show bone marrow to bone, and bone marrow to liver concentration ratios of approximately 50:1 and 1:1. Tissues other than bone marrow, liver, and spleen, contain little or no activity. The colloid preparation is formed in the presence of carrier-free ionic ^{68}Ga by controlled heating of a dilute solution of ferric chloride. Gelatin is added as a stabilizing agent and the pH is adjusted with sodium acetate. The effect of the rate of heating (which affects the particle size) on distribution is now under investigation.

The Laboratory Evaluation of Rats Progressing Through a Fatty-liver Cycle Caused by Cerium

G. C. Kyker, J. J. Rafter, V. Z. Holten, A. Webb, B. Chastain, and M. K. Ballenger

Our studies of the metabolic effects of rare earths in experimental animals have emphasized primarily the fatty liver in rats caused by intravenous doses of cerium, and various physiologic and nutritional factors that prevent or effect this acute but transient response. Se-

102716h

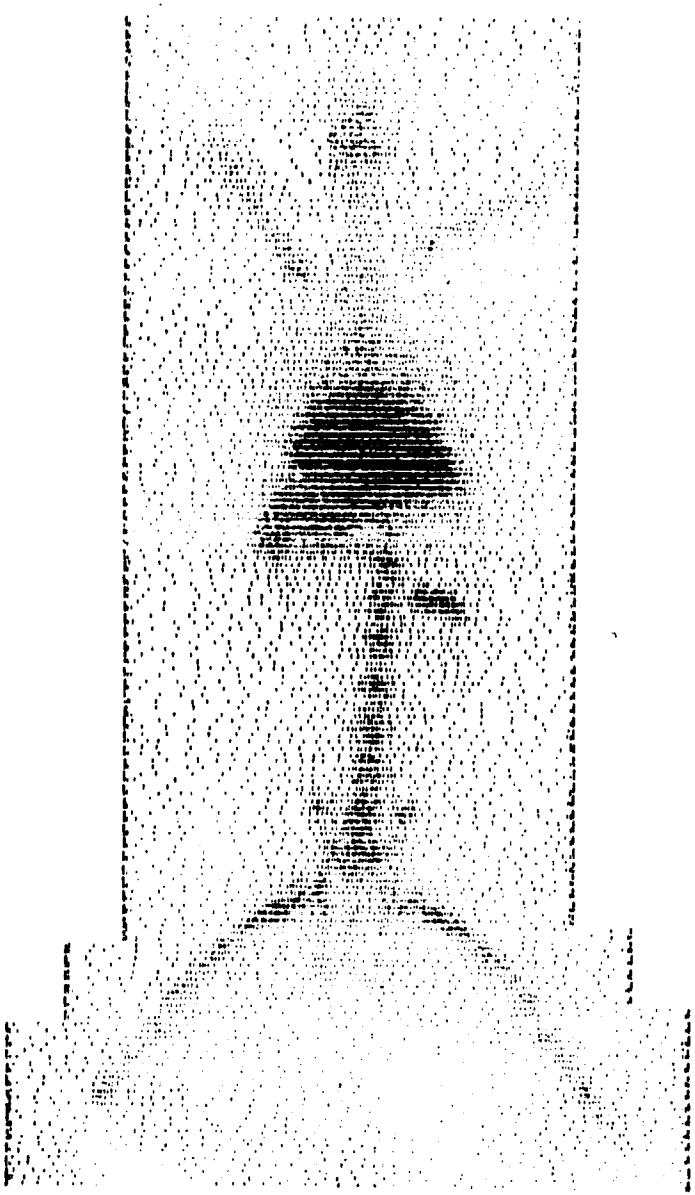

Fig. 35. Gallium-68 labeled hydrous ferric oxide colloid scan of a rabbit showing liver, spleen, and bone marrow. Scan made 1 hr after administration of 2.5 mg Fe/kg.

lected other measurements have been made to reflect the general scope of related effects.

Series of female Carworth Farms Nelson (CFN) rats were examined with the use of a battery of laboratory procedures at various intervals after intravenous doses of cerium. The measurements included total liver lipids, serum electrolytes, serum enzymes, serum bilirubin, hematocrit, serum protein patterns (electrophoresis, gel filtration), urinalysis, and other miscellaneous tests. In the first series of rats, the standard dose of cerium (2 mg/kg as the chloride) appeared more toxic than in some earlier experiments. This observation was made in animals produced in the laboratory breeding colony that has been maintained continuously for the past seven years. A lower-dose series, 1 mg Ce/kg, was added for comparison. Also, two other series of freshly purchased CFN animals were used to duplicate both dose levels used in the Institute-produced stock.

The results showed differences for the two dose levels and, in general, close agreement between the old and fresh stock of animals. Typical fatty livers gave an accumulation of 2.5 to 3 times the normal total liver lipids at two to three days after 2 mg Ce/kg. The lower dose, 1 mg/kg, caused only a slight increase in liver lipids. No detectable differences occurred in the serum levels of chlorides, sodium, or potassium in either group except that in the higher dose series potassium showed an elevation within 6 hr that continued through three days.

Serum enzyme measurements included (1) glutamic-pyruvic transaminase (SGPT), (2) glutamic-oxaloacetic transaminase (SGOT), (3) isocitric dehydrogenase (ICD), and (4) lactic dehydrogenase (LDH). The first, SGPT, increased 10 to 12 times normal at the lower dose level and more than 50 times at the higher dose within 48 hours. The second, SGOT, showed no difference in the lower-dose series at any of six intervals after treatment through the peak of fatty infiltration (72 hr). This enzyme did, however, show a difference between the old and fresh stock of CFN rats that received the higher dose of 2 mg/kg. The maximum serum SGOT level occurring at 48 hr, was about 100 and 50 times normal in the old and fresh stock of CFN rats, respectively. Both dehydrogenases, ICD and LDH, showed no significant increase in the 1-mg/kg series and both increased sharply to reach a maximum at 48 hr in the 2-mg/kg series. The ICD increased as much as 250- to 300-fold in both the old and fresh stock animals. The LDH showed a larger relative increase in the old stock animals, about 50 times normal compared to a 15-fold increase in the fresh stock.

Serum bilirubin remained normal after the lower dose but after

the higher dose peaked sharply at 48 hr and came down to normal at 72 hr. The hematocrit increased sharply from 0.45 to 0.65 during induction of fatty infiltration to its peak at 48 hr; variations between individual animals were quite small.

Serum proteins showed little change by electrophoresis (cellulose acetate, microzone; polyacrylamide, disc method). Gel filtration, however, showed consistent differences. Separation on Sephadex G-200 gave four fractions, the first and last of which were unchanged. The second and third fractions showed compensating changes in amount, the second decreasing and the third increasing at 48 to 72 hr *(Fig. 36)*.

Results by qualitative urinalysis were negative (protein, bilirubin, blood, ketone bodies, reducing sugar, pH). Quantitative interpretation of results by disc and vertical gel electrophoresis continues in progress. The results indicate that no renal impairment occurs and suggest that further studies should consist of application of a wide spectrum of representative liver function tests; these should afford new insight into the physiologic basis of the acute metabolic effect that produces these gross changes in the livers of rats.

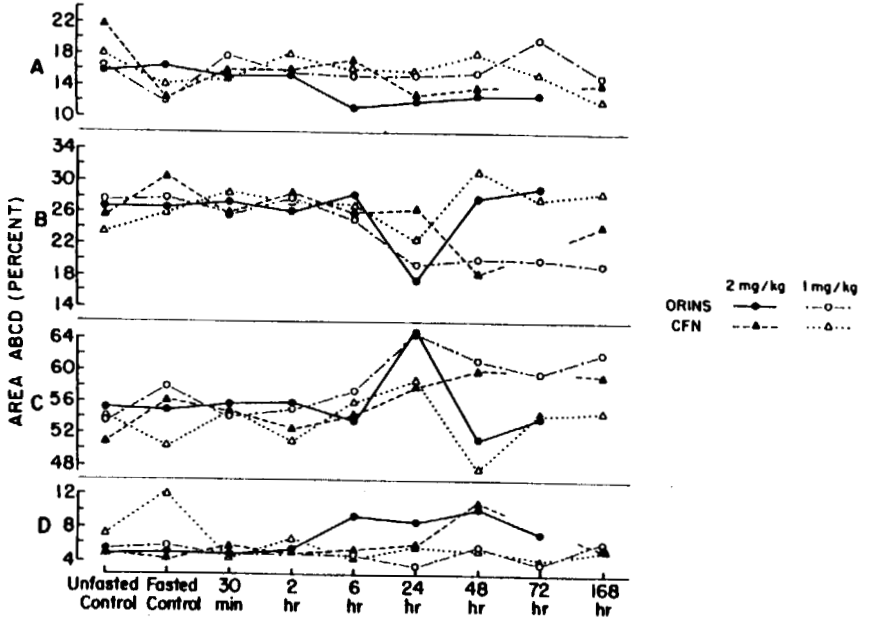

Fig. 36. Sephadex G-200 fractions of rat serum after $CeCl_2$ administration. Results are expressed as percentage of area under transmittance curves from absorptiometric measurement at 2537 A.

1027765

Production of Lanthanide Radioisotopes for Clinical Use

G. C. Kyker and J. J. Rafter

The studies of bone-marrow scanning in animals summarized last year[1] made use of an equilibrium mixture of ^{144}Ce and ^{141}Pr as a convenient and available long-lived lanthanide tracer. We presumed, based on other experience, that the results would serve as an accurate prototype of other lanthanide radioisotopes selected for suitability in clinical work. After consideration of about a score of short-lived gamma-emitting lanthanide radioisotopes, two were selected for verifying measurements and possible use in hospital patients.

The two selected radioisotopes are ^{165}Dy ($t_{1/2}$, 165 min) and ^{159}Gd ($t_{1/2}$, 18 hr). Availability of highly enriched stable isotopes, ^{161}Dy and ^{158}Gd, made the reactor production of the selected radioisotopes quite practical. Preparations showed high radiochemical purity and specific activity. In a neutron flux of 10^{13}, Low Intensity Testing Reactor (LITR) of Oak Ridge National Laboratory, the calculated maximum yield of ^{165}Dy and ^{159}Gd is about 2 curies and 3.75 millicuries per milligram of enriched ^{164}Dy and ^{158}Gd, respectively; similarly for a flux of 2×10^{14}, Oak Ridge Reactor (ORR) of Oak Ridge National Laboratory, the respective maximum yields are about 40 curies and 75 millicuries per milligram of the enriched target. In practice, 10 mg of enriched ^{164}Dy (about 90%) as the oxide was bombarded 30 min in LITR (estimated yield, 2,400 millicuries) and processed 6 hr later in about 5 ml 1.0 N hydrochloric acid. At this point about 80 millicuries per milliliter remained for dose preparation and animal studies. Similarly 10 mg of enriched ^{158}Gd (about 95%) as the oxide was in the ORR 48 hr, yielding about 650 millicuries at the time of discharge. Processed later the same day as convenient and delivered the next 24 hr after removing from the reactor, the 1.0 N HCl preparation (5 ml) contained about 50 millicuries per milliliter. Evaluation of purity by their rate of decay and by their gamma-ray spectrum obtained with a 400-channel analyzer showed each to be essentially free of radiochemical contaminants.

Colloidal citrated hydrous oxide sols of dysprosium and of gadolinium labeled with their respective tracers were prepared in the same way as had been those of cerium in previous studies.[1] Used for scanning bone marrow in rabbits, gadolinium gave results equal to or better than those with cerium. It was believed that for clinical use of the dysprosium preparation it would be necessary to allow for significant decay after administration, because better localization for scans

was obtained 4 to 6 hours after intravenous doses of the sol. The production of ^{159}Gd was carried out several times for preliminary evaluation in hospital patients. (See Clinical Studies, page 90).

REFERENCE

1. Kyker, G. C. and Rafter, J. J. Scanning of bone marrow in animals. *In:* Research Report for 1964, Medical Division, Oak Ridge Institute of Nuclear Studies, USAEC Report ORINS-49, pp. 68–69.

Effects of Lanthanide Chlorides on Selected Enzymes

*V. Z. Holten, G. C. Kyker, and M. Pulliam**

This study was undertaken as part of an effort to explain the profound metabolic effects caused by rare-earth chlorides in rats and certain other laboratory animals. An explanation at the level of a molecular mechanism must take under consideration the heavy-metal effect of these elements on metabolic enzymes. Enzymes selected for *in vitro* measurements include (1) aldolase and lactate dehydrogenase, (2) glucose 6-phosphate dehydrogenase, and (3) isocitrate and malate dehydrogenases to represent equilibrium reactions in (1) the Krebs cycle, (2) the hexose monophosphate shunt, and (3) the tricarboxylic acid cycle.

The metals used in the measurements included yttrium and the lanthanides: lanthanum, cerium, praseodymium, neodymium, gadolinium, dysprosium, holmium, and lutetium. The first four of the lanthanides in the order listed cause acute fatty liver in rats and the last four do not. In these *in vitro* measurements all the metals inhibited lactate, isocitrate and glucose 6-phosphate dehydrogenases, and the reverse direction of glutamate dehydrogenase; the forward direction of the latter was inhbited only by lanthanum and by cerium, as well as by mercury which was used for comparison. The degree of inhibition appeared random for the various combinations of enzyme and lanthanide and ranged widely from very slight to almost complete inhibition. The results suggest that the lanthanide inhibition of selected enzymes in the *in vitro* situation is a typical heavy-metal effect.

*Summer Student Trainee, Birmingham Southern College.

1027166

The Effect of Glucose Inhibitors on Gold-thioglucose-induced Hypothalamic Obesity in Mice*

H. J. Likuski,† A. F. Debons,† and R. J. Cloutier

The syndrome of hyperphagia and obesity in mice following the administration of gold-thioglucose was first reported in 1949.[1] It was later established that gold-thioglucose caused damage to hypothalamic neurones known to be associated with satiety in normal feeding behavior. The administration of other gold compounds, such as gold-thiogalactose and gold-thiomalate, failed to induce comparable hypothalamic damage and obesity. These observations support the glucostatic theory of the regulation of food intake. In an earlier study, Debons *et al.*[2] obtained further evidence in support of this theory by demonstrating the full extent of gold deposition at the site of the hypothalamic lesion. The amount of gold was determined by neutron activation analysis and its location by autoradiography of tissue sections. The Division has a continuing interest in both these techniques, hence, this collaborative effort.

It is well established that 2-deoxy-D-glucose and 2-amino-2-deoxy-D-glucose inhibit the intracellular transfer and oxidation of glucose in peripheral and central nervous tissue and raise blood glucose levels. The dose requirement of 2-amino-2-deoxy-D-glucose needed to inhibit glucose metabolism has been shown in *in vivo* studies to be attributed to steric factors which are known to play an important role in the rates of entry or metabolism of these glucose analogs or both. Phosphorylated derivatives of these glucose antimetabolites are unable to serve as metabolic substrates for either the phosphohexosisomerase or glucose-6-phosphate reaction.

Female CBA mice were used to determine the effect of the glucose inhibitors, 2-deoxy-D-glucose and 2-amino-2-deoxy-D-glucose on gold-thioglucose-induced hypothalamic obesity. A marked inhibition in obesity resulted when gold-thioglucose was administered to mice receiving 2-deoxy-D-glucose (1 g/kg body weight) or 2-amino-2-deoxy-D-glucose (3 g/kg body weight). Deposits of gold at the site of the hypothalamic lesion were readily observed after neutron activation

*This project was begun as a collaborative study with A. F. Debons when he was affiliated with the University of Alabama Medical School. It is supported, in part, by Public Health Service Grants AM-07037 and AM-08667 to the Downstate Medical Center, New York.

†Radioisotope Service, Veterans Administration Hospital, and State University of New York, Downstate Medical Center, Brooklyn, N. Y.

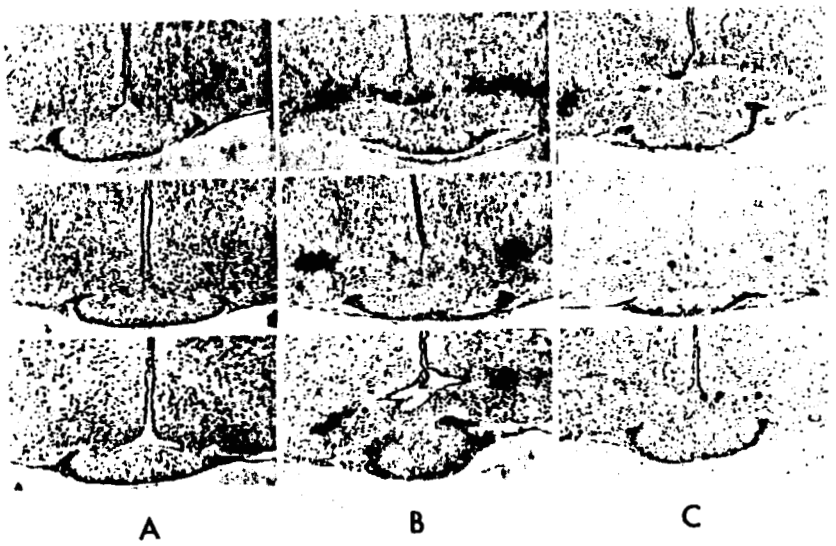

Fig. 37. Typical autoradiograms illustrating hypothalamic localization of ^{198}Au: Upper Row: A, control; B, gold-thioglucose-treated obese; C, gold-thioglucose-treated nonobese. Middle Row: A, 2-deoxy-D-glucose-treated control; B, 2-deoxy-D-glucose- and gold-thioglucose-treated obese; C, 2-deoxy-D-glucose- and gold-thioglucose-treated nonobese. Lower Row: A, 2-amino-2-deoxy-D-glucose-treated control; B, 2-amino-2-deoxy-D-glucose- and gold-thioglucose-treated obese; C, 2-amino-2-deoxy-D-glucose- and gold-thioglucose-treated nonobese.

using autoradiographic techniques in all gold-thioglucose-treated animals *(Fig. 37)*. These deposits were more extensive in obese than in nonobese mice. The results indicate that 2-deoxy-D-glucose and its amino analog interact with cells in the "satiety center" to inhibit gold-thioglucose-induced hypothalamic damage and obesity. It was also noted that a hyperphagic response occurred during the administration of 2-deoxy-D-glucose. This finding supports further the contention that 2-deoxy-D-glucose interacts with cells in the "satiety center."

L9LL701

REFERENCES

1. Brecher, G. and Waxler, S. H. Obesity in albino mice due to single injections of gold-thioglucose. Proc Soc Exp Biol Med 70, 498–501, 1949.
2. Debons, A. F., Silver, L., Cronkite, E. P., Johnson, H. A., Brecher, G., Tenzer, D., and Schwartz, I. L. Localization of gold in mouse brain in relation to gold thioglucose obesity. Amer J Phys 202 (4): 743–750, 1962.

Therapy with Radiation

The objective is to develop and assess improved methods of therapy with radiation, both internal and external. Main areas of effort are (1) total-body irradiation in the treatment of certain kinds of cancer and especially lymphoma, polycythemia, and the leukemias; (2) local external radiation therapy in selected patients, applying experimental methods that have been suggested by results in animal studies; and (3) continued study and follow-up on patients given internal radioisotopes for therapy. This includes a long-range study on the use of ^{131}I for cancer of the thyroid.

Total-body Irradiation Program

D. A. White, C. L. Edwards, F. V. Comas, G. A. Andrews, and R. M. Kniseley

An ongoing major project of the Division has been the study of total-body irradiation in human beings who have disseminated malignant disease, especially leukemia and lymphoma. For many years therapists have controlled with some success the progression of certain disorders by giving "spray" irradiation with X-ray machines or internally administered radiation, particularly with ^{32}P. The evaluation and comparison of various therapies have been complicated by differences in fractionations of doses, energy of the treatment beams, and uniformity of exposures to various parts of the body.

Our objective has been to improve the use of total-body irradiation by determining the best selection of patients, radiation dose, and dose rate. Uniform protocols have been established so that careful assessments of the patients can be carried out through an adequate follow-up period.

An earlier phase of the study dealt with marrow-graft attempts, mostly in patients with acute leukemia who were given high exposures (300 to 900 R). Because of the difficulties and failures experienced by us and by other groups, the marrow-graft attempts have been halted until new experimental information suggests a more promising pathway. The use of lower exposures (50 to 100 R) has been continued

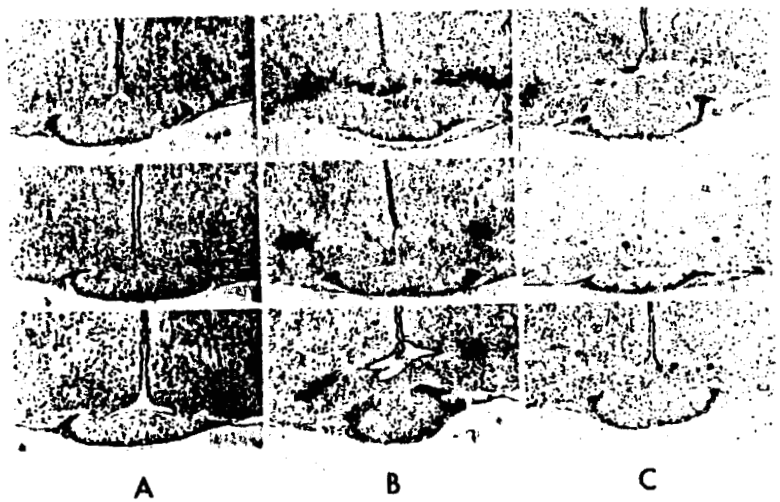

Fig. 37. Typical autoradiograms illustrating hypothalamic localization of ^{198}Au: Upper Row: A, control; B, gold-thioglucose-treated obese; C, gold-thioglucose-treated nonobese. Middle Row: A, 2-deoxy-D-glucose-treated control; B, 2-deoxy-D-glucose- and gold-thioglucose-treated obese; C, 2-deoxy-D-glucose- and gold-thioglucose-treated nonobese. Lower Row: A, 2-amino-2-deoxy-D-glucose-treated control; B, 2-amino-2-deoxy-D-glucose- and gold-thioglucose-treated obese; C, 2-amino-2-deoxy-D-glucose- and gold-thioglucose-treated nonobese.

using autoradiographic techniques in all gold-thioglucose-treated animals *(Fig. 37)*. These deposits were more extensive in obese than in nonobese mice. The results indicate that 2-deoxy-D-glucose and its amino analog interact with cells in the "satiety center" to inhibit gold-thioglucose-induced hypothalamic damage and obesity. It was also noted that a hyperphagic response occurred during the administration of 2-deoxy-D-glucose. This finding supports further the contention that 2-deoxy-D-glucose interacts with cells in the "satiety center."

REFERENCES

1. Brecher, G. and Waxler, S. H. Obesity in albino mice due to single injections of gold-thioglucose. Proc Soc Exp Biol Med 70, 498–501, 1949.
2. Debons, A. F., Silver, L., Cronkite, E. P., Johnson, H. A., Brecher, G., Tenzer, D., and Schwartz, I. L. Localization of gold in mouse brain in relation to gold thioglucose obesity. Amer J Phys 202 (4), 743–750, 1962.

1027168

Therapy with Radiation

The objective is to develop and assess improved methods of therapy with radiation, both internal and external. Main areas of effort are (1) total-body irradiation in the treatment of certain kinds of cancer and especially lymphoma, polycythemia, and the leukemias; (2) local external radiation therapy in selected patients, applying experimental methods that have been suggested by results in animal studies; and (3) continued study and follow-up on patients given internal radioisotopes for therapy. This includes a long-range study on the use of ^{131}I for cancer of the thyroid.

Total-body Irradiation Program

D. A. White, C. L. Edwards, F. V. Comas, G. A. Andrews, and R. M. Kniseley

An ongoing major project of the Division has been the study of total-body irradiation in human beings who have disseminated malignant disease, especially leukemia and lymphoma. For many years therapists have controlled with some success the progression of certain disorders by giving "spray" irradiation with X-ray machines or internally administered radiation, particularly with ^{32}P. The evaluation and comparison of various therapies have been complicated by differences in fractionations of doses, energy of the treatment beams, and uniformity of exposures to various parts of the body.

Our objective has been to improve the use of total-body irradiation by determining the best selection of patients, radiation dose, and dose rate. Uniform protocols have been established so that careful assessments of the patients can be carried out through an adequate follow-up period.

An earlier phase of the study dealt with marrow-graft attempts, mostly in patients with acute leukemia who were given high exposures (300 to 900 R). Because of the difficulties and failures experienced by us and by other groups, the marrow-graft attempts have been halted until new experimental information suggests a more promising pathway. The use of lower exposures (50 to 100 R) has been continued

principally in patients with chronic leukemia and lymphomas, and a few patients with acute leukemia have been given higher doses without marrow-graft attempts. These investigations, in addition to providing information of value to the field of radiotherapy, also as a by product have given data needed by the Atomic Energy Commission and the National Aeronautics and Space Administration on radiation [illegible]. A summary of the program to date is given in *Table 10.*

[illegible] improvement. Some experience a marked subjective improvement such as increased exercise tolerance and feeling of well-being. More commonly, the improvement can be characterized as moderate, and only a few show no subjective improvement. The objective responses, regression of palpable disease (lymphadenopathy, hepatosplenomegaly), are moderate in the majority of patients, and relatively few patients fail to show improvement. As might be anticipated, additional therapy is required with the passage of time. Depending on the clinical features, repeat total-body irradiation may be given or, if indicated, ^{32}P, chemotherapy, corticosteroids, or local radiotherapy may be required for the optimum management of the patient. In general, we find the benefits of low-dosage (50 to 100 R) total-body irradiation to be comparable to conventional forms of therapy for these diseases.

Our experience with polycythemia vera has to date included five patients who have received 100 R. Three were women and two were men. Their ages ranged between 55 and 73 years. Three had received previous ^{32}P therapy, and one also had been treated with busulfan. Three patients were symptomatic, one was asymptomatic, and the other patient's symptoms were caused predominantly by cardiac and gastrointestinal diseases. The patients with symptoms had moderate to pronounced subjective improvement by the third week after total-body irradiation. The most significant improvement was observed in a patient with thrombocytosis and severe hemorrhagic phenomena. Her bleeding tendency disappeared as her platelet counts fell toward normal values *(Fig. 38).* In four patients, hepatomegaly and splenomegaly decreased during the first four weeks after irradiation. The regression in spleen size was greater than the reduction in liver enlargement. All patients had a decrease in peripheral blood values during the third to fifth week after treatment *(Fig. 39).* Four patients had a slight reduction in red-cell values. In three of four patients with leukocytosis, the white blood counts returned to a normal range. All patients had a significant decrease in platelet counts. In four patients,

all peripheral blood values had returned to pretreatment levels after three to four months. An appreciably greater and more sustained decrease in the leukocyte and platelet counts was observed in a patient who received 5 millicuries of ^{32}P three months after total-body irradiation. Seven months later, white blood counts and platelet counts were lower than at any time after total-body irradiation. Erythrocyte values were more difficult to evaluate because it was considered desirable to place the patient on oral iron therapy before treatment with ^{32}P. It is our impression that 5 millicuries of ^{32}P may have a greater myelosuppressive effect than 100 R total-body irradiation in patients with polycythemia vera.

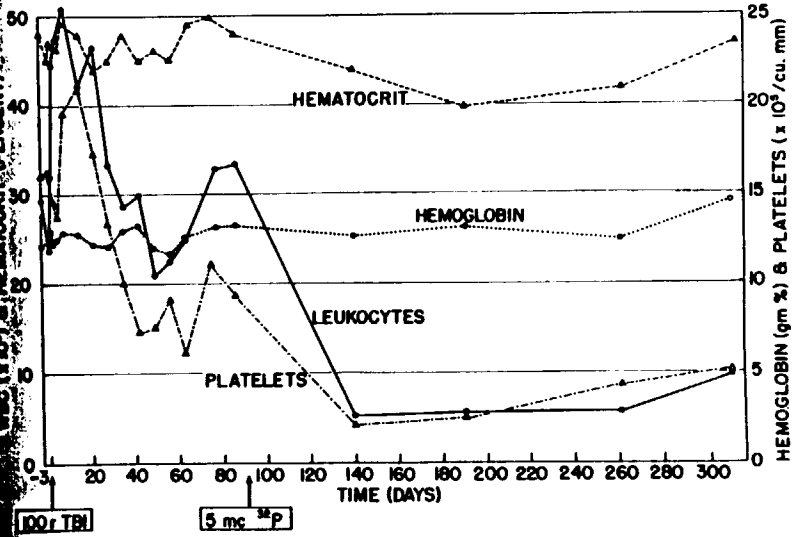

Fig. 38. *The patient, a woman, age 73, with polycythemia vera complicated by thrombocythemia and an associated bleeding tendency responded well to 100 R total-body irradiation with prompt decrease in platelet values and relief of hemorrhagic phenomena. On day 92 after the irradiation, 5 millicuries of ^{32}P were given because of ascending blood values. The response of platelet and leukocyte values, though slower, was quite pronounced, and persisted for a longer period.*

0027769

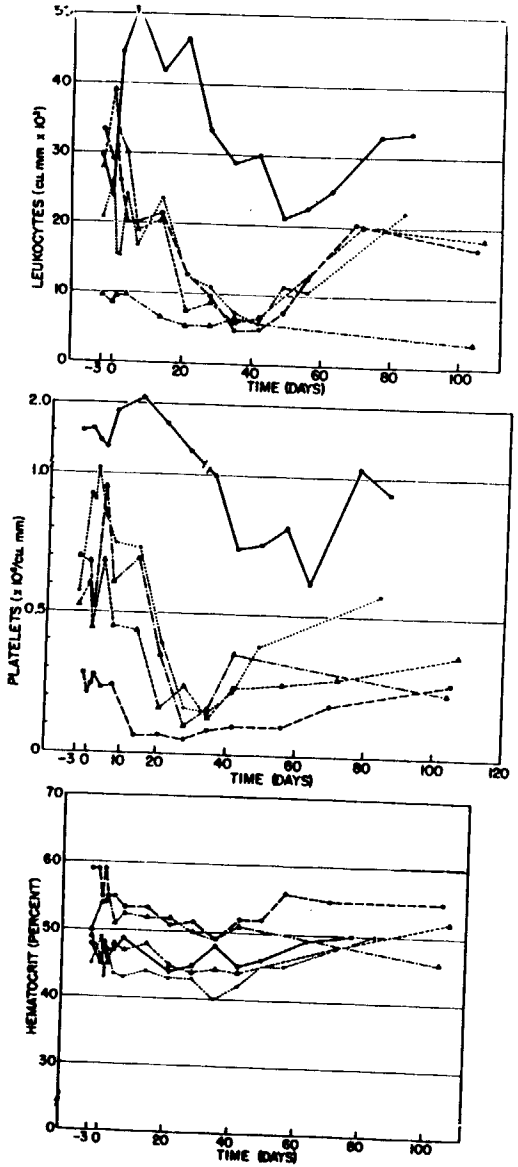

Fig. 39. Blood values after 100 R total-body irradiation in five patients with polycythemia vera. In most patients 100 R appears inadequate to produce a persistent remission, as judged by red-cell values.

1027770

TABLE 10
Total-body Irradiations Through 1964

	50R	100R	200R	3-900R	Total
Acute leukemia	2	4	1	19	
Chronic lymphocytic leukemia	13	12	0	0	
Chronic granulocytic leukemia	7	1	0	1	
Lymphosarcoma	5	20	0	0	
Hodgkin's disease	1	2	0	1	
Polycythemia vera	0	1	0	0	
Miscellaneous neoplasms	0	3	1	3	
	28	43	2	24	97
Total-body Irradiations in 1965					
Acute leukemia	0	1	0	1	
Chronic lymphocytic leukemia	0	5	0	0	
Chronic granulocytic leukemia	1	1	0	0	
Lymphosarcoma	0	2	0	0	
Multiple myeloma	0	0	1	0	
Polycythemia vera	0	4	0	0	
	1	13	1	1	16
				Total	113

Variations in Leukocyte Alkaline Phosphatase Scores After Radiation Therapy in Some Blood Dyscrasias

G. L. Humason, C. C. Lushbaugh, and F. V. Comas

A modification of the histochemical method of Kaplow[1] for leukocyte alkaline phosphatase (LAP) was devised to improve the histochemical quantitation of this enzyme for scoring. This modification produces green leukocytic cytoplasm when little or no phosphatase reacts and brilliant scarlet granules when phosphatase activity is

high. This distinct contrast allows easy scoring using the semiquantitative scale of one to four plus activity. Modifying technical factors such as incubation temperatures and optimal duration, substrate concentrations and pH, or poisoning by impure solutions were rigidly controlled.

Buffy coats were obtained from 13 patients before and at intervals after 100 R total-body irradiation,[2] and similarly from 11 patients with chronic myelogenous leukemia (CML) treated with fractionated radiotherapy (up to 1500 R) to the spleen (7 cases) and to the liver (4 cases) for comparative purposes.[3]

Analysis of LAP scores suggested that changes in them correlated with clinical improvement. For example, two patients with CML treated with 100 R total-body irradiation showed little clinical improvement, and no significant increase in their typically low LAP score (28 and 30). Local splenic (but not hepatic) irradiation, on the other hand, produced a progressive increase in LAP over 2 to 3 months that persisted at normal levels for several months in five of seven patients that showed good hematologic and clinical improvement. Total-body irradiation with 100 R, on the other hand, was followed by a steadily increasing LAP score to pathologically high levels in the three patients with chronic lymphocytic leukemia and in three patients with lymphosarcoma. In two out of three cases with polycythemia rubra vera, total-body irradiation caused a lowering of initially high scores to normal levels within 30 days.

In general these LAP scores after radiation therapy tended to change toward the normal score (about 130) whether the initial score was pathologically high (150 to 350) or low (0 to 13). Although the mechanisms whereby radiation affects these changes are not known, LAP scoring appears to be a useful adjunct in appraisal of radiotherapeutic effectiveness.

REFERENCES

1. Kaplow, L. S. Cytochemistry of leukocyte alkaline phosphatase. Amer J Clin Path 39, 439–449, 1963.
2. White, D. A., Edwards, C. L., Comas, F. V., Andrews, G. A., and Kniseley, R. M. Total-body irradiation program. This report, pp. 75–78.
3. Comas, F. V. In progress.

1027771

Immunotherapy of Acute Leukemia: An Experimental Approach

C. L. Edwards, C. C. Congdon, N. Gengozian, H. Vodopick, and G. A. Andrews*

The role of the immune mechanism in the control of neoplastic disease in man remains the object of intensive investigation. Antigenic differences between normal and autochthonous neoplastic tissue has been demonstrated in many experimental tumors. This differential permits the production of tumor-specific antibodies, some of which can be demonstrated by serological techniques. A tumor-suppressive immunologic effect has been elicited against certain murine tumors, with the use of thoracic duct lymphocytes from rats previously immunized against the tumor.[1,2] Similarly an antileukemic effect has been demonstrated for isologous hematopoietic tissue taken from an immunized animal.[3]

In an effort to determine whether an analogous situation exists for human leukemia, we have begun a study patterned after the experiment of Delorme and Alexander using thoracic duct lymphocytes from an immunized homologous donor. Our protocol calls for (1) obtaining leukemic bone-marrow cells from a patient with untreated acute leukemia; (2) killing the leukemic cells with 10,000 R; (3) injection of the irradiated leukemic cells into a normal volunteer donor, in whom 2 weeks or more is allowed for an immune response; (4) temporary treatment of the patient with conventional chemotherapy to suppress the population of leukemic cells; and (5) cannulation of the donor's thoracic duct with collection and separation of the donor lymphocytes and infusion into the patient.

The anticipated hazards to the patient include (1) deprivation of total continuous conventional therapy; (2) antiphylactoid or other immediate reaction to the infusion of lymphocytes; and (3) a graft versus host reaction (secondary disease). Possible hazards to the donor include immediate reaction to the injected cells; risk inherent in a surgical procedure (cannulation of thoracic duct); depletion of immunoglobulins and other constituents of the thoracic duct lymph; and conceivably the transmission of leukemia, although efforts by others to transmit leukemia even using viable cells have been unsuccessful.

One patient, a 3-year-old boy with acute lymphoblastic leukemia was treated under this protocol *(Fig. 40)*. His mother served as the donor of lymphocytes. Two billion bone-marrow cells (90% lympho-

*Biology Division, Oak Ridge National Laboratory.

blasts) were irradiated *in vitro* and injected intramuscularly into the mother. The patient was treated with Methotrexate and prednisone during the immunizing period of 17 days after which the Methotrexate was discontinued and the prednisone dose was tapered. A total of 1.6×10^{10} thoracic-duct lymphocytes was collected and infused into the patient over a 4-day period.

The donor experienced moderate postoperative discomfort but little disability. Although there was a minor drop in the serum albumin, no quantitative change was noted in the serum globulins or peripheral leukocytes. The patient experienced only moderate fever during the infusion period. His bone marrow, which had been blastic, was hypocellular at the onset of the infusion, and became normal within two weeks after infusion. Four weeks after the infusion the patient developed a transient maculopapular eruption. Nothing otherwise resembled a secondary disease type of reaction. He remained clinically in remission without further therapy until at 16 weeks his

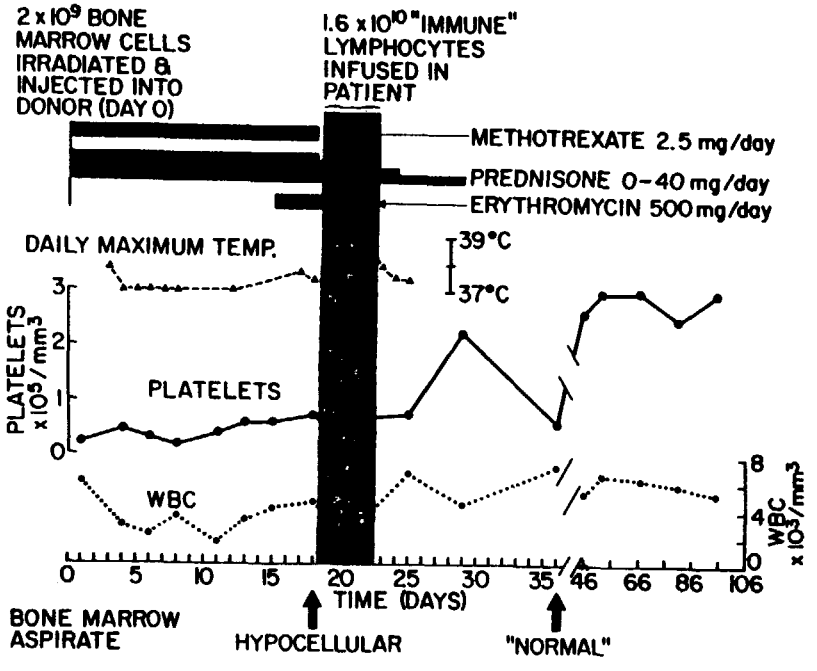

Fig. 40. Summary of the clinical course of a patient treated with "immune" thoracic-duct lymphocytes.

1027772

bone marrow revealed a predominance of lymphoblasts resembling the original aspirate.

Serologic tests failed to exhibit antibody reaction between the mother's serum and the patient's circulating (normal) leukocytes. More refined techniques for detecting and measuring the immune response are planned for subsequent efforts.

REFERENCES

1. Delorme, E. J., and Alexander, Peter. Treatment of primary fibrosarcoma in the rat with immune lymphocytes. The Lancet 2: 171–120, 1964.
2. Woodruff, M. F. A., Symes, M. O., and Anderson, N. F. The effect of intraperitoneal injection of thoracic duct lymphocytes from normal and immunized rats in mice inoculated with Landshutz ascites tumor. Brit J Cancer 17 (3), 482–486, 1963.
3. Mathe, G. Secondary syndrome: A stumbling block to the treatment of leukemia by whole-body irradiation and transfusion of allogenic hematopoietic cells. *In* Diagnosis and Treatment of Acute Radiation Injury, World Health Organization, International Documents Service, New York, 1961.

Lipid Embolism to the Brain After Lymphography[1]

B. Nelson, E. A. Rush,* M. Takasugi, and J. Wittenberg†

Lymphography has been used at the Division to determine node involvement by malignant lymphoma. This permits appropriate radiation therapy and, because the oily radiopaque medium remains in the nodes for months, the effect of local or systemic treatment can be observed. Even with accepted precautions, rare respiratory deaths have occurred in patients with pulmonary disease, but fatal cerebral embolism after lymphography has not previously been reported. Many medical procedures of great value carry slight but definite risk. On the rare occasions when a procedure causes unfortunate reactions, it is important to describe and document the event for the benefit of physicians and patients everywhere.

The death described here probably resulted from injection of what proved to be too much ethiodized oil into a lymphatic system with a capacity greatly reduced by intensively treated malignant lymphoma.

*Present address: Resident, Department of Internal Medicine, University of Tennessee, Memphis. Work done while an ORINS Trainee in Clinical Investigation.
†Present address: Resident, Department of Radiology, Massachusetts General Hospital, Boston. Work done while assigned as a short-term resident to the Medical Division.

Coma with onset about 2 hr after completion of injection persisted until death 14 days later. Microemboli in various tissues and microinfarcts in the brain resembled those of fatal fat embolism associated with trauma or with a fatty liver. Microradiography* was useful in confirming the radiopacity of the emboli and demonstrating their surprising abundance in cerebral capillaries even after 14 days *(Fig. 41)*.

*Performed with special instrumentation by Joel W. Garber at the Oak Ridge Y-12 Plant, operated for the U. S. Atomic Energy Commission by Union Carbide Corporation.

REFERENCE

1. Nelson B., Rush, E. A., Takasugi, M., and Wittenberg, J. Lipid embolism to the brain after lymphography. New Engl J Med 273: 1132–1134, 1965.

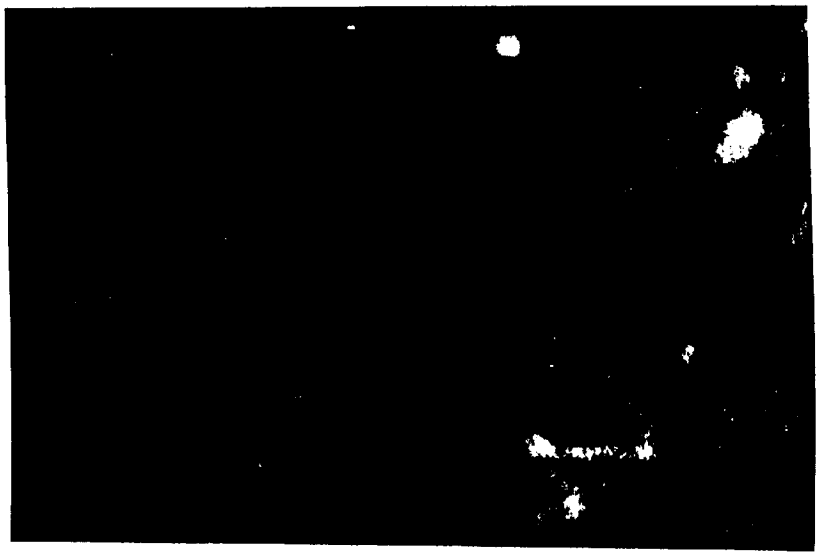

Fig. 41. Photographic enlargement of low-voltage X-ray of thin slice of brain, showing radiopaque emboli within capillaries. Larger spherules are probably extravasitions of ethiodized oil (100X). This work was done with the use of special facilities of the Y-12 plant in Oak Ridge. To our knowledge this is the first use of microradiography to demonstrate radiopaque emboli of the ethiodized oil used for lymphography.

1027773

Radioisotopes in Diagnosis

The objective is to apply radioisotopic test compounds in (1) the detection of tumors, (2) the measurement of functional disorders, and (3) the diagnosis of metabolic defects. The agents are radioactive compounds, either already available or newly synthesized and tested in animals; the subjects are patients in the Division's research hospital; and the procedures involved emphasize whole-body counting and scanning. Special techniques for radioassay and autoradiography on biopsy and autopsy material are applied to these problems.

New emphasis is being placed upon theoretical and mathematical approaches to diagnostic radioisotope studies and this is reflected in several of the following reports.

The work on radioiodine-labeled fibrinogen represents a pilot study; more extensive work on this subject has been done at other institutions and the limited effort here was undertaken to explore in a preliminary way the possible use of this potential diagnostic material with the scanning devices available here.

Gallium-68 Citrate in Bone Scanning

J. Ahumada, R. L. Hayes, R. Tanida, and C. L. Edwards

Many human tumors metastasize to bone. The metastases may be asymptomatic, but frequently become painful before being visible on roentgenograms. The pain may be poorly localized and difficult to distinguish from that of less serious musculoskeletal disorders. When bone metastases are detected, the tumor therapy may be significantly altered. Palliation of the pain can often be achieved with localized irradiation.

Most metastatic malignant lesions of bone are associated with increased new bone formation, or increased exchange of bone salts, or both. If the lesion is osteoblastic, these features may exist throughout it; if it is mainly destructive, these changes are likely to exist only at the periphery. The changes in uptake of certain bone-seeking radioisotopes can often be detected before there is sufficient change in the bone density to appear on roentgenograms. However, the radioactive isotopes of calcium are not good scanning agents. Calcium-45 is a pure beta emitter and the gamma photons of ^{47}Ca are too energetic (1.3

Mev) to permit convenient collimation. Strontium-85, ^{87m}Sr and ^{18}F are more desirable scanning agents, but each is less than ideal. The long physical half-life of ^{85}Sr (64 days) subjects patients to more radiation at doses adequate for scanning than is acceptable for general use. The half-lives of both ^{87m}Sr (2.8 hr) and ^{18}F (110 min) are better; however, neither is likely to become generally available. Fluorine-18 is usable only near the reactor facilities where it is produced. Strontium-87m is obtained from an accelerator-produced parent (^{87}Y) with a half-life of only 80 hr.

As reported last year Hayes and associates demonstrated that ^{68}Ga as the citrate could be used in scanning bones in animals. The bone-seeking properties of gallium citrate had been investigated in the early 1950's by Brucer and associates[1] at the Institute in the course of their investigation into the therapeutic properties of the longer half-lived isotopes of gallium. The use of ^{68}Ga awaited the development of the ^{68}Ge cow generator. The chief advantage of ^{68}Ga over other bone scan-

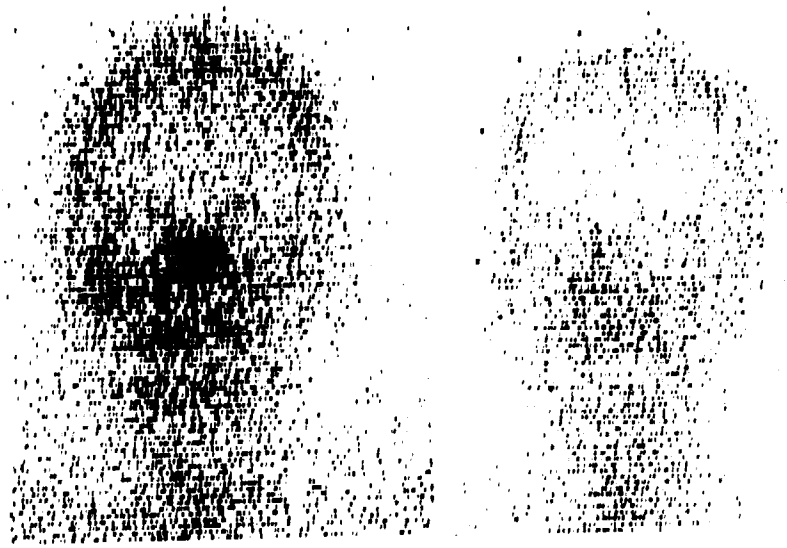

Fig. 42. Area scans of the head obtained 1½–2 hr after an intravenous dose of 6.5 to 6.8 millicuries of ^{68}Ga citrate with 4mg/kg of stable gallium carrier. The scan on the left was obtained of a patient with carcinoma of the nasopharynx with bone involvement compared to the normal scan on the right.

1027774

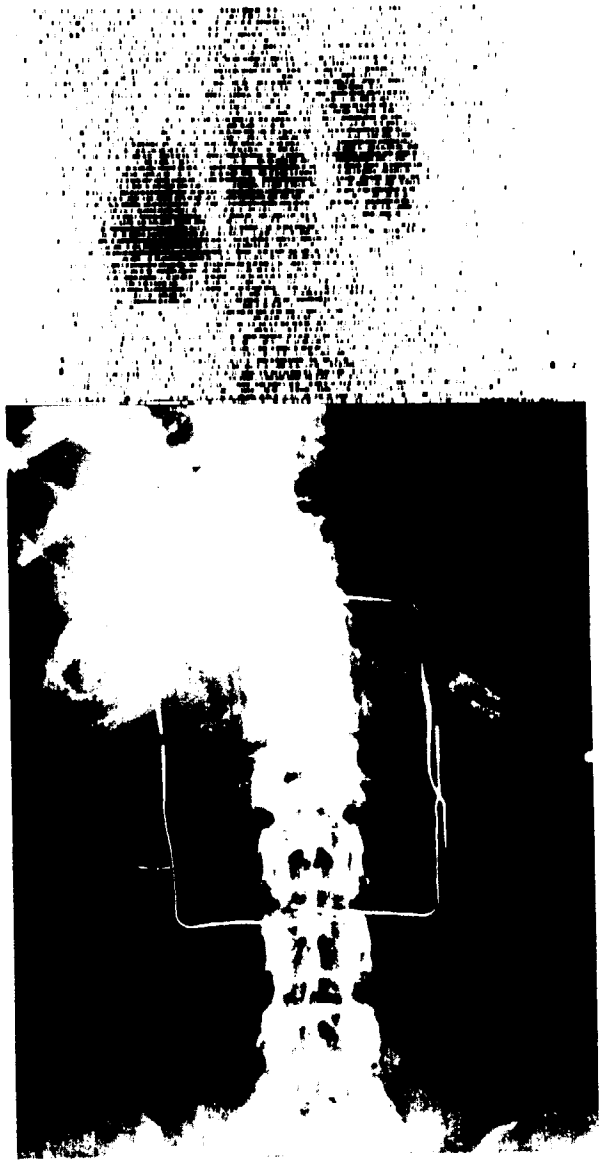

Fig. 43. Scan of the lumbar vertebrae obtained 30 min after an intravenous dose of 6 millicuries of ^{68}Ga citrate with 2 mg/kg carrier. The area of increased radioactivity corresponds to the second lumbar vertebra, which subsequently was demonstrated to have an osteolytic lesion on the X-ray.

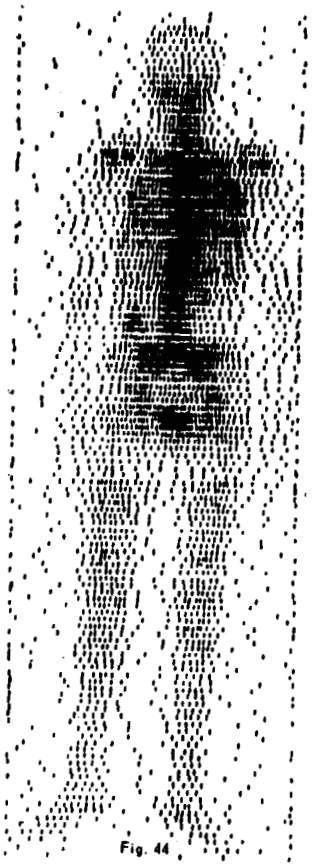

Fig. 44

^{68}Ga 8.0 mc I.V.
Carrier Ga^{+++} 2 mg/kg
Time Interval: 3 hours

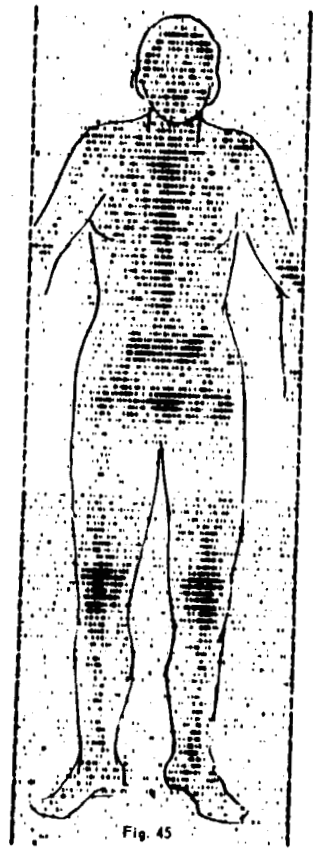

Fig. 45

July 16, 1965
^{68}Ga 9.0 mc I.V.
Carrier Ga^{+++} 2 mg/kg
Time Interval: 3 hours

Fig. 44. *Whole-body scan obtained 3 hr after an intravenous dose of 8 millicuries of ^{68}Ga citrate with 2 mg/kg carrier gallium. Note the increased radioactivity of the spine and posterior pelvic bones corresponding to the marked osteofibrosis known to be present in these bones. A displaced right kidney is demonstrated.*

Fig. 45. *Whole-body scan obtained 3 hr after an intravenous dose of 9 millicuries of ^{68}Ga citrate and 2 mg/kg of carrier stable gallium. Note the increased radioactivity in the region of the knees, which exhibited severe degenerative arthritis. Activity is also greater over the spine and pelvis affected by myelofibrosis.*

1027775

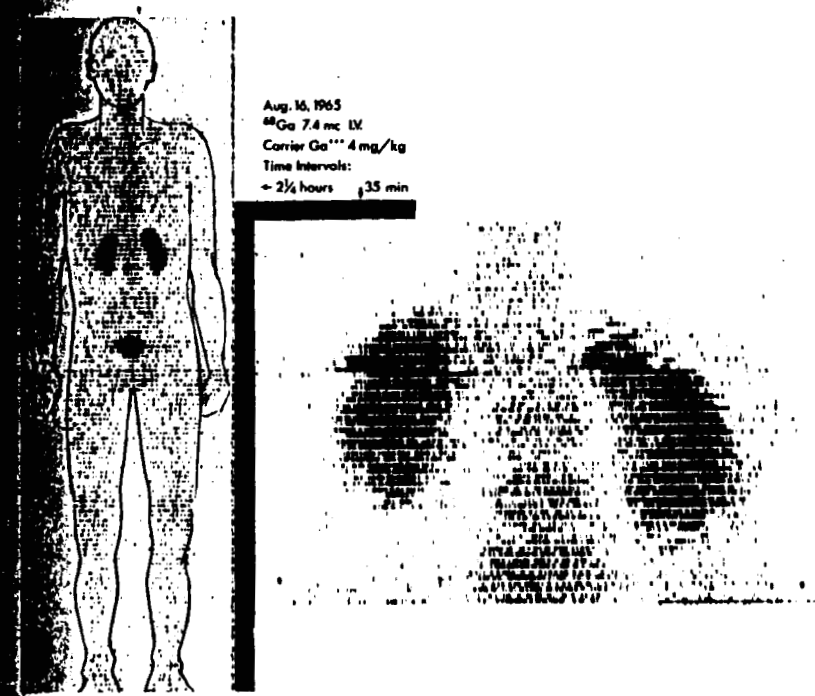

Fig. 46. *Whole-body and area scan obtained at 135 and 35 min respectively after an intravenous dose of 7.4 millicuries of ^{68}Ga citrate with 4 mg/kg of stable gallium. Note the good quality renal scan and the clearer delineation of the vertebral bodies.*

ning agents are (1) the short half-life (68 min), and (2) ready availability from the long half-lived (280 days) germanium generator.

During the past year we have used ^{68}Ga citrate in 49 skeletal scans of 41 patients with known or suspected bone lesions. As with other bone scanning agents, it has been possible to demonstrate metastatic bone lesions with ^{68}Ga scans *(Fig. 42)* sometimes before the lesions are detected on roentgenograms *(Fig. 43)*. Other skeletal disorders that are found to give abnormal scans include myelofibrosis *(Fig. 44)*, and degenerative arthritis *(Fig. 45)*.

As was found in the preliminary animal experiments, the quality of the scans can be improved by increasing the amount of carrier gallium from 2 mg/kg used initially to 4 mg/kg. The only adverse reaction ob-

served to date has been transient chills without fever in several patients. A useful by-product of the skeletal scans has been renal scans of good quality, which suggests other applications for this nuclide *(Fig. 46)*.

REFERENCE

1. Brucer, M. *et al.* A study of gallium^{72}. Radiology 61, 534–613, 1953.

Clinical Bone-marrow Scanning

R. M. Kniseley, G. A. Andrews, R. Tanida, C. L. Edwards and G. C. Kyker

This program, devoted to the study of the distribution of functioning bone marrow in patients with a variety of disorders affecting the blood-forming organ, has shown further progress. The whole-body scanner has proved to be a useful tool in this work. We have continued to rely on colloidal ^{198}Au *(Fig. 47)*, given intravenously to show the distribution of reticuloendothelial tissue, which in the marrow correlates well with hematopoietic tissue. *Fig. 48* demonstrates some of the difficulties in interpretation of scans. The depth of the collimator focus is critically important, and factors of scatter and attenuation also are significant.

Even at the present stage of development, bone-marrow scanning is a useful adjunct to understanding the patient's hematopoietic status *(Fig. 49)*. Responses to destruction of marrow, the patterns of extension of the active marrow into the extremities, the sites and shape of local lesions, and the hyperplasia seen in some anemias can be shown, sometimes in dramatic detail. To produce better marrow scans, improved radioactive colloids are needed. Clearly, both particle size and chemical properties of particle surfaces are important, and a material that would concentrate more in the marrow and less in the liver and spleen would be desirable. The present choices of colloids have been influenced by availability, half-life, and gamma energy of a convenient radioactive label. One of the main needs is to reduce the radiation dose to the patient so that the diagnostic test can be performed without concern, even in patients without serious disease. We have been able to initiate clinical trials with colloidal preparations of ^{99m}Tc and ^{159}Gd, since they offer some advantages (*Table 11*).

1027776

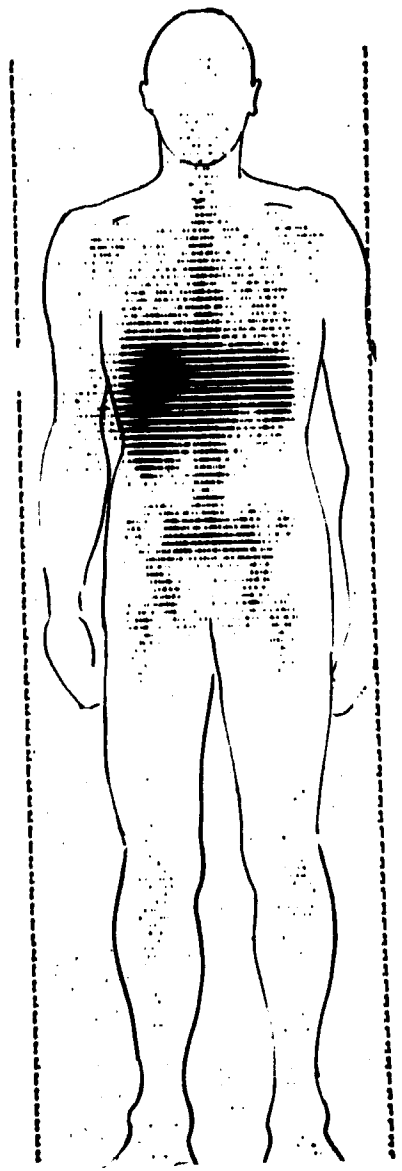

Fig. 47. Typical whole-body scan with intravenous colloidal ^{198}Au. This man, age 28, had a metastatic soft-tissue tumor, with no known bone involvement. Distribution of functioning marrow is essentially normal.

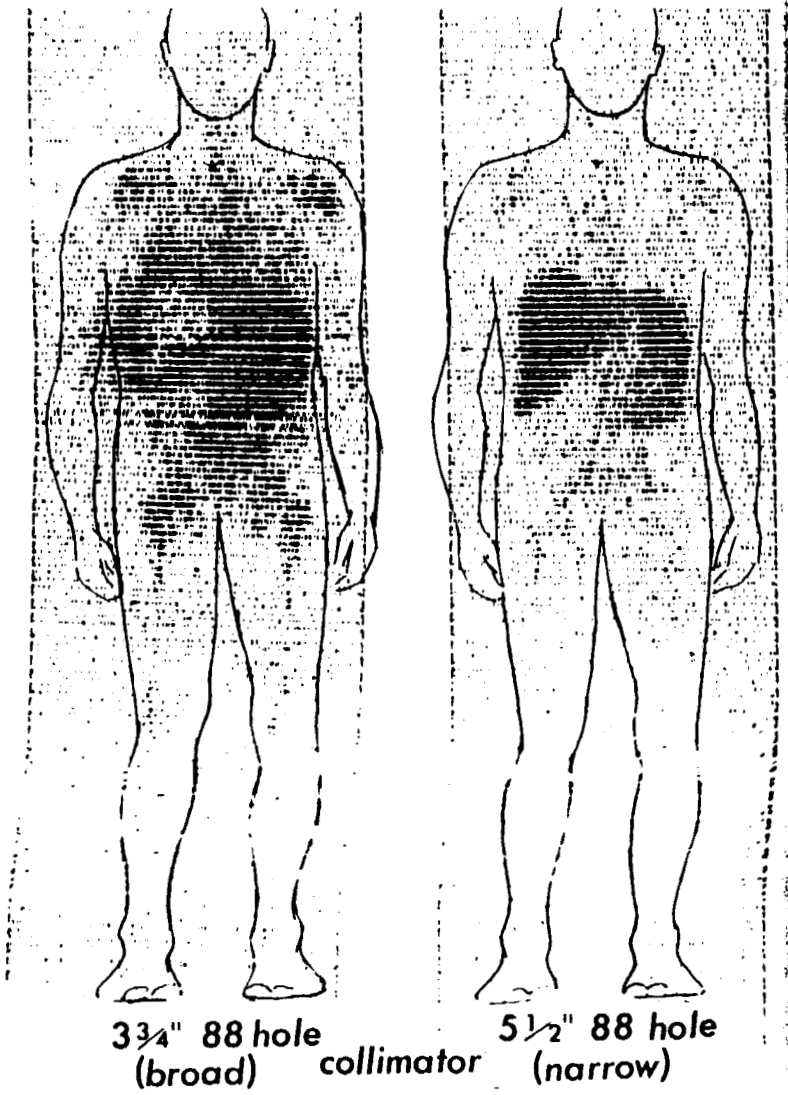

Fig. 48. Scans obtained after colloidal ^{198}Au in a patient with chronic granulocytic leukemia. Care in interpretation is necessary: although marrow expansion is obvious with the "broad" collimator, the "narrow" collimator less readily shows this alteration. These are mechanical dot scans, and the hole in the midportion of the liver is overload freezing of the tapper.

1027777

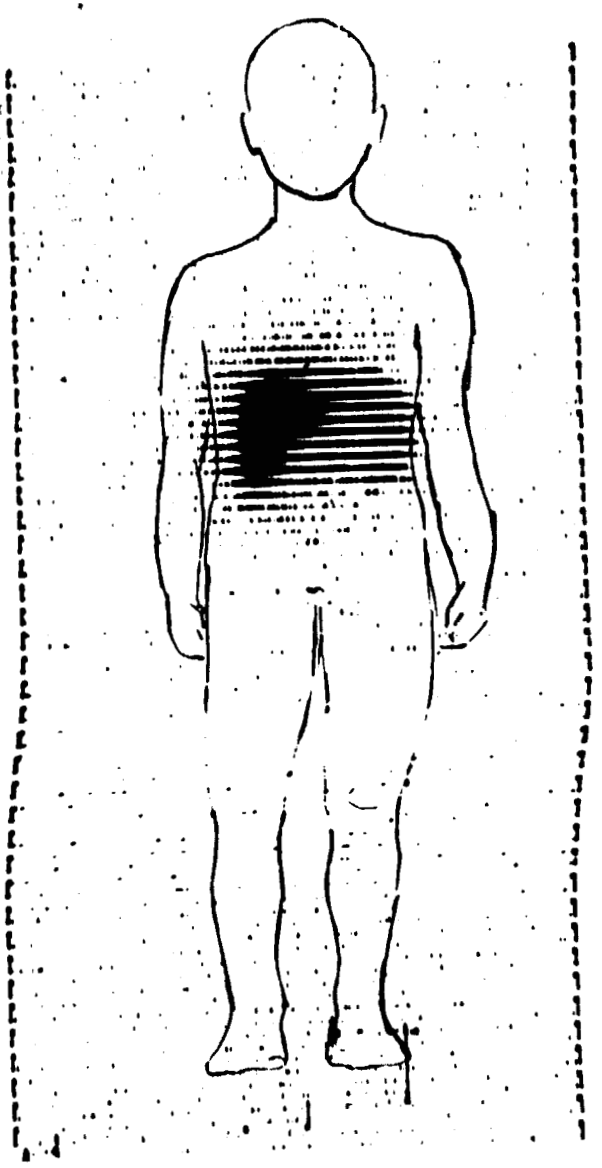

Fig. 49. A boy, age 4 years, with acute lymphoblastic leukemia in relapse. Scan was taken 18½ hr after intravenous colloidal ^{198}Au. Note absence of marrow uptake.

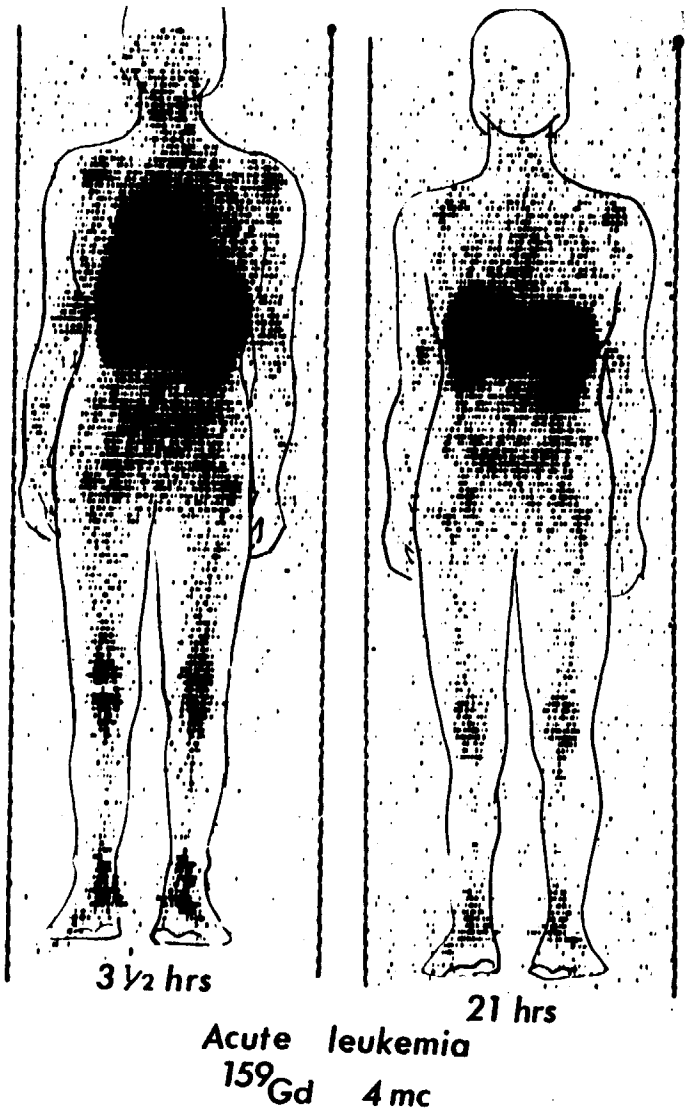

Fig. 50. A woman, age 44, with acute granulocytic leukemia, after intravenous ^{159}Gd hydroxycitrate. The scan on the left, taken at 3½ hr, shows lung activity, less on the left side where there was a pleural effusion. Improved marrow delineation was obtained at 21 hr. Note pronounced marrow expansion into the lower extremities.

1027178

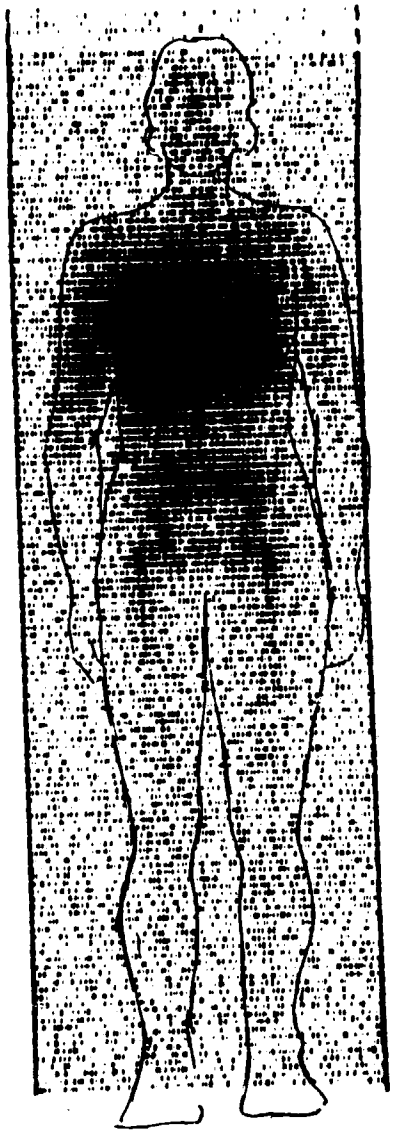

Fig. 51. A woman, age 40, with Hodgkin's disease, was scanned 4½ hr after 4 millicuries of ^{99m}Tc. The spectrometer was set at 125-kev base with a 100-kev window, yet scatter in the trunk and especially in the arms, from the high liver activity, is significant.

The initial trials with ^{159}Gd hydroxycitrate show that it clears from the blood less rapidly than colloidal gold *(Fig. 50)*, although it appears to have larger colloidal size. The scans show a pattern resembling that observed with ^{198}Au. The gadolinium isotope is inexpensive to produce. Animal studies have shown a relatively high concentration in the marrow. If it can be shown for the human, this may be an asset.

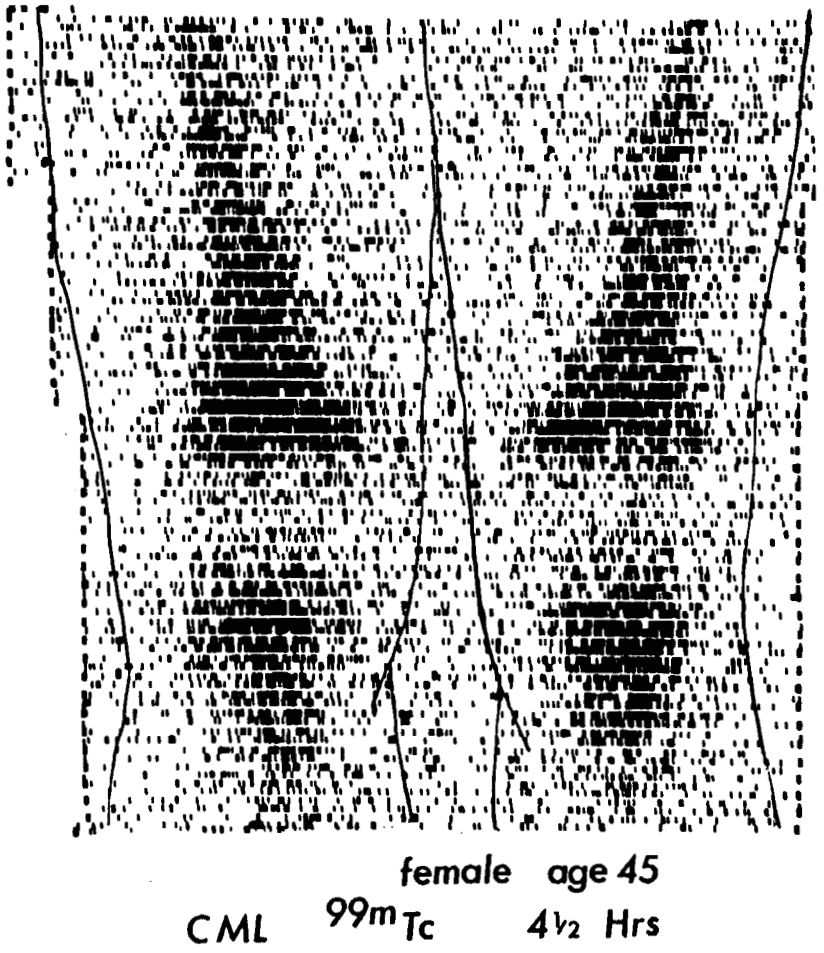

Fig. 52. Scan of the knees after ^{99m}Tc colloid (research area scanner) in a patient with chronic granulocytic leukemia whose whole-body scan showed marrow expansion. The detail is good and scatter effects are absent.

1027779

This has not yet been reflected in improved clinical scans, and the early concentration in the lung along with the slow removal from the blood stream suggest that its colloidal properties may not be uniform or ideal with the present methods of preparation and amounts of carrier.

We have also been able to delineate the functioning reticuloendothelial activity with the sulfur colloid of ^{99m}Tc, and its distribution corresponds with that observed with gadolinium and gold colloids. Preparations of ^{99m}Tc have not been extensively studied for colloidal properties, and the particle size is not known. The currently available methods of colloid preparation are probably not optimum. A compound of uniform particle size and completely free of pertechnitate ion is needed. This isotope, because of its low energy, will not lend itself to quantitation *in vivo* because of variations in attenuation by tissue. Even higher-energy emissions such as the 410 kev of colloidal ^{198}Au are attenuated, and the variability in tissue thickness in different parts of the marrow organ have prevented quantitations by linear scanning. The problem of degradation scatter of the low-energy gamma emission of the ^{99m}Tc is serious and has received relatively little attention. Instrumentation problems for bone-marrow scanning are more complex than for any other organ scanning, especially because of the variable depth of the marrow from the surface of the body. In some of our initial results with the use of ^{99m}Tc and the whole-body scanner, difficulties caused by scatter characteristic of the 140-kev energy emission have been encountered *(Fig. 51)*. In spite of difficulties, scans of good quality have been produced *(Fig. 52)*.

TABLE 11

Characteristics of Three Isotopes Used for Marrow Scanning

	^{198}Au	^{99m}Tc	^{159}Gd
Half-time	2.67 days	6 hr	18 hr
Emissions	γ0.41; β0.97	γ0.14; β0.014	γ0.37, 0.057; β0.95
Production	^{197}Au (n,γ)	^{99}Mo generator	enriched ^{158}Gd (n,γ)
Daughter	^{198}Hg (stable)	^{99}Tc (stable)	^{159}Tb (stable)
Rads to liver/millicurie	32 - 42	0.2 to 0.3	10 to 13

Based on 1 millicurie given intravenously with 70 to 90% concentration in liver, remaining until complete decay.

Whole-body Scans After Absorption of ^{131}I-Fatty Acids in a Patient with Chylothorax

E. A. Rush and F. Snyder*

Chylothorax results in a reservoir for products transported from the intestinal lacteals by way of the thoracic duct into the pleural space. Studies have shown that long-chain fatty acids are transported via the thoracic duct, but that short- and medium-chain fatty acids enter the circulation by way of the portal vein.[1-3] Recently, a patient with chylothorax gave us the opportunity to study the differential absorption of ^{131}I-labeled fatty acids of varying chain lengths (C_8, C_{11}, and C_{18}) by whole-body scans. The labeled ^{131}I-lipids of the pleural fluid after the oral administration of these acids were also examined chromatographically. Lipid extracts of the pleural fluid were prepared by drying in a freeze-dry apparatus before extraction with 2:1 chloroform:methanol (v/v). Purification of the lipid extract was done according to the procedure of Folch *et al.*[4] Thin-layer chromatograms (2 × 20 cm) of the total lipid extracts were developed in a solvent system of hexane:diethyl ether:acetic acid [illegible]. The radioactivity distribution along the chromatographic lane was determined by zonal scanning.[5]

The whole-body scans in our experiments showed that after ingestion, only oleic acid *(Fig. 53)* was absorbed into the lymphatic system; while the shorter-chain fatty acids were not. The scans vividly demonstrated the abnormal communication between the thoracic duct and the pleural cavity by the peak of radioactivity in the left side of the chest. Thin-layer chromatography showed that the label in the chylous fluid after administration of oleic-^{131}I-acid was entirely in the triglyceride fraction *(Fig. 54)*. Although radioactivity was present in the chylous fluid after octenoic acid and unedecenoic acid ingestion, none of it was found in the lipid fraction. Our results obtained with the use of ^{131}I-whole-body scans correlate well with previous nonisotopic and ^{14}C studies of patients with chylothorax or chyluria, and demonstrate the usefulness of whole-body scans in metabolic studies.

*Work done while a trainee in clinical investigation. Present address: Resident, Department of Medicine, University of Tennessee, Memphis.

1027180

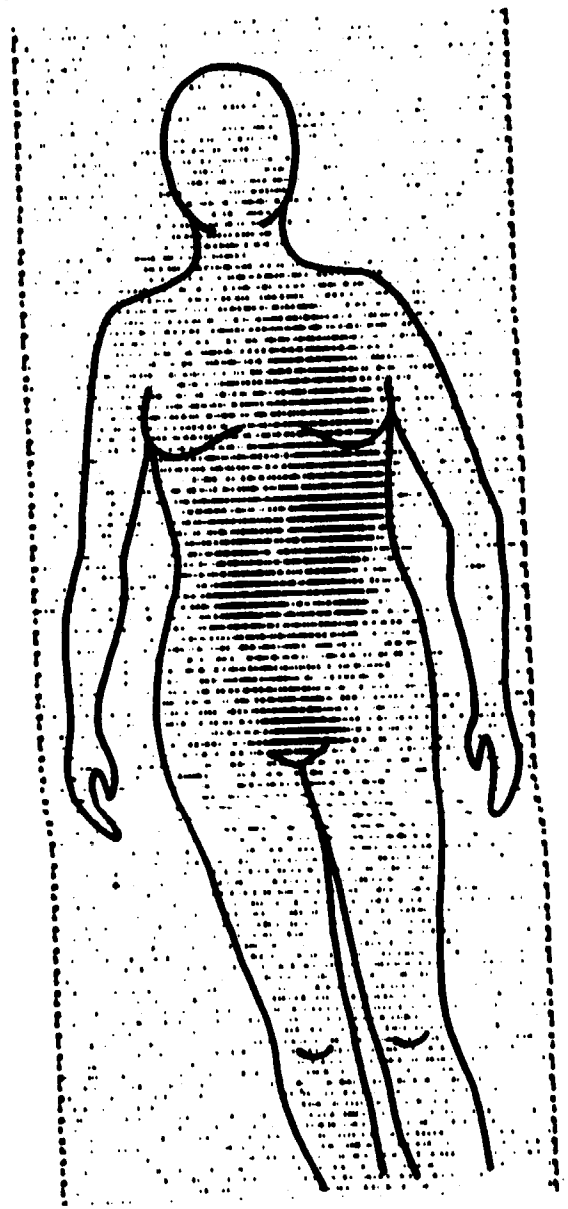

Fig. 53. Whole-body scan 3 hr after the administration of ^{131}I-labeled oleic acid.

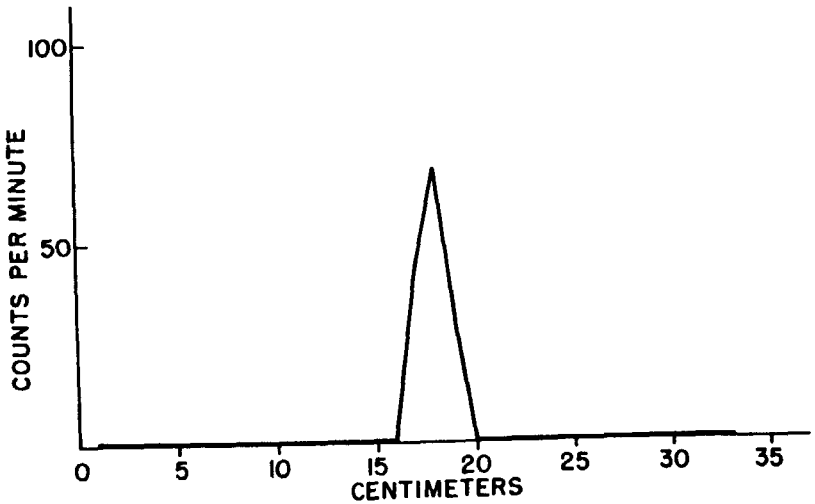

Fig. 54. Thin-layer chromatographic zonal scan of ^{131}I-labeled lipids from pleural fluid 6 hr after the administration of ^{131}I-labeled oleic acid.

REFERENCES

1. Fernandes, J., Van de Kamer, J. H., and Weijers, H. A. The absorption of fats studied in a child with chylothorax. J Clin Invest 34, 1026–1036, 1960.
2. Karmen, A., Whyte, M., and Goodman, D. Fatty acid esterification and chylomicron formation during fat absorption. I. Triglycerides and cholesterol esters. J Lipid Res 4, 312–321, 1963.
3. Bloom, B., Chaikoff, I. L., and Reinhardt, W. O. Intestinal lymph as pathway for transport of absorbed fatty acids of different chain lengths. Amer J Physiol 166, 451–455, 1951.
4. Folch, J., Lees, M., and Stanley, G. H. S. A simple method for the isolation and purification of total lipides from animal tissues. J Biol Chem 226, 497–509, 1957.
5. Snyder, F. Radioassay of thin-layer chromatograms; A high-resolution zonal scraper for quantitative C^{14} and H^3 Scanning of thin-layer chromatograms. Anal Biochem 9, 183–196, 1964.

1027781

^{131}I-Fibrinogen Plasma Disappearance and Evaluation as a Scanning Agent

*E. A. Rush**

Several investigators have reported significant concentration of ^{131}I-labeled fibrinogen in tumors of animals and man. To determine whether or not this preparation might be useful as a scanning agent, with the techniques and facilities available here, to obtain information on the distribution and excretion of this material, a study was made of 11 patients who were each given about 4 mg of fibrinogen labeled with 400 microcuries of ^{131}I, prepared by Abbott Laboratories. Because there is published evidence that fibrinolysis may hasten the removal of deposited labeled fibrin, in five patients an attempt was made to prevent this by giving epsilon amino caproic acid (EACA)†, which prevents fibrinolysis by competitive inhibition of enzymatic activation of plasminogen.

Of the 11 patients studied, seven had hematologic disorders and were evaluated by plasma disappearance curves and by other measures of general retention. Only four patients had localized tumors that might have been expected to show specific localization. One of these, who had a lymphoma and was not given EACA, showed some transient localization of the radioisotope in the lesions. Of three who were given EACA along with the labeled fibrinogen, one showed fairly good concentration in the tumor by scan. In another a rescan technique made visible a very slight accentuation in counting rate over the tumor. A third patient, in whom no concentration in the tumor could be shown by scanning, died seven days after the dose was given, and autoradiograms from the postmortem specimen *(Fig. 55)* showed definite localization of the label in areas of tumor; tissue assays showed a concentration of radioactivity in the metastases seven times as high as that in the normal liver. It appeared that late studies, five to seven days after the dose was injected, gave the best chance for visualization of tumors. High general body levels of radioactivity interfered with detection of localization.

The general result of this limited study was to show that, although labeled fibrinogen does show a tendency to concentrate in tumors to a higher level than in most normal tissues, the differential uptake is so

*Present address: Resident, Department of Internal Medicine, University of Tennessee, Memphis. Work done while an ORINS Trainee in Clinical Investigation.

†Amicar – Lederle Laboratories

slight as to be difficult to detect by current scanning methods; it is unlikely that small, unknown tumors could be detected by this technique without improvements in the localization of the compound or in the scanning equipment.

Plasma disappearance half-time averaged 2.6 days.

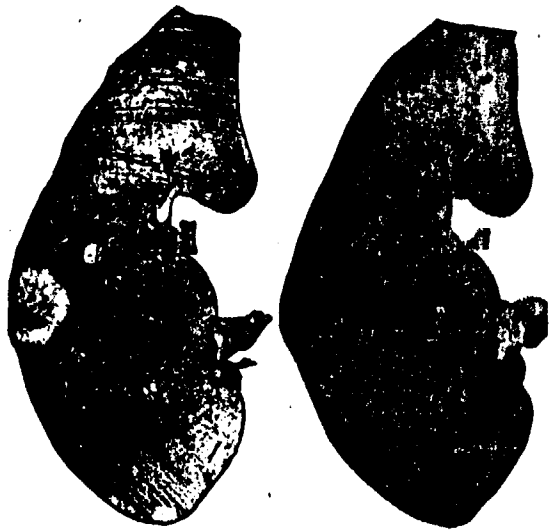

Fig. 55. Photograph and gross autoradiogram of liver with metastases of poorly differentiated squamous cell malignancy from a primary in the esophagus. Autopsy seven days after tracer dose of ^{131}I-labeled fibrinogen.

On the Ergodic Properties of the Tracer System*

P.-E. E. Bergner

The "system" (the organism) is considered such that a particle, belonging to a definite class of particles in the system, can attain a finite number of Markovian states; each state can contain more than one

*Abstract of a paper presented at the Biometric Society Meeting, Tallahassee, Fla., May 1, 1965.

1027182

particle. The state of a particle in the system thus constitutes a finite Markov process, assumed to be homogeneous in time. The system is defined as open when all the states have finite mean time of sojourn. A constant input of particles into such a system eventually results in a steady-state distribution of particles over the set of states.

Problem: How is the stochastic process of the individual particle related to the steady-state distribution? It is shown that, in terms of appropriate space means and time means, such relations exist. A comparison is also made with the closed system, especially the irreducible one, which is the system usually considered in classic theory. When the closed system is considered, the steady-state distribution, used at the analysis of the open system, is replaced by the more common stationary, limiting distribution.

The results seem to have some immediate practical consequences, particularly in the biomedical use of radioactive tracers. For instance, let us consider potassium metabolism in man and assume steady state. If there is a "proper" instantaneous supply of $^{42}K^+$, it can be shown that the area under the whole-body tracer curve determines the mean exit probability of potassium ions, the mean being taken over the steady state distribution of potassium in the body.[1] As a general conclusion, the theory shows that, to make a physicobiologically significant interpretation of tracer data, one has to consider the whole tracer process (from $t = 0$ to $t = \infty$). This invalidates many earlier methods, where attempts are made to draw conclusions from parts of the tracer curves, e.g., the use of the so-called "last linear slope" for determination of "biological half-life." The theory also indicates certain connections with classic statistical mechanics, and gives suggestions for principles to be followed in the future work.

REFERENCE

1. Bergner, P.-E. E. Tracer dynamics and the determination of turnover factors and pool-sizes in metabolic systems. J Theor Biol 6, 137–158, 1964.

Exchangeable Mass: Determination Without Assumption of Isotopic Equilibrium

P.-E. E. Bergner

The method of isotope dilution[1] for determining the exchangeable mass is, at best, approximate. A formally exact method, defining the mass is proposed. The new otherwise vague concept of exchangeable mass, is proposed. The new

method may serve as a standard for determining errors in results obtained by the earlier method; the magnitude of these errors will give information on the "structure" of the metabolic system, like, in intuitive terms, the efficiency of internal mixing. The theory seems ready to be applied to studies of potassium and sodium metabolism in man, with the use of whole-body counting techniques; the required period of observation in each case is about 30 days.

The difference between the new method and the old one is illustrated by the following equations:

The "new" method

$$\int_0^\infty \frac{b_s(t)}{b_s^0}\,dt = \int_0^\infty \frac{b(t)}{b^0}\,dt$$

The "old" method

$$\frac{b_s(t)}{b_s^0} = \frac{b(t)}{b^0}$$

where $b_s(t)$ and $b(t)$ is the total tracer amount in the whole system (body) and in a volume element of blood; b_s^0 and b^0 are the corresponding amounts of mother substance (i.e. the naturally present isotope). The whole-body counter could be used to determine $b_s(t)$ and blood samples for $b(t)/b^0$. Hence, in the equation, every entity except b_s^0 can be directly observed and, therefore, the equations determine the total content of mother substance in the whole body. Actually, b_s^0 denotes the exchangeable mass rather than the total mass. One could say that the equations define the otherwise vague concept of exchangeable mass. However, it has been shown by several authors that the second equation (the old method) is basically incorrect. On the other hand, the first equation can be derived from a quite general and physically precise theory.[1]

A drawback with the new method suggested is that the theoretical exactness is received at the expense of experimental simplicity: the new method requires observation over perhaps a quite long period of time, whereas the old method is satisfied with one single observation. [This is a consequence of the ergodic theory (See Ergodic Properties of the Tracer System pp. 102–103)].

REFERENCE

1 Bergner, P.-E. E. Exchangeable mass. Determination without assumption of isotopic equilibrium. Science [illegible]

1027183

On Stationary and Nonstationary Red-cell Survival Curves*

P.-E. E. Bergner

The communication presents an extension of a previously reported analysis, at the same time as the work is confined to a more specific type of cell-survival data: essentially to the kind of data that can be obtained from studies with $DF^{32}P$-labeled red cells. The analysis is partly motivated by clinical requirements; e.g., it has become desirable to extend the former analyses to the clinically more realistic nonstationary system.

The first part of the communication is devoted to conceptual problems: the physicobiologic significance of death probability. An analysis of the stationary system then follows, and a formal model for the normal system is formulated.

The nonstationary (nonnormal) system is studied in terms of perturbations of the stationary, normal system. Only simple perturbations are studied, but some general conclusions for further work seem possible.

The experimentally most useful result of the analysis is probably a theorem, according to which the initial slope of a survival curve always determines the mean death probability of the cells; the classical concept of mean life span comes out to be less useful under nonstationary conditions than is the mean death probability.

*Abstract of paper in J Theor Biol. 9, 366 (1965).

Determination of Red-cell Destruction from $DF^{32}P$-Data

P.-E. E. Bergner and J. D. Lawson

Earlier theoretical analysis has proved that the red-cell destruction can be determined from the initial slope of the red-cell survival curve obtained with $DF^{32}P$-labeled red cells.[1,2] A preliminary computer program has been constructed for the data processing, and tested against different sets of hypothetical data. The results indicate that reasonable estimates of the red-cell destruction can be obtained with a rather short time of observation, provided the experimental technique is sufficiently accurate. For example, if the standard deviation in the observed values of the survival curve is 0.5%, 10 observations per day

over a period of 10 days will give an estimate of the mean life span with a standard deviation of approximately 8.5%, when the true mean life span is put equal to 100 days (120 days is the normal value). When the mean life span is further decreased, the time of observation can be shortened.

The investigation shows that improvements in the experimental precision and in the data processing technique will make possible a reduction of the time of observations. Clinical methods today, using ^{51}Cr-labeled cells, usually require at least 10 days of observation. Moreover, while the new method actually determines the red-cell destruction, the physical significance of the chromium method is uncertain. One reason for this is the so-called "elution phenomenon" that takes place with chromium-labeled red cells (see page 107–112 by Lawson, Bergner, Lushbaugh, Gibbs and Lushbaugh). Another reason is that the analysis of chromium data usually has been done fundamentally in terms of the mean life span of red cells: the two equations

$$(\text{Destruction}) = \begin{pmatrix}\text{Mean death probability}\\ \text{density}\end{pmatrix} \times \begin{pmatrix}\text{Total number of}\\ \text{circulating RBC}\end{pmatrix}$$

$$\begin{pmatrix}\text{Mean death probability}\\ \text{density}\end{pmatrix} = \frac{1}{\begin{pmatrix}\text{Mean life}\\ \text{span}\end{pmatrix}} \times (\text{Some function of time})$$

are generally valid, the mean being with respect to the age distribution of the red-cell population. The mean death-probability density is always determined by the initial slope of the DF^{32}P-curve and, because this is the only method we know of today for determination of that quantity, the mean life span is determinable only if the time function in the second equation is known. This function is constant and equal to unity when the red-cell population is stationary, but it is otherwise undetermined experimentally. Consequently, as in many clinical situations, the assumption of stationarity must be doubted, the concept of mean life span appears unsatisfactory (see also page 105 On Stationary and Nonstationary Red-cell Survival Curves).

REFERENCES

1. Bergner, P.-E. E. Stochastic concepts in clinical red-cell survival studies. Nature 205, 975–977, 1965.
2. Bergner, P.-E. E. On stationary and nonstationary red-cell survival curves. J Theor Biol In press.

1027784

A Mathematical Description of the Discrepancy between Whole-body and Peripheral Blood Retention of ^{51}Cr given as Labeled Red Cells

J. D. Lawson, P.-E. E. Bergner, C. C. Lushbaugh, W. D. Gibbs, and D. H. Lushbaugh*

It is well accepted that red cells labeled *in vitro* with ^{51}Cr lose their tag through elution in the peripheral blood so that a spuriously short RBC survival time is obtained by this method. The "eluted" tag is allegedly excreted quickly in the urine. However, when simultaneous measurements of ^{51}Cr activity in the whole body and whole blood are made, an increasingly large discrepancy is found, which appears to be due to sequestration of labeled RBC by the reticuloendothelial system.[1] The whole-body t_{50} of the tag in normal man is about 45 days (t_{50} is the time required for the first 50% of the ^{51}Cr to leave the body).[2] Observations from 30 simultaneously performed whole-body and peripheral blood ^{51}Cr survival studies in normal persons and those with hematologic disease,[3] lead to the conclusion that the rate of sequestration of the chromium-labeled cell depends not only upon the degree of cell damage caused by disease, but also on the amount of chromium used in the tagging procedure itself. Red-cell damage from a variety of causes leads to an increased rate of removal of red cells from the blood. These conclusions encourage a less rigid mathematical description of the data[2] than the commonly used single compartmental model based upon an exponential elution rate for chromium-labeled red cells.

The following description appears to explain the experimental and clinical findings and to enable fitting of the whole-body and peripheral-blood data by analog computer:

We consider whole-body counts W(t), blood counts B(t) and reticuloendothelial systems counts R(t) due to erythrocyte labeling by $Na_2{}^{51}CrO_4$ at time $t = 0$.

We assume first that

$$W(t) = B(t) + R(t) \qquad (1)$$

The removal of cells from the blood stream is, in a "normal" human, essentially due to senescence: by some yet unknown mechanism the cells are removed from the circulation when they reach a certain and, as it seems, rather definite age X($\approx$ 120 days).[4] In addition, removal

*Visiting scientist, Waterloo University, Department of Mathematics, Waterloo, Ontario.

might often be caused by some mechanism that acts independently of the cell age; in the following this is referred to as random removal. Random removal is usually negligible in normal subjects.

It is now assumed that some of the cells contributing to B(t) are damaged by the chromium label and that this damage introduces a random destruction. This part of B(t) is denoted by $B_1(t)$: these cells might be removed either by a random mechanism or by senescence. Cells removed by this particular random mechanism are assumed to be captured by a part of the reticuloendothelial system R_1, whereas senescent cells are assumed to be captured by another part R_2; thus $R_1(t) + R_2(t) = R(t)$. The rest of B(t) is denoted by $B_2(t)$ (i.e. $B_1 + B_2 = B$), corresponding to the cells that are labeled but unaltered by the label: the body treats them as normal cells, and they are, in normal subjects, removed by senescence only, which means that these cells, when being removed, are captured by R_2.

In the following, the analysis is based on the assumption that the labeling in B_1, as well as in B_2, is independent of the cell age.

The random removal of B_1 cells by R_1 proceeds at a rate λB_1 and the clearance of R_1 at a rate $\kappa_1 R_1$. All cells in B_2 and those cells of B_1 which escape random removal by R_1 are removed by R_2 and cleared from R_2 at a rate $\kappa_2 R_2$.

For $B_1(t)$, $t < X$, we have according to,[4] assuming steady state:

$$\frac{dB_1}{dt} = -\lambda B_1 - \frac{B_1^0}{X} e^{-\lambda t}; \; B_1(0) = B_1^0 . \tag{2}$$

The term $(B_1^0/X)e^{-\lambda t}$ is the rate of removal of cells in B_1 by system R_2. The solution is:

$$B_1(t) = B_1^0 e^{-\lambda t} (1 - t/X), \; t < X: \tag{3}$$

$$B_1(t) = 0, \; t > X.$$

Similarly, for $B_2(t)$, $t < X$, we have:

$$\frac{dB_2}{dt} = -B_2^0/X; \; B_2(0) = B_2^0 \tag{4}$$

$$B_2(t) = B_2^0 (1 - t/X), \; t < X; \tag{5}$$

$$B_2(t) = 0, \; t > X .$$

Note that in Eq. 4 we assume a nonrandom removal of uninjured

1027785

senescent cells. If the red-cell population suffers from an abnormal destruction mechanism, then Eq. 4 must be modified. Both Eq. 2 and Eq. 4 are based on an assumed uniform age distribution in the labeled sample.

For $R(t) = R_1(t) + R_2(t)$ we have the equations:

$$\frac{dR_1}{dt} = \lambda B_1 - \kappa_1 R_1; \; R_1(0) = 0; \tag{6}$$

$$\frac{dR_2}{dt} = (B_2^0 + B_1^0 e^{-\lambda t})/X - \kappa_2 R_2; \; R_2(0) = 0. \tag{7}$$

Finally $W(t) = R_1(t) + R_2(t) + B_1(t) + B_2(t)$.

Attempts to make curve fits to some of the data on the analog computer reveal that:

(i) Both B_1 and B_2 are necessary to avoid a poor fit at the "tail" of the blood curve;

(ii) Some clearance of B_1 to R_2 is necessary for most cases;

(iii) Some cases require that the senescent cells in B_1 be cleared to R_1.

If a steady-state random red-cell loss is present due to bleeding or hemolysis, we may account for this by a somewhat more complex analysis.[4] We assume a fractional random destruction rate of u per unit time and divide the labeled population in two groups as before. For B_1 we now consider senescence, random removal of B_1 cells by R_1 and random loss. For B_2 we consider senescence plus random loss. Using this method of analysis,[4] we obtain:

$$B_1(t) = B_1^0 \exp(-\lambda t) \; [\exp(-ut) - \exp(-uX)]/[1 - \exp(-uX)];$$

$$B_2(t) = B_2^0 \; [\exp(-ut) - \exp(-uX)]/[1 - \exp(-uX)]$$

To facilitate analog simulation, we give the differential equations for B_1 and B_2 as follows:

$$\frac{dB_1}{dt} = -(\lambda + u) B_1 - uB_1^0 \exp(-\lambda t)/[\exp(uX) - 1];$$

$$\frac{dB_2}{dt} = -uB_2 - uB_2^0/[\exp(uX) - 1]$$

The term λB_1 represents random removal of B_1 cells by R_1. The

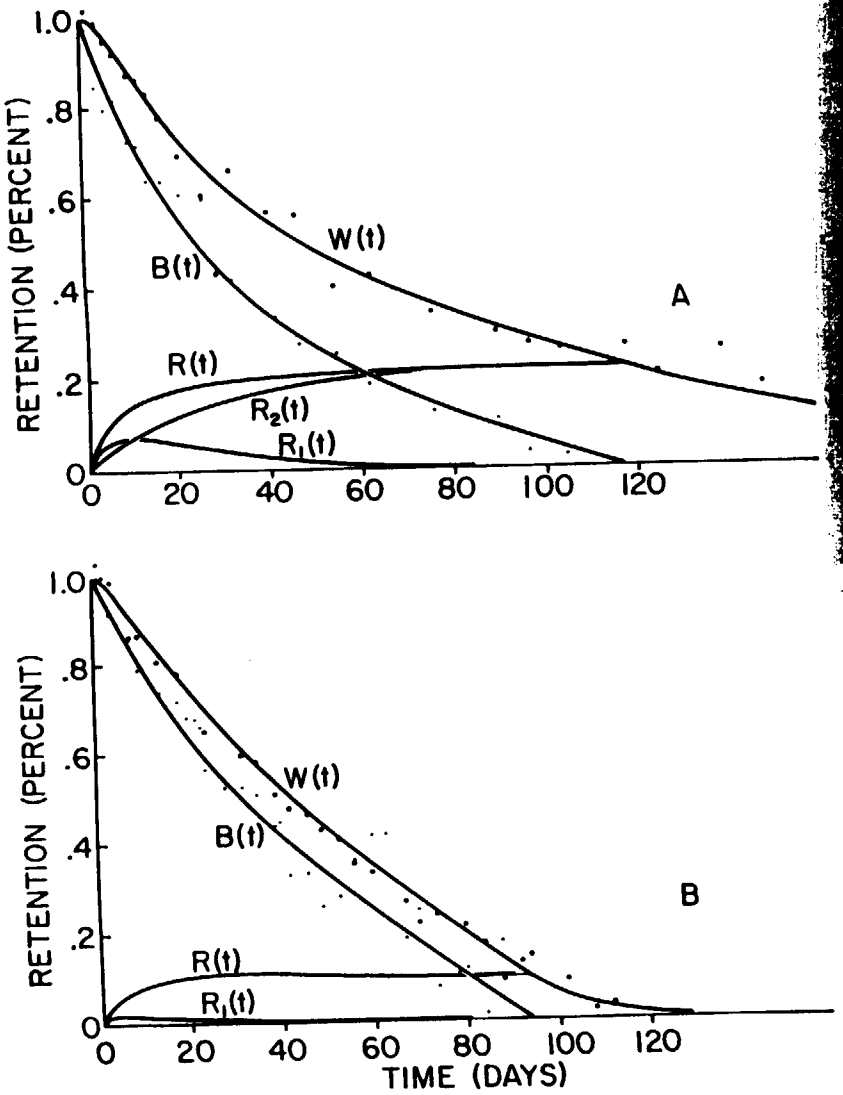

Fig. 56. Typical analog computer fits of blood [B(t)] and whole-body [W(t)] ^{51}Cr-retention data (dots) in (A) a person without hematologic disease and (B) in a patient with hemolytic anemia in partial remission under cortisone therapy. The parameters are described in the text.

terms uB_1 and uB_2 represent random loss due to disease, and the final terms represent removal of senescent cells by R_2.

The differential equation for R_1 is unchanged but for R_2 we have:

$$\frac{dR_2}{dt} = -\kappa_2 R_2 + u[B_1^0 \exp(-\lambda t) + B_2^0]/[\exp(uX) - 1].$$

In *Fig. 56*, two typical sets of data are shown fitted by the analog computer using these formulations: Graph A shows the peripheral blood and whole-body retention of the ^{51}Cr tag in a person without hematologic disease whose cells were tagged with 300 microcuries of ^{51}Cr contained in 3 mg of $Na_2{}^{51}CrO_4$, to illustrate the effect of a large chromium dose upon nondiseased red cells; Graph B depicts data similarly fitted from a patient with hemolytic anemia and acute leukemia in clinical but incomplete hematologic remission under vigorous cortisone therapy. These cells were tagged with high specific activity $Na_2{}^{51}CrO_4$ to minimize chromium damage. The parameters in *Table 12* of these two red-cell survival studies illustrate that the normal patient had cells with a normal life span but a large damaged fraction B_1^0: the red cells in the ill subject had a shortened maximum life span X, but reticuloendothelial clearance rates κ_1 and κ_2 were increased three to five times. The discrepancies in retention between whole-body and blood in these examples are therefore explained as being due principally to the differences in clearance rates of the reticuloendothelial systems.

These results and this mathematical description suggest that chromium "elution" may be explained as random loss of labeled cells into the reticuloendothelial system rather than the loss of label from cells; and the amount of chromium as well as red-cell disease (or both) contribute to the red-cell defect seen clinically as exponential disappearance of ^{51}Cr label from the peripheral blood. The large discrepancy between retention in whole-body and peripheral blood does not seem explainable in any other way.

REFERENCES

1. Lushbaugh, C. C., Marvin, H., and Hale, D. B. The life-span of the radiochromated erythrocyte, Fed Proc 18, 1935, 1959.
2. Bergner, P.-E. E. Stochastic concepts in clinical red-cell survival studies, Nature 205, 975–977, 1965.
3. Unreported work done at H-4 Biomedical Research Group, Los Alamos Scientific Laboratory.
4. Bergner, P.-E. E. On stationary and nonstationary red-cell survival curves, J Theor Biol 9, 366–388, 965.

TABLE 12

Parameters	Study Case A	Study Case B
Peripheral Blood		
Life Span (X) days	116	94
RBC Fraction		
Damaged by Chromium (B_1^0)	0.65	0.35
Nondamaged by Chromium (B_2^0)	0.35	0.65
Random Removal Rate Constant		
Due to Chromium Damage (λ)	0.034	0.038
Due to Disease (u)	0.000	0.006
Reticuloendothelial System Clearance Constants		
For R_1 (κ_1)	0.20	0.60
For R_2 (κ_2)	0.014	0.075

Feasibility of Using *in vivo* $DF^{32}P$ and Whole-body Counting in Red-cell Survival Studies.

C. C. Lushbaugh, W. L. Scott, M. C. Yarbrough, R. Queener, and W. D. Gibbs*

The use of difluorophosphate phosphorus-32 ($DF^{32}P$) instead of ^{51}Cr as a red-cell label is becoming more widely accepted clinically, because it is easy to use and affords a linear measure of red-cell survival.[1] Its bremsstrahlung can be seen by external scanning[2] and whole-body counting.[3] Phantom studies indicate that it will be feasible to obtain quantitative results with this isotope, provided distribution within the body does not change radically with time. However, when injected intramuscularly in the most accepted manner, DFP is known to become bound to other tissues and plasma proteins besides red cells.[1] Whole-body counting to determine red-cell survival would be feasible, therefore, only if these nonred-cell labels were lost rapidly or were relatively small and inconspicuous.

*Summer research participant, Southeastern Louisiana College, Hammond, La.

1027787

This feasibility was tested experimentally by using two groups of 15 rats each, one injected intravenously and the other intraperitoneally with 30 microcuries of $DF^{32}P$ as 0.3 mg of DFP per rat. The animal weights ranged from 180 to 210 g. All rats were whole-body counted immediately after injection and at 1, 3, 7, and 14 days. Three randomly selected animals from each group were killed each time after whole-body counts, and selected tissues were removed for radioassay. Results shown in *Table 13* indicate that radioactivity decreases steadily in liver, kidney, and lung with increasing time after dose in all animals, regardless of route of injection of the dose. After 14 days the marrow in both groups contains more $DF^{32}P$ than at earlier times. The extremely high figure for marrow from the intraperitoneally dosed animals seems valid since two of the three animals killed at this time had marrow concentrations in excess of 1.6% dose per gram. Cortical bone shows a steady rise in radioactivity with time. It is noteworthy that blood levels decrease rapidly with time indicating relative inefficient labeling of blood elements in this species by this *in vivo* method. A suggestion of slight increase of blood radioactivity at 14 days could reflect poor counting statistics. The rapid elimination of $DF^{32}P$ during the first day is probably caused by the relatively large chemical dose that was administered as shown by a parallel study of optimal conditions for *in vitro* blood labeling.

This study demonstrated that *in vivo* $DF^{32}P$ labeling of tissues other than red cells precludes the use of whole-body counting for red-cell survival studies, and an *in vitro* labeling method is required.

REFERENCES

1. Cohen, J. A. and Warringa, M.G.P.J. Fate of P^{32} labeled diisopropylfluorophosphate in human body and its use as a labeling agent in study of turnover of blood plasma and red cells. J Clin Invest 33, 459, 1954.
2. Mehl, H. G. The distribution of a pure beta-emitter in the human body. Problems and preliminary results of Bremsstrahlung measurements *in vivo*. Medical Radioisotope Scanning, IAEA, Vienna, 1959, pp. 125–142.
3. Gibbs, W. D., Hodges, H. D., and Lushbaugh, C. C. Standardization and calibration of a whole-body counter. This report, page 145.

TABLE 13
Distribution of $DF^{32}P$ in Selected Tissues of the Rat

Intravenous

Tissues	Days After Dose 1	3	7	14
	(% dose/gram)			
Adrenal	0.000	0.036	0.000	0.050
Marrow	0.000	0.044	0.000	0.189
Spleen	0.075	0.009	0.004	0.017
Liver	0.504	0.313	0.109	0.031
Kidney	0.269	0.117	0.030	0.013
Lung	0.142	0.084	0.040	0.027
Muscle	0.003	0.008	0.003	0.011
Bone	0.000	0.016	0.022	0.053
Blood	0.078	0.023	0.007	0.008

Intraperitoneal

Tissues	Days After Dose 1	3	7	14
	(% dose/gram)			
Adrenal	0.000	0.094	0.028	0.274
Marrow	0.000	0.100	0.049	1.192
Spleen	0.106	0.016	0.005	0.018
Liver	0.569	0.350	0.107	0.035
Kidney	0.091	0.089	0.023	0.011
Lung	0.118	0.086	0.044	0.030
Muscle	0.026	0.011	0.008	0.016
Bone	0.011	0.017	0.022	0.073
Blood	0.037	0.018	0.007	0.008

1027188

An *in vitro* Method for $DF^{32}P$ Labeling of Red Cells for Intravenous Administration

C. C. Lushbaugh, R. Queener, and W. D. Gibbs

Since whole-body counting cannot be used to estimate difluorophosphate phorphorus-32 ($DF^{32}P$) labeled red blood cell (RBC) survival if the unbound drug is administered directly to the patient by intraperitoneal, intravenous, or intramuscular routes,[1] an *in vitro* method that restricts the label to red cells was developed based on a study of optimal incubation time, carrier effect, and *in vitro* stability of the red-cell label.

Maximum labeling was found to occur in 1 hr of incubation at room temperature in acid citrate dextrose (ACD) solution. The typical rate of incorporation of the drug by red cells under these conditions is shown in *Fig. 57*. Maximum labeling is prevented by carrier DFP as previously shown by Garby.[2] *Figure 58* shows that with 0.01 mg DFP/100 ml of whole blood, 50% of the $DF^{32}P$ was found on the washed red cells and any increase in amount of DFP decreased the labeling efficiency. Increasing amounts of DFP were also found to influence the subsequent *in vitro* release of label, but not the rate of red-cell death as shown in *Fig. 59*.

Based on these findings a simple, efficient method for *in vitro* red-cell labeling with $DF^{32}P$ would be to (1) add less than 0.01 mg of DFP containing $DF^{32}P$ to 100 ml of whole blood in 10 ml of ACD solution; (2) incubate at room temperature for 1 hr; (3) wash three times with saline; and (4) reconstitute to original volume and inject intravenously as in other RBC survival studies.

The use of low specific activity solution that requires more than 0.01 mg DFP/100 ml of blood to obtain a sufficiently large radioactive label may require overnight *in vitro* storage, and additional saline washes immediately before administration to the patient to circumvent injection of ^{32}P no longer bound to red cells.

REFERENCES

1. Lushbaugh, C. C., Scott, W. L., Yarbrough, M. C., Queener, R., and Gibbs, W. D. Feasibility study of using *in vivo* $DF^{32}P$ and whole-body counting in red-cell survival studies. This report.
2. Garby, L. Analysis of red-cell survival curves in clinical practice and the use of Di-isopropylfluorophosphate ($DF^{32}P$) as a label for red cells in man. Brit J Haemat 8:15–27, 1962.

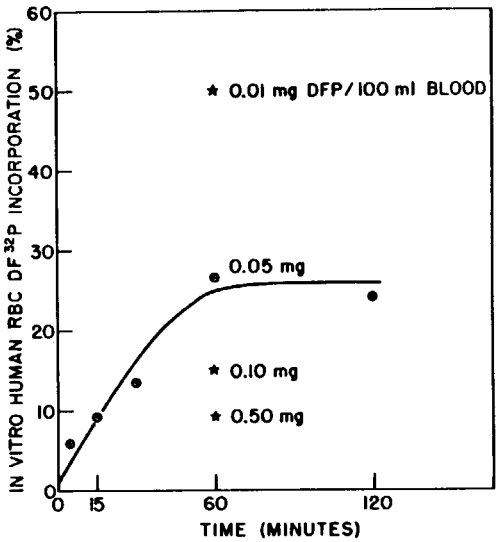

Fig. 57. In vitro incorporation of $DF^{32}P$ in human blood showing effects of time of incubation and carrier levels.

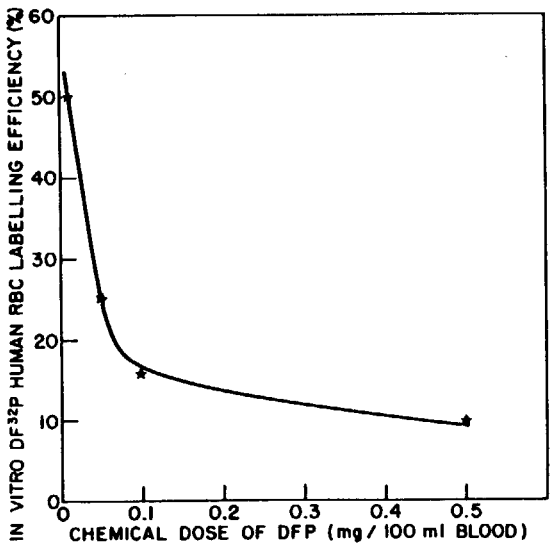

Fig. 58. In vitro incorporation of $DF^{32}P$ in human blood showing decrease in labeling efficiency with increase of carrier DFP.

1027789

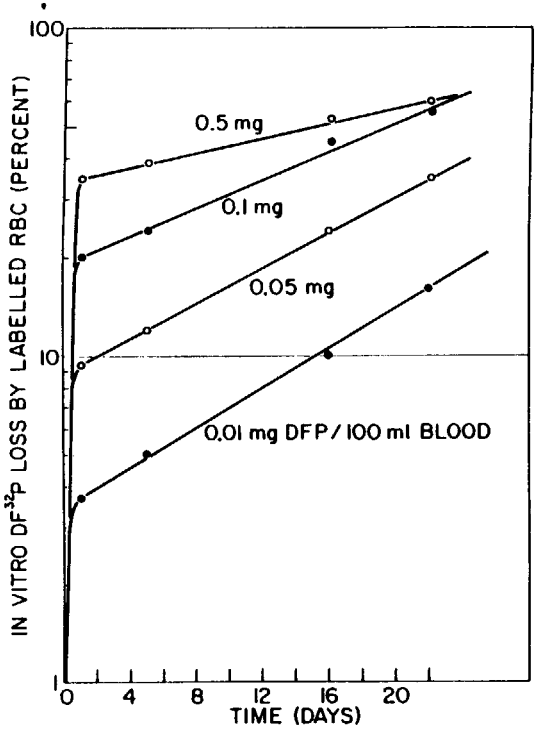

Fig. 59. Early in vitro release of $DF^{32}P$ Label from human blood showing dependence upon carrier DFP level.

A Test of the Extravascular Concept of the Dynamics of Rose Bengal Blood Clearance in the Rat

C. C. Lushbaugh, M. L. Davis, and W. D. Gibbs*

An analog computer model was devised that simulated satisfactorily the hepatic uptake and arm and blood clearance of ^{131}I rose bengal in patients with hepatic disease.[1] This model, based upon the compartmental concept, considered the equilibria of the blood, liver, and extravascular spaces. The extravascular space was thought to be enlarged in hepatic disease and to provide a reservoir into which the

*Summer student employee.

intravenously-injected dye diffused in increased amounts when early blood clearance was impaired by hepatic dysfunction. The dye concentration in this reservoir then controlled blood concentration and thereby further limited hepatic extraction. The practical result of this phenomenon was rapid blood clearance but slow arm clearance of the dye, since arm counting detected both blood and extravascular space. In parenchymal hepatic diseases, high activity in the extravascular

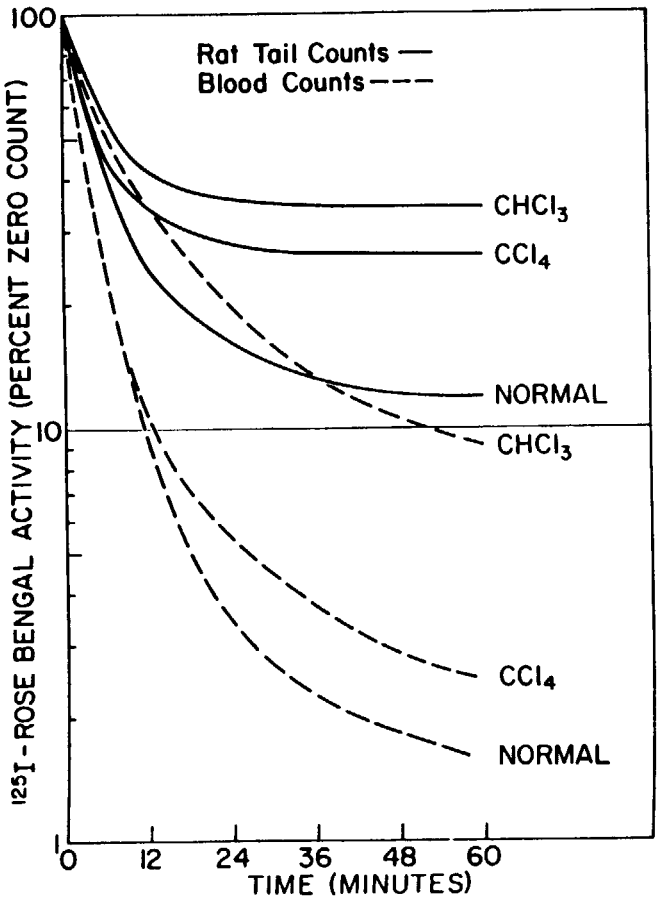

Fig. 60. Rose bengal ^{125}I activity in total circulating blood and tails of normal and CH_3Cl and CCl_4 poisoned rats showing the early cessation of tail clearance due to the blood-extravascular equilibrium enhanced by hepatic damage.

1027790

space obscured the clearance rate of the dye circulating in the blood of the arm.

To test whether the early establishment of an equilibrium between blood and extravascular space was related directly to hepatic damage, this model was tested experimentally in rats. After ^{125}I rose bengal was injected intravenously, the disappearance of the dye from the blood was measured as the mean blood activity of total circulating blood/rat, while the "arm" clearance curve was simulated by continuous counting of the radioactivity of the distal 8 cm of the tail coiled in a lead shield against the face of a 3-in. diameter NaI crystal detector. Hepatic disease was produced by intraperitoneal injection of 0.2 to 0.4 ml of chloroform or carbon tetrachloride in peanut oil 48 hr before test.

The results of this study are summarized in *Fig. 60*, which shows that the percentage clearance of both blood and tail was rapid initially, but that blood continued to clear at a rapid rate even in the presence of severe hepatic damage, while tail clearance seemed to almost stop at levels of radioactivity 4 to 10 times higher than the levels of residual blood activity. These levels appeared to be related to the amount of hepatic damage assessed microscopically and to be due, as previously surmised, to diffusion of the dye into the extravascular tissues. The residual tail activity, therefore, measures the increased amount of dye lost into the extravascular space by diffusion when hepatic blood clearance is impaired. Gross blood clearance, on the other hand, consists of the total amount of dye lost by hepatic clearance and extravascular diffusion and is not a direct measurement of hepatic extraction alone.

The presence of a blood-extravascular space equilibrium was also shown by autoradiography using the Auger electrons of ^{125}I. Although some postfixation diffusion of the labeled rose bengal was obvious, the distribution of the dye conformed well to the predictions of the model: at 1 hr, maximum concentration was in biliary canaliculi, little or none in areas of chloroform necrosis, large amounts in spared hepatic parenchymal cells, and small amounts distributed equally between blood and extravascular portal connective tissues.

REFERENCE

1. Lushbaugh, C. C., Kretchmar, A., and Gibbs, W. Liver function measured by the blood clearance of rose bengal-^{131}I. A review and a model based on compartmental analysis of changes in arm, blood, and liver radioactivity. *In:* Dynamic Clinical Studies with Radioisotopes, Kniseley, R. M. and Tauxe, W. M., USAEC Report TID-7678, June 1964, pp. 319–357, 1964.

Biologically Important Radioisotopic Materials: Absorption, Whole-body Retention, and Deposition in Specific Organs

The objective is to determine quantitatively the rates of absorption, patterns of distribution, and rates of excretion for tracer metals, radioisotopes of medical interest, and environmental and occupational contaminants. Emphasis is on human data in normal persons and patients with malignant disease, obtained with modern scanning and whole-body counting equipment. Work in experimental animals is done before the studies with radioisotopes administered to the human being. The reports this year do not fully reflect the total program in this area.

Clinical Evaluation of the ORINS Medium-level Whole-body Counter

M. Takasugi, C. C. Lushbaugh, C. L. Edwards, and W. D. Gibbs

The ORINS Medium-level Whole-body Counter (MLWBC) was described in the 1964 Research Report of the Division. It was designed to measure gamma-emitting radionuclides with an activity range from 0.1 to 100 microcuries, which includes most clinical diagnostic doses. To evaluate the MLWBC clinically, 39 patients receiving diagnostic doses of ^{131}I were studied.

The distribution of iodine during the course of its ingestion, metabolism, and excretion changes radically. These changes require the instrument to compare focal sources with diffuse sources. As reported in the 1964 report,[1] the spectral changes produced by distribution changes, as observed using compartmentalized phantoms, are minimized if the counting rates are taken as the scatter energy range (200 to 300 kev for ^{131}I) rather than peak energies (300 to 400 kev for ^{131}I).[2] This finding was confirmed in patients *(Table 14)*.

Whole-body counting is generally concerned with retention, expressed as a fraction of an administered dose or other reference rather than an absolute assay. Because counting rate becomes maximum at about 2 hr after the dose is ingested, this becomes a convenient 100% reference. Most patients are able to retain their urine for this period of time.

Using the 2-hr determination as a 100% reference, whole-body retention determined on the MLWBC compares within 10% with values

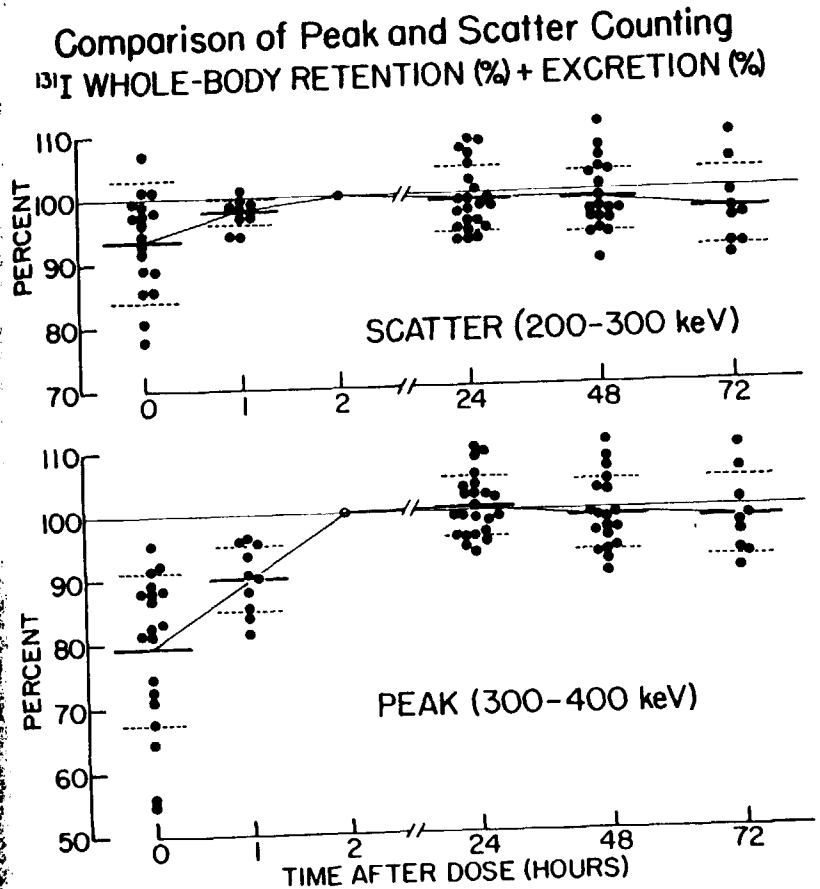

Fig. 61. Whole-body counting of ^{131}I at scatter-energy range (200 to 300 kev) and at peak energy range (300 to 400 kev). The two techniques of whole-body counting are compared at 1, 2, 24, 48, and 72 hr by plotting the percentage of the administered dose that can be accounted for by adding the percentage of the dose excreted in stools and urine to the whole-body retention; the latter value is computed from the whole-body-counting value with the use of 2 hr counting rate as the 100% reference.

1027791

computed from urine and fecal excretion data *(Fig. 61)*. When whole-body retention is compared with thyroid uptake we find better correlation than with retention computed from excretion studies *(Fig. 62)*, pointing up the unreliability of collection of excreta for retention studies.

Previous studies using the Los Alamos whole-body counters (Humco I and II) showed that whole-body counting was an applicable

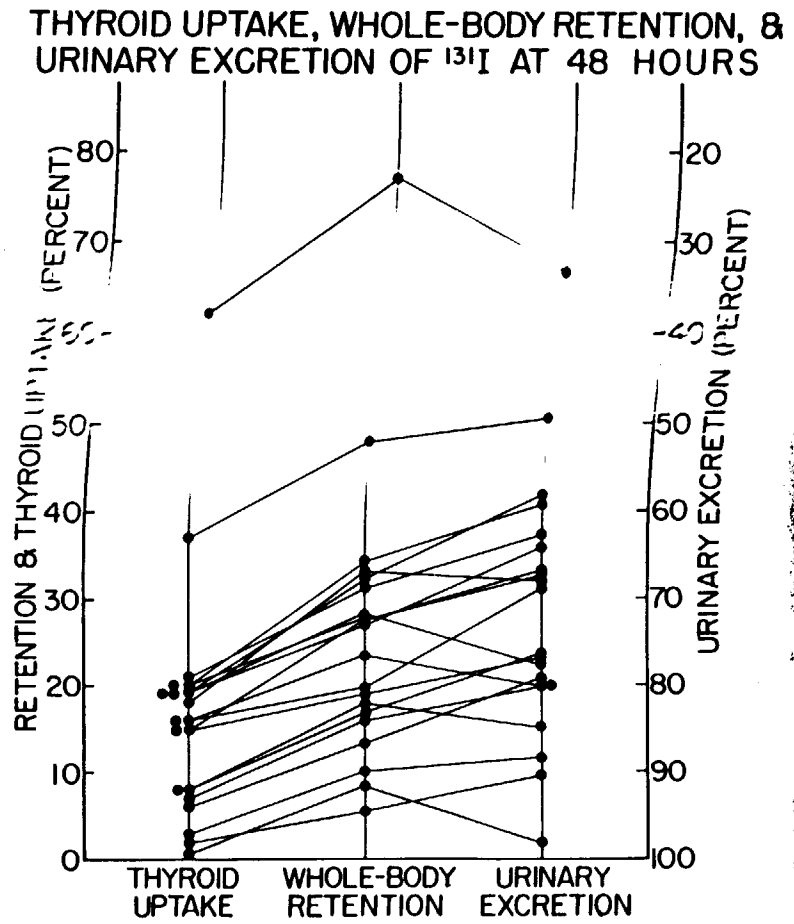

Fig. 62. Whole-body retention of ^{131}I as determined on the ORINS Medium-level Whole-body Counter compared with the thyroid uptake and urinary excretion at 48 hr.

1027792

technique for determining thyroid function with ^{131}I in man[3] and other vertebrates.[4]

Comparing thyroid uptake with whole-body retention obtained using the MLWBC reveals a correlation coefficient of .85 at 24 hr and 0.98 at 48 hr *(Fig. 63)*. The regression lines are calculated to be $Y = 0.835\ X + 24.6$ at 24 hr, and $Y = 1.16\ X + 6.8$ at 48 hr *(Fig. 64)*. These intercepts represent the nonthyroidal iodine and compare well

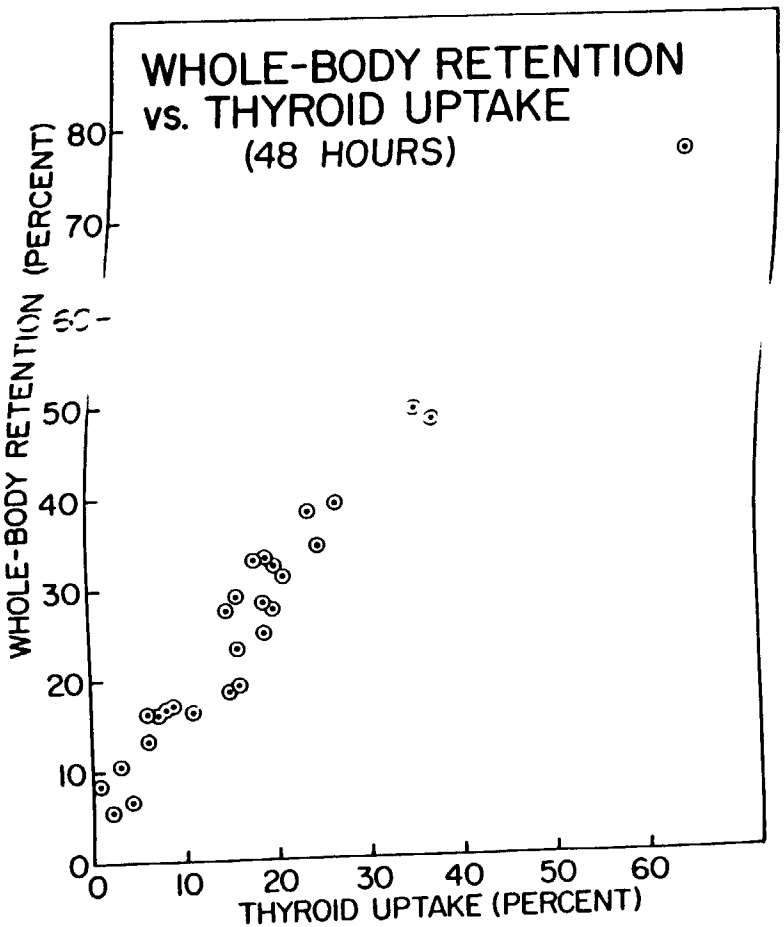

Fig. 63. Whole-body retention of ^{131}I determined on the ORINS Medium-level Whole-body Counter plotted against the thyroid uptake at 48 hr.

with the hypothetical values obtained from the formula, $Y = (1 - e^{-\lambda})X + 100\, e^{-\lambda}$, where Y = the whole-body retention, X is the thyroid uptake and λ is the biological elimination constant for inorganic iodine assuming a biological half-life of 12 hr for inorganic iodine. The slopes of the hypothetical regression lines are not the same as those calculated from the observed data because the formula erroneously assumes no release of hormonal or organically bound iodine from the thyroid gland. In hyperthyroid states in which there is an increase in the thyroid uptake, there is also rapid turnover of thyroidal iodine and release of thyroid hormone with a longer biological half-life than inorganic iodine.

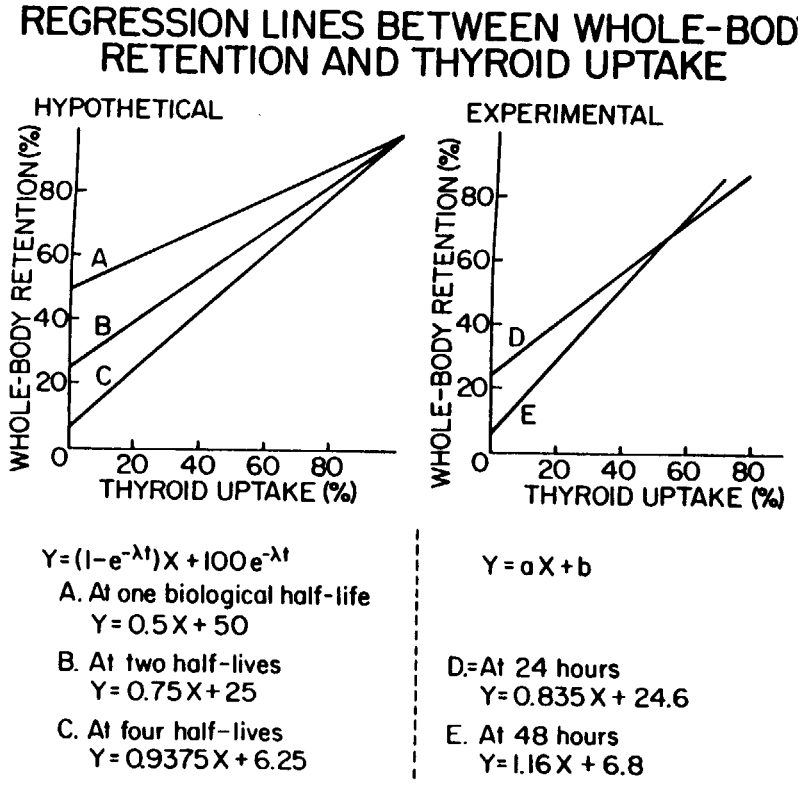

Fig. 64. Hypothetical and experimental regression lines for whole-body retention plotted against thyroid uptake. Hypothetical: A. at one biological half-life $Y = 0.5 \times +50$, B. at two half-lives $Y = 0.75 \times +25$, C. at four half-lives $Y = 0.9375 \times +6.25$. Experimental: D. at 24 hr $Y = 0.835 + 24.6$, E. at 48 hr $Y = 1.16 \times +6.8$.

1027793

TABLE 14

	0 Hour	1 Hour
Scatter energies (200–300 kev)	93.5 ± 9.5	97.8 ± 2.1
Peak energies (300–400 kev)	79.3 ± 11.8	90 ± 5.1

Comparison of counting rates obtained immediately and 1 hr after administering the dose of ^{131}I. The values are percentages of the counting rate obtained at 2 hr for each range of energies.

REFERENCES

1. Morris, A. C., Jr., Lushbaugh, C. C., Hayes, R. L., Kakehi, H., and Gibbs, W. D. Whole-body counters: Diagnostic-level counter. *In:* Research Report for 1964, Medical Division, Oak Ridge Institute of Nuclear Studies, USAEC Report ORINS-49, 1964, pp. 115–122.
2. Gibbs, W. D. Hot-patient counter. *In:* Research Report for 1962, Medical Division, Oak Ridge Institute of Nuclear Studies, USAEC Report ORINS-42, pp. 45–47, 1962.
3. Lushbaugh, C. C. and New, P. S. Clinical applications of whole body scintillometry. II. A comparison of three different methods of determining retention and thyroid uptake of orally administered I^{131}. Los Alamos Scientific Laboratory semiannual report LAMS-2445, pp. 348–360, 1960.
4. Lushbaugh, C. C. A universally applicable method for assaying thyroid function in vertebrates. Nature 198, 862–864, 1963.

The Possibility that Tobacco Contributes to Human Radioactive Body Burdens

W. D. Gibbs, C. C. Lushbaugh, and H. D. Hodges

The correlation of cigarette smoking with lung cancer has led to a search for carcinogens in tobacco. Although carcinogenic tars are known to be produced from the smoke condensate, Radford's finding[1] of ^{210}Po in the urine of heavy smokers as well as in cigarette tars suggests that exposure to radioactivity from tobacco or its by-products may also play an etiologic role. If so, the necessary contamination by radioactivity is not measureable by external counting techniques as

shown by whole-body counting of 69 adult male smokers.[2] Furthermore, we were unable to detect by external counting any unusual amount of gamma radioactivity in the mediastinum and lungs of a heavy smoker who died with primary bronchogenic carcinoma. However, cigarette tobacco does contain many gamma-emitting radioisotopes, which vary widely in amount among the different brands even from the same manufacturer.[2] The search for gamma radioactivity in cigarettes was extended to include study of fresh burley, flue- and fire-cured tobacco as obtained in wholesale markets from 21 tobacco producing areas in this country.

The gamma-ray spectra were obtained as previously described. Routine counting time was 100 min. These spectra were compared with those from cigarettes and found identical qualitatively, all gamma peaks in cigarettes being present in crude leaf tobacco. When results were expressed per gram of dry tobacco, quantitative differences in most gamma peaks were noted between cigarettes and leaf tobacco; types of leaf tobacco; samples of the same type of tobacco grown in different areas; and different brands of cigarettes. However, the burley tobacco samples contained less ^{54}Mn than other types of tobacco regardless of the area in which they were grown. The ^{40}K content of burley was, in general, higher than that of other tobaccos but varied from sample to sample by a factor of 1.8. Flue-cured tobacco contained more ^{137}Cs and ^{54}Mn than fire-cured. These radioisotopes are present in flue-cured tobacco in amounts higher than in burley by a factor of about 2 regardless of the areas in which they were grown. Typical spectra obtained from these samples are shown in *Fig. 65 A, B, and C.*

The dilemma posed by the presence of significant amounts of gamma-emitting radioisotopes in tobacco, but not in tobacco users, appears to be resolved as Radford suggests[1] by the boiling points of the isotopes tentatively identified as being present *(Table 15)*. Cesium-137 and ^{40}K are the only ones of these isotopes carried over in tobacco smoke. Manganese-54 is probably a tobacco contaminant introduced in the drying process like ^{210}Po.[3] This metal would not be released in cigarette smoke because of its greater than 2000°C boiling point. The absence of gamma-emitting isotopes other than ^{137}Cs and ^{40}K in tobacco tars[2] is therefore expected. These observations suggest that tobacco and its products are not a major source of environmental gamma-ray isotopic contamination of man.

1027794

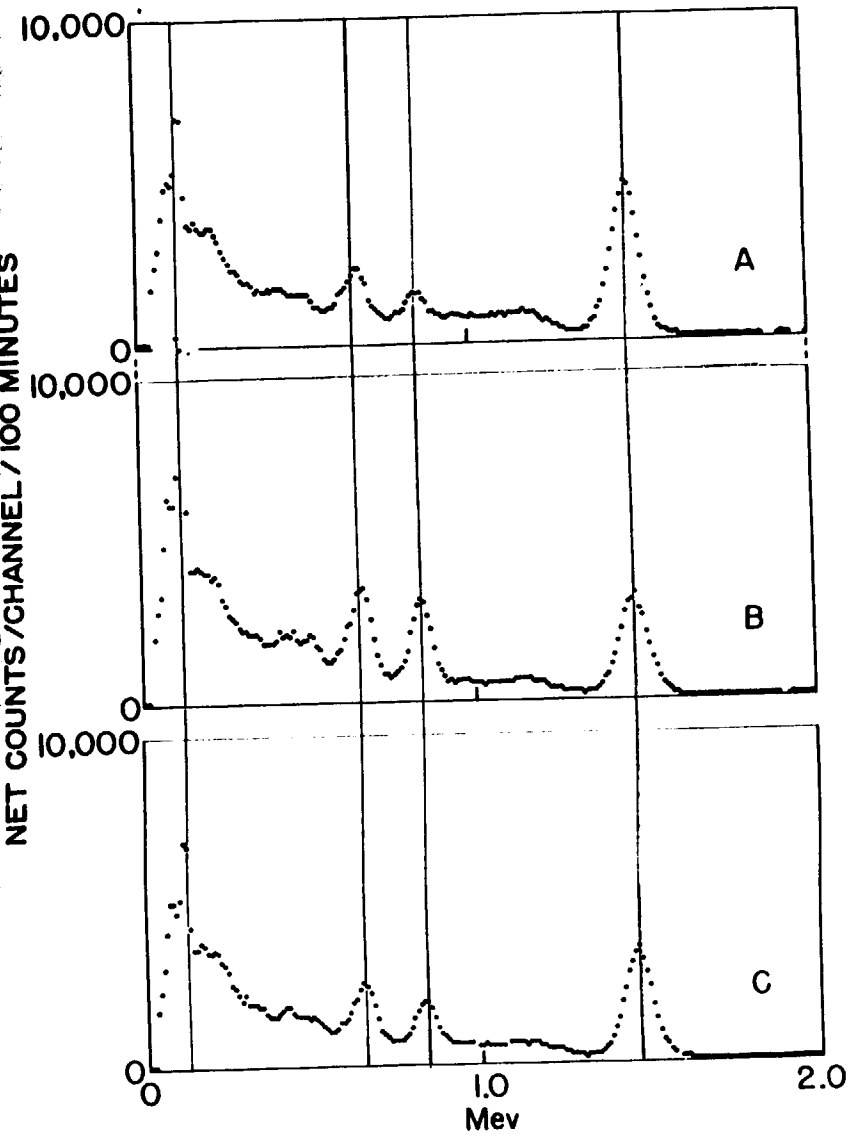

Fig. 65. Gamma-ray spectra of fresh burley A, flue-cured B, and fire-cured C, tobacco showing the increases in isotopic contamination associated with tobacco processing.

LEAF TOBACCO
TABLE 15

Energy (Mev)	Probable Isotope	Boiling Point (°C)
0.09	Thorium-232	4230
0.135	Cerium-144	2417
0.180	Radium-226	1140
0.235	Lead-212	1515
0.300	Lead-214	1515
0.350	Lead-214	1515
0.510	Many	—
0.662	Cesium-137	670
0.835	Manganese-54	2152
0.96	Actinium-228	3000
1.46	Potassium-40	760
1.76	Bismuth-214	1470
2.2	Thallium-208	1457
2.6	Thallium-208	1457

REFERENCES

1. Radford, E. P., Jr. and Hunt, V. R. Polonium-210: A volatile radioelement in cigarettes. Science 143, 247-249, 1964.
2. Gibbs, W. D., Lushbaugh, C. C., and Hodges, H. D. Radioactivity of cigarettes. *In:* Research Report, Oak Ridge Institute of Nuclear Studies, USAEC Report ORINS 49, 1964, pp. 105-107.
3. Berger, K. C., Erhardt, W. H., and Francis, C. W. Polonium-210 analysis of vegetables, cured and uncured tobacco, and associated soils. Science 150, 1738-1739, 1965.

Whole-body Retention and Distribution of Manganese-54 Chloride in the Rat

W. D. Gibbs, A. Hendrix, and H. D. Hodges*

Interest in ^{54}Mn was aroused by the highly variable concentration of this isotope in crude tobacco and cigarettes, which raised questions concerning the location in the organs of the body and the turnover of

*Summer student trainee

1027795

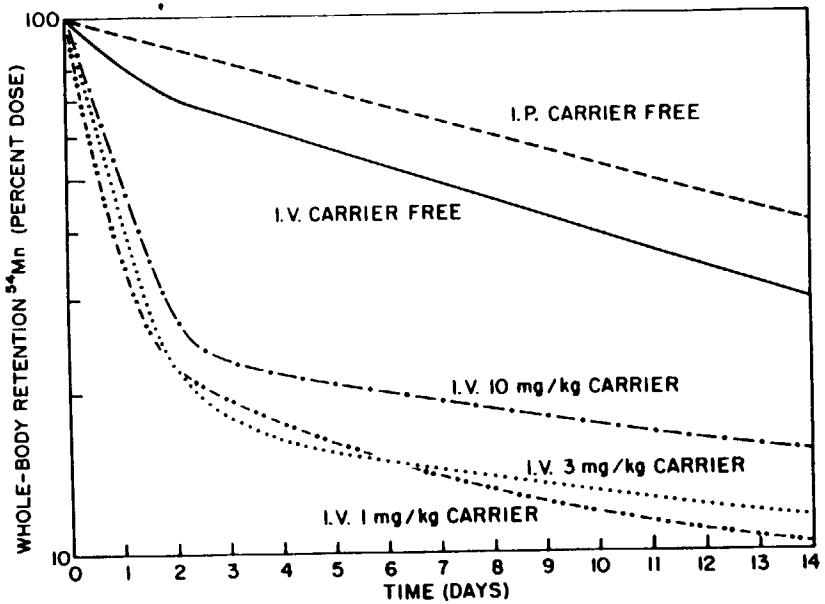

Fig. 66. The effect of route of administration and dose of carrier upon ^{54}Mn whole-body retention in the rat.

greater than trace amounts of this metal in smokers and other users of tobacco products. Little is known of the role and fate of this trace element in normal man and experimental animals[1] but previous whole-body retention studies have indicated that retention is neither unusually high nor prolonged in disease and that gastrointestinal absorption is relatively low[2] and greatly affected by carrier metal. Most studies have suggested that no particular organ has an unusually great affinity for this trace metal but Cotzias[1] has observed cohort red-cell labeling with ^{54}Mn after intravenous administration. These conflicting but provocative observations led us to investigate whether this element was applicable to diagnostic radioisotope procedures such as red-cell survival studies.

Manganese-54 chloride was injected into male albino rats according to the schedule shown in *Table 16*. They were whole-body counted immediately after injection and then at approximately daily intervals for 14 days or more. The animals were randomly selected, killed at intervals as indicated in *Table 17*, autopsied and tissue samples were

collected for radioassay. *Table 17* also shows the average ^{54}Mn contents of selected tissues expressed as percentage of dose per gram. Average whole-body retention for each dose group is shown in *Figs. 66* and *67*. It is evident that carrier decreases percentage dose retention by causing increased excretion for a short time. The 10 mg/kg carrier level is quite toxic. Nine of 15 animals given this dose died immediately after injection.

With low carrier or carrier-free solutions relative adrenal content increases remarkably with time. Paradoxically an increase in carrier level increases the concentration in femoral bone. Different carrier levels also affect the organic retention and excretion rates to variable degrees with time.

The tissue assays of group IV, given carrier free ^{54}Mn and then injected with 3 mg/kg carrier after 14 days, show extremely high adrenal

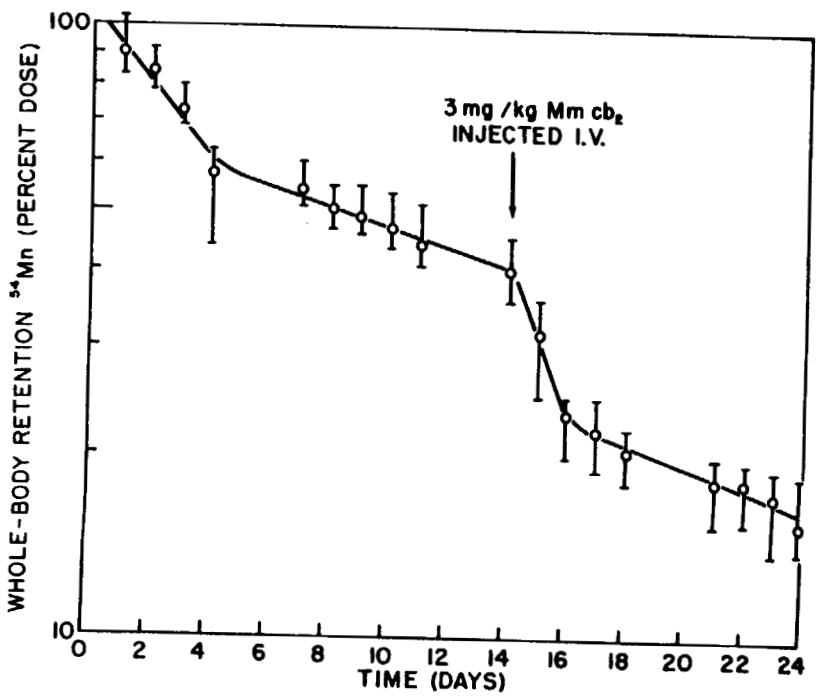

Fig. 67. The effect of an intravenous dose of carrier upon an established rate of ^{54}Mn excretion as measured by whole-body retention in the rat.

concentrations at 24 days, but most other tissues are quite low. This preferential retention of manganese by the adrenal suggests that some form of a manganese label might possibly serve as a scanning agent for adrenals, although the absolute amount present when the body background is lowest may not be sufficient for external scanning. The physical half-life of 314 days and high-energy gamma radiation of ^{54}Mn may make it an undesirable radioisotope for organ location in humans if large doses are necessary. Manganese-52 ($T\frac{1}{2}$ = 5.7 days) would overcome this objection because positron scanning methods could be used, but this approach would require accelerating adrenal uptake to compensate for this short half-life.

This study also showed that red-cell labeling by manganese was insignificant in the rat and that the relatively rapid turnover rate and small size of the manganese metabolic pool minimized the potential hazard of this element from accidental or environmental contamination, should this occur.

REFERENCES

1. Cotzias, G. C. Trace metals: Essential or detrimental to life. USAEC Report BNL-828, April 10, 1963.
2. Furchner, J. E., Drake, G. A., and Richmond, C. R. The retention of manganese-54 by mice, rats, dogs, and monkeys. LASL Annual Report LA-3132, MS, July 1963 through June 1964.

TABLE 16

Group No.	No. of Rats	Injection Route	Carrier Level
I	12	I. V.	1 mg/kg
II	12	I. V.	3 mg/kg
III	6	I. V.	10 mg/kg
IV	8	I. V.	*
V	12	I. P.	carrier free
VI	12	I. V.	carrier free

*3 mg/kg injected 14 days after carrier-free dose.

TABLE 17

Distribution of Intravenous ^{54}Mn in the Rat

Carrier (mg/kg)	Tissue	Time after Dose 2 Days	4 Days	7 Days	21 Days	24 Days
				% dose/gram		
0	Pancreas	2.564	2.013	1.529	0.455	†
	Adrenal	1.612	1.886	3.920	2.528	
	Kidney	2.953	1.789	1.414	0.341	
	Liver	3.548	2.105	1.575	0.323	
	Femur	0.170	0.174	0.179	0.160	
	Blood	0.005	0.009	0.005	0.002	
1	**Tissue**	**1 Day**	**3 Days**	**7 Days**	**14 Days**	**24 Days**
	Pancreas	0.923	0.402	0.220	0.256	†
	Adrenal	0.167	0.114	0.225	0.305	
	Liver	0.426	0.278	0.231	0.156	
	Kidney	0.289	0.161	0.117	0.088	
	Femur	0.197	0.188	0.154	0.147	
	Blood	0.002	0.001	0.001	0.001	
3	Pancreas	0.751	0.233	0.134	0.019	†
	Adrenal	0.164	0.080	0.146	0.041	
	Kidney	0.198	0.099	0.074	0.013	
	Liver	0.197	0.169	0.100	0.022	
	Femur	0.281	0.271	0.320	0.044	
	Blood	0.001	0.001	0.001	0.000	
10	Pancreas	1.182	†	0.052	0.059	†
	Adrenal	0.075		0.056	0.083	
	Kidney	0.149		0.036	0.037	
	Liver	0.105		0.068	0.064	
	Femur	0.807		0.224	0.402	
	Blood	0.001		0.001	0.001	
*	Pancreas	†	†	†	†	0.158
	Adrenal					0.740
	Kidney					0.184
	Liver					0.205
	Femur					0.087
	Blood					0.002

*Injected carrier free; 3 mg/kg carrier injected at 14 days
† No Data

1027197

Aestival Variation of Thyroid Function in the Box Turtle

C. C. Lushbaugh, G. L. Humason, M. C. Yarbrough, R. Queener, and W. D. Gibbs

A previous study[1] was designed to test the hypothesis that whole-body counting of ^{131}I retention could be used universally to assay thyroid function in animals with thyroid glands of unknown location and size.[2] The box turtle, *Terrapene carolina carolina*, was chosen because of obvious difficulties encountered in measuring the thyroid radioactivity in this species by other external counting procedures. A remarkably large variation was found in the amount of ^{131}I retained by different turtles.[1] Analysis of these data indicated that the variation was caused by increasing retention as the study progressed during the summer. It had been suggested earlier that this variation was merely due to dehydration that land turtles are said to experience under laboratory conditions,[3] but a histologic study disclosed epithelial changes in the thyroid glands that seemed to correlate logically with degree of retention and to suggest that the turtle thyroid became hyperfunctional during the summer months. To test the veracity of this explanation, an experiment was designed to correlate whole-body iodine retention, thyroid iodine uptake, histologic appearance, and time of year in this species.

Six groups of 10 box turtles were chosen at random. On June 24, July 22, August 19, September 2 and 16, and October 4, the turtles in a group were injected intraperitoneally with 5 microcuries of carrier-free ^{131}I sodium iodide. Whole-body counts were obtained immediately after injection and at 1, 5, 7, 11, and 14 days. On the 14th day the turtles were killed; their thyroids were removed, assayed for radioactivity, and prepared for autoradiography and histologic study.

The results are summarized in the figures. The mean whole-body iodine retention curves for the groups injected on June 24, September 2, and October 4 are shown in *Fig. 68*. The progressively higher iodine retention as autumn approaches is well demonstrated. The parallel increase of thyroid iodide binding and retention at 14 days after injection is shown in *Fig. 69* in which the means and 90% confidence intervals of the data for thyroid iodine retention are graphed. The variation in each group is wide but the increase of thyroid iodine retention with passage of calendar time is evident. This variation is also to be found in the histologic appearance of glands from any one group except that of the group labeled in early fall (October).

The thyroid glands of the turtles killed during the summer are of

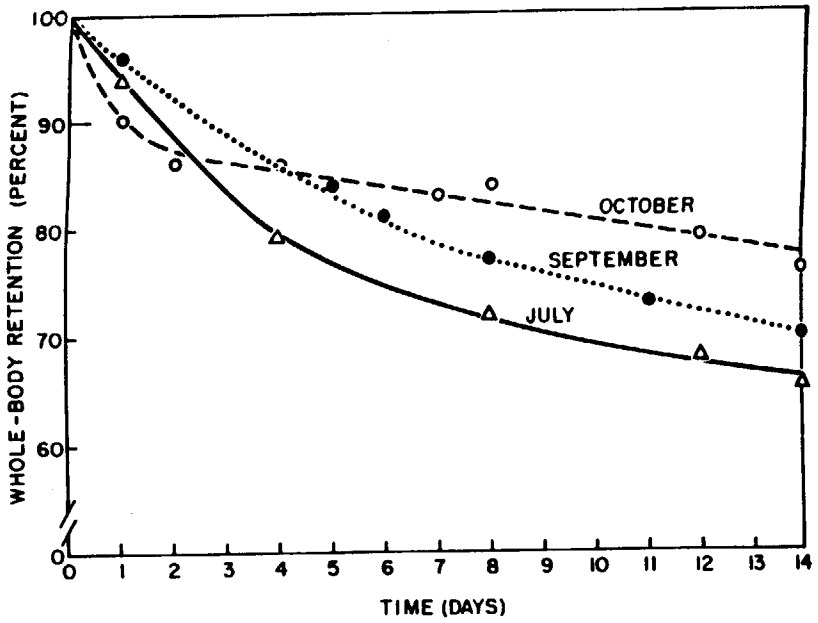

Fig. 68. The mean whole-body retention curves of 30 box turtles, labeled in groups of 10 in July, September, and October, showing increased prehibernal iodine retention.

four main types, as shown in *Fig. 70A, B, C, and D*, arranged in the order that correlates best with the respective thyroid ^{131}I activity on the 14th day after injection. Low retention occurred in glands showing a colloid goiterous appearance as in *Fig. 70A*. The epithelium was flattened, colloid was abundant, acini were greatly distended, interstitial tissue and blood vessels were inconspicuous. The next stage, *Fig. 70B*, accompanied by thyroid retention of from 30–50%, was typified by large irregular vacuoles in the colloid adjacent to the epithelium, which was now cuboidal. Colloid continued to be diminished in amount in the next phase *(Fig. 70C)*, stained poorly with the PAS reaction and was diffusely granular. The epithelium was tall cuboidal. The interstitial connective tissue was prominent. *Figure 70D* shows the most hyperplastic appearance of the gland; crowded columnar epithelium surrounding a small acinus filled with vacuolated PAS positive colloid or faint traces of granular colloidal detritus. The histologic stages C and D were accompanied by uptakes in the 50 to

1027798

70% range, but surprisingly not with the highest uptakes (70 to 95%, see *Fig. 69*).

The greatest retention was associated with the histologic appearance seen in *Fig. 70E*, which resembles that in *Fig. 70A*, except for prominent connective tissue, hyperemic blood vessels (arrow), cuboidal epithelium, and colloid that varied from acinus to acinus as watery, granular, or solid PAS positive abundant material as depicted. These observations are supported further by comparison of the thyroid iodine content with the whole-body iodine retention at 14 days, which

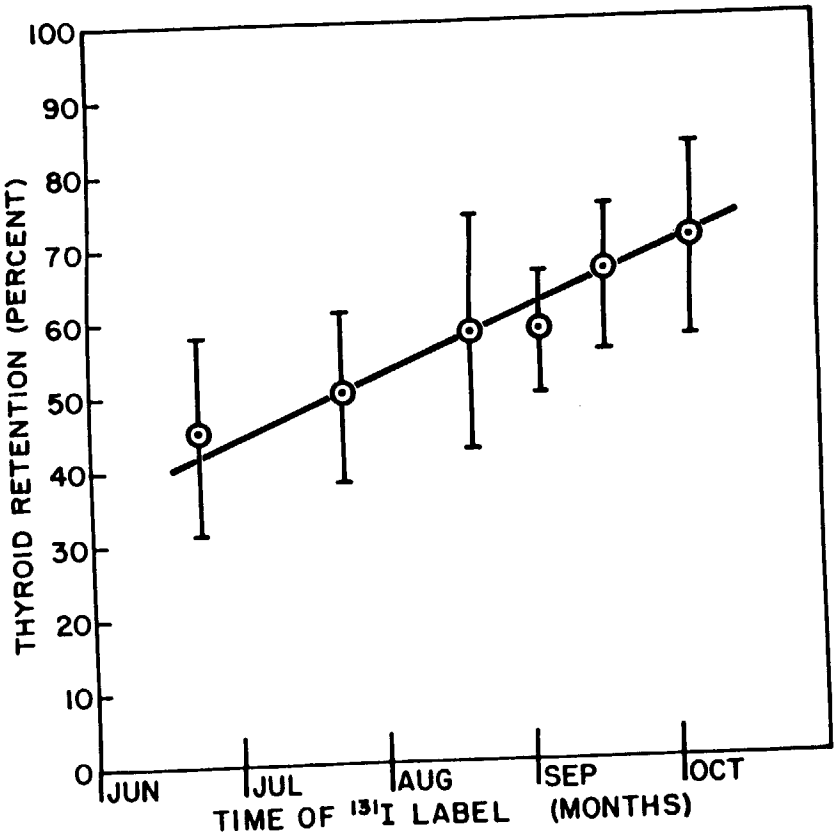

Fig. 69. The thyroid iodine retention 14 days after intraperitoneal ^{131}I injection as a function of the calendar month during which the study was made.

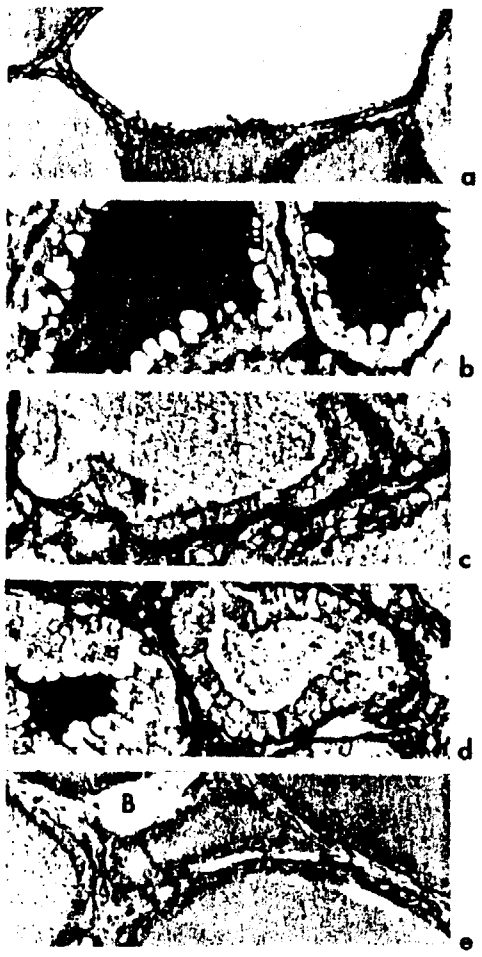

Fig. 70. Photomicrograph (X275) of the histologic stages (Periodic Acid Schiff (PAS) stain) of aestival hyperplasia and prehibernal colloid storage arranged in the temporal order this study suggests: A, in early summer, flattened acinar epithelium and abundant colloid becoming granular; B, cuboidal epithelium and peripherally vacuolated colloid; C, columnar epithelium and diminished coarsely granular colloid; D, tall columnar epithelium, small acini, minute foci of residual (?) colloid; and E, in early autumn, cuboidal to flattened epithelium and colloid becoming increasingly abundant, less granular and more PAS positive. In E, at arrow, a distended capillary is seen, typical of the hyperemia present.

1027799

shows that in early summer the extrathyroidal tissue contained 30% of the total-body bound iodide but only 8% in the autumn.

These observations suggest that the large variation found in turtles' thyroid iodine uptake or whole-body iodine retention is due to a wide variation in individual thyroid function; that on merging from hibernation the thyroid contained acini distended with colloid lined by atrophic epithelium, and that during the summer months the gland goes through a hyperplastic cycle during which old colloid is lost and new colloid, rich in newly bound iodide, is formed and stored in the follicle. This aestival change, because of its correlation with calendar time, may be an annual prehibernal process controlled by environmental conditions.

REFERENCES

1. Gibbs, W. D., Wilson, E., Hodges, H. D., and Lushbaugh, C. C. Comparative study of thyroid and whole body retention of iodine in box turtles. *In:* Second Annual Oak Ridge Radioisotope Conference, April 19–22, 1964. USAEC Report TID-7689, pp. 20–21.
2. Lushbaugh, C. C. A universally applicable method for assaying thyroid function in vertebrates. Nature (Lond.) 198:862–864, 1963.
3. Shellabarger, C. J., Gorbman, A., Schatzlein, F. C., and McGill, D. Some quantitative and qualitative aspects of I^{131} metabolism in turtles. Endocrinology 59, 331–339, 1956.

NASA Study on Radiation Effects

This project is supported by the National Aeronautics and Space Administration and the U.S. Atomic Energy Commission. Its objective is to establish the radiosensitivity of man from information obtained from therapeutic trials and radiation accidents.

Radiobiologic knowledge useful in predicting the responses of man to ionizing radiation has in the past been largely based on experiments on laboratory animals. The great need for human data leads to this type of study, which uses information from clinical and accidental irradiation. The many difficulties in collecting and analyzing this information we overcome, in part, by the use of modern data processing equipment. The major effort up to the present has been in collecting and analyzing in great detail the information available in hospital records at the Division, and at other institutions.

First emphasis has been placed on developing an analytical system basic to probit analysis of apparent dose-response relationships that will finally result in probit regression equations and effective doses (ED_{50}) with fiducial confidence limitations. These data will be used to appraise the extent to which man will be endangered from radiation during space travel in conjunction with probability estimates of what doses, rates, and quality of radiation of energies will be met during two-week to two-year missions. Determination of effective doses for eliciting the prodromal symptoms of radiation sickness has been the first goal since such symptoms are detrimental to man's efficient performance. Thus dose estimates were initially worked out with 100 patients at the Division, then strengthened by 60 additional cases from the University of Cincinnati and the City of Hope Hospital in Duarte, Calif. The base is being further broadened by data from approximately 700 other cases of total-body exposure of man. A major part of time has been expended recently in attempting to reduce the sensitizing bias of disease upon these figures. In many clinical instances prodromal-like responses are caused by disease and not radiation.

Plans are under way for the collection of new information on radiation exposure, and to this end the construction of a new low-dose-rate irradiation facility has been begun at the Division.

1027800

Human Radiosensitivity as Measured by Study of Clinical Data From Therapeutic Total-body Irradiation

C.C. Lushbaugh, G. A. Andrews, R. Hofstra, and F. V. Comas*

The effects of total-body irradiation on man have been studied clinically since Walsh[1] first described "radiation sickness" in 1897. The dose-response relationships, however, are still poorly known and present estimates are based largely upon conjectures derived by extrapolation from animal experiments or from experience with radiation accident victims, atomic bomb casualties, and therapeutically irradiated patients.[2-5] These estimates are not sufficiently accurate to allow prediction of the doses of radiation required to cause deleterious functional effects or significant decrements in performance. More accurate dose-response relationships are needed for man before the success or failure of a space flight through a radiation field can be predicted on the basis of radiobiologic probability equations.

At present it is not known with certainty whether the prodromal radiation syndrome – anorexia, nausea, vomiting, diarrhea, listlessness (apathy), and increased fatigability – would lead to delayed or lowered performance capabilities, but it seems justifiable to assume that it would. This group of effects probably constitutes the earliest physiologic threat at the clinical level to man's continued performance during, or shortly after, irradiation. For these reasons emphasis was placed on determining directly with probit equations the radiation dose-symptomatic response relationships for these six commonest symptoms of the prodromal radiation syndrome.

Ninety-three patients irradiated for therapeutic purposes in the Institute's total-body irradiation facility and seven nuclear radiation accident victims who were treated at the Medical Division comprised the 100 cases studied. A three-day period of study preceded the single therapeutic radiation exposures. After radiation exposure, clinical and laboratory observations were made for six weeks. To relate the absorbed dose from exposure to different kinds of radiations to an acceptable standard unit, the midline exposures were converted to midepigastric rads on the basis of the depth-dose measurements for ^{137}Cs and ^{60}Co, and appropriate quality factors for neutrons and gamma rays from critical excursions.[6] The resulting 100 midepigastric doses were found to be clustered in four groups of unequal numbers of cases.

*Mathematics Division, Oak Ridge National Laboratory.

The arithmetic and geometric means of each group were used respectively for the subsequent linear and logarithmic line-fitting programs.

An encodement was made of symptoms, signs, and laboratory and nursing observations, so that pertinent information from the clinical chart could be extracted and coded digitally by trained clerical personnel. Although it was well known that some of these patients were exhibiting the symptoms without radiation, no correction for these nonradiobiologic responses was made. The coded observations were arranged and stored on magnetic tape. Programs were devised for data retrieval, and probit analyses were made of the percent responses in relation to dose and the dose transformed to logarithms. The Chi-square goodness-of-fit of the resulting regression lines and 95% confidence limits were then obtained. The results are shown in *Table 18* and *Fig. 71* as the ED_{50} for these responses; they agree well with the

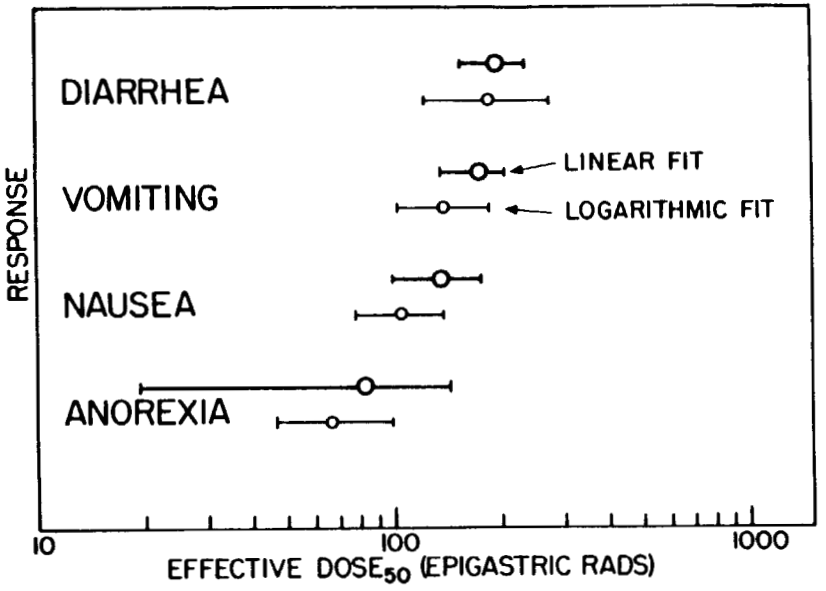

Fig. 71. Comparison of the ED_{50}'s and their respective 95% confidence limits derived from linear and logarithmic dose-probit analyses of percent incidence of anorexia, nausea, vomiting, and diarrhea in 100 hospital patients. The responses are arranged in order of increasing clinical severity assumed from the rank of the effective doses.

1027801

TABLE 18

Probit Analysis of Effective Doses for Gastrointestinal and Systemic Clinical Responses to Total-body Irradiation in Man

A. Using arithmetic dose:

Clinical Response	Equation P = a(dose) + b		$ED_{50} \pm$ S.E. (m)	
	Probit Units (a)	(b)	Epigastric Dose (rads)	Midline Air Dose* (R)
Anorexia†	0.017	3.609	82 ± 32	124
Nausea†	0.008	3.837	138 ± 20	209
Vomiting†	0.008	3.588	173 ± 18	262
Fatigue‡	0.004	4.428	136 ± 36	206
Diarrhea‡	0.008	3.441	194 ± 19	294

B. Using logarithmic dose:

Clinical Response	P = a (log dose) + b	$ED_{50} \pm$ S.E. (m)		
	Probit Units (a) (b)	Epigastric Dose (Log_{10} rads)	(rads)	Midline Air Dose* (R)
Anorexia†	3.431 − 1.275	1.8291 ± 0.0837	68	101
Nausea†	2.301 + 0.362	2.0152 ± 0.0640	104	157
Vomiting†	2.369 − 0.061	2.1360 ± 0.0640	137	201
Fatigue‡	1.329 + 2.360	1.9868 ± 0.1068	97	147
Diarrhea‡	1.895 + 0.712	2.2622 ± 0.0900	183	277

*As if all doses were from ^{137}Cs gamma rays, so 66 absorbed tissue rads = 100 R measured in air at theoretical midline without the patient present.
†Incidence of response through 2 days.
‡Incidence of response through 42 days.

majority of dose-response estimates derived in other studies and reviews.[2,3] The 95% confidence limits about the regression lines indicate, however, that these numbers can be used only with prudent restrictions.

These results show an internal agreement, however, that appears

logical as well as intuitively fortunate as shown in *Fig. 72*. Clinically assumed severity of response varies in proportion with effective dosage.

The actual ED_{50}'s obtained by the two methods are not significantly different as the overlapping 95% confidence limits illustrate. Because these data are from people suffering from diseases these ED_{50}'s should be considered the least doses required for these responses, and probably should be increased for normal adult man. No dose-correction factor for converting these ED_{50}'s from sick to well man is now available, but it is believed that the bias caused by disease can be minimized by the expansion of these studies to include the data of other investigators who gave total-body irradiation to patients with nonhematologic diseases.

REFERENCES

1. Walsh, D. Deep tissue traumatism from roentgen ray exposure. Brit Med J 2, 272 1897.
2. Langham, W. H., Brooks, P. M., and Grahn, D. Radiation biology and space environmental parameters in manned spacecraft design and operations. Aerospace Med 36, #2, section 2, 1-55, 1965.
3. Bord, V. P., Fliedner, T. M., and Archambeau, J. O. Mammalian radiation lethality, a disturbance in cellular kinetics, Academic Press, New York, 1965, pp. 101-114.
4. Oughterson, A. W., and Warren, S., eds. Medical effects of the atomic bomb in Japan. McGraw-Hill Book, Inc., New York, 1956.
5. Gerstner, H. B. Reaction to short-term radiation in man. Ann Rev Med 11, 289-302, 1960.
6. Hayes, R. L., Oddie, T. H., and Brucer, M. Dose comparison of two total-body irradiation facilities. Intern J Appl Radiat 15, 313-318, 1964.

1027802

Instrument Development and Methodology

The success of modern biomedical research often depends on inventiveness and the ability to devise new tools and new methods. These technological outputs require much effort, and it is important to report and share these advances. One objective is to develop and apply refined instrumentation for detecting and localizing radioactivity to meet specific needs in the research effort. Examples have been scanning systems, whole-body counting facilities, and other detection apparatus for quantitating the radioactivity in an organ. Some developments are not directly related to measurement of radioactivity; for example, this year a major effort was in the design of a hemolyzometer, which is used for studying red-cell changes as related to radiation injury and hematologic diseases.

Color and Contrast Enhancing Rescanner

G. Uchiyama, A. C. Hitchcock, and A. C. Morris, Jr.*

Color recording in radioisotope scanning has been developed to improve the diagnostic ability of radioisotope scanning. A color rescanner[1] has been developed to combine color recording with the rescanning technique. High quality black and white photoscan records, which contain all available information about radioisotope concentrations expressed as a degree of density on film, are first obtained from the patient by an area scanner. The new instrument rescans these films and demonstrates by color patterns the degree of contrast. This permits easy interpretation of subtle changes in density or concentration of the radioisotope. The device has a photoelectric densitometer that provides a color signal proportional to the density of the original photoscan. A photocell signal rotates a color-wheel disc through an optical servomechanism to a position set by the film opacity. Light passing from a source up through a slit in the color

*Work done while a Fellow in Radiological Research of the James Picker Foundation. Present address: Department of Radiology, Chiba University, Chiba, Japan.

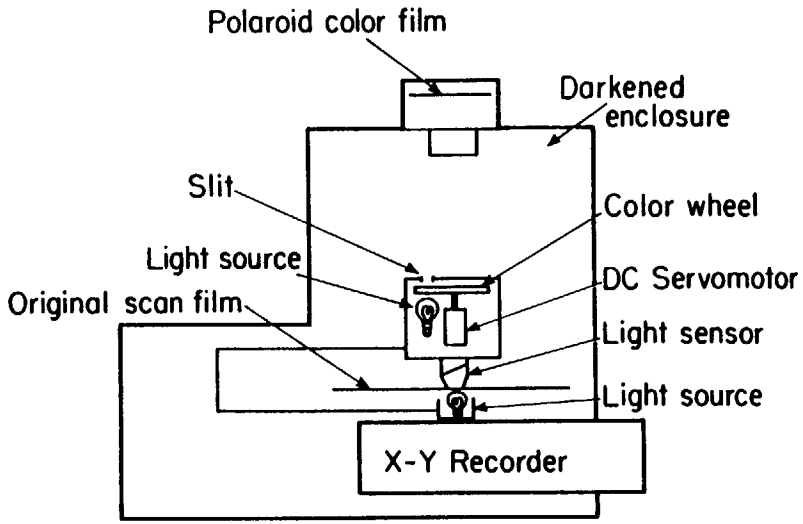

Fig. 72. Block diagram of the color rescanner.

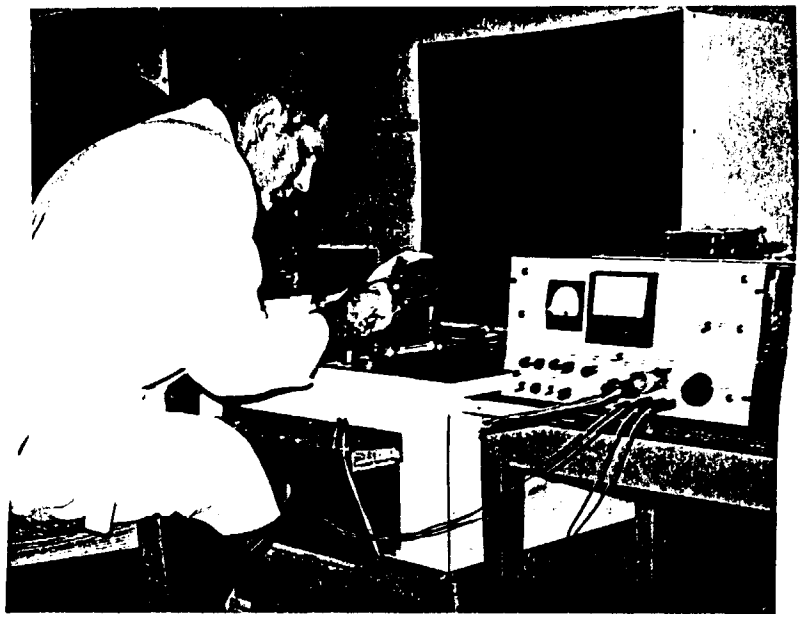

Fig. 73. Color rescanner with the operator changing the color-wheel disc.

1027803

wheel is used to expose Polaroid color film. *Figure 72* shows a block diagram.

This color rescanner, a joint development with the Medical Nuclear Instrumentation Group, Oak Ridge National Laboratory, was completed this year. The color sequences to be used for various kinds of original scan records have been examined carefully. In this study, linear, logarithmic, and reverse-logarithmic color wheels were produced and used. *Figure 73* shows the color rescanner with an operator changing the color-wheel disc. An early rescan[2] result was shown on the cover of the 1964 Research Report.[3]

REFERENCES

1. Harris, C. C., Satterfield, M. M., Uchiyama, G., and Kimble, H. E. A "rescanner" with photographic color readout. Manuscript in preparation.
2. Uchiyama, G., Hitchcock, A. A. C., and Morris, A. C., Jr. Clinical results with a color-recording rescanner. Manuscript in preparation.
3. USAEC Report ORINS-49.

Standardization and Calibration of a Whole-body Counter for Clinical Research

W. D. Gibbs, H. D. Hodges, C. C. Lushbaugh

The application of whole-body counting to clinical diagnostic and medical problems depends upon precise daily quantitation of radioisotopes that change their location in various organs. Reliability and reproducibility of results under these circumstances require that the response of the counter be independent of body size and distribution of the radioisotope. No whole-body counter at this time meets these specifications. In using[1] the Institute's whole-body counter (see cover illustration), a method was developed that satisfies these requirements within narrow limits by using empirically determined correction curves for different body sizes and a system for each radioisotope of analyzing selected portions of the scatter spectrum rather than the photopeak. The integrated photopeak counts can be used quantitatively only if the radioisotope is uniformly distributed because counting efficiency in this situation is primarily dependent upon body thickness rather than body mass. For ^{40}K such integrated photopeak assays can be easily corrected for various body thicknesses by the use of the counting efficiency–body thickness relationships shown in *Fig. 74*. Similar curves have been determined for ^{137}Cs with the use of adult, adolescent, and child water phantoms.[2] The anteroposterior diameter

of the chest measured with calipers at the xiphoid was found to approximate the value obtained for the average body thickness from the equation:

$$\bar{T} = \sqrt{\frac{\text{body weight (g)}}{\text{height (cm)}}}$$

The small effect of body length upon the efficiency of this whole-body counter is illustrated by the displacement of the curves for the child, adolescent,and adult phantoms *(Fig. 74)*, which require less than 6% correction between children and adults.

The response of the counter to point sources was studied with ^{131}I, ^{51}Cr, ^{59}Fe, ^{137}Cs, ^{60}Co, and ^{198}Au in many locations in phantoms representing various body sizes and body builds. Results for these nonuniformly distributed radioisotopes indicate that if photopeak counts are used, counter response may vary more than 100% depending upon location of the radioisotope. However, for every radioisotope studied an energy band in the scatter spectrum was found in which the observed counting rate varied by less than ±15% regardless of the location of the source within the phantom. This method of data analysis requires immediate assay of the patient after administration of the isotope to

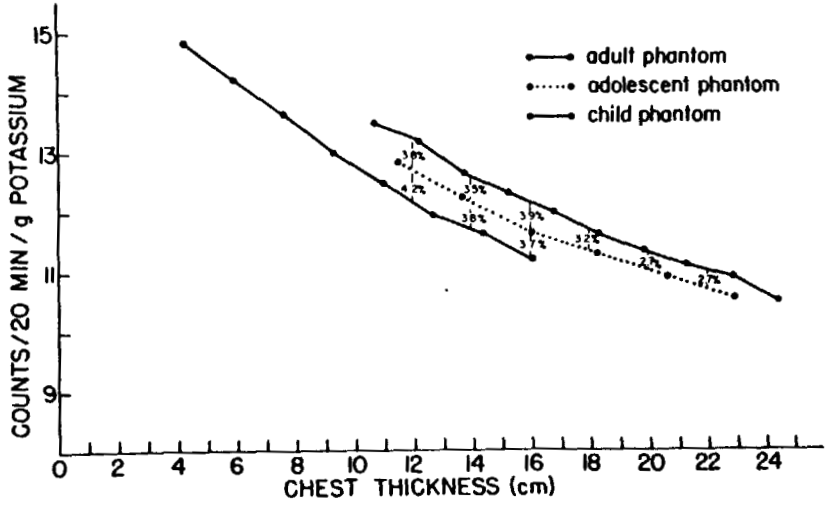

Fig. 74. Correction curves for child, adolescent, and adult phantoms showing the large dependency of counting efficiency upon average body thickness rather than length (body height).

1027804

obtain a 100% dose count for the individual. All subsequent measurements on any one subject are then expressed as percentage of initial count after correction for physical decay. *Table 19* illustrates these differences obtained by the two methods of data analysis for ^{131}I. The technique of scatter counting is not, of course, generally suitable for simultaneous studies of multiple isotopes, or when the nuclide present is unknown.

A further complication to accurate daily quantitations of radioisotope retention has resulted from unpredictable background fluctuations caused by radon leakage in the counter cave. The radon comes from the lead shield located beneath the inner stainless steel lining of the iron room. Attempts to reduce this contamination by negative pressure and by plastic paint are only temporarily beneficial. Until

TABLE 19

Difference in radioactivity measurements of an ^{131}I source in various body locations, when the integrated photopeak or the scatter peak is used. Shaded areas indicate variations greater than ±10% from the standard position in the center of the trunk.

Percent Response From ^{131}I Point Source in Water Phantom

Body Section	Peak Response*			Scatter Response**		
	Source Location			Source Location		
	Front (%)	Center (%)	Back (%)	Front (%)	Center (%)	Back (%)
Lt. Leg	169	156	198	103	112	107
Rt. Leg	180	163	203	104	115	112
Lt. Thigh	156	129	178	99	104	100
Rt. Thigh	159	133	187	102	109	104
Pelvis	148	109	177	103	104	106
Trunk	151	100	178	102	100	102
Neck	148	121	176	99	100	99
Head	157	115	184	97	92	92
Lt. Arm	159	150	156	97	106	106
Rt. Arm	173	151	179	103	106	110

*310 410 kev
**150 310 kev

a solution of this problem is found, nightly background determinations are required to assess the variations shown in *Fig. 75*. If radon is allowed to reach equilibrium inside the "cave" a background increase of 35% over the minimum is seen with prominent gamma-ray peaks at 0.30, 0.35, 0.61, and 1.77 Mev.

The absolute efficiency of the counter is being determined in cooperation with the AEC Committee for Whole-Body Counter Calibration to provide worldwide cross reference for future measurements.

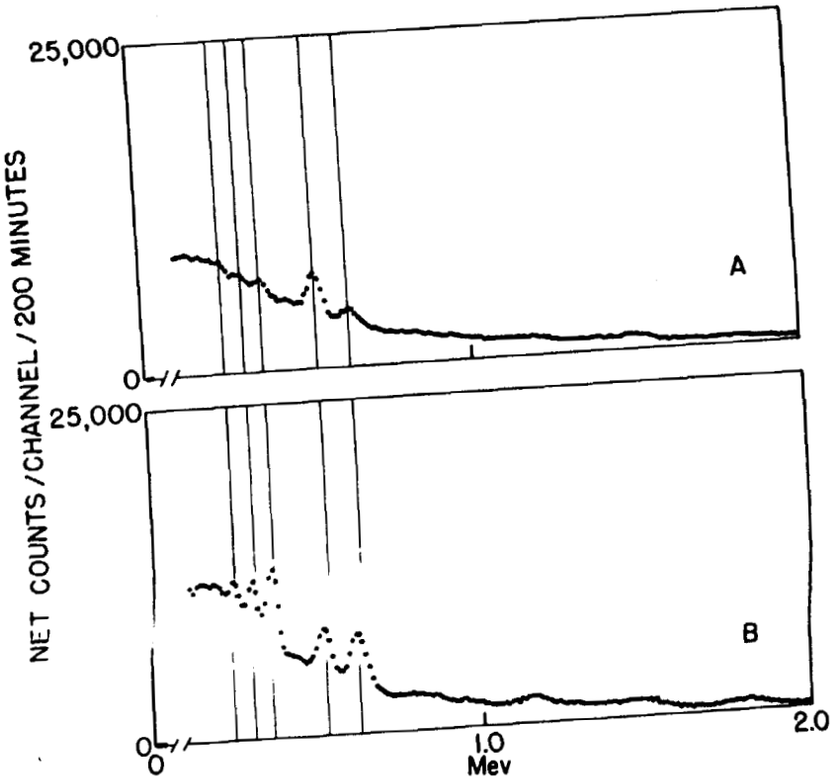

Fig. 75. Gamma-ray spectra of 200 minute nightly background radioactivity determination in the cave: A. after vacuum pumping and B. after reestablishment of equilibrium with the lead contaminant, 3 days after pumping was stopped.

1027805

These studies have necessarily preceded the complete development of a research program. However, 565 measurements have now been made in normal and ill persons. Retention studies have been started with the use of ^{140}La, ^{47}Ca, ^{28}Mg, ^{99m}Tc, ^{68}Ga, ^{131}I, ^{159}Gd, ^{198}Au, ^{51}Cr, ^{60}Co, ^{160}Tb, and ^{22}Na. The determination of retention of ^{60}Co-labeled vitamin B_{12} in patients with pernicious anemia has proved to be a useful adjunct to long-term management.

REFERENCES

1. Gibbs, W. D., Lushbaugh, C. C., and Morris, A. C., Jr. Preliminary efficiency and calibration studies with a new whole-body counter with an ultralow background shield. J Nucl Med 6, 337, 1965.
2. Hayes, R. L., Oddie, T. H., and Brucer, M. Dose comparison of two total-body irradiation facilities. Int J Appl Radiat 15, 313-318, 1964.

A Rapid Electronic Method for Measuring Red-cell Fragility in Hemolytic Systems

*A. C. Morris, Jr., C. C. Lushbaugh, D. H. Lushbaugh, and R. H. Corley**

In 1956, Danon developed a dialysis method for gradually decreasing the salt concentration of a red-cell suspension[1]; this method was later extended through instrumentation to measure automatically osmotic red-cell fragility.[2] In this system the change in tonicity is determined by measurement of increasing conductivity of the distilled water bath in which the dialysis chamber containing red cells in normal saline is suspended, and hemolysis is measured by means of an optical system. The utility as well as the accuracy of the method depends upon maintenance of uniformity of the dialyzing membranes, which must be changed at intervals because of wear. The difficulties in obtaining uniform membrane-diffusion-time characteristics (which cause changes in osmotic tonicity that are uniform in relation to time), and the inability to conduct parallel studies of other hemolytic systems on the same time base, do not interfere with the clinical usefulness of this instrument[3,4] but can be limiting experimentally.

*Student Trainee from State College of Louisiana.

To provide greater control of changes in concentrations of chemical hemolysins, an instrumented method was devised in which changes in concentrations of solute are produced by precise metering pumps.[5] Hemolysis is measured by recording with a strip chart[6] the net increase in light transmitted by a red-cell suspension; the suspension becomes less turbid, i.e., more transparent, as progressively more cells are hemolysed. The prototype instrument (*Figs.* 76 and 77) has two transparent cuvettes, each of which holds initially 30 ml of isotonic saline containing 0.1 ml of heparinized whole blood. The fluid in both chambers is constantly circulated by small stainless steel propellers revolving at 240 rpm. Light from a small pilot lamp is focused through each solution onto a solar cell mounted at the opposite end of each chamber. The solar-cell outputs are connected to two potentiometers in an opposed-voltage bridge circuit. The recorder signal is taken from the two potentiometers and represents the difference in light transmission through the two chambers. Permanently mounted, long surgical hypodermic needles feed fluid from metering pumps to a point just under the stirring propellers. For an osmotic fragility test, one pump delivers isotonic saline to the balancing chamber, while the other pump delivers distilled water at the same rate to the hemolyzing chamber. With the use of this balanced-chamber arrangement the effect of dilu-

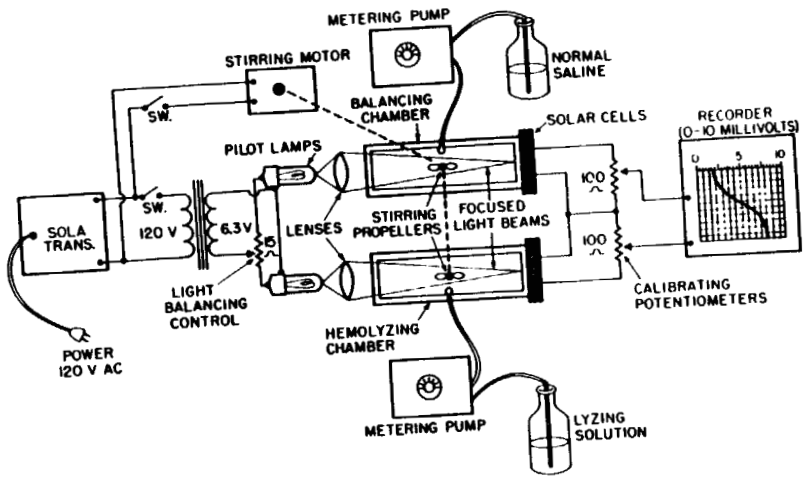

Fig. 76. Block diagram of the prototype instrument devised for measuring red-cell hemolysis caused by change in solute concentration controlled by precise metering pumps.

1027806

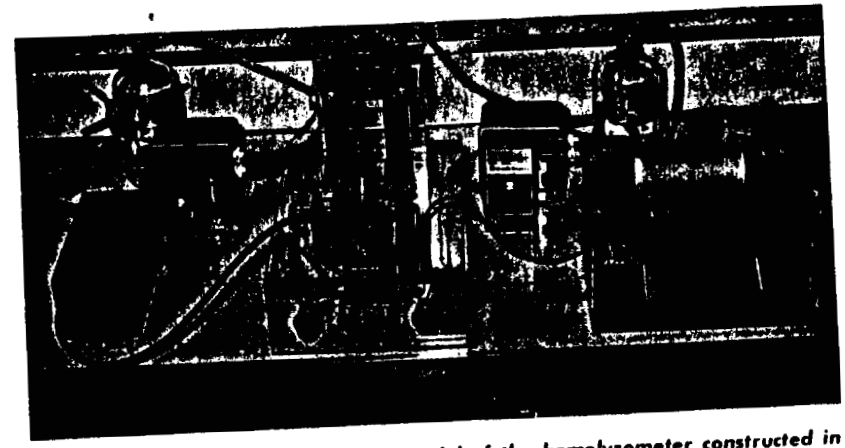

Fig. 77. Photograph of the working model of the hemolyzometer constructed in transparent plastic and connected to the accessory equipment as diagrammed in Fig. 76.

tion upon the transparency of the hemolysis chamber is subtracted out by the electrical signal from the saline chamber where dilution but no hemolysis is occurring. Maximum light transmission by the hemoglobin solution is obtained in this system by avoidance of the violet region of the spectrum (*Fig.* 78), through the use of incandescent light in an unfiltered optical system with solar cells maximally sensitive to red wave lengths. The voltage output of this type of solar cell is linear when operating into low resistance loads, and the voltage subtraction is valid over the range of operation. The potentiometric recorder has a 10 millivolt full-scale sensitivity.

In the osmotic fragility tests now being performed with this instrument, the pumps deliver 6 ml/min of buffered 0.9% saline (pH 6.7) and distilled water to the balancing and test chambers respectively. *Table 20* shows the resulting highly reproducible changes in suspension volume and tonicity with pumping time; it also shows the graph traversed for each time interval at this pumping rate. With this system no demonstrable change in fragility was found with changes in pumping rates from 1.0 to 9.0 ml/min. The rate of 6.0 ml/min was chosen as optimal because it permitted easiest inspection of the chart, and required significantly less time for the test than slower rates, which could be used if desired. The different mass of red cells in anemic and polycythemic blood is compensated for by adjusting, on the basis of the patient's hematocrit, the amount of blood added initially to

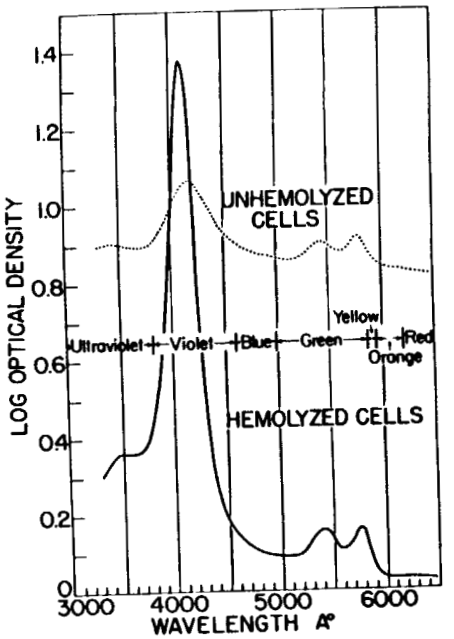

Fig. 78. Spectrophotometric analysis of light transmission by hemolyzed and non-hemolyzed red-cell suspensions.

give 0.05 ml of packed red cells. In *Fig. 79*, typical osmotic fragility curves are shown for a normal person, for a patient with acquired hemolytic anemia, and for one with iron-deficiency anemia. The direct measurements are shown in A, and in B are shown derived curves of the frequency distribution of change in red-cell fragility with change in tonicity. The time scale, which is linear in these graphs, has been converted to percent saline concentration. The distinct differences in effective tonicity for 50% hemolysis of the sample (ET_{50}) for each of these clinical examples are obvious, as are those in frequency distribution and slope of the integrated increment in light output (hemolysis).

Since normally the ET_{50} is about 0.42% saline, referral to *Table 20* indicates that this method can determine normal osmotic fragility in about 6 min, allowing application of the method to rapid screening of large volumes of blood samples daily for red-cell abnormalities as reflected in altered osmotic fragility. The application of the instrument to measuring red-cell sensitivities to saponin, venoms, and other hemolytic systems is in progress.

1027807

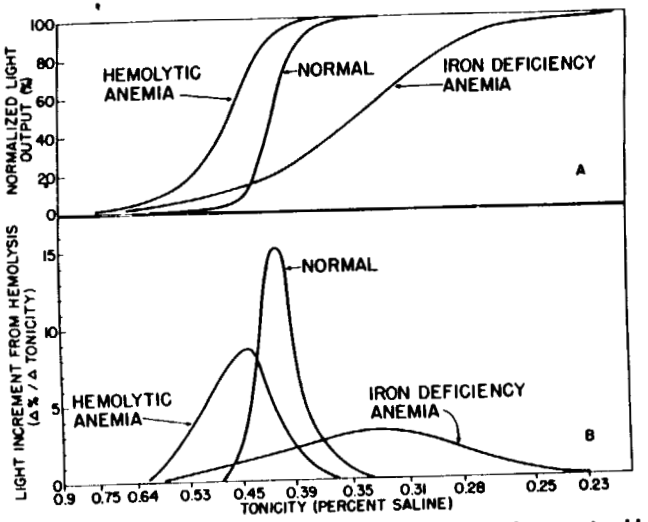

Fig. 79. A typical normal red-cell osmotic fragility curve, one for acquired hemolytic anemia, and one for iron-deficiency anemia; A. Integrated amount of hemolysis as measured by amount of light output of the system in respect to pumping time expressed as resulting tonicity (saline concentration); B. The first derivative of these sigmoid response curves in these clinical cases showing the frequency distribution of red-cell sensitivity with respect to change in time converted to saline concentration.

TABLE 20

Pump Time (6 ml/min)	Chamber Volume	Chart Units	Tonicity
(min)	(ml)	(4/50 sec)	(% NaCl)
0	30	0	0.9
5	60	24	0.45
10	90	48	0.30
15	120	72	0.225
20	150	96	0.18

REFERENCES

1. Danon, D., Nevo, A., and Marikovsky, Y. Preparation of erythrocyte ghosts by gradual hemolysis in hypotonic aqueous solution. Bull Res Council Israel, 6E 36–39, 1956.
2. Danon, D., Frei, E. H., Frei, Y. F., and Lipkin, Y. An instrument for automatically recording the osmotic fragility curve of red cells and/or its derivative. I.E.E.E. Transaction on Bjomedical Electronics 10, 24–28, 1963.

3. Danon, D. A rapid micro method for recording red cell osmotic fragility by continuous decrease of salt concentration. J Clin Path 16, 337, 1963.
4. Danon, D., Frei, Y. F., Rimon, A., and Ben-David, A. Simple rapid osmotic fragility test proposed as a routine in blood banks. Transfusion 4, 339–342, 1964.
5. Beckman Instrument Company, Metering Pump Model 746.
6. Nesco Instruments, Inc. Costa Mesa, California.

Measurement of Plutonium in Wounds: Self-absorption by Plutonium

R. J. Cloutier and E. E. Watson

The fate of metallic particles of plutonium in subcutaneous wounds in machinists is a continuing problem of the atomic fuel industry[1] and is under cooperative study* at the Division.[2] Accurate determination of the plutonium content is difficult when the plutonium is deeply embedded in a wound or is present in microgram amounts. Lack of information about the attenuation and self-absorption of the ^{239}Pu 17-keV X ray accounts for the uncertainty of the measurement.

If the more energetic photons emitted during plutonium decay are counted, measurement accuracy can be improved, but the small number of photons emitted reduces the sensitivity of this method. Sensitivity can be retained and accuracy can be improved by measuring the 60-keV gamma ray of the plutonium contaminant, ^{241}Am, and the Am/Pu curie ratio. The Am/Pu curie ratio can be determined by alpha spectroscopy of a small specimen of the material from the wound. Almost all plutonium contains a small amount of Am as a result of the Pu decay. The amount of americium present depends on the past interaction history of the plutonium and the length of time since it was purified.

The ability to monitor plutonium is related to the number of photons per curie of plutonium multiplied by the correction factors for self-absorption. This product is called the Relative Monitoring Ability (RMA).[4] *Figure 80* shows the RMA factor for 17-, 60-, and 100-keV photons as affected by the size of the plutonium particle when the curie ratio of Am/Pu is 0.1. *Figure 81* shows the RMA factor as the Am/Pu curie ratio increases. Both figures assume only self-absorption of the photons by the plutonium itself; however, the general shape of the curves will remain the same when other causes of attenuation are included.

*S. Gusak, Department of Industrial Medicine, Dow Chemical Company, Rocky Flats, Colo.

1027808

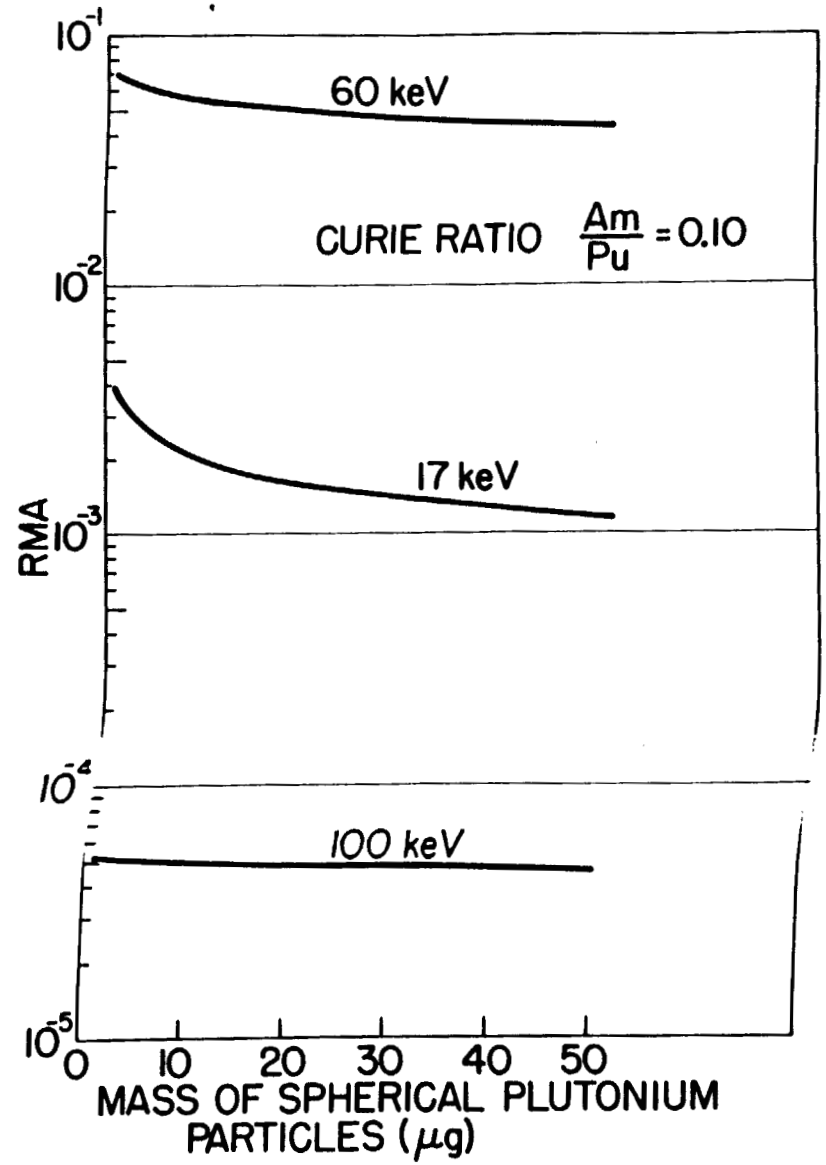

Fig. 80. Relative Monitoring Ability (RMA) factors for ^{239}Pu and ^{241}Am photons as related to plutonium particle mass.

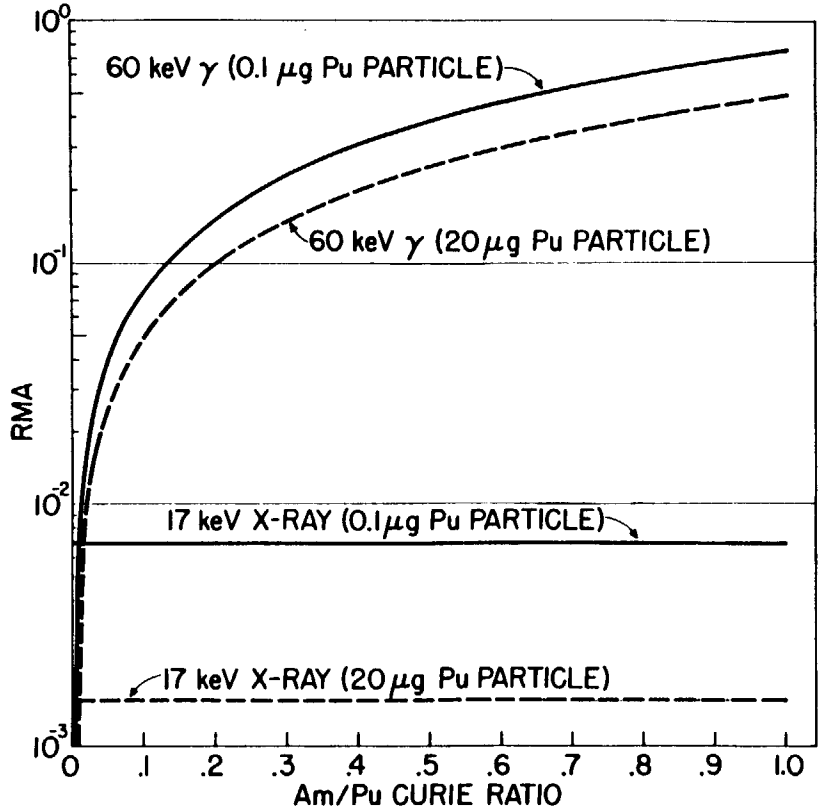

Fig. 81. Relative Monitoring Ability (RMA) factors for ^{239}Pu and ^{241}Am photons as related to Am/Pu curie ratio and particle mass.

REFERENCES

1. Lushbaugh, C. C. and Langham, J. A dermal lesion from implanted plutonium, AMA Arch Derm 86: 461-464, 1962.
2. Cloutier, R. J. and Lushbaugh, C. C. Analysis of wounds and tissue for plutonium, USAEC Report ORINS-49, 107-109, 1964.
3. Dawson, F. G., Deonigi, D. E., and Eschbach, E. A. Plutonium buildup and depletion, Nucleonics 23 (8), 101-105, 1965.
4. Cloutier, R. J. and Watson, E. E. Measurement of Plutonium in wounds: self-absorption by plutonium, submitted for publication.

1027809

Gas-liquid Chromatography Analysis of Long-chain Isomeric Glyceryl Ethers *

R. Wood† *and F. Snyder*

A quantitative method was developed for the gas chromatographic analysis of glyceryl ethers with the use of their trifluoroacetate (TFA) and trimethylsilyl (TMS) ether derivatives. Both derivatives are prepared at room temperature by reactions that proceed virtually to completion in less than 15 min, eliminating time-consuming deriva-

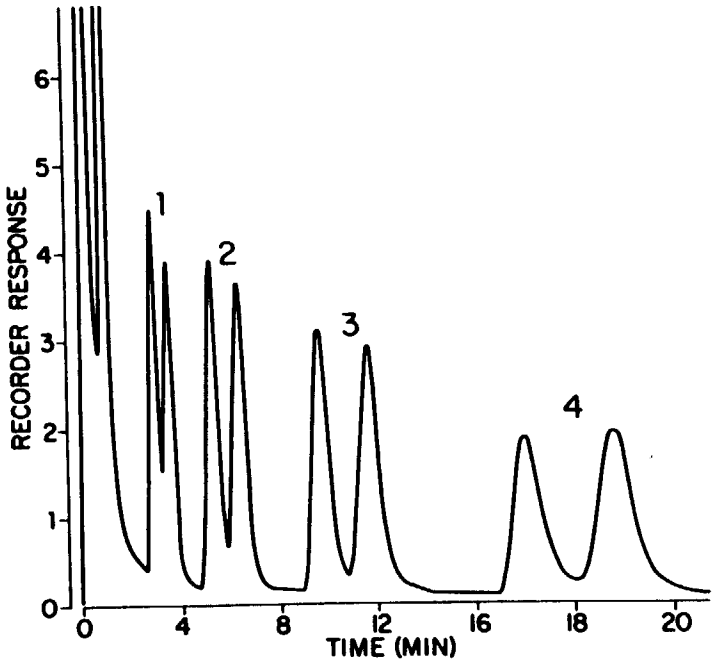

Fig. 82. A typical chromatogram showing the resolution of a purified synthetic mixture of 1- and 2-glyceryl ether trifluoroacetate derivatives. The separations were obtained with a 5-ft × 1/8-in stainless steel column packed with 10.5% EGSS-X on 100 to 120 mesh Gas-Chrom P operating at 170°C. The numbered peaks are (1) 12:0; (2) 14:0; (3) 16:0; and (4) 18:0. The 1-isomers were eluted ahead of the 2-isomers. The isomeric trimethylsilyl derivatives were not resolved on this column.

*Presented at the American Oil Chemists' Fall Meeting, October 10–13, 1965, Cincinnati, Ohio. Lipids (Inaugural issue), 1, 62–72, 1966.

†USAEC Postdoctoral Fellow.

tive preparations and laborious clean-up steps of unreacted materials required by other methods.

Gas-liquid chromatography resolves the 1- and 2- isomers of the glyceryl ether TFA derivatives, which have not been separated previously *(Fig. 82)*. Purified synthetic 1- and 2-glyceryl ethers, including saturated and mono- and di-unsaturated, were used to evaluate several polar and nonpolar liquid phases for the analysis of the TFA and TMS derivatives. Analyses can be made on some liquid phases normally used for methyl esters, while others are unsatisfactory. A mixture of isomeric C_{18} saturated and mono- and di-unsaturated TFA derivatives was partially resolved; however, a complete analysis of this mixture can be made by preliminary separation of the unsaturates on silver-ion-impregnated thin-layer plates or by gas-liquid chromatography alone with three different phases.

Modified Silver Ion Thin-layer Chromatography*

R. Wood† and F. Snyder

Thin-layer chromatography plates of Silica Gel G impregnated with 12.5% silver nitrate were prepared from aqueous and ammonium hydroxide solutions. Several comparisons of the plates from the two different preparations were made. Ammonical silver ion plates had a longer shelf life, and they gave greater resolution to methyl esters according to degree of unsaturation than that obtained on plates prepared from aqueous solutions. Discoloration caused by exposure to light was greatly reduced when the silver ion plates were prepared from ammonium hydroxide solutions. A 12.5% solution of silver nitrate in ammonium hydroxide was found to be less corrosive toward many metals than the same concentration in an aqueous solution. The superiority of the ammonium hydroxide prepared silver ion plates was given a chemical interpretation that agrees well with the experimental observations.

*Journal of the American Oil Chemists' Society, 43, 53–54, 1966.
†USAEC Postdoctoral Fellow.

1027810

A Modified Applicator for the Uniform Coating of Thin-layer Plates*

R. Wood† and F. Snyder

The application of uniform layers of adsorbent to thin-layer chromatography (TLC) plates is the most difficult and important step in TLC. The need for a uniform layer becomes even more critical when photometric methods are used for quantitative analysis on the chromatoplate. Uniform adsorbent layers are difficult to prepare because of the variation in the thickness of the glass chromatoplates, and because most commercial applicators use a smooth surface template upon which the glass plates are placed. The spreader is passed over the uneven top surfaces of the plates resulting in a nonuniform adsorbent layer.

A commercially available applicator has been modified to enable the preparation of uniform adsorbent layers on TLC plates. Advantage was taken of the inflatable bag arrangement available in an applicator distributed by Colabs that permits the top surface of the glass plate to be even and perfectly flat during the application of the adsorbent layers. Nonuniformity of adsorbent layers resulting from variation in chromatoplate thickness is eliminated by the leveled top surface. To accommodate the 2- × 20-cm plates used for zonal-scan analysis and the selection of desired solvent systems, the bed rollers originally supplied with the plate holder were removed and an 8- × 45- × 1/8-in. aluminum bed plate (a) was used instead as shown in *Fig. 83*. A 1/2- × 3/8-in. piece of foam rubber (b) affixed to each side of the bed plate holds the chromatoplates (g) firmly against the securing edges (c) when the leveling bag (h) is inflated. The addition of guide bars (d) equipped with ball bushings (e), also shown in *Fig. 83*, allow the spreader (f) to be moved evenly and smoothly across the plate, producing a very uniform layer of adsorbent on all plate sizes ranging from 2 × 20 cm up to 20 × 20 cm. Micrometer heads can also be added on the applicator's adjustable plate to allow quick, accurate, and reproducible selection of layer thicknesses.

*J Chromatog, in press, 1965.
†USAEC Postdoctoral Fellow.

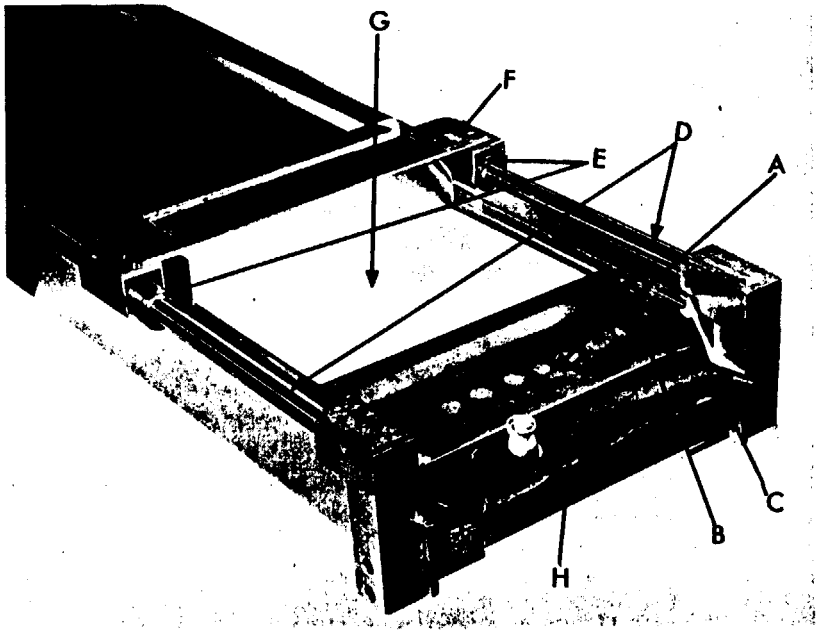

Fig. 83. A modified thin-layer chromatography applicator for the preparation of uniform layers. The labeled parts are: (A) aluminum bed plate; (B) foam rubber strip; (C) securing edge; (D) stainless steel guide bars; (E) ball bushings; (F) spreader; (G) chromatoplate; and (H) the inflatable bag.

A Comparison of Zonal Scans, Strip Scans, and Autoradiographic Scans of Thin-layer Chromatograms

Fred Snyder

Zonal scanning, strip scanning, and autoradiographic scanning to determine the distribution of radioactivity along a thin-layer chromatographic strip have been compared. The zonal scans were prepared with an automatic scraping device.[1] A Packard Radiochromatogram Scanner, Model 7200 was used to scan the chromatostrips before the scraping of 2-mm zones. Densitometric autoradiographic scanning was accomplished according to a procedure already described.[2]

Figure 84 demonstrates the increased sensitivity and superiority of resolution of zonal-scan analysis over windowless strip scanning detectors for quantitative radioassay of thin-layer chromatograms. When the disintegrations per minute of a ^{14}C-lipid mixture applied

1027811

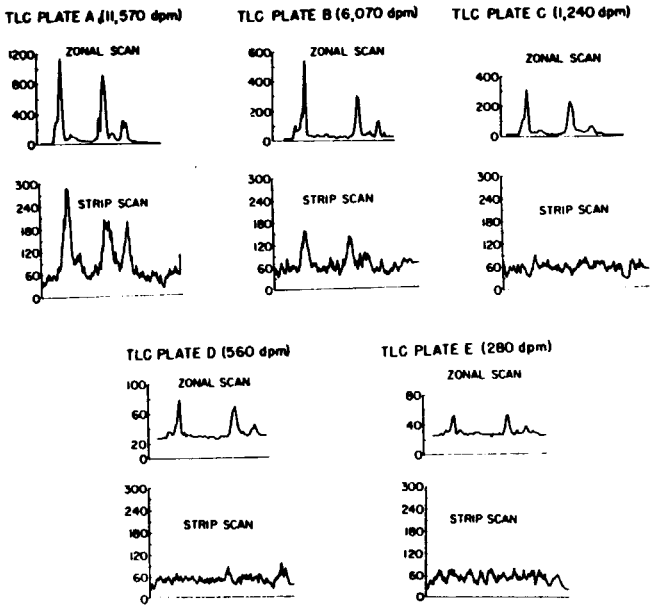

Fig. 84. Strip and zonal scans (2mm) of a ^{14}C-labeled lipid mixture separated on Silica Gel G in a solvent system of hexane:diethyl ether:glacial acetic acid (80:20:1). The numbers along the ordinate represent counts per minute.

to the chromatostrip were below 6000, the various activity peaks along the chromatographic lane became obscure if strip scanning was used for their detection. On the other hand, zonal-scanning analysis as accomplished with the automatic scraper and sample collector, revealed the same radioactivity peaks for the plate containing only 280 dpm (Plate E) as seen for the plate containing the highest quantity of radioactivity (Plate A - 11,570 dpm). Obviously, not only the sensitivity is much greater when minute zones are scraped into liquid scintillation vials for assay, but also the degree of resolution for detecting the separations is significantly better.

The third technique, photodensitometric analysis of autoradiograms, requires less expensive equipment to obtain the radioactive distribution curves, but has the disadvantages of being more time-consuming and of providing poorer resolution and quantitation than the zonal scans *(Fig. 85)*.

Densitometric analysis cannot resolve radioactive peaks as well as liquid-scintillation zonal analysis because the film response is poor

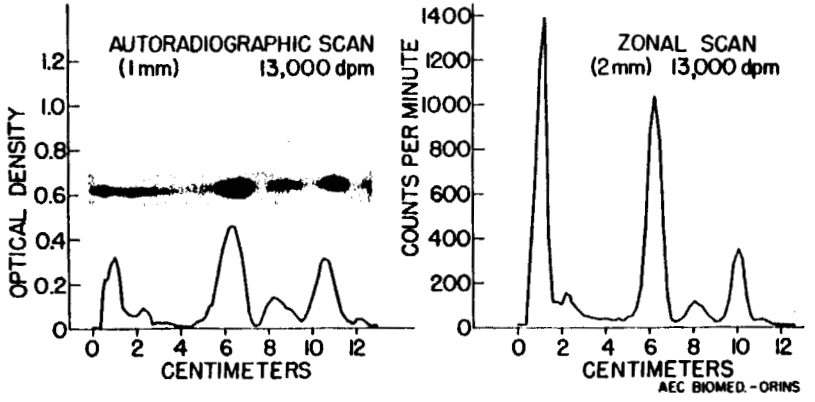

Fig. 85. Comparison of a 2-mm zonal scan (liquid scintillation) and a photodensitometric scan (autoradiogram) of an impure ^{14}C-tripalmitin sample chromatographed by thin-layer chromatography on Silica Gel G in a solvent system of hexane:diethyl ether:acetic acid (80:20:1). The autoradiogram was exposed for 14 days.

over a wide range of disintegrations per minute at any given exposure time. This is demonstrated in *Fig. 85* showing the relatively narrow range of film density response for a wide range of disintegrations per minute. Overloading causing maximum density response must be avoided for quantification of the autoradiograms. One should also note that while major radioactive peaks are shown on both densitometric and zonal scans, the latter gives much sharper resolution of the low activity area. The time required to obtain both scans shown in *Fig. 85* emphasizes one of the most important features of zonal scan analysis: the preparation of the zonal scan required approximately 2 hr while the preparation of the densitometric scan required approximately 14.5 days including exposure.

The author expresses thanks to Nelson Stephens of the Oak Ridge Institute of Nuclear Studies and Michael Frosolono of the University of North Carolina, department of biochemistry, for assistance in this work.

REFERENCES

1. Snyder, F. and Kimble, H., An automatic zonal scraper and sample collector for radioassay of thin-layer chromatograms, Anal Biochem 11, 510–518, (1965).
2. Snyder, F., Quantitative radioassay methods for thin-layer chromatography: zonal and autoradiographic scans. International Atomic Energy Agency Symposium on Radioisotope Sample Measurement Techniques in Medicine and Biology, Vienna, Austria, May, 1965, In Press.

1027812

Publications

1965

Reprints from the open literature and additional information on publications can be obtained by contacting Mrs. Edward H. Anderson, Technical Editor, Medical Division, Oak Ridge Institute of Nuclear Studies, Box 117, Oak Ridge, Tennessee 37830. Complete lists of Medical Division publications are available.

ARTICLES IN JOURNALS

Andrews, G. A. and Cloutier, R. J. Accidental acute radiation injury: The need for recognition. AMA Arch Environ Health 10, 498–507, 1965.

Bergner, P.-E. E. Exchangeable mass: Determination without assumption of isotopic equilibrium. Science 150, 1048–1050, 1965.

Bergner, P.-E. E. Stochastic concepts in clinical red cell survival studies. Nature (Lond) 205, 975–977, 1965.

Edwards, C. L. and Gengozian, N. Autoimmune hemolytic anemia treated with d-penicillamine. Ann Intern Med 62: 576–579, 1965.

Gengozian, N., Rabette, B., and Congdon, C. C. Abnormal immune mechanism in allogeneic radiation chimeras. Science 149, 645–647, 1965.

Hayes, R. L., Carlton, J. E., and Byrd, B. L. Bone scanning with gallium-68: A carrier effect. J. Nucl Med 605–610, 1965.

Hubner, K. and Brown, D. W. Scanning of the spinal subarachnoid space after intrathecal injection of ^{131}I labeled human serum albumin. J Nucl Med 6, 465–472, 1965.

Hubner, K. and Gengozian, N. Depression of the primary immune response by dl-penicillamine. Proc Soc Exp Biol Med 118, 561–565, 1965.

Kretchmar, A. L., McArthur, W. H., and Congdon, C. C. Shift in the relative distribution of body nitrogen between skin and carcass in mouse radiation chimeras. J Nutr 87, 261–266, 1965.

Lushbaugh, C. C. and Lushbaugh, D. B. Rapid electronic cell sizing as an aid in clinical diagnosis. Southern Med J 58, 1208–1212, 1965.

Meyer, L. M., Schiffer, L. M., White, D. A., and Cronkite, E. P. The plasma disappearance of radioactive cobalamin: Effect of prior administration of vitamin B_{12} analogues. Brit J Haematol 11, 370–379, 1965.

Miller, B., Anderson, C. E., Kyker, G. C., Yarbro, C. L., and Cress, E. A. Plasmalogen in rare earth-induced fatty infiltration in rat liver. J. Elisha Mitchell Sci Soc 81, Suppl. 1, 12–18, April 1965.

Morris, A. C., Jr. A diagnostic-level whole-body counter. J Nucl Med 6, 481–488, 1965.

Nelson, B., Rush, E. A., Takasugi, M., and Wittenberg, J. Lipid embolism to the brain after lymphography. New Engl J Med 273, 1132–1134, 1965.

Snyder, F. and Kimble, H. An automatic zonal scraper and sample collector for radioassay of thin-layer chromatograms. Anal Biochem 11, 510–518, 1965.

Snyder, F. Fatty acid oxidation in irradiated bone marrow cells. Nature (Lond) 206, 733, 1965.

Snyder, F. and Wright, Reba. Effect of localized irradiation of the metabolism of bone marrow lipids. Radiat Res 25, 417–422, 1965.

Steckel, R. J., Hendrix, E. L. and Bigelow, R. R. Malignant solid teratoma of the ovary in an 8-year-old child. Obstet Gynec (N Y) 25, 249–252, 1965.

CHAPTERS IN BOOKS

Andrews, G. A., Auxier, J. A., and Lushbaugh, C. C. The importance of dosimetry to the medical management of persons accidentally exposed to high levels of ionizing radiation. In: Personnel Dosimetry for Radiation Accidents. Vienna, IAEA, 1965, pp. 3–16.

Snyder, F. Zonal scanning of thin-layer chromatograms. In: Advances in Tracer Methodology, Vol. 2. New York, Plenum Press, 1965, pp. 107–113.

PUBLISHED ABSTRACTS

Bergner, P.-E. E. and Lawson, J. D. Red cell survival: On the analysis of DF^{32}P-data. (Introduced by G. A. Andrews) Clin Res 13, 66, 1965.

Gengozian, N., Edwards, L., and Hubner, K. Clinical and experimental studies on the effect of penicillamine on antibody formation. (Introduced by R. C. Hartmann) Clin Res 13, 68, 1965.

Gibbs, W. D., Lushbaugh, C. C., and Morris, A. C., Jr. Preliminary efficiency and calibration studies with a new whole-body counter with an ultralow background shield. J Nucl Med 6, 337, 1965.

Goh, K. O. Cytogenetic interrelation of the myeloproliferative disorders. Clin Res 13, 273, 1965.

Harris, C. C., Satterfield, M. M., Kimble, H. E., and Uchiyama, G. A "rescanner" with photographic readout. J Nucl Med 6, 332, 1965.

Hayes, R. L., Carlton, J. E., and Byrd, B. L.^{68}Gallium as a bone scanning agent. J Nucl Med 6, 358, 1965.

Kniseley, R. M., Andrews, G. A., Tanida, R., Edwards, C. L., and Kyker, G. C. Whole-body scanning of the bone marrow organ. J Nucl Med 6, 361, 1965.

Kretchmar, A. L. Stability and response characteristics of the red blood cell system: A computer study. (Introduced by R. C. Hartmann) Clin Res 13, 67, 1965.

Kyker, G. C. and Rafter, J. J. Scanning of bone marrow in animals. J. Nucl Med 6, 361 1965.

Lushbaugh, C. C., Hofstra, R., Roth, R. E., and Andrews, G. A. ED_{50} for gastrointestinal responses in man. Radiat Res 25, 213–214, 1965, abstr. 114.

Miller, I. H., Jr. and Kyker, G. C. Nutritional protection against fatty liver due to cerium. Fed Proc 24, 564, 1965, abstr. 2404.

Pfannenstiel, P., Andrews, G. A., and Brown, D. W. Congential hypothyroidism from intrauterine ^{131}I damage. In: Volume of abstracts of papers presented at The Fifth International Thyroid Conference, Rome, May 23–27, 1965, abstr. 16.

Snyder, F., Piantadosi, C., and Oswald, E. The deposition and metabolism of α-batyl alcohol-1-^{14}C in the rat. J Amer Oil Chem Soc 42, 461A, 1965, abstr. 91.

1027813

Uchiyama, G., Harris, C. C., Kimble, H., and Morris, A. C., Jr. Color recording for a rescanning device. (Introduced by G. A. Andrews) Clin Res 13, 82, 1965.

MISCELLANEOUS

Andrews, G. A. Editorial: Radiation accidents. JAMA 191, 151–152, 1965.

Goh, K. O. Book Review: Human Chromosome Methodology. Edited by J. J. Yunis, Academic Press, New York and London, 1965. Ann Intern Med 63, 925–926, 1965.

ARTICLES IN PRESS

Andrews, G. A. Radiation accidents and their management. Radiat Res.

Andrews, G. A Total-body irradiation in the human being. In: Proceedings of the XI International Congress of Radiology, Rome. September 1965.

Bergner, P.-E. E. On Stationary and nonstationary red-cell survival curves. J Theor Biol.

Bollinger, J. N. The incorporation of dietary linoleic acid into triglycerides of irradiated bone marrow. Radiat Res.

Goh, K. O. Smaller G chromosome in man. Lancet.

Hayes, R. L. Isotopes of gallium. In: Radioactive Pharmaceuticals. AEC Symposium Series CONF-651111, edited by G. A. Andrews, R. M. Kniseley, and H. N. Wagner, Jr.

Johnson, G. T. and Kyker, G. C. The mechanism of cerium uptake by *Saccharomyces cerevisiae*. J Bacteriol.

Kniseley, R. M. Diseases of the bone marrow. In: Principles of Nuclear Medicine. H. N. Wagner, Jr., ed., W. B. Saunders.

Kniseley, R. M., Andrews, G. A., Tanida, R., Edwards, C. L., and Kyker, G. C. Delineation of active marrow by whole-body scanning with radioactive colloids. J Nucl Med.

Kyker, G. C. and Rafter, J. J. Colloidal properties of the lanthanides. In: Radioactive Pharmaceuticals. AEC Symposium Series CONF-651111, edited by G. A. Andrews, R. M. Kniseley, and H. N. Wagner, Jr.

Lushbaugh, C. C., Comas, F., and Hofstra, R. Clinical studies of radiation effects in man: A preliminary report of a retrospective search for dose-response relationships in the prodromal syndrome. Radiat Res.

Morris, A. C., Jr. and Ross, D. A. The design and construction of a low-background whole-body counting facility. USAEC Report ORINS-51.

Nelson, B., Cosgrove, G. E., and Gengozian, N. Diseases in a laboratory colony of the primate *Tamarinus nigricollis*. Lab Animal Care.

Rogers, W. A., Jr. and Nelson, B. Strongyloidiasis and malignant lymphoma: "Opportunistic infection" by a nematode. JAMA.

Snyder, F. Book Review of Proceedings of an International Symposium on Lipid Transport. Southern Med J.

Snyder, F. Triglyceride biosynthesis in irradiated bone marrow. Radiat Res.

Snyder, F. Quantitative radioassay methods for thin-layer chromatography: Zonal and autoradiographic scans. In: Proceedings of the International Atomic Energy Agency Symposium on Radioisotope Sample Measurement Techniques in Medicine and Biology, Vienna, Austria, May 1965.

Snyder, F. and Piantadosi, C. Labeling and radiopurity of lipids. In: Advances in Lipid Research, Volume 4, edited by D. Kritchevsky and R. Paoletti.

Snyder, F. and Piantadosi, C. The synthesis and purity of labeled lipids. In: Radioactive Pharmaceuticals, AEC Symposium Series CONF-651111, edited by G. A. Andrews, R. M. Kniseley, and H. N. Wagner, Jr.

Wood, R. and Snyder, F. A modified applicator for the uniform coating of thin-layer plates. J Chromatog.

Wood, R. and Snyder, F. Gas-liquid chromatography analyses of isomeric glyceryl ethers. Lipids.

Wood, R. and Snyder, F. Modified silver ion thin-layer chromatography. J Amer Oil Chem Soc.

LEGAL NOTICE

This report was prepared as an account of Government sponsored work. Neither the United States, nor the Commission, nor any person acting on behalf of the Commission

A. Makes any warranty or representation, expressed or implied, with respect to the accuracy, completeness, or usefulness of the information contained in this report, or that the use of any information, apparatus, method, or process disclosed in this report may not infringe privately owned rights; or

B. Assumes any liabilities with respect to the use of, or for damages resulting from the use of any information, apparatus, method, or process disclosed in this report.

As used in the above, "person acting on behalf of the Commission" includes any employee or contractor of the Commission, or employee of such contractor, to the extent that such employee or contractor of the Commission, or employee of such contractor prepares, disseminates, or provides access to, any information pursuant to his employment or contract with the Commission, or his employment with such contractor.

1027814

Acknowledgements

Research collaboration has involved many staff members from the Oak Ridge National Laboratory, university and medical school members of the Institute, consultants, and other persons and institutions. These associations are to some extent recognized in the authorship of reports in this publication.

The Medical Nuclear Instrument Group from the Oak Ridge National Laboratory, especially P. R. Bell, C. C. Harris, and D. A. Ross, have continued to aid in the development of the instrument program, particularly with the color-recording rescanner.

Several physicians have been of special help to the clinical program. Knoxville physicians who have helped as consultants in the care of patients are Doctors Edmund Andrews, James B. Cox, Margaret Maynard, Robert W. Newman, and Eidson Smith. Dr. P. M. Huggin and the East Tennessee Tuberculosis Hospital have also been of assistance. In Oak Ridge, the following physicians have given consultation and special services: Doctors Robert Ball, Louis Bryan, R. R. Bigelow, Betty Cooper, Kenneth Crounse, Dexter Davis, Earl Eversole, Ernest Lee Hendrix, Avery P. King, Raymond Johnson, Dana Nance, W. W. Pugh, Jr., Henry Ruley, Paul Spray, George Stevens, III, and Joseph Tittle. Dr. B. B. Blevins has been the dental consultant. Dr. C. W. Sensenbach has contributed helpfully by attending clinical rounds each week. Valuable aid has been given by the surgeons and operating room group of the Oak Ridge Hospital and by the pathology department under Dr. Alex Carabia.

The Information Services Department of Oak Ridge Associated Universities handled publication of this report.

Author Index

Ahumada, J. 85
Allen, E. 35
Andrews, G. A. 75, 81, 90, 139
Ballenger, M. K. 68
Bergner, P.-E. E. 103, 105, 107
Bollinger, J. N. 18, 21
Byrd, B. L. 64, 68
Carlson, D. 35
Carlton, J. E. 64, 68
Chastain, B. 68
Cheng, S. 23
Cloutier, R. J. 73, 154
Comas, F. V. 53, 75, 79, 139
Congdon, C. C. 38, 81
Conover, W. R. 50
Corley, R. H. 149
Cosgrove, G. E. 34
Davis, M. L. 117
Debons, A. F. 73
Edwards, C. L. 75, 81, 85, 90, 120
Gengozian, N. 26, 28, 31, 34, 35, 38, 81
Gibbs, W. D. 107, 112, 115, 117, 120, 125, 128, 133, 145
Goh, K. O. 55, 56
Hayes, R. L. 64, 68, 85
Hendrix, A. 128
Hitchcock, A. A. C. 143
Hodges, H. D. 125, 128, 145
Hofstra, R. 139
Holten, V. Z. 68, 72
Humason, G. L. 31, 79, 133
Kniseley, R. M. 31, 75, 90
Kretchmar, A. L. 41, 47, 50, 51
Kyker, G. C. 68, 71, 72, 90
Lawson, J. D. 105, 107
Likuski, H. J. 73
Lim, J. 15
Lushbaugh, C. C. 31, 79, 107, 112, 115, 117, 120, 125, 133, 139, 145, 149
Lushbaugh, D. H. 107, 149
Merritt, C. 26
Morris, A. C., Jr. 143, 149
Nelson, B. 5, 7, 34, 84
Oswald, E. 19
Pfleger, R. 12
Phipps, C. E. 51
Piantodosi, C. 12, 15, 19, 23
Pulliam, M. 72
Queener, R. 112, 115, 133
Rabette, B. 38
Rafter, J. J. 68, 71
Rogers, W. A., Jr. 5
Rupp, E. 47
Rush, E. A. 84, 98, 101
Scott, W. L. 112
Snyder, F. 9, 12, 15, 19, 23, 98, 157, 158, 159, 160
Takasugi, M. 84, 120
Tanida, R. 85, 90
Uchiyama, G. 143
Vodopick, H. 81
Watson, E. E. 154
Webb, A. 68
White, D. A. 61, 75
Wittenberg, J. 84
Wood, R. 157, 158, 159
Yarbrough, M. C. 112, 133

1027815

US-ORINS PROPE
ORINS-49

RESEARCH REPORT

Medical Division

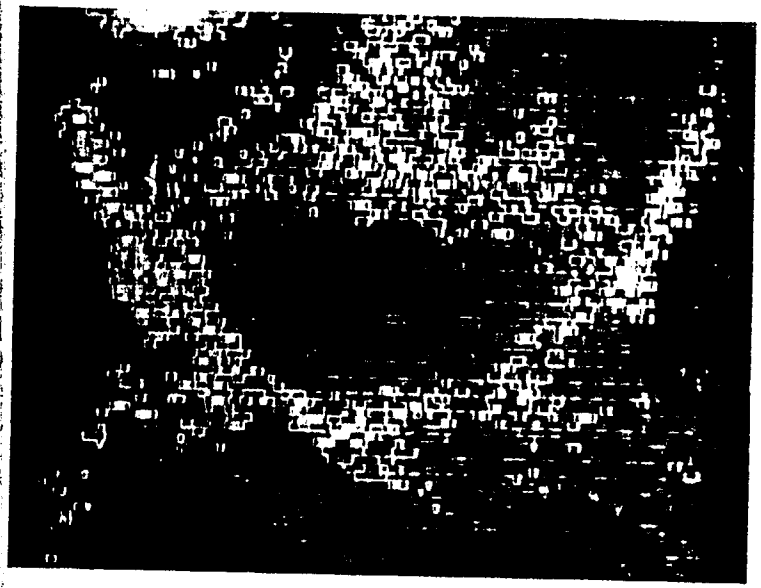

Oak Ridge Institute Of Nuclear Studies

Oak Ridge Institute for Science and Education, Medical Sciences Division
REPOSITORY Oak Ridge Associated Universities Annual Research Reports, Medical and Health Sciences Division
COLLECTION Vance Road Facility, Room 202A
BOX No. No folder title.
FOLDER Document No: ORAU-30002, Part 1 of 6

1027816

OAK RIDGE INSTITUTE OF NUCLEAR STUDIES
MEDICAL DIVISION—RESEARCH REPORT

COVER: *The reproduction on the front cover was made by analyzing a photo-recording scan of the pelvic region of a patient with a recording densitometer known as the "ORNL rescanner." The apparatus, including its color readout, was devised by the Medical Nuclear Instrumentation Group of Oak Ridge National Laboratory. Construction was a cooperative project between this group and the Technical Services Department of the Oak Ridge Institute of Nuclear Studies. The continued development (including this picture) is being carried out by Dr. G. Uchiyama of Chiba University, Japan, on a Picker Fellowship at the Medical Division of the Oak Ridge Institute of Nuclear Studies.*

1027817

OPERATING UNDER CONTRACT WITH THE
UNITED STATES ATOMIC ENERGY COMMISSION

DECEMBER 31, 1964

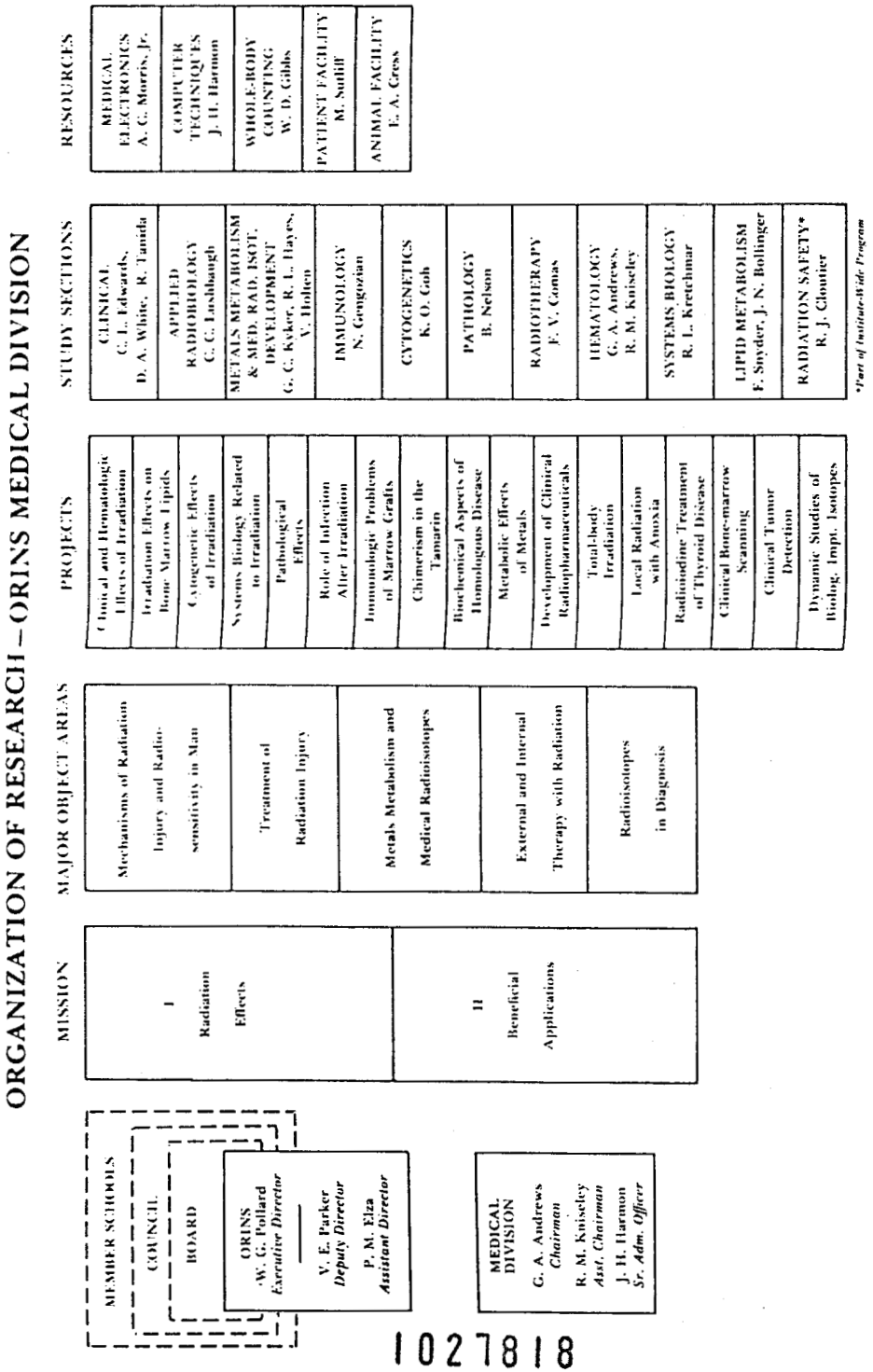

10278 18

Contents

Page

FOREWORD 7

MECHANISMS OF RADIATION INJURY 9

Correlation Between Kidney Muramidase Activity and Plasma Iron Removal in Rats with Walker-256 Carcinosarcoma. *A. L. Kretchmar and F. V. Comas* 9

Infections in Patients Exposed to Total-body Irradiation. *G. A. Andrews, B. W. Sitterson, and B. M. Nelson* 11

Hematologic Responses to Total-body Irradiation in the Human Being. *G. A. Andrews and Mary Smyser* 13

Effects of Irradiation on Lipid Metabolism in the Walker-256 Tumor. *J. N. Bollinger* 16

Effect of Vitamin Deficiency on the Growth Rate of the Walker-256 Tumor. *J. N. Bollinger* 19

Effect of Localized Irradiation on the Metabolism of Bone-marrow Lipids. *F. Snyder and Reba Wright* 21

Lipid Classes of Hematopoietic and Fatty Bone Marrow. *F. Snyder and E. A. Cress* 24

Lipid Metabolism in Fatty and Nonfatty Bone-marrow Fractions. *F. Snyder and E. A. Cress* 26

Effect of Dietary Fat and Total-body Irradiation on Fatty Acid Composition of Bone-marrow Lipids. *J. N. Bollinger*.. 31

Fatty Acid Oxidation in Irradiated Bone-marrow Cells. *F. Snyder* 34

Rapid Electronic Red Blood Cell Sizing as an Aid in Clinical Diagnosis. *C. C. Lushbaugh and D. B. Lushbaugh* 35

STUDIES RELATED TO TREATMENT OF RADIATION INJURY 40

Nitrogen Balance in Radiation Chimeras. *W. H. McArthur, C. C. Congdon, and A. L. Kretchmar* 40

Change in the Partition of Total-body Nitrogen in Irradiation Chimeras. *A. L. Kretchmar, W. H. McArthur, and C. C. Congdon* 42

Lipid Composition of Tissues After Isologous and Homologous Marrow Transplants in Mice. *J. N. Bollinger, F. Snyder, and C. C. Congdon* 44

Transplantation of Rat Bone Marrow in Irradiated Mice as a Function of Exposure Rate. *N. Gengozian* 46

Autoimmune Hemolytic Anemia Treated with d-Penicillamine. *C. L. Edwards and N. Gengozian* 46

Depression of the Primary Immune Response by dl-Penicillamine. *K. Hubner and N. Gengozian* 49

Human A- and B-like Antigens on Red Cells of Marmosets. *N. Gengozian* 52

Hematologic and Cytogenetic Evidence for Chimerism in the Marmoset, *Tamarinus nigricollis*. *N. Gengozian, J. S. Batson, and P. Eide* 55

Bone-marrow Grafting Attempts in Tamarins after Total-body Irradiation. *N. Gengozian, J. S. Batson, and Bill M. Nelson* 58

Allotypic Specificities in Four Strains of Inbred Mice as Revealed by Reciprocal Immunizations. *N. Gengozian and G. Doria* 61

METALS METABOLISM AND MEDICAL RADIOISOTOPE DEVELOPMENT 63

Plasmalogen in Rare-earth-induced Fatty Infiltration in Rat Liver. *B. Miller, C. E. Anderson, G. C. Kyker, C. L. Yarbro, and E. A. Cress* 63

Trigylceride Accumulation and Release in the Rare-earth Fatty Liver. *F. Snyder and G. C. Kyker* 65

The Mechanism of Cerium Uptake by *Saccharomyces cerevisiae*. *G. T. Johnson and G. C. Kyker* 66

Rare-earth Fatty Liver Induced by Lanthanon Chelates. *G. C. Kyker and J. J. Rafter* 66

Iron and Aluminum Antagonism to Rare-earth Binding by Yeast. *G. T. Johnson and G. C. Kyker* 67

Scanning of Bone Marrow in Animals. *G. C. Kyker and J. J. Rafter* 68

1027819

Nutritional Protection Against Fatty Liver Due to Cerium. *I. H. Miller, Jr. and G. C. Kyker* 69

In vivo Redistribution of Barium-137m. *R. L. Hayes and J. E. Carlton* 70

THERAPY WITH RADIATION 72

Use of Thyrotropic Hormone (TSH) for Demonstration and Postoperative Treatment of Thyroid Cancer with Radioiodine. *P. Pfannenstiel, B. W. Sitterson, and G. A. Andrews* 72

RADIOISOTOPES IN DIAGNOSIS 79

Bone Scanning with Gallium-68. *R. L. Hayes and J. E. Carlton* 79

Clinical Bone-marrow Scanning. *R. M. Kniseley, G. A. Andrews, and R. Tanida* 81

Stability and Response Characteristics of the Red Blood Cell System: A Computer Study. *A. L. Kretchmar* 89

Red Cell Survival: On the Analysis of DF^{32}P Data. *P.-E. E. Bergner and J. D. Lawson* 91

Diagnostic Uses for Iodine-130. *P. Pfannenstiel and G. A. Andrews* 91

ABSORPTION, WHOLE-BODY, AND ORGAN RETENTION OF BIOLOGICALLY IMPORTANT RADIOISOTOPIC MATERIALS 98

Whole-body Counting Research Program. *W. D. Gibbs, C. C. Lushbaugh, and H. D. Hodges* 98

Evaluation of Thyroid Function in Infants with the ORINS Low-level Whole-body Counter. *P. Pfannenstiel and W. D. Gibbs* 103

Radioactivity of Cigarettes. *W. D. Gibbs, C. C. Lushbaugh, and H. D. Hodges* 105

Analysis of Wounds and Tissue for Plutonium. *R. J. Cloutier and C. C. Lushbaugh* 107

Determination of Fraction of Blood Volume "Seen" in the Human Forearm by the "Armac" Arm Counter. *W. D. Gibbs, H. D. Hodges, and C. C. Lushbaugh* 110

DETECTING AND LOCALIZING RADIOACTIVITY IN PATIENTS 111

Whole-body Counters. *A. C. Morris, Jr., C. C. Lushbaugh, R. L. Hayes, H. Kakehi, and W. D. Gibbs* 111

Computer Program for Calculation of Response of Detector-collimator Systems. *W. D. Gibbs* 122

Thermoluminescent Dosimetry. *Young Ja Lee, R. J. Cloutier, and P. Dalton* 123

The Whole-body Scanner. *A. C. Morris, Jr.* 124

NASA RETROSPECTIVE STUDY ON IRRADIATION EFFECTS 127

Radiosensitivity in Man: A Study Based on Therapeutic and Accidental Exposure. *C. C. Lushbaugh, R. Hofstra, R. E. Roth, and G. A. Andrews* 128

METHODOLOGY 132

Processing of Feces for Analysis. *A. M. Webb and G. C. Kyker* 132

Automatic Zonal Scraper and Sample Collector for Radioassay of Thin-layer Chromatograms. *F. Snyder, H. Kimble, and N. Stephens* 134

PUBLICATIONS 136

ACKNOWLEDGEMENTS 139

AUTHOR INDEX 140

1027820

Foreword

The Medical Division is one of the major "on-site" biomedical programs with clinical emphasis supported by the Division of Biology and Medicine of the U.S. Atomic Energy Commission. Some additional financial support has come to the Medical Division from the U.S. Air Force, which has funded a project on radiation studies in tamarins, and from the Oak Ridge Institute of Nuclear Studies, which on occasion makes available corporate funds for special needs. The National Aeronautics and Space Administration requested the Medical Division, through the Atomic Energy Commission Division of Biology and Medicine, to undertake a retrospective study of the effects of total-body irradiation in humans based on our experience and the experience of others who have treated patients or managed the treatment of accident victims. The information is vital in the prediction of effects and design criteria needed for long-term space flights.

The present report dealing with research during calendar 1964 does not fully portray the activities in the Division because some of our major object areas involve long-range studies that do not lend themselves by their nature to annual reporting. The productivity of the Division has shown gratifying growth and the staff was strengthened appreciably during the year. The chart on page 2 indicates the major areas of research and staff assignments. In addition to the members of the staff, major contributions are made by consultants and collaborators both in Oak Ridge and at a distance.

We are pleased to announce that Dr. Kong-oo Goh, formerly of the University of Rochester (N.Y.), joined the staff to direct the cytogenetics program. Late in the year Dr. Beecher Sitterson resigned from our staff to accept a position in the Boston area. Dr. Sitterson served here as chief of clinical services and managed the care of patients with skill and devotion. We appreciate his contribution to the program and regret his departure. His successor, Dr. C. Lowell Edwards, will assume his duties about March 1, 1965, and we welcome him to our program. Dr. Virginia Holten, whose main research area is enzyme kinetics, will join the group early in 1965 to work with Dr. G. C. Kyker in the program on metals metabolism and medical radioisotope development.

During the year several distinguished visiting scientists enhanced our program. Dr. Hirotake Kakehi, Professor of Radiology, Chiba University (Japan), produced an outstanding calibration study of

the characteristics of the ORINS medium-level whole-body counter. Dr. Per-Erik Bergner, Karolinska Institutet, a theoretical biologist, and Douglas Lawson, University of Waterloo (Ontario), a mathematician, have been working with Dr. A. L. Kretchmar in the development of theoretical systems applicable to certain of our major research projects. Dr. Peter Pfannenstiel from Freiburg, Germany, spent the year at the Medical Division as a trainee in clinical investigation.

The staff is indebted to Elizabeth Anderson, technical editor, Jeanne Simmons, medical illustrator, and Rush King, photographer, for much assistance in preparing this report.

GOULD A. ANDREWS
Chairman

1027821

Mechanisms of Radiation Injury

The objective is to elucidate selected mechanisms of radiation damage, both acute and subacute, with emphasis on those effects characterized by hematologic, biochemical, immunologic, and cytogenetic changes. These studies are made on human beings where possible. It is expected that this approach will lead to information of value in (1) better management of unwanted radiation injury and (2) improved therapeutic use of radiation.

Correlation Between Kidney Muramidase Activity and Plasma Iron Removal in Rats With Walker-256 Carcinosarcoma

A. L. Kretchmar and F. V. Comas

Muramidase activity in kidneys of rats with transplanted tumors is increased 2 to 12 times.[1,2,3] Suu *et al.*[4,5] found a similar large increase in kidney muramidase activity in irradiation chimeras. The highest level of enzyme activity was found in bone marrow, spleen, and kidney. Because the kidney muramidase activity increased at a time when hemopoietic regeneration was known to be occurring,[6] Suu *et al.* suggested that muramidase activity in kidney was related in some way to the proliferating grafted hemopoietic cells in the irradiation chimeras. The observation to be reported here, that there is a positive correlation between plasma iron turnover and kidney muramidase in tumor-bearing rats, is of interest in this connection.

Male rats, weighing 230 to 340 g, were injected with Walker-256 carcinosarcoma cells into the femoral muscle of both legs. At 4, 8, 12, and 16 days after the transplantation of the tumor the animals were given 1 microcurie of ^{59}Fe intravenously as ferrous citrate. Plasma clearance of ^{59}Fe and total plasma iron were determined and the rats were killed and lysozyme content of kidneys was determined.

Figure 1 shows the muramidase activity plotted against the rate of iron removal from plasma. The muramidase level in kidney four days after implantation of tumor is slightly elevated (0.75 mg equivalents per gram) with no increase in the rate of removal of iron. At 16 days both are about four times the control value (2.00 and 45 vs. 0.60 and 12). The 12-day muramidase extracts were unfortunately lost; iron removal was 30.4 micrograms per hour. The levels of mura-

midase activity are similar to those reported by Cappuccino *et al.*[2] for rats with this tumor.

The level of muramidase in kidney is increased when the reticuloendothelial system is stimulated.[7] Radioactive colloidal gold has been shown to concentrate in the regions of active hemopoiesis in bone marrow of humans and this uptake of colloidal gold is presumably a function of the reticuloendothelial system.[8,9] Possibly there is some relation between rate of hemopoiesis and activity of the reticuloendothelial system, and through this relation muramidase levels are increased in animals with an activated hemopoietic system.

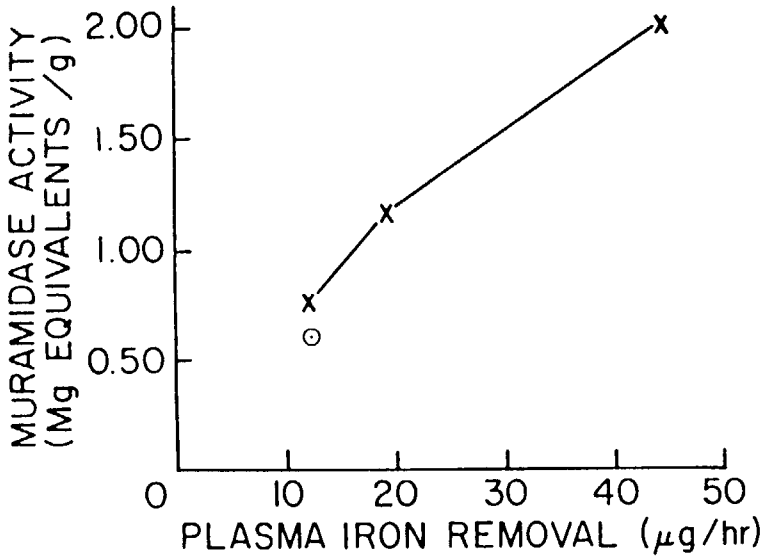

Fig. 1. Kidney muramidase against rate of plasma iron removal in tumor-bearing rats. ⊙ = control animals; X = tumor-bearing rats, 4, 8, and 16 days after implantation. The iron data are averages of separate determinations on six rats at each point. The muramidase data are averages of four determinations on the pooled extracts from kidneys of six rats for each point.

REFERENCES

1. Perri, G. C., Faulk, M., Mellors, J. and Stock, C. C. Crystallization of a basic protein (lysozyme) from kidneys of tumor-bearing rats (Jensen sarcoma). Nature (Lond) 193, 649-651, 1962.

1027822

2. Cappuccino, J. G., Reilly, H. C. and Winston, S. Elevation of lysozyme in extracts of kidneys and spleens from tumor-bearing animals. Cancer Res 22, 850-856, 1962.
3. Perri, G. C., Cappuccino, J. G., Faulk, M., Mellors, J. and Stock, C. C. Variations of the content of lysozyme in normal rats and in rats bearing Jensen sarcoma following surgery. Cancer Res 23, 431-435, 1963.
4. Suu, Vu-Thi, Congdon, C. C. and Kretchmar, A. L. Increase in lysozyme activity in kidneys of irradiation chimeras. Proc Soc Exp Biol Med 113, 481-485, 1963.
5. Suu, Vu-Thi, Congdon, C. C. and Kretchmar, A. L. Lysozyme activity in radiation chimeras. Proc Soc Exp Biol Med 115, 825-829, 1964.
6. Congdon, C. C. and Urso, I. S. Homologous bone marrow in the treatment of radiation injury in mice. Amer J Path 33, 749-767, 1957.
7. Perri, G. C., Faulk, M. and Money, W. L. Thyroid function and kidney muramidase. Proc Soc Exp Biol Med 115, 185-188, 1964.
8. Root, S. W., Andrews, G. A., Kniseley, R. M. and Tyor, M. P. The distribution and radiation effects of intravenously administered colloidal Au^{198} in man. Cancer 7, 856-866, 1954.
9. Edwards, C. L., Andrews, G. A., Sitterson, B. W. and Kniseley, R. M. Clinical bone marrow scanning with radioisotopes. Blood 23, 741-756, 1964.

Infections in Patients Exposed to Total-body Irradiation

G. A. Andrews, B. W. Sitterson, and Bill M. Nelson

In the course of total-body irradiation therapy we have had the opportunity to study infections that occurred after exposure. Twenty-six doses of from 200 to 940 r (midbody air dose) were given, 20 in patients with acute or subacute leukemia (one treated twice), and five in patients with disseminated neoplasms of other types. Almost all these patients were in a late stage of their disease and had been previously treated by multiple techniques. Some of the patients were given bone marrow after irradiation in an attempt to achieve grafts.

Almost all patients had fever, presumably or demonstrably due to infection, during the six weeks after therapy. Figure 2 illustrates the outcome in these patients. Of 13 who died within 45 days after therapy, infections were a prominent feature in 10. Infections were more severe in leukemic patients than in those with other neoplasms. The timing of deaths, with quite a number occurring during the first 25 days, may suggest that in some instances death was in part due to irradiation. On the other hand, some of the reduction in deaths after the first month is definitely attributable to radiation-induced remissions in some patients with leukemia.

The following are the findings at autopsy in 12 of the 13 patients who died within 45 days. Because of the occurrence of multiple infec-

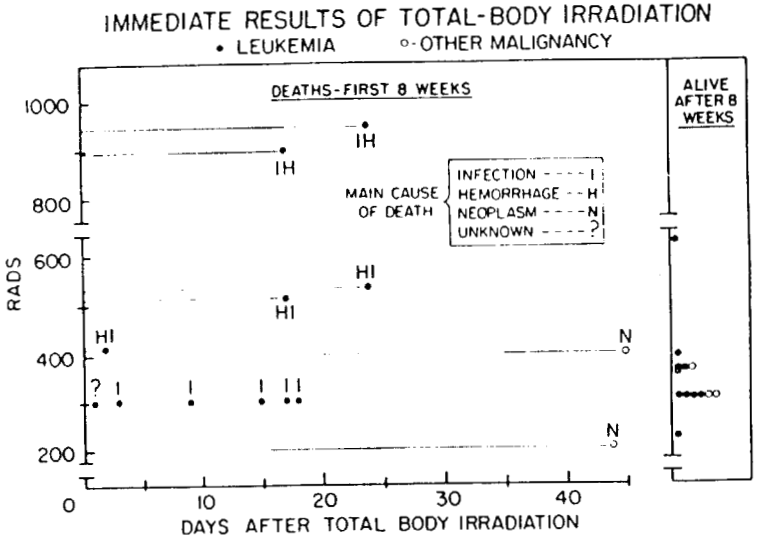

Fig. 2. Twenty-six treatments with total-body irradiation, 200 to 940 r midbody air dose, were given to patients with late stages of leukemia and malignancy. Half the patients died within eight weeks and the causes of death are indicated. Infection was the major cause of early death.

tions, some patients are included more than once. Two patients had no evidence of infection. Eight patients had hemorrhagic pulmonary lesions with the following organisms:

3 *Pseudomonas* (all with bacillemia; one also had pulmonary aspergillosis).
2 *E. coli* (both with positive blood cultures).
1 *Klebsiella-Aerobacter* group (with bacilli in many organs).
2 *Staphylococcus epidermidis*, coagulase negative (found only by culture).
2 Gram-positive cocci (not cultured).
2 Aspergillosis (1 with pulmonary lesions, listed above; the other with lung, G. I., liver lesions).

Other Infections:

3 *Candida* (all in G. I. tract; one also in many other organs).
1 Small pleomorphic bacterium in bladder wall (positive blood culture for *E. coli*, but no coliform bacilli were seen in sections).

1027823

Among the patients who survived, a variety of infections was encountered. Superficial skin infections with *Staphylococcus aureus* were common and three patients had deep abscesses caused by this organism. One patient recovered from a septicemia caused by *Staphylococcus aureus*. In several instances infections due to gram-negative organisms were not recognized until autopsy; one patient had *E. coli* septicemia confirmed by culture early enough to allow a trial of vigorous therapy, but the outcome was fatal. *Candida* infections of the mouth and throat occurred in several patients.

There were also instances in which severe febrile responses were believed due to infection, but the exact site or nature of the infection could not be determined.

This experience indicates the importance of infection as a post-radiation complication. It was not possible to show any clear difference in the type of infections after radiation in leukemic patients and those seen in leukemic patients treated by other means. The prominence of gram-negative infections and fungi is emphasized in this series. Diffuse pulmonary hemorrhage associated with infection was frequent and may be rather characteristic of irradiation injury. Leukopenia appears to be the most important feature in susceptibility to infection. In those patients developing remissions in acute leukemia as a result of irradiation, there was a prompt lysis of fever as soon as normal granulocytes began to increase.

These studies will be continued in an effort to elucidate the prevention, pathogenesis, diagnosis, and treatment of infections occurring after irradiation.

Hematologic Responses to Total-body Irradiation in the Human Being

G. A. Andrews and Mary Smyser

Because responses of the blood picture are extremely important in estimation of radiation dose and in planning therapy, we have attempted to establish typical patterns for various doses of total-body irradiation in the previously normal human being. The preliminary results are shown in Figs. 3, 4, 5, and 6. These curves were derived in part from accident data, most of which are unsatisfactory because of lack of accurate information on radiation doses. The curves are also based partly on clinical total-body irradiation studies, partic-

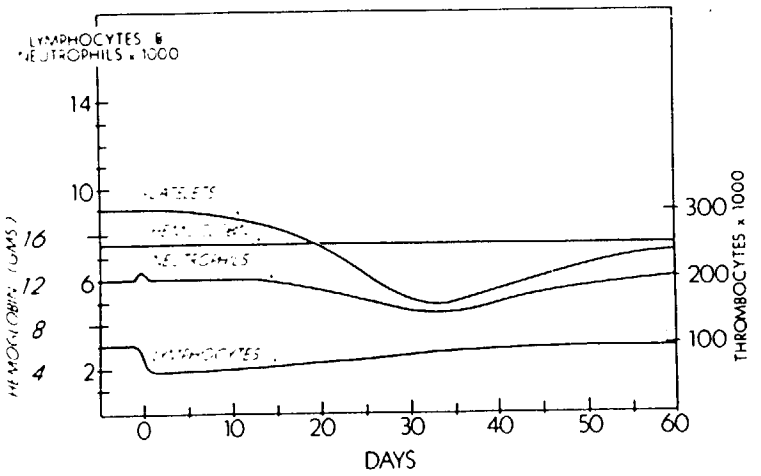

Fig. 3. Typical hematologic response to 100 rads.

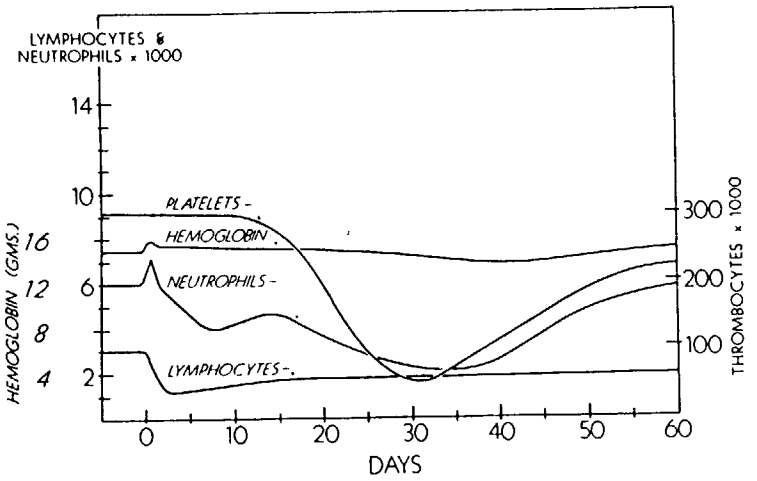

Fig. 4. Typical hematologic response to 200 rads.

ularly those done at the Medical Division, but data from patients with leukemia were obviously not applicable and the number of patients with approximately normal pretreatment hematologic status was small. In the literature on clinical total-body irradiation, very few reports include systematic hematologic data for a period of two months or more after therapy.

A special problem was encountered with the effects in the range of 100 rads; the data available show very inconsistent responses at this level. Sometimes there is a rather prolonged mild depression in the leukocyte count. In drawing the pattern shown in Fig. 3 we did not give full weight to the data that seemed to show completely erratic responses, and drew the curve mainly on the basis of the data suggesting that responses at this dose are a less severe version of those occurring after higher doses. Further information may show that this is not correct.

The curves shown, although open to many criticisms, represent our best knowledge at present. The extensive compilations of data now being undertaken here for the National Aeronautics and Space Administration are expected to yield information of this type based on a larger series of patients and including information on range of variation in response.

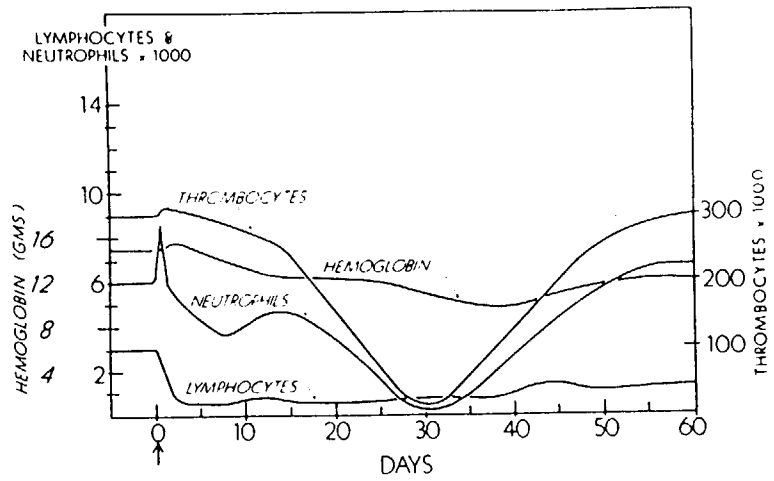

Fig. 5. Typical hematologic response to 300 rads.

1027824

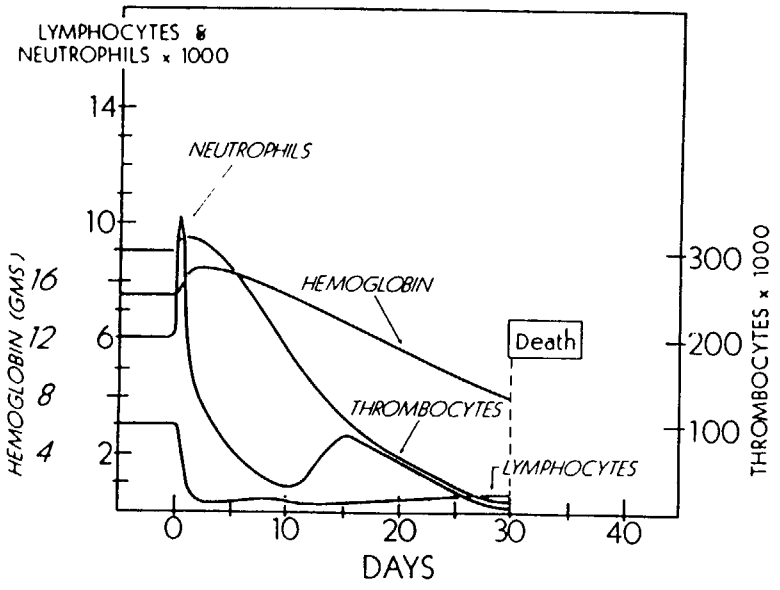

Fig. 6. Typical hematologic response to 450 rads.

Effect of Irradiation on Lipid Metabolism in the Walker-256 Tumor

J. N. Bollinger

Fatty acid metabolism is being studied in the Walker-256 tumor before and after irradiation. The work was initiated on the basis that it should be possible to control the nature of fat mobilized to tumor tissue by dietary means and subsequently hinder tumor growth by irradiation via free-radical formation of the polyunsaturated fats incorporated into tumor tissue.

Female rats (an average weight of 250 g) were fed two different diets. A control group received fat-free diet for one month and a second group of rats was fed the control diet containing a supplement of 10% safflower oil for one month before tumor implants.

1027825

Walker-256 tumor cells from donor rats were macerated in a micro Waring-type blender and the homogenized cells were diluted in saline solution. They were then injected subcutaneously into the animal's right rear leg. Ten days after the tumor implantation, the tumor area was exposed to approximately 1000 r (70 r/min) ^{137}Cs irradiation. The animals were anesthetized with Nembutal and securely taped to a board so that only the right rear leg and tumor were exposed to the radiation field. Four days after irradiation the animals were anesthetized with ether and killed by exsanguination. The tumors, livers, and genital fat pads were removed for lipid analysis. The liver and tumor tissue samples were ground in an Elvejhem-Potter type of homogenizer and freeze-dried. Total lipids were extracted from all tissues with a 2:1 chloroform:methanol mixture. Total lipids of liver and tumor were fractionated into phospholipids and neutral lipids with silicic acid. The fatty acid composition of both the neutral and phospholipid fractions was determined by gas-liquid chromatography in an 8-inch x ½-inch column packed with 15% ethylene glycol succinate coated on 100 to 120 mesh Chromosorb-W.

The tumor growth (4 to 14 g) was very poor in animals fed the fat-free and 10% fat diets when compared with that of animals receiving a commercial chow (Gambril-Dietrich). Average tumor weights obtained with the commercial chow diets were in the range of 20 to 40 g two weeks after implantation.' A subsequent experiment showed that the retarded growth was the result of inadequate vitamin supplement and not the level of fat in the diet.

The ratio of neutral lipids to phospholipids of tumor tissue was generally in the range of 45:55; however, this was not consistent. Gas-liquid chromatography showed that fat in the diet (Table 1) affected the fatty acid composition of the neutral lipids. A threefold increase of linoleic acid in the neutral lipids was seen after feeding the 10% safflower oil diet. Irradiation prevented this increase in linoleic acid and caused a significant increase in the stearic acid level of the neutral lipids. The fatty acid composition of the phospholipid fraction of tumors appeared to be unaffected by either diet or irradiation.

Irradiation had no effect on the liver lipids; however, the presence of a tumor produced fatty livers. The increase was due to an increase in the neutral lipid fraction, which consequently reversed the ratios of neutral lipid to phospholipid (Table 2). Although the implanted tumor tissue was rejected in four animals and the total liver lipids were not increased, the ratio of neutral lipids to phospholipids was

TABLE 1

Lipid Fatty Acid Analysis of Walker-256 Carcinoma

Diet	No. of tumors	Treatment	Fatty Acids*						
			14:0	16:0	16:1	18:0	18:1	18:2	20:4
			%	%	%	%	%	%	%
			Neutral lipids of Walker-256 carcinoma						
Fat-free	2	None	2.0	28.2	6.0	9.43	32.4	12.1	10.0
Fat-free	2	1000 r	2.8	26.2	2.9	25.7	32.2	11.1	—
10% Saff. oil	2	None	1.8	19.9	2.9	7.8	26.1	37.9	6.3
10% Saff. oil	3	1000 r	1.1	21.9	1.5	22.7	20.4	17.6	14.7
			Phospholipids of Walker-256 carcinoma						
Fat-free	2	None	0.9	23.8	2.8	27.2	28.1	4.6	18.0
Fat-free	2	1000 r	0.4	22.1	1.3	28.8	21.1	6.8	19.3
10% Saff. oil	2	None	1.4	24.9	0.8	30.2	13.1	11.1	18.7
10% Saff. oil	3	1000 r	0.8	26.2	1.0	28.9	16.4	9.1	18.2

*Based on gas-liquid chromatography fatty acid analysis; mean percentage of total lipid in fraction.

TABLE 2

Effect of Irradiation on Liver Lipids From Rats Subcutaneously Implanted With Cells From a Walker-256 Carcinoma and Fed a Fat-free Diet and a 10% Safflower Oil Diet

Treatment		Total lipids* %	Neutral lipids† %	Phospholipids‡ %
		Fat-free Diet		
None (control)	(3)	11.2	33.2	66.8
Tumor implant (−)	(1)	13.3	54.0	46.0
Tumor implant (+)	(2)	19.2	64.0	36.0
1000 r	(3)	10.2	35.7	64.3
Tumor implant with 1000 r (−)	(1)	8.9	50.6	49.4
Tumor implant with 1000 r (+)	(2)	19.5	67.4	32.6
		10% Safflower oil Diet		
None (controls)	(3)	9.3	33.4	66.6
Tumor implant (−)	(1)	11.2	44.5	55.5
Tumor implant (+)	(2)	8.4	62.1	38.0
1000 r§	(3)	10.9	30.6	70.0
Tumor implant (+) with 1000 r	(3)	25.3	70.8	29.2

* 75 68 r/min; right leg only by using a 6 x 6 cm collimator.
† Based on dry tissue weight; mean-values.
‡ Total lipid extract separated with silicic acid; the mean percent is based on total lipids.
(−) No visible tumor; (+) Visible tumor.
The numbers in parentheses represent the number of rats per group.

1027826

also reversed. This could be explained as an immunologic response[2] to foreign tissue.

REFERENCES

1. Comas, F. Personal communication.
2. Klein, G. The usefulness and limitations of transplantation in cancer research. A review. Cancer Res 19, 343-358, 1959.

Effect of Vitamin Deficiency on the Growth Rate of the Walker-256 Tumor

J. N. Bollinger

A research problem under investigation is a study of the effect of irradiation on lipid metabolism in the Walker-256 tumor. Since the rats used in these experiments were fed purified diets, it soon became evident that the vitamin level in these diets had a significant effect on the eventual growth of the transplanted tumor. For this reason an experiment was performed to determine what effect the lack or absence of a particular vitamin (over a relatively short two-month prefeeding period) had on the growth of the Walker-256 tumor. The design of this experiment was expected to reveal which vitamins were critical for maximum uniform growth of the Walker-256 tumor.

Rats fed the thiamine-deficient diet were the only ones showing acute visual signs of a vitamin deficiency and only one animal from this group survived long enough for the intramuscular implantation of the tumor. The tumors in animals receiving diets deficient in vitamins A, C, B_{12}, folic acid, choline, pantothenic acid, and pyridoxine grew as well as those tumors implanted in animals fed the complete vitamin-supplement diet. When compared with the controls, the rats receiving diets deficient in riboflavin and niacin showed a significant decrease in growth rate and size of tumor. Tocopherol-deficient diets produced a reduced tumor growth, but the effect was not so great as that produced in animals fed diets deficient in riboflavin and niacin. On the other hand, diets deficient in vitamin D and biotin yielded greater tumor growth rates and larger tumors than those of the controls (Fig. 7).

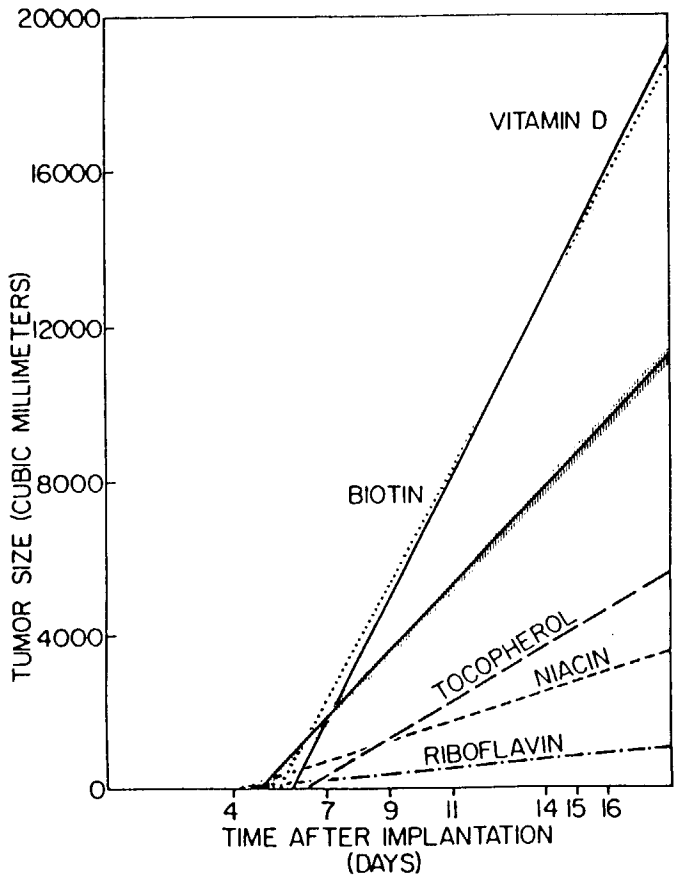

Fig. 7. A complete vitamin-fortified diet and 13 vitamin-deficient diets were fed to rats for two months before implantation with Walker-256 tumor tissue. Tumor growth was studied in animals receiving the following vitamin-deficient diets: A, C, D, E, biotin, choline, folic acid, panthothenic acid, riboflavin, niacin, B_1, B_6, and B_{12}. The tumor tissue was implanted intramuscularly in the right rear leg, and progressive tumor size was determined from the difference in the diameter of the right and left rear leg of the same animal. Only vitamins recorded in Fig. 7 showed a definite deviation from those of the controls (shaded line).

1027827

Effect of Localized Irradiation on the Metabolism of Bone-marrow Lipids*

F. Snyder and Reba Wright†

We have observed[1] that the administration of radioactive-labeled fatty acids to animals exposed to total-body irradiation results in a significant increase in the total amount of radioactivity in the bone-marrow organ, mostly present as fatty acid esters in the triglyceride fraction. This stimulation of fat-cell formation and fatty acid esterification in the bone marrow of irradiated animals reflects the degree of irradiation injury to the marrow. Two contrasting avenues of explanation for such stimulation are (1) that it is due to direct exposure of the bone-marrow cells to irradiation and (2) that a systemic factor, such as a hormone or hormonal imbalance, is responsible. To investigate this problem, chemical and metabolic studies were performed on rats after a 1080-r exposure of a single femur and after a similar exposure of the head only.

The data obtained conclusively demonstrate that only bone marrow directly exposed to the field of irradiation becomes fatty. Table 3 shows that localized irradiation (1080 r) of a single femur causes an increase in total lipids (triglyceride accumulation) of this particular marrow tissue at 4, 7, and 8 days after exposure. Neither total lipids nor fatty acid esterification in marrow cells were elevated in the non-irradiated femur of these animals nor in the femur marrow of rats whose heads only were exposed to 928 r. These facts we take to mean that the biochemical lesion in bone marrow caused by irradiation is manifested in the marrow cells and that no systemic factors are involved.

The autoradiogram (Fig. 8) depicts the labeling of lipid classes in bone marrow six hours after the oral administration of palmitic, stearic, and oleic-1-^{14}C-labeled acids; data obtained when these same compounds were administered intravenously gave essentially the same results. Although mono- and diglycerides, and in some instances the free fatty acids, contained some radioactivity, the fatty acids administered were primarily incorporated into triglycerides. Esterification of ^{14}C-labeled palmitic and stearic acids increased at the irradiation marrow site as early as 24 hours after irradiation exposure (Table 3), but the incorporation of oleic-1-^{14}C into marrow triglycer-

* In press, Radiation Research.

† University Relations Division student trainee from Southwestern University, Memphis, Tenn.

Fig. 8. An autoradiogram of bone-marrow lipids separated by thin-layer chromatography as described in the text. The triglyceride zone (a) clearly shows that the direct irradiation of bone-marrow cells causes an increase in the labeling of triglycerides six hours after feeding palmitic-1-^{14}C and stearic-1-^{14}C acid. The numbers represent 1, left irradiated femur four days after irradiation (1080 r), and 2, control right femur; 3, left irradiated femur one day after irradiation (1080 r), and 4, control right femur; 5, left irradiated femur four days after irradiation (1080 r), and 6, control right femur. Numbers 1, 2, 3, and 4 are from rats given palmitic-1-^{14}C orally. Numbers 5 and 6 are from rats given stearic-1-^{14}C acid orally.

ides of exposed marrow resembled that of controls. These data obtained for the incorporation of saturated and unsaturated fatty acids into triglycerides of a localized area of bone marrow directly exposed to irradiation agree with those obtained for rats exposed to total-body irradiation.[1] Why doesn't irradiation affect the incorporation of oleic-1-^{14}C acid into bone-marrow triglycerides when incorporation of both palmitic and stearic acids is doubled? Possibly the precursor lipid structure acting as a receptor for fatty acid esterification in the irradiated marrow is a diglyceride derived from phosphatidic acid,

1027828

TABLE 3

Effect of Localized Irradiation on Bone-marrow Lipids

Days after irradiation	% Lipid (Dry weight)		% ^{14}C as triglyceride, 6 hr after fatty acid injection							
			Palmitic-1-^{14}C+		Stearic-1-^{14}C+		Oleic-1-^{14}C+	
	Oral	I.V.	Oral	I.V.	Oral	I.V.	Oral	I.V.
Right femur control								
0	25,13,9,18			42	30	—	86	—
	16,18,21	26,29,21	45					
	13,15		39,40,46					
Left femur only irradiated (1080 r)								
1	18,18	24	69,74	74	—	—	—	—
4	38,30,32	41,46	83,91	81	66	—	88	104,85
7	55,34,44	—	—	—	—	—	—	—
8	60	—	—	—	—	—	—	—
Head only irradiated (928 r)								
4	7	—	26	—	—	—	—	—
8	21,18	—	—	—	—	—	—	—

and specific positioning of saturated fatty acids occurs at this position in the marrow. Our data lend strong support to this idea, but it can only be firmly established by pancreatic lipase studies of the fatty acid positioning in the marrow triglycerides. However, it has already been reported that oleic acid is primarily incorporated into the 2 position, and palmitic acid into the 1 and 3 positions, of rat liver triglycerides.[2]

REFERENCES

1. Snyder, F. Bone marrow lipids and their metabolism. USAEC Report ORINS-43. 13-18. 1964.
2. Gransson, G. The incorporation of palmitic and oleic acid into liver lipids by the rat. Biochem J 92, No. 1, 41-42, 1964.

Lipid Classes of Hematopoietic and Fatty Bone Marrow

F. Snyder and E. A. Cress

To determine how marrow lipid composition is related to cell population, the lipid composition of fatty marrow sites from various animals has previously been compared with that of other sites containing mostly hematopoietic cells.[1] In the current investigation the marrow-cell population was broken down into hematopoietic and lipid fractions by centrifugation, and the lipid composition of the fractions was analyzed and compared.

Fresh bone-marrow cells were extruded from rat and dog femurs under nitrogen pressure into an ice-cold buffer solution. Approximately 30 to 50 mg of fresh marrow was used per milliliter of buffer. The samples were centrifuged for 10 minutes at 600, 2,000, or 33,000 x *g* at approximately 4° C. Under these conditions, the fat cells formed a pellicle on the surface of the buffer. This was removed with a spatula for lipid extraction with chloroform:methanol (2:1) and designated as Fraction I. Fraction II consisted of the clear solution between the fat pellicle and the cellular sediment called Fraction III. Fractions II and III were freeze-dried before the lipids were extracted. Each fraction was examined chemically and histologically.

Histologically, Fraction I (fat pellicle) consisted of many well-preserved fat cells with a fairly uniform diameter of 40 to 60 microns. Although the volume of fat cells in this fraction greatly exceeded hematopoietic elements, many leukocytes and other smaller cells (but only occasional red blood cells) were associated with the fat cell

1027829

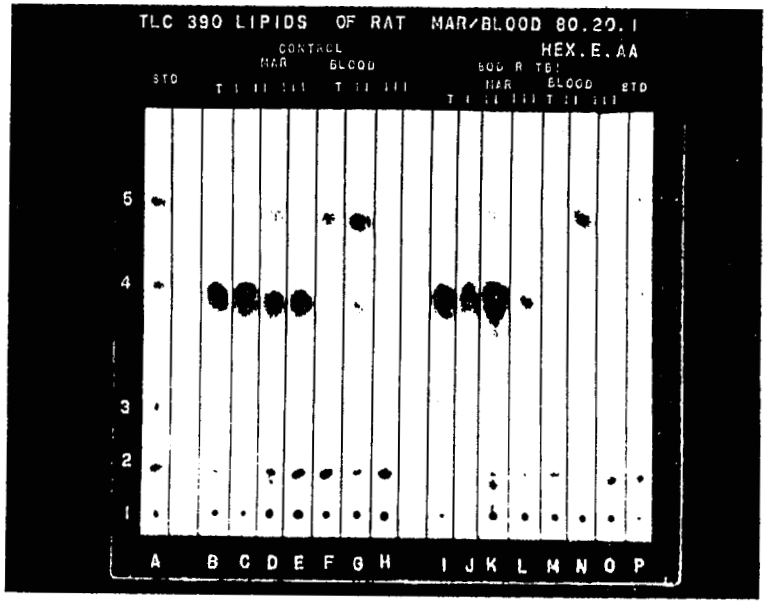

Fig. 9. Thin-layer chromatogram of lipids obtained from bone-marrow fractions isolated by centrifugation.

fraction. Fraction II was essentially cell-free, while Fraction III consisted of layers: (a) top, principally platelets and small fragments of debris; (b) a deeper layer of nuclei with very little cytoplasm and a layer mass with red cells dominating; and (c) a lower layer with megakaryocytes predominating. Scattered fat cells (1%) were trapped in the middle portion of the sediment.

Biochemically the lipid layer, Fraction I, was essentially indistinguishable from perirenal fat consisting mainly of triglycerides (Fig. 9). The lipids of the soluble layer, Fraction II, and of the hematopoietic cells, Fraction III, were similar qualitatively, although Fraction II contained more free fatty acids, long-chain fatty alcohols, and an unknown area directly beneath the triglycerides. Cholesterol esters, absent in Fraction I, were found in the soluble fraction and, to a lesser degree, in the sedimented cells. Chromatography of the lipids present in the total marrow extract did not reveal many of the compounds present in trace amounts even at relatively high chromatographic loading levels, primarily because of the diluting effect of the large amount of triglycerides present (Fig. 9). A thin-layer chromat-

ogram showing the lipid patterns of sedimented cells (Fraction III) and supernatant (Fraction I and II combined) separated at 33,000 x *g* indicated that the same lipid classes are present in the respective fractions for the rat and the dog. The weanling rat has very little lipid in the active marrow and most of it is phospholipid. However, in both the young and adult rat, the blood lipids showed the expected patterns for the serum and cellular fractions; no lipid layer formed with blood samples. The blood cells contained only cholesterol and phospholipids; the serum contained these in addition to traces of free fatty acids, triglycerides, and cholesterol esters. Unlike the sedimented cells of blood (Fig. 9), the marrow hematopoietic cells contain a remarkably high level of triglyceride in adult animals.

REFERENCE

1. Snyder, F. Bone marrow lipids and their metabolism. USAEC Report ORINS-43, 13-18, 1964.

Lipid Metabolism in Fatty and Nonfatty Bone-marrow Fractions

F. Snyder and E. A. Cress

Early microscopic work by Clark and Clark,[1] who used transparent chambers installed in the ears of rabbits, revealed that preadipose cells were indistinguishable in form from fibroblasts. There is no biochemical evidence available regarding the origin of fat cells. To investigate their origin, metabolic studies were made on floating fat cells and sedimented cells of marrow separated by centrifugation.

Lipids of fatty and nonfatty bone-marrow fractions. Triglyceride was essentially the only class present in the lipid layer (Fraction I) from either control or irradiated marrow (Fig. 10). The lipids of the soluble layer (Fraction II) and of the hematopoietic cells (Fraction III) contained similar classes; however, the cell-free fraction had more free fatty acids, long-chain fatty alcohols, and an unknown area directly beneath the triglycerides. Cholesterol esters were found in the cell-free fraction and to a lesser degree in the sedimented cells. These qualitative findings did not differ whether the animals had been irradiated or not.

1027830

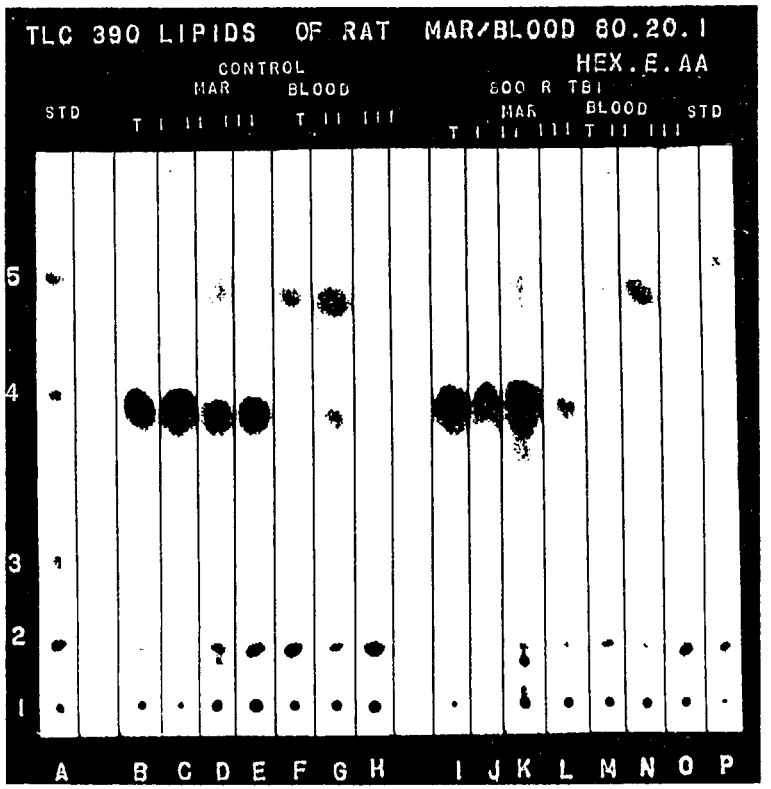

Fig. 10. Thin-layer chromatogram of fatty and nonfatty bone-marrow fraction separated by centrifugation (2000 x g). A and J: standard mixture (1, lecithin; 2, cholesterol; 3, oleic acid; 4, triolein; 5, cholesteryl oleate). B, F: total lipids from whole marrow. C, G: lipids from Fraction I. D, H: lipids from Fraction II. E, I: lipids from Fraction III. B, C, D, and E are from control rats. F, G, H, and I are from rats that had received 800 r total-body irradiation.

The bone-marrow accumulation of fat induced by irradiation was accompanied by an increase in the triglycerides of Fractions I and II, while the active cells decreased in triglyceride content. This decrease could result from a release of triglycerides from the cells, or from a change in the density (flotation) of a particular cell type.

Comparison of the lipids from the marrow fractions with those from blood plasma and cells was also made. As expected, the blood

plasma contains phospholipids, cholesterol, free fatty acids, triglycerides, and cholesterol esters. The cells contain only cholesterol and phospholipids, with a trace of cholesterol esters. Thin-layer chromatograms of the blood lipids were identical for the control and irradiated animals.

Incorporation of ^{14}C-fatty acids into lipids of fatty and nonfatty bone-marrow fractions. Table 4 shows that the ratio of ^{14}C-lipids in fat cells of the marrow (Fraction I) to those in the hematopoietic elements (Fraction III) was altered by irradiation. After 800 r, the percentage of total radioactivity present in the fat-cell fraction increased, while the percentage of total radioactivity found in the hematopoietic fraction decreased. The soluble layer (Fraction II) contained less than 5% of the total radioactivity. The zonal scans shown in Fig. 11 indicated that essentially all the radioactivity in the fat cells of marrow in both control and irradiated rats was present as triglyceride. On the other hand, although total radioactivity in the hematopoietic cells decreased after irradiation (Table 4), the percentage of this radioactivity present as triglyceride in that fraction

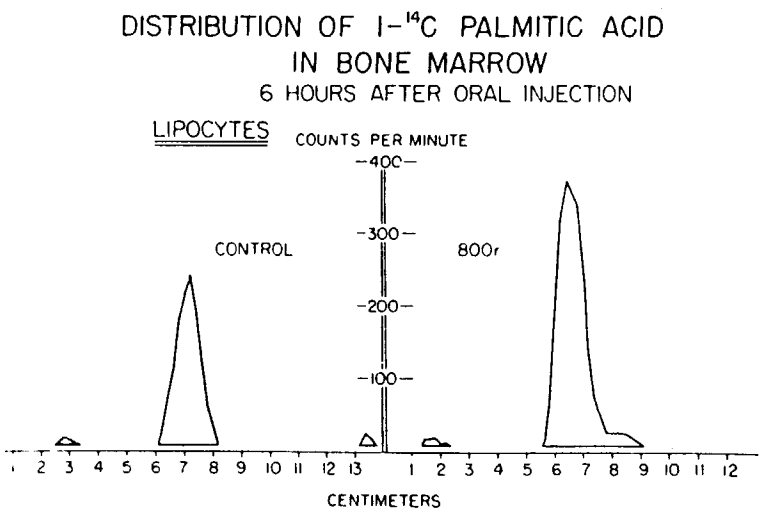

Fig. 11. A zonal scan of the ^{14}C-lipid distribution in the fat cell fraction of control and irradiated rats. Almost all the radioactivity incorporated was in the form of triglycerides (at 6 to 8 cm).

1027831

TABLE 4

Incorporation of 1-^{14}C-fatty Acids into Bone Marrow Lipids of Irradiated Rats*

Experiment	Fatty Acid-^{14}C	Total Lipids mg		Marrow-ACD Suspension	% of Lipids per Fraction		% of ^{14}C per Fraction		% of ^{14}C per Fraction as Triglyceride	
		Control	TBI†	Fraction	Control	TBI	Control	TBI	Control	TBI
A.	Palmitic-1-^{14}C	13.2	27.1	I Fat Cells	24	86	30	84	87	100
				II Soluble	23	3	5	2	—	—
				III Sedimented Cells	53	11	65	14	8	78
B.	Potassium Palmitate-1-^{14}C	36.8	58.7	I Fat Cells	13	83	60	74	96	90
				II Soluble	11	4	13	8	—	—
				III Sedimented Cells	76	13	27	18	12	81
		—	14.7	I Fat Cells	—	68	—	58	—	104
				II Soluble	—	14	—	27	—	—
				III Sedimented Cells	—	18	—	15	—	57
C.	Potassium Stearate-1-^{14}C	20.3	36.0	I Fat Cells	4	62	6	60	—	104
				II Soluble	30	16	7	12	—	—
				III Sedimented Cells	66	21	86	28	6	60

* 4 days after 800 r total-body irradiation, six hours after oral injection of ^{14}C.
† Total-body irradiation.

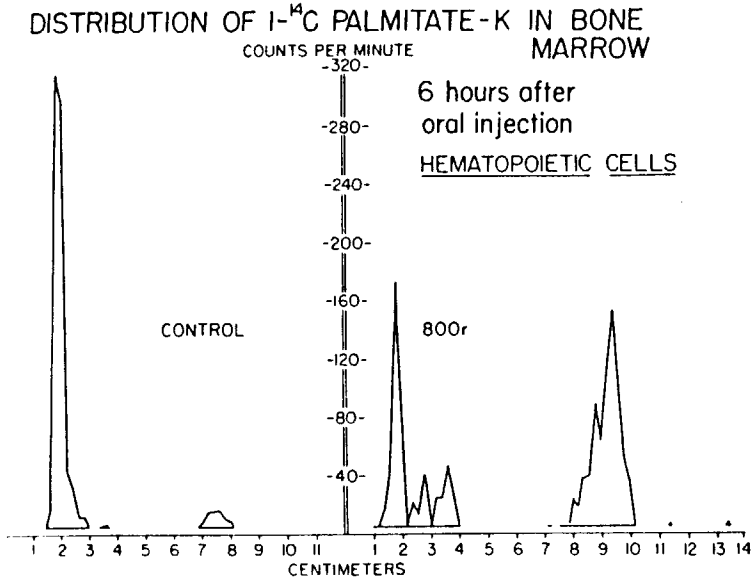

Fig. 12. A zonal scan of the ^{14}C-lipid distribution in the sedimented cell fraction of control and irradiated rats: triglycerides (10 to 13 cm), phospholipids (1 to 2 cm); other minor components present, diglycerides and fatty acids.

increased almost tenfold whether the precursor administered was palmitic or stearic acid. Furthermore, the zonal scans depicted in Fig. 12 show that radioactivity was also present in the phospholipids and diglycerides isolated from control and irradiated marrow. These zonal scans demonstrate in a strikingly visual manner the fact that irradiation stimulates the biosynthesis of triglycerides in hematopoietic cells.

Our conclusion is that the major effect of irradiation on marrow lipid metabolism is to stimulate the esterification of fatty acids into newly formed triglycerides in the hematopoietic cellular fraction and to depress fatty acid oxidation[2] and *de novo* synthesis of fatty acids.[3]

REFERENCES

1. Clark, E. R. and Clark, E. L. Microscopic studies of the new formation of fat in living adult rabbits. Amer J Anat 67, 255-285, 1940.
2. Snyder, F. Fatty acid oxidation in irradiated bone marrow. (See abstract in USAEC Report ORINS-49).
3. Miras, C. J., Mantzos, J. D. and Levis, G. M. Lipid biosynthesis by human bone marrow cell cultures and gamma radiation. Radiat Res 22, 682-692, 1964.

1027832

Effect of Dietary Fat and Total-body Irradiation on the Fatty Acid Composition of Bone-marrow Lipids

J. N. Bollinger

Recent reports[1] have shown that gamma irradiation drastically increases the lipid content of rat bone marrow, and that the increase in bone-marrow fat cells is due to an increase in triglyceride synthesis.[2] This study was undertaken in an effort to determine whether the fat incorporated into bone marrow after total-body irradiation could be modified by the quality or quantity of dietary fat.

In two experiments rats were fed a diet containing 1% safflower oil one month before total-body irradiation. On the day of irradiation the rats were divided into six groups; three groups served as controls and received no irradiation while three groups received 800 r total-body irradiation at a dose rate of approximately 4 r per minute. Both control and irradiated groups were further divided as follows: (a) one group was retained on the 1% safflower oil diet; (b) a second group was placed on a 10% safflower oil diet; and (c) a third group was placed on a 10% coconut oil diet. The animals were maintained on these diets for one week postirradiation after which they were killed by exsanguination. In a third experiment rats (after the initial one month 1% safflower oil dietary regimen) were placed on a 10% safflower oil diet or a 10% coconut oil diet one week before irradiation and maintained on these diets one week after receiving total-body irradiation (800 r). A third group of animals in this experiment was starved for one week postirradiation. Adipose, liver, plasma, and bone-marrow tissue samples were removed from all animals when killed. Total lipids were extracted from the freeze-dried tissues and fractionated into neutral and phospholipids. Thin-layer and gas-liquid chromatographic analysis was performed on all lipid samples.

Neither the level of fat in the diet nor the type of fat (saturated versus unsaturated) present in the diet had an effect on the total amount of fat accumulated in the bone marrow of rats exposed to total-body irradiation (Table 5). On the other hand, the fatty acid composition of the dietary triglycerides greatly influenced the fatty acid composition of the irradiated bone marrow (Fig. 13). In the animals fed the 10% safflower oil diet the level of linoleic acid in the neutral lipid fraction (primarily triglycerides) of the bone marrow lipids was twice that found in the control marrow. Similarly, the level of lauric acid in irradiated marrow increased 4 to 5 times over that found in control marrow from animals fed the 10% coconut oil

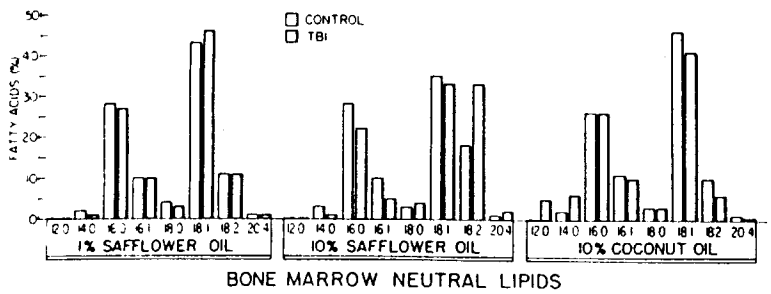

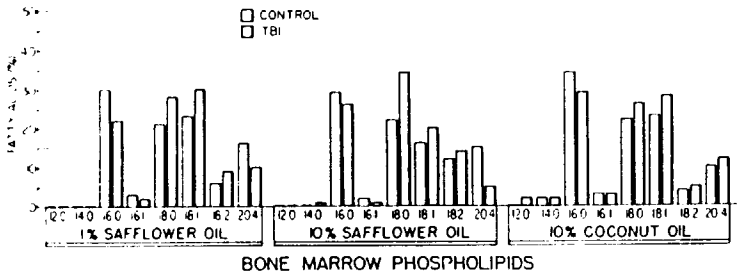

Fig. 13. The effect of dietary fat on the fatty acid composition of bone-marrow lipids one week after total-body irradiation.

diet. The concentration of these acids in the plasma, liver, or genital lipids remained unchanged by the irradiation treatment. The data suggest that the fatty acids used for the increased bone-marrow triglyceride synthesis can be derived from chylomicrons immediately after absorption.

An additional observation was a pronounced decrease in the concentration of arachidonic acid and concomitant increase in stearic acid of phospholipids of bone marrow and plasma after irradiation.

1027833

Since these phenomena occurred only in animals fed a diet (10% safflower oil) relatively high in linoleic acid, it is believed that the radiation altered the linoleic acid molecule or inhibited the enzymatic conversion of linoleic acid to arachidonic acid.

REFERENCES

1. Snyder, F. and Cress, E. A. Bone marrow lipids in rats exposed to total-body irradiation. Radiat Res 19, 129-141, 1963.
2. Snyder, F. Bone marrow lipids and their metabolism. USAEC Report ORINS-43, 13-18, 1964.

TABLE 5

Effect of Dietary Fat on the Accumulation of Fat in the Bone Marrow Of Rats One Week After Total-body Irradiation (TBI)*

Diet	Experiment No.	I†	II†	III‡
	Treatment	Total bone-marrow lipids §		
		%	%	%
1% Safflower Oil	Control	32.3	27.4	
" "	TBI	74.8	77.8	
10% Safflower Oil	Control	26.8	31.9	32.1
" "	TBI	69.5	72.0	72.1
10% Coconut Oil	Control	23.9	33.5	16.2
" "	TBI	78.2	77.7	77.7
Starved¶	Control			30.9
	TBI			76.4

* Total-body irradiation; 800 r at a rate of 4 r per minute.

† Rats were fed a diet containing 1% safflower oil for one month before irradiation; on the day of irradiation they were either retained on this diet or changed to the indicated diet for one week at which time they were killed.

‡ Animals in Experiment III were treated similarly except the diets were switched one week before irradiation.

§ Based on dry tissue weight.

¶ Starved for one week postirradiation.

Fatty Acid Oxidation in Irradiated Bone-marrow Cells*

F. Snyder

A primary event of the acute radiation syndrome is depressed hematopoiesis and an associated accumulation of fat cells' in the bone-marrow cavity. Our work has shown that the fatty change occurs only at bone-marrow sites directly exposed to ionizing irradiation. On the basis of metabolic studies, we have concluded that irradiation stimulates the biosynthesis of triglycerides in nonfatty stem cells of the hematopoietic complex. Although *de novo* synthesis of fatty acids by irradiated marrow cells is impaired,[2] both the uptake of lipid and the esterification of fatty acids into triglycerides by marrow cells are stimulated in irradiated animals.[3] However, fatty acid oxidation by irradiated marrow cells has not been investigated. This study conclusively demonstrated that fatty acid oxidation is severely inhibited by gamma radiation and that the effect is related to the total dose of radiation received.

The data in Fig. 14 show that total-body irradiation significantly inhibits the oxidation of palmitic-1-^{14}C acid by marrow cells. As little as 100 r caused fatty acid oxidation to be inhibited; as long as 55 days after the irradiation exposure, the bone marrow oxidized the fatty acid at only one-half the normal rate. The largest degree of inhibition by 800 r occurred one day after exposure. This emphasizes that the data demonstrating a depressed oxidative rate are not affected by dilution due to a high degree of lipid deposition, since at this time the total lipid level of irradiated bone marrow is essentially normal.[1] The fat cell formation in irradiated bone marrow appears to be primarily caused by the stimulation of the biosynthesis of fatty acid esters and the inhibition of fatty acid oxidation.

* In press. Nature (Lond).

REFERENCES

1. Snyder, F. and Cress, E. A. Bone marrow lipids in rats exposed to total-body irradiation. Radiat Res 19, 129-141, 1963.
2. Miras, C. J., Mantzos, J. D. and Levis, G. M. Lipid biosynthesis by human bone marrow cell cultures and gamma radiation. Radiat Res 22, 682-692, 1964.
3. Snyder, F. Bone marrow lipids and their metabolism. USAEC Report ORINS-43, 13-18a, 1964.

1027834

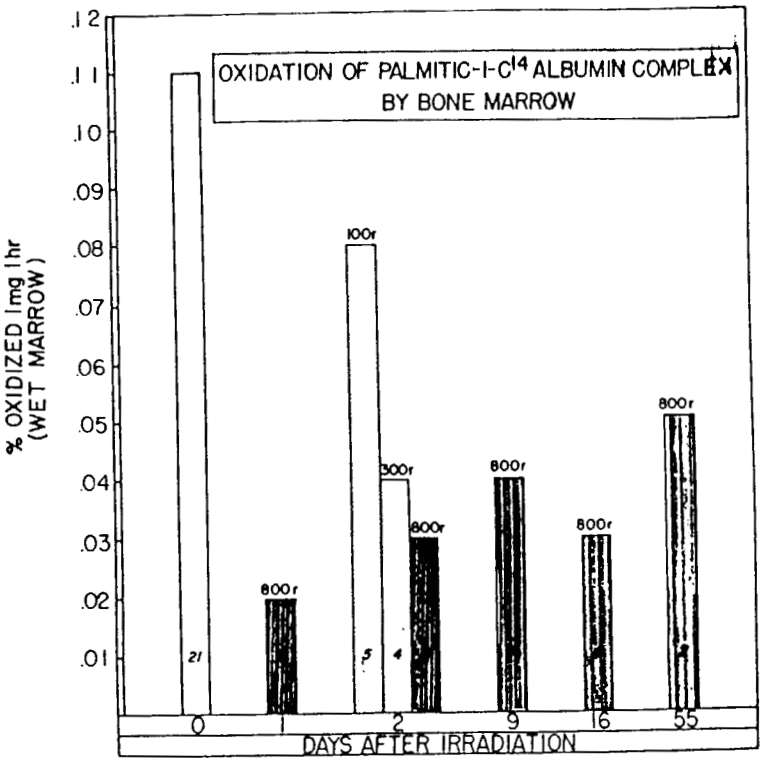

Fig. 14. The effect of total-body irradiation on the oxidation of palmitic-1-^{14}C acid by rat bone marrow.

Rapid Electronic Red Blood Cell Sizing as an Aid in Clinical Diagnosis

C. C. Lushbaugh and D. B. Lushbaugh

The use of the electronic particle-enumeration apparatus to determine cell volume is infrequent in the clinical pathology laboratory even though the mean corpuscular volume (MCV) is a more useful clinical pathologic measurement than the red blood cell count alone. Most laboratories are content to determine MCV indirectly through the use of the hematocrit and the red blood cell count. The propor-

Fig. 15. Electronic cell-volume analyzer unit built around the Coulter Particle Counter. The components are (right to left): The Coulter Counter, Model B, and its glass transducer assembly; the pulse-height analyzer, live oscilloscopic display unit; and oscilloscope camera; preset counting module and parallel-to-serial converter; and electric typewriter.

tionality between the volume of the particle (cell) and the height of the electronic pulse transduced by the passage of a cell through the Coulter Counter* aperture affords a more accurate means of measuring cell volumes directly.

A system was developed and given clinical trials which seemed to overcome many of the difficulties commonly encountered with the Coulter principle of transducing particle volume into pulse-height information electronically for making clinical hematologic diagnoses rapidly. This cell-volume analyzing unit and its components are shown in Fig. 15. In these studies a small amount of blood was obtained in a heparinized glass capillary tube, then diluted with 250 ml saline buffered at 6.7 pH, at room temperature and mixed thoroughly by aeration. The resulting diluted sample contains approximately 45,000 RBC per cubic centimeter. Approximately one to two minutes of analyzer time is then required to size 100,000 cells, and this rate

* Coulter Electronics, Hialeah, Fla.

1027835

of sorting causes slightly less than 10% analyzer "dead time." The frequency distribution of RBC sizes is photographed and the data are typed out as number of "cells" per analyzer-channel number per 100,000 RBC sorted; then the curve is integrated and the "mean channel" is determined. This value is converted to MCV in cubic microns by multiplication with a previously determined scaling factor. For clinical purposes, the ratio of mean channel number to mean cell volume as derived from the hematocrit and red blood cell count is a sufficiently accurate means of calibration (Fig. 16) by graphing for each blood sample the hematocrit-derived MCV and the electronically determined mean channel.

Studies made of the blood of reptiles, amphibia, birds, and mammals (including man), have shown almost universally that under the conditions used in this study, red blood cell volumes are distributed log-normally at low aperture currents, or bimodally at relatively high aperture currents. The electronic method using high aperture currents described here helps in an, as yet, unexplained way to accentu-

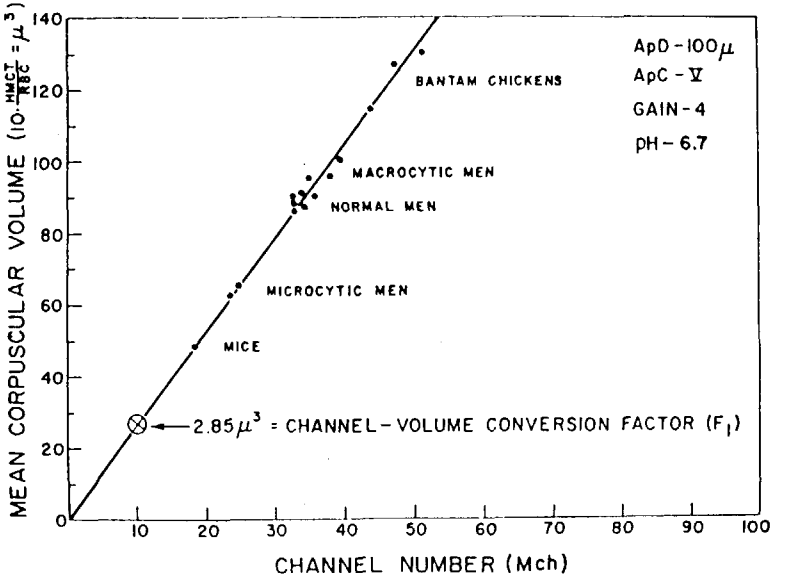

Fig. 16. Graphic correlation of hematocrit and mean anlyzer channel number of various-sized RBC showing method of establishing the scaling factor for converting channel number to cubic microns.

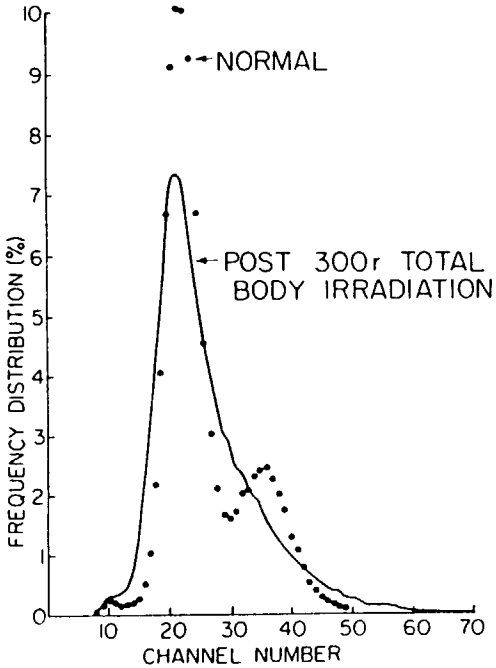

Fig. 17. Normal frequency distribution curve of RBC volumes compared with those of the RBC of a patient nine days after 300 r total-body gamma irradiation, showing the disappearance of the young population as bone-marrow activity stops.

ate the size differences in young and old cells. Artifactual or not, during normal homeostasis this second subpopulation of young cells and reticulocytes is quite reproducible in size, shape, and distribution in relation to the population of old cells of smaller individual volumes. In some diseases affecting the survival, production, and mature size of the erythrocyte, our clinical studies show that changes occur in the position, size, and distribution of the second subpopulation of young cells to a greater extent than in those of the old population.

To date, 27 patients have been studied by this method: seven acute leukemias with anemia; two chronic myelogenous and one chronic lymphocytic leukemia; three refractory anemias of unknown etiology; one thalassemia minor; one polycythemia rubra vera; two vitamin B_{12} deficiencies, one due to malabsorption syndrome and the

1027836

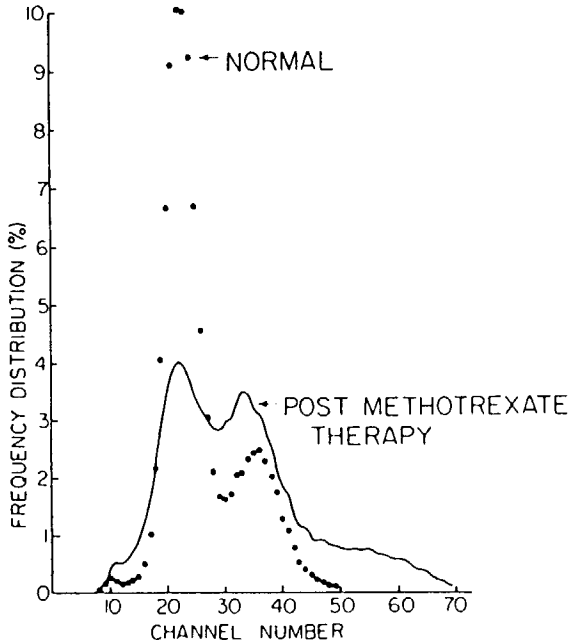

Fig. 18. Normal frequency distribution curve of RBC volumes compared with those of the RBC of a patient with folic acid blockade produced by Methotrexate (R), showing the appearance of a new population of abnormally large young cells.

other to lack of intrinsic factor; two anemias associated with thyroid malignancy; two lymphosarcomas; one multiple myeloma; and five terminal cases with anemia secondary to widespread carcinoma metastases. Figure 17 shows how under identical conditions of measurement the small subpopulation of large RBC was found to disappear from the blood of a child with acute leukemia, during the two weeks after 300 r of total-body gamma irradiation. Figure 18 shows the trimodal pattern that was found in the RBC population of children with acute leukemia in the course of treatment with Methotrexate.*

* 4-amino-N^{10}-methyl-pteroglutamic acid (Lederle Laboratories).

Studies Related to Treatment of Radiation Injury

The objective is to prevent or correct the infections and hemorrhagic manifestations that follow severe radiation damage to bone marrow and lymphatic structures. Intensive studies are done on patients intentionally irradiated for therapy and, when opportunity arises, on victims of radiation accidents. The treatment in part hinges on the feasibility of successful marrow grafts in patients. Animal experimentation has shown that lethal irradiation can be countered by marrow grafts, but homologous disease is a serious potential handicap. Hence, immunologic and biochemical studies on homologous disease comprise a major approach to this objective.

Nitrogen Balance in Radiation Chimeras

W. H. McArthur, C. C. Congdon,† and A. L. Kretchmar*

We have previously reported[1] that food intake is comparable in irradiated mice given isologous or homologous bone-marrow cells. Despite this, the animals given homologous cells develop a secondary syndrome characterized by loss of body weight (homologous disease). We undertook the experiments summarized to determine whether overall nitrogen metabolism was abnormal. The results indicate that nitrogen balance is positive both in animals treated with isologous marrow and in mice given homologous marrow after irradiation.

Mice were irradiated (900 r total-body) and given 40 x 10^6 isologous or homologous bone-marrow cells intravenously on the day of irradiation. They were then kept in special metabolism cages where food intake could be measured, and urine and feces could be collected in dilute sulfuric acid so that nitrogen excretion could be determined. The nitrogen balance was computed as nitrogen excreted minus nitrogen intake. The food was found to contain 33.6 to 36.0 mg of nitrogen per gram of pellet.

The data summarized in Table 6 show that animals treated with isologous marrow maintain a normal rate of gain in body weight

*Knoxville College, Knoxville, Tenn.

†Biology Division, Oak Ridge National Laboratory.

1027837

through 90 days, but retain significantly more nitrogen than normal animals. The animals given homologous marrow fail to gain weight but retain twice as much nitrogen as normal mice. Both marrow-treated groups show the same degree of increased positive nitrogen balance.

We presume that the elevated positive balance in irradiated animals given isologous marrow is the sum of the nitrogen retained for growth, as in the normal mice, and the nitrogen required to complete repair of the damage induced by the lethal irradiation. Despite this elevated retention of nitrogen, which in animals given isologous marrow is sufficient for both growth and repair, the mice treated with homologous cells are unable to grow normally. We speculate that nitrogen is directed into some abnormal compartment or compartments in animals with secondary disease and that this is related in some way to the immunologic conflict between grafted homologous cells and the host animals. If nitrogen in these abnormal forms is retained with less water, glycogen, and solutes than in normal tissues (muscle, for example, contains approximately 75% water, 20% protein, and 5% glycogen and solutes), then the nitrogen balance can be strongly positive even with loss of, or no gain, in gross body weight.

REFERENCE

1. McArthur, W. H., Kretchmar, A. and Congdon, C. C. Study of nitrogen balance in irradiated mice given foreign bone marrow. Blood 22, 502-503, 1963, abstr.

TABLE 6

Average Weight Gain and Nitrogen Balance for the Period 10 to 90 Days of Normal Mice and of Mice Given 900 r Total-body Irradiation and Isologous or Homologous Bone-marrow Cells

Group	Wt. Gain, g/day	Nitrogen balance mg/hr
Normal	0.06 ±0.009	0.34 ± 0.08
Isologous	0.05 ±0.011	0.67 ± 0.09
Homologous	0.009 ±0.011	0.72 ± 0.09

(± Standard error of mean.)

Change in the Partition of Total-body Nitrogen in Irradiation Chimeras

A. L. Kretchmar, W. H. McArthur, and C. C. Congdon†*

We have previously reported[1] that nitrogen balance in irradiated mice given homologous bone-marrow cells was positive and that these animals retained as much nitrogen as did irradiated mice given isologous cells. Despite this equally favorable nitrogen balance, the homologous chimeras failed to gain weight, whereas mice given isologous cells showed good weight recovery and growth. Both irradiated bone-marrow treated groups retained more nitrogen over the 90 days following irradiation than normal unirradiated control mice.

It was tentatively concluded that the nitrogen retained by irradiated mice treated with isologous cells was utilized in synthesis of protein for the regenerating hemopoietic system, other repair processes and growth. We speculated that, since homologous chimeras retained as much nitrogen but failed to gain in body weight, there was a shift in the distribution of body nitrogen in these mice with homologous marrow grafts. If, for example, nitrogen were bound up in the protein of antigen-antibody complexes of a graft-versus-host reaction and these complexes were deposited extracellularly, or on the surface of cells of the graft and host,[2] then a considerable amount of nitrogen could be retained without increasing the body weight to the same degree as if this same amount of nitrogen were retained in protein of normal protoplasm where there is approximately 4 grams of water for each gram of protein. Further, if the formation of antibody occurred at a rate high enough to mobilize body protein, then the shifting of nitrogen from normal tissue compartments to extracellular antigen-antibody complexes could result in loss of gross body weight not reflected in nitrogen balance studies where only nitrogen intake and excretion are measured.

To test this suggestion the total-body nitrogen of mice was determined 4 and 25 days after lethal X-irradiation and injection of isologous or homologous bone-marrow cells (20×10^6). The animals were arbitrarily divided into four sections by gross dissection: (1) blood and thoracic viscera; (2) abdominal viscera; (3) skin, tail, and head; and (4) carcass. These sections were completely digested in sulfuric acid, and the nitrogen content was determined. The total-body nitrogen was thus partitioned into four compartments.

*Knoxville College, Knoxville, Tenn.
†Biology Division, Oak Ridge National Laboratory.

1027838

The results are summarized in Table 7. The numbers shown were calculated by dividing the total nitrogen content of Section III by that of Section IV. When the ratios for each animal were plotted together against body weight, there was no correlation in normal and isologous marrow-treated animals. This showed that the total content in each section varied together with body weight (thus, small animals had less nitrogen in both skin and carcass) but that the relative amount of the total-body nitrogen in skin or carcass was not different in 25-g animals from that in 14-g animals (14 to 24 g was the weight range of animals in the normal group). In contrast, in homologous chimeras the skin/carcass ratio was negatively correlated to body weight. That is, the lightest chimeras had the highest ratios.

The data in Table 7 show that distribution of nitrogen is changed in homologous chimeras and that there is relatively more nitrogen in skin than in carcass, especially in animals of less than 18 g and, therefore, presumably suffering from homologous disease. The data also show that this shift can be detected early (four days) but is probably progressive. The result suggests that a major target of the graft-anti-host reaction is the skin and that nitrogen is deposited in this tissue at the expense of the carcass tissues.

REFERENCES

1. McArthur, W. H., Congdon, C. C. and Kretchmar, A. L. Nitrogen balance in radiation chimeras. Proc Soc Exp Biol Med 117, 171-175, 1964.
2. Hager, E. B., DuPuy, M. P. and Wallach, D. F. H. Immunologic suicide and studies on the role of antibody and complement in canine kidney homograft rejection. Ann NY Acad Sci 120, 447-457, 1964.

TABLE 7

Ratio of Nitrogen in Skin to that in Carcass of Mice Given 950 r Total-body Irradiation and 20 x 10⁶ Bone-marrow Cells

Group and Marrow Treatment	Days after Irradiation	Skin/Carcass N ratio
Normal	(4-day control)	1.0
	(25-day control)	1.0
Isologous	4	1.0
	25	1.0
Homologous	4	1.24*
	25	1.43*

* Ratios are for chimeras with body weight less than 18 g. Animals above this weight showed normal skin/carcass ratios.

Lipid Composition of Tisssues After Isologous and Homologous Marrow Transplants in Mice

*J. N. Bollinger, F. Snyder, and C. C. Congdon**

These experiments were undertaken to asses the degree of lipid involvement in the metabolic consequence of tissue transplantation terminating in homologous disease. Previous data' suggested that a form of metabolic starvation (including the gross observation of adipose fat depletion) occurs in animals affected with this secondary disease, thereby implicating that stored fat might be used preferentially over other metabolites for the energy requirements of these animals. The evaluation of this supposition has led to this report on the lipid content and composition of various tissues obtained from irradiated mice given homologous and isologous marrow. Fed, three-day fasted, and irradiated (950 r) mice served as control groups in this study.

Total lipids, the lipid classes separated by thin-layer chromatography (TLC), and the total fatty acid composition of each tissue as determined by gas-liquid chromatography were measured on lipid extracts obtained from the liver, serum, bone marrow, genital fat pad, and carcass.

The data obtained reveal that transplantation of homologous marrow in irradiated mice has essentially no effect on the lipid class composition of liver, marrow, serum, adipose tissue, or carcass. An exception was the observation of long-chain fatty alcohols present in the carcass lipids of the 90-day chimeras only. The finding of these alcohols in the chimeras might just be related to the age or mouse strain used and not to the experimental treatment. The TLC chromatograms also revealed the triglyceride fatty liver of all mice that were starved for three days (Fig. 19).

We observed that depletion of adipose fat occurred in some of the animals that received homologous transplants and not in others. The healthy looking animals had ample fat in the genital areas, but such animals had no visible depot fat. These differences in adipose fat in homologous mice showed up in the total lipid determination and complicated the interpretation of these results. Perhaps longer term studies will give more consistency to this pattern. Our data conclusively show that, if mobilization of adipose fat to liver does occur in the homologous mice, it is readily used for energy requirements, since in no instance was there any accumulation of liver triglycerides or buildup of serum free fatty acids.

* Oak Ridge National Laboratory, Biology Division.

1027839

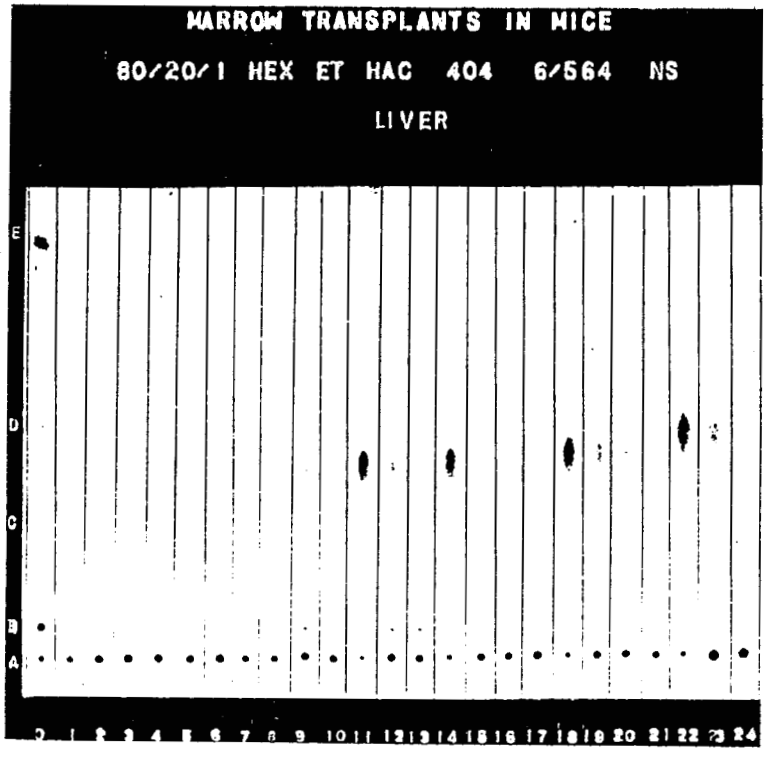

Fig. 19. (O) Lipid standard (A) lecithin (B) cholesterol (C) oleic acid (D) triolein (E) cholesterol oleate; (1) (2) (8) (17), control mice; (3) (4) (5) (6), 90-day chimeras; (7) (12), one week after irradiation alone. Groups of mice irradiated for the two- and three-week study died of irradiation syndromes; (9) (16), one week after homologous transplants; (10) (15), one week after isologous transplants; (20) (24), two and three weeks respectively after homologous transplants; (19) (23), two and three weeks respectively after isologous transplants; (11) (14) (18) and (22), three-day starved controls. The mouse strains used in this study were male and female. (101XC$_3$H)FI and (C$_{57}$BL-6 DBA-2)FI.

Gas-liquid chromatography analysis of adipose fat showed that no alterations in the total fatty acid composition occurred in any of the experimental groups. The high content of linoleic acid demonstrated no essential fatty acid deficiency in the mice. The marrow lipids of the mice revealed a much more complex mixture of lipids

than that previously observed for hematopoietic or fatty marrow from other species. Additional data on the lipid patterns of donor and recipient bone marrow before and after transplants would be valuable to determine the role that transplanted marrow cells and diet have in determining the type of lipids deposited.

REFERENCE

1. Snyder, F. and Cress, E. A. Bone marrow lipids in rats exposed to total-body irradiation. Radiat Res 19, 129-141, 1963.

Transplantation of Rat Bone Marrow in Irradiated Mice As a Function of Exposure Rate

N. Gengozian

Mice were given 900 r total-body irradiation at varying exposure rates with either the ^{137}Cs total-body irradiator designed for the treatment of patients or a ^{60}Co Westinghouse therapy unit. Within two hours after irradiation, groups of mice from each exposure rate received intravenously 100 x 10^6 nucleated rat (CFN) bone-marrow cells. At varying intervals after treatment the animals were tested both for the presence of the donor graft and for the formation of serum antibodies directed against the graft. Table 8 shows that the success of the foreign marrow transplantation depended on the radiation exposure rate to which the recipient mice were subjected. Erythrocytes characteristic of the donor were found in none of the mice receiving 900 r at 3.75 r/min. Of recipients irradiated at 19.8 r/min, only one mouse of 24 tested on day 10 was positive for rat erythrocytes, and this animal was negative when tested on day 30. Of mice irradiated at 39.7 and 53.4 r/min, increasing numbers showed some signs of a transplant. Among all four groups, only six mice were true radiation chimeras, and five of these had been subjected to the highest exposure rate. Failure of the transplantation indicated an immunologic rejection phenomenon as shown by the presence of agglutinating antibodies in the serum of some of the treated mice (Table 8). This was most evident in the group subjected to 3.75 r/min, where nine of 20 animals tested on day 20 showed some agglutinating antibodies to rat erythrocytes. As the exposure rate increased, the number of animals showing agglutinins decreased.

1027840

The data in this demonstrated that, independent of the total irradiation dose, the exposure rate is an important factor in the degree of suppression and rate of recovery of the immune mechanism. The operation of this phenomenon in a heterograft system was demonstrated by: (1) a transient or only temporary take in the low exposure-rate groups with permanent grafts only in the two higher exposure-rate groups; (2) early active antibody formation after disappearance of the graft in the low exposure-rate group; (3) a longer persistence of the foreign cells with an increase in exposure rate; and (4) greater survival value from the foreign graft at the highest exposure rate. It is not yet known whether the exposure-rate dependent immune phenomenon shown here in mice is also operating in larger animals such as dogs and primates, including man. Studies are also needed to determine the association of mortality with immunologic suppression in view of the increased mortality obtained with an increase in exposure rates.

TABLE 8

Tests for the Presence of Rat Erythrocytes, and Agglutinins for Rat Erythrocytes, in the Blood of Irradiated Mice Injected with Rat Bone Marrow. All Mice Received a Total of 900 r.

Days after injection of bone marrow	Exposure rate (r/min)			
	3.75	19.8	39.7	53.4
	Tests for rat erythrocytes*			
10	0/34†	1/24	10/33	18/32
20	0/20	1/20	3/13	8/17
30	0/16	0/19	1/13	5/12
	Tests for rat erythrocyte agglutinins			
20	9/20(1-4)‡	1/19(1)	0/10	0/9
30	10/16(2-6)	3/19(2-4)	2/12(3,4)	1/7(5)
50	11/15(2-9)	4/18(1-5)	2/10(2,3)	2/6(4,6)

* Exposure-rate difference significant by chi-square test.

† Fractions represent number of animals showing positive test over number tested.

‡ Values in parentheses represent agglutinin titer (log_2) or range in titer on positive serum samples.

Autoimmune Hemolytic Anemia Treated with d-Penicillamine

C. L. Edwards and N. Gengozian

The mercaptan, penicillamine (dimethyl-cysteine), has been used clinically as a chelating agent to promote the excretion of copper in Wilson's disease. The *in vivo* depolymerization of macroglobulins in Waldenstrom's macroglobulinemia has also been reported to follow the oral administration of penicillamine,[1] and Ritzmann and Levin[2] reported the successful treatment of cold-agglutinin disease with two mercaptans, dl-penicillamine and mercaptopyridoxine.

A patient at the Division with autoimmune hemolytic anemia associated with multiple neoplasms did not respond to corticosteroid therapy or treatment with 6-mercaptopurine. *In vitro* reaction of the patient's serum antibody with the sulfhydryl compounds, 2-mercaptoethanol and d-penicillamine, resulted in inactivation of the autoagglutinin, suggesting that it was a macroglobulin. Treatment of the patient with d-penicillamine orally for eight consecutive days was followed by a decrease in the autoagglutinin titer, resulting in disappearance of the antibody within a few days after cessation of therapy. This permitted successful transfusion with restoration of previous red blood cell values and without further evidence of excessive destruction of the transfused cells (Fig. 20). Although the patient remained Coombs positive after d-penicillamine treatment and throughout the ensuing months, the serum autoagglutinins did not reappear.

The results would suggest that penicillamine, in this instance, exerted its beneficial effects by affecting the cellular level of the immunologic process rather than through any *in vivo* depolymerizing effect on circulating macroglobulins. More definitive answers on the mode of action of penicillamine on immunologic processes may be obtained by studies on experimental animals where one can control the course of an experimentally induced antibody-forming mechanism.

REFERENCES

1. Bloch, H. S., Prasad, A., Anastasi, A. and Briggs, D. R. Serum protein changes in Waldenstrom's macroglobulinemia during administration of a low molecular weight thiol (penicillamine). J Lab Clin Med 56, 212-217, 1960.
2. Ritzmann, S. E. and Levin, W. C. Effect of mercaptans in cold agglutinin disease. J Lab Clin Med 57, 718-732, 1961.

1027841

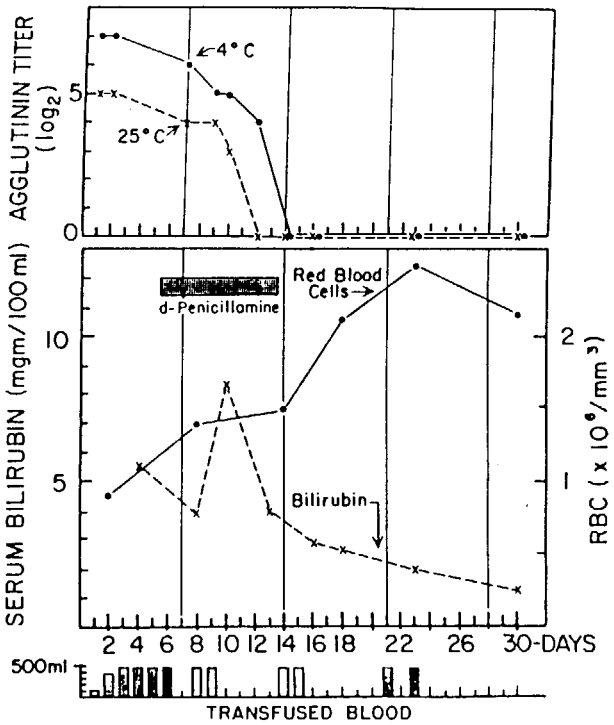

Fig. 20. Changes in autoagglutinins and hemolysis after penicillamine treatment of a patient with autoimmune hemolytic anemia.

Depression of the Primary Immune Response by dl-Penicillamine

K. Hubner and N. Gengozian*

Limited studies in patients with macroglobulin-associated disorders have suggested a beneficial effect derived from the administration of penicillamine, one of the mercaptan compounds. The SH-radical of penicillamine, active in the chelation of copper and other heavy metals, also appears to be effective in the depolymerization of macroglobulins *in vitro* and *in vivo*. Treatment of a patient with auto-

*Present address: 74 Tubingen Herrenbergerstrasse 23, West-Germany.

immune hemolytic anemia in our laboratory with dl-penicillamine resulted in prompt and complete disappearance of the auto-agglutinin (see p. 48). The effectiveness of penicillamine in reducing the clinical syndromes associated with macroglobulinemias of hemolytic anemia, Waldenstrom's disease, and rheumatoid arthritis suggested that a basic study be made of its effect on an experimentally induced antibody-synthesizing mechanism.

Groups of mice were treated with dl-penicillamine (Table 9) before or after stimulation with a bacterial antigen, *S. typhosa*, which stimulates in most species the formation of a macromolecular antibody in the early phases of a primary immune response. Figure 21 shows the typhoid H agglutinin titers for the normal and experimental groups. Figure 22 shows the agglutinin titers for the same groups after treatment of the sera with 2-mercaptoethanol (2-ME), a sulfhydryl compound that depolymerizes and inactivates macroglobulin antibodies. Considering the total antibody formed (i.e., non-2-ME treated sera, Fig. 21) from the seventh through the thirty-fifth day after antigen injection, a response significantly lower ($P<0.001$) than the normal group A was obtained in three groups, C, D, and E. The depression was greatest in group E, which had received daily subcutaneous injections of penicillamine before and after antigen injection.

Among the four experimental groups, only B showed a response comparable to the normal, and this group received penicillamine only after antigen injection. In those groups showing depression of antibody response, the formation of both 19S and 7S antibody was reduced, the latter type also showing a delay in appearance but subsequently reaching levels comparable to those seen in normal animals. Administration of penicillamine intravenously to animals having only 19S antibody in the serum resulted in an immediate but transient reduction of antibody titer. This observation, along with that showing failure of penicillamine to affect the formation of both 19S and 7S antibody when given after antigen injection, suggests that the depressive effect is primarily at the cellular level of the immunologic mechanism rather than through an intravascular dissociation process.

1027842

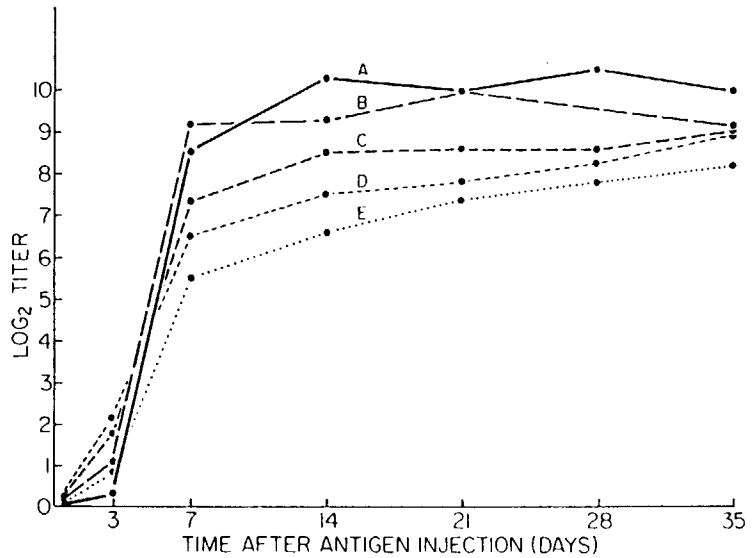

Fig. 21. Agglutinin response to typhoid H antigen in normal mice and mice treated with dl-penicillamine (see Table 9 for legend).

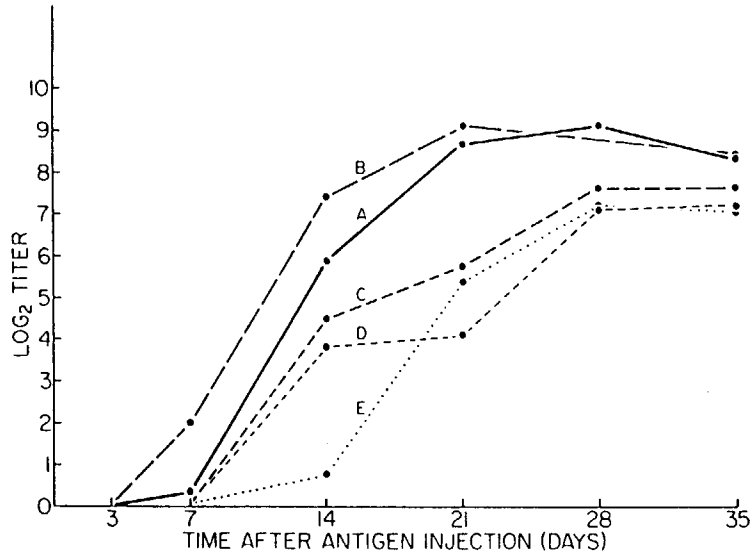

Fig. 22. Agglutinin titers following treatment of the immune sera with 2-mercaptoethanol (see Table 9 for legend).

TABLE 9

Penicillamine Treatment Schedule Relative to Antigen Injection

Group	Day −21 to Day 0	Day 0	Day 0 to Day +23
A	No treatment	Ag	No treatment
B	No treatment	Ag	5.5 mg q.d. (x8), i.p.
C	5.5 mg q.o.d., i.p.	Ag	No treatment
D	5.5 mg q.o.d., i.p.	Ag	5.5 mg q.o.d., i.p.
E	5.5 mg q.d., s.c.	Ag	5.5 mg q.d., s.c.

Human A- and B-like Antigens on Red Cells of Marmosets

N. Gengozian

Studies are being conducted in this laboratory on the use of the South American marmoset, *Tamarinus nigricollis*, for total-body irradiation effects. Since we are interested in the therapeutic value of bone-marrow transfusions in lethally irradiated animals, it is desirable to know whether red cell antigenic differences exist among these primates that would permit identification of any transplanted donor elements in the irradiated host.

In the present study, the red blood cells of the marmoset were tested for the presence of human A and B antigens with specific antisera reagents. As shown in Table 10, absorption tests with human anti-A and anti-B sera suggested the presence of a B-like antigen on their red cells and the absence of any A-like antigen. Reaction of specific anti-A and anti-B eluates with the marmoset's cells confirmed the absorption tests. Eluates prepared from the absorption of the anti-A and anti-B reagent with marmoset red cells suggested, however, the presence of an A-like antigen in addition to the B-like antigen on their red cells (Table 11).

Tests of 40 marmosets failed to reveal any red cell antigenic differences with respect to their human A- and B-like antigens. Inhibition tests on marmoset saliva indicated the presence of the A antigen and

1027843

TABLE 10

Reaction of Anti-A and Anti-B Reagents with Marmoset Cells Before and After Specific Absorptions

Reagent	Agglutinin reaction with:		
	A rbc	B rbc	M* rbc
	Titer (log_2)		
Antiserum:			
Anti-A			
Unabsorbed	9	—†	4
Absorbed with A rbc	0	—	4
Anti-B			
Unabsorbed	—	9	9
Absorbed with B rbc	—	0	5
Eluate:			
Anti-A			
Unabsorbed	6	—	0
Absorbed with A rbc	0	—	—
Absorbed with M rbc	6	—	—
Anti-B			
Unabsorbed	—	5	4
Absorbed with B rbc	—	0	0
Absorbed with M rbc	—	0	0

* M = marmoset

† Test not performed

TABLE 12

Analysis for Sex Drumstick in Neutrophils of 22 Female and 20 Male Tamarins

Animal No. and Sex	Neutrophil drumsticks (per 500 cells)	Animal No. and Sex	Neutrophil drumsticks (per 500 cells)
1-F	14	1-M	0
2-F	12	2-M	0
3-F	10	3-M	0
4-F	9	4-M	0
5-F	9	5-M	0
6-F	9	6-M	1
7-F	9	7-M	1
8-F	8	8-M	1
9-F	8	9-M	1
10-F	6	10-M	1
11-F	5	11-M	2
12-F	4	12-M	4
13-F	3	13-M	4
14-F	3	14-M	4
15-F	3	15-M	4
16-F	2	16-M	4
17-F	2	17-M	5
18-F	0.5*	18-M	5
19-F	0	19-M	7
20-F	0	20-M	7
21-F†	7		
22-F†	7		

* Scoring done on 1000 neutrophils

† Female twins born in this laboratory

among several males the drumstick neutrophil was found in a frequency comparable to that seen in some of the female tamarins. The results in a comparison between the drumstick marker and sex chromosomes in the evaluation for chimerism are shown in Table 13.

Analysis of the data for both male and female tamarins shows there was no agreement between the frequency of drumstick neutrophils in the peripheral blood and the percentage of these same cells having the female sex chromosome. Spleen, bone marrow, and lymph-node cells of female 19 were also cultivated for sex-chromosome analysis; as with the blood, male chimerism was found in all tissues. A high percentage of male chimerism was found in this female, where

1027844

approximately 90% of the cells scored in the blood, spleen, and lymph node were of male origin.

Although in our study the neutrophil drumstick did not provide a good quantitative index of chimerism, its distribution among the male and female tamarins suggests that this criterion can be used as presumptive evidence for heterosexual chimerism. Thus, if fraternal twinning, with its 50% probability that twins will be of the opposite sex, is a consistent occurrence, prenatal vascular anastomosis would result in a decreased number of drumstick neutrophils in 50% of the females and a corresponding increase among 50% of the males. The data in Table 12 indeed suggest that this may be occurring. Marmosets are only the second species (after cattle) in which dizygotic twinning associated with blood-cell chimerism is the rule rather than

TABLE 13

Comparison of Neutrophil Drumstick and Sex-chromosome Analysis in Evaluation for Chimerism

Animal No. and Sex	Neutrophil drumsticks (per 500 cells)	Sex-chromosome Analysis			
		Tissue	Cells containing: XX	XY	Percent Chimerism
1-M	0	Blood	0	50	0
2-M	0	Blood	0	50	0
17-M	5	Blood	23	27	46
19-M	7	Blood	8	42	16
1-F	14	Blood	50	0	0
3-F	10	Bone Marrow	50	0	0
4-F	9	Blood	50	0	0
18-F	1	Bone Marrow	63	27	30
19-F	0	Blood	6	59	91
		Spleen	3	25	89
		Bone Marrow	16	49	75
		Lymph Node	6	59	91

TABLE 11

Reaction of Anti-A and Anti-B Reagents Following Absorption with Marmoset Red Blood Cells

Reagent	Agglutinin reaction with:		
	A rbc	B rbc	M* rbc
	Titer (log_2)		
Antiserum:			
Anti-A			
Unabsorbed	9	—†	4
1st absorption	8	—	0
2nd absorption	8	—	—
3rd absorption	8	—	—
4th absorption	8	—	—
Anti-B			
Unabsorbed	—	9	9
1st absorption	—	7	0
2nd absorption	—	6	—
3rd absorption	—	5	—
4th absorption	—	5	—
Eluate:			
Anti-M(A)‡	5	—	0
Anti-M(B)‡	—	5	3

* M = marmoset

† Test not performed

‡ Eluates prepared after absorption of anti-A(A) and anti-B(B) reagents with marmoset rbc.

the absence of the B and H antigenic substances in their saliva. Initial limited tests for the presence of natural agglutinins to human A and B cells were negative. Subsequent testing during an iso- and heteroimmunization study revealed the presence of anti-B agglutinins in the sera of 18 of 30 marmosets tested with only two showing weak

1027845

agglutinins to human A cells. Natural isohemagglutinins among these animals have as yet not been found, which is not surprising in view of the established hematopoietic chimerism presumed to exist in these primates, a phenomenon that would lead to suppression of any development of isohemagglutinins through immunologic tolerance. In any event, the data thus far suggest the nonidentity of the marmoset red cell antigens to that of the human A and B.

Hematologic and Cytogenetic Evidence for Chimerism in the Marmoset, *Tamarinus nigricollis*

N. Gengozian, J. S. Batson, and P. Eide

Recent studies in this laboratory have been conducted on the feasibility of developing a species of the Hapalidae family of small South American primates, *Tamarinus nigricollis*, as an experimental animal for the study of radiation effects. In the absence of a suitable red blood cell antigen marker, consideration was given to the possible use of the characteristic chromatin body ("drumstick") of female neutrophils as a marker for detecting transplantation of female donor cells in an irradiated male host. Sexual differentiation on the basis of this nuclear drumstick appendage of female leukocytes is well established among humans and other primates. In preliminary analyses of peripheral blood smears, it was evident that, although the neutrophil drumstick was readily identified, the presence of these cells was not limited to the female, and furthermore, it could not be found at all in the cells of some female tamarins. This observation suggested a possible heterosexual chimerism among these animals; this supposition was supported by the report of Wislocki[1] describing the high frequency of fraternal twinning in marmosets and the occurrence of placental anastromosis between the twins.

Table 12 shows the results obtained upon scoring the blood smears of male and female tamarins for neutrophils having the drumstick appendage. Since the animals were randomly selected and were not heterosexual twin pairs, they were arbitrarily tabulated in Table 12 in order of their scoring for the neutrophil drumsticks; i.e., in decreasing order for the females and ascending order for the males. Two females showed the absence of cells bearing the drumstick and

the exception. In view of this, we believe that as a small laboratory primate this animal offers unique opportunities for the study of immunologic phenomena as related to its naturally acquired state of tolerance, i.e., hematopoietic chimerism.

REFERENCE

1. Wislocki, G. B. Observations on twinning in marmosets. Amer J Anat 64, 445-483, 1939.

Bone-marrow Grafting Attempts in Tamarins After Total-body Irradiation

N. Gengozian, J. S. Batson, and Bill M. Nelson

The efficacy of bone-marrow cells in promoting recovery from lethal radiation injury has been extensively studied and effectively accomplished in several species of animals. Successful therapeutic marrow transplants have been effected in mice, rabbits, dogs, hamsters, guinea pigs, and pigeons. Less promising have been the attempts in primates, human and subhuman. The present study was undertaken to determine the effectiveness of homologous marrow transfusions in protecting the South American marmoset, *Tamarinus nigricollis*, from lethal and supralethal total-body irradiation.

Groups of tamarins exposed to 400 r, 600 r, or 800 r were injected with homologous marrow within two to four hours postirradiation. To evaluate the effectiveness of marrow treatment in prolonging survival, the mean survival times of tamarins receiving similar radiation exposures without marrow treatment is shown in Table 14. Table 15 shows the day of death of the individual animals in the three groups after radiation and marrow treatment. Only in the 600 r and 800 r groups did bone marrow increase survival time. In the former group, three of seven tamarins survived significantly longer than the radiation controls. In the 800 r group, five of seven survived significantly beyond the time of the control group. In contrast, injection of homologous bone marrow in the 400 r group did not extend the survival time but apepared to have the opposite effect, two animals dying before the expected time of death as indicated by the controls in Table 14. Definitive evidence for marrow transplants was obtained only in four of the 800 r treated animals (Table 15). Two of these

1027846

TABLE 14

Survival Time in Days Among Tamarins Receiving Lethal Doses of Total-body Irradiation

Dose (r)					
400		600		800	
Animal No. and Sex	Day of Death*	Animal No. and Sex	Day of Death	Animal No. and Sex	Day of Death
2-2-3 (M)	9	24-3-2 (M)	7	26-6-2 (M)	5
14-1-3 (F)	9	26-5-2 (F)	7	26-4-1 (F)	7
14-4-2 (F)	10	14-2-4 (F)	7	25-2-2 (F)	8
7-2-3 (M)	10	26-4-4 (F)	9	21-7-1 (M)	8
14-1-4 (F)	11	21-2-2 (M)	10	21-2-4 (F)	9
14-4-3 (M)	12	2-6-2 (M)	11	26-2-4 (F)	9
2-2-1 (F)	12	26-6-1 (M)	12		
26-5-3 (F)	13				
2-6-3 (M)	13				
27-5-4 (M)	14				
Mean	11.3		9		7.7
Standard Deviation	1.67		1.92		1.38

* Each value represents the day of death of a single animal after treatment.

were determined by sex chromosome analyses of bone-marrow tissues obtained at the time of death and two by the appearance of drumstick neutrophils within two weeks after treatment. Attempts to detect marrow grafts by the sex chromosome method were also made on the remaining animals in this group and in the 600 r group, but technical problems prevented obtaining cells suitable for scoring.

The results of this study substantiate further the reports of others on the difficulties of obtaining therapeutic homologous grafts in irradiated primates. Failure of homologous marrow to extend the survival times of animals receiving 400 r suggests that this was due to an active immunologic rejection of the graft by the host. Although survival was extended significantly in some of the 600 r and 800 r mar-

10278471

TABLE 15

Effect of Homologous Bone Marrow on Survival Time of Tamarins Receiving Lethal Doses of Total-body Irradiation

Dose (r)								
400			600			800		
Animal No. and Sex	Day of Death*	Relative Deviate†	Animal No. and Sex	Day of Death	Relative Deviate	Animal No. and Sex	Day of Death	Relative Deviate
9-4-4 (F)	8	2.0	25-3-1 (M)	7	1.0	21-21-2 (F)	7	0.5
24-3-1 (M)	8	2.0	25-2-3 (M)	8	0.5	22-1-1 (F)	7	0.5
22-1-3 (F)	9	1.4	25-2-1 (M)	9	0	23-1-1 (M)	11	2.4‡
10-3-2 (F)	10	0.8	14-2-3 (M)	10	0.5	22-1-2 (F)	13	3.8
21-13-2 (F)	11	0	25-4-1 (F)	18	4.7	21-17-1 (M)	13	3.8§
24-3-3 (M)	11	0	14-1-1 (F)	20	5.7	22-3-2 (M)	16	6.0¶
			21-13-4 (F)	33	12.5	21-7-4 (M)	26	13.2¶

* Each value represents the day of death of a single animal following treatment.

† Relative deviate expresses the distance from the mean time of death of the controls (Table 14) in units of the standard deviation.

‡ Presence of female cells (25%) in male host indicated by sex chromosome analysis of bone marrow obtained from host at time of death.

§ Presence of female cells (100%) in male host indicated by sex chromosome analysis of bone marrow obtained from host at time of death.

¶ Presence of donor female cells indicated by drumstick-bearing neutrophils in peripheral blood smears.

row-treated animals, the reasons for failure of hematopoietic recovery resulting finally in death of the animals is not clear. One contributory factor may have been the chronic parasitism prevalent in these animals, which would compound the radiation damage to the tissues and thus place greater metabolic stress on the animals. This, however, would not explain the death of those animals in which marrow histology showed active hematopoietic sites at time of death. A more plausible explanation, and one that is more germane to the problem, is the genetic incompatibility of donor and host in this homologous transfer that may result in immunologic reactions leading to early death of the animals.

Allotypic Specificities in Four Strains of Inbred Mice as Revealed by Reciprocal Immunizations

*N. Gengozian and G. Doria**

Allotypes are those serum proteins differentiated within any one species by their antigenic specificities and have been reported in rabbits, mice, guinea pigs, and man. It has been generally convenient to study the allotypes of gamma globulin since this protein can be obtained immunobiologically in a relatively pure form. Thus, the induction of antibody formation to an antigen in one animal, followed by the reaction of the immune serum *in vitro* with the antigen, provides the specific antibody protein of that animal in an immune precipitate. Subsequent injections of this precipitate into another animal of the same species but of different genetic constitution yields an immune serum that can then be used as a reagent to reveal allotypic specificities of gamma globulin.

In the present study, reciprocal immunizations among four strains of highly inbred mice with their respective gamma globulin protein (in antigen-antibody immune precipitates) was performed to determine allotypic specificity. Up to the present, the determination of allotypes in mice has been based on the development of an isoprecipitin reagent in one strain of mouse followed by testing its activity against serum of other inbred strains. The isoimmune sera obtained were tested *in vitro* by tannic acid hemagglutination, immunodiffusion and immunoelectrophoresis to determine the allotypic relation

*Present address: Biology Division of Euratom, Laboratorio Di Radiobiologia Animale, C. S. N. Della Casaccia (Rome) Italy.

m and Medical Radioisotope evelopment

iomedical studies of lanthanon metabo- l during the year and more emphasis on rations has resumed. The summaries deal- s, plasmalogens, accumulation and release factors, and microbiological uptake give hemical properties and effects of these ele- dioisotopes of these same elements have ing bone marrow, and other radioisotopes valuated for bone scanning and diagnostic y included improvements in fecal analysis trophoresis using polyacrylamide gels for om patients given total-body irradiation. er new approaches are, however, prelimi- ter.

---

arth-induced Fatty Infiltration

on,[1] G. C. Kyker, C. L. Yarbro,[†]

ere measured at various intervals during of rare-earth fatty liver in rats, caused by anum, cerium, praseodymium, and neody- ed similarly after treatment with each of f plasmalogens was observed after treat- um, neodymium, which correlated closely iver lipids; after praseodymium, plasmalo- unchanged throughout. Confirming pre- effect of cerium, the level of phospholipid ent in any of the four groups.

ased plasmalogens in liver caused by rare comprise a group of lipids considered to be

i Soc.
, Chapel Hill, N. C.

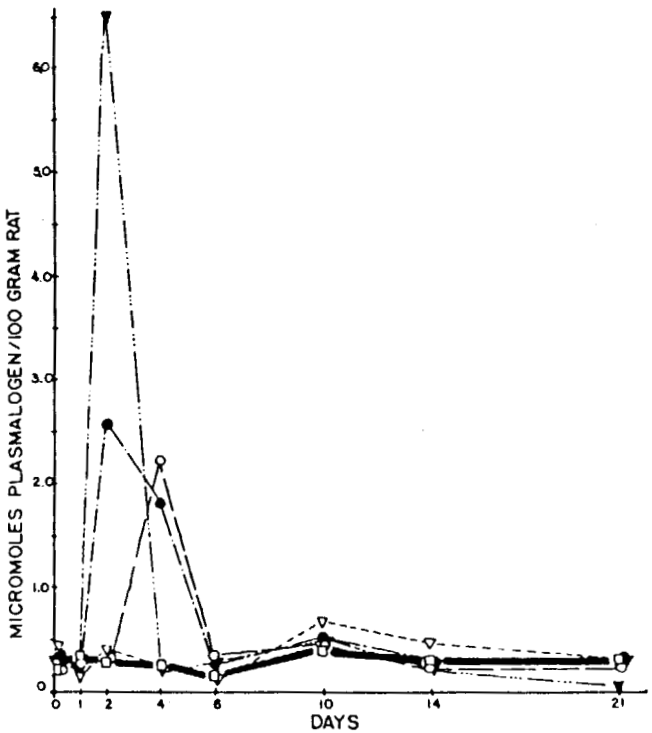

Fig. 23. Plasmalogen in the rare-earth fatty liver. □ physiological saline; O lanthanum; ⊙ cerium; ▽ praseodymium; ▼ neodymium.

derivatives of 1-alkenyl ethers of glycerol with positions 2 and 3 resembling a phospholipid or neutral lipid. Although their metabolic function is unknown, their occurrence in animal and in plant tissues is widely reported in micromolar amounts. There is evidence of increased plasmalogens during metabolic stress. The present results are therefore consistent with present knowledge. The very low normal level of this fraction of lipids could be due to very active metabolic turnover. The increase could then be explained by the decreased utilization of liver lipids during rare-earth fatty liver. The results also give the first indication of difference in the fatty liver caused by different elements in the cerium group of lanthanons. (See Fig. 23).

1027849

Triglyceride Accumulation and Release in the Rare-earth Fatty Liver*

F. Snyder and G. C. Kyker

The hyperlipemic response to Triton (p-isooctyl polyoxyethylene phenol polymer) caused by decreased removal of triglycerides from plasma was used to evaluate hepatic accumulation and release of lipid during infiltration caused by cerium.

Others have shown that most of the triglycerides in plasma after Triton come from liver so that a blocked hepatic release of triglyceride reduces or prevents the hyperlipemia. Measurements comparing the effect of cerium and ethionine indicated a sharp difference in mechanism. No significant block in the release of triglyceride from liver to plasma occurs during the accumulation. This conclusion is evident according to the tabulated results (Table 16). At 48 hours after cerium the hyperlipemic effect of Triton is less. This period approximates the time of highest level of accumulated lipid and maximum injury to the liver. Accordingly, the capacity to release lipid may be less because of reduced liver function.

* Proc Soc Exp Biol Med 116, 890-893, 1964.

TABLE 16

Effect of Cerium and Ethionine on the Release of Esterified Fatty Acids from Liver

Treatment		μEq esterified fatty acid in neutral lipids/100 ml plasma	Liver %
Control	(35)	138	6.04
6-hr Triton	(6)	6108	7.10
1-day cerium, 6-hr Triton	(6)	5256	12.55
2-day cerium, 6-hr Triton	(5)	3167	14.09
3-day cerium, 6-hr Triton	(5)	4444	13.78
1-day ethionine, 6-hr Triton	(4)	1547	—
2-hr Triton	(8)	1838	6.44
1-day cerium, 2-hr Triton	(8)	2125	9.30
3-day cerium, 2-hr Triton	(6)	1719	—
1-day ethionine, 2-hr Triton	(4)	576	15.85

The values in parentheses represent the number of rats used to obtain a pooled sample for analysis.

The Mechanism of Cerium Uptake by *Saccharomyces cerevisiae*

G. T. Johnson and G. C. Kyker

A large fraction of the total uptake of tracer cerium by washed resting yeast cells occurs quite rapidly (less than 15 minutes). Optimum uptakes occur in acidic environments (pH 2.5-4.0) and are higher with living than with dead cells. Data presented suggest that cerium uptake by yeast involves primarily an adsorption of the element by some solid phase in or on the cell, rather than an active transport process in which metabolic energy is required.

The uptake is independent of temperature over the range from 4 to 38° C, is as high under anaerobic as under aerobic conditions, and is not affected by the common inhibitors of respiratory and glycolytic pathways. The cerium of labeled cells is extensively leached by chelating agents and is rapidly replaced by apparent exchange with stable cerium. Yeast resting cells show a relatively constant cerium binding capacity (about 1×10^{-3} mg/mg dry weight, measured after two hours' contact time). The formation of insoluble cerium ribonucleate on the cell membrane is an interpretation of the rapid initial uptake that is consistent with the observations.

Rare-earth Fatty Liver Induced by Lanthanon Chelates*

G. C. Kyker and J. J. Rafter

The mechanism of fatty livers induced in rats by certain lanthanons is unknown. As previously described here, this fatty liver response is among the most intense and regular that has appeared in biochemical reports. In contrast to fatty livers due to other acutely toxic agents, recovery is equally regular without detectable residual injury. The characteristic cycle of disturbed metabolism and fat distribution is initiated immediately by an intravenous dose (2 mg/kg) of the metal; once initiated, it appears irreversible although preventable by several hormonal and nutritional factors.

* Presented at the American Society of Biological Chemists, Federation Meetings, Chicago, April, 1964.

1027850

This study compares three series of lanthanon complexes (Ce, Nd, Sm) of increasing stability ranging from citric to diethylenetriaminepentaacetic acid (DTPA); their respective stability also increases with the atomic number of the lanthanon. Liver enlargement, total liver lipids, hepatic localization, and excretion of the metal correlate with the graded stability of the chelates. Cerium complexed with citric acid, hydroxyethyliminodiacetic acid (HEIDA), or nitrilotriacetic acid (NTA) induced fatty infiltration as well as chloride; and its more stable chelates did not. For samarium, only the citrate acted like the chloride and the neodymium series gave intermediate results. These responses give a relative measure of the stability of the unknown binding site critical to originating this fatty liver cycle.

Iron and Aluminum Antagonism to Rare-earth Binding by Yeast*

G. T. Johnson† and G. C. Kyker

Yeast cells readily accumulate radiocerium from solutions containing tracer quantities of the element.[1] We have now studied the effect of other trivalent cations on cerium uptake by yeast. Divalent cations were included for comparison. The studies primarily involved magnesium, calcium, strontium, cobalt, manganese, chromium, aluminum, and iron. Measurements were made in solutions using washed cells without the addition of nutrient. Some of the measurements compared the effect of various cations at different concentrations (0.1, 0.01, and 0.001 M) on cerium uptake by *Saccharomyces cerevisiae*. Although relatively dilute solutions of the cations were used, they were present in preponderant excess by comparison with the concentration of tracer cerium. Both aluminum and iron were very effective in reducing cerium uptake. The other ions had only slight effect or no effect.

In other experiments, cells labeled with cerium were washed and placed in solutions of the various cations. Solutions of aluminum and iron each removed most of the cerium associated with the cells where-

* Abstract of paper presented at the meeting of the American Institute of Biological Sciences, Denver, August 1964.

† University of Arkansas, Fayetteville.

as solutions of the other ions again showed little or no effect. Comparable experiments on the uptake and removal of tracer iron with yeast disclosed that iron uptake is very slight under conditions where cerium uptake is quite high. The data suggest a degree of specificity among available yeast-cell trivalent-cation binding sites.

REFERENCE

1. Johnson, G. T. and Kyker, G. C. J Bacteriol 81:733, 1961.

Scanning of Bone Marrow in Animals*

G. C. Kyker and J. J. Rafter

Evaluation of the functional size and distribution of bone marrow has wide potential medical use. The consistent correlation between localization of colloids within marrow and its hematopoietic activity offers a practical approach.[1] The properties favoring localization of particles in marrow over other organs (liver, lung, spleen) are only obscurely defined. With similar chemical properties size is, however, an important factor.[2]

We have compared scans of six colloidal preparations of one rare-earth metal, cerium, differing in pH and presumably differing in colloidal size. These were made by titrating acid solutions of cerium citrate containing ^{141}Ce tracer to pH 3.5, 5.0, and 7.0. A cloud of hydrolytic product varied according to the extent of titration and much of it remained dispersed as a sol. Direct use of these supernatants comprised three of the six preparations and the other three were their corresponding centrifugates (2500 rpm, 5 minutes). In rabbits, each of these six preparations gave a clear delineation of the femoral, pelvic, spinal, and other marrow sites. The scan pattern was both quickly evident and persistent (from one hour to one week). The optimal time and sharpness of the scan varied slightly among preparations and correlated with the radioassay data.

After the last serial scan, the animals were killed and heart, kidney, lung, spleen, liver, marrow, and bone were radioassayed. These preparations at pH 3.5, 5.0, and 7.0 gave marrow/liver ratios of 1.8, *1.3*, 0.9, *1.7*, 1.8, and *1.0*, respectively. (The italicized values represent the centrifuged supernatants.) Similarly, the marrow/bone ratios were 96, *26*, 27, *24*, 21, and *41*. These marrow/liver ratios greatly exceed those for radiocolloidal gold[3] which is now finding practical use for the clinical scanning of marrow[1] although it largely localizes in liver (90% to 95%). A short-lived (few hours), low-energy (less than 150 kev), pure-gamma emitter would serve ideally for marrow scanning. Technetium-99m, which is so rapidly gaining medical usefulness,[4] has all these physical characteristics, but we have observed poor marrow localization with presently described sols of this isotope.[5] The ^{141}Ce used here has none of these desired physical characteristics, but the series of chemically similar rare-earth elements include numerous radioisotopes, some of which do meet these physical criteria.

* Abstract of paper presented at the Society of Nuclear Medicine, annual meeting of Southeastern Chapter, Atlanta, October 1964.

1027851

REFERENCES

1. Edwards, C. L., Andrews, G. A., Sitterson, B. W. and Kniseley, R. M. Clinical bone marrow scanning with radioisotopes. Blood 23, 741-756, 1964.
2. Gofman, J. W. Studies with colloids containing radioisotopes of yttrium, zirconium, columbium, and lanthanum. I. Chemical principles and methods involved in preparation of colloids of yttrium, zirconium, columbium, and lanthanum. J Lab Clin Med 34, 297-304, 1949.
3. Ganz, A. and Brucer, M. Blood clearance and tissue distribution studies in the dog following intravenous administration of radioactive colloidal gold (Aurocoloid). J Lab Clin Med 52, 20-26, 1958.
4. Harper, P. V., Beck, R., Charleston, D. and Lathrop, K. A. Optimization of a scanning method using Tc^{99m}. Nucleonics 22 (1), 50-54, 1964.
5. Richards, P. Brookhaven National Laboratory. Personal communication.

Nutritional Protection Against Fatty Liver Due to Cerium*

I. H. Miller, Jr.,† and G. C. Kyker

Earlier characterization of acute fatty liver in rats (3-fold, 2 days; recovery, 1 week) shows protection by chemical, hormonal, and nutritional factors. The nutritional factors were pursued further to evaluate essential and nonessential amino acids and total calories. Under standard conditions, young adult CFN female rats were kept on a complete liquid diet (2 Cal/ml; Winitz, *et al.*) which conveniently

* Abstract of paper prepared for Federation Meetings, Atlantic City, April 1965.

† Meharry Medical College, Nashville, Tenn.

serves changes in dietary composition and quantitative forced feeding. This special diet proved adequate for maintaining and for the typical fatty-liver response. The results correlate total lipid, protein, glycogen, and water in liver with dietary intake. Voluntary intake of the liquid diet decreased after intravenous cerium the same as with ordinary ration. With less glucose, the diet (1 Cal/ml) protected the rats against fatty liver. By intubation of the standard formula, one-third of normal intake gave protection and one-fifth gave partial protection. Total lipid and glycogen varied inversely, their sum being about 11% of fresh liver. Isonitrogenous modification containing no methionine and choline gave as good or better protection than the unmodified diet. These results and other nitrogenous modifications show that cerium involves the protein and carbohydrate metabolism of liver along with gross fatty infiltration.

In vivo Redistribution of Barium-137m

R. L. Hayes and J. E. Carlton

In the rat, the daughter ^{137m}Ba (2.6 min T) level in whole blood is three times that of the secular equilibrium value to be expected from the parent ^{137}Cs (30 yr T) content of the blood. The overage of ^{137m}Ba in blood is a fascinating phenomenon, potentially of clinical usefulness. An investigation has been under way to determine whether this redistribution phenomenon can be put to practical use in diagnosis.

Studies have been made mainly in the rat. Initially, it was found that the ratio of ^{137m}Ba to ^{137}Cs in the blood rises with time after administration of ^{137}Cs. The rise continues for as long as 24 days postadministration. This is caused by a more rapid loss of ^{137}Cs activity from the vascular compartment as compared to that from the extravascular compartments. On the other hand, the overage of ^{137m}Ba in the vascular compartment expressed as percentage of the extravascular ^{137}Cs remains constant with time. States of anesthesia, hypothermia, and hyperthermia produced very significant alterations in the percentage of "mobilization" of ^{137m}Ba. Recent work has shown that alteration of metabolic rate by radiation thyroidectomy and surgical thyroidectomy do not produce any significant change in the mobilization of ^{137m}Ba in the anesthetized or the conscious state. Administration of propylthiouracil also produced no effect. Since the

1027852

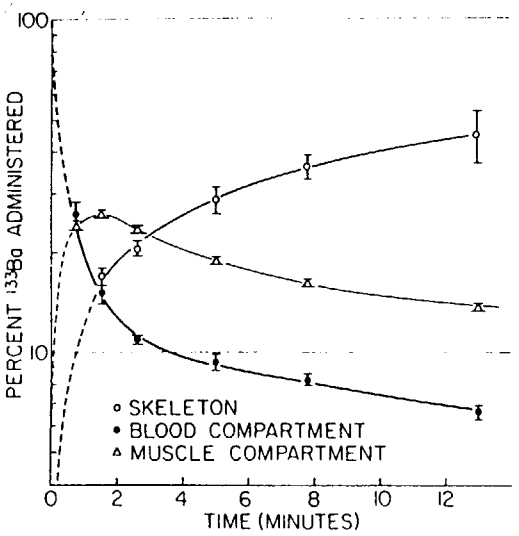

Fig. 24. Distribution of ^{133}Ba in the rat at short intervals after intravenous administration.

half-life of ^{137m}Ba is so short (2.6 minutes), a parallel investigation of the distribution of long-lived ^{133}Ba in rats at short intervals after intravenous administration was carried out to determine the distribution pattern of barium immediately after its entry into the vascular compartment. The average life of ^{137m}Ba is only 3.8 minutes and therefore the study was limited to measurements at short intervals over a period of only 13 minutes postadministration. After 13 minutes, only a few percent of any ^{137m}Ba initially entering the vascular compartment would remain. The long-lived ^{133}Ba was thus used as a semitracer of ^{137m}Ba.

The results of this study show that excretory mechanisms have little effect on the vascular level of barium over this period of time, as judged by the level of ^{133}Ba in the kidneys, bladder, and intestinal tract. The uptake of ^{133}Ba in the bone during this period is very rapid and it appears that bone uptake is one of the main factors controlling the level of excess ^{137m}Ba in the blood. The activity of other tissues parallels that of blood. Figure 24 shows the distribution of ^{133}Ba among various compartments as a function of time after intravenous administration.

Therapy With Radiation

The objective is to develop and assess refined methods of using radiation in therapy, as with total-body and local irradiation and radioiodine treatment.

1. Total-body irradiation is used in the treatment of cancer, polycythemia, and leukemias. Since it may be possible to exploit dose-rate dependent differences in responses of normal and malignant tissues, comparison of effects of different dose rates is undergoing clinical investigation.
2. Local irradiation is used under local anoxia to improve the relative sensitivity of tumors; this approach is based on the fact that sensitivity is related to oxygenation. To improve local radiation therapy—palliative and curative—responses to specific teletherapy treatment plans are measured in certain other clinical situations, e.g., mechanism of effect of local radiation to the spleen in chronic granulocytic leukemia.
3. Internal radioisotopes for cancer therapy have been investigated by long-range (14+ years) study and follow-up of patients with thyroid cancer given radioiodine. An improved treatment has evolved at the Division, using surgery and radioiodine with special emhasis on early radiodetection of regional lymph-node metastases.

Use of Thyrotropic Hormone (TSH) for Demonstration and Postoperative Treatment of Thyroid Cancer with Radioiodine

P. Pfannenstiel, B. W. Sitterson, and G. A. Andrews

The effectiveness of pretreatment with exogenous animal TSH on the radioiodine metabolism in malignant thyroid tissue was studied. Nineteen courses of 100 USP units of TSH were given to 11 patients (nine women and two men) with histologically proved thyroid cancer, most commonly a mixture of papillary and follicular lesions. The radioiodine study was done not earlier than three to four weeks after surgical ablation of all accessible thyroid tissue to allow for a biologic change in the function of the residual normal or malignant thyroid tissue to respond to increased endogenous TSH levels, secondary to deficiency of thyroid hormones. In addition to surgery, six of the patients had previous ^{131}I therapy. In the later patients, replacement therapy with desiccated thyroid was discontinued four weeks before the study. All patients had definite manifestations of myxedema, both clinically and on the basis of low levels of serum protein-bound iodine (PBI) as well as of low T_3 indexes.

To minimize statistical randomness, rather large test doses of ^{130}I were given, ranging from 0.5 to 5.0 millicuries depending on the time interval between the serial tests. The ^{130}I was more conveniently administered by mouth since comparable results could be obtained with either intravenous or oral administration. In each individual test series the size of the dose, route of administration, time intervals, instrument settings, etc., were kept exactly the same to exclude all possible technical variables.

For the thyrotropic stimulation we used a heterologous TSH preparation (beef thyrotropin*). Since others had suggested[1] that the TSH dose necessarily does not exceed 100 USP units, we adopted this regimen. Usually, 10 single intramuscular injections of TSH were given over a period of 72 hours, the last dose not later than five to six hours before the ^{130}I administration. Before repeating a TSH course, usually one USP unit of TSH in 0.2 cc normal saline was injected into the superficial skin layer on the forearm. Only one patient exhibited redness, induration, and edema of the subcutaneous tissues about six hours later, and no thyrotropic stimulation was given. Of six other patients, two developed minimal allergic reactions in form of slight skin rash and nausea. These reactions occurred after the seventh or eighth TSH injection of a repeated stimulative course and were well controlled by antihistaminics.

In five of the eleven patients an increase of the ^{130}I whole-body retention was observed after TSH, determined through total-body counts or urinary ^{130}I excretion. This did not appear to be completely accounted for by the enhanced ^{130}I accumulation in the remaining functioning normal or malignant thyroid tissue, as determined by uptake measurements and area scans over the lesions, or by output of slightly increased amounts of $PB^{130}I$. The PBI and T_3 indexes remained in the hypothyroid range after the thyrotropic stimulation. Linear scans gave no evidence that other iodide-concentrating tissues such as salivary and gastric glands respond to TSH. Two normals

*"Thytropar" from Armour Laboratories, Kankakee, Ill.

1027853

with $KClO_4$-blocked thyroid glands did not retain more ^{130}I after TSH.

One of the patients who had three TSH courses and always retained somewhat increased amounts of radioiodine in the circulation after TSH had a decreased 24-hour urine volume (from 1990 ml to 1290 ml), a decreased creatinine clearance (38.6 ml/min compared to 131 ml min), and a drop of the blood pressure (from 160/80 to 105 65) after TSH. Therefore, the possibility should be considered that the TSH preparation made from beef pituitary glands occasionally contains posterior pituitary hormones with an antidiuretic and vasopressive effect resulting in a decreased urinary ^{130}I excretion. Benua *et al.*[1] also observed that the whole-body retention of the

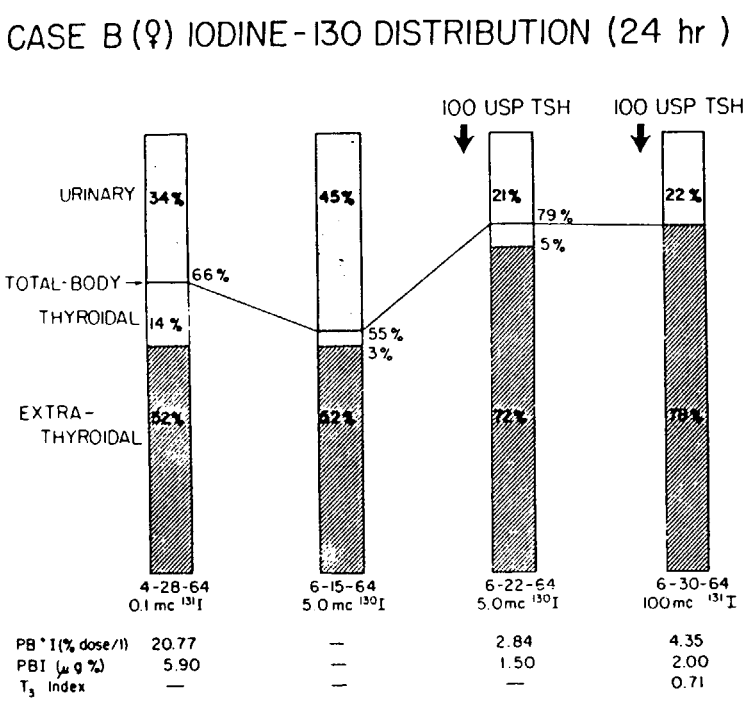

Fig. 25. Prethyrotropin and postthyrotropin results in a patient with well-differentiated adenocarcinoma of the thyroid gland.

1027854

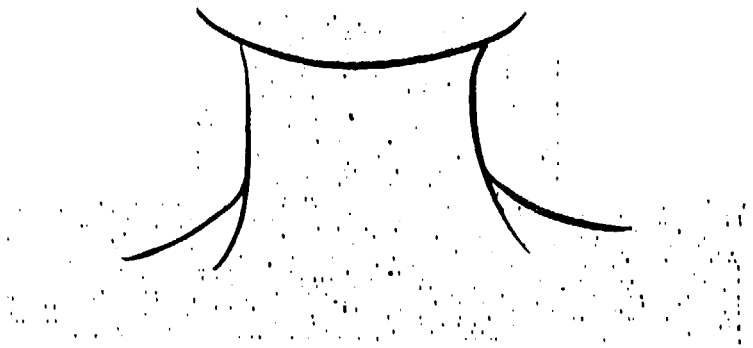

3wk after total thyroidectomy &
24 hr after 5.0 mc ^{130}I p.o.
6-15-64 Dot factor: 2

Fig. 26. Postoperative neck scan before TSH.

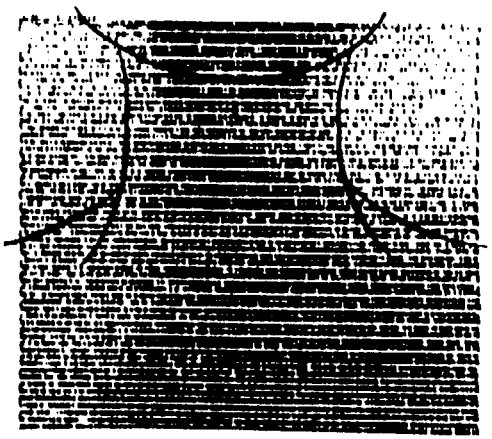

24 hr after 5.0 mc ^{130}I p.o.
6-23-64 Dot factor: 2
Thyrotropic Stimulation: 100 USP TSH

Fig. 27. Postoperative neck scan of the same patient as in Fig. 26 after TSH under the same physical conditions.

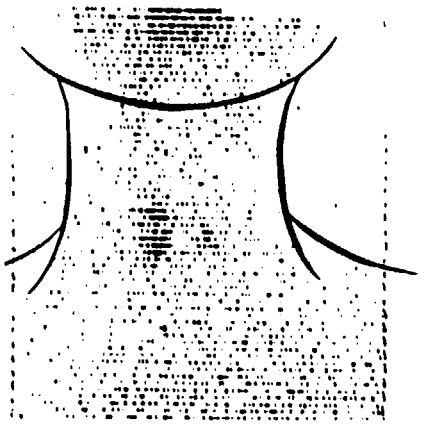

24 hr after 5.0 mc ^{130}I p.o.
6-23-64 Dot factor: 4
Thyrotropic Stimulation: 100 USP TSH

Fig. 28. Postoperative neck scan of the patient shown in Figs. 25 and 26 with changed recording parameters.

radioiodine was in their patients on the average 25% higher after TSH.

Even though the observation of an increased radioiodine retention in these patients remains puzzling, three of the patients also showed definite areas of ^{130}I concentration in the neck while the pre-TSH scans were "blank." These areas probably represented malignant residuals of thyroid tissue in which ^{130}I uptake was induced by the administration of the exogenous TSH. All three patients had only partially treated thyroid cancer without previous ^{131}I therapy.

Figure 25 summarizes the prethyrotropin and postthyrotropin results in one illustrative patient with well-differentiated adenocarcinoma of the thyroid gland. Three weeks after total thyroidectomy the patient retained 55% of 5.0-millicurie ^{130}I test dose at 24 hours with 3% in the neck area. After thyrotropic stimulation, the whole-body ^{130}I retention increased to 79% with 5% in the area of the removed thyroid gland. Figures 26 and 27 show the postoperative neck scans in this patient before and after TSH, obtained under the same physical conditions. Note the significant increase in the body back-

1027855

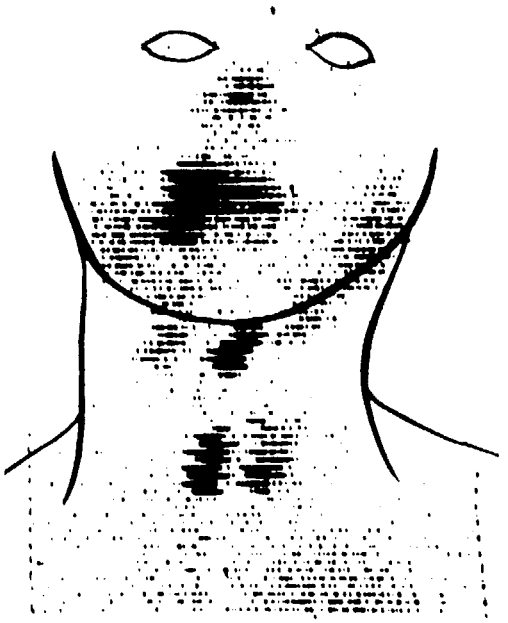

8 days after 100 mc ^{131}I p.o.
6-30-64 Dot factor: 4
Thyrotropic Stimulation: 100 USP TSH

Fig. 29. Postoperative neck scan of the same patient shown in Figs. 25, 26, and 27 after a therapeutic dose of 100 millicuries of ^{131}I after a second course of TSH.

ground in the scan after TSH. After changing the recording parameters, definite areas of residual functioning thyroid tissue could be demonstrated (Fig. 28). Because of the good response to TSH, the patient was given a therapeutic dose of 100 millicuries of ^{131}I after a second course of thyrotropic stimulation with similar results as obtained with the ^{130}I test dose (Figs. 25 and 29).

Even though we were unable to demonstrate the same degree of success in enhancing radioiodine uptake by malignant thyroid tissue

as others reported,[1-4] this preliminary investigation suggests that TSH pretreatment makes ^{131}I therapy more effective in some patients with thyroid carcinoma. Before definite conclusions can be drawn from these experiments, a large and representative series of patients with endocrinologically active thyroid cancer needs to be studied.

REFERENCES

1. Benua, R. S., Sonenberg, M., Leeper, R. D. and Rawson, R. W. An 18 year study of the use of beef thyrotropin to increase ^{131}I uptake in metastatic thyroid cancer. J Nucl Med 5, 796-801, 1964.
2. Sheline, G. E. and Miller, E. R. Studies with radioiodine. VI. Evaluation of radioiodine treatment of carcinoma of the thyroid based on the experience at the University of California from 1938-1954. Radiology 69, 527-545, 1957.
3. Catz, B., Petit, D. W. and Starr, P. The diagnostic and therapeutic value of thyrotropic hormone and heavy dosage scintigrams for the demonstration of thyroid cancer metastases. Amer J Med Sci 237, 158-164, 1959.
4. Rose, R. G. and Kelsey, M. P. Radioactive iodine in the diagnosis and treatment of thyroid cancer. Cancer 16, 896-913, 1963.

1027856

Radioisotopes in Diagnosis

The objective is to apply radioisotopic test compounds in (1) the detection of tumors, (2) the measurement of functional disorders, and (3) the diagnosis of metabolic defects. The agents are radioactive compounds, either already available or newly synthesized and tested in animals; the subjects are patients in the Division's research hospital; and the procedures involved emphasize whole-body counting and scanning. Special techniques for radioassay and autoradiography on biopsy and autopsy material are applied to these problems.

Bone Scanning with Gallium-68

R. L. Hayes and J. E. Carlton

Germanium-68 ($T_{\frac{1}{2}}$ = 280 d) decays by positron emission to ^{68}Ga ($T_{\frac{1}{2}}$ = 68 minutes). Gallium-68 can be milked from a ^{68}Ge cow with the use of dilute EDTA. This chelate solution of ^{68}Ga has been used by a number of investigators for brain scanning. An obvious advantage of ^{68}Ga is its short half-life and the fact that it is readily separated from a long-lived parent. Studies have been carried out in the rat with the ^{68}Ga chelate solution and with separated ^{68}Ga plus various levels of carrier gallium in the citrate form to determine whether ^{68}Ga can be used to scan for bone lesions. Gallium-68 was separated from EDTA by a solvent extraction technique. As expected, the gallium-EDTA chelate preparation was more or less uniformly distributed throughout the animal body. As the level of carrier gallium in the gallium citrate preparations was increased, uptake in the bone became more pronounced and apparently adequate scans of the skeleton of the rat can be made at levels of 1 to 10 mg/kg of gallium carrier at one to two hours after intravenous administration. (See Fig. 30.)

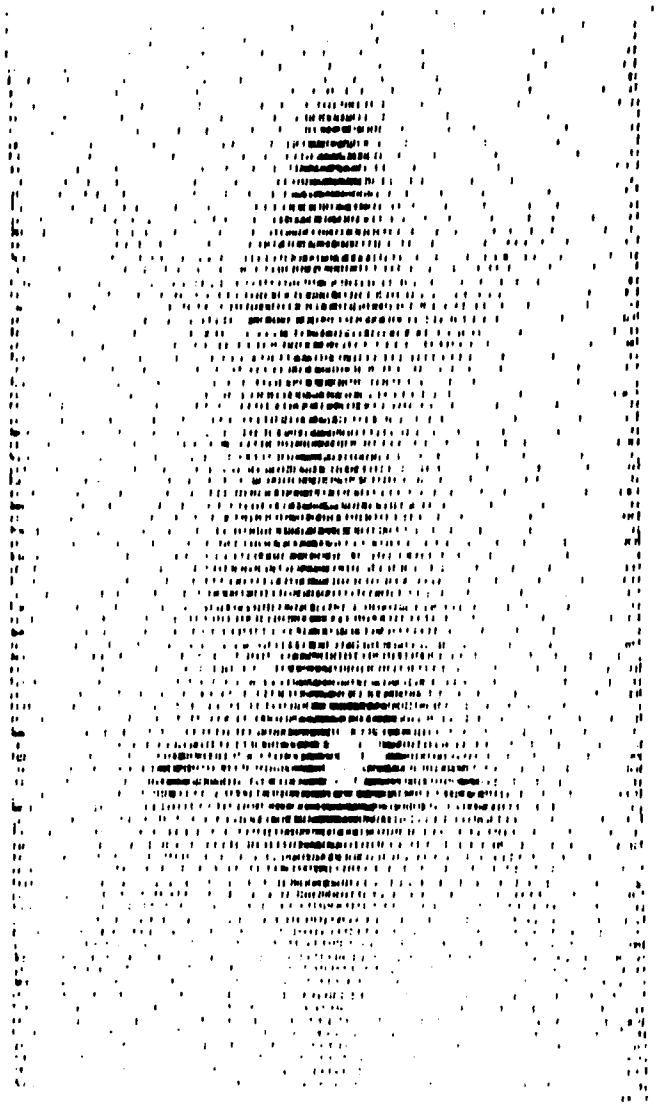

Fig. 30. Bone scan of rat 1½ hours after intravenous ^{68}Ga citrate (1 mg/kg).

1027857

Clinical Bone-marrow Scanning

R. M. Kniseley, G. A. Andrews, and R. Tanida

The distribution of functioning bone marrow has been studied further by means of scanning during the past year and a recent review was made of scans on 27 patients examined since January 1964. The isotope used is colloidal ^{198}Au given intravenously; this shows the distribution of reticuloendothelial tissue which, in the marrow, correlates extremely well with the hematopoietic tissue. The scanning procedure has proved especially valuable in showing the various degrees of myelofibrosis. The first patient with an active, severe hemolytic anemia was studied recently. He showed, surprisingly, only a moderate increase in size of the marrow organ. Much more severe degrees of extension have been seen in a patient who had an obscure anemia with hyperplastic marrow and in a patient who had an unusual myeloproliferative disorder subsequent to polycythemia vera.

We have compared linear scans made with ^{198}Au and ^{59}Fe and find that they tend to be very similar in marrow pattern, but the relative size of the liver-spleen peak may be quite different with the two isotopes. The linear scanner, although not showing details of the marrow pattern, has the advantage of requiring only small doses of the radioisotope. We have followed with interest the work of Anger and Van Dyke[1,2] who used ^{52}Fe with a special gamma-ray camera. Their marrow area scans are similar in quality to those we obtain with colloidal ^{198}Au, but they are able to use small doses of the radioisotope. Their findings in various disease states seem to fit a reasonably orderly pattern of predictable expansion and contraction of the marrow organ in relation to hematopoietic need, while we are more impressed with the unexpected and unexplained findings in some patients. These unexpected findings include expansion of the marrow organ where none was predicted, lack of expansion in situations where it would be expected, and unexplained asymmetry, especially of expansion of marrow into the lower extremities. (See Figs. 31 and 32.)

REFERENCES

1. Anger, H. O. and Van Dyke, D. C. Human bone marrow distribution shown *in vivo* by iron-52 and the positron scintillation camera. Science 144, 1587-1589, 1964.
2. Van Dyke, D. C., Anger, H. O. and Pollycove, M. The effect of erythropoietic stimulation on marrow distribution in man, rabbit and rat as shown by Fe^{59} and Fe^{52}. Blood 24, 356-371, 1964.

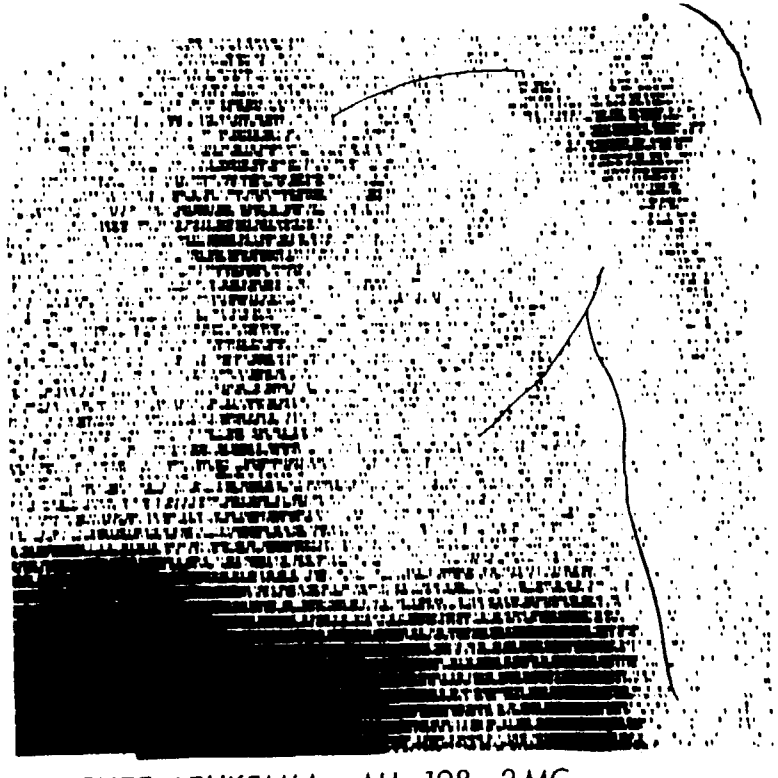

Fig. 31. Marrow scans on a patient with acute leukemia given colloidal ^{198}Au. Expansion of the marrow organ is pronounced, with increased uptake both in usual sites and extension into extremities. This pattern is not consistently found in all cases of acute leukemia. 31a Anterior view of chest.

1027858

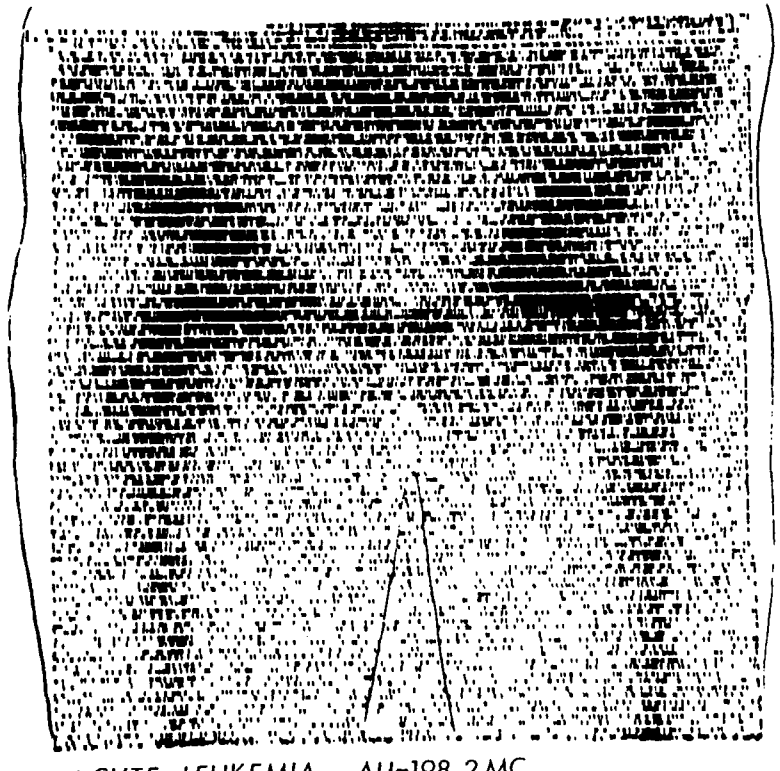

31b Anterior pelvis

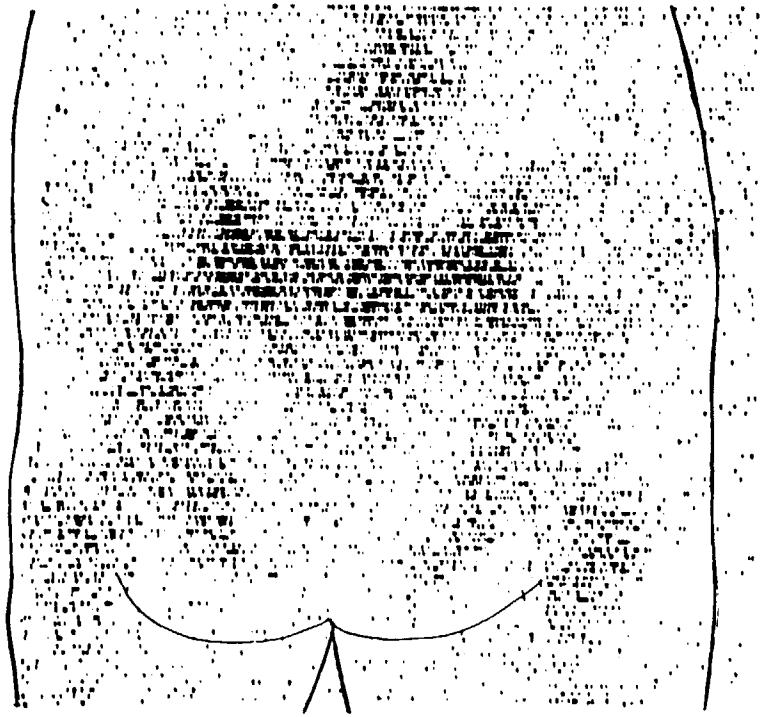

31c Posterior pelvis

1027859

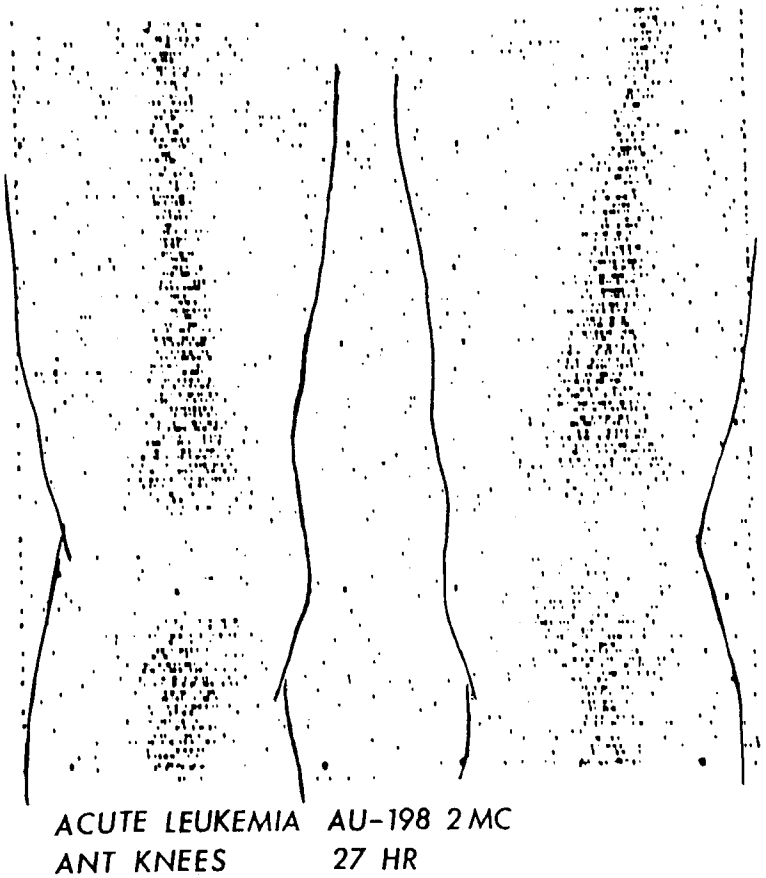

31d Lower extremities

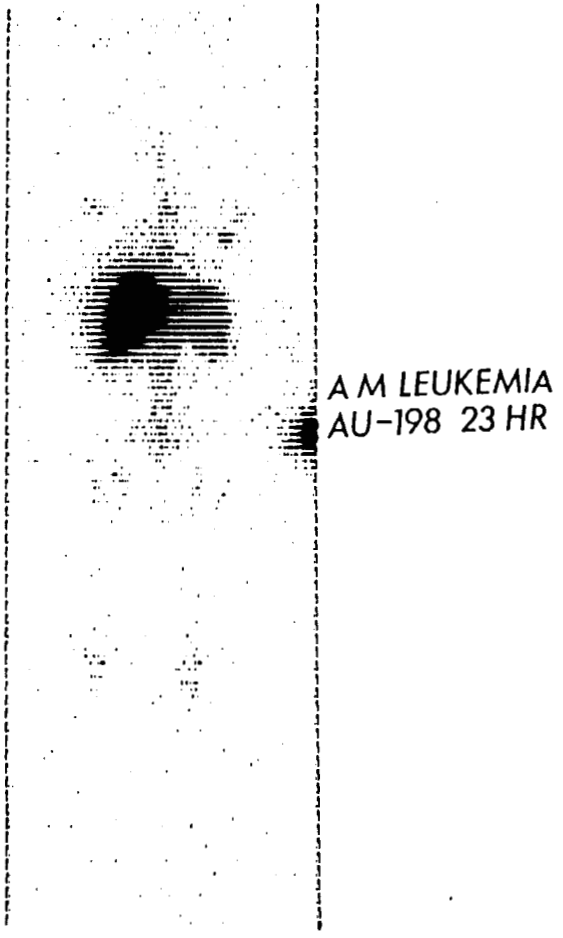

Fig. 32. Examples of whole-body scans with a broad focus collimator showing distribution of colloidal ^{198}Au given intravenously. The large concentrations of activity in the midtrunk are liver and spleen. Fig. 32a is acute myeloblastic leukemia in an adult showing some extension of marrow into regions of knees and with decrease in pelvic marrow. Note activity on patient's left side, at the site of extravasation at injection site in the arm. There is also local uptake in the left axillary lymph node, lymphatic drainage from extravasated gold in injection site.

1027860

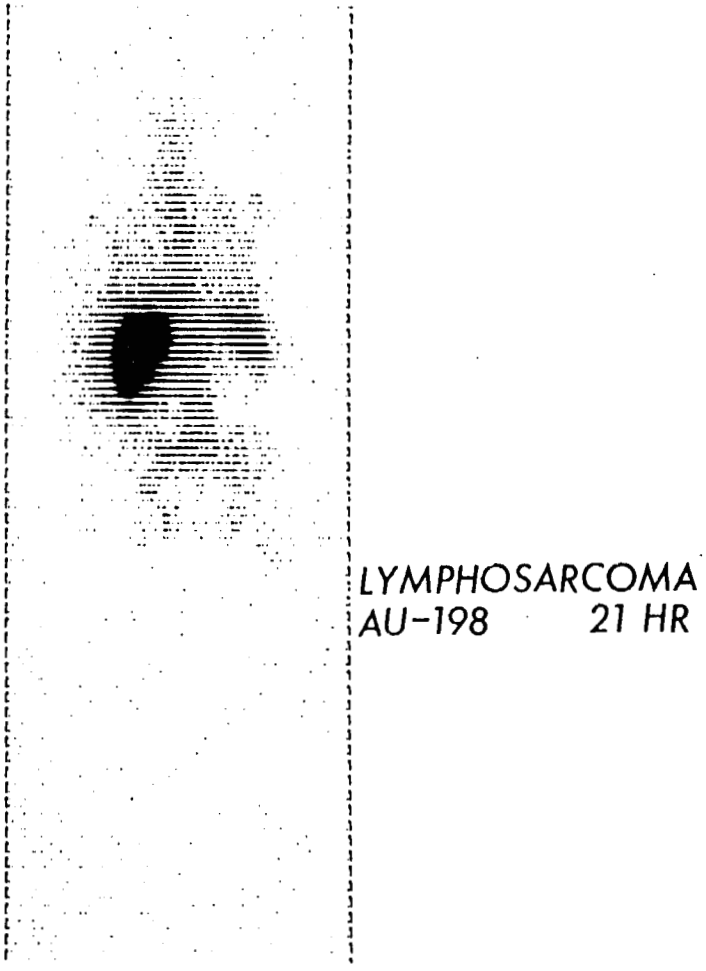

32b Patient with lymphosarcoma showing usual marrow distribution in an adult.

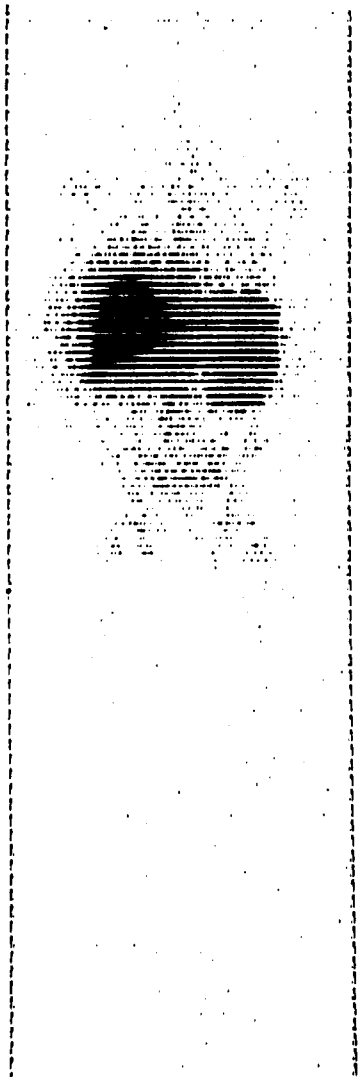

32c Patient with chronic lymphocytic leukemia showing slightly decreased marrow uptake in pelvis. Note massive splenic enlargement.

1027861

Stability and Response Characteristics of the Red Blood Cell System: A Computer Study

A. L. Kretchmar

A model of the red blood cell system is derived utilizing the concept of *maturation probability* Φ (x). This parameter is defined as the likelihood that a randomly chosen cell, of age x, from a specified precursor-cell class, will develop the physiologic and biochemical characteristics of the next more mature cell class in unit time. Stem-cell maturation is considered to take place in fixed hematopoietic sites and cell death to occur primarily in the oldest cells of the circulating elements. The model is programmed for an analog computer in such a way that various assumptions about cell maturation and death can be simulated and the consequences can be observed in the behavior of the analog system. The model fulfills the basic requirements of Lajtha *et al.*[1] for models of a stem-cell system; it can (1) start from a beginning and reach a steady state equilibrium; (2) respond to changes in circulating red blood cell population in a stable fashion; (3) recover from acute damage to stem cells; and (4) maintain function under conditions of limited continuous damage.

Figure 33 is one example of the output from this model. The curves show the size of the population of stem cells, S, and of the dividing erythroid cells, D, in the marrow for two different assumed conditions of competition between these populations. The system oscillates and has a pronounced overshoot above the population size that obtains at equilibrium. This kind of analysis may be helpful in understanding the recovery of hemopoiesis after irradiation in animals. Oscillations in the size of the population of cells in recovering irradiated animals have been experimentally observed.

REFERENCE

1. Lajtha, L. G., Oliver, R. and Gurney, C. W. Kinetic model of a bone-marrow stem-cell population. Brit J Haemat 8:442-460, 1962.

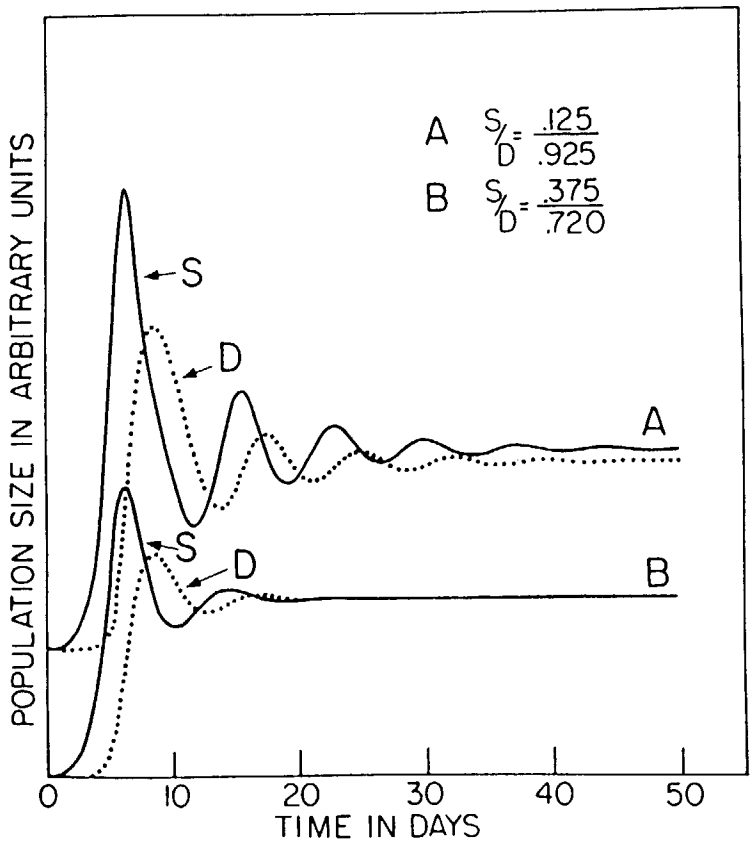

Fig. 33. The ratio S/D is a measure of relative competition between S and D cells. In curves A the S and D cells compete equally; in curves B competition between cells of the same population—the S cells —is greater than with cells of the other population—D cells.

1027862

Red Cell Survival: On the Analysis of DF^{32}P Data

P.-E. E. Bergner and J. D. Lawson

In the literature on red cell survival data, one can find statements about the significance of the initial slope of survival curves. The earlier theoretical analysis has proved these statements for systems in steady state. Our work, however, shows that the initial slope can be given a quite general significance also under nonsteady state conditions, provided the proper concepts are chosen.

Consequently, short-term studies can in principle be used for a theoretically correct estimate of the total destruction rate (number of circulating red cells destroyed per unit of time). Deficiencies in the labeling technique are, however, likely to introduce certain difficulties, and we are at present performing theoretical studies of different systems to see what experimental precision is necessary to give sufficiently accurate estimates of the destruction rate. Also, we hope that these studies will reveal other survival-curve parameters of biomedical significance.

Diagnostic Uses for Iodine-130

P. Pfannenstiel and G. A. Andrews

The use of ^{132}I in repeated tracer studies of the effect of various measures on radioiodine uptake in malignant thyroid tissue met with serious problems because of the very short half-life (2.3 hours) and difficulties in counting the strong gamma emission (~2 Mev) *in vivo*.[1] Iodine-130 with a physical half-life of 12.6 hours and less potent gamma radiation seemed to be more promising. Cyclotron-produced ^{130}I (^{130}Te [d, 2 n] ^{130}I) was one of the first radioisotopes of iodine used for studies of thyroid function and detection of metastatic thyroid lesions with a Geiger-Muller counter.[2,3] After 1946, ^{130}I was replaced completely by ^{131}I. Reactor-produced ^{130}I (^{129}I [n, α] ^{130}I), available from Oak Ridge National Laboratory, has not found clinical use since. We do not know of reports in which ^{130}I was applied to diagnostic techniques with modern equipment.

From the five different gamma energies of ^{130}I in the range from 0.409 to 1.15 Mev, we selected the region from 600-800 kev for

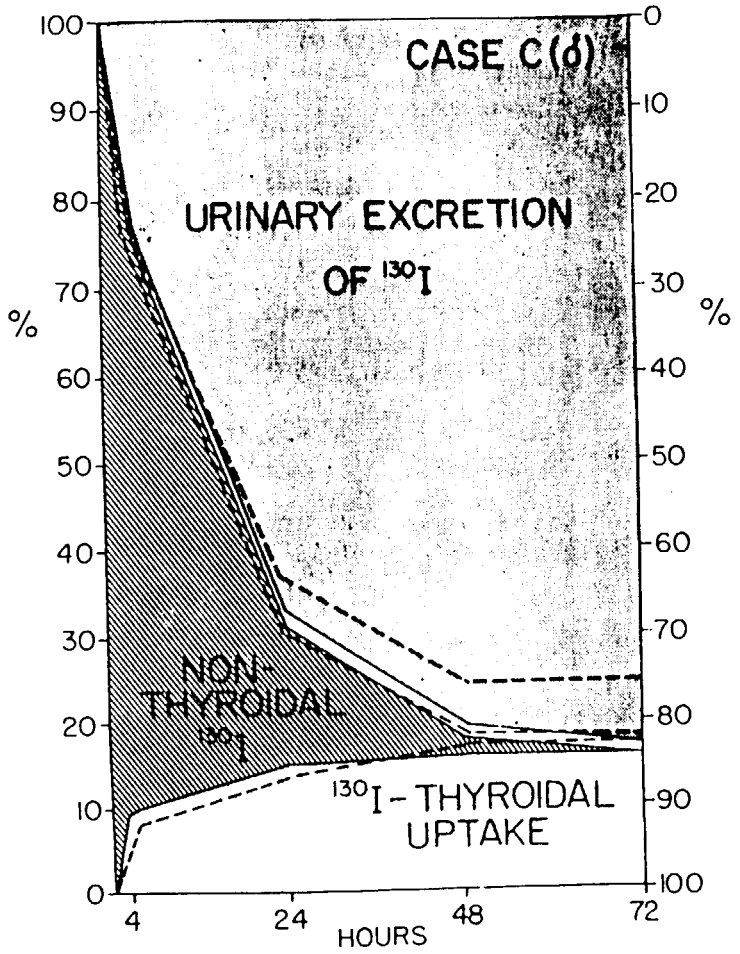

Fig. 34. Iodine-130 balance study.

counting. The existing standard arrangement for thyroidal ^{131}I uptake measurements with a 2-inch NaI crystal was used. No major instrumental modifications were undertaken except for increasing the thickness of the B-filter from ½-inch thickness to 2-inch thickness to screen out about 98% of the high-energy gamma radiation of ^{130}I. Figure 34 shows the results of an ^{130}I balance study in terms of per-

1027863

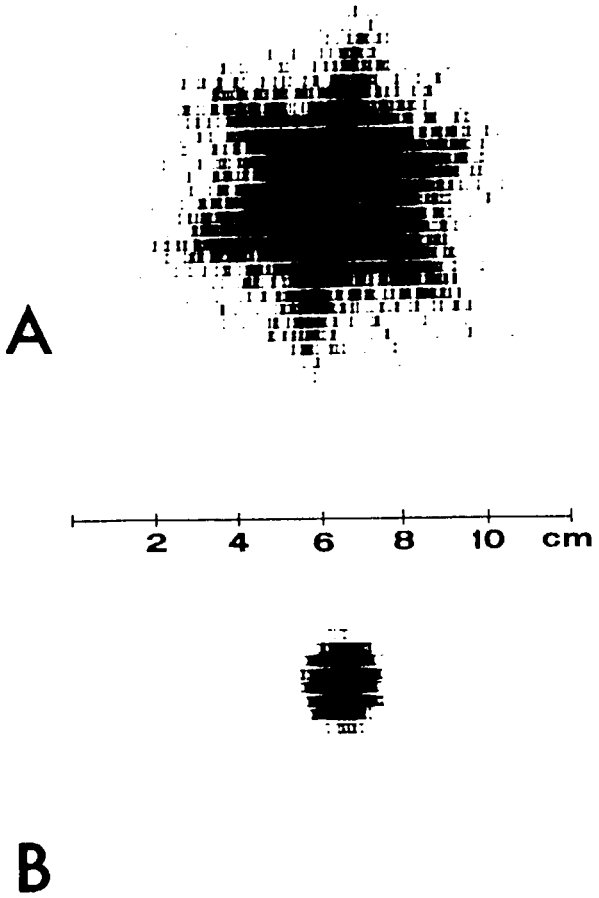

Fig. 35. Area scan of ^{130}I point source (ϕ 1.0 cm) in Oak Ridge Institute of Nuclear Studies thyroid phantom, placed 2.0 in. under collimator of Oak Ridge National Laboratory research scanner. Recording speed 0.3 in./sec (2A: dot factor 4; 2B: dot factor 32).

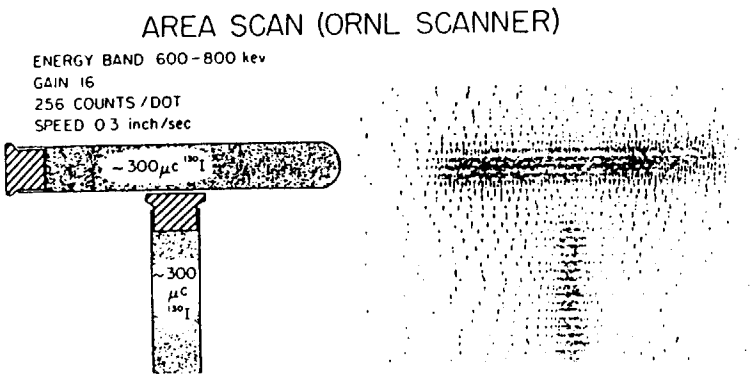

Fig. 36. Demonstration of decreased radioactivity in the area of a rubber stopper.

centage of the given dose at different time intervals (4, 24, 48, and 72 hours) after oral administration of 114 microcuries in one of five normals studied. The size of the nonthyroidal radioiodine pool represents the difference between whole-body ^{130}I retention (as measured with the ORINS linear scanner) and thyroidal radioiodine uptake. The dotted lines indicate the results after 114 microcuries of ^{131}I were given under the same condition. Thus ^{130}I behaves physiologically in exactly the same way as ^{131}I.

Area scans were performed with the Oak Ridge National Laboratory research scanner with a 37-hole gold collimator in a tungsten side shield. Even with this superior shielding a starfish-like distortion in the scan image of an ^{130}I point source was obtained with high sensitivity recordings (Fig. 35) because of leakage of the high-energy gamma radiation through the hexagonal arrangement of the hexagonal holes in the collimator.[4] This distortion was reduced considerably by changing the dot factor (Fig. 35). As a result of good resolution, decreased radioactivity in the area of the rubber stopper is recorded in the simple experiment demonstrated in Fig. 36.

Figure 37 shows an example of an ^{130}I scan of a thyroid gland with a definite area (anaplastic carcinoma) in the right upper lobe that failed to concentrate radioiodine. Figure 38 shows, in comparison, the neck scan on the same patient obtained after ^{131}I two days earlier. The "cold" nodule appears somewhat sharper because the gamma rays of ^{131}I are more efficiently collimated, and the ^{131}I gamma rays emerging from tissue posterior to the nodule are more readily ab-

1027864

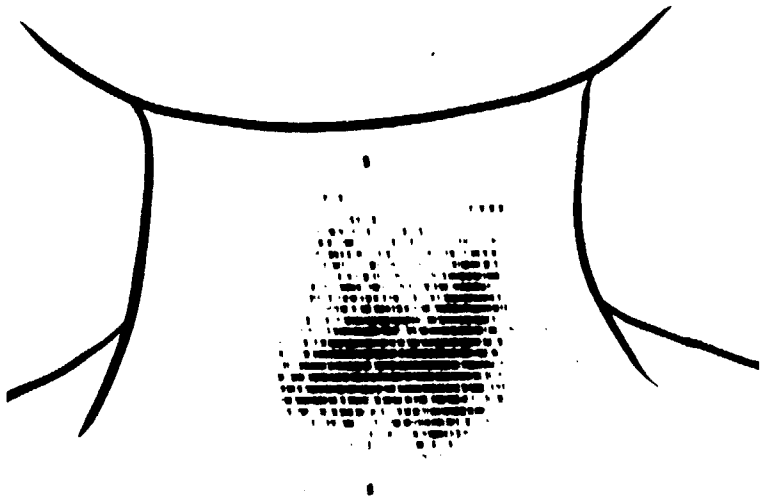

Fig. 37. Iodine-130 scan.

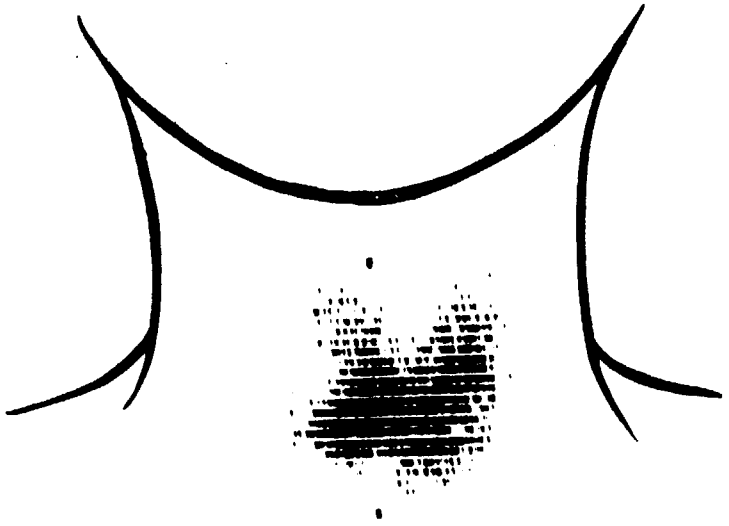

Fig. 38. Iodine-131 scan of the same patient as in Fig. 37.

sorbed than are the more energetic gamma rays of ^{130}I. However, to study radioiodine uptake in malignant thyroid lesions the harder gamma rays of ^{130}I will render the detection of tracer amounts of radioiodine even easier.

Since the lower-energy photons of ^{131}I are screened out by our pulse-height selection of 600-800 kev (except for the 640 kev and 720 kev minor components), it is possible to use ^{131}I and ^{130}I simultaneously. Evaluation of the influence of TSH on poorly functioning thyroid glands or of triiodothyronine on so-called "hot" nodules in

1027865

hyperthyroidism may be done without waiting for the ^{131}I initially present to decay, when ^{130}I is used after an ^{131}I base-line study.

In a series of forty ^{130}I studies in 18 different patients with doses ranging from 0.5 to 5.0 millicuries orally or intravenously, the 12.6-hour half-life of ^{130}I proved to be adequate for most diagnostic procedures. It allows serial tracer studies at fairly short intervals since the residual radioactivity in the patient decreases rather rapidly. Possible variables arising from long intervals between repeated ^{131}I studies will be reduced. Iodine-130 is in our experience a useful isotope to evaluate responses of normal, hyperthyroid, and thyroid carcinoma patients to various drugs and manipulations. In general, ^{130}I thyroidal uptake measurements and ^{130}I scans are comparable to those obtained with ^{131}I.

REFERENCES

1. Pascasio, F., Sitterson, B. W. and Andrews, G. A. Iodine-132 studies in thyroid carcinoma. USAEC Report ORINS-34, p. 32.
2. Livingood, J. J. and Seaborg, G. T. Radioactive isotopes of iodine. Phys Rev 54, 775-782, 1938.
3. Frantz, V. K., Ball, R. P., Keston, A. S. and Palmer, W. W. Thyroid carcinoma with metastases. Studied with radioactive iodine. Ann Surg 119, 666-689, 1944.
4. Harris, C. C., Bell, P. R., Francis, J. E., Jr., Satterfield, M. M., Jordan, J. C. and Murray, J. P., Jr. Collimators for radioisotope scanning. *In* Progress in Medical Radioisotope Scanning. Edited by R. M. Kniseley *et al.* USAEC Report TID-7673, 25-65, 1963.

Absorption, Whole-body, and Organ Retention of Biologically Important Radioisotopic Materials

The objective is to determine absorption and retention rates of tracer metals, dietary essentials, radioisotopes, and environmental and occupational contaminants in normal, diseased, and particularly cancerous man, by means of an especially designed ultrasensitive whole-body counting, spectral analyzer, and electronic systems for determining organic localization.

Whole-body Counting Research Program

W. D. Gibbs, C. C. Lushbaugh, and H. D. Hodges

Early in September the low-level whole-body counting facility was sufficiently complete to allow the instrumentation to be tested and the NaI crystals to be installed. After some initial delay because one of the crystals was not meeting specifications for resolution, eight crystals were finally installed and their positions were modified slightly to obtain a flat field of response. Background measurements were obtained at once to establish the level of inadvertent contamination by fallout materials, and daily measurements were begun to determine fluctuations due to changes in environment or systems stability. The air-filtration equipment was found a most necessary adjunct to the system of physical exclusion of sources of contamination. The air filters themselves proved to be an excellent means of determining the efficiency of the filtration and also the concentration of environmental air contaminants.

After stabilization of the assay techniques, data recording and readout of measurements were begun in normal man to determine the efficiency of the apparatus for the measurement of ^{137}Cs and ^{40}K and to establish the optimum compromise between long counting times for statistical purposes and patient comfort. In this study, 175 normal persons were assayed and their natural gamma-ray spectrum was established as a reference pool for future control of experimental programs. Use of this material will also be made in the projected health

10278bb

physics surveillance of the personnel of the Oak Ridge Institute of Nuclear Studies.

Routine techniques were established to minimize variation due to uncontrollable variables. The human subjects showered, and shampooed their hair, and dressed in hospital scrub suits. Only they and the bioassayist were allowed admission to the counting facility itself. Histories were taken of each subject's dietary habits, diseases, and isotope exposure. Installation of lights and an FM auditory system were successful in allaying most apprehensions and preventing claustrophobia. Study of the spectra under these conditions showed that 20-minute counting times of normal, uncontaminated man gave reproducible total-body counts and sufficient activity per channel to easily identify and quantitate radioactive cesium and potassium. An automatic subtraction of background based on a 200-minute background taken previously, or during the preceding night, was used to help visualize the spectra on the X-Y plotter readouts.

Data handling consisted of storing the pulse-height analyses in 200 channels in an analyzer carefully standardized by simultaneous measurements of ^{137}Cs and ^{60}Co standards. The sorted counts were then punched on paper tape, printed as an X-Y plot, typed digitally, and stored. Computer processing of the assays at this stage is under development.

The counts of the 175 normal men and women indicate that, although the spectrum of normal men and women are similar, some differences are readily detectable between drinkers and nondrinkers of milk; slender and obese persons in relation to their body weight and composition of lean versus total weight; and between women and men matched carefully for height, weight, age, and diet. Some of these changes are shown in Figs. 39-42.

Measurements have begun at the feasibility level with intentionally contaminated volunteers and patients, to establish for this facility typical spectra of the commonly used diagnostic radioisotopes. These assays are being used to establish criteria for body-burden estimates of radioisotope residues in man on a nanocurie per kilogram basis. The limits of the detection of various energies of radioactive spectra are being determined as well as the length of effective retention times relative to counter sensitivity.

Only one clinical study has been completed so far. The study was an emergency in the sense that previous determinations of thyroid activity in this child were suspect because of difficulties in establishing with confidence the child's apparent complete lack of thyroid function. This study (see p. 103) established with ease that the

child in question was a true cretin, for he retained less than 1% of the ^{131}I dose after three days. Further clinical trials are being delayed for completion of the standardization studies just described; however, many studies are projected. One such study not previously feasible is the spectral analysis of radioactivity of patients with different kinds of untreated cancers to determine whether or not previous radioisotope contamination from dietary or other habits and situations may have been a contributing factor in their disease. Another study will involve the long-term follow-up of patients exposed to radioisotopes diagnostically and therapeutically to determine whether unsuspected amounts of unknown contaminants of long half-lives might have accumulated in such persons and play a role in their continuing ill health.

The studies of normal persons in relation to their dietary habits, environmental habitats, pregnancy, age, and sex will be expanded. The facility will also be used to monitor the neutron-activation exposure dosages in the experimental radiation-therapy program. It will be used in metabolic studies of iron and vitamin utilizations in leukemia and allied blood dyscrasias.

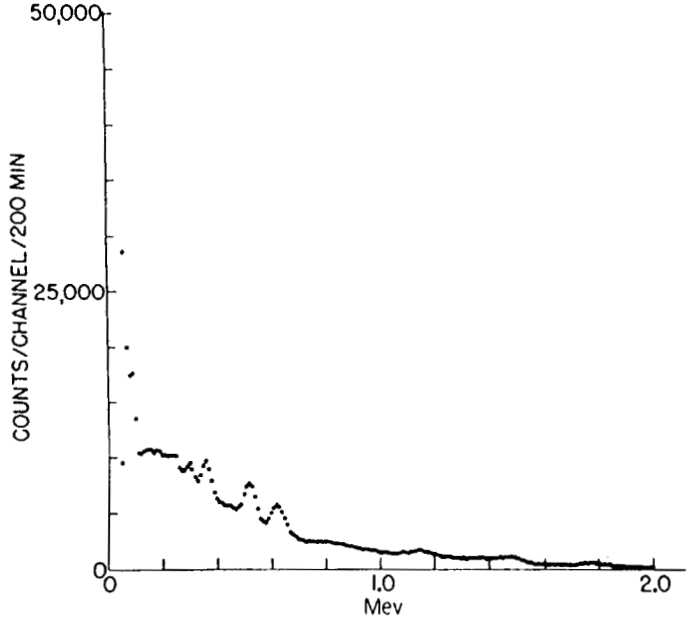

Fig. 39. Spectrum of cave background (200-min assay, 0-2.0 Mev).

1027867

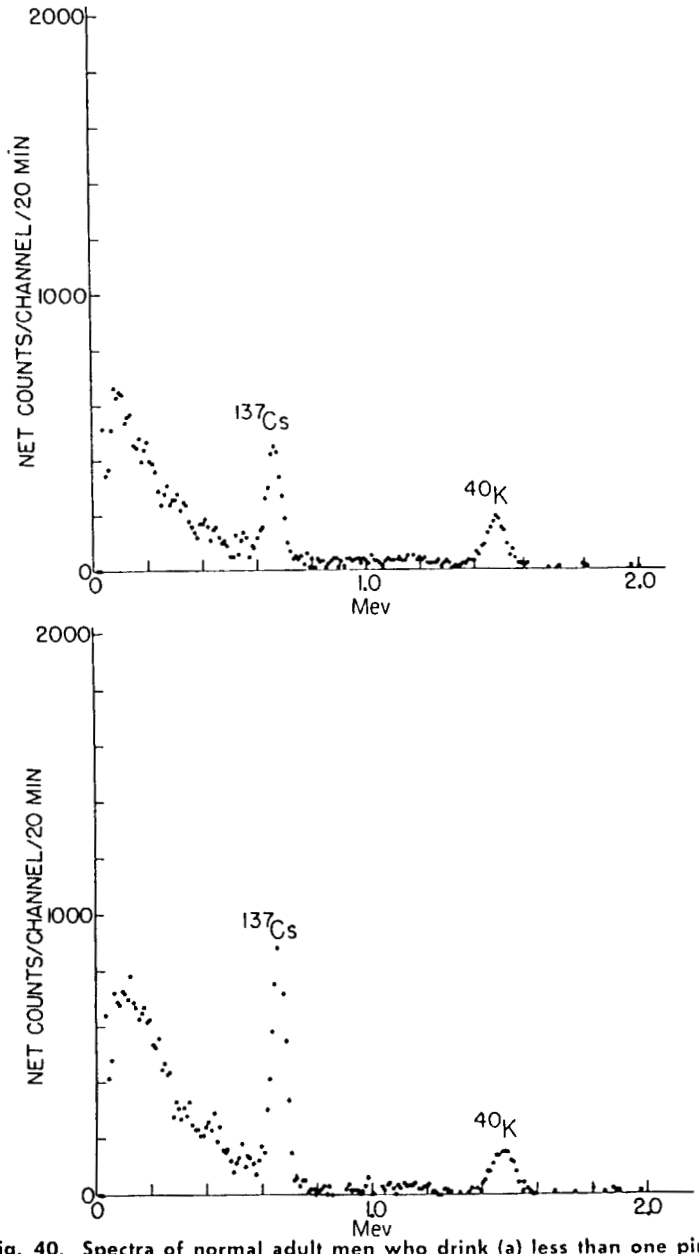

Fig. 40. Spectra of normal adult men who drink (a) less than one pint of milk a day; (b) more than one quart of milk a day.

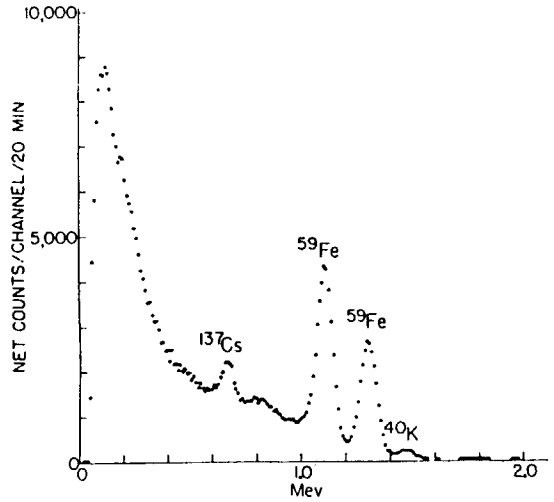

Fig. 41. Spectrum of normal man containing ^{59}Fe in his hemoglobin and iron stores.

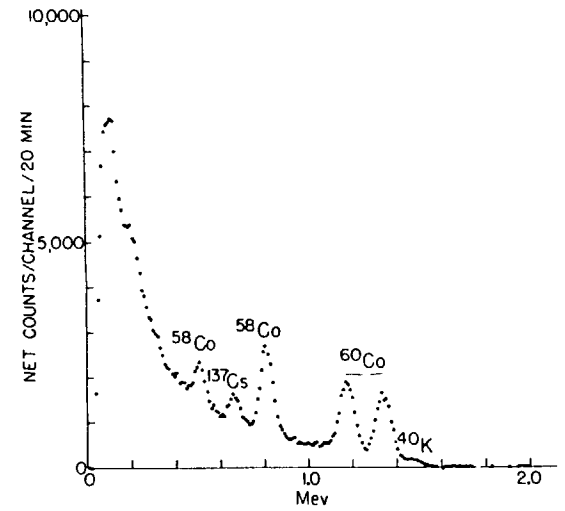

Fig. 42. Spectrum of normal man six months post-Schilling tests using ^{60}Co and ^{58}Co labeled vitamin B_{12}.

1027868

Evaluation of Thyroid Function in Infants with the ORINS Low-level Whole-body Counter

P. Pfannenstiel and W. D. Gibbs

Radioiodine damage to the fetal thyroid gland may occur when ^{131}I is inadvertently given in large therapeutic doses during pregnancy. Four such instances of iatrogenic congenital hypothyroidism are reported in the literature.[1,2,3] We treated, in the tenth week of an unsuspected pregnancy, a young woman having residual thyroid carcinoma, with 99 millicuries of ^{131}I. Subsequently, we have observed her infant for the past two years. The male child was born at term and appeared normal to the patient's personal physician. Unfortunately, it was not until the age of about eight months that clinical appearance, a serum PBI of 2.8 micrograms per 100 milliliters (normal range at this age is 6.3±1.0 micrograms per 100 milliliters) and a roentgenologic bone age of less than three months suggested thyroid insufficiency. For his hypothyroidism, the child has been treated since with desiccated thyroid. The infant seems to be improving for length, weight, and bone age are almost normal. However, his mental development is retarded.

To prove the tentative diagnosis of congenital hypothyroidism, we discontinued the thyroid replacement therapy for one week. Twenty-four hours after the administration of 10 USP units of thyrotropic hormone (TSH), we administered 0.001 millicurie of ^{131}I intramuscularly and measured the ^{131}I total-body retention in the new ORINS low-level whole-body counter. The fast ^{131}I disappearance shown in Fig. 43 is consistent with a total absence of functioning thyroid tissue in this patient.[4] Only about 1% of the administered dose was retained at three days. A causal relationship of the child's athyroidism and the maternal ^{131}I therapy seems a strong possibility.

The indirect ^{131}I thyroid uptake measurement in the low-level whole-body counter has proved very efficacious after tracer doses as low as one microcurie ^{131}I; direct uptake techniques with such low doses in infants are extremely difficult. Low sensitivity of the detectors and difficulty in reproducing the positions of the gland and the crystal, owing to movements of the child, make counting unreliable. Thyroid metabolism can be studied accurately by whole-body counting in newborn infants, especially those suspected to have congenital hypo- or athyroidism. Since early detection and early adequate treatment are important factors for the mental prognosis in cretinism, the application of the low-level whole-body counter in ^{131}I-retention stud-

ies appears to be valuable in diagnosis of thyroid abnormalities in infancy.

REFERENCES

1. Russell, K. P., Rose, H. and Starr, P. Radioiodine during pregnancy. Effects on maternal and fetal functions. Trans Pacif Coast Obstet Gynec Soc 24, 62-70, 70-73 (discussion) 1956.
2. Ray, E. W., Sterling, K. and Gardner, L. I. Congenital cretinism associated with ^{131}I therapy of the mother. AMA J Dis Child 98, 506-507, 1959.
3. Hamill, G. C., Jarman, J. A. and Wynne, M. Fetal effects of radioactive iodine therapy in a pregnant woman with thyroid cancer. Amer J Obstet Gynec 81, 1018-1023, 1961.
4. Lushbaugh, C. C. A universally applicable method for assaying thyroid function in vertebrates. Nature (Lond) 198, 862-864, 1963.

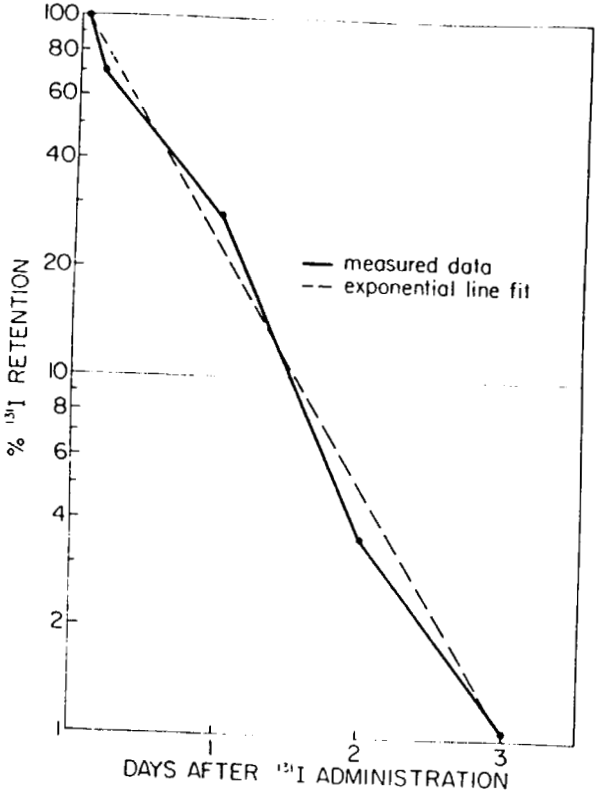

Fig. 43. Whole-body retention of 0.001 millicurie ^{131}I administered intramuscularly.

1027869

Radioactivity of Cigarettes

W. D. Gibbs, C. C. Lushbaugh, and H. D. Hodges

A study of the radioactivity of 14 brands of cigarettes was done with the ORINS low-level sample counter. Ten cartons of each brand, removed from cartons and packages, were counted for 1000 minutes and 200-channel gamma-ray spectra were obtained for energy ranges 0-0.4 Mev, 0-1.0 Mev, 0-2.0 Mev, and 0-4.0 Mev for each brand.

All cigarettes contained ^{40}K (1.46 Mev) and ^{137}Cs (0.662 Mev) as was expected. Other definite peaks seen in all cigarettes:

Energy (Mev)	*Isotope*
0.08-0.09	^{232}Th
0.135	^{144}Ce
0.180	^{226}Ra
0.235	^{212}Pb
0.300	^{214}Pb
0.350	^{214}Pb
0.510	many
0.96	^{228}Ac
1.76	^{214}Bi
2.2	^{208}Tl
2.6	^{208}Tl

Except for the very prominent 0.135 and 0.51 Mev peaks, all these gamma rays are consistent with the presence of ^{232}Th and ^{226}Ra and their many daughters. The 0.510 Mev peak is probably due to a number of fission products. In addition, the 0.835 Mev peak of ^{54}Mn was present in nine brands and was especially prominent in two brands manufactured by the same company. Antimony-125 (0.43 Mev) was seen in 12 of the 14 brands.

If the data for all brands are normalized on the ^{40}K peak, the total activity per pound of tobacco varies by a factor of about 2 from the least to the most radioactive brands. The two most highly radioactive brands are manufactured by the same company. Figure 44 shows a spectrum obtained from the most radioactive cigarettes and Fig. 45 is the spectrum of the least radioactive brand.

A gamma-ray spectrum was obtained from 100 grams of cigarette tar supplied by Dr. Paul Kotin and Hans Falk of the National Cancer Institute. This sample of tar contained minute amounts of ^{137}Cs and ^{40}K. No other radioiosotopes were detectable. This would indicate

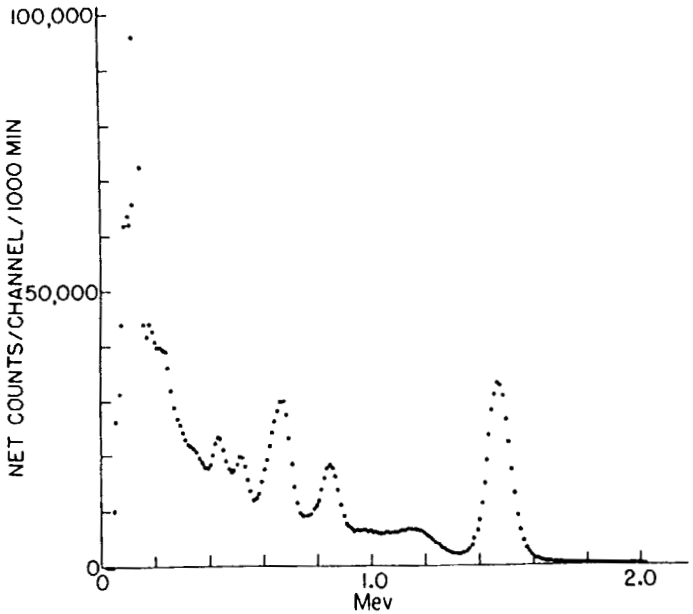

Fig. 44. Spectrum of the most radioactive cigarettes.

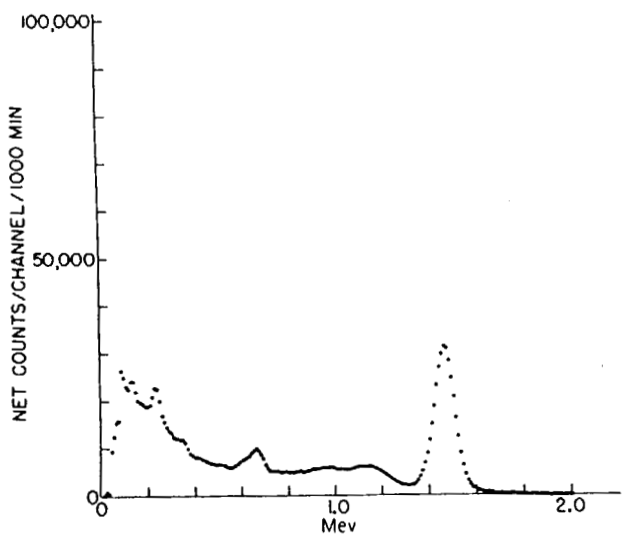

Fig. 45. Spectrum of the least radioactive cigarettes.

1027870

that no appreciable amounts of radioactivity are ingested as a result of cigarette smoking.

Preliminary studies done with the ORINS low-level whole-body counter on 120 normal adult men (51 nonsmokers, 69 smokers) show no difference in whole-body activity between smokers and nonsmokers.

The variations in cigarette radioactivity from one brand to another are probably due to (1) tobaccos of different age; (2) geographic area in which the tobacco was grown.

Possibly some cigarette manufacturers do not age tobacco so long as others. This young tobacco would contain fairly short-lived radioisotopes that would have decayed below detectable levels in older tobacco. Also, since fallout levels vary from year to year, this could account for some of the differences.

Natural radioactivity and fallout vary from one geographic area to another. This could also be responsible for the differences in radioactivity of cigarettes. Studies of samples of the 1964 tobacco crop are under way on samples obtained from 21 different areas throughout the tobacco-growing region.

Analysis of Wounds and Tissue for Plutonium

R. J. Cloutier and C. C. Lushbaugh

Because plutonium decays primarily by alpha emission, determining the amount of plutonium in a wound contaminated with it is very difficult. Some success in monitoring wounds has been achieved by measuring the low-energy X rays emitted with about 0.01 of the decays. The low-energy X rays are usually measured with a thin NaI(Tl) crystal.[1]

As a result of an accidental explosion in a chemical processing plant this year, considerable plutonium was embedded in the thumb and index finger of a technician. The *in vivo* estimate of plutonium in the thumb was 400 micrograms. The index finger was estimated to contain three micrograms. Because of the deep distribution of embedded plutonium in the thumb and finger, debriding the material was impossible. The thumb and finger were amputated to prevent the plutonium from relocating to the bones of the body. The amputated appendages were sent to the Division for plutonium analysis and for histologic examination.

Superficial external counting of the tissue after division into

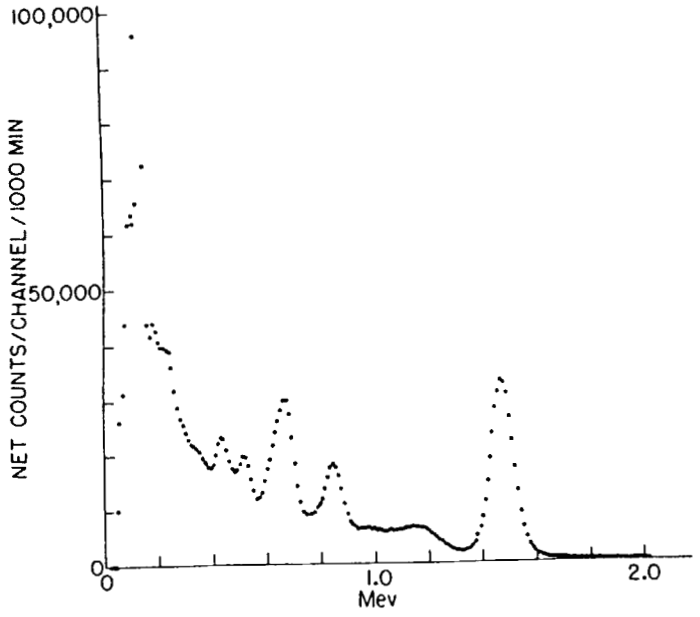

Fig. 44. Spectrum of the most radioactive cigarettes.

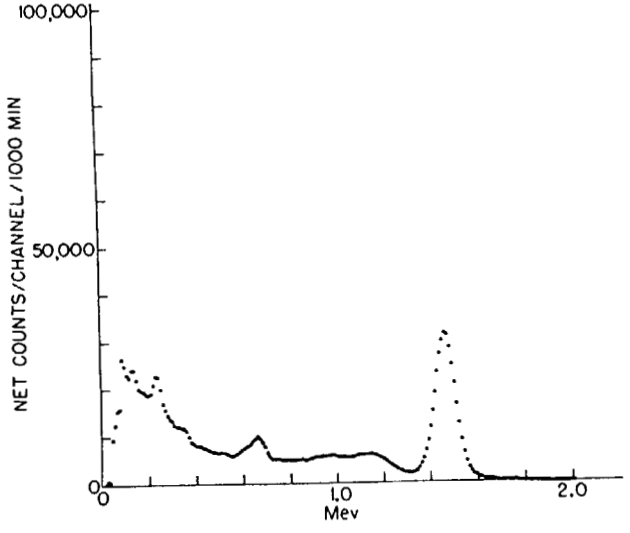

Fig. 45. Spectrum of the least radioactive cigarettes.

1027871

that no appreciable amounts of radioactivity are ingested as a result of cigarette smoking.

Preliminary studies done with the ORINS low-level whole-body counter on 120 normal adult men (51 nonsmokers, 69 smokers) show no difference in whole-body activity between smokers and nonsmokers.

The variations in cigarette radioactivity from one brand to another are probably due to (1) tobaccos of different age; (2) geographic area in which the tobacco was grown.

Possibly some cigarette manufacturers do not age tobacco so long as others. This young tobacco would contain fairly short-lived radioisotopes that would have decayed below detectable levels in older tobacco. Also, since fallout levels vary from year to year, this could account for some of the differences.

Natural radioactivity and fallout vary from one geographic area to another. This could also be responsible for the differences in radioactivity of cigarettes. Studies of samples of the 1964 tobacco crop are under way on samples obtained from 21 different areas throughout the tobacco-growing region.

Analysis of Wounds and Tissue for Plutonium

R. J. Cloutier and C. C. Lushbaugh

Because plutonium decays primarily by alpha emission, determining the amount of plutonium in a wound contaminated with it is very difficult. Some success in monitoring wounds has been achieved by measuring the low-energy X rays emitted with about 0.01 of the decays. The low-energy X rays are usually measured with a thin NaI(Tl) crystal.[1]

As a result of an accidental explosion in a chemical processing plant this year, considerable plutonium was embedded in the thumb and index finger of a technician. The *in vivo* estimate of plutonium in the thumb was 400 micrograms. The index finger was estimated to contain three micrograms. Because of the deep distribution of embedded plutonium in the thumb and finger, debriding the material was impossible. The thumb and finger were amputated to prevent the plutonium from relocating to the bones of the body. The amputated appendages were sent to the Division for plutonium analysis and for histologic examination.

Superficial external counting of the tissue after division into

smaller parts showed that it contained more plutonium than was originally estimated. The final estimate, based on four different methods (Table 17), showed that the thumb contained 4000 micrograms of plutonium. The original estimate was most likely low because of self-absorption of the low-energy X rays by bone and the plutonium particles themselves. A scan of the bones (Fig. 46) showed that most of the plutonium was embedded in the fractured proximal phalanx and consisted of relatively large particles. Of the external counting methods used to estimate the amount of plutonium *in vivo*, only the measurement of the higher energy ^{241}Am gamma ray minimized the error due to self-absorption. To use this method, it was necessary to know the Pu Am ratio. This ratio was determined by obtaining a sample of material similar to that in the wound and performing an alpha-spectrum analysis.

The autoradiogram of histologic sections of the thumb and finger showed microscopically only traumatic damage to bone, connective tissue, and muscle without unusual inflammatory reaction. Microscopically large metallic dust particles were embedded deep in the bone and surrounding connective tissue. The photographic emulsion showed abundant "sunbursts" of alpha particle activity.

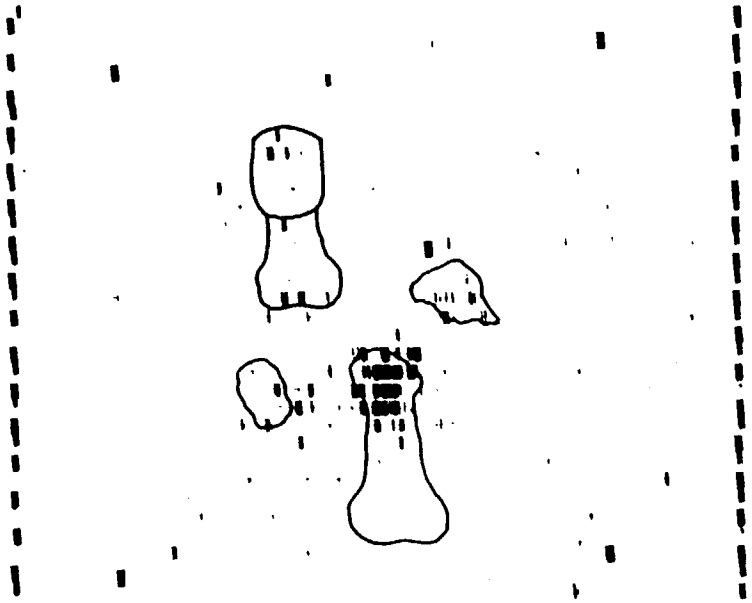

Fig. 46. Plutonium in wounds.

1027872

TABLE 17

Estimated Micrograms ^{239}Pu in Tissue and Bone Samples

Sample Number	ORNL* H.P. Estimate	ORNL α Lab Estimate	ORINS Estimate†	ORINS Estimate‡
1	51.8	—	79.1	82.0
2	37.3	—	45.3	59.2
3	48.6	—	68.6	72.9
4	56.7	—	89.3	86.6
5	56.7	64.8	73.1	72.9
6	51.8	—	53.1	50.1
7	53.5	—	77.5	77.4
8	35.6	—	39.7	45.6
9	64.8	—	74.1	86.6
10	47.0	—	49.6	59.2
11	66.4	—	79.3	82.0
12	30.8	—	32.1	36.4
Deboned finger	9.23	—	—	—
Thumb bones	1782	—	3425	2825
All but histology sections and sample No. 5	—	2590	—	—
TOTAL SAMPLES 1-12	601.0	—	760.8	810.9

* Oak Ridge National Laboratory.

† Estimate based on 93-kev to 112-kev peak of samples and a 5-μg ^{239}Pu standard.

‡ Estimate based on average Pu to Am ratio. (Am amount based on Pu results as calculated by ORNL α Lab for sample No. 5.)

REFERENCE

1. Putzier, E. A., Mann, J. R. and Johnson, V. P. Use of a gamma ray spectrometer for investigation of plutonium contaminated wounds. Am Ind Hyg Ass J 19, 384-385, 1958.

Determination of Fraction of Blood Volume "Seen" in the Human Forearm by the "Armac" Arm Counter

W. D. Gibbs, H. D. Hodges, and C. C. Lushbaugh

Radioisotope studies with the Armac* arm counter have been performed at the Division during the last two years. Some of the radioisotopes and labeled compounds used have been ^{198}Au, ^{59}Fe, ^{51}Cr, ^{131}I rose bengal, ^{131}I human serum albumin, ^{60}Co, and ^{58}Co vitamin B_{12}.

Predetermination of rate-meter sensitivity so that maximum recorder deflection of 50% to 80% full scale could be obtained was made possible by determining the average "arm" blood volume of the subjects with a standard intravenous isotope dose.

Five patients, three men and two women, were given red cells labeled with ^{51}Cr (50 microcuries) and arm counts were done. Simultaneous blood samples (5 ml) were obtained from the other arm at 5, 10, 20, and 30 minutes for blood volume determinations. Each patient was then given ^{131}I human serum albumin and these procedures were repeated. A known fraction of each dose of radioisotope was counted in an arm phantom in the arm counter. The actual arm counts were compared with the count obtained with the arm phantom and the percentage of dose present in the arm of each patient was calculated.

The results showed that 1% of the intravenously injected radioisotope level was present in the blood circulating through the portion of arm being counted. The range of "arm" blood volumes was 0.98 to 1.03% total blood volume, indicating that the forearm or cubitus is a fairly reliable portion of the total body mass regardless of sex and body size.

This 1% of any gamma-emitting isotope to be studied can be placed in the arm phantom and used as the theoretical 100% standard for arm activity and rate-meter and window settings predetermined individually. Use of a constant total dose in arm-counter studies effectively "normalizes" the data for all body types.

These data are also basic to the analog computer model of the mechanism of rose-bengal blood clearance, since it shows that arm blood volume is a constant that does not complicate the computer equations.

* Packard Instrument Company, La Grange, Ill.

1027873

Detecting and Localizing Radioactivity in Patients

The objective is to develop and apply refined instrumentation for detecting and localizing radioactivity to meet specific needs in the research effort. Examples have been scanning systems, whole-body counting facilities, and miscellaneous detection apparatus for quantitating the radioactivity in an organ.

Whole-body Counters

A. C. Morris, Jr., C. C. Lushbaugh, R. L. Hayes, H. Kakehi, and W. D. Gibbs

Low-level Counter—For several years the Division has been developing a series of three whole-body counters for clinical use. Construction has been completed, and they are now in operation. The use of one or more of these counters allows whole-body retention counts to be made over the entire range of activities from therapeutic dose levels down to the natural body background. One of the several important studies to be undertaken will be whole-body retention of radioisotopes over many biological half-lives. Here the system of three counters has the advantage that when the activity to be counted reaches the lower limit of sensitivity with one instrument, the counting procedure is shifted to the next, more sensitive counter. Thus, the activity of a therapeutic dose may be followed until it ultimately disappears into the natural body background.

During construction of the now completed low-level whole-body counter many careful tests were made of the steel, stainless steel, and lead of the primary shield. Additional tests were made on the olivine fill, concrete, and all other materials lying within six feet of the counting chamber to insure the lowest possible background count. In all, more than 100 separate tests were made. Some construction materials were rejected because of unacceptable radioactive content, and acceptable substitute materials were obtained. The result of these efforts has produced a counter in which the construction materials have met or exceeded the designed background requirements. On completion of the contractor's work, Institute staff installed the

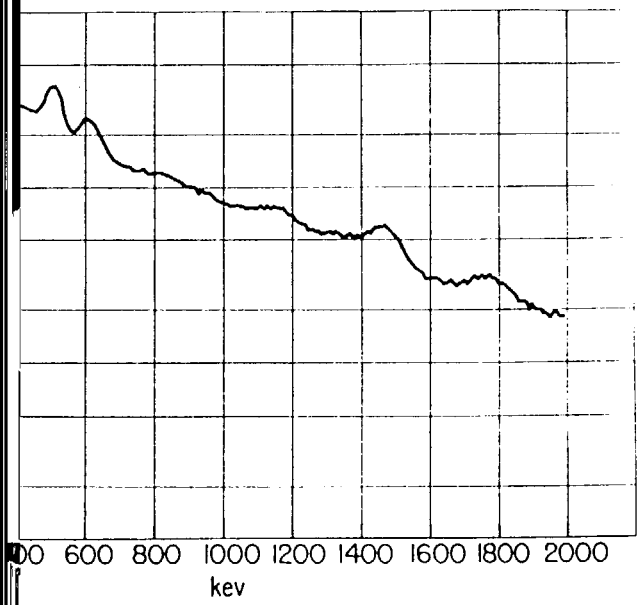

background gamma radioactivity of the completed cave.

ns entering the counting shield also must shower to
es of fallout that might be on the skin.
rocedure for a patient to be counted is to enter the
, place his clothes in a basket, and then enter the
After a shower he goes into the gowning room where
ns foot scuffs and a scrub suit. He then enters the
and reclines on the transport stretcher (Fig. 47).
into the counting shield and the heavy steel shield-
d. Equipment inside the counting chamber includes
comfort a ventilation system, intercommunications
system, high-fidelity music, and a "panic button."
e to count body background (no administered test

doses) is approximately 20 minutes, and thus far patients have commented that they are comfortable and do not feel "closed in." Patients then leave the instrument room and go into the dressing room where they redress. With this procedure patients can be counted with minimum delay.

Typical background gamma radioactivity of the completed cave is shown in Fig. 48. Figure 49 shows the response of the whole-body

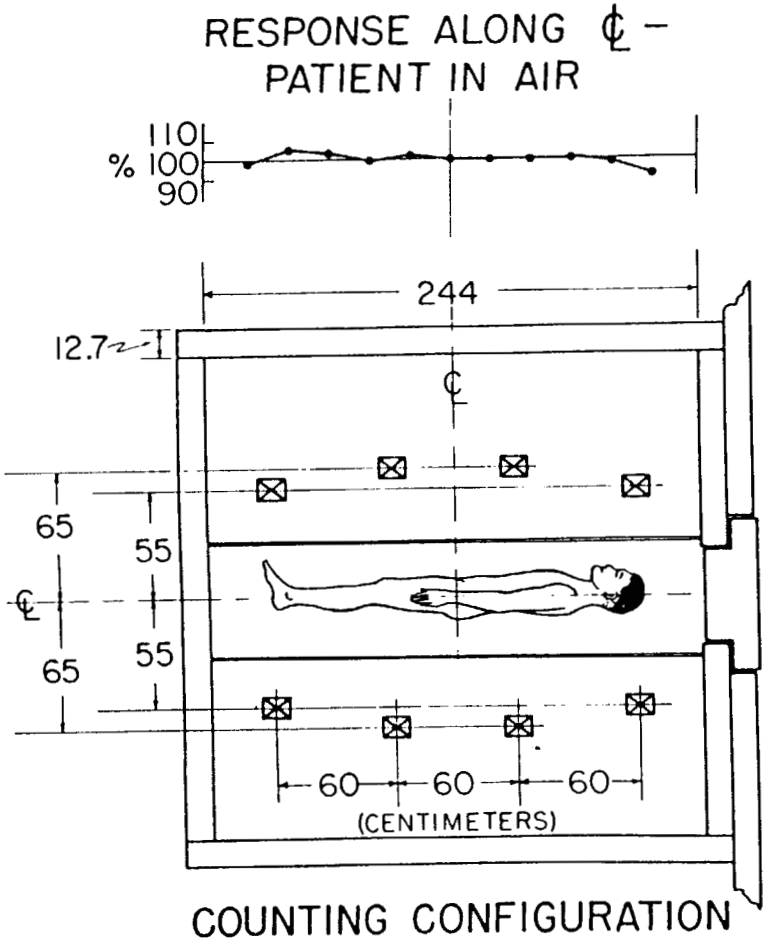

Fig. 49. Response of the whole-body counts to a point source of ^{137}Cs in air.

1027875

counts to a point source of ^{137}Cs in air placed at 20-cm intervals along the midline of the stretcher bed. This uniform response for the whole counter was obtained by studying the individual detector responses to the source at these positions.

Diagnostic-level Counter — The diagnostic-level, whole-body counter consists of a long lead trough in which are mounted four three-inch diameter by three-inch thick scintillation crystals (Fig. 50). All crystals view the entire length of a subject suspended above the lead trough on a Transaver stretcher with a radiolucent bottom (Fig. 51). The output of all four detectors is combined into one input for a single-channel analyzer system. Spectrometry is normally used because of a sizable amount of scattered radiation.

Several experiments were performed to evaluate the uniformity of response and clinical usefulness of the counter. The longitudinal response curve from head to foot in air is shown in Fig. 52 and the transverse curve from right to left is shown in Fig. 53. These curves show that for measurements in air the response from head to foot, and from right to left sides is reasonably uniform. Another set of data was obtained by adding to an 8-liter polyethylene bottle filled with water increasing amounts of ^{131}I. The isotope was mixed thoroughly in the solution and was then counted at the center of the stretcher.

DIAGNOSTIC-LEVEL, WHOLE-BODY COUNTER SHIELD CONSTRUCTION
(SUPPORTING FRAMEWORK NOT SHOWN)

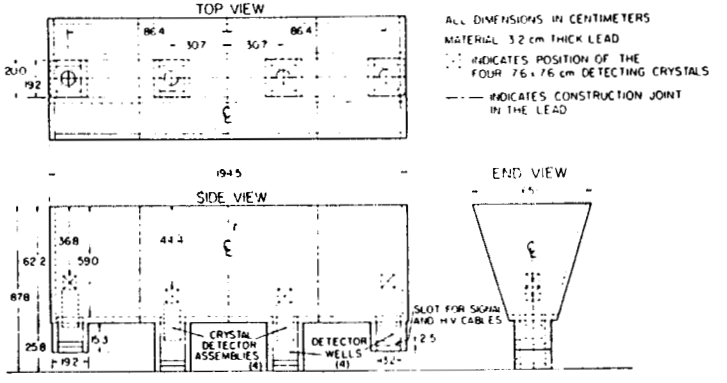

Fig. 50. Construction drawing.

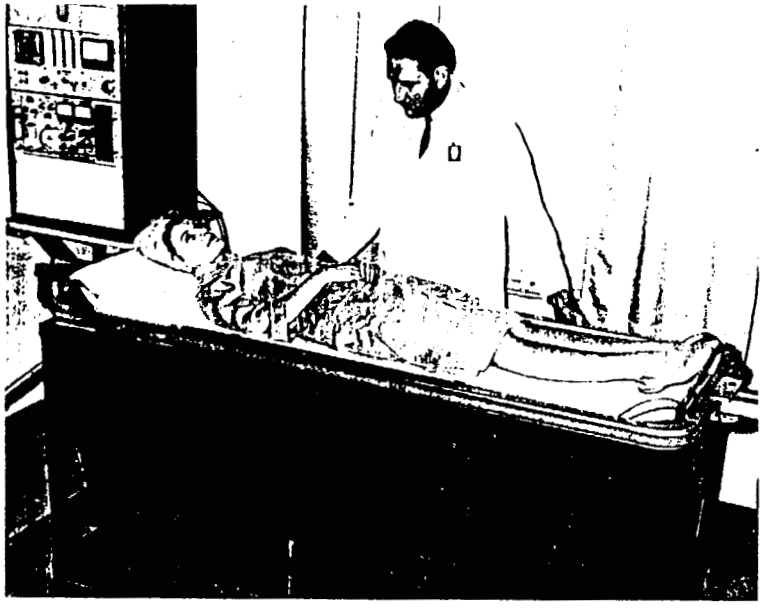

Fig. 51. Photograph of diagnostic-level whole-body counter.

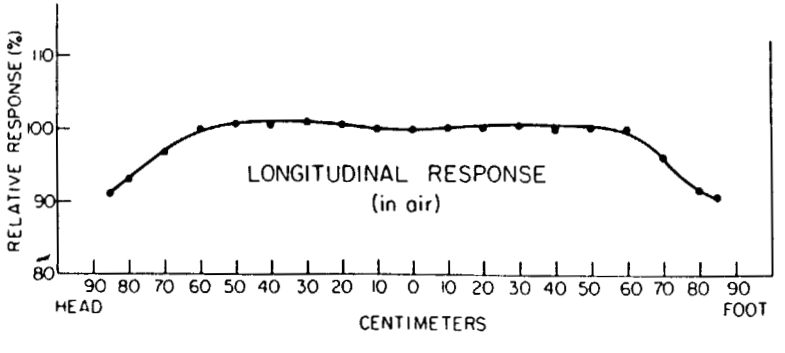

Fig. 52. Longitudinal response.

1027876

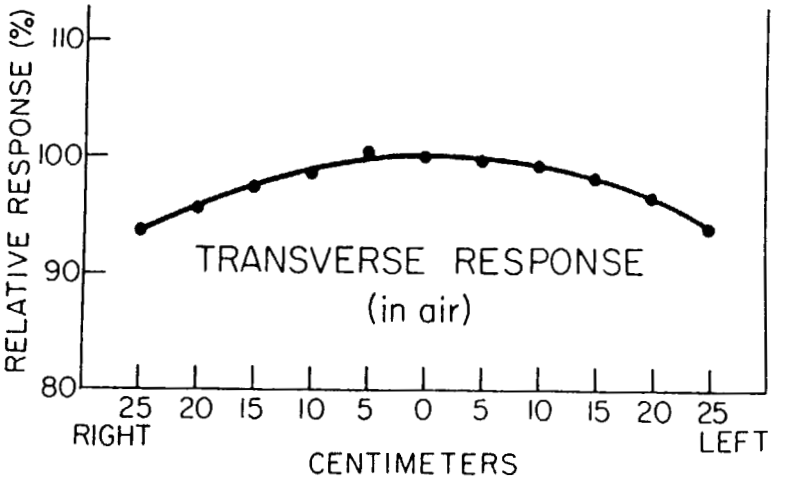

Fig. 53. Transverse response.

The counts recorded are given in Table 18 and are plotted in Fig. 54. The results show that over the design range of 0.1 to 100 microcuries this diagnostic-level counter gives a reasonably uniform response.

When using a diagnostic-level whole-body counter, one is usually concerned with the retention of radioactivity as a function of time rather than an absolute assay of the whole-body content, and here it is necessary only to compare the counting rate of the patient with that of an appropriate aliquot of the dose. Initial counts on the standard and on the subject before any excretion establish a ratio for subsequent measurements as a "100% retention value."

Here it is necessarily assumed that the distribution pattern of the radioisotope is fixed shortly after administration and remains fixed during the course of the study, but most radioisotopes change their distribution pattern in the human body with time. For example, when a patient swallows a capsule of ^{131}I, it acts as a point source in the stomach. After it has dissolved, the ^{131}I content is then absorbed into the blood through the intestinal mucosa. Now the detectors of a whole-body counter will "see" the radioactivity as a diffuse source in the patient's whole body. The ^{131}I will then gradually accumulate in the thyroid gland, bladder, salivary glands, etc. After 24 hours, most of the retained radioiodine will be accumulated in the thyroid gland. Thus the radioactivity will have changed its distribution in the body from a point source to a diffuse source and back to a point source.

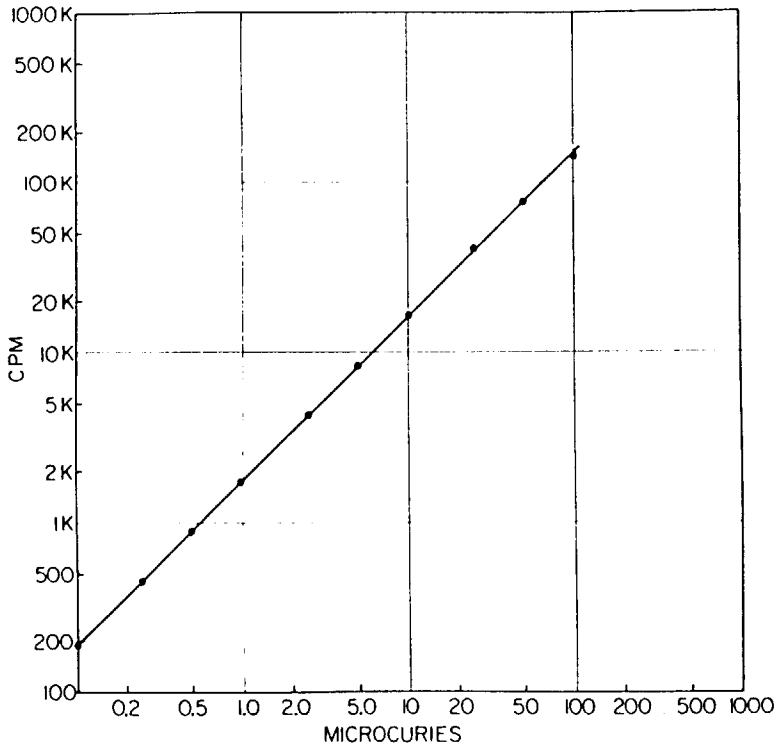

Fig. 54. Activity versus counting rate.

Such changes in distribution can have profound effects on the whole-body counting rate and, in turn, the apparent retention value, depending on how the subject is counted.

To determine how best to count subjects with this new whole-body counting facility, an extensive phantom study was made of the counting characteristics of various radionuclides of medical interest. Point sources (at various positions) and diffuse sources in a compartmentalized water phantom were compared with each other. Some typical data from this study are shown in Figs. 55, 56, and 57. In general, the counting rate was least dependent on distribution of the isotope when counts were made in the scatter region of the spectrum. On the basis of these phantom measurements, the following energy ranges appear best: ^{131}I, 200-300 kev; ^{198}Au, 150-350 kev; ^{137}Cs, 300-

1027877

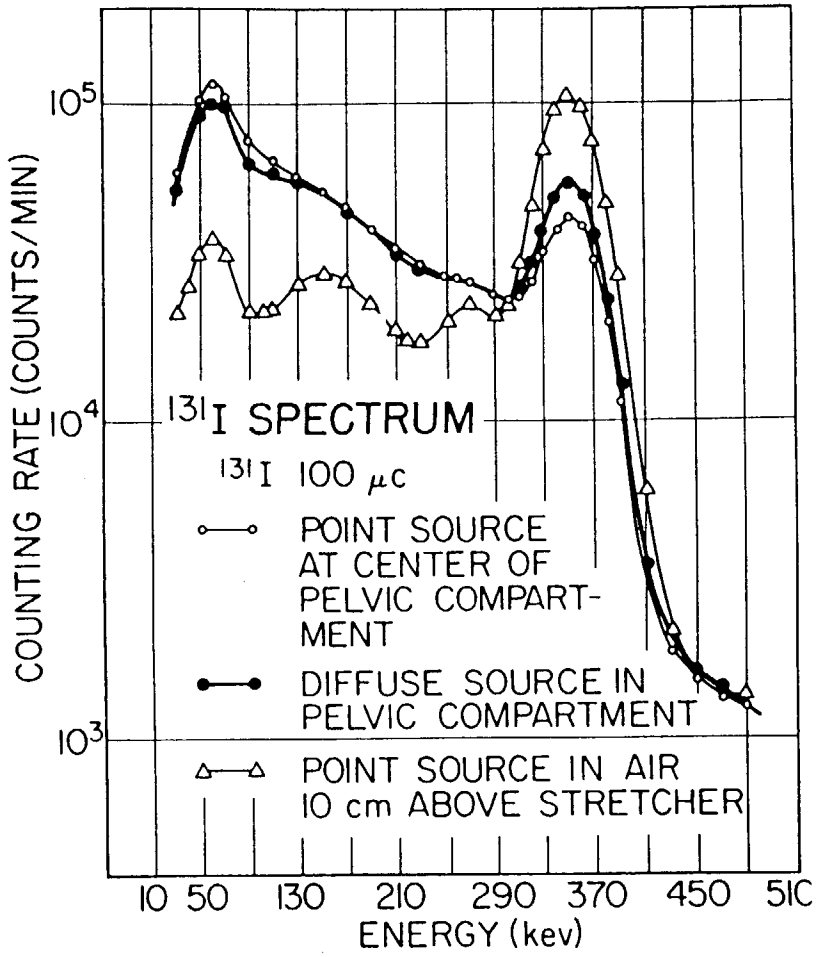

Fig. 55. Iodine-131 spectra for different source geometries.

500 kev; ^{60}Co, integral above 500 kev. These ranges are, of course, estimates based on phantom measurements. A study of counting-rate changes with time (distribution) with various energy ranges using human subjects is in progress. Figure 58 shows a comparison of the

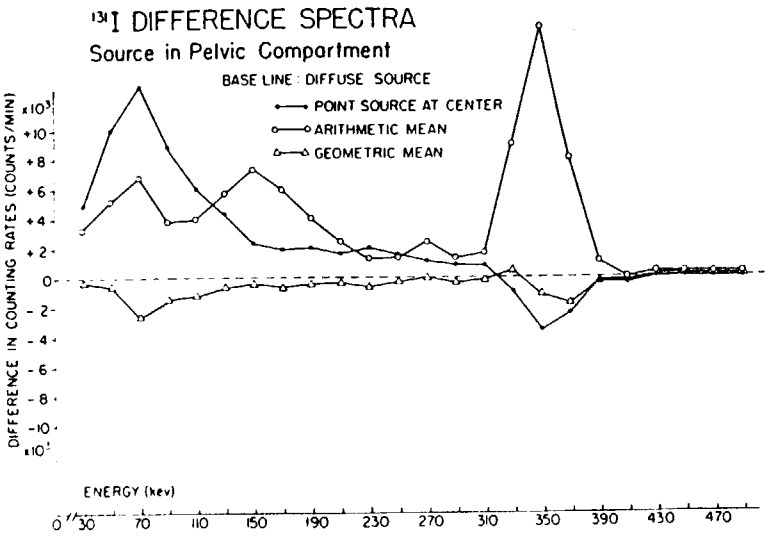

Fig. 56. Iodine-131 counting-rate differences as a function of energy for different source geometries, diffuse source taken as the base line.

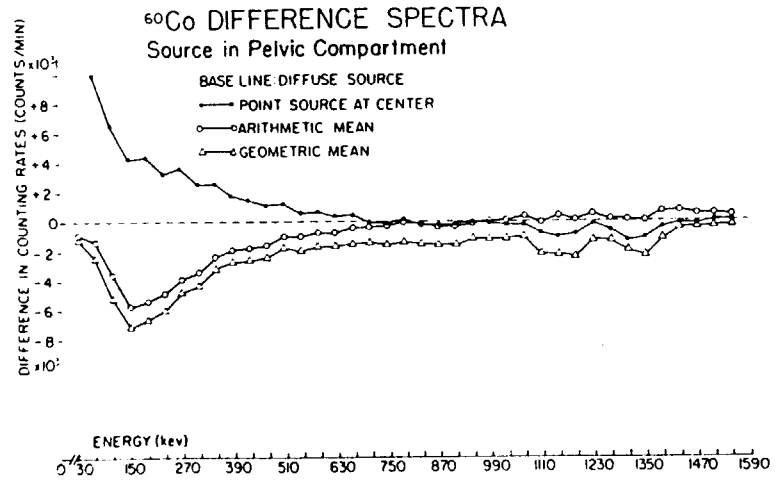

Fig. 57. Cobalt-60 counting-rate differences as a function of energy for different source geometries, diffuse source taken as the base line.

1027878

SENSITIVITY OF MEDIUM-LEVEL WHOLE-BODY COUNTER

RADIOISOTOPE	ENERGY RANGE (kev)	BKGD CTS (cpm)	SMALL VOLUME SOURCE (net cpm/μc)	2 GAL BOTTLE DIFFUSE SOURCE (net cpm/μc)	PATIENT (net cpm/μc)
^{131}I	200 ~ 300	3330	1080	1340	1270
	300 ~ 400	1690	2840	1800	1440
	250 ~ 400	3060	3380	2410	2000
^{198}Au	160 ~ 390	8180	2060	2720	
	360 ~ 460	1560	2500	1700	
^{137}Cs	350 ~ 450	1550	1150	570	
	600 ~ 700	870	3470	1030	
^{60}Co	ABOVE 500 INTEGRAL	2840	3330	2030	
^{59}Fe	ABOVE 500 INTEGRAL	2710	1570	1140	940

Fig. 58. Sensitivity of medium-level whole-body counter for different isotopes and geometries.

TABLE 18

Sensitivity Calibration Results*

ACTIVITY† (Microcuries ^{131}I)	NET COUNT (Counts/min)
0.1	191
0.25	458
0.5	896
1.0	1725
2.5	4273
5.0	8314
10	16,527
25	40,580
50	77,494
100	143,857

* Background counts were subtracted to give the net counts in this table. A typical background for a spectrometer passband of 330 to 390 kev is 1,147 counts per minute.

† Isotope was ^{131}I dissolved in an 8-liter water-filled plastic bottle.

sensitivity of the diagnostic-level whole-body counter for selected isotopes with various energy ranges.

With the current design of the diagnostic-level whole-body counter, it is necessary to count subjects both supine and prone. However, the diagnostic-level counter has a distinct advantage in that it allows whole-body retention studies to be made concurrently with other clinical tracer investigations. In contrast to the low-background whole-body counters now in use it is relatively inexpensive. Moreover, the subject is in an unconfined, comfortable position, and the counting times are short. Our experience with phantoms and patient studies indicates that this will be a useful instrument for following whole-body measurements in the diagnostic dose range.

High-level Counter—The high-level whole-body counter continues to be a useful clinical instrument. The recent incorporation of a transistorized spectrometer system has resulted in more stability and easier operation.[1]

REFERENCE

1. USAEC Report ORINS-43, p. 99-100.

Computer Program for Calculation of Response Of Detector-Collimator Systems

W. D. Gibbs

A computer program was designed to calculate the isoresponse and volume response of a detector-collimator system. The calculations follow the method outlined last year.[1]

The program was written specifically for data obtained at 546 points but can be simply generalized for any number of points.

This problem was run on an IBM 1620 computer.* Computations and readout time required less than 30 minutes. Similar calculations done by hand would require about three days of work by an experienced person.

The program as written in Fortran is available by writing to the author.

* Courtesy of Douglas Lawson, University of Waterloo, Waterloo, Canada.

REFERENCE

1. USAEC Report ORINS-43, p. 75.

1027879

Thermoluminescent Dosimetry

Young Ja Lee, R. J. Cloutier, and P. Dalton*

Thermoluminescent dosimetry is currently being used to mea the dose to patients during total-body irradiation. Small caps containing 100 mg of lithium fluoride powder are taped to the ski the patients. When exposed to radiation, the lithium fluoride crys absorb energy and later emit this energy as light when the crys are heated. The amount of light is related to the radiation dose. ' system has excellent linearity of response and has been calibr against a standard condenser R-meter. Table 19 shows the ther luminescent dosimetry data compared to earlier work on dosim of an anthropomorphic phantom exposed to total-body irradiation

* International Atomic Energy Agency Fellow from Korea.

REFERENCE

1. Hayes, R. L., Oddie, T. H. and Brucer, M. Dose comparison of two t body irradiation facilities. Int J Appl Radiat 15, 313-318, 1964.

TABLE 19

Comparison of Thermoluminescent Dosimetry of Three Patients Giv Total-body Irradiation with Ionization Chamber Measurement of Irradiated Phantom

Location	^{137}Cs Total-body irradiation facility. Dose expressed as percentage dose in air at the middle of the bed.				
	Adult Phantom (1)	Thermoluminescent Dosimetry of Patients			
		1	2	3	Avera
Head	91	96	85	90	90
Neck	90	88	82	82	84
Chest	88	93	90	80	88
Abdomen	85	82	90	74	82
Pelvis	91	80	—	—	—
Lower Leg	97	100	107	91	99
Feet	91	94	—	—	—

The Whole-body Scanner

A. C. Morris, Jr.

The whole-body scanner system being developed at the Division is essentially complete. This scanner uses a 5-inch diameter by 4-inch thick NaI scintillation detector mounted underneath the patient-supporting bed. The scanner permits the selection of different line spacings ranging between 1/16 inch and 1-1/16 inches and scanning speeds ranging between 0 and 40 inches/minute.

The original formica bed-top was ⅜ inch thick and prevented use of the collimator's long focal length of 3⅞ inches to advantage, so a bed-top of ⅛ inch epoxy fiber glass sheet was substituted. This fiber glass sheet deflected about ¾ inch under a heavy subject. Therefore two washing-machine rollers were installed on each side of the collimator to support the weight. Now the deflection caused by the patient's weight is negligible and the collimator face can be moved just under the surface of the support. The detector moves under the patient and the operator cannot visually localize the focal point of the collimator hidden from view by the bed top; therefore a supporting system was installed over the scanner with a small, movable slide projector to beam a spot of light onto the patient, moving synchronously with the collimating head. Also, the bed-top was modified so that the maximum scan width could be increased from 23 to 25 inches.

The electronic system includes both multidot and photoscan recording. This system also incorporates a selection of separate dot factors for both photoscan and multidot modes of recording.

Dr. Orhan Ternar, a visiting scientist from Turkey, designed and developed an effective light source for use with the photoscan recorder. It focuses a sharp, bright beam of light onto the recording film from a crater-lamp that gives a bright burst of light in a 10-microsecond pulse. With this photoscan recorder it will be possible to produce well-defined scans at very low dot factors. The scanner chassis as received had a mechanical reduction factor of 5 to 1 from scanner movement to recorder movement. A new mechanical drive system has been incorporated so that this ratio can be changed from either 5 to 1 or 1 to 1 as desired. Thus areas of interest seen with the 5 to 1 ratio can be further investigated in larger detail with the 1 to 1 setting. Figure 59 shows the thin table top, the overhead localizing light projector, the electronic system for driving the scanner motor and recorders to the rear, and on the table to the right, the multidot and the photoscan recorder boxes.

1027880

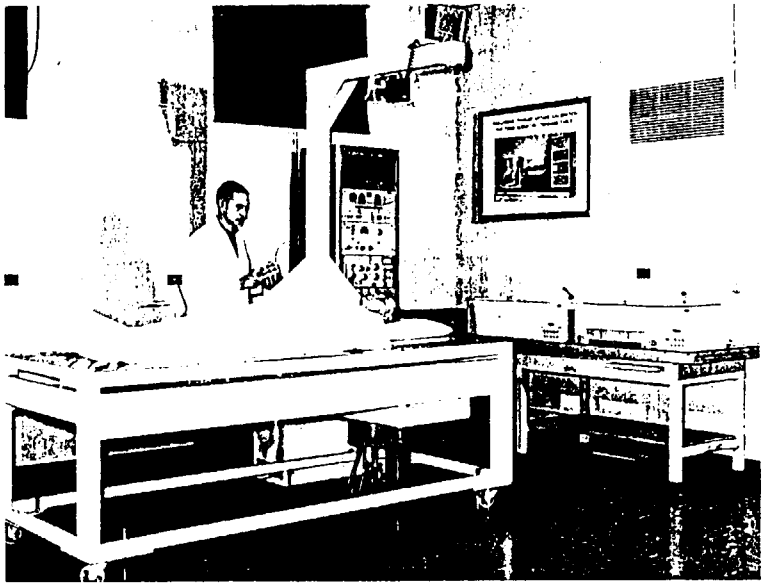

Fig. 59. Photograph of the whole-body scanner.

Its original collimator was developed by C. C. Harris, *et al.* of Oak Ridge National Laboratory. It has a 96-hole focusing insert and a focal distance of 3⅞ inches, designed so that various inserts having other numbers of holes and focal lengths could be inserted to meet different scan requirements. This original insert gave an extremely high resolution. Subsequently, a broader resolving collimator insert was developed to use when resolution is less important than higher sensitivity. It gives a focal diameter approximately twice that of the high-resolution collimator and increases the sensitivity by a factor of 4. Figure 60 shows the TsuyaTscan' response patterns of these collimators in air and in water, giving a general indication for ^{131}I of what the scanner is seeing. The pattern of the high-resolution collimator is very sharp, and the response of both collimators is reduced in depth with the water phantom.

REFERENCE

1. USAEC Report ORINS-24.

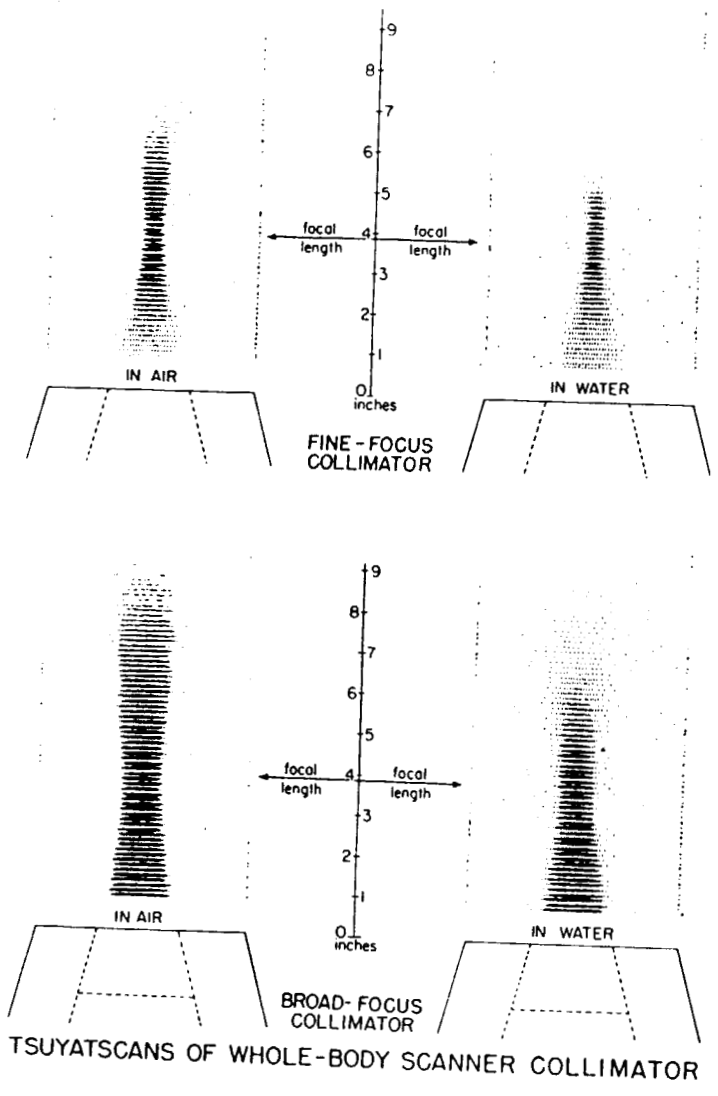

Fig. 60. TsuyaTscan patterns of collimators.

1027881

NASA Retrospective Study on Irradiation Effects

The long range goal of this project is to establish the radiosensitivity of man from human data obtained during therapeutic trials and from accidental exposures.

Radiobiologic knowledge useful in predicting the physiologic or morphologic responses of man to ionizing radiation is largely derived from animal experimentation. Analyses of human exposure data are relatively scarce and little confidence can be placed upon their conjectures concerning the levels of radiation that will cause detrimental human reactions. Much of this paucity is due to the difficulties encountered in evaluation of such data because of the numerous variables involved. Modern research methods employing easily manipulatable computers with large memory storage capacity, however, are now available for such data accumulation and evaluation.

The actual clinical data recorded in all human whole-body radiation exposures will be obtained, extracted, and encoded in such a form that the volume of data and its complexity will be minimized by modern mathematical electronic computer methods. The Division's patient material obtained in a radiotherapeutic program since 1957 will constitute the first study group and will be used to test the feasibility of the system. Additional human data will then be obtained from other hospital centers with similar studies and from the therapeutic and accident literature concerning specific physiologic or morphologic radiation effects in man. These data will be incorporated into the study to extend the original observations and test the validity of original appraisals. Specific studies will be directed toward determining from these data the dose relations in man for anorexia, nausea, vomiting, diarrhea, fatigue, weight loss, fever, erythema, epilation, lymphopenia, granulocytopenia, anemia, thrombocytopenia, cytogenetic damage, decreased resistance to infection, decreased antibody synthesis, increased aging, carcinogenesis, and lethality. The values obtained will be evaluated for degree of clinical and mathematical confidence to permit the use of these data in predicting man's reaction to the ambient radiations of space, and to direct further clinical exploration on the effect of ionizing radiation upon cancerous and normal processes.

Radiosensitivity in Man: A Study Based on Therapeutic and Accidental Exposure

C. C. Lushbaugh, R. Hofstra, R. E. Roth,† and G. A. Andrews*

Nausea and vomiting are not considered a significant clinical problem in patients who have received less than 200 r to the abdomen, as partial or total-body therapeutic irradiation. Most radiologists and radiobiologists would not debate the view that an exposure of about 200 r is required to cause nausea and vomiting in man but few, if any, can predict with any stated degree of certainty for man what the probability is that any exposure to less than 200 r of total-body irradiation will elicit nausea or vomiting. Recently, it has become urgent to obtain such information as precisely as possible to predict the probability of total mission failure for manned space flight because of detrimental physiologic responses of the astronaut. Vomiting, per se, or nausea if severe enough, is conceivably an effect of radiation exposure, which, if not anticipated, could be disastrous in space flight.

The case histories of 94 patients who had received total-body irradiation in the course of therapy, or as the result of a criticality accident, were encoded and processed to determine the incidence of anorexia, nausea, and vomiting. As shown in Table 20, the patients were divided into five dosage groups for which geometric mean doses of 49.6, 105.2, 300, 370.3, and 540.5 r were determined. In Table 21, the percentage of cases in each group that showed anorexia, nausea, and vomiting are shown. Probability (probit) analyses were then done with these data to estimate the total-body irradiation dose required to produce the particular response in 50% of the patients. The resulting machine-fitted regression lines are shown in Fig. 61, as charted directly by a Control Data Corporation computer (#1604) used in these studies. Table 22 contains the probit equations, the chi-square confidence limits, and the effective dose (ED_{50}) for these responses. The values are expressed as common logarithm to define the standard deviations of the estimates, and the midline air dose (roentgens), and the absorbed dose (rads) to the gastrointestinal tract.

* Oak Ridge National Laboratory, Oak Ridge, Tenn.
† St. Bonaventure College, St. Bonaventure, N.Y.

1027882

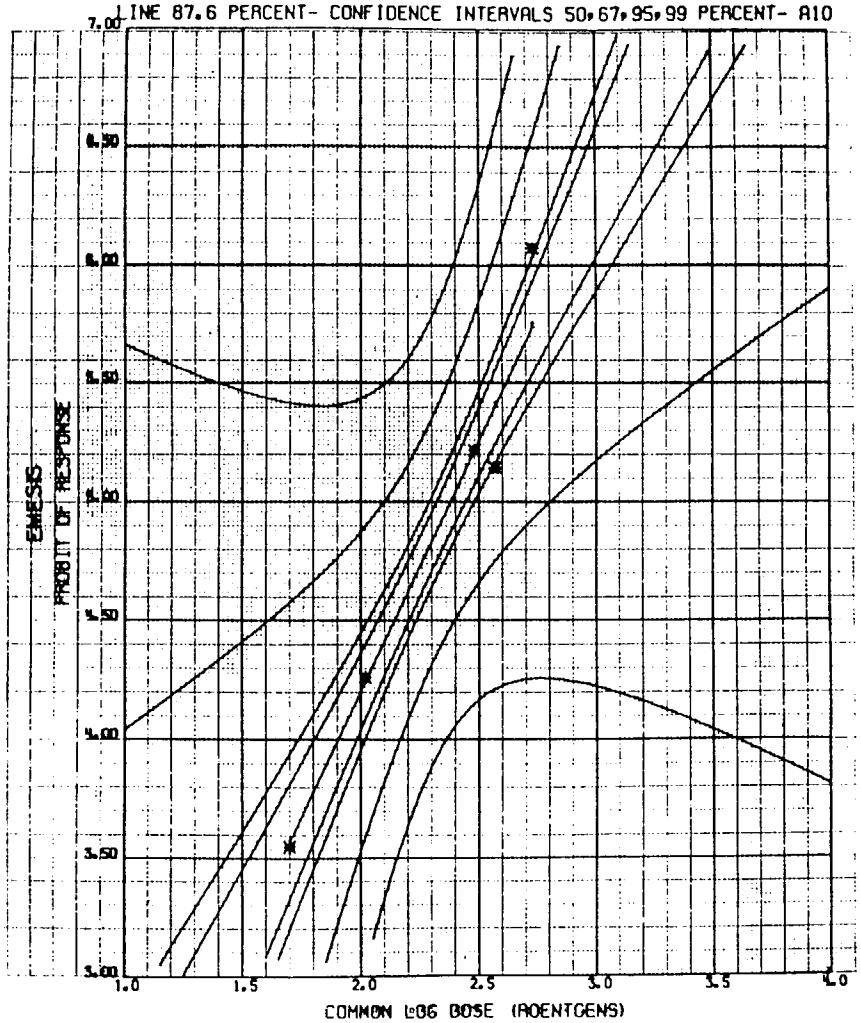

Fig. 61. Photograph of chart made directly by the Control-Data Corporation Computer.

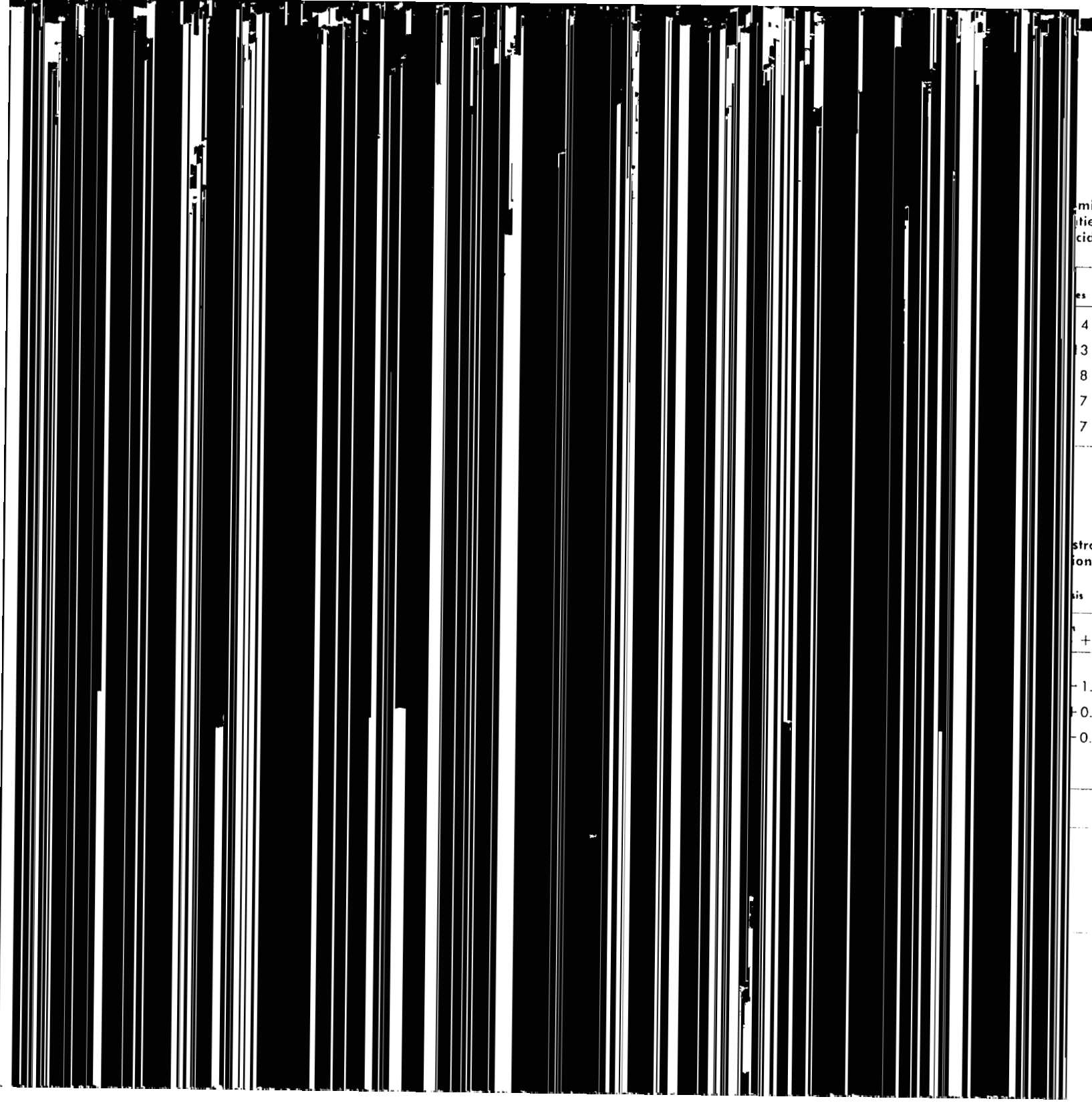

miting in the Division's Radio-
tients, Including Division's
cident Patients

es	Nausea %	Vomiting Yes	%
4	14.8	2	7.4
3	33.3	9	23.1
8	66.7	7	58.3
7	77.8	5	55.5
7	100.0	6	85.7

strointestinal Responses
ion in Man

sis

+ b	Chi-square Confidence
(b)	(%)
- 1.849	91.2
+ 0.066	82.4
- 0.005	87.6

Midline Air Dose	Absorbed Dose to GI Tract
(r)	(rads)
104.9	69.2
157.9	104.2
240.5	158.7

Methodology

Although the goals in the research program are not aimed at methodology, success often depends on inventiveness and the ability to devise new tools. Much effort may be expended in such developments, and it is important to report and share these advances.

Processing of Feces for Analysis*

A. M. Webb and G. C. Kyker

Inconvenience in processing feces for quantitative analysis hinders general use of potentially valuable clinical determinations. An example is fecal urobilinogen in diagnosing hepatic and hemolytic disorders. Its chemical determination by the Ehrlich aldehyde reagent is well established. Quantitative application of this and other methods depends, however, on homogeneous mixing and aliquoting of unpleasant material.

A system is described for adapting common laboratory items to avoid the unpleasantness associated with collecting, processing, sampling, and discarding stool specimens. A numbered plastic receptacle is weighed before use. The specimen is conveniently collected with the apparatus described by Hayes' and weighed by difference. In the hood, water and 10-12 glass marbles are added for rotary mixing. For average stools, dilution (ml) equals the specimen (g); for watery stools, dilution is less, judged by experience. Warm water (50 to 60° C) is used for reducing the pressure during cooling, the sealed container is inverted, and the rim is filled with rubber cement. The sealed container is mounted horizontally under tension and rotated at 60 rpm for 30 to 45 minutes. A multipurpose rotator with a modified head is used for one specimen or a spring-loaded canister on a ball mill serves two.

Aliquots are drawn by piercing the plastic lid with a needle (No. 15, 5 inches) on a calibrated syringe. The puncture is sealed with tape or a drop of Duco cement for disposal. The procedure can conveniently serve various chemical, radioisotopic, and other quantitative procedures.

* Abstract of paper presented at the annual meeting of the American Association of Clinical Chemistry, Boston, August 1964.

REFERENCE
1. Amer J Clin Path 39, 203-205, 1963.

1027884

An Automatic Zonal Scraper and Sample Collector for Radioassay of Thin-layer Chromatograms*†

F. Snyder, H. E. Kimble, and N. Stephens

Zonal radioscanning of thin-layer chromatoplates can be done with a specially designed manual scraper[1,2,3] capable of removing 1-, 2-, or 5-mm zones. Liquid scintillation counting of the zones provides 4-pi counting geometry and efficiencies comparable to those observed for nonquenched liquid systems containing ^{14}C and tritium. Plotting the radioactivity counted as a continuum of zones results in a curve of the activity according to its position on the thin-layer chromatoplates. Specific activities can readily be calculated when this apparatus is used in conjunction with photodensitometric quantitation of the unlabeled compound. The high resolution obtainable with this scraper also makes its utility applicable outside the realm of radiometric analysis. The scraping of minute zones has indeed made possible the monitoring of a chromatostrip in predetermined fractions analogously to the mass and radioactivity monitoring of liquid and gas flow columns. The manual scraper has served as the prototype for the construction of the completely automatic zonal scraper and sample collector.

Production cost of the automatic unit will vary somewhat because of variation in labor cost, overhead, profit, etc. Actual construction time for the prototype, not including development and drawings, was 186 man-hours. Cost of materials for the unit was $218.

The scraper-sample collector (Fig. 62) consists of an aluminum frame and housing assembly containing the mechanism and electrical controls. A carriage (A) travels on guide rods (B) and is driven by the intermittent rotation of a lead screw (C) whose movement is adjustable by a lever (D) causing movement of the glass plate (E) under the spring-loaded scraper blade (F) in increments of 1 mm, 2 mm, or 5 mm.

A knob (G) disengages the carriage from the lead screw allowing rapid traverse (manually) of the carriage and another knob (H) allows manual rotation of the lead screw for initial positioning.

As the glass plate is intermittently pushed under the scraper blade, the adsorbent falls into the vials (I), which are placed in a "Tri-Carb" tray holding 24 vials. The turntable (X) on which the tray is placed moves intermittently and reciprocates with the movement of the glass plates. A solenoid is energized at the end of each

* In press. Analytical Biochemistry.
† Blueprints are available as USAEC Report ORINS-47.

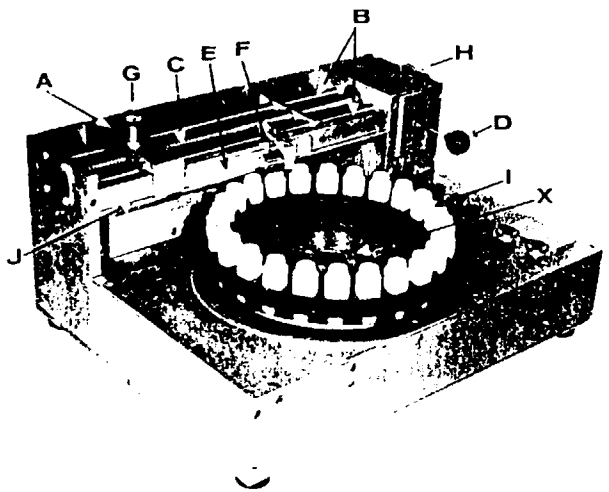

Fig. 62. Front view of automatic zonal scraper and sample collector. See text for description of parts designated by letters.

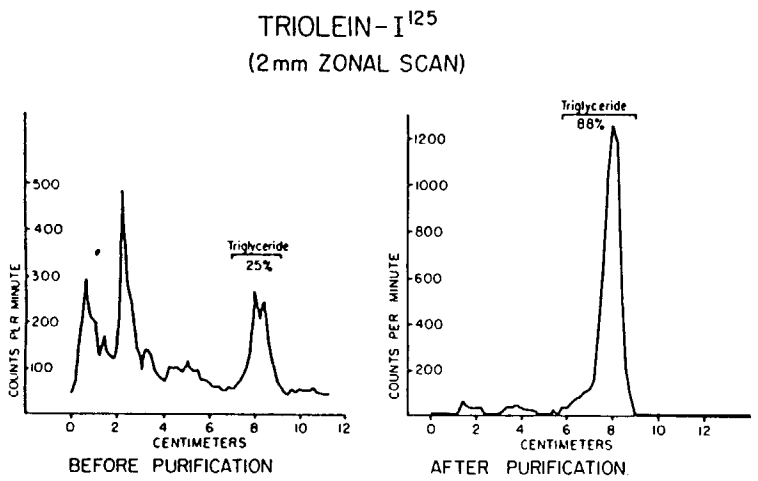

Fig. 63. A zonal scan of ^{125}I-triolein before and after purification by thin-layer chromatography. The solvent system used for development of the chromatogram was hexane:diethyl ether:acetic acid (80:20:1).

1027885

scraping stroke vibrating the plate (J) on which the glass plate is resting, causing any remaining loose adsorbent to fall into the vial.

With this automatic scraper, the 24 samples on a tray may be scraped and collected in one minute. After collection is completed, the turntable tray is removed and new trays of empty vials are placed on the turntable for repeated cycles until the desired number of zones have been collected. A volume of 15 ml liquid scintillator[1,2] is then added to each vial and the tray is placed on a shelf of a Packard 4000 series Tri-Carb for radioassay; if a 4000 series Tri-Carb is not available, the vials are removed in consecutive order and positioned correspondingly in the sample holder of any liquid scintillation spectrometer. The spectrometer controls are placed at the proper settings to program the radioassay, which is then done in continuous order corresponding to a distance along the chromatographic path of approximately 1 cm below the origin to approximately 1 cm above the solvent front as described earlier. [1,2]

The data obtained from the liquid scintillation spectrometer are plotted on graph paper. Better still, a rate meter with recorder can be attached to the spectrometer so that the counting rate may be graphed automatically. Graphs of this type may, for example, demonstrate the contamination of a commercially available ^{125}I-triolein by a mixture of ^{14}C-labeled components. Figure 63 shows the resolution thus obtainable and demonstrates that the contaminants can be removed by chromatographic purification on thin-layer chromatoplates.

REFERENCES

1. Snyder, F. Radioassay of thin-layer chromatograms: A high resolution zonal scraper for quantitative ^{14}C and ^{3}H scanning of thin-layer chromatograms. Anal Biochem 9, 183-196, 1964.
2. Snyder, F. Zonal scanning of thin-layer chromatograms, "Atomlight," Vol. 38, June 1964, pp. 7-12, a technical bulletin available from New England Nuclear Corporation. Presented at the Eighth Symposium on Advances in Tracer Methodology, Chicago, 1963. Symposia on Advances in Tracer Methodology, Vol. II, 1964.
3. Snyder, F., Alford, T. J. and Kimble, H. Radioassay of thin-layer chromatograms: Blueprints for zonal scaper. USAEC Report ORINS-44, April 1964.

Publications

1964

Reprints from the open literature and additional information on publications can be obtained by contacting Mrs. Edward H. Anderson, Technical Editor, Medical Division, Oak Ridge Institute of Nuclear Studies, Box 117, Oak Ridge, Tenn. 37831. Complete lists of Medical Division publications are available.

ARTICLES IN JOURNALS

Burger, C. L., Harris, W. W., Anderson, N. G., Bartlett, T. W., and Kniseley, R. M. Virus-like particles in human leukemic plasma. Proc Soc Exp Biol Med 115, 151-156, 1964.

Comas, F. V. Comparative changes in radiosensitivity between bone marrow and a rat tumor irradiated under anoxia. Radiology 83, 528-533, 1964.

Edwards, C. L., Andrews, G. A., Sitterson, B. W., and Kniseley, R. M. Clinical bone marrow scanning with radioisotopes. Blood 23, 741-756, 1964.

Fliedner, T. M., Andrews, G. A., Cronkite, E. P., and Bond, V. P. Early and late cytologic effects of whole body irradiation on human marrow. Blood 23, 471-487, 1964.

Gengozian, N. Heterotransplantation of human antibody-forming cells in diffusion chambers. Ann NY Acad Sci 120, 91-118, 1964.

Gengozian, N. Human A- and B-like antigens on red cells of marmosets. Proc Soc Exp Biol Med 117, 858-861, 1964.

Gengozian, N. Transplantation of rat bone marrow in irradiated mice: Effect of exposure rate. Science 146, 663-664, 1964.

Gengozian, N. and Doria, G. Allotypic specificities in four strains of inbred mice as revealed by reciprocal immunizations. J Immunol 93, 426-432, 1964.

Hayes, R. L., Carlton, J. E., and Nelson, Bill. Lanthanum-140 as a measure of the completeness of stool collections: Demonstration of delayed excretion of iron-59. J Nucl Med 5, 200-208, 1964.

Hayes, R. L., Oddie, T. H., and Brucer, M. Dose comparison of two total-body irradiation facilities. Int J Appl Radiat 15, 313-318, 1964.

Kretchmar, A. L. and Comas, F. V. Correlation between kidney muramidase activity and plasma iron removal in rats with Walker-256 carcinosarcoma. Proc Soc Exp Biol Med 116, 275-277, 1964.

McArthur, W. H., Congdon, C. C., and Kretchmar, A. L. Nitrogen balance in radiation chimeras. Proc Soc Exp Biol Med 117, 171-175, 1964.

MacLeod, J., Hotchkiss, R. S., and Sitterson, B. W. Recovery of male fertility after sterilization by nuclear radiation. JAMA 187, 637-641, 1964.

Morris, A. C., Jr., Ross, D. A., and Travis, J. C. A high-level whole-body counter. Int J Appl Radiat 15, 391-396, 1964.

Nelson, Bill M. and Andrews, G. A. Breast cancer and cytologic dysplasia in many organs after busulfan (Myleran). Amer J Clin Path 42, 37-44, 1964.

1027886

Snyder, F. Radioassay of thin-layer chromatograms: A high-resolution zonal scraper for quantitative C^{14} and H^3 scanning of thin-layer chromatograms. Anal Biochem 9, 183-196, 1964.

Snyder, F. and Kyker, G. C. Triglyceride accumulation and release in the rare-earth fatty liver. Proc Soc Exp Biol Med 116, 890-893, 1964.

Snyder, F. and Lewis, W. Phospholipid patterns in livers accumulating fat. Proc Soc Exp Biol Med 116, 459-462, 1964.

Vu-Thi, Suu, Congdon, C. C., and Kretchmar, A. L. Lysozyme acivity in radiation chimeras. Proc Soc Exp Biol Med 115, 825-829, 1964.

Urso, P. and Gengozian, N. Immunofluorescent detection of proliferating human antibody-forming cells. Nature 203, 1391-1392, 1964.

CHAPTERS IN BOOKS

Kniseley, R. M., Andrews, G. A., Edwards, C. L., and Tanida, R. Scanning of bone marrow in hematopoietic disorders. In: Medical Radioisotope Scanning, Vol. II Vienna, International Atomic Energy Agency, 1964, pp. 207-220, discussion 220-225.

Lushbaugh, C. C., Kretchmar, A., and Gibbs, W. Liver function measured by the blood clearance of rose bengal-I^{131}: A review and a model based on compartmental analysis of changes in arm, blood, and liver radioactivity. In: Dynamic Clinical Studies with Radioisotopes, USAEC Report TID-7678, June 1964, pp. 319-357 (AEC Symposium Series No. 3).

GOVERNMENT DOCUMENTS

Available from the Office of Technical Services, Department of Commerce, Washington, D.C. 20230:

Dynamic Clinical Studies with Radioisotopes. Proceedings of a symposium held at the Oak Ridge Institute of Nuclear Studies, October 21-25, 1963. Edited by R. M. Kniseley and W. N. Tauxe, U.S. Atomic Energy Commission Report TID-7678, June 1964, No. 3. AEC Symposium Series, 634 pp. Price, $4.50.

Saito, H. and Nagai, T. Labeling of myeloma cells and leukemic leukocytes in short-term culture with tagged precursors of nucleic acid and protein. USAEC Report ORINS-45, August 1964, 18 pp. Price, $0.50.

Snyder, F., Alford, T. S., and Kimble, H. Radioassay of thin-layer chromatograms: Blueprints for zonal scraper. USAEC Report ORINS-44, April 1964, 4 pp. Price, $0.50.

Available from the Clearinghouse for Federal Scientific and Technical Information, National Bureau of Standards, U.S. Department of Commerce, Springfield, Virginia:

Snyder, F. and Kimble, H. Blueprints of an automatic zonal scraper and sample collector for radioassay of thin-layer chromatograms. USAEC Report ORINS-47, November 1964, 10 pp. Price, $1.00.

Microfiche:

Kretchmar, A. L. and Congdon, C. C. The metabolic problem in secondary disease. USAEC Report ORNL-P-656, 1964.

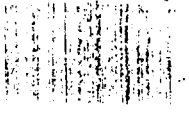

PUBLISHED ABSTRACTS

Gibbs, W. D. and Lushbaugh, C. C. A new counter for radioactive samples. J Nucl Med 5, 726, 1964, abstr.

Gibbs, W., Wilson, E., Hodges, H., and Lushbaugh, C. C. Comparative study of thyroid and whole-body retention of iodine in box turtles. In: Second Annual Oak Ridge Radioisotope Conference, April 19-22, 1964, USAEC Report TID-7689, pp. 20-21, abstr.

Hayes, R. L. and Carlton, J. E. *In vivo* mobilization of barium-137m. J Nucl Med 5, 378, 1964, abstr.

Kakehi, H. and Hayes, R. L. Counting characteristics of a medium-level whole-body counter. J Nucl Med 5, 372, 1964, abstr.

Kyker, G. C. and Rafter, J. Rare earth fatty liver induced by lanthanon chelates. Fed Proc 23, 375, 1964, abstr. 1647.

Kyker, G. C. and Rafter, J. Scanning of bone marrow in animals. J Nucl Med 5, 726-727, 1964, abstr.

Lushbaugh, C. C. and Gibbs, W. A rapid screening method for detecting abnormal plasma vitamin B_{12} binding sites in chronic myelogenous leukemia using arm counting. Abstr. In: Second Annual Oak Ridge Radioisotope Conference, April 19-22, 1964, USAEC Report TID-7689, pp. 11-14.

Morris, A. C., Jr. A diagnostic-level whole-body counter. J Nucl Med 5, 364, 1964, abstr.

Nelson, Bill M., Vichai Poshyachinda, and Makumkrong Wasanasomsithi. A method for comparing collimator systems applied to external counting of Cr^{51} in the spleen. J Nucl Med 5, 725-726, 1964, abstr.

Pfannenstiel, P. and Sitterson, B. W. Clinical usefulness of iodine-130 in serial tracer-studies in patients with functioning thyroid cancer. J Nucl Med 5, 727, 1964, abstr.

Wilson, E. D., Gibbs, W. D., and Lushbaugh, C. C. Thyroid uptake and whole-body retention of I^{131} in box turtles. Texas Rep Biol Med 22, 211-212, 1964, abstr.

MISCELLANEOUS

Andrews, G. A. Book review: Silver, Solomon. Radioactive Isotopes in Medicine and Biology: Medicine. Quimby, Edith and Feitelberg, Sergei. Radioactive Isotopes in Medicine and Biology: Basic Physics and Instrumentation. AMA Arch Int Med 113, 310-311, 1964.

Andrews, G. A. Discussion of: Cronkite, E. P. The diagnosis, treatment, and prognosis of human radiation injury from whole-body exposure. Ann NY Acad Sci 114, 349-354, 1964.

Andrews, G. A. Mexican Co^{60} radiation accident. Isotopes and Radiation Technology 1, 200-201, Winter, 1963-1964.

Kniseley, R. M. Meeting report: Radioisotope Scanning. Science 145, 416-418, 1964.

Snyder, F. Book review: Randerath, Kurt. Thin-Layer Chromatography. J Chem Educ, 1964.

Snyder, F. Zonal scanning of thin-layer chromatograms. Atomlight 38, 7-12, 1964. Symposia on Advances in Tracer Methodology, Vol. II, 1964.

1027887

ARTICLES IN PRESS

Andrews, G. A. and Cloutier, R. J. Accidental acute radiation injury: The need for recognition. AMA Arch Environ Health

Bergner, P.-E. E. Brief note: A plea for certain stochastic concepts in clinical red cell survival studies. Nature (Lond).

Edwards, C. L. and Gengozian, N. Autoimmune hemolytic anemia treated with d-penicillamine. Ann Int Med.

Gengozian, N., Batson, J. S., and Eide, P. Hematologic and cytologic evidence for chimerism in the marmoset *Tamarinus nigricollis*. Cytogenetics.

Hubner, K. and Brown, D. W. Myelography with radioactive iodinated serum albumin. J Nucl Med.

Hubner, K. and Gengozian, N. Depression of the primary immune response by dl-penicillamine. Proc Soc Exp Biol Med.

Johnson, J., Privett, O. S., and Snyder, F. Special report: Radiopurity of lipids. J Lipid Res.

Lushbaugh, C. C. and Lushbaugh, D. B. Rapid electronic red blood cell sizing as an aid in clinical diagnosis. Southern Med J.

Meyer, L. M., Schiffer, L. M., White, D. A., and Cronkite, E. P. The plasma disappearance of radioactive cobalamin: Effect of prior administration of vitamin B_{12} analogues. Brit J Haematol.

Snyder, F. An automatic zonal scraper and sample collector for radioassay of thin-layer chromatograms. Anal Biochem.

Snyder, F. Fatty acid oxidation in irradiated bone-marrow cells. Nature (Lond).

Snyder, F. and Wright, Reba. Effect of localized irradiation on the metabolism of bone marrow lipids. Radiat Res.

Steckel, R. J., Hendrix, E. L., and Bigelow, R. R. Malignant solid teratoma of the ovary in an 8-year-old child. Obstet Gynec (NY).

Acknowledgements

The research program is indebted to many individuals and groups. The care of patients has been assisted by consultations with physicians in Knoxville and Oak Ridge. In particular, we wish to express our appreciation to Doctors R. R. Bigelow, B. B. Blevins, Louis Bryan, Betty Cooper, James B. Cox, Kenneth L. Crounse, Dexter Davis, Earl Eversole, Ernest Lee Hendrix, R. A. Johnson, Avery P. King, W. G. Laing, Margaret Maynard, Dana Nance, Robert W. Newman, E. Converse Pierce, W. W. Pugh, C. Julian Ragan, Henry B. Ruley, C. W. Sensenbach, Eidson Smith, Paul Spray, George M. Stevens, II, and Joe Tittle.

The surgeons and operating room group at the Oak Ridge Hospital have rendered valuable aid. The Medical Nuclear Instrument Group at ORNL offered generously of their skills and knowledge. P. R. Bell, C. C. Harris, and D. A. Ross have been especially helpful. Others from Oak Ridge National Laboratory have given freely of their time to help with specific problems. All these resources have enhanced the program of the Division.

Author Index

Anderson, C. E. 63
Andrews, G. A. 11, 13, 72, 81, 91, 128
Batson, J. S. 55, 58
Bergner, P.-E. E. 91
Bollinger, J. N. 16, 19, 31, 44
Carlton, J. E. 70, 79
Cloutier, R. J. 107, 123
Comas, F. V. 9
Congdon, C. C. 40, 42, 44
Cress, E. A. 24, 26, 63
Dalton, Patricia 123
Doria, D. 61
Edwards, C. L. 48
Eide, P. 55
Gengozian, N. 46, 48, 49, 52, 55, 58, 61
Gibbs, W. D. 98, 103, 105, 110, 111, 122
Hayes, R. L. 70, 79, 111
Hodges, H. D. 98, 105, 110
Hofstra, Ruth 128
Hubner, K. 49
Johnson, G. T. 66, 67
Kakehi, H. 111
Kimble, H. 134
Kniseley, R. M. 81
Kretchmar, R. L. 9, 40, 42, 89
Kyker, G. C. 63, 65, 66, 67, 68, 69, 132
Lawson, J. D. 91
Lee, Young Ja 123
Lushbaugh, C. C. 35, 98, 105, 107, 110, 111, 128
Lushbaugh, D. B. 35
Miller, B. 63
Miller, I. H., Jr. 69
Morris, A. C., Jr. 111, 124
McArthur, W. H. 40, 42
Nelson, Bill M. 11, 58
Pfannenstiel, P. 72, 91, 103
Rafter, J. J. 66, 68
Roth, R. E. 128
Sitterson, B. W. 11, 72
Smyser, Mary 13
Snyder, F. 21, 24, 26, 34, 44, 65, 134
Stephens, N. 134
Tanida, R. 81
Webb, A. M. 132
Wright, Reba 21
Yarbro, C. L. 63

10217888